$$\nabla \times \vec{E} = -\frac{\partial \vec{B}}{\partial t}$$

$$\nabla \times \vec{H} = \vec{J} + \frac{\partial \vec{D}}{\partial t}$$

$$\nabla \cdot \vec{D} = \rho$$

$$\nabla \cdot \vec{B} = 0$$

ELECTROMAGNETICS

Branislav M. Notaroš

Electromagnetics

Branislav M. Notaroš

Department of Electrical and Computer Engineering
Colorado State University

Prentice Hall

Upper Saddle River Boston Columbus San Francisco New York
Indianapolis London Toronto Sydney Singapore Tokyo Montreal
Dubai Madrid Hong Kong Mexico City Munich Paris Amsterdam Cape Town

Contents

Preface xi

1 Electrostatic Field in Free Space 1

1.1 Coulomb's Law 2
1.2 Definition of the Electric Field Intensity Vector 7
1.3 Continuous Charge Distributions 8
1.4 On the Volume and Surface Integration 9
1.5 Electric Field Intensity Vector due to Given Charge Distributions 10
1.6 Definition of the Electric Scalar Potential 16
1.7 Electric Potential due to Given Charge Distributions 18
1.8 Voltage 21
1.9 Differential Relationship between the Field and Potential in Electrostatics 22
1.10 Gradient 23
1.11 3-D and 2-D Electric Dipoles 26
1.12 Formulation and Proof of Gauss' Law 28
1.13 Applications of Gauss' Law 31
1.14 Differential Form of Gauss' Law 35
1.15 Divergence 36
1.16 Conductors in the Electrostatic Field 39
1.17 Evaluation of the Electric Field and Potential due to Charged Conductors 43
1.18 Electrostatic Shielding 46
1.19 Charge Distribution on Metallic Bodies of Arbitrary Shapes 48
1.20 Method of Moments for Numerical Analysis of Charged Metallic Bodies 49
1.21 Image Theory 51

2 Dielectrics, Capacitance, and Electric Energy 61

2.1 Polarization of Dielectrics 62
2.2 Polarization Vector 63
2.3 Bound Volume and Surface Charge Densities 64
2.4 Evaluation of the Electric Field and Potential due to Polarized Dielectrics 68
2.5 Generalized Gauss' Law 70
2.6 Characterization of Dielectric Materials 71
2.7 Maxwell's Equations for the Electrostatic Field 75
2.8 Electrostatic Field in Linear, Isotropic, and Homogeneous Media 75
2.9 Dielectric-Dielectric Boundary Conditions 79
2.10 Poisson's and Laplace's Equations 82
2.11 Finite-Difference Method for Numerical Solution of Laplace's Equation 84
2.12 Definition of the Capacitance of a Capacitor 86
2.13 Analysis of Capacitors with Homogeneous Dielectrics 88
2.14 Analysis of Capacitors with Inhomogeneous Dielectrics 95
2.15 Energy of an Electrostatic System 102
2.16 Electric Energy Density 104
2.17 Dielectric Breakdown in Electrostatic Systems 108

3 Steady Electric Currents 124

3.1 Current Density Vector and Current Intensity 125
3.2 Conductivity and Ohm's Law in Local Form 128
3.3 Losses in Conductors and Joule's Law in Local Form 132
3.4 Continuity Equation 133
3.5 Boundary Conditions for Steady Currents 137

3.6 Distribution of Charge in a Steady Current Field 138
3.7 Relaxation Time 139
3.8 Resistance, Ohm's Law, and Joule's Law 140
3.9 Duality between Conductance and Capacitance 146
3.10 External Electric Energy Volume Sources and Generators 149
3.11 Analysis of Capacitors with Imperfect Inhomogeneous Dielectrics 152
3.12 Analysis of Lossy Transmission Lines with Steady Currents 156
3.13 Grounding Electrodes 162

4
Magnetostatic Field in Free Space 173

4.1 Magnetic Force and Magnetic Flux Density Vector 174
4.2 Biot-Savart Law 177
4.3 Magnetic Flux Density Vector due to Given Current Distributions 179
4.4 Formulation of Ampère's Law 185
4.5 Applications of Ampère's Law 187
4.6 Differential Form of Ampère's Law 193
4.7 Curl 195
4.8 Law of Conservation of Magnetic Flux 198
4.9 Magnetic Vector Potential 201
4.10 Proof of Ampère's Law 204
4.11 Magnetic Dipole 206
4.12 The Lorentz Force and Hall Effect 209
4.13 Evaluation of Magnetic Forces 211

5
Magnetostatic Field in Material Media 221

5.1 Magnetization Vector 222
5.2 Behavior and Classification of Magnetic Materials 223
5.3 Magnetization Volume and Surface Current Densities 227
5.4 Generalized Ampère's Law 234
5.5 Permeability of Magnetic Materials 236
5.6 Maxwell's Equations and Boundary Conditions for the Magnetostatic Field 239
5.7 Image Theory for the Magnetic Field 241
5.8 Magnetization Curves and Hysteresis 243
5.9 Magnetic Circuits – Basic Assumptions for the Analysis 247
5.10 Kirchhoff's Laws for Magnetic Circuits 250
5.11 Maxwell's Equations for the Time-Invariant Electromagnetic Field 258

6
Slowly Time-Varying Electromagnetic Field 263

6.1 Induced Electric Field Intensity Vector 264
6.2 Slowly Time-Varying Electric and Magnetic Fields 269
6.3 Faraday's Law of Electromagnetic Induction 271
6.4 Maxwell's Equations for the Slowly Time-Varying Electromagnetic Field 276
6.5 Computation of Transformer Induction 277
6.6 Electromagnetic Induction due to Motion 283
6.7 Total Electromagnetic Induction 289
6.8 Eddy Currents 294

7
Inductance and Magnetic Energy 311

7.1 Self-Inductance 312
7.2 Mutual Inductance 318
7.3 Analysis of Magnetically Coupled Circuits 324
7.4 Magnetic Energy of Current-Carrying Conductors 331
7.5 Magnetic Energy Density 334
7.6 Internal and External Inductance in Terms of Magnetic Energy 342

8
Rapidly Time-Varying Electromagnetic Field 351

8.1 Displacement Current 352
8.2 Maxwell's Equations for the Rapidly Time-Varying Electromagnetic Field 357
8.3 Electromagnetic Waves 361
8.4 Boundary Conditions for the Rapidly Time-Varying Electromagnetic Field 363
8.5 Different Forms of the Continuity Equation for Rapidly Time-Varying Currents 364
8.6 Time-Harmonic Electromagnetics 366
8.7 Complex Representatives of Time-Harmonic Field and Circuit Quantities 369

8.8 Maxwell's Equations in Complex Domain 373
8.9 Lorenz Electromagnetic Potentials 376
8.10 Computation of High-Frequency Potentials and Fields in Complex Domain 381
8.11 Poynting's Theorem 389
8.12 Complex Poynting Vector 397

9
Uniform Plane Electromagnetic Waves 408

9.1 Wave Equations 409
9.2 Uniform-Plane-Wave Approximation 411
9.3 Time-Domain Analysis of Uniform Plane Waves 412
9.4 Time-Harmonic Uniform Plane Waves and Complex-Domain Analysis 416
9.5 The Electromagnetic Spectrum 425
9.6 Arbitrarily Directed Uniform TEM Waves 427
9.7 Theory of Time-Harmonic Waves in Lossy Media 429
9.8 Explicit Expressions for Basic Propagation Parameters 433
9.9 Wave Propagation in Good Dielectrics 436
9.10 Wave Propagation in Good Conductors 439
9.11 Skin Effect 441
9.12 Wave Propagation in Plasmas 447
9.13 Dispersion and Group Velocity 452
9.14 Polarization of Electromagnetic Waves 458

10
Reflection and Transmission of Plane Waves 471

10.1 Normal Incidence on a Perfectly Conducting Plane 472
10.2 Normal Incidence on a Penetrable Planar Interface 483
10.3 Surface Resistance of Good Conductors 492
10.4 Perturbation Method for Evaluation of Small Losses 497
10.5 Oblique Incidence on a Perfect Conductor 499
10.6 Concept of a Rectangular Waveguide 505
10.7 Oblique Incidence on a Dielectric Boundary 507
10.8 Total Internal Reflection and Brewster Angle 513
10.9 Wave Propagation in Multilayer Media 520

11
Field Analysis of Transmission Lines 533

11.1 TEM Waves in Lossless Transmission Lines with Homogeneous Dielectrics 534
11.2 Electrostatic and Magnetostatic Field Distributions in Transversal Planes 538
11.3 Currents and Charges of Line Conductors 539
11.4 Analysis of Two-Conductor Transmission Lines 540
11.5 Transmission Lines with Small Losses 547
11.6 Attenuation Coefficients for Line Conductors and Dielectric 550
11.7 High-Frequency Internal Inductance of Transmission Lines 556
11.8 Evaluation of Primary and Secondary Circuit Parameters of Transmission Lines 557
11.9 Transmission Lines with Inhomogeneous Dielectrics 563
11.10 Multilayer Printed Circuit Board 567

12
Circuit Analysis of Transmission Lines 576

12.1 Telegrapher's Equations and Their Solution in Complex Domain 577
12.2 Circuit Analysis of Lossless Transmission Lines 581
12.3 Circuit Analysis of Low-Loss Transmission Lines 581
12.4 Reflection Coefficient for Transmission Lines 583
12.5 Power Computations of Transmission Lines 589
12.6 Transmission-Line Impedance 592
12.7 Complete Solution for Line Voltage and Current 597
12.8 Short-Circuited, Open-Circuited, and Matched Transmission Lines 601
12.9 Transmission-Line Resonators 608
12.10 Quality Factor of Resonators with Small Losses 610
12.11 The Smith Chart – Construction and Basic Properties 614
12.12 Circuit Analysis of Transmission Lines Using the Smith Chart 618

12.13 Transient Analysis of Transmission Lines 628
12.14 Thévenin Equivalent Generator Pair and Reflection Coefficients for Line Transients 630
12.15 Step Response of Transmission Lines with Purely Resistive Terminations 634
12.16 Analysis of Transmission Lines with Pulse Excitations 640
12.17 Bounce Diagrams 646
12.18 Transient Response for Reactive or Nonlinear Terminations 649

13
Waveguides and Cavity Resonators 662

13.1 Analysis of Rectangular Waveguides Based on Multiple Reflections of Plane Waves 663
13.2 Propagating and Evanescent Waves 666
13.3 Dominant Waveguide Mode 668
13.4 General TE Modal Analysis of Rectangular Waveguides 671
13.5 TM Modes in a Rectangular Waveguide 676
13.6 Cutoff Frequencies of Arbitrary Waveguide Modes 677
13.7 Wave Impedances of TE and TM Waves 680
13.8 Power Flow along a Waveguide 681
13.9 Waveguides with Small Losses 684
13.10 Waveguide Dispersion and Wave Velocities 688
13.11 Waveguide Couplers 692
13.12 Rectangular Cavity Resonators 696
13.13 Electromagnetic Energy Stored in a Cavity Resonator 700
13.14 Quality Factor of Rectangular Cavities with Small Losses 703

14
Antennas and Wireless Communication Systems 713

14.1 Electromagnetic Potentials and Field Vectors of a Hertzian Dipole 715
14.2 Far Field and Near Field 720
14.3 Steps in Far-Field Evaluation of an Arbitrary Antenna 722
14.4 Radiated Power, Radiation Resistance, Antenna Losses, and Input Impedance 730
14.5 Antenna Characteristic Radiation Function and Radiation Patterns 736
14.6 Antenna Directivity and Gain 740
14.7 Antenna Polarization 745
14.8 Wire Dipole Antennas 745
14.9 Image Theory for Antennas above a Perfectly Conducting Ground Plane 751
14.10 Monopole Antennas 754
14.11 Magnetic Dipole (Small Loop) Antenna 758
14.12 Theory of Receiving Antennas 760
14.13 Antenna Effective Aperture 766
14.14 Friis Transmission Formula for a Wireless Link 768
14.15 Antenna Arrays 772

APPENDICES

1
Quantities, Symbols, Units, and Constants 791

2
Mathematical Facts and Identities 796

3
Vector Algebra and Calculus Index 801

4
Answers to Selected Problems 802

Bibliography 806
Index 809

Preface

Electromagnetic theory is a fundamental underpinning of technical education, but, at the same time, one of the most difficult subjects for students to master. In order to help address this difficulty and contribute to overcoming it, here is another textbook on electromagnetic fields and waves for undergraduates, entitled, simply, *Electromagnetics*. This text provides engineering and physics students and other users with a comprehensive knowledge and firm grasp of electromagnetic fundamentals by emphasizing both mathematical rigor and physical understanding of electromagnetic theory, aimed toward practical engineering applications.

The book is designed primarily (but by no means exclusively) for junior-level undergraduate university and college students in electrical and computer engineering, physics, and similar departments, for both two-semester (or two-quarter) course sequences and one-semester (one-quarter) courses. It includes 14 chapters on electrostatic fields, steady electric currents, magnetostatic fields, slowly time-varying (low-frequency) electromagnetic fields, rapidly time-varying (high-frequency) electromagnetic fields, uniform plane electromagnetic waves, transmission lines, waveguides and cavity resonators, and antennas and wireless communication systems.

Apparently, there are an extremely large number of quite different books for undergraduate electromagnetics available (perhaps more than for any other discipline in science and engineering), which are all very good and important. This book, however, aims to combine the best features and advantages of all of them. It also introduces many new pedagogical features not present in any of the existing texts.

This text provides many nonstandard theoretically and practically important sections and chapters, new style and approaches to presenting challenging topics and abstract electromagnetic phenomena, innovative strategies and pedagogical guides for electromagnetic field and wave computation and problem solving, and, most importantly, outstanding (by the judgment of students so far) worked-out examples, homework problems, conceptual questions, and MATLAB exercises. The goal is to significantly improve students' understanding of electromagnetics and their attitude toward it. Overall, the book is meant as an ***"ultimate resource" for undergraduate electromagnetics***.

The distinguishing features of the book are:

- *371 realistic examples with very detailed and instructive solutions, tightly coupled to the theory, including strategies for problem solving*
- *650 realistic end-of-chapter problems, strongly and fully supported by solved examples (there is a demo example for every homework problem)*
- *Clear, rigorous, complete, and logical presentation of material, balance of breadth and depth, balance of static (one third) and dynamic (two thirds) fields, with no missing steps*
- *Flexibility for different options in coverage, emphasis, and ordering the material in a course or courses, including the transmission-lines-first approach*
- *Many nonstandard topics and subtopics and new derivations, explanations, proofs, interpretations, examples, pedagogical style, and visualizations*
- *500 multiple-choice conceptual questions (on the Companion Website), checking conceptual understanding of the book material*
- *400 MATLAB computer exercises and projects (on the Companion Website), many with detailed solutions (tutorials) and MATLAB codes (m files)*

www.pearsonhighered.com/notaros

The following sections explain these and other features in more detail.

WORKED EXAMPLES AND HOMEWORK PROBLEMS

The most important feature of the book is an extremely large number of realistic examples, with detailed and pedagogically instructive solutions, and end-of-chapter (homework) problems, strongly and fully supported by solved examples. There are a total of 371 worked examples, all tightly coupled to the theory, strongly reinforcing theoretical concepts and smoothly and systematically developing the problem-solving skills of students, and a total of 650 end-of-chapter problems, which are essentially offered and meant as end-of-section problems (indications appear at the ends of sections as to which problems correspond to that section).

Most importantly, for each homework problem or set of problems, there is always an example or set of examples in the text whose detailed solution provides the students and other readers with all necessary instruction and guidance to be able to solve the problem on their own, and to complete all homework assignments and practice for tests and exams. The abundance and quality of examples and problems are enormously important for the success of the course and class: students always ask for more and more solved examples, which must be relevant for the many problems that follow (for homework and exam preparation) – and this is exactly what this book attempts to offer.

Examples and problems in the book emphasize physical conceptual reasoning and mathematical synthesis of solutions, and not pure formulaic (plug-and-chug) solving. They also do not carry dry and too complicated pure mathematical formalisms. The primary goal is to teach the readers to reason through different (more or less challenging) situations and to help them gain confidence and really understand and like the material. Many examples and problems have a strong practical engineering context.

Solutions to examples show and explain every step, with ample discussions of approaches, strategies, and alternatives. Very often, solutions are presented in more than one way to aid understanding and development of true electromagnetic problem-solving skills. By acquiring such skills, which are definitely not limited to a skillful browsing through the book pages in a quest for a suitable "black-box" formula or set of formulas nor a skillful use of pocket calculators to plug-and-chug, the reader also acquires true confidence and pride in electromagnetics, and a strong appreciation for both its theoretical fundamentals and its practical applications.

"Physical" nontrivial examples are good also for instructors – for lectures and recitations – as they are much more interesting and suitable for logical presentation and discussion in the class than the "plug-and-chug" or purely "mathematical" examples.

CLARITY, RIGOR, AND COMPLETENESS

Along with the number and type of examples and problems (and questions and exercises), the most characteristic feature of the book is its consistent attention to clarity, completeness, and pedagogical soundness of presentation of the material throughout the entire text, aiming for an optimal balance of breadth and depth. Electromagnetics, as a fundamental science and engineering discipline, provides complete physical explanations for (almost) everything within its scope and rigorous mathematical models for everything it covers. Thus, besides a couple of experimental fundamental laws (like Coulomb's law) that have to be taken for granted for the model to build on, all other steps in building the most impressive and exciting structure called the electromagnetic theory can be readily presented to the reader in a consistent and meaningful manner and with enough detail to be understandable and appreciable. This is exactly what this book attempts to do.

Simply speaking, literally everything is derived, proved, and explained (except for a couple of experimental facts), with many new derivations, explanations, proofs, interpretations, and visualizations. Difficult and important concepts and derivations are regularly presented in more than one way to help students understand and master the subject at hand. Maximum effort has been devoted to a continuous logical flow of topics, concepts, equations, and ideas, with practically no "intentionally skipped" steps and parts. This, however, is done in a structural and modular manner, so that the reader who feels that some steps, derivations, and proofs can be bypassed at the time (with an opportunity of redoing it later) can do so, but this is left to the reader's discretion (or to the discretion and advice of the course instructor), not the author's.

Overall, my approach is to provide all possible (or all necessary) explanations, guidance, and detail

in the theoretical parts and examples in the text, whereas students' actual understanding of the material, their thinking "on their own feet," and ability to do independent work are tested and challenged through numerous and relevant end-of-chapter problems and conceptual questions, and not through filling the missing gaps in the text.

On the other hand, I am fully aware that brevity may seem attractive to students at first glance because it typically means fewer pages for reading assignments. However, most students will readily acknowledge that it is indeed much easier and faster to read, grasp, and use several pages of thoroughly explained and presented material as opposed to a single page of condensed material with too many missing parts. During my dealings with students over so many years, I have been constantly told that they in fact prefer having everything derived and explained, and host of sample problems solved, to a lower page count and too many important parts, steps, and explanations missing, and too few detailed solutions, and this was the principal motivation for my writing this book.

This approach, in my opinion, is also good for instructors, as they have a self-contained, ready-to-use continuous "story" for each of their lectures, instead of a set of discrete formulas and sample facts with little or no explanations and detail. On the other hand, the instructor may choose to present only main facts for a given topic in class and rely on students for the rest, as they will be able to quickly and readily understand all reading assignments from the book. Indeed, I expect that every instructor using this text will have different "favorite" topics presented in class with all details and in great depth, including a number of examples, while "giving away" some other topics to students to cover on their own, with more or less depth, including worked examples.

OPTIONS IN COVERAGE OF THE MATERIAL

This book promotes and implements the direct or chronological and not inverse order of topics in teaching/learning electromagnetics, which can briefly be characterized as: first static and then dynamic topics, or first fields (static, quasistatic, and rapidly time-varying) and then waves (uniform plane waves, transmission lines, waveguides, and antennas). In addition, the book features a favorable balance of static (one third) and dynamic (two thirds) fields. Ideally, a course or a sequence of courses using this text would completely cover the book material, with a likelihood that some portions would be given to students as a reading assignment only. However, the book allows a lot of flexibility and many different options in actually covering the material, or parts of it, and ordering the topics in a course (or courses).

One scenario is to quickly go through Chapters 1–7, do just basic concepts and equations, and a couple of examples in each chapter, quickly reach Chapter 8 (general Maxwell's equations, etc.), and then do everything else as applications of general Maxwell's equations, including selected topics from Chapters 1–7 and more or less complete coverage of all other chapters. This scenario would essentially reflect the inverse (nonchronological) order of topics in teaching/learning electromagnetics. In fact, there may be many different scenarios suitable for different areas of emphasis and specialized outcomes of the course and the available time, all of them advancing in chronological order, through Chapters 1–14 of the book, just with different speeds and different levels of coverage of individual chapters.

To help the instructors create a plan for using the book material in their courses and students and other readers prioritize the book contents in accordance with their learning objectives and needs, Tables 1 and 2 provide classifications of all book chapters and sections, respectively, in two levels, indicating which chapters and sections within chapters are suggested as more likely candidates to be skipped or skimmed (covered lightly). This is just a guideline, and I expect that there will be numerous extremely creative, effective, and diverse combinations of book topics and subtopics constituting course outlines and learning/training plans, customized to best meet the preferences, interests, and needs of instructors, students, and other book users.

Most importantly, if chapters and sections are skipped or skimmed in the class, they are not skipped nor skimmed in the book, and the student will always be able to quickly find and apprehend additional information and fill any missing gaps using pieces of the book material from chapters and sections that are not planned to be covered in detail.

Table 1. **Classification of book chapters in two groups**, where "mandatory" chapters are those that would likely be covered in most courses, while some of the "elective" chapters could be skipped (or skimmed) based on specific areas of emphasis and desired outcomes of the course or sequence of courses and the available time. In selecting the material for the course(s), this classification at the chapter level could be combined with the classification at the section level given in Table 2.

"Mandatory" Chapters: 1, 3, 4, 6, 8, 9, 12	"Elective" Chapters: 2, 5, 7, 10, 11, 13, 14
1. Electrostatic Field in Free Space	2. Dielectrics, Capacitance, and Electric Energy
3. Steady Electric Currents	5. Magnetostatic Field in Material Media
4. Magnetostatic Field in Free Space	7. Inductance and Magnetic Energy
6. Slowly Time-Varying Electromagnetic Field	10. Reflection and Transmission of Plane Waves
8. Rapidly Time-Varying Electromagnetic Field	11. Field Analysis of Transmission Lines
9. Uniform Plane Electromagnetic Waves	13. Waveguides and Cavity Resonators
12. Circuit Analysis of Transmission Lines	14. Antennas and Wireless Communication Systems

Table 2. **Classification of book sections in two "tiers"** in terms of the suggested priority for coverage; if one or more sections in any of the chapters are to be skipped (or skimmed) given the areas of emphasis and specialized outcomes of the course or courses and the available time, then it is suggested that they be selected from the "tier two" sections, which certainly does not rule out possible omission (or lighter coverage) of some of the "tier one" sections as well.

Chapter	"Tier One" Sections	"Tier Two" Sections
1. Electrostatic Field in Free Space	1.1–1.4, 1.6, 1.8–1.10, 1.13–1.16	1.5, 1.7, 1.11, 1.12, 1.17–1.21
2. Dielectrics, Capacitance, and Electric Energy	2.1, 2.6, 2.7, 2.9, 2.10, 2.12, 2.13, 2.15, 2.16	2.2–2.5, 2.8, 2.11, 2.14, 2.17
3. Steady Electric Currents	3.1–3.4, 3.8, 3.10, 3.12	3.5–3.7, 3.9, 3.11, 3.13
4. Magnetostatic Field in Free Space	4.1, 4.2, 4.4–4.7, 4.9	4.3, 4.8, 4.10–4.13
5. Magnetostatic Field in Material Media	5.1, 5.5, 5.6, 5.8, 5.11	5.2–5.4, 5.7, 5.9, 5.10
6. Slowly Time-Varying Electromagnetic Field	6.2–6.5	6.1, 6.6–6.8
7. Inductance and Magnetic Energy	7.1, 7.4, 7.5	7.2, 7.3, 7.6
8. Rapidly Time-Varying Electromagnetic Field	8.2, 8.4, 8.6–8.8, 8.11, 8.12	8.1, 8.3, 8.5, 8.9, 8.10
9. Uniform Plane Electromagnetic Waves	9.3–9.7, 9.11, 9.14	9.1, 9.2, 9.8–9.10, 9.12, 9.13
10. Reflection and Transmission of Plane Waves	10.1, 10.2, 10.4–10.7	10.3, 10.8, 10.9
11. Field Analysis of Transmission Lines	11.4–11.6, 11.8	11.1–11.3, 11.7, 11.9, 11.10
12. Circuit Analysis of Transmission Lines	12.1–12.6, 12.11, 12.12, 12.15	12.7–12.10, 12.13, 12.14, 12.16–12.18
13. Waveguides and Cavity Resonators	13.1–13.3, 13.6, 13.8, 13.9, 13.12	13.4, 13.5, 13.7, 13.10, 13.11, 13.13, 13.14
14. Antennas and Wireless Communication Systems	14.1, 14.2, 14.4–14.6, 14.8, 14.14, 14.15	14.3, 14.7, 14.9–14.13

Table 3. **Ordering the book material for the transmission-lines-first approach**; Chapter 12 (Circuit Analysis of Transmission Lines) is written using only pure circuit-theory concepts (all field-theory aspects of transmission lines are placed in Chapter 11 – Field Analysis of Transmission Lines), so it can be taken at the very beginning of the course (or at any other time in the course). Note that two sections introducing (or reviewing) complex representatives of time-harmonic voltages and currents (Sections 8.6 and 8.7) must be done before Chapter 12.

Section 8.6: Time-Harmonic Electromagnetics
Section 8.7: Complex Representatives of Time-Harmonic Field and Circuit Quantities
Chapter 12: Circuit Analysis of Transmission Lines (or a selection of sections from Chapter 12 – see Table 2)
Chapters 1-11, 13, 14 or a selection of chapters (see Table 1) and sections (see Table 2)

TRANSMISSION-LINES-FIRST APPROACH

One possible exception from the chronological sequence of chapters (topics) in using this text implies a different placement of Chapter 12 (Circuit Analysis of Transmission Lines), which is written in such a manner that it can be taken at any time, even at the very beginning of the course, hence constituting the transmission-lines-first approach to teaching the course and learning the material. Namely, the field and circuit analyses of transmission lines are completely decoupled in the book, so that any field-theory aspects are placed in Chapter 11 (Field Analysis of Transmission Lines) and only pure circuit-theory concepts are used in Chapter 12 with per-unit-length characteristics (distributed parameters) of the lines being taken for granted (are assumed to be known) from the field analysis if the circuit analysis is done first. Table 3 shows the transmission-lines-first scenario using this book.

MULTIPLE-CHOICE CONCEPTUAL QUESTIONS

The book provides, on the *Companion Website*, a total of 500 conceptual questions. These are multiple-choice questions that focus on the core concepts of the material, requiring conceptual reasoning and understanding rather than calculations. They serve as checkpoints for readers following the theoretical parts and worked examples (like homework problems, conceptual questions are referred to at the ends of sections). Generally, conceptual questions may appear simple, but students often find them harder than the standard problems. Pedagogically, they are an invaluable resource. They are also ideal for in-class questions and discussions (so-called active teaching and learning) to be combined with traditional lecturing – if so desired.

In addition, conceptual questions are perfectly suited for class assessments, namely, to assess students' performance and evaluate the effectiveness of instruction, usually as the "gain" between the course "pretest" and "posttest" scores, and especially in light of ABET and similar accreditation criteria (the key word in these criteria is "assessment"). Selected conceptual questions from the large collection provided in the book can readily be used by instructors as partial and final assessment instruments for individual topics at different points in the course and for the entire class.

MATLAB EXERCISES, TUTORIALS, AND PROJECTS

The book provides, on the *Companion Website*, a very large and comprehensive collection of MATLAB computer exercises, strongly coupled to the book material, both the theory and the worked examples, and designed to help students develop a stronger intuition and a deeper understanding of electromagnetics, and find it more attractive and likable. MATLAB is chosen principally because it is a generally accepted standard in science and engineering education worldwide.

There are a total of 400 MATLAB exercises, which are referred to regularly within all book chapters, at the ends of sections, to supplement problems and conceptual questions. Each section of this collection starts with a comparatively very large number of tutorial exercises with detailed completely

worked out solutions, as well as MATLAB codes (m files). This resource provides abundant opportunities for instructors for assigning in-class and homework projects – if so desired.

VECTOR ALGEBRA AND CALCULUS

Elements of vector algebra and vector calculus are presented and used gradually across the book sections with an emphasis on physical insight and immediate links to electromagnetic field theory concepts, instead of having a purely mathematical review in a separate chapter. They are fully integrated with the development of the electromagnetic theory, where they actually belong and really come to life.

The mathematical concepts of gradient, divergence, curl, and Laplacian, as well as line (circulation), surface (flux), and volume integrals, are literally derived from physics (electromagnetics), where they naturally emanate as integral parts of electromagnetic equations and laws and where their physical meaning is almost obvious and can readily be made very visual. Furthermore, the text is written in such a way that even a reader with little background in vector algebra and vector calculus will indeed be able to learn or refresh vector analysis concepts directly through the first several chapters (please see Appendix 3 – Vector Algebra and Calculus Index).

LINKS TO CIRCUIT THEORY

The book provides detailed discussions of the links between electromagnetic theory and circuit theory throughout all of its chapters. It contains physical explanations for all elements of circuit theory, for both dc and ac regimes. All basic circuit-theory equations (circuit laws, element laws, etc.) are derived from electromagnetic theory. The goal is for the reader to develop both an appreciation of electromagnetic theory as a foundation of circuit theory and electrical engineering as a whole, as well as an understanding of limitations of circuit theory as an approximation of field theory.

HISTORICAL ASIDES

Throughout almost all chapters of the book, dozens of Historical Asides appear with quite detailed and fascinating biographies of famous scientists and pioneers in the field of electricity and magnetism. There are a total of 40 biographies, which are, in my view, not only very interesting historically and informative in terms of providing the factual chronological review of the development of one of the most impressive, consistent, and complete theories of the entire scientific and technological world – the electromagnetic theory – but they also often provide additional technical facts and explanations that complement the material in the text. I also feel that some basic knowledge about the discoverers – who made such epochal scientific achievements and far-reaching contributions to humanity – like Faraday, Maxwell, Henry, Hertz, Coulomb, Tesla, Heaviside, Oersted, Ampère, Ohm, Weber, and others should be made an irreplaceable part of a sort of "general education" of our engineering and physics students.

SUPPLEMENTS

The book is accompanied by the Solutions Manual (for instructors) with detailed solutions to all end-of-chapter problems (written in the same manner as the solutions in the examples in the book), answers to all conceptual questions, and MATLAB codes (m files) for all MATLAB computer exercises and projects, as well as by PowerPoint slides with all illustrations from the text and by other supplements. *Pearson eText* of the book is also available.

www.pearsonhighered.com/notaros

ACKNOWLEDGMENTS

This text is based on my electromagnetics teaching and research over more than 20 years at the University of Belgrade, Yugoslavia (Serbia), University of Colorado at Boulder, University of Massachusetts Dartmouth, and Colorado State University, in Fort Collins, U.S.A. I gratefully acknowledge my colleagues and/or former Ph.D. students at these institutions whose discussions, advice, ideas, enthusiasm, initiatives, co-teaching, and co-authorships have shaped my knowledge, teaching style, pedagogy, and writing in electromagnetics, including: Prof. Branko Popović (late), Prof. Milan Ilić, Prof. Miroslav Djordjević, Prof. Antonije Djordjević, Prof. Zoya Popović, Gradimir Božilović, Prof. Momčilo Dragović (late), Prof.

Branko Kolundžija, Prof. Vladimir Petrović, and Prof. Jovan Surutka (late). All I know in electromagnetics and about its teaching I learned from them or with them or because of them, and I am enormously thankful for that.

I am grateful to all my students in all my classes over all these years for all the joy I have had in teaching them electromagnetics and for teaching me to teach better.

I especially thank my current Ph.D. students Nada Šekeljić, Ana Manić, and Sanja Manić for their invaluable help in writing MATLAB computer exercises, tutorials, and codes, checking the derivations and examples in the book, and solving selected end-of-chapter problems. I owe a particular debt of gratitude to my colleague and former Ph.D. student Prof. Milan Ilić, for his outstanding work and help with the initial electronic artwork in the book. My colleagues and former students Andjelija Ilić and Prof. Miroslav Djordjević, as well as Olivera Notaroš, also contributed very significantly to the artwork, for which I am sincerely indebted.

I would like to express my gratitude to the reviewers of the manuscript for their extremely detailed, useful, positive, and competent comments that I feel helped me to significantly improve the quality of the book, including: Professors Indira Chatterjee, Robert J. Coleman, Cindy Harnett, Jianming Jin, Leo Kempel, Edward F. Kuester, Yifei Li, Krzysztof A. Michalski, Michael A. Parker, Andrew F. Peterson, Costas D. Sarris, and Fernando L. Teixeira.

Special thanks to all members of the Pearson Prentice Hall team, who all have been excellent, and particularly to my editor Andrew Gilfillan, who has been extremely helpful and supportive, and whose input was essential at many stages in the development of the manuscript and book, my production manager Scott Disanno, for expertly leading the book production, Marcia Horton, Vice President and Editorial Director with Prentice Hall, for great conversations and support in the initial phases of the project, and Tom Robbins, former Publisher at Prentice Hall, for the first encouragements. I hope they enjoyed our dealings and discussions as extensively as I did.

I thank my wife Olivera Notaroš, who also teaches in the ECE Department at Colorado State University, not only for her great and constant support and understanding but also for her direct involvement and absolutely phenomenal ideas, advice, and help in all phases of writing the manuscript and production of the book. Without her, this book would not be possible or would, at least, be very different. I also acknowledge extraordinary support by my wonderful daughters Jelena and Milica, and I hope that I will be able to keep my promise to them that I will now take a long break from writing. I am very sad that the writing of this book took me so long that my beloved parents Smilja and Mile did not live to receive the first dedicated copy of the book from me, as had been the case with my previous books.

Finally, on a very personal note as well, I really love electromagnetics and teaching it, and I hope that this book will convey at least a portion of my admiration and enthusiasm to the readers and help more and more students start liking and appreciating this fascinating discipline with endless impacts. I am proud of being able to do that in my classes, and am now excited and eager to try to spread that message to a much larger audience using this text. Please send me your comments, suggestions, questions, and corrections (I hope there will not be many of these) regarding the book to notaros@colostate.edu.

Branislav M. Notaroš
Fort Collins, Colorado

"I believe but cannot explain that the author's confidence is somehow transferred to the student as a trust that the text they are reading and learning from is worth their time."
—Anonymous reviewer of the book manuscript

1 Electrostatic Field in Free Space

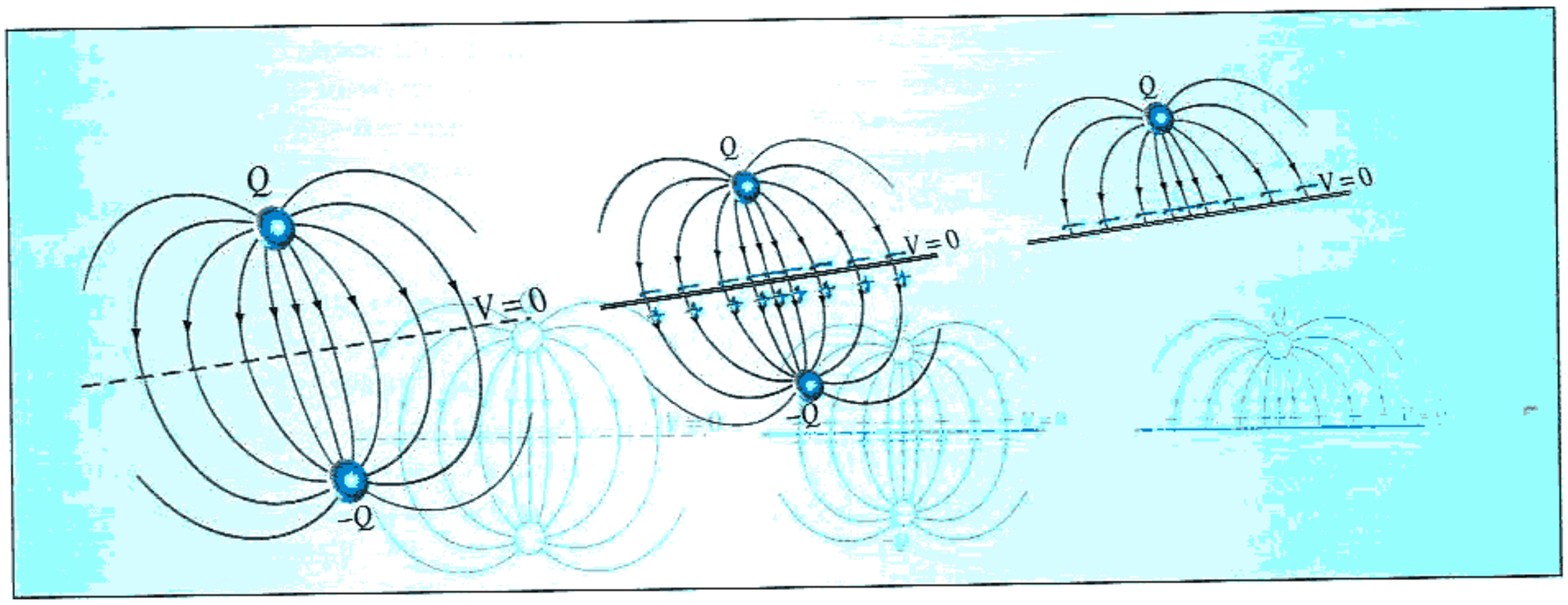

Introduction:

Electrostatics is the branch of electromagnetics that deals with phenomena associated with static electricity, which are essentially the consequence of a simple experimental fact – that charges exert forces on one another. These forces are called electric forces, and the special state in space due to one charge in which the other charge is situated and which causes the force on it is called the electric field. Any charge distribution in space with any time variation is a source of the electric field. The electric field due to time-invariant charges at rest (charges that do not change in time and do not move) is called the static electric field or electrostatic field. This is the simplest form of the general electromagnetic field, and its physics and mathematics represent the foundation of the entire electromagnetic theory. On the other hand, a clear understanding of electrostatics is essential for many practical applications that involve static electric fields, charges, and forces in electrical and electronic devices and systems.

We shall begin our study of electrostatics by investigating the electrostatic field in a vacuum or air (free space), which will then be extended to the analysis of electrostatic structures composed of charged conductors in free space (also in this chapter). In the next chapter, we shall evaluate the electrostatic field in the presence of dielectric materials, and include such materials in our discussion of general electrostatic systems.

HISTORICAL ASIDE

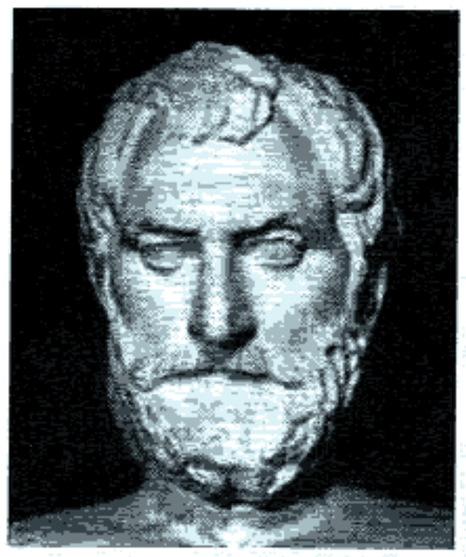

The first record of our experiences with electricity dates back to the sixth century B.C., when **Thales of Miletus** (624 B.C.–546 B.C.), an ancient Greek philosopher and mathematician, one of the greatest minds of all time, wrote that amber rubbed in wool attracts pieces of straw or feathers – which we now know is a manifestation of electrification by friction. In relation to this, the name "electron" for the subatomic particle carrying the smallest amount of (negative) charge comes from the Greek word ἤλεκτρον (*elektron*) for amber. Our experiences with magnetism, on the other side, also trace back to ancient times. The origin of the word "magnet" relates to the region in Greece named Magnesia (*Μαγνησία*), in which ancient Greeks first noticed (ca. 800 B.C.) that pieces of the black rock they were standing on, now known as the iron mineral magnetite (Fe_3O_4), attracted one another.

Charles Augustin de Coulomb (1736–1806) was a colonel in the Engineering Corps of the French Army and a brilliant experimentalist in electricity and magnetism. He graduated in 1761 from the School of the Engineering Corps (*École du Génie*), and was in charge of building the Fort Bourbon on Martinique, in the West Indies, where he showed his engineering and organizational skills. In 1772, Coulomb returned to France with impaired health, and began his research in applied mechanics. In 1777, he invented a torsion balance to measure small forces, and as a result of his 1781 memoir on friction, he was elected to the French Academy (*Académie des Sciences*). Between 1785 and 1791, he wrote a series of seven papers on electricity and magnetism, out of which by far the most important and famous is his work on the theory of attraction and repulsion between charged bodies. Namely, Coulomb formulated in 1785 the basic law for the electrostatic force between like and unlike charges (i.e., between two charges of the same or opposite polarity) using his genuine torsion balance apparatus, in a course of experiments originally aimed at improving the mariner's compass. He measured the electric force of attraction or repulsion that two charged small pith balls exerted on one another by the amount of twist produced on the torsion balance, and demonstrated an inverse square law for such forces – the force is proportional to the product of the charges of each of the balls and inversely proportional to the square of the distance between their centers. This result came out to be an underpinning of the whole area of science and engineering now known as electromagnetics, and of all of its applications. Upon the outbreak of the French Revolution in 1789, Coulomb retired to a small estate near Blois, to work in peace on his scientific memoirs. His last post was that of the inspector general of public instruction, under Napoleon, from 1802 to 1806. The law of electric forces on charges now bears his name – Coulomb's law – and his name is further immortalized by the use of coulomb (C) as the unit of charge.

1.1 COULOMB'S LAW

The basis of electrostatics is an experimental result called Coulomb's law. It states that the electric force $\mathbf{F}_{e12}$ on a point charge Q_2 due to a point charge Q_1 in a

vacuum (or air) is given by[1] (Fig. 1.1)

$$\boxed{\mathbf{F}_{e12} = \frac{1}{4\pi\varepsilon_0}\frac{Q_1 Q_2}{R^2}\hat{\mathbf{R}}_{12}.} \qquad (1.1)$$ *Coulomb's law*

With $\mathbf{R}_{12}$ denoting the position vector of Q_2 relative to Q_1, $R = |\mathbf{R}_{12}|$ is the distance between the two charges, $\hat{\mathbf{R}}_{12} = \mathbf{R}_{12}/R$ is the unit vector[2] of the vector $\mathbf{R}_{12}$, and ε_0 is the permittivity of a vacuum (free space),

$$\boxed{\varepsilon_0 = 8.8542 \text{ pF/m}} \qquad (1.2)$$ *permittivity of a vacuum*

(p $\equiv 10^{-12}$ and F is farad, the unit for capacitance, which will be studied in the next chapter). By point charges we mean charged bodies of arbitrary shapes whose dimensions are much smaller than the distance between them. The SI (International System of Units[3]) unit for charge is the coulomb (abbreviated C), named in honor of Charles Coulomb. This is a very large unit of charge. The charge of an electron, which is negative, turns out to be

$$\boxed{e = 1.602 \times 10^{-19} \text{ C}} \qquad (1.3)$$ *charge of electron, magnitude*

in magnitude ($Q_{\text{electron}} = -e$). The unit for force ($\mathbf{F}$) is the newton (N). The expression $Q_1 Q_2/(4\pi\varepsilon_0 r^2)$ in Eq. (1.1) represents the algebraic intensity (can be of arbitrary sign) of the vector $\mathbf{F}_{e12}$ with respect to the unit vector $\hat{\mathbf{R}}_{12}$. If Q_1 and Q_2 are of the same sign or polarity (like charges), this intensity is positive, $\mathbf{F}_{e12}$ has the same orientation as $\hat{\mathbf{R}}_{12}$, and the force between charges is repulsive. Conversely, the electric force between unlike charges ($Q_1 Q_2 < 0$) is attractive.

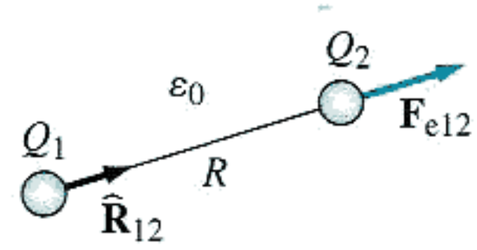

Figure 1.1 Notation in Coulomb's law, given by Eq. (1.1).

By reversing the indices 1 and 2 in Eq. (1.1) and noting that $\hat{\mathbf{R}}_{21} = -\hat{\mathbf{R}}_{12}$, we obtain that $\mathbf{F}_{e21} = -\mathbf{F}_{e12}$; i.e., the force on Q_1 due to Q_2 is equal in magnitude and opposite in direction to the force on Q_2 due to Q_1. This result is essentially an expression of Newton's third law – to every action (force) in nature, there is an opposed equal reaction.

If we have more than two point charges, we can use the principle of superposition, which also is a result of experiments, to determine the resultant force on a particular charge – by adding up vectorially the partial forces exerted on it by each of the remaining charges individually.

In the general case, vector addition is carried out component by component (for an arbitrary number of vectors), most frequently in the Cartesian coordinate system. Cartesian (or rectangular) coordinates, x, y, and z, and coordinate unit vectors, $\hat{\mathbf{x}}$, $\hat{\mathbf{y}}$, and $\hat{\mathbf{z}}$ (unit vectors along the x, y, and z directions), are shown in Fig. 1.2. The unit vectors are mutually perpendicular, and an arbitrary vector $\mathbf{a}$ in Cartesian coordinates can be represented as

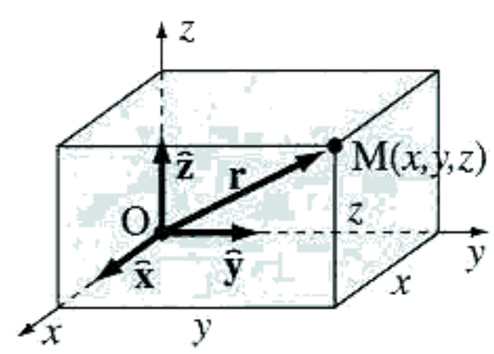

Figure 1.2 Point M(x, y, z) and coordinate unit vectors in the Cartesian coordinate system.

$$\boxed{\mathbf{a} = a_x\,\hat{\mathbf{x}} + a_y\,\hat{\mathbf{y}} + a_z\,\hat{\mathbf{z}}.} \qquad (1.4)$$ *Cartesian vector components*

[1] In typewritten work, vectors are commonly represented by boldface symbols, e.g., $\mathbf{F}$, whereas in handwritten work, they are denoted by placing a right-handed arrow over the symbol, as $\vec{F}$.

[2] All unit vectors in this text will be represented using the "hat" notation, so the unit vector in the x direction (in the rectangular coordinate system), for example, is given as $\hat{\mathbf{x}}$ (note that some of the alternative widely used notations for unit vectors would represent this vector as $\mathbf{a}_x$, $\mathbf{i}_x$, and $\mathbf{u}_x$, respectively).

[3] SI is the modernized version of the metric system. The abbreviation is from the French name *Système International d'Unités*.

Here, a_x, a_y, and a_z are the components of vector $\mathbf{a}$ in the Cartesian coordinate system, and its magnitude is

$$a = |\mathbf{a}| = \sqrt{a_x^2 + a_y^2 + a_z^2}. \tag{1.5}$$

The unit vector of $\mathbf{a}$ is $\hat{\mathbf{a}} = \mathbf{a}/a$. Of course, the magnitude of $\hat{\mathbf{a}}$, and of any unit vector, is unity, $|\hat{\mathbf{a}}| = |\mathbf{a}|/a = 1$. The sum of two vectors is given by

$$\mathbf{a} + \mathbf{b} = (a_x + b_x)\,\hat{\mathbf{x}} + (a_y + b_y)\,\hat{\mathbf{y}} + (a_z + b_z)\,\hat{\mathbf{z}}. \tag{1.6}$$

Shown in Fig. 1.2 is also the position vector $\mathbf{r}$ of an arbitrary point M(x, y, z) in space, with respect to the coordinate origin (O),

position vector of a point

$$\boxed{\mathbf{r} = x\,\hat{\mathbf{x}} + y\,\hat{\mathbf{y}} + z\,\hat{\mathbf{z}},} \tag{1.7}$$

where, using Eq. (1.5), $r = |\mathbf{r}| = \sqrt{x^2 + y^2 + z^2} = \overline{\text{OM}}$ is the distance[4] between points O and M.

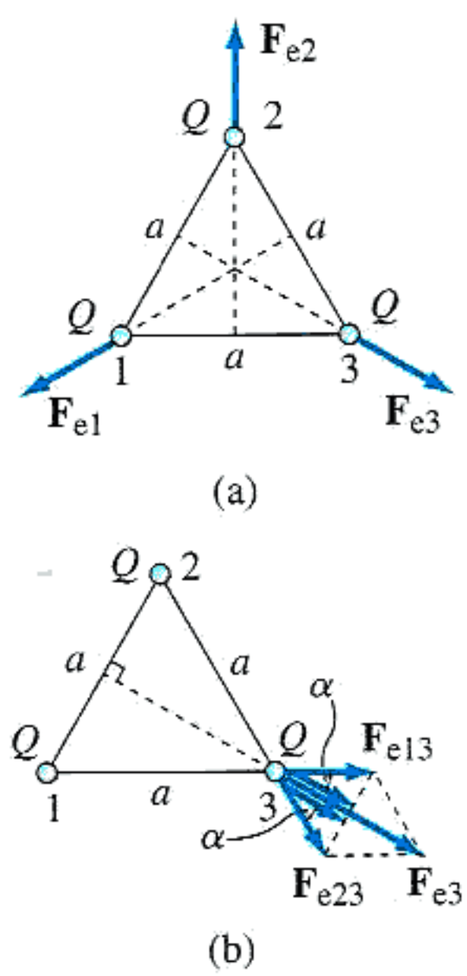

Figure 1.3 (a) Three equal point charges at the vertices of an equilateral triangle and (b) computation of the resultant electric force on one of the charges; for Example 1.1.

Example 1.1 Three Equal Point Charges at Triangle Vertices

Three small charged bodies of charge Q are placed at three vertices of an equilateral triangle with sides a, in air. The bodies can be considered as point charges. Find the direction and magnitude of the electric force on each of the charges.

Solution Even with no computation whatsoever, we can conclude from the symmetry of this problem that the resultant forces on the charges, $\mathbf{F}_{e1}$, $\mathbf{F}_{e2}$, and $\mathbf{F}_{e3}$, all have the same magnitude and are positioned in the plane of the triangle as indicated in Fig. 1.3(a). Let us compute the resultant force on the lower right charge – charge 3. Using the principle of superposition, this force represents the vector sum of partial forces due to charges 1 and 2, respectively, that is [Fig. 1.3(b)],

$$\mathbf{F}_{e3} = \mathbf{F}_{e13} + \mathbf{F}_{e23} \quad \text{(vector superposition)}. \tag{1.8}$$

From Coulomb's law, Eq. (1.1), magnitudes of the individual partial forces are given by

$$F_{e13} = F_{e23} = \frac{Q^2}{4\pi\varepsilon_0 a^2}, \tag{1.9}$$

and both forces are repulsive.

We note that the vector $\mathbf{F}_{e3}$ is positioned along the symmetry line between charges 1 and 2, i.e., between vectors $\mathbf{F}_{e13}$ and $\mathbf{F}_{e23}$, and it makes the angle $\alpha = \pi/6$ with both vectors. The magnitude of the resultant vector is therefore twice the projection of any of the partial vectors on the symmetry line, which yields

$$F_{e3} = 2\,(F_{e13}\cos\alpha) = 2F_{e13}\frac{\sqrt{3}}{2} = F_{e13}\sqrt{3} = \frac{\sqrt{3}Q^2}{4\pi\varepsilon_0 a^2}. \tag{1.10}$$

[4]While dealing with a wide variety of vector quantities in electromagnetics, we shall regularly visualize (draw) them as arrows in space, like the force vector $\mathbf{F}_{e12}$ in Fig. 1.1, to aid the analysis and computation. However, we shall always have in mind that only position vectors, like $\mathbf{r}$ in Fig. 1.2, and some other length vectors to be introduced later have this feature of their magnitude being the actual geometrical distance in space. Magnitudes of all other vectors are measured in units different from meter, and the sizes (lengths) of arrows in space that they are associated with can only be indicative of relative magnitudes of quantities of the same nature (with the same unit), like two forces acting on the same body, which is equally useful and will be utilized extensively in this text as well.

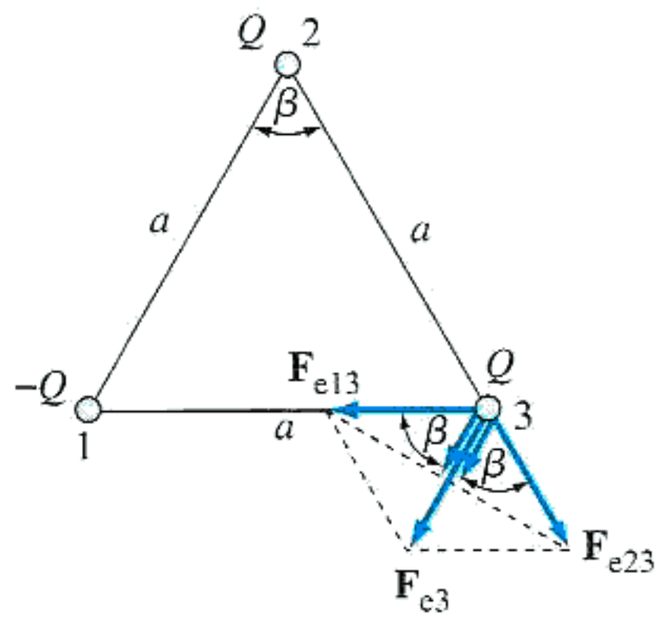

Figure 1.4 Three point charges equal in magnitude but with different polarities at the vertices of an equilateral triangle – computation of the resultant electric force on charge 3; for Example 1.2.

Example 1.2 Three Unequal Point Charges at Triangle Vertices

Determine the resultant force on the lower right charge in the configuration shown in Fig. 1.4. Assume that Q and a are given quantities.

Solution The only difference with respect to the configuration in Fig. 1.3 is that the force $\mathbf{F}_{e13}$ is now attractive, as indicated in Fig. 1.4. The resultant force on charge 3 is parallel to the line connecting charges 2 and 1, and the angle it makes with any of the partial forces, $\mathbf{F}_{e13}$ and $\mathbf{F}_{e23}$, is $\beta = \pi/3$. Its magnitude is hence

$$F_{e3} = 2\,(F_{e13}\cos\beta) = 2F_{e13}\frac{1}{2} = F_{e13} = \frac{Q^2}{4\pi\varepsilon_0 a^2}. \tag{1.11}$$

Example 1.3 Three Point Charges in Cartesian Coordinate System

Point charges $Q_1 = 1\ \mu\text{C}$, $Q_2 = -2\ \mu\text{C}$, and $Q_3 = 2\ \mu\text{C}$ are situated in free space at points defined by Cartesian coordinates $(1\text{ m}, 0, 0)$, $(0, 1\text{ m}, 0)$, and $(0, 0, 1\text{ m})$, respectively. Compute the resultant electric force on charge Q_1.

Solution From Coulomb's law and Fig. 1.5(a), the magnitudes of the individual forces on the charge Q_1 are

$$F_{e21} = F_{e31} = \frac{Q_1 Q_3}{4\pi\varepsilon_0 R^2} = 9\text{ mN}, \tag{1.12}$$

where R is the distance of Q_1 from Q_2 (or Q_3). In order to add together vectors $\mathbf{F}_{e21}$ and $\mathbf{F}_{e31}$, we decompose them into convenient components, in this case – into components in the Cartesian coordinate system. Based on Figs. 1.5(b) and (c),

$$\mathbf{F}_{e21} = -F_{e21}\cos\alpha\ \hat{\mathbf{x}} + F_{e21}\sin\alpha\ \hat{\mathbf{y}}, \quad \alpha = \frac{\pi}{4}, \tag{1.13}$$

$$\mathbf{F}_{e31} = F_{e31}\cos\beta\ \hat{\mathbf{x}} - F_{e31}\sin\beta\ \hat{\mathbf{z}}, \quad \beta = \frac{\pi}{4}, \tag{1.14}$$

so the resultant force is

$$\mathbf{F}_{e1} = \mathbf{F}_{e21} + \mathbf{F}_{e31} = F_{e21}\frac{\sqrt{2}}{2}(\hat{\mathbf{y}} - \hat{\mathbf{z}}). \tag{1.15}$$

The Cartesian components of the vector $\mathbf{F}_{e1}$ amount to

$$F_{e1x} = 0, \quad F_{e1y} = -F_{e1z} = F_{e21}\frac{\sqrt{2}}{2} = 6.36\text{ mN}, \tag{1.16}$$

and its magnitude [Eq. (1.5)] comes out to be

$$F_{e1} = \sqrt{F_{e1x}^2 + F_{e1y}^2 + F_{e1z}^2} = F_{e21} = 9\text{ mN}. \tag{1.17}$$

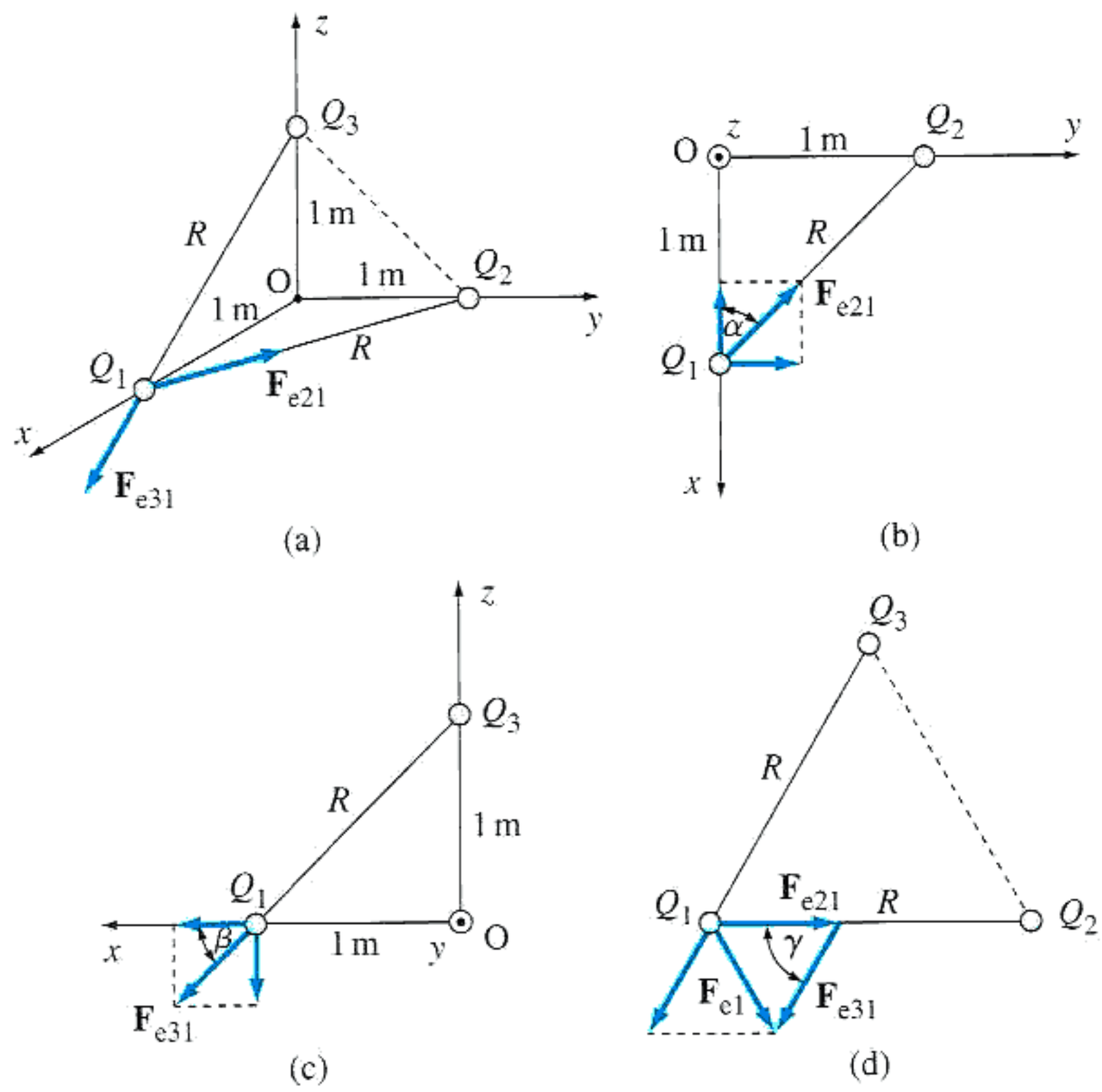

Figure 1.5 Summation of electric forces in the Cartesian coordinate system: (a) three point charges in space, with partial force vectors $\mathbf{F}_{e21}$ and $\mathbf{F}_{e31}$, (b) component decomposition of $\mathbf{F}_{e21}$, (c) decomposition of $\mathbf{F}_{e31}$, and (d) alternative addition of forces using the head-to-tail rule and the cosine formula; for Example 1.3.

Note that F_{e1} can alternatively be obtained using the head-to-tail rule, as portrayed in Fig. 1.5(d),[5] in combination with the cosine formula,[6] which yields

$$F_{e1} = \sqrt{F_{e21}^2 + F_{e31}^2 - 2F_{e21}F_{e31}\cos\gamma} = F_{21} = 9 \text{ mN}, \quad \gamma = \frac{\pi}{3}. \tag{1.18}$$

Note also that the vector $\mathbf{F}_{e1}$ is parallel to the line connecting charges Q_3 and Q_2, and that it is positioned at an angle of $\pi/4$ with respect to the plane xy.

Example 1.4 Four Charges at Tetrahedron Vertices

Four point charges Q are positioned in free space at four vertices of a regular (equilateral) tetrahedron with the side length a. Find the electric force on one of the charges.

[5]By the head-to-tail rule for vector addition, to obtain graphically the vector sum $\mathbf{c} = \mathbf{a} + \mathbf{b}$, we first arrange the two vectors (usually translate $\mathbf{b}$ from its original position) in such a way that the tail of $\mathbf{b}$ (second vector) is placed at the head of $\mathbf{a}$ (first vector). In other words, the head of the first vector is "connected" to the tail of the second, and hence the term "head-to-tail" for this arrangement. Then we draw $\mathbf{c}$ (resultant vector) as a vector extending from the tail of $\mathbf{a}$ to the head of $\mathbf{b}$, as in Fig. 1.5(d). An equivalent graphical method to add two vectors together is the parallelogram rule, where $\mathbf{c} = \mathbf{a} + \mathbf{b}$ corresponds to a diagonal of the parallelogram formed by $\mathbf{a}$ and $\mathbf{b}$, which can also be seen in Fig. 1.5(d). To add more than two vectors, e.g., $\mathbf{d} = \mathbf{a} + \mathbf{b} + \mathbf{c}$, we simply apply the head-to-tail rule to add $\mathbf{c}$ to the already found $\mathbf{a} + \mathbf{b}$, and so on – the resultant vector extends from the tail of the first vector to the head of the last vector in the multiple head-to-tail chain, and a polygon is thus obtained, which is why this procedure is often referred to as the polygon rule.

[6]In an arbitrary triangle of side lengths a, b, and c and angles α, β, and γ, the square of the length c of the side opposite to the angle γ equals $c^2 = a^2 + b^2 - 2ab\cos\gamma$ (and analogously for a^2 and b^2 using $\cos\alpha$ and $\cos\beta$, respectively), and this is known as the cosine formula (rule) or law of cosines.

Solution Note that this configuration actually represents a spatial version of the planar configuration of Fig. 1.3. Referring to Fig. 1.6, let us find the force on the charge on the top of the tetrahedron – charge 4. This force is given by

$$\mathbf{F}_{e4} = \mathbf{F}_{e14} + \mathbf{F}_{e24} + \mathbf{F}_{e34}, \tag{1.19}$$

where all the three partial forces are of the same magnitude, equal to $F_{e14} = Q^2/(4\pi\varepsilon_0 a^2)$. The horizontal components of the force vectors all lie in one plane and the angle between each two is 120°, so that they vectorially add up to zero. Thus, the resultant vector $\mathbf{F}_{e4}$ has a vertical component only, whose magnitude amounts to three times that of the vertical component of each partial force,

$$F_{e4} = 3\,(F_{e14}\cos\alpha)\,. \tag{1.20}$$

To determine $\cos\alpha$ (as H/a) from the right-angled triangle $\triangle$O14 in Fig. 1.6, we first find the distance b (between charge 1 and point O) from the equilateral triangle $\triangle$123 (the base of the tetrahedron), as 2/3 of the height of this triangle,[7] so we have

$$b = \frac{2}{3}\left(\frac{\sqrt{3}}{2}a\right) = \frac{\sqrt{3}}{3}a \quad\longrightarrow\quad \cos\alpha = \frac{H}{a} = \frac{\sqrt{a^2-b^2}}{a} = \sqrt{\frac{2}{3}}, \tag{1.21}$$

which substituted in Eq. (1.20) results in

$$F_{e4} = 3F_{e14}\frac{\sqrt{6}}{3} = \frac{\sqrt{6}Q^2}{4\pi\varepsilon_0 a^2}. \tag{1.22}$$

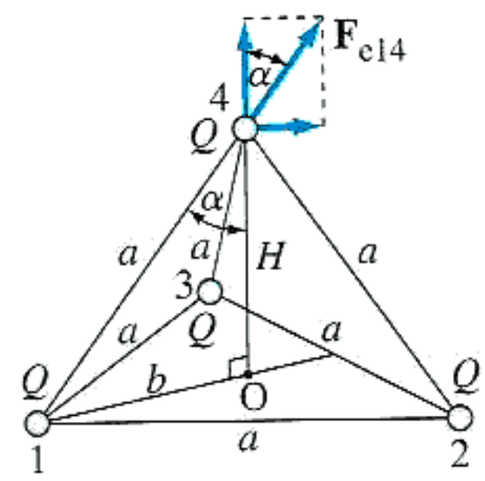

Figure 1.6 Four point charges at tetrahedron vertices; for Example 1.4.

Problems: 1.1–1.7; *Conceptual Questions* (on Companion Website): 1.1 and 1.2; *MATLAB Exercises* (on Companion Website).

1.2 DEFINITION OF THE ELECTRIC FIELD INTENSITY VECTOR

The electric field is a special physical state existing in a space around charged objects. Its fundamental property is that there is a force (Coulomb force) acting on any stationary charge placed in the space. To quantitatively describe this field, we introduce a vector quantity called the electric field intensity vector, **E**. By definition, it is equal to the electric force $\mathbf{F}_e$ on a probe (test) point charge Q_p placed in the electric field, divided by Q_p, that is,

$$\boxed{\mathbf{E} = \frac{\mathbf{F}_e}{Q_p} \quad (Q_p \to 0).} \tag{1.23}$$

definition of **E** *(unit: V/m)*

The probe charge has to be small enough in magnitude in order to practically not affect the distribution of charges which are the sources of **E**. The unit for the electric field intensity we use is volt per meter (V/m).

From the definition in Eq. (1.23) and Coulomb's law, Eq. (1.1), we obtain the expression for the electric field intensity vector of a point charge Q at a distance R from the charge (Fig. 1.7)

$$\boxed{\mathbf{E} = \frac{1}{4\pi\varepsilon_0}\frac{Q}{R^2}\hat{\mathbf{R}},} \tag{1.24}$$

electric field due to a point charge in free space

[7] Note that the orthocenter (point O in Fig. 1.6) of an equilateral triangle partitions its heights (h) in the ratio 2 : 1, so into segments $2h/3$ and $h/3$ long. Note also that $h = \sqrt{3}a/2$ (in an equilateral triangle), a being the side length of the triangle.

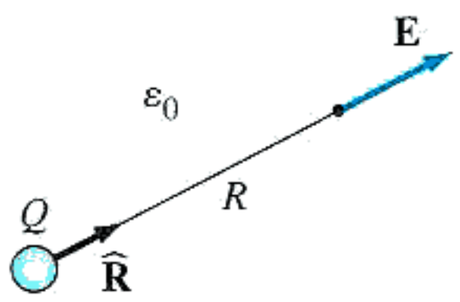

Figure 1.7 Electric field intensity vector due to a point charge in free space.

where $\hat{\mathbf{R}}$ is the unit vector along R directed from the center of the charge (source point) toward the point at which the field is (to be) determined (field or observation point).

By superposition, the electric field intensity vector produced by N point charges $(Q_1, Q_2, \ldots, Q_N)$ at a point that is at distances $R_1, R_2, \ldots, R_N$, respectively, from the charges can be obtained as

$$\mathbf{E} = \mathbf{E}_1 + \mathbf{E}_2 + \cdots + \mathbf{E}_N = \frac{1}{4\pi\varepsilon_0} \sum_{i=1}^{N} \frac{Q_i}{R_i^2} \hat{\mathbf{R}}_i, \tag{1.25}$$

where $\hat{\mathbf{R}}_i$, $i = 1, 2, \ldots, N$, are the corresponding unit vectors.

Problems: 1.8; *MATLAB Exercises* (on Companion Website).

1.3 CONTINUOUS CHARGE DISTRIBUTIONS

A point charge is the simplest case of a charge distribution, which, mathematically, corresponds to the space (three-dimensional) delta function. In the general case, however, charge can be distributed throughout a volume, on a surface, or along a line. Each of these three characteristic continuous charge distributions is described by a suitable charge density function. The volume charge density (in a volume v) is defined as [Fig. 1.8(a)]

volume charge density (unit: C/m³)

$$\boxed{\rho = \frac{\mathrm{d}Q}{\mathrm{d}v},} \tag{1.26}$$

the surface charge density (on a surface S) is given by [Fig. 1.8(b)]

surface charge density (unit: C/m²)

$$\boxed{\rho_s = \frac{\mathrm{d}Q}{\mathrm{d}S},} \tag{1.27}$$

and the line charge density (along a line l) is [Fig. 1.8(c)]

line charge density (unit: C/m)

$$\boxed{Q' = \frac{\mathrm{d}Q}{\mathrm{d}l}.} \tag{1.28}$$

Note that the symbol ρ_v is sometimes used instead of ρ, σ instead of ρ_s, and ρ_l instead of Q'. In the above equations, $\mathrm{d}Q$ represents the elemental charge in a volume element $\mathrm{d}v$, on a surface element $\mathrm{d}S$, and along a line element $\mathrm{d}l$, respectively, and the corresponding units for charge densities are C/m³, C/m², and C/m.

The total charge Q for the three characteristic charge distributions in Fig. 1.8 is obtained as $\int \mathrm{d}Q$ (adding charge elements $\mathrm{d}Q$), which leads to

$$Q_{\text{in } v} = \int_v \rho \, \mathrm{d}v, \quad Q_{\text{on } S} = \int_S \rho_s \, \mathrm{d}S, \quad \text{and} \quad Q_{\text{along } l} = \int_l Q' \, \mathrm{d}l. \tag{1.29}$$

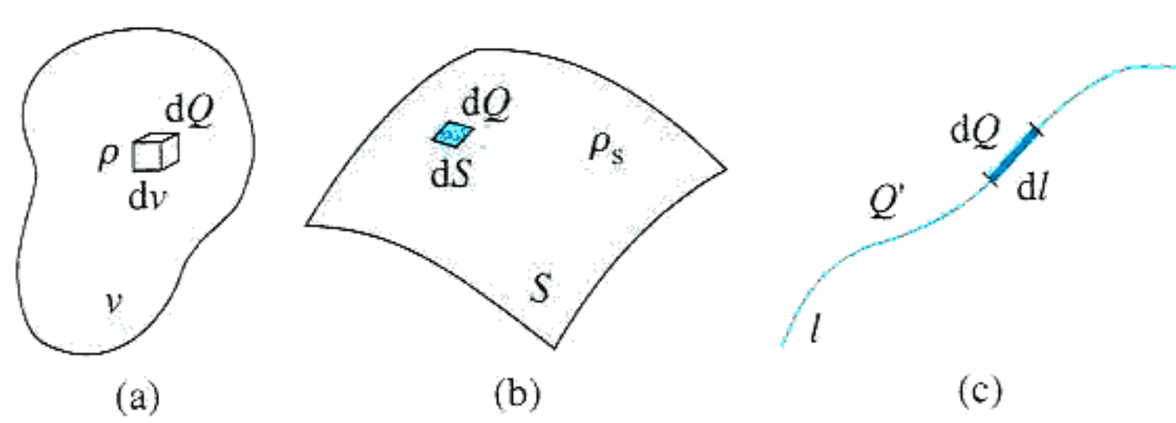

Figure 1.8 Three characteristic continuous charge distributions and charge elements: (a) volume charge, (b) surface charge, and (c) line charge.

respectively. Special, but important, cases of continuous charge distributions are uniform volume, surface, and line charge distributions. A charge distribution is said to be uniform if the associated charge density is constant over the entire region (v, S, or l) with charges. The expressions in Eqs. (1.29) then become much simpler,

$$Q_{\text{in } v} = \rho v \quad (\rho = \text{const}), \quad Q_{\text{on } S} = \rho_s S \quad (\rho_s = \text{const}),$$
$$Q_{\text{along } l} = Q' l \quad (Q' = \text{const}). \tag{1.30}$$

Note that Q' ($Q' = \text{const}$) is also used to represent the so-called charge per unit length (p.u.l.) of a long uniformly charged structure (e.g., thin or thick cylinder), defined as the charge on one meter (unit of length) of the structure divided by 1 m,

$$\boxed{Q' = Q_{\text{p.u.l.}} = \frac{Q_{\text{along } l}}{l} = \frac{Q_{\text{for 1 m length}}}{1\,\text{m}},} \tag{1.31}$$

charge per unit length, in C/m

and hence Q' numerically equals the charge on each meter of the structure.

Example 1.5 **Nonuniform Volume Charge Distribution in a Sphere**

A volume charge is distributed in free space inside a sphere of radius a. The charge density is

$$\rho(r) = \rho_0 \frac{r}{a} \quad (0 \le r \le a), \tag{1.32}$$

where r stands for the radial distance from the sphere center, and ρ_0 is a constant. Find the total charge of the sphere.

Solution Since the charge density depends on r only, we need to integrate in the first expression in Eqs. (1.29) only with respect to that coordinate, and we adopt $\mathrm{d}v$ in the form of a thin spherical shell of radius r and thickness $\mathrm{d}r$, as shown in Fig. 1.9. The volume of the shell is

$$\mathrm{d}v = 4\pi r^2\,\mathrm{d}r, \tag{1.33}$$

which can be visualized as the volume of a thin flat slab of the same thickness ($\mathrm{d}r$) and the same surface area ($S = 4\pi r^2$), $\mathrm{d}v = S\,\mathrm{d}r$. The total charge of the sphere comes out to be

$$Q = \int_v \rho\,\mathrm{d}v = \int_{r=0}^{a} \rho_0 \frac{r}{a}\, 4\pi r^2\,\mathrm{d}r = \rho_0 \pi a^3. \tag{1.34}$$

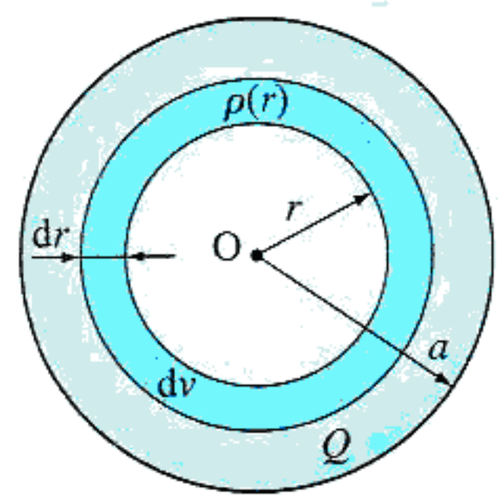

Figure 1.9 Integration of nonuniform volume charge density in a sphere; for Example 1.5.

Problems: 1.9–1.12.

1.4 ON THE VOLUME AND SURFACE INTEGRATION

A few additional comments about the volume integration performed in Eq. (1.34), and similar multiple integrations, may be useful at this point. In general, our strategy for solving volume integrals, $\int_v f\,\mathrm{d}v$, is to adopt as large volume elements $\mathrm{d}v$ as possible, the only restriction being the condition that $f = \text{const}$ in $\mathrm{d}v$. For instance, for the function $\rho = \rho(r)$ in Eq. (1.32) and a sphere as the domain of integration, the largest volume element over which $\rho = \text{const}$ is a thin spherical shell, with $\mathrm{d}v$ given in Eq. (1.33). This adoption enables us to perform the volume integration in Eq. (1.34) by integrating along r only, from 0 to a, whereas the adoption of the standard differential volume element (elementary curvilinear cuboid) in the spherical coordinate system (Fig. 1.10),

$$\mathrm{d}v' = \mathrm{d}r\,(r\,\mathrm{d}\theta)\,(r\sin\theta\,\mathrm{d}\phi) = r^2 \sin\theta\,\mathrm{d}r\,\mathrm{d}\theta\,\mathrm{d}\phi, \tag{1.35}$$

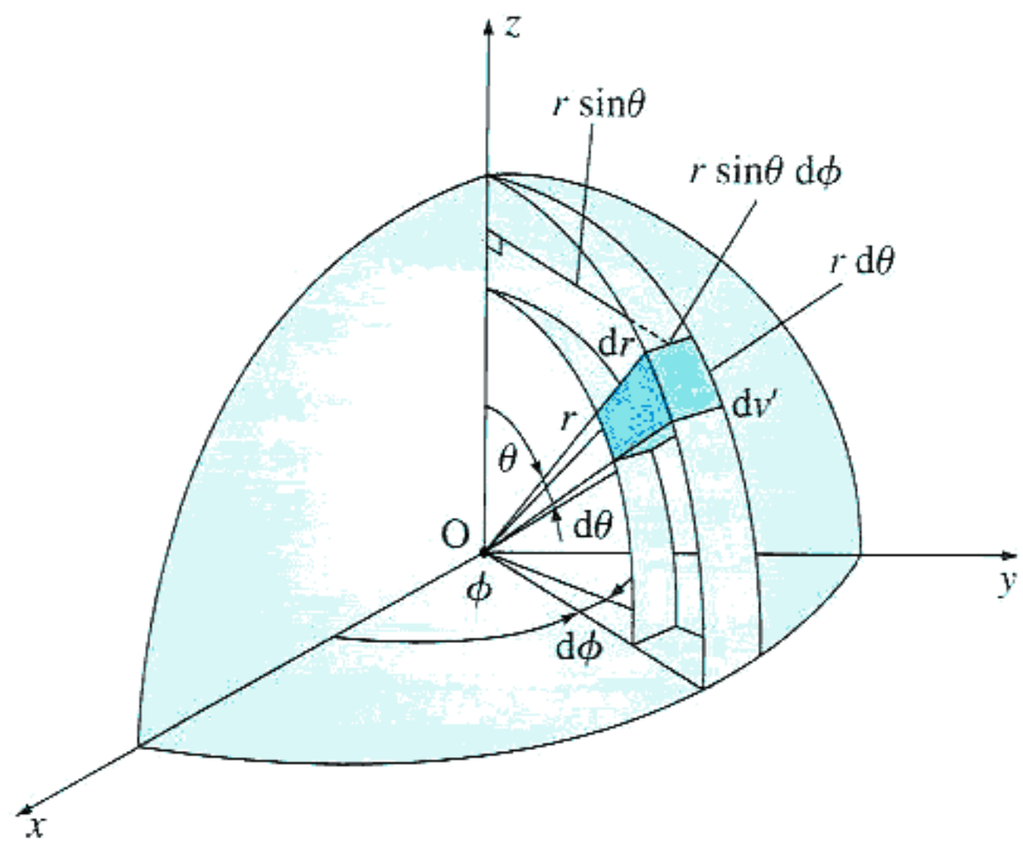

Figure 1.10 Standard differential volume element ($\mathrm{d}v'$) in the spherical coordinate system.

would require two additional integrations, i.e., the integration in θ from 0 to π and the integration in ϕ from 0 to 2π. Note, however, that these two integrations are implicitly contained in the expression for $\mathrm{d}v$ in Eq. (1.33), as

$$\int_{\theta=0}^{\pi}\int_{\phi=0}^{2\pi} \sin\theta \,\mathrm{d}\theta \,\mathrm{d}\phi = 4\pi. \tag{1.36}$$

Note also that the elementary cuboid $\mathrm{d}v'$ would be necessary for a charge density depending on all three coordinates in the spherical coordinate system, $\rho = \rho(r, \theta, \phi)$. Similar considerations apply to volume integrations associated with the cylindrical and Cartesian coordinate systems.

A trivial example for our integration strategy is the adoption of v in place of $\mathrm{d}v$ in cases when $f = \text{const}$ in the entire integration domain v, yielding $\int_v f \,\mathrm{d}v = fv$ [e.g., the first expression in Eqs. (1.30)].

The same principle is utilized for adopting surface elements $\mathrm{d}S$ for solving surface integrals.

1.5 ELECTRIC FIELD INTENSITY VECTOR DUE TO GIVEN CHARGE DISTRIBUTIONS

Using the superposition principle, the electric field intensity vector due to each of the (uniform or nonuniform) charge distributions ρ, ρ_s, and Q' can be regarded as the vector summation of the field intensities contributed by the numerous equivalent point charges making up the charge distribution. Thus, by replacing Q in Eq. (1.24) with charge element $\mathrm{d}Q = \rho \,\mathrm{d}v$, $\rho_s \,\mathrm{d}S$, or $Q' \,\mathrm{d}l$ and integrating, we get

electric field due to volume charge

$$\mathbf{E} = \frac{1}{4\pi\varepsilon_0}\int_v \frac{\rho \,\mathrm{d}v}{R^2}\,\hat{\mathbf{R}}, \tag{1.37}$$

electric field due to surface charge

$$\mathbf{E} = \frac{1}{4\pi\varepsilon_0}\int_S \frac{\rho_s \,\mathrm{d}S}{R^2}\,\hat{\mathbf{R}}, \tag{1.38}$$

electric field due to line charge

$$\mathbf{E} = \frac{1}{4\pi\varepsilon_0}\int_l \frac{Q' \,\mathrm{d}l}{R^2}\,\hat{\mathbf{R}}. \tag{1.39}$$

Note that, in the general case, R and $\hat{\mathbf{R}}$ vary as the integrals in Eqs. (1.37)–(1.39) are evaluated, along with the functions ρ, ρ_s, and Q'. We shall now apply these expressions to some specific charge distributions and field points, for which the integrals can be evaluated analytically. It is very important that we develop analytical skills for solving these (and similar), true three-dimensional (3-D), vector problems. There is not a unique recipe for an optimal solution algorithm. A general advice, however, is to use superposition whenever possible – to break up a complex problem into simpler ones, and then add up (integrate) their solutions to get the solution to the original problem. In doing this, sometimes we use directly the expressions in Eqs. (1.37)–(1.39), which essentially imply breaking up the structure into equivalent point charges. Often, on the other hand, we do not go directly all the way down to point charges. Instead, we decompose the structure and apply superposition "layer by layer," modularly, going down toward simpler structures level by level. In this, we always try to incorporate already known solutions to relevant simpler problems into the solution to the problem under consideration.

Example 1.6 **Charged Ring**

A line charge of uniform charge density Q' is distributed around the circumference of a ring of radius a in air. Find the electric field intensity vector along the axis of the ring normal to its plane.

Solution We subdivide the ring (contour C) into elemental segments of length $\mathrm{d}l$, as shown in Fig. 1.11, and apply Eq. (1.39). The contribution to the electric field at a point P on the ring axis (z-axis) by each charged segment is

$$\mathrm{d}\mathbf{E} = \frac{Q'\,\mathrm{d}l}{4\pi\varepsilon_0 R^2}\hat{\mathbf{R}}, \quad R = \sqrt{z^2 + a^2}, \tag{1.40}$$

with the position of P along the axis being defined by the coordinate z ($-\infty < z < \infty$). The total electric field intensity vector is obtained as

$$\mathbf{E} = \oint_C \mathrm{d}\mathbf{E}. \tag{1.41}$$

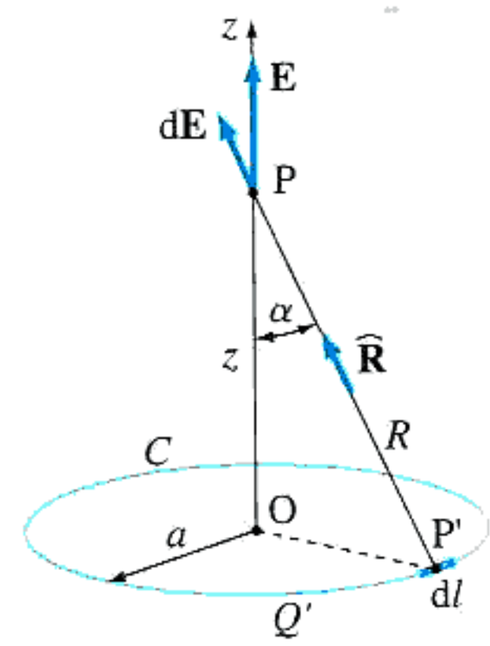

Figure 1.11 Evaluation of the electric field along the axis of a charged ring normal to its plane; for Example 1.6.

Due to symmetry, the horizontal (radial) component of the vector $\mathbf{E}$ is zero (for every element $\mathrm{d}l$ there is a corresponding diametrically opposite element that gives an equal but opposite horizontal electric field component, so that the two contributions cancel each other), and hence $\mathbf{E}$ has a vertical (axial) component only (Fig. 1.11),

$$E = E_z = \oint_C \mathrm{d}E_z, \quad \mathrm{d}E_z = \mathrm{d}E\cos\alpha = \mathrm{d}E\,\frac{z}{R}. \tag{1.42}$$

Substituting the expression for $\mathrm{d}E$ from Eq. (1.40) into Eq. (1.42), we get

$$E_z = \frac{Q'z}{4\pi\varepsilon_0 R^3}\oint_C \mathrm{d}l = \frac{Q'az}{2\varepsilon_0 R^3} \quad \left(\oint_C \mathrm{d}l = l = 2\pi a\right) \tag{1.43}$$

or

$$\boxed{\mathbf{E} = \frac{Qz}{4\pi\varepsilon_0\left(z^2 + a^2\right)^{3/2}}\hat{\mathbf{z}},} \tag{1.44}$$

electric field due to a ring of charge

where $Q = Q'2\pi a$ is the total charge of the ring.

Note that for $|z| \gg a$, $z^2 + a^2 \approx z^2$, and Eq. (1.44) yields

$$E \approx \frac{Q}{4\pi\varepsilon_0 z^2} \quad (|z| \gg a). \tag{1.45}$$

This means that far away from the ring, its charge is equivalent to a point charge Q located at its center. In other words, when the distance of the field point from the ring is much larger than the ring dimensions, the ring can be considered as a point charge and the actual shape of the ring (or any other charged body) does not matter. This in fact is the definition of a point charge or a small charged body.

Example 1.7 Semicircular Line Charge

A line charge in the form of a semicircle of radius a is situated in free space, as shown in Fig. 1.12(a). The line charge density is Q'. Compute the electric field intensity vector at an arbitrary point along the z-axis.

Solution The electric field intensity vector along the z-axis due to an elemental charge $Q'\,\mathrm{d}l$ on the semicircle [Fig. 1.12(a)] is given by the expression in Eq. (1.40). To be able to perform the integration in Eq. (1.39), we need to decompose this vector into convenient components. With reference to Fig. 1.12(b), we first represent $\mathrm{d}\mathbf{E}$ by its horizontal and vertical components,

$$\mathrm{d}\mathbf{E} = \mathrm{d}\mathbf{E}_\mathrm{h} + \mathrm{d}E_z\,\hat{\mathbf{z}}, \quad \mathrm{d}E_\mathrm{h} = \mathrm{d}E\sin\alpha, \quad \sin\alpha = \frac{a}{R},$$

$$\mathrm{d}E_z = \mathrm{d}E\cos\alpha, \quad \cos\alpha = \frac{z}{R}. \tag{1.46}$$

Since the direction of the vector $\mathrm{d}\mathbf{E}_\mathrm{h}$ varies as the integral is evaluated (i.e., as the point P′ moves along the semicircle), we need to decompose it further [Fig. 1.12(c)],

$$\mathrm{d}\mathbf{E}_\mathrm{h} = \mathrm{d}E_x\,\hat{\mathbf{x}} + \mathrm{d}E_y\,\hat{\mathbf{y}}, \quad \mathrm{d}E_x = -\mathrm{d}E_\mathrm{h}\cos\phi, \quad \mathrm{d}E_y = -\mathrm{d}E_\mathrm{h}\sin\phi \tag{1.47}$$

(the range for the azimuthal angle ϕ is $-\pi/2 \le \phi \le \pi/2$). From the above expressions and the relationship $\mathrm{d}l = a\,\mathrm{d}\phi$ (segment $\mathrm{d}l$ is an arc of radius a defined by the angle $\mathrm{d}\phi$, and its length thus equals the radius times the angle), we obtain

$$E_x = \int_l \mathrm{d}E_x = -\frac{Q'a^2}{4\pi\varepsilon_0 R^3}\int_{-\pi/2}^{\pi/2}\cos\phi\,\mathrm{d}\phi = -\frac{Q'a^2}{2\pi\varepsilon_0 R^3}, \tag{1.48}$$

$$E_y = \int_l \mathrm{d}E_y = -\frac{Q'a^2}{4\pi\varepsilon_0 R^3}\int_{-\pi/2}^{\pi/2}\sin\phi\,\mathrm{d}\phi = 0, \tag{1.49}$$

$$E_z = \int_l \mathrm{d}E_z = \frac{Q'az}{4\pi\varepsilon_0 R^3}\int_{-\pi/2}^{\pi/2}\mathrm{d}\phi = \frac{Q'az}{4\varepsilon_0 R^3}, \tag{1.50}$$

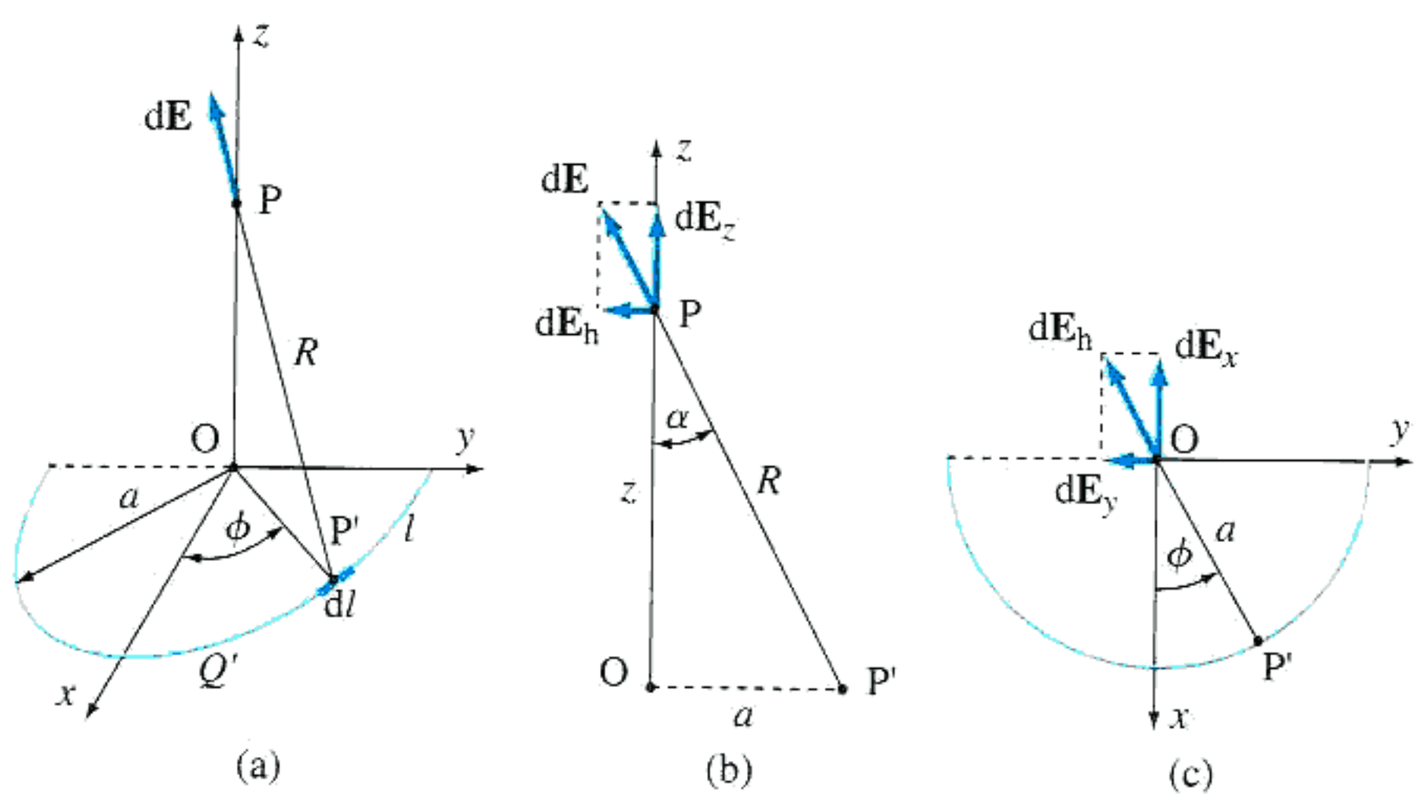

Figure 1.12 Evaluation of the electric field due to a line charge in the form of a semicircle; for Example 1.7.

so that the final expression for the electric field vector is

$$\mathbf{E} = \frac{Q'a}{2\varepsilon_0 R^3}\left(-\frac{a}{\pi}\,\hat{\mathbf{x}} + \frac{z}{2}\,\hat{\mathbf{z}}\right), \quad R = \sqrt{z^2 + a^2}. \tag{1.51}$$

Example 1.8 Straight Line Charge of Finite Length

Find the expression for the **E** field at an arbitrary point in space due to a straight line of length l uniformly charged with a total charge Q. The ambient medium is air.

Solution Let the line charge and the field point (P) be in the plane of drawing (Fig. 1.13). The geometry of this problem can be defined using three parameters: angles θ_1 and θ_2, and the perpendicular distance from the line to the point, d (for the particular position of the point P shown in Fig. 1.13, $\theta_1 < 0$ and $\theta_2 > 0$). In Eq. (1.39), $Q' = Q/l$, $R = \sqrt{z^2 + d^2}$, $dl = dz$, and

$$\hat{\mathbf{R}} = \cos\theta\,\hat{\mathbf{x}} - \sin\theta\,\hat{\mathbf{z}}, \tag{1.52}$$

where z ($z_1 \le z \le z_2$) and θ ($\theta_1 \le \theta \le \theta_2$) are the length and angular coordinates, respectively, each determining the position of the source point, P′, along the line. From Fig. 1.13, the following trigonometric relationship exists between these two coordinates:

$$\tan\theta = \frac{z}{d}, \tag{1.53}$$

and its differential form (by taking the differential of both sides of the equation) reads

$$\frac{\mathrm{d}\theta}{\cos^2\theta} = \frac{\mathrm{d}z}{d} \quad (d = \text{const}), \tag{1.54}$$

which, given that $\cos\theta = d/R$, is equivalent to

$$\frac{\mathrm{d}z}{R^2} = \frac{\mathrm{d}\theta}{d}. \tag{1.55}$$

Finally, substituting the expressions from Eqs. (1.52) and (1.55) into Eq. (1.39), we have

$$\mathbf{E} = \frac{Q}{4\pi\varepsilon_0 l d}\left(\int_{\theta_1}^{\theta_2} \cos\theta\,\mathrm{d}\theta\,\hat{\mathbf{x}} - \int_{\theta_1}^{\theta_2} \sin\theta\,\mathrm{d}\theta\,\hat{\mathbf{z}}\right)$$

$$\longrightarrow \quad \boxed{\mathbf{E} = \frac{Q}{4\pi\varepsilon_0 l d}\left[(\sin\theta_2 - \sin\theta_1)\,\hat{\mathbf{x}} + (\cos\theta_2 - \cos\theta_1)\,\hat{\mathbf{z}}\right].} \tag{1.56}$$

electric field due to a line charge of finite length

Note that the expression in Eq. (1.56) can be combined for computing the electric field due to an arbitrary structure assembled from straight line segments of charge.

Example 1.9 Infinite Line Charge

An infinite line charge of uniform density Q' resides in air. Determine the electric field intensity vector at an arbitrary point in space.

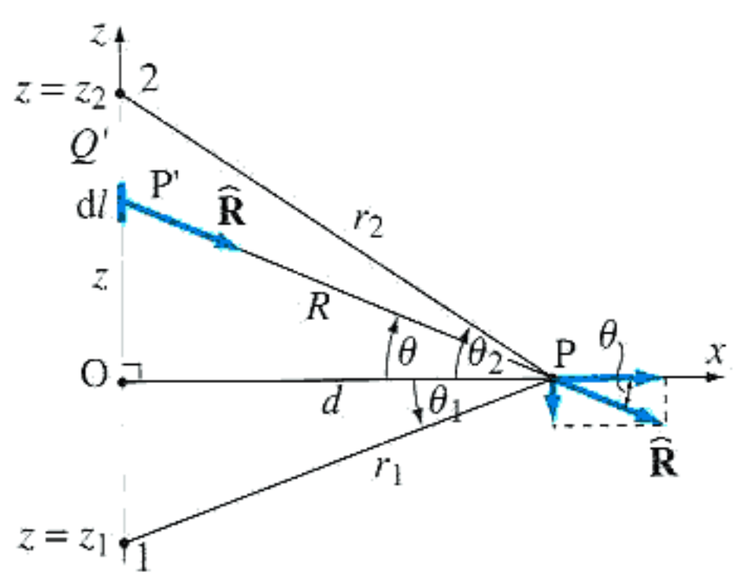

Figure 1.13 Evaluation of the electric field due to a line charge of finite length; for Example 1.8.

Solution Let r be the perpendicular (radial) distance of a field (observation) point, P, from the line charge, and $\hat{\mathbf{r}}$ the unit vector along this distance directed from the line to the point P. We use the expression for the field due to a finite line charge in Eq. (1.56) and let $\theta_1 \to -\pi/2$ and $\theta_2 \to \pi/2$ (the line extends to $z \to -\infty$ and $z \to \infty$, respectively), as well as $Q/l = Q'$, $d = r$, and $\hat{\mathbf{x}} = \hat{\mathbf{r}}$. What we obtain is exactly the field expression for the infinite line charge with density Q':

electric field due to an infinite line charge

$$\boxed{\mathbf{E} = \frac{Q'}{2\pi\varepsilon_0 r}\,\hat{\mathbf{r}}.} \tag{1.57}$$

We see that the vector $\mathbf{E}$ is radial with respect to the line charge axis, and its magnitude varies in space as a function of the radial distance r only, with E being inversely proportional to r.

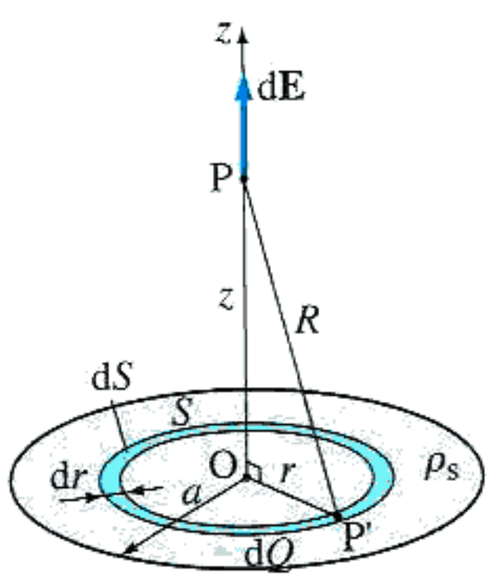

Figure 1.14 Evaluation of the electric field due to a charged disk; for Example 1.10.

Example 1.10 Disk of Charge

Consider a very thin charged disk (i.e., a circular sheet of charge), of radius a and a uniform surface charge density ρ_s, in free space. Calculate the electric field intensity vector along the disk axis normal to its surface.

Solution Instead of directly applying Eq. (1.38), we subdivide the disk into elemental rings of width $\mathrm{d}r$, as shown in Fig. 1.14. The field due to a ring of radius r ($0 \le r \le a$) at a point P along the z-axis is [see Eq. (1.44)]

$$\mathrm{d}\mathbf{E} = \frac{\mathrm{d}Qz}{4\pi\varepsilon_0 R^3}\,\hat{\mathbf{z}}, \quad R = \sqrt{r^2 + z^2}, \tag{1.58}$$

with $\mathrm{d}Q$ standing for the charge of the ring, given by

$$\mathrm{d}Q = \rho_s\,\mathrm{d}S. \tag{1.59}$$

The surface area of the ring, $\mathrm{d}S$, can be computed as the area of a thin strip of length equal to the ring circumference, $2\pi r$, and width $\mathrm{d}r$, that is,

$$\mathrm{d}S = 2\pi r\,\mathrm{d}r. \tag{1.60}$$

By superposition,

$$\mathbf{E} = \int_S \mathrm{d}\mathbf{E} = \frac{\rho_s z}{2\varepsilon_0}\,\hat{\mathbf{z}} \int_{r=0}^{a} \frac{r\,\mathrm{d}r}{R^3}. \tag{1.61}$$

Taking the differential of the relationship $R^2 = r^2 + z^2$, we obtain

$$R\,\mathrm{d}R = r\,\mathrm{d}r, \tag{1.62}$$

so that the substitution of $r\,\mathrm{d}r$ by $R\,\mathrm{d}R$ in Eq. (1.61) yields

electric field due to a charged disk

$$\mathbf{E} = \frac{\rho_s z}{2\varepsilon_0}\int_{r=0}^{a} \frac{\mathrm{d}R}{R^2}\,\hat{\mathbf{z}} = \frac{\rho_s z}{2\varepsilon_0}\left(-\frac{1}{R}\right)\Bigg|_{r=0}^{a}\hat{\mathbf{z}} \quad \longrightarrow \quad \boxed{\mathbf{E} = \frac{\rho_s}{2\varepsilon_0}\left(\frac{z}{|z|} - \frac{z}{\sqrt{a^2+z^2}}\right)\hat{\mathbf{z}},} \tag{1.63}$$

where $R|_{r=0} = \sqrt{z^2} = |z|$, to allow a negative z as well ($-\infty < z < \infty$).

Example 1.11 Infinite Sheet of Charge

Find the electric field intensity vector due to an infinite sheet of charge of density ρ_s in free space.

Solution We note that the infinite sheet of charge can be obtained from the disk in Fig. 1.14 by extending its radius to infinity. Consequently, the field due to the infinite sheet can be obtained from the field due to the disk by letting $a \to \infty$ in Eq. (1.63). With this, the second term in parentheses in the final field expression in Eq. (1.63) vanishes. The first term, $z/|z|$,

is either 1 (for $z > 0$) or -1 (for $z < 0$), and we conclude that the field intensity around the infinite sheet of charge is uniform (constant) in both half-spaces cut by the sheet, and given by

$$\boxed{E = \frac{\rho_s}{2\varepsilon_0}} \tag{1.64}$$

electric field due to an infinite sheet of charge

with respect to the reference directions indicated in Fig. 1.15. Namely, for a positive charge ($\rho_s > 0$) of the sheet, the actual orientations of **E** are those in Fig. 1.15 (field lines are directed outward from the positive charge), while the situation for a negative ρ_s is just opposite (the field vector points toward the negative charge).

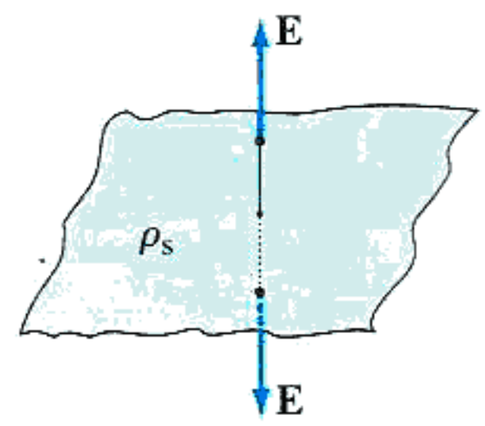

Figure 1.15 Infinite sheet of charge; for Example 1.11.

Example 1.12 Hemispherical Surface Charge

A hemispherical surface of radius a is uniformly charged with a charge density ρ_s. The medium is air. Compute the electric field intensity vector at the center of the hemisphere (center of the corresponding full sphere).

Solution We perform a similar procedure as in Example 1.10 and subdivide the hemisphere into thin rings, as depicted in Fig. 1.16. The radius of a ring whose position on the hemisphere is defined by an angle θ ($0 \le \theta \le \pi/2$) is $a_r = a \sin\theta$. Its charge is

$$\mathrm{d}Q = \rho_s\,\mathrm{d}S = \rho_s \underbrace{2\pi a \sin\theta}_{C_r}\,\underbrace{a\,\mathrm{d}\theta}_{\mathrm{d}l_r}, \tag{1.65}$$

where C_r and $\mathrm{d}l_r$ denote the ring circumference and width, respectively. Using Eq. (1.44), the electric field intensity $\mathrm{d}\mathbf{E}$ at the point O due to the charge $\mathrm{d}Q$ is found as follows:

$$z_r = -a\cos\theta \quad \text{and} \quad R = a \quad \longrightarrow \quad \mathrm{d}\mathbf{E} = \frac{\mathrm{d}Q(-a\cos\theta)}{4\pi\varepsilon_0 a^3}\,\hat{\mathbf{z}}, \tag{1.66}$$

with z_r being the local z-coordinate of the point O with respect to the ring center (Fig. 1.16). Therefore, the resultant field vector amounts to

$$\mathbf{E} = \int_{\theta=0}^{\pi/2} \mathrm{d}\mathbf{E} = -\frac{\rho_s}{2\varepsilon_0}\int_0^{\pi/2} \underbrace{\sin\theta\cos\theta}_{(\sin 2\theta)/2}\,\mathrm{d}\theta\,\hat{\mathbf{z}} = -\frac{\rho_s}{4\varepsilon_0}\,\hat{\mathbf{z}}. \tag{1.67}$$

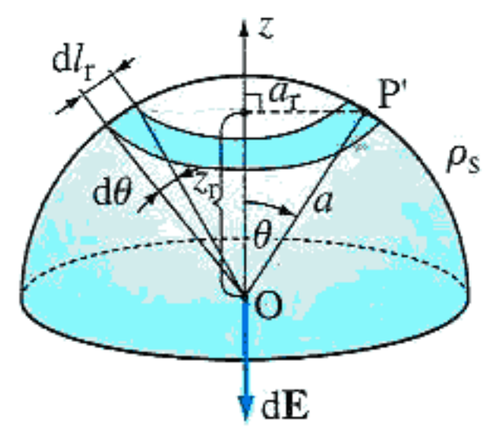

Figure 1.16 Evaluation of the electric field at the center (point O) of a hemispherical surface charge; for Example 1.12.

Example 1.13 Force on a Line Charge due to a Charged Semicylinder

A uniform charge of density ρ_s is distributed in free space over a surface in the form of a half of a very long circular cylinder of radius a, as shown in Fig. 1.17(a). A line charge of uniform density Q' is positioned along the semicylinder axis. Find the electric force on the line charge per unit of its length.

Solution From Eqs. (1.23) and (1.31), the per-unit-length electric force on the line charge, that is, the force on one meter (unit length) of the structure (line charge) divided by 1 m (the unit is N/m), is given by

$$\boxed{\mathbf{F}'_e = Q'\mathbf{E},} \tag{1.68}$$

per-unit-length Coulomb force on a line charge (unit: N/m)

with **E** standing for the electric field intensity vector due to the charged semicylinder at its axis. We subdivide the semicylinder into elemental strips, of width $\mathrm{d}l$, and find **E** using the superposition principle. The field due to each strip can be approximated by that of a very long line charge with charge density $\mathrm{d}Q' = \rho_s\,\mathrm{d}l$; namely, the charge of the elemental strip of length h, $\rho_s h\,\mathrm{d}l$, must be equal to the charge of the equivalent line charge of the same length, so $\mathrm{d}Q'h$, which yields this expression for $\mathrm{d}Q'$. Having in mind Eq. (1.57), the electric field vector due to the line charge is radial with respect to the line, and its magnitude at the semicylinder axis [Fig. 1.17(b)] comes out to be

$$\mathrm{d}E = \frac{\mathrm{d}Q'}{2\pi\varepsilon_0 a} = \frac{\rho_s\,\mathrm{d}\phi}{2\pi\varepsilon_0}, \tag{1.69}$$

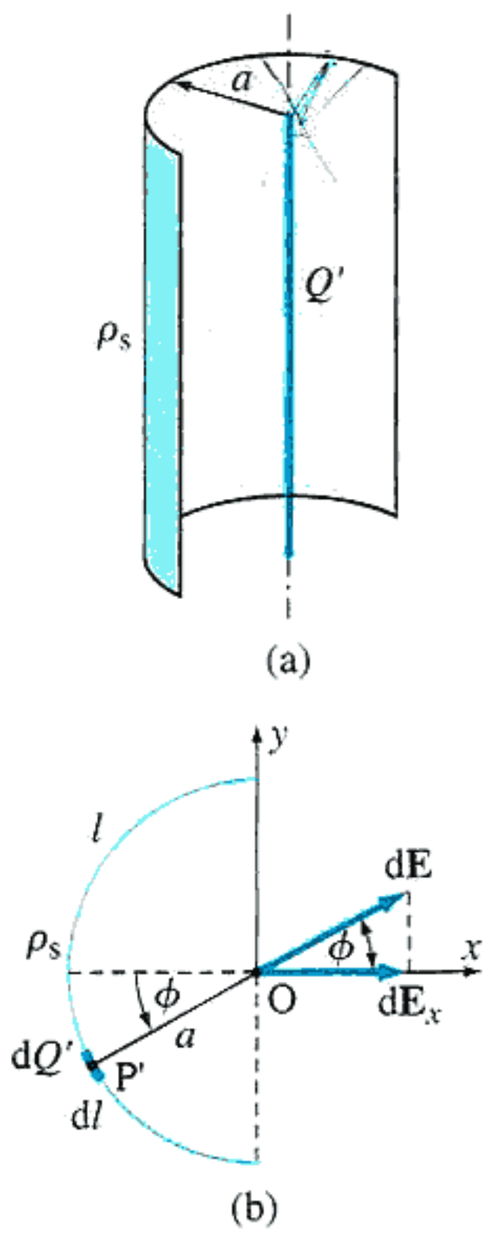

Figure 1.17 Evaluation of the electric force on a line charge positioned along the axis of a charged semicylinder: (a) three-dimensional view showing the structure geometry and (b) cross-sectional view for field computations; for Example 1.13.

since $r = a$ and $\mathrm{d}l = a\,\mathrm{d}\phi$. By symmetry, the resultant field has an x-component only, computed as

$$E_x = \int_l \mathrm{d}E_x = \int_l \mathrm{d}E \cos\phi = \frac{\rho_s}{2\pi\varepsilon_0}\int_{\phi=-\pi/2}^{\pi/2} \cos\phi\,\mathrm{d}\phi = \frac{\rho_s}{\pi\varepsilon_0}, \tag{1.70}$$

where l denotes the line (semicircle) representing the semicylinder cross section. Finally, Eqs. (1.68) and (1.70) result in

$$\mathbf{F}'_e = \frac{Q'\rho_s}{\pi\varepsilon_0}\,\hat{\mathbf{x}}. \tag{1.71}$$

Problems: 1.13–1.28: *Conceptual Questions* (on Companion Website): 1.3–1.6; *MATLAB Exercises* (on Companion Website).

1.6 DEFINITION OF THE ELECTRIC SCALAR POTENTIAL

The electric scalar potential is a scalar quantity that can be used instead of the electric field intensity vector for the description of the electrostatic field. Dealing with the potential is mathematically simpler than dealing with the field vector. Three different integrations are needed in general for the evaluation of **E**, one integration for each vector component, while a single integration is required for the potential, and **E**, in turn, can easily be found from the potential by differentiation. In addition, using the electric potential we are able to connect the electric field with the voltage, as a fundamental bridge between the field theory and the circuit theory.

The electric scalar potential is defined through the work done by the electric field, that is, by the electric force, $\mathbf{F}_e$, in moving a test point charge, Q_p. The work $\mathrm{d}W_e$ done by $\mathbf{F}_e$ while moving Q_p along an elementary vector distance $\mathbf{dl}$ equals the dot product[8] of $\mathbf{F}_e$ and $\mathbf{dl}$,

$$\mathrm{d}W_e = \mathbf{F}_e \cdot \mathbf{dl} = F_e\,\mathrm{d}l\cos\alpha, \tag{1.72}$$

where α is the angle between the two vectors in the product, as shown in Fig. 1.18. We note that $\mathrm{d}W_e$ can be negative (for $\pi/2 < \alpha \le \pi$), meaning that the work $|\mathrm{d}W_e|$ is being performed against the electric field by an external agent. Based on Eq. (1.72), the electric scalar potential, V, at a point P in an electric field is defined as the work done by the field in moving a test charge from P to a reference point $\mathcal{R}$ (Fig. 1.18),

$$W_e = \int_P^{\mathcal{R}} \mathbf{F}_e \cdot \mathbf{dl}, \tag{1.73}$$

divided by Q_p. Having in mind Eq. (1.23), this becomes

definition of the electric potential (unit: V)

$$\boxed{V = \frac{W_e}{Q_p} = \int_P^{\mathcal{R}} \frac{\mathbf{F}_e}{Q_p} \cdot \mathbf{dl} = \int_P^{\mathcal{R}} \mathbf{E} \cdot \mathbf{dl}.} \tag{1.74}$$

Thus, the potential V at the point P with respect to the reference point $\mathcal{R}$ turns out to not depend on Q_p and to be equal to the line integral of vector **E** from P to $\mathcal{R}$.[9]

[8]The dot product (also known as the scalar product) of vectors **a** and **b** is a scalar given by $\mathbf{a}\cdot\mathbf{b} = |\mathbf{a}||\mathbf{b}|\cos\alpha$, α being the angle between **a** and **b**.

[9]The line integral of a vector function (field) **a** along a line (curve) l, from a point A to a point B, is defined as $\int_l \mathbf{a}\cdot\mathbf{dl} = \int_A^B \mathbf{a}\cdot\mathbf{dl}$, where $\mathbf{dl}$ is the differential length vector tangential to the curve (as in

Obviously, the potential at the reference point is zero (integral from $P \equiv \mathcal{R}$ to $\mathcal{R}$). The unit for the potential is volt (abbreviated V), and hence the unit V/m for the electric field intensity. Note that Φ is also used to denote the electric potential.

By the principle of conservation of energy, the net work done by the electrostatic field in moving Q_p from a point A to some point B and then moving it back to A along a different path is zero (because after the round trip, the system is the same as at the beginning). This means that the line integral of the electric field intensity vector along an arbitrary closed path (contour) is zero,

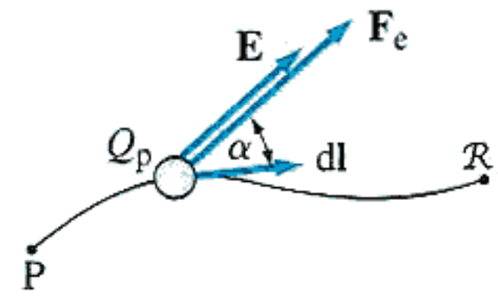

Figure 1.18 Displacement of a test charge in an electrostatic field.

$$\boxed{\oint_C \mathbf{E} \cdot d\mathbf{l} = 0,} \tag{1.75}$$

conservative nature of the electrostatic field

which constitutes Maxwell's first equation for the electrostatic field. We see that the circulation (closed line integral) of **E** in electrostatics is always zero, and hence the electrostatic field belongs to a class of conservative vector fields.[10]

Eq. (1.75) can alternatively be derived from Coulomb's law, i.e., from the expression for the electric field intensity vector due to a single point charge, Q, given by Eq. (1.24) and Fig. 1.7. To do this, we break the contour C up into elemental segments ($dl \to 0$) parallel and normal to **E**, as indicated in Fig. 1.19. We realize that contributions to the overall line integral in Eq. (1.75) occur only for the segments parallel to **E**, while no contribution for the segments normal to **E** ($\alpha = 90°$ and $\mathbf{E} \cdot d\mathbf{l} = 0$). In specific, along the segments parallel to **E** (segments radial with respect to the charge Q), $\mathbf{E} \cdot d\mathbf{l}$ equals either $E\,dl$ ($\alpha = 0$) or $-E\,dl$ ($\alpha = 180°$), resulting in a zero net line integral (sum) along C. By superposition, this result is

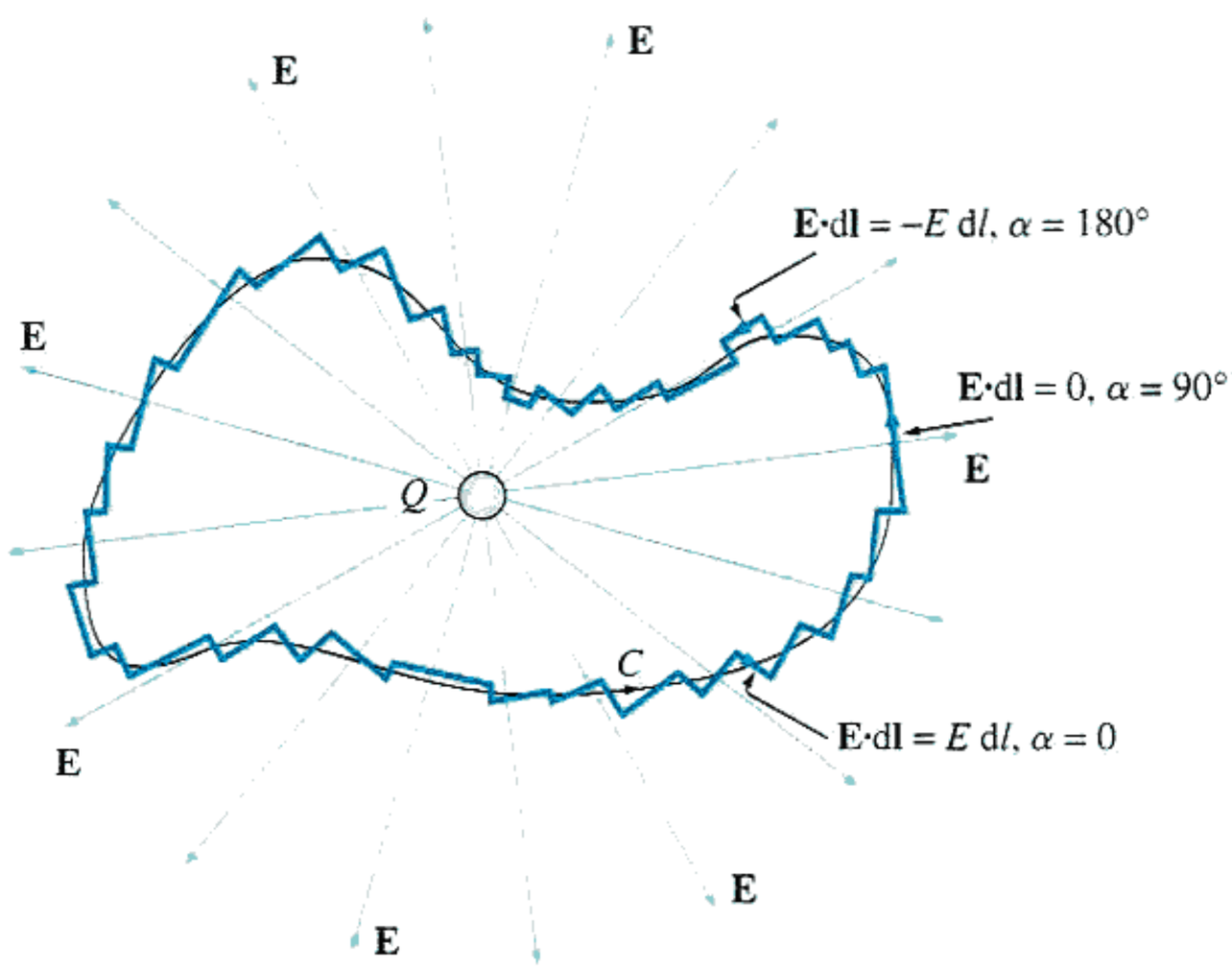

Figure 1.19 Derivation of Maxwell's first equation for the electrostatic field starting with Coulomb's law.

Fig. 1.18) oriented from A toward B. If the line is closed (for example, a circle or a square), we call it contour (and usually mark it C), and the corresponding line integral, $\oint_C \mathbf{a} \cdot d\mathbf{l}$, is termed the circulation of **a** along C. The reference direction of $d\mathbf{l}$ coincides with the orientation of the contour.

[10] By definition, a vector field is said to be conservative when its circulation is zero for a closed path of arbitrary shape.

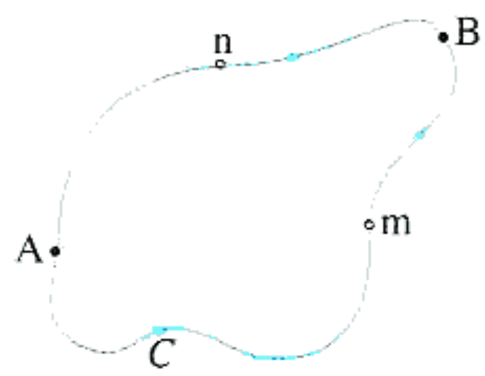

Figure 1.20 For the proof that the line integral of an electrostatic field vector between two points is the same for any path of integration.

also valid for any charge distribution (which, as we know, can be represented as a system of equivalent point charges, and for which the resultant field can be obtained as a vector sum of individual fields due to point charges).

The line integral of **E** between two points in an electrostatic field does not depend on the path of integration. To prove this, let us refer to Fig. 1.20 and write the circulation of **E** along a contour C as

$$\oint_C \mathbf{E}\cdot d\mathbf{l} = \int_{\mathrm{AmBnA}} \mathbf{E}\cdot d\mathbf{l} = \int_{\mathrm{AmB}} \mathbf{E}\cdot d\mathbf{l} + \int_{\mathrm{BnA}} \mathbf{E}\cdot d\mathbf{l}$$
$$= \int_{\mathrm{AmB}} \mathbf{E}\cdot d\mathbf{l} - \int_{\mathrm{AnB}} \mathbf{E}\cdot d\mathbf{l}, \tag{1.76}$$

so that, from Eq. (1.75), the integral from A to B along the path containing the point m is the same as the integral along the path with the point n,

path independence for the line integral of **E**

$$\boxed{\int_{\mathrm{AmB}} \mathbf{E}\cdot d\mathbf{l} = \int_{\mathrm{AnB}} \mathbf{E}\cdot d\mathbf{l},} \tag{1.77}$$

or along any other path. This also means that, for an adopted reference point, the electric potential at any point in the field is a uniquely determined quantity, having the same value for any path of moving the test charge.

Finally, let us see what happens with the potential at an arbitrary point P in the field after a new reference point, $\mathcal{R}'$, is adopted. The new potential is

$$V' = \int_{\mathrm{P}}^{\mathcal{R}'} \mathbf{E}\cdot d\mathbf{l} = \underbrace{\int_{\mathrm{P}}^{\mathcal{R}} \mathbf{E}\cdot d\mathbf{l}}_{V} + \int_{\mathcal{R}}^{\mathcal{R}'} \mathbf{E}\cdot d\mathbf{l}, \tag{1.78}$$

and thus the change in potential amounts to

change in potential due to a new reference point

$$\boxed{\Delta V = V' - V = \int_{\mathcal{R}}^{\mathcal{R}'} \mathbf{E}\cdot d\mathbf{l}.} \tag{1.79}$$

It is very important to note that ΔV does not depend on the position of the point P in the field; if the reference point is changed, the potential at all points changes by the same constant value, i.e., by an additive constant.

Problems: 1.29 and 1.30; *Conceptual Questions* (on Companion Website): 1.7 and 1.8; *MATLAB Exercises* (on Companion Website).

1.7 ELECTRIC POTENTIAL DUE TO GIVEN CHARGE DISTRIBUTIONS

Let us determine the electric scalar potential due to a point charge in free space. In general, it is customary to adopt the reference point, $\mathcal{R}$, at infinity whenever possible, namely, when the charge distribution is finite. As we shall see in an example, this choice is impossible, or at least inadequate, for infinite charge distributions, such as an infinite straight line charge. From Fig. 1.21 and Eqs. (1.74) and (1.24), the potential at a distance R from the charge Q, and with respect to the reference point at infinity, is

electric potential due to a point charge

$$V = \int_{\mathrm{P}}^{\mathcal{R}} \mathbf{E}\cdot d\mathbf{l} = \int_{x=R}^{\infty} E\,dx = \int_{R}^{\infty} \frac{Q}{4\pi\varepsilon_0 x^2}\,dx \quad\longrightarrow\quad \boxed{V = \frac{Q}{4\pi\varepsilon_0 R}.} \tag{1.80}$$

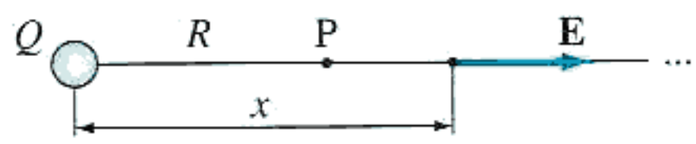

Figure 1.21 Evaluation of the electric potential due to a point charge in free space.

The potential function (of R) obtained for a reference point at an arbitrary (finite) distance from the charge differs from this result by an additive constant, as determined by Eq. (1.79).

Shown in Fig. 1.22 is a sketch of electric-field lines (in general, lines to which vector **E** is tangential at all points) and equipotential surfaces (surfaces having the same potential, $V = \text{const}$, at all points) around the point charge in Fig. 1.21. Of course, based on Eqs. (1.24) and (1.80), field lines are radial "beams" starting at the charge and equipotentials are spherical surfaces (graphed as circles – equipotential lines – in the figure) centered at the charge, respectively. Field lines are perpendicular to equipotential surfaces, and this conclusion holds always, for an arbitrary electrostatic field. Namely, since a movement of a probe charge Q_p (in Fig. 1.18) over an equipotential surface results in no work by electric forces (no change in V), **E** does not have a component along that movement, meaning that it is perpendicular to the surface. The density of field lines (the number of lines per unit area of the equipotential surface) is representative of the magnitude of the field vector, i.e., it decreases as $1/R^2$ (the area of equipotential surfaces increases as R^2) away from the charge in Fig. 1.22.

Starting with Eq. (1.80) and applying the superposition principle, the expression for the resultant electric potential, similar to the field expression in Eq. (1.25), is obtained for the system of N point charges, which reads

$$V = \frac{1}{4\pi\varepsilon_0}\sum_{i=1}^{N}\frac{Q_i}{R_i}, \tag{1.81}$$

as well as for the three characteristic continuous charge distributions, corresponding to Eqs. (1.37)–(1.39) for the field vector,

$$\boxed{V = \frac{1}{4\pi\varepsilon_0}\int_v \frac{\rho\,\mathrm{d}v}{R},} \tag{1.82}$$

electric potential due to volume charge

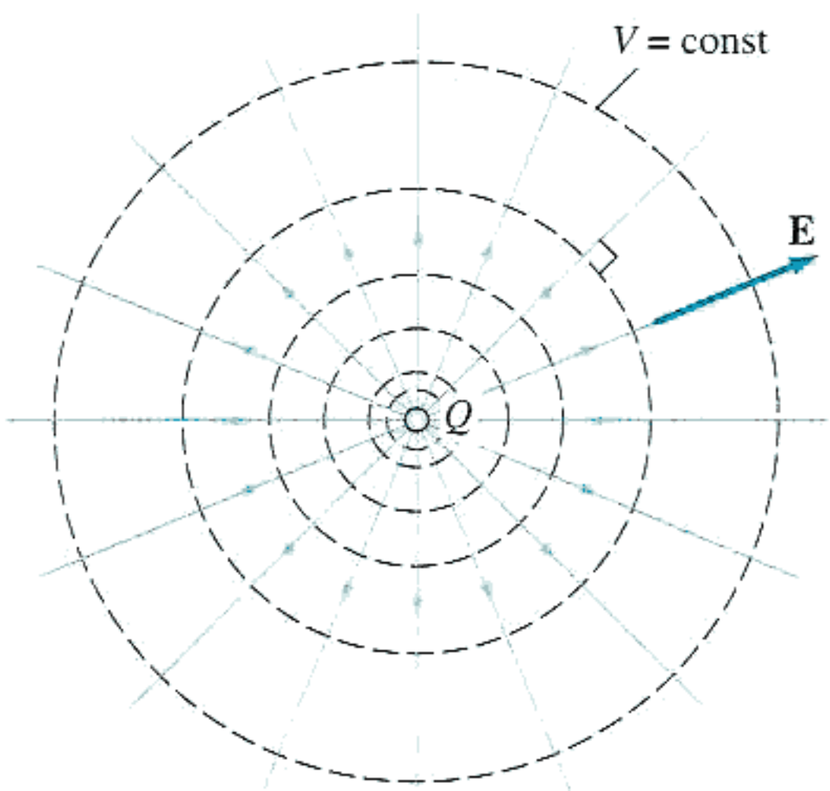

Figure 1.22 Field and equipotential lines for a point charge in Fig. 1.21.

electric potential due to surface charge

$$V = \frac{1}{4\pi\varepsilon_0}\int_S \frac{\rho_s\,\mathrm{d}S}{R}, \tag{1.83}$$

electric potential due to line charge

$$V = \frac{1}{4\pi\varepsilon_0}\int_l \frac{Q'\,\mathrm{d}l}{R}. \tag{1.84}$$

Obviously, these integrals are substantially simpler than the respective field integrals, and the same holds true for the resulting solutions for the potential due to charge distributions on various characteristic geometries, for which we have already evaluated the electric field vector in Section 1.5.

Example 1.14 **Electric Potential due to a Charged Ring**

Find the electric scalar potential along the axis of a uniformly charged ring in free space normal to the ring plane. The line charge density of the ring is Q' and its radius is a.

Solution From Eq. (1.84) and Fig. 1.11, the potential at an arbitrary point P on the z-axis (for $-\infty < z < \infty$) is given by

$$V = \frac{1}{4\pi\varepsilon_0}\oint_C \frac{Q'\,\mathrm{d}l}{R} = \frac{Q'}{4\pi\varepsilon_0 R}\oint_C \mathrm{d}l = \frac{Q'a}{2\varepsilon_0\sqrt{z^2+a^2}}. \tag{1.85}$$

Example 1.15 **Potential due to an Infinite Line Charge**

Compute the electric potential at an arbitrary point in space due to an infinite uniform line charge of density Q' in air.

Solution The expressions for potential computations given in Eqs. (1.81)–(1.84) all imply that the reference point is at infinity. These expressions cannot therefore be used for the evaluation of the potential due to infinite charge distributions (because the potential due to an infinite charge distribution with respect to the reference point taken at infinity is infinite). In such cases, we invoke Eq. (1.74) instead – to compute the potential, and an infinite straight line charge, the field of which is given by Eq. (1.57), is a typical, and a very important, example. To find the potential due to this charge, at a point whose radial distance from the charge line is r, we apply Eq. (1.74) to a convenient integration path shown in Fig. 1.23, which

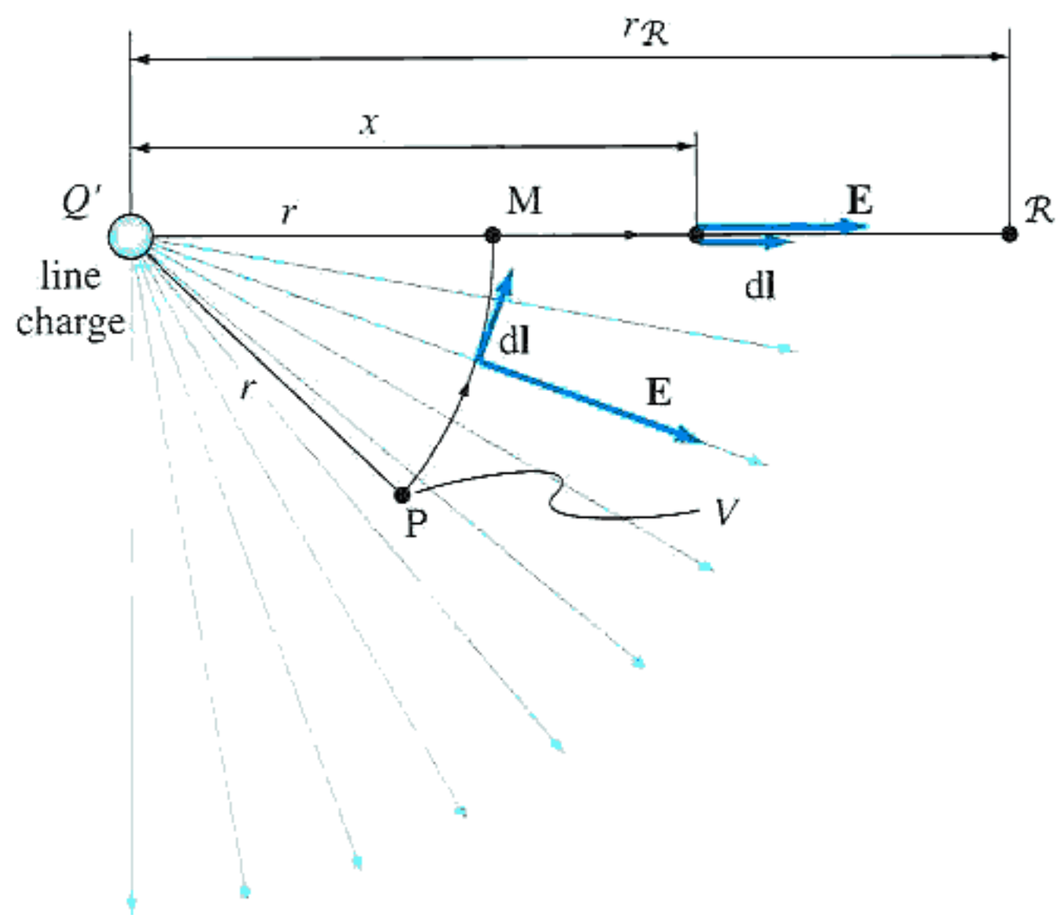

Figure 1.23 Evaluation of the electric potential due to an infinite line charge – cross section of the structure; for Example 1.15.

consists of an arc between points P and M and a straight line segment between points M and $\mathcal{R}$, and obtain

$$V = \int_{\mathrm{P}}^{\mathcal{R}} \mathbf{E} \cdot \mathrm{d}\mathbf{l} = \int_{\mathrm{P}}^{\mathrm{M}} \mathbf{E} \cdot \mathrm{d}\mathbf{l} + \int_{\mathrm{M}}^{\mathcal{R}} \mathbf{E} \cdot \mathrm{d}\mathbf{l} = \int_{x=r}^{r_{\mathcal{R}}} E\,\mathrm{d}x = \int_{r}^{r_{\mathcal{R}}} \frac{Q'}{2\pi\varepsilon_0 x}\,\mathrm{d}x. \tag{1.86}$$

The line integral between points P and M is zero because $\mathbf{E}$ is perpendicular to $\mathrm{d}\mathbf{l}$ along the path. Thus, the potential at a distance r from the line charge with respect to the reference point that is a distance $r_{\mathcal{R}}$ away from it comes out to be

$$\boxed{V = \frac{Q'}{2\pi\varepsilon_0} \ln \frac{r_{\mathcal{R}}}{r}.} \tag{1.87}$$

electric potential due to an infinite line charge

Note that the adoption of the reference point at infinity in this case, which implies that $r_{\mathcal{R}} \to \infty$ in Eq. (1.87), would result in $V \to \infty$. Note, furthermore, that this result, so an infinite potential regardless of the location of the observation point, is also "correct" in a sense that it can be understood as the potential distribution (function of r) given by Eq. (1.87) plus an infinite constant, as a consequence of the change of the reference point from $\mathcal{R}$ in Fig. 1.23 to infinity [see Eqs. (1.78) and (1.79)]. In other words, the potential at all points in space is changed by the same constant value after the new reference point (at infinity) is adopted, which, being infinite ($\Delta V \to \infty$), masks the correct potential distribution. However, this result, although "correct," is useless for the analysis, since the actual function $V(r)$ cannot be extracted from an infinite additive constant, and that is why we say that in potential evaluations due to infinite charge distributions reference point cannot be taken at infinity.

Problems: 1.31–1.36; *MATLAB Exercises* (on Companion Website).

1.8 VOLTAGE

By definition, the voltage between two points is the potential difference between them. The unit is V. The voltage between points A and B is denoted by V_{AB}, so we have

$$\boxed{V_{\mathrm{AB}} = V_{\mathrm{A}} - V_{\mathrm{B}}.} \tag{1.88}$$

definition of voltage (unit: V)

where V_{A} and V_{B} are the potentials at point A and point B, respectively, with respect to the same reference point.

Combining Eqs. (1.74) and (1.88), we get

$$V_{\mathrm{AB}} = \int_{\mathrm{A}}^{\mathcal{R}} \mathbf{E} \cdot \mathrm{d}\mathbf{l} - \int_{\mathrm{B}}^{\mathcal{R}} \mathbf{E} \cdot \mathrm{d}\mathbf{l} = \int_{\mathrm{A}}^{\mathcal{R}} \mathbf{E} \cdot \mathrm{d}\mathbf{l} + \int_{\mathcal{R}}^{\mathrm{B}} \mathbf{E} \cdot \mathrm{d}\mathbf{l} \tag{1.89}$$

or

$$\boxed{V_{\mathrm{AB}} = \int_{\mathrm{A}}^{\mathrm{B}} \mathbf{E} \cdot \mathrm{d}\mathbf{l}.} \tag{1.90}$$

voltage via a line integral of $\mathbf{E}$

Therefore, the voltage between two points in an electrostatic field equals, in turn, the line integral of the electric field intensity vector along any path between these points. Obviously, $V_{\mathrm{BA}} = -V_{\mathrm{AB}}$.

If a new reference point is adopted for the electric potential in a system, voltages in the system remain unchanged. To prove this statement, we recall that the potential at all points in the system changes by the same constant value (ΔV) after the new reference point is adopted [see Eq. (1.79)]. Since a voltage is the difference of the potential values at the respective points in the system, Eq. (1.88), the new voltage between points A and B is given by

$$V'_{\mathrm{AB}} = V'_{\mathrm{A}} - V'_{\mathrm{B}} = (V_{\mathrm{A}} + \Delta V) - (V_{\mathrm{B}} + \Delta V) = V_{\mathrm{A}} - V_{\mathrm{B}} = V_{\mathrm{AB}}, \tag{1.91}$$

i.e., it equals the old voltage between these points.

Note that, in terms of voltages, Eq. (1.75) can be written as

Kirchhoff's voltage law

$$\boxed{\sum_{\text{along } C} V_i = 0,} \tag{1.92}$$

which, if applied to a closed path in a dc circuit, represents Kirchhoff's circuital law for voltages. This law tells us that the algebraic sum of voltages around any closed path in a circuit is zero.[11] Kirchhoff's voltage law for dc circuits, Eq. (1.92), is therefore just a special form of Maxwell's first equation for the electrostatic field, Eq. (1.75). We shall see in a later chapter that with some restrictions and approximations, Kirchhoff's voltage law in the form in Eq. (1.92) can also be used for the analysis of ac circuits.

Problems: 1.37; *Conceptual Questions* (on Companion Website): 1.9.

HISTORICAL ASIDE

The SI unit for the voltage, electric potential, and electromotive force (to be studied in a later chapter), volt (V), was named in honor of **Alessandro Volta** (1745–1827), an Italian physicist and inventor, a professor of experimental physics at the University of Pavia, who is famous for his invention of the electric battery (voltaic pile) in 1800. In experiments, he used his tongue to sense and measure the electricity and voltage — the first voltmeter. Volta's battery was a series of electrochemical cells made as a pile of alternating silver and zinc plates separated by cardboard disks soaked in salty water (electrolyte). *(Portrait: Edgar Fahs Smith Collection, University of Pennsylvania Libraries)*

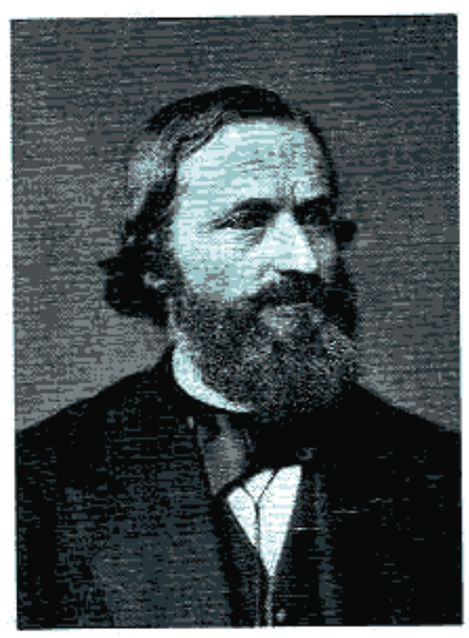

Gustav Robert Kirchhoff (1824–1887), a German physicist and chemist, taught at Universities of Berlin, Breslau, and Heidelberg. Kirchhoff received his doctoral degree from the University of Königsberg in 1847, under Neumann (1798–1895). Extending the work of Ohm (1789–1854), he formulated, in 1850, the fundamental relations between currents and voltages in an electric circuit with multiple loops, which we call Kirchhoff's circuital laws for currents and voltages. Kirchhoff also made seminal contributions to spectroscopy and thermal emission. *(Portrait: Edgar Fahs Smith Collection, University of Pennsylvania Libraries)*

1.9 DIFFERENTIAL RELATIONSHIP BETWEEN THE FIELD AND POTENTIAL IN ELECTROSTATICS

Eq. (1.74) represents an integral relationship between the electric field intensity vector and the potential in electrostatics, which enables us to determine V if we know $\mathbf{E}$. In this section, we shall derive an equivalent, differential, relationship between these two quantities, and then use it for evaluating $\mathbf{E}$ from V.

[11] Algebraic sum means that the voltages in the sum can be of arbitrary sign, where the sign with which the voltage is taken depends on the agreement or disagreement of the orientation (polarity) of the voltage with the orientation of the contour.

Consider a point A in an electrostatic field at which the potential is V_A. Let us move from that point for an elementary distance $dl = dx$ along the x-axis, to a point B, as shown in Fig. 1.24. The resulting change in the potential amounts to the potential at B (new potential) minus the potential at A (starting potential), that is,

$$dV = V_B - V_A. \tag{1.93}$$

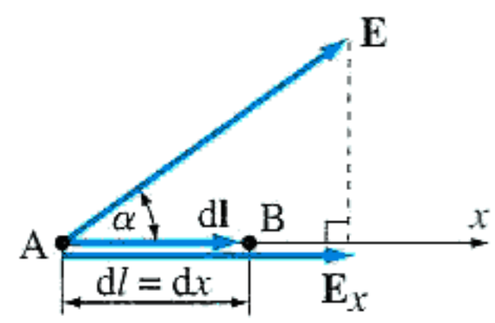

Figure 1.24 Derivation of the differential relationship between **E** and V in electrostatics.

On the other hand, Eq. (1.90) tells us that the potential difference (voltage) between points A and B is related to the electric field intensity vector as

$$V_A - V_B = \mathbf{E} \cdot d\mathbf{l} = E\,dl\cos\alpha = \underbrace{E\cos\alpha}_{E_x}\,dx = E_x\,dx, \tag{1.94}$$

with E_x standing for the x-component of **E**, which equals the projection of **E** on the x-axis, $E\cos\alpha$. Combining Eqs. (1.93) and (1.94), we have

$$\boxed{E_x = -\frac{dV}{dx}.} \tag{1.95}$$

1-D differential relationship between **E** *and* V

Similarly, the projections of the vector **E** on the other two axes of the Cartesian coordinate system are obtained as

$$E_y = -\frac{dV}{dy}, \quad E_z = -\frac{dV}{dz}. \tag{1.96}$$

Hence, the complete vector expression for **E** is given by

$$\mathbf{E} = E_x\,\hat{\mathbf{x}} + E_y\,\hat{\mathbf{y}} + E_z\,\hat{\mathbf{z}} = -\left(\frac{\partial V}{\partial x}\,\hat{\mathbf{x}} + \frac{\partial V}{\partial y}\,\hat{\mathbf{y}} + \frac{\partial V}{\partial z}\,\hat{\mathbf{z}}\right), \tag{1.97}$$

where we use partial derivatives instead of ordinary ones because the potential is a function of all three coordinates (multivariable function), $V = V(x, y, z)$. This differential relationship is an important general means for computing the field **E** from the potential V in electrostatics.

Example 1.16 **1-D Problem**

In an electrostatic system, the potential is constant in any individual plane normal to the Cartesian x-axis, while it varies along that axis as

$$V(x) = V_0 + V_1\frac{x}{d} + V_2\frac{x^2}{d^2}, \tag{1.98}$$

where V_0, V_1, V_2, and d are constants. Find the electric field intensity vector in the system.

Solution Since $dV/dy = 0$ and $dV/dz = 0$, we are left with an x-component of the vector **E** only, according to Eq. (1.97), which comes out to be

$$E_x = -\frac{dV}{dx} = -\frac{V_1}{d} - \frac{2V_2x}{d^2}. \tag{1.99}$$

Problems: 1.38; *Conceptual Questions* (on Companion Website): 1.10; *MATLAB Exercises* (on Companion Website).

1.10 GRADIENT

The expression in the parentheses in Eq. (1.97) is called the gradient of the scalar function (V). It is sometimes written as grad V, but much more frequently we write

it using the so-called del operator or nabla operator, defined as

del operator

$$\boxed{\nabla = \frac{\partial}{\partial x}\,\hat{\mathbf{x}} + \frac{\partial}{\partial y}\,\hat{\mathbf{y}} + \frac{\partial}{\partial z}\,\hat{\mathbf{z}}.} \tag{1.100}$$

So, we have

E from V in electrostatics

$$\boxed{\mathbf{E} = -\operatorname{grad} V = -\nabla V,} \tag{1.101}$$

where, in the Cartesian coordinate system (Fig. 1.2),

gradient in Cartesian coordinates

$$\boxed{\operatorname{grad} V = \nabla V = \frac{\partial V}{\partial x}\,\hat{\mathbf{x}} + \frac{\partial V}{\partial y}\,\hat{\mathbf{y}} + \frac{\partial V}{\partial z}\,\hat{\mathbf{z}}.} \tag{1.102}$$

The other two best-known and most commonly used coordinate systems are the cylindrical and the spherical. An arbitrary point (M) in the cylindrical coordinate system is represented as (r, ϕ, z), where r is the radial distance from the z-axis to the point M, ϕ the azimuthal angle measured from the x-axis in the xy-plane, and z the same as in the Cartesian coordinate system, as shown in Fig. 1.25. The ranges of the coordinates are

$$0 \le r < \infty, \quad 0 \le \phi < 2\pi \quad (\text{or } -\pi \le \phi < \pi), \quad -\infty < z < \infty. \tag{1.103}$$

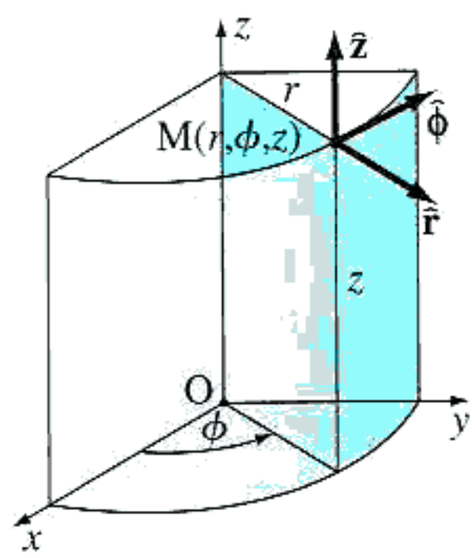

Figure 1.25 Point $M(r, \phi, z)$ and coordinate unit vectors in the cylindrical coordinate system.

The coordinate unit vectors, $\hat{\mathbf{r}}$, $\hat{\boldsymbol{\phi}}$, and $\hat{\mathbf{z}}$, are, by definition, directed in directions of increasing r, ϕ, and z, respectively. They are all mutually perpendicular (the cylindrical coordinate system belongs to the class of orthogonal coordinate systems), and the vector $\mathbf{E}$ in cylindrical coordinates can be expressed as

$$\mathbf{E} = E_r\hat{\mathbf{r}} + E_\phi\hat{\boldsymbol{\phi}} + E_z\,\hat{\mathbf{z}}. \tag{1.104}$$

Since ϕ is not a length coordinate but an angular one, an incremental distance $\mathrm{d}l$ corresponding to an elementary increment in the coordinate, $\mathrm{d}\phi$, equals $\mathrm{d}l = r\,\mathrm{d}\phi$ (the length of an arc of radius r defined by the angle $\mathrm{d}\phi$), and this exactly is the displacement $\mathrm{d}l$ in Fig. 1.24 in computing the change in potential $\mathrm{d}V$ in Eqs. (1.93)–(1.95) now in the ϕ direction. Therefore, the ϕ-component of the electric field vector at the point M in Fig. 1.25 equals $E_\phi = -\,\mathrm{d}V/\mathrm{d}l = -\,\mathrm{d}V/(r\,\mathrm{d}\phi)$ and not just $-\,\mathrm{d}V/\mathrm{d}\phi$. The other two cylindrical coordinates, r and z, are length coordinates, so no modification is needed, $E_r = -\,\mathrm{d}V/\mathrm{d}r$ and $E_z = -\,\mathrm{d}V/\mathrm{d}z$. Consequently, having in mind Eqs. (1.104) and (1.101), the gradient of $V = V(r, \phi, z)$ in the cylindrical coordinate system is, in place of Eq. (1.102), given by

gradient in cylindrical coordinates

$$\boxed{\operatorname{grad} V = \nabla V = \frac{\partial V}{\partial r}\,\hat{\mathbf{r}} + \frac{1}{r}\frac{\partial V}{\partial \phi}\,\hat{\boldsymbol{\phi}} + \frac{\partial V}{\partial z}\,\hat{\mathbf{z}}.} \tag{1.105}$$

In the spherical coordinate system, a point M is defined by (r, θ, ϕ), with r being the radial distance from the coordinate origin (O) to M, θ the zenith angle between the z-axis and the position vector of M, and ϕ the same as in the cylindrical coordinate system, as illustrated in Fig. 1.26. The ranges of spherical coordinates are

$$0 \le r < \infty, \quad 0 \le \theta \le \pi, \quad 0 \le \phi < 2\pi, \tag{1.106}$$

and the component representation of the vector $\mathbf{E}$ reads

$$\mathbf{E} = E_r\hat{\mathbf{r}} + E_\theta\hat{\boldsymbol{\theta}} + E_\phi\hat{\boldsymbol{\phi}}, \tag{1.107}$$

where $\hat{\mathbf{r}}$, $\hat{\boldsymbol{\theta}}$, and $\hat{\boldsymbol{\phi}}$ are mutually perpendicular coordinate unit vectors (directed in directions of increasing r, θ, and ϕ, respectively). As depicted in Fig. 1.10, the

corresponding incremental distances $\mathrm{d}l$ along these vectors equal to $\mathrm{d}r$, $r\,\mathrm{d}\theta$, and $r\sin\theta\,\mathrm{d}\phi$, and hence the following expression for the gradient of $V = V(r, \theta, \phi)$ in the spherical coordinate system:

$$\boxed{\operatorname{grad} V = \nabla V = \frac{\partial V}{\partial r}\,\hat{\mathbf{r}} + \frac{1}{r}\frac{\partial V}{\partial \theta}\,\hat{\boldsymbol{\theta}} + \frac{1}{r\sin\theta}\frac{\partial V}{\partial \phi}\,\hat{\boldsymbol{\phi}}.} \tag{1.108}$$

gradient in spherical coordinates

It is important to note that there is no equivalent in the cylindrical or spherical coordinates to the expression for the del operator, ∇, in Eq. (1.100), essentially because all the unit vectors in Figs. 1.25 and 1.26 except $\hat{\mathbf{z}}$ (of course, their directions and not magnitudes) depend on the location (on coordinates) of the point M. So, ∇ can be formally treated as a vector, given by Eq. (1.100), only in Cartesian coordinates.

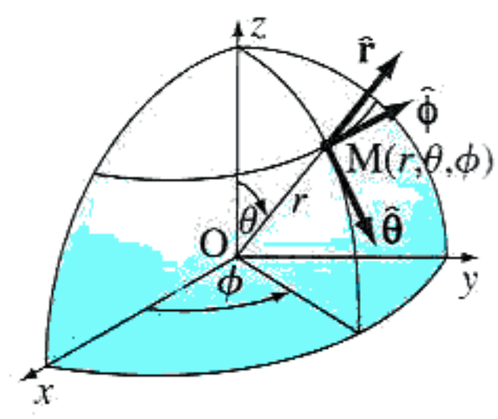

Figure 1.26 Point $\mathrm{M}(r, \theta, \phi)$ and coordinate unit vectors in the spherical coordinate system.

The expression in Eq. (1.102) and the corresponding expressions associated with other coordinate systems enable us to calculate ∇V for any multivariable scalar function V (not necessarily the electric potential). We shall now derive the relationship between the gradient and so-called directional derivative of a scalar field, which will provide us with a new physical interpretation of the gradient operation in general.

Combining Eqs. (1.94), (1.95), and (1.101), we have

$$-\frac{\mathrm{d}V}{\mathrm{d}x} = E_x = \mathbf{E}\cdot\hat{\mathbf{x}} = -\nabla V\cdot\hat{\mathbf{x}} \quad\longrightarrow\quad \frac{\mathrm{d}V}{\mathrm{d}x} = \nabla V\cdot\hat{\mathbf{x}}. \tag{1.109}$$

We can now formally proclaim the Cartesian x-axis to be an arbitrarily positioned linear axis in space, and call it an l-axis, with respect to which (Fig. 1.27)

$$\boxed{\frac{\mathrm{d}V}{\mathrm{d}l} = \nabla V\cdot\hat{\mathbf{l}} = |\nabla V|\cos\beta,} \tag{1.110}$$

directional derivative

where $\hat{\mathbf{l}}$ is the associated unit vector ($|\hat{\mathbf{l}}| = 1$) and β the angle between the vector ∇V and the l-axis. The derivative $\mathrm{d}V/\mathrm{d}l$ is referred to as the directional derivative of V in the l direction. It represents the rate of change of V in this direction, and equals the projection (component) of the vector ∇V on (along) the l-axis. Eq. (1.110) is an equivalent mathematical definition of the gradient of a scalar, and, although obtained specifically for the electrostatic potential, it is valid for any scalar field V (for which the necessary derivatives exist).

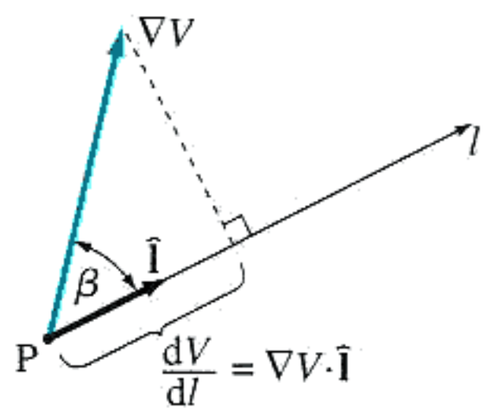

Figure 1.27 Relationship between the gradient and the directional derivative of a scalar field.

In addition, Eq. (1.110) has a very important physical meaning and practical implications. We note that for a given scalar field V, ∇V at a point P in Fig. 1.27 is a fixed vector. By steering the l-axis around P, i.e., by varying the angle β, we obtain different derivatives $\mathrm{d}V/\mathrm{d}l$ at the location P. For $\beta = \pm 90°$, $\mathrm{d}V/\mathrm{d}l = 0$ [from Eq. (1.110)]; for $\beta = 0$, however, we reach the maximum in $\mathrm{d}V/\mathrm{d}l$ ($\cos\beta = 1$), which becomes

$$\boxed{\left.\frac{\mathrm{d}V}{\mathrm{d}l}\right|_{\max} = |\nabla V| \quad (\beta = 0).} \tag{1.111}$$

physical meaning of the gradient

This means that (1) the magnitude of ∇V equals the maximum space rate of change in the function V per unit distance [$|\nabla V| = (\mathrm{d}V/\mathrm{d}l)_{\max}$] and (2) ∇V points in the direction of the maximum space rate of change in V ($\beta = 0$). We conclude that the gradient of a scalar field V is a vector that provides us with both the direction in which V changes most rapidly and the magnitude of the maximum space rate of change. This property of the gradient operation is extensively used in numerous applications, in all areas of science and engineering.

Example 1.17 **Field from Potential, Charged Ring**

From the electric potential due to a charged ring given by Eq. (1.85), find the electric field intensity vector along the ring axis normal to its plane.

Solution By symmetry, the vector **E** along the z-axis (Fig. 1.11) has a z-component only, so that a combination of Eqs. (1.101), (1.105), and (1.85) gives

$$\mathbf{E} = -\nabla V = -\frac{\mathrm{d}V}{\mathrm{d}z}\hat{\mathbf{z}} = -\frac{\mathrm{d}}{\mathrm{d}z}\left(\frac{Q'a}{2\varepsilon_0\sqrt{z^2+a^2}}\right)\hat{\mathbf{z}} = \frac{Q'az}{2\varepsilon_0\left(z^2+a^2\right)^{3/2}}\hat{\mathbf{z}}, \tag{1.112}$$

which, of course, is the same result as in Eq. (1.44).

Conversely, according to Eq. (1.74), the expression for the potential due to the ring can be found from the expression for the field, in Eq. (1.44), by integration along the z-axis from the point P (with a coordinate z) to the reference point at infinity ($z \to \infty$), as

$$V = \int_z^\infty E_z\,\mathrm{d}z, \tag{1.113}$$

and it is a simple matter to verify that the solution of this integral is exactly the potential in Eq. (1.85).

Problems: 1.39–1.45; *Conceptual Questions* (on Companion Website): 1.11; *MATLAB Exercises* (on Companion Website).

1.11 3-D AND 2-D ELECTRIC DIPOLES

An electric dipole is a very important, fundamental electrostatic system consisting of two point charges Q of opposite polarities separated by a distance d. We alternatively refer to this system as a three-dimensional (3-D) dipole, to distinguish it from an analogous 2-D system combining line charges, which will be analyzed later in this section. So, let us first derive the expressions for the electrostatic scalar potential and field intensity vector due to a 3-D dipole at large distances compared to d.

Introducing a spherical coordinate system whose origin is at the dipole center as shown in Fig. 1.28 and using Eq. (1.80) for the electric potential due to a single point charge and superposition, the potential due to the dipole at a point P is

$$V = \frac{Q}{4\pi\varepsilon_0}\left(\frac{1}{r_1} - \frac{1}{r_2}\right) = \frac{Q}{4\pi\varepsilon_0}\frac{r_2 - r_1}{r_1 r_2}. \tag{1.114}$$

Since $r \gg d$, $r_2 - r_1 \approx d\cos\theta$ and $r_1 r_2 \approx r^2$, and Eq. (1.114) becomes

electric dipole potential

$$\boxed{V \approx \frac{Q}{4\pi\varepsilon_0}\frac{d\cos\theta}{r^2} = \frac{p\cos\theta}{4\pi\varepsilon_0 r^2} = \frac{\mathbf{p}\cdot\hat{\mathbf{r}}}{4\pi\varepsilon_0 r^2},} \tag{1.115}$$

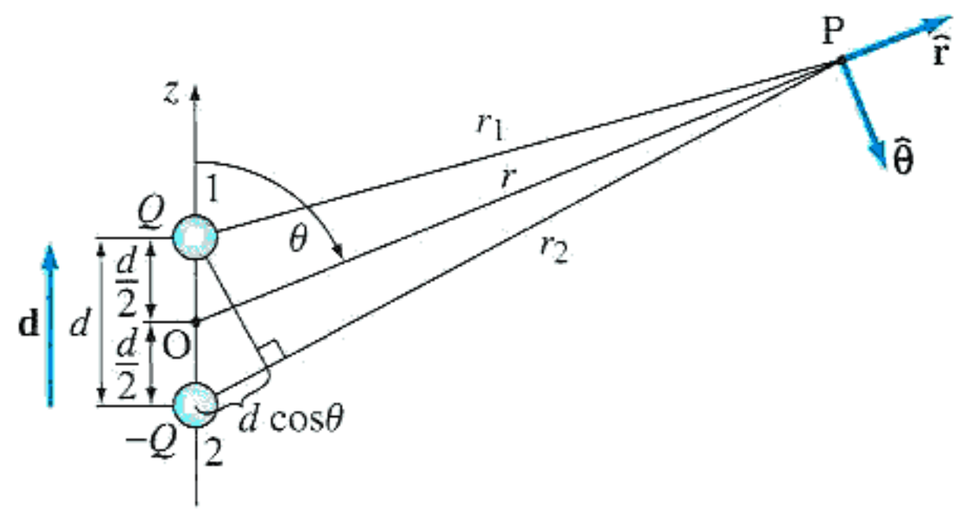

Figure 1.28 Electric dipole.

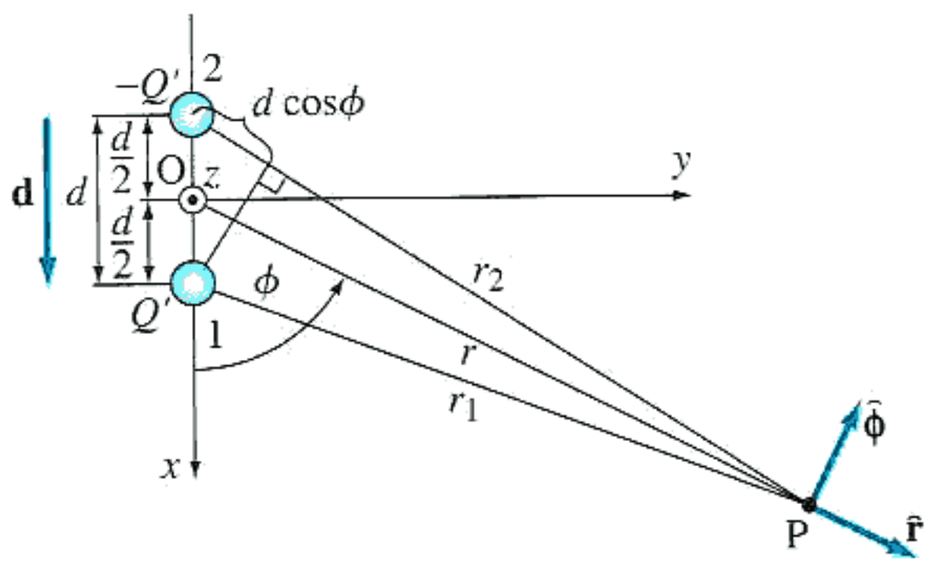

Figure 1.29 Cross section of a line dipole.

where

$$\boxed{\mathbf{p} = Q\mathbf{d}} \tag{1.116}$$

electric dipole moment

is the dipole moment ($p = Qd$). The unit for $\mathbf{p}$ is C · m.

Applying the formula for the gradient in spherical coordinates, Eq. (1.108), to the expression for V in Eq. (1.115) yields

$$\boxed{\mathbf{E} = -\nabla V = -\frac{\partial V}{\partial r}\hat{\mathbf{r}} - \frac{1}{r}\frac{\partial V}{\partial \theta}\hat{\boldsymbol{\theta}} = \frac{p}{4\pi\varepsilon_0 r^3}\left(2\cos\theta\,\hat{\mathbf{r}} + \sin\theta\,\hat{\boldsymbol{\theta}}\right).} \tag{1.117}$$

electric dipole field

We note that V and $\mathbf{E}$ due to an electric dipole vary with distance as $1/r^2$ and $1/r^3$, respectively.

We shall see in the next chapter that electric dipoles are fundamental for the discussion of dielectric polarization. In addition, a dipole concept is used in electromagnetic interference (EMI) considerations, since the quasistatic (low-frequency) electric field produced by an electrical device can often be approximated by the field due to a single electric dipole, given in Eq. (1.117).

The combination of two equal parallel infinite line charges Q' of opposite polarities separated by a distance d constitutes a line or two-dimensional (2-D) electric dipole. Let us find the potential due to this system.

Fig. 1.29 shows the cross section of a line dipole with the following per-unit-length dipole moment:

$$\mathbf{p}' = Q'\mathbf{d}. \tag{1.118}$$

The cylindrical coordinate system is adopted such that the z-axis is normal to the plane of drawing and coincides with the central line of the dipole. Taking the point O ($r = 0$) for the reference point for potential and applying Eq. (1.87), we have

$$V = \frac{Q'}{2\pi\varepsilon_0}\ln\frac{r_{\mathcal{R}1}}{r_1} + \frac{-Q'}{2\pi\varepsilon_0}\ln\frac{r_{\mathcal{R}2}}{r_2} = \frac{Q'}{2\pi\varepsilon_0}\ln\frac{r_2}{r_1}, \tag{1.119}$$

where $r_{\mathcal{R}1} = d/2$ and $r_{\mathcal{R}2} = d/2$ are the distances of the reference point from charges 1 and 2, respectively. At large distances from the dipole ($r \gg d$),

$$V \approx \frac{Q'}{2\pi\varepsilon_0}\ln\frac{r_1 + d\cos\phi}{r_1} \approx \frac{Q'}{2\pi\varepsilon_0}\ln\left(1 + \frac{d\cos\phi}{r}\right). \tag{1.120}$$

Since $\ln(1 + x) \approx x$ for $x \ll 1$, the final expression for the electric potential due to a line dipole turns out to be

$$\boxed{V \approx \frac{p'\cos\phi}{2\pi\varepsilon_0 r},} \tag{1.121}$$

line dipole potential

with $p' = Q'd$.

Note that for quasistatic electric field evaluations, transmission lines (telecommunication lines, power lines, computer buses, etc.) can sometimes be approximately modeled by a single line electric dipole, with the potential computed by Eq. (1.121). Such evaluations are important in studying undesired couplings between transmission lines, as well as associated EMI field levels.

Problems: 1.46–1.50; *MATLAB Exercises* (on Companion Website).

1.12 FORMULATION AND PROOF OF GAUSS' LAW

Gauss' law represents one of the fundamental laws of electromagnetism. It is an alternative statement of Coulomb's law and a direct consequence of the mathematical form of the electric field intensity vector due to a point charge. Gauss' law involves the flux (surface integral) of the vector **E** through a closed mathematical surface,[12] and can equivalently be formulated in a differential form, which is based on a differential operation called divergence on **E**. This important equation, in either form, provides an easy means of calculating the electric field due to highly symmetrical charge distributions, including problems with spherical, cylindrical, and planar symmetry, respectively.

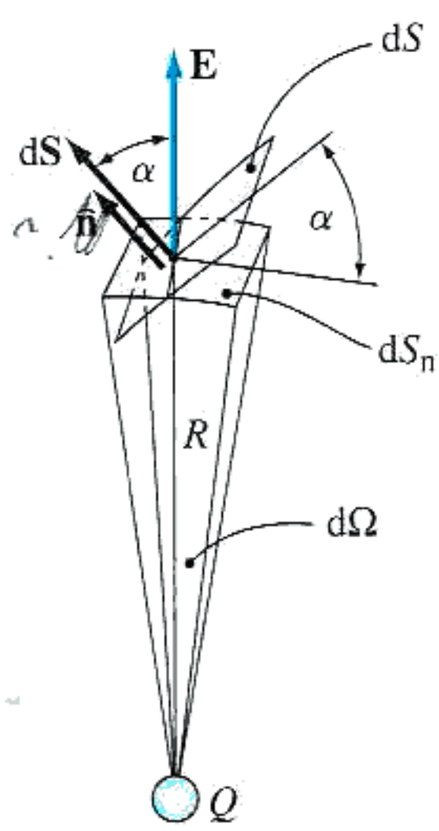

Figure 1.30 Evaluation of the flux of the vector **E** due to a point charge through a surface element dS, whose area vector, $d\mathbf{S}$, is oriented from the charge outward.

Gauss' law states that the outward flux of the electric field intensity vector through any closed surface in free space is equal to the total charge enclosed by that surface, divided by ε_0. To prove it, let us consider first a single point charge Q in free space and evaluate the flux of vector **E** through an arbitrarily positioned surface element (differentially small patch) of area dS, whose surface area vector is $d\mathbf{S}$, as shown in Fig. 1.30. This elementary flux is given by

$$d\Psi_E = \mathbf{E} \cdot d\mathbf{S}, \quad d\mathbf{S} = dS\,\hat{\mathbf{n}}, \tag{1.122}$$

where $\hat{\mathbf{n}}$ is the unit vector normal to dS directed from the charge outward. Using Eq. (1.24), we have

$$d\Psi_E = E\,dS\cos\alpha = E\,dS_n = \frac{Q}{4\pi\varepsilon_0}\frac{dS_n}{R^2}, \tag{1.123}$$

with dS_n standing for the projection of dS on the plane perpendicular to R (Fig. 1.30). This projection can be considered as the base of a cone with the apex at the charge. The solid angle of the cone is, by definition,

elementary solid angle

$$\boxed{d\Omega = \frac{dS_n}{R^2}} \tag{1.124}$$

[a solid angle is measured in steradians (sr or srad)], yielding

$$d\Psi_E = \frac{Q}{4\pi\varepsilon_0}\,d\Omega. \tag{1.125}$$

Assume now that the charge Q is enclosed by an arbitrary closed surface S, as depicted in Fig. 1.31(a). From Eq. (1.125), by integration, the outward flux of the

[12] The flux of a vector function **a** through an open or closed surface S is defined as $\int_S \mathbf{a} \cdot d\mathbf{S}$, where $d\mathbf{S}$ (to be discussed in this section) is the vector element of the surface perpendicular to it, and directed in accordance to the orientation of the surface.

HISTORICAL ASIDE

Johann Karl Friedrich Gauss (1777–1855) was a German mathematician and a director of the Göttingen Observatory. Gauss was born in Braunschweig (Brunswick) as a son of a gardener and a servant girl, and he showed his mathematical genius very early. At the age of seven, to the astonishment of his elementary school teacher, he summed the integers from 1 to 100 within seconds by realizing that the sum equaled 50 pairs of numbers from opposite ends of the list, each pair adding up to 101 ($1 + 100 = 101$, $2 + 99 = 101, \ldots$), so $50 \times 101 = 5{,}050$. He attended Universities of Braunschweig, Göttingen, and Helmstedt, and received his doctoral degree in 1799. Gauss made numerous seminal contributions to the number theory, algebra, geometry, and calculus, proved several fundamental theorems in different branches of mathematics, and is considered by many to be one of the three greatest mathematicians of all time, others being Archimedes (287 B.C.–212 B.C.) and Newton (1642–1727). He developed in 1813 the divergence theorem, providing the mathematical form for the famous law of electricity that relates the flux of the electric field intensity vector through a closed surface to the enclosed net charge and now carries his name – the law which first came out from experiments with charged concentric metallic spheres by Faraday (1791–1867) and was later translated into the Gaussian mathematical form by Maxwell (1831–1879). Upon Weber's (1804–1891) arrival at Göttingen in 1831, they worked together on a variety of topics in electricity and magnetism (see Weber's biography in Section 4.8).

vector $\mathbf{E}$ through the entire surface S ($\hat{\mathbf{n}}$ is directed from the surface outward) is

$$\Psi_E = \oint_S d\Psi_E = \frac{Q}{4\pi\varepsilon_0} \oint_S d\Omega = \frac{Q}{4\pi\varepsilon_0}\,\Omega, \tag{1.126}$$

where Ω is the full solid angle, which, in turn, can be interpreted as the angular measure for a spherical surface of arbitrary radius r and area $S_0 = 4\pi r^2$, resulting in (for spherical surfaces, $dS_n = dS$)

$$\boxed{\Omega = \oint_{S_0} d\Omega = \oint_{S_0} \frac{dS_n}{r^2} = \frac{1}{a^2}\oint_{S_0} dS = \frac{S_0}{r^2} = 4\pi.} \tag{1.127}$$

full solid angle

As the full solid angle turns out to equal 4π (sr), the total flux becomes

$$\Psi_E = \oint_S \mathbf{E}\cdot d\mathbf{S} = \frac{Q}{\varepsilon_0}, \quad \text{for a point charge } Q \text{ enclosed by } S. \tag{1.128}$$

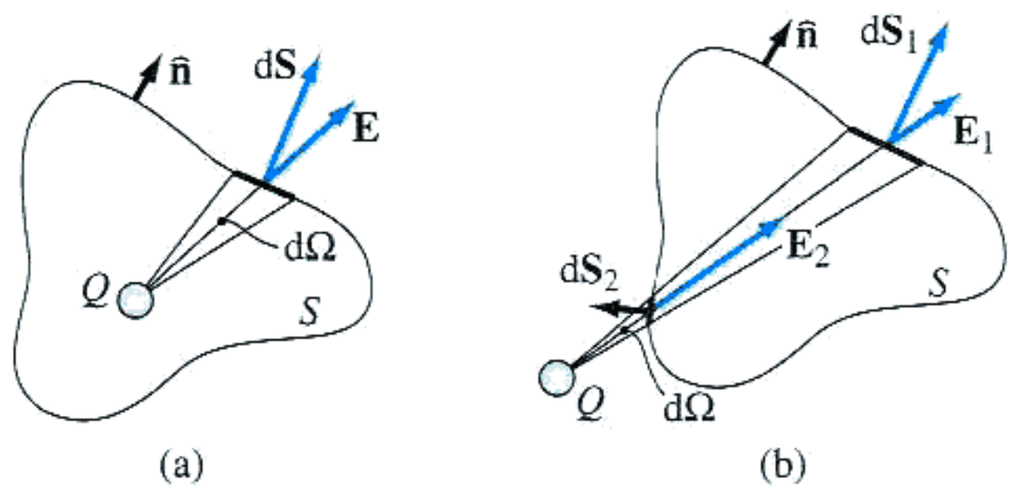

Figure 1.31 Evaluation of the outward flux of $\mathbf{E}$ due to a point charge through a closed surface S, the charge being enclosed by S (a) or located outside S (b).

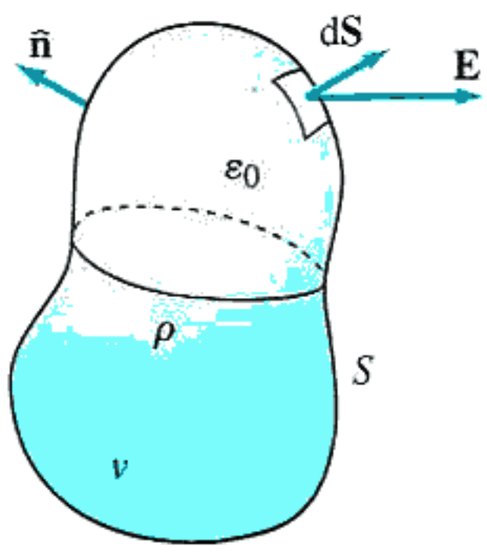

Figure 1.32 Arbitrary closed surface containing a volume charge distribution in free space.

For a point charge Q outside the surface S, we realize that the elementary fluxes through the two surface elements shown in Fig. 1.31(b), which have opposite orientations, are

$$(\mathrm{d}\Psi_E)_{\text{through } \mathrm{d}S_1} = \frac{Q}{4\pi\varepsilon_0}\,\mathrm{d}\Omega \quad \text{and} \quad (\mathrm{d}\Psi_E)_{\text{through } \mathrm{d}S_2} = -\frac{Q}{4\pi\varepsilon_0}\,\mathrm{d}\Omega, \tag{1.129}$$

respectively, so that their contributions to the flux integral cancel each other, and the total flux of $\mathbf{E}$ through S is

$$\Psi_E = \oint_S \mathbf{E}\cdot\mathrm{d}\mathbf{S} = 0, \quad \text{for a point charge outside } S. \tag{1.130}$$

By means of the superposition principle, Eq. (1.128) can then readily be generalized to the case of N point charges enclosed by a (closed) surface S:

$$\oint_S \mathbf{E}\cdot\mathrm{d}\mathbf{S} = \oint_S (\mathbf{E}_1 + \mathbf{E}_2 + \cdots + \mathbf{E}_N)\cdot\mathrm{d}\mathbf{S}$$

$$= \oint_S \mathbf{E}_1\cdot\mathrm{d}\mathbf{S} + \oint_S \mathbf{E}_2\cdot\mathrm{d}\mathbf{S} + \cdots + \oint_S \mathbf{E}_N\cdot\mathrm{d}\mathbf{S} = \frac{Q_1}{\varepsilon_0} + \frac{Q_2}{\varepsilon_0} + \cdots + \frac{Q_N}{\varepsilon_0}, \tag{1.131}$$

where $\mathbf{E}_i$ is the field due to a charge Q_i, $i = 1, 2, \ldots, N$. With the notation

$$Q_S = \sum_{i=1}^{N} Q_i, \tag{1.132}$$

we have

Gauss' law

$$\boxed{\oint_S \mathbf{E}\cdot\mathrm{d}\mathbf{S} = \frac{Q_S}{\varepsilon_0}.} \tag{1.133}$$

There may also be charges located outside the surface S; recall from Eq. (1.130), however, that the contribution to the total flux resulting from such charges is zero. As we know, any (continuous or discontinuous) charge distribution can be represented as a system of equivalent point charges. This means that Eq. (1.133) holds true for any charge distribution (in free space), where

$$Q_S = \text{total charge enclosed by } S \quad \text{(arbitrary charge distribution)}. \tag{1.134}$$

Eq. (1.133) is the mathematical formulation of Gauss' law.

The most general case of continuous charge distributions is the volume charge distribution, Fig. 1.32, in terms of which Gauss' law can be written as

Gauss' law for volume charge

$$\boxed{\oint_S \mathbf{E}\cdot\mathrm{d}\mathbf{S} = \frac{1}{\varepsilon_0}\int_v \rho\,\mathrm{d}v,} \tag{1.135}$$

with v denoting the volume enclosed by the surface S and ρ the volume charge density. This particular form of Gauss' law is usually referred to as Maxwell's third equation for the electrostatic field in free space.

The principle of conservation of energy in the electrostatic field, Eq. (1.75), and Gauss' law, Eq. (1.135), are the two fundamental integral equations (Maxwell's equations) describing the electrostatic field in free space.[13] As shown here and

[13]Gauss' law is the second equation out of a total of two Maxwell's equations used in electrostatics. Nevertheless, we term it Maxwell's third equation because it is customarily positioned as the third equation in the complete set of four general Maxwell's equations for the electromagnetic field, as we shall see in later chapters.

in Fig. 1.19, both equations can be derived from Coulomb's law, i.e., from the expression for the electrostatic field due to a point charge in free space.

Problems: 1.51 and 1.52; *Conceptual Questions* (on Companion Website): 1.12–1.16.

1.13 APPLICATIONS OF GAUSS' LAW

Let us now discuss procedures for using Gauss' law to determine the electric field intensity if the charge distribution is known. Gauss' law is always true, and we can apply it to any charge distribution and any problem. However, it enables us to analytically solve only for the field due to highly symmetrical charge distributions. To understand this, note that Gauss' law is mathematically formulated by an integral equation [Eq. (1.133)] in which the unknown quantity to be determined ($\mathbf{E}$) appears inside the integral. We can use the law to obtain a solution, therefore, only in cases in which we are able to bring the field intensity, E, outside the integral sign, and solve for it. These cases involve highly symmetrical charge distributions, for which we are able to choose a closed surface S, known as a Gaussian surface, that satisfies two conditions: (1) $\mathbf{E}$ is everywhere either normal or tangential to S and (2) $E = \text{const}$ on the portion of S on which $\mathbf{E}$ is normal. When $\mathbf{E}$ is tangential to the surface, $\mathbf{E} \cdot d\mathbf{S}$ in Eq. (1.133) becomes zero. When $\mathbf{E}$ is normal to the surface, $\mathbf{E} \cdot d\mathbf{S}$ becomes $E\,dS$, and since we have also that E is constant, it can be brought outside the integral sign in Eq. (1.133). We shall now apply these basic ideas to problems with spherical, cylindrical, and planar symmetry, respectively, in four characteristic examples.

Example 1.18 Example of a Problem with Spherical Symmetry

The first class of problems for which Gauss' law can be used to solve for the field involve charge distributions that depend only on the radial coordinate in the spherical coordinate system. Due to spherical symmetry, only the radial component of the electric field intensity vector is present, and this component is a function of the radial coordinate only. Based on these facts, the solution procedure is simple to perform. As an example, consider a sphere of radius a with a uniform volume charge density ρ, in free space, and determine (a) the field distribution both inside and outside the sphere and (b) the electric scalar potential at the sphere center.

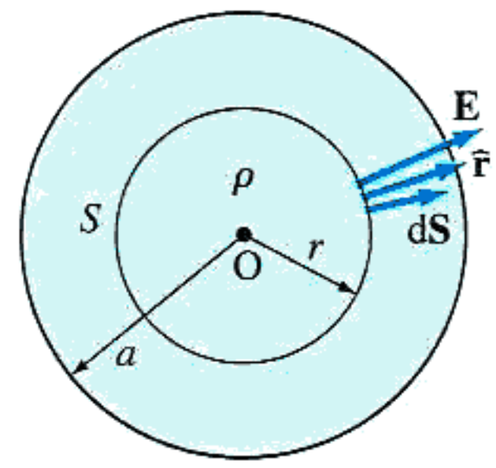

Figure 1.33 Application of Gauss' law to a problem with spherical symmetry – Example 1.18.

Solution

(a) The electric field vector at an arbitrary point in space is of the form

$$\boxed{\mathbf{E} = E(r)\,\hat{\mathbf{r}},} \tag{1.136}$$

$\mathbf{E}$ in a problem with spherical symmetry

where r is the radial coordinate in the spherical coordinate system and $\hat{\mathbf{r}}$ is the radial unit vector, as shown in Fig. 1.33. The Gaussian surface S is a spherical surface of radius r centered at the origin. On S,

$$d\mathbf{S} = dS\,\hat{\mathbf{r}} \quad \longrightarrow \quad \mathbf{E} \cdot d\mathbf{S} = E\,\hat{\mathbf{r}} \cdot dS\,\hat{\mathbf{r}} = E\,dS\,\hat{\mathbf{r}} \cdot \hat{\mathbf{r}} = E\,dS. \tag{1.137}$$

The outward flux of the vector $\mathbf{E}$ through S is hence

$$\Psi_E = \oint_S \mathbf{E} \cdot d\mathbf{S} = \oint_S E(r)\,dS = E(r) \oint_S dS = E(r)\,S = E(r)\,4\pi r^2 \quad (0 \le r < \infty)\,. \tag{1.138}$$

Since $\rho = \text{const}$ (uniform charge distribution), the charge enclosed by S is computed, according to Eq. (1.30), as ρ times the corresponding volume, which is that of either the

entire domain inside S, for $r < a$, or the charged sphere of radius a (there is no charge outside this sphere), for $r \geq a$, so Q_S amounts to

$$Q_S = \begin{cases} \rho 4\pi r^3/3 & \text{for } r < a \\ \rho 4\pi a^3/3 & \text{for } r \geq a \end{cases}. \tag{1.139}$$

According to Gauss' law, $\Psi_E = Q_S/\varepsilon_0$, yielding

$$E(r) = \begin{cases} \rho r/(3\varepsilon_0) & \text{for } r < a \\ \rho a^3/(3\varepsilon_0 r^2) & \text{for } r \geq a \end{cases}. \tag{1.140}$$

Note that the field for $r \geq a$ is identical to that of a point charge $Q = \rho 4\pi a^3/3$ (the total charge of the sphere) placed at the sphere center. This means that the point charge and the charged sphere are equivalent sources with respect to the region outside the sphere. Concept of equivalent sources is often used in electromagnetics.

(b) To find the electric potential at the sphere center (with respect to the reference point at infinity[14]), we first conclude that the potential outside the charged sphere is identical to the potential of the equivalent point charge, because the fields are identical, so that the potential at the sphere surface ($r = a$) is obtained directly from Eq. (1.80):

$$V(a) = \frac{Q}{4\pi\varepsilon_0 a}. \tag{1.141}$$

Invoking Eq. (1.90), the potential difference (voltage) between the sphere center and surface equals the line integral of $\mathbf{E}$ from the center to the surface, which results in the following for the potential at the center:

$$V(0) = \int_{r=0}^{a} E(r)\,\mathrm{d}r + V(a) = \frac{3Q}{8\pi\varepsilon_0 a} = \frac{\rho a^2}{2\varepsilon_0}. \tag{1.142}$$

Example 1.19 Example of a Problem with Cylindrical Symmetry

The second class of problems we deal with using Gauss' law involve infinitely long charge distributions that depend only on the radial coordinate in the cylindrical coordinate system. As an example, consider an infinitely long charged cylinder of radius a and volume charge density

$$\rho(r) = \rho_0 \frac{r^2}{a^2} \quad (0 \leq r \leq a) \tag{1.143}$$

in free space, where ρ_0 is a constant and r the radial coordinate (i.e., the distance from the cylinder axis), and find the electric field everywhere.

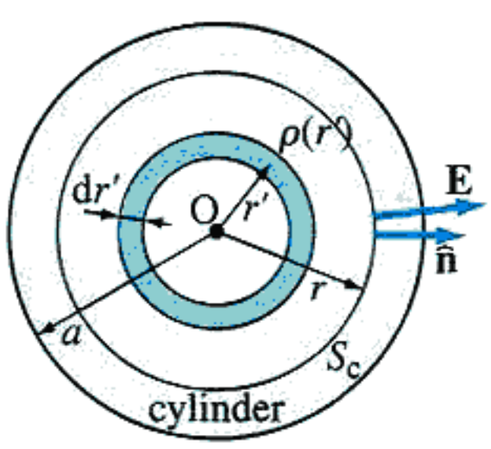

Figure 1.34 Application of Gauss' law to a problem with cylindrical symmetry – Example 1.19.

Solution Shown in Fig. 1.34 is a cross section of the cylinder. Due to cylindrical symmetry of the charge distribution in this case, the field is radial with respect to the cylinder axis and is of the form given in Eq. (1.136), r being here the radial cylindrical coordinate and $\hat{\mathbf{r}}$ the associated unit vector. The Gaussian surface is a cylinder of radius r and height (length) h, positioned coaxially with the charged cylinder.

To determine $\mathbf{E}$ inside the charge distribution, we apply Gauss' law, Eq. (1.135), to a Gaussian cylinder of radius $r \leq a$,

$$E(r)\underbrace{2\pi r h}_{S_c} = \frac{1}{\varepsilon_0}\int_{r'=0}^{r} \underbrace{\rho_0 \frac{r'^2}{a^2}}_{\rho} \underbrace{2\pi r'\,\mathrm{d}r' h}_{\mathrm{d}v}, \tag{1.144}$$

[14]Whenever the reference point for the potential to be determined is not specified, we assume that it is at infinity, except for infinite charge distributions, where such assumption would give us an infinite potential [e.g., Eq. (1.87) for $r_{\mathcal{R}} \to \infty$].

where S_c is the lateral surface area of the cylinder, and dv is the volume of a thin cylindrical shell of radius r' ($0 < r' \leq r$), thickness dr', and height h (we adopt as large as possible dv, as explained in Section 1.4). This volume is computed as that of a thin flat rectangular slab with edges equal to $2\pi r'$ (circumference of the cylindrical shell), h, and dr' (for the purpose of the volume computation, the shell is flattened into a rectangular slab). The flux of the vector $\mathbf{E}$ through the top and bottom surfaces of the Gaussian cylinder is zero since $\mathbf{E}$ is tangential to those surfaces ($\mathbf{E} \cdot d\mathbf{S} = 0$). By integration in Eq. (1.144),

$$E(r) = \frac{\rho_0 r^3}{4\varepsilon_0 a^2}, \quad \text{for } r \leq a. \tag{1.145}$$

For a field point outside the charged cylinder ($r > a$), the upper limit in the integral in Eq. (1.144) becomes a, which results in

$$E(r) = \frac{\rho_0 a^2}{4\varepsilon_0 r}, \quad \text{for } r > a. \tag{1.146}$$

Note that this field is identical to the field due to an infinite line charge positioned along the cylinder axis with the same charge per unit length Q' as the cylinder [see Eqs. (1.31) and (1.57)].

Example 1.20 Example of a Problem with Planar Symmetry

Finally, this and the following example illustrate how problems involving charge distributions that depend on one Cartesian coordinate only – problems with planar symmetry – can be solved using Gauss' law. Consider first a layer of volume charges in free space with the volume charge density being the following even function of the Cartesian coordinate x:

$$\rho(x) = \rho_0 \left(1 - \frac{x^2}{a^2}\right), \quad |x| \leq a. \tag{1.147}$$

where ρ_0 and a ($a > 0$) are constants and $\rho(x) = 0$ for $|x| > a$. Determine the electric field intensity vector everywhere, i.e., inside and outside the charge layer.

Solution Fig. 1.35 shows the charge distribution. Due to planar symmetry, vector $\mathbf{E}$ at an arbitrary point of space has an x-component only, and E_x depends on the coordinate x only (it is constant in any plane $x = \text{const}$), so we can write

$$\boxed{\mathbf{E} = E_x(x)\,\hat{\mathbf{x}}.} \tag{1.148}$$

$\mathbf{E}$ in a problem with planar symmetry

In addition, since the charge distribution is symmetrical with respect to the plane $x = 0$, vector $\mathbf{E}$ in the plane defined by $x' = x$ ($x > 0$) in Fig. 1.35 is equal in magnitude and opposite in

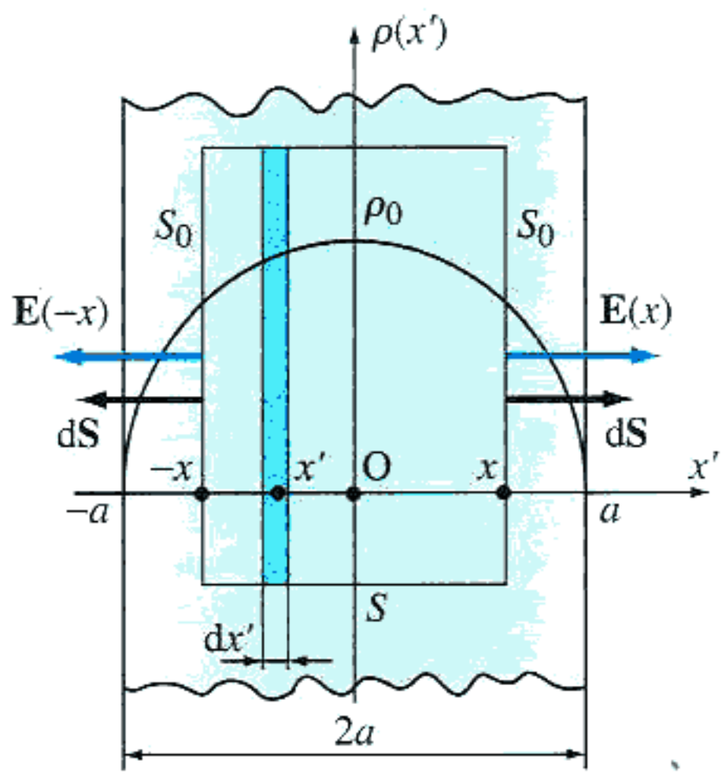

Figure 1.35 Application of Gauss' law to a problem with planar symmetry – Example 1.20.

direction to that in the plane $x' = -x$. The Gaussian surface is a right-angled parallelepiped (rectangular box) that is cut symmetrically by the plane $x = 0$ and has two of its faces, with areas S_0, positioned in the planes $x' = x$ and $x' = -x$, respectively.

Let us first determine the field intensity $E_x(x)$ inside the charge layer ($-a \le x \le a$). Noting that $\mathbf{E}$ and $\mathrm{d}\mathbf{S}$ are oriented in the same direction at both faces S_0, as well as that $\mathbf{E}$ and $\mathrm{d}\mathbf{S}$ are mutually perpendicular on the remaining portions of the Gaussian surface, we have

$$2\,E_x(x)\,S_0 = \frac{1}{\varepsilon_0}\int_{x'=-x}^{x} \rho(x')\,\underbrace{S_0\,\mathrm{d}x'}_{\mathrm{d}v}. \tag{1.149}$$

where $\mathrm{d}v$ is the volume of a thin slice of the parallelepiped with thickness $\mathrm{d}x'$. The integration in x' yields

$$E_x(x) = \frac{\rho_0 x}{\varepsilon_0}\left(1 - \frac{x^2}{3a^2}\right), \quad \text{for } |x| \le a. \tag{1.150}$$

Let us now bring the parallelepiped faces S_0 onto the boundaries of the charge layer. If we then start moving them toward infinity, symmetrically with respect to the plane $x = 0$, nothing will change in the application of Gauss' law, since there is no charge beyond the layer boundaries. This reasoning gives us directly the field intensity outside the charge layer:

$$E_x(x) = E_x(a) = \frac{2\rho_0 a}{3\varepsilon_0}, \quad \text{for } x > a, \tag{1.151}$$

$$E_x(x) = E_x(-a) = -\frac{2\rho_0 a}{3\varepsilon_0}, \quad \text{for } x < -a. \tag{1.152}$$

Example 1.21 **Planar Symmetry, Antisymmetrical Charge Distribution**

Repeat the previous example but for the following odd function of x as the charge density of the $2a$-thick layer:

$$\rho(x) = \rho_0\,\frac{x}{a}, \quad |x| \le a\,; \tag{1.153}$$

there is no charge outside the layer.

Solution As this is an antisymmetrical charge distribution with respect to the plane $x = 0$, the total charge of the layer is zero, which implies that the electric field outside the layer is zero; namely, this field is as if due to an equivalent infinite sheet of charge (Fig. 1.15) with zero surface charge density ($\rho_s = 0$). In other words, if we subdivide the charge layer described by Eq. (1.153) into differentially thin layers of thicknesses $\mathrm{d}x'$ and add (integrate) the fields, given by Eq. (1.64), due to all these thin layers (observed outside all of them), the positives and negatives exactly cancel out, and the result (total field for $x < -a$ or $x > a$) is zero. In place of Eqs. (1.151) and (1.152) we thus have

$$\int_{x'=-a}^{a} \rho(x')\,\mathrm{d}x' = 0 \quad \longrightarrow \quad E_x(x) = 0 \quad (|x| > a). \tag{1.154}$$

Positioning the Gaussian rectangular surface in Fig. 1.35 such that one of its parallel faces with area S_0 is in the region $x' < -a$ (on the left of the charge layer) and the other is in the plane $x' = x$ where $-a \le x \le a$ (inside the layer), Gauss' law gives [instead of Eqs. (1.149) and (1.150)]

$$E_x(x)\,S_0 = \frac{1}{\varepsilon_0}\int_{x'=-a}^{x} \rho_0\,\frac{x'}{a}\,S_0\,\mathrm{d}x' \quad \longrightarrow \quad E_x(x) = \frac{\rho_0}{2\varepsilon_0 a}\left(x^2 - a^2\right) \quad (|x| \le a). \tag{1.155}$$

since the flux of $\mathbf{E}$ through the face outside the charge layer is zero, from Eq. (1.154), and the volume integration effectively starts at $x' = -a$, where the charge distribution begins.

Problems: 1.53–1.64; *Conceptual Questions* (on Companion Website): 1.17 and 1.18; *MATLAB Exercises* (on Companion Website).

1.14 DIFFERENTIAL FORM OF GAUSS' LAW

Gauss' law is an integral equation in the spatial domain (the integrations involved are carried out with respect to spatial coordinates), and, in the general case, it represents an integral relationship between the electric field intensity vector, **E**, and the volume charge density, ρ [Eq. (1.135)]. In this section, we shall derive an equivalent, differential, relationship between **E** and ρ, that is, the differential form of Gauss' law.

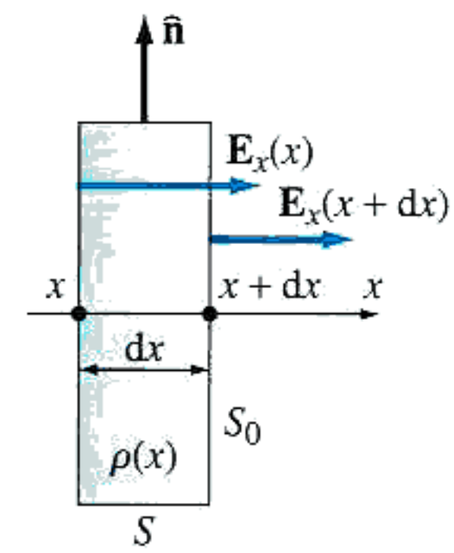

Figure 1.36 For derivation of the one-dimensional Gauss' law in differential form.

Assume first that ρ is a function of the Cartesian coordinate x only, $\rho = \rho(x)$ (1-D charge distribution), so that the only present component of **E** is $E_x = E_x(x)$. Let us apply Gauss' law, Eq. (1.135), to a rectangular closed surface S, the dimension of which in the x direction is dx and the sides normal to that direction are S_0 in area, as indicated in Fig. 1.36. The field being constant on both surfaces S_0, no integration is needed on the left-hand side of Eq. (1.135). In addition, since dx is differentially small, we can take $\rho(x)$ as constant in the volume enclosed by S, so that no integration is needed on the right-hand side of Eq. (1.135) either. Noting that on the left-hand side of S, **E** and $d\mathbf{S}$ are directed in opposite directions, we have

$$-E_x(x)\, S_0 + E_x(x + dx)\, S_0 = \frac{1}{\varepsilon_0}\, \rho(x)\, S_0\, dx. \tag{1.156}$$

The differential of E_x corresponding to the displacement dx,

$$dE_x = E_x(x + dx) - E_x(x), \tag{1.157}$$

divided by dx, is, by definition, the derivative of E_x with respect to x. From Eq. (1.156), this derivative comes out to be

$$\boxed{\frac{dE_x}{dx} = \frac{\rho}{\varepsilon_0}.} \tag{1.158}$$

1-D differential Gauss' law

This is a differential equation in the spatial domain, and it represents the one-dimensional Gauss' law in differential form. It states that, in cases when the charge distribution changes with a single linear spatial coordinate in free space, the rate of change of the electric field intensity with that coordinate equals the local density of volume charge, divided by ε_0.

The generalization of Eq. (1.158) to the three-dimensional case is straightforward. The charge density is now a function of all three coordinates, $\rho = \rho(x, y, z)$, and the Gaussian surface S has to be differentially small in all three dimensions, as shown in Fig. 1.37. We break the flux integral over S in Eq. (1.135) up into three pairs of integrals, each pair being carried out over two parallel sides of S. All sides being differentially small, the flux over each of them can be approximated by taking a constant value of the field component normal to the side and multiplying it by the side area. This gives us the result for each individual pair of integrals that has exactly the same form as in the one-dimensional case above [Eqs. (1.156)–(1.158)].

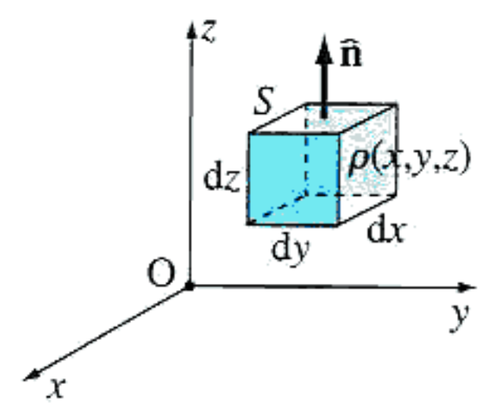

Figure 1.37 For derivation of Gauss' law in differential form for an arbitrary charge distribution.

For the first pair of integrals, we have that the outward flux of **E** through sides normal to the x direction (front side and back side in Fig. 1.37) is

$$\int_{\text{front}} \mathbf{E} \cdot d\mathbf{S} + \int_{\text{back}} \mathbf{E} \cdot d\mathbf{S} = (\text{change of } E_x \text{ across } dx) \times (dy\, dz)$$

$$= \frac{\partial E_x}{\partial x}\, dx\, (dy\, dz), \tag{1.159}$$

and adding the results for other two pairs of integrals, we obtain the total flux

$$\oint_S \mathbf{E} \cdot d\mathbf{S} = \frac{\partial E_x}{\partial x}\, dx\,(dy\, dz) + \frac{\partial E_y}{\partial y}\, dy\,(dx\, dz) + \frac{\partial E_z}{\partial z}\, dz\,(dx\, dy). \tag{1.160}$$

The volume enclosed by S is $\Delta v = dx\, dy\, dz$, with which the above equation becomes

$$\oint_S \mathbf{E} \cdot d\mathbf{S} = \left(\frac{\partial E_x}{\partial x} + \frac{\partial E_y}{\partial y} + \frac{\partial E_z}{\partial z}\right) \Delta v \quad (\Delta v \to 0). \tag{1.161}$$

Since Δv is very small, the total charge in it can be found with no integration in Eq. (1.135), simply as

$$Q_S = \rho\, \Delta v = \rho\,(dx\, dy\, dz). \tag{1.162}$$

Finally, interconnecting the flux and charge by means of Eq. (1.135), we have

Gauss' law in differential form

$$\boxed{\frac{\partial E_x}{\partial x} + \frac{\partial E_y}{\partial y} + \frac{\partial E_z}{\partial z} = \frac{\rho}{\varepsilon_0}.} \tag{1.163}$$

This is Gauss' law in differential form, i.e., Maxwell's third differential equation for the electrostatic field in free space. It is a partial differential equation or PDE (partial derivatives with respect to individual coordinates enter into the equation) in three unknowns (three components of the vector **E**). This equation provides us with valuable information about the way **E** varies in space. It relates the rate of change of field components with spatial coordinates to the local charge density. We see that changes of individual components along the direction of that component only (change of E_x along x, and not along y and z, etc.) contribute in this relationship.

Problems: 1.65 and 1.66; *Conceptual Questions* (on Companion Website): 1.19; *MATLAB Exercises* (on Companion Website).

1.15 DIVERGENCE

The expression on the left-hand side of Eq. (1.163) is called the divergence of a vector function (**E**), and is written as div **E**. Applying formally the formula for the dot product of two vectors in the Cartesian (rectangular) coordinate system,

$$\mathbf{a} \cdot \mathbf{b} = (a_x\, \hat{\mathbf{x}} + a_y\, \hat{\mathbf{y}} + a_z\, \hat{\mathbf{z}}) \cdot (b_x\, \hat{\mathbf{x}} + b_y\, \hat{\mathbf{y}} + b_z\, \hat{\mathbf{z}}) = a_x b_x + a_y b_y + a_z b_z, \tag{1.164}$$

to the del operator, Eq. (1.100), and vector **E**, we get

$$\begin{aligned} \nabla \cdot \mathbf{E} &= \left(\frac{\partial}{\partial x}\, \hat{\mathbf{x}} + \frac{\partial}{\partial y}\, \hat{\mathbf{y}} + \frac{\partial}{\partial z}\, \hat{\mathbf{z}}\right) \cdot (E_x\, \hat{\mathbf{x}} + E_y\, \hat{\mathbf{y}} + E_z\, \hat{\mathbf{z}}) \\ &= \frac{\partial E_x}{\partial x} + \frac{\partial E_y}{\partial y} + \frac{\partial E_z}{\partial z}, \end{aligned} \tag{1.165}$$

and this is exactly div **E**, in Eq. (1.163). Note that the divergence is an operation that is performed on a vector, but the result is a scalar. The differential Gauss' law now can be written in a short form

Gauss' law using divergence notation

$$\boxed{\operatorname{div} \mathbf{E} = \frac{\rho}{\varepsilon_0} \quad \text{or} \quad \nabla \cdot \mathbf{E} = \frac{\rho}{\varepsilon_0},} \tag{1.166}$$

where, in the Cartesian coordinate system,

divergence in Cartesian coordinates

$$\boxed{\operatorname{div} \mathbf{E} = \nabla \cdot \mathbf{E} = \frac{\partial E_x}{\partial x} + \frac{\partial E_y}{\partial y} + \frac{\partial E_z}{\partial z}.} \tag{1.167}$$

In nonrectangular coordinate systems, the corresponding formulas are more complex, due to curvature (or nonrectangularity) of differential volume cells in place of the one in Fig. 1.37. For instance, if, in analogy to the situation in Fig. 1.36, we consider a one-dimensional spherical volume charge distribution with $\rho = \rho(r)$, r being the radial spherical coordinate in Fig. 1.26, the only component of $\mathbf{E}$ is $E_r = E_r(r)$, as in Eq. (1.136), and applying Gauss' law, Eq. (1.135), to the inner (radius r) and outer (radius $r + \mathrm{d}r$) surfaces of a thin spherical shell in Fig. 1.9, Eq. (1.156) becomes

$$-E_r(r)\,4\pi r^2 + E_r(r + \mathrm{d}r)\,4\pi(r + \mathrm{d}r)^2 = \frac{1}{\varepsilon_0}\,\rho(r)\,4\pi r^2\,\mathrm{d}r, \tag{1.168}$$

where the use is made of the expression for $\mathrm{d}v$ in Eq. (1.33). After eliminating 4π on both sides of the equation, the expression on the left-hand side is the differential [see Eq. (1.157)] of the function $r^2 E_r$ corresponding to the coordinate increment $\mathrm{d}r$, which divided by $\mathrm{d}r$ represents the derivative of $r^2 E_r$ with respect to r, and hence

$$\frac{1}{r^2}\,\frac{\mathrm{d}(r^2 E_r)}{\mathrm{d}r} = \frac{\rho}{\varepsilon_0}, \tag{1.169}$$

analogously to Eq. (1.158). This is a one-dimensional differential Gauss' law in the spherical coordinate system, and its generalization to the 3-D case of $\rho = \rho(r, \theta, \phi)$ mimics the derivation in Eqs. (1.159)–(1.163) accommodated to the elemental spherical cuboid in Fig. 1.10, and similarly for $\rho = \rho(r, \phi, z)$ (Fig. 1.25). The resulting formula for the cylindrical coordinate system is

$$\boxed{\operatorname{div}\mathbf{E} = \nabla\cdot\mathbf{E} = \frac{1}{r}\,\frac{\partial}{\partial r}(rE_r) + \frac{1}{r}\,\frac{\partial E_\phi}{\partial \phi} + \frac{\partial E_z}{\partial z},} \tag{1.170}$$

divergence in cylindrical coordinates

and that for spherical coordinates

$$\boxed{\operatorname{div}\mathbf{E} = \nabla\cdot\mathbf{E} = \frac{1}{r^2}\,\frac{\partial}{\partial r}\left(r^2 E_r\right) + \frac{1}{r\sin\theta}\,\frac{\partial}{\partial\theta}(\sin\theta E_\theta) + \frac{1}{r\sin\theta}\,\frac{\partial E_\phi}{\partial\phi}.} \tag{1.171}$$

divergence in spherical coordinates

As the vector expression for the operator ∇ in Eq. (1.100) is valid only in the Cartesian coordinate system, the dot product in $\nabla\cdot\mathbf{E}$ actually makes sense only in rectangular coordinates. However, we shall still use extensively the notation $\nabla\cdot\mathbf{E}$ in cylindrical and spherical coordinate systems as well – to simply mean the divergence of $\mathbf{E}$ ($\operatorname{div}\mathbf{E}$) and a symbolic representation of the respective formulas in Eqs. (1.170) and (1.171). In general, we shall often draw conclusions about gradient, divergence, and other operations involving vector field quantities by treating ∇ as a vector, Eq. (1.100), and performing formally vector operations with it, like in Eq. (1.165). Most importantly, these conclusions, properties, and relations, although derived in Cartesian coordinates, hold true (as identities) in all possible (cylindrical, spherical, and other) coordinate systems, because the properties of a physical quantity and relations between two or more quantities are the same regardless of the choice of a coordinate system.

Combining Eqs. (1.161) and (1.167), we obtain the equation

$$\boxed{\operatorname{div}\mathbf{E} = \nabla\cdot\mathbf{E} = \lim_{\Delta v\to 0}\frac{\oint_S \mathbf{E}\cdot\mathrm{d}\mathbf{S}}{\Delta v},} \tag{1.172}$$

physical meaning of the divergence

which tells us that the divergence of $\mathbf{E}$ at a given point is the net outflow of the flux of $\mathbf{E}$ per unit volume as the volume shrinks about the point. Eq. (1.172) is an equivalent

mathematical definition of the divergence of a vector. From it, we may regard div **E** physically as a measure of how much the field diverges from the point. In general, a positive divergence of any vector field indicates a local source of the field at that point producing radial field components with respect to the point – the outward flow of flux is positive, which means that the vector diverges (spreads out) at the point. Possible field components that are tangential to S do not contribute to the flux, and are not related to the divergence. Similarly, a negative divergence indicates a sink at the point (local negative source) – the outward flux flow is negative, and the vector field converges at the point. Finally, the divergence is zero where there is neither source nor sink of locally radial field components. Gauss' law simply tells us that these positive and negative sources in the case of the electric field, **E**, are positive and negative charges, $\rho\,\Delta v$. Quantitatively, the divergence represents the volume density of sources, and in our case this density is ρ.

Let us now replace ρ in the integral form of Gauss' law, Eq. (1.135), by its equal, $\varepsilon_0 \nabla \cdot \mathbf{E}$ – from the differential form of the law, Eq. (1.166):

divergence theorem

$$\boxed{\oint_S \mathbf{E} \cdot \mathrm{d}\mathbf{S} = \int_v \nabla \cdot \mathbf{E}\,\mathrm{d}v.} \tag{1.173}$$

This equation is called the divergence theorem (or Gauss-Ostrogradsky theorem). Although we have obtained it specifically for the electrostatic field in free space, the theorem is true for any vector field (for which the appropriate partial derivatives exist) and is one of the basic theorems of vector calculus. It applies to an arbitrary closed surface S and, in words, states that the net outward flux of a vector field through S equals the volume integral of the divergence of that field throughout the volume v bounded by S.

Example 1.22 **Problem with Spherical Symmetry Using Differential Gauss' Law**

Redo Example 1.18, part (a), but now employing Gauss' law in differential form.

Solution As we already know, from the spherical symmetry of the problem, that the electric field vector both inside the charged sphere and outside it has the form in Eq. (1.136), the formula for the divergence in spherical coordinates, given by Eq. (1.171), retains only the first term. For a point inside the charge distribution in Fig. 1.33, Gauss' law in differential form, Eq. (1.166), thus reduces to the following differential equation in a single coordinate, r:

$$\nabla \cdot \mathbf{E} = \frac{1}{r^2}\frac{\partial}{\partial r}\left[r^2 E(r)\right] = \frac{\rho}{\varepsilon_0} \quad (0 \le r < a)\,, \tag{1.174}$$

which can be directly solved by integration. Since $\rho = \text{const}$, we have

$$r^2 E(r) = \frac{\rho}{\varepsilon_0}\int r^2\,\mathrm{d}r + C_1 = \frac{\rho r^3}{3\varepsilon_0} + C_1 \quad \longrightarrow \quad E(r) = \frac{\rho r}{3\varepsilon_0} + \frac{C_1}{r^2}. \tag{1.175}$$

and the integration constant, C_1, is found from the "initial" condition $E(0) = 0$ at the center of the sphere (for $r = 0$). Namely, given that there is not a point charge (Q_0) at the point O in Fig. 1.33, the field at this point is zero, and hence $C_1 = 0$ [otherwise, the constant would amount to $C_1 = Q_0/(4\pi\varepsilon_0)$, from Eq. (1.24)], which yields the result for E in Eq. (1.140).

Outside the charge distribution in Fig. 1.33, $\rho = 0$, which substituted in Eq. (1.174) results in

$$\frac{\partial}{\partial r}\left[r^2 E(r)\right] = 0 \quad \longrightarrow \quad r^2 E(r) = C_2 \quad \longrightarrow \quad E(r) = \frac{C_2}{r^2} \quad (a < r < \infty). \tag{1.176}$$

The new constant of integration, C_2, is determined by means of the "boundary" condition at the boundary of the charged sphere, $r = a$; the field intensity on the inner side of the

boundary, computed from Eq. (1.175), must be the same (since there exist no surface charges on the boundary) as that on the outer side of it, from Eq. (1.176),

$$E(a^-) = E(a^+) = E(a) \quad \longrightarrow \quad C_2 = \frac{\rho a^3}{3\varepsilon_0}. \tag{1.177}$$

With this, the result for E in Eq. (1.176) agrees with the solution in Eq. (1.140).

Example 1.23 **Problem with Planar Symmetry by the Differential Gauss' Law**

Redo Example 1.20 but with the use of the differential Gauss' law.

Solution As this is a problem with planar symmetry, the electric field intensity vector everywhere is of the form in Eq.(1.148). Hence, Gauss' law given by the differential equation in Eq. (1.158) applies, which we solve by integration with respect to x (also see the previous example). For the observation point inside the charge layer ($-a \le x \le a$) in Fig. 1.35,

$$E_x(x) = \frac{1}{\varepsilon_0}\int \rho(x)\,\mathrm{d}x + C_1 = \frac{\rho_0 x}{\varepsilon_0}\left(1 - \frac{x^2}{3a^2}\right) + C_1, \quad \text{for } |x| \le a. \tag{1.178}$$

Because of symmetry (Fig. 1.35),

$$E_x(a) = -E_x(-a) \quad \longrightarrow \quad \frac{2\rho_0 a}{3\varepsilon_0} + C_1 = \frac{2\rho_0 a}{3\varepsilon_0} - C_1 \quad \longrightarrow \quad C_1 = 0, \tag{1.179}$$

which, substituted in Eq. (1.178), gives the same result as in Eq. (1.150).

For the point outside the layer ($|x| > a$), $\rho = 0$, so that Eq. (1.158) yields $E_x(x) = C_2$. Matching this field value to the one from Eqs. (1.178) and (1.179) in the "boundary" condition at the layer boundary defined by $x = a$, $E_x(a^+) = E_x(a^-) = E_x(a)$, we obtain $C_2 = 2\rho_0 a/(3\varepsilon_0)$, and thus $E_x(x) = 2\rho_0 a/(3\varepsilon_0)$ for $x > a$, the same as in Eq. (1.151). On the other side of the layer, the vector $\mathbf{E}$ has this same magnitude but opposite direction, resulting in the field expression in Eq. (1.152).

Note that the application of Gauss' law in differential form to a problem with planar symmetry and an antisymmetrical charge distribution is presented in Example 2.6.

Problems: 1.67–1.74; *MATLAB Exercises* (on Companion Website).

1.16 CONDUCTORS IN THE ELECTROSTATIC FIELD

So far, we have considered electrostatic fields in free space (a vacuum or air). We shall now extend our theory to electrostatic fields in the presence of materials. As we shall see, most of the formulas derived and solution techniques developed and used for the electrostatic field in free space are directly applicable to the analysis of electrostatic fields in material space, although some require modification. Materials can broadly be classified in terms of their electrical properties as conductors (which conduct electric current) and dielectrics (insulators). In the rest of this chapter, we shall study the interaction of the electrostatic field with conductors, in which case essentially no theoretical modification is needed to the electrostatic equations, whereas the behavior of dielectrics in the electrostatic field will be discussed in the next chapter.

Conductors have a large proportion of freely movable electric charges (free electrons and ions) that make the electric conductivity (ability to conduct electric current) of the material. Best conductors (with highest conductivity) are metals (such as silver, copper, gold, aluminum, etc.). In many applications, we consider

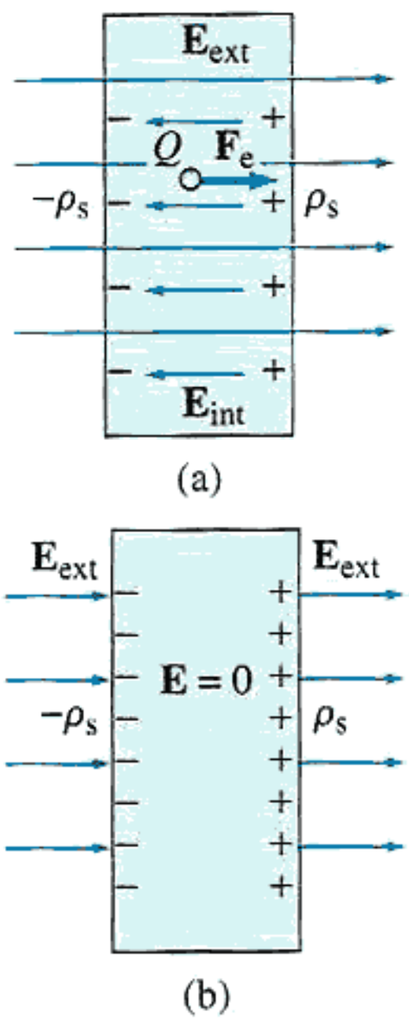

Figure 1.38 (a) A conductor in an external electrostatic field. (b) After a transitional process, there is no electrostatic field inside the conductor.

metallic conductors as perfect electric conductors (with infinite conductivity). There are also many other, less conductive conductors such as water, earth (ground), so-called semiconductors (e.g., silicon and germanium), etc. Practically all insulators (glass, paper, rubber, etc.) have some (usually extremely low) conductivity, and thus theoretically are (very poor) conductors, although almost always (in electrostatics) they may be considered as perfect dielectrics (with zero conductivity), i.e., non-conductors. In our studies of electrostatic fields, by conductor we normally mean a metallic conductor.

Consider an isolated conductor, shown in Fig. 1.38(a). Assume that it is uncharged or electrically neutral (its net charge is zero). When an external electrostatic field $\mathbf{E}_{ext}$ is applied, the free charges in the conductor are influenced by the electric force [see Eq. (1.23)]

$$\mathbf{F}_e = Q\mathbf{E}_{ext}. \tag{1.180}$$

This force pushes the positive charges along the direction of $\mathbf{E}_{ext}$, that is from left to right, while the negative charges move in the opposite direction. Consequently, the right-hand side of the conductor becomes progressively more positive, and the left-hand side progressively more negative. In fact, for a metallic conductor, what actually happens is movement of free electrons (negative charges) toward the left side leaving an equal number of positive charges, namely, a deficiency of electrons, on the other side of the conductor. Accumulated free charges form two layers of surface charge, of densities $-\rho_s$ ($\rho_s > 0$) and ρ_s, on the conductor sides. Creation of surplus charges in the body caused by an external electrostatic field is called the electrostatic induction. The induced charges, in turn, set up an internal induced electric field in the conductor, $\mathbf{E}_{int}$, which is directed from the positive to the negative layer, i.e., oppositely to $\mathbf{E}_{ext}$. As ρ_s increases, $\mathbf{E}_{int}$ becomes progressively stronger, and it opposes the migration of charges from left to right. In the equilibrium, $\mathbf{E}_{int}$ completely cancels out $\mathbf{E}_{ext}$ in the conductor, so that the total field $\mathbf{E}$ in the conductor is zero, and the motion of charges stops, as illustrated in Fig. 1.38(b). Note that the conductor remains uncharged as a whole. The entire transitional process is extremely fast, and the electrostatic steady state is established practically instantaneously. In fact, based on the length of the time needed for this process of movement of charges to the surface of a material body, i.e., their redistribution in such a way that the total electric field inside the body becomes zero, we determine whether a material is a conductor or dielectric. For example, as we shall see in a later chapter, the time to reach the equilibrium for the most commonly used metallic conductor – copper – is as brief as $\sim 10^{-19}$ s, whereas it takes as long as ~ 50 days for the charge rearrangement across a piece of fused quartz (very good insulator).

In the case of a conductor that had been charged (with a positive or negative excess charge) prior to being situated in the external field, a similar process takes place. All free charges (for a metallic conductor, free electrons of the conductor, which abundantly exist in the material also when it is electrically neutral as a whole, plus excess charge[15]) are exposed to the force $\mathbf{F}_e$ and produce the internal field that cancels out the externally applied field in the electrostatic equilibrium.

[15]Note that excess charge on a metallic body may be produced by bringing electrons to the body (negative excess charge) or by taking some of its free electrons away (positive excess charge), where the number of these extra or missing electrons is always much smaller than the total count of free electrons of the body.

We conclude that under electrostatic conditions, there cannot be electric field in a conductor,

$$\boxed{\mathbf{E} = 0.} \tag{1.181}$$

no electrostatic field inside a conductor

This is the first fundamental property of conductors in electrostatics. Starting from it, we derive all other fundamental conclusions about the behavior of conductors in the electrostatic field.

According to Eqs. (1.181), (1.90), and (1.88), the voltage between any two points in the conductor, including points on its surface, is zero. This means that a conductor is an equipotential body, i.e., the potential is the same everywhere in the conductor and on its surface,

$$\boxed{V = \text{const.}} \tag{1.182}$$

interior and surface of a conductor are equipotential

From Eq. (1.181), $\nabla \cdot \mathbf{E} = 0$ in a conductor, implying that [Eq. (1.166)] there cannot be surplus volume charges inside it,

$$\boxed{\rho = 0.} \tag{1.183}$$

no volume charge inside a conductor

So, any locally surplus charge of a conductor (whether it is neutral as a whole or not) must be located at the surface of the conductor.

Let us now derive so-called boundary conditions that the electric field must satisfy on a conductor surface. The electric field intensity vector $\mathbf{E}$ near the conductor in a vacuum can be decomposed into the normal and tangential components with respect to the boundary surface, as shown in Fig. 1.39(a). The two components are

$$E_n = E\cos\alpha \quad \text{and} \quad E_t = E\sin\alpha, \tag{1.184}$$

respectively, where α is the angle that $\mathbf{E}$ makes with the normal to the surface. We apply Eq. (1.75) to the narrow rectangular elementary contour C in Fig. 1.39(a). The field is zero along the lower side of C ($\mathbf{E} = 0$ in conductors), and we let the contour side Δh shrink to zero pressing the sides Δl tightly onto the boundary surface, so that the only contribution to the line integral in Eq. (1.75) is $\mathbf{E} \cdot \Delta\mathbf{l}$ along the upper side of C (no integration is needed, because Δl is small),

$$\oint_C \mathbf{E} \cdot d\mathbf{l} = \mathbf{E} \cdot \Delta\mathbf{l} = E\Delta l \sin\alpha = E_t\,\Delta l = 0. \tag{1.185}$$

Hence, there is no tangential component of $\mathbf{E}$ over the surface of a conducting body in electrostatics,

$$\boxed{E_t = 0.} \tag{1.186}$$

zero tangential electric field on a conductor surface

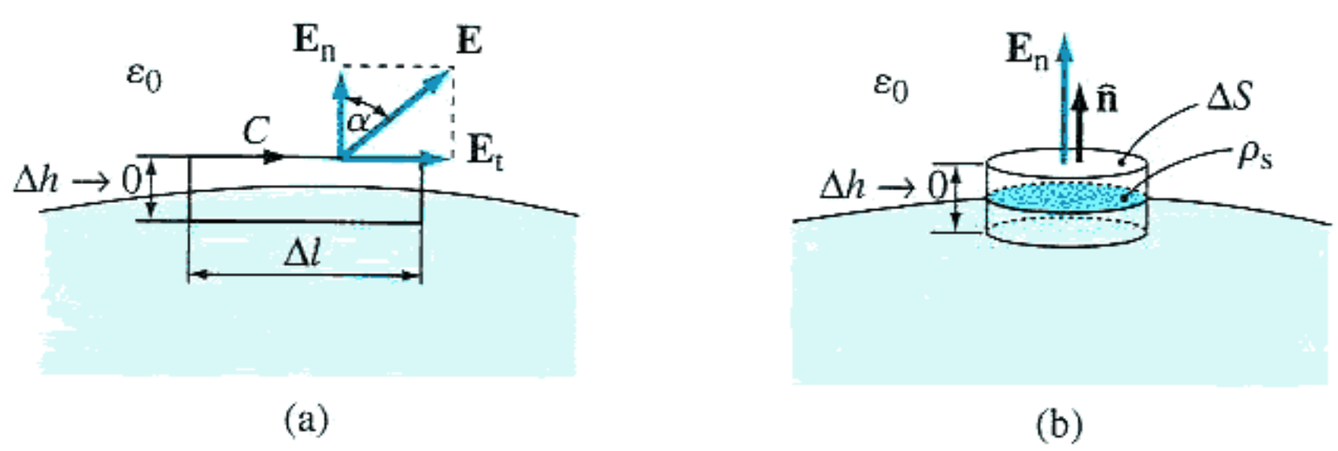

Figure 1.39 Deriving boundary conditions for the electrostatic field ($\mathbf{E}$) near a conductor surface: (a) narrow rectangular elementary contour (used for the boundary condition for the tangential component of $\mathbf{E}$) and (b) pillbox elementary closed surface (for the boundary condition for the normal component of $\mathbf{E}$).

In other words, the electric field intensity vector on the surface of a conductor is always normal to the surface,

$$\mathbf{E} = E_n \hat{\mathbf{n}}, \tag{1.187}$$

where $\hat{\mathbf{n}}$ is the normal unit vector on the surface, directed from the surface outward.

To obtain the boundary condition for the normal (the only existing) component of $\mathbf{E}$, we apply Eq. (1.133) to the pillbox Gaussian surface, with bases ΔS and height Δh (shrinking to zero), shown in Fig. 1.39(b). For similar reasons as in obtaining Eq. (1.185), the flux in Eq. (1.133) reduces to $\mathbf{E} \cdot \Delta\mathbf{S}$ over the upper side of S. Because the charge enclosed by S is $\rho_s \, \Delta S$,

$$\oint_S \mathbf{E} \cdot d\mathbf{S} = \mathbf{E} \cdot \Delta\mathbf{S} = (E_n \hat{\mathbf{n}}) \cdot (\Delta S \hat{\mathbf{n}}) = E_n \, \Delta S = \frac{1}{\varepsilon_0} \rho_s \, \Delta S, \tag{1.188}$$

providing the relationship between the normal component of the electric field intensity vector near a conductor surface and the surface charge density on the surface:

normal electric field component on a conductor surface

$$\boxed{E_n = \frac{\rho_s}{\varepsilon_0}.} \tag{1.189}$$

The lines of the electric field are normal to the surface of a conductor. We should always remember that the normal component E_n in Eq. (1.189) is defined with respect to the outward normal $\hat{\mathbf{n}}$. When $\rho_s > 0$, the field lines start from the conductor ($E_n > 0$), whereas they end on it ($E_n < 0$) when $\rho_s < 0$.

In analyzing complex conducting structures, we usually do not know in advance the orientation of the electric field intensity vector at specific portions of conducting surfaces. In such cases, the following expression for ρ_s in terms of the field vector, obtained noting that $E_n = \hat{\mathbf{n}} \cdot \mathbf{E}$ from Eq.(1.187), is useful:

$$\rho_s = \varepsilon_0 \, \hat{\mathbf{n}} \cdot \mathbf{E}. \tag{1.190}$$

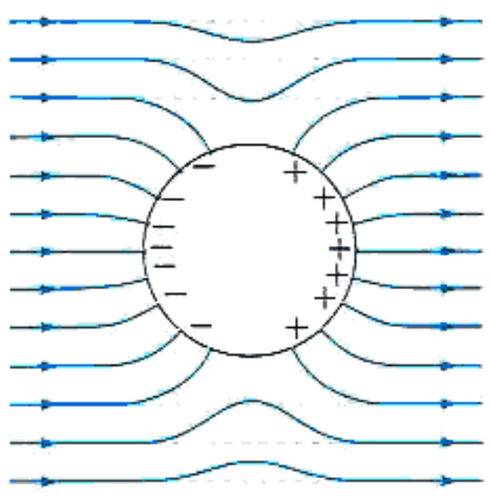

Figure 1.40 Uncharged metallic sphere in a uniform external electrostatic field; for Example 1.24.

Example 1.24 **Metallic Sphere in a Uniform Electrostatic Field**

An uncharged metallic sphere is brought into a uniform electrostatic field, in air. Sketch the field lines around the sphere after electrostatic equilibrium is reached.

Solution The field lines in the new electrostatic state are sketched in Fig. 1.40. Because the field due to induced charges on the sphere surface (this field exists both inside and outside the sphere) is superimposed to the external field, the field inside the sphere becomes zero, and that outside it is not uniform any more. Negative induced charges are sinks of the field lines on the left-hand side of the sphere, whereas the positive induced charges are sources of the field lines on the right-hand side. The field lines on both sides are normal to the sphere surface, and they therefore bend near the sphere. At points in air close to the left- and right-hand side of the sphere, the electric field is stronger (the field lines are denser) than in the remaining space. This is obvious as well from noting that near the left-hand side of the sphere, in air, the field due to negative induced charges dominates over the field due to positive charges on the opposite side of the sphere, it is directed toward the negative charges, and adds to the external field intensity. The field due to positive induced charges dominates near the right-hand side of the sphere, which results in the same strengthening of the external field at these points in air. The field at distances from the sphere a few times the sphere diameter is practically equal to the external field (the field due to induced charges is negligible).

1.17 EVALUATION OF THE ELECTRIC FIELD AND POTENTIAL DUE TO CHARGED CONDUCTORS

Assume that we know the charge distribution ρ_s over the surface of a conductor situated in free space. The electric field intensity at points close to the conductor surface can be evaluated from Eq. (1.189). How do we obtain the electric field and potential at an arbitrary point in space? The answer is straightforward. Because $\mathbf{E} = 0$ inside the conductor, nothing will change, as far as the field outside the conductor is concerned, if we remove the conductor and fill the space previously occupied by it with a vacuum, keeping the charge distribution ρ_s on the surface unchanged. With this useful equivalence, we are left with the problem of evaluating the field and potential due to a known surface charge distribution in free space, and we can use Eqs. (1.38), (1.83), (1.101), (1.133), and (1.165) to solve the problem.

Example 1.25 Charged Metallic Sphere

A metallic sphere of radius a is situated in air and charged with a charge Q. Find (a) the charge distribution of the sphere, (b) the electric field intensity vector in air, and (c) the potential of the sphere.

Solution

(a) Due to symmetry, the charge distribution over the sphere surface is uniform, and hence the associated surface charge density turns out to be

$$\rho_s = \frac{Q}{S_0} = \frac{Q}{4\pi a^2}, \tag{1.191}$$

where S_0 stands for the surface area of the sphere.

(b) The electric field around the sphere is radial, and has the form given by Eq. (1.136). Applying Gauss' law, Eq. (1.133), to a spherical surface of radius r ($a < r < \infty$), positioned concentrically with the metallic sphere [see Eqs. (1.137) and (1.138)], we obtain

$$\boxed{E(r) = \frac{Q}{4\pi\varepsilon_0 r^2} \quad (a < r < \infty).} \tag{1.192}$$

electric field due to a charged metallic sphere

Note that

$$E(a^+) = \frac{Q}{4\pi\varepsilon_0 a^2} = \frac{\rho_s}{\varepsilon_0}, \tag{1.193}$$

which is in agreement with Eq. (1.189).[16]

(c) We realize that the field outside the charged metallic sphere, Eq. (1.192), is identical to that due to a point charge Q placed at the sphere center, and so is the potential. The potential at the surface $r = a$ is thus given by Eq. (1.141). This is the potential of the sphere, the same at any point of its interior and surface [see Eq. (1.182)].

Example 1.26 Charged Cylindrical Conductor

Repeat the previous example but for an infinitely long cylindrical conductor of radius a in air, if the charge per unit length of the conductor is Q'.

[16] $E(a^+)$ or $E(a+0)$ [$E(a+\delta)$, $\delta \to 0$] designates the field in air very close to the conductor surface at $r = a$.

Solution

(a) Using Eq. (1.31), the charge per length h of the conductor is

$$Q_h = Q'h, \tag{1.194}$$

so the surface charge density amounts to

$$\rho_s = \frac{Q_h}{S_0} = \frac{Q_h}{2\pi a h} = \frac{Q'}{2\pi a}, \tag{1.195}$$

where S_0 is the surface area of that part of the conductor.

(b) The electric field is radial (with respect to the conductor axis). From Gauss' law [Eq. (1.133)] applied to the cylindrical surface of radius r ($a < r < \infty$) and height (length) h, coaxial with the conductor [see the left-hand side of Eq. (1.144)],

electric field due to a charged cylindrical conductor

$$\boxed{E(r) = \frac{1}{2\pi r h}\frac{Q_h}{\varepsilon_0} = \frac{Q'}{2\pi\varepsilon_0 r} \quad (a < r < \infty).} \tag{1.196}$$

(c) This is an infinite charge distribution, and the reference point for the potential cannot be adopted at infinity. The field in Eq. (1.196) being identical to the field due to an infinite line charge of density Q', Eq. (1.57), the potential due to the charged cylindrical conductor is given by the expression in Eq. (1.87). In particular, this expression for $r = a$ represents the potential of the conductor:

potential due to a charged cylindrical conductor

$$\boxed{V = \frac{Q'}{2\pi\varepsilon_0}\ln\frac{r_R}{r} \quad (r \geq a)} \quad \longrightarrow \quad V_{\text{conductor}} = \frac{Q'}{2\pi\varepsilon_0}\ln\frac{r_R}{a} \quad (r = a), \tag{1.197}$$

where r_R ($r_R \geq a$) is the distance of the reference point from the conductor axis.

Example 1.27 Charged Sphere Enclosed by an Uncharged Shell

A metallic sphere, of radius a and charge Q ($Q > 0$), is enclosed by an uncharged concentric metallic spherical shell, of inner radius b and outer radius c ($a < b < c$). The medium everywhere is air. Find the potential at the center of the sphere.

Solution As a result of the electrostatic induction, there is induced surface charge on the surfaces of the shell. As we know, there cannot be volume charges in the metal under electrostatic conditions, Eq. (1.183). Let Q_b and Q_c denote the total induced charges on the inner and outer surface of the shell, respectively. On the surface of the sphere, $Q_a = Q$. Since every line of the electric field originating at a positive charge on the sphere terminates at a negative charge on the inner surface of the shell, the relationship between total charges on two surfaces is

$$Q_b = -Q_a. \tag{1.198}$$

This can be obtained also from Gauss' law, Eq. (1.133), applied to a closed surface that is entirely inside the metal of the shell, so that $\Psi_E = 0$ [because of Eq. (1.181)], which implies that $Q_S = 0$, i.e., $Q_a + Q_b = 0$. On the other hand, since the shell is uncharged,

$$Q_b + Q_c = 0, \tag{1.199}$$

and hence $Q_c = -Q_b = Q_a$. Because of symmetry, charges on individual surfaces are distributed uniformly, and the electric field everywhere in air is in the form given by Eq. (1.136). Distributions of the charge and field in the system are sketched in Fig. 1.41.

By means of Gauss' law, the electric field for $a < r < b$ and $c < r < \infty$ is

$$E(r) = \frac{Q_a}{4\pi\varepsilon_0 r^2} \quad \text{(in air)}, \tag{1.200}$$

whereas for $0 \leq r \leq a$ and $b \leq r \leq c$,

$$E(r) = 0 \quad \text{(in metal)}. \tag{1.201}$$

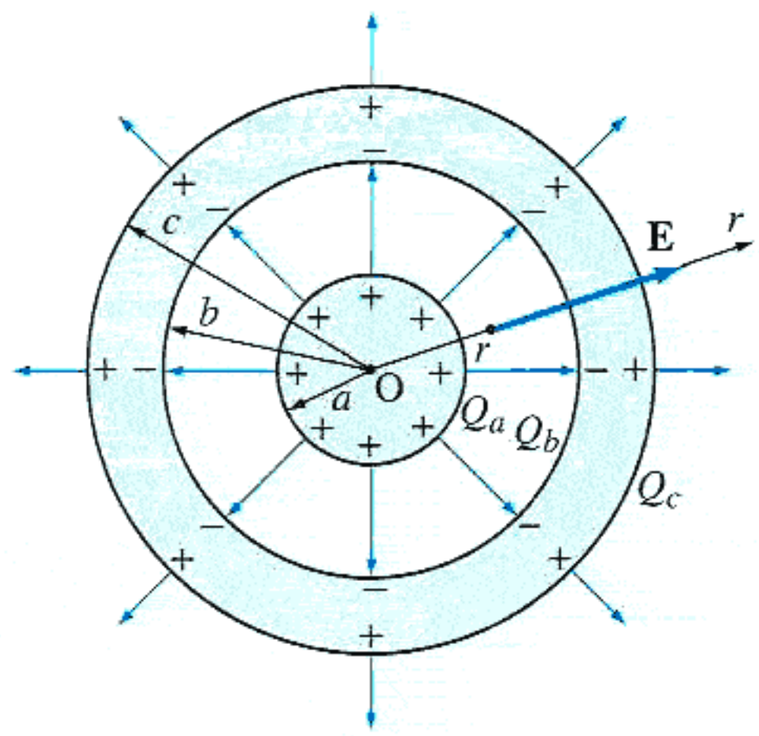

Figure 1.41 Charge and field distributions in the system of Example 1.27.

The potential at the point O in Fig. 1.41 is thus [Eq. (1.74)]

$$V = \int_{r=0}^{\infty} E(r)\,\mathrm{d}r = \frac{Q_a}{4\pi\varepsilon_0}\left(\int_a^b \frac{\mathrm{d}r}{r^2} + \int_c^{\infty} \frac{\mathrm{d}r}{r^2}\right) = \frac{Q}{4\pi\varepsilon_0}\left(\frac{1}{a} - \frac{1}{b} + \frac{1}{c}\right)$$

$$= \frac{Q(bc - ac + ab)}{4\pi\varepsilon_0 abc}. \tag{1.202}$$

Example 1.28 Five Parallel Large Flat Electrodes

Consider five parallel large metallic electrodes situated in air, as shown in Fig. 1.42(a). The thickness of each electrode, as well as the distance between each two adjacent electrodes, is $d = 2$ cm. The surface area of sides of electrodes facing each other is $S = 1\ \mathrm{m}^2$. The first, fourth, and fifth electrodes are grounded, the potential of the second electrode with respect to the ground is $V = 2$ kV, and the charge of the third electrode is $Q = 2\ \mu$C. Find the electric field intensity between the electrodes.

Solution Since the dimensions of the electrodes are much larger than the separation between them, we can neglect the fringing effects, i.e., we can ignore the nonuniformity of the electric field near the electrode edges, as well as the existence ("leakage") of the field lines outside the spaces between electrodes. We assume, thus, that the electric field is localized only in spaces between the electrode sides S, that vector $\mathbf{E}$ is normal to those sides, and that the field in each space is uniform. Charge distributions over electrode sides are also uniform. In

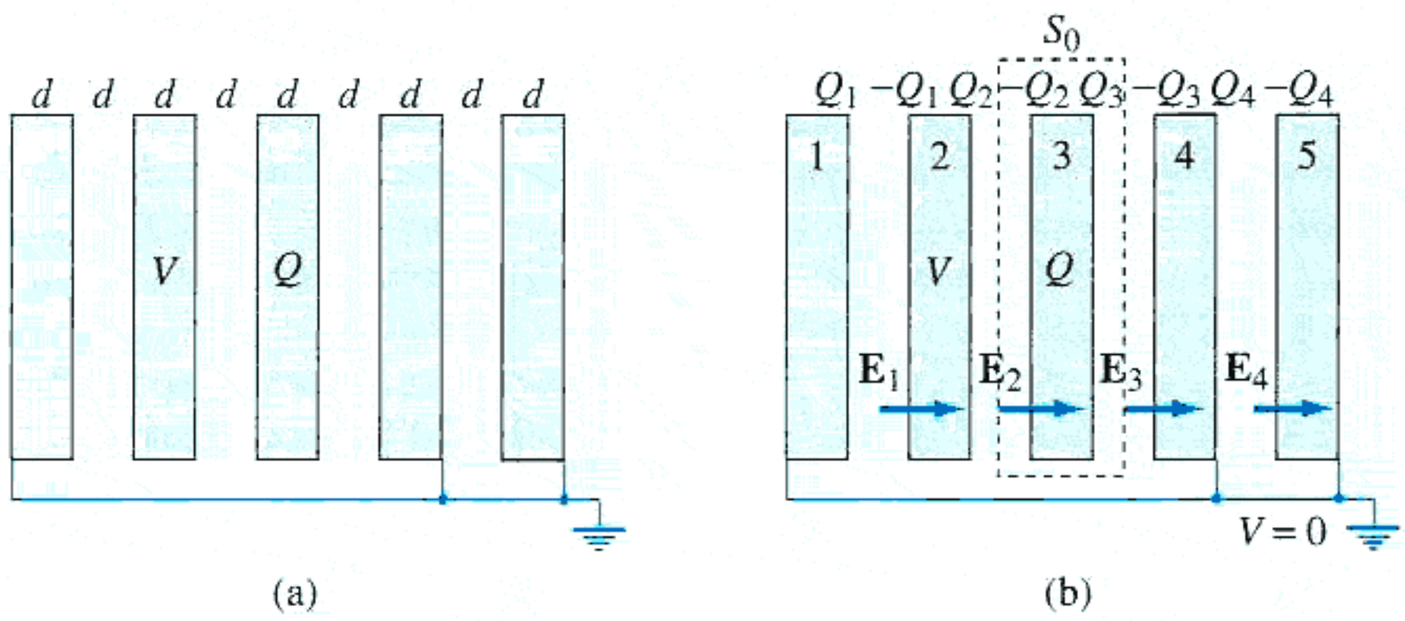

Figure 1.42 Electrostatic analysis of a system of five large electrodes in air: (a) geometry of the system and (b) charges on electrodes and fields between them; for Example 1.28.

each space between electrodes, neighboring sides of electrodes must be charged with charges of equal amounts, but of opposite polarities, as indicated in Fig. 1.42(b).

The potential V (which we know) of the second electrode with respect to the ground can be expressed in terms of the line integral of $\mathbf{E}$ from that electrode, to the left, to the first electrode, which is grounded (its potential is zero). The field is uniform, and the line integral is simply

$$V = \int_{\text{second electrode}}^{\text{first electrode}} \mathbf{E} \cdot d\mathbf{l} = -E_1 d. \tag{1.203}$$

Hence, the field intensity between the first and second electrodes is $E_1 = -V/d = -100$ kV/m. On the other side, the same potential can be expressed as the line integral of $\mathbf{E}$ to the right, to the fourth electrode, which is also grounded, yielding

$$V = E_2 d + E_3 d. \tag{1.204}$$

By a similar token, the field between the fourth and fifth electrodes is zero, $E_4 = 0$, and so are the associated charges on the sides of electrodes facing each other ($Q_4 = 0$), because these electrodes are at the same (zero) potential.

To solve for field intensities E_2 and E_3, we need one more equation with them as unknowns. Applying Gauss' law, Eq. (1.133), to the surface S_0 that encloses the third electrode (the charge of which is known), we obtain

$$-E_2 + E_3 = \frac{Q}{\varepsilon_0 S}. \tag{1.205}$$

The solution of the system of equations composed from Eqs. (1.204) and (1.205) is $E_2 = -62.94$ kV/m and $E_3 = 162.94$ kV/m.

Problems: 1.75–1.82; *Conceptual Questions* (on Companion Website): 1.20–1.22; *MATLAB Exercises* (on Companion Website).

1.18 ELECTROSTATIC SHIELDING

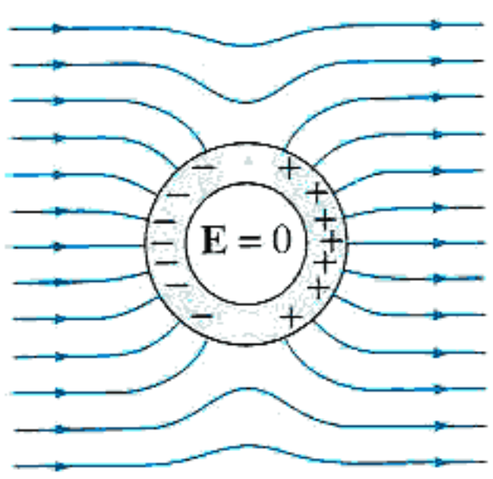

Figure 1.43 Metallic shell in an electrostatic field – Faraday cage.

Let us consider again the metallic sphere in the external electrostatic field shown in Fig. 1.40. Because there is no field throughout the sphere interior, we can remove it, without affecting the field outside the sphere. We thus obtain a domain with no field, bounded by a metallic shell (Fig. 1.43). This means that the space inside the shell cavity is perfectly protected (isolated) from the external electrostatic field. The thickness of the shell can be arbitrary, and its shape does not need to be spherical. Hence, an arbitrary closed conducting shell represents a perfect electrostatic shield or screen for its interior domain. We call such a shield a Faraday cage. If the field outside the cage is changed, the charge on the cage walls will redistribute itself so that the field inside will remain zero.

We see that a Faraday cage provides an absolute protection to its interior from an external electrostatic field. Let us now reverse the problem. Can an electrostatic field be encapsulated by a metallic shell so that the domain outside the shell is protected from the sources inside it? The answer to this important question is twofold. Let us get to it by analyzing two simple examples.

Consider first a single positive point charge Q positioned arbitrarily inside an uncharged spherical conducting shell. The distribution of induced charges on the shell surfaces and the field lines are sketched in Fig. 1.44(a). The total induced charges on the inner and outer shell surfaces are $-Q$ and Q, respectively (see

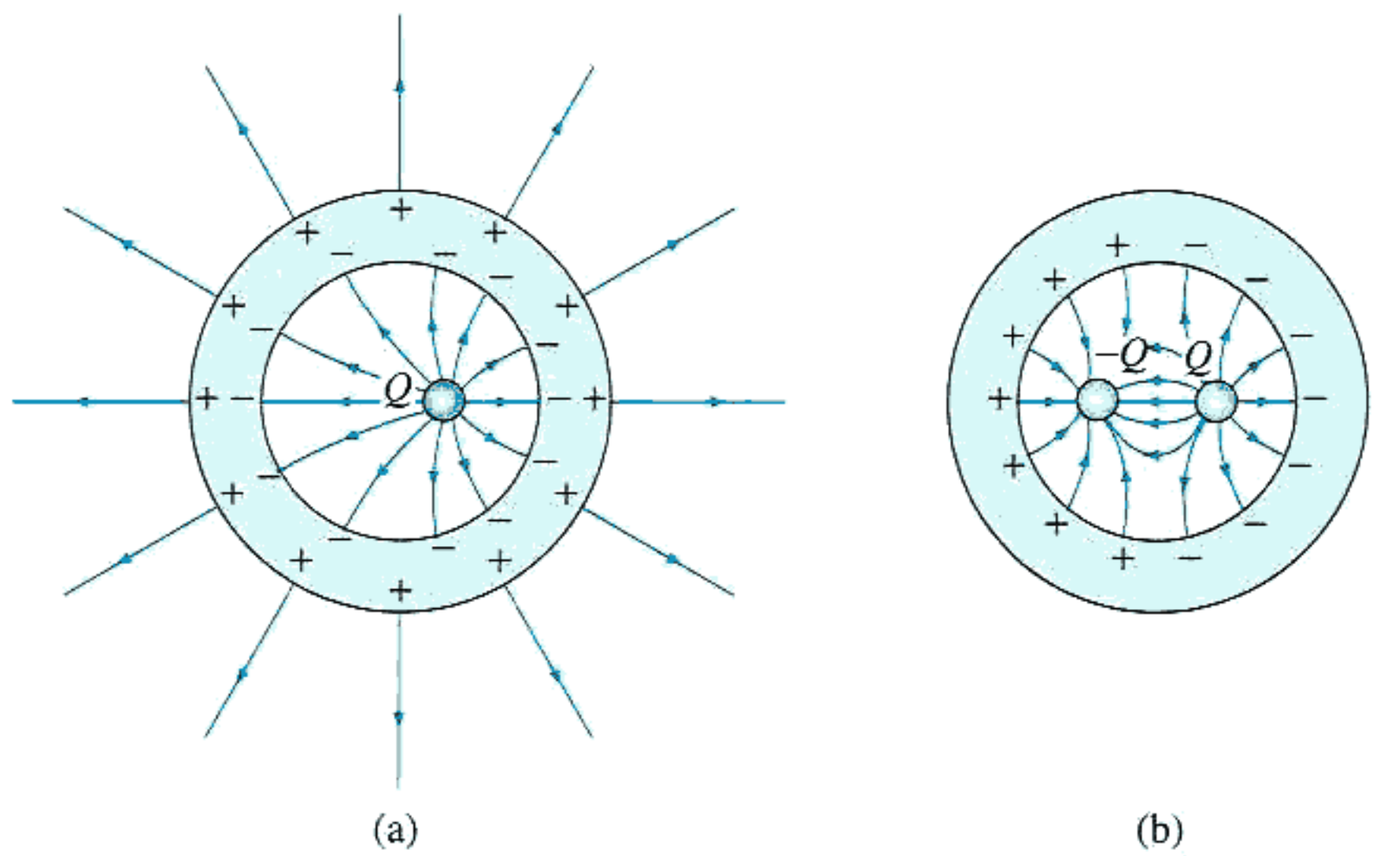

Figure 1.44 Single point charge (a) and two point charges amounting to a zero total charge (b) in a Faraday cage.

Example 1.27). The concentration of induced negative charges is higher on the side of the inner surface closer to the point charge. Because there is no field in the shell wall, the positive charge on the outer shell surface is distributed irrespective of the position of the point charge inside the cavity, which means uniformly in this case (the surface is smooth and symmetrical).

Let us now add another point charge in the cavity, and let it be exactly $-Q$, as shown in Fig. 1.44(b). The total negative and total positive induced charges on the inner surface of the shell are both less than Q in magnitude, because some field lines originating at the positive point charge end at the negative one inside the cavity, but mutually they are equal in magnitude and opposite in polarity. The net induced charge on the inner surface is therefore zero, implying that there is no charges whatsoever on the outer shell surface. This means, in turn, that there is no field outside the shell, which is also in agreement with Gauss' law, applied to a spherical surface enclosing the shell.

We conclude that a Faraday cage can completely encapsulate an interior electrostatic field, with a zero field outside, only if the total charge inside the cage is zero. This is true for any interior charge distribution, provided that the object or the system of objects (devices) inside the cage is electrically neutral (uncharged) as a whole. In cases when the total interior charge is not zero, the exterior domain (and neighboring objects) is in the field of induced charges on the outer surface of the cage. The exterior field, however, is totally independent of the distribution of interior sources. Its relative distribution in space depends only on the shape of the outer cage surface, whereas its absolute values at individual points in space are also proportional to the total amount of interior charge.

It is interesting to note that even very thin metallic shells represent ideal electrostatic shields, either in the mode of operation illustrated in Fig. 1.43 or in the one illustrated in Fig. 1.44(b). However, as we shall see in a later chapter, this is not necessarily the case with time-varying fields, where the effectiveness of a shield of a given thickness depends on the metal conductivity and on the rate with which the field varies in time (that is, frequency in the case of time-harmonic fields).

Conceptual Questions (on Companion Website): 1.23 and 1.24.

1.19 CHARGE DISTRIBUTION ON METALLIC BODIES OF ARBITRARY SHAPES

In the general case of a charged metallic body of an arbitrary shape, the charge distribution over the body surface is not uniform. The determination of this distribution for a given body with nonsymmetrical and/or nonsmooth surface is a rather complex problem. In this section, we shall get some qualitative insight about how the charge is distributed over the surface of an arbitrarily shaped isolated conducting body, and in the next section we shall present a general numerical method for determining approximately the charge density function over conducting objects.

Consider a system composed of two charged metallic spheres of different radii, a and b, whose centers are a distance d apart, in free space. Let the spheres be connected by a very thin conductor, as shown in Fig. 1.45. Assume, for simplicity, that $d \gg a, b$, so that the electric potential of each sphere can be evaluated as if the other one were not present. In addition, we assume that the charge along the connecting conductor is zero, because the conductor is very thin, and ignore its influence on the field between the spheres. Therefore, the potentials of spheres are [see Example 1.25 and Eq. (1.141)]

$$V_a = \frac{Q_a}{4\pi\varepsilon_0 a} \quad \text{and} \quad V_b = \frac{Q_b}{4\pi\varepsilon_0 b}, \tag{1.206}$$

respectively, where Q_a and Q_b are the associated total charges of spheres. The spheres being galvanically connected together, and thus representing a single conducting body, which must be equipotential, Eq. (1.182), these potentials are the same,

$$V_a = V_b. \tag{1.207}$$

So, by equating the expressions in Eq. (1.206), we obtain

$$\frac{Q_a}{Q_b} = \frac{a}{b}. \tag{1.208}$$

Using Eq. (1.191), the sphere charges can be expressed in terms of the corresponding surface charge densities, with which Eq. (1.208) becomes

charge density ∝ surface curvature

$$\boxed{\frac{\rho_{sa}}{\rho_{sb}} = \frac{b}{a}}, \tag{1.209}$$

and, from Eq. (1.193), the corresponding relationship between the electric field intensities near the surfaces of spheres turns out to be

local field intensity ∝ surface curvature

$$\boxed{\frac{E_a}{E_b} = \frac{b}{a}}. \tag{1.210}$$

We see from Eqs. (1.209) and (1.210) that the charge is distributed between the two spheres in Fig. 1.45 in such a way that the surface charge density on and electric

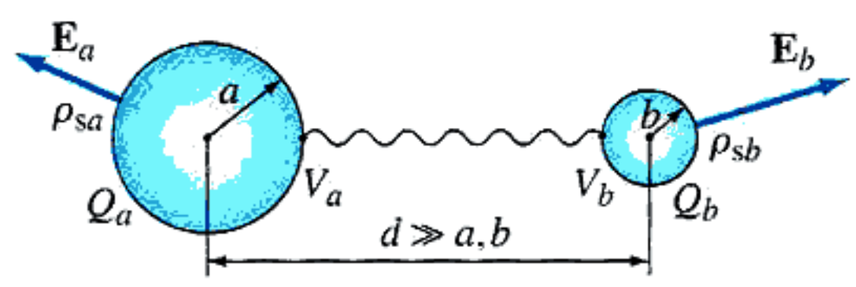

Figure 1.45 Two metallic spheres of different radii at the same potential.

field intensity near the surface of individual spheres is inversely proportional to the sphere radius. The surface charge is denser and the field stronger on the smaller sphere.

The importance of Eqs. (1.209) and (1.210) is much beyond the particular system in Fig. 1.45. They imply a general conclusion that the surface charge density and the nearby field intensity at different parts of the surface of an arbitrarily shaped conducting body are approximately proportional to the local curvature of the surface, as long as it is convex.[17] This means, generally, that the largest concentration of charge and the strongest electric field are around sharp parts of conducting bodies. Note that this phenomenon is essential for the operation of lightning arresters, as we shall see in the next chapter.

Problems: 1.83; *Conceptual Questions* (on Companion Website): 1.25–1.27.

1.20 METHOD OF MOMENTS FOR NUMERICAL ANALYSIS OF CHARGED METALLIC BODIES

Consider a charged metallic body of an arbitrary shape situated in free space. Let the electric potential of the body with respect to the reference point at infinity be V_0. Our goal is to determine the charge distribution of the body. The potential at an arbitrary point on the body surface, S, can be expressed in terms of the surface charge density, ρ_s, over the entire S [Eq. (1.83)]. On the other hand, this potential equals V_0 (the body is equipotential), and hence

$$\boxed{\frac{1}{4\pi\varepsilon_0}\int_S \frac{\rho_s\,\mathrm{d}S}{R} = V_0 \qquad \text{(at an arbitrary point on } S\text{).}} \tag{1.211}$$

surface integral equation for charge distribution

This is an integral equation with the function ρ_s over S as unknown quantity, to be determined.

Eq. (1.211) cannot be solved analytically – in a closed form, but only numerically, with the aid of a computer. The method of moments (MoM) is a common numerical technique used in solving integral equations such as Eq. (1.211) in electromagnetics and in other disciplines of science and engineering. MoM can be implemented in numerous ways, but the simplest MoM solution in this case implies subdivision of the surface S into small patches ΔS_i, $i = 1, 2, \ldots, N$, with a constant approximation of the unknown function ρ_s on each patch. That is, we assume that each patch is uniformly charged,

$$\boxed{\rho_s \approx \rho_{si} \quad (\text{on } \Delta S_i), \quad i = 1, 2, \ldots, N.} \tag{1.212}$$

piece-wise constant approximation for charge

With this approximation, we reduce Eq. (1.211) to its approximate form:

$$\sum_{i=1}^{N} \rho_{si} \int_{\Delta S_i} \frac{\mathrm{d}S}{4\pi\varepsilon_0 R} = V_0, \tag{1.213}$$

in which the unknown quantities are N charge-distribution coefficients, $\rho_{s1}, \rho_{s2}, \ldots, \rho_{sN}$. Shown in Fig. 1.46 is an example of the application of this method to a metallic

[17] If the surface of a conducting body is concave (curved inward), the effect is just opposite; for a deep incurvature, we actually have a partial effect of a Faraday cage (cavity), Fig.1.43, and a decrease of the local field intensity.

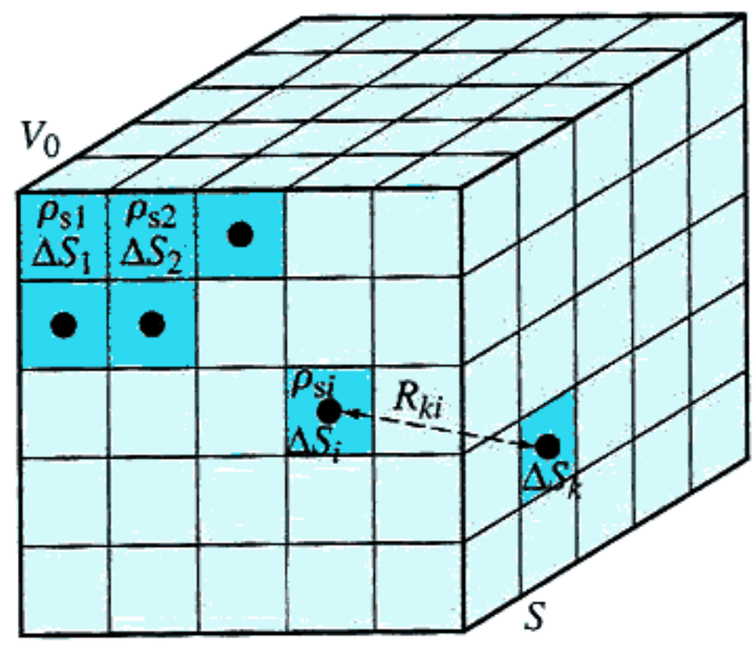

Figure 1.46 Method of moments (MoM) for analysis of charged metallic bodies: approximation of the surface charge distribution on a cube by means of N small square patches with constant charge densities.

cube, where square patches are used [for the particular subdivision shown in the figure, $N = 6 \times (5 \times 5) = 150$, which is a rather coarse model].

By stipulating that Eq. (1.213) be satisfied at centers of every small patch, individually, we obtain[18]

$$\begin{aligned} A_{11}\rho_{s1} + A_{12}\rho_{s2} + \cdots + A_{1N}\rho_{sN} &= V_0 \quad \text{(at the center of } \Delta S_1\text{)}, \\ A_{21}\rho_{s1} + A_{22}\rho_{s2} + \cdots + A_{2N}\rho_{sN} &= V_0 \quad \text{(at the center of } \Delta S_2\text{)}, \\ &\vdots \\ A_{N1}\rho_{s1} + A_{N2}\rho_{s2} + \cdots + A_{NN}\rho_{sN} &= V_0 \quad \text{(at the center of } \Delta S_N\text{)}. \end{aligned} \tag{1.214}$$

This is a system of N linear algebraic equations in N unknowns, $\rho_{s1}, \rho_{s2}, \ldots, \rho_{sN}$. In matrix form,

MoM matrix equation

$$\boxed{[A][\rho_s] = [B],} \tag{1.215}$$

where $[\rho_s]$ is a column matrix whose elements are the unknown charge-distribution coefficients, while elements of the column matrix $[B]$ are known and all equal V_0. Elements of matrix $[A]$, which is a square matrix, are given by

point-matching at centers of patches

$$\boxed{A_{ki} = \int_{\Delta S_i} \frac{\mathrm{d}S}{4\pi\varepsilon_0 R} \quad \text{(at the center of } \Delta S_k\text{)}, \quad k, i = 1, 2, \ldots, N,} \tag{1.216}$$

and they can be computed irrespective of the particular charge distribution. Physically, A_{ki} is the potential at the center of patch ΔS_k due to patch ΔS_i that is uniformly charged with unit (1 C/m^2) surface charge density. In the case of commonly used square or triangular flat patches, this potential can be evaluated analytically (exactly), while it is evaluated numerically (approximately) if some other surface elements are used (for example, curvilinear quadrilateral or triangular patches). Once matrix $[A]$ is filled, i.e., all its elements computed, we can use matrix inversion,

$$[\rho_s] = [A]^{-1}[B], \tag{1.217}$$

or any other standard method for solving systems of linear algebraic equations (e.g., Gaussian elimination method), to obtain the numerical results for the charge-distribution coefficients, which constitute an approximate surface charge distribution of the body, and a numerical solution to the integral equation, Eq. (1.211).

[18]The variant of the method of moments in which the left-hand side and the right-hand side of an integral equation [in our case, Eq. (1.211)] are "matched" to be equal at specific points of the definition domain of the equation (surface S in our case) is called the point-matching method. The idea of point-matching is similar to the concept of taking moments in mechanics, and hence the generic name method of moments.

The larger the number of subdivisions, N, the more accurate (but more computationally demanding in terms of computer resources) solution.

The crudest approximation in computing the elements of matrix $[A]$ is given by

$$A_{ki} = \begin{cases} \Delta S_i/(4\pi\varepsilon_0 R_{ki}) & \text{for } k \neq i \\ \sqrt{\Delta S_i}/(2\sqrt{\pi}\varepsilon_0) & \text{for } k = i \end{cases}. \tag{1.218}$$

Here, all nondiagonal elements of $[A]$ $(k \neq i)$ are evaluated by approximating the charged patch ΔS_i by an equivalent point charge, $\Delta Q_i = 1\ (\mathrm{C/m^2}) \times \Delta S_i$, placed at the patch center, and using the expression for the electric potential due to a point charge in free space, Eq. (1.80), with R_{ki} being the distance between centers of patches ΔS_k and ΔS_i (Fig. 1.46). In filling diagonal elements (self terms) of $[A]$ $(k = i)$, the potential due to a (square or triangular) patch ΔS_i at the center of that same patch is evaluated by approximating the patch by the equivalent circular patch of the same surface area and radius $\sqrt{\Delta S_i/\pi}$, and employing the potential expression given in Problem 1.34 with $z = 0$ and $\rho_s = 1\ \mathrm{C/m^2}$.

Starting from the result for $[\rho_s]$, we can now obtain any other quantity of interest (potential and field at any point in space, etc.). For instance, the total charge of the body can be found using the approximate version of the surface integral expression in Eqs. (1.29):

$$Q = \sum_{i=1}^{N} \rho_{si} \Delta S_i. \tag{1.219}$$

Problems: 1.84–1.86; *MATLAB Exercises* (on Companion Website).

1.21 IMAGE THEORY

Often, electrostatic systems include charge configurations in the presence of grounded conducting planes. Examples are charged conductors near grounded metallic plates or large flat bodies, transmission lines in which one of the conductors is a ground plane (such as microstrip transmission lines), various charged objects (power lines, charged clouds, charged airplanes, lightning rods, etc.) above the earth's surface, and so on. There is a very useful theory (theorem) by means of which we can remove the conducting plane from the system, and replace it by the equivalent charge distribution in free space. In this section, we shall derive this theorem, and apply it to problems which otherwise could not be analytically solved.

Consider two point charges of equal magnitudes and opposite polarities, Q and $-Q$, in free space. By symmetry, the total electric field intensity vector due to the charges is normal to the plane of symmetry of the charges (the tangential components due to individual charges are of equal magnitudes and opposite directions, so they cancel each other out), as shown in Fig. 1.47(a). The plane of symmetry is equipotential, and at the potential $V = 0$ (the potentials due to individual charges are of the same magnitudes and opposite signs, and they cancel out). Hence, nothing will change in the entire space if we insert an infinite grounded metallic foil (conducting plane) in the plane of symmetry, as is done in Fig. 1.47(b), because the boundary condition in Eq. (1.186) is automatically satisfied and $V = 0$ over the plane of symmetry (the foil is grounded). In the new system, surface charges will be induced on both sides of the foil, according to Eq. (1.190). We note that the foil actually separates the entire space onto two completely independent half-spaces, i.e., it

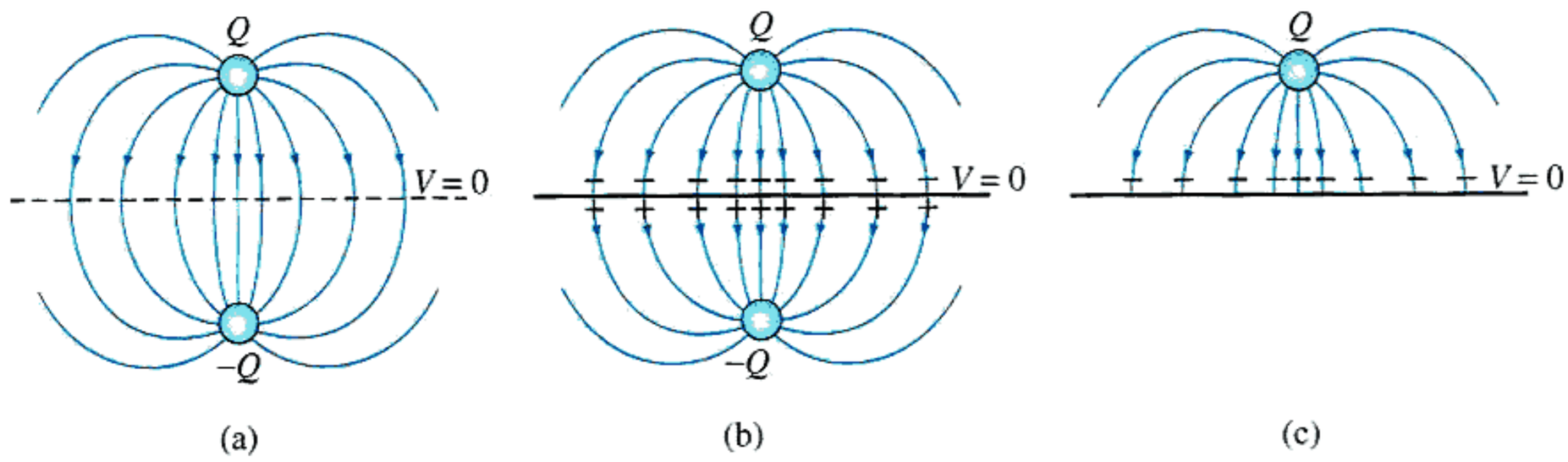

Figure 1.47 Deriving image theory: systems (a), (b), and (c) are equivalent with respect to the electric field in the upper half-space.

acts as a perfect electrostatic screen (see Section 1.18) between the two half-spaces. Because of that, nothing will change in the upper half-space if we, furthermore, remove the point charge $-Q$ and the induced charge on the lower side of the foil from the system. (Note that we can put whatever we want below the foil, and the field above it will remain the same, in the electrostatic state.) We are thus left with the point charge Q above the foil and the induced charge on its upper side (and nothing in the lower half-space), as depicted in Fig. 1.47(c).

We conclude that, as far as the electrostatic field in the upper half-space is concerned, systems in Figs. 1.47(a) and (c) are equivalent. This is so-called image theory, which, generalized to more than one point charge, i.e., to a (discrete or continuous) charge distribution, states that an arbitrary charge configuration above an infinite grounded conducting plane can be replaced by a new charge configuration in free space consisting of the original charge configuration itself and its negative image in the (former) conducting plane. The equivalence is with respect to the electric field above the conducting plane, whose component due to the induced charge on the plane is equal to the field of the image.

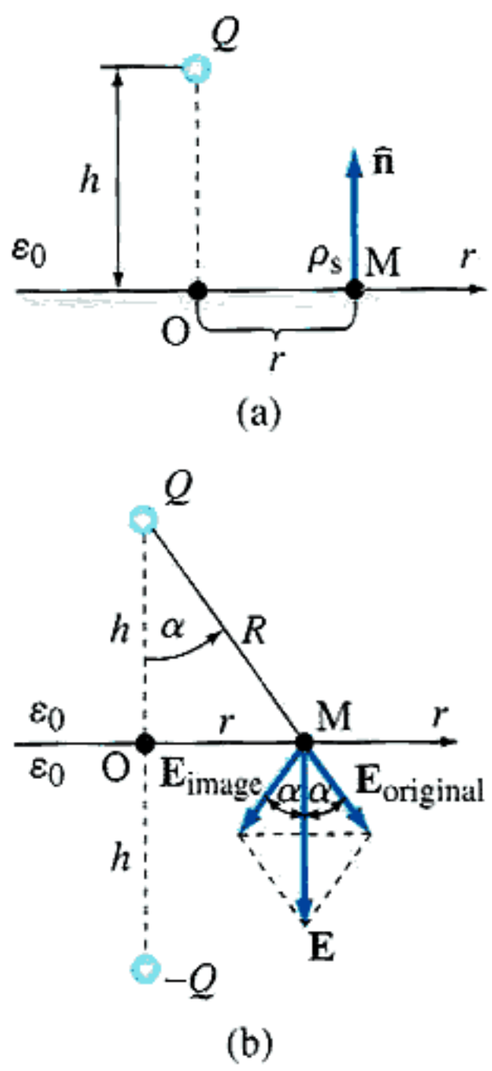

Figure 1.48 Computation of the induced surface charge density, ρ_s, on a conducting plane underneath a point charge Q: (a) original system and (b) equivalent system using image theory; for Example 1.29.

Example 1.29 Induced Charge Distribution on a Conducting Plane

A point charge Q is placed in air at a height h above a grounded conducting plane. (a) Determine the density of induced surface charges at an arbitrary point on the plane. (b) Find the total induced charge on the plane.

Solution

(a) The surface charge density ρ_s at a point M on the conducting plane, in Fig. 1.48(a), is given by Eq. (1.190), with the unit vector $\hat{\mathbf{n}}$ being vertical and directed from the plane upward, and $\mathbf{E}$ representing the electric field intensity vector in air, at a point that is "glued" to the point M from its upper side. This field is produced by the point charge Q and the induced surface charges on the conducting plane. According to the image theory, however, the field due to the induced charges equals that due to the negative image of Q in free space, as shown in Fig. 1.48(b). Let the position of the point M be defined by a radial distance r from the projection of Q on the plane (point O). Vector $\mathbf{E}$ is given by

$$\mathbf{E} = \mathbf{E}_{\text{original}} + \mathbf{E}_{\text{image}} = 2E_Q \cos\alpha\ (-\hat{\mathbf{n}}),$$

$$E_Q = \frac{Q}{4\pi\varepsilon_0 R^2}, \quad R = \sqrt{r^2 + h^2}, \quad \cos\alpha = \frac{h}{R}, \tag{1.220}$$

and the charge density comes out to be

$$\rho_s(r) = \varepsilon_0 \hat{\mathbf{n}} \cdot \mathbf{E} = -\frac{Qh}{2\pi\left(r^2 + h^2\right)^{3/2}}. \tag{1.221}$$

(b) The total induced charge on the conducting plane is

$$Q_{\text{ind}} = \int_S \rho_s(r) \underbrace{2\pi r\,\mathrm{d}r}_{\mathrm{d}S} = -Qh \int_{r=0}^{\infty} \frac{r\,\mathrm{d}r}{R^3} = -Qh \int_{r=0}^{\infty} \frac{\mathrm{d}R}{R^2} = Qh \frac{1}{R}\bigg|_{r=0}^{\infty} = -Q, \tag{1.222}$$

where $\mathrm{d}S$ is the surface area of an elemental ring of width $\mathrm{d}r$ and radius r $(0 \le r < \infty)$ around the point O (see Fig. 1.14), and the use is made of Eq. (1.62) to change variables in integration. The result in Eq. (1.222) is expected, because all field lines terminating on the image, $-Q$, in the equivalent system [(Fig. 1.48(b)] terminate on the surface charges of the conducting plane in the original system [Fig. 1.48(a)].

Example 1.30 Infinite Line Charge above a Conducting Plane

An infinite line charge of uniform density Q' is situated in air and is parallel to a grounded conducting plane at a distance h from it. Compute the electric force on the line charge per unit of its length.

Solution Under the influence of the electric field of the line charge, surface charges are induced on the conducting plane. The electric force on each meter of the line charge is therefore [Eq. (1.68)]

$$\mathbf{F}'_e = Q'\mathbf{E}_2, \tag{1.223}$$

where $\mathbf{E}_2$ represents the electric field vector at points along the line charge due to the induced charges on the plane. By image theory, this field is equal to the field due to a line charge in free space obtained as a negative image of Q', Fig. 1.49, and hence the following for its intensity [see Eq. (1.57)] and the per-unit-length force:

$$E_2 = \frac{Q'}{2\pi\varepsilon_0(2h)} \quad \longrightarrow \quad F'_e = Q'E_2 = \frac{Q'^2}{4\pi\varepsilon_0 h} \tag{1.224}$$

(the distance between the original and the image is $2h$). The force is attractive. –

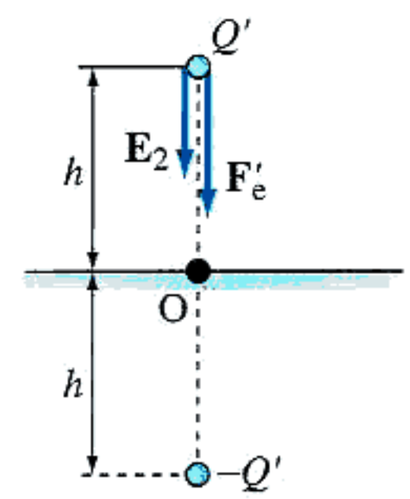

Figure 1.49 Force on a line charge above a conducting plane; for Example 1.30.

Problems: 1.87–1.89; *Conceptual Questions* (on Companion Website): 1.28–1.30; *MATLAB Exercises* (on Companion Website).

Problems

1.1. Three unequal charges in a triangle. Repeat Example 1.1 but assuming that one of the three charges in Fig. 1.3(a) amounts to (a) $3Q$ and (b) $-3Q$, respectively.

1.2. Three charges in equilibrium. The distance between point charges $Q_1 = 36$ pC and $Q_2 = 9$ pC is $D = 3$ cm. If the third charge, Q_3, is placed at the line connecting Q_1 and Q_2, at a distance d from Q_1, as shown in Fig. 1.50, find Q_3 and d which ensure that all the charges in this system are in the electrostatic equilibrium, i.e., that the resultant Coulomb force on each charge is zero.

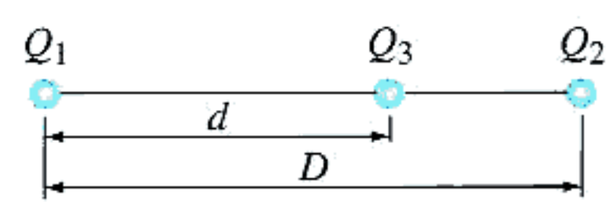

Figure 1.50 Three point charges along a line; for Problem 1.2.

1.3. Four charges at rectangle vertices. Four small charged bodies of equal charges $Q = -1$ nC are placed at four vertices of a rectangle with sides $a = 4$ cm and $b = 2$ cm. Determine the direction and magnitude of the electric force on each of the bodies.

1.4. Five charges in equilibrium. Four small charged balls of equal charges $Q_1 = 5$ pC are positioned at four vertices of a square, whereas the fifth ball of unknown charge Q_2 is at the square center. Find Q_2 such that all the balls are in the electrostatic equilibrium.

1.5. Three point charges in space. (a) For the three charges from Example 1.3, find the resultant electric force on the charge Q_2 ($\mathbf{F}_{e2}$). (b) Determine the force $\mathbf{F}_{e3}$ (on Q_3). (c) What is the sum of all the three forces, $\mathbf{F}_{e1} + \mathbf{F}_{e2} + \mathbf{F}_{e3}$?

1.6. Five charges at pyramid vertices. Four point charges Q are positioned in air at the corners of the square base of a pyramid. A fifth charge $-Q$ is positioned at the top vertex of the pyramid. All sides of the pyramid have the same length, a. Compute the electric force on the top charge.

1.7. Eight charges at cube vertices. Eight small charged bodies of equal charges Q exist at the vertices of a cube with sides of length a, in free space. Find the magnitude and direction of the electric force on one of the charges.

1.8. Electric field due to three point charges in space. For the three charges from Example 1.3, determine the magnitude and direction of the electric field intensity vector at (a) the coordinate origin and (b) the point at the z-axis defined by $z = 100$ m.

1.9. Nonuniform volume charge in a cylinder. An infinitely long cylinder of radius a in free space is charged with a volume charge density $\rho(r) = \rho_0(a - r)/a$ $(0 \le r \le a)$, where ρ_0 is a constant and r the radial distance from the cylinder axis. Find the charge per unit length of the cylinder.

1.10. Nonuniform volume charge in a cube. A cube of edge length a in free space is charged over its volume with a charge density $\rho(x) = \rho_0 \sin(\pi x/a)$, $0 \le x \le a$, where ρ_0 is a constant and x is the normal distance from one of the cube sides. Compute the total charge of the cube.

1.11. Nonuniform surface charge on a disk. A surface charge is distributed in free space over a circular disk of radius a. The charge density is $\rho_s(r) = \rho_{s0} r^2/a^2$ $(0 \le r \le a)$, where r is the radial distance from the disk center, and ρ_{s0} is a constant. Obtain the total charge of the disk.

1.12. Nonuniform line charge along a rod. A rod of length l in air is charged with a line charge of density $Q'(x) = Q'_0[1 - \sin(\pi x/l)]$ $(0 \le x \le l)$, where Q'_0 is a constant and x is the length coordinate along the rod. Calculate the total charge of the rod.

1.13. Field maximum at the axis of a ring. (a) For the charged ring in Fig. 1.11, assume $Q > 0$, and find z for which the electric field intensity along the z-axis is maximum. (b) Plot the function $E_z(z)$, $-\infty < z < \infty$.

1.14. Point charge equivalent to a charged semicircle. Show that far away along the z-axis, the semicircular line charge in Fig. 1.12(a) is equivalent to a point charge with the same amount of charge located at the coordinate origin.

1.15. Charged contour of complex shape. Fig. 1.51 shows a contour consisting of two semicircular parts, of radii a and b $(a < b)$, and two linear parts, each of length $b - a$. The contour is situated in air and carries a charge Q uniformly distributed along its length. Compute the electric field intensity vector at the contour center (point O).

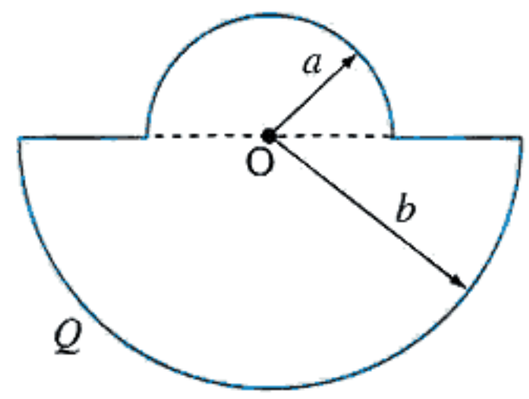

Figure 1.51 Uniformly charged contour with two semicircular and two linear parts; for Problem 1.15.

1.16. Nonuniform line charge along a semicircle. Consider the geometry in Fig. 1.12(a), and assume that the charge along the semicircle is nonuniform, given by $Q'(\phi) = Q'_0 \sin\phi$ $(-\pi/2 \le \phi \le \pi/2)$, where Q'_0 is a constant. (a) Find the total charge of the semicircle.

(b) Prove that the electric field intensity vector along the z-axis equals $\mathbf{E} = -Q'_0 a^2\,\hat{\mathbf{y}}/[8\varepsilon_0(z^2 + a^2)^{3/2}]$.

1.17. Line charge along three-quarters of a circle. A uniform line charge in the form of an arc that is 3/4 of a circle of radius a is situated in air. The total charge of the arc is Q. Calculate the electric field intensity vector at the arc center.

1.18. Line charge along a quarter of a circle. A charge of density Q' in free space is distributed uniformly along an arc representing a quarter of a circle of radius a. Determine the electric field intensity vector at an arbitrary point along the axis that contains the arc center and is normal to the arc plane.

1.19. Semi-infinite line charge. A line charge of uniform charge density Q' is distributed in free space along the negative part of the x-axis in the Cartesian coordinate system ($-\infty < x \leq 0$). Find the expression for the electric field intensity vector at an arbitrary point in the xy-plane.

1.20. Half-positive, half-negative infinite line charge. A line charge in free space is distributed along the x-axis in the Cartesian coordinate system. The line charge density is Q' ($Q' > 0$) for $-\infty < x \leq 0$ and $-Q'$ for $0 < x < \infty$. Derive the expression for the electric field intensity vector at a point M with coordinates $(0, d, 0)$, where $d > 0$.

1.21. Charged square contour. A line charge of uniform charge density Q' is distributed along a square contour a on a side. The medium is air. Find the electric field intensity vector at a point that is at a distance a from each of the square vertices.

1.22. Point charge equivalent to a charged disk. Consider the charged disk in Fig. 1.14, and show that for $|z| \gg a$, the $\mathbf{E}$ field in Eq. (1.63) is equivalent to the field of a point charge $Q = \rho_s \pi a^2$ placed at the disk center.

1.23. Field due to a nonuniformly charged disk. Consider the disk with a nonuniform charge distribution from Problem 1.11, and find the electric field intensity vector along the disk axis normal to its plane.

1.24. Nonuniformly charged spherical surface. A sphere of radius a in free space is nonuniformly charged over its surface such that the charge density is given by $\rho_s(\theta) = \rho_{s0} \sin 2\theta$, where ρ_{s0} is a constant and the angle θ ($0 \leq \theta \leq \pi$) is defined as in Fig. 1.10 or 1.16. Compute (a) the total charge of the sphere and (b) the electric field intensity vector at the sphere center.

1.25. Infinite charged sheet with a circular hole. An infinite sheet of charge with a constant density ρ_s has a hole of radius a in it. The sheet is in the xy-plane of the Cartesian coordinate system and the center of the hole is at the coordinate origin. The ambient medium is air. Under these circumstances, determine the electric field intensity vector at an arbitrary point along the z-axis – in the following two ways, respectively: (a) integrating the fields due to elementary rings as in Fig. 1.14 and (b) combining the results of Examples 1.11 (infinite sheet of charge, with no hole) and 1.10 (charged disk).

1.26. Force on a charged semicylinder due to a line charge. For the structure composed from a line charge and a charged semicylinder shown in Fig. 1.17(a) and described in Example 1.13, find the force per unit length on the semicylinder.

1.27. Charged strip. Consider an infinitely long uniformly charged strip of width a and surface charge density ρ_s in air. Using the geometrical representation of the cross section of the problem as in Fig. 4.11 in Chapter 4 (also see Fig. 1.13) and change of integration variables given by Eqs. (4.43) and (4.44), obtain the expression for the $\mathbf{E}$ field at an arbitrary point in space due to this charge.

1.28. Two parallel oppositely charged strips. Two parallel, very long strips are uniformly charged with charge densities ρ_s and $-\rho_s$, respectively ($\rho_s > 0$). The cross section of the structure is shown in Fig. 1.52. The width of the strips is the same as the distance between them ($a = d$), and the medium is air. Find the electric field

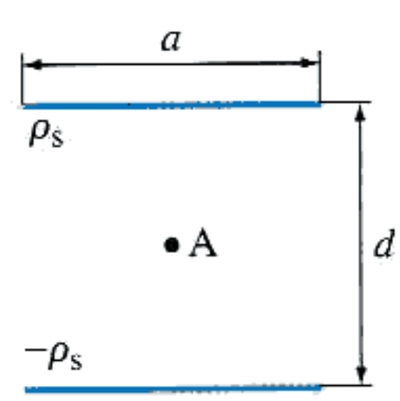

Figure 1.52 Cross section of two parallel, very long charged strips; for Problem 1.28.

intensity vector at the center of the cross section (point A).

1.29. Work in an electrostatic field. What is the work done by electric forces in moving a charge $Q = 1$ nC from the coordinate origin to the point (1 m, 1 m, 1 m) in the electrostatic field given by $\mathbf{E}(x, y, z) = (x\hat{\mathbf{x}} + y^2\hat{\mathbf{y}} - \hat{\mathbf{z}})$ V/m (x, y, z in m) in the Cartesian coordinate system along the straight line joining the two points?

1.30. Work in the field of a point charge. A point charge $Q_1 = 10$ nC is positioned at the center of a square contour $a = 10$ cm on a side, as shown in Fig. 1.53. Find the work done by electric forces in carrying a charge $Q_2 = -1$ nC from the point M_1 to the point M_2 marked in the figure.

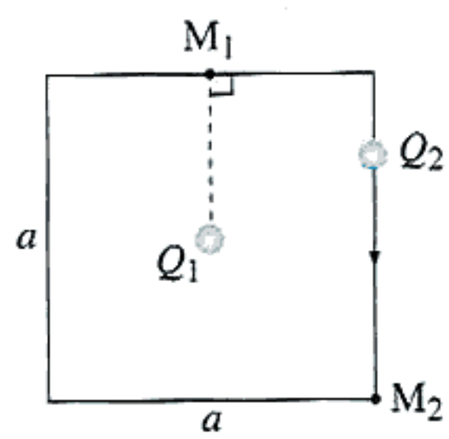

Figure 1.53 Movement of a charge Q_2 in the field of a charge Q_1 positioned at the center of a square contour; for Problem 1.30.

1.31. Electric potential due to three point charges in space. For the three charges from Example 1.3, calculate the electric potential at points defined by (a) (0, 0, 2 m) and (b) (1 m, 1 m, 1 m), respectively.

1.32. Point charge and an arbitrary reference point. Derive the expression for the potential at a distance r from a point charge Q in free space with respect to the reference point which is an arbitrary (finite) distance $r_{\mathcal{R}}$ away from the charge.

1.33. Potential due to a semicircular line charge. Prove that the electric scalar potential at an arbitrary point along the z-axis in the field of the semicircular line charge shown in Fig. 1.12(a) and described in Example 1.7 is $V = Q'a/(4\varepsilon_0\sqrt{z^2 + a^2})$.

1.34. Potential due to a charged disk. For the charged disk from Example 1.10, derive the following expression for the electric scalar potential along the z-axis ($-\infty < z < \infty$): $V = \rho_s(\sqrt{a^2 + z^2} - |z|)/(2\varepsilon_0)$.

1.35. Potential due to a hemispherical surface charge. Consider the hemispherical surface charge from Example 1.12, and find the electric scalar potential at the hemisphere center ($z = 0$).

1.36. Potential due to a nonuniform spherical surface charge. Determine the electric potential at the center of the nonuniformly charged spherical surface from Problem 1.24.

1.37. Voltage due to two point charges. Two point charges, $Q_1 = 7\ \mu$C and $Q_2 = -3\ \mu$C, are located at the two nonadjacent vertices of a square contour $a = 15$ cm on a side. Find the voltage between any of the remaining two vertices of the square and the square center.

1.38. Sketch field from potential. The electrostatic potential V in a region is a function of a single rectangular coordinate x, and $V(x)$ is shown in Fig. 1.54. Sketch the electric field intensity $E_x(x)$ in this region.

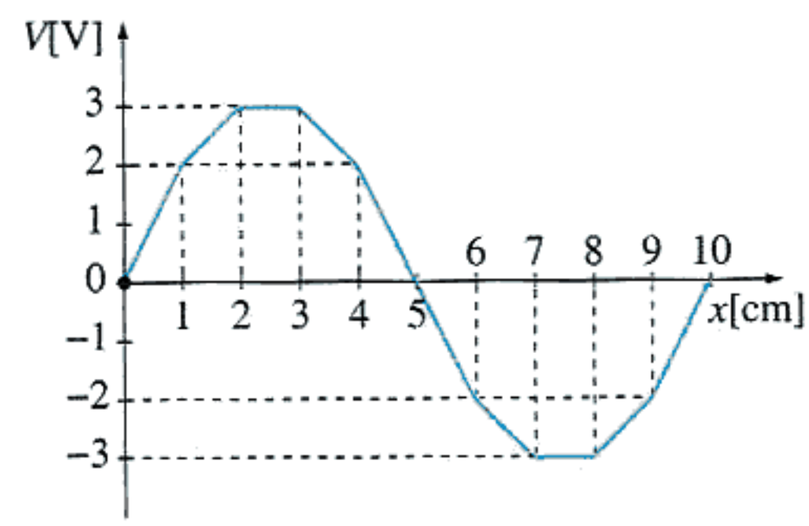

Figure 1.54 1-D potential distribution; for Problem 1.38.

1.39. Field from potential, point charge. For a point charge in free space, obtain the expression for $\mathbf{E}$ in Eq. (1.24) from the expression for V in Eq. (1.80).

1.40. Field from potential, charged semicircle. For the semicircular line charge from Example 1.7, (a) obtain the expression for E_z in Eq. (1.50) from the expression for V given in Problem 1.33 and (b) explain why it is impossible to obtain the expression for E_x in Eq. (1.48) from this same expression for V.

1.41. Field from potential, charged disk. For the charged disk from Example 1.10, obtain the expression for $\mathbf{E}$ in Eq. (1.63) from the expression for V given in Problem 1.34.

1.42. Field from potential, charged hemisphere. For the hemispherical surface charge from Example 1.12, explain why we cannot obtain the expression for **E** at the hemisphere center ($z = 0$), given in Eq. (1.67), from the expression for V computed in Problem 1.35.

1.43. Angle between field lines and equipotential surfaces. Using the concept of gradient, prove that in an arbitrary electrostatic field, field lines are perpendicular to equipotential surfaces (as in Fig. 1.22).

1.44. Direction of the steepest ascent. The terrain elevation in a region is given by a function $h(x, y) = 100x \ln y$ [m] (x, y in km), where x and y are coordinates in the horizontal plane and $1 \text{ km} \leq x, y \leq 10$ km. (a) What is the direction of the steepest ascent at (3 km, 3 km)? (b) How steep, in degrees, is the ascent in (a)?

1.45. Maximum increase in electrostatic potential. The electrostatic field intensity vector in a region is given by $\mathbf{E}(x, y, z) = (4\hat{\mathbf{x}} - z^2\hat{\mathbf{y}} + 2yz\hat{\mathbf{z}})$ V/m (x, y, z in m). Find the direction of the maximum increase in the electric scalar potential at a point (1 m, 1 m, −1 m).

1.46. Large and small electric dipole. Two point charges, $Q_1 = 1$ nC and $Q_2 = -1$ nC, are situated in free space at points along the z-axis defined by $z = 1$ m and $z = -1$ m, respectively. Compute the electric potential and field intensity vector at the point defined by Cartesian coordinates (a) (0, 0, 0), (b) (0, 1 m, 0), and (c) (100 m, 100 m, 100 m), respectively.

1.47. Potential and field due to a small electric dipole. An electric dipole with a moment $\mathbf{p} = 1$ pCm $\hat{\mathbf{z}}$ is located at the origin of a spherical coordinate system. The length of the dipole is $d = 1$ cm. Find V and **E** at the following points defined by spherical coordinates: (a) (1 m, 0, 0), (b) (1 m, $\pi/2$, $\pi/2$), (c) (1 m, π, 0), (d) (1 m, $\pi/4$, 0), (e) (10 m, $\pi/4$, 0), and (f) (100 m, $\pi/4$, 0).

1.48. Dipole equivalent to a nonuniform line charge. Consider the nonuniform line charge distribution along the semicircle from Problem 1.16, and show that far away along the z-axis ($|z| \gg a$) this charge distribution can be replaced by an equivalent electric dipole located at the coordinate origin. Find the moment, **p**, of the equivalent dipole.

1.49. Expression for the electric field due to a line dipole. For the line dipole in Fig. 1.29, obtain the expression for **E** from the expression for V in Eq. (1.121).

1.50. Near and far potential and field due to a line dipole. Two infinite line charges, with densities $Q_1' = 100$ pC/m and $Q_2' = -100$ pC/m, are positioned along lines defined by (1 m, 0, z) and (−1 m, 0, z), $-\infty < z < \infty$, in the Cartesian coordinate system. The medium is air. Calculate V and **E** at the point defined by Cartesian coordinates (a) (2 m, 0, 0) and (b) (100 m, 100 m, 0), respectively.

1.51. Flux of the electric field vector through a cube side. A point charge Q is located at the center of a cube in free space. The cube edges are a long. Find the outward flux of the electric field intensity vector due to this charge through each of the cube sides.

1.52. Flux for a different placement of the point charge. If the point charge Q from the previous problem is placed at the center of a side of the cube, determine the total outward flux of the electric field vector due to the charge through the surface composed of the remaining five sides of the cube.

1.53. Field of a point charge from Gauss' law. Using Gauss' law, derive the expression for the electric field intensity vector of a point charge in free space [Eq. (1.24)].

1.54. Uniformly charged thin spherical shell. An infinitely thin spherical shell of radius a in free space is uniformly charged over its surface with a total charge Q. Determine: (a) the electric field intensity vector inside and outside the shell, (b) the potential of the shell, and (c) the potential at the shell center.

1.55. Sphere with a nonuniform volume charge. Find the distribution of the electric scalar potential inside and outside the sphere with the volume charge density given by Eq. (1.32).

1.56. Field of an infinite line charge from Gauss' law. Using Gauss' law, derive the expression for the electric field intensity vector of an infinite line charge in free space [Eq. (1.57)].

1.57. Uniformly charged thin cylindrical shell. An infinitely long and infinitely thin cylindrical shell of radius a is situated in free space. The shell is charged over its surface with a uniform

charge density ρ_s. Find the electric field intensity vector inside and outside the shell.

1.58. Cylinder with uniform volume charge. Compute the voltage between the surface and the axis of a uniformly charged infinite cylinder of radius a in free space, if the volume charge density in the cylinder is ρ.

1.59. Field of an infinite sheet of charge from Gauss' law. Using Gauss' law, derive the expression for the electric field intensity vector of an infinite sheet of charge in free space [Eq. (1.64)].

1.60. Two parallel oppositely charged sheets. Two parallel infinite sheets of charge with densities ρ_s and $-\rho_s$ are situated in free space. (a) Find the electric field intensity vector inside and outside the space between the sheets. (b) What is the voltage between the sheets?

1.61. Equivalent sheet of charge. An infinitely large layer of charge in free space has a uniform volume charge density ρ and thickness d. (a) Compute the electric field vector inside the layer. (b) Show that, as far as the field outside the layer is concerned, the layer can be replaced by an equivalent infinite sheet of charge, and find the surface charge density, ρ_s, of this sheet.

1.62. Layer with a cosine volume charge distribution. The density of a volume charge in free space depends on the Cartesian coordinate x only and is given by $\rho(x) = \rho_0 \cos(\pi x/a)$ $(|x| \leq a)$ and $\rho(x) = 0$ $(|x| > a)$, where ρ_0 and a $(a > 0)$ are constants. (a) Determine the electric field intensity vector in the entire space. (b) Find the voltage between planes $x = -a$ and $x = a$.

1.63. Layer with a sine charge distribution. Repeat the previous problem but for the following charge density function: $\rho(x) = \rho_0 \sin(\pi x/a)$ for $|x| \leq a$ (there is no charge outside the layer).

1.64. Exponential charge distribution in the entire space. A volume charge distribution in free space is described in the rectangular coordinate system as $\rho(x) = \rho_0 \, e^{x/a}$ for $x < 0$, $\rho(0) = 0$, and $\rho(x) = -\rho_0 \, e^{-x/a}$ for $x > 0$, with ρ_0 and a being positive constants. Calculate the electric field intensity vector for $-\infty < x < \infty$.

1.65. Uniform electric field. In a certain region, there is a uniform electric field, $\mathbf{E}_0$. What is the volume charge density in that region?

1.66. Charge distribution from 1-D field distribution. Find the volume charge density $\rho(x)$ in the electrostatic system from Example 1.16, assuming that the permittivity of the medium is ε_0.

1.67. Charge from field, planar symmetry. From the field expressions in Eqs. (1.150)–(1.152), obtain the corresponding charge distribution in free space [Eq. (1.147)].

1.68. Charge from field, cylindrical symmetry. From the field with a radial cylindrical component only given by Eqs. (1.145) and (1.146), obtain the corresponding charge distribution in free space [Eq. (1.143)].

1.69. Charge from field, spherical symmetry. Using Gauss' law in differential form, show that the field with a radial spherical component only given by Eq. (1.140) is produced by a uniformly charged sphere of radius a and charge density ρ in free space.

1.70. Nonuniformly charged sphere using differential Gauss' law. For the nonuniform volume charge distribution in a sphere defined by Eq. (1.32) and analyzed in Problem 1.55 (based on Gauss' law in integral form), compute the electric field intensity vector everywhere using the differential Gauss' law.

1.71. Problem with cylindrical symmetry by differential Gauss' law. Redo Example 1.19 but with the use of Gauss' law in differential form.

1.72. Problem with planar symmetry using differential Gauss' law. Redo Problem 1.61 employing differential Gauss' law.

1.73. Antisymmetrical charge, differential Gauss' law. Redo Example 1.21 applying differential Gauss' law.

1.74. Gauss' law in differential and integral form. In a certain region, the electric field is given by $\mathbf{E} = (4xy\,\hat{\mathbf{x}} + 2x^2\,\hat{\mathbf{y}} + \hat{\mathbf{z}})$ V/m (x, y in m). The medium is air. (a) Calculate the charge density. (b) From the result in (a), find the total charge enclosed in a cube situated in the first coordinate octant ($x, y, z \geq 0$), with one vertex at the coordinate origin, and the edges, of length 1 m, parallel to coordinate axes. (c) Confirm the validity of Gauss' law in integral form and the divergence theorem by evaluating the net outward flux of $\mathbf{E}$ through the surface of the cube defined in (b).

1.75. Excentric charged sphere inside an uncharged shell. Consider the structure from Example 1.27, and assume that the sphere is moved toward the shell wall so that the centers of the sphere and the shell are separated by a distance d. Find the potential of the shell in the new electrostatic state if (a) $d = (b - a)/2$ and (b) $d = b - a$ (the sphere is pressed against the shell wall).

1.76. Point charge inside a charged shell. A point charge $2Q$ is placed at the center of an air-filled spherical metallic shell, charged with Q and situated in air. The inner and outer radii of the shell are a and b ($a < b$). (a) What is the total charge on the inner and on the outer surface of the shell, respectively? (b) Find the potential of the shell.

1.77. Three concentric shells, one uncharged. Three concentric spherical metallic shells are situated in air. The outer radius of the inner shell is $a = 30$ mm, and its charge $Q = 10$ nC. The inner and outer radii of the middle shell are $b = 50$ mm and $c = 60$ mm, and its potential $V = 1$ kV with respect to the reference point at infinity. The inner and outer radii of the outer shell are $d = 90$ mm and $e = 100$ mm, and it is uncharged. Calculate (a) the charge of the middle shell and (b) the voltage between the inner and the outer shell.

1.78. Three concentric shells, two at the same potential. Consider a structure with the same geometry as in the previous problem, and assume that the charges of the inner and outer shells are $Q_1 = 2$ nC and $Q_3 = -2$ nC, respectively, as well as that their potentials are the same ($V_1 = V_3$). Under these circumstances, compute (a) the charge of the middle shell (Q_2) and (b) the potentials of the inner and the middle shells (V_1 and V_2) with respect to the reference point at infinity.

1.79. Four coaxial cylindrical conductors. Four very long conductors, each in the form of a cylindrical shell with thickness $d = 1$ cm, are positioned in air coaxially with respect to each other, as indicated in Fig. 1.55, which shows a detail of the cross section of the system. The first and the fourth conductor are grounded, and the potential of the third conductor with respect to the ground is $V_3 = 1$ kV. The second conductor is uncharged. Find the charges per unit length of the first and the third conductor, Q_1' and Q_3'.

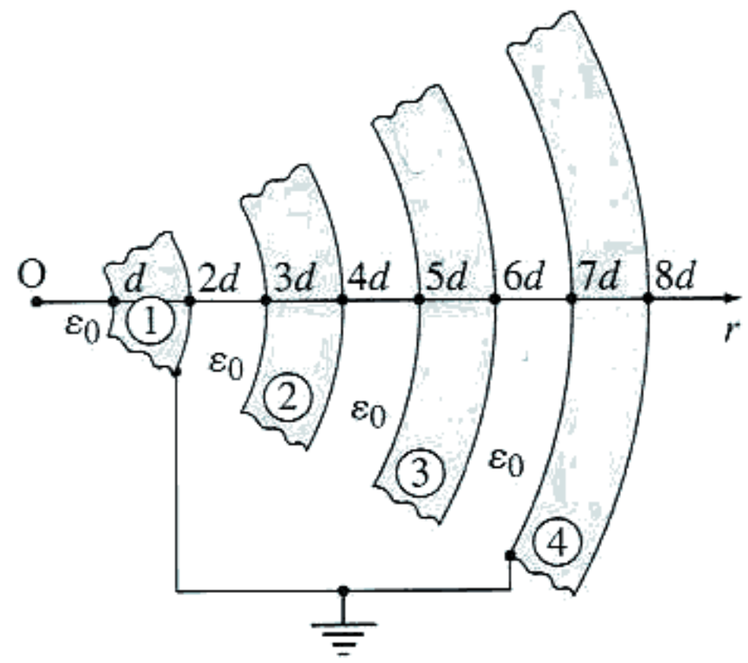

Figure 1.55 Detail of the cross section of a system of four cylindrical conductors; for Problem 1.79.

1.80. Three concentric conductors, one grounded. Shown in Fig. 1.56 is a system consisting of three concentric spherical conductors (the inner conductor is a solid sphere, while the remaining two are spherical shells). The radius of the inner conductor is $a = 2$ mm. The inner radius of the middle conductor is $b = 5$ mm, and outer $c = 6$ mm. The inner radius of the outer conductor is $d = 8$ mm. The space between the conductors is air-filled. The outer conductor is grounded, and the potentials of the inner and middle conductors with respect to the ground are $V_1 = 15$ V and $V_2 = 10$ V, respectively. Determine total charges of the inner and middle conductors, Q_1 and Q_2.

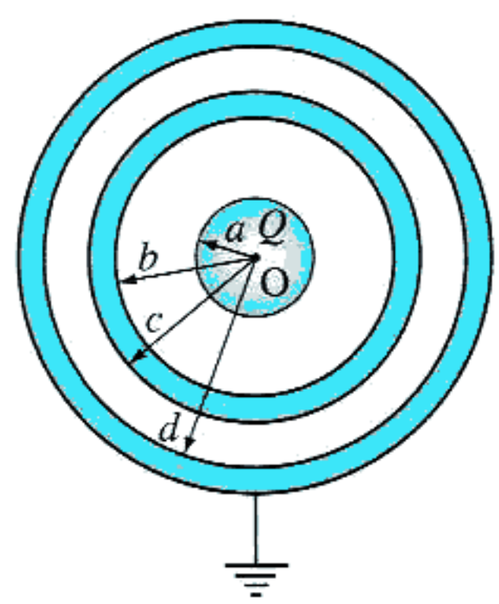

Figure 1.56 System of three concentric spherical conductors; for Problem 1.80.

1.81. Charged metallic foil. An infinitely large flat metallic foil is situated in air and charged uniformly with the surface charge density $\rho_s = 1$ nC/m^2. Find the electric field intensity vector everywhere.

1.82. Two metallic slabs. An infinitely large metallic slab of thickness $d = 1$ cm is situated in air and charged such that the surface charge density at each of the slab surfaces is $\rho_s = 1\ \mu C/m^2$. Another metallic slab of the same thickness, which is uncharged, is then introduced and placed parallel to the charged slab such that the distance between the surfaces of the two slabs facing each other is $D = 3$ cm. In the new electrostatic state, calculate (a) the surface charge densities at all four surfaces of the slabs, (b) electric field intensity vector everywhere, and (c) the voltage between the slabs.

1.83. Two metallic spheres at the same potential. Consider the system in Fig. 1.45, and assume that $a = 5$ cm, $b = 1$ cm, and $d = 1$ m, as well as that the total charge of the two spheres is $Q = 600$ pC. Find (a) the potential of the spheres and (b) the electric field intensities E_a and E_b near the surfaces of the spheres.

1.84. MoM-based computer program for a charged plate. Using the method of moments as presented in Section 1.20, write a computer program to determine the charge distribution on a very thin charged square plate of edge length a at a potential V_0, in free space. Subdivide the plate into N square patches, and assume that $a = 1$ m and $V_0 = 1$ V. (a) Tabulate and plot the results for the surface charge density (ρ_s) of the patches, taking $N = 100$ (ten partitions in each dimension). (b) Compute the total charge of the plate, taking (i) $N = 9$, (ii) $N = 25$, (iii) $N = 49$, and (iv) $N = 100$, respectively.

1.85. MoM computation for a charged cube. Write a computer program for the method-of-moments analysis of a charged metallic cube, Fig. 1.46, with edge length $a = 1$ m, and compute the total charge of the cube for $V_0 = 1$ V and ten, or as many as possible (given available computational resources), subdivisions per cube edge ($N = 600$ if ten subdivisions per edge are adopted).

1.86. Approximate integral expression for the electric field vector. (a) Write the approximate integral expression for the evaluation of the electric field intensity vector at an arbitrary point in space due to a charged body (e.g., the cube in Fig. 1.46), whose charge distribution is approximately described by Eq. (1.212). (b) Using the expression in (a) and the associated computer program, compute the electric field along the axis of the plate from Problem 1.84 perpendicular to its plane at points that are $a/2$, $2a$, and $100a$, respectively, distant from the plate surface (for $N = 100$). (c) Also compute the electric field inside the cube from the previous problem (Problem 1.85), at a quarter of its space diagonal (body diagonal) and at its center.

1.87. Force on a point charge due to its image. Find the electric force on the point charge Q in Fig. 1.48(a).

1.88. Imaging a line charge. For the structure defined in Example 1.30, determine the distribution of induced surface charges on the conducting plane.

1.89. Charged wire parallel to a corner screen. Fig. 1.57 shows a cross section of the structure consisting of a metallic wire of radius a and a 90° corner metallic screen in air. The distance of the wire from both the horizontal and vertical half-planes constituting the screen is h, where $h \gg a$. If the wire is charged with Q' per unit length, calculate the voltage between the wire and the screen.

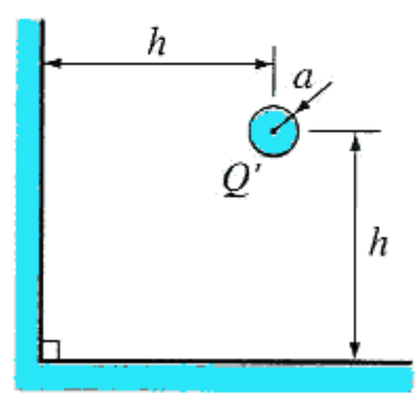

Figure 1.57 Cross section of a charged metallic wire parallel to a metallic corner screen; for Problem 1.89.

2 Dielectrics, Capacitance, and Electric Energy

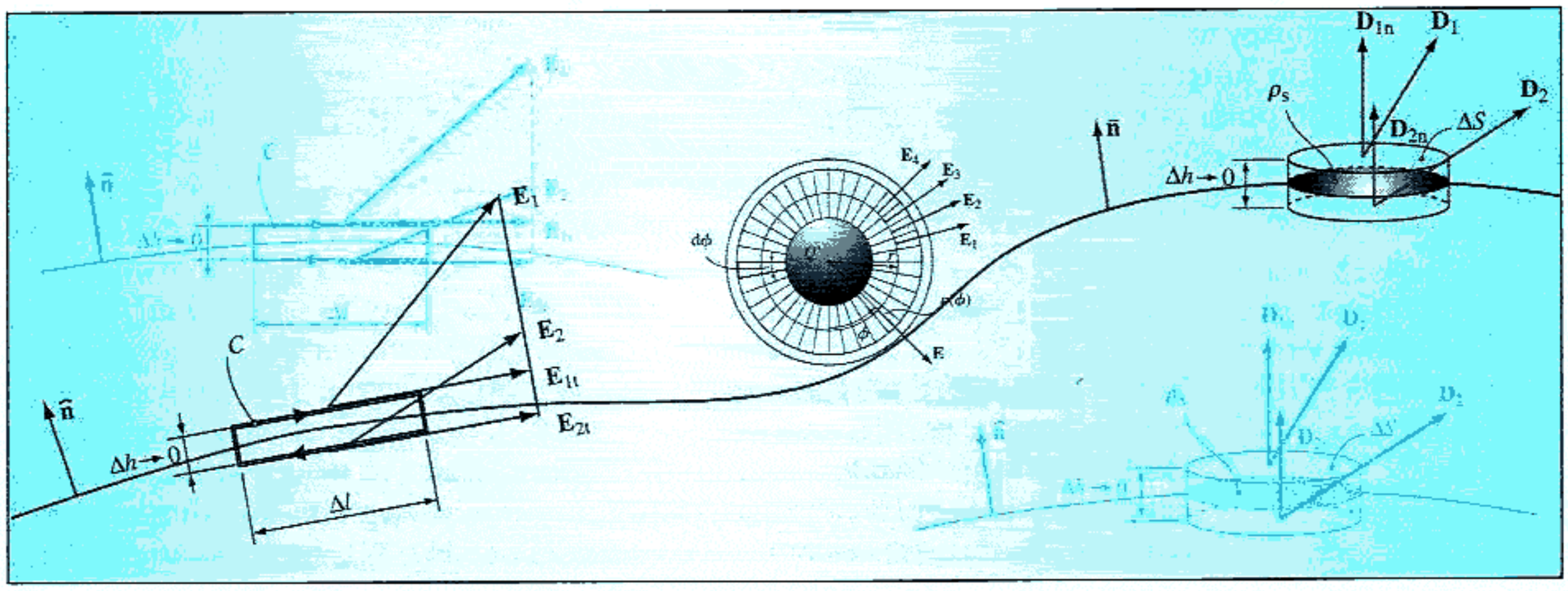

Introduction:

In this chapter, we shall analyze electrostatic fields in the presence of dielectrics and study several important related topics. Dielectrics or insulators are nonconducting materials, having very little free charges inside them (theoretically, perfect dielectrics have no free charges). In addition, redistribution of any free charges (e.g., electrons) deposited inside the material lasts much longer than in metallic conductors, a typical example, as already indicated in Section 1.16, being the charge rearrangement time of ~ 50 days for fused quartz compared to $\sim 10^{-19}$ s for copper. We shall see, however, that another type of charges, called bound or polarization charges, exist in a polarized dielectric. We shall first investigate the mechanisms of the polarization of dielectrics, caused by an external electric field. By introducing the macroscopic quantities such as the polarization vector, and the volume and surface density of bound charges, it is possible to evaluate the electric field intensity vector and the electric potential due to polarized dielectrics using free-space formulas and techniques from the previous chapter. Gauss' law will be generalized for an electrostatic system that includes arbitrary media (conductors and dielectrics), and characterization of dielectric materials in terms of their linearity, homogeneity, and isotropy will be presented. Dielectric-dielectric boundary conditions will be derived and used. The chapter will also introduce Poisson's and Laplace's second-order differential equations for the potential and their solution.

Having both conductors and dielectrics, we shall then put them together to form capacitors and related electrostatic systems. The capacitor is a fundamental element in electrical engineering. Its basic property is its capacitance. We shall analyze capacitors with electrodes of different shapes and with different types of dielectrics, and evaluate capacitance per unit length of various two-conductor

transmission lines as well. In addition, we shall evaluate the electric energy contained in charged capacitors, transmission lines, and other systems of conducting bodies, and introduce the electric energy density to help us find and quantify the localization and distribution of the energy in such systems. Dielectric breakdown, occurring for exceedingly strong electric fields in a dielectric material causing it to become conducting, will also be discussed for various electrostatic structures. We shall analyze structures with electric fields close to breakdown levels in order to predict critical values of voltages and other circuit quantities for the structure at breakdown. Such parameters (e.g., the breakdown voltage of a capacitor or a transmission line) define maximal permissible extents of quantities for the safe operation of the structure prior to an eventual breakdown.

The electrostatic analysis of capacitors and transmission lines, to determine their capacitance, energy, and breakdown characteristics, represents a culmination of the theory of the electrostatic field. It represents, on the other hand, a gateway to many practical applications of this theory. Finally, a clear understanding of concepts that will be presented in this chapter is essential for many similar, dual, and analogous concepts in other areas of electromagnetics, which are to be introduced later in the text.

2.1 POLARIZATION OF DIELECTRICS

Each atom or molecule in a dielectric is electrically neutral. For most dielectrics, centers of "gravity" of the positive and negative charges in an atom or molecule coincide – in the absence of the external electric field. When a dielectric is placed in an external field, of intensity $\mathbf{E}_{\text{ext}}$, however, the positive and negative charges shift in opposite directions against their mutual attraction, and produce a small electric dipole (Fig. 1.28), which is aligned with the electric field lines. The moment of this equivalent dipole is given by $\mathbf{p} = Q\mathbf{d}$ [Eq. (1.116)], where Q is the positive charge of the atom or molecule ($-Q$ is the negative charge), and $\mathbf{d}$ is the vector displacement of Q with respect to $-Q$. The charges are displaced from their equilibrium positions by forces

$$\mathbf{F}_{e1} = Q\mathbf{E}_{\text{ext}} \quad \text{and} \quad \mathbf{F}_{e2} = -Q\mathbf{E}_{\text{ext}}, \tag{2.1}$$

respectively, and thus Q shifts in the direction of $\mathbf{E}_{\text{ext}}$, while $-Q$ moves in the opposite direction, so that $\mathbf{p}$ and $\mathbf{E}_{\text{ext}}$ are collinear and have the same direction. The displacement $\mathbf{d}$ is very small, smaller than the dimensions of atoms and molecules. The charges Q and $-Q$ are bound in place by atomic and molecular forces and can only shift positions slightly in response to the external field. So, the two charges in an equivalent small dipole cannot separate one from the other and migrate across the material in opposite directions run by the electric field. Hence, these charges are called bound charges (in contrast to free charges).

Some dielectrics, such as water, have molecules with a permanent displacement between the centers of the positive and negative charge, so that they act as small electric dipoles even with no applied electric field. Such molecules are known as polar molecules, and the dielectrics are called polar dielectrics (those with no built-in dipoles are nonpolar dielectrics). In the absence of the electric field, all the dipoles are oriented in a random way. If a polar molecule, which we model by an electric dipole, is brought into an electric field, however, the forces on the two dipole charges, given in Eq. (2.1), act as indicated in Fig. 2.1. The torques (moments) of forces with respect to the center of the dipole (point O) are

$$\mathbf{T}_1 = \mathbf{r}_1 \times \mathbf{F}_{e1} \quad \text{and} \quad \mathbf{T}_2 = \mathbf{r}_2 \times \mathbf{F}_{e2}, \tag{2.2}$$

with $\mathbf{r}_1$ and $\mathbf{r}_2$ denoting the position vectors of Q and $-Q$ with respect to the dipole center. We notice that $\mathbf{r}_1 - \mathbf{r}_2 = \mathbf{d}$, and hence the resultant torque on the dipole turns out to be

$$\boxed{\mathbf{T}_{\text{on dipole}} = \mathbf{T}_1 + \mathbf{T}_2 = Q(\mathbf{r}_1 - \mathbf{r}_2) \times \mathbf{E}_{\text{ext}} = Q\mathbf{d} \times \mathbf{E}_{\text{ext}} = \mathbf{p} \times \mathbf{E}_{\text{ext}},} \tag{2.3}$$

torque on an electric dipole in an external electric field

where we assume that $\mathbf{E}_{\text{ext}}$ is practically uniform along the dipole. Vector $\mathbf{T}_{\text{on dipole}}$ is normal to the plane of $\mathbf{p}$ and $\mathbf{E}_{\text{ext}}$ (the plane of drawing in Fig. 2.1), and its magnitude amounts to

$$T_{\text{on dipole}} = |\mathbf{p} \times \mathbf{E}_{\text{ext}}| = p\, E_{\text{ext}} \sin\alpha. \tag{2.4}$$

We see that the torque given by Eq. (2.3) tends to rotate the dipole about the axis passing through the dipole center and being normal to the dipole and the plane of drawing, i.e., about the vector $T_{\text{on dipole}}$. The action of such torques in the dielectric is against random intermolecular thermic forces, and is to align the dipoles, to some extent, in the same direction – toward the field lines. We also see that the stronger the field, the larger $T_{\text{on dipole}}$, and the larger the component of the resultant dipole moment of all the molecules, $\sum \mathbf{p}$, along the direction of $\mathbf{E}_{\text{ext}}$. A sufficiently strong field may even produce an additional displacement between the positive and negative charges in a polar molecule, resulting in a larger p.

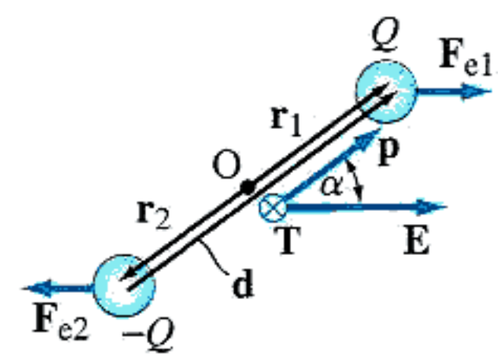

Figure 2.1 Polarization of polar dielectrics: model of a polar molecule in an external electric field.

We conclude that both an unpolar and polar dielectric in an electric field can be viewed as an arrangement of (more or less) oriented microscopic electric dipoles. The process of making atoms and molecules in a dielectric behave as dipoles and orienting the dipoles toward the direction of the external field is termed the polarization of the dielectric, and bound charges are sometimes referred to as polarization charges. This process is extremely fast, practically instantaneous, and the dielectric in the new electrostatic state is said to be polarized or in the polarized state. For almost all materials, the removal of the external electric field results in the return to their normal, unpolarized, state. A very few dielectrics, called electrets, remain permanently polarized in the absence of an applied electric field (an example is a strained piezoelectric crystal).

Conceptual Questions (on Companion Website): 2.1 and 2.2.

2.2 POLARIZATION VECTOR

When polarized (by an external electric field), a dielectric is a source of its own electric field, and the total field at an arbitrary point in space (inside or outside the dielectric) is a sum of the external (primary) field and the field due to the polarized dielectric (secondary field). To determine the secondary field, we replace the dielectric by a collection of equivalent small dipoles, which can be considered to be in a vacuum, as the rest of the material does not produce any field.

Theoretically, we could use the expression for the electric field due to an electric dipole, Eq. (1.117), and obtain the field due to a polarized dielectric by superposition. However, as many atoms or molecules in a dielectric body that many equivalent small dipoles in it, and, with the "microscopic" approach to the evaluation of the field due to the polarized dielectric, we would need to consider every single dipole, which is practically impossible [there is on the order of as many as 10^{30} atoms per unit volume (1 m^3) in solid and liquid dielectrics].

We rather adopt a "macroscopic" approach, and introduce a macroscopic quantity called the polarization vector to describe the polarized state of a dielectric and

the resulting field. We first average dipole moments in an elementary volume dv,

average dipole moment in an elementary volume of a polarized dielectric

$$\boxed{\mathbf{p}_{av} = \frac{\left(\sum \mathbf{p}\right)_{\text{in } dv}}{N_{\text{in } dv}},} \tag{2.5}$$

and then multiply this average by the concentration of dipoles (i.e., concentration of atoms or molecules in the dielectric), which equals

$$N_v = \frac{N_{\text{in } dv}}{dv}. \tag{2.6}$$

What we get is, by definition, the polarization vector:

polarization vector (unit: C/m^2)

$$\boxed{\mathbf{P} = N_v\, \mathbf{p}_{av} = \frac{\left(\sum \mathbf{p}\right)_{\text{in } dv}}{dv}.} \tag{2.7}$$

Note that $\mathbf{P}$ would represent the resultant dipole moment in a unit volume ($1\ m^3$) if it were polarized uniformly (equally) throughout the volume. Note also that

$$\mathbf{P}\, dv = \left(\sum \mathbf{p}\right)_{\text{in } dv} \tag{2.8}$$

is the dipole moment of an electric dipole equivalent to an element dv of the polarized dielectric, i.e., to all the dipoles within it.[1] The unit for $\mathbf{P}$ is C/m^2.

In any dielectric material, the polarization vector at a point is a function of the (total) electric field intensity vector at that point,

$$\mathbf{P} = \mathbf{P}(\mathbf{E}). \tag{2.9}$$

For linear (in the electrical sense) materials, this relationship is linear, i.e.,

χ_e - electric susceptibility of a linear dielectric

$$\boxed{\mathbf{P} = \chi_e \varepsilon_0 \mathbf{E},} \tag{2.10}$$

where χ_e is the electric susceptibility of the dielectric. It is a pure number, i.e., a dimensionless quantity, obtained by measurements on individual materials, and is always nonnegative ($\chi_e \geq 0$). For a vacuum, $\chi_e = 0$, whereas $\chi_e \approx 0$ for air.

2.3 BOUND VOLUME AND SURFACE CHARGE DENSITIES

We shall now derive the expressions for calculating the macroscopic distribution of excess bound charges in a polarized dielectric body from a given distribution of the polarization vector, $\mathbf{P}$, which, in turn, is obtained by averaging the microscopic dipoles in the dielectric material. These expressions will be used in the next section for free-space evaluations of the electric field due to polarized dielectrics.

Let us first find the total bound (polarization) charge Q_{pS} enclosed by an arbitrary imaginary closed surface S situated (totally or partly) inside a polarized dielectric body, as shown in Fig. 2.2. Knowing that bound charge actually consists of a vast collection of small electric dipoles, each dipole being composed from a

[1] An elementary volume dv, as we use it in macroscopic electromagnetic theory, is small in a physical sense, and cannot be infinitely small in a mathematical sense. Within the definition of the polarization vector, for instance, that means that dv is large enough to contain many small dipoles to be treated "on average," but yet sufficiently small so that $\mathbf{P}$ can be considered constant in dv from the macroscopic point of view. Such dv still contains a vast number (millions) of atoms or molecules.

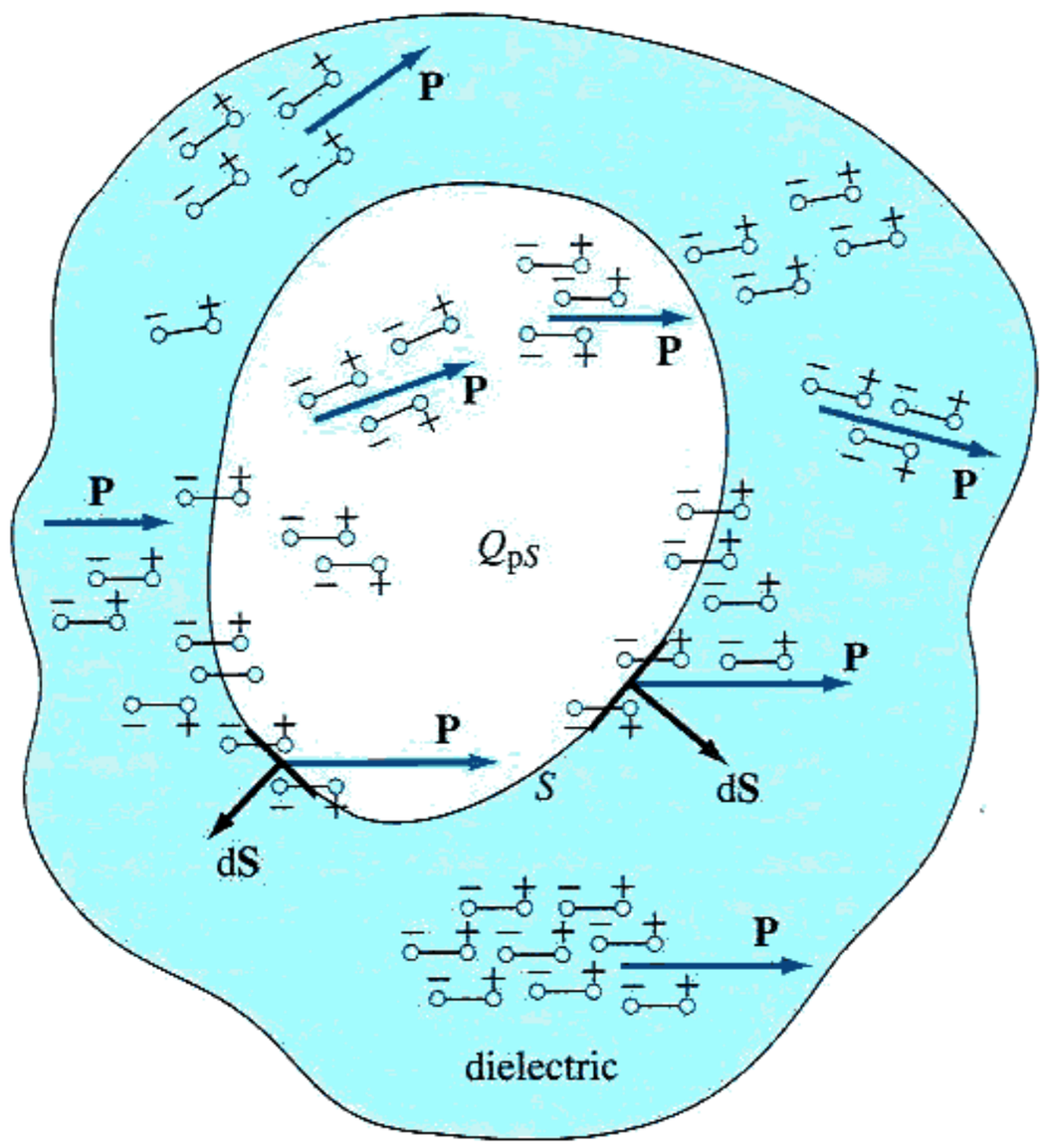

Figure 2.2 Closed surface S in a polarized dielectric body.

positive Q and a negative $-Q$, we realize that all the dipoles that appear inside S with both their ends, Q and $-Q$, as well as dipoles that are totally outside S, contribute with zero net charge to Q_{pS}. Only dipoles whose one end is inside S (and the other end outside S) contribute actually to the total bound charge in S. (We notice right away that $Q_{pS} = 0$ when S encloses the entire dielectric body.) To evaluate Q_{pS} (in the general case), we therefore count the dipoles that cross the surface S. In doing that, we count the contribution of such dipoles as either Q or $-Q$ (note that Q, generally, differ from dipole to dipole), by inspecting which end of the dipole is inside S.

Consider an element $\mathrm{d}S$ of S and the case when the angle α between the vector $\mathbf{P}$ (or vector $\mathbf{p}_{av}$) and vector $\mathrm{d}\mathbf{S}$, which is oriented from S outward, is less than 90°, as depicted in Fig. 2.3(a). Note that negative ends of dipoles that extend across $\mathrm{d}S$ with one (negative) end inside S are in a cylinder with bases $\mathrm{d}S$ and height

$$h = d\cos\alpha, \tag{2.11}$$

so that the number of these dipoles equals the concentration of dipoles, N_v, times the volume of the cylinder, $\mathrm{d}v = \mathrm{d}S\,h$. The dipole ends on the inner side of $\mathrm{d}S$ being all negative, and with an assumption that all dipoles in $\mathrm{d}v$ are with the same moments and charge, the corresponding bound charge is given by

$$\mathrm{d}Q_p = N_v\,\mathrm{d}S\,d\cos\alpha\,(-Q) \qquad (0 \le \alpha < 90°). \tag{2.12}$$

In the case when $\alpha > 90°$, portrayed in Fig. 2.3(b),

$$h = d\,\cos(\pi - \alpha) = d\,(-\cos\alpha), \tag{2.13}$$

and, because the ends of dipoles on the inner side of $\mathrm{d}S$ are all positive,

$$\mathrm{d}Q_p = N_v\,\mathrm{d}S\,d\,(-\cos\alpha)\,Q \qquad (90° < \alpha \le 180°), \tag{2.14}$$

which turns out to be the same result as in Eq. (2.12).

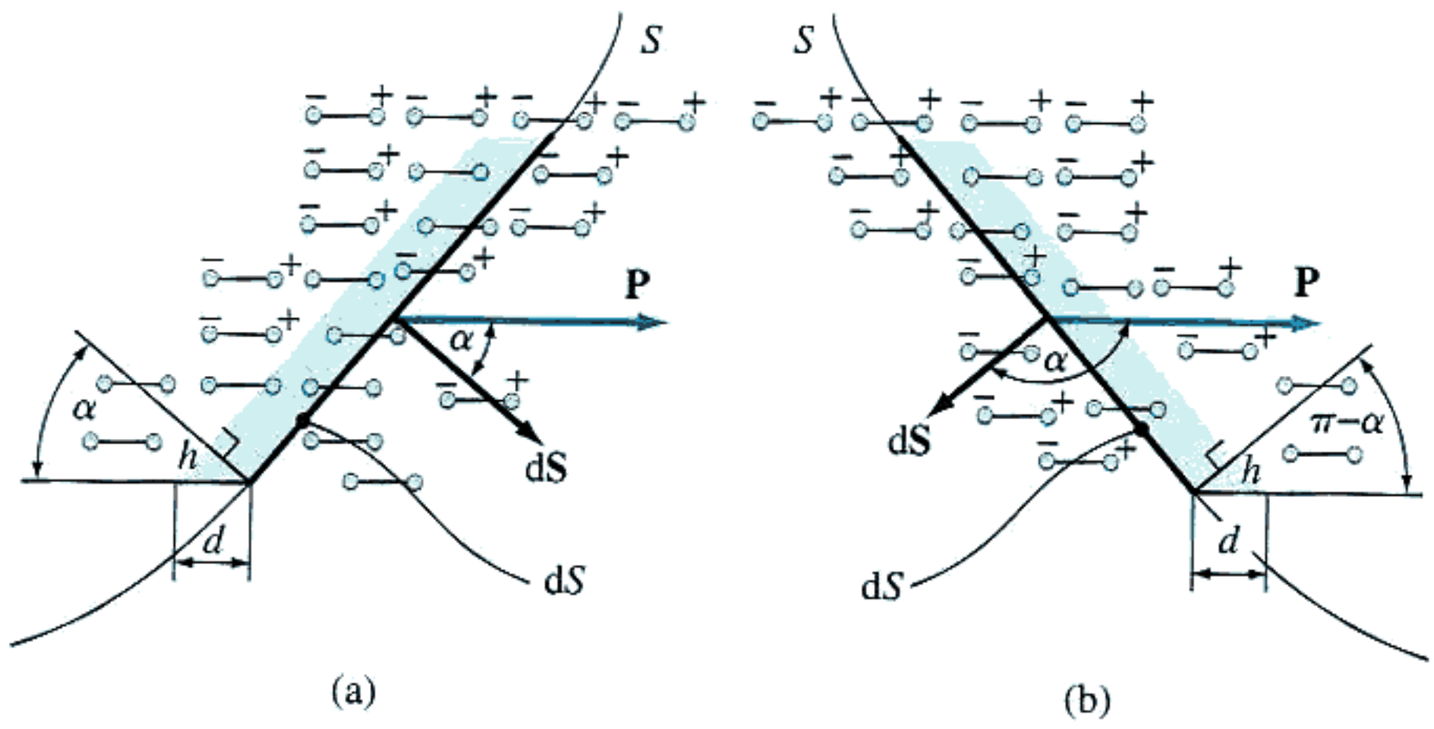

Figure 2.3 Element of surface S in Fig. 2.2, in two cases with regards to the angle α between $\mathbf{P}$ and $d\mathbf{S}$: (a) $0 \le \alpha < 90°$ and (b) $90° < \alpha \le 180°$.

For unpolar dielectrics, $\mathbf{p}_{av} = \mathbf{p}$, and $\mathbf{P} = N_v\mathbf{p} = N_v Q\mathbf{d}$. For polar dielectrics, where not all dipole moments are mutually parallel, we can consider the dipoles in small cylinders in Figs. 2.3(a) and (b) to be equivalent dipoles with moments $\mathbf{p}_{av} = Q\mathbf{d}$, so that $\mathbf{P} = N_v\mathbf{p}_{av} = N_v Q\mathbf{d}$. Hence, for an arbitrary α ($0 \le \alpha \le 180°$), we have

$$dQ_p = -N_v Q d\, dS \cos\alpha = -P\, dS \cos\alpha = -\mathbf{P}\cdot d\mathbf{S} \tag{2.15}$$

(note that the boundary case, $\alpha = 90°$ and $dQ_p = 0$, is also properly included in this formula). Finally, by integrating the result for dQ_p over the entire surface S, we obtain

total bound (polarization) charge enclosed by a closed surface S

$$\boxed{Q_{pS} = -\oint_S \mathbf{P}\cdot d\mathbf{S}.} \tag{2.16}$$

This is an integral equation similar in form to Gauss' law, Eq. (1.133). It tells us that the outward flux of the polarization vector through an arbitrary closed surface in an electrostatic system that includes dielectric materials is equal to the total bound (polarization) charge enclosed by that surface, multiplied by -1.

Eq. (2.16) is true for any closed surface S. Let us now apply it to the surface S enclosing an elementary volume Δv inside a polarized dielectric:

$$\frac{(Q_p)_{\text{in}\,\Delta v}}{\Delta v} = \frac{-\oint_S \mathbf{P}\cdot d\mathbf{S}}{\Delta v} \quad (\Delta v \to 0), \tag{2.17}$$

with both sides of the equation being also divided by Δv. The expression on the left-hand side of Eq. (2.17) represents the density of excess volume bound charge,

$$\rho_p = \frac{(Q_p)_{\text{in}\,\Delta v}}{\Delta v}, \tag{2.18}$$

while the expression on its right-hand side is, by definition [Eq. (1.172)], the negative of the divergence of the polarization vector. Hence,

bound volume charge density

$$\boxed{\rho_p = -\operatorname{div}\mathbf{P} = -\nabla\cdot\mathbf{P}.} \tag{2.19}$$

If $\mathbf{P} = \text{const}$ inside the dielectric (uniformly polarized dielectric), all spatial derivatives of $\mathbf{P}$ are zero, and using Eq. (2.19),

no volume bound charge in a uniformly polarized dielectric

$$\boxed{\mathbf{P} = \text{const} \quad \longrightarrow \quad \rho_p = 0.} \tag{2.20}$$

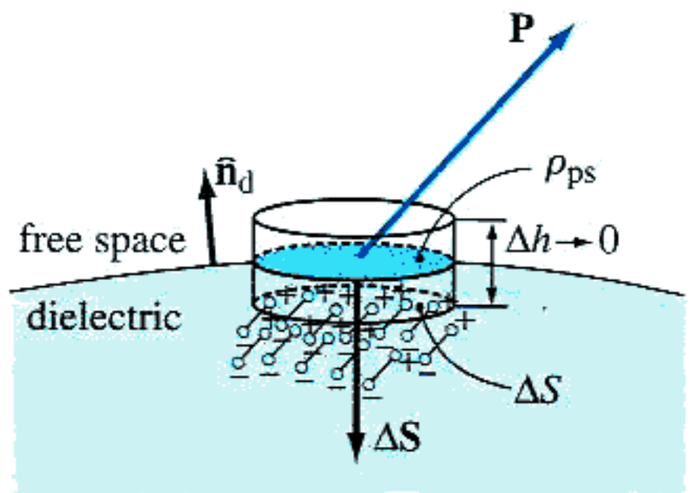

Figure 2.4 Elementary closed surface used for deriving the boundary condition for the vector **P** on a surface dielectric-free space, Eq. (2.23).

If $\mathbf{P} \neq$ const, however, then excess volume bound charge exists only if the polarization vector varies throughout the volume of the dielectric (nonuniformly polarized dielectric) in a way that its divergence is nonzero, otherwise $\rho_p = 0$.

On the surface of a polarized dielectric, there always exists excess surface bound charge (there are ends of dipoles pressed onto the surface that cannot be compensated by oppositely charged ends of neighboring dipoles), except on parts of the surface where **P** and the dipoles are tangential to the surface. To determine the associated bound (or polarization) surface charge density, ρ_{ps}, we apply Eq. (2.16) to a small pillbox surface, with bases ΔS and height Δh ($\Delta h \to 0$), shown in Fig. 2.4. There is no polarization in free space (a vacuum or air),

$$\boxed{\mathbf{P} = 0,} \tag{2.21}$$

no polarization in a vacuum or air

so that the flux of vector **P** in Eq. (2.16) is reduced to $\mathbf{P} \cdot \Delta\mathbf{S}$ over the lower side of S, and we have [also see the similar derivation in Eq. (1.188)]

$$\rho_{ps} \Delta S = -\mathbf{P} \cdot \Delta\mathbf{S}. \tag{2.22}$$

With $\hat{\mathbf{n}}_d$ denoting the normal unit vector oriented from the dielectric body outward, $\Delta\mathbf{S} = -\Delta S \hat{\mathbf{n}}_d$, which yields

$$\boxed{\rho_{ps} = \hat{\mathbf{n}}_d \cdot \mathbf{P}.} \tag{2.23}$$

bound surface charge density; $\hat{\mathbf{n}}_d$ outward normal on a dielectric surface

This is the boundary condition for the vector **P** on a surface dielectric-free space, connecting the polarization vector in the dielectric near the boundary surface and the bound surface charge density on the surface. Note that only the normal component of **P** contributes to ρ_{ps}.

Example 2.1 Nonuniformly Polarized Dielectric Cube

The polarization vector in a dielectric cube shown in Fig. 2.5 is given by

$$\mathbf{P}(x, y) = P_0 \frac{xy}{a^2} \hat{\mathbf{x}}, \tag{2.24}$$

where P_0 is a constant. The surrounding medium is air. Find the distribution of bound charges of the cube.

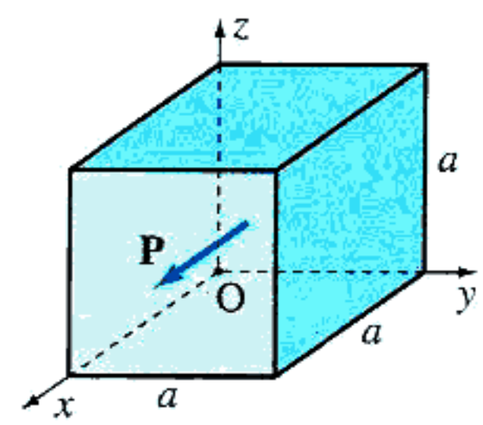

Figure 2.5 Dielectric cube with polarization $\mathbf{P}(x, y)$; for Example 2.1.

Solution Using Eqs. (2.19) and (1.167), the bound volume charge density inside the cube is

$$\rho_p = -\frac{\partial P_x}{\partial x} = -\frac{P_0 y}{a^2}, \tag{2.25}$$

whereas Eq. (2.23) tells us that bound surface charge exists on the front side of the cube only, and its density amounts to

$$\rho_{ps} = \hat{\mathbf{x}} \cdot \mathbf{P}(a^-, y) = \frac{P_0 y}{a}, \tag{2.26}$$

with $\mathbf{P}(a^-, y)$ denoting the polarization vector in the dielectric very close to the boundary surface at $x = a$. On the back side, $\rho_{ps} = 0$ since $P(0^+, y) = 0$, while on the remaining four sides $\rho_{ps} = 0$ because $\hat{\mathbf{n}}_d$ and $\mathbf{P}$ are mutually perpendicular.

Note that, with v designating the volume of the cube and S its boundary surface,

$$Q_p = \int_v \rho_p \, dv + \oint_S \rho_{ps} \, dS = \int_{y=0}^{a} \left(-\frac{P_0 y}{a^2}\right) a^2 \, dy + \int_{y=0}^{a} \frac{P_0 y}{a} a \, dy = 0, \tag{2.27}$$

as expected (the total bound charge of a dielectric body is always zero), where, in accordance with our general integration strategy explained in Section 1.4, dv is adopted to be a slice of the cube of thickness dy, and dS a strip of width dy on the front cube side.

Problems: 2.1.

2.4 EVALUATION OF THE ELECTRIC FIELD AND POTENTIAL DUE TO POLARIZED DIELECTRICS

In this section, we shall evaluate the electric field intensity vector and electric scalar potential due to polarized dielectric bodies in several characteristic cases. We assume that the state of polarization of a dielectric body is described by a given distribution of the polarization vector, $\mathbf{P}$, inside the body. From $\mathbf{P}$, using Eqs. (2.19) and (2.23), we first find the distribution of volume and surface bound charge densities, ρ_p and ρ_{ps}, throughout the body volume and over its surface, respectively. Then, we calculate the field $\mathbf{E}$ and potential V (and any other related quantity of interest) using the appropriate free-space formulas and equations [Eqs. (1.37), (1.38), (1.82), (1.83), (1.133), etc.] and solution techniques suitable to specific geometries and source distributions.

Example 2.2 Uniformly Polarized Dielectric Disk

A dielectric disk of radius a and thickness d is situated in free space. The disk is uniformly polarized throughout its volume, the polarization vector being normal to the disk bases and its magnitude being P. Find (a) the distribution of bound charges of the disk and (b) the electric field intensity vector at the disk center.

Solution

(a) Eq. (2.20) tells us that there is no bound volume charge inside the disk. According to Eq. (2.23) and Fig. 2.6, the bound surface charge densities on the upper and lower disk bases are

$$\rho_{ps1} = \hat{\mathbf{n}}_{d1} \cdot \mathbf{P} = P \quad \text{and} \quad \rho_{ps2} = \hat{\mathbf{n}}_{d2} \cdot \mathbf{P} = -P, \tag{2.28}$$

respectively, while on the side disk surface, $\rho_{ps3} = \hat{\mathbf{n}}_{d3} \cdot \mathbf{P} = 0$.

(b) The electric field due to the polarized disk equals the field due to two circular sheets of charge with densities ρ_{ps1} and ρ_{ps2} in free space. We use the expression for the field due to a circular sheet of charge (thin charged disk) in Eq. (1.63) and the superposition principle to add up the fields due to two sheets, $\mathbf{E}_1$ and $\mathbf{E}_2$. The charge densities are $\rho_s = \pm P$ and the distance from each sheet at the disk center (point O) is $d/2$, so the two fields are the same, and the total field comes out to be

$$\mathbf{E} = \mathbf{E}_1 + \mathbf{E}_2 = 2\mathbf{E}_1 = -\frac{P}{\varepsilon_0}\left[1 - \frac{d}{2\sqrt{a^2 + (d/2)^2}}\right]\hat{\mathbf{z}}. \tag{2.29}$$

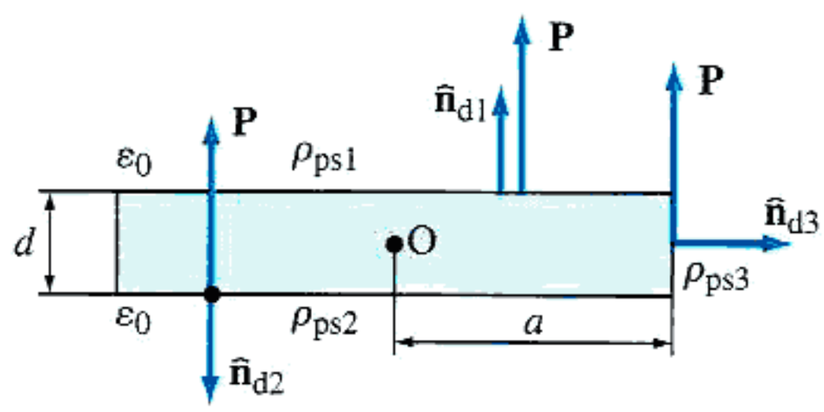

Figure 2.6 Bound surface charge on a uniformly polarized dielectric disk; for Example 2.2.

Example 2.3 Uniformly Polarized Dielectric Sphere

A dielectric sphere of radius a, in free space, is uniformly polarized, and the polarization vector is $\mathbf{P}$. Compute (a) the distribution of bound charge of the sphere, (b) the electric scalar potential at the sphere center, and (c) the electric field intensity vector at the sphere center.

Solution

(a) Let us adopt a spherical coordinate system with the origin at the sphere center and the z-axis parallel to the vector $\mathbf{P}$, as shown in Fig. 2.7. The bound volume charge density is $\rho_p = 0$. The bound surface charge density at a point M on the sphere surface, defined by the angle θ, is

$$\rho_{ps} = \hat{\mathbf{n}}_d \cdot \mathbf{P} = P \cos \angle(\hat{\mathbf{n}}_d, \mathbf{P}) = P \cos\theta, \qquad 0 \le \theta \le \pi. \tag{2.30}$$

We now replace the polarized sphere by a nonuniform spherical sheet of charge in free space, whose charge density is the function of θ given in Eq. (2.30), and compute V and $\mathbf{E}$ at the sphere center (point O) using free-space concepts and equations.

(b) From Eq. (1.83) and Fig. 2.7, the potential at the point O turns out to be

$$V = \frac{1}{4\pi\varepsilon_0} \oint_S \frac{\rho_{ps}\, dS'}{a} = \frac{1}{4\pi\varepsilon_0 a} \oint_S \rho_{ps}\, dS' = \frac{1}{4\pi\varepsilon_0 a} Q_p = 0, \tag{2.31}$$

because the total bound charge of the sphere, Q_p, is zero.

(c) Due to symmetry, vector $\mathbf{E}$ at the point O in Fig. 2.7 has a (negative) z-component only, which is computed essentially in the same way as in Fig. 1.16, subdividing the sphere surface into thin rings and integrating the fields $d\mathbf{E}$ due to individual rings, the only two differences being that the surface charge density is now a function of θ, Eq. (2.30), and

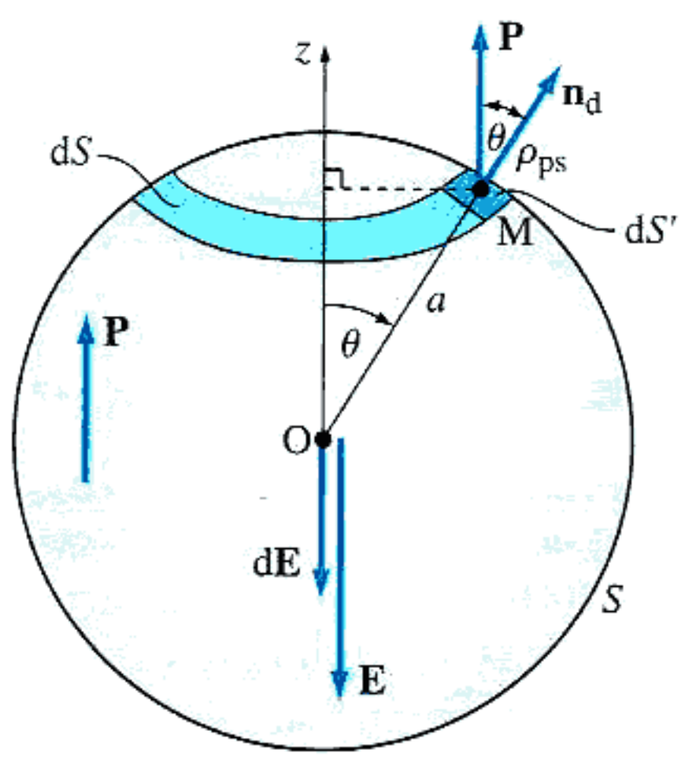

Figure 2.7 Dielectric sphere with a uniform polarization; for Example 2.3.

that the upper limit in the integration is now $\theta = \pi$. With this, Eq. (1.67) becomes

$$\mathbf{E} = \oint_S \mathrm{d}\mathbf{E} = -\frac{1}{2\varepsilon_0}\int_{\theta=0}^{\pi} \rho_{\mathrm{ps}}(\theta)\sin\theta\cos\theta\,\mathrm{d}\theta\,\hat{\mathbf{z}} = -\frac{P}{2\varepsilon_0}\int_0^{\pi} \underbrace{\cos^2\theta}_{u^2}\underbrace{\sin\theta\,\mathrm{d}\theta}_{-\mathrm{d}u}\,\hat{\mathbf{z}}$$

electric field inside a uniformly polarized dielectric sphere

$$= -\frac{P}{3\varepsilon_0}\hat{\mathbf{z}} \quad \longrightarrow \quad \boxed{\mathbf{E} = -\frac{\mathbf{P}}{3\varepsilon_0},} \tag{2.32}$$

where the substitution given by $u = \cos\theta$ is used to solve the integral in θ. It can be shown that $\mathbf{E}$ has this same (constant) value at any point inside the polarized sphere.

Example 2.4 Nonuniformly Polarized Dielectric Sphere

A nonuniformly polarized dielectric sphere, of radius a, is situated in free space. In a spherical coordinate system whose origin coincides with the sphere center, the polarization vector is given by the expression

$$\mathbf{P}(r) = P_r(r)\,\hat{\mathbf{r}} = P_0\frac{r}{a}\,\hat{\mathbf{r}} \tag{2.33}$$

(P_0 is a constant). Determine (a) the bound volume and surface charge densities of the sphere and (b) the electric scalar potential inside and outside the sphere.

Solution

(a) Using the expression for the divergence in spherical coordinates, Eq. (1.171), the bound volume charge density of the sphere amounts to

$$\rho_{\mathrm{p}} = -\nabla\cdot\mathbf{P} = -\frac{1}{r^2}\frac{\partial}{\partial r}\left(r^2 P_r\right) = -\frac{3P_0}{a} \tag{2.34}$$

(it is the same at all points inside the sphere). The bound surface charge density is

$$\rho_{\mathrm{ps}} = \hat{\mathbf{r}}\cdot\mathbf{P}(a^-) = P_0. \tag{2.35}$$

(b) The field outside the sphere (for $r > a$) is zero, because it is identical to the field of the equivalent point charge $Q_{\mathrm{p}} = 0$ (total charge of the sphere) placed at the sphere center. Hence, the potential outside the sphere is also zero,

$$V(r) = 0, \quad a < r < \infty. \tag{2.36}$$

From Eq. (1.140), the electric field inside the sphere is given by

$$E(r) = \frac{\rho_{\mathrm{p}} r}{3\varepsilon_0} = -\frac{P_0 r}{\varepsilon_0 a}, \quad 0 \le r < a. \tag{2.37}$$

The potential inside the sphere is thus

$$V(r) = \int_{r'=r}^{a} E(r')\,\mathrm{d}r' = -\frac{P_0 a}{2\varepsilon_0}\left(1 - \frac{r^2}{a^2}\right), \quad 0 \le r \le a. \tag{2.38}$$

Problems: 2.2–2.6; *Conceptual Questions* (on Companion Website): 2.3 and 2.4; *MATLAB Exercises* (on Companion Website).

2.5 GENERALIZED GAUSS' LAW

We now consider the most general electrostatic system containing both conductors and dielectrics. The equivalent field sources are now both free and bound charges, in free space, and Gauss' law, Eq. (1.133), becomes

Gauss' law for a system with conductors and dielectrics

$$\boxed{\oint_S \mathbf{E}\cdot\mathrm{d}\mathbf{S} = \frac{Q_S + Q_{\mathrm{p}S}}{\varepsilon_0},} \tag{2.39}$$

where Q_S and Q_{pS} are the total free charge and the total bound charge, respectively, enclosed by an arbitrary closed surface S. Multiplying this equation by ε_0, moving Q_{pS} to the left-hand side of the equation, then substituting it by the negative of the flux of the polarization vector, $\mathbf{P}$, from Eq. (2.16), and finally joining the two integrals over S into a single integral, we obtain the equivalent integral equation:

$$\oint_S (\varepsilon_0 \mathbf{E} + \mathbf{P}) \cdot d\mathbf{S} = Q_S. \tag{2.40}$$

To shorten the writing, we define a new vector quantity,

$$\boxed{\mathbf{D} = \varepsilon_0 \mathbf{E} + \mathbf{P},} \tag{2.41}$$

electric flux density vector (unit: C/m^2)

which is called the electric flux density vector (also known as the electric displacement vector or electric induction vector). Accordingly, the flux of $\mathbf{D}$ is termed the electric flux (symbolized by Ψ),

$$\boxed{\Psi = \int_{S'} \mathbf{D} \cdot d\mathbf{S},} \tag{2.42}$$

electric flux (unit: C)

where S' is any designated surface (open or closed). In place of Eq. (2.40),

$$\boxed{\oint_S \mathbf{D} \cdot d\mathbf{S} = Q_S.} \tag{2.43}$$

generalized Gauss' law

This is an equivalent form of Gauss' law for electrostatic fields in arbitrary media, which is more convenient than the form in Eq. (2.39) because it has only free charges on the right-hand side of the integral equation, and not the bound charges, and thus is simpler to use. It is referred to as the generalized Gauss' law, and, in words, it states that the outward electric flux through any closed surface in any electrostatic system including conductors and dielectrics equals the total free charge enclosed by the surface. From Eq. (2.43), the unit for the electric flux is C, so that the unit for its density, $\mathbf{D}$, is C/m^2.

In the general case, free charge is represented by means of the volume charge density, ρ, yielding

$$\boxed{\oint_S \mathbf{D} \cdot d\mathbf{S} = \int_v \rho \, dv,} \tag{2.44}$$

generalized Gauss' law in terms of the volume charge density

with v denoting the volume bounded by S. Since this integral relation is true regardless of the choice of v, the divergence theorem, Eq. (1.173), gives the differential form of the generalized Gauss' law:

$$\boxed{\nabla \cdot \mathbf{D} = \rho.} \tag{2.45}$$

generalized differential Gauss' law

Problems: 2.7–2.11; *Conceptual Questions* (on Companion Website): 2.5.

2.6 CHARACTERIZATION OF DIELECTRIC MATERIALS

The polarization properties of materials can be described by the relationship between the polarization vector, $\mathbf{P}$, and the electric field intensity vector, $\mathbf{E}$, Eq. (2.9). We now employ the electric flux density vector, $\mathbf{D}$, and substituting Eq. (2.9) into Eq. (2.41), obtain the equivalent relationship

$$\boxed{\mathbf{D} = \varepsilon_0 \mathbf{E} + \mathbf{P}(\mathbf{E}) = \mathbf{D}(\mathbf{E}),} \tag{2.46}$$

constitutive equation of an arbitrary (nonlinear) dielectric

which is more often used for characterization of dielectric materials and is termed a constitutive equation of the material. For linear dielectrics, Eq. (2.10) applies, and Eq. (2.46) becomes

constitutive equation of a linear dielectric

$$\boxed{\mathbf{D} = (\chi_e + 1)\varepsilon_0\mathbf{E} = \varepsilon_r\varepsilon_0\mathbf{E} \quad \text{or} \quad \mathbf{D} = \varepsilon\mathbf{E},} \tag{2.47}$$

where ε is the permittivity and ε_r the relative permittivity of the medium (ε_r is sometimes referred to as the dielectric constant of the material). The unit for ε is farad per meter (F/m), while ε_r is dimensionless, obtained as

$$\varepsilon_r = \chi_e + 1, \tag{2.48}$$

and hence

$$\varepsilon_r \geq 1. \tag{2.49}$$

The value of ε_r shows how much the permittivity of a dielectric material,

permittivity of a linear dielectric (unit: F/m)

$$\boxed{\varepsilon = \varepsilon_r\varepsilon_0,} \tag{2.50}$$

is higher than the permittivity of free space (vacuum), given in Eq. (1.2). For free space and nondielectric materials (such as metals), $\varepsilon_r = 1$ and

constitutive equation for free space

$$\boxed{\mathbf{D} = \varepsilon_0\mathbf{E}.} \tag{2.51}$$

Table 2.1 shows values of the relative permittivity of a number of selected materials, for electrostatic or low-frequency time-varying (time-harmonic) applied electric fields,[2] at room temperature (20°C).

For nonlinear dielectrics, the constitutive relation between **D** and **E**, Eq. (2.46), is nonlinear. This also means that the polarization properties of the material depend on the electric field intensity, E (for linear dielectrics, χ_e and ε are constants, independent of E).

In so-called ferroelectric materials, Eq. (2.46) is not only nonlinear, but also shows hysteresis effects. The function $D(E)$ has multiple branches, so that D is not uniquely determined by a value of E, but it depends also on the history of polarization of the material, i.e., on its previous states. A notable example is barium titanate ($BaTiO_3$), used in ceramic capacitors and various microwave devices (e.g., ceramic filters and multiplexers).

Another concept in characterization of materials is homogeneity. A material is said to be homogeneous when its properties do not change from point to point in the region being considered. In a linear homogeneous dielectric, ε is a constant independent of spatial coordinates. Otherwise, the material is inhomogeneous [e.g., $\varepsilon = \varepsilon(x, y, z)$ in the region].

Finally, we introduce the concept of isotropy in classifying dielectric materials. Generally, properties of isotropic media are independent of direction. In a linear isotropic dielectric, ε is a scalar quantity, and hence **D** and **E** are always collinear and in the same direction, regardless of the orientation of **E**. In an anisotropic medium, however, individual components of **D** depend differently on different components of **E**, so that Eq. (2.47) becomes a matrix equation,

$[\varepsilon]$ – permittivity tensor of an anisotropic dielectric

$$\boxed{\begin{bmatrix} D_x \\ D_y \\ D_z \end{bmatrix} = \begin{bmatrix} \varepsilon_{xx} & \varepsilon_{xy} & \varepsilon_{xz} \\ \varepsilon_{yx} & \varepsilon_{yy} & \varepsilon_{yz} \\ \varepsilon_{zx} & \varepsilon_{zy} & \varepsilon_{zz} \end{bmatrix} \begin{bmatrix} E_x \\ E_y \\ E_z \end{bmatrix}.} \tag{2.52}$$

[2] At higher frequencies, when viewed over very wide frequency ranges, the permittivity generally (for most materials) is not a constant, but depends on the operating frequency of electromagnetic waves propagating through the material.

Table 2.1. Relative permittivity of selected materials*

Material	ε_r	Material	ε_r
Vacuum	1	Quartz	5
Freon	1	Diamond	5–6
Air	1.0005	Wet soil	5–15
Styrofoam	1.03	Mica (ruby)	5.4
Polyurethane foam	1.1	Steatite	5.8
Paper	1.3–3	Sodium chloride (NaCl)	5.9
Wood	2–5	Porcelain	6
Dry soil	2–6	Neoprene	6.6
Paraffin	2.1	Silicon nitride (Si_3N_4)	7.2
Teflon	2.1	Marble	8
Vaseline	2.16	Alumina (Al_2O_3)	8.8
Polyethylene	2.25	Animal and human muscle	10
Oil	2.3	Silicon (Si)	11.9
Rubber	2.4–3	Gallium arsenide	13
Polystyrene	2.56	Germanium	16
PVC	2.7	Ammonia (liquid)	22
Amber	2.7	Alcohol (ethyl)	25
Plexiglass	3.4	Tantalum pentoxide	25
Nylon	3.6–4.5	Glycerin	50
Fused silica (SiO_2)	3.8	Ice	75
Sulfur	4	Water	81
Glass	4–10	Rutile (TiO_2)	89–173
Bakelite	4.74	Barium titanate ($BaTiO_3$)	1,200

* For static or low-frequency applied electric fields, at room temperature.

Thus, instead of a single scalar ε, we have a tensor $[\varepsilon]$ (permittivity tensor), i.e., nine (generally different) scalars corresponding to different pairs of spatial components of **D** and **E**. Crystalline dielectric materials, in general, are anisotropic; the periodic nature of crystals causes dipole moments to be formed and oriented by means of the applied electric field much more easily along the crystal axes than in other directions. An example is rutile (TiO_2), whose relative permittivity is $\varepsilon_r = 173$ in the direction parallel to a crystal axis and $\varepsilon_r = 89$ at right angles. For many crystals the change in permittivity with direction is small. For example, quartz has $\varepsilon_r = 4.7 - 5.1$, and it is customary to adopt a rounded value $\varepsilon_r = 5$ for its average relative permittivity and treat the material as isotropic.

The theory of dielectrics we have discussed so far assumes normal designed regimes of operation of electrical systems – when the electric field intensity, E, in individual dielectric parts of a system is below a certain "breakdown" level. Namely, the intensity E in a dielectric cannot be increased indefinitely: if a certain value is exceeded, the dielectric becomes conducting. It temporarily or permanently loses its insulating property, and is said to break down. The breaking field value, i.e., the maximum electric field intensity that an individual dielectric material can withstand without breakdown, is termed the dielectric strength of the material. We denote it by E_{cr} (critical field intensity). The values of E_{cr} for different materials are obtained by measurement. For air,

$$\boxed{E_{cr0} = 3\ \text{MV/m}.} \tag{2.53}$$

dielectric strength of air

In gaseous dielectrics, like air, because of a very strong applied electric field, the free electrons and ions are accelerated, by Coulomb forces [see Eq. (1.23)], to velocities high enough that in collisions with neutral molecules, they are able to knock electrons out of the molecule (so-called impact ionization). The newly created free electrons and positively charged ions are also accelerated by the field, they collide with molecules, liberate more electrons, and the result is an avalanche process of impact ionization and very rapid generation of a vast number of free electrons that constitute a substantial electric current in the gas (usually sparking occurs as well). In other words, the gas, normally a very good insulator, is suddenly transformed into an excellent conductor. Note that many air breakdowns occur at any instant of time in thunderstorms all over the earth. Basically, they are caused by large atmospheric electric fields (fields due to charged clouds), reaching the breakdown value in Eq. (2.53), and their most obvious manifestation is, of course, lightning.

Similar avalanche processes occur at high enough electric field intensities in liquid and solid dielectrics. For solids, these processes are enhanced and the value of the dielectric strength (E_{cr}) of the particular piece of a dielectric is lowered by impurities and structural defects in the material, by certain ways the material is manufactured, and even by microscopic air-filled cracks and voids in the material. In addition, when, under the influence of a strong electric field, the local heat due to leakage currents flowing in lossy (low-loss) dielectrics is generated faster than it can be dissipated in the material, the resulting rise of temperature may cause a change in the material (melting) and lead to a so-called thermal breakdown of the dielectric. Such breakdown processes depend on the duration of the applied strong field and the ambient temperature. Breakdowns in solid dielectrics most often cause a permanent damage to the material (e.g., formation of highly conductive channels of molten material, sometimes including carbonized matter, that irreversibly damage the texture of the dielectric).

The values of E_{cr} for some selected dielectric materials are presented in Table 2.2. Dielectric strengths of dielectrics other than air are larger than the value in Eq. (2.53). Note that, by definition, the dielectric strength of a vacuum is infinite.

Conceptual Questions (on Companion Website): 2.6.

Table 2.2. Dielectric strength of selected materials*

Material	E_{cr} (MV/m)	Material	E_{cr} (MV/m)
Air (atmospheric pressure)	3	Bakelite	25
Barium titanate ($BaTiO_3$)	7.5	Glass (plate)	30
Freon	~8	Paraffin	~30
Germanium	~10	Silicon (Si)	~30
Wood (douglas fir)	~ 10	Alumina	~35
Porcelain	11	Gallium arsenide	~40
Oil (mineral)	15	Polyethylene	47
Paper (impregnated)	15	Mica	200
Polystyrene	20	Fused quartz (SiO_2)	~1000
Teflon	20	Silicon nitride (Si_3N_4)	~1000
Rubber (hard)	25	Vacuum	∞

* At room temperature.

2.7 MAXWELL'S EQUATIONS FOR THE ELECTROSTATIC FIELD

We note that Maxwell's first equation for the electrostatic field, Eq. (1.75), does not depend on the material properties, and is the same in all kinds of dielectrics as it is in free space. Eq. (2.44) is Maxwell's third equation, and we now write down the full set of Maxwell's equations for the electrostatic field in an arbitrary medium, together with the constitutive equation, Eq. (2.46) or (2.47):

$$\boxed{\begin{cases} \oint_C \mathbf{E} \cdot d\mathbf{l} = 0 \\ \oint_S \mathbf{D} \cdot d\mathbf{S} = \int_v \rho \, dv \\ \mathbf{D} = \mathbf{D}(\mathbf{E}) \; [\mathbf{D} = \varepsilon \mathbf{E}] \end{cases}} \quad (2.54)$$

Maxwell's first equation in electrostatics
Maxwell's third equation
constitutive equation for **D**

We shall see later in this text that these equations represent a subset of the full set of Maxwell's equations for the electromagnetic field, specialized for the electrostatic case. In the general case, the set contains four Maxwell's equations and three constitutive equations. As we shall see, the third equation (generalized Gauss' law) retains this same form also under nonstatic conditions. Constitutive equations are not Maxwell's equations, but are associated with them and are needed to supply the information about the materials involved.

2.8 ELECTROSTATIC FIELD IN LINEAR, ISOTROPIC, AND HOMOGENEOUS MEDIA

Most often we deal with linear, isotropic, and homogeneous dielectrics, in which Eq. (2.47) applies, and the permittivity ε is independent of the intensity of the applied field, is the same for all directions, and does not change from point to point. For such media, we can bring ε outside the integral sign in the integral form of the generalized Gauss' law, Eq. (2.43),

$$\boxed{\oint_S \mathbf{E} \cdot d\mathbf{S} = \frac{Q_S}{\varepsilon},} \quad (2.55)$$

Gauss' law for a homogeneous dielectric

or outside the operator (div) sign in the differential generalized Gauss' law, Eq. (2.45),

$$\nabla \cdot \mathbf{E} = \frac{\rho}{\varepsilon}. \quad (2.56)$$

We notice that Eqs. (2.55) and (2.56) are identical to the corresponding free-space laws, Eqs. (1.133) and (1.165), except for ε_0 being substituted by ε. Recall that the expression for the electric field intensity vector due to a point charge in free space, and with it also Coulomb's law, can be derived from Gauss' law (see Problem 1.53). Based on this, we can now reconsider all charge distributions in free space we have considered so far, and all structures with conductors in free space we have analyzed, and by merely replacing ε_0 with ε in all the equations, obtain the solutions for the same (free) charge distributions and the same conducting structures situated in a homogeneous dielectric of permittivity ε.[3] This is the power of the concept

[3] In what follows (in this entire text), we shall always assume linear and isotropic media, except when we explicitly specify that the medium under consideration is nonlinear and/or anisotropic.

of dielectric permittivity. We emphasize again that, with using the electric flux density vector and the dielectric permittivity, we are left to deal with free charges in the system only, while the contribution of bound charges to the field is properly added through ε. Thus, for example, Eq. (1.82) implies that the potential due to a free volume charge distribution in a homogeneous dielectric with permittivity ε is given by

$$V = \frac{1}{4\pi\varepsilon}\int_v \frac{\rho\,\mathrm{d}v}{R}. \tag{2.57}$$

Also, the free surface charge density on the surface of a conductor surrounded by a dielectric with permittivity ε is [from Eq. (1.190)]

$$\rho_s = \varepsilon\,\hat{\mathbf{n}}\cdot\mathbf{E} \tag{2.58}$$

(boundary condition for the normal component of $\mathbf{E}$), and so on. Note, however, that the boundary condition for the tangential component of $\mathbf{E}$ near a conductor surface, Eq. (1.186), is always the same, irrespective of the properties (ε) of the surrounding dielectric.

Once we find the electric field in a structure filled with a homogeneous dielectric, we can calculate the polarization vector in the dielectric as [Eqs. (2.41) and (2.47)]

polarization vector in a linear dielectric

$$\boxed{\mathbf{P} = \mathbf{D} - \varepsilon_0\mathbf{E} = (\varepsilon - \varepsilon_0)\mathbf{E},} \tag{2.59}$$

and then the distribution of volume and surface bound charges of the dielectric – using Eqs. (2.19) and (2.23).

Note that, from Eqs. (2.19), (2.59), (2.56), and (2.50), the bound volume charge density, ρ_p, at a point in the dielectric can be obtained directly from the free volume charge density, ρ, at that point as

$$\rho_p = -\nabla\cdot\mathbf{P} = -(\varepsilon - \varepsilon_0)\nabla\cdot\mathbf{E} = -\frac{\varepsilon - \varepsilon_0}{\varepsilon}\rho = -\frac{\varepsilon_r - 1}{\varepsilon_r}\rho. \tag{2.60}$$

In an analogous manner, we derive the relationship between the bound and free surface charge densities on the surface of a conductor surrounded by a dielectric with relative permittivity ε_r. Shown in Fig. 2.8 is a detail of the surface. Combining Eqs. (2.23), (2.59), (2.58), and (2.50), and noting that $\hat{\mathbf{n}}_d = -\hat{\mathbf{n}}$ [in Eq. (2.23), $\hat{\mathbf{n}}_d$ is directed from the dielectric outward; in Eq. (2.58), $\hat{\mathbf{n}}$ is directed from the conductor outward], we obtain

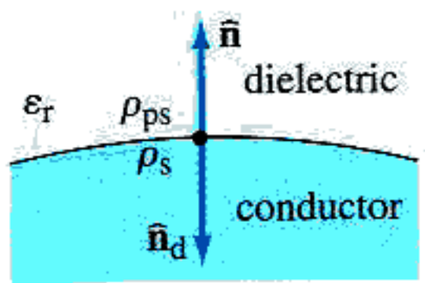

Figure 2.8 Detail of a conductor-linear dielectric surface.

$$\rho_{ps} = \hat{\mathbf{n}}_d\cdot\mathbf{P} = -(\varepsilon - \varepsilon_0)\hat{\mathbf{n}}\cdot\mathbf{E} = -\frac{\varepsilon_r - 1}{\varepsilon_r}\rho_s. \tag{2.61}$$

Although the free surface charge density, ρ_s, is actually localized on the conductor side of the boundary surface and the bound surface charge density, ρ_{ps}, is localized on the dielectric side of the surface, they can be treated as a single sheet of charge with the total density

$$\rho_{s\,tot} = \rho_s + \rho_{ps} = \left(1 - \frac{\varepsilon_r - 1}{\varepsilon_r}\right)\rho_s = \frac{\rho_s}{\varepsilon_r}. \tag{2.62}$$

Example 2.5 Dielectric Sphere with Free Volume Charge

A homogeneous dielectric sphere, of radius a and relative permittivity ε_r, is situated in air. There is a free volume charge density $\rho(r) = \rho_0 r/a$ $(0 \le r \le a)$ throughout the sphere volume, where r is the distance from the sphere center (spherical radial coordinate) and ρ_0 is a constant. Determine (a) the electric scalar potential for $0 \le r < \infty$ and (b) the bound charge distribution of the sphere.

Solution

(a) Because of spherical symmetry of the problem, the electric flux density vector, **D**, is purely radial and depends only on r. From the generalized Gauss' law [Eq. (2.44)], applied in a similar fashion to that in Example 1.19 accommodated for spherical symmetry (see also Example 1.18), the magnitude of **D** is found to be

$$D(r) = \begin{cases} \rho_0 r^2/(4a) & \text{for } r \le a \\ \rho_0 a^3/(4r^2) & \text{for } r > a \end{cases}. \tag{2.63}$$

The electric field intensity vector is of the same form, and its magnitude is given by

$$E(r) = \begin{cases} D(r)/(\varepsilon_r \varepsilon_0) & \text{for } r \le a \\ D(r)/\varepsilon_0 & \text{for } r > a \end{cases}. \tag{2.64}$$

The potential at a distance r from the sphere center is hence:

$$V(r) = \frac{1}{\varepsilon_0} \int_{r'=r}^{\infty} D(r')\,\mathrm{d}r' = \frac{\rho_0 a^3}{4\varepsilon_0 r}, \qquad \text{for } r \ge a, \tag{2.65}$$

and [also see Eq. (1.142)]

$$V(r) = \frac{1}{\varepsilon_r \varepsilon_0} \int_{r'=r}^{a} D(r')\,\mathrm{d}r' + V(a) = \frac{\rho_0 a^2}{4\varepsilon_0}\left[1 + \frac{1}{3\varepsilon_r}\left(1 - \frac{r^3}{a^3}\right)\right], \qquad \text{for } r < a. \tag{2.66}$$

(b) According to Eq. (2.60), the bound volume charge density inside the sphere amounts to

$$\rho_p(r) = -\frac{\varepsilon_r - 1}{\varepsilon_r}\rho(r) = -\frac{\rho_0(\varepsilon_r - 1)r}{\varepsilon_r a}. \tag{2.67}$$

Using Eqs. (2.23), (2.59), (2.47), and (2.63), the bound surface charge density on the sphere surface comes out to be

$$\rho_{ps} = P(a^-) = \frac{\varepsilon_r - 1}{\varepsilon_r} D(a^-) = \frac{\rho_0(\varepsilon_r - 1)a}{4\varepsilon_r}. \tag{2.68}$$

Example 2.6 Model of a *pn* Junction

Sketched in Fig. 2.9(a) is a *pn* junction between two semiconducting half-spaces, doped p-type and n-type, respectively. The volume charge distribution in the semiconductor can be approximated by the following function:

$$\rho(x) = \begin{cases} -\rho_0\,\mathrm{e}^{x/a} & \text{for } x < 0 \\ 0 & \text{for } x = 0 \\ \rho_0\,\mathrm{e}^{-x/a} & \text{for } x > 0 \end{cases}, \tag{2.69}$$

where ρ_0 and a are positive constants. The permittivity of the semiconductor is ε. Find (a) the electric field intensity vector in the semiconductor, (b) the electric scalar potential in the semiconductor, and (c) the voltage between the ends of the semiconductor, from the end on the n-type side to the end on the p-type side of the junction.

Solution

(a) This is a problem with planar symmetry (see Examples 1.20, 1.21, and 1.23), and the electric field intensity vector in the semiconductor is given by $\mathbf{E} = E_x(x)\,\hat{\mathbf{x}}$ [Eq. (1.148)]. The differential generalized Gauss' law, Eq. (2.56), becomes

$$\frac{\mathrm{d}E_x(x)}{\mathrm{d}x} = \frac{\rho(x)}{\varepsilon}. \tag{2.70}$$

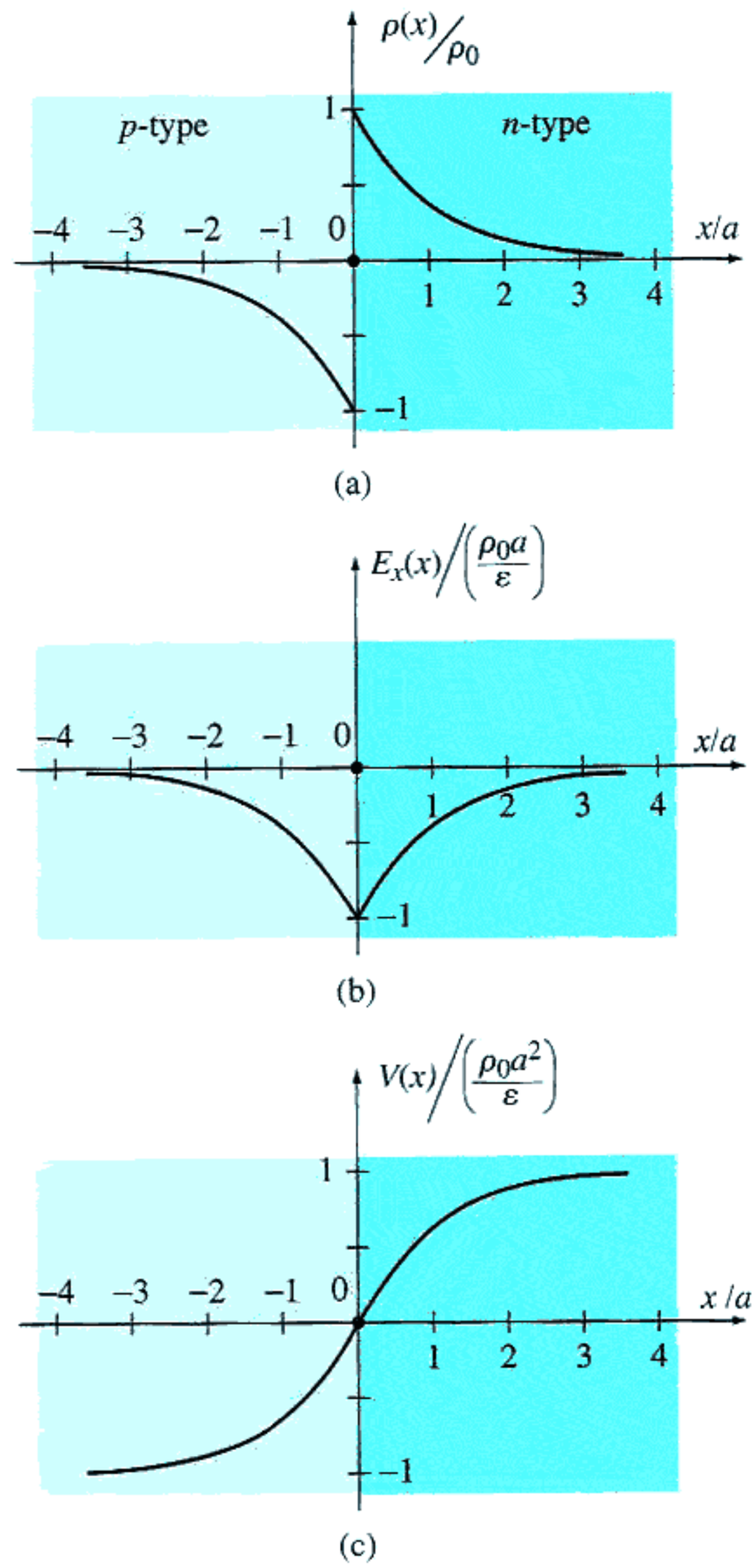

Figure 2.9 Model of a *pn* junction: (a) volume charge density, (b) electric field intensity, and (c) electric scalar potential; for Example 2.6.

This is a first-order differential equation in x, and we solve it by integrating with respect to x [as in Eq. (1.178)]:

$$E_x(x) = \frac{1}{\varepsilon}\int_{x'=-\infty}^{x} \rho(x')\,\mathrm{d}x' + C, \tag{2.71}$$

where C is the constant of integration, which represents the field E_x in the plane $x \to -\infty$. We note that

$$\int_{-\infty}^{\infty} \rho(x')\,\mathrm{d}x' = 0, \tag{2.72}$$

meaning that the total charge of the semiconductor is zero. This means, in turn, that no field can exist far from the junction [see also Eq. (1.154)],

$$E_x(x \to \mp\infty) = 0, \tag{2.73}$$

and hence $C = 0$. Substituting Eq. (2.69), the integration for the field points in the p-type region of the semiconductor yields

$$E_x(x) = -\frac{\rho_0}{\varepsilon}\int_{-\infty}^{x} e^{x'/a}\,dx' = -\frac{\rho_0 a}{\varepsilon}\,e^{x/a} \quad (-\infty < x \le 0). \tag{2.74}$$

In the n-type region, we have to break the integration up into two parts:

$$E_x(x) = \frac{\rho_0}{\varepsilon}\left(-\int_{-\infty}^{0} e^{x'/a}\,dx' + \int_{0}^{x} e^{-x'/a}\,dx'\right) = -\frac{\rho_0 a}{\varepsilon}\,e^{-x/a} \quad (0 < x < \infty). \tag{2.75}$$

Fig. 2.9(b) shows the electric field intensity $E_x(x)$ in the semiconductor. We see that the field is oriented from the n-type doped region to the p-type doped region. This field is called the built-in field of a pn junction, as it exists in the junction even when an external voltage is not applied (e.g., when the terminals of a pn diode are not connected to an external voltage source). In the equilibrium state established after the pn junction is formed, the built-in field prevents further diffusion of positive charges (holes) to the right and negative charges (electrons) to the left across the junction.[4]

(b) Let us arbitrarily adopt our reference point for potential ($\mathcal{R}$) at the center of the junction, $x = 0$, so that the potential at points in the p-type region is [Eq. (1.74)]

$$\begin{aligned} V(x) &= \int_{\mathrm{P}}^{\mathcal{R}} \mathbf{E}\cdot d\mathbf{l} = \int_{x'=x}^{0} E_x(x')\,dx' = -\frac{\rho_0 a}{\varepsilon}\int_{x}^{0} e^{x'/a}\,dx' \\ &= \frac{\rho_0 a^2}{\varepsilon}\left(e^{x/a} - 1\right), \quad -\infty < x \le 0. \end{aligned} \tag{2.76}$$

In the n-type region, we reverse the direction of integration for convenience,

$$\begin{aligned} V(x) &= \int_{\mathrm{P}}^{\mathcal{R}} \mathbf{E}\cdot d\mathbf{l} = -\int_{\mathcal{R}}^{\mathrm{P}} \mathbf{E}\cdot d\mathbf{l} = -\int_{0}^{x} E_x(x')\,dx' \\ &= \frac{\rho_0 a}{\varepsilon}\int_{0}^{x} e^{-x'/a}\,dx' = \frac{\rho_0 a^2}{\varepsilon}\left(1 - e^{-x/a}\right), \quad 0 < x < \infty. \end{aligned} \tag{2.77}$$

The distribution of the potential, $V(x)$, along the semiconductor is shown in Fig. 2.9(c).

(c) The voltage between the n-type and p-type ends of the semiconductor turns out to be

$$V(x \to \infty) - V(x \to -\infty) = \frac{2\rho_0 a^2}{\varepsilon}. \tag{2.78}$$

This voltage is called the built-in voltage of a pn junction (diode).

Problems: 2.12–2.15; *MATLAB Exercises* (on Companion Website).

2.9 DIELECTRIC-DIELECTRIC BOUNDARY CONDITIONS

So far, we have considered boundary surfaces conductor-free space (Fig. 1.39), dielectric-free space (Fig. 2.4), and conductor-dielectric (Fig. 2.8), and analyzed the fields close to surfaces and surface charge densities on the surfaces [Eqs. (1.186), (1.189), (2.23), and (2.58)]. Let us now consider a dielectric-dielectric boundary

[4]Note that initially there are excess holes to the left of the plane $x = 0$ (p-type semiconductor is positively charged over its entire volume) and excess electrons to the right (n-type semiconductor is negatively charged by doping). In a brief transient, a diffusion of holes occurs from the p-region into the n-region and electrons diffuse in the opposite direction, until an electric field is built up in such a direction that the diffusion current drops to zero.

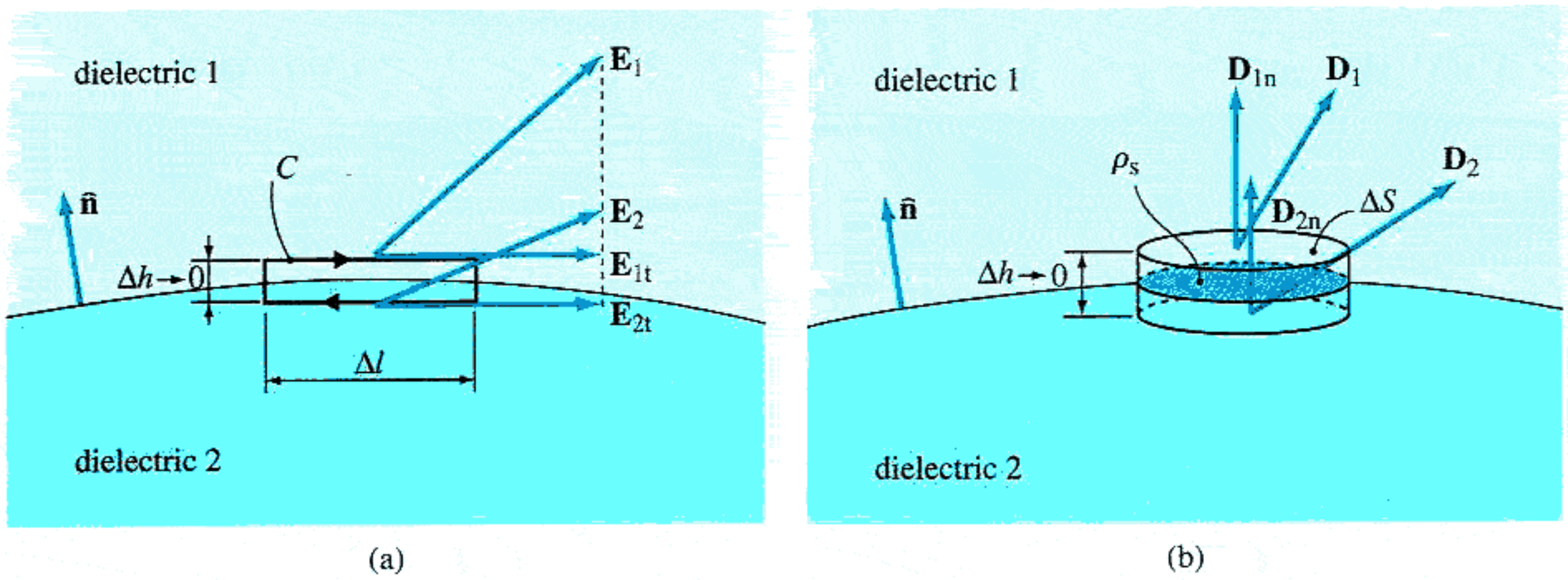

Figure 2.10 Dielectric-dielectric boundary surface: deriving boundary conditions for (a) tangential components of **E** and (b) normal components of **D**.

surface, shown in Fig. 2.10, and derive the boundary conditions for field components near the surface. We apply the same technique as in deriving the corresponding boundary conditions for the conductor-free space case, Eqs. (1.186) and (1.189). The main difference is that now the field exists at both sides of the boundary. Let $\mathbf{E}_1$ and $\mathbf{D}_1$ be, respectively, the electric field intensity vector and electric flux density vector close to the boundary in medium 1, whereas $\mathbf{E}_2$ and $\mathbf{D}_2$ stand for the same quantities in medium 2.

Applying Eq. (1.75) to a narrow rectangular elementary contour C, Fig. 2.10(a), we obtain

continuity of the tangential component of **E**

$$\oint_C \mathbf{E} \cdot d\mathbf{l} = E_{1t}\,\Delta l - E_{2t}\,\Delta l = 0 \quad \longrightarrow \quad \boxed{E_{1t} = E_{2t}.} \tag{2.79}$$

This boundary condition tells us that the tangential components of **E** are the same on the two sides of the boundary, i.e., that $\mathbf{E}_t$ is continuous across the boundary.

On the other hand, an application of Eq. (2.43) to a pillbox Gaussian elementary surface, Fig. 2.10(b), gives

$$\oint_S \mathbf{D} \cdot d\mathbf{S} = D_{1n}\,\Delta S - D_{2n}\,\Delta S = \rho_s\,\Delta S \quad \longrightarrow \quad D_{1n} - D_{2n} = \rho_s \tag{2.80}$$

(we employ vector **D** to avoid dealing with bound charges), where the normal components of **D** are defined with respect to the unit normal $\hat{\mathbf{n}}$ directed from region 2 to region 1, and ρ_s is the free surface charge density that may exist on the surface. In the absence of charge,

continuity of the normal component of **D**, *charge-free surface*

$$\boxed{D_{1n} = D_{2n} \qquad (\rho_s = 0).} \tag{2.81}$$

This boundary condition enforces that the normal components of **D** be the same on the two sides of a boundary with no free charge on it. In other words, $\mathbf{D}_n$ is continuous across the boundary free of charge.

Relationships in Eqs. (2.79) and (2.80) represent two primary boundary conditions for the electrostatic field at the interface between two arbitrary media. When the dielectrics 1 and 2 are linear, $\mathbf{D}_1 = \varepsilon_1 \mathbf{E}_1$ and $\mathbf{D}_2 = \varepsilon_2 \mathbf{E}_2$, so we obtain an additional pair of (secondary) boundary conditions – for the tangential components of **D** and normal components of **E**. From Eq. (2.79), the boundary condition for $\mathbf{D}_t$ reads

$$\frac{D_{1t}}{\varepsilon_1} = \frac{D_{2t}}{\varepsilon_2}, \tag{2.82}$$

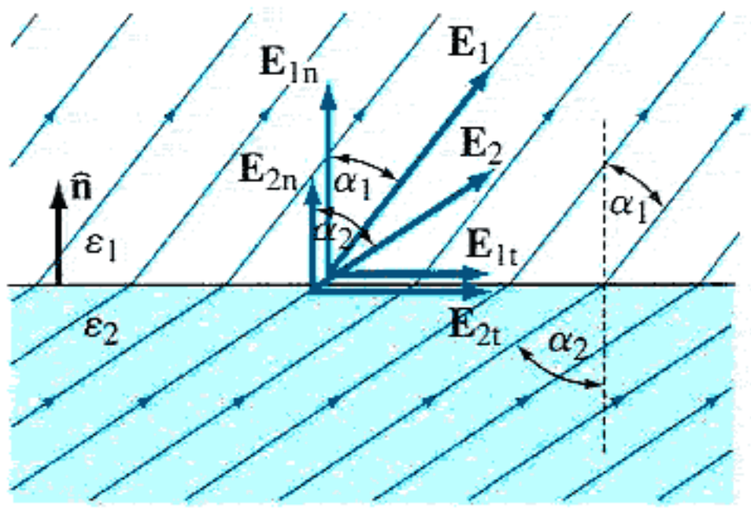

Figure 2.11 Refraction of electric field lines at a dielectric-dielectric interface.

and we see that $\mathbf{D}_t$ is discontinuous across the boundary. Similarly, Eq. (2.81) yields the boundary condition for $\mathbf{E}_n$ (if $\rho_s = 0$ at the interface):

$$\varepsilon_1 E_{1n} = \varepsilon_2 E_{2n}, \tag{2.83}$$

which shows that $\mathbf{E}_n$ is also discontinuous across the boundary.

Note that the boundary conditions for $\mathbf{E}$ and $\mathbf{D}$, that is, for $\mathbf{E}_t$ and $\mathbf{D}_n$, in Eqs. (2.79) and (2.80) can be written in vector form:

$$\boxed{\begin{aligned} \hat{\mathbf{n}} \times \mathbf{E}_1 - \hat{\mathbf{n}} \times \mathbf{E}_2 &= 0, \\ \hat{\mathbf{n}} \cdot \mathbf{D}_1 - \hat{\mathbf{n}} \cdot \mathbf{D}_2 &= \rho_s, \end{aligned} \quad (\hat{\mathbf{n}} \text{ directed from region 2 to region 1}),} \qquad \begin{aligned} &(2.84) \\ &(2.85) \end{aligned}$$

boundary condition for $\mathbf{E}_t$
boundary condition for $\mathbf{D}_n$

which is often more convenient for use in analyzing complex structures.

Let us consider again the interface between two dielectric media and the angles α_1 and α_2 that field lines in region 1 and region 2 make with the normal to the interface, as depicted in Fig. 2.11. The tangents of these angles can be expressed as

$$\tan\alpha_1 = \frac{E_{1t}}{E_{1n}} \quad \text{and} \quad \tan\alpha_2 = \frac{E_{2t}}{E_{2n}}. \tag{2.86}$$

We divide the tangents and use Eqs. (2.79) and (2.83) to get

$$\boxed{\frac{\tan\alpha_1}{\tan\alpha_2} = \frac{\varepsilon_1}{\varepsilon_2}.} \tag{2.87}$$

law of refraction of electric field lines

This is the law of refraction of the electric field lines at a dielectric-dielectric boundary that is free of charge ($\rho_s = 0$). Bending of field lines is, essentially, a result of unequal bound charges on the two sides of the boundary.

Finally, let us find the distribution of bound surface charges on a dielectric-dielectric interface (Fig. 2.10). From Eq. (2.23), the bound charge densities that accumulate on the two sides of the interface are

$$\rho_{ps1} = \hat{\mathbf{n}}_{d1} \cdot \mathbf{P}_1 \quad \text{and} \quad \rho_{ps2} = \hat{\mathbf{n}}_{d2} \cdot \mathbf{P}_2, \tag{2.88}$$

where $\hat{\mathbf{n}}_{d1} = -\hat{\mathbf{n}}$ and $\hat{\mathbf{n}}_{d2} = \hat{\mathbf{n}}$ [$\hat{\mathbf{n}}_d$ in Eq. (2.23) is directed from the dielectric outward]. Hence, by adding ρ_{ps1} and ρ_{ps2} together, the total bound surface charge density at the interface is given by

$$\boxed{\rho_{ps} = \hat{\mathbf{n}} \cdot \mathbf{P}_2 - \hat{\mathbf{n}} \cdot \mathbf{P}_1.} \tag{2.89}$$

boundary condition for $\mathbf{P}_n$

This is the boundary condition for the normal components of vector $\mathbf{P}$ at a dielectric-dielectric boundary.

Problems: 2.16–2.18; *Conceptual Questions* (on Companion Website): 2.7 and 2.8; *MATLAB Exercises* (on Companion Website).

2.10 POISSON'S AND LAPLACE'S EQUATIONS

Consider the electric field intensity vector, **E**, and scalar potential, V, in a homogeneous dielectric region of permittivity ε. The spatial derivatives of **E** at a point in the region are related to the free volume charge density, ρ, that may exist at that point by Eq. (2.56), which is a first-order differential equation. **E**, in turn, is related to the spatial derivatives of V through Eq. (1.101). It is obvious, then, that the second-order spatial derivatives of V are related to ρ by means of a second-order differential equation. This equation is Poisson's equation, which is easily derived by substituting Eq. (1.101) into Eq. (2.56):

$$\nabla \cdot (\nabla V) = -\frac{\rho}{\varepsilon}. \tag{2.90}$$

The double-∇ operation in Poisson's equation is performed by evaluating first the gradient of V, and then the divergence of the result. In the Cartesian coordinate system, gradient and divergence are calculated using Eqs. (1.102) and (1.167), respectively, and we have

$$\nabla \cdot (\nabla V) = \text{div}\,(\text{grad}\, V) = \nabla \cdot \left(\frac{\partial V}{\partial x}\,\hat{\mathbf{x}} + \frac{\partial V}{\partial y}\,\hat{\mathbf{y}} + \frac{\partial V}{\partial z}\,\hat{\mathbf{z}}\right)$$

$$= \frac{\partial}{\partial x}\left(\frac{\partial V}{\partial x}\right) + \frac{\partial}{\partial y}\left(\frac{\partial V}{\partial y}\right) + \frac{\partial}{\partial z}\left(\frac{\partial V}{\partial z}\right) = \frac{\partial^2 V}{\partial x^2} + \frac{\partial^2 V}{\partial y^2} + \frac{\partial^2 V}{\partial z^2}. \tag{2.91}$$

We note that the same result would have been obtained by applying formally the formula for the dot product in the Cartesian coordinate system, Eq. (1.164), to the dot product of two identical vectors (∇) in $(\nabla \cdot \nabla)V$, where ∇ is expressed as in Eq. (1.100). Hence, we can write

$$\nabla \cdot (\nabla V) = (\nabla \cdot \nabla)V. \tag{2.92}$$

The operator $\nabla \cdot \nabla$ is abbreviated ∇^2 ("del squared"), and Poisson's equation becomes

Poisson's equation

$$\boxed{\nabla^2 V = -\frac{\rho}{\varepsilon},} \tag{2.93}$$

where

Laplacian in Cartesian coordinates

$$\boxed{\nabla^2 V = \frac{\partial^2 V}{\partial x^2} + \frac{\partial^2 V}{\partial y^2} + \frac{\partial^2 V}{\partial z^2}.} \tag{2.94}$$

In a charge-free region ($\rho = 0$),

Laplace's equation

$$\boxed{\nabla^2 V = 0,} \tag{2.95}$$

which is known as Laplace's equation. The ∇^2 operator is called the Laplacian. We see that the Laplacian operates on a scalar (e.g., V), and the result is another scalar (e.g., $-\rho/\varepsilon$ or 0).

The expressions for $\nabla^2 V$ in the cylindrical coordinate system (Fig. 1.25) and the spherical coordinate system (Fig. 1.26) can be obtained in the same manner, i.e., by first taking the gradient of V [Eqs. (1.105) and (1.108)], and then the divergence [Eqs. (1.170) and (1.171)] of the result. In cylindrical coordinates, the Laplacian of $V = V(r, \phi, z)$ thus comes out to be

Laplacian in cylindrical coordinates

$$\boxed{\nabla^2 V = \frac{1}{r}\frac{\partial}{\partial r}\left(r\frac{\partial V}{\partial r}\right) + \frac{1}{r^2}\frac{\partial^2 V}{\partial \phi^2} + \frac{\partial^2 V}{\partial z^2},} \tag{2.96}$$

HISTORICAL ASIDE

Siméon Denis Poisson (1781–1840), French mathematician, was a student of Laplace (1749–1827) and Lagrange (1736–1813), and successor of Fourier (1768–1830) as a professor, at École Polytechnique, Paris. He is best known for his work on probability (Poisson's distribution), and his contributions to mathematics as applied to electricity and magnetism. In 1813, he published a generalization of Laplace's differential equation for the potential theory, valid for a nonzero mass density, so inside a solid, in mechanics or for a nonzero charge density, so inside a charge distribution, in electromagnetics.

Pierre Simon de Laplace (1749–1827), French mathematician and astronomer, was President of *Académie des Sciences* (French Academy). His work in mathematical astronomy was summed up in a monumental five-volume book on celestial mechanics (*Mécanique Céleste*), published between 1799 and 1825, in which the second-order partial differential equation for potential that we now name after him, Laplace's equation, appeared. He also wrote a treatise on the theory of probability, and worked on specific heats of substances. Laplace was a minister and senator under Napoleon, and was made a marquis by Louis XVIII.

and that of $V = V(r, \theta, \phi)$ in spherical coordinates

$$\boxed{\nabla^2 V = \frac{1}{r^2}\frac{\partial}{\partial r}\left(r^2\frac{\partial V}{\partial r}\right) + \frac{1}{r^2 \sin\theta}\frac{\partial}{\partial \theta}\left(\sin\theta\frac{\partial V}{\partial \theta}\right) + \frac{1}{r^2\sin^2\theta}\frac{\partial^2 V}{\partial \phi^2}.} \tag{2.97}$$

Laplacian in spherical coordinates

Example 2.7 Application of a 1-D Poisson's Equation

A free volume charge of a uniform density ρ exists in a homogeneous dielectric, of permittivity ε, between two flat metallic electrodes, as shown in Fig. 2.12. The electrodes are connected to a voltage V_0, and the distance between them is d. Neglecting the fringing effects, find (a) the electric potential and (b) the electric field intensity vector in the dielectric.

Solution

(a) Neglecting the fringing effects is equivalent to assuming that the electrodes are infinitely large, in which case the potential in the dielectric varies with the distance from the electrodes only. Let x be the normal distance from the left electrode (Fig. 2.12). Poisson's equation, given by Eqs. (2.93) and (2.94), becomes

$$\frac{d^2 V(x)}{dx^2} = -\frac{\rho}{\varepsilon} \quad (0 < x < d). \tag{2.98}$$

By integrating it twice, we get

$$V(x) = -\frac{\rho x^2}{2\varepsilon} + C_1 x + C_2, \tag{2.99}$$

where C_1 and C_2 are the constants of integration. The boundary condition $V(0) = V_0$ results in $C_2 = V_0$, and the condition on the other boundary, $V(d) = 0$, gives $C_1 = \rho d/(2\varepsilon) - V_0/d$. Hence,

$$V(x) = \frac{\rho x(d-x)}{2\varepsilon} + V_0\left(1 - \frac{x}{d}\right). \tag{2.100}$$

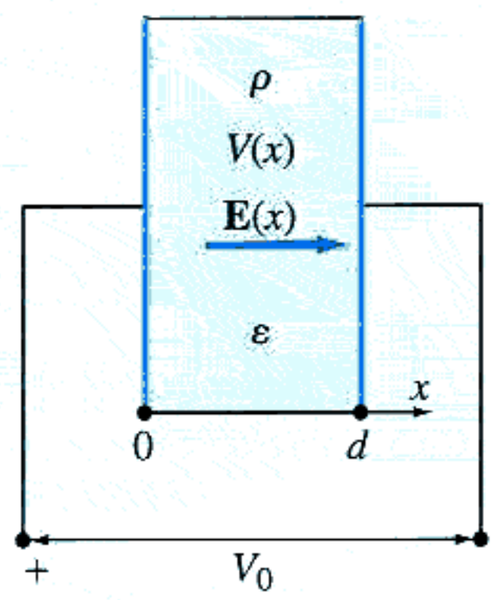

Figure 2.12 Uniform volume charge between metallic plates: application of a 1-D Poisson's equation (fringing neglected); for Example 2.7.

(b) Using Eqs. (1.101) and (1.102), we obtain the electric field vector from the potential:

$$\mathbf{E}(x) = -\nabla V = -\frac{\mathrm{d}V(x)}{\mathrm{d}x}\hat{\mathbf{x}} = \left[\frac{\rho}{\varepsilon}\left(x - \frac{d}{2}\right) + \frac{V_0}{d}\right]\hat{\mathbf{x}}. \tag{2.101}$$

Problems: 2.19–2.22; *Conceptual Questions* (on Companion Website): 2.9.

2.11 FINITE-DIFFERENCE METHOD FOR NUMERICAL SOLUTION OF LAPLACE'S EQUATION

In many practical cases, Poisson's or Laplace's equation cannot be solved analytically, but only numerically. The most popular and perhaps the simplest numerical method for solving these equations (and other types of differential equations generally) is the finite-difference (FD) method. It consists of replacing the derivatives in the differential equation by their finite-difference approximations and solving the resulting algebraic equations. To illustrate this, consider an air-filled coaxial cable with conductors of square cross section, shown in Fig. 2.13(a). Let the cross-sectional dimensions of the cable be a and b ($a < b$). The cable is charged by time-invariant charges, and the potentials of the conductors, V_a and V_b, are known. Our goal is to determine the distribution of the potential V in the space between the cable conductors.

This is a two-dimensional electrostatic problem for which, according to Fig. 2.13(b), Laplace's equation, Eqs. (2.95) and (2.94), is given by

$$\nabla^2 V = \frac{\partial^2 V}{\partial x^2} + \frac{\partial^2 V}{\partial y^2} = 0. \tag{2.102}$$

We discretize the region between the conductors by introducing a grid with cells of sides d [Fig. 2.13(b)], and employ the FD method in order to approximately compute the potentials at the grid points (nodes). Obviously, the accuracy of the computation depends on the grid resolution, i.e., the smaller the spacing of the grid, d, the more accurate (but computationally slower) the solution.

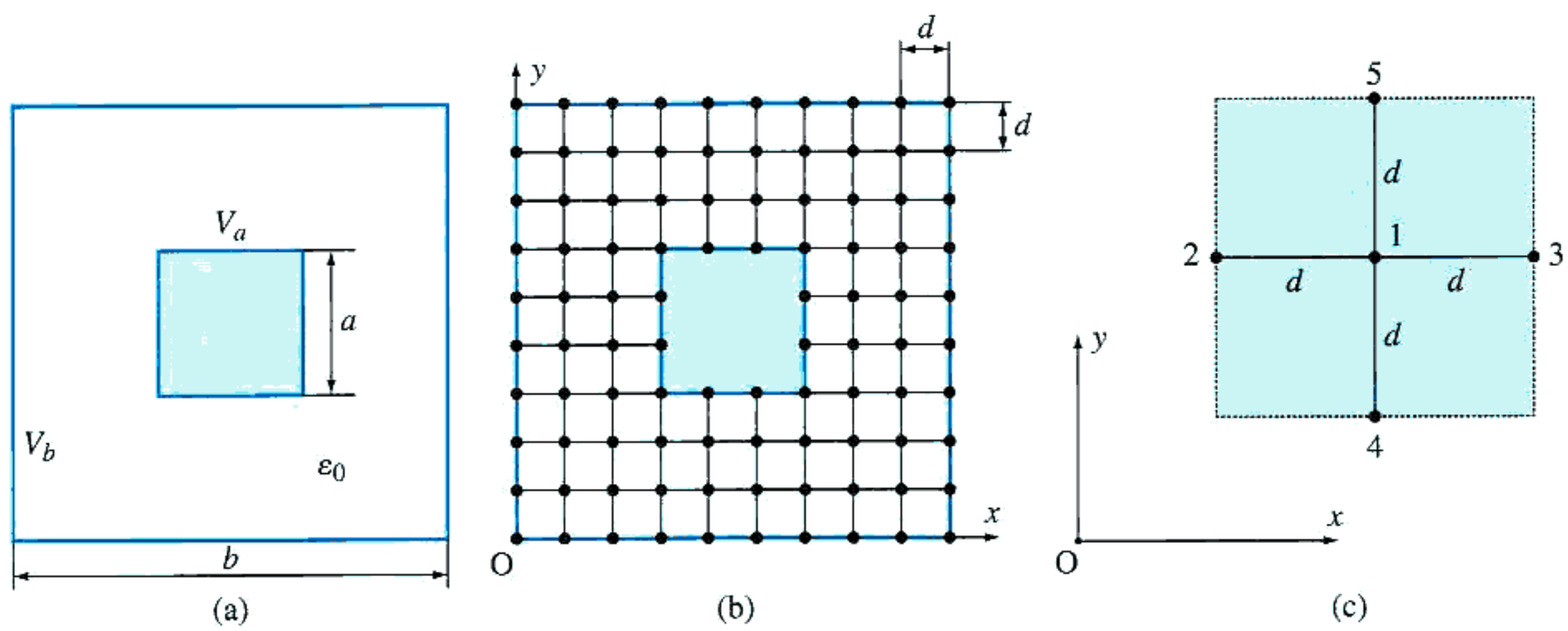

Figure 2.13 Finite-difference analysis of a coaxial cable of square cross section: (a) structure geometry, (b) nodes with discrete potential values as unknowns, and (c) detail of the grid for approximating Laplace's equation in terms of finite differences.

Fig. 2.13(c) shows a detail of the grid in Fig. 2.13(b). At the node 1, the backward-difference approximation for the first partial derivative of V with respect to the x-coordinate turns out to be

$$\boxed{\left.\frac{\partial V}{\partial x}\right|_1 \approx \frac{V_1 - V_2}{d},} \tag{2.103}$$

finite-difference (FD) approximation of a derivative

which, combined with the forward-difference approximation for the second partial derivative with respect to x, yields

$$\left.\frac{\partial^2 V}{\partial x^2}\right|_1 = \frac{\partial}{\partial x}\left(\frac{\partial V}{\partial x}\right)\bigg|_1 \approx \frac{1}{d}\left(\left.\frac{\partial V}{\partial x}\right|_3 - \left.\frac{\partial V}{\partial x}\right|_1\right) \approx \frac{1}{d}\left(\frac{V_3 - V_1}{d} - \frac{V_1 - V_2}{d}\right)$$

$$= \frac{V_2 + V_3 - 2V_1}{d^2}. \tag{2.104}$$

Analogously,

$$\left.\frac{\partial^2 V}{\partial y^2}\right|_1 \approx \frac{V_4 + V_5 - 2V_1}{d^2}, \tag{2.105}$$

so that the FD approximation for Laplace's differential equation at point 1 in Fig. 2.13(c) is

$$\boxed{\nabla^2 V\big|_1 \approx \frac{V_2 + V_3 + V_4 + V_5 - 4V_1}{d^2} = 0} \quad \longrightarrow \quad V_1 = \frac{1}{4}(V_2 + V_3 + V_4 + V_5). \tag{2.106}$$

FD approximation of Laplace's equation

The simplest technique to solve the above finite-difference equation with the aid of a computer is an iterative technique expressed as

$$\boxed{V_1^{(k+1)} = \frac{1}{4}\left[V_2^{(k)} + V_3^{(k)} + V_4^{(k)} + V_5^{(k)}\right], \quad k = 0, 1, \ldots} \tag{2.107}$$

iterative solution to the FD Laplace's equation

When some of the nodes 2, 3, 4, and 5 belong to one of the surfaces of conductors, the potential at such nodes is in all iteration steps equal to the respective given potential of the conductor (V_a or V_b). For the initial solution, at the zeroth ($k = 0$) iteration step, we can adopt $V^{(0)} = 0$ at all nodes between the conductors. By traversing the grid in a systematic manner, node by node, the average of the four neighboring potentials is computed at the $(k+1)$th step for each node and is used to replace the potential at that node, Eq. (2.107), and thus improve the solution from the kth step. This procedure is repeated until the changes of the solution (residuals) with respect to the previous iteration at all nodes are small enough, i.e., until a final set of values for the unknown potentials consistent with the criterion

$$\left|V_1^{(k+1)} - V_1^{(k)}\right| < \delta_V \tag{2.108}$$

is obtained, where δ_V stands for the specified tolerance of the potential.

Once the approximate solution for the potential distribution is known, numerical results for the electric field intensity vector, $\mathbf{E}$, at the grid nodes can be obtained by approximating the gradient operator involved in Eqs. (1.101) and (1.102) in terms of finite differences. For example, $\mathbf{E}$ at the node 1 in Fig. 2.13(c) is computed approximately as

$$\boxed{\mathbf{E}_1 = -\nabla V|_1 = -\left.\frac{\partial V}{\partial x}\right|_1 \hat{\mathbf{x}} - \left.\frac{\partial V}{\partial y}\right|_1 \hat{\mathbf{y}} \approx \frac{V_2 - V_3}{2d}\,\hat{\mathbf{x}} + \frac{V_4 - V_5}{2d}\,\hat{\mathbf{y}}} \tag{2.109}$$

FD approximation of the electric field vector

(central-difference approximation). Additionally, the surface charge density, ρ_s, on the conducting surfaces can be found by means of the boundary condition in Eq. (1.190). For example, assuming that the node 4 in Fig. 2.13(c) belongs to the surface of the inner conductor in Fig. 2.13(a), ρ_s at that point can be approximately evaluated as

$$\rho_{s4} = \varepsilon_0\, \hat{\mathbf{y}} \cdot \mathbf{E}_4 = \varepsilon_0\, E_{y4} = -\varepsilon_0 \left.\frac{\partial V}{\partial y}\right|_4 \approx -\varepsilon_0 \frac{V_1 - V_4}{d} = \varepsilon_0 \frac{V_a - V_1}{d}. \tag{2.110}$$

Finally, the total charge per unit length of each of the conductors, Eq. (1.31), can be found by numerically integrating ρ_s, that is, summing ρ_{si}, along the individual conductor contours. Thus, the per-unit-length charge of the inner conductor is given by

$$Q'_a = \oint_{C_a} \rho_s \, \mathrm{d}l \approx \sum_{i=1}^{N_a} \rho_{si} d, \tag{2.111}$$

where N_a denotes the total number of nodes along the contour C_a of the conductor, and similarly for the outer conductor.

Problems: 2.23 and 2.24; *MATLAB Exercises* (on Companion Website).

2.12 DEFINITION OF THE CAPACITANCE OF A CAPACITOR

Fig. 2.14 shows a system consisting of two metallic bodies (electrodes) embedded in a dielectric, and charged with equal charges of opposite polarities, Q and $-Q$. This system is referred to as a capacitor. The principal property of a capacitor is its capability to store the charge. The potential difference between the electrode carrying Q and the one with $-Q$ is called the capacitor voltage. The capacitor is linear if its dielectric is linear. The dielectric can be homogeneous or inhomogeneous.

In linear capacitors, the capacitor charge, Q, is linearly proportional to the capacitor voltage, V, i.e., $Q \propto V$. To prove this, assume for the moment that the capacitor charge is changed to $2Q$. The surface charge density, ρ_s, will remain distributed in the same way over the surfaces of electrodes, and its magnitude will

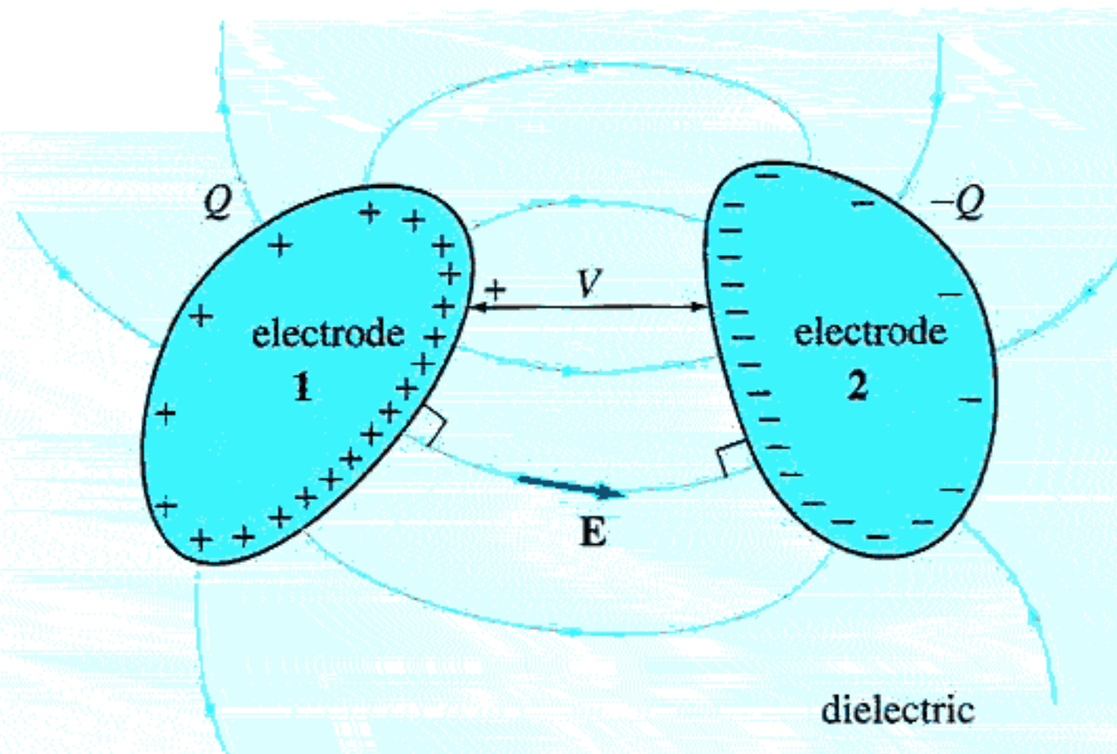

Figure 2.14 Capacitor.

double everywhere. The electric field intensity vector at an arbitrary point in the dielectric also becomes twice its previous value; for homogeneous dielectrics this is obvious from Eq. (1.38) with ε_0 replaced by ε, while for inhomogeneous dielectrics we first note that the vector $\mathbf{D}$ doubles [e.g., generalized Gauss' law, Eq. (2.43)], and then, since $\mathbf{E} \propto \mathbf{D}$ at any point of the dielectric [Eq. (2.47)], we find the same for the vector $\mathbf{E}$. Finally, because the capacitor voltage equals the line integral of $\mathbf{E}$ (along any path) between the electrodes [Eq. (1.90)], we conclude that the voltage doubles as well. Summarily, V doubles because Q is doubled, meaning that Q and V are linearly proportional to each other. This proportionality is customarily written as

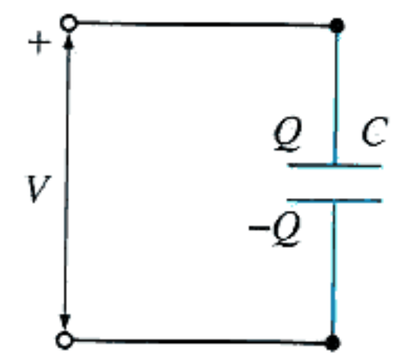

Figure 2.15 Circuit-theory representation of a capacitor.

$$Q = CV, \tag{2.112}$$

from which the constant C, termed the capacitance of the capacitor, is defined as

$$\boxed{C = \frac{Q}{V}.} \tag{2.113}$$

capacitance of a capacitor (unit: F)

The capacitance is a measure of the ability of a capacitor to hold the charge – per a volt of the applied voltage between the electrodes. It depends on the shape, size, and mutual position of the electrodes, and on the properties of the dielectric of the capacitor. For nonlinear capacitors, however, the capacitance depends also on the applied voltage,

$$\boxed{C = C(V),} \tag{2.114}$$

nonlinear capacitor

and a notable example is a varactor diode. The capacitance of a capacitor is always positive ($C > 0$), and the unit is the farad (F). For two-conductor transmission lines (two-body systems with very long conductors of uniform cross section), we define the capacitance per unit length of the line, that is, the capacitance for one meter (unit length) of the structure divided by 1 m,

$$\boxed{C' = C_{\text{p.u.l.}} = \frac{C}{l} = \frac{Q'}{V},} \tag{2.115}$$

capacitance p.u.l. of a transmission line (unit: F/m)

where C, l, and Q' are the total capacitance, length, and charge per unit length of the structure [see Eq. (1.31)]. The unit for C' is F/m.

Shown in Fig. 2.15 is the circuit-theory representation of a capacitor. In circuit theory, it is assumed that the charge is stored only in the capacitors in a circuit (i.e., on the capacitor electrodes), while the connecting conductors are considered as ideal short-circuiting elements with zero capacitance (and also with zero resistance and inductance, as we shall see in later chapters).

Finally, let us introduce another related concept, the capacitance of an isolated metallic body situated in a linear dielectric. It is defined as

$$\boxed{C = \frac{Q}{V_{\text{isolated body}}}.} \tag{2.116}$$

capacitance of an isolated metallic body

where Q is the charge of the body and $V_{\text{isolated body}}$ is its potential with respect to the reference point at infinity. Note that this definition can also be regarded as a special case of the definition in Eq. (2.113), for the capacitance of a two-body system, with the assumption that the second body, carrying $-Q$, is at infinity.

2.13 ANALYSIS OF CAPACITORS WITH HOMOGENEOUS DIELECTRICS

We now consider various examples of the analysis of capacitors with homogeneous dielectrics. The examples cover several characteristic types of capacitors and transmission lines of both theoretical and practical importance. The analysis of capacitors and transmission lines with different types of inhomogeneous dielectrics will be presented in the next section.

Example 2.8 **Spherical Capacitor**

Consider a spherical capacitor, which consists of two concentric spherical conductors, as shown in Fig. 2.16. Let the radius of the inner conductor be a and the inner radius of the outer conductor be b ($b > a$). Find the capacitance of the capacitor if it is filled with a homogeneous dielectric of permittivity ε.

Solution Assume that the capacitor is charged with a charge Q (the inner electrode carries $+Q$). Due to spherical symmetry, the electric field in the dielectric is radial and has the form given by Eq. (1.136). Applying the generalized Gauss' law in Eq. (2.55) to the spherical surface S of radius r ($a < r < b$) positioned concentrically with the capacitor electrodes [see the flux computation in Eq. (1.138)], we obtain

$$E(r) = \frac{Q}{4\pi\varepsilon r^2} \quad (a < r < b). \tag{2.117}$$

The capacitor voltage is [Eq. (1.90)]

$$V = \int_a^b E(r)\,\mathrm{d}r = \frac{Q}{4\pi\varepsilon}\left(\frac{1}{a} - \frac{1}{b}\right), \tag{2.118}$$

so that the capacitance comes out to be

capacitance of a spherical capacitor

$$\boxed{C = \frac{Q}{V} = \frac{4\pi\varepsilon ab}{b-a}.} \tag{2.119}$$

Example 2.9 **Capacitance of an Isolated Spherical Conductor**

Determine the expression for the capacitance of a metallic sphere of radius a situated in air.

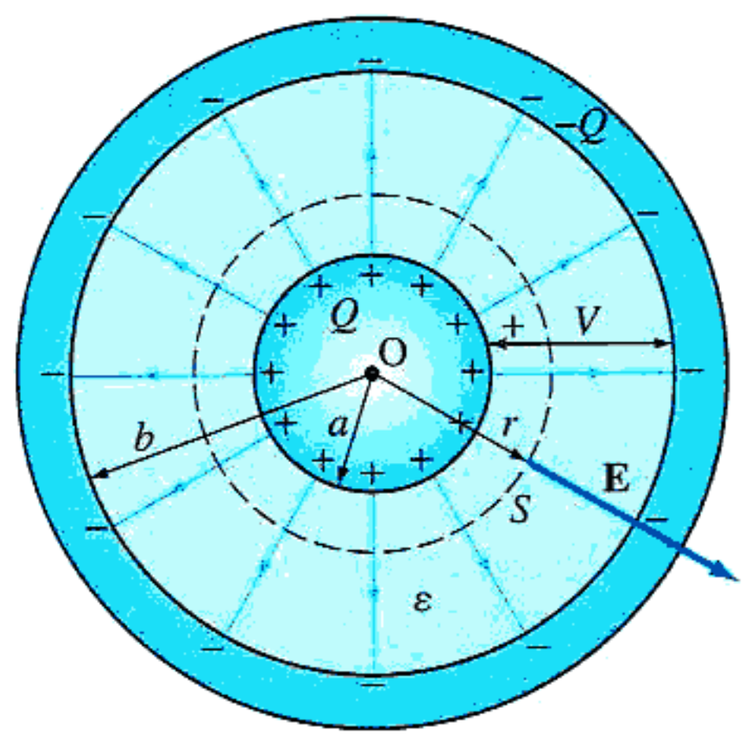

Figure 2.16 Spherical capacitor with a homogeneous dielectric; for Example 2.8.

Solution We use the definition of the capacitance of an isolated body, Eq. (2.116). The potential of the sphere if it carries a charge Q is (see Example 1.25)

$$V_{\text{sphere}} = \frac{Q}{4\pi\varepsilon_0 a}. \tag{2.120}$$

Its capacitance is hence

$$\boxed{C = \frac{Q}{V_{\text{sphere}}} = 4\pi\varepsilon_0 a.} \tag{2.121}$$

capacitance of an isolated metallic sphere in air

Note that an isolated sphere can be regarded as the inner electrode of a spherical capacitor whose outer electrode has an infinite radius, and that the same result for the sphere capacitance is obtained from Eq. (2.119) with $b \to \infty$.

Example 2.10 Coaxial Cable

A coaxial cable is a transmission line consisting of an inner cylindrical conductor (a wire) and an outer hollow cylindrical (tubular) conductor, with the conductors being coaxial with respect to each other, as depicted in Fig. 2.17. Note that this structure is sometimes referred to as a cylindrical capacitor. The inner conductor has a radius a, and the outer conductor has an inner radius b ($b > a$). The cable is filled with a homogeneous dielectric of permittivity ε. Find the capacitance per unit length, C', of the cable.

Solution This is a problem with cylindrical symmetry. The electric field is radial with respect to the cable axis (Fig. 2.17). By means of the generalized Gauss' law applied to a cylindrical surface S positioned in the dielectric coaxially with the cable conductors (see Example 1.26), we obtain the field intensity, and from it the voltage between the conductors,

$$E(r) = \frac{Q'}{2\pi\varepsilon r} \quad (a < r < b) \quad \longrightarrow \quad V = \int_a^b E(r)\,\mathrm{d}r = \frac{Q'}{2\pi\varepsilon}\ln\frac{b}{a}, \tag{2.122}$$

where Q' is the charge per unit length of the cable. Hence, the capacitance per unit length of the cable, Eq. (2.115), equals

$$\boxed{C' = \frac{Q'}{V} = \frac{2\pi\varepsilon}{\ln(b/a)}.} \tag{2.123}$$

capacitance p.u.l. of a coaxial cable

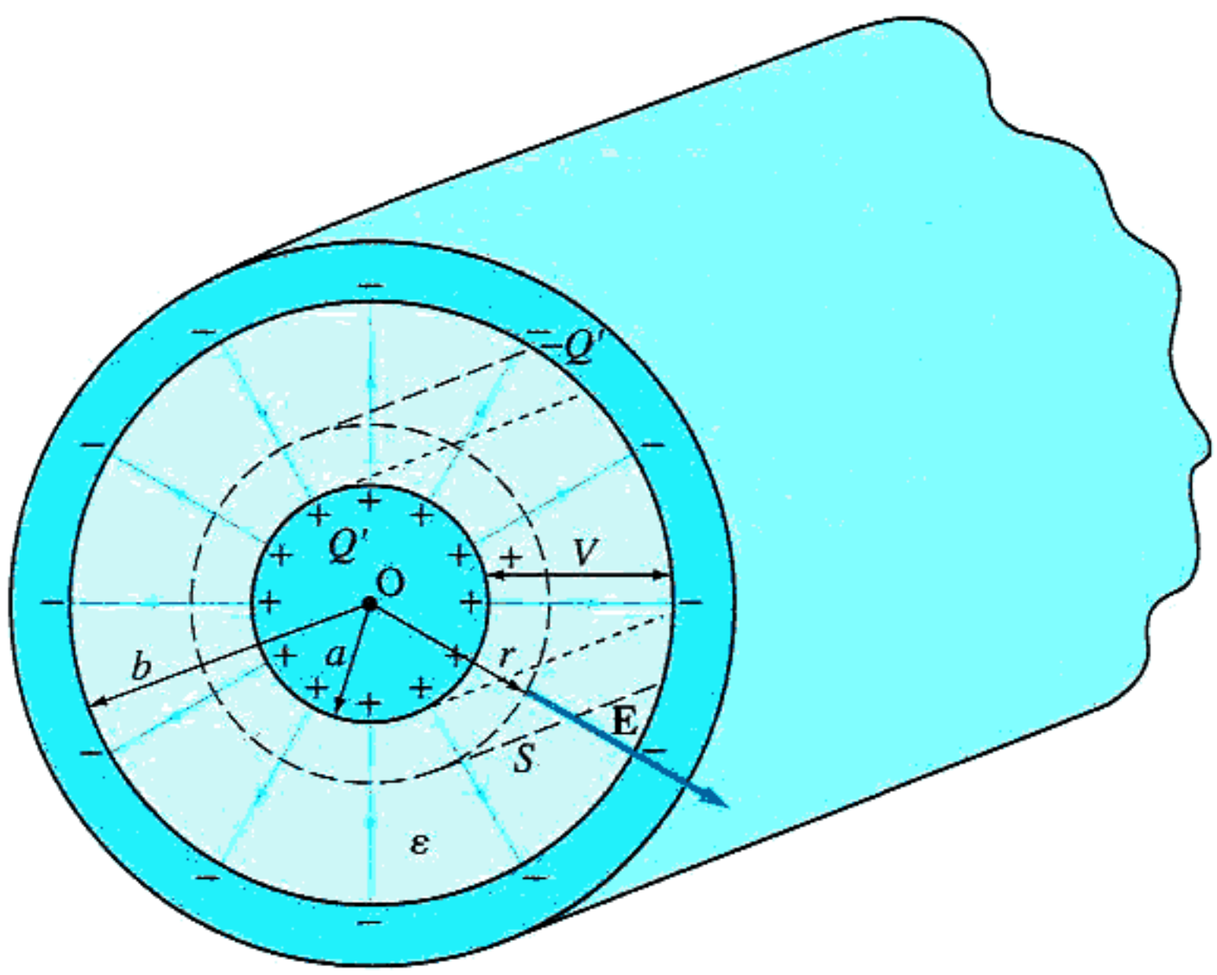

Figure 2.17 Coaxial cable (cylindrical capacitor) with a homogeneous dielectric; for Example 2.10.

We note that, combining together Eqs. (2.122),

electric field in a coaxial cable

$$\boxed{E(r) = \frac{V}{r\ln(b/a)},} \tag{2.124}$$

which is a very useful expression for the field intensity (in terms of the voltage) in a coaxial cable.

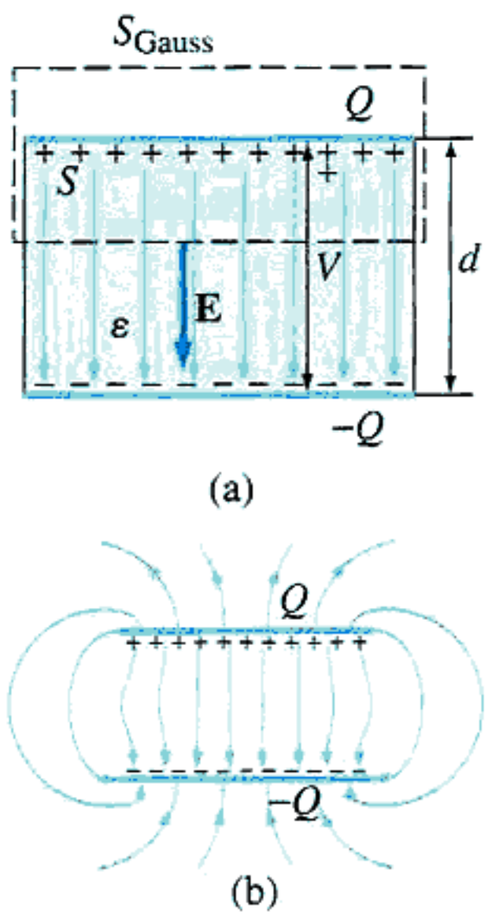

Figure 2.18 (a) Parallel-plate capacitor with a homogeneous dielectric and (b) fringing field for $\varepsilon_r = 1$; for Example 2.11.

Example 2.11 Parallel-Plate Capacitor

Consider a parallel-plate capacitor, which consists of two parallel metallic plates, each of area S, charged with Q and $-Q$. Let the space between the plates be filled with a homogeneous dielectric of permittivity ε, as shown in Fig. 2.18(a). Assume that the plate separation, d, is very small compared to the dimensions of the plates, so that the fringing effects can be neglected. Calculate the capacitance of the capacitor.

Solution Under given assumptions, the electric field in the dielectric is uniform, and there is no field outside the dielectric. Applying the generalized Gauss' law to a rectangular closed surface that encloses the upper plate [Fig. 2.18(a)], we get [see the left-hand side of Eq. (1.155)]

$$ES = \frac{Q}{\varepsilon}, \tag{2.125}$$

and hence $E = Q/(\varepsilon S)$. The voltage between the plates is

$$V = Ed = \frac{Qd}{\varepsilon S}, \tag{2.126}$$

and the capacitance of the capacitor

capacitance of a parallel-plate capacitor, fringing neglected

$$\boxed{C = \frac{Q}{V} = \varepsilon\frac{S}{d}.} \tag{2.127}$$

For arbitrary capacitor dimensions, there is a considerable fringing field extending far outside the capacitor and the field between the capacitor plates close to plate edges is not uniform (edge effects), as illustrated in Fig. 2.18(b) for $\varepsilon_r = 1$. With this, the actual capacitance is larger than the value obtained from Eq. (2.127).

Example 2.12 Electric Forces on Capacitor Plates

Electrodes of an air-filled capacitor are parallel square plates of edge lengths a. The distance between the plates is d, where $d \ll a$. The capacitor voltage is V. Find the electric forces on electrodes.

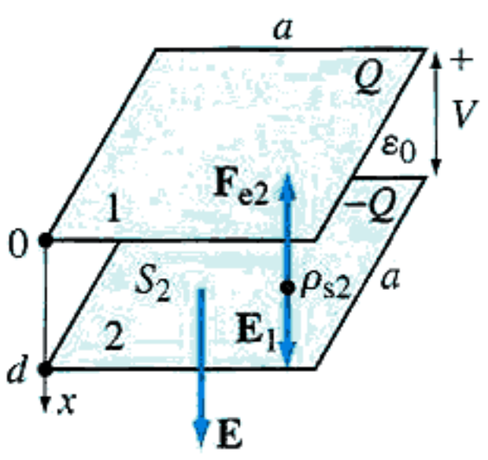

Figure 2.19 Evaluation of the electric force on the lower electrode of an air-filled parallel-plate capacitor; for Example 2.12.

Solution To find the net electric force on the lower plate (Fig. 2.19), we subdivide it into differentially small patches of surface areas $\mathrm{d}S$, and add up (integrate) the forces on individual patches that are due to the electric field of the other charged plate (the upper plate). Each charged patch can be considered as a point charge and the force $\mathrm{d}\mathbf{F}_{e2}$ on it can be calculated using Eq. (1.23), so that

$$\mathbf{F}_{e2} = \int_{S_2} \mathrm{d}\mathbf{F}_{e2} = \int_{S_2} \underbrace{\rho_{s2}\,\mathrm{d}S}_{\mathrm{d}Q_2}\,\mathbf{E}_1. \tag{2.128}$$

Here, ρ_{s2} is the surface charge density of the lower plate and $\mathbf{E}_1$ is the electric field intensity vector due to the charge of the upper plate. Since $d \ll a$, the fringing effects can be neglected, and these quantities are

$$\rho_{s2} = -\frac{Q}{S} \quad \text{and} \quad \mathbf{E}_1 = \frac{Q}{2\varepsilon_0 S}\hat{\mathbf{x}} \quad (S = a^2). \tag{2.129}$$

We realize that $\mathbf{E}_1$ equals a half of the total electric field intensity between the plates (the other half is due to the charge of the lower plate) and can also be obtained as the field of an infinite sheet of charge, Eq. (1.64). Q is the charge of the capacitor,

$$Q = CV = \frac{\varepsilon_0 SV}{d}, \tag{2.130}$$

and C is its capacitance. The force on the lower plate is hence

$$\mathbf{F}_{e2} = -\frac{\varepsilon_0 a^2 V^2}{2d^2}\,\hat{\mathbf{x}}. \tag{2.131}$$

The force on the upper electrode is opposite. The forces are attractive.

Note that, from Eq. (2.131),

$$\frac{F_{e2}}{S} = \frac{\varepsilon_0 V^2}{2d^2}. \tag{2.132}$$

By definition, this is the pressure of the force $\mathbf{F}_{e2}$ on the surface of the plate. We term it the electric pressure. The unit for pressure is Pa (pascal), where Pa = N/m^2. By introducing the total electric field intensity of the capacitor, $E = V/d$, the electric pressure can be expressed as

$$\boxed{p_e = \frac{1}{2}\varepsilon_0 E^2.} \tag{2.133}$$

electric pressure (unit: Pa)

This expression is valid for any conducting surface, with E standing for the local electric field intensity in the dielectric (air) near the surface. The pressure acts from the conductor toward the dielectric.

Example 2.13 **Microstrip Transmission Line**

Consider the transmission line shown in Fig. 2.20. It consists of a conducting strip of width w, resting on a dielectric substrate of permittivity ε and thickness h, and a ground plane beneath the substrate, and is called a microstrip line. Neglecting the fringing effects, determine the capacitance per unit length of this line.

Solution Without taking into account the fringing effects, the electric field of the line is uniform and localized in the dielectric below the strip only. The capacitance of the part of the line with length l is, from Eq. (2.127),

$$C = \varepsilon \frac{wl}{h}, \tag{2.134}$$

and the capacitance per unit length of the line comes out to be

$$\boxed{C' = \frac{C}{l} = \varepsilon \frac{w}{h}.} \tag{2.135}$$

capacitance p.u.l. of a microstrip line, fringing neglected

Note, however, that this expression is accurate only for $h \ll w$. Namely, as pointed out in Example 2.11, the actual electric field distribution in the structure with an arbitrary ratio w/h is quite different from that in Fig. 2.20. In a later chapter (on field analysis of transmission

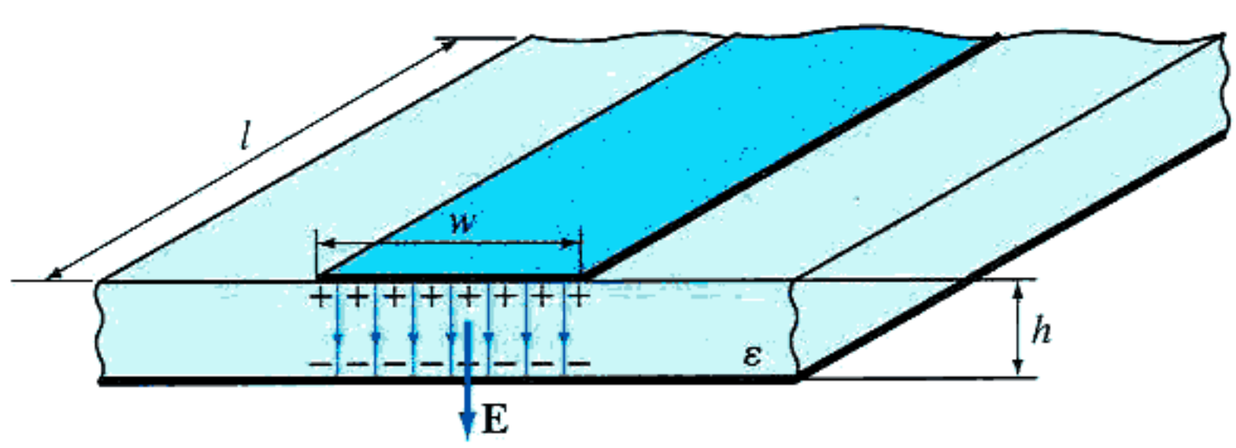

Figure 2.20 Microstrip transmission line; for Example 2.13.

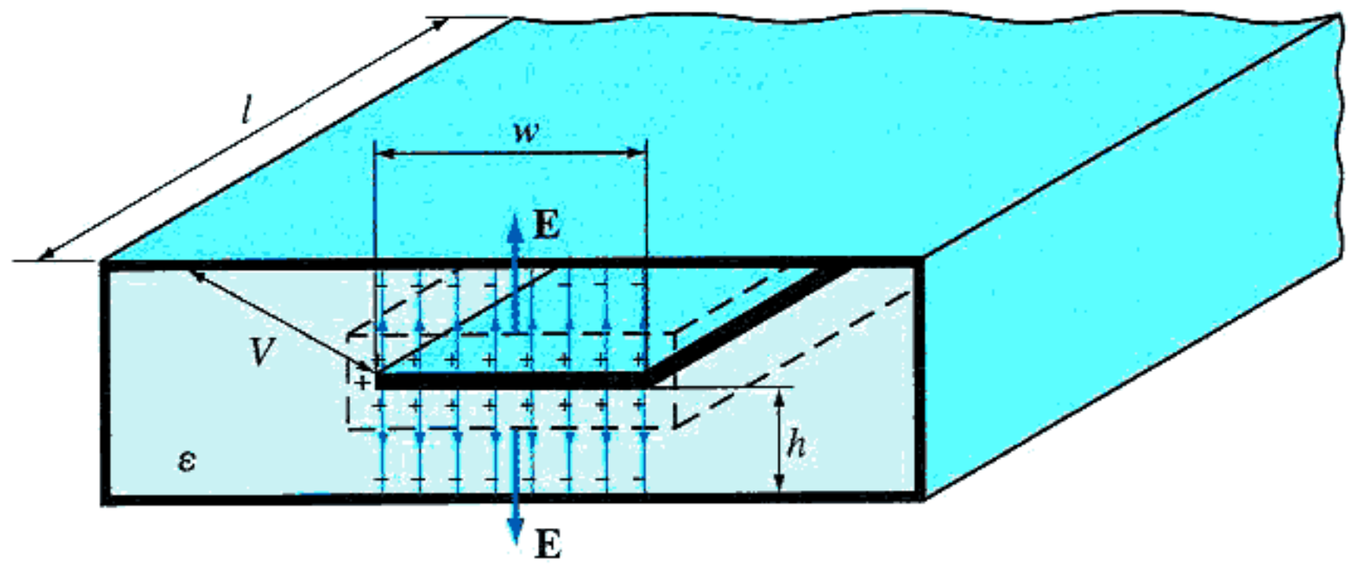

Figure 2.21 Strip transmission line; for Example 2.14.

lines), we shall present accurate empirical formulas for the electrostatic analysis of microstrip lines for all values of w/h.

Example 2.14 Strip Transmission Line

The transmission line consisting of a strip conductor between two conducting planes (large plates) at the same potential, as depicted in Fig. 2.21, is called a strip line. Let the width of the strip be w and its distance from each of the planes be h. The permittivity of the dielectric is ε. Assuming that $h \ll w$, find the capacitance per unit length of the line.

Solution Neglecting the fringing fields (as $h \ll w$) and applying the generalized Gauss' law to a rectangular closed surface of length l (along the line) that encloses the strip (Fig. 2.21), we have [see the left-hand side of Eq. (1.149)]

$$2Ewl = \frac{Q'l}{\varepsilon}, \tag{2.136}$$

where E is the electric field intensity between the line conductors and Q' the charge per unit length of the line. The voltage between the conductors is $V = Eh$, from which the per-unit-length capacitance of the line amounts to

capacitance p.u.l. of a strip line, fringing neglected

$$\boxed{C' = \frac{Q'}{V} = \frac{2\varepsilon w}{h}.} \tag{2.137}$$

Accurate analysis for an arbitrary ratio w/h will be presented in a later chapter.

Example 2.15 Thin Symmetrical Two-Wire Transmission Line

Fig. 2.22 shows a thin symmetrical two-wire transmission line in air. The charge per unit length of the line is Q', and the radii of the wire conductors, a, are much smaller than the distance between the conductor axes, d. Under these circumstances, compute the capacitance per unit length of the line.

Solution By superposition, the total electric field intensity vector in air is given by

$$\mathbf{E} = \mathbf{E}_1 + \mathbf{E}_2, \tag{2.138}$$

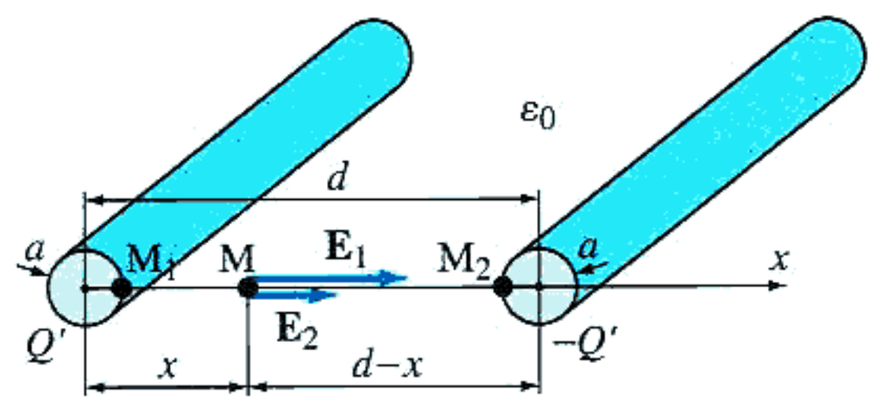

Figure 2.22 Two-wire transmission line with $d \gg a$ in air; for Example 2.15.

where $\mathbf{E}_1$ and $\mathbf{E}_2$ are the fields due to the individual charged conductors. Since $d \gg a$, these fields can be evaluated independently from each other, so we use the expression for the field of an isolated charged wire conductor in air, Eq. (1.196). At a point M in the plane containing the axes of conductors, Fig. 2.22, vectors $\mathbf{E}_1$ and $\mathbf{E}_2$ are collinear, and thus the resultant field intensity turns out to be

$$E = E_1 + E_2 = \frac{Q'}{2\pi\varepsilon_0}\left(\frac{1}{x} + \frac{1}{d-x}\right), \tag{2.139}$$

where x stands for the coordinate defining the position of the point M.

The voltage between the conductors is

$$\begin{aligned} V &= \int_{x=a}^{d-a} E\,\mathrm{d}x = \frac{Q'}{2\pi\varepsilon_0}\left[\int_a^{d-a}\frac{dx}{x} - \int_a^{d-a}\frac{\mathrm{d}(d-x)}{d-x}\right] \\ &= \frac{Q'}{2\pi\varepsilon_0}\left[\ln x|_a^{d-a} - \ln(d-x)|_a^{d-a}\right] = \frac{Q'}{2\pi\varepsilon_0}\left(\ln\frac{d-a}{a} - \ln\frac{a}{d-a}\right) \\ &= \frac{Q'}{\pi\varepsilon_0}\ln\frac{d-a}{a} \approx \frac{Q'}{\pi\varepsilon_0}\ln\frac{d}{a}, \end{aligned} \tag{2.140}$$

where the use is made of the approximate relation $d - a \approx d$. The capacitance per unit length of the line is

$$\boxed{C' = \frac{Q'}{V} = \frac{\pi\varepsilon_0}{\ln(d/a)}.} \tag{2.141}$$

capacitance p.u.l. of a thin two-wire line

Let us now obtain the same result in a different way, using the expression for the potential due to an isolated charged wire conductor in air, Eq. (1.197) for $r \geq a$, and the superposition principle. We adopt a point M_2 on the surface of the right conductor (Fig. 2.22) to be the reference point for potential ($V_{\mathrm{M}_2} = 0$). The potential at a point M_1 on the surface of the other conductor (with respect to the reference point) amounts to

$$V_{\mathrm{M}_1} = \frac{Q'}{2\pi\varepsilon_0}\ln\frac{d-a}{a} + \frac{-Q'}{2\pi\varepsilon_0}\ln\frac{a}{d-a}, \tag{2.142}$$

with the two terms representing the potentials [Eq. (1.197)] due to the conductors with per-unit-length charges Q' and $-Q'$, respectively. The capacitance per unit length of the line is

$$C' = \frac{Q'}{V_{\mathrm{M}_1} - V_{\mathrm{M}_2}} = \frac{Q'}{V_{\mathrm{M}_1}}, \tag{2.143}$$

which yields the same expression as in Eq. (2.141).

Example 2.16 Three Parallel Equidistant Wires

Three parallel thin wire conductors are situated in air, as depicted in Fig. 2.23. The wire radii are $a = 1$ mm and the distance between the axes of conductors is $d = 50$ mm. Two wires are galvanically connected to each other. Determine the capacitance per unit length of this system.

Solution This is a two-conductor transmission line, which we analyze as a capacitor of infinite length. The first electrode of the capacitor (the first conductor of the transmission line) is the isolated (free) wire (wire 1), while the other electrode (the other line conductor) consists of the two short-circuited wires (wires 2 and 3), which are at the same potential. Let the electrodes be charged by Q' and $-Q'$ per unit of their length, respectively. Because of symmetry, the charge $-Q'$ of the second electrode is distributed equally between wires 2 and 3, as indicated in Fig. 2.23. We assume that there is no charge on the short-circuiting conductor.

Let us proclaim the second electrode of the capacitor to be at a zero potential. The potential of the first electrode, i.e., the potential at the point M_1 on the surface of wire 1 (Fig. 2.23), with respect to the reference point M_2 taken on the surface of wire 3 ($V_{\mathrm{M}_2} = 0$)

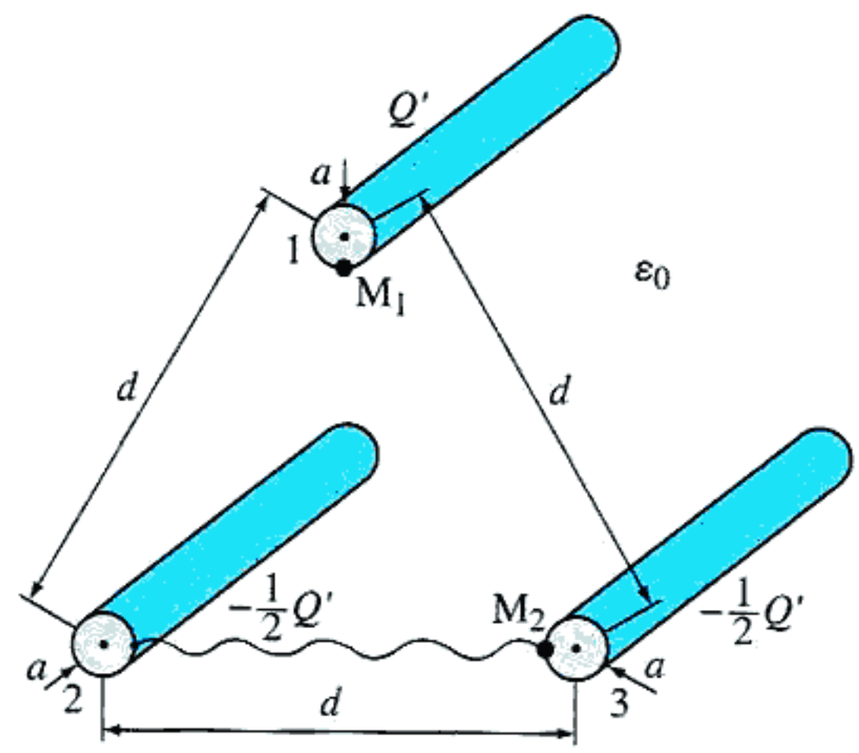

Figure 2.23 Transmission line consisting of an isolated (free) wire and two galvanically interconnected wires in air; for Example 2.16.

is the sum of the corresponding potentials due to wires 1, 2, and 3, respectively. By means of Eq. (1.197) for $r \geq a$,

$$V_{M_1} = \frac{Q'}{2\pi\varepsilon_0}\ln\frac{d}{a} + \frac{-Q'/2}{2\pi\varepsilon_0}\ln\frac{d}{d} + \frac{-Q'/2}{2\pi\varepsilon_0}\ln\frac{a}{d} = \frac{3Q'}{4\pi\varepsilon_0}\ln\frac{d}{a}. \tag{2.144}$$

The capacitance per unit length of the line (capacitor) is

$$C' = \frac{Q'}{V_{M_1}} = \frac{4\pi\varepsilon_0}{3\ln(d/a)} = 9.48 \text{ pF/m}. \tag{2.145}$$

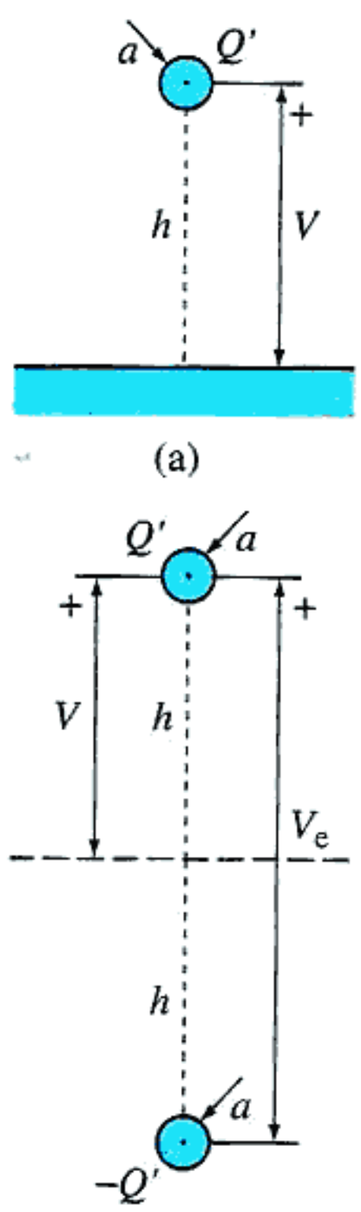

Figure 2.24 (a) Thin wire conductor above a grounded conducting plane in air and (b) equivalent two-wire line; for Example 2.17.

Example 2.17 Thin Wire Conductor above a Ground Plane

Consider a transmission line that consists of a thin wire conductor and a grounded conducting plane, as shown in Fig. 2.24(a). The medium is air, the wire is parallel to the plane, the height of the wire axis with respect to the plane is h, and the wire radius is a ($a \ll h$). Find the capacitance per unit length of this line.

Solution Assume that the charge per unit length of the line is Q', namely, that the wire is charged by Q' and the plane by $-Q'$ per unit length. By image theory (Figs. 1.47 and 1.49), we can replace the conducting plane by a negative image of the charged wire and obtain the equivalent thin two-wire line in Fig. 2.24(b), with the distance between the conductor axes $d = 2h$. Of course, the two systems are equivalent only in the upper half-space. The voltage between the conductors in the original system (wire-plane) equals a half of the voltage in the equivalent system (wire-wire). Hence, the capacitance per unit length of the wire-plane transmission line comes out to be (see Fig. 2.24)

$$C' = \frac{Q'}{V} = \frac{Q'}{V_e/2} = 2\frac{Q'}{V_e} = 2C'_e = \frac{2\pi\varepsilon_0}{\ln(2h/a)}, \tag{2.146}$$

where C'_e is the capacitance per unit length of the equivalent two-wire line, which is computed from Eq. (2.141).

Problems: 2.25–2.41; *Conceptual Questions* (on Companion Website): 2.10–2.18; *MATLAB Exercises* (on Companion Website).

2.14 ANALYSIS OF CAPACITORS WITH INHOMOGENEOUS DIELECTRICS

In this section, we deal with systems (capacitors) containing inhomogeneous dielectrics, and, specifically, with two basic classes of systems with dielectric inhomogeneity. The first class includes systems in which the dielectric permittivity varies (abruptly or continuously[5]) in the direction of the electric field lines of the same system if air-filled. In the second class of systems, the dielectric permittivity varies in the direction normal to the electric field lines of the air-filled system. As we shall see, the way in which the electric flux density vector, **D**, varies in the first class of dielectrics is the same as in the corresponding air-filled system, while in the second class of dielectrics this is true for the electric field intensity vector, **E**. Hence, the two classes of systems are referred to as D- and E-systems, respectively.

To illustrate these concepts, consider the two parallel-plate capacitors with piece-wise homogeneous dielectrics shown in Fig. 2.25. The permittivities of dielectric pieces are ε_1 and ε_2. Assume that the fringing effects are negligible, and that the field in each dielectric piece is uniform.

The capacitor in Fig. 2.25(a) belongs to the first class of systems with dielectric inhomogeneity – the dielectric permittivity (abruptly) changes in the direction of the field lines, perpendicularly to the capacitor plates, so it is a D-system. From the generalized Gauss' law, Eq. (2.43), applied to a rectangular closed surface enclosing the plate charged with Q, with the right-hand side positioned in either one of the dielectrics, we have

$$\boxed{D_1 = D_2 = D = \frac{Q}{S},} \tag{2.147}$$

D = const, capacitor in Fig. 2.25(a)

where S is the surface area of the plates. That $D_1 = D_2$ is also obvious from the boundary condition for the normal components of **D**, Eq. (2.81), applied to the interface between the two dielectrics. The electric field intensities in the dielectrics are not the same,

$$E_1 = \frac{D}{\varepsilon_1} = \frac{Q}{\varepsilon_1 S} \quad \text{and} \quad E_2 = \frac{D}{\varepsilon_2} = \frac{Q}{\varepsilon_2 S}. \tag{2.148}$$

The voltage of the capacitor comes out to be

$$V = E_1 d_1 + E_2 d_2 = \frac{Q}{S}\left(\frac{d_1}{\varepsilon_1} + \frac{d_2}{\varepsilon_2}\right), \tag{2.149}$$

with d_1 and d_2 standing for thicknesses of the layers. The capacitance is

$$C = \frac{Q}{V} = \frac{\varepsilon_1 \varepsilon_2 S}{\varepsilon_2 d_1 + \varepsilon_1 d_2}. \tag{2.150}$$

In the capacitor in Fig. 2.25(b), the change of dielectric characteristics is in the direction normal to the field lines – this is an E-system (the second class of systems). By means of Eq. (1.90) applied to a straight path between the capacitor plates, positioned in either one of the dielectrics,

$$\boxed{E_1 = E_2 = E = \frac{V}{d},} \tag{2.151}$$

E = const, capacitor in Fig. 2.25(b)

[5]Inhomogeneous dielectrics composed of a number of homogeneous pieces of different permittivities are called piece-wise homogeneous dielectrics; continuously inhomogeneous dielectrics, on the other side, are characterized by continuous spatial variations of permittivity.

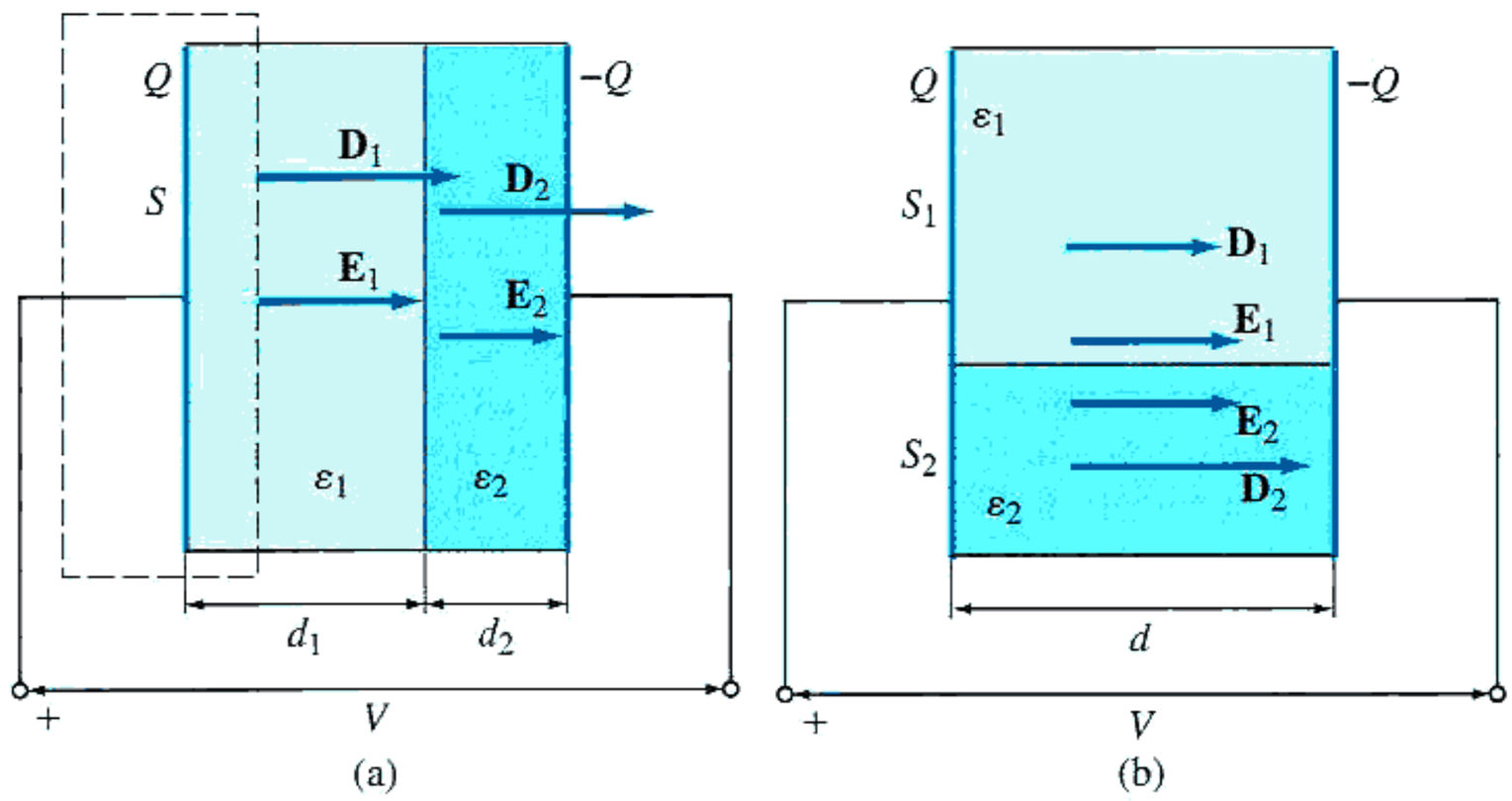

Figure 2.25 Capacitors with two-layer dielectrics representing a D-system (a) and E-system (b).

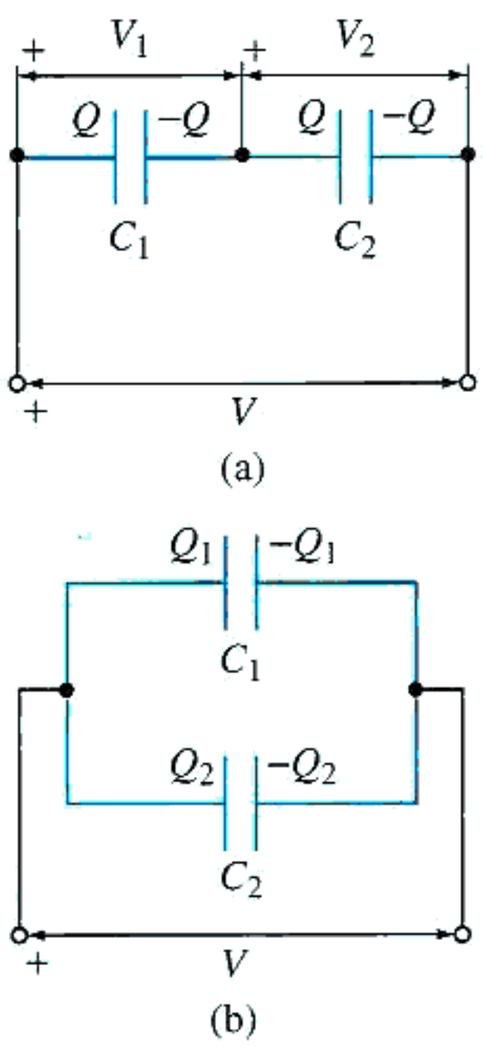

Figure 2.26 Equivalent circuits for two capacitors in series (a) and parallel (b).

where V is the capacitor voltage and d the separation between plates [$E_1 = E_2$ is also obtained from the boundary condition for tangential components of $\mathbf{E}$, Eq. (2.79), applied to the dielectric-dielectric interface]. The electric flux density is discontinuous across the interface,

$$D_1 = \varepsilon_1 E = \frac{\varepsilon_1 V}{d} \quad \text{and} \quad D_2 = \varepsilon_2 E = \frac{\varepsilon_2 V}{d}. \tag{2.152}$$

Applying the generalized Gauss' law to a rectangular surface positioned about the plate with the charge Q yields

$$Q = D_1 S_1 + D_2 S_2 = (\varepsilon_1 S_1 + \varepsilon_2 S_2)\frac{V}{d}, \tag{2.153}$$

with S_1 and S_2 being surface areas of the parts of the plate interfacing the individual dielectric layers, and the capacitance is

$$C = \frac{Q}{V} = \frac{\varepsilon_1 S_1 + \varepsilon_2 S_2}{d}. \tag{2.154}$$

The systems in Fig. 2.25 can be explained also from the circuit-theory point of view. Such a view is usually much simpler than the full field-theory view, and is sufficient for some evaluations. Let us compute the capacitances of capacitors in Fig. 2.25 using the associated equivalent circuits.

Note that the interface between the dielectric layers of the capacitor in Fig. 2.25(a) is equipotential, and nothing will change in the system if we metalize this surface, i.e., insert a metallic foil between the layers. We thus obtain two capacitors in series, as indicated in the equivalent circuit in Fig. 2.26(a). The charges of both capacitors are the same, and therefore

$$V = V_1 + V_2 = \frac{Q}{C_1} + \frac{Q}{C_2} = Q\left(\frac{1}{C_1} + \frac{1}{C_2}\right), \tag{2.155}$$

from which the total capacitance of the system amounts to

equivalent capacitance of two capacitors in series

$$\boxed{C = \frac{Q}{V} = \frac{C_1 C_2}{C_1 + C_2}.} \tag{2.156}$$

With the use of Eq. (2.127), the capacitances of individual capacitors are

$$C_1 = \varepsilon_1 \frac{S}{d_1} \quad \text{and} \quad C_2 = \varepsilon_2 \frac{S}{d_2}, \tag{2.157}$$

resulting in the same expression for C as in Eq. (2.150).

On the other hand, the system in Fig. 2.25(b) represents two capacitors in parallel, the equivalent circuit of which is shown in Fig. 2.26(b). The voltages of both capacitors are the same, so that

$$Q = Q_1 + Q_2 = C_1 V + C_2 V = (C_1 + C_2)\, V. \tag{2.158}$$

The total capacitance of the system is

$$\boxed{C = \frac{Q}{V} = C_1 + C_2,} \tag{2.159}$$

equivalent capacitance of two capacitors in parallel

where,

$$C_1 = \varepsilon_1 \frac{S_1}{d} \quad \text{and} \quad C_2 = \varepsilon_2 \frac{S_2}{d}, \tag{2.160}$$

which gives the same result as in Eq. (2.154).

Example 2.18 Spherical Capacitor with Two Concentric Dielectric Layers

A spherical capacitor is filled with two concentric dielectric layers. The relative permittivity of the layer near the inner electrode of the capacitor is $\varepsilon_{r1} = 4$, and that of the other layer $\varepsilon_{r2} = 2$. The radius of the inner electrode is $a = 10$ mm, the radius of the boundary surface between the layers is $b = 25$ mm, and the inner radius of the outer electrode is $c = 35$ mm. If the voltage between the inner and outer electrode is $V = 10$ V, what are (a) the charge of the capacitor and (b) the total bound charge on the interface between the layers?

Solution

(a) This is a D-system, and the electric flux density vector is of the form

$$\mathbf{D} = D(r)\,\hat{\mathbf{r}}, \tag{2.161}$$

where r and $\hat{\mathbf{r}}$ are the radial coordinate and the radial unit vector in the spherical coordinate system with the origin at the capacitor center, as shown in Fig. 2.27. The generalized Gauss' law applied to a spherical surface placed in either the first or the second layer tells us that

$$D(r) = \frac{Q}{4\pi r^2}, \quad a < r < c, \tag{2.162}$$

where Q is the capacitor charge – to be determined.

The electric field intensity vector is $\mathbf{E}_1 = \mathbf{D}/\varepsilon_1$ in the first layer and $\mathbf{E}_2 = \mathbf{D}/\varepsilon_2$ in the second one. The capacitor voltage is given by

$$V = \int_a^b E_1(r)\,\mathrm{d}r + \int_b^c E_2(r)\,\mathrm{d}r = \frac{Q}{4\pi}\left[\frac{1}{\varepsilon_1}\left(\frac{1}{a} - \frac{1}{b}\right) + \frac{1}{\varepsilon_2}\left(\frac{1}{b} - \frac{1}{c}\right)\right], \tag{2.163}$$

from which

$$Q = 4\pi\varepsilon_0 \left(\frac{b-a}{\varepsilon_{r1} ab} + \frac{c-b}{\varepsilon_{r2} bc}\right)^{-1} V = CV = 53.7 \text{ pC}, \tag{2.164}$$

where $C = 5.37$ pF is the capacitance of the capacitor.

Note that the capacitor charge can also be found by computing C as the equivalent total capacitance of a series connection of two spherical capacitors with homogeneous dielectrics, Eq. (2.156), where, using Eq. (2.119),

$$C_1 = \frac{4\pi\varepsilon_{r1}\varepsilon_0 ab}{b-a} = 7.4 \text{ pF} \quad \text{and} \quad C_2 = \frac{4\pi\varepsilon_{r2}\varepsilon_0 bc}{c-b} = 19.5 \text{ pF}. \tag{2.165}$$

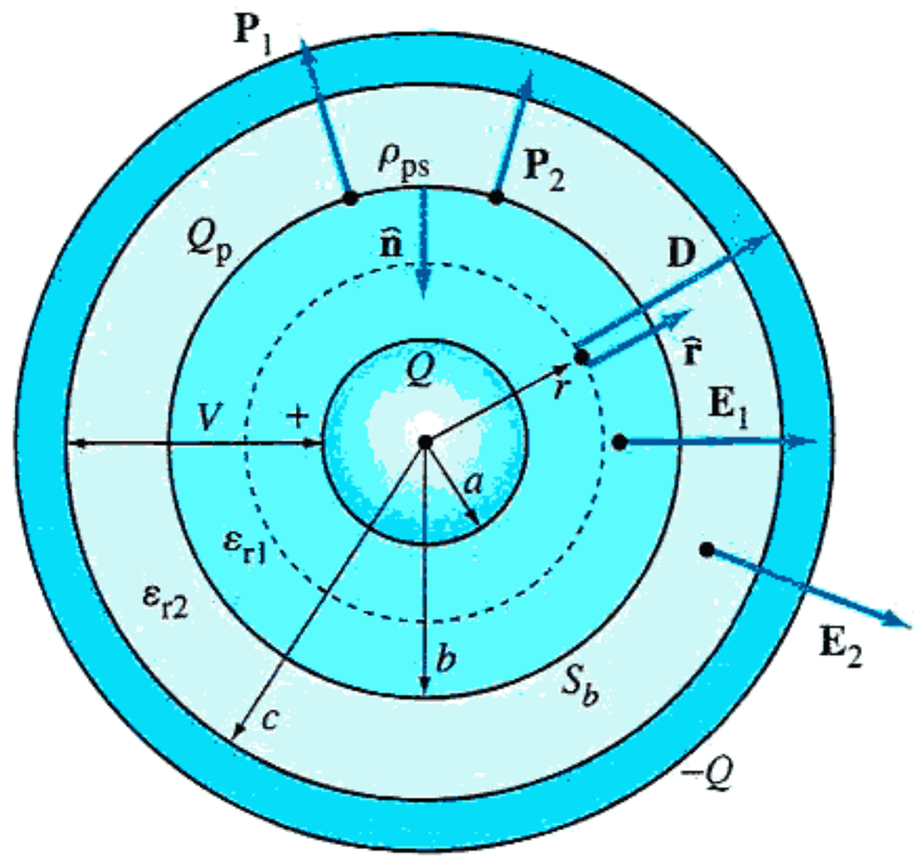

Figure 2.27 Spherical capacitor with two concentric homogeneous dielectric layers; for Example 2.18.

(b) From Eqs. (2.59) and (2.47), the intensities of the polarization vector in the dielectric layers with respect to the positive (outward) radial direction (Fig. 2.27) are

$$P_1(r) = \frac{\varepsilon_{r1} - 1}{\varepsilon_{r1}} D(r) \quad \text{and} \quad P_2(r) = \frac{\varepsilon_{r2} - 1}{\varepsilon_{r2}} D(r). \tag{2.166}$$

By means of Eq. (2.89), the bound surface charge density on the boundary surface S_b between the layers turns out to be

$$\rho_{ps} = \hat{\mathbf{n}} \cdot \mathbf{P}_2 - \hat{\mathbf{n}} \cdot \mathbf{P}_1 = -P_2(b^+) + P_1(b^-) = \left(\frac{\varepsilon_{r1} - 1}{\varepsilon_{r1}} - \frac{\varepsilon_{r2} - 1}{\varepsilon_{r2}} \right) D(b), \tag{2.167}$$

and hence the total bound charge on the surface

$$Q_p = \rho_{ps} S_b = \rho_{ps} 4\pi b^2 = \left(\frac{\varepsilon_{r1} - 1}{\varepsilon_{r1}} - \frac{\varepsilon_{r2} - 1}{\varepsilon_{r2}} \right) Q = 13.43 \text{ pC}. \tag{2.168}$$

Example 2.19 Spherical Capacitor with a Continuously Inhomogeneous Dielectric

A spherical capacitor is filled with a continuously inhomogeneous dielectric, whose permittivity depends on the distance r from the capacitor center and is given by the function $\varepsilon(r) = 3\varepsilon_0 b/r$, $a < r < b$, where a and b are radii of the inner and outer capacitor electrode, respectively. The outer electrode is grounded and the potential of the inner electrode is V. Find (a) the capacitance of the capacitor and (b) the bound charge distribution of the dielectric. (c) By integrating the charge densities in (b), prove that the total bound charge of the dielectric is zero.

Solution

(a) Let us subdivide the dielectric into thin spherical concentric layers of radii r and thicknesses $\mathrm{d}r$, $a < r < b$, as shown in Fig. 2.28. Each thin layer can be considered as being homogeneous, of permittivity $\varepsilon(r)$. It is now obvious that this capacitor represents a generalization of that in Fig. 2.27, which has only two such layers. Therefore, the electric flux density vector in the two capacitors is the same, given by Eqs. (2.161) and (2.162). Here, $\mathbf{E} = \mathbf{D}/\varepsilon(r)$, and the potential of the inner electrode with respect to the ground (outer electrode) and the capacitance of the capacitor can be obtained as

$$V = \int_a^b E(r)\,\mathrm{d}r = \frac{Q}{4\pi} \int_a^b \frac{\mathrm{d}r}{r^2 \varepsilon(r)} \quad \longrightarrow \quad C = \frac{Q}{V} = 4\pi \left[\int_a^b \frac{\mathrm{d}r}{r^2 \varepsilon(r)} \right]^{-1}. \tag{2.169}$$

Specifically, for the given function $\varepsilon(r)$, $C = 12\pi\varepsilon_0 b/\ln(b/a)$.

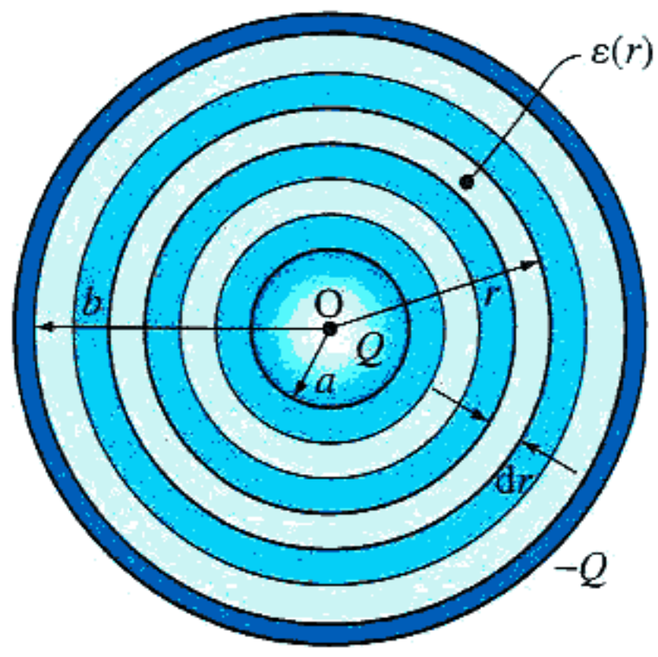

Figure 2.28 Spherical capacitor with a continuously inhomogeneous dielectric of permittivity $\varepsilon(r)$, subdivided into differentially thin homogeneous layers; for Example 2.19.

(b) The polarization vector in the dielectric is radial, with intensity [Eqs. (2.59) and (2.47)]

$$P(r) = \frac{\varepsilon(r) - \varepsilon_0}{\varepsilon(r)} D(r) = \frac{\varepsilon_0(3b - r)V}{r^2 \ln(b/a)}. \tag{2.170}$$

By means of Eqs. (2.19) and (1.171), the bound volume charge density inside the dielectric amounts to

$$\rho_p = -\nabla \cdot \mathbf{P} = -\frac{1}{r^2}\frac{d}{dr}\left[r^2 P(r)\right] = \frac{\varepsilon_0 V}{r^2 \ln(b/a)}, \tag{2.171}$$

while, from Eq. (2.23), the bound surface charge densities on the surfaces of the dielectric near the inner and outer capacitor electrodes are

$$\rho_{psa} = -P(a^+) = -\frac{\varepsilon_0(3b - a)V}{a^2 \ln(b/a)} \quad \text{and} \quad \rho_{psb} = P(b^-) = \frac{2\varepsilon_0 V}{b \ln(b/a)}, \tag{2.172}$$

respectively.

(c) To verify that the total bound charge of the dielectric is zero, we write

$$\begin{aligned} Q_p &= \int_a^b \rho_p(r) \underbrace{4\pi r^2\, dr}_{dv} + \rho_{psa} \underbrace{4\pi a^2}_{S_a} + \rho_{psb} \underbrace{4\pi b^2}_{S_b} \\ &= \frac{4\pi\varepsilon_0(b - a)V}{\ln(b/a)} - \frac{4\pi\varepsilon_0(3b - a)V}{\ln(b/a)} + \frac{8\pi\varepsilon_0 bV}{\ln(b/a)} = 0, \end{aligned} \tag{2.173}$$

where dv is the volume of the thin layer of radius r in Fig. 2.28, while S_a and S_b are the areas of surfaces of inner and outer capacitor electrodes, respectively.

Example 2.20 Spherical Capacitor Half Filled with a Liquid Dielectric

A spherical capacitor has a liquid dielectric occupying a half of the space between the electrodes. The radii of electrodes are a and b ($a < b$), and the permittivity of the dielectric is ε. Determine the capacitance of the capacitor.

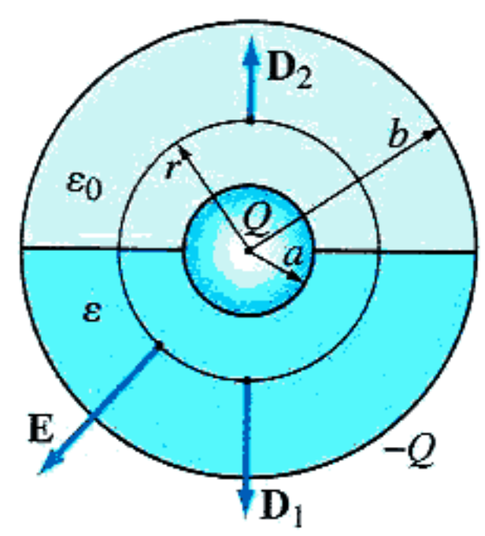

Figure 2.29 Analysis of a spherical capacitor half filled with a liquid dielectric; for Example 2.20.

Solution Assume that the capacitor is charged by Q, as indicated in Fig. 2.29. This is an E-system, and the electric field intensity vector, $\mathbf{E}$, is entirely radial. From the boundary condition for tangential components of the electric field intensity vector, Eq. (2.79), its magnitude depends on the radial spherical coordinate, r, only, i.e., it is the same at all points of a sphere of radius r ($a < r < b$), shown in Fig. 2.29.

The electric flux density vector is $\mathbf{D}_1 = \varepsilon_r\varepsilon_0\mathbf{E}$ in the dielectric and $\mathbf{D}_2 = \varepsilon_0\mathbf{E}$ in air. Applying the generalized Gauss' law to the sphere of radius r (Fig. 2.29), we obtain

$$D_1 2\pi r^2 + D_2 2\pi r^2 = Q \quad \longrightarrow \quad (\varepsilon_r + 1)\varepsilon_0 E(r) 2\pi r^2 = Q, \tag{2.174}$$

and hence

$$E(r) = \frac{Q}{2\pi(\varepsilon_r + 1)\varepsilon_0 r^2}. \tag{2.175}$$

The capacitor voltage and capacitance then come out to be

$$V = \int_a^b E(r)\,\mathrm{d}r = \frac{Q}{2\pi(\varepsilon_r + 1)\varepsilon_0}\left(\frac{1}{a} - \frac{1}{b}\right) \quad \longrightarrow \quad C = \frac{Q}{V} = \frac{2\pi(\varepsilon_r + 1)\varepsilon_0 ab}{b - a}. \tag{2.176}$$

We note that this expression for C represents the equivalent total capacitance of a parallel connection of two hemispherical capacitors with homogeneous dielectrics, Eq. (2.159), where $C_1 = 2\pi\varepsilon_r\varepsilon_0 ab/(b - a)$ and $C_2 = 2\pi\varepsilon_0 ab/(b - a)$.

Example 2.21 Coaxial Cable with a Continuously Inhomogeneous Dielectric

Shown in Fig. 2.30(a) is a cross section of a coaxial cable with a continuously inhomogeneous dielectric, the permittivity of which is given by a function $\varepsilon(\phi) = (3 + \sin\phi)\varepsilon_0$, $\phi \in [0, 2\pi]$. The voltage between the inner and outer conductor of the cable is V. Compute (a) the capacitance per unit length of the cable and (b) the distribution of free charges on the cable conductors.

Solution

(a) Let us subdivide the dielectric into thin sectors (slices) defined by elemental azimuthal angles $\mathrm{d}\phi$, as depicted in Fig. 2.30(b). Each such sector can be considered as being homogeneous, of permittivity $\varepsilon(\phi)$. This way it becomes obvious that dielectric inhomogeneities in the systems in Figs. 2.29 and 2.30 are of the same type.

Because of symmetry, the electric field intensity vector in the dielectric is radial, and, based on the boundary condition in Eq. (2.79), $\mathbf{E}_1 = \mathbf{E}_2$, $\mathbf{E}_2 = \mathbf{E}_3$, $\mathbf{E}_3 = \mathbf{E}_4$, ... [Fig. 2.30(b)]. This means that E is constant on a cylindrical surface of radius r ($a < r < b$), i.e., it is a function of the radial cylindrical coordinate, r, only. The electric flux density vector is $\mathbf{D}(r, \phi) = \varepsilon(\phi)\mathbf{E}(r)$. Generalized Gauss' law applied to a cylinder of radius r and height (length) h gives

$$\int_{\phi=0}^{2\pi} \underbrace{\varepsilon(\phi)E(r)}_{D}\,\underbrace{r\,\mathrm{d}\phi h}_{\mathrm{d}S} = \underbrace{Q'h}_{Q_S} \quad \longrightarrow \quad E(r) = \frac{Q'}{r\int_0^{2\pi}\varepsilon(\phi)\,\mathrm{d}\phi}, \tag{2.177}$$

where $\mathrm{d}S$ is the area of an elemental strip of width $r\,\mathrm{d}\phi$ and height h, and Q' is the charge per unit length of the cable. The voltage between the cable conductors and the

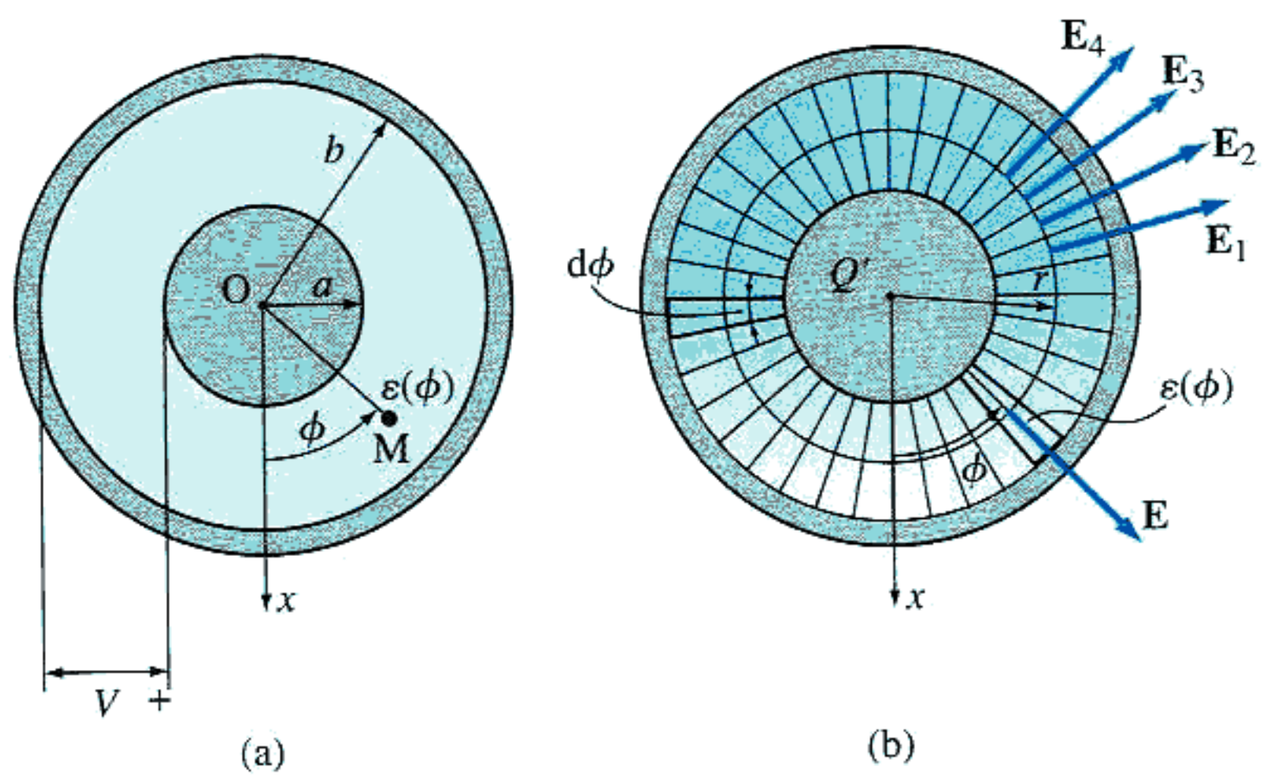

Figure 2.30 Analysis of a coaxial cable with a continuously inhomogeneous dielectric of permittivity $\varepsilon(\phi)$: (a) cross-sectional view of the structure and (b) subdivision of the dielectric into differentially thin homogeneous sectors; for Example 2.21.

capacitance per unit length are then obtained as

$$V = \int_{r=a}^{b} E(r)dr = \frac{Q' \ln(b/a)}{\int_0^{2\pi} \varepsilon(\phi)\, d\phi} \quad \longrightarrow \quad C' = \frac{Q'}{V} = \frac{\int_0^{2\pi} \varepsilon(\phi)\, d\phi}{\ln(b/a)} = \frac{6\pi\varepsilon_0}{\ln(b/a)}. \quad (2.178)$$

(b) From Eqs. (2.177) and (2.178), the electric field intensity, $E(r)$, is the same as in the air-filled coaxial cable, Eq. (2.124), which is expected, because this is an E-system. Using Eq. (2.58), the free surface charge density on the inner conductor of the cable is

$$\rho_{sa}(\phi) = \varepsilon(\phi)E(a^+) = \frac{\varepsilon_0(3+\sin\phi)V}{a\ln(b/a)}, \quad (2.179)$$

while on the outer conductor,

$$\rho_{sb}(\phi) = -\varepsilon(\phi)E(b^-) = -\frac{\varepsilon_0(3+\sin\phi)V}{b\ln(b/a)}. \quad (2.180)$$

Example 2.22 Two-Wire Line with Dielectrically Coated Conductors

Each conductor of a thin symmetrical two-wire transmission line, with the distance between the conductor axes d and conductor radii a ($d \gg a$), is coated by a coaxial dielectric layer of permittivity ε and thickness a. Find the expression for the capacitance per unit length of this line if situated in air.

Solution Let the line be charged by Q' per unit of its length, as shown in Fig. 2.31. Similarly to the analysis of a thin-wire line with bare conductors in Fig. 2.22, the electric fields due to the individual charged conductors can be evaluated independently from each other, because the line is thin. Thus, the electric flux densities due to the conductors 1 and 2 evaluated at the point M in Fig. 2.31 are

$$D_1 = \frac{Q'}{2\pi x} \quad \text{and} \quad D_2 = \frac{Q'}{2\pi(d-x)}, \quad (2.181)$$

respectively. The total electric flux density is $D = D_1 + D_2$. To simplify the computation, however, we take that $D \approx D_1$ in the first dielectric coating (the second conductor is far away) and $D \approx D_2$ in the second coating. Having in mind that the electric field intensity in dielectric coatings is $\mathbf{E} = \mathbf{D}/\varepsilon$, while $\mathbf{E} = \mathbf{D}/\varepsilon_0$ in air, the voltage between the conductors is given by

$$\begin{aligned} V &= \int_a^{d-a} E\,dx = \frac{1}{\varepsilon}\int_a^{2a} D_1\,dx + \frac{1}{\varepsilon_0}\int_{2a}^{d-2a}(D_1+D_2)\,dx + \frac{1}{\varepsilon}\int_{d-2a}^{d-a} D_2\,dx \\ &= \frac{Q'}{2\pi}\left[\frac{1}{\varepsilon}\ln 2 + \frac{1}{\varepsilon_0}\left(\ln\frac{d-2a}{2a} - \ln\frac{2a}{d-2a}\right) + \frac{1}{\varepsilon}\ln 2\right] \approx \frac{Q'}{\pi}\left(\frac{1}{\varepsilon}\ln 2 + \frac{1}{\varepsilon_0}\ln\frac{d}{2a}\right) \end{aligned} \quad (2.182)$$

[see the integration in Eq. (2.140)]. The capacitance per unit length of the line is

$$C' = \frac{Q'}{V} = \pi\left(\frac{1}{\varepsilon}\ln 2 + \frac{1}{\varepsilon_0}\ln\frac{d}{2a}\right)^{-1}. \quad (2.183)$$

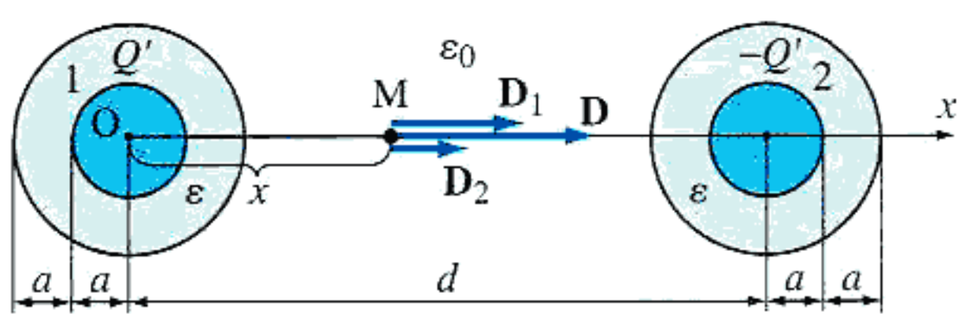

Figure 2.31 Cross section of a thin two-wire line with dielectric coatings over conductors, in air; for Example 2.22.

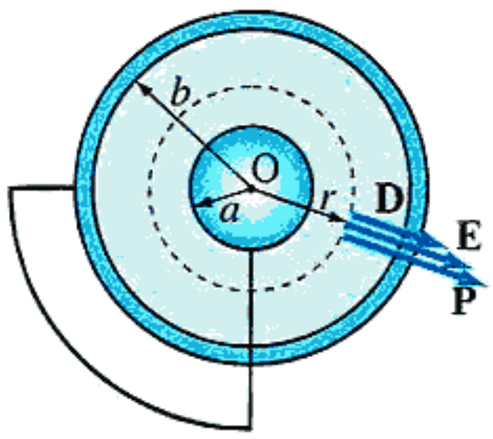

Figure 2.32 Nonlinear spherical capacitor with short-circuited electrodes and remanent polarization; for Example 2.23.

Example 2.23 Spherical Capacitor with a Nonlinear Dielectric

Consider a spherical capacitor with radii of electrodes a and b ($a < b$), filled with a ferroelectric. After being connected to a voltage generator, the capacitor electrodes are short-circuited, and there is a remanent (residual) polarization in the dielectric in the new steady state (Fig. 2.32). The polarization vector is radial, with magnitude $P(r) = P_0 b/r$, where P_0 is a constant and r is the distance from the capacitor center. Calculate the electric field intensity vector in the dielectric.

Solution Since this is a nonlinear capacitor (ferroelectrics are nonlinear materials), relationship in Eq. (2.112) does not hold, and there is a charge, Q and $-Q$, on the capacitor electrodes although the voltage between them is zero in the new state. From spherical symmetry and the given form of the vector $\mathbf{P}$ in the dielectric, the electric flux density vector in the dielectric, $\mathbf{D}$, has that same form (radial vector that depends on r only), as in Eq. (2.161). This means that the capacitor in Fig. 2.32 represents a D-system. Then, using the generalized Gauss' law, Eq. (2.43), which is true for arbitrary (including nonlinear) media, the magnitude of the vector $\mathbf{D}$ is found to be that in Eq. (2.162).

To determine the electric field intensity vector, $\mathbf{E}$, from $\mathbf{D}$, however, we cannot use the relationship in Eq. (2.47), as the dielectric is not linear, but we can use the definition of the vector $\mathbf{D}$ in Eq. (2.41), which yields

$$\mathbf{E} = \frac{\mathbf{D} - \mathbf{P}}{\varepsilon_0}. \tag{2.184}$$

From the condition $V = 0$,

$$\int_{r=a}^{b} E(r)\,\mathrm{d}r = \frac{1}{\varepsilon_0}\int_a^b [D(r) - P(r)]\,\mathrm{d}r = 0, \tag{2.185}$$

that is,

$$\int_a^b \left(\frac{Q}{4\pi r^2} - \frac{P_0 b}{r}\right)\mathrm{d}r = \frac{Q}{4\pi}\left(\frac{1}{a} - \frac{1}{b}\right) - P_0 b \ln\frac{b}{a} = 0. \tag{2.186}$$

Hence, $Q = 4\pi P_0 \ln(b/a)\, ab^2/(b-a)$ and

$$\mathbf{E} = \frac{P_0 b}{\varepsilon_0 r}\left[\frac{ab\ln(b/a)}{(b-a)r} - 1\right]\hat{\mathbf{r}}. \tag{2.187}$$

Problems: 2.42–2.56; *Conceptual Questions* (on Companion Website): 2.19–2.26; *MATLAB Exercises* (on Companion Website).

2.15 ENERGY OF AN ELECTROSTATIC SYSTEM

Every charged capacitor and every system of charged conducting bodies contain a certain amount of energy, which, by the principle of conservation of energy, equals the work done in the process of charging the system. This energy is called the electric energy and is related to the charges and potentials of the conducting bodies in the system. To find this relationship, we perform a numerical experiment in which a system that was initially uncharged is being gradually charged, by bringing elementary charges to the conducting bodies by an external agent. We evaluate the net work done against the electric forces while the charges of the bodies are being changed from zero to their final values.

Consider first a linear capacitor of capacitance C. Let the charges of the electrodes of the capacitor be Q and $-Q$, and their potentials with respect to a reference point be V_1 and V_2, respectively. The capacitor voltage is

$$V = V_1 - V_2 = \frac{Q}{C}. \tag{2.188}$$

If we add an elementary positive charge $\mathrm{d}Q$ to the first electrode and $-\mathrm{d}Q$ to the second one, the change of the energy of the capacitor is equal to the work done against the electric forces in moving $\mathrm{d}Q$ from the reference point (i.e., from the zero potential level) to the first electrode (which is at the potential V_1) and $-\mathrm{d}Q$ to the second electrode (at the potential V_2). By the definition of the electric scalar potential, the potential of a point on either one of the electrodes equals the work done by the electric field in moving a charge from the electrode to the reference point, or, conversely, the work done against the electric field in moving a charge from the reference point to the electrode, divided by the charge [Eq. (1.74)]. This is exactly what we have in our experiment, so the elementary work done while moving $\mathrm{d}Q$ and $-\mathrm{d}Q$ is given by

$$\mathrm{d}W_\mathrm{e} = \mathrm{d}Q\,V_1 + (-\mathrm{d}Q)\,V_2, \tag{2.189}$$

or, equivalently,

$$\mathrm{d}W_\mathrm{e} = \mathrm{d}Q\,(V_1 - V_2) = \mathrm{d}Q\,V = \mathrm{d}Q\,\frac{Q}{C}. \tag{2.190}$$

When uncharged, the capacitor has no energy. The total energy stored in the capacitor when it is charged with Q is therefore equal to the net work done in changing the capacitor charge from $q = 0$ to $q = Q$, and is obtained by adding up all elementary works $\mathrm{d}W_\mathrm{e}$ in Eq. (2.190):

$$W_\mathrm{e} = \int_{q=0}^{q=Q} \mathrm{d}W_\mathrm{e} = \frac{1}{C}\int_{q=0}^{Q} q\,\mathrm{d}q = \frac{1}{C}\,\frac{Q^2}{2}. \tag{2.191}$$

Hence, the equivalent expressions for the energy of a capacitor are

$$\boxed{W_\mathrm{e} = \frac{Q^2}{2C} = \frac{1}{2}\,QV = \frac{1}{2}\,CV^2.} \tag{2.192}$$

energy of a capacitor (unit: J)

The unit for the electric energy is the joule (J). As a special case, the electric energy of an isolated charged metallic body in a linear dielectric is

$$\boxed{W_\mathrm{e} = \frac{1}{2}\,CV^2_{\text{isolated body}},} \tag{2.193}$$

energy of an isolated metallic body

where C here is the capacitance of the single body, given by Eq. 2.116, $V_{\text{isolated body}}$ is its potential with respect to the reference point at infinity, and two additional equivalent expressions, like in Eq. 2.192, can be written as well.

Note that the energy of a capacitor can also be expressed in terms of the charges and potentials of individual electrodes as

$$W_\mathrm{e} = \frac{1}{2}\,QV = \frac{1}{2}\,Q(V_1 - V_2) = \frac{1}{2}\,(Q_1V_1 + Q_2V_2). \tag{2.194}$$

Generally, for a linear multibody system with N charged conducting bodies,

$$\boxed{W_\mathrm{e} = \frac{1}{2}\sum_{i=1}^{N} Q_iV_i.} \tag{2.195}$$

energy of a multibody electrostatic system

Finally, if a system also includes a volume charge distributed throughout the dielectric between the conductors, in addition to surface charges over the conductors, the

total electric energy of the system is

energy of a multibody system with volume charge in the dielectric

$$\boxed{W_e = \frac{1}{2}\sum_{i=1}^{N} Q_i V_i + \frac{1}{2}\int_v \rho V \, dv,} \tag{2.196}$$

where ρ is the charge density and V the electric scalar potential in the dielectric, and energy $(\rho \, dv) \, V/2$ of an elemental charge $dQ = \rho \, dV$ is integrated throughout the volume v of the dielectric.

2.16 ELECTRIC ENERGY DENSITY

Expression in Eq. (2.196) enables us to find the total energy associated with the charge distribution of an electrostatic system. As the charges are sources of the electric field, it turns out that the energy of the system can be expressed also in terms of the electric field intensity throughout the system. This leads to an assumption that the electric energy is actually localized in the electric field, and therefore in the dielectric (which can be air and a vacuum) between the conductors of an electrostatic system. Quantitatively, as we shall see, the concentration (density) of energy at specific locations in the dielectric is proportional to the local electric field intensity squared.

Let us consider first a simple case of a homogeneous electric field in the dielectric of a parallel-plate capacitor, with plate areas S, plate separation d (d is small compared to the dimensions of the plates), and dielectric permittivity ε [Fig. 2.18(a)]. From Eqs. (2.192), (2.127), and (2.126), the energy of the capacitor is

$$W_e = \frac{1}{2}CV^2 = \frac{1}{2}\varepsilon\frac{S}{d}(Ed)^2 = \frac{1}{2}\varepsilon E^2 Sd = \frac{1}{2}\varepsilon E^2 v, \tag{2.197}$$

where E is the electric field intensity in the dielectric and $v = Sd$ is the volume of the dielectric, i.e., the volume of the domain where the electric field exists. We define the electric energy density as

$$w_e = \frac{W_e}{v} = \frac{1}{2}\varepsilon E^2, \tag{2.198}$$

or, by employing Eq. (2.47),

electric energy density (unit: J/m^3)

$$\boxed{w_e = \frac{1}{2}\varepsilon E^2 = \frac{1}{2}ED = \frac{D^2}{2\varepsilon}.} \tag{2.199}$$

The unit is J/m^3 (volume density). The energy of the capacitor can now be written in the form

$$W_e = w_e v. \tag{2.200}$$

We shall now generalize this result to obtain a field-based expression for the energy contained in an arbitrary capacitor (Fig. 2.14) and an arbitrary electrostatic system. Let us subdivide the domain between the conducting bodies of a system into elementary flux tubes containing the lines of vector **D**, that start and terminate at surfaces of the bodies. We then cut each tube along its length into small cells of volume dv, such that the interfaces between the neighboring cells are perpendicular to the field lines. We can metalize these interfaces, without changing the field, and get an array of small parallel-plate capacitors along the tube. The entire space between the conducting bodies of the system, i.e., the domain with the electric

field, is thus partitioned into volume cells, and each cell represents an elementary parallel-plate capacitor with a homogeneous dielectric and uniform electric field between the plates. The energy contained in each capacitor is

$$\mathrm{d}W_\mathrm{e} = w_\mathrm{e}\,\mathrm{d}v, \tag{2.201}$$

where the energy density is given by Eq. (2.199). Summing the energies contained in all capacitors, that is, integrating the energy $\mathrm{d}W_\mathrm{e}$ throughout the entire dielectric between the conducting bodies of the system (volume v), we obtain the electric energy of the entire system:

$$\boxed{W_\mathrm{e} = \int_v w_\mathrm{e}\,\mathrm{d}v = \frac{1}{2}\int_v ED\,\mathrm{d}v.} \tag{2.202}$$

electric energy of an electromagnetic system, via the energy density

The expressions for the electric energy in Eqs. (2.196) and (2.202) are equivalent, namely, they give the same result for the total energy of an electrostatic system. The latter expression, however, implies that the actual localization of electric energy is throughout the electric field, that is, in the dielectric between the conductors of the system (even if the dielectric is a vacuum), and not in the conductors, nor on their surfaces. It also provides us with a means, the energy density in Eq. (2.199), for evaluating and analyzing the exact distribution of energy throughout the dielectric.

On the other hand, reconsidering Eq. (2.196) and reinspecting its terms, we might now come up with an alternative viewpoint on the actual energy localization in electrostatics, which implies that the stored electric energy of a system resides in the system charge, and not the field. Accordingly, $\rho V/2$ might be considered to be the volume energy density at points where $\rho \neq 0$ throughout the volume of the dielectric [from the second term of the energy expression in Eq. (2.196)]. The corresponding surface energy density, equal to $\rho_\mathrm{s} V/2$, would then quantify energy localization in the surface charge distribution over the surfaces of the conductors in the system [constituting the first term of the energy expression in Eq. (2.196)]. Both viewpoints have merit and are equally "correct." Nevertheless, the assumption that the energy is actually "contained" in the field, and not in the charge producing it, turns out to be much better suited for energy considerations in the analysis of electromagnetic waves (to be done in a later chapter). Namely, an electromagnetic wave consists of time-varying electric and magnetic fields which travel through space (even in a vacuum) and carry energy independent of the sources (charges and currents) that produced them (the sources might not even exist any more). Therefore, it is much simpler and more natural to describe the energy distribution of a system with traveling waves in terms of the fields, which change in time and travel in space, than to associate it with the stationary distribution of sources at previous instants of time. This is why we have adopted the field-based energy localization approach in the first place and the associated energy density expressions, those in Eq. (2.199), to quantify the energy distribution in an arbitrary (linear) system (with static or time-varying charges and fields).

Example 2.24 Energy of Parallel-Plate Capacitors with Two Dielectric Layers

Find the energy of each of the capacitors in Fig. 2.25, neglecting the fringing effects. Express the energy in terms of the capacitor charge in case (a) and the capacitor voltage in case (b).

Solution Based on Eqs. (2.202), (2.147), (2.192), (2.157), and (2.150), the energy of the capacitor in Fig. 2.25(a) can be found using either (1) the electric flux density in the dielectric, or (2) the capacitances of two capacitors corresponding to individual dielectric layers, or

(3) the equivalent total capacitance of a series connection of capacitors with homogeneous dielectrics:

$$W_e = \underbrace{\frac{D^2}{2\varepsilon_1} S d_1 + \frac{D^2}{2\varepsilon_2} S d_2}_{(1)} = \underbrace{\frac{Q^2}{2C_1} + \frac{Q^2}{2C_2}}_{(2)} = \underbrace{\frac{Q^2}{2C}}_{(3)} = \frac{(\varepsilon_2 d_1 + \varepsilon_1 d_2) Q^2}{2\varepsilon_1 \varepsilon_2 S}. \tag{2.203}$$

Similarly, the energy of the capacitor in Fig. 2.25(b) can be computed by employing either (1) the electric field intensity in the dielectric, or (2) the capacitances of the two capacitors with homogeneous dielectrics, or (3) the total capacitance of a parallel connection of capacitors:

$$W_e = \underbrace{\frac{\varepsilon_1 E^2}{2} S_1 d + \frac{\varepsilon_2 E^2}{2} S_2 d}_{(1)} = \underbrace{\frac{C_1 V^2}{2} + \frac{C_2 V^2}{2}}_{(2)} = \underbrace{\frac{CV^2}{2}}_{(3)} = \frac{(\varepsilon_1 S_1 + \varepsilon_2 S_2) V^2}{d} \tag{2.204}$$

[see Eqs. (2.151), (2.160), and (2.154)].

Example 2.25 Energy Per Unit Length of a Coaxial Cable

Determine (a) the energy density and (b) the energy per unit length of a coaxial cable, with conductor radii a and b ($a < b$) and dielectric permittivity ε, if the voltage between the cable conductors is V.

Solution

(a) The electric field intensity in the dielectric of the cable is given by Eq. (2.124), and hence the electric energy density at a distance r from the cable axis is

$$w_e = \frac{1}{2} \varepsilon E(r)^2 = \frac{\varepsilon V^2}{2r^2 \ln^2(b/a)} \quad (a < r < b). \tag{2.205}$$

(b) The electric energy per unit length of the cable can be evaluated as

electric energy per unit length of a transmission line (unit: J/m)

$$\boxed{W'_e = (W_e)_{\text{p.u.l.}} = \frac{W_e}{l} = \frac{1}{l} \int_v w_e \underbrace{\mathrm{d}S\, l}_{\mathrm{d}v} = \int_S w_e \, \mathrm{d}S,} \tag{2.206}$$

where W_e is the energy contained in a part of the cable of length l, S is the cross-sectional area of the dielectric between the cable conductors, and $\mathrm{d}v = \mathrm{d}S\, l$. The unit for W'_e is J/m. Because the energy density is a function of the coordinate r only, we adopt $\mathrm{d}S$ in the form of an elementary ring of radius r and width $\mathrm{d}r$, Eq. (1.60), and obtain

$$W'_e = \int_{r=a}^{b} w_e(r) \underbrace{2\pi r \, \mathrm{d}r}_{\mathrm{d}S} = \frac{\pi \varepsilon V^2}{\ln^2(b/a)} \int_a^b \frac{\mathrm{d}r}{r} = \frac{\pi \varepsilon V^2}{\ln(b/a)}. \tag{2.207}$$

This result is, of course, in agreement with the expression

p.u.l. electric energy via p.u.l. capacitance

$$\boxed{W'_e = \frac{1}{2} C' V^2.} \tag{2.208}$$

where C' is the capacitance per unit length of the cable, given in Eq. (2.123).

Example 2.26 Energy in a Coaxial Cable with a Dielectric Spacer

Shown in Fig. 2.33 is a cross section of a coaxial cable that is partly filled with a dielectric of relative permittivity ε_r. The dielectric is in the form of a spacer between the cable conductors defined by an angle α. The remaining space between the conductors is air-filled. The conductor radii are a and b ($a < b$), and the voltage between the conductors is V. Find

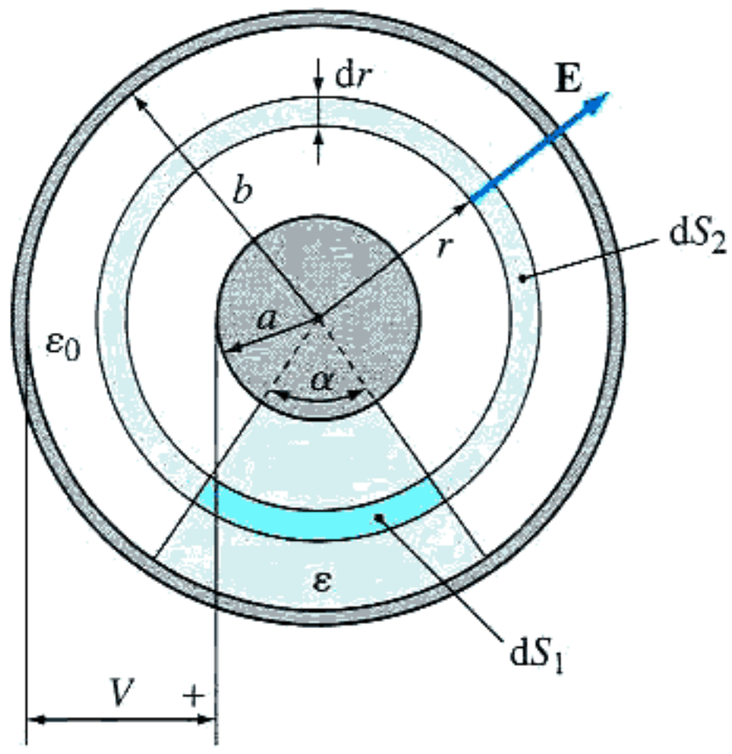

Figure 2.33 Coaxial cable with a dielectric spacer; for Example 2.26.

α for which the electric energy contained in the dielectric equals a half of the total energy in the cable.

Solution Electric energy densities in the dielectric and air part of the cable interior are

$$w_{e1} = \frac{1}{2}\varepsilon_r\varepsilon_0 E^2 \quad \text{and} \quad w_{e2} = \frac{1}{2}\varepsilon_0 E^2, \tag{2.209}$$

respectively, where the electric field intensity E in the cable is continuous across the interface between the dielectric and air. This is an E-system (see Example 2.21), and E is the same as in the air-filled coaxial cable, Eq. (2.124).

By the requirement in the statement of the example, the energy per unit length of the cable contained in the dielectric spacer and that in the air are stipulated to be the same, $W'_{e1} = W'_{e2}$, which means that (Fig. 2.33)

$$\int_{r=a}^{b} \underbrace{\frac{1}{2}\varepsilon_r\varepsilon_0 E(r)^2}_{w_{e1}} \underbrace{\alpha r\,\mathrm{d}r}_{\mathrm{d}S_1} = \int_{r=a}^{b} \underbrace{\frac{1}{2}\varepsilon_0 E(r)^2}_{w_{e2}} \underbrace{(2\pi - \alpha) r\,\mathrm{d}r}_{\mathrm{d}S_2}. \tag{2.210}$$

Here, $\mathrm{d}S_1$ and $\mathrm{d}S_2$ are surface areas of the parts of a thin ring of radius r and width $\mathrm{d}r$ determined by angles α and $2\pi - \alpha$, respectively. Even without any integration, Eq. (2.210) gives

$$\varepsilon_r\alpha = 2\pi - \alpha \quad \longrightarrow \quad \alpha = \frac{2\pi}{\varepsilon_r + 1}. \tag{2.211}$$

Example 2.27 Energy of a System with Volume Charges

Calculate the electric energy of the system from Example 2.5.

Solution This system does not contain conductors. The electric energy densities in the dielectric sphere and air are

$$w_e = \frac{D(r)^2}{2\varepsilon_r\varepsilon_0} \quad (0 \le r \le a) \qquad \text{and} \qquad w_{e0} = \frac{D(r)^2}{2\varepsilon_0} \quad (a < r < \infty), \tag{2.212}$$

respectively, where the electric flux density, D, is given in Eq. (2.63). Hence, the electric energy of the system is

$$W_e = \int_0^a w_e(r)\,4\pi r^2\,\mathrm{d}r + \int_a^\infty w_{e0}(r)\,4\pi r^2\,\mathrm{d}r = \frac{\rho_0^2\pi a^5}{56\varepsilon_0}\left(7 + \frac{1}{\varepsilon_r}\right), \tag{2.213}$$

where $\mathrm{d}v$ is adopted in the form of a thin spherical shell of radius r and thickness $\mathrm{d}r$, Eq. (1.33).

The above result can also be obtained employing the expression in Eq. (2.196),

$$W_e = \frac{1}{2}\int_v \rho V \, dv = \frac{1}{2}\int_0^a \rho(r)V(r)\,4\pi r^2 \, dr = \frac{\rho_0^2 \pi a^5}{56\varepsilon_0}\left(7 + \frac{1}{\varepsilon_r}\right), \tag{2.214}$$

with v being the volume of the sphere, ρ the volume charge density given in Example 2.5, and V the electric scalar potential in Eq. (2.66).

Note that the integration in Eq. (2.213) is over both the dielectric sphere and the air, while that in Eq. (2.214) is over the sphere only. This is because the electric field exists in the entire space, whereas the volume charge occupies the volume of the sphere only.

Problems: 2.57–2.68; *Conceptual Questions* (on Companion Website): 2.27–2.31; *MATLAB Exercises* (on Companion Website).

2.17 DIELECTRIC BREAKDOWN IN ELECTROSTATIC SYSTEMS

We shall now analyze electrostatic systems in high-voltage applications, i.e., in situations where the electric field in the dielectric is so strong that there is a danger of dielectric breakdown in the system. As discussed in Section 2.6, dielectric breakdown occurs when the largest field intensity in the dielectric reaches the critical value for that particular material – dielectric strength of the material, E_{cr}. Under the influence of such strong electric fields, a dielectric material is suddenly transformed from an insulator into a very good conductor, causing an intense current to flow. While systems with gaseous and liquid dielectrics can completely recover after a breakdown, those with solid dielectrics are most often permanently damaged by breakdown fields, as insulating properties of the dielectric are irreversibly degraded. In this section, our goal is not to analyze local breakdown processes in materials nor the overall behavior of systems resulting from these processes (these phenomena are largely nonlinear and are not electrostatic), but to evaluate the systems and their performance in linear electrostatic states close to the breakdown occurrences. In fact, our goal here is basically to determine the maximum extent of values of various quantities in a system (or device) that are "permitted" for its safe operation prior to an eventual breakdown.

In systems (devices) with nonuniform electric field distributions, the principal task is to identify the most vulnerable spot for dielectric breakdown, and to relate the corresponding largest electric field intensity to the charges or potentials of conducting bodies in the system. In the case of a capacitor or a two-conductor transmission line, the voltage that corresponds to the critical field in the dielectric is called the breakdown voltage of the capacitor or line. This is the highest possible voltage that can be applied to the system (before it breaks down), and is sometimes also referred to as the voltage rating of the system.[6] In some applications, we optimize individual parameters of a system (e.g., the radius of the inner conductor

[6]Since the dielectric strength of a given material may vary considerably depending on the actual conditions under which the material is used, as well as the way the particular piece of a solid dielectric is manufactured, the voltage rating and critical values of other quantities for a system in practice are always defined with a certain safety factor included. For example, with a safety factor of 10, the voltage rating of a given capacitor equals a tenth of the voltage that would lead to a breakdown under ideal conditions and assumptions.

of a coaxial cable) such that the breakdown voltage is maximum. It is also of interest to evaluate the critical (breakdown) values for the capacitor charge and energy, and the corresponding values for forces on conductors (charge, energy, and forces per unit length for transmission lines), as these are the largest possible charge, energy, and forces for that particular system.

For systems filled with a homogeneous dielectric, the strongest electric field in the dielectric is most frequently right next to one of the conducting bodies of the system. In addition, this is most likely in the vicinity of sharp parts of a conducting surface [see Eq. (1.210)]. In systems with heterogeneous dielectrics, on the other side, the most vulnerable spots can be close to a boundary surface between dielectric parts with different permittivities, where the normal component of the electric field intensity is discontinuous. In such systems, furthermore, the largest field intensity in a given dielectric part is not necessarily the breakdown field, because the dielectric strength vary from material to material, and only an electrostatic analysis (or an experiment) can tell which of the dielectric parts would break down first after a voltage of critical value is applied to the system.

For a system of conducting bodies situated in air (or any other gas), the breakdown region, where the air is ionized by an avalanche breakdown mechanism (see Section 2.6) and behaves like a conducting material, is usually localized only in the immediate vicinity of "hot" spots on conductor surfaces, as the field farther away from the conductor is not sufficiently strong to sustain the breakdown. Due to an avalanche of impact ionization of air molecules, vast numbers of free electrons and positive ions are created, so that the air near the conductor becomes more and more conducting. The ionized air might even glow (at night), appearing as a luminous "crown" around the conductor, and hence such a local discharge close to a conductor surface is referred to as a corona discharge. A corona discharge on a conductor is equivalent to an enlargement of the conductor, since a layer of conducting material (ionized air) is added over the conductor surface. It substantially increases losses on power transmission lines and also emits electromagnetic waves that can interfere with nearby communication devices and systems. On some occasions, the field intensities in the system are so high that breakdowns occur even away from the conductors. A continuously ionized path is formed from a part of a conductor surface with an exceedingly high charge density to the nearest conductor with opposite charge polarity. This path is apparent as a bright luminous arc carrying a current of a very large intensity (typically hundreds to thousands of amperes, sometimes as large as 100 kA). As a result, a very rapid and violent discharge of the conductors occurs, known as arc discharge. The most apparent and spectacular arc discharges certainly are intense cloud-to-ground lightning discharges in the form of giant sparks in thunderstorms. Lightning strikes are, as we know, a frequent cause of loss of human lives and property.

Analysis of electrostatic systems with fields close to breakdown levels and predicting critical values of voltages, charges, and other quantities at breakdown require no new theory, and is just a matter of applying what we already know in an appropriate way and order, having in mind the above general comments. The rest of this section consists therefore of a number of characteristic examples.

Example 2.28 Breakdown in a Parallel-Plate Capacitor

Consider the capacitor in Fig. 2.19 for $a = 1$ m and $d = 2$ cm, and determine its breakdown voltage and the corresponding charge and energy, as well as the electric pressure and forces on capacitor electrodes at breakdown.

Solution The electric field between the capacitor plates is approximately uniform, and its breakdown intensity is

$$E = E_{\mathrm{cr0}} = 3\ \mathrm{MV/m} \tag{2.215}$$

[dielectric strength of air, Eq. (2.53)], from which the breakdown voltage of the capacitor, Eq. (2.126), charge of the capacitor, Eq. (2.125), and capacitor energy, Eq. (2.192), come out to be

$$V = E_{\mathrm{cr0}} d = 60\ \mathrm{kV}, \quad Q = \varepsilon_0 a^2 E_{\mathrm{cr0}} = 26.56\ \mu\mathrm{C}, \quad \text{and} \quad W_{\mathrm{e}} = \frac{1}{2} QV = 0.8\ \mathrm{J}, \tag{2.216}$$

respectively. According to Eqs. (2.133) and (2.132), the electric pressure and electric forces on electrodes at breakdown amount to

$$p_{\mathrm{e}} = \frac{1}{2}\varepsilon_0 E_{\mathrm{cr0}}^2 = 39.84\ \mathrm{Pa} \quad \text{and} \quad F_{\mathrm{e}} = p_{\mathrm{e}} a^2 = 39.84\ \mathrm{N}. \tag{2.217}$$

Note that the above values for energy and force are quite small compared to energies and forces of nonelectrical origin, and these are the largest possible values for this (quite large) capacitor.

Example 2.29 Maximum Breakdown Voltage of a Coaxial Cable

Conductor radii of a coaxial cable are a and $b = 7$ mm ($a < b$). The cable is filled with a homogeneous dielectric of relative permittivity $\varepsilon_{\mathrm{r}} = 2.56$ and dielectric strength $E_{\mathrm{cr}} = 20$ MV/m (polystyrene). (a) Find a for which the breakdown voltage of the cable is maximum. (b) What is the maximum breakdown voltage of the cable?

Solution

(a) Assume that the voltage between the cable conductors is V. The electric field intensity in the cable is given by Eq. (2.124). Obviously, the field is the strongest right next to the inner conductor of the cable,

maximum electric field of a coaxial cable

$$\boxed{E(a^+) = \frac{V}{a \ln(b/a)},} \tag{2.218}$$

meaning that dielectric breakdown occurs when this field intensity reaches the critical value – dielectric strength,

$$E(a^+) = E_{\mathrm{cr}}. \tag{2.219}$$

For a given radius a, the breakdown voltage, i.e., the largest voltage that the cable can withstand, is therefore

$$V_{\mathrm{cr}}(a) = E_{\mathrm{cr}}\, a \ln \frac{b}{a}. \tag{2.220}$$

To find the optimal radius a, for which the voltage V_{cr} is the largest, we impose the condition

$$\frac{\mathrm{d}V_{\mathrm{cr}}}{\mathrm{d}a} = 0 \quad \longrightarrow \quad E_{\mathrm{cr}}\left(\ln \frac{b}{a} - 1\right) = 0. \tag{2.221}$$

The solution is

coaxial cable radii ratio for a maximum breakdown voltage

$$\boxed{\frac{b}{a} = \mathrm{e} = 2.718} \quad \longrightarrow \quad a_{\mathrm{opt}} = \frac{b}{\mathrm{e}} = 2.57\ \mathrm{mm}. \tag{2.222}$$

Because the second derivative of $V_{\mathrm{cr}}(a)$ for $a = a_{\mathrm{opt}}$ is negative (equals $-E_{\mathrm{cr}}/a_{\mathrm{opt}}$), the function $V_{\mathrm{cr}}(a)$ has indeed a maximum (and not a minimum) at that point.

(b) The maximum breakdown voltage of the cable is

$$(V_{\mathrm{cr}})_{\mathrm{max}} = V_{\mathrm{cr}}(a_{\mathrm{opt}}) = E_{\mathrm{cr}}\, a_{\mathrm{opt}} = 51.5\ \mathrm{kV}. \tag{2.223}$$

HISTORICAL ASIDE

The lightning rod was invented around the middle of the eighteenth century by **Benjamin Franklin** (1706–1790), an American statesman and scientist, a prolific inventor in the area of electricity (e.g., principle of conservation of charge, labeling positive and negative charges, investigation of lightning, etc.), as well as in numerous other areas of scientific inquiry (e.g., bifocal glasses, Franklin stove, improved printing press, Gulf Stream chart, etc.). Franklin speculated that lightning was electricity, and proposed that upright sharp-pointed iron rods be mounted on roofs of buildings and connected by conducting wires to the iron bars buried in the earth (grounding electrodes). One of the first lightning rods with grounding conductors based on his design was that installed in 1752 on the Pennsylvania State House (now Independence Hall), in Philadelphia. With several improvements by Franklin and others in decades to follow, grounded lightning rods soon proved to be an efficient way of protecting buildings from lightning damage. *(Portrait: Library of Congress)*

Example 2.30 Breakdown Voltage of a Thin Two-Wire Line

Consider a symmetrical two-wire line with conductor radii $a = 1$ mm and the distance between conductor axes $d = 0.5$ m. The line is situated in air. Compute (a) the breakdown voltage of the line and (b) the largest possible forces on line conductors per unit length.

Solution

(a) Let $Q' > 0$ and $-Q'$ be the charges per unit length of the line conductors, as in Fig. 2.22. The electric field intensity of the line is the largest very close to the surface of each of the conductors. At these points, the total field (due to both charged conductors), Eq. (2.138), can approximately be evaluated as the field due to a single isolated charged wire conductor, because the other conductor is far away ($d \gg a$). Thus, by means of Eq. (1.196),

$$\boxed{E_{\max} = \frac{Q'}{2\pi\varepsilon_0 a},} \tag{2.224}$$

maximum electric field of a thin two-wire line

and, at breakdown, the critical charge per unit length of the line turns out to be

$$E_{\max} = E_{\text{cr}0} = 3\ \text{MV/m} \quad \longrightarrow \quad Q'_{\text{cr}} = 2\pi\varepsilon_0 a E_{\text{cr}0} = 167\ \text{nC/m}. \tag{2.225}$$

The breakdown voltage of the line amounts to

$$V_{\text{cr}} = \frac{Q'_{\text{cr}}}{C'} = \frac{Q'_{\text{cr}}}{\pi\varepsilon_0}\ln\frac{d}{a} = 2aE_{\text{cr}0}\ln\frac{d}{a} = 37.29\ \text{kV}, \tag{2.226}$$

where C' is the capacitance per unit length of the line [Eq. (2.141)].

(b) Since $a \ll d$, the corresponding intensity of electric forces on line conductors per unit length can be computed as in Eqs. (1.223) and (1.224), and the result is

$$F'_{\text{e}} = \frac{Q'^2_{\text{cr}}}{2\pi\varepsilon_0 d} = 1\ \text{mN/m}, \tag{2.227}$$

which is the largest possible force for this line.

Example 2.31 Grounded Wire Conductor as a Lightning Arrester

A wire conductor, of radius $a = 5$ mm, is positioned horizontally above the surface of the earth, at a height $h = 6$ m, as shown in Fig. 2.34. The conductor is grounded. A uniform

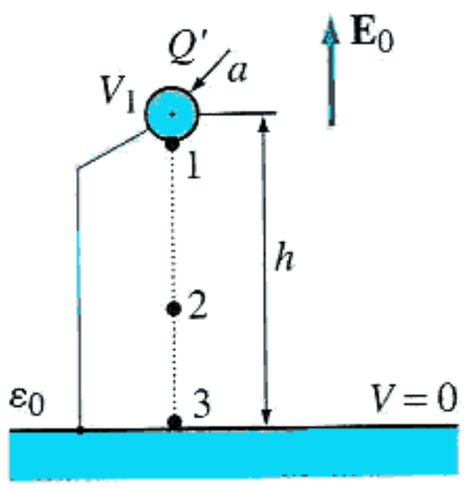

Figure 2.34 Grounded wire conductor in a uniform atmospheric electric field; for Example 2.31.

atmospheric electric field of intensity E_0, due to a large charged cloud, exists above the earth's surface. The vector $\mathbf{E}_0$ is vertical and directed upward.[7] Assuming that E_0 is known ($E_0 > 0$), find (a) the charge induced in the conductor per unit of its length and (b) the electric field intensity on the surface of the conductor. (c) Consider a cloud discharge to the ground and discuss the protection that the wire conductor provides to the space below it.

Solution

(a) The earth's surface represents a conducting plane. Let the potential of the plane be zero. Since the wire conductor is connected to the earth, a charge of opposite polarity to that of the lower part of the cloud, that is, of positive polarity, is induced in the conductor (pulled out from the earth) under the influence of the atmospheric field. Let Q' designate this charge per unit length of the conductor ($Q' > 0$), as indicated in Fig. 2.34. The potential of the conductor, V_1, can be expressed as the sum of the potential due to charge Q' and the potential produced by the external field $\mathbf{E}_0$. This first component can be obtained as the potential at the surface of the wire due to both Q' and its image in the conducting plane, as in Fig. 1.49, and thus using Eq. (1.119) with $r_1 = a$ (distance of the point at which the potential is computed form the axis of the original wire equals the wire radius) and $r_2 = 2h$ (since $2h \gg a$). The other component of the potential can be found from Eq. (1.90), by integrating the field $\mathbf{E}_0$ from the conductor to the earth's surface along the straight, vertical path. As this field is uniform, the voltage is simply $-E_0$ times the length of the path, and the total potential of the conductor is given by

$$V_1 = \frac{Q'}{2\pi\varepsilon_0} \ln \frac{2h}{a} - E_0 h. \tag{2.228}$$

From the condition that the conductor is grounded, we now have

$$V_1 = 0 \quad \longrightarrow \quad Q' = \frac{2\pi\varepsilon_0 E_0 h}{\ln(2h/a)}. \tag{2.229}$$

(b) The electric field intensity on the surface of the wire conductor (point 1 in Fig. 2.34) is approximately [Eq. (2.224)]

$$E_1 = \frac{Q'}{2\pi\varepsilon_0 a} = \frac{E_0 h}{a \ln(2h/a)} = 154 E_0. \tag{2.230}$$

(c) On the other hand, having in mind Eq. (2.139), the electric field intensity below the conductor at a height $H = 2$ m, for instance, with respect to the ground level (point 2 in Fig. 2.34) amounts to

$$E_2 = -\frac{Q'}{2\pi\varepsilon_0}\left(\frac{1}{r} + \frac{1}{2h - r}\right) + E_0 = 0.71 E_0 \tag{2.231}$$

($\mathbf{E}_2$ is directed upward), where $r = h - H = 4$ m. Similarly, the field intensity below the conductor close to the earth's surface (point 3) turns out to be $E_3 = -Q'/(\pi\varepsilon_0 h) + E_0 = 0.743 E_0$ ($r = h$).

As the atmospheric field becomes stronger and stronger, in a thunderstorm, the field intensity E_1 reaches the breakdown value [Eq. (2.225)]

$$E_1 = E_{\mathrm{cr0}}. \tag{2.232}$$

The air ionizes and becomes conductive, so that a portion of the negative charge of the cloud flows through this conducting air channel to the wire conductor and down to the

[7] In cold clouds, that contain water and ice, and cause eventual lightning discharges, there is a positive charge buildup at the top of a cloud and a negative one in its base. The bottom buildup induces another positively charged area at the earth's surface, and these two charge layers, like a giant charged capacitor, generate an electric field above the earth that is directed vertically upward, as in Fig. 2.34.

ground. The field intensities E_2 and E_3, however, are much lower than critical,

$$E_2 = 0.71E_0 = \frac{0.71}{154}E_1 = \frac{E_{cr0}}{217} \quad \text{and} \quad E_3 = 0.743E_0 = \frac{0.743}{154}E_1 = \frac{E_{cr0}}{207}, \tag{2.233}$$

meaning that a structure or a person that may be underneath the conductor is safe from breakdown and cloud discharge (or lightning strike). The grounded conductor protects therefore the space below it and serves principally as a lightning arrester.[8]

Example 2.32 Breakdown in a Spherical Capacitor with Two Dielectrics

The dielectric of a spherical capacitor consists of two concentric layers. The relative permittivity of the inner layer is $\varepsilon_{r1} = 2.5$ and its dielectric strength $E_{cr1} = 50$ MV/m. For the outer layer, $\varepsilon_{r2} = 5$ and $E_{cr2} = 30$ MV/m. Electrode radii are $a = 3$ cm and $c = 8$ cm, and the radius of the boundary surface between the layers is $b = 5$ cm. Calculate (a) the breakdown voltage and (b) the corresponding energy of the capacitor.

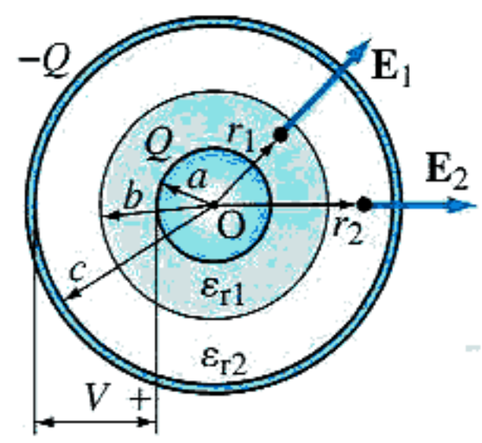

Figure 2.35 Evaluation of the breakdown voltage of a spherical capacitor with a two-layer dielectric; for Example 2.32.

Solution

(a) Let Q be the charge of the capacitor. The electric flux density in the dielectric is given by Eq. (2.162). With reference to Fig. 2.35, the electric field intensities in individual layers are

$$E_1(r) = \frac{Q}{4\pi\varepsilon_{r1}\varepsilon_0 r^2} = E_1(a^+)\frac{a^2}{r^2}, \quad a < r < b, \tag{2.234}$$

$$E_2(r) = \frac{Q}{4\pi\varepsilon_{r2}\varepsilon_0 r^2} = E_2(b^+)\frac{b^2}{r^2}, \quad b < r < c, \tag{2.235}$$

where r is the radial spherical coordinate. Note that $E_1(a^-)$ is the largest field intensity in the inner layer, while $E_2(b^+)$ represents the strongest field in the outer layer. Combining Eqs. (2.234) and (2.235), we arrive to the following relationship between these field intensities:

$$\varepsilon_{r1}a^2E_1(a^+) = \varepsilon_{r2}b^2E_2(b^+). \tag{2.236}$$

We do not know in advance which dielectric layer would break down first after a voltage of critical value is applied across the capacitor electrodes. Let us first check the possibility of a breakdown in the inner layer, which implies that

$$E_1(a^+) = E_{cr1}. \tag{2.237}$$

At the same time, from Eq. (2.236),

$$E_2(b^+) = E_{cr1}\frac{\varepsilon_{r1}a^2}{\varepsilon_{r2}b^2} = 9 \text{ MV/m}. \tag{2.238}$$

As $E_2(b^+) < E_{cr2}$, we conclude that the electric field intensity at all points in the outer dielectric layer is lower than the critical value for that dielectric. This means that the assumption of a breakdown occurring in the inner dielectric layer is correct.

[8]Note that this is the principle of operation of lightning arresters, in general. Grounded lightning rods, placed as high as possible, protect exposed objects (buildings or other structures, as well as humans and animals) and their immediate surroundings from violent atmospheric electrical discharges by enforcing that an eventual dielectric breakdown leading to a lightning strike is "induced" near the surface of the rod, and not at some other part of the object. Then, the rod routes the lightning discharge through an insulated wire conductor to a grounding electrode, rather than through the object. In addition to simple vertical metallic rods with pointed ends, designs of lightning arresters include rods with spherical metallic tops or umbrella-like wire extensions, which have capacity for carrying much larger amounts of induced charge.

The other possibility, which assumes that an eventual breakdown occurs in the outer layer, gives

$$E_2(b^+) = E_{\mathrm{cr}2}, \tag{2.239}$$

and $E_1(a^+) = E_{\mathrm{cr}2}\varepsilon_{\mathrm{r}2}b^2/(\varepsilon_{\mathrm{r}1}a^2) = 166.7$ MV/m. This is impossible, as E_1 cannot be larger than $E_{\mathrm{cr}1}$ under the assumption that the inner layer is in a normal regime, while the outer layer breaks down.

With the field-intensity values in Eqs. (2.237) and (2.238), the breakdown voltage of the capacitor is

$$V_{\mathrm{cr}} = E_1(a^+)\,a^2\int_a^b \frac{\mathrm{d}r}{r^2} + E_2(b^+)\,b^2\int_b^c \frac{\mathrm{d}r}{r^2} = \varepsilon_{\mathrm{r}1}a^2E_{\mathrm{cr}1}\left(\frac{b-a}{\varepsilon_{\mathrm{r}1}ab} + \frac{c-b}{\varepsilon_{\mathrm{r}2}bc}\right) = 769\ \mathrm{kV}. \tag{2.240}$$

This voltage can also be obtained by considering the critical value of the capacitor charge for breakdown. Let us denote by $Q_{\mathrm{cr}}^{(1)}$ and $Q_{\mathrm{cr}}^{(2)}$ the charge in the case of an eventual breakdown in the inner and outer dielectric layer, respectively. Based on Eqs. (2.234), (2.235), (2.237), and (2.239),

$$Q_{\mathrm{cr}}^{(1)} = 4\pi\varepsilon_{\mathrm{r}1}\varepsilon_0 a^2 E_{\mathrm{cr}1} \quad \text{and} \quad Q_{\mathrm{cr}}^{(2)} = 4\pi\varepsilon_{\mathrm{r}2}\varepsilon_0 b^2 E_{\mathrm{cr}2}. \tag{2.241}$$

As Q becomes larger and larger, the breakdown occurs when it reaches the smaller of the two charges in Eqs. (2.241). The critical charge of the capacitor is thus

$$Q_{\mathrm{cr}} = \min\left\{Q_{\mathrm{cr}}^{(1)}, Q_{\mathrm{cr}}^{(2)}\right\}. \tag{2.242}$$

For the given numerical data, $Q_{\mathrm{cr}}^{(1)} < Q_{\mathrm{cr}}^{(2)}$ $[Q_{\mathrm{cr}}^{(1)} = 0.3Q_{\mathrm{cr}}^{(2)}]$, meaning that the breakdown occurs in the inner dielectric layer. Hence,

$$Q_{\mathrm{cr}} = Q_{\mathrm{cr}}^{(1)} = 12.52\ \mu\mathrm{C}. \tag{2.243}$$

The corresponding voltage is

$$V_{\mathrm{cr}} = \frac{Q_{\mathrm{cr}}}{C} = 769\ \mathrm{kV}, \tag{2.244}$$

where $C = 16.28$ pF is the capacitance of the capacitor [Eq. (2.164)].

(b) The largest possible energy of the capacitor is

$$W_{\mathrm{e}} = \frac{1}{2}CV_{\mathrm{cr}}^2 = 4.81\ \mathrm{J}. \tag{2.245}$$

Problems: 2.69–2.81; *Conceptual Questions* (on Companion Website): 2.32–2.34; *MATLAB Exercises* (on Companion Website).

Problems

2.1. Nonuniformly polarized dielectric parallelepiped. A rectangular dielectric parallelepiped is situated in air in the first octant of the Cartesian coordinate system $(x, y, z \geq 0)$, with one vertex at the coordinate origin, and the edges, of lengths a, b, and c, parallel to coordinate axes x, y, and z, respectively. The polarization vector in the parallelepiped is given by $\mathbf{P}(x, y, z) = P_0[(x/a)\,\hat{\mathbf{x}} + (y/b)\,\hat{\mathbf{y}} + (z/c)\,\hat{\mathbf{z}}]$, where P_0 is a constant. (a) Find the densities of volume and surface bound charge of the parallelepiped. (b) Show that the total bound charge of the parallelepiped is zero.

2.2. Uniformly polarized disk on a conducting plane. A uniformly polarized dielectric disk surrounded by air is lying at a conducting plane, as shown in Fig. 2.36. The polarization vector

in the disk is $\mathbf{P} = P\hat{\mathbf{z}}$, the disk radius is a, and thickness d. Calculate the electric field intensity vector along the disk axis normal to the conducting plane (z-axis).

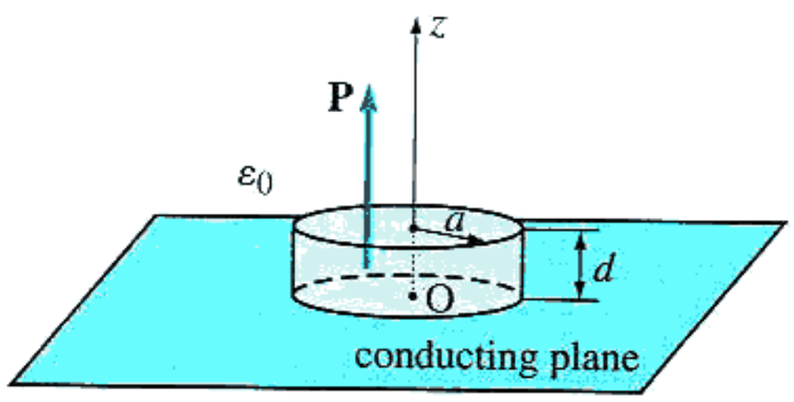

Figure 2.36 Dielectric disk with a uniform polarization lying at a conducting plane; for Problem 2.2.

2.3. Uniformly polarized hollow dielectric cylinder. A hollow dielectric cylinder of radii a and b, and height $2h$, is uniformly polarized and situated in free space. The polarization vector, of magnitude P, is parallel to the cylinder axis, as shown in Fig. 2.37. Find the electric field intensity vector at the center of the cylinder (point O).

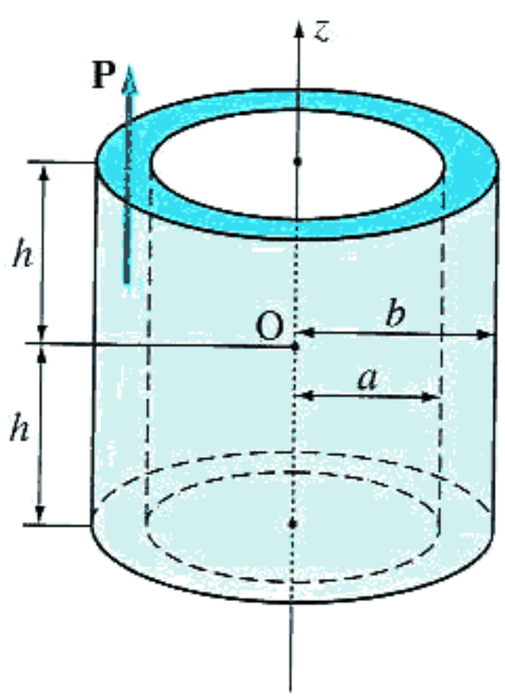

Figure 2.37 Hollow dielectric cylinder with a uniform polarization; for Problem 2.3.

2.4. Nonuniformly polarized thin dielectric disk. A very thin dielectric disk, of radius a and thickness d ($d \ll a$), is polarized throughout its volume. In the cylindrical coordinate system shown in Fig. 2.38, the polarization vector is defined by the expression $\mathbf{P} = P_0 r\hat{\mathbf{r}}/a$, where P_0 is a constant. The medium around the disk is air. Determine (a) the distribution of bound charge and (b) the electric field intensity vector along the z-axis.

2.5. Uniformly polarized dielectric hemisphere. A dielectric hemisphere of radius a is situated in

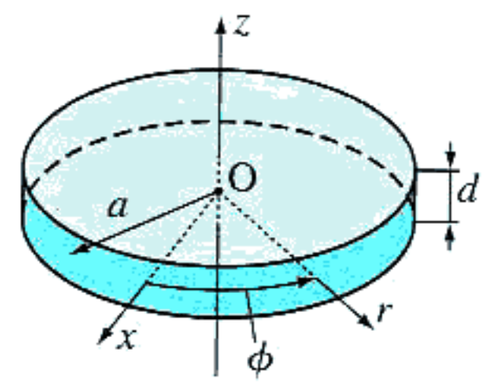

Figure 2.38 Very thin dielectric disk with a nonuniform polarization; for Problem 2.4.

free space and is lying at a conducting plane. The polarization vector is $\mathbf{P}$, and it is normal to the plane, as depicted in Fig. 2.39. Find (a) the bound surface charge density at the flat and spherical surfaces of the hemisphere and (b) the electric field intensity vector at the center of the flat surface (point O in the figure), assuming that it is on the dielectric side of the boundary surface (dielectric-conductor), very close to the surface.

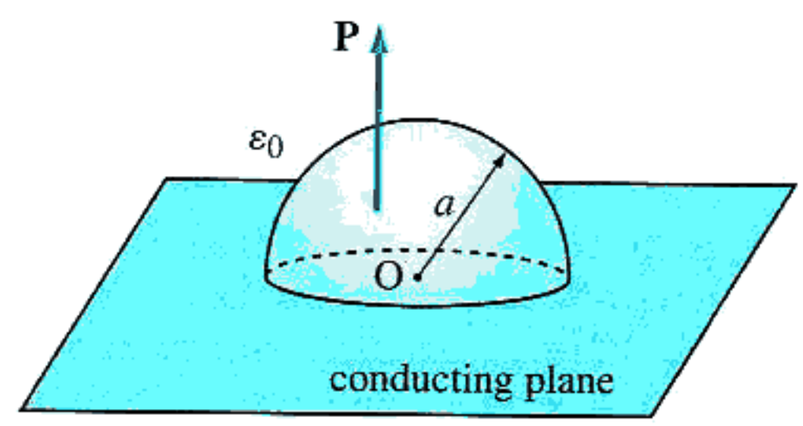

Figure 2.39 Dielectric hemisphere with a uniform polarization lying at a conducting plane; for Problem 2.5.

2.6. Nonuniformly polarized large dielectric slab. An infinitely large dielectric slab of thickness $d = 2a$, shown in Fig. 2.40, is polarized such that the polarization vector is $\mathbf{P} = P_0 x^2 \hat{\mathbf{x}}/a^2$, where P_0 is a constant. The medium outside the slab is air. Compute (a) the distribution of volume and surface bound charge of the slab, (b) the electric field intensity vector everywhere, and (c) the voltage between the boundary surfaces of the slab.

2.7. Electric flux density vector. Find the electric flux density vector, $\mathbf{D}$, (a) at the center of the polarized dielectric sphere in Fig. 2.7 and (b) along the axis of the polarized dielectric disk (z-axis) in Fig. 2.36.

2.8. Total (free plus bound) volume charge density. The electric field intensity vector in a dielectric, $\mathbf{E}$, is a known function of spatial coordinates. (a) Prove that the total (free plus

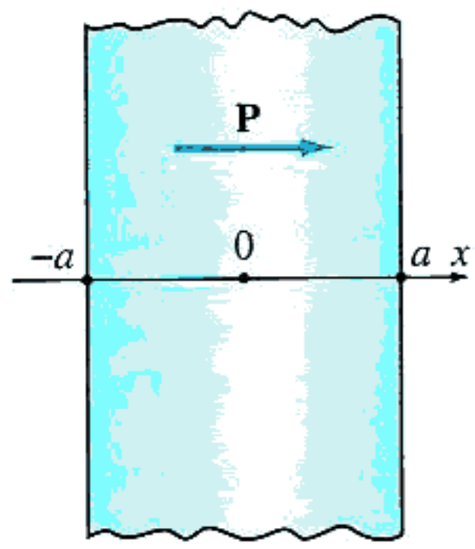

Figure 2.40 Infinitely large dielectric slab with a nonuniform polarization; for Problem 2.6.

bound) volume charge density in the dielectric, $\rho_{tot} = \rho + \rho_p$, can be obtained as $\rho_{tot} = \varepsilon_0 \nabla \cdot \mathbf{E}$. (b) Specifically, find ρ_{tot} for $\mathbf{E}$ given as the following function of Cartesian coordinates: $\mathbf{E}(x, y, z) = [4xyz\,\hat{\mathbf{x}} + (2x^2z - y^3)\,\hat{\mathbf{y}} + (2x^2y + z^3)\,\hat{\mathbf{z}}]$ V/m (x, y, z in m).

2.9. Uniform field in a dielectric. There is a uniform electric field in a certain dielectric region. The free volume charge density is ρ. Determine the bound volume charge density, ρ_p.

2.10. Closed surface in a uniform field. Considering an arbitrary closed surface in a uniform electric field, in a charge-free ($\rho_{tot} = 0$) region (Fig. 2.41), prove the following vector identity: $\oint_S d\mathbf{S} = 0$.

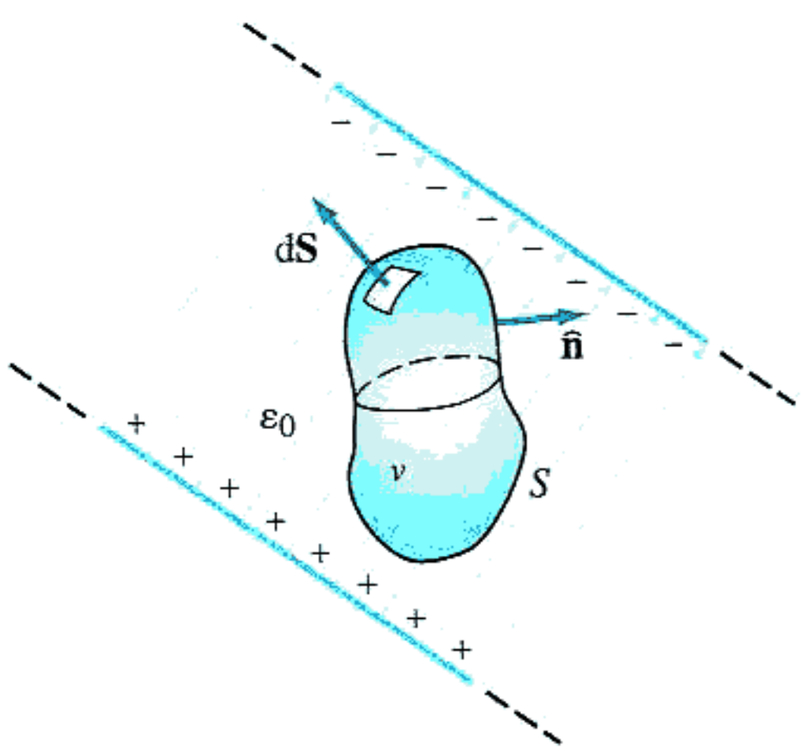

Figure 2.41 Closed surface in a region with a uniform electric field and no volume charge; for Problem 2.10.

2.11. Flux of the electric field intensity vector. The polarization vector, $\mathbf{P}$, and free volume charge density, ρ, are known at every point of a dielectric body. Find the expression for the flux of the electric field intensity vector, Ψ_E, through a closed surface S situated entirely inside the body.

2.12. Total enclosed bound and free charge. Consider an imaginary closed surface S inside a homogeneous dielectric of permittivity ε. The total free charge enclosed by S is Q_S. What is the total bound charge Q_{pS} enclosed by S?

2.13. Charge-free homogeneous medium. Prove that in a homogeneous linear medium with no free volume charge, there is no bound volume charge either.

2.14. Dielectric cylinder with free volume charge. A very long homogeneous dielectric cylinder, of radius a and relative permittivity ε_r, is charged uniformly with free charge density ρ throughout its volume. The cylinder is surrounded by air. (a) Calculate the voltage between the axis and the surface of the cylinder. (b) Find the bound charge distribution of the cylinder.

2.15. Linear-exponential volume charge distribution. Repeat Example 2.6 but for a model of a *pn* junction given by the volume charge density $\rho(x) = \rho_0(x/a)\,e^{-|x|/a}$, where ρ_0 and a are positive constants, as shown in Fig. 2.42.

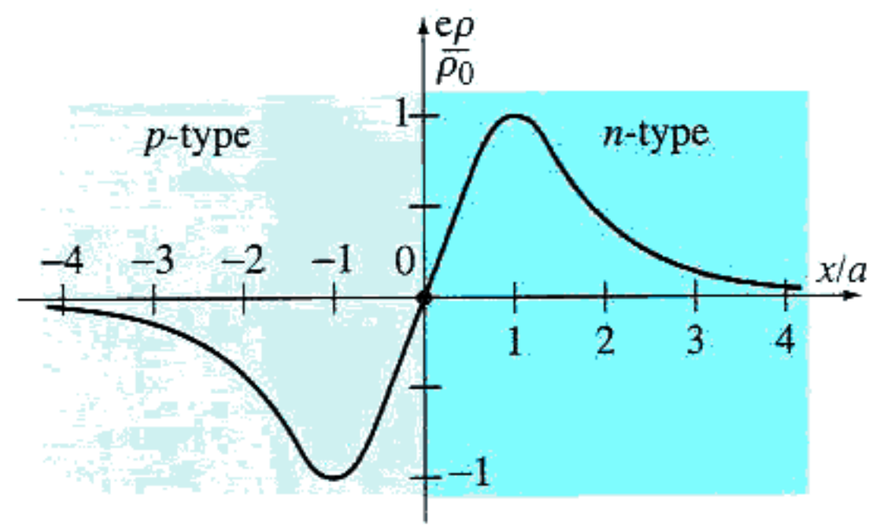

Figure 2.42 Model of a *pn* junction with a linear-exponential charge distribution; for Problem 2.15.

2.16. Dielectric-dielectric boundary conditions. Assume that the plane $z = 0$ separates medium 1 ($z > 0$) and medium 2 ($z < 0$), with relative permittivities $\varepsilon_{r1} = 4$ and $\varepsilon_{r2} = 2$, respectively. The electric field intensity vector in medium 1 near the boundary (for $z = 0^+$) is $\mathbf{E}_1 = (4\,\hat{\mathbf{x}} - 2\,\hat{\mathbf{y}} + 5\,\hat{\mathbf{z}})$ V/m. Find the electric field intensity vector in medium 2 near the boundary (for $z = 0^-$), $\mathbf{E}_2$, if (a) no free charge exists on the boundary ($\rho_s = 0$) and (b) there is a surface charge of density $\rho_s = 53.12$ pC/m^2 on the boundary.

2.17. Conductor-dielectric boundary conditions. Obtain conductor-dielectric and conductor-free space boundary conditions, Eqs. (1.186), (2.58), and (1.190), from Eqs. (2.84) and (2.85).

2.18. Water-air boundary. Sketch the field lines emerging from water ($\varepsilon_r = 80$) into air, if the "incident" angle (in water) is $\alpha = 45°$.

2.19. Poisson's equation for inhomogeneous media. (a) Derive Poisson's equation for an inhomogeneous medium. (b) Write Laplace's equation for an inhomogeneous medium.

2.20. Vacuum diode. Fig. 2.43 shows a vacuum diode, which consists of two flat electrodes, the cathode and the anode, and a charge distribution in a vacuum between them. Let the potential of the cathode be zero and the potential of the anode V_0 ($V_0 > 0$). The distribution of the potential in the diode can be described as $V(x) = V_0(x/d)^{4/3}$, $0 \le x \le d$, where d is the distance between the electrodes. Find (a) the volume charge density in the diode, (b) the surface charge density on the cathode, (c) the surface charge density on the anode, and (d) the total charge of the diode.

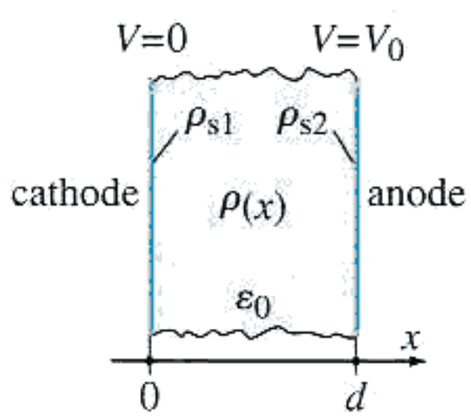

Figure 2.43 Vacuum diode; for Problem 2.20.

2.21. Application of Poisson's equation in spherical coordinates. Consider a system of two spherical concentric metallic electrodes (a solid sphere enclosed by a shell) as the one in Fig. 1.41, with $a = 1$ cm and $b = 5$ cm, and assume that a nonuniform free volume charge whose density is the function $\rho(r)$ given in Eq. (1.32), with $\rho_0 = 3$ C/m^3, exists between the electrodes, for $a < r < b$, where the permittivity is ε_0. In addition, let the potential of the inner electrode (sphere) with respect to the outer one (shell) be $V_0 = 10$ V. Under these circumstances, compute (a) the electric potential and (b) the electric field vector at an arbitrary point between the electrodes.

2.22. Application of Laplace's equation in spherical coordinates. Repeat the previous problem but for $\rho(r) = 0$ (no volume charge) between the electrodes (for $a < r < b$).

2.23. FD computer program – iterative solution. Write a computer program for the finite-difference analysis of a coaxial cable of square cross section (Fig. 2.13) based on Eq. (2.107). Assume that $a = 1$ cm, $b = 3$ cm, $V_a = 1$ V, and $V_b = -1$ V. (a) Plot the results for the distribution of the potential and the electric field intensity in the space between the conductors, and the surface charge density on the surfaces of conductors, taking the grid spacing to be $d = a/10$ and the tolerance of the potential $\delta_V = 0.01$ V. (b) Compute the total charge per unit length of the inner and the outer conductor, taking $d = a/N$ and $N = 2, 3, 5, 7, 9, 10$, and 12, respectively.

2.24. FD computer program – direct solution. As an alternative to the iterative technique based on Eq. (2.107), write a computer program for the FD analysis of a square coaxial cable by directly solving the system of linear algebraic equations with the potentials at interior grid nodes in Fig. 2.13(b) as unknowns [applying Eq. (2.106) to each interior grid node, we get a set of simultaneous equations the number of which equals the number of unknown potentials]. The system of equations, in which known potentials at nodes on the surface of conductors appear on the right-hand side of equations, should be solved by the Gaussian elimination method (or by matrix inversion). Compute and plot the same quantities as in the previous problem, and compare the results obtained by the two programs.

2.25. Capacitance of the earth. Find the capacitance of the earth assuming that it is a conducting sphere of radius $R = 6378$ km (grounds and waters are conducting media).

2.26. Capacitance of a person. It can be shown that the capacitance C of an arbitrary conducting body is in between the capacitance of the sphere inscribed in the body and that of the sphere overscribed about the body, that is [Eq. (2.121)], $4\pi\varepsilon_0 R_{\min} < C < 4\pi\varepsilon_0 R_{\max}$, where $R_{\min}$ and $R_{\max}$ are the radii of the two spheres. Based on that, estimate the capacitance of an average human body (human tissues are conducting media).

2.27. Capacitance of a metallic cube, computed by the MoM. Find the capacitance of the metallic cube numerically analyzed by the method of moments in Problem 1.85, and compare the result with capacitances of the following metallic spheres, respectively: (a) the sphere inscribed in the cube, (b) the sphere overscribed about the cube, (c) the sphere whose radius is the arithmetic mean of the radii of spheres in (a) and (b), (d) the sphere having the same surface as the cube, and (e) the sphere with the same volume as the cube.

2.28. RG-55/U coaxial cable. A RG-55/U coaxial cable has conductor radii $a = 0.5$ mm and $b = 3$ mm. The dielectric is polyethylene ($\varepsilon_r = 2.25$). Determine the capacitance per unit length of the cable.

2.29. Capacitance p.u.l. of a square coaxial cable, FD analysis. Compute the capacitance per unit length of the coaxial cable of square cross section numerically analyzed by a finite-difference technique in Problems 2.23 and 2.24, and compare the result (using the grid spacing of $d = a/10$) with the per-unit-length capacitance of a (standard) coaxial cable (of circular cross section) having the same ratio of conductor radii ($b/a = 3$) and dielectric (air) as the square cable.

2.30. Parallel-plate capacitor model of a thundercloud. A thundercloud can be approximately represented, as far as its electrical properties are concerned, as a parallel-plate capacitor with horizontal plates of area $S = 15$ km^2 and vertical separation $d = 1$ km. Assume that the upper plate has a total charge $Q = 300$ C and the lower plate an equal amount of negative charge. Neglecting the fringing effects, find (a) the capacitance of this capacitor, (b) the voltage between the top and bottom of the cloud, and (c) the electric field intensity in the cloud.

2.31. MoM numerical analysis of a parallel-plate capacitor. Consider the parallel-plate capacitor in Fig. 2.19, and write a computer program based on the method of moments to evaluate its capacitance (C). In specific, subdivide each of the plates into $N = 10 \times 10 = 100$ square patches, and assume constant charge densities on individual patches (as in Fig. 1.46). Additionally, assume that the upper and lower plates in Fig. 2.19 are at potentials $V_1 = 1$ V and $V_2 = -1$ V, respectively, as well as that the charge densities of pairs of corresponding patches that are right above/below each other on the two plates are equal in magnitude and opposite in polarity. With this, the unknowns in the procedure are charge densities $\rho_{s1}, \rho_{s2}, \ldots, \rho_{sN}$ on the upper plate only, and matching points, at which the potentials are computed, are centers of the same patches; however, these potentials are due to pairs of patches on both plates, with charge densities ρ_{si} and $-\rho_{si}$ ($i = 1, 2, \ldots, N$). Using the MoM program, find C for $a = 1$ m and the following d/a ratios: (i) 0.1, (ii) 0.5, (iii) 1, (iv) 2, and (v) 10, and compare the results with the corresponding C values obtained from Eq. (2.127), which neglects the fringing effects.

2.32. Nonsymmetrical thin two-wire line. Derive the expression for the capacitance per unit length of a nonsymmetrical thin two-wire transmission line in air. The radii of the conductors are a and b ($a \neq b$), and the distance between the axes of conductors is d ($d \gg a, b$).

2.33. Thick symmetrical two-wire line. Consider a symmetrical two-wire line with conductors of arbitrary thickness (radius of wires, a, is not necessarily small compared to the distance between wire axes, d) in air. Using a version of image theory for line charges in the vicinity of conducting cylinders, it can be shown that the capacitance per unit length of this line is given by $C' = \pi\varepsilon_0 / \ln\{d/(2a) + \sqrt{[d/(2a)]^2 - 1}\}$. Take d/a to be 3, 5, 10, 20, and 100, and calculate C' using this expression and the expression in Eq. (2.141), obtained for thin two-wire lines. Compare the two sets of results and evaluate the error due to thin-wire approximation of the line for individual distance to radius ratios.

2.34. Two small metallic spheres in air. A capacitor consists of two small metallic spheres of equal radii, a, placed in air at a center-to-center distance d ($d \gg a$). Find the capacitance of this capacitor.

2.35. Four parallel wires in air. The transmission line shown in Fig. 2.44 consists of two pairs of galvanically interconnected thin wire conductors, situated in air. The distance between the axes

of adjacent wires is $d = 200$ mm and the wire radii are $a = 1$ mm. Compute the capacitance per unit length of the line.

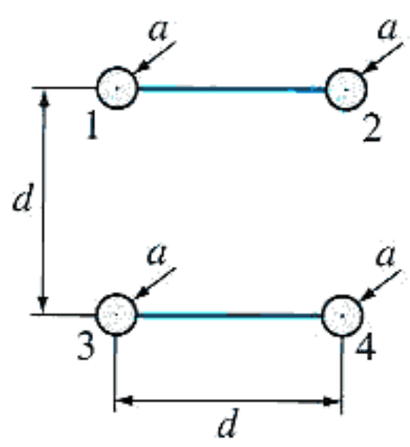

Figure 2.44 Cross section of a transmission line consisting of two pairs of short-circuited wires in air; for Problem 2.35.

2.36. Two wires at the same potential and a foil. A short-circuited two-wire line is parallel to a large flat metallic foil, as portrayed in Fig. 2.45. The geometry parameters are $a = 1$ mm, $h = 20$ mm, and $d = 30$ mm, and the medium is air. (a) What is the capacitance per unit length of a two-conductor transmission line whose one conductor is the two-wire line and the other conductor is the foil? (b) If the voltage between the line and the foil is $V = 20$ V, find the induced surface charge density at the central point O on the foil.

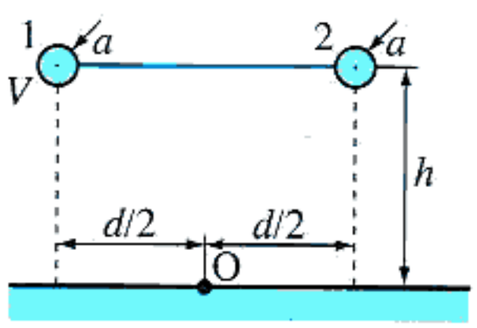

Figure 2.45 Short-circuited horizontal two-wire line over a large metallic foil; for Problem 2.36.

2.37. Capacitance per unit length of a wire-corner line. Consider the system composed of a wire parallel to a corner screen in Fig. 1.57, and assume that $a = 2$ mm and $h = 10$ cm. Calculate the capacitance per unit length of this system (transmission line).

2.38. Equivalent circuit with two spherical capacitors. (a) Consider the system described in Example 1.27, and show that it can be replaced by the equivalent circuit given in Fig. 2.46. (b) What are the capacitances of the capacitors in this schematic diagram? (c) Obtain the expression for the potential at the center of the structure in Fig. 1.41, Eq. (1.202), that is, repeat Example 1.27, by solving this circuit.

2.39. Equivalent circuit with three spherical capacitors. (a) Repeat Problem 1.77 by generating

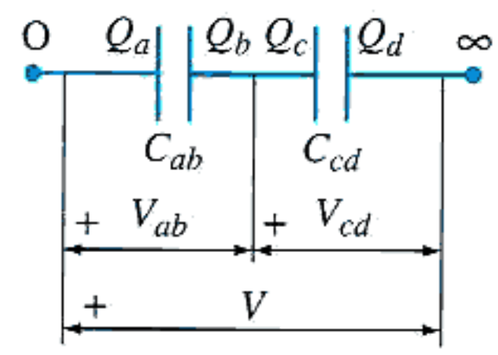

Figure 2.46 Equivalent circuit for the system in Fig. 1.41; for Problem 2.38.

and solving an equivalent circuit with three capacitors. (b) Repeat Problem 1.78 using the same circuit and the corresponding set of conditions.

2.40. Equivalent circuit with parallel-plate capacitors. Repeat Example 1.28 by solving the equivalent circuit shown in Fig. 2.47.

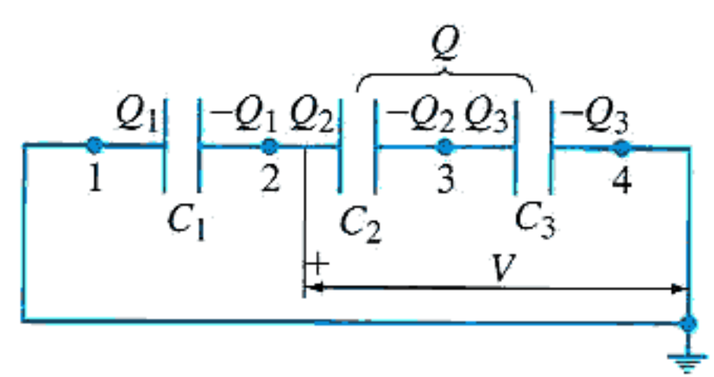

Figure 2.47 Equivalent circuit for the system in Fig. 1.42; for Problem 2.40.

2.41. Equivalent circuit with cylindrical capacitors. Repeat Problem 1.79 by generating and solving an equivalent circuit with capacitors.

2.42. Spherical capacitor with a solid and liquid dielectric. Consider the spherical capacitor in Fig. 2.27 and assume that the inner dielectric layer is made from mica ($\varepsilon_{r1} = 5.4$), whereas the outer layer is oil ($\varepsilon_{r2} = 2.3$). The geometrical parameters are $a = 2$ cm, $b = 8$ cm, and $c = 16$ cm. The capacitor is connected to a source of voltage $V = 100$ V. The source is then disconnected, and the oil is drained from the capacitor. Find the voltage between the electrodes of the capacitor in the new electrostatic state.

2.43. Oil drain without disconnecting the source. If the oil in the capacitor from the previous problem is drained without disconnecting the voltage source, determine the flow of electricity through the source circuit (that is, the difference in the charge of the capacitor) between the two electrostatic states.

2.44. Metallic sphere with dielectric coating. A metallic sphere of radius $a = 1$ cm is covered

with a concentric dielectric layer of relative permittivity $\varepsilon_r = 4$ and thickness $b - a = 2$ cm and situated in air, as shown in Fig. 2.48. The potential of the sphere with respect to the reference point at infinity is $V = 1$ kV. Compute (a) the capacitance of the sphere, (b) the free surface charge density on the sphere surface, (c) the bound volume charge density in the dielectric, and (d) the bound surface charge densities on dielectric interfaces.

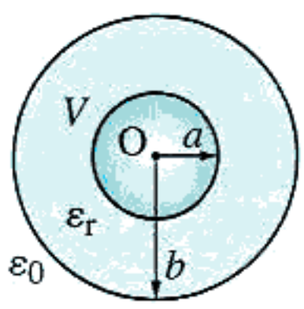

Figure 2.48 Metallic sphere with a dielectric coating in air; for Problem 2.44.

2.45. Charge densities in a half-filled spherical capacitor. Consider the half-filled spherical capacitor from Fig. 2.29, and assume that $a = 2$ cm, $b = 10$ cm, $\varepsilon_r = 3$, and $Q = 10$ nC. Find the distributions of (a) free surface charges on metallic surfaces and (b) bound surface charges on dielectric surfaces.

2.46. Empty and half-filled spherical capacitor. An air-filled spherical capacitor with conductor radii $a = 3$ cm and $b = 15$ cm is connected to a source of voltage $V = 15$ kV. After an electrostatic state is established, the source is disconnected. The capacitor is then half filled with a liquid dielectric of relative permittivity $\varepsilon_r = 2.5$. What is the new voltage between the electrodes of the capacitor?

2.47. Metallic sphere half embedded in a dielectric. A metallic sphere of radius a is pressed into a dielectric half-space of permittivity ε up to a half of its volume, as shown in Fig. 2.49. The medium in the upper half-space is air. (a) Find the capacitance of the sphere. (b) If the sphere is charged with Q, determine what portion of this charge is located on the upper half of the sphere surface.

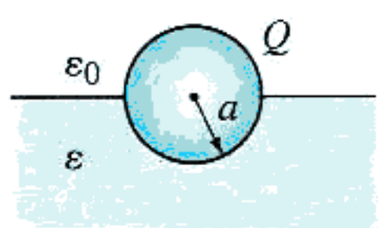

Figure 2.49 Charged metallic sphere half embedded in a dielectric half-space; for Problem 2.47.

2.48. Coaxial cable with two coaxial dielectric layers. Fig. 2.50 shows a cross section of a coaxial cable with two coaxial dielectric layers. The geometry parameters are $a = 1$ mm, $b = 2$ mm, and $c = 4$ mm. The dielectric parameters are $\varepsilon_{r1} = 5$ and $\varepsilon_{r2} = 2$. Calculate the capacitance per unit length of the cable.

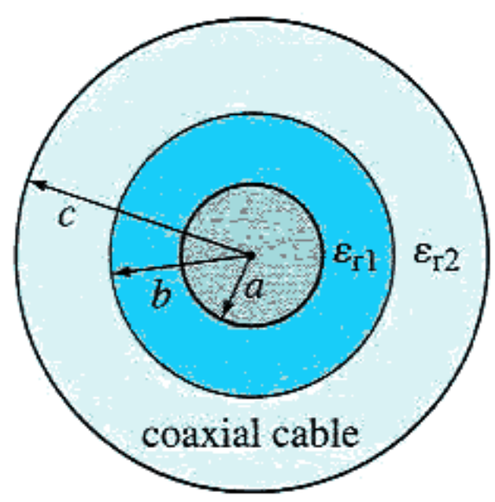

Figure 2.50 Cross section of a coaxial cable with two dielectric layers; for Problem 2.48.

2.49. Coaxial cable with a radial variation of permittivity. Consider a coaxial cable with a continuously inhomogeneous dielectric, whose relative permittivity is given by the following function of the radial distance r from the cable axis: $\varepsilon_r(r) = r/a$ $(a \le r \le b)$, where a and $b = 5a$ are the cable conductor radii. If the potential difference between the cable conductors is V, find (a) the capacitance per unit length of the cable and (b) the bound charge distribution of the dielectric.

2.50. Coaxial cable with four dielectric sectors. A coaxial cable is filled with a piece-wise homogeneous dielectric composed of four 90° sectoral parts with different permittivities, as shown in Fig. 2.51. Let the relative permittivities of the sectors be $\varepsilon_{r1} = 6$, $\varepsilon_{r2} = 2$, $\varepsilon_{r3} = 1$, and $\varepsilon_{r4} = 10$, the radii of the cable conductors $a = 2$ mm and $b = 7$ mm, and the potential of the outer conductor with respect to the inner conductor $V = 25$ V. Compute (a) the capacitance per unit length of the cable and (b) the free charge density at an arbitrary point on the surface of the inner conductor.

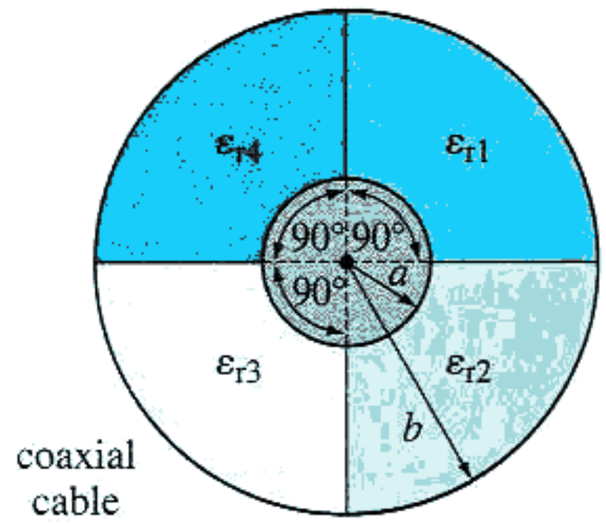

Figure 2.51 Cross section of a coaxial cable with four 90° dielectric sectors; for Problem 2.50.

2.51. Charge distribution for two coated wires. Consider the two-wire line with dielectric coatings in Fig. 2.31, and assume that $a = 1$ mm, $d = 25$ mm, $\varepsilon_r = 4$, and $V = 10$ V. Under these circumstances, find the distribution of (a) free charge and (b) bound charge in the system.

2.52. Two metallic spheres with dielectric coating. If two identical metallic spheres with dielectric coating as the one described in Problem 2.44 are placed in air so that the distance between their centers is $d = 1$ m, determine the capacitance of such a capacitor.

2.53. Two metallic spheres half embedded in a dielectric. Two metallic spheres of radii $a = 5$ mm are half embedded in a dielectric half-space of relative permittivity $\varepsilon_r = 4$, as shown in Fig. 2.52. The distance between the centers of the spheres is $d = 30$ cm. The upper medium is air. The spheres are charged with charges of equal magnitudes and opposite polarities. The potential difference between the spheres is $V = 200$ V. For such a capacitor, find (a) the capacitance, (b) the distribution of free charges over conductors, and (c) distribution of bound charges in the dielectric.

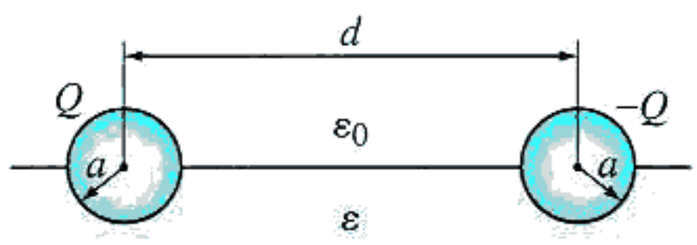

Figure 2.52 Two charged metallic spheres pressed into a dielectric half-space; for Problem 2.53.

2.54. Permittivity gradient normal to capacitor plates. Fig. 2.53 shows a parallel-plate capacitor with rectangular plates of dimensions a and b and continuously inhomogeneous dielectric of thickness d. The permittivity of the dielectric is given by the following function of the x-coordinate: $\varepsilon(x) = 2(1 + 3x/d)\varepsilon_0$ $(0 \le x \le d)$. Neglecting fringing, calculate the capacitance of this capacitor.

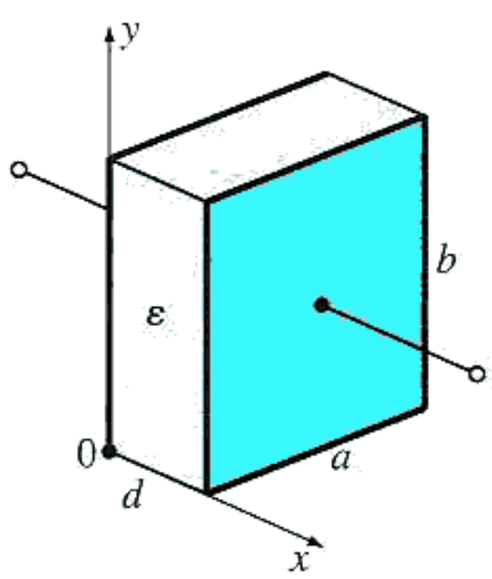

Figure 2.53 Parallel-plate capacitor with a continuously inhomogeneous dielectric; for Problem 2.54.

2.55. Permittivity gradient parallel to capacitor plates. Assume that the permittivity of the dielectric in Fig. 2.53 is a function of the y-coordinate, $\varepsilon(y) = 2[1 + 3\sin(\pi y/b)]\varepsilon_0$ $(0 \le y \le b)$, and find the capacitance of the capacitor. Neglect fringing.

2.56. Capacitor with a nonlinear dielectric layer. Fig. 2.54 shows a parallel-plate capacitor that is half filled with a ferroelectric. The other part of the capacitor is air-filled. The capacitor is charged by being connected to a voltage source. The source is then disconnected, and the capacitor electrodes are short-circuited. In the new electrostatic state, there is a remanent uniform polarization throughout the volume of the dielectric, with the polarization vector being normal to the capacitor plates and its magnitude being P. Determine the electric field intensity vector between the capacitor plates in (a) air and (b) dielectric. Fringing can be neglected.

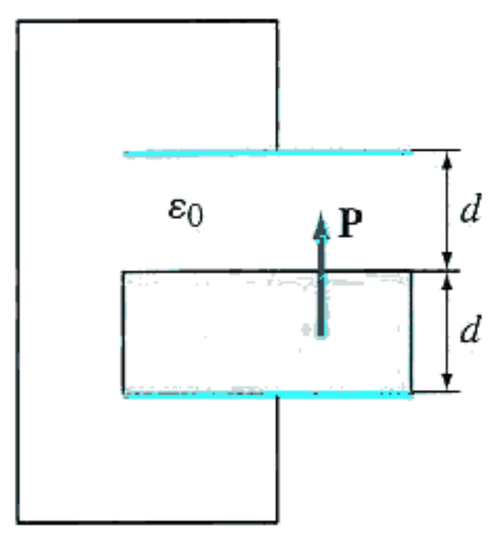

Figure 2.54 Short-circuited parallel-plate capacitor containing a nonlinear dielectric layer with a uniform remanent polarization; for Problem 2.56.

2.57. Energy of a spherical capacitor with two layers. For the spherical capacitor with two concentric dielectric layers from Example 2.18, compute the electric energy stored in each of the layers by (a) integrating the electric energy density over the volume of each layer and (b) representing the capacitor as a series connection of two spherical capacitors with homogeneous dielectrics.

2.58. Change in energy of a spherical capacitor. For the spherical capacitor with solid and liquid

dielectric layers from Problem 2.42, find the change in energy of the capacitor between the electrostatic state with the capacitor connected to the voltage source and the final electrostatic state.

2.59. Energy of a coated metallic sphere. For the charged metallic sphere with a dielectric coating from Problem 2.44, determine the radius b such that 1/2 of the total energy of the system is stored in the coating.

2.60. Energy of a coaxial cable with two coaxial layers. For the coaxial cable with two coaxial dielectric layers from Problem 2.48, assume that the voltage between the cable conductors is $V = 100$ V and find the per-unit-length electric energy contained in each of the layers by (a) integrating the electric energy density over the cross section of each layer and (b) representing the cable as a series connection of two coaxial cylindrical capacitors with homogeneous dielectrics.

2.61. Energy of a half-filled spherical capacitor. For the spherical capacitor half filled with a liquid dielectric from Example 2.20, calculate the electric energy stored in the liquid, if the charge of the capacitor is Q.

2.62. Energy of a coaxial cable with four sectors. For the coaxial cable with four dielectric sectors from Problem 2.50, find the per-unit-length electric energy contained in each of the sectors.

2.63. Energy of a capacitor with a variable permittivity. Consider the parallel-plate capacitor with a permittivity variation normal to plates from Problem 2.54. Determine what percentage of the total electric energy of the capacitor, when charged, is contained in the first half of the dielectric, from $x = 0$ to $x = d/2$.

2.64. Energy of a capacitor with an inhomogeneous dielectric. For the parallel-plate capacitor with a permittivity variation parallel to plates from Problem 2.55, find what percentage of the total electric energy of the capacitor, if charged, is stored in the lower half of the dielectric, from $y = 0$ to $y = b/2$.

2.65. Energy of a system of spherical conductors. Calculate the energy of the system of three spherical conductors from Problem 1.80.

2.66. Energy of a system of flat electrodes. Compute the electric energy stored in the system of five parallel large flat electrodes from Example 1.28 in the following two ways: (a) using the electric field intensities between electrodes (found in Example 1.28) and the corresponding energy densities and (b) using the equivalent circuit in Fig. 2.47 and the involved capacitances, respectively.

2.67. Energy of a system with free volume charge. Find the electric energy per unit length of the system with a volume free charge distribution from Problem 2.14.

2.68. Energy of a *pn* junction. Calculate the electric energy contained in the *pn* junction from Example 2.6, assuming that the area of the junction cross section perpendicular to the x-axis is S.

2.69. Breakdown charge and energy of the earth. Determine the maximum possible charge and electric energy that could be stored on the earth, as described in Problem 2.25, and in the electric field around it, limited by an eventual dielectric breakdown of air near the earth's surface.

2.70. Maximum breakdown voltage of a spherical capacitor. A spherical capacitor has electrodes of radii a and $b = 10$ cm ($a < b$). It is filled with a homogeneous dielectric of relative permittivity $\varepsilon_r = 5$ and dielectric strength $E_{cr} = 25$ MV/m. (a) Find a for which the breakdown voltage of the capacitor is maximum. (b) What is the maximum breakdown voltage of the capacitor? (c) What is the energy of the capacitor at breakdown?

2.71. Breakdown in a wire-plane transmission line. (a) Compute the breakdown voltage of the wire-plane transmission line in Fig. 2.24(a), assuming that $a = 1$ cm and $h = 1$ m. (b) What is the maximum energy per unit length of this line? (c) Determine the largest possible electric force on the wire conductor per unit of its length.

2.72. Grounded metallic sphere as a lightning arrester. Repeat Example 2.31 but for a grounded small metallic sphere (instead of the wire) in a uniform atmospheric electric field above the surface of the earth. Adopt the same radius and the same height of the conductor.

2.73. Parallel-plate capacitor with two dielectric layers. Consider the parallel-plate capacitor with

two dielectric layers in Fig. 2.25(a), and assume that $d_1 = 2$ mm, $d_2 = 4$ mm, $\varepsilon_{r1} = 3$, and $\varepsilon_{r2} = 5$, as well as that the dielectric strengths for the layers are $E_{cr1} = 20$ MV/m and $E_{cr2} = 11$ MV/m, respectively. Find the breakdown voltage of the capacitor. Neglect fringing.

2.74. Parallel-plate capacitor with two dielectric sectors. Repeat the previous problem but for the parallel-plate capacitor with two dielectric sectors from Fig. 2.25(b) and $d = d_1 + d_2$.

2.75. Breakdown in a spherical capacitor with two layers. Find the breakdown voltage of the spherical capacitor with two concentric dielectric layers from Problem 2.42 in (a) the first state (outer layer is oil) and (b) the second state (outer layer is air). The dielectric strengths for mica and oil are $E_{cr1} = 200$ MV/m and $E_{cr2} = 15$ MV/m, respectively.

2.76. Breakdown potential of a coated metallic sphere. (a) Determine the breakdown potential of the metallic sphere with a dielectric coating from Problem 2.44 if the dielectric strength for the coating is $E_{cr} = 30$ MV/m. (b) What is the maximum energy of this structure?

2.77. Breakdown in a coaxial cable with two layers. (a) Find the breakdown voltage of the coaxial cable with two coaxial dielectric layers from Problem 2.48. The dielectric strengths of the inner and outer layer are $E_{cr1} = 40$ MV/m and $E_{cr2} = 20$ MV/m, respectively. (b) Calculate the maximum energy that this cable can store per unit of its length.

2.78. Simultaneous breakdown in two spherical layers. Consider the spherical capacitor with two concentric dielectric layers in Fig. 2.27. Let the dielectric strengths of the inner and outer layer be E_{cr1} and E_{cr2}, respectively. Find the relationship between the parameters of this capacitor (a, b, c, ε_{r1}, ε_{r2}, E_{cr1}, and E_{cr2}) such that, for sufficiently large capacitor voltage, dielectric breakdown will occur in both dielectric layers simultaneously.

2.79. Simultaneous breakdown in two coaxial layers. Repeat the previous problem but for a coaxial cable with two coaxial dielectric layers (Fig. 2.50).

2.80. Metallic sphere half immersed in a liquid dielectric. A metallic sphere of radius $a = 2$ cm is half immersed in a liquid dielectric, as in Fig. 2.49. The relative permittivity of the dielectric is $\varepsilon_r = 3$ and its dielectric strength is $E_{cr} = 20$ MV/m. The upper medium is air. Calculate the maximum potential of this sphere such that dielectric breakdown will not occur after it is removed from the liquid and raised high above the interface.

2.81. Breakdown in a coaxial cable with a dielectric spacer. Consider the coaxial cable with a dielectric spacer in Fig. 2.33, and assume that $a = 2$ mm, $b = 6$ mm, $\alpha = 60°$, and $\varepsilon_r = 5$, as well as that the dielectric strength for the spacer is $E_{cr} = 200$ MV/m. Find (a) the breakdown voltage of the cable and (b) the electric energy per unit length of the cable at breakdown.

3 Steady Electric Currents

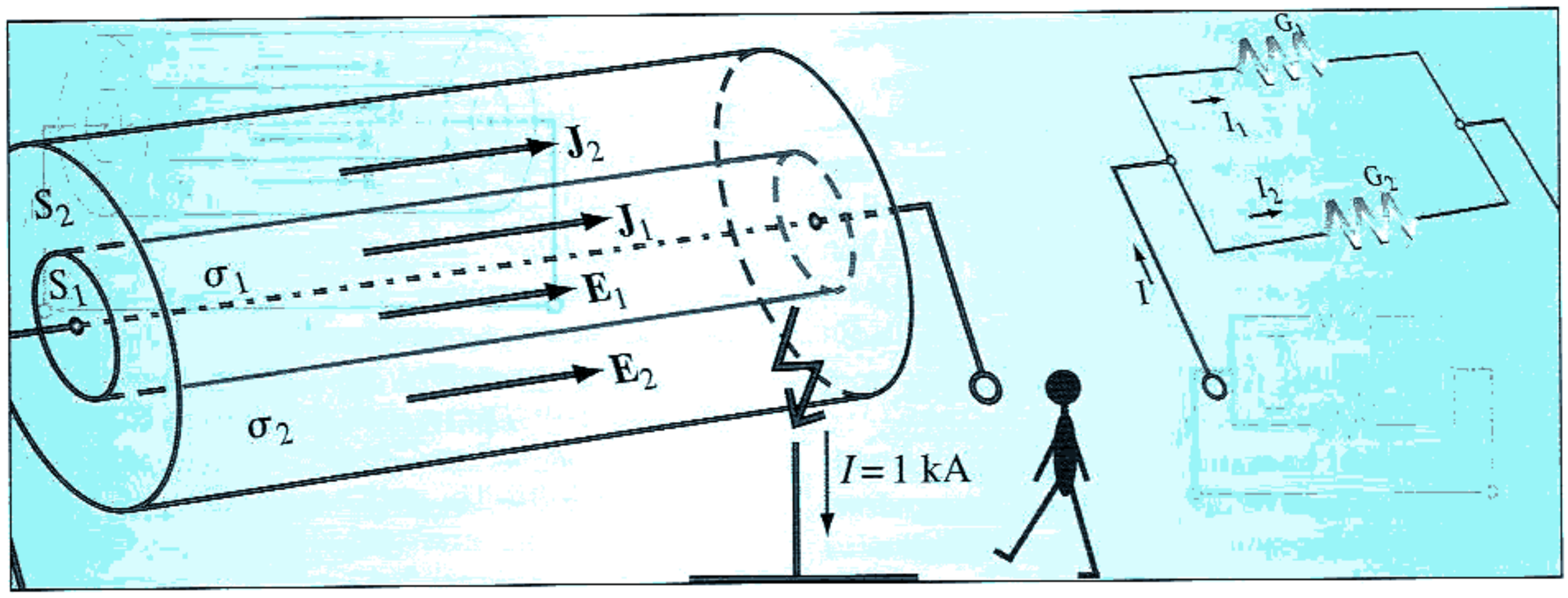

Introduction:

So far, we have dealt with electrostatic fields, associated with time-invariant charges at rest. We now consider the charges in an organized macroscopic motion, which constitute an electric current. Our focus in this chapter is on the steady flow of free charges in conducting materials, i.e., on steady (time-invariant) electric currents, whose macroscopic characteristics (like the amount of current through a wire conductor) do not vary with time. Steady currents are also called direct currents, abbreviated dc. The subject of steady electric currents links field theory to several important concepts of circuit theory, such as Ohm's law, Kirchhoff's current and voltage laws, Joule's law, resistance, conductance, voltage and current generators, and power balance in a circuit. Discussions of steady electric currents will bring us to the field and circuit analysis of transmission lines with losses in a time-invariant (dc) regime, and help us further develop and understand the concept of a transmission line as a circuit with distributed parameters.

We shall derive and discuss integral and differential field equations for steady electric currents and their electric field, along with the corresponding boundary conditions. We shall also study the mechanism of conduction for various materials, introduce models of energy sources, and derive expressions for power and energy calculations. These equations and concepts will enable us to develop and demonstrate techniques for analysis of several general configurations with steady currents, such as resistors of various composition and shapes, capacitors with imperfect inhomogeneous dielectrics, transmission lines with imperfect conductors and imperfect inhomogeneous dielectrics, and grounding electrodes buried in the earth.

3.1 CURRENT DENSITY VECTOR AND CURRENT INTENSITY

In the absence of an externally applied electric field, free charges in a conductor are in a state of random (chaotic) motion due to their thermal energy. This is so-called thermal motion of charges. The corresponding velocity is the thermal velocity, denoted as $\mathbf{v}_t$. Generally, v_t is rather large. In metallic conductors, free electrons move at thermal velocities on the order of $v_t \sim 10^5$ m/s at room temperature, between collisions with the atoms and with one another.[1] Because of the entirely random nature of thermal motion of charges (without any external electric field applied), there is no net macroscopic motion in any given direction, i.e., the macroscopic average vectorial resultant of thermal velocities of individual charges at any point in the conductor is zero. For an electric current, defined as a macroscopic net flow of free charges, to exist, there must be a nonzero macroscopic average velocity of microscopic velocities of charges in some direction in a conductor. This can be achieved, as we shall see, by establishing and maintaining an external (i.e., externally applied) electric field within a conductor.

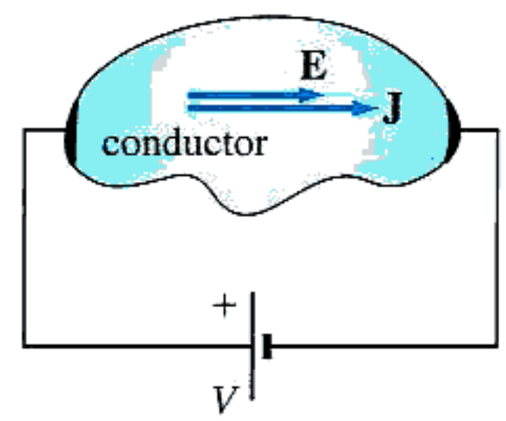

Figure 3.1 Conductor whose two ends are maintained at a potential difference.

Consider a conducting body whose two ends are connected to a generator of voltage V, as shown in Fig. 3.1. Because a potential difference is maintained between the conductor ends, there is an electric field of intensity $\mathbf{E}$ inside the conductor [the line integral of $\mathbf{E}$, Eq. (1.90), through the conductor is nonzero]. Note that this situation is essentially different from the situation in Fig. 1.38, where the transient redistribution of charge occurred and electrostatic equilibrium with zero field inside the conductor was established. Here, the conductor is not isolated but wired to a source of electromotive force (generator), providing a mechanism that forces the free charges to move and prevents them from piling up, which would tend to reduce the field in the conductor. Assume, for simplicity, that the free charge carriers in the conductor are electrons only (as in metallic conductors). The electric force on each charge is thus [Eq. (1.23)]

$$\mathbf{F}_e = -e\mathbf{E}, \tag{3.1}$$

where the charge amount e ($e > 0$) is given in Eq. (1.3). This force compels the electrons to move through the conductor, between its ends. However, since the electrons are not in free space, they cannot accelerate indefinitely under the influence of the electric field. Before they can acquire any appreciable speed, the electrons collide with the atomic lattice and acquire new random velocities $\mathbf{v}_t$. Since the field $\mathbf{E}$ essentially has to start accelerating the electrons all over again every $\Delta t_c \sim 10^{-14}$ s (typical average time interval between collisions at room temperature), it can change the random thermal velocities of the electrons only slightly, but in a systematic manner. This relatively slight systematic drift of the free electrons is the basis of electric conduction (current). After a brief initial transient, the electrons acquire a steady-state average velocity, determined by the balance between the accelerating force of the applied field, $\mathbf{F}_e$, and the scattering effect of the collisions with the lattice. This velocity is termed the drift velocity and symbolized by $\mathbf{v}_d$.

[1]The free electrons in a metallic conductor are so-called conduction-band electrons (or valence electrons), which are very loosely bound to their atoms and are essentially free to move about the crystalline structure of the metal. For example, each atom of copper has 29 electrons, 28 of which are bound electrons (tightly bound in their shells), while the outermost one is a free electron.

In general, $v_d \ll v_t$, since the electric field makes only a slight change in the velocity distribution that existed before the field was applied, and $\mathbf{v}_d$ is a macroscopic resultant of microscopic velocities of free charges in a direction along the electric field lines. In most cases, its magnitude is not larger than $v_d \sim 10^{-4}$ m/s in metals, for reasonable amounts of current carried (as we shall see in an example). The drift velocity is linearly proportional to the electric field intensity vector,

drift velocity

$$\boxed{\mathbf{v}_d = -\mu_e \mathbf{E},} \tag{3.2}$$

where the constant μ_e is the so-called mobility of electrons in the given material. The mobility is measured in the units of $m^2/(Vs)$ and is positive by definition. For electrons, the direction of $\mathbf{v}_d$, as well as the direction of $\mathbf{F}_e$, is opposite to the direction of $\mathbf{E}$. Good conductors have high mobility.

We can now say that charge carriers in the conductor move through its volume with the macroscopic average velocity $\mathbf{v}_d$. This is an organized, directive motion of charges, which constitute an electric current throughout the conductor volume. We introduce then a new field quantity, to describe the current at a point: the current density vector, $\mathbf{J}$. By definition,

current density vector (unit: A/m^2)

$$\boxed{\mathbf{J} = N_v(-e)\mathbf{v}_d,} \tag{3.3}$$

where N_v is the concentration of charge carriers, i.e., their number per unit volume or per 1 m^3 (the unit is m^{-3}).[2]

The current density can alternatively be defined by means of the current intensity, I, which, in turn, is defined as a rate of movement of charge passing through a surface (e.g., cross section of a cylindrical conductor). That is,

current intensity or, simply, current (unit: A)

$$\boxed{I = \frac{dQ}{dt}.} \tag{3.4}$$

In other words, I equals the total amount of charge that flows through the surface during an elementary time dt, divided by dt. The unit for current intensity, which is usually referred to as, simply, current, is ampere or amp (A), equal to C/s. The current density vector is directed along the macroscopic motion of charges, i.e., along the current lines. If we set an elementary surface of area dS perpendicular to the current lines, as in Fig. 3.2(a), the magnitude of the current density vector is given by

current density vs. intensity

$$\boxed{J = \frac{dI}{dS}.} \tag{3.5}$$

where dI is the current flowing through dS. We see that the unit for $\mathbf{J}$ is A/m^2, which means that it actually represents a surface density of a volume current.

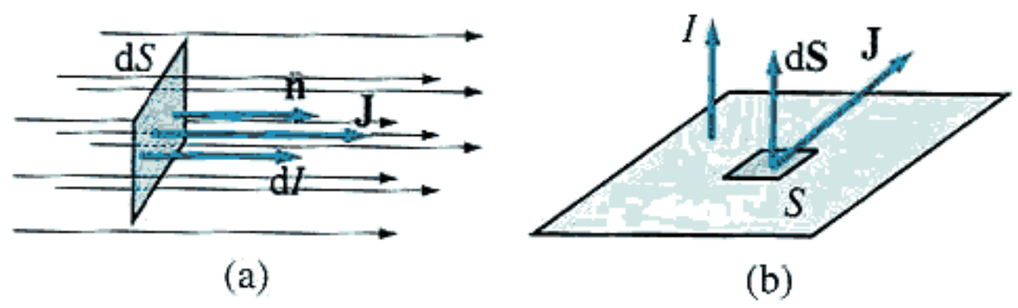

Figure 3.2 (a) Definition of the current density by means of the current intensity. (b) Evaluation of the total current through a surface.

[2]For example, the concentration of conduction electrons in copper is $N_v = 8.45 \times 10^{28}$ m^{-3}. It equals the number of copper atoms per unit volume, since copper has one conduction-band electron per atom. The number of atoms per unit volume is approximately the same for all solids.

To show that the definitions of current density, J, in Eqs. (3.3) and (3.5) are equivalent, we realize that the total amount of charge that crosses $\mathrm{d}S$ during the time interval $\mathrm{d}t$ is

$$\mathrm{d}Q = N_\mathrm{v} \underbrace{\mathrm{d}S v_\mathrm{d}\,\mathrm{d}t}_{\Delta v} (-e) \tag{3.6}$$

(in the time interval $\mathrm{d}t$, a charge moves a distance $v_\mathrm{d}\,\mathrm{d}t$, and all charges in the volume $\Delta v = \mathrm{d}S v_\mathrm{d}\,\mathrm{d}t$, the number of which is the concentration N_v times Δv, pass through $\mathrm{d}S$). Using the definition of J in Eq. (3.3), this becomes

$$\mathrm{d}Q = J\,\mathrm{d}S\,\mathrm{d}t. \tag{3.7}$$

Dividing by $\mathrm{d}t$, we obtain the current intensity $\mathrm{d}I$ through $\mathrm{d}S$ in terms of J:

$$\mathrm{d}I = J\,\mathrm{d}S, \tag{3.8}$$

which indeed is the same as in Eq. (3.5).

In the case where the current density vector is not perpendicular to the surface element, the current through the element is

$$\mathrm{d}I = J\,\mathrm{d}S_\mathrm{n} = J\,\mathrm{d}S\cos\alpha = \mathbf{J}\cdot\mathrm{d}\mathbf{S}, \tag{3.9}$$

where $\mathrm{d}S_\mathrm{n}$ is the projection of $\mathrm{d}S$ on the plane normal to $\mathbf{J}$ and α is the angle between $\mathbf{J}$ and $\mathrm{d}\mathbf{S}$ (see Fig. 1.30). Hence, the total current through an arbitrary surface S, Fig. 3.2(b), equals the flux of the current density vector through the surface,

$$\boxed{I = \int_S \mathbf{J}\cdot\mathrm{d}\mathbf{S}.} \tag{3.10}$$

total current through a surface

If there are several types of free charge carriers in a conductor drifting with different average velocities, the resultant current density vector is a vector sum of current densities in Eq. (3.3),

$$\mathbf{J} = \sum_{i=1}^{M} N_{\mathrm{v}i} q_i \mathbf{v}_{\mathrm{d}i}, \tag{3.11}$$

that correspond to individual types of carriers (e.g., electrons and holes in a semiconductor). Equivalently, the net charge flow is taken in evaluating the resultant current intensity in Eq. (3.4). Positive charges move in the direction of $\mathbf{E}$, negative charges in the opposite direction, but both add to the total current. Eqs. (3.4), (3.5), and (3.10) are therefore valid for any conductor and any combination of charge carriers.

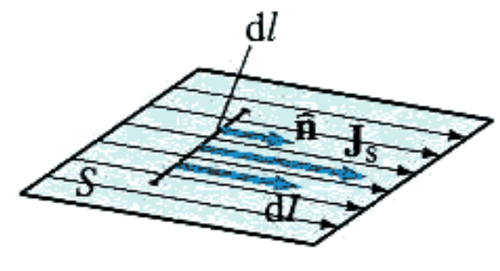

Figure 3.3 Surface current density vector ($\mathbf{J}_\mathrm{s}$).

In many situations, current flow is localized in a very thin (theoretically infinitely thin) film over a surface, as shown in Fig. 3.3. This is so-called surface current, described by the surface current density vector, $\mathbf{J}_\mathrm{s}$, which is defined as

$$\boxed{\mathbf{J}_\mathrm{s} = N_\mathrm{s} q \mathbf{v}_\mathrm{d},} \tag{3.12}$$

surface current density vector (unit: A/m)

where N_s is the surface concentration of charge carriers (number of carriers per unit surface area, in m^{-2}). Note that the surface current density vector is sometimes denoted as $\mathbf{K}$. In terms of the current intensity, the surface current density is given by

$$\boxed{J_\mathrm{s} = \frac{\mathrm{d}I}{\mathrm{d}l},} \tag{3.13}$$

surface current density vs. current intensity

where dI is the current flowing across a line element dl set normal to the current flow (Fig. 3.3). The unit for $\mathbf{J}_s$, which represents a line density of a surface current, is A/m. For example, the surface current density of a very thin aluminum strip (foil) with a current I that is uniformly distributed across the strip width, w, equals $J_s = I/w$, and $\mathbf{J}_s$ is directed parallel to the strip axis.

Example 3.1 Electron Drift along a 1-km Copper Wire

A copper wire of length $l = 1$ km and radius $a = 3$ mm carries a steady current of intensity $I = 10$ A. The current is uniformly distributed across the wire cross section. Find the time in which the electrons drift along the wire.

Solution As the current is distributed uniformly across the cross section (S) of the wire, the current density in the wire is [Eq. (3.10)]

$$J = \frac{I}{S} = \frac{I}{\pi a^2} = 3.54 \times 10^5 \text{ A/m}^2. \tag{3.14}$$

From Eq. (3.3), the drift velocity of electrons is

$$v_d = \frac{J}{N_v e} = 2.62 \times 10^{-5} \text{ m/s}, \tag{3.15}$$

where $N_v = 8.45 \times 10^{28}$ m^{-3} is the concentration of conduction electrons in copper and e is the absolute value of the charge of an electron, Eq. (1.3). The time it takes for an electron to drift along the wire is hence

$$t = \frac{l}{v_d} = 3.82 \times 10^7 \text{ s}, \tag{3.16}$$

which is approximately 442 days.[3]

3.2 CONDUCTIVITY AND OHM'S LAW IN LOCAL FORM

Consider again a metallic conductor (the charge is carried by electrons), with the current density $\mathbf{J}$. Substituting Eq. (3.2) into Eq. (3.3), we obtain

current density in a metallic conductor

$$\boxed{\mathbf{J} = N_v e \mu_e \mathbf{E}.} \tag{3.17}$$

This equation can be rewritten as

Ohm's law in local form

$$\boxed{\mathbf{J} = \sigma \mathbf{E},} \tag{3.18}$$

where the proportionality constant,

conductivity of metallic conductors (unit: S/m)

$$\boxed{\sigma = N_v e \mu_e,} \tag{3.19}$$

is a macroscopic parameter of the medium called conductivity. It is always positive, and represents, in general, a measure of the ability of materials to conduct electric current. The unit for conductivity is siemens per meter (S/m). The reciprocal of σ is denoted by the symbol ρ and termed resistivity. The unit is ohm × meter (Ωm).

[3]We know that, of course, we do not need to wait 442 days to receive a communication signal sent via a 1-km long transmission line. We shall see in a later chapter that time-varying signals traveling along transmission lines propagate as electromagnetic waves outside the conductors that constitute the line, and not via the drifting motion of electrons within the conductors. The conductors actually serve as guides for the waves along the line. That is why signals travel at the velocity of electromagnetic waves in the medium surrounding the line conductors. If the medium is air, the velocity is 3×10^8 m/s (speed of light in a vacuum), and the travel time is only 3.33 μs for a 1-km line.

Using resistivity, Eq. (3.18) becomes

$$\boxed{\mathbf{E} = \rho \mathbf{J}, \quad \rho = \frac{1}{\sigma}.} \tag{3.20}$$

ρ – resistivity (unit: Ωm)

Both Eqs. (3.18) and (3.20) are known as Ohm's law in local or point form.

Note that Eq. (3.18) is one of the three general electromagnetic constitutive equations for characterization of materials [another one being Eq. (2.46)]. It can be written in the following form:

$$\boxed{\mathbf{J} = \mathbf{J}(\mathbf{E}),} \tag{3.21}$$

*constitutive equation for **J**, for an arbitrary material*

to encompass all possible conducting properties of materials. However, in terms of their conductivity, most conducting materials are linear and isotropic, i.e., $\mathbf{J}(\mathbf{E}) = \sigma \mathbf{E}$, where σ is independent of electric field intensity and current density (the property of linearity), and is the same for all directions (isotropy). In homogeneous conductors, σ does not change from point to point in the region being considered. For inhomogeneous conductors, on the other hand, σ is a function of spatial coordinates [e.g., $\sigma = \sigma(x, y, z)$ in the region].

Almost always, the conductivity is a function of temperature, T. One of the few exceptions is an alloy called constantan (55% copper, 45% nickel), whose conductivity is practically constant in a temperature range 0–100°C. For metallic conductors, the mobility of electrons decreases with an increase in temperature (because the average time interval between collisions with vibrating atoms, Δt_c, decreases). Hence, the conductivity decreases and resistivity increases with a temperature rise. Around a room temperature of $T_0 = 293$ K (20°C), the resistivity varies almost linearly with T, and we can write

$$\rho(T) = \rho_0 [1 + \alpha (T - T_0)], \tag{3.22}$$

where $\rho_0 = \rho(T_0)$. For most metals (copper, aluminum, silver, etc.), the temperature coefficient of resistivity, α, is approximately 0.4% per kelvin.

For some materials the resistivity drops abruptly to zero below a certain temperature:

$$\boxed{\rho(T) = 0 \quad \text{for} \quad T < T_{cr},} \tag{3.23}$$

superconductors

where T_{cr} is called the critical temperature of the material. This property, discovered by Kamerlingh Onnes in 1911, is called superconductivity, and the materials are said to behave like superconductors. Most superconductors are metallic elements that exhibit transition into superconducting states at a temperature of a few kelvin. Examples are aluminum ($T_{cr} = 1.2$ K), lead ($T_{cr} = 7.2$ K), and niobium ($T_{cr} = 9.2$ K), as well as their alloys and compounds. More recently, new ceramic materials were discovered that become superconducting at considerably higher (and thus less expensive to produce and maintain) temperatures. For example, yttrium-barium-copper oxide ($YBa_2Cu_3O_7$), discovered in 1986, has $T_{cr} = 80$ K, so its superconductivity can be utilized by cooling with liquid nitrogen. Interestingly, some of the best of the normal conductors, such as silver and copper, cannot become superconducting at any temperature, while the ceramic superconductors are normally good insulators – when they are not at low enough temperatures to be in a superconducting state.

Ohm's law in local form holds also for conductors with more than one type of charge carriers [see Eq. (3.11)]. In plasmas and gases, the charge carriers are electrons and positive ions (electron-deficient atoms or molecules). In liquid conductors, called electrolytes, the charge is carried by positive and negative ions. In all cases,

both positively and negatively charged particles (ions and electrons) contribute to the conductivity.

In semiconductors (e.g., silicon and germanium), vacancies in the atomic crystal lattice left by electrons, called holes, can move from atom to atom and behave like positive charge carriers, each hole carrying charge e. The conductivity of a semiconductor is therefore

conductivity of semiconductors

$$\boxed{\sigma = N_{\text{ve}} e \mu_{\text{e}} + N_{\text{vh}} e \mu_{\text{h}},} \tag{3.24}$$

where the first term represents the contribution to the conductivity from electrons, moving opposite to the field $\mathbf{E}$, while the second term represents the contribution from holes, which move with $\mathbf{E}$. The concentrations N_{ve} and N_{vh} rapidly increase with an increase in temperature (temperature rise accelerates generation of free electrons and holes). Consequently, the conductivity of semiconductors increases with increasing the temperature, which is opposite to the temperature behavior of metallic conductors.

By adding very small amounts of impurities to pure (intrinsic) semiconductors, the conductivity may be increased dramatically. Impurities called donors (e.g., phosphorus) provide additional electrons and form n-type semiconductors, while acceptors (e.g., boron) introduce extra holes, forming p-type semiconductors. This procedure is known as doping of semiconductors. Note that the boundary between p-type and n-type parts of a single semiconductor crystal forms a junction region, called pn junction (see Fig. 2.9), which is utilized in semiconductor devices (diodes and transistors).[4]

Unlike the relative permittivity (ε_{r}), shown in Table 2.1, the conductivity of materials varies over an extremely wide range of values, as we go from the best insulators to semiconductors, to the finest conductors. In S/m, σ (at room temperature) ranges from around 10^{-17} for fused quartz, 10^{-9} for bakelite, 10^{-2} for fresh water, and 2.2 for germanium to 6.17×10^{7} for silver. We see that the range in conductivity from quartz to silver is as large as 25 orders of magnitude (10^{25}), and then it goes to infinity for superconductors. Table 3.1 lists values of the conductivity of selected materials.

Copper (Cu), the most commonly used metallic conductor, has a conductivity of

conductivity of copper, at 20°C

$$\boxed{\sigma_{\text{Cu}} = 58 \text{ MS/m}.} \tag{3.25}$$

In many applications, we consider copper and other metallic conductors as perfect electric conductors (PEC), with

perfect electric conductor (PEC)

$$\boxed{\sigma \to \infty.} \tag{3.26}$$

Of course, superconductors also fall under this category. From Eqs. (3.18) and (3.26), we conclude that

no electric field inside a PEC body

$$\boxed{\mathbf{E} = \frac{\mathbf{J}}{\sigma} = 0,} \tag{3.27}$$

[4] Generally, the current density in semiconductor devices is composed of two components: a drift current density, $\mathbf{J} = \sigma \mathbf{E}$, and a diffusion current density, $\mathbf{J}_{\text{dif}}$, which depends on the gradient of the concentration of charge carriers in a material and, therefore, does not satisfy Ohm's law in local form. Consequently, the relationship between the total current density vector and the electric field intensity vector, Eq. (3.21), in semiconductor devices is, in general, nonlinear.

Table 3.1. Conductivity of selected materials*

Material	σ (S/m)	Material	σ (S/m)
Quartz (fused)	$\sim 10^{-17}$	Carbon (graphite)	7.14×10^4
Wax	$\sim 10^{-17}$	Bismuth	8.70×10^5
Polystyrene	$\sim 10^{-16}$	Cast iron	$\sim 10^6$
Sulfur	$\sim 10^{-15}$	Nichrome	10^6
Mica	$\sim 10^{-15}$	Mercury (liquid)	1.04×10^6
Paraffin	$\sim 10^{-15}$	Stainless steel	1.1×10^6
Rubber (hard)	$\sim 10^{-15}$	Silicon steel	2×10^6
Porcelain	$\sim 10^{-14}$	Titanium	2.09×10^6
Carbon (diamond)	2×10^{-13}	Constantan (45% Ni)	2.26×10^6
Glass	$\sim 10^{-12}$	German silver	3×10^6
Polyethylene	1.5×10^{-12}	Lead	4.56×10^6
Wood	$10^{-11} - 10^{-8}$	Solder	7×10^6
Bakelite	$\sim 10^{-9}$	Niobium	8.06×10^6
Marble	10^{-8}	Tin	8.7×10^6
Granite	10^{-6}	Platinum	9.52×10^6
Dry soil	10^{-4}	Bronze	10^7
Distilled water	2×10^{-4}	Iron	1.03×10^7
Silicon (intrinsic)	4.4×10^{-4}	Nickel	1.45×10^7
Clay	5×10^{-3}	Brass (30% Zn)	1.5×10^7
Fresh water	10^{-2}	Zinc	1.67×10^7
Wet soil	$\sim 10^{-2}$	Tungsten	1.83×10^7
Animal fat**	4×10^{-2}	Sodium	2.17×10^7
Animal muscle ($\perp$ to fiber)**	8×10^{-2}	Magnesium	2.24×10^7
Animal, body (average)**	0.22	Duralumin	3×10^7
Animal muscle ($\parallel$ to fiber)**	0.4	Aluminum	3.5×10^7
Animal blood**	0.7	Gold	4.1×10^7
Germanium (intrinsic)	2.2	Copper	5.8×10^7
Seawater	3–5	Silver	6.17×10^7
Ferrite	10^2	Mercury (at <4.1 K)	∞
Tellurium	$\sim 5 \times 10^2$	Niobium (at <9.2 K)	∞
Silicon (doped)	1.18×10^3	$YBa_2Cu_3O_7$ (at <80 K)	∞

* For dc or low-frequency currents, at room temperature.
** Also for humans.

i.e., the electric field is always zero in perfect conductors. This, in turn, implies that the voltage between any two points of a perfect conductor [Eq. (1.90)] is zero.

Finally, so-called convection currents, which are the result of the motion of positively or negatively charged particles in a vacuum or rarefied gas (where $\sigma = 0$), are not governed by Ohm's law. Examples are electron beams in a cathode ray tube and a violent motion of charged particles in a thunderstorm. The convection current density is given by

$$\boxed{\mathbf{J} = \rho \mathbf{v},} \tag{3.28}$$

convection current density

where $\mathbf{v}$ is the velocity of particles and ρ is the volume density of charges (charge per unit volume) in the vacuum or rarefied gas. Noting that $\rho = N_v q$, N_v being the concentration of particles and q an elementary charge, we observe the equivalency of the definitions of convection and conduction current densities given by Eqs. (3.28)

and (3.3), respectively. However, the velocity $\mathbf{v}$ in Eq. (3.28) is not a drift velocity ($\mathbf{v}_d$) of charges and Eq. (3.2) is not satisfied.

Conceptual Questions (on Companion Website): 3.1 and 3.2.

HISTORICAL ASIDE

Heike Kamerlingh Onnes (1853–1926), Dutch physicist and professor at the University of Leyden, was awarded a Nobel Prize in Physics in 1913 for his investigations of the properties of matter at extremely low temperatures. His experiments led him as close to absolute zero as 0.9 K, which was a fascinating result at that time. He was the first to produce liquid helium (in 1908). Onnes demonstrated in 1911 that the resistivity of mercury absolutely disappears at temperatures below about 4 K, and thus discovered superconductivity.

The SI unit of power, the watt, was named in honor of **James Watt** (1736–1819), a Scottish mechanical engineer and inventor, who is famous for his revolutionary improvements of the steam engine in the 1760s, which led to great advancements in the Industrial Revolution, and is also known for devising the "horsepower" – to measure the power of his steam engines.

3.3 LOSSES IN CONDUCTORS AND JOULE'S LAW IN LOCAL FORM

Let us now consider the current flow in a conductor from the energy point of view. As we know, free charge carriers (e.g., electrons) are accelerated on their paths between collisions with vibrating atoms, and at every collision they lose their acquired kinetic energy. Energy is thus transmitted from the electric field, $\mathbf{E}$, via charge carriers to the atoms, enhancing their thermal vibration and ultimately resulting in a higher temperature of the conductor. This means that in a conductor with electric current, electric energy is constantly converted into heat. We wish to derive the expression for the rate (power) of this energy transformation.

We start with the electric force on a charge $\mathrm{d}Q$ given in Eq. (3.7), which equals $\mathrm{d}Q\,\mathbf{E}$. The work done by this force in moving $\mathrm{d}Q$ a distance $\mathrm{d}l$ along the field lines is [Eq. (1.72)]

$$\mathrm{d}W_e = \mathrm{d}Q\,E\,\mathrm{d}l = J\,\mathrm{d}S\,\mathrm{d}t E\,\mathrm{d}l = JE\,\mathrm{d}v\,\mathrm{d}t \quad (\mathrm{d}v = \mathrm{d}S\,\mathrm{d}l), \tag{3.29}$$

where $\mathrm{d}v$ is an elementary volume in the conductor. This work is converted (lost) to heat, known as Joule's heat. The rate of this conversion, $\mathrm{d}W_e/\mathrm{d}t$ (J/s), is power, called the power of Joule's losses or ohmic losses. Thus, the power of Joule's losses in the volume $\mathrm{d}v$ is

$$\mathrm{d}P_J = \frac{\mathrm{d}W_e}{\mathrm{d}t} = JE\,\mathrm{d}v. \tag{3.30}$$

The volume density of this power is

Joule's law in local form; p_J – ohmic power density (unit: W/m^3)

$$\boxed{p_J = \frac{\mathrm{d}P_J}{\mathrm{d}v} = JE = \frac{J^2}{\sigma} = \sigma E^2,} \tag{3.31}$$

and this is known as Joule's law in local (point) form. The unit for power is watt (W), and hence the unit for power density is W/m^3.

The total power of Joule's losses (the electric power that is lost to heat) in a domain of volume v (e.g., in the entire conducting body) is obtained by integration of power $\mathrm{d}P_\mathrm{J}$ throughout v:

$$\boxed{P_\mathrm{J} = \int_v \underbrace{p_\mathrm{J}\,\mathrm{d}v}_{\mathrm{d}P_\mathrm{J}} = \int_v JE\,\mathrm{d}v.} \tag{3.32}$$

power of Joule's (ohmic) losses (unit: W)

Conceptual Questions (on Companion Website): 3.3.

3.4 CONTINUITY EQUATION

We now consider one of the fundamental principles of electromagnetics – the continuity equation, which is the mathematical expression of the principle of conservation of charge. Charge is indestructible, and cannot be lost or created. It can move from place to place, but can never appear from nowhere nor disappear. Let an arbitrary closed surface, S, enclosing volume v, be situated in a region with time-varying currents, as shown in Fig. 3.4(a), and let Q_S and $Q_S + \mathrm{d}Q_S$ denote the net charges in v at instants of time t and $t + \mathrm{d}t$, respectively. The change in charge, $\mathrm{d}Q_S$, cannot be created in v, but only brought in from the domain outside the surface S, and it is brought by the current flowing through S. So, the charge $\mathrm{d}Q_S$ passes the surface S during the time $\mathrm{d}t$, and this is exactly what we have in the definition of current intensity in Eq. (3.4). Therefore,

$$I_\mathrm{in} = \frac{\mathrm{d}Q_S}{\mathrm{d}t} \tag{3.33}$$

is the intensity of the current flowing across the surface S into the region v. The current crossing the surface in the opposite direction, i.e., the current leaving the region, is hence

$$I_\mathrm{out} = -I_\mathrm{in} = -\frac{\mathrm{d}Q_S}{\mathrm{d}t}. \tag{3.34}$$

On the other hand, by virtue of Eq. (3.10), the current leaving v across S equals the total outward flux of the current density vector through S (which is a closed surface), that is,

$$I_\mathrm{out} = \oint_S \mathbf{J}\cdot\mathrm{d}\mathbf{S}. \tag{3.35}$$

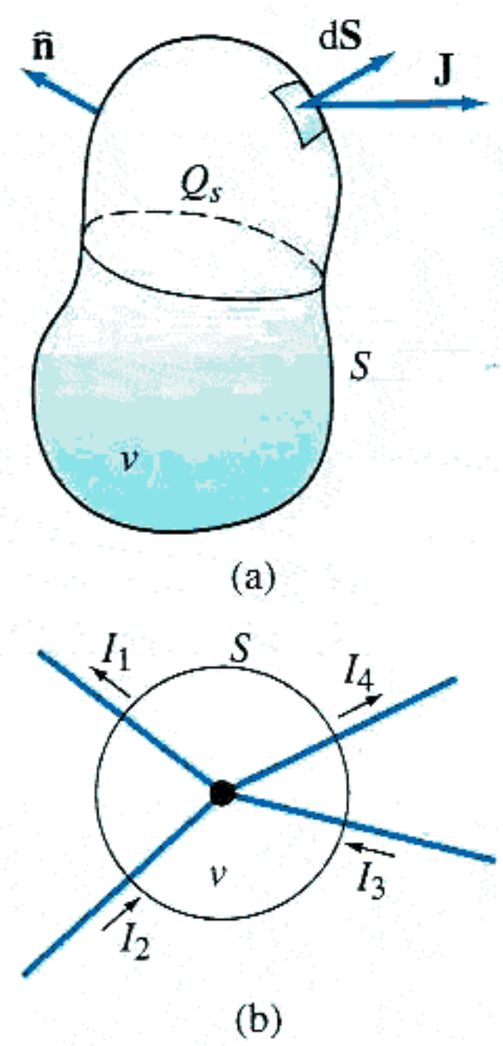

Figure 3.4 Arbitrary closed surface in a region with currents: (a) general case and (b) current flow through wires meeting at a node.

Combining the two preceding equations, we obtain

$$\boxed{\oint_S \mathbf{J}\cdot\mathrm{d}\mathbf{S} = -\frac{\mathrm{d}Q_S}{\mathrm{d}t}.} \tag{3.36}$$

continuity equation, for currents of any time dependence

This is the continuity equation (in integral form). It tells us that the outward flux of the current density vector through any closed surface is equal to the negative of the derivative in time of the total charge enclosed by that surface.

By expressing the charge in terms of the volume charge density, ρ, the continuity equation becomes

$$\oint_S \mathbf{J}\cdot\mathrm{d}\mathbf{S} = -\frac{\mathrm{d}}{\mathrm{d}t}\int_v \rho\,\mathrm{d}v. \tag{3.37}$$

If the surface S does not change in time, the time derivative can be moved inside the volume integral, yielding

continuity equation in terms of the volume charge density

$$\boxed{\oint_S \mathbf{J} \cdot d\mathbf{S} = -\int_v \frac{\partial \rho}{\partial t}\, dv.} \tag{3.38}$$

The ordinary derivative is replaced by a partial derivative because ρ, generally, is a multivariable function of time and space coordinates.

By applying the divergence theorem, Eq. (1.173), to Eq. (3.38) or simply by analogy to the differential form of the generalized Gauss' law, Eq. (2.45), we get the differential form of the continuity equation:

continuity equation in differential form

$$\boxed{\nabla \cdot \mathbf{J} = -\frac{\partial \rho}{\partial t}.} \tag{3.39}$$

It tells us that the divergence of $\mathbf{J}$ at a given point equals the negative of the time rate of variation in charge density at that point, and is also called the continuity equation at a point.

For steady (time-invariant) currents, the charge density is constant in time, $\partial \rho / \partial t = 0$, and the integral form of the continuity equation reduces to

continuity equation for steady currents, integral form

$$\boxed{\oint_S \mathbf{J} \cdot d\mathbf{S} = 0.} \tag{3.40}$$

The differential equation of continuity of steady currents is given by

differential continuity equation for steady currents

$$\boxed{\nabla \cdot \mathbf{J} = 0.} \tag{3.41}$$

Thus, time-invariant current density vector has zero divergence everywhere, and under all circumstances. We say that steady electric currents are divergenceless or solenoidal. The zero divergence of a vector field indicates that there are no sources or sinks in the field for the lines of flux to originate from or terminate on. This means that the streamlines of steady currents close upon themselves (steady currents must flow in closed loops), unlike the streamlines of the electrostatic field intensity, which originate and end on charges.

If the steady current is carried into and out of the volume v by a number (N) of wire conductors meeting at a point, as indicated in Fig. 3.4(b), then Eq. (3.40) implies that the algebraic sum of all the currents leaving the junction is zero,

Kirchhoff's current law

$$\boxed{\sum_{k=1}^{N} I_k = 0.} \tag{3.42}$$

For the situation and notation in Fig. 3.4(b), $I_1 - I_2 - I_3 + I_4 = 0$. Eq. (3.42), if applied to a node in a dc circuit, represents Kirchhoff's circuital law for currents. Like Kirchhoff's voltage law, Eq. (1.92), Kirchhoff's current law in the above form also applies to time-varying situations and ac circuits, with certain restrictions and assumptions, which will be discussed later in this text.

In studying steady current fields, we always have in mind that time-invariant currents in a conductor are produced by a static electric field, which is a conservative field, meaning that the line integral (circulation) of the electric field intensity vector, $\mathbf{E}$, along an arbitrary contour (closed path) is zero,

conservative nature of $\mathbf{E}$ in steady current field

$$\boxed{\oint_C \mathbf{E} \cdot d\mathbf{l} = 0.} \tag{3.43}$$

We also have in mind that **J** and **E** are related at any point in the conductor by the constitutive equation for the current density, Eq. (3.21) [or Eq. (3.18) for linear media].

Example 3.2 Element Law for a Capacitor

Prove that the current through a capacitor equals the product of the capacitor capacitance and the time rate of change of the voltage drop across the capacitor.

Solution Fig. 3.5 shows a capacitor of capacitance C connected to a time-varying voltage[5] v. We assume that the capacitor is ideal, i.e., its dielectric is perfect (nonconducting), as well as that there is no excess charge along the connecting conductors in the circuit (charge is localized only on the capacitor electrodes). To relate the current through the capacitor, i, to the capacitor charge, Q, we apply the continuity equation for time-varying currents in integral form, Eq. (3.36), to a surface S enclosing completely only the upper electrode of the capacitor (Fig. 3.5). The total current leaving the enclosed domain (left-hand side of the equation) equals $-i$, whereas the total enclosed charge (appearing on the right-hand side of the equation) equals the charge of the upper electrode, i.e., the capacitor charge: $Q_S = Q$. Thus, Eq. (3.36) becomes

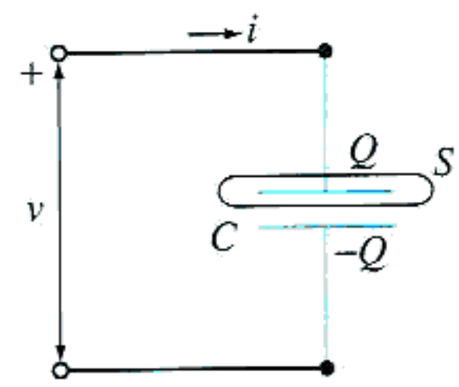

Figure 3.5 Capacitor with a time-varying current; for Example 3.2.

$$-i = -\frac{dQ}{dt}. \tag{3.44}$$

Substituting $Q = Cv$ [Eq. (2.112)] yields

$$\boxed{i = C\frac{dv}{dt}.} \tag{3.45}$$

element law (current-voltage characteristic) for a capacitor with a time-varying current

We see that i is linearly proportional to the rate of change of v in time, with C as the proportionality constant. This is the element law (current-voltage characteristic) for a capacitor, which is widely used in circuit theory, in conjunction with Kirchhoff's laws and other element laws.

Example 3.3 Spherical Capacitor with an Imperfect Dielectric

A spherical capacitor is filled with an imperfect homogeneous dielectric of conductivity σ. The radius of the inner electrode is a and the inner radius of the outer electrode is b ($b > a$). The electrodes have a conductivity that is much larger than σ, so that they can be considered as perfect conductors. The capacitor is connected to a generator of time-invariant voltage V. Find (a) the current density vector in the dielectric and (b) the power of Joule's losses in the capacitor.

Solution

(a) Since $\sigma \neq 0$, there exists a steady current of intensity I in the capacitor circuit, as indicated in Fig. 3.6. To determine the current density vector in the dielectric, we apply the continuity equation for steady currents in integral form, Eq. (3.40). In general, application of the continuity equation is analogous to application of the generalized Gauss' law, Eq. 2.43. This problem is one with spherical symmetry (see Example 1.18), and the current density vector is of the form

$$\boxed{\mathbf{J} = J(r)\,\hat{\mathbf{r}},} \tag{3.46}$$

volume current distribution with spherical symmetry

where r is the radial coordinate in the spherical coordinate system and $\hat{\mathbf{r}}$ is the radial unit vector (Fig. 3.6). The surface S for applying the continuity equation is a spherical surface

[5] We use lowercase (small letter) symbols for the voltage and current here to emphasize that those are time-varying quantities.

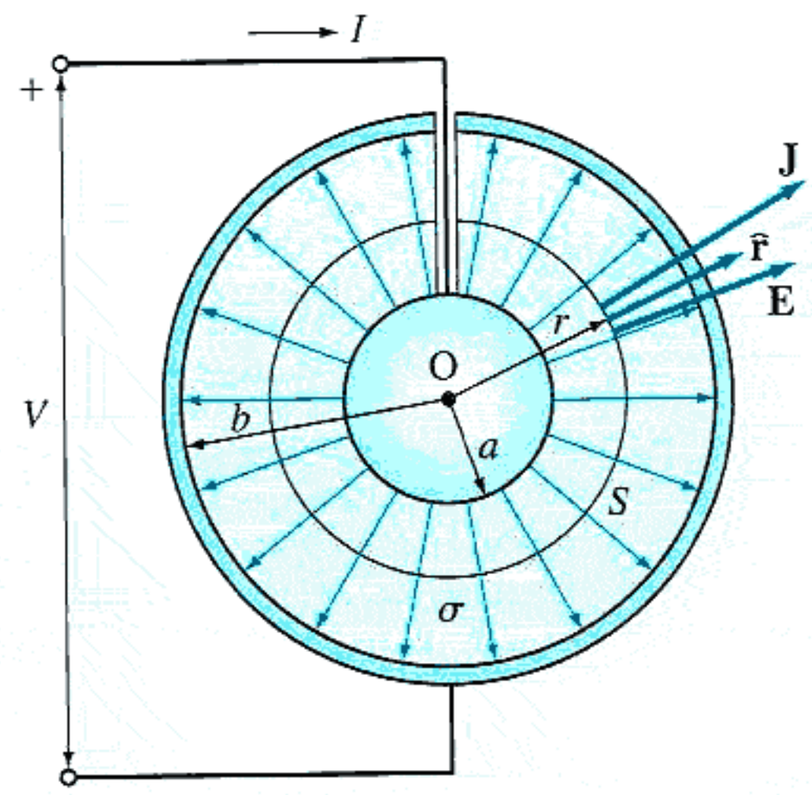

Figure 3.6 Spherical capacitor with an imperfect homogeneous dielectric and time-invariant current; for Example 3.3.

of radius r ($a < r < b$) centered at the origin (the same as the corresponding Gaussian surface in electrostatics, e.g., that in Fig. 2.16). The total current flowing through S in the outward direction is zero, that is,

$$J(r)\,4\pi r^2 - I = 0. \tag{3.47}$$

This means that the outward flux of $\mathbf{J}$ through S equals the current I through the capacitor terminals. Hence,

$$J(r) = \frac{I}{4\pi r^2} \quad (a < r < b). \tag{3.48}$$

From Eq. 3.18, the electric field intensity in the dielectric is

$$E(r) = \frac{J(r)}{\sigma} = \frac{I}{4\pi\sigma r^2}. \tag{3.49}$$

The voltage between the electrodes is given by

$$V = V_a - V_b = \int_{r=a}^{b} E\,\mathrm{d}r = \frac{I}{4\pi\sigma}\left(\frac{1}{a} - \frac{1}{b}\right), \tag{3.50}$$

where V_a and V_b are the potentials of the electrodes (each electrode is equipotential because $\sigma_{\text{electrodes}} \gg \sigma$). Combining Eqs. (3.48) and (3.50), we get

$$J(r) = \frac{\sigma abV}{(b-a)r^2}. \tag{3.51}$$

(b) Using Eq. (3.32), the power of Joule's losses in the dielectric is

$$P_{\mathrm{J}} = \int_v p_{\mathrm{J}}\,\mathrm{d}v = \int_{r=a}^{b} \frac{J(r)^2}{\sigma}\underbrace{4\pi r^2\,\mathrm{d}r}_{\mathrm{d}v} = \frac{4\pi\sigma a^2b^2V^2}{(b-a)^2}\int_a^b \frac{\mathrm{d}r}{r^2} = \frac{4\pi\sigma abV^2}{b-a}, \tag{3.52}$$

with $\mathrm{d}v$ adopted in the form of a thin spherical shell of radius r and thickness $\mathrm{d}r$ [Eq. (1.33)]. There are no losses in the electrodes (perfect conductors), so this is the overall loss power in the capacitor.

Conceptual Questions (on Companion Website): 3.4–3.6; *MATLAB Exercises* (on Companion Website).

3.5 BOUNDARY CONDITIONS FOR STEADY CURRENTS

Applications of steady current fields involve considerations of interfaces between conducting media of different conductivity. In this section, we shall formulate the boundary conditions that govern the manner in which the current density vector, **J**, and the electric field intensity vector, **E**, behave across such interfaces.

Comparing the integral form of the continuity equation for time-varying currents, Eq. (3.38), to the integral form of the generalized Gauss' law, Eq. (2.44), we conclude that the boundary condition for normal components of the vector **J** is of the same form as the boundary condition for normal components of the vector **D**, Eq. (2.85). The only difference is on the right-hand side of the equation, where ρ_s (the surface charge density that may exist on the surface) is replaced by $-\partial\rho_s/\partial t$. With this,

$$\boxed{\hat{\mathbf{n}} \cdot \mathbf{J}_1 - \hat{\mathbf{n}} \cdot \mathbf{J}_2 = -\frac{\partial \rho_s}{\partial t},} \tag{3.53}$$

boundary condition for $\mathbf{J}_n$, time-varying currents

where $\hat{\mathbf{n}}$ is the normal unit vector on the surface, directed from region 2 to region 1.

For steady currents, $-\partial\rho_s/\partial t = 0$ in Eq. (3.53), and the boundary condition that corresponds to Eq. (3.43) is that in Eq. (2.84) [Eq. (3.43) is the same as for the electrostatic field], so the complete set of boundary conditions for steady currents is given by

$$\hat{\mathbf{n}} \times \mathbf{E}_1 - \hat{\mathbf{n}} \times \mathbf{E}_2 = 0 \quad \text{or} \quad E_{1t} = E_{2t}, \tag{3.54}$$

boundary condition for $\mathbf{E}_t$

$$\hat{\mathbf{n}} \cdot \mathbf{J}_1 - \hat{\mathbf{n}} \cdot \mathbf{J}_2 = 0 \quad \text{or} \quad J_{1n} = J_{2n}. \tag{3.55}$$

boundary condition for $\mathbf{J}_n$, dc regime

We see that in the steady current field, the tangential component of the electric field intensity vector and the normal component of the current density vector, $\mathbf{E}_t$ and $\mathbf{J}_n$, are both continuous across the boundary. As we shall see in a later chapter, the boundary condition for $\mathbf{E}_t$ in Eq. (3.54) has this same form for fields of any time variation.

By analogy to the procedure of deriving Eq. (2.87) for the electrostatic field, we obtain the law of refraction of the current density lines at a boundary between two linear conducting media of conductivities σ_1 and σ_2:

$$\boxed{\frac{\tan\alpha_1}{\tan\alpha_2} = \frac{\sigma_1}{\sigma_2},} \tag{3.56}$$

law of refraction of current streamlines

where α_1 and α_2 are the angles that current lines in region 1 and region 2 make with the normal to the interface, as shown in Fig. 3.7.

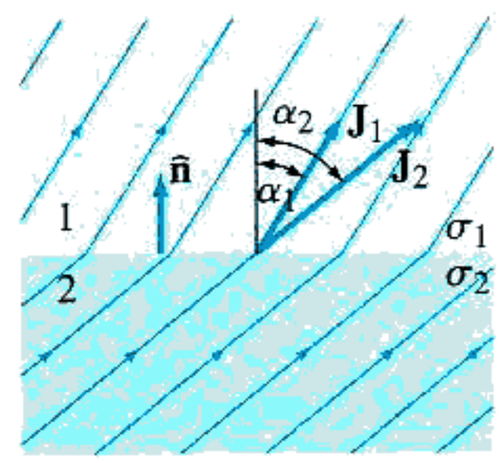

Figure 3.7 Refraction of steady current lines at a conductor-conductor interface.

Note that if medium 2 is a good conductor and medium 1 is a low-loss dielectric, then $\sigma_2 \gg \sigma_1$, i.e., $\sigma_1/\sigma_2 \approx 0$, and Eq. (3.56) gives $\tan\alpha_1 \approx 0$ for any α_2. Therefore,

$$\alpha_1 \approx 0 \quad (\sigma_2 \gg \sigma_1), \tag{3.57}$$

meaning that the current lines always leave (or enter) a good conductor at a right angle to the boundary (zero angle to the normal on the boundary).

Note also that if medium 1 is a perfect dielectric (e.g., air), then $\sigma_1 = 0$, and $\tan\alpha_2 \to \infty$, from which

$$\alpha_2 = 90^\circ \quad (\sigma_1 = 0). \tag{3.58}$$

This means that the lines of current flow are always parallel to the surface of a conductor surrounded by a nonconducting medium.

Conceptual Questions (on Companion Website): 3.7 and 3.8.

3.6 DISTRIBUTION OF CHARGE IN A STEADY CURRENT FIELD

The electric field intensity vector, **E**, in a steady current field is produced by stationary excess charges in the system. In the general case, these charges exist not only on the surfaces of conductors, but also inside their volume. Distribution of charges in the system is conditioned by the distribution of currents, and can be determined only after the current distribution is determined first.

The distribution of the current density vector, **J**, inside conductors can be obtained by solving the basic equations that govern steady current fields, which we summarize here:

Maxwell's first equation for static fields

dc continuity equation

constitutive equation for **J**

$$\boxed{\begin{cases} \oint_C \mathbf{E} \cdot d\mathbf{l} = 0 \\ \oint_S \mathbf{J} \cdot d\mathbf{S} = 0 \\ \mathbf{J} = \mathbf{J}(\mathbf{E}) \; [\mathbf{J} = \sigma \mathbf{E}] \end{cases}} \quad (3.59)$$

Once the solution for **J** is known, the charge distribution can be obtained from the generalized Gauss' law in conjunction with the constitutive equation for the electric flux density vector, **D**:

Maxwell's third equation

constitutive equation for **D**

$$\boxed{\begin{cases} \oint_S \mathbf{D} \cdot d\mathbf{S} = Q_S \\ \mathbf{D} = \mathbf{D}(\mathbf{E}) \; [\mathbf{D} = \varepsilon \mathbf{E}] \end{cases}} \quad (3.60)$$

Note that, assuming that the medium is linear, both **D** and **J** are linearly proportional to **E**. As a result, we have a linear relationship between **D** and **J**:

duality of **D** *and* **J**

$$\boxed{\mathbf{D} = \varepsilon \mathbf{E} = \frac{\varepsilon}{\sigma} \mathbf{J}.} \quad (3.61)$$

This duality relationship will be used on many occasions.

Starting from the differential form of the generalized Gauss' law, Eq. (2.45), and using Eqs. (3.61) and (3.41), the volume charge density in the conductor is[6]

volume charge in a steady current field

$$\boxed{\rho = \nabla \cdot \mathbf{D} = \nabla \cdot \left(\frac{\varepsilon}{\sigma} \mathbf{J}\right) = \left[\nabla \left(\frac{\varepsilon}{\sigma}\right)\right] \cdot \mathbf{J} + \frac{\varepsilon}{\sigma} (\nabla \cdot \mathbf{J}) = \mathbf{J} \cdot \nabla \left(\frac{\varepsilon}{\sigma}\right).} \quad (3.62)$$

We see that $\nabla \cdot \mathbf{J} = 0$ does not imply that $\rho = 0$. Volume charge density is nonzero in inhomogeneous conducting media where $\varepsilon/\sigma \neq$ const, and its magnitude is proportional to the gradient of ε/σ. On the other hand, we also conclude that there cannot be volume excess charges ($\rho = 0$) inside homogeneous media (σ and ε do not vary with position) with steady currents.

The corresponding boundary condition for **D**, Eq. (2.85), in combination with Eqs. (3.61) and (3.55), gives the surface charge density on the interface between medium 1 (with parameters σ_1 and ε_1) and medium 2 (with σ_2 and ε_2):

surface charge in a steady current field

$$\boxed{\rho_s = \hat{\mathbf{n}} \cdot \mathbf{D}_1 - \hat{\mathbf{n}} \cdot \mathbf{D}_2 = \frac{\varepsilon_1}{\sigma_1} \hat{\mathbf{n}} \cdot \mathbf{J}_1 - \frac{\varepsilon_2}{\sigma_2} \hat{\mathbf{n}} \cdot \mathbf{J}_2 = \left(\frac{\varepsilon_1}{\sigma_1} - \frac{\varepsilon_2}{\sigma_2}\right) J_n,} \quad (3.63)$$

[6]Having in mind the rule for calculating the derivative of a product of two functions, we apply the divergence operator, which is a differential operator, to a product of a scalar and a vector function, and get $\nabla \cdot (f\mathbf{a}) = (\nabla f) \cdot \mathbf{a} + f(\nabla \cdot \mathbf{a})$.

where $J_n = \hat{\mathbf{n}} \cdot \mathbf{J}_1 = \hat{\mathbf{n}} \cdot \mathbf{J}_2$ is the normal component of the current density vector across the boundary ($\hat{\mathbf{n}}$ is directed as in Figs. 2.10 and 3.7). Note that $\rho_s = 0$ only for the special case of $\varepsilon_1/\sigma_1 = \varepsilon_2/\sigma_2$. If both media are metallic conductors, we have approximately $\varepsilon_1 = \varepsilon_2 = \varepsilon_0$, so that Eq. (3.63) becomes

$$\rho_s = \varepsilon_0 \left(\frac{1}{\sigma_1} - \frac{1}{\sigma_2} \right) J_n. \tag{3.64}$$

Finally, the distribution of bound (polarization) charge in the dielectric can be found by computing first the polarization vector, $\mathbf{P}$, from Eq. (2.59), and then bound volume and surface charge densities, ρ_p and ρ_{ps}, using Eqs. (2.19) and (2.89), respectively.

Problems: 3.1; *Conceptual Questions* (on Companion Website): 3.9 and 3.10; *MATLAB Exercises* (on Companion Website).

3.7 RELAXATION TIME

We know from electrostatics that charge placed in the interior of a conductor will move to the conductor surface and redistribute itself in such a way that $\mathbf{E} = 0$ in the conductor under electrostatic equilibrium conditions. With the continuity equation (for time-varying currents) now in hand, we can quantitatively analyze this nonelectrostatic transitional process and calculate the time it takes to reach an equilibrium.

Consider a homogeneous conducting medium of conductivity σ and permittivity ε. The current density vector, $\mathbf{J}$, and electric flux density vector, $\mathbf{D}$, in the medium are interconnected by the duality relationship in Eq. (3.61). Combining the differential form of the generalized Gauss' law, Eq. (2.45), and that of the continuity equation, Eq. (3.39), we can write

$$\rho = \nabla \cdot \mathbf{D} = \nabla \cdot \left(\frac{\varepsilon}{\sigma} \mathbf{J} \right) = \frac{\varepsilon}{\sigma} \nabla \cdot \mathbf{J} = -\frac{\varepsilon}{\sigma} \frac{\partial \rho}{\partial t}, \tag{3.65}$$

where the ratio ε/σ can be brought outside the divergence sign because it is a constant (the medium is homogeneous). Rewriting, we have that the charge density, ρ, in the medium satisfies the equation

$$\frac{\partial \rho}{\partial t} + \frac{\sigma}{\varepsilon} \rho = 0, \tag{3.66}$$

which is a first-order partial differential equation in time, t. Its solution is given by

$$\boxed{\rho = \rho_0 \, e^{-(\sigma/\varepsilon)t} = \rho_0 \, e^{-t/\tau},} \tag{3.67}$$

redistribution of charge

where ρ_0 is the initial value of the charge density at $t = 0$. In general, ρ is a function of the space coordinates as well, e.g., $\rho = \rho(x, y, z, t)$. Eq. (3.67) tells us that the charge density at a given location in the conductor decreases with time exponentially, completely independent of any applied electric field. The time constant

$$\boxed{\tau = \frac{\varepsilon}{\sigma}} \tag{3.68}$$

relaxation time

is referred to as the relaxation time (the unit is s) and it equals the time required for the charge density at any point to decay to 1/e (36.8%) of its initial value. It can easily be shown that ρ decreases to 1% of ρ_0 after approximately 4.6τ, while at $t = 10\tau$, $\rho \approx 4.5 \times 10^{-5} \rho_0$, i.e., $\rho \approx 0$.

For metallic conductors, τ is so short that it can hardly be measured or observed. For example, copper has $\tau_{Cu} \approx 10^{-19}$ s. Even much poorer conductors than metals have very short relaxation times (e.g., $\tau_{H_2O} \approx 10^{-5}$ s for distilled water). On the other hand, the relaxation time for good dielectrics (insulators) is relatively long (e.g., $\tau_{glass} \approx 1$ minute, $\tau_{mica} \approx 15$ hours, and $\tau_{quartz} \approx 50$ days).

While this chapter is devoted to time-invariant currents and fields, we note here that the concept of relaxation time is also used to determine the electrical nature (in terms of conducting and dielectric properties) of materials for time-varying currents and fields. Namely, whether a material of parameters σ and ε is considered a good conductor or a good dielectric is decided on the basis of the relaxation time, as compared to times of interest in a given application. Thus, for a time-harmonic (sinusoidal) field of frequency f, the relaxation time, given by Eq. (3.68), is compared to the time period,[7] $T = 1/f$. If $\tau \ll T$, the medium is classified as a good conductor. In particular, if $\tau = 0$ ($\sigma \to \infty$), the material is said to be a perfect electric conductor (PEC). On the other hand, the material is considered a good dielectric (insulator) if $\tau \gg T$. In a limit, $\tau \to \infty$ for perfect (lossless) dielectrics ($\sigma = 0$). For all other (intermediate) values of τ, the material is classified as a quasi-conductor. We can now understand that some materials that are considered as good conductors at certain frequencies may behave like good dielectrics at sufficiently higher frequencies (i.e., shorter time periods). For example, at frequencies $f_1 = 1$ kHz, $f_2 = 10$ MHz, and $f_3 = 30$ GHz, average rural ground ($\varepsilon_r = 14$ and $\sigma = 10^{-2}$ S/m, assuming no change in the parameters as a function of frequency) behaves like (1) a good conductor, (2) a quasi-conductor, and (3) a good dielectric, respectively. Further discussions of conducting and dielectric properties of materials at different frequencies, in a context of general Maxwell's equations and electromagnetic wave propagation, are provided in later chapters.

3.8 RESISTANCE, OHM'S LAW, AND JOULE'S LAW

Consider an arbitrarily shaped conductor made from a linear (generally inhomogeneous) material of conductivity σ, as shown in Fig. 3.8. Let the end surfaces S_A and S_B of the conductor be coated with perfectly conducting material (or with material of conductivity much greater than σ). If the voltage V is applied between the conductor ends, the current, of density $\mathbf{J}$, in the conductor flows normal to the end surfaces [Eq. (3.57)] and parallel to the sides of the resistor [Eq. (3.58)]. By virtue of the continuity equation, the same total current must pass through every cross section of the conductor. This current is given by

$$I = \int_S \mathbf{J} \cdot d\mathbf{S} = \int_S \sigma \mathbf{E} \cdot d\mathbf{S}, \tag{3.69}$$

where $\mathbf{E}$ is the electric field intensity vector in the conductor. On the other hand, the voltage between S_A and S_B equals the line integral of the same vector, $\mathbf{E}$, along any path in the conductor connecting these surfaces [Eq. (1.90)], that is,

$$V = \int_A^B \mathbf{E} \cdot d\mathbf{l}. \tag{3.70}$$

[7]The time period (T) is defined as an interval after which a time-harmonic (or other time-periodic) function repeats itself over time, whereas the frequency (f) is the number of repetitions of the function per unit time (one second), so that f times T equals unity.

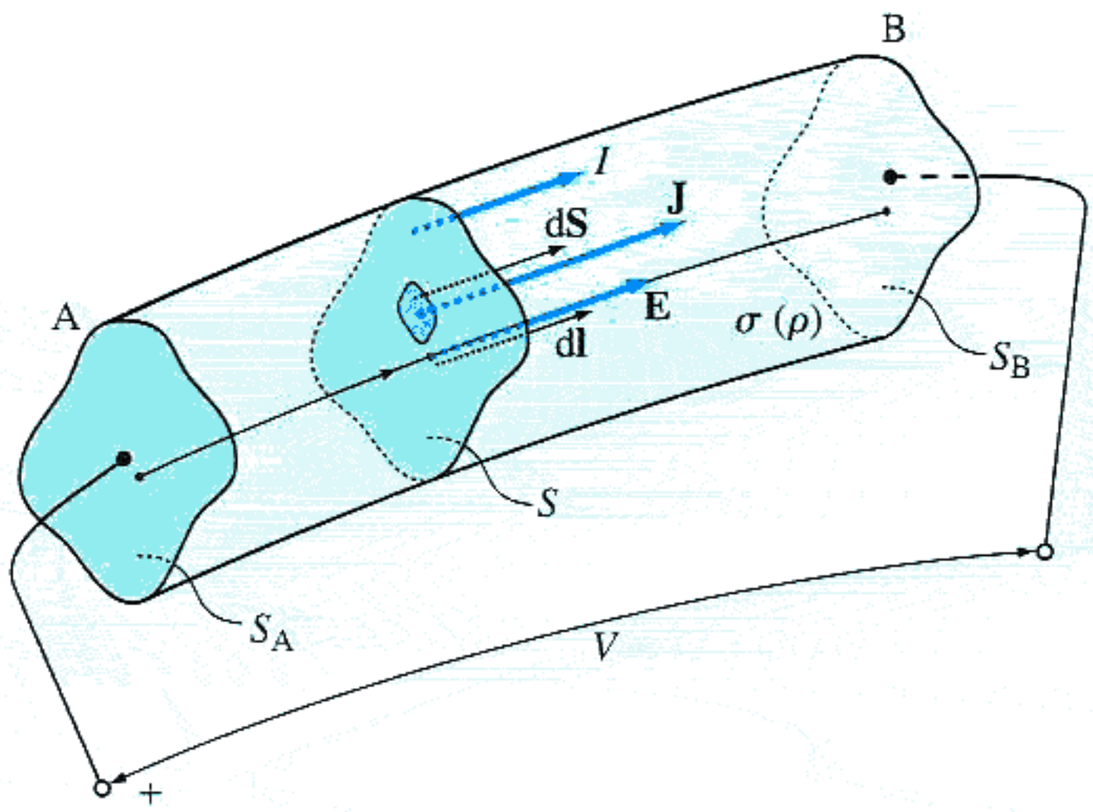

Figure 3.8 Arbitrarily shaped conductor – resistor.

Now, we note that if V is increased (for some reason), the electric field lines do not change shape, but $\mathbf{E}$ proportionally increases everywhere within the conductor, and, by means of Eq. (3.69), so does the current I. The ratio of V and I is thus a constant,

$$\boxed{R = \frac{V}{I},} \qquad (3.71) \quad \textit{resistance (unit: } \Omega\textit{)}$$

called the resistance of the conductor. A conductor with two terminals and a (substantial) resistance R is usually referred to as a resistor. The relation between the voltage, current, and resistance of a resistor is known as Ohm's law:

$$\boxed{V = RI.} \qquad (3.72) \quad \textit{Ohm's law}$$

The resistance is always nonnegative ($R \geq 0$), and the unit is the ohm (Ω), equal to V/A. The value of R depends on the shape and size of the conductor (resistor), and on the conductivity σ (or resistivity ρ) of the material.

HISTORICAL ASIDE

Georg Simon Ohm (1789–1854), a German physicist and mathematician, was a professor at the University of Munich. As a child, Ohm received a fine mathematical and scientific education from his father, who was a locksmith and an entirely self-taught man. In 1811, he received a doctorate in mathematics from the University of Erlangen. He was also interested in physics, where he studied analogies between the flow of electricity and flow of heat. In a series of papers in 1825 and 1826, he gave a mathematical description of conduction in electric circuits modeled after Fourier's study of heat conduction. He assumed that, just as the rate at which heat flowed between two points depended on the temperature difference between the points and on the ease with which heat was conducted by the material between the points, the electric current between two points should depend on the difference in electric potential between the points and on the electric conductivity of the material between the points. By experimenting with wires of different lengths and thicknesses, he found that

the current intensity through a wire, for a given potential difference between the wire ends, was inversely proportional to the length and directly proportional to the cross-sectional area of the wire. As very knowledgeable of both mathematics and physics, Ohm was able to deduce mathematical relationships based on the experimental evidence that he had tabulated. He defined the resistance of a wire and showed, in 1827, that a simple relation existed among the resistance, potential difference (voltage), and current intensity of a wire. This is now known as Ohm's law. The fully developed presentation of his theory of electric conduction appeared in his famous book "Die Galvanische Kette, Mathematisch Bearbeitet" (The Galvanic Circuit, Analyzed Mathematically), published in 1827 in Berlin. At first, Ohm's work was received with little enthusiasm, and a full acknowledgement and recognition of his results, including Ohm's law, did not come until 1841, when he was awarded the Copley Medal of the Royal Society and soon after became member of several European academies. Only in 1852, two years before his death, Ohm achieved his lifelong ambition of being appointed to the chair of physics at the University of Munich. Ohm's name was further immortalized in 1881, when the International Electrical Congress established the ohm as the unit of resistance. *(Portrait: Edgar Fahs Smith Collection, University of Pennsylvania Libraries)*

The siemens is adopted as the SI unit for conductance in honor of brothers Werner and Wilhelm von Siemens, German engineers and inventors. **Ernst Werner von Siemens** (1816–1892) contributed to then new discipline of electrical engineering with several inventions in telegraphy (needle telegraph), cable transmission (large undersea cables), and energy generation, and was one of the first great entrepreneurs in electrical industry. In 1847, he founded, together with the mechanic Johann Georg Halske (1814–1890), the "Siemens & Halske Telegraph Construction Company" in Berlin, later known as "Siemens." **Karl Wilhelm von Siemens** (1823–1883) was a mechanical engineer by training and successful businessman. His most important inventions are the regenerative furnace and electric pyrometer. He later became British subject, Sir Charles William Siemens.

The reciprocal of resistance is called the conductance and symbolized by G. From Ohm's law,

conductance (unit: S)

$$\boxed{G = \frac{1}{R} = \frac{I}{V}.} \tag{3.73}$$

Its unit is the siemens (S), where $\mathrm{S} = \Omega^{-1} = \mathrm{A/V}$. Note that sometimes the mho (ohm spelled backwards) is used instead of the siemens.

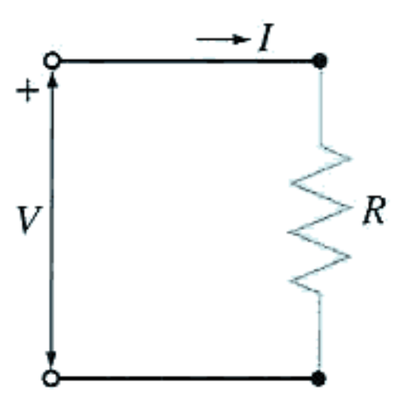

Figure 3.9 Circuit-theory representation of a resistor.

Fig. 3.9 shows the circuit-theory representation of a resistor. In circuit theory, it is assumed that the resistances are located only in the resistors in a circuit, while the interconnecting conductors are considered as perfectly conducting. Each connecting conductor has therefore zero resistance and is equipotential (acts as a short circuit). The only voltage drops in the circuit occur across circuit elements. Note that Ohm's law, Eq. (3.72), is valid also for time-varying voltage (v) and current (i) of a resistor ($v = Ri$). It represents the element law for a resistor, as one of the basic elements in circuit theory [another element law being Eq. (3.45) for a capacitor].

For linear resistors, R remains constant for different voltages and currents, V and I. For nonlinear resistors, however, the conductivity of the material depends on the applied electric field, $\mathbf{E}$, and R therefore depends on the applied voltage (or current),

nonlinear resistor

$$\boxed{R = R(V).} \tag{3.74}$$

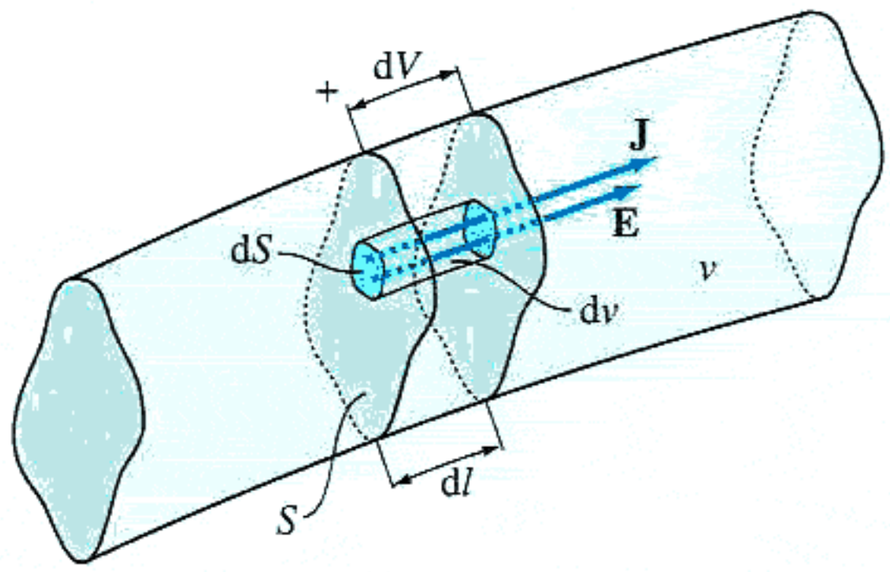

Figure 3.10 Evaluation of the power of Joule's (ohmic) losses in a resistor of general shape.

Examples are semiconductor (pn) diodes, whose current-voltage characteristics, $I = I(V)$, are nonlinear functions.

The total power of Joule's or ohmic losses in the resistor in Fig. 3.8 is given by Eq. (3.32), where v is the volume of the resistor. To carry out the volume integration, we first cut v into thin slices with bases chosen to be equipotential surfaces (perpendicular to current lines). We then subdivide each slice along the current lines into small tubular cells of volume $\mathrm{d}v = \mathrm{d}S\,\mathrm{d}l$, as depicted in Fig. 3.10, and write

$$P_J = \int_v JE\,\mathrm{d}v = \int_A^B \int_S JE\,\underbrace{\mathrm{d}S\,\mathrm{d}l}_{\mathrm{d}v}. \tag{3.75}$$

Note that $E\,\mathrm{d}l$ equals the voltage $\mathrm{d}V$ between the bases of the cell, which is the same for all cells within a slice (because of the equipotentiality of interfaces between adjacent slices). Therefore, $\mathrm{d}V$ is a constant for cross-sectional integration over S, and can be taken out of that integral. We have thus separated the overall integration throughout v into two independent integrals:

$$P_J = \int_A^B \int_S J\,\mathrm{d}S\,\underbrace{E\,\mathrm{d}l}_{\mathrm{d}V} = \left(\int_A^B E\,\mathrm{d}l\right)\left(\int_S J\,\mathrm{d}S\right) = VI, \tag{3.76}$$

which equal, respectively, the voltage V [Eq. (3.70)] and the current I [Eq. (3.69)] of the resistor. Employing Eqs. (3.72) and (3.73), the equivalent expressions for the power of Joule's losses in a resistor are

$$\boxed{P_J = VI = RI^2 = \frac{V^2}{R} = GV^2 = \frac{I^2}{G}.} \tag{3.77}$$

Joule's law

This is known as Joule's law.

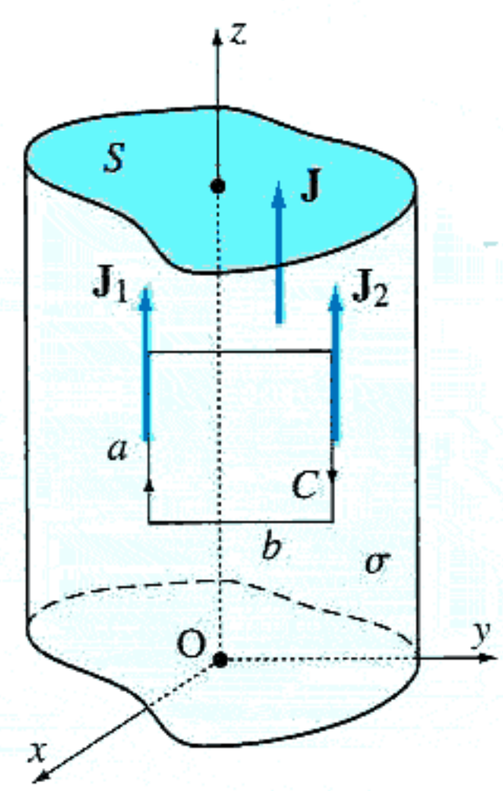

Figure 3.11 Steady current in a homogeneous conductor of a uniform cross section; for Example 3.4.

Example 3.4 **Current Uniformity in Conductors with Uniform Cross Section**

A steady current is flowing through a long conductor made of a homogeneous material and having a uniform cross section of an arbitrary shape. Prove that the current density is the same in the entire conductor.

Solution With reference to Fig. 3.11, the current density vector in the conductor has a z-component only, $\mathbf{J} = J_z(x, y, z)\,\hat{\mathbf{z}}$. From the continuity equation for steady currents in differential form, Eq. (3.41), and the expression for divergence in the Cartesian coordinate system, Eq. (1.167), we have

$$\nabla \cdot \mathbf{J} = \frac{\partial J_z}{\partial z} = 0, \tag{3.78}$$

which means that J_z is not a function of z, i.e., it does not vary along the conductor.

HISTORICAL ASIDE

James Prescott Joule (1818–1889), an English scientist, was a member of the Royal Society. As a son of a wealthy Salford brewer, Joule was educated by private tutors, including the famous English chemist and physicist John Dalton (1766–1844). Later, while working in the family brewery, he studied in his spare time the subject of electricity (new at that time) and was especially interested in the efficiency of electric motors. After several attempts to design a superefficient electric motor that would produce infinite power (this possibility had been suggested in previous papers) and thus offer an ideal alternative to steam engines, he realized that this goal was not achievable and became interested in studying the heat generated by electricity. Joule lacked in mathematical rigor, but was a fanatic experimentalist. Based on extensive measurements of heat in electric motors and other electric circuitry, he discovered, in 1840, that the heat produced by a current in an electric circuit over a certain interval of time equals the square of the current intensity multiplied by the resistance of the circuit and time. This came to be called Joule's law. He measured the heat produced by every process he could think of, and studied the relationship between the amount of work entering the system and the amount of heat exiting the system. In his famous "paddle wheel" experiment in 1847, he used a falling weight to spin a paddle wheel in an insulated barrel of water and measured very precisely the increase in the water temperature produced by the friction of the wheel – to determine the mechanical equivalent of the heat dissipated in the water. His general conclusion was that heat was only one of many forms of energy, which can be converted from one form to another but the total energy of a closed system remains constant. With this, he contributed fundamentally to the discovery and recognition of the principle of conservation of energy. We honor Joule also by using joule as the unit for work and energy. *(Portrait: National Bureau of Standards Archives, courtesy AIP Emilio Segrè Visual Archives, E. Scott Barr Collection)*

To prove that **J** does not change in a cross section of the conductor either, we apply Eq. (3.43) to a rectangular contour C placed inside the conductor, with sides of length a set parallel to current lines (Fig. 3.11). Using also Eq. (3.18), we can write

$$\oint_C \mathbf{E} \cdot d\mathbf{l} = \oint_C \frac{\mathbf{J}}{\sigma} \cdot d\mathbf{l} = \frac{1}{\sigma} \oint_C \mathbf{J} \cdot d\mathbf{l} = 0, \tag{3.79}$$

where σ is the conductivity of the medium, and $1/\sigma$ can be taken out of the integral because the medium is homogeneous ($\sigma = \text{const}$). Hence,

$$\oint_C \mathbf{J} \cdot d\mathbf{l} = J_1 a - J_2 a = 0, \tag{3.80}$$

with J_1 and J_2 standing for the current densities along the two sides of the contour parallel to **J**. We conclude that these current densities are the same:

$$J_1 = J_2. \tag{3.81}$$

Note that C can be translated to any position in the conductor, so that J_1 and J_2 can be associated to any pair of points in the conductor cross section. This implies that **J** does not depend on x and y, namely, it is the same in the entire cross section of the conductor. Combined with our previous conclusion about the current uniformity in the z-direction, we have that

dc current uniformity in a homogeneous conductor of a uniform cross section

$$\boxed{J = \text{const}} \tag{3.82}$$

everywhere inside the conductor.

Example 3.5 **Resistance of a Resistor of a Uniform Cross Section**

Determine the resistance of a homogeneous resistor with a uniform cross section of an arbitrary shape and surface area S. The length of the resistor is l and the conductivity of the material is σ.

Solution Eq. (3.82) tells us that the current is distributed uniformly in the resistor. The current density in the resistor is thus

$$J = \frac{I}{S}, \tag{3.83}$$

where I is the current intensity through the resistor, Eq. (3.69). Using Eq. (3.70), the voltage across the resistor is

$$V = El = \frac{J}{\sigma} l = \frac{Il}{\sigma S}. \tag{3.84}$$

Hence, the resistance of the resistor comes out to be

$$\boxed{R = \frac{V}{I} = \frac{l}{\sigma S}.} \tag{3.85}$$

resistance of a homogeneous resistor with a uniform cross section

Example 3.6 **Two Resistors in Series**

Fig. 3.12(a) shows a cylindrical resistor of radius a consisting of two parts of lengths l_1 and l_2. Conductivities of the parts are σ_1 and σ_2 ($\sigma_1 \neq \sigma_2$). The voltage across the resistor is V. Find the current through the resistor.

Solution The current through the two parts of the resistor is the same, and they can be represented as two homogeneous resistors connected in series, as shown in Fig. 3.12(b). The total resistance of the connection is

$$\boxed{R = R_1 + R_2,} \tag{3.86}$$

equivalent resistance of two resistors in series

where, using Eq. (3.85), the resistances of individual resistors amount to

$$R_1 = \frac{l_1}{\sigma_1 \pi a^2} \quad \text{and} \quad R_2 = \frac{l_2}{\sigma_2 \pi a^2}, \tag{3.87}$$

respectively. The current through the resistor in Fig. 3.12(a) is hence

$$I = \frac{V}{R_1 + R_2} = \frac{\pi \sigma_1 \sigma_2 a^2 V}{\sigma_2 l_1 + \sigma_1 l_2}. \tag{3.88}$$

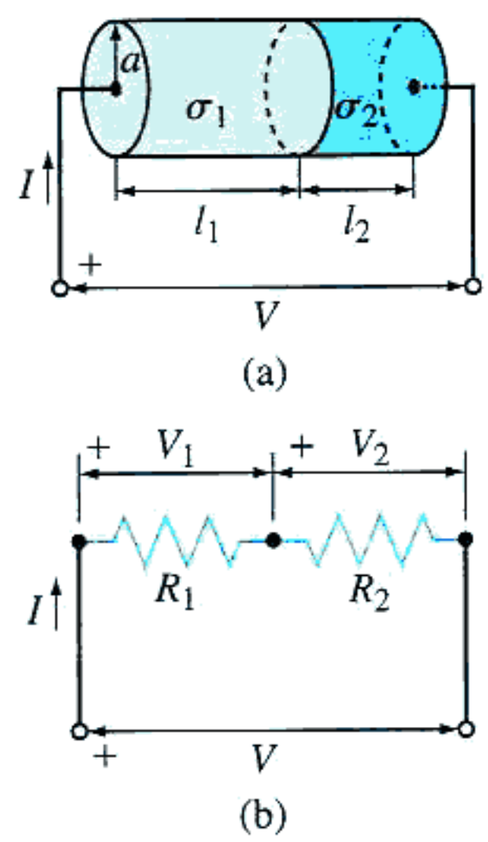

Figure 3.12 Cylindrical resistor with two parts of different conductivities: (a) geometry and (b) network representation; for Example 3.6.

Example 3.7 **Two Resistors in Parallel**

A cylindrical resistor of length l consists of two coaxial layers of different conductivities, σ_1 and σ_2, as shown in Fig. 3.13(a). The cross-sectional surface areas of the layers are S_1 and S_2. The current through the resistor is I. Compute (a) the current density in the resistor and (b) the voltage across the resistor.

Solution

(a) Eq. (3.54) tells us that the electric field intensities in the two layers are the same:

$$E_1 = E_2 = E. \tag{3.89}$$

Hence, the current densities in the layers are not the same, as $J_1 = \sigma_1 E$ and $J_2 = \sigma_2 E$. The total current through the resistor is given by

$$I = J_1 S_1 + J_2 S_2 = (\sigma_1 S_1 + \sigma_2 S_2) E, \tag{3.90}$$

from which

$$E = \frac{I}{\sigma_1 S_1 + \sigma_2 S_2} \tag{3.91}$$

and

$$J_1 = \frac{\sigma_1 I}{\sigma_1 S_1 + \sigma_2 S_2} \quad \text{and} \quad J_2 = \frac{\sigma_2 I}{\sigma_1 S_1 + \sigma_2 S_2}. \tag{3.92}$$

(b) The voltage across the resistor is

$$V = El = \frac{Il}{\sigma_1 S_1 + \sigma_2 S_2}. \tag{3.93}$$

Note that V can also be found using the equivalent circuit shown in Fig. 3.13(b). Namely, since the voltage across the two layers of the resistor is the same, they can be represented as two homogeneous resistors connected in parallel. The total conductance of the connection turns out to be

equivalent conductance of two resistors in parallel

$$\boxed{G = G_1 + G_2,} \tag{3.94}$$

that is [Eq. (3.85)],

$$G = \frac{\sigma_1 S_1}{l} + \frac{\sigma_2 S_2}{l}. \tag{3.95}$$

The voltage of the resistors is $V = I/G$.

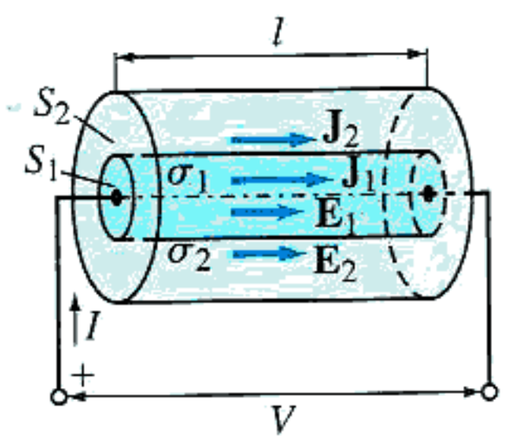

(a)

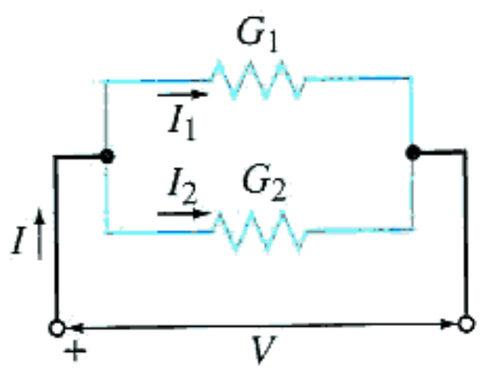

(b)

Figure 3.13 Resistor with two coaxial layers (a), which can be represented as two homogeneous resistors connected in parallel (b); for Example 3.7.

Example 3.8 Conductance of a Spherical Capacitor

Find the conductance of the spherical capacitor with an imperfect (conducting) dielectric (of conductivity σ) from Fig. 3.6.

Solution Using Eqs. (3.73) and (3.50), the conductance of the nonideal spherical capacitor is, by definition,

leakage conductance of a nonideal spherical capacitor

$$\boxed{G = \frac{I}{V} = \frac{4\pi\sigma ab}{b-a}.} \tag{3.96}$$

This, actually, is the so-called leakage conductance of the capacitor. (An ideal capacitor has a perfect dielectric and zero leakage conductance.) Note, however, that the system in Fig. 3.6 may also represent a spherical resistor, with resistance

$$R = \frac{1}{G} = \frac{\rho(b-a)}{4\pi ab}. \tag{3.97}$$

where $\rho = 1/\sigma$ is the resistivity of a (resistive) material between the electrodes.

Note also that, employing the conductance (or resistance) and Joule's law, Eq. (3.77), the power of Joule's losses in the capacitor (resistor) can now easily be found as

$$P_J = GV^2 = \frac{V^2}{R} = \frac{4\pi\sigma abV^2}{b-a}, \tag{3.98}$$

which, of course, is the same result as in Eq. (3.52).

Problems: 3.2–3.9; *Conceptual Questions* (on Companion Website): 3.11–3.17; *MATLAB Exercises* (on Companion Website).

3.9 DUALITY BETWEEN CONDUCTANCE AND CAPACITANCE

Consider a pair of metallic bodies (electrodes) placed in a homogeneous conducting medium of conductivity σ and permittivity ε, as shown in Fig. 3.14. The conductivity of electrodes is much larger than σ. Let the voltage between the electrodes be V. From Eq. (3.62), there is no volume charges ($\rho = 0$) in the medium (σ and ε are constants). Having in mind Eq. (3.57), the current (and field) lines are normal to the surfaces of electrodes. We now use the duality relationship between the current

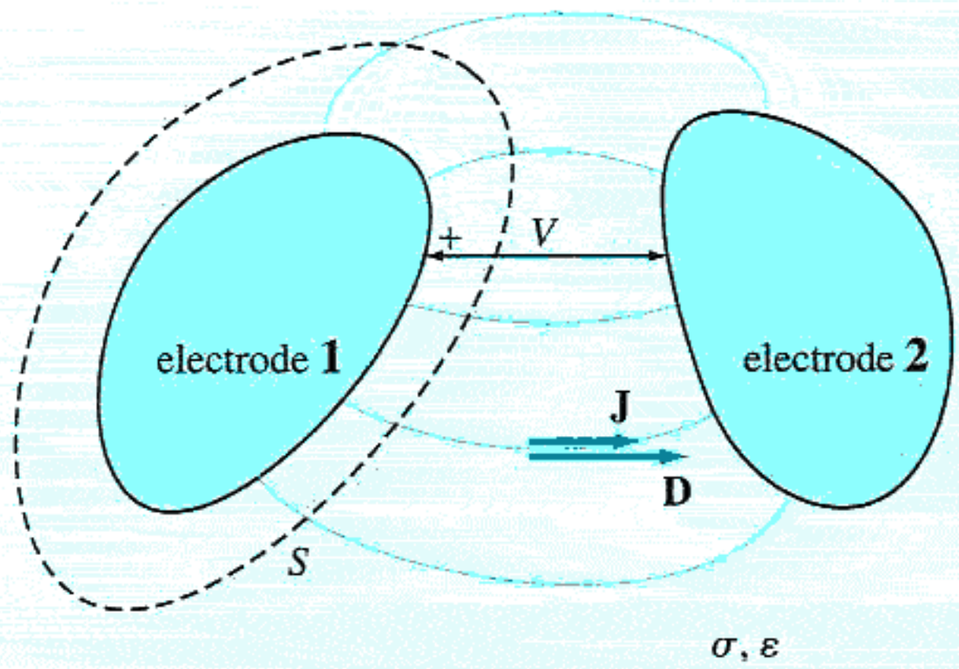

Figure 3.14 Two metallic electrodes in a homogeneous conducting medium.

density vector, **J**, and electric flux density vector, **D**, in the medium, Eq. (3.61), to relate the conductance, G, and capacitance, C, between the electrodes.

Applying the continuity equation for steady currents, Eq. (3.40), and generalized Gauss' law, Eqs. (3.60), to an arbitrary surface S completely enclosing the positive electrode (Fig. 3.14) gives

$$I = \int_S \mathbf{J} \cdot d\mathbf{S} = \frac{\sigma}{\varepsilon} \int_S \mathbf{D} \cdot d\mathbf{S} = \frac{\sigma}{\varepsilon} Q, \tag{3.99}$$

where I is the total current leaving the positive electrode through the conducting medium (and entering the negative electrode), Q is the total charge of the positive electrode (the total charge of the negative electrode is $-Q$), and σ/ε can be brought outside the integral sign because it is a constant, i.e., the medium is homogeneous.[8] By dividing this equation by V, we obtain

$$\frac{I}{V} = \frac{\sigma}{\varepsilon} \frac{Q}{V}, \tag{3.100}$$

which, by means of Eqs. (3.73) and (2.113), yields the following duality relationship between G and C:

$$\boxed{G = \frac{\sigma}{\varepsilon} C.} \tag{3.101}$$

duality of G and C

Note that, since the definition of C, Eq. (2.113), depends on the existence of charges Q and $-Q$ on the electrodes and is independent of whether or not a current also exists in the dielectric medium (of permittivity ε), G and C in Eq. (3.101) do not necessarily represent the conductance and capacitance of a system with an imperfect dielectric of parameters σ and ε. They can also be associated with two independent dual systems, representing the capacitance (C) between a pair of electrodes when placed in a perfect dielectric (of permittivity ε, including the case $\varepsilon = \varepsilon_0$, and zero conductivity) and the conductance (G) between the same electrodes when placed in a conducting medium (of conductivity σ and totally arbitrary permittivity), respectively.

[8] Note, however, that this is true also for inhomogeneous media for which functions σ and ε are such that $\sigma/\varepsilon =$ const.

In terms of the resistance, R, between the electrodes, Eq. (3.101) can be rewritten as

R-C analogy

$$\boxed{RC = \frac{\varepsilon}{\sigma} = \tau,} \tag{3.102}$$

where τ, given by Eq. (3.68), is the relaxation time of the material between the electrodes. Fig. 3.15 shows the circuit-theory representation of the system in Fig. 3.14. This is a first-order capacitive circuit, whose time constant ($\tau_C = RC$) is equal, by virtue of Eq. (3.102), to the relaxation time of the material ($\tau = \varepsilon/\sigma$).

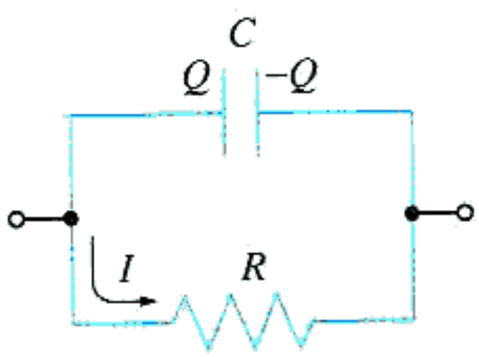

Figure 3.15 Network representation of the system in Fig. 3.14.

The relations in Eqs. (3.101) and (3.102) are very useful in deriving expressions for conductance and resistance of electrode configurations for which we already have the capacitance, or vice versa. For example, from the expression for the capacitance of a spherical capacitor with dielectric permittivity ε (and zero conductivity) and electrode radii a and b ($a < b$), given in Eq. (2.119), we can immediately determine the expression for the conductance of the same capacitor if filled with a conducting medium of conductivity σ:

$$G = \frac{\sigma}{\varepsilon} C = \frac{4\pi\sigma ab}{b - a} \tag{3.103}$$

[the same as in Eq. (3.96)].

Example 3.9 **Self-Discharging of a Nonideal Capacitor**

A parallel-plate capacitor is filled with an imperfect dielectric of relative permittivity $\varepsilon_r = 6$ and conductivity $\sigma = 10^{-14}$ S/m. The capacitor was connected to an ideal battery and fully charged to a voltage of 20 V between its plates, and then disconnected from the battery. Find the time after which the voltage of the capacitor decays to 1 V.

Solution The capacitor can be represented by the equivalent network in Fig. 3.15, where C and R are the capacitance and resistance between the capacitor plates, respectively. With no battery in the circuit, the current discharging C is also the current across R, which, with help of Eqs. (3.45) and (3.72), gives

$$-C\frac{dv}{dt} = \frac{v}{R} \quad \longrightarrow \quad \frac{dv}{dt} + \frac{v}{\tau_C} = 0, \tag{3.104}$$

where the time constant $\tau_C = RC$ is found from Eq. (3.102). The solution of this differential equation is

self-discharging of a capacitor with an imperfect dielectric

$$\boxed{v(t) = v(0)\,e^{-t/(RC)} = v(0)\,e^{-(\sigma/\varepsilon)t}.} \tag{3.105}$$

Finally, we take the natural logarithms of both sides of the equation, and obtain the time we seek:

$$t = -\frac{\varepsilon_r\varepsilon_0}{\sigma} \ln\frac{v(t)}{v(0)} = 265 \text{ minutes}, \tag{3.106}$$

where $v(0) = 20$ V and $v(t) = 1$ V.

We realize that discharging of a charged capacitor with homogeneous imperfect dielectric that is left to itself (open-circuited) is completely independent of its shape (geometry) and size, and completely analogous to redistribution of charge in a conductor described by Eq. (3.67). The capacitor voltage, $v(t)$, and charge, $Q(t) = Cv(t)$, decrease exponentially with time, at a rate that is set by the relaxation time of the lossy dielectric filling the space between the capacitor electrodes.

Conceptual Questions (on CD): 3.18–3.21: *MATLAB Exercises* (on Companion Website).

3.10 EXTERNAL ELECTRIC ENERGY VOLUME SOURCES AND GENERATORS

We observed in connection with Fig. 3.1 that an external voltage source (e.g., a chemical battery) is required to maintain a steady current in a conductor. This source creates a rise in potential in the circuit and a potential difference between the ends of the conductor. From the energy standpoint, an external source of energy is necessary to maintain steady electric current flow through the circuit by continuously supplying the energy that is then dissipated in the conductor as Joule's heat. In concrete situations, various forms of the external energy (chemical energy, mechanical energy, thermal energy, light energy, etc.) are converted to the energy of the electric field in conductors and ultimately lost to heat. Generally, in analogy to circuit-theory generators, we use two field-theory models of volume-distributed energy sources capable of transmitting energy to electric charges: sources analogous to voltage generators and sources analogous to current generators.

Consider a source region of volume v shown in Fig. 3.16(a) in which a nonelectric external force, $\mathbf{F}_i$, termed the impressed force, acts on charge carriers (e.g., electrons) and separates positive and negative excess charges. An example is the force on electrons in a metallic wire moving in a magnetic field (as we shall see in a later chapter). We can formally divide $\mathbf{F}_i$ by the charge of a carrier, q ($q = -e$ for electrons), and what we get is a quantity expressed in V/m:

$$\mathbf{E}_i = \frac{\mathbf{F}_i}{q}, \tag{3.107}$$

which we call the impressed electric field intensity vector. This field, however, although of the same dimension and unit as $\mathbf{E}$, is not a true electric field (a field due to charges). Since there is also a field due to charges in the domain v, the total force on q is

$$\mathbf{F}_{tot} = \mathbf{F}_i + q\mathbf{E} = q(\mathbf{E}_i + \mathbf{E}), \tag{3.108}$$

and this is the force that compels the charges to move through the region. The current density vector in the region is, therefore, given by

$$\boxed{\mathbf{J} = \sigma(\mathbf{E} + \mathbf{E}_i),} \tag{3.109}$$

where σ is the conductivity of the material in v. It is very important to note that $\mathbf{E}_i$ does not depend on $\mathbf{J}$.

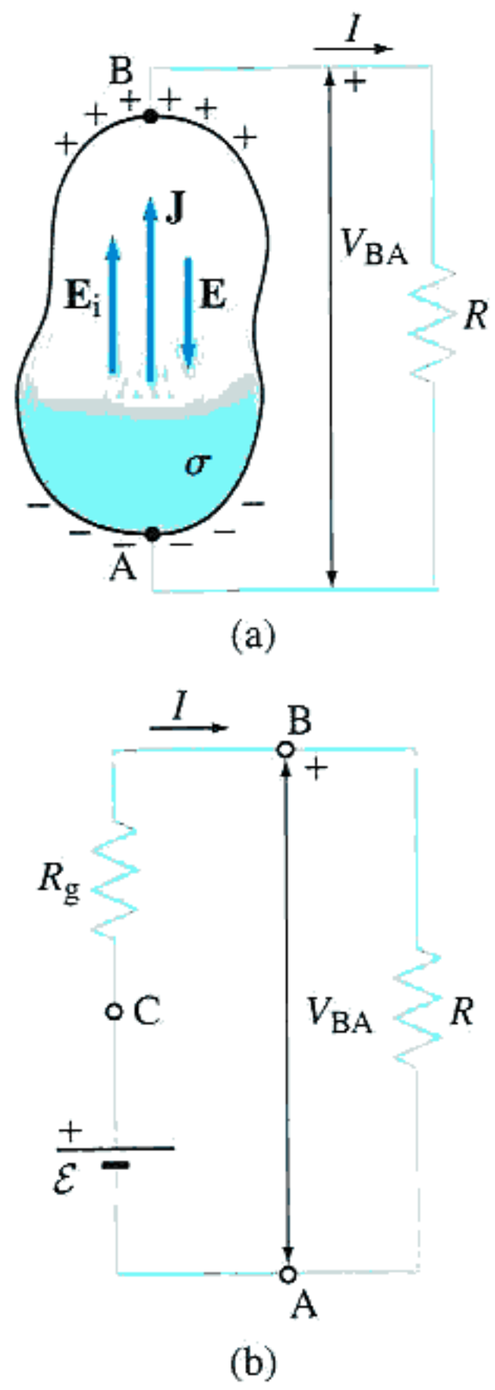

Figure 3.16 (a) External electric energy sources modeled by an impressed electric field, of intensity $\mathbf{E}_i$. (b) Voltage generator in circuit theory.

$\mathbf{E}_i$ – impressed electric field intensity vector (unit: V/m)

The model with a volume distribution (throughout v) of energy sources modeled by an impressed electric field, of intensity $\mathbf{E}_i$, can be used in many different electromagnetic situations, as we shall see later in this text. However, we note here that the particular situation in Fig. 3.16(a) actually represents a voltage generator in circuit theory. The generator is connected to a resistor of resistance R. Combining Eqs. (1.90) and (3.109), the voltage between the ends B and A of the source region (generator), can be written as

$$V_{BA} = \int_B^A \mathbf{E} \cdot d\mathbf{l} = \int_B^A \left(-\mathbf{E}_i + \frac{\mathbf{J}}{\sigma}\right) \cdot d\mathbf{l}. \tag{3.110}$$

Reversing the order of integration limits, we have

$$V_{BA} = \int_A^B \mathbf{E}_i \cdot d\mathbf{l} - \int_A^B \frac{\mathbf{J}}{\sigma} \cdot d\mathbf{l}. \tag{3.111}$$

The first term on the right-hand side of this equation is, by definition, the electromotive force (emf) of the generator:

electromotive force — emf (unit: V)

$$\boxed{\mathcal{E} = \int_{A}^{B} \mathbf{E}_i \cdot d\mathbf{l}.} \tag{3.112}$$

Note that $\mathcal{E}$ equals the work done by the external force, $\mathbf{F}_i$, in moving the charge q through the generator, from its negative terminal (A) to its positive terminal (B), divided by q. The unit for emf is V. The second integral in Eq. (3.111) is linearly proportional to the current I in the circuit:

$$\int_{A}^{B} \frac{\mathbf{J}}{\sigma} \cdot d\mathbf{l} = R_g I, \tag{3.113}$$

where the constant of proportionality, R_g, is called the internal resistance of the generator. Hence, Eq. (3.111) becomes

voltage generator

$$\boxed{V_{BA} = \mathcal{E} - R_g I.} \tag{3.114}$$

Fig. 3.16(b) shows the equivalent circuit-theory representation of the generator. Note that if the generator terminals A and B are open-circuited ($R \to \infty$), no current flows through the generator ($I = 0$), and we can write [Fig. 3.16(b)]

$$(V_{BA})_{\text{open-circuited}} = V_{CA} = \mathcal{E} \quad (I = 0). \tag{3.115}$$

Thus, the emf of the generator also equals its voltage when open-circuited.

An ideal voltage generator is one with a zero internal resistance ($R_g = 0$), i.e., no internal losses, implying that the voltage of such a generator is always equal to its emf, irrespective of the current flowing through it. That is,

ideal voltage generator

$$\boxed{V_{BA} = \mathcal{E}} \tag{3.116}$$

for all values of I and all values of R. This, essentially, is a consequence of the impressed electric field intensity, $\mathbf{E}_i$, being completely independent of the current density, $\mathbf{J}$, in the generator.

By Ohm's law, Eq. (3.72), on the other hand, the voltage V_{BA} in Fig. 3.16 can be written as

$$V_{BA} = RI, \tag{3.117}$$

which, combined with Eq. (3.114), gives

$$\mathcal{E} = R_g I + RI. \tag{3.118}$$

In general, for a closed path in a circuit with many emf sources and resistors (including the internal resistances of the sources), we have

Kirchhoff's voltage law in terms of emf's and voltage drops RI

$$\boxed{\sum_{j=1}^{M} \mathcal{E}_j = \sum_{k=1}^{N} R_k I_k.} \tag{3.119}$$

This equation is an expression of Kirchhoff's voltage law, Eq. (1.92). It states that the algebraic sum of the emf's (voltage rises) around a closed path in a circuit equals the algebraic sum of the voltage drops (RI) across the resistances around the path.

Multiplying both sides of Eq. (3.118) by I, we obtain

$$\mathcal{E}I = R_g I^2 + RI^2. \tag{3.120}$$

By Joule's law, Eq. (3.77), the expressions appearing on the right-hand side of this equation represent the power of Joule's losses in the generator and that in the resistor of resistance R, respectively. Both these powers are lost to heat. Therefore, by the principle of conservation of energy, the expression on the left-hand side of the equation,

$$P_{\mathrm{i}} = \mathcal{E} I, \tag{3.121}$$

must be the power generated by the emf of the generator. In local form, the volume density (in $\mathrm{W/m^3}$) of the power of the impressed electric field of intensity $\mathbf{E}_{\mathrm{i}}$ is [see Eq. (3.31)]

$$p_{\mathrm{i}} = \frac{\mathrm{d}P_{\mathrm{i}}}{\mathrm{d}v} = \mathbf{E}_{\mathrm{i}} \cdot \mathbf{J}. \tag{3.122}$$

The total power of sources in the domain v is thus [see Eq. (3.32)]

$$\boxed{P_{\mathrm{i}} = \int_v \mathbf{E}_{\mathrm{i}} \cdot \mathbf{J}\, \mathrm{d}v.} \tag{3.123}$$

power generated by impressed field

Let now the charges in a source region be carried by an impressed nonconduction current of density $\mathbf{J}_{\mathrm{i}}$, as depicted in Fig. 3.17(a), independent of the electric field intensity, $\mathbf{E}$. This is the second general model of energy sources we use in electromagnetics.[9] The current density $\mathbf{J}_{\mathrm{i}}$ does not enter Ohm's law in local form, and the total current density vector in the region is given by[10]

$$\boxed{\mathbf{J} = \sigma \mathbf{E} + \mathbf{J}_{\mathrm{i}},} \tag{3.124}$$

$\mathbf{J}_{\mathrm{i}}$ – impressed current density vector (unit: $\mathrm{A/m^2}$)

which, in scalar notation [for the situation in Fig. 3.17(a)], becomes

$$J = -\sigma E + J_{\mathrm{i}}. \tag{3.125}$$

This is analogous to a current generator in circuit theory, shown in Fig. 3.17(b) and described by

$$\boxed{I = -G_{\mathrm{g}} V + I_{\mathrm{g}},} \tag{3.126}$$

current generator

where I_{g} and G_{g} are the current intensity and internal conductance of the generator, respectively. Note that I_{g} equals the current of the generator with its terminals short-circuited ($V = 0$). An ideal current generator has a zero internal conductance ($G_{\mathrm{g}} = 0$), or an infinite internal resistance. This means that the current of such a generator is always constant,

$$\boxed{I = I_{\mathrm{g}},} \tag{3.127}$$

ideal current generator

i.e., it is independent of the generator terminal voltage (and of the conductance G).

---

[9]A classical example is so-called Van de Graaff generator, where the impressed current consists of charges transported mechanically on a moving dielectric belt, so that the velocity at which the belt moves actually represents an equivalent drift velocity ($\mathbf{v}_{\mathrm{d}}$) of charges. Here, however, the velocity of charges (i.e., the velocity of the belt) obviously does not depend on the electric field intensity vector, $\mathbf{E}$, and Eq. (3.2) does not make sense.

[10]Note that both Eq. (3.109), for a region with energy sources modeled by an impressed electric field, and Eq. (3.124), for a region with an impressed current, can be regarded as versions of the general constitutive equation for the current density, Eq. (3.21). In other words, Eq. (3.21) generally includes models of volume energy sources based on impressed fields and impressed currents, along with conduction properties of materials.

The power density of sources represented by an impressed current of density $\mathbf{J}_i$ amounts to

$$p_i = -\mathbf{E} \cdot \mathbf{J}_i, \tag{3.128}$$

where the minus sign is necessary because vectors $\mathbf{E}$ (the electric field intensity vector, due to positive and negative charges) and $\mathbf{J}_i$ (the impressed current density vector, which, like any other current density vector, carries positive charges in its direction and negative charges in the opposite direction) are directed oppositely. For the situation in Fig. 3.17(a), $p_i = EJ_i$. The total power of sources in v is

power generated by impressed current

$$\boxed{P_i = -\int_v \mathbf{E} \cdot \mathbf{J}_i \, dv.} \tag{3.129}$$

Note that the power generated by I_g in Fig. 3.17(b) is given by

$$P_i = VI_g. \tag{3.130}$$

This power is delivered to the rest of the circuit and dissipated to heat in the two resistors, the total power of Joule's losses being $G_g V^2 + GV^2$.

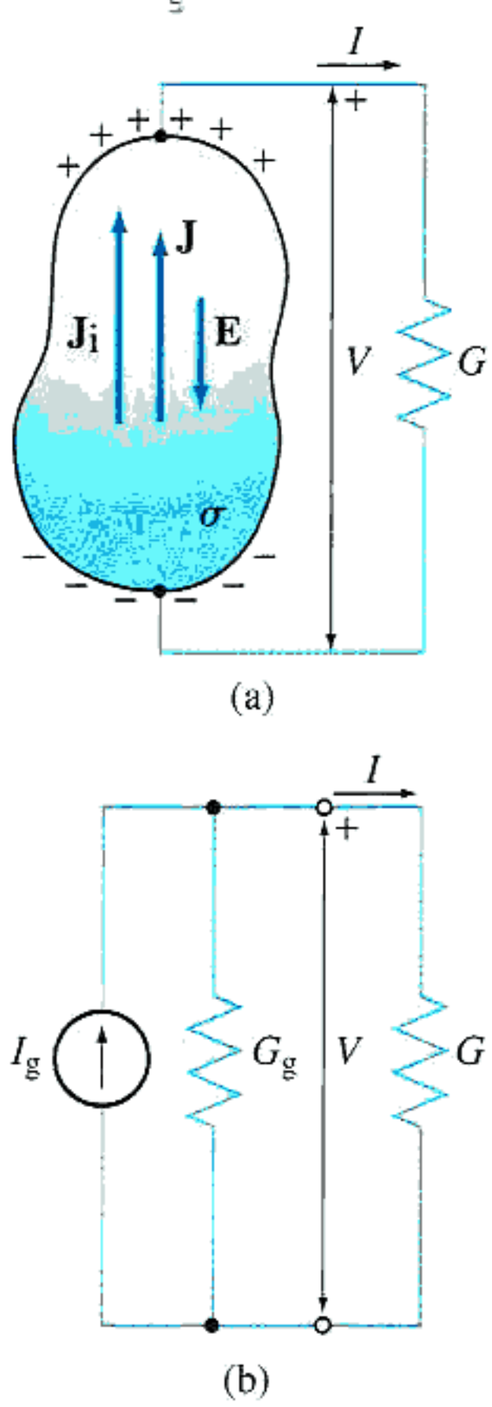

Figure 3.17 (a) External electric energy sources modeled by an impressed electric current, of density $\mathbf{J}_i$. (b) Current generator in circuit theory.

3.11 ANALYSIS OF CAPACITORS WITH IMPERFECT INHOMOGENEOUS DIELECTRICS

We now deal with steady current fields in capacitors containing piece-wise homogeneous and continuously inhomogeneous imperfect (lossy) dielectrics. Generally, charges in these systems exist not only on the surfaces of capacitor electrodes, but also on the boundary surfaces between homogeneous dielectric layers and over the volume of continuously inhomogeneous dielectrics. The analysis starts with the evaluation of the current distribution, i.e., the computation of the current density vector, $\mathbf{J}$, in the dielectric. The electric field intensity vector, $\mathbf{E}$, is then determined by Ohm's law in local form. By integrating $\mathbf{E}$ through the dielectric, we find the voltage between the electrodes and the conductance (and resistance) of the capacitor. Finally, the distribution of charge in the system can be found from the electric flux density vector, $\mathbf{D}$, using the generalized Gauss' law in differential form and the corresponding boundary condition.

As an illustration, consider a parallel-plate capacitor with two imperfect dielectric layers shown in Fig. 3.18(a). Let the permittivities of the layers be ε_1 and ε_2, their conductivities σ_1 and σ_2, and thicknesses d_1 and d_2, respectively. The surface area of each of the plates is S. The plates can be considered as perfect conductors. Let us analyze this capacitor, assuming that it is connected to an ideal generator of time-invariant voltage V.

The current density vector in the dielectric is normal to the plates [Eq. (3.57)] and uniform in each dielectric layer [Eq. (3.82)]. From the boundary condition for the normal components of $\mathbf{J}$, Eq. (3.55), applied to the interface between the two dielectrics and the continuity equation for steady currents in integral form, Eq. (3.40), applied to a rectangular closed surface enclosing the positive plate [Fig. 3.18(a)], with the right-hand side positioned in either one of the dielectrics, we have

$$J_1 = J_2 = J = \frac{I}{S}, \tag{3.131}$$

where I is the current through the capacitor. The electric field intensities in the dielectrics are

$$E_1 = \frac{J}{\sigma_1} = \frac{I}{\sigma_1 S} \quad \text{and} \quad E_2 = \frac{J}{\sigma_2} = \frac{I}{\sigma_2 S}. \tag{3.132}$$

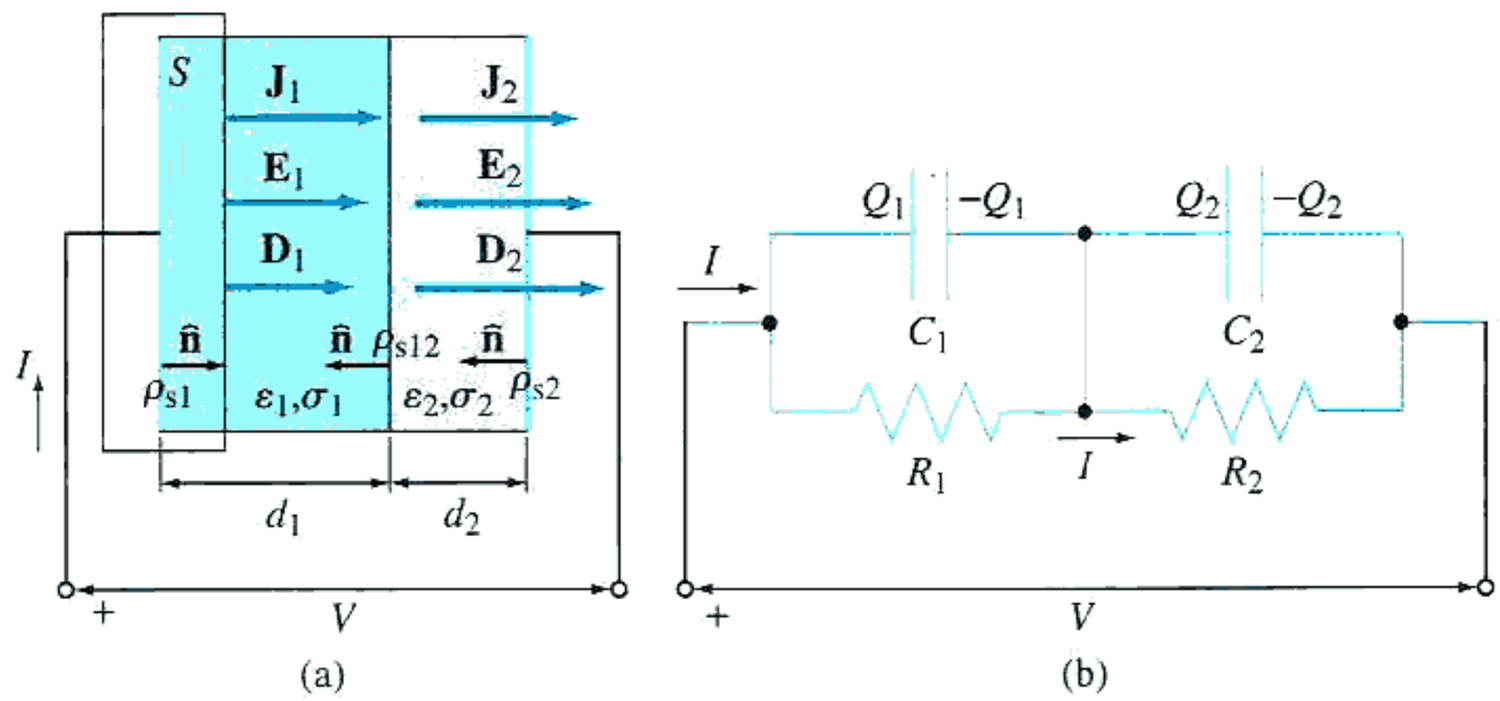

Figure 3.18 Analysis of a capacitor with a two-layer imperfect dielectric: (a) geometry of the structure with vectors **J**, **E**, and **D** in individual layers and (b) equivalent circuit of the system.

The voltage across the capacitor is given by

$$V = E_1 d_1 + E_2 d_2 = \frac{I}{S}\left(\frac{d_1}{\sigma_1} + \frac{d_2}{\sigma_2}\right), \tag{3.133}$$

so that the conductance of the capacitor[11] comes out to be

$$G = \frac{I}{V} = \frac{\sigma_1 \sigma_2 S}{\sigma_2 d_1 + \sigma_1 d_2}. \tag{3.134}$$

The electric flux densities in the layers are[12]

$$D_1 = \varepsilon_1 E_1 = \frac{\varepsilon_1 G V}{\sigma_1 S} \quad \text{and} \quad D_2 = \varepsilon_2 E_2 = \frac{\varepsilon_2 G V}{\sigma_2 S}. \tag{3.135}$$

Eq. (3.62) tells us that, since the dielectric layers are homogeneous, there is no volume charge in them. Using Eq. (3.63), the surface charge on the boundary surface between the layers amounts to

$$\rho_{s12} = D_2 - D_1 = \left(\frac{\varepsilon_2}{\sigma_2} - \frac{\varepsilon_1}{\sigma_1}\right) J = \frac{(\varepsilon_2 \sigma_1 - \varepsilon_1 \sigma_2) V}{\sigma_1 d_2 + \sigma_2 d_1}, \tag{3.136}$$

where we take $J_n = -J$ in Eq. (3.63) because the unit vector $\hat{\mathbf{n}}$ in the corresponding boundary condition is directed from medium 2 to medium 1. Note that if $\varepsilon_1/\sigma_1 = \varepsilon_2/\sigma_2$, $\rho_{s12} = 0$. From Eq. (2.58), the surface charge densities on the plates are

$$\rho_{s1} = D_1 = \frac{\varepsilon_1 \sigma_2 V}{\sigma_1 d_2 + \sigma_2 d_1} \quad \text{and} \quad \rho_{s2} = -D_2 = -\frac{\varepsilon_2 \sigma_1 V}{\sigma_1 d_2 + \sigma_2 d_1}. \tag{3.137}$$

The system in Fig. 3.18(a) can be explained and analyzed also invoking the circuit-theory point of view and concepts. The interface between the dielectric layers is equipotential, and can, therefore, be metalized. We thus get two nonideal capacitors in series, each of them being represented by a parallel connection of an ideal

[11] Note that the current field in the resistor of Fig. 3.12(a) can be analyzed in the same way.

[12] Note that $D_1 \neq D_2$, contrary to Eq. (2.147) for the same capacitor with two perfect dielectric layers, shown in Fig. 2.25(a). The capacitor with a perfect dielectric represents an electrostatic system (with no current), and the analysis starts with the generalized Gauss' law. The capacitor with an imperfect dielectric represents a system with steady current, and the analysis starts with the continuity equation.

capacitor and an ideal resistor, as shown in the equivalent circuit in Fig. 3.18(b). The characteristics of the elements in the circuit are:

$$C_1 = \frac{\varepsilon_1 S}{d_1}, \quad C_2 = \frac{\varepsilon_2 S}{d_2}, \quad R_1 = \frac{d_1}{\sigma_1 S}, \quad R_2 = \frac{d_2}{\sigma_2 S}, \tag{3.138}$$

where the resistances R_1 and R_2 can be obtained either from the corresponding capacitances, C_1 and C_2 [also see Eqs. (2.157)], using the relationship in Eq. (3.102), or from Eq. (3.85).

Using the expression for the equivalent total resistance of a series connection of resistors, Eq. (3.86), the conductance of the system is

$$G = \frac{1}{R_1 + R_2} = \frac{\sigma_1 \sigma_2 S}{\sigma_2 d_1 + \sigma_1 d_2}. \tag{3.139}$$

The charges of the capacitors in Fig. 3.18(b) are computed as

$$Q_1 = C_1 V_1 = C_1 R_1 I = C_1 R_1 G V = \frac{\varepsilon_1}{\sigma_1} G V, \tag{3.140}$$

$$Q_2 = C_2 V_2 = C_2 R_2 I = C_2 R_2 G V = \frac{\varepsilon_2}{\sigma_2} G V, \tag{3.141}$$

with V_1 and V_2 standing for the voltages across individual dielectric layers.[13] Finally, the surface charge densities in Fig. 3.18(a) are given by the expressions

$$\rho_{s1} = \frac{Q_1}{S}, \quad \rho_{s12} = \frac{Q_2 - Q_1}{S}, \quad \text{and} \quad \rho_{s2} = \frac{-Q_2}{S}, \tag{3.142}$$

which give the same results as in Eqs. (3.136) and (3.137).

Example 3.10 Spherical Capacitor with a Continuously Inhomogeneous Imperfect Dielectric

A spherical capacitor is filled with a continuously inhomogeneous imperfect dielectric. The permittivity and conductivity of the dielectric depend on the distance r from the capacitor center and are given by the expressions $\varepsilon(r) = 3\varepsilon_0 b/r$ and $\sigma(r) = \sigma_0 b^2/r^2$ $(a < r < b)$, where a and b are radii of the inner and outer capacitor electrodes, and σ_0 is a (positive) constant. The capacitor is connected to a time-invariant voltage V. Find: (a) the conductance of the capacitor, (b) the free charge distribution of the capacitor, (c) the bound charge distribution of the dielectric, and (d) the total free charge in the capacitor.

Solution

(a) Because of spherical symmetry, the current density vector in the dielectric is of the form given by Eq. (3.46). From the continuity equation, $J(r)$ is the same as in Eq. (3.48), so that the electric field intensity vector in the dielectric is (Fig. 3.19)

$$\mathbf{E} = \frac{\mathbf{J}}{\sigma(r)} = \frac{I}{4\pi\sigma(r) r^2}\hat{\mathbf{r}} = \frac{I}{4\pi\sigma_0 b^2}\hat{\mathbf{r}} = E\hat{\mathbf{r}}, \tag{3.143}$$

with I being the current intensity of the capacitor. We note that the electric field intensity turns out to be the same in the entire dielectric ($E = \text{const}$). The voltage between the

[13] Note that the voltages of the elements in Fig. 3.18(b) are determined by the resistors: $V_1 = VR_1/(R_1 + R_2)$ and $V_2 = VR_2/(R_1 + R_2)$ – resistive voltage divider. In the case of the same system with perfect dielectric layers [Figs. 2.25(a) and 2.26(a)], which is an electrostatic system, the voltages are determined by the capacitors: $V_1 = VC_2/(C_1 + C_2)$ and $V_2 = VC_1/(C_1 + C_2)$ – capacitive voltage divider.

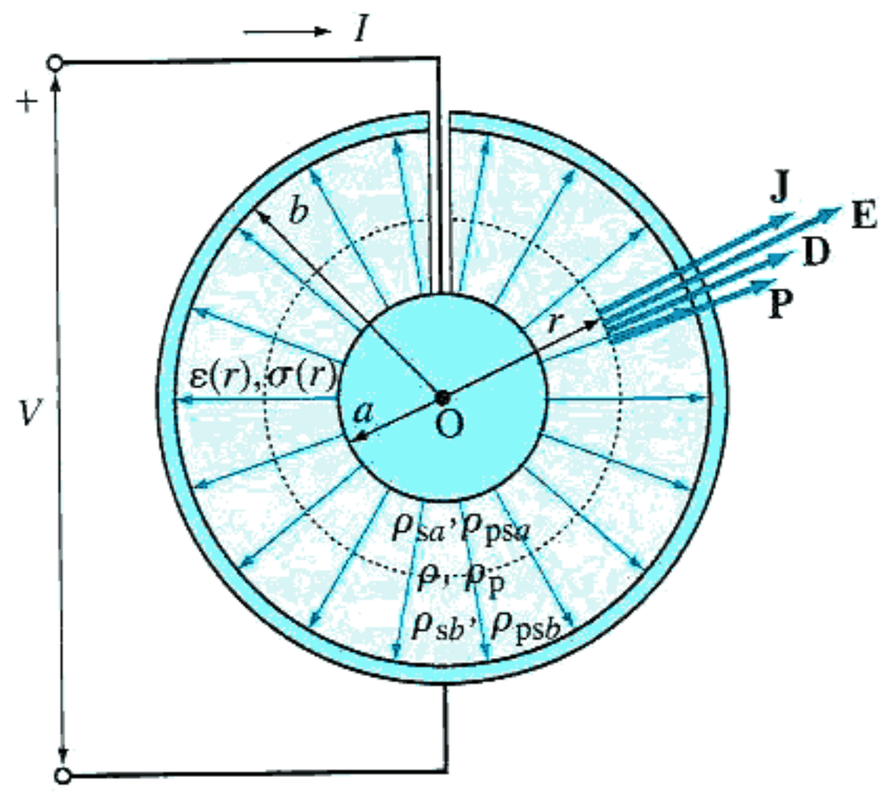

Figure 3.19 Spherical capacitor with a continuously inhomogeneous dielectric with losses; for Example 3.10.

electrodes and the capacitor conductance amount to[14]

$$V = \int_a^b E\,\mathrm{d}r = E(b-a) \quad \longrightarrow \quad G = \frac{I}{V} = \frac{4\pi\sigma_0 b^2}{b-a}. \tag{3.144}$$

(b) The electric flux density vector in the dielectric is given by

$$\mathbf{D} = \varepsilon(r)E\,\hat{\mathbf{r}}, \tag{3.145}$$

where $E = V/(b-a)$. By means of Eqs. (3.62) and (1.171), the free volume charge density inside the dielectric is

$$\rho = \nabla\cdot\mathbf{D} = \frac{1}{r^2}\frac{\mathrm{d}}{\mathrm{d}r}\left[r^2 D(r)\right] = \frac{E}{r^2}\frac{\mathrm{d}}{\mathrm{d}r}\left(r^2\varepsilon\right) = \frac{3\varepsilon_0 bV}{(b-a)r^2}. \tag{3.146}$$

The free surface charge density on the surfaces of the inner and outer capacitor electrodes are

$$\rho_{sa} = D(a^+) = \varepsilon(a^+)E = \frac{3\varepsilon_0 bV}{a(b-a)} \quad \text{and} \quad \rho_{sb} = -D(b^-) = -\varepsilon(b^-)E = -\frac{3\varepsilon_0 V}{b-a}, \tag{3.147}$$

respectively.

(c) From Eq. (2.59), the polarization vector in the dielectric is given by

$$\mathbf{P} = [\varepsilon(r) - \varepsilon_0]E\,\hat{\mathbf{r}}. \tag{3.148}$$

Using Eq. (2.19), the bound volume charge density over the volume of the dielectric is

$$\rho_{\mathrm{p}} = -\nabla\cdot\mathbf{P} = -\frac{1}{r^2}\frac{\mathrm{d}}{\mathrm{d}r}\left[r^2 P(r)\right] = -\frac{\varepsilon_0 V(3b-2r)}{r^2(b-a)}, \tag{3.149}$$

while Eq. (2.23) gives us the bound surface charge density on the surfaces of the dielectric:

$$\rho_{\mathrm{psa}} = -P(a^+) = -\frac{\varepsilon_0(3b-a)V}{a(b-a)} \quad \text{and} \quad \rho_{\mathrm{psb}} = P(b^-) = \frac{2\varepsilon_0 V}{b-a}. \tag{3.150}$$

(d) The total free charge Q in the capacitor is zero. To prove that, we write

$$Q = \int_a^b \rho(r)\underbrace{4\pi r^2\,\mathrm{d}r}_{\mathrm{d}v} + \rho_{sa}S_a + \rho_{sb}S_b = 12\pi\varepsilon_0 bV + \frac{12\pi\varepsilon_0 abV}{b-a} - \frac{12\pi\varepsilon_0 b^2 V}{b-a} = 0, \tag{3.151}$$

[14]Note that, since $\varepsilon(r)/\sigma(r) \neq$ const, G is not proportional to C, i.e., Eq. (3.101) is not satisfied. The capacitance C is found in Example 2.19.

where dv is adopted to be the volume of a spherical shell of radius r and thickness dr [see Fig. 1.9 and Eq. (1.33)], $S_a = 4\pi a^2$ (surface area of the inner electrode), and $S_b = 4\pi b^2$ (surface area of the outer electrode).

Problems: 3.10–3.16; *Conceptual Questions* (on Companion Website): 3.22 and 3.23; *MATLAB Exercises* (on Companion Website).

3.12 ANALYSIS OF LOSSY TRANSMISSION LINES WITH STEADY CURRENTS

In this section, we analyze transmission lines with losses in a time-invariant (dc) regime. Consider, as an example, a coaxial cable with imperfect conductors of (finite) conductivity σ_c and an imperfect dielectric of (nonzero) conductivity σ_d. The radius of the inner conductor of the cable is a, the inner and outer radii of the outer conductor are b and c, respectively ($a < b < c$), and the length of the cable is l. The cable is fed by a time-invariant (dc) voltage generator of electromotive force $\mathcal{E}$ and internal resistance R_g, as shown in Fig. 3.20. A load of resistance R_L is connected to the other end of the cable.

Let I designate the current flowing through the inner conductor of the cable. The same current returns through the outer conductor. Since the dielectric in the cable is imperfect, there is a leakage (stray) current through the dielectric, between the cable conductors. Due to cylindrical symmetry of the structure, this current is radial with respect to the cable axis and its density, J, depends only on the radial distance r from the axis. The current leakage, in turn, causes a continual decrease of the current intensity I along the cable, meaning that I is a function of the coordinate z along the cable, $I = I(z)$. Applying the continuity equation, Eq. (3.40), to a cylindrical closed surface S of radius r and length Δz (Fig. 3.20) gives

$$\underbrace{I(z+\Delta z) - I(z)}_{\Delta I} + \underbrace{J 2\pi r}_{I'_d}\,\Delta z = 0 \tag{3.152}$$

[currents $I(z+\Delta z)$ and $I'_d \Delta z$ leave S, while $I(z)$ enters it], where ΔI is the change in current I along a distance Δz, and I'_d is the leakage current per unit length (p.u.l.) of the cable (in A/m). Hence,

current leakage in a transmission line with an imperfect dielectric

$$\boxed{\frac{\Delta I}{\Delta z} = -I'_d = -(I_d)_{\text{p.u.l.}},} \tag{3.153}$$

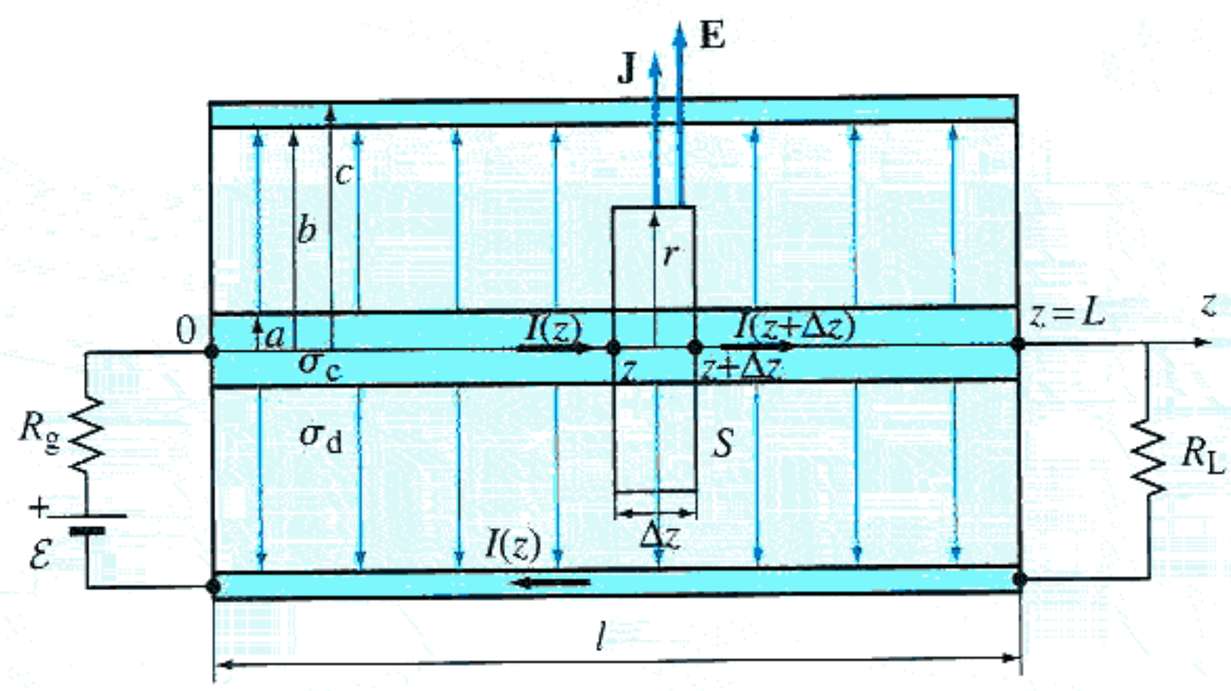

Figure 3.20 Coaxial cable with imperfect conductors and dielectric in a dc regime.

and

$$J = \frac{I'_{\mathrm{d}}}{2\pi r}. \tag{3.154}$$

Using Ohm's law in local form, Eq. (3.18), the electric field intensity vector in the dielectric is computed as

$$\mathbf{E} = \frac{\mathbf{J}}{\sigma_{\mathrm{d}}} = \frac{I'_{\mathrm{d}}}{2\pi\sigma_{\mathrm{d}} r}\,\hat{\mathbf{r}}, \tag{3.155}$$

so that the voltage between the inner and outer conductor of the cable amounts to

$$V = \int_a^b E\,\mathrm{d}r = \frac{I'_{\mathrm{d}}}{2\pi\sigma_{\mathrm{d}}} \ln\frac{b}{a}. \tag{3.156}$$

By definition, the conductance per unit length of a transmission line, i.e., the conductance for one meter (unit length) of the line divided by 1 m, is

$$\boxed{G' = G_{\mathrm{p.u.l.}} = \frac{I'_{\mathrm{d}}}{V}.} \tag{3.157}$$

conductance per unit length of a transmission line (unit: S/m)

It is also referred to as the p.u.l. leakage conductance. The unit is S/m. For a coaxial cable, from Eq. (3.156),

$$\boxed{G' = \frac{2\pi\sigma_{\mathrm{d}}}{\ln(b/a)}.} \tag{3.158}$$

conductance p.u.l. of a coaxial cable

The drop of the current I along a distance Δz equals $\Delta I = \Delta G V$, where

$$\Delta G = G'\Delta z \tag{3.159}$$

is the conductance through the dielectric at the length Δz.

As Δz approaches zero, the expression on the left-hand side of Eq. (3.153) becomes the derivative of I with respect to z. Therefore, combining Eqs. (3.153) and (3.157), we have

$$\boxed{\frac{\mathrm{d}I}{\mathrm{d}z} = -G'V.} \tag{3.160}$$

transmission line with a lossy dielectric

This is a first-order differential equation in z for the current and voltage of a transmission line with a lossy dielectric. It tells us that the rate of change of the current along the line is proportional to the negative of the line voltage, with the conductance per unit length of the line as the proportionality constant. In the case of a transmission line with a perfect dielectric (no losses in the dielectric), $G' = 0$, so that $\mathrm{d}I/\mathrm{d}z = 0$, yielding

$$\boxed{I = \text{const.}} \tag{3.161}$$

transmission line with a perfect dielectric

Because of losses in the conductors ($1/\sigma_{\mathrm{c}} \neq 0$), the voltage between conductors varies along the cable, i.e., $V = V(z)$. From Eq. (3.85), the total resistance (for time-invariant currents) of the cable turns out to be

$$R = R_1 + R_2 = \frac{l}{\sigma_{\mathrm{c}} S_1} + \frac{l}{\sigma_{\mathrm{c}} S_2}, \tag{3.162}$$

where R_1 and R_2 are the resistances of the inner and outer conductor, respectively, and S_1 and S_2 are cross-sectional surface areas of the conductors. The resistance per unit length of the line is given by

$$\boxed{R' = R_{\mathrm{p.u.l.}} = \frac{R}{l}} \tag{3.163}$$

resistance per unit length of a transmission line (unit: Ω/m)

(the unit is Ω/m), so that

dc resistance p.u.l. of a coaxial cable

$$\boxed{R' = \frac{1}{\pi\sigma_c}\left(\frac{1}{a^2} + \frac{1}{c^2 - b^2}\right).} \tag{3.164}$$

The resistance along the length Δz of the line is

$$\Delta R = R'\Delta z, \tag{3.165}$$

and the voltage drop across that resistance

$$V(z) - V(z + \Delta z) = \Delta R I. \tag{3.166}$$

This equation can be rewritten as

$$\underbrace{V(z + \Delta z) - V(z)}_{\Delta V} = -R'\Delta z I, \tag{3.167}$$

which, as Δz approaches zero, becomes

transmission line with lossy conductors

$$\boxed{\frac{\mathrm{d}V}{\mathrm{d}z} = -R'I.} \tag{3.168}$$

We see that the rate of change of the voltage along a transmission line with lossy conductors is proportional to the negative of the line current, with the resistance per unit length of the line being the proportionality constant. For a transmission line with perfect electric conductors (PEC), $R' = 0$ and $\mathrm{d}V/\mathrm{d}z = 0$, so that

transmission line with perfect conductors

$$\boxed{V = \text{const.}} \tag{3.169}$$

Eqs. (3.167), (3.153), and (3.157) tell us that each section of a transmission line of length Δz can be represented by a circuit cell consisting of a series resistor of resistance $R'\Delta z$ and a shunt (parallel) resistor of conductance $G'\Delta z$, and the entire transmission line can be replaced by many cascaded equal small cells, as indicated in Fig. 3.21. Thus, a transmission line is said to be a circuit with distributed parameters (parameters per unit length), and Eqs. (3.160) and (3.168) are in fact based on Kirchhoff's laws and Ohm's law for the cells of the circuit.

Eqs. (3.160) and (3.168) are called transmission-line equations or telegrapher's equations for time-invariant currents and voltages on transmission lines. For a transmission line with both $R' \neq 0$ and $G' \neq 0$, these two equations are coupled differential equations in two unknowns: $I(z)$ and $V(z)$. By taking the derivative with respect to z of one equation and substituting its right-hand side by the corresponding expression from the other equation, we can eliminate one unknown (current

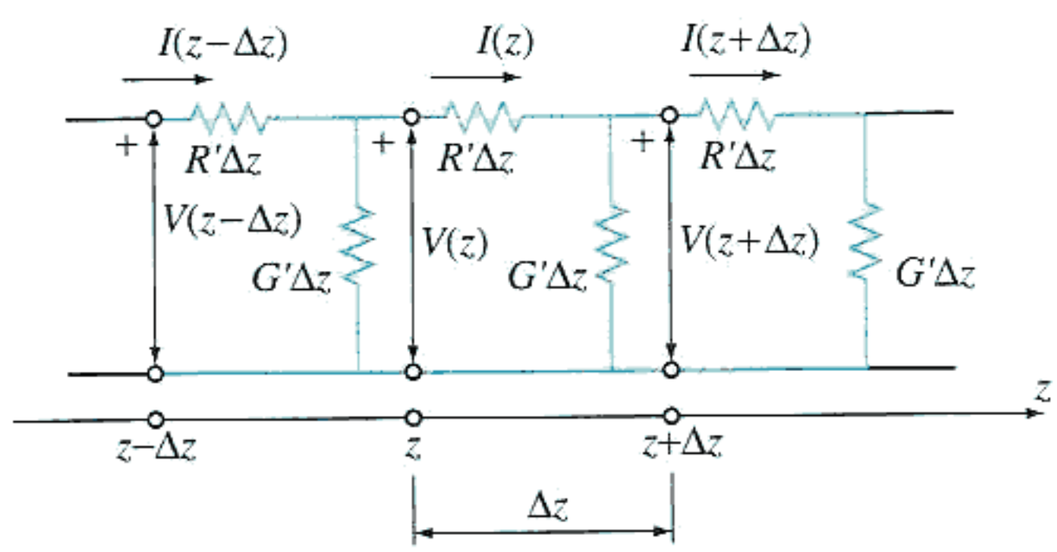

Figure 3.21 Circuit-theory representation of a transmission line with losses in conductors and dielectric in a dc regime.

or voltage) and obtain the following second-order differential equations with only voltage and only current as unknowns:

$$\frac{d^2V}{dz^2} - R'G'V = 0 \quad \text{and} \quad \frac{d^2I}{dz^2} - R'G'I = 0 \quad (R' \neq 0,\ G' \neq 0). \tag{3.170}$$

Their solutions are exponential functions for the voltage and current along the line. If $R' = 0$ and $G' \neq 0$, $V = \text{const}$ along the line [Eq. (3.169)], and the solution to Eq. (3.160) is a linear function for the current along the line. Conversely, if $G' = 0$ and $R' \neq 0$, $I = \text{const}$ along the line [Eq. (3.161)], and the solution to Eq. (3.168) is a linear function for the voltage along the line. Finally, if both $G' = 0$ and $R' = 0$, both current and voltage do not vary along the line.

Note that using the duality relationship in Eq. (3.101), the leakage conductance per unit length of a transmission line with homogeneous imperfect dielectric can be found from the capacitance per unit length of the line as

$$\boxed{G' = \frac{\sigma_d}{\varepsilon} C',} \tag{3.171}$$

duality of G′ and C′

where ε is the permittivity of the dielectric [for a coaxial cable, see Eqs. (3.158) and (2.123)]. Note also that $R' \neq 1/G'$ in Eqs. (3.170).

The power of Joule's losses per unit length of a transmission line, P'_J, can be obtained as the power of Joule's losses in one cell in Fig. 3.21, divided by Δz. The unit is W/m. Specifically, in conductors of the line (series resistor in Fig. 3.21),

$$\boxed{(P'_J)_c = \frac{\Delta R I^2}{\Delta z} = R'I^2.} \tag{3.172}$$

Joule's or ohmic losses p.u.l. in line conductors (unit: W/m)

In the dielectric (shunt resistor in Fig. 3.21),

$$\boxed{(P'_J)_d = \frac{\Delta G V^2}{\Delta z} = G'V^2.} \tag{3.173}$$

Joule's (ohmic) losses p.u.l. in line dielectric (unit: W/m)

The total power of Joule's losses per unit length of the line is hence

$$P'_J = R'I^2 + G'V^2. \tag{3.174}$$

Example 3.11 Transmission Line with Perfect Conductors and Imperfect Dielectric

A transmission line of length l and conductance per unit length G' is connected to an ideal voltage generator of time-invariant emf $\mathcal{E}$. The other end of the line is terminated in a load of resistance R_L. The losses in the conductors of the line can be neglected. Find: (a) the distribution of current along the line conductors, (b) the total power of Joule's losses in the line, and (c) the power of the generator.

Solution

(a) With reference to Fig. 3.22,[15] since there are no losses in the line conductors, $R' = 0$, the voltage along the line is [Eq. (3.169)]

$$V(z) = \mathcal{E} \quad (0 \leq z \leq l). \tag{3.175}$$

[15] Although resembles a two-wire line, a pair of parallel horizontal lines in Fig. 3.22 is a symbolic representation of an arbitrary two-conductor transmission line, with conductors of completely arbitrary cross section and generally inhomogeneous dielectric.

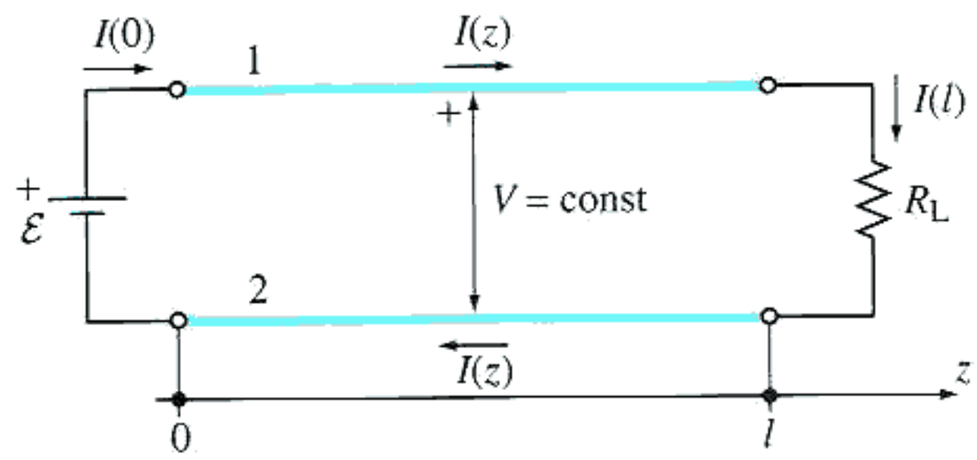

Figure 3.22 Transmission line with lossless conductors and lossy dielectric in a dc regime; for Example 3.11.

Eq. (3.160) becomes

$$\frac{dI}{dz} = -G'\mathcal{E}, \tag{3.176}$$

and by integrating it, we obtain

$$I(z) = -G'\mathcal{E}z + I_0 \quad (0 \le z \le l). \tag{3.177}$$

From the condition $I(l) = V/R_L = \mathcal{E}/R_L$ (the line current at $z = l$ equals the current through the load), the integration constant is found to be $I_0 = G'\mathcal{E}l + \mathcal{E}/R_L$ [$I_0 = I(0)$ is the current of the generator], so that

$$I(z) = G'\mathcal{E}(l - z) + \frac{\mathcal{E}}{R_L} \quad (R' = 0,\ G' \neq 0). \tag{3.178}$$

(b) Based on Eq. (3.173), the power of Joule's losses per unit length of the line is given by

$$P'_J = (P'_J)_d = G'V^2 = G'\mathcal{E}^2 = \text{const} \quad (0 \le z \le l). \tag{3.179}$$

As P'_J does not vary along the line, the total power of Joule's losses in the line, including the losses in the load, comes out to be

$$P_J = \underbrace{P'_J l}_{\text{line}} + \underbrace{\frac{\mathcal{E}^2}{R_L}}_{\text{load}} = \left(G'l + \frac{1}{R_L}\right)\mathcal{E}^2. \tag{3.180}$$

(c) Eq. (3.121) tells us that the power of the generator is

$$P_i = \mathcal{E}I(0) = \mathcal{E}\left(G'\mathcal{E}l + \frac{\mathcal{E}}{R_L}\right). \tag{3.181}$$

Note that

$$P_i = P_J, \tag{3.182}$$

which, of course, is in agreement with the principle of conservation of energy and power; namely, the power generated by the generator is delivered to the rest of the circuit, and dissipated to heat in the lossy dielectric of the transmission line and in the resistive load.

Example 3.12 Thin Two-Wire Line with Losses

Determine the resistance and conductance per unit length of a thin symmetrical two-wire line with lossy conductors and a lossy dielectric. The conductivities of both conductors and of the dielectric are σ_c and σ_d, respectively. The conductor radii are a and the distance between their axes is d ($d \gg a$).

Solution The resistance per unit length of the line is twice that of a single wire:

dc resistance p.u.l. of a thin two-wire line

$$\boxed{R' = 2\frac{1}{\sigma_c \pi a^2}} \tag{3.183}$$

[see also Eq. (3.164)].

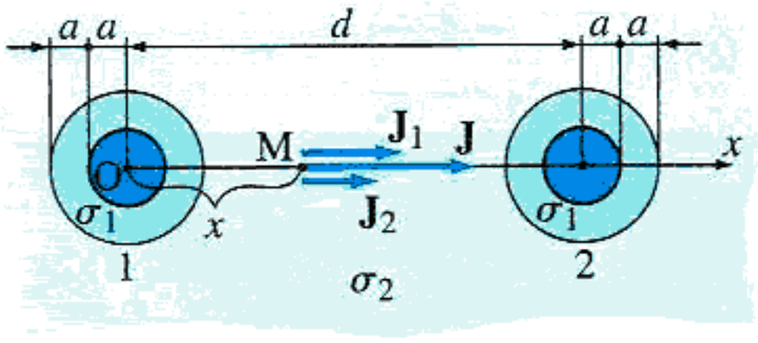

Figure 3.23 Cross section of a thin symmetrical two-wire line with imperfect dielectric coatings immersed in a conducting liquid; for Example 3.13.

From Eqs. (3.171) and (2.141), the conductance per unit length of the line is

$$G' = \frac{\sigma_d}{\varepsilon} C' = \frac{\pi \sigma_d}{\ln(d/a)}. \tag{3.184}$$

conductance p.u.l. of a thin two-wire line

Example 3.13 Two-Wire Line with Imperfect Coatings in a Conducting Liquid

Conductors of a thin two-wire line are coated with thin coaxial layers of imperfect dielectric of conductivity σ_1. The radius of each wire is a, the thickness of coatings is also a, and the distance between wire axes is d ($d \gg a$). The line is immersed in a liquid of conductivity σ_2. What is the conductance per unit length of this line?

Solution The evaluation of the (leakage) conductance per unit length of the line, whose cross section is shown in Fig. 3.23, can be performed completely in parallel to the evaluation of the capacitance per unit length of the line in Fig. 2.31. Here, instead of Q' we have I'_d – the current that leaks from conductor 1 of the line through the coatings and the liquid to conductor 2 of the line, per unit of its length. The leakage current densities due to the individual conductors, i.e., the current density due to the leakage from conductor 1 and that due to the leakage into conductor 2, evaluated at the point M in Fig. 3.23, are

$$J_1 = \frac{I'_d}{2\pi x} \quad \text{and} \quad J_2 = \frac{I'_d}{2\pi(d-x)}, \tag{3.185}$$

respectively. The total current density along the x-axis between the conductors is $J = J_1 + J_2$. The electric field intensity is $E = J/\sigma_1$ in the coatings and $E = J/\sigma_2$ in the liquid. The voltage between the conductors, V, is calculated as in Eq. (2.182), and the conductance per unit length of the line comes out to be

$$G' = \frac{I'_d}{V} = \pi \left(\frac{1}{\sigma_1} \ln 2 + \frac{1}{\sigma_2} \ln \frac{d}{2a} \right)^{-1}. \tag{3.186}$$

Note that this expression for G' can be obtained also by substituting the permittivities in the expression for C' in Eq. (2.183) by the corresponding conductivities. Namely, the inhomogeneity in terms of σ in the system in Fig. 3.23 is of the same form as the inhomogeneity in terms of ε in the system in Fig. 2.31, and a sort of duality between the conductance and capacitance of the two systems can be exploited.

Example 3.14 Planar Line with Two Imperfect Dielectric Layers

Fig. 3.24 shows a planar transmission line consisting of two parallel metallic strips of width w and a two-layer dielectric between the strips. The strips are perfectly conducting, whereas both dielectric layers are imperfect, with conductivities σ_1 and σ_2. The thicknesses of layers are d_1 and d_2, and the length of the line is l. The line is connected at one end to an ideal voltage generator of time-invariant emf $\mathcal{E}$. The other end of the line is open. Calculate (a) the conductance per unit length of the line and (b) the current along the strips.

Solution

(a) An application of the continuity equation to a rectangular closed surface S portrayed in Fig. 3.24, much like that in Eq. (3.152), yields

$$Jw\Delta z = I(z) - I(z + \Delta z) = I'_d \Delta z \tag{3.187}$$

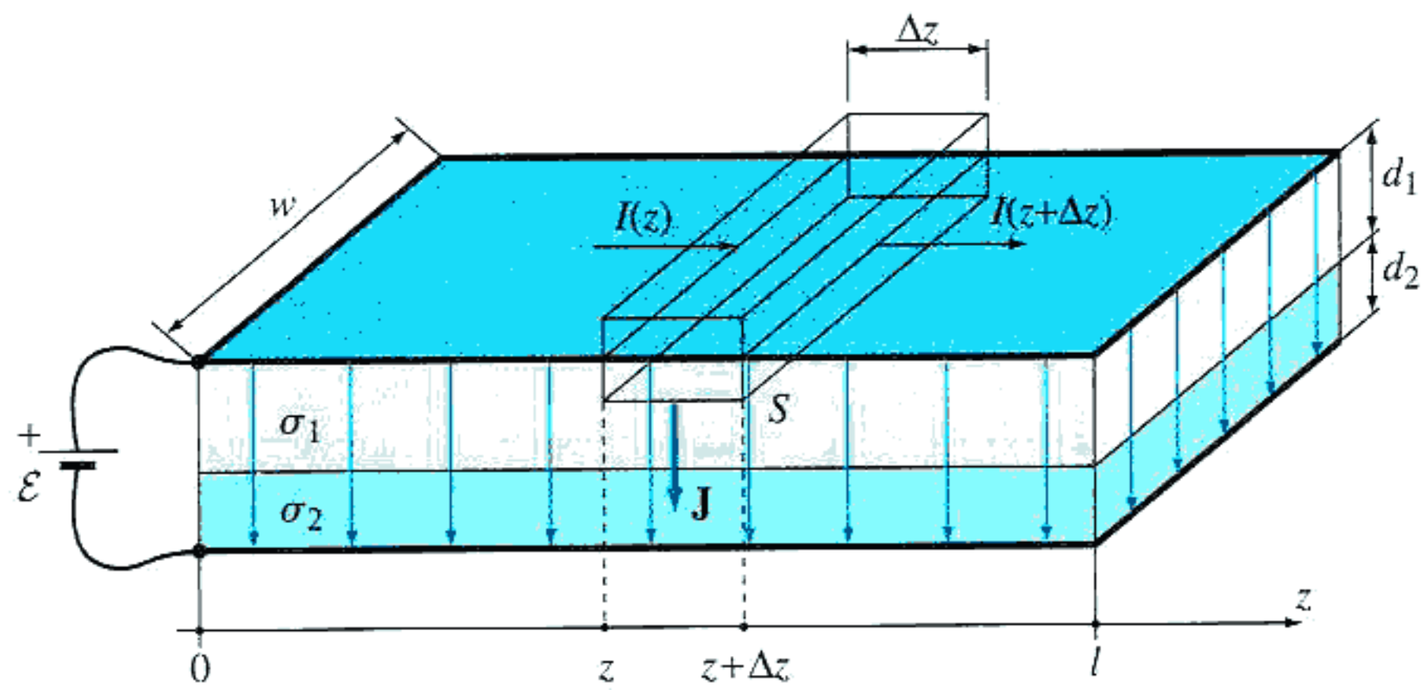

Figure 3.24 Planar transmission line with a two-layer imperfect dielectric; for Example 3.14.

(I'_{d} is the leakage current per unit length of the line), from which, the current density in both dielectric layers is

$$J = \frac{I'_{\mathrm{d}}}{w}. \tag{3.188}$$

Having in mind Eqs. (3.133) and (3.157), the voltage between the strips and the conductance per unit length of the line are obtained as

$$V = \frac{J}{\sigma_1} d_1 + \frac{J}{\sigma_2} d_2 = \frac{I'_{\mathrm{d}}}{w}\left(\frac{d_1}{\sigma_1} + \frac{d_2}{\sigma_2}\right) \quad \longrightarrow \quad G' = \frac{I'_{\mathrm{d}}}{V} = w\left(\frac{d_1}{\sigma_1} + \frac{d_2}{\sigma_2}\right)^{-1}. \tag{3.189}$$

(b) The current along the line is given by Eq. (3.178) with $R_{\mathrm{L}} \to \infty$ (the line is open):

$$I(z) = G'\mathcal{E}(l - z) = \frac{w\mathcal{E}(l - z)}{d_1/\sigma_1 + d_2/\sigma_2}. \tag{3.190}$$

Problems: 3.17–3.22; *Conceptual Questions* (on Companion Website): 3.24–3.26; *MATLAB Exercises* (on Companion Website).

3.13 GROUNDING ELECTRODES

Consider a metallic body (electrode) of arbitrary shape buried under the flat surface of the earth. This body may represent a grounding electrode for some electrical or electronic device (residing on the earth's surface).[16] Assume that the conductivity of the earth is the same, σ, in the entire lower half-space. Let a time-invariant current of intensity I flow from the electrode into the earth (this current is supplied to the electrode through a thin insulated wire), as shown in Fig. 3.25(a). As the conductivity of the electrode is much larger than σ, Eq. (3.57) tells us that the current lines leaving the electrode are perpendicular to its surface. From Eq. (3.58), on the other side, the current lines in the earth near to its boundary with air are tangential (parallel) to the boundary surface.

[16]Grounding electrodes, in general, are used for draining static electricity induced on parts of a device, for equalizing the electric potential of a device housing with the neighboring conducting objects, for reducing the so-called conduction interference (undesired currents induced in a device, interfering with "regular" currents in the device and with neighboring devices), for routing (together with lightning rods) the charge flow in lightning to the ground, etc.

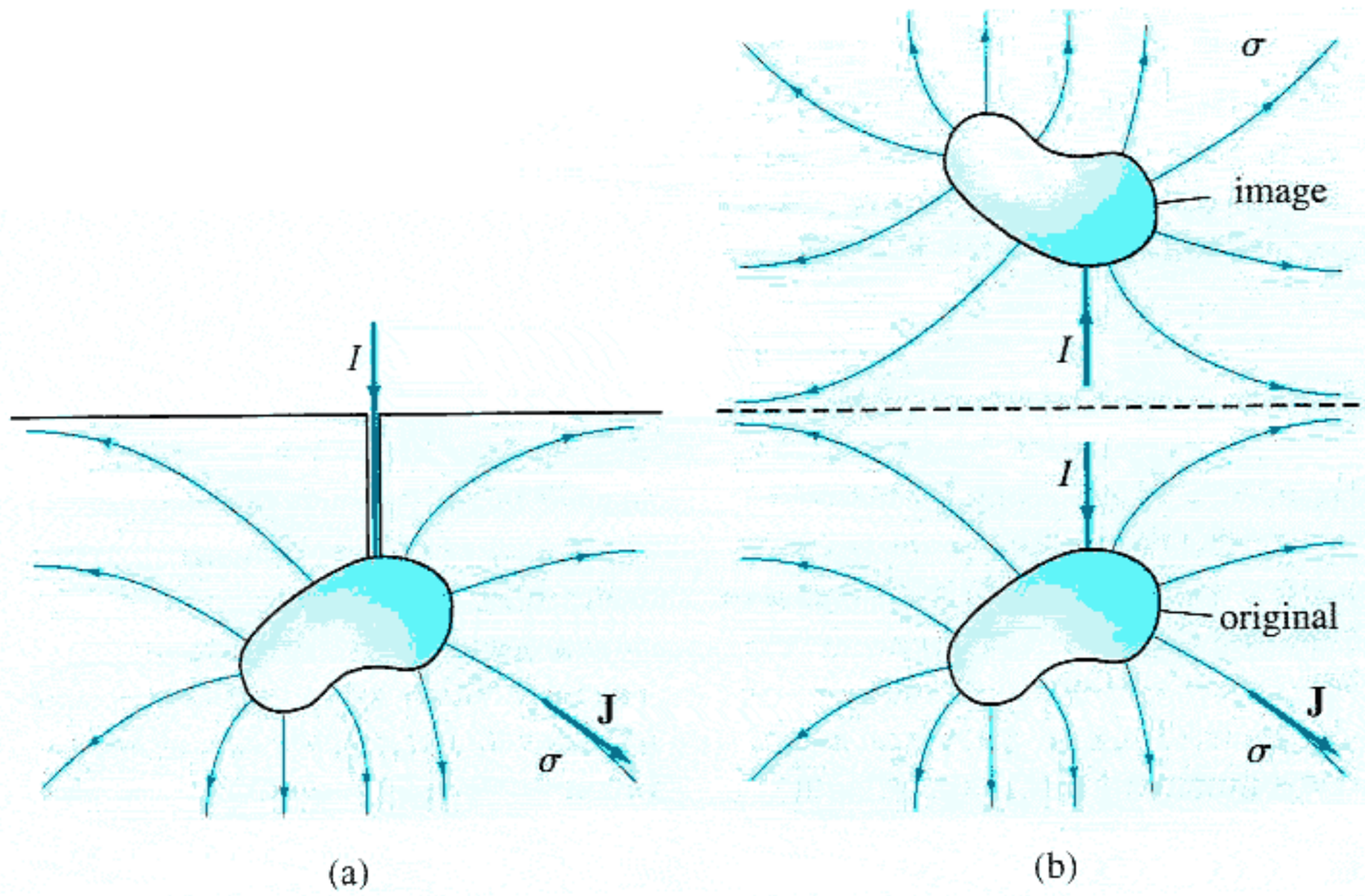

Figure 3.25 Grounding electrode with a steady current (a) and the equivalent system with the earth-air boundary removed (b) – image theory for steady currents.

Consider now the system shown in Fig. 3.25(b), obtained by taking an image of the lower half-space of Fig. 3.25(a) in the earth-air boundary plane. Namely, the grounding electrode in the lower half-space is the same as in the original system and a symmetrical electrode (image electrode) with respect to the boundary plane is introduced in the upper half-space, while the entire space around the electrodes is filled with the medium of conductivity σ. The current of the image electrode is the same as that of the original one (I), and it flows also out of the electrode (positive image). By symmetry, the total current density vector (due to both electrodes) at an arbitrary point of the plane of symmetry in the system in Fig. 3.25(b) has a horizontal component only. This means that the resultant current lines are tangential to the plane of symmetry, and this plane corresponds to the ground-air interface in the system in Fig. 3.25(a). We conclude that the distributions of current in the lower half-space in the systems in Figs. 3.25(a) and (b) are the same. This is the so-called image theory (or theorem) for steady currents, which states that an arbitrary steady-current source (e.g., a grounding electrode with a steady current flowing into the ground) situated in a conducting half-space near a flat boundary surface with a nonconducting medium (e.g., earth-air interface) can be replaced by a new system of sources in an infinite conducting medium. The new system consists of the original source configuration itself and its positive image in the boundary plane. The image electrode (i.e., the charge on its surface) actually represents an equivalent for the surface charge on the boundary between two half-spaces in the original system. There is no direct way to determine this charge and take its contribution to the total electric field into account in the original system, and that is why the equivalent (homogenized) system, with the boundary removed, is generally much simpler for analysis.

After the current density vector, $\mathbf{J}$, in the earth for a given current I of a grounding electrode is determined by analyzing the equivalent system in Fig. 3.25(b), all other quantities of interest for a specific application can be found – in the original system in Fig. 3.25(a). The electric field intensity vector in the ground and on its surface is $\mathbf{E} = \mathbf{J}/\sigma$. An important parameter of a grounding electrode is its grounding

resistance, defined as

grounding resistance

$$\boxed{R_{gr} = \frac{V_{gr}}{I},} \tag{3.191}$$

where V_{gr} is the potential of the electrode with respect to the reference point at infinity. According to Eq. (1.74), this potential is given by

potential of a grounding electrode (reference point at infinity)

$$\boxed{V_{gr} = \int_{\text{electrode}}^{\text{infinity}} \mathbf{E} \cdot d\mathbf{l}.} \tag{3.192}$$

By integrating **E** along the field lines on the earth's surface between two points that are a distance equal to an average person's step apart, we get the so-called voltage of a step, V_{step}, around the grounding electrode. This voltage corresponds to the potential difference between the feet of a person walking in the direction along the field lines on the earth's surface. The maximum voltage of a step in the region above a grounding electrode is a parameter important for applications where a large current intensity of the electrode may cause exceedingly large values of V_{step}, with even fatal consequences.

Example 3.15 Hemispherical Grounding Electrode

A hemispherical grounding electrode of radius $a = 1$ m is buried in the earth of conductivity $\sigma = 10^{-3}$ S/m, with its base up, as shown in Fig. 3.26(a). The current of the electrode is $I = 1000$ A. Find (a) the grounding resistance of the electrode and (b) the voltage of a step between points on the earth's surface that are $r_1 = 2$ m and $r_2 = r_1 + b$ away from the electrode center, where $b = 0.75$ m (average person's step).

Solution

(a) Using the image theory for steady currents, Fig. 3.25, we get the equivalent system shown in Fig. 3.26(b), which consists of two hemispherical electrodes pressed onto each other, forming thus a spherical electrode with current $2I$ flowing into a homogeneous medium of conductivity σ. Due to spherical symmetry, the current density vector, **J**, in the medium is radial. Consequently, **J** in the original system is also radial and of the form given by Eq. (3.46). Applying the continuity equation to a spherical surface S of radius r

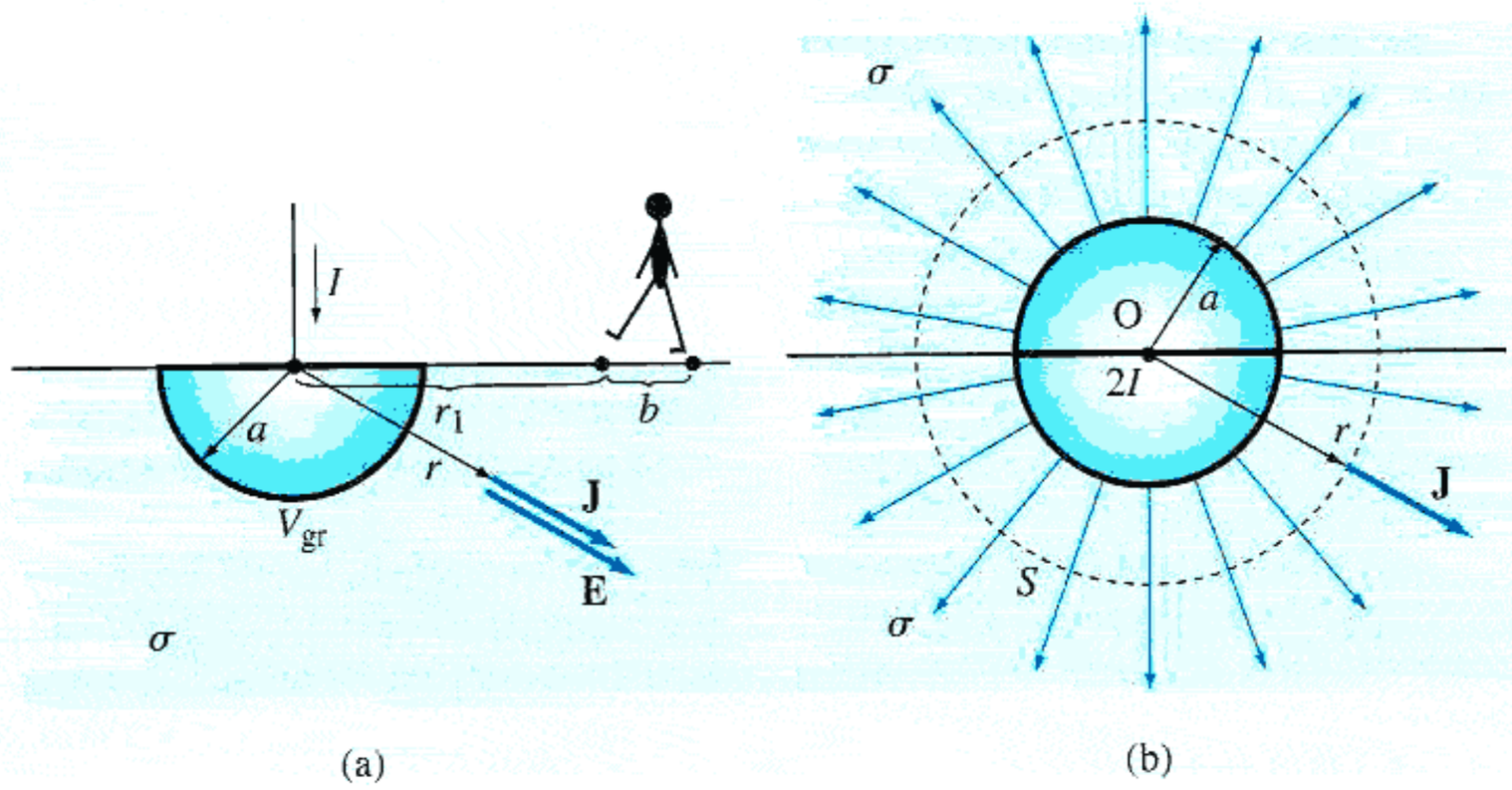

Figure 3.26 (a) Hemispherical grounding electrode and (b) equivalent spherical electrode in a homogeneous medium; for Example 3.15.

positioned around the electrode gives

$$J(r) = \frac{2I}{4\pi r^2} = \frac{I}{2\pi r^2} \quad (a < r < \infty). \tag{3.193}$$

Note that the same result is obtained by applying the continuity equation to a hemispherical surface of radius r in the original system – in Fig. 3.26(a).

Combining Eqs. (3.18) and (3.193), the electric field intensity in the earth is

$$E(r) = \frac{J(r)}{\sigma} = \frac{I}{2\pi\sigma r^2}. \tag{3.194}$$

With the use of Eqs. (3.192) and (3.191), the potential of the electrode with respect to the reference point at infinity and its grounding resistance come out to be

$$V_{gr} = \int_{r=a}^{\infty} E\,dr = \frac{I}{2\pi\sigma a} \quad \longrightarrow \quad \boxed{R_{gr} = \frac{V_{gr}}{I} = \frac{1}{2\pi\sigma a} = 159\ \Omega.} \tag{3.195}$$

grounding resistance of a hemispherical electrode

(b) The voltage of a step is as large as

$$\boxed{V_{step} = \int_{r_1}^{r_2} E\,dr = \frac{I}{2\pi\sigma}\left(\frac{1}{r_1} - \frac{1}{r_2}\right) = \frac{Ib}{2\pi\sigma r_1 r_2} = 21.7\ \text{kV} \quad (b = r_2 - r_1).} \tag{3.196}$$

voltage of a step; b is an average person's step

Example 3.16 Two Hemispherical Grounding Electrodes

The electric circuit shown in Fig. 3.27 consists of an ideal voltage generator of emf $\mathcal{E} = 100$ V, a wire of negligible resistance, and two hemispherical grounding electrodes. The radius of each electrode is $a = 2$ m, the conductivity of the earth is $\sigma = 10$ mS/m, and the distance between the electrode centers is $d = 100$ m. Compute the current in the circuit.

Solution Since $d \gg a$, the potentials with respect to the reference point at infinity of the individual electrodes can be evaluated independently from each other, that is, as for a single isolated grounding electrode. The equivalent resistance seen by the generator equals therefore $2R_{gr}$, where the expression for R_{gr} is given in Eqs. (3.195). As the resistance of the wire is negligible, the current in the circuit is

$$I = \frac{\mathcal{E}}{2R_{gr}} = \pi\sigma a\mathcal{E} = 6.28\ \text{A}. \tag{3.197}$$

Example 3.17 Hemispherical Grounding Electrode in a Two-Layer Earth

Conductivity of a layer of earth around a hemispherical grounding electrode shown in Fig. 3.28 is $\sigma_1 = 5 \times 10^{-3}$ S/m and that of the rest of the earth $\sigma_2 = 10^{-3}$ S/m. The radii of the electrode and the boundary surface between the earth layers are $a = 1$ m and $b = 2$ m, respectively. The current intensity of the electrode is $I = 100$ A. Determine (a) the grounding resistance of the electrode and (b) the power of Joule's losses in the earth.

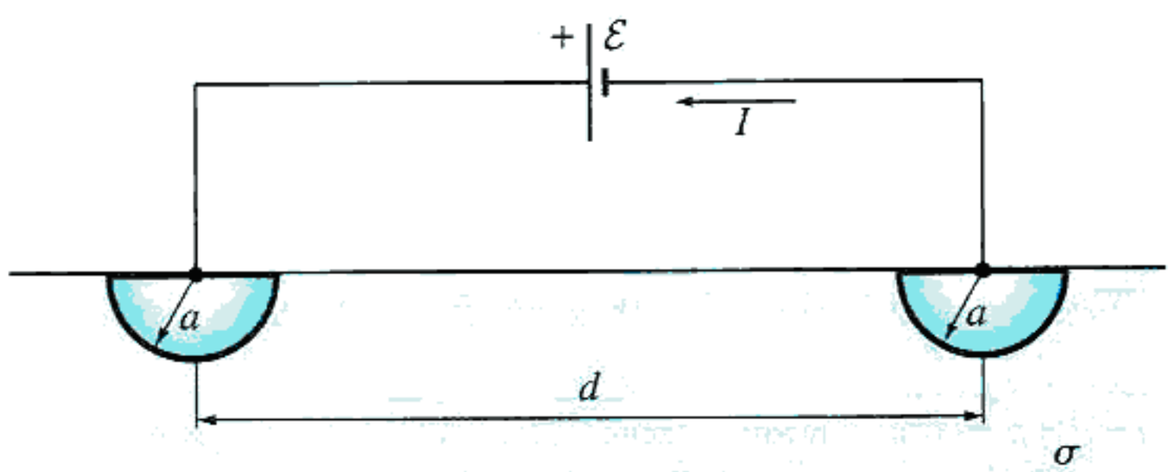

Figure 3.27 Two hemispherical grounding electrodes in a dc circuit; for Example 3.16.

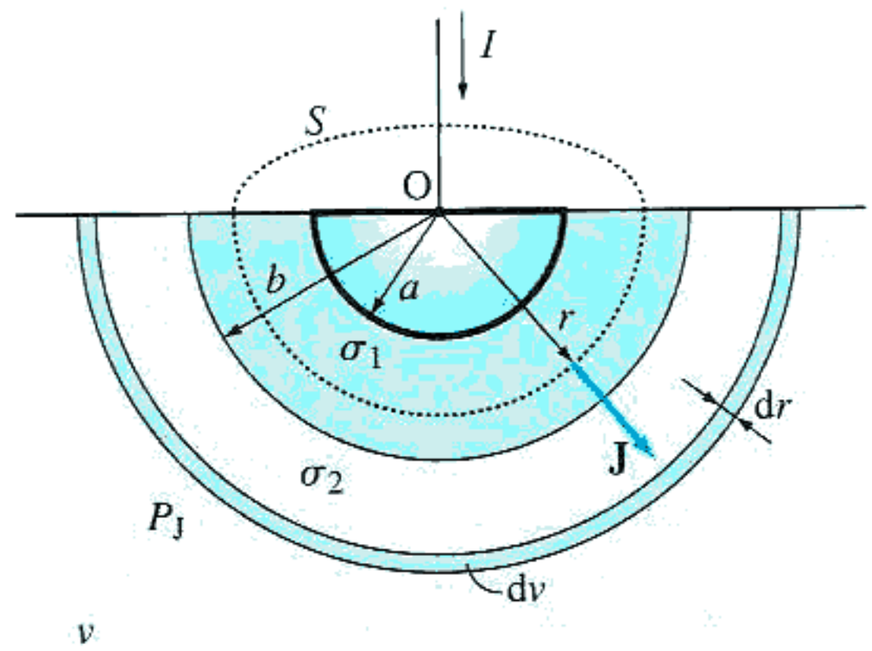

Figure 3.28 Hemispherical grounding electrode in an earth consisting of two concentric layers; for Example 3.17.

Solution

(a) Because of symmetry, the current flow in both layers of earth is radial. Applying the continuity equation to the closed surface S shown in Fig. 3.28, we obtain the same expression for the current density J in the earth as in Eq. (3.193). The electric field intensity vector in the earth is $\mathbf{E}_1 = \mathbf{J}/\sigma_1$ for $a < r < b$ and $\mathbf{E}_2 = \mathbf{J}/\sigma_2$ for $b < r < \infty$. By means of Eq. (3.192), the potential of the electrode with respect to the reference point at infinity is given by

$$V_{\text{gr}} = \int_a^\infty E\,\mathrm{d}r = \int_a^b E_1\,\mathrm{d}r + \int_b^\infty E_2\,\mathrm{d}r = \frac{I}{2\pi}\left[\frac{1}{\sigma_1}\left(\frac{1}{a} - \frac{1}{b}\right) + \frac{1}{\sigma_2 b}\right], \tag{3.198}$$

from which the grounding resistance, Eq. (3.191), is

$$R_{\text{gr}} = \frac{V_{\text{gr}}}{I} = \frac{1}{2\pi b}\left(\frac{b-a}{\sigma_1 a} + \frac{1}{\sigma_2}\right) = 95.5\ \Omega. \tag{3.199}$$

(b) Using Eq. (3.32), and combining it with Eq. (3.193), the power of Joule's losses in the earth turns out to be

$$P_{\text{J}} = \int_v JE\,\mathrm{d}v = \int_a^\infty \frac{I}{2\pi r^2} E\,\underbrace{2\pi r^2\,\mathrm{d}r}_{\mathrm{d}v} = I\int_a^\infty E\,\mathrm{d}r, \tag{3.200}$$

where $\mathrm{d}v$ is the volume of a hemispherical shell of radius r and thickness $\mathrm{d}r$ (portrayed in Fig. 3.28). Noting that the last integral in this equation equals V_{gr} [Eq. (3.198)], we have

power of Joule's losses in the earth surrounding a grounding electrode

$$\boxed{P_{\text{J}} = V_{\text{gr}} I = R_{\text{gr}} I^2,} \tag{3.201}$$

and $P_{\text{J}} = 955$ kW for given numerical data.[17]

Example 3.18 Spherical Grounding Electrode Deep in the Earth

A spherical grounding electrode of radius $a = 30$ cm is buried in a homogeneous earth of conductivity $\sigma = 10^{-2}$ S/m such that its center is at a depth $d = 6$ m with respect to the ground surface, as shown in Fig. 3.29(a). There is a steady current flowing through the electrode, and its potential with respect to the reference point at infinity is $V_{\text{gr}} = 15$ kV. Calculate the maximum tangential component of the electric field intensity vector on the earth's surface.

[17] Although derived for a specific grounding electrode, that in Fig. 3.28, the expression for the power of Joule's losses in the earth in Eq. (3.201) is true for an arbitrary grounding electrode, with grounding resistance R_{gr} and current I. Note that this is actually an expression of Joule's law, Eq. (3.77).

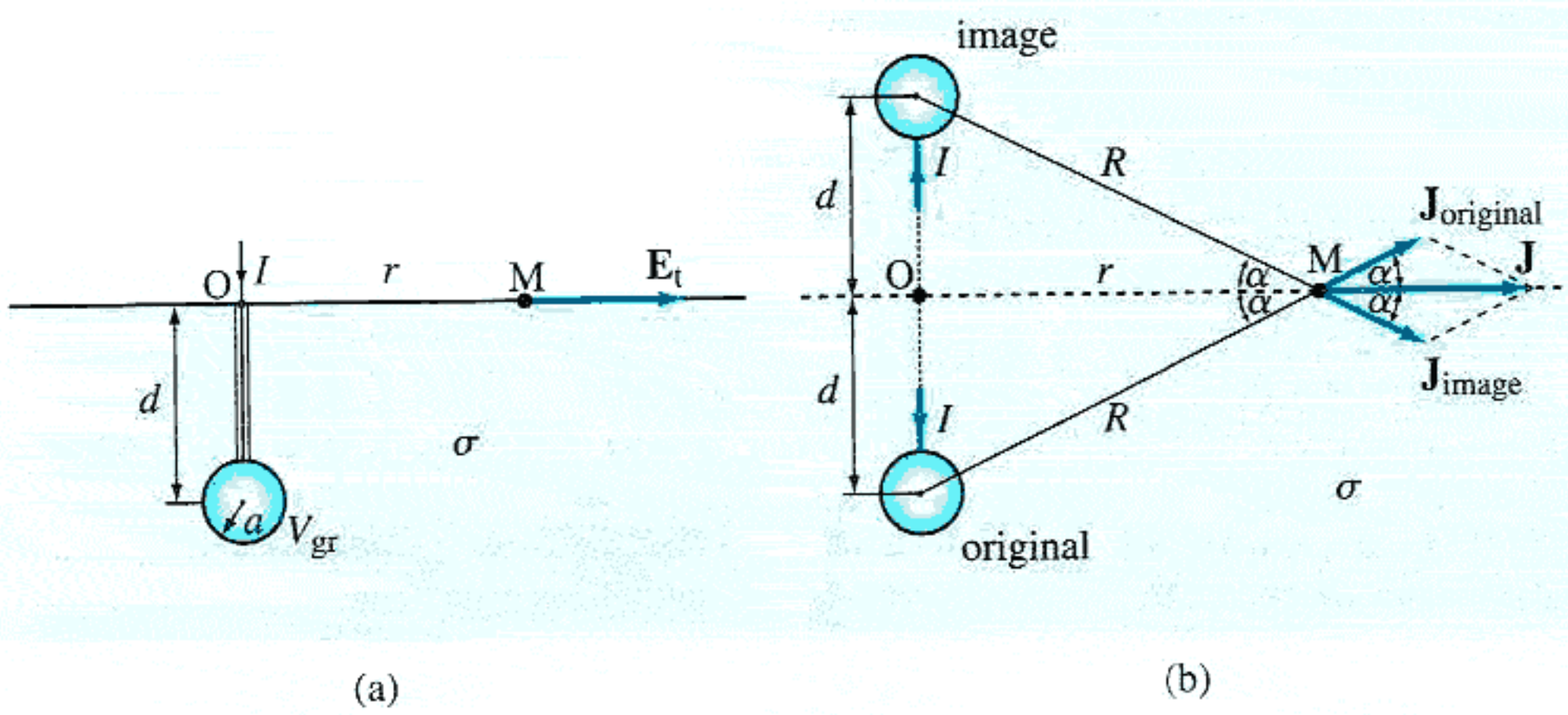

Figure 3.29 (a) Spherical grounding electrode buried deep in the earth and (b) equivalent system – by virtue of the image theory for steady currents; for Example 3.18.

Solution Since $d \gg a$, the influence of the boundary with air on the grounding resistance of the electrode can be neglected, meaning that R_{gr} can be evaluated as for an electrode in the infinite homogeneous medium of conductivity σ. Invoking the duality relationship in Eq. (3.102), we can further relate R_{gr} to the capacitance (C) of the same metallic sphere situated in an infinite dielectric medium of permittivity ε. Eq. (2.121) gives this capacitance for $\varepsilon = \varepsilon_0$, so that

$$\boxed{R_{gr} = \frac{\varepsilon_0}{\sigma C} = \frac{1}{4\pi\sigma a} = 26.5\ \Omega.} \tag{3.202}$$

grounding resistance of a spherical electrode buried deep in the earth

Hence, the current of the electrode is $I = V_{gr}/R_{gr} = 565.5$ A.

Applying the image theory for steady currents (Fig. 3.25) and the superposition principle, the resultant current density vector at a point M in Fig. 3.29(b), the position of which is determined by a radial distance r from the projection of the electrode centers on the plane of symmetry (point O), can be obtained as

$$\mathbf{J} = \mathbf{J}_{\text{original}} + \mathbf{J}_{\text{image}}, \tag{3.203}$$

where $\mathbf{J}_{\text{original}}$ and $\mathbf{J}_{\text{image}}$ are the current density vectors due to the current flow from individual electrodes. Making use of the fact that $d \gg a$, these current densities can be evaluated independently from each other, which results in

$$J_{\text{original}} = J_{\text{image}} = \frac{I}{4\pi R^2} \quad \longrightarrow \quad J = 2J_{\text{original}} \cos\alpha = \frac{Ir}{2\pi R^3} \tag{3.204}$$

($\cos\alpha = r/R$ and $R = \sqrt{r^2 + d^2}$).

The tangential component of the electric field intensity vector on the earth's surface in the original system, Fig. 3.29(a), is

$$E_t(r) = \frac{J}{\sigma} = \frac{Ir}{2\pi\sigma(r^2 + d^2)^{3/2}}. \tag{3.205}$$

From the condition

$$\frac{\mathrm{d}E_t(r)}{\mathrm{d}r} = 0, \tag{3.206}$$

we get that the field intensity E_t is maximum on a circle of radius $r_{max} = d/\sqrt{2} = 4.24$ m, centered at the point O. This maximum field is

$$(E_t)_{max} = E_t(r_{max}) = \frac{I\sqrt{3}}{9\pi\sigma d^2} = 96\ \text{V/m}. \tag{3.207}$$

Note that the maximum voltage of a step, taking $b = 0.75$ m as an average person's step, is approximately

$$(V_{step})_{max} \approx (E_t)_{max}\, b = 72\ \text{V}, \tag{3.208}$$

which is much less than the voltage found in Eq. (3.196), for instance. This is expected, because the electrode in Fig. 3.29(a) is buried deep in the earth.

Problems: 3.23–3.29; *Conceptual Questions* (on Companion Website): 3.27–3.30; *MATLAB Exercises* (on Companion Website).

Problems

3.1. Charge density in terms of the conductivity gradient. In a region with steady currents, the conductivity of the material varies with spatial coordinates, $\sigma \neq$ const, whereas permittivity does not, $\varepsilon =$ const. If the electric potential in the region is V, show that the volume charge density is given by $\rho = (\varepsilon/\sigma)\nabla\sigma \cdot \nabla V$.

3.2. Various computations for a copper wire with steady current. For a copper wire with a steady current described in Example 3.1, compute: (a) the number of electrons that pass through a cross section of the wire during one hour, (b) the electric field intensity in the wire, (c) the voltage between the wire ends, (d) the volume density of the power of Joule's losses in the wire material, (e) the total power of ohmic losses in the wire, (f) the resistance of the wire at room temperature, and (g) the wire resistance at the temperature of 100°C ($\alpha_{Cu} = 0.0039\ \mathrm{K}^{-1}$).

3.3. Parallel-plate capacitor with an imperfect dielectric. A parallel-plate capacitor has a homogeneous imperfect dielectric of permittivity ε and conductivity σ. The separation between plates is d and the plate area is S. If the voltage between the plates is V (time-invariant), find (a) the current distribution in the dielectric, (b) the current through the capacitor terminals, (c) the conductance of the capacitor, (d) the power of Joule's losses in the capacitor, (e) the free charge distribution in the capacitor, and (f) the bound charge distribution in the capacitor.

3.4. Spherical capacitor half filled with a conducting liquid. A spherical capacitor has a poorly conducting liquid dielectric occupying a half of the space between the electrodes. The radii of electrodes are a and b ($a < b$), and the conductivity of the dielectric is σ. Determine the conductance of this capacitor.

3.5. Hollow steel-reinforced aluminum wire conductor. Consider a hollow steel-reinforced aluminum wire conductor of length $l = 100$ m. The radius of the cylindrical hole in the central part of the conductor is $a = 5$ mm, the thickness of the stainless-steel ($\sigma_{steel} = 1.1$ MS/m) reinforcement is $b - a = 5$ mm, and the rest of the conductor, whose overall radius is $c = 2$ cm, is aluminum ($\sigma_{Al} = 35$ MS/m). What is the resistance of this wire, and what is the ratio of current intensities I_{Al}/I_{steel} in the two materials for a given dc voltage drop between the two ends of the wire?

3.6. Resistor with two cuboidal parts. A resistor is formed from two rectangular cuboids of the same size, with sides $a = 8$ mm, $b = 2$ mm, and $c = 4$ mm. The cuboids are made out from different resistive materials, with conductivities $\sigma_1 = 10^5$ S/m and $\sigma_2 = 4 \times 10^5$ S/m. The voltage between the resistor terminals is $V = 50$ V. Find the electric field intensity, current density, current intensity, and power of Joule's losses in each of the two cuboids if they are connected as in (a) Fig. 3.30(a) and (b) Fig. 3.30(b).

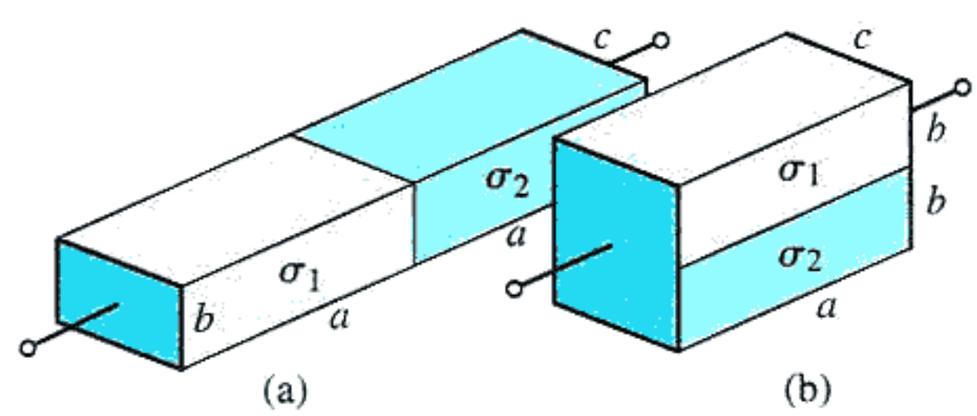

Figure 3.30 Two rectangular cuboids made out from different resistive materials connected in (a) series and (b) parallel; for Problem 3.6.

3.7. Conductivity gradient along the resistor current. Fig. 3.31 shows a right-angled cuboidal resistor of dimensions a, b, and c, made out

from a continuously inhomogeneous resistive material. The conductivity of the material is given by the following function of the x-coordinate: $\sigma(x) = \sigma_0/(1 + 9x/a)$ $(0 \le x \le a)$, where σ_0 is a constant. Calculate the resistance of this resistor.

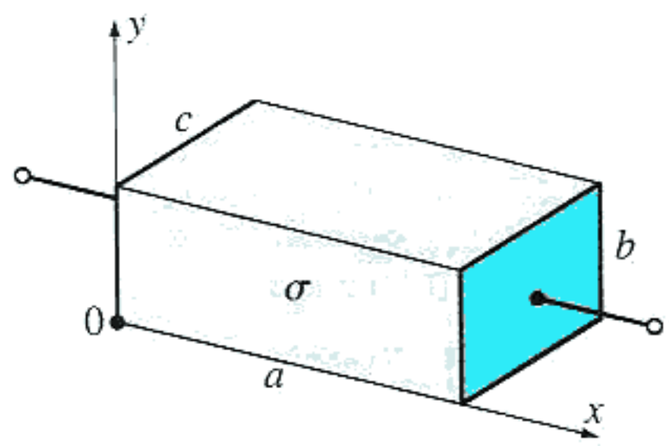

Figure 3.31 Right-angled cuboidal resistor made out from a continuously inhomogeneous resistive material; for Problems 3.7–3.9.

3.8. **Conductivity gradient normal to the resistor current.** Assume that the conductivity of the material in Fig. 3.31 is a function of the y-coordinate, $\sigma(y) = \sigma_0[1 + 9\sin(\pi y/b)]$ $(0 \le y \le b$, $\sigma_0 = \text{const})$, and find the resistance of the resistor.

3.9. **Integrated-circuit resistor with exponential conductivity profile.** An integrated-circuit (IC) resistor is built by diffusing a layer of p-type impurity into an n-type background material. As a consequence of the diffusion process, the concentration of impurity is not uniform across the treated region, so that the obtained IC resistor can essentially be represented by the structure in Fig. 3.31 with the conductivity varying as $\sigma = \sigma(y)$. In specific, $\sigma(y)$ exponentially decreases from $\sigma_1 = 100$ S/m at the air-resistor surface to $\sigma_2 = 0.1$ S/m at the interface with the n-type background, which is considered to be nonconducting, and the length, thickness, and width of the p-type region are $a = 4\ \mu$m, $b = 1\ \mu$m, and $c = 2\ \mu$m, respectively. Determine the resistance of the IC resistor.

3.10. **Spherical capacitor with two lossy dielectric layers.** The dielectric of a spherical capacitor with electrode radii $a = 5$ cm and $c = 15$ cm is composed of two concentric imperfect dielectric layers, where the radius of the boundary surface between the layers is $b = 10$ cm. The relative permittivity and conductivity of the layer near the inner electrode are $\varepsilon_{r1} = 12$ and $\sigma_1 = 4 \times 10^{-4}$ S/m, and those of the other layer $\varepsilon_{r2} = 7$ and $\sigma_2 = 5 \times 10^{-6}$ S/m. The capacitor is connected to a time-invariant voltage $V = 100$ V. (a) Find the current distribution in the dielectric. Using this result and integration (field-theory approach), compute (b) the conductance of the capacitor, (c) the power of Joule's losses in each of the layers, and (d) the free charge on each of the boundaries of radii a, b, and c.

3.11. **Solution using equivalent circuit with ideal elements.** Repeat parts (b)–(d) of the previous problem but using the equivalent circuit with two ideal capacitors and two ideal resistors in Fig. 3.18(b) (circuit-theory approach).

3.12. **Continuously inhomogeneous imperfect dielectric.** Fig. 3.32 shows a parallel-plate capacitor with circular plates of radius a and a continuously inhomogeneous imperfect dielectric. The permittivity and conductivity of the dielectric are the following functions of the z-coordinate: $\varepsilon(z) = 2(1 + 3z/d)\varepsilon_0$ and $\sigma(z) = \sigma_0/(1 + 3z/d)$, $0 \le z \le d$, where σ_0 is a constant and d is the separation between the plates. The capacitor is connected to a time-constant voltage V. Find (a) the current distribution in the dielectric, (b) the conductance of the capacitor, (c) the power of Joule's losses in the capacitor, (d) the free charge distribution in the capacitor, and (e) the bound charge distribution in the capacitor.

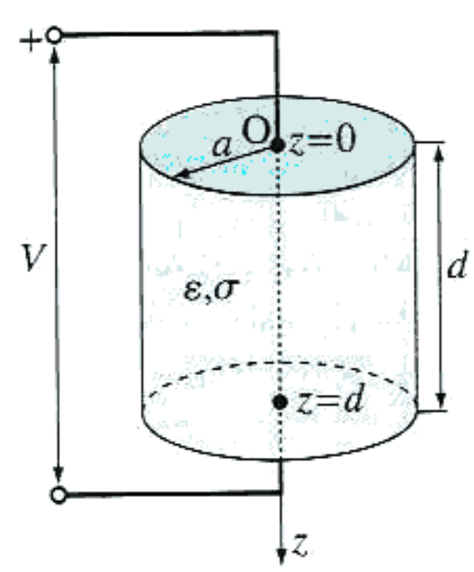

Figure 3.32 Parallel-plate capacitor with a continuously inhomogeneous lossy dielectric; for Problem 3.12.

3.13. **Parallel-plate capacitor with two lossy dielectrics.** Consider a parallel-plate capacitor with a piece-wise homogeneous dielectric shown in Fig. 3.33. The permittivities of the dielectric parts are ε_1 and ε_2. Both parts

are lossy, with conductivities σ_1 and σ_2. The separation between the plates is d and the cross-sectional areas of the dielectric parts are S_1 and S_2. The voltage between the electrodes is V. By employing a field-theory approach (based on determining the current and field distribution in the dielectric), calculate (a) the current through the capacitor terminals, (b) the conductance of the capacitor, (c) the power of Joule's losses in each of the dielectric parts, and (d) the free charge distribution in the capacitor.

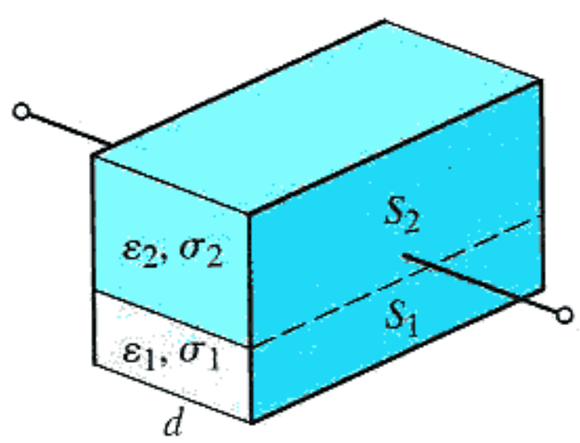

Figure 3.33 Parallel-plate capacitor with two imperfect dielectric parts; for Problem 3.13.

3.14. Equivalent circuit with ideal capacitors and resistors. Repeat the previous problem but employing a circuit-theory approach, i.e., generating and solving an equivalent circuit with ideal capacitors and resistors.

3.15. Current distribution through circular plates. Find the distribution of current through the upper and lower plate of the parallel-plate capacitor with imperfect dielectric from Problem 3.12. Assume that the plates are thin enough so that the current through them can be described using the surface current density vector.

3.16. Current distribution through a thin spherical electrode. Consider the spherical capacitor with imperfect dielectric from Example 3.3, and assume that the inner electrode is hollow, with a very thin wall. With this assumption, determine the distribution of current through the inner electrode. Represent this current using the surface current density vector.

3.17. Coaxial cable with two lossy dielectric layers. Fig. 3.34 shows a longitudinal cross section of a coaxial cable with two coaxial layers of imperfect dielectric. The conductors are perfectly conducting, and their radii are $a = 3$ mm, $c = 10$ mm, and $d = 12$ mm. The radius of the boundary surface between the dielectric layers is $b = 7$ mm and the length of the cable is $l = 100$ m. The relative permittivities of the layers are $\varepsilon_{r1} = 4$ and $\varepsilon_{r2} = 8$, and the conductivities are $\sigma_1 = 10^{-12}$ S/m and $\sigma_2 = 5 \times 10^{-12}$ S/m. The cable is connected at one end to an ideal voltage generator of time-invariant emf $\mathcal{E} = 30$ V, and the other end of the cable is terminated in a load of resistance $R_L = 1$ kΩ. Compute (a) the current density in the dielectric, (b) the conductance per unit length of the cable, (c) the current intensity along the conductors, (d) the current density in each of the conductors, (e) the power of Joule's losses in the cable and in the load, (f) the power of the generator, and (g) the free surface charge density on the boundary between the dielectric layers.

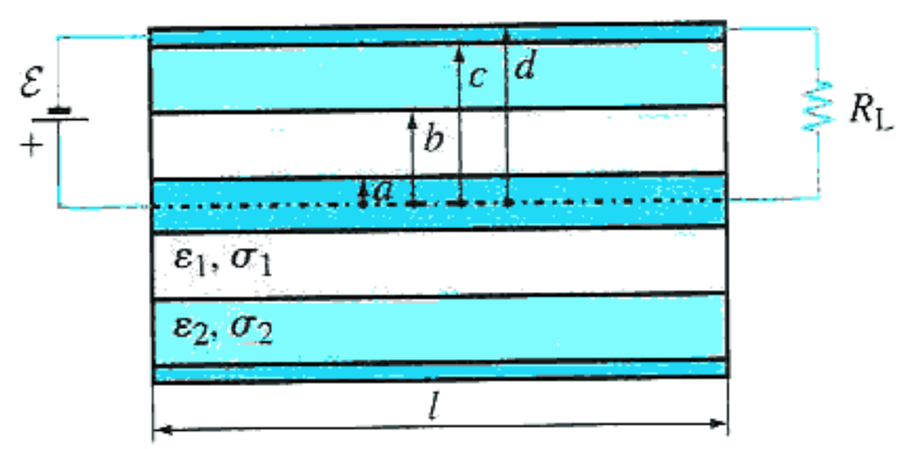

Figure 3.34 Coaxial cable with two coaxial imperfect dielectric layers in a dc regime; for Problem 3.17.

3.18. Coaxial cable with an inhomogeneous imperfect dielectric. A coaxial cable with perfect conductors is filled with an inhomogeneous imperfect dielectric of parameters $\varepsilon = \varepsilon_0(1 + r^2/a^2)$ and $\sigma_d = \sigma_0/(1 + r^2/a^2)$ $(a < r < b)$, where a and b are the radius of the inner cable conductor and the inner radius of the outer conductor, and σ_0 is a constant. The voltage between the cable conductors is V (dc). Calculate (a) the conductance per unit length of the cable and (b) the density of volume free charges in the dielectric.

3.19. Coaxial cable partly filled with a lossy dielectric. A coaxial cable with perfect conductors is partly filled with an imperfect dielectric of conductivity σ, as shown in Fig. 3.35. The conductor radii are a and b, the cable length is l, and the length of the air-filled part of the cable is c. The cable is fed by an ideal dc voltage generator of emf $\mathcal{E}$, and the other end of the cable is open. Find the expression for the current intensity through the cable conductors.

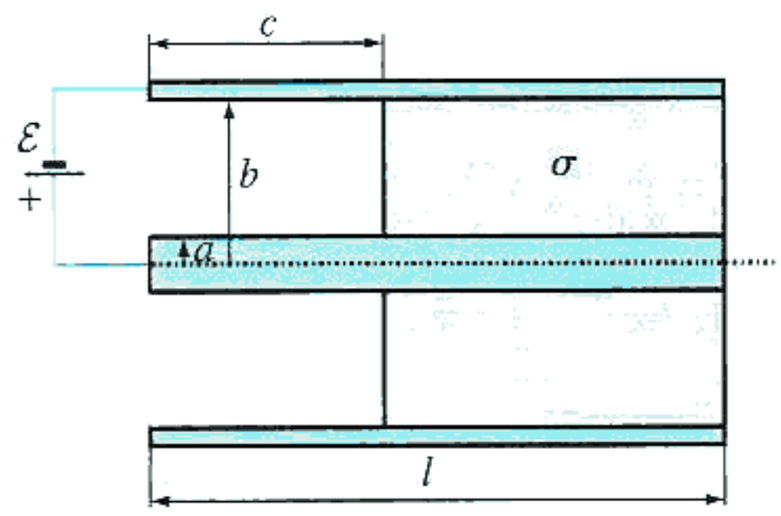

Figure 3.35 Coaxial cable partly filled with a conducting dielectric in a dc regime; for Problem 3.19.

3.20. Coaxial cable with a poorly conducting spacer. Shown in Fig. 3.36 is a cross section of an air-filled coaxial cable with a spacer between the conductors. The spacer is made out of an imperfect dielectric of conductivity σ and its cross section is defined by an angle α. The conductor radii are a and b. What is the conductance per unit length of this cable?

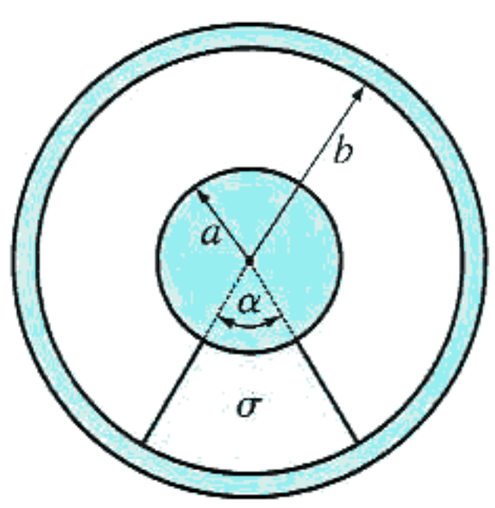

Figure 3.36 Cross section of a coaxial cable with a poorly conducting spacer between conductors; for Problem 3.20.

3.21. Planar line with imperfect conductors. If the strips of the planar transmission line in Fig. 3.24 are not perfectly conducting, but have a finite conductivity σ_c, find the dc resistance per unit length of the line. Assume that the thickness of each of the strips is t.

3.22. Planar line with an inhomogeneous lossy dielectric. Consider a planar (two-strip) transmission line shown in Fig. 3.37. The strips are perfectly conducting, very thin, w wide, l long, and d apart from each other. The dielectric between the strips is imperfect and continuously inhomogeneous, with parameters $\varepsilon(x) = (4 + 3x/d)\varepsilon_0$ and $\sigma(x) = \sigma_0/(1 + 9x/d)$, $0 \le x \le d$, where σ_0 is a constant. The line is connected to an ideal dc voltage generator of emf $\mathcal{E}$, and is open-circuited at the other end. Calculate the distributions of (a) volume current in the dielectric, (b) surface current over the strips, and (c) volume free charge in the dielectric.

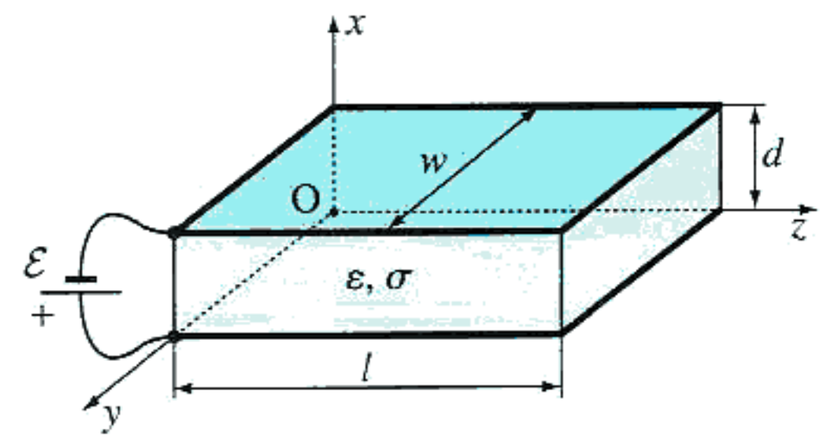

Figure 3.37 Planar line with a continuously inhomogeneous imperfect dielectric in a dc regime; for Problem 3.22.

3.23. Grounding electrode in an inhomogeneous earth. Conductivity of the earth around a hemispherical grounding electrode shown in Fig. 3.38 can be described as the following function of the radial coordinate r: $\sigma(r) = \sigma_0\sqrt{a/r}$ $(a < r < \infty)$, where a is the radius of the electrode and σ_0 is a constant. The current intensity of the electrode is I. Find (a) the grounding resistance of the electrode, (b) the total power of Joule's losses in the earth, and (c) the power of Joule's losses in a layer with thickness a around the electrode $(a < r < 2a)$.

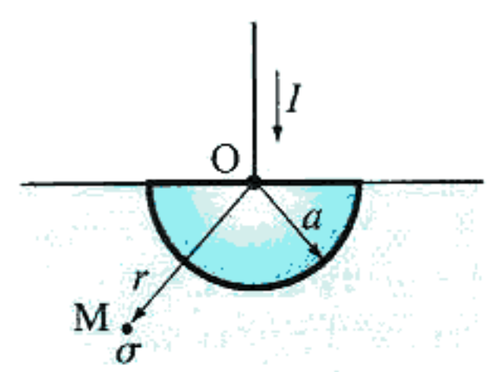

Figure 3.38 Hemispherical grounding electrode in a continuously inhomogeneous earth; for Problem 3.23.

3.24. Grounding electrode in a two-sector earth. The earth around a hemispherical grounding electrode of radius $a = 1$ m can be represented as two sectors with conductivities $\sigma_1 = 2 \times 10^{-3}$ S/m and $\sigma_2 = 8 \times 10^{-3}$ S/m, as shown in Fig. 3.39. The current intensity of the electrode amounts to $I = 50$ A. Compute (a) the grounding resistance of the electrode and (b) the power of Joule's losses in each of the two earth sectors.

3.25. Two short-circuited grounding electrodes. Two identical hemispherical grounding electrodes of radii a are galvanically connected to each other by a wire of negligible resistance, as

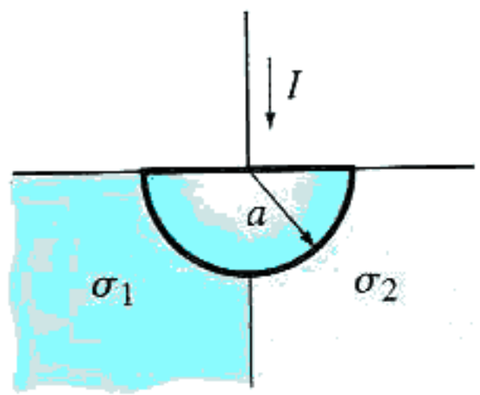

Figure 3.39 Hemispherical grounding electrode in a two-sector earth; for Problem 3.24.

shown in Fig. 3.40. The conductivity of the earth is σ and the distance between the electrode centers is d ($d \gg a$). Determine the grounding resistance of such a system of electrodes.

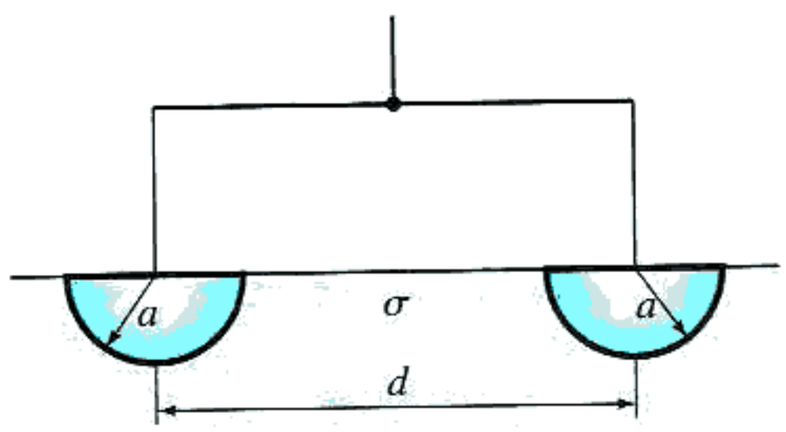

Figure 3.40 Two short-circuited hemispherical grounding electrodes; for Problem 3.25.

3.26. Two grounding electrodes in a layered earth. The electric circuit shown in Fig. 3.41 consists of an ideal current generator of current intensity $I = 100$ A, a wire of negligible resistance, and two identical hemispherical grounding electrodes of radii $a = 2$ m. The conductivity of the earth near the electrodes, within the radius $b = 4$ m, is $\sigma_1 = 10^{-2}$ S/m. The conductivity elsewhere is $\sigma_2 = 10^{-3}$ S/m. The distance between the electrode centers is $d = 80$ m. What is the voltage between the electrodes?

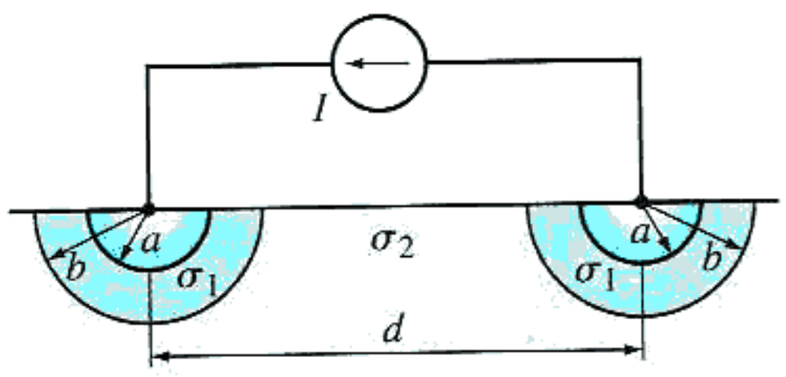

Figure 3.41 Two hemispherical grounding electrodes in a layered earth; for Problem 3.26.

3.27. Two deep spherical grounding electrodes. Consider two identical spherical grounding metallic electrodes of radii a in a homogeneous earth of conductivity σ. Both the distance between the sphere centers and their depth with respect to the ground surface equal d, where $d \gg a$. What is the resistance between the two electrodes?

3.28. Cylindrical grounding electrode deep in the earth. A cylindrical grounding electrode of radius $a = 20$ cm and length $l = 5$ m is buried in a homogeneous earth of conductivity $\sigma = 10^{-2}$ S/m such that its axis is at a depth $d = 4$ m below the ground surface, as depicted in Fig. 3.42. If a steady current of intensity $I = 200$ A flows through the electrode, find the maximum voltage of a step on the earth's surface. Adopt $b = 0.75$ m as an average person's step. Neglect end effects due to the finite length of the cylinder.

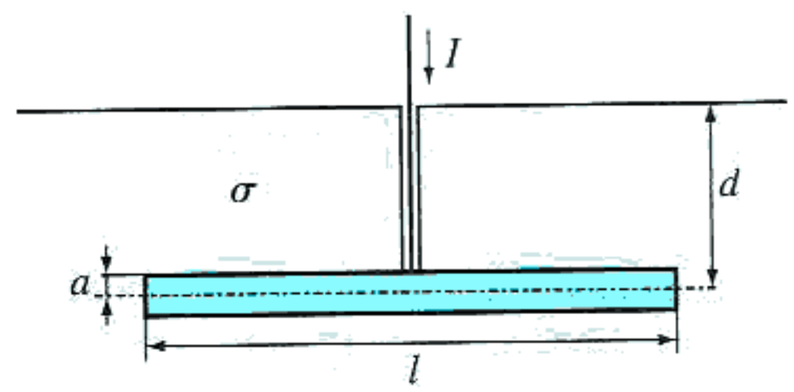

Figure 3.42 Cylindrical grounding electrode buried deep in the earth; for Problem 3.28.

3.29. Two deep parallel cylindrical electrodes. Two identical cylindrical grounding electrodes as the one in Fig. 3.42 are placed parallel to each other (at the same depth with respect to the earth's surface) so that the distance between their axes is $D = 6$ m. If they are connected together in a circuit with an ideal current generator as in Fig. 3.41 (with $I = 200$ A), compute (for the numerical data given in the previous problem) the voltage between the electrodes.

4 Magnetostatic Field in Free Space

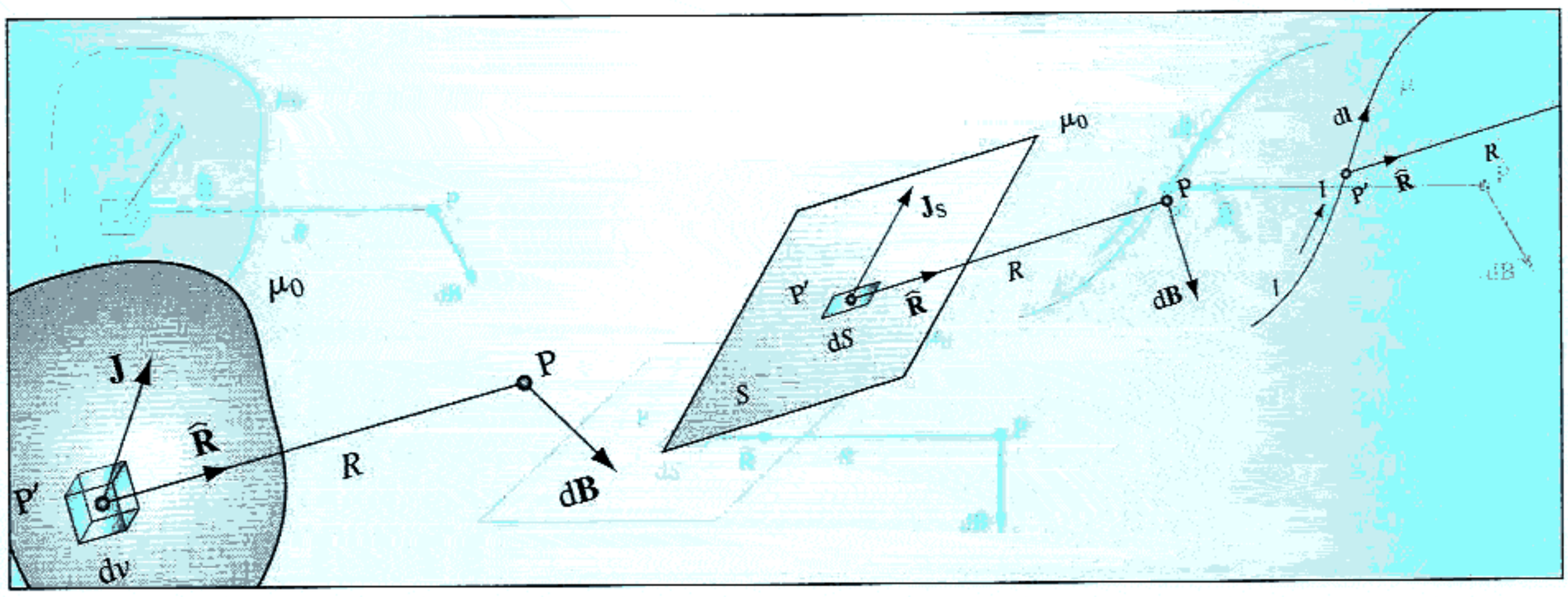

Introduction:

In our studies of steady electric currents in the preceding chapter, we introduced and discussed physical laws and mathematical techniques for determining the distribution of currents for given geometry, material properties, and excitation of various structures. We now introduce a series of new phenomena associated with steady electric currents, which are essentially the consequence of a new simple experimental fact – that conductors with currents exert forces on one another. These forces are called magnetic forces, and the field due to one current conductor in which the other conductor is situated and which causes the force on it is called the magnetic field. Any motion of electric charges and any electric current are followed by the magnetic field. The magnetic field due to steady electric currents is termed the steady (static) magnetic field or magnetostatic field. The theory of the magnetostatic field, the magnetostatics, restricted to a vacuum and nonmagnetic media is the subject of this chapter. The magnetic materials will be discussed in the following chapter.

Starting from the experimental law of the magnetic force between two point charges that move in free space (a vacuum or air) – Coulomb's law for the magnetic field, we shall derive the Biot-Savart law, which, in turn, will serve as a starting point for the derivation of Ampère's law. Both laws represent a means for evaluating the magnetic field due to given steady-current distributions, and we shall apply them to many theoretically and practically important configurations that do not include magnetic materials. The differential form of Ampère's law will introduce a new differential operator, the curl. We shall derive the law of conservation of magnetic flux (Gauss' law for the magnetic field), and complete the full set of Maxwell's equations for the magnetostatic field in nonmagnetic media. The magnetic vector potential will be introduced as a counterpart of the electric scalar potential and the magnetic dipole as the equivalent of the electric dipole. Examples involving evaluation of magnetic forces and torques will also be presented.

4.1 MAGNETIC FORCE AND MAGNETIC FLUX DENSITY VECTOR

The magnetic field is a special physical state existing in a space around moving electric charges and, thus, electric currents in conductors. Its fundamental property is that there is a force acting on any electric charge placed in the space, provided that the charge is moving. That wires carrying electric currents produce magnetic fields was first discovered by Oersted in 1820. To quantitatively describe this field, we introduce a vector quantity called the magnetic flux density vector, **B**. It is defined through the force on a small probe point charge Q_p moving at a velocity **v** in the field, which equals the cross product[1] of vectors $Q_p\mathbf{v}$ and **B**,

definition of **B** *(unit:* T*)*

$$\boxed{\mathbf{F}_m = Q_p\mathbf{v} \times \mathbf{B} \quad (Q_p \to 0).} \tag{4.1}$$

This force is called the magnetic force. The unit for **B** is tesla (abbreviated T). We note that the magnetic flux density vector, which is also referred to as the magnetic induction vector, is defined analogously to the electric field intensity vector, **E**, in electrostatics [Eq. (1.23)].

The basis for determining the magnetic flux density vector due to steady currents is an experimental law describing the magnetic force between two point charges that move in a vacuum. This law represents the equivalent of Coulomb's law, Eq. (1.1), of electrostatics, and is an underpinning for the entire magnetostatic theory. With reference to Fig. 4.1, it states that the magnetic force on a point charge Q_2 that moves at a velocity $\mathbf{v}_2$ in the magnetic field due to a point charge Q_1 moving with a velocity $\mathbf{v}_1$ in a vacuum (or air) is given by

magnetic force

$$\boxed{\mathbf{F}_{m12} = \frac{\mu_0}{4\pi}\frac{Q_2\mathbf{v}_2 \times \left(Q_1\mathbf{v}_1 \times \hat{\mathbf{R}}_{12}\right)}{R^2},} \tag{4.2}$$

where the notation of vectors is the same as for Coulomb's law in Fig. 1.1, and μ_0 is the permeability of a vacuum (free space),

permeability of a vacuum

$$\boxed{\mu_0 = 4\pi \times 10^{-7}\ \text{H/m}} \tag{4.3}$$

(H is henry, the unit for inductance, which will be studied in a later chapter). Eq. (4.2), as mentioned, is the result of experiments, but it can also be derived from Coulomb's law using the special theory of relativity. Note that it is sometimes referred to as Ampère's law of force.

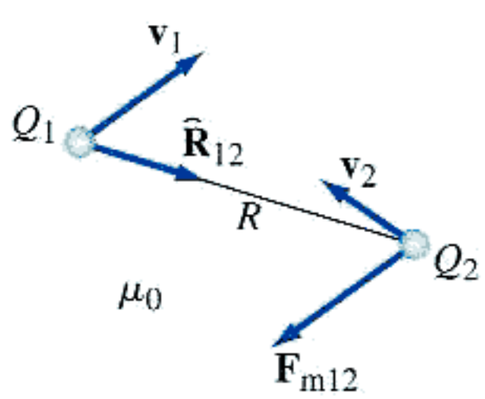

Figure 4.1 Magnetic force between two moving point charges in a vacuum, given by Eq. (4.2).

Although of the similar form, the magnetic force law in Eq. (4.2) is mathematically more complicated than Coulomb's law, because two vector cross products are implied in the equation. We first need to determine the vector resulting from the cross product $Q_1\mathbf{v}_1 \times \hat{\mathbf{R}}_{12}$, and then the cross product of $Q_2\mathbf{v}_2$ and that vector [and, of course, multiply the result by $\mu_0/(4\pi R^2)$]. Let us apply this rule to the situation shown in Fig. 4.2, where vectors $Q_1\mathbf{v}_1$ and $Q_2\mathbf{v}_2$ are parallel to each other and normal to the line joining them. We see that the force between the charges is attractive

[1] The cross product (also referred to as the vector product) of vectors **a** and **b**, $\mathbf{a} \times \mathbf{b}$, is a vector whose magnitude is given by $|\mathbf{a} \times \mathbf{b}| = |\mathbf{a}||\mathbf{b}| \sin\alpha$, where α is the angle between the two vectors in the product. It is perpendicular to the plane defined by the vectors **a** and **b**, and its direction (orientation) is determined by the right-hand rule when the first vector (**a**) is rotated by the shortest route toward the second vector (**b**). In this rule, the direction of rotation is defined by the fingers of the right hand when the thumb points in the direction of the cross product.

HISTORICAL ASIDE

Hans Christian Oersted (1777–1851), a Danish physicist, was a professor of physics and chemistry at the University of Copenhagen. As part of a classroom demonstration, he discovered, apparently by accident, that an electric current flowing through a wire produces a magnetic field around the wire. Namely, while preparing an evening lecture on electricity and magnetism in April of 1820, in which he wanted to demonstrate the heating effects of the electric current in a wire connected between the terminals of a voltaic source (battery), Oersted noticed that the magnetic needle of a compass sitting next to the wire spun off of the north position every time the battery was in use. It was generally believed at that time that electricity and magnetism were not related. Therefore, he was extremely surprised and excited with what he saw. He continued experimenting during that lecture, which eventually led him to the conclusion that an electric current creates a magnetic field – and electromagnetism was born. He also discovered that, not only is a magnetic needle deflected by an electric current, but that a wire with a current is also deflected in a magnetic field (by the magnetic force), thus laying the foundation for the construction of the electric motor. His epoch-making discovery of the magnetic effects of electric currents was announced to the French Academy of Sciences on September 4, 1820. It immediately set off an explosion of research activity by many brilliant minds, including Ampère (1775–1836), Biot (1774–1862), and Savart (1791–1841). Oersted's experiment was the first demonstration of a connection between electricity and magnetism, and is considered the foundation of the modern study of electromagnetism. In 1829, Oersted became the first director of the Polytechnic Institute in Copenhagen, now the Technical University of Denmark. *(Portrait: AIP Emilio Segrè Visual Archives, Brittle Books Collection)*

if the vectors are in the same direction [Fig. 4.2(a)], and repulsive if they are in opposite directions [Fig. 4.2(b)]. This is formally just opposite to Coulomb's law, where like charges repel and unlike attract each other.

Combining Eqs. (4.1) and (4.2), and assuming that the second charge in Fig. 4.1 is a probe charge ($Q_2 = Q_p$), we can identify the expression for the magnetic flux density vector of a point charge Q moving with a velocity $\mathbf{v}$:

$$\boxed{\mathbf{B} = \frac{\mu_0}{4\pi}\frac{Q\mathbf{v} \times \hat{\mathbf{R}}}{R^2},} \tag{4.4}$$

B *due to a moving point charge in free space*

where R is the distance from the charge and $\hat{\mathbf{R}}$ is the unit vector along R directed from the source point toward the field point, as shown in Fig. 4.3. Vector $\mathbf{B}$ is perpendicular to R and perpendicular to the plane of the vectors $Q\mathbf{v}$ and $\hat{\mathbf{R}}$. Its

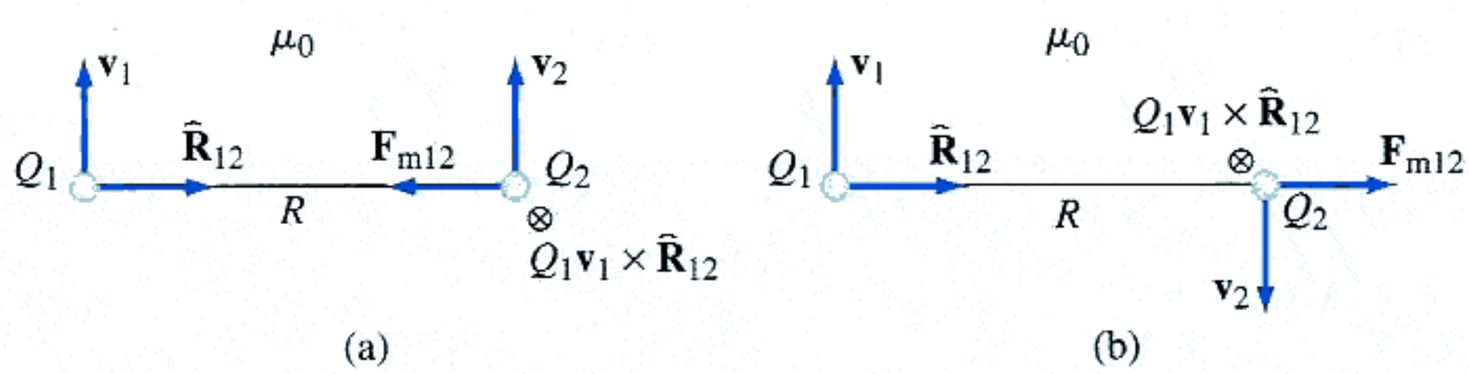

Figure 4.2 Two charges moving parallel to each other in the same direction (a) and in opposite directions (b) in a vacuum.

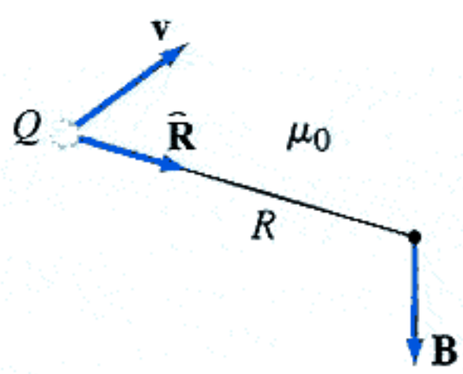

Figure 4.3 Magnetic flux density vector due to a point charge moving in a vacuum.

orientation comes from the definition of the cross product of vectors, i.e., it is determined by the right-hand rule in rotating $Q\mathbf{v}$ by the shortest route to $\hat{\mathbf{R}}$.

Note that the magnetic flux density is proportional to the product $Q\mathbf{v}$, which can be regarded as a measure of sources of the magnetostatic field (the measure of sources of the electrostatic field is a charge Q). Comparing Eq. (4.4) to the expression for the electric field intensity vector due to a point charge, Eq. (1.24), we observe the same dependence on the amount of sources ($Q|\mathbf{v}|$ and Q) and on distance R. The constant μ_0 corresponds to the constant $1/\varepsilon_0$. The only formal difference is the direction of the field vector with respect to the source. The electric field intensity vector, $\mathbf{E}$, due to Q is radial with respect to Q (Fig. 1.7), whereas the magnetic flux density vector, $\mathbf{B}$, due to $Q\mathbf{v}$ is circular with respect to $Q\mathbf{v}$ (Fig. 4.3). In other words, the lines of $\mathbf{E}$ are radials starting at Q, while the lines of $\mathbf{B}$ are circles centered on the line containing the vector $Q\mathbf{v}$.

Conceptual Questions (on Companion Website): 4.1 and 4.2.

HISTORICAL ASIDE

Nikola Tesla (1856–1943), an American inventor, was a brilliant electrical engineer with no complete formal education. He made alternating current (ac) practical and had about 250 patents issued in the U.S. and other countries. Tesla was born in Smiljan near Gospić, Lika, in Croatia (then in the Habsburg Empire of Austria), in a Serbian family. He studied mechanical engineering at the Polytechnic School in Graz from 1875 to 1878 and then natural philosophy at the University of Prague until 1880, but never graduated due to a shortage of funds after his father's death. While working as electrical engineer for companies in Budapest and Paris, he came up with an idea of the principle of the rotating magnetic field and polyphase alternating currents producing it in 1882 and constructed the world's first induction (ac) motor in 1883, both during after-work hours. He emigrated to America in 1884, with four cents in his pocket, and worked for a year for Thomas Edison (1847–1931). He failed to get Edison interested in the induction motor and alternating current, and later established his own "Tesla Electric Company" in New York City. Tesla obtained most of his best known U.S. patents in the area of polyphase alternating currents and polyphase systems, including ac generators, motors, and transformers, as well as principles of power distribution using alternating currents, in 1887 and 1888, and delivered his famous lecture "A New System of Alternate Current Motors and Transformers" before the American Institute of Electrical Engineers (now IEEE) on May 16, 1888. In June of 1888, George Westinghouse (1846–1914), head of the "Westinghouse Electric Company" in Pittsburgh, bought the first seven of Tesla's patents for polyphase systems. This marked the beginning of the five-year "war of currents" to decide whether Edison's existing dc systems or newly proposed Tesla-Westinghouse ac systems would be the chosen technology for the global electric power distribution of the future in America. Tesla invented an air-core resonant transformer known as a Tesla coil (or Tesla transformer) in 1891, which was capable of generating alternating currents of extremely high frequencies for that time (up to a hundred of thousands of cycles per second or 100 kHz in today's notation). The coil could also build up tremendously high voltages and cause spectacular spark discharges. Tesla's new electric lamps based on a high-frequency power supply were the forerunners of our fluorescent tubes and neon signs. In a series of spectacular lectures-demonstrations in America

and Europe from 1891 to 1893 aimed at promoting alternating current and high-frequency technology, he was able to power electric lamps without wires, either through air or by allowing high-frequency electricity to flow through his body, produce artificial lightning flashes of different shapes, and even shoot large lightning bolts from his coils to the audience without harm. In early 1893, he proposed a complete radio system with a transmitter and receiver in the form of Tesla coils tuned to resonate at the same frequency as a basis for wireless communications. The "war of currents" ended on the evening of May 1, 1893, with the opening of the Chicago World Exposition, spectacularly illuminated by a hundred thousand lamps with alternating current from Tesla's generators. Only couple of months later, Westinghouse was awarded the contract to build the world's first ac hydroelectric power plant on Niagara Falls, based on Tesla's design, which was put into operation on November 16, 1896. Tesla filed his basic radio patent applications in 1897, and this is, in fact, the invention of radio, although it was Guglielmo Marconi (1874–1937) who put it into practical and commercial use, and was awarded Nobel Prize in Physics in 1909 for the development of wireless telegraphy. In 1898, Tesla demonstrated the world's first wireless remote control (of a boat model) at Madison Square Garden. He continued his investigations of the wireless transmission of power in 1899 and 1900 in Colorado Springs, where he built a huge, 200-kW radio transmitter consisting of a 142-foot metal mast with a spherical top and the world's largest Tesla coil 51 feet in diameter. Tesla also patented a bladeless disk turbine, so-called Tesla turbine, in 1913, as well as many other devices and systems in various areas of science and engineering. The SI unit for the magnetic flux density, the tesla, was named in his honor in 1960. *(Portrait: © Nikola Tesla Museum, Belgrade, Serbia)*

4.2 BIOT-SAVART LAW

If we have many point charges moving in free space, the total magnetic flux density vector is, by the principle of superposition, a vector sum of the magnetic flux density vectors due to individual charges. In a current, a vast number of elementary free charges moves through a conductor in an organized manner with the macroscopic average velocity $\mathbf{v}_\mathrm{d}$ (drift velocity). The sum of products $Q\mathbf{v}$ for all charges in an elementary volume $\mathrm{d}v$ is given by

$$\left(\sum Q\mathbf{v}\right)_{\text{in } \mathrm{d}v} = N_{\text{in } \mathrm{d}v}\, Q\mathbf{v}_\mathrm{d} = N_\mathrm{v}\, \mathrm{d}v\, Q\mathbf{v}_\mathrm{d} = \mathbf{J}\, \mathrm{d}v, \tag{4.5}$$

where $\mathbf{J}$ is the current density vector, defined by Eq. (3.3). We assume that the permeability everywhere[2] is μ_0. Hence, the magnetic flux density vector due to the charges in $\mathrm{d}v$ is computed as

$$\boxed{\mathrm{d}\mathbf{B} = \frac{\mu_0}{4\pi} \frac{(\mathbf{J}\, \mathrm{d}v) \times \hat{\mathbf{R}}}{R^2},} \tag{4.6}$$ *Biot-Savart law*

which is known as the Biot-Savart law. We see that the product $\mathbf{J}\, \mathrm{d}v$ represents a macroscopic volume elemental source of the magnetic field, and we call it accordingly the volume current element. By integrating Eq. (4.6), we obtain the expression

[2]We shall see in the next chapter that most materials we encounter in science and engineering are nonmagnetic materials, that is, their permeability is practically that of a vacuum. Examples are commonly used metallic conductors such as copper, aluminum, silver, gold, etc., most frequently encountered natural environments (air, water, and ground), biological tissues, and practically all insulators and semiconductors. Some materials, such as iron, steel, cobalt, nickel, ferrites, etc., on the other hand, have permeability much greater than μ_0.

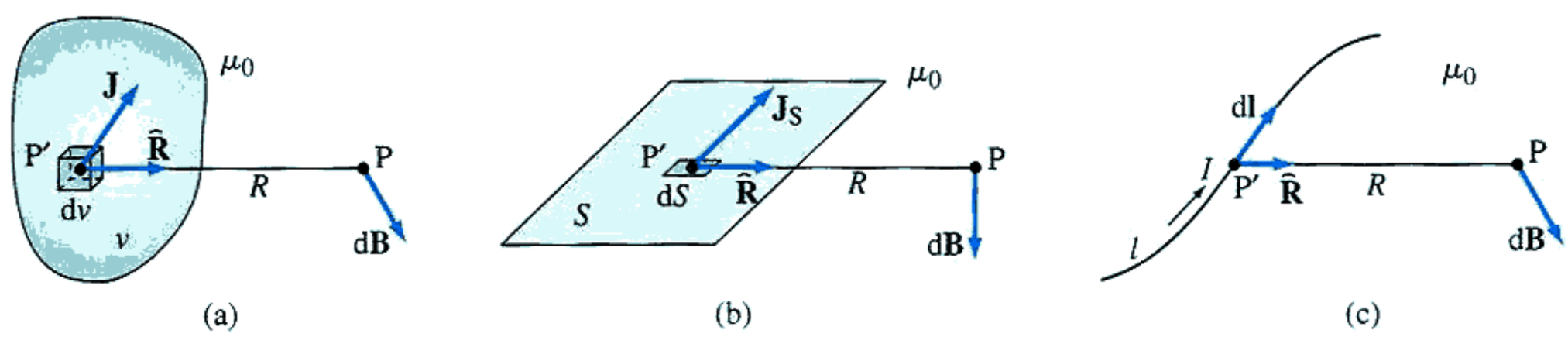

Figure 4.4 Magnetic flux density vector due to three characteristic current distributions – volume current (a), surface current (b), and line current (c).

for the resultant magnetic flux density vector due to a current distribution in an entire volume v [Fig. 4.4(a)]:

Biot-Savart law for volume current

$$\boxed{\mathbf{B} = \frac{\mu_0}{4\pi}\int_v \frac{(\mathbf{J}\,\mathrm{d}v)\times\hat{\mathbf{R}}}{R^2}.} \tag{4.7}$$

HISTORICAL ASIDE

Jean Baptiste Biot (1774–1862), a French physicist, was a student of Lagrange (1736–1813) at the École Polytechnique and a junior professor of mechanics under sponsorship of Laplace (1749–1827) at the Collège de France. Biot's most important contributions to science are in the theory of polarized light and effects on it by organic substances. **Fèlix Savart** (1791–1841), another French physicist, was also a professor at the Collège de France, where he taught experimental physics and acoustics, and a member of the Paris Academy. His most important scientific work was in vibration and acoustics, and particularly in the physics of the violin. Biot and Savart showed experimentally in October of 1820, soon after Oersted's discovery of magnetic effects of electric currents, that the magnetic field produced by a current in a long, straight wire is inversely proportional to the distance from the wire.

In the case of a surface current flowing over a surface S [see Eqs. (3.12) and (3.13)], we have $N_s\,\mathrm{d}S$ instead of $N_v\,\mathrm{d}v$ in Eq. (4.5), yielding $\mathbf{J}_s\,\mathrm{d}S$ as a surface current element, where $\mathbf{J}_s$ is the surface current density vector. The magnetic flux density vector due to a surface current distribution is thus [Fig. 4.4(b)]

Biot-Savart law for surface current

$$\boxed{\mathbf{B} = \frac{\mu_0}{4\pi}\int_S \frac{(\mathbf{J}_s\,\mathrm{d}S)\times\hat{\mathbf{R}}}{R^2}.} \tag{4.8}$$

Finally, for a line current along a line l, e.g., a current of intensity I flowing through a (generally curvilinear) thin wire of length l and cross-sectional area S, $\mathrm{d}v = S\,\mathrm{d}l$, $J = I/S$ [Eq. (3.5)], and $J\,\mathrm{d}v = JS\,\mathrm{d}l = I\,\mathrm{d}l$, where $\mathrm{d}l$ is an elemental segment along l. We conclude that the line current element equals $I\,\mathrm{d}\mathbf{l}$, where $\mathrm{d}\mathbf{l}$ is oriented in the reference direction of the current flow. For curved lines, $\mathrm{d}\mathbf{l}$ is tangential to the line. The magnetic flux density vector due to a line current is hence [Fig. 4.4(c)]

Biot-Savart law for line current

$$\boxed{\mathbf{B} = \frac{\mu_0}{4\pi}\int_l \frac{I\,\mathrm{d}\mathbf{l}\times\hat{\mathbf{R}}}{R^2}.} \tag{4.9}$$

In summary, we note that Eqs. (4.7)–(4.9) have the same generic mathematical form: integral of μ_0(current element) $\times\,\hat{\mathbf{R}}/(4\pi R^2)$, with the following three current

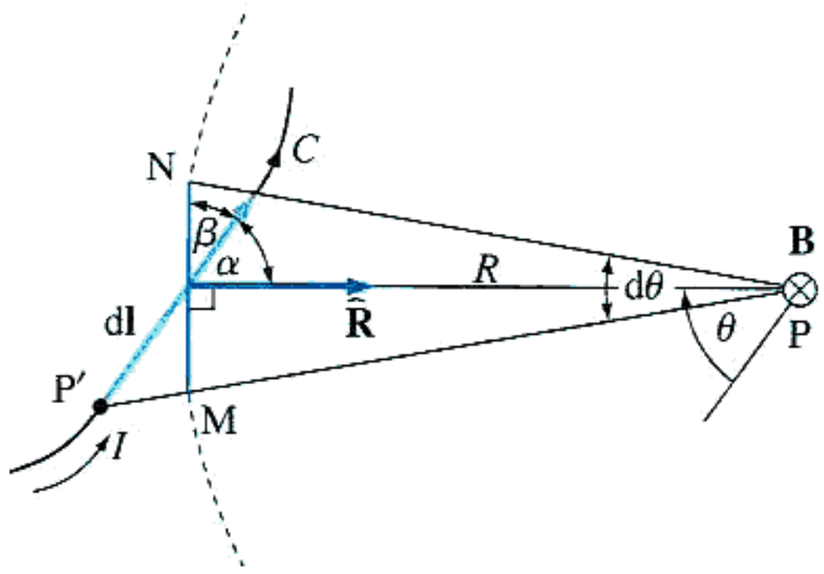

Figure 4.5 Part of a planar current loop C and a field point P in the same plane.

elements as different source functions:

$$\boxed{\mathbf{J}\,\mathrm{d}v \longleftrightarrow \mathbf{J}_s\,\mathrm{d}S \longleftrightarrow I\,\mathrm{d}\mathbf{l},} \tag{4.10}$$

volume, surface, and line current elements (unit: A · m)

and they all represent one physical law – the Biot-Savart law.

In addition, the general form of the Biot-Savart law for line currents, Eq. (4.9), can considerably be simplified in the case of a planar current contour (contour lying in one plane) and a field point P (at which the magnetic flux density vector is calculated) in the same plane, shown in Fig. 4.5. Here, the vector **B** is normal to the plane of the contour (the plane of drawing), and its magnitude is given by

$$B = \frac{\mu_0}{4\pi}\oint_C \frac{I|\mathrm{d}\mathbf{l}\times\hat{\mathbf{R}}|}{R^2}. \tag{4.11}$$

Because (Fig. 4.5)

$$|\mathrm{d}\mathbf{l}\times\hat{\mathbf{R}}| = \mathrm{d}l\sin\alpha = \mathrm{d}l\cos\beta = \overline{\mathrm{MN}} = R\,\mathrm{d}\theta \tag{4.12}$$

($R\,\mathrm{d}\theta$ is the length of an arc representing a differentially small portion of a circle of radius R centered at the point P), we have that

$$\boxed{B = \frac{\mu_0}{4\pi}\oint_C \frac{I\,\mathrm{d}\theta}{R},} \tag{4.13}$$

B for a loop and field point in one plane

where θ is the angle between R and an arbitrarily adopted reference axis in the contour plane. The reference rise of θ corresponds to the reference flow of I, and the reference direction of **B** is related to the direction of I by the right-hand rule (fingers – field; thumb – current).

Note that the integral expression in Eq. (4.13) implies only scalar integration and the function that needs to be integrated is much simpler than that in Eq. (4.9). We shall, therefore, use the simplified form of the Biot-Savart law whenever possible, i.e., when dealing with planar current contours and calculating the magnetic flux density vector in the same plane. Eq. (4.13) can also be used in cases when a planar part of a nonplanar contour and a field point are in one plane.

Conceptual Questions (on Companion Website): 4.3.

4.3 MAGNETIC FLUX DENSITY VECTOR DUE TO GIVEN CURRENT DISTRIBUTIONS

Eqs. (4.7)–(4.9), with Eq. (4.13) added, are general means for evaluating (by superposition and integration) the magnetic flux density vector, **B**, due to

given current distributions in free space (or any nonmagnetic medium), just as Eqs. (1.37)–(1.39) are the means for evaluating the electric field intensity vector, **E**, due to given charge distributions in free space. In this section, we shall consider various characteristic examples of the application of the Biot-Savart law. The examples include current distributions that are theoretically and practically important on one hand and for which the integrals can be evaluated analytically on the other. Most of the magnetostatic structures we shall analyze have their electrostatic counterparts in Section 1.5, so that many solution strategies introduced and developed in that section apply also here.

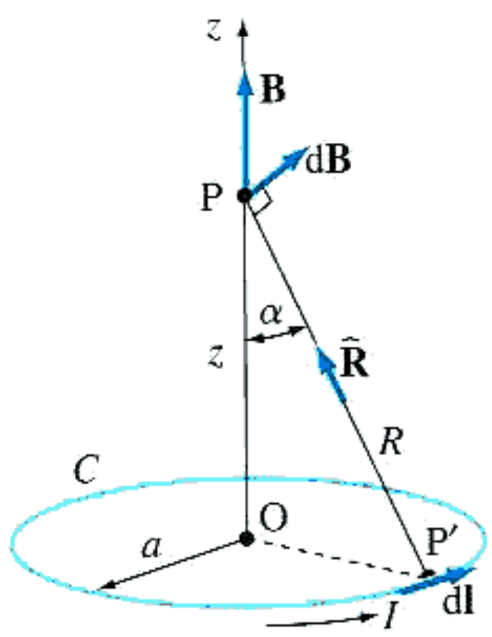

Figure 4.6 Evaluation of the magnetic flux density vector along the axis of a circular current loop normal to its plane; for Example 4.1.

Example 4.1 Magnetic Field of a Circular Current Loop

Consider a circular loop of radius a carrying a steady current of intensity I in air. Calculate the magnetic flux density vector along the axis of the loop normal to its plane.

Solution We subdivide the loop (contour C) into elemental segments and apply Eq. (4.9), analogously to the electric field computation in Example 1.6. With reference to Fig. 4.6, the contribution to the magnetic flux density vector at a point P on the loop axis (z-axis) of a current element $I\,\mathrm{d}\mathbf{l}$ at a point P′ on the contour is

$$\mathrm{d}\mathbf{B} = \frac{\mu_0 I\,\mathrm{d}\mathbf{l} \times \hat{\mathbf{R}}}{4\pi R^2}, \tag{4.14}$$

where $R = \sqrt{z^2 + a^2}$ (z is the coordinate of the point P). As $\mathrm{d}\mathbf{l}$ and $\hat{\mathbf{R}}$ are mutually perpendicular and $|\hat{\mathbf{R}}| = 1$ (unit vector), $|\mathrm{d}\mathbf{l} \times \hat{\mathbf{R}}| = \mathrm{d}l$. Hence, the magnitude of the vector $\mathrm{d}\mathbf{B}$ equals

$$\mathrm{d}B = \frac{\mu_0 I\,\mathrm{d}l}{4\pi R^2}. \tag{4.15}$$

The total magnetic flux density vector at the point P is obtained as

$$\mathbf{B} = \oint_C \mathrm{d}\mathbf{B}. \tag{4.16}$$

Because of symmetry, the radial (horizontal) components of the vector $\mathrm{d}\mathbf{B}$ in Fig. 4.6 cancel out in the integral (much like in Fig. 1.11, in the electrical case), and only the axial (vertical) components

$$\mathrm{d}B_z = \mathrm{d}B\cos(90^\circ - \alpha) = \mathrm{d}B\sin\alpha = \mathrm{d}B\frac{a}{R} = \frac{\mu_0 I a\,\mathrm{d}l}{4\pi R^3} \tag{4.17}$$

contribute to the final result. Consequently,

$$\mathbf{B} = \oint_C \mathrm{d}B_z\,\hat{\mathbf{z}} = \frac{\mu_0 I a}{4\pi R^3}\,\hat{\mathbf{z}} \oint_C \mathrm{d}l, \tag{4.18}$$

which yields [see Eq. (1.43)]

B due to a circular current loop

$$\boxed{\mathbf{B} = \frac{\mu_0 I a^2}{2(z^2 + a^2)^{3/2}}\,\hat{\mathbf{z}}.} \tag{4.19}$$

Example 4.2 Magnetic Field of a Finite Straight Wire Conductor

Consider a straight conductor of length l representing a part of a wire contour with a steady current of intensity I in free space. Find the expression for the **B** field at an arbitrary point in space due to this current conductor.

Solution The conductor and an arbitrary field point (P) always determine one plane, which means that we can use the simplified form of the Biot-Savart law in Eq. (4.13). From Fig. 4.7,

$\cos\theta = d/R$, so that the magnetic flux density is given by

$$B = \frac{\mu_0}{4\pi}\int_l \frac{I\,\mathrm{d}\theta}{R} = \frac{\mu_0 I}{4\pi d}\int_{\theta=\theta_1}^{\theta_2} \cos\theta\,\mathrm{d}\theta. \tag{4.20}$$

The solution to this integral is

$$\boxed{B = \frac{\mu_0 I}{4\pi d}(\sin\theta_2 - \sin\theta_1),} \tag{4.21}$$

B due to a straight wire conductor of finite length

where θ_1 and θ_2 are the angles defining the starting and ending point of the conductor, respectively, and d is the perpendicular distance from the conductor to the point P.

The expression in Eq. (4.21) can be combined for computing the magnetic field due to any structure assembled from straight line segments with steady current. In addition, it can be used for the evaluation of the contribution to the total field of straight segments contained in structures that also include curvilinear segments.

By taking $\theta_1 = -\pi/2$ and $\theta_2 = \pi/2$ in Fig. 4.7 and in Eq. (4.21), we obtain the expression for the magnetic flux density due to an infinitely long straight wire conductor carrying a current I in free space. With a notation $d = r$, r standing for the radial coordinate in the cylindrical coordinate system whose z-axis coincides with the axis of the wire conductor, this expression reads

$$\boxed{B = \frac{\mu_0 I}{2\pi r}.} \tag{4.22}$$

B due to an infinite wire conductor

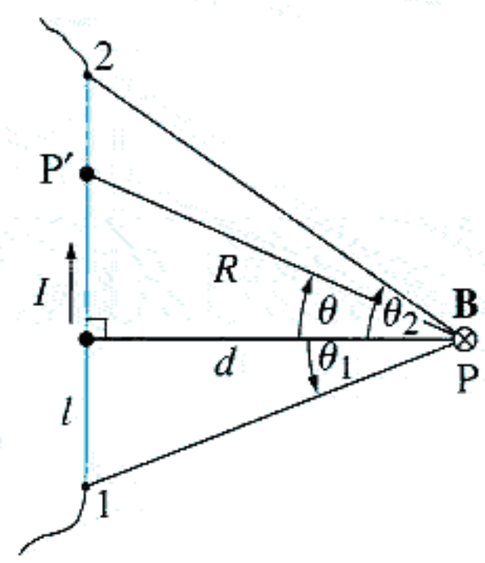

Figure 4.7 Evaluation of the magnetic field of a finite straight wire conductor; for Example 4.2.

Example 4.3 Magnetic Field of a Square Current Loop

A square loop of side length a in free space carries a steady current of intensity I. Obtain the expression for the magnetic flux density vector at the loop center.

Solution The magnetic flux density at the loop center due to the current along one of the square sides, B_1, is given by Eq. (4.21) with $d = a/2$, $\theta_1 = -\pi/4$, and $\theta_2 = \pi/4$, as can be seen in Fig. 4.8. By means of the superposition principle, the magnitude of the total magnetic flux density vector amounts to

$$B = 4B_1 = \frac{2\sqrt{2}\mu_0 I}{\pi a}, \tag{4.23}$$

with respect to the reference direction of **B** indicated in Fig. 4.8.

Example 4.4 Magnetic Field of a Loop with a Semicircular Part

Fig. 4.9(a) shows a wire contour consisting of a semicircle (of radius a) and a straight line (of length $2a$). The contour is situated in air and lies in the xy-plane of the Cartesian coordinate system. If the contour carries a steady current of intensity I, calculate the magnetic flux density vector at an arbitrary point along the z-axis.

Solution Let $\mathrm{d}\mathbf{B}'$ denote the magnetic flux density vector at a point P on the z-axis due to a current element $I\,\mathrm{d}\mathbf{l}$ that belongs to the semicircular part of the contour [Fig. 4.9(a)]. This vector is given by Eq. (4.14), and we need to break it up into components suitable for integration, which are x-, y-, and z-components in this case, and this is very similar to the decomposition of the vector $\mathrm{d}\mathbf{E}$ in Fig. 1.12 and Eqs. (1.46) and (1.47). So, we first decompose $\mathrm{d}\mathbf{B}'$ in the plane of the triangle $\triangle$POP′ [Fig. 4.9(b)]:

$$\mathrm{d}\mathbf{B}' = \mathrm{d}\mathbf{B}'_{\mathrm{h}} + \mathrm{d}B'_z\,\hat{\mathbf{z}}, \quad \mathrm{d}B'_{\mathrm{h}} = \mathrm{d}B'\cos\alpha, \quad \cos\alpha = \frac{z}{R}, \quad \mathrm{d}B'_z = \mathrm{d}B'\sin\alpha, \quad \sin\alpha = \frac{a}{R}, \tag{4.24}$$

where $\mathrm{d}B'$ is given in Eq. (4.15). We then represent the horizontal vector $\mathrm{d}\mathbf{B}'_{\mathrm{h}}$ by its x- and y-components [Fig. 4.9(c)]:

$$\mathrm{d}\mathbf{B}'_{\mathrm{h}} = \mathrm{d}B'_x\,\hat{\mathbf{x}} + \mathrm{d}B'_y\,\hat{\mathbf{y}}, \quad \mathrm{d}B'_x = \mathrm{d}B'_{\mathrm{h}}\cos\phi, \quad \mathrm{d}B'_y = \mathrm{d}B'_{\mathrm{h}}\sin\phi. \tag{4.25}$$

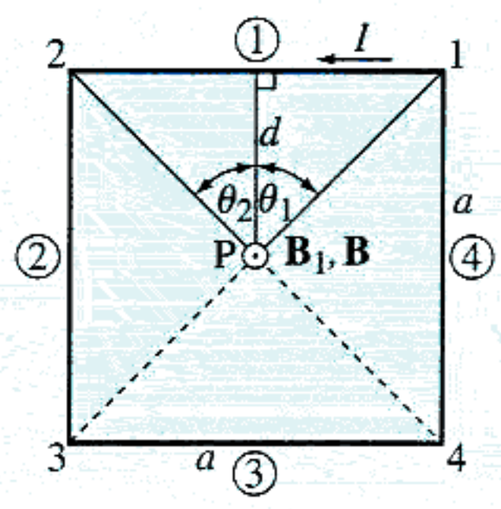

Figure 4.8 Evaluation of the magnetic field at the center of a square current loop; for Example 4.3.

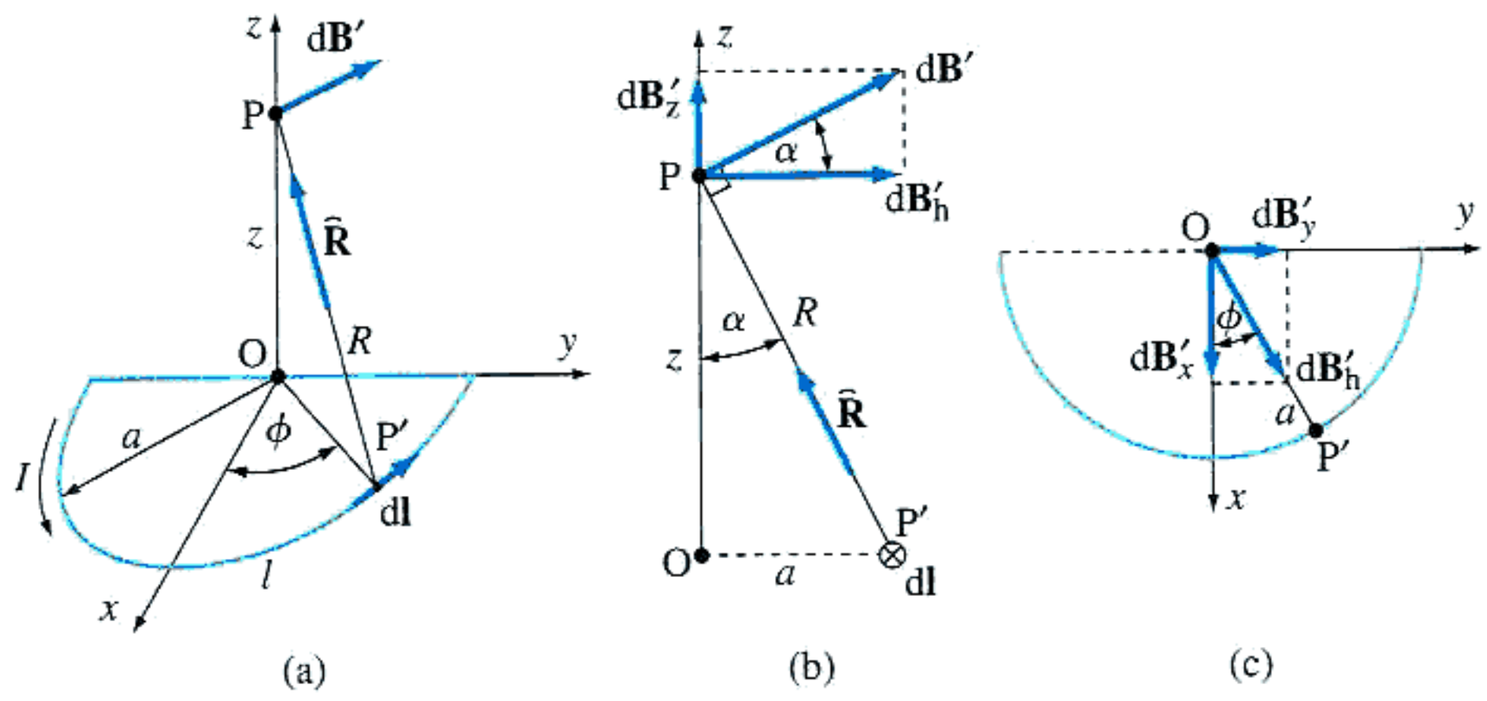

Figure 4.9 Evaluation of the magnetic field due to a current contour with a semicircular and a linear part; for Example 4.4.

Finally, we integrate, as in Eqs. (1.48)–(1.50) in the electrical case, the three Cartesian components of $\mathrm{d}\mathbf{B}'$ along the semicircle, with respect to the azimuthal angle ϕ $(-\pi/2 \le \phi \le \pi/2)$ as the integration variable [note that $\mathrm{d}l = a\,\mathrm{d}\phi$ in Eq. (4.15)]:

$$B'_x = \int_l \mathrm{d}B'_x = \frac{\mu_0 I a z}{4\pi R^3}\int_{-\pi/2}^{\pi/2}\cos\phi\,\mathrm{d}\phi = \frac{\mu_0 I a z}{2\pi R^3}, \quad B'_y = \int_l \mathrm{d}B'_y$$

$$= \frac{\mu_0 I a z}{4\pi R^3}\int_{-\pi/2}^{\pi/2}\sin\phi\,\mathrm{d}\phi = 0, \quad B'_z = \int_l \mathrm{d}B'_z = \frac{\mu_0 I a^2}{4\pi R^3}\int_{-\pi/2}^{\pi/2}\mathrm{d}\phi = \frac{\mu_0 I a^2}{4R^3}. \tag{4.26}$$

Hence, the resultant magnetic flux density vector due to the semicircular part of the contour comes out to be

$$\mathbf{B}' = \frac{\mu_0 I a}{2R^3}\left(\frac{z}{\pi}\,\hat{\mathbf{x}} + \frac{a}{2}\,\hat{\mathbf{z}}\right). \tag{4.27}$$

The magnetic flux density vector at the point P due to the linear part of the contour, on the other hand, is determined from Eq. (4.21) with $d = z$, $\theta_1 = -\alpha$, and $\theta_2 = \alpha$:

$$\mathbf{B}'' = \frac{\mu_0 I}{4\pi z}2\sin\alpha(-\hat{\mathbf{x}}) = -\frac{\mu_0 I a}{2\pi z R}\,\hat{\mathbf{x}}. \tag{4.28}$$

The total $\mathbf{B}$ field along the z-axis is

$$\mathbf{B} = \mathbf{B}' + \mathbf{B}'' = \frac{\mu_0 I a^2}{2R^3}\left(-\frac{a}{\pi z}\,\hat{\mathbf{x}} + \frac{1}{2}\,\hat{\mathbf{z}}\right), \quad R = \sqrt{z^2 + a^2}. \tag{4.29}$$

Example 4.5 Magnetic Field of a Finite Solenoid

Fig. 4.10(a) shows a solenoid (cylindrical coil) consisting of N turns of an insulated thin wire wound uniformly and densely in one layer on a cylindrical nonmagnetic support with a circular cross section of radius a. The length of the solenoid is l and the current through the wire is I. The medium is air. Find the expression for the magnetic flux density vector along the solenoid axis.

Solution Because of the coil being closely wound in a spiral and the wire being thin, the current flowing through the turns of the solenoid can be regarded as a thin cylindrical current sheet with surface current density [Eq. (3.13)]

$$J_s = \frac{NI}{l}. \tag{4.30}$$

The current over an elemental length $\mathrm{d}z$ along the solenoid, shown in Fig. 4.10(b),

$$\mathrm{d}I = J_s\,\mathrm{d}z = \frac{NI\,\mathrm{d}z}{l}, \tag{4.31}$$

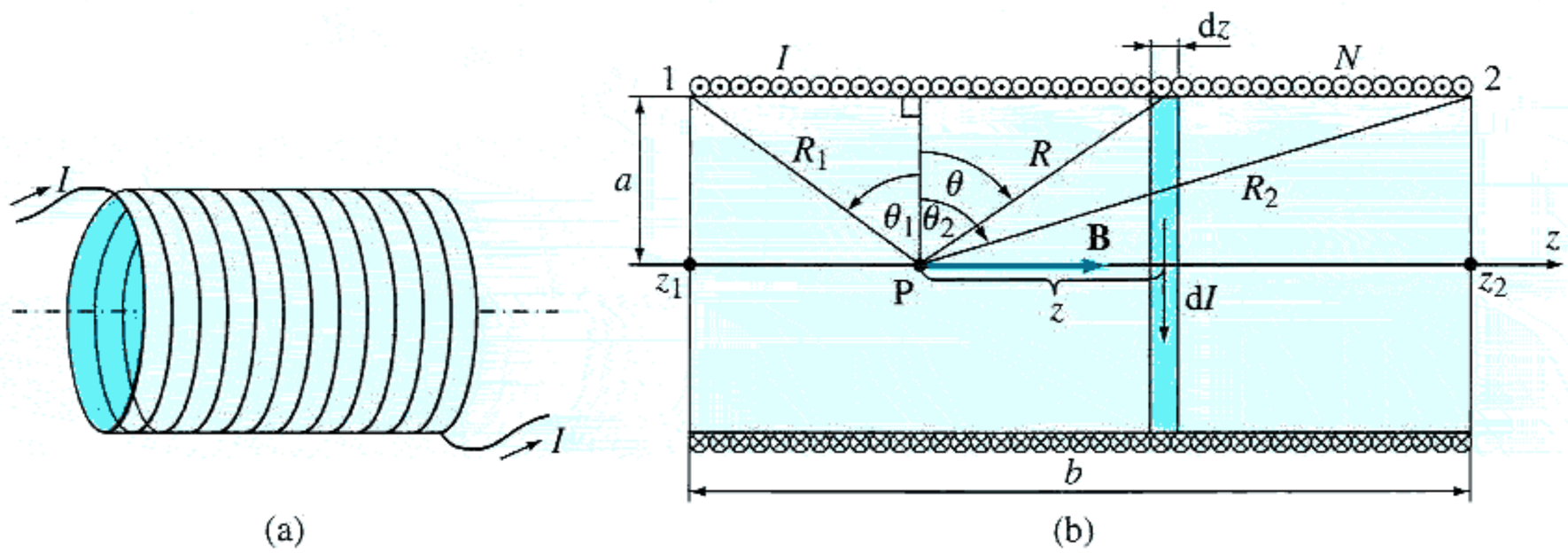

Figure 4.10 (a) Uniformly and densely wound solenoidal coil with a steady current and (b) evaluation of the magnetic flux density vector along the solenoid axis; for Example 4.5.

can be viewed as the current of an equivalent circular current loop of radius a and wire diameter $\mathrm{d}z$. From Eq. (4.19), the magnetic flux density vector of this loop at an arbitrary point P at the solenoid axis [Fig. 4.10(b)] is

$$\mathrm{d}\mathbf{B} = \frac{\mu_0 \, \mathrm{d}I a^2}{2R^3} \, \hat{\mathbf{z}}. \tag{4.32}$$

To find the total field $\mathbf{B}$ at the point P, we integrate $\mathrm{d}\mathbf{B}$ to sum the contributions of all equivalent loops along the solenoid (superposition principle):

$$\mathbf{B} = \int_{z=z_1}^{z_2} \mathrm{d}\mathbf{B} = \frac{\mu_0 N I a^2}{2l} \int_{z_1}^{z_2} \frac{\mathrm{d}z}{R^3} \, \hat{\mathbf{z}}, \qquad R = \sqrt{z^2 + a^2}. \tag{4.33}$$

In order to solve this integral, however, we note that the relationship in Eq. (1.55), with d substituted here by a, exists between the length coordinate z (measured from the point P) and the angular coordinate θ of the position of the equivalent loop along the solenoid axis. Multiplying it by $a/R = \cos\theta$ yields

$$\frac{a^2 \, \mathrm{d}z}{R^3} = \cos\theta \, \mathrm{d}\theta. \tag{4.34}$$

With this, the integral in Eq. (4.33) is reduced to a simple form:

$$\mathbf{B} = \frac{\mu_0 N I}{2l} \int_{\theta=\theta_1}^{\theta_2} \cos\theta \, \mathrm{d}\theta \, \hat{\mathbf{z}}, \tag{4.35}$$

which results in

$$\boxed{\mathbf{B} = \frac{\mu_0 N I}{2l} (\sin\theta_2 - \sin\theta_1) \, \hat{\mathbf{z}}.} \tag{4.36}$$

$\mathbf{B}$ along the axis of a finite solenoid

This expression is valid for an arbitrary field point along the solenoid axis, both inside and outside the solenoid, with the position of the point being defined by angles θ_1 and θ_2. Note, however, that the position of the point P can also be defined by coordinates z_1 and z_2, where $z_1 = a \tan\theta_1$ and $z_2 = a \tan\theta_2$.

In the case of an infinitely long solenoid, $\theta_1 = -\pi/2$ ($z_1 \to -\infty$) and $\theta_2 = \pi/2$ ($z_2 \to \infty$) in Fig. 4.10(b) and in Eq. (4.36), so that

$$\boxed{B = \mu_0 N' I,} \tag{4.37}$$

B inside an infinite solenoid

where $N' = N/l$ is the number of wire turns per unit length of the solenoid. The magnetic field is uniform, with flux density given in Eq. (4.37), within an infinite solenoid even at points off of its axis, as we shall show in a later example.

Example 4.6 **Magnetic Field of an Infinitely Long Strip Conductor**

An infinitely long conductor in the form of a thin strip of width a carries a steady current of intensity I. The permeability everywhere is μ_0. Determine the expression for the magnetic flux density vector at an arbitrary point in space.

Solution This is a two-dimensional problem, and we solve it in the cross-sectional plane shown in Fig. 4.11. Eq. (3.82) tells us that the current I must be uniformly distributed in the cross section of the conductor. Because of the conductor being thin, however, its current can be regarded as a surface current, Fig. 3.3, with density

$$J_s = \frac{I}{a}. \tag{4.38}$$

By virtue of the superposition principle, we subdivide the conductor into elemental strips of width $\mathrm{d}l = \mathrm{d}y$, and each such strip can be considered as an infinitely long line current of intensity

$$\mathrm{d}I = J_s\,\mathrm{d}l = \frac{I\,\mathrm{d}y}{a}. \tag{4.39}$$

The magnetic flux density vector due to individual line currents is circular with respect to the line, and, from Eq. (4.22), its magnitude at an arbitrary point P in space (Fig. 4.11) is

$$\mathrm{d}B = \frac{\mu_0\,\mathrm{d}I}{2\pi R}, \qquad R = \sqrt{y^2 + d^2}, \tag{4.40}$$

where d is the perpendicular distance of P from the plane of the strip. We decompose vector $\mathrm{d}\mathbf{B}$ into its x- and y-components,

$$\mathrm{d}B_x = \mathrm{d}B\sin\theta, \qquad \mathrm{d}B_y = \mathrm{d}B\cos\theta, \tag{4.41}$$

and integrate them over the width of the strip conductor to sum the contributions of all elemental strips,

$$B_x = \frac{\mu_0 I}{2\pi a}\int_{y=y_1}^{y_2}\frac{\sin\theta\,\mathrm{d}y}{R}, \qquad B_y = \frac{\mu_0 I}{2\pi a}\int_{y_1}^{y_2}\frac{\cos\theta\,\mathrm{d}y}{R}. \tag{4.42}$$

We now use the relationship in Eq. (1.55), where z is y here, to change the integration variable from y to θ. Multiplying its left-hand side by $R\cos\theta$ and right-hand side by d, which is justified by the fact that $\cos\theta = d/R$ in Fig. 4.11, we obtain

$$\frac{\cos\theta\,\mathrm{d}y}{R} = \mathrm{d}\theta. \tag{4.43}$$

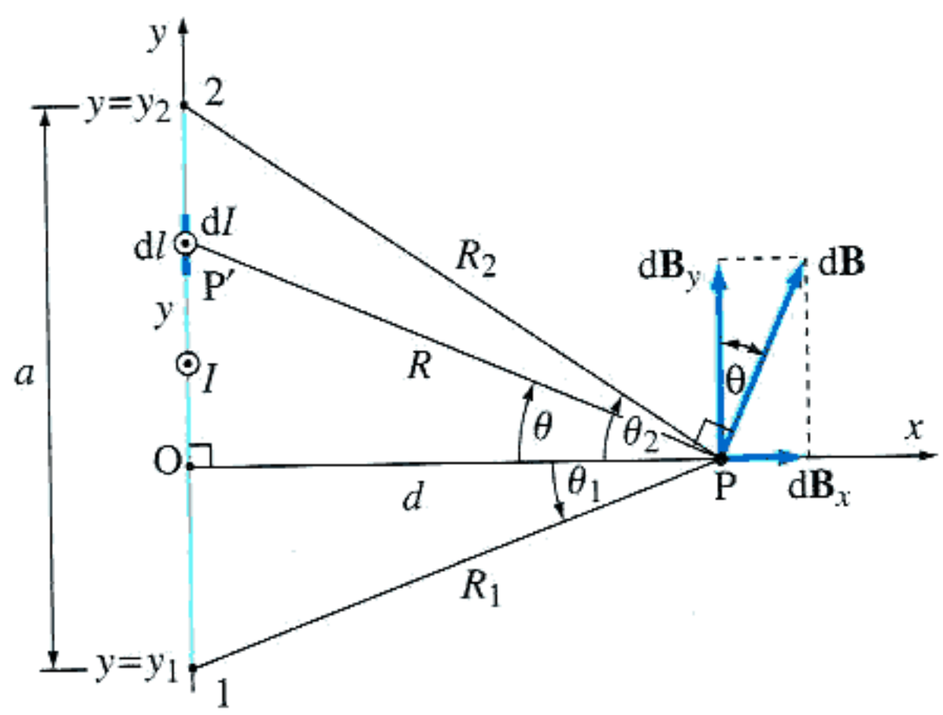

Figure 4.11 Evaluation of the magnetic field due to an infinitely long strip conductor (cross-sectional view); for Example 4.6.

which, multiplied by $\sin\theta/\cos\theta (= \tan\theta)$ gives, in turn,

$$\frac{\sin\theta\,\mathrm{d}y}{R} = \frac{\sin\theta}{\cos\theta}\,\mathrm{d}\theta. \tag{4.44}$$

Based on these two relations, the integrals in Eqs. (4.42) are simple to solve:

$$B_x = \frac{\mu_0 I}{2\pi a}\int_{\theta_1}^{\theta_2}\frac{\sin\theta}{\cos\theta}\,\mathrm{d}\theta = \frac{\mu_0 I}{2\pi a}\ln\frac{\cos\theta_1}{\cos\theta_2}, \quad B_y = \frac{\mu_0 I}{2\pi a}\int_{\theta_1}^{\theta_2}\mathrm{d}\theta = \frac{\mu_0 I}{2\pi a}(\theta_2-\theta_1), \tag{4.45}$$

where the use is made of the substitution $u = \cos\theta$ ($\mathrm{d}u = -\sin\theta\,\mathrm{d}\theta$) in the first integration. Hence, the total magnetic flux density vector due to the strip conductor turns out to be

$$\boxed{\mathbf{B} = \frac{\mu_0 I}{2\pi a}\left[\hat{\mathbf{x}}\ln\frac{R_2}{R_1} + (\theta_2-\theta_1)\,\hat{\mathbf{y}}\right],} \tag{4.46}$$

B due to a strip conductor

with R_1 and R_2 being the distances of the point P from the starting and ending point, respectively, of the line representing the cross section of the strip conductor, in Fig. 4.11.

Note that if we let $a \to \infty$ while keeping $I/a = \text{const}$, we get an infinitely wide and infinitely long planar current sheet with a uniform surface current density $J_s = I/a$. Then, $R_1 = R_2$ (infinite), $\theta_1 = -\pi/2$, and $\theta_2 = \pi/2$, with which Eq. (4.46) becomes

$$\boxed{\mathbf{B} = \frac{\mu_0 J_s}{2}\,\hat{\mathbf{y}}.} \tag{4.47}$$

B due to an infinite current sheet

We conclude that the magnetic field due to an infinite planar sheet of current is uniform at each side of the sheet, with field lines parallel to the sheet.

Problems: 4.1–4.9; *Conceptual Questions* (on Companion Website): 4.4–4.6; *MATLAB Exercises* (on Companion Website).

4.4 FORMULATION OF AMPÈRE'S LAW

We saw in Chapter 1 that the electric field due to highly symmetrical charge distributions in free space can be determined much more easily using Gauss' law, Eq. (1.133), than by direct application of Coulomb's law and the superposition principle, i.e., Eqs. (1.37)–(1.39). In magnetostatics, Eqs. (4.7)–(4.9) (the Biot-Savart law) provide general solution procedures analogous to those in Eqs. (1.37)–(1.39), whereas the law that helps us evaluate the magnetic field due to highly symmetrical current distributions in free space more easily is known as Ampère's law (also called Ampère's circuital law or Ampère's work law). It states that the line integral (circulation) of the magnetic flux density vector around any contour (C) in a vacuum (free space) is equal to μ_0 times the total current enclosed by that contour, which we mark as I_C,

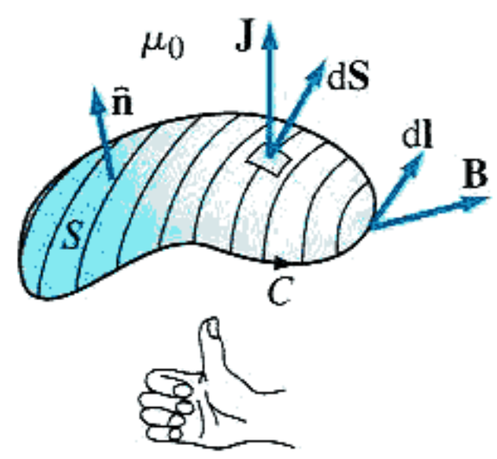

Figure 4.12 Arbitrary contour in a magnetostatic field – for the formulation of Ampère's law.

$$\boxed{\oint_C \mathbf{B}\cdot\mathrm{d}\mathbf{l} = \mu_0 I_C.} \tag{4.48}$$

Ampère's law

The reference direction of the current flow is related to the reference direction of the contour by means of the right-hand rule: the current is in the direction defined by the thumb of the right hand when the other fingers point in the direction of the contour, as shown in Fig. 4.12. This law may be derived from the Biot-Savart law (we recall that Gauss' law is derived from Coulomb's law), and the derivation is carried out in Section 4.10. For the present, we accept Ampère's law temporarily as another law capable of experimental proof. Eq. (4.48) represents Maxwell's second

HISTORICAL ASIDE

André-Marie Ampère (1775–1836), a French mathematician and physicist, was a professor of mathematics, physics, and chemistry in Bourg and Paris, and inspector general of the national university system under Napoleon. Although with little formal education, Ampère acquired the best possible knowledge of mathematics and sciences for that time by reading many books and articles, with a great support and guidance from his father. As a teenager, he was already deriving his own mathematical theories and writing papers on some geometrical problems. However, his life was soon to be shattered when his father was sent to the guillotine by the Jacobins in Lyon in 1793 during the French Revolution. The effect on Ampère of his father's death was devastating, and he did not return to his studies of mathematics for almost two years. After several years of tutoring mathematics in Lyon, he was appointed professor of physics and chemistry at Bourg École Centrale in 1802, and then professor of mathematics at the École Polytechnique in Paris in 1809. His mathematics research included a wide variety of topics in probability, calculus, analytic geometry, and partial differential equations. He contributed also to the theory of light, chemistry, and, most importantly, to electricity and magnetism. Only a few weeks after hearing of Oersted's experimental results, Ampère was ready, before the end of September of 1820, to report to the French Academy of Sciences his discovery of magnetic forces between wires carrying electric currents. He discovered experimentally that two parallel wires carrying currents in the same direction attracted each other, whereas the wires with currents flowing in opposite directions repelled each other. His experiments founded the science of the magnetic field due to electric currents. He described the magnetic force circling around a current-carrying wire in a way which is now known as the right-hand rule. On November 6, 1820, Ampère gave a talk on his circuital law of addition of magnetic forces – a basis of a general equation that we call now Ampère's (circuital) law. He was the first to describe current as the flow of electricity along a wire, analogous to the surge of water through a pipe. He predicted theoretically that a wire helix with current would behave as it were a bar permanent magnet, and called such a helix a solenoid. Ampère also explained permanent magnets as a collection of tiny electric currents circling eternally within them, and in this he was three-quarters of a century ahead of his time. A comprehensive presentation of his findings in electricity and magnetism, including both description of experiments and mathematical derivations, appeared in his most important publication "Memoir on the Mathematical Theory of Electrodynamic Phenomena, Uniquely Deduced from Experience" in 1826. The same year, Ampère was appointed to a chair at the Université de France, which he held until his death. In his honor, the intensity of electric current is measured in amperes. *(Portrait: Edgar Fahs Smith Collection, University of Pennsylvania Libraries)*

equation for static fields in free space (as we know, there is a total of four Maxwell's equations for the general electromagnetic field). By expressing the current in terms of the volume current density, **J**, Ampère's law becomes

Ampère's law for volume current

$$\boxed{\oint_C \mathbf{B} \cdot d\mathbf{l} = \mu_0 \int_S \mathbf{J} \cdot d\mathbf{S},} \tag{4.49}$$

where S is a surface of arbitrary shape spanned over (bounded by) the contour C and oriented in accordance to the right-hand rule with respect to the orientation of C (Fig. 4.12).

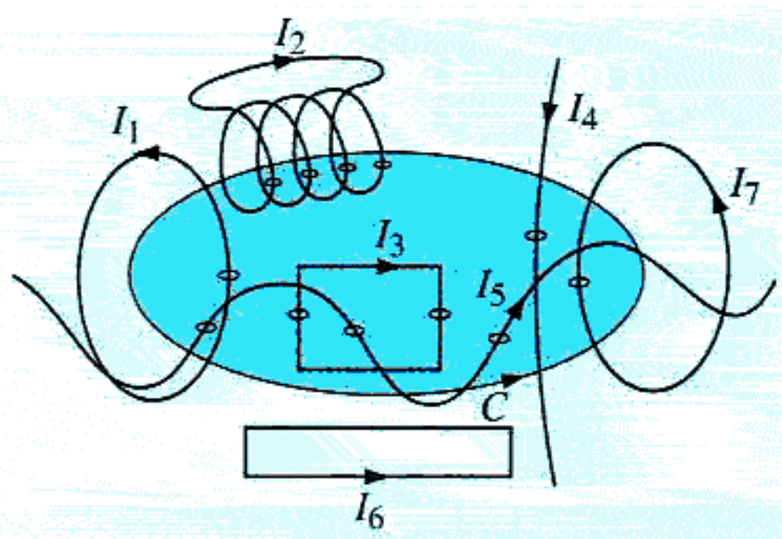

Figure 4.13 Closed path C and seven line currents in air; for Example 4.7.

Example 4.7 **Algebraic Total Enclosed Current**

What is the circulation of the magnetic flux density vector along the contour C in Fig. 4.13? The medium is air.

Solution According to the right-hand rule given with respect to the reference direction of the contour C indicated in Fig. 4.13, the reference orientation of the surface S spanned over C, i.e., the reference direction of the vector $d\mathbf{S}$ in Eq. (4.49), is from S upward. From Ampère's law, the line integral of the magnetic flux density vector along C equals μ_0 times the algebraic sum of all current intensities passing through S. We note that current I_1 pierces S once in the positive direction (direction in agreement with the orientation of S), I_2 passes it four times, I_4 and I_7 once each but in the negative direction, I_3 once in the positive and once in the negative direction, I_5 twice in the positive and once in the negative direction, while I_6 does not traverse S at all. Hence,

$$\oint_C \mathbf{B} \cdot d\mathbf{l} = \mu_0 (I_1 + 4I_2 - I_4 + I_5 - I_7) . \tag{4.50}$$

What is very important, the same result for the algebraic total current, and thus for the circulation of $\mathbf{B}$, is obtained for any other surface we imagine with the contour C as the perimeter and totally arbitrary shape.

Example 4.8 **Contour inside a Conductor**

Fig. 4.14 shows the cross section of a very long cylindrical copper conductor that carries a steady current of intensity I ($I > 0$). Is the circulation of the magnetic flux density vector along the contour C less than, equal to, or greater than $\mu_0 I$?

Solution From Ampère's law,

$$\oint_C \mathbf{B} \cdot d\mathbf{l} < \mu_0 I, \tag{4.51}$$

since the total current appearing on the right-hand side of Eq. (4.49) equals exactly that portion of the total current of the conductor (I) enclosed by the contour.

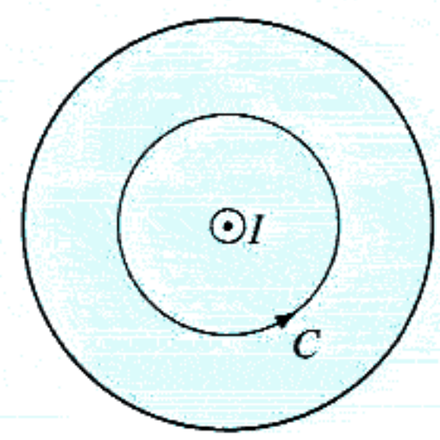

Figure 4.14 Contour inside a conductor with a steady current; for Example 4.8.

Conceptual Questions (on Companion Website): 4.7–4.10.

4.5 APPLICATIONS OF AMPÈRE'S LAW

This section is devoted to the application of Ampère's law in evaluating the magnetic field due to given steady current distributions in nonmagnetic media. As is the case with Gauss' law, the use of Ampère's law will also require

careful consideration of the symmetry of the problem to determine which field components are present in the structure and which spatial variables the present components depend on. Eq. (4.48), although always true, enables us to analytically solve for the field only due to highly symmetrical current distributions. Namely, as the unknown quantity to be determined (**B**) appears inside the integral in Eq. (4.48), we can use Ampère's law to obtain a solution only in cases in which we are able to bring the magnetic flux density, B, outside the integral sign, and solve for it. These cases involve current distributions for which we are able to adopt a closed path C, called the Amperian contour, that satisfies two requirements: (1) **B** is everywhere either tangential or normal to C and (2) $B = \text{const}$ along sections of C where **B** is tangential. Along the portion of the path where **B** is normal to it (if such portion exists), the dot product $\mathbf{B} \cdot \mathbf{dl}$ in Eq. (4.48) becomes zero. Along the remaining part of the contour, $\mathbf{B} \cdot \mathbf{dl}$ becomes $B\,\mathrm{d}l$, and the second requirement (constancy) then permits us to remove B from the integral sign in Eq. (4.48). The integration we are left with is usually trivial and consists of finding the length of that portion of the path to which **B** is tangential.

In this discussion, we notice and exploit the parallelism with the application of Gauss' law, discussed in Section 1.13. All similarities and differences in the mathematical formalism are direct consequences of the mathematical form of the fields **E** and **B** due to the elementary sources Q and $Q\mathbf{v}$, Eqs. (1.24) and (4.4). With Gauss' law, we integrate over a closed surface (Gaussian surface) on the left-hand side of the equation, while Ampère's law implies integration along a closed path (Amperian contour). The field component contributing to the integral is a component normal to the Gaussian surface and tangential to the Amperian contour, respectively. On the right-hand side of the equation, Gauss' law involves finding the total charge enclosed by the surface, whereas the application of Ampère's law involves finding the total current enclosed by the contour. For sources expressed by volume charge and current densities [Eqs. (1.135) and (4.49)], this means volume integration over the volume enclosed by the Gaussian surface and surface integration over the surface bounded by the Amperian contour, respectively.

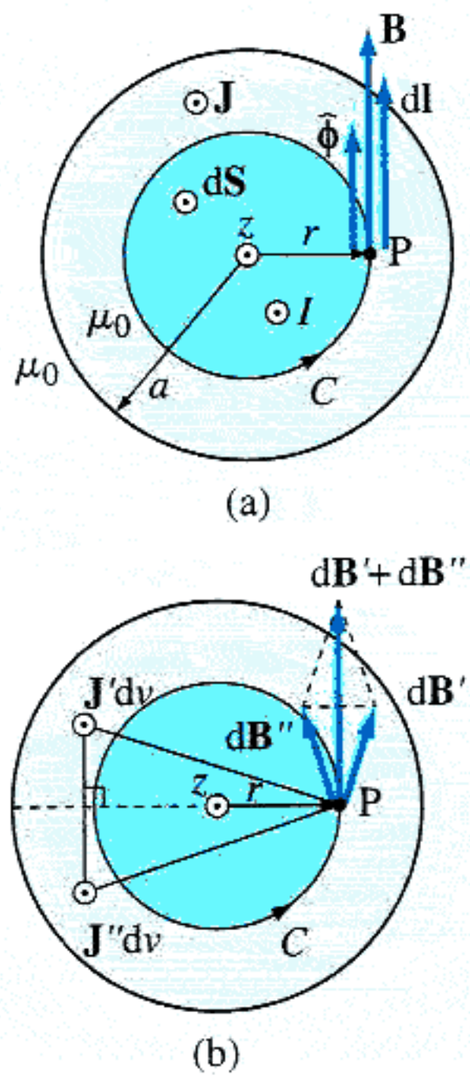

Figure 4.15 Cross section of a cylindrical conductor with a steady current I: (a) application of Ampère's law and (b) proof that the magnetic field lines are circles; for Example 4.9.

Example 4.9 Magnetic Field of a Cylindrical Conductor

An infinitely long cylindrical copper conductor of radius a carries a steady current of intensity I. The conductor is situated in air. Find the magnetic flux density vector inside and outside the conductor.

Solution Fig. 4.15(a) shows a cross section of the conductor. According to Eq. (3.82), the current is uniformly distributed in the cross section, so that its density is

$$J = \frac{I}{\pi a^2}. \tag{4.52}$$

Because of symmetry, the lines of the magnetic field due to the conductor current are circles centered at the conductor axis. To show this, consider the direction of the magnetic flux density vector, **B**, at an arbitrary point P in space, either inside or outside the conductor. Let the distance of the point from the conductor axis be r, and let $\mathrm{d}\mathbf{B}'$ and $\mathrm{d}\mathbf{B}''$ represent the fields at P due to two symmetrical current elements denoted as $\mathbf{J}'\,\mathrm{d}v$ and $\mathbf{J}''\,\mathrm{d}v$ and shown in Fig. 4.15(b). In accordance to the Biot-Savart law, Eq. (4.6), these two elementary field vectors are such that their sum $\mathrm{d}\mathbf{B}' + \mathrm{d}\mathbf{B}''$ is tangential to the circular contour C of radius r centered at the conductor axis. The same is true for any other pair of symmetrical current elements, which can also be in a plane that does not contain the point P, and all current elements constituting the current I in the conductor can be grouped in such symmetrical

pairs. We conclude that the resultant vector **B** at the point P is tangential to the contour C. In addition, symmetry also implies that $B = \text{const}$ along C, i.e., the magnitude of **B** depends only on the radial coordinate r of the cylindrical coordinate system whose z-axis coincides with the conductor axis. Hence, we can write

$$\mathbf{B} = B(r)\,\hat{\boldsymbol{\phi}}, \tag{4.53}$$

where $\hat{\boldsymbol{\phi}}$ is the circular unit vector in the system.

Based on the preceding discussion, it is now obvious that the contour C in Fig. 4.15 satisfies both requirements for the Amperian contour for our problem. Along C, $\mathrm{d}\mathbf{l} = \mathrm{d}l\,\hat{\boldsymbol{\phi}}$, so that $\mathbf{B}\cdot\mathrm{d}\mathbf{l} = B\,\mathrm{d}l$ [Fig. 4.15(a)]. The circulation of **B** along C thus turns out to be

$$\oint_C \mathbf{B}\cdot\mathrm{d}\mathbf{l} = \oint_C B(r)\,\mathrm{d}l = B(r)\oint_C \mathrm{d}l = B(r)\,l = B(r)\,2\pi r, \quad 0 \le r < \infty, \tag{4.54}$$

whereas the current enclosed by C amounts to

$$I_C = \begin{cases} J\pi r^2 & \text{for } r < a \\ I & \text{for } r \ge a \end{cases}. \tag{4.55}$$

Eqs. (4.54) and (4.55) combined in Ampère's law, Eq. (4.48), finally give

$$\boxed{B = \begin{cases} \mu_0 I r/(2\pi a^2) & \text{for } r < a \\ \mu_0 I/(2\pi r) & \text{for } r \ge a \end{cases}}. \tag{4.56}$$

B due to a thick cylindrical conductor with a steady current

Note that the magnetic field outside the conductor (for $r \ge a$) is identical to that of a line current of intensity I placed along the conductor axis, Eq. (4.22). This means that the line current (e.g., a thin wire with current I) and the (thick) conductor of Fig. 4.15 are equivalent sources with respect to the region outside the conductor.

Example 4.10 Cylindrical Conductor with an Excentric Cavity

A very long cylindrical nonmagnetic conductor of radius b has an excentric cylindrical cavity of radius a along its entire length, as shown in Fig. 4.16. The axis of the cavity is offset from the axis of the conductor by a vector **d** ($a + d \le b$). The medium in the cavity and outside the conductor is air. Compute the magnetic flux density vector in the cavity, assuming a steady current of density J flowing through the conductor.

Solution The current density in the cavity is zero, and it can be considered to result from two currents of the same density (J) flowing in opposite directions. Accordingly, we can represent the current distribution in the hollow conductor, including the cavity, as a sum of current distributions of a cylindrical conductor of radius b carrying a current of density J without a cavity and another one of radius a with a current of the same density but flowing in the opposite direction, as depicted in Fig. 4.16. By the superposition principle, the magnetic flux density vector of the original (resultant) current distribution, **B**, can be obtained as

$$\mathbf{B} = \mathbf{B}_1 + \mathbf{B}_2, \tag{4.57}$$

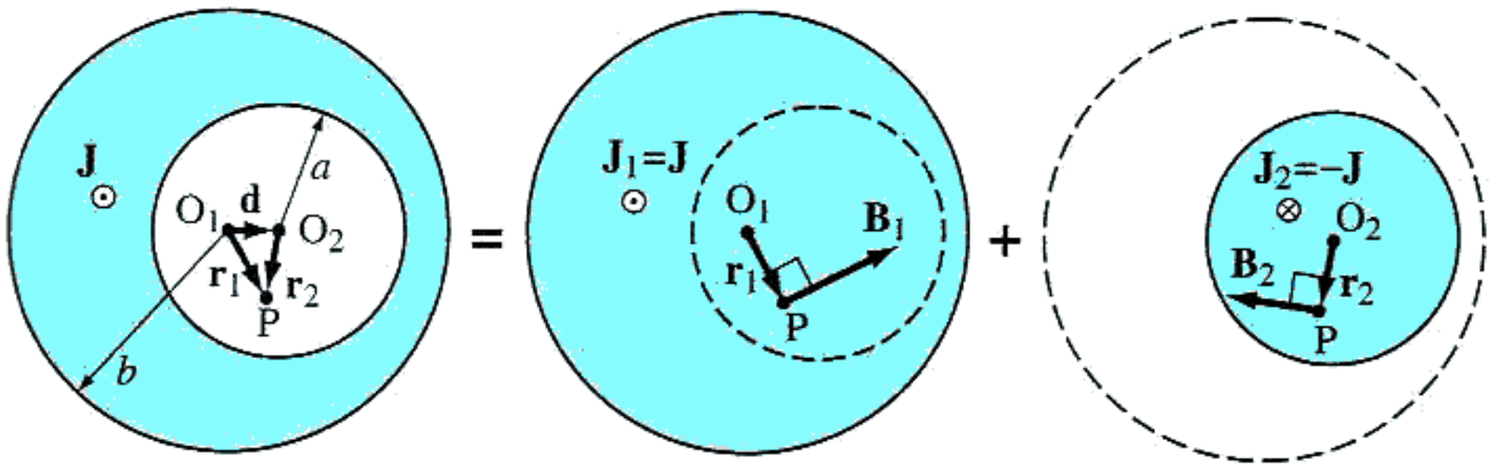

Figure 4.16 Cylindrical conductor with an excentric cylindrical cavity, viewed as a superposition of two solid conductors with currents of the same density but opposite directions; for Example 4.10.

where $\mathbf{B}_1$ and $\mathbf{B}_2$ are the magnetic flux density vectors due to the partial current distributions $\mathbf{J}_1$ and $\mathbf{J}_2$ in Fig. 4.16. These vectors, according to Eq. (4.56), can be written in the form[3]

$$\mathbf{B}_1 = \frac{\mu_0 \mathbf{J} \times \mathbf{r}_1}{2} \quad \text{and} \quad \mathbf{B}_2 = \frac{\mu_0(-\mathbf{J}) \times \mathbf{r}_2}{2}. \tag{4.58}$$

where $\mathbf{r}_1$ and $\mathbf{r}_2$ are the position vectors of the field point (P) with respect to the conductor axis (O_1) and cavity axis (O_2), respectively. Finally, combining the preceding equations, we get

$$\mathbf{B} = \frac{\mu_0 \mathbf{J} \times (\mathbf{r}_1 - \mathbf{r}_2)}{2} = \frac{\mu_0 \mathbf{J} \times \mathbf{d}}{2}, \tag{4.59}$$

and $B = \mu_0 J d/2$. We conclude that the magnetic field inside the cavity is uniform, as the above expression for the resultant magnetic flux density vector does not depend on the position of the point P. The field lines are parallel to the plane of the conductor cross section and at right angles to the vector $\mathbf{d}$.

Example 4.11 Magnetic Field of a Coaxial Cable

Conductors of a coaxial cable are made from copper, and its dielectric is air. The radius of the inner conductor is a, whereas the inner and outer radii of the outer conductor are b and c, respectively ($a < b < c$). A steady current of intensity I is established in the cable. Find the magnetic flux density vector everywhere.

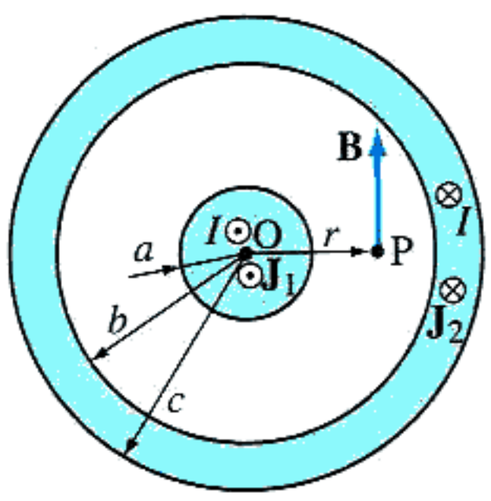

Figure 4.17 Evaluation of the magnetic field of a coaxial cable; for Example 4.11.

B in the dielectric of a coaxial cable

Solution Referring to Fig. 4.17, current densities in the cable conductors are

$$J_1 = \frac{I}{\pi a^2} \quad \text{and} \quad J_2 = \frac{I}{\pi(c^2 - b^2)}. \tag{4.60}$$

Due to symmetry, the magnetic flux density vector, $\mathbf{B}$, is circular with respect to the cable axis. Following a similar procedure as in Example 4.9, we apply Ampère's law to the circular contour C of radius r ($0 \le r < \infty$). The circulation of $\mathbf{B}$ along C is the same as in Eq. (4.54), for all values of r, while the expression for the total current enclosed by C is different for four different characteristic positions of the contour. The field inside the inner conductor and between the conductors is identical to that found in Example 4.9 for a single conductor,

$$B = \frac{\mu_0 J_1 r}{2} = \frac{\mu_0 I r}{2\pi a^2} \quad (0 \le r \le a), \qquad \boxed{B = \frac{\mu_0 I}{2\pi r} \quad (a < r < b).} \tag{4.61}$$

For the contour positioned inside the outer conductor, the enclosed net current equals the entire current of the inner conductor minus that portion of the current of the outer conductor which is enclosed by the contour, so that

$$B = \frac{1}{2\pi r}\mu_0 \underbrace{[I - J_2\pi(r^2 - b^2)]}_{I_C} = \frac{\mu_0 I(c^2 - r^2)}{2\pi(c^2 - b^2)r} \quad (b \le r \le c). \tag{4.62}$$

Finally, if the radius r is larger than the outer radius of the outer conductor,

$$B = \frac{1}{2\pi r}\mu_0(I - I) = 0 \quad (c < r < \infty). \tag{4.63}$$

So, the external magnetic field (for $r > c$) is zero. This, we see, results from currents of equal intensities and opposite directions in cable conductors (making zero total enclosed current in Ampère's law), much as the external electric field of a charged coaxial cable is zero because of charges of equal magnitudes and opposite polarities per unit length of cable

[3]Note that the magnetic flux density inside the solid cylindrical conductor in Fig. 4.15 can be written as $B = \mu_0 J r/2$, and, in vector form, $\mathbf{B} = \mu_0 \mathbf{J} \times \mathbf{r}/2$, where $\mathbf{r}$ is the position vector of the field point with respect to the conductor axis.

conductors (making zero total enclosed charge in Gauss' law). [Such (equal positive and negative) charges and currents are standard in operations of all two-conductor transmission lines.] This is a very important property of a coaxial cable; the electrostatic and magnetostatic fields of the cable are concentrated exclusively inside the cable, and its exterior is perfectly decoupled (shielded) with respect to the interior, and vice versa.

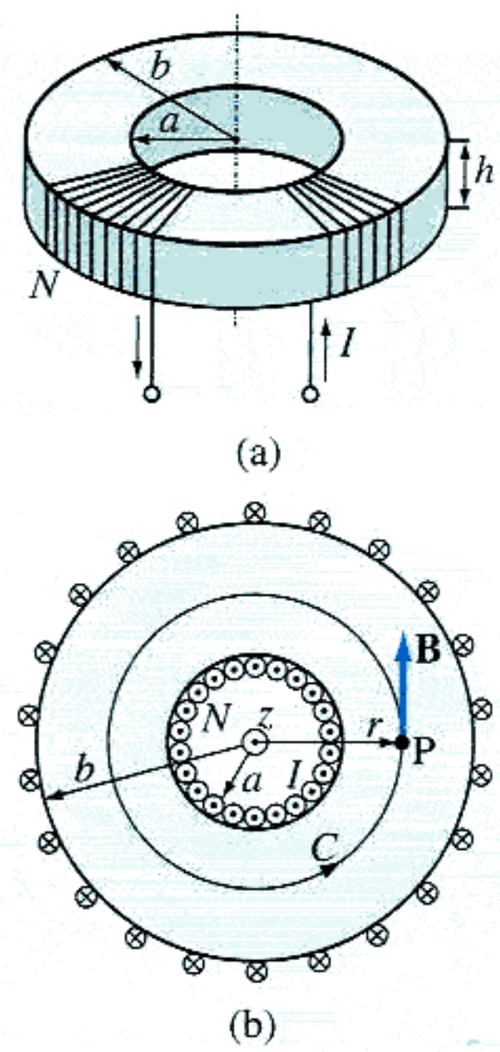

Figure 4.18 Evaluation of the magnetic field of a toroidal coil: (a) three-dimensional view showing the winding and (b) cross-sectional view showing Amperian contours ($0 \le r < \infty$); for Example 4.12.

Example 4.12 Magnetic Field of a Toroidal Coil

Shown in Fig. 4.18(a) is a toroidal ("doughnut"-shaped) coil with a rectangular cross section. The coil consists of N turns of wire that are uniformly and densely wound along the length of the toroid and carry a steady current of intensity I. The inner and outer radii of the toroid are a and b ($a < b$), and its height is h. The medium inside and outside the coil is nonmagnetic. Calculate the magnetic flux density vector inside and outside the coil.

Solution Fig. 4.18(b) portrays a horizontal cut of the toroid in Fig. 4.18(a). Because of symmetry, the lines of the magnetic field density vector, $\mathbf{B}$, due to the current in the coil are circles centered at the toroid axis [z-axis in Fig. 4.18(b)], and the magnitude of $\mathbf{B}$ depends only on the distance r from the axis. This means that the vector $\mathbf{B}$ is of the form given in Eq. (4.53). Applying Ampère's law to a circular contour of radius r ($0 \le r < \infty$), we obtain the following equations for three characteristic locations of the contour:

$$B(r)\,2\pi r = 0 \quad (0 \le r \le a), \qquad B(r)\,2\pi r = \mu_0 NI \quad (a < r < b),$$

$$B(r)\,2\pi r = \mu_0(NI - NI) = 0 \quad (b \le r < \infty). \tag{4.64}$$

Hence, $B = 0$ outside the toroid, while inside it

$$B(r) = \frac{\mu_0 NI}{2\pi r} \quad \text{(inside a thick toroidal coil)}. \tag{4.65}$$

Note that this result is valid for an arbitrary shape of the toroid (vertical) cross section (not only rectangular).

If the toroid is thin, i.e., $b - a \ll a$, we can assume that $r \approx c$ inside it, where $c = (a + b)/2$ is its mean radius. This implies that the magnetic field inside the toroid can be considered to be uniform, with the flux density

$$\boxed{B = \frac{\mu_0 NI}{2\pi c} = \frac{\mu_0 NI}{l} = \mu_0 N' I,} \tag{4.66}$$

B inside a thin toroidal coil

where $l = 2\pi c$ is the length of the toroid and $N' = N/l$ is the number of wire turns per unit length.

We realize that the final expression for B in Eq. (4.66) is the same as that in Eq. (4.37), found for an infinite solenoid. Namely, we can visualize an infinitely long solenoid as a toroid with an infinite radius.

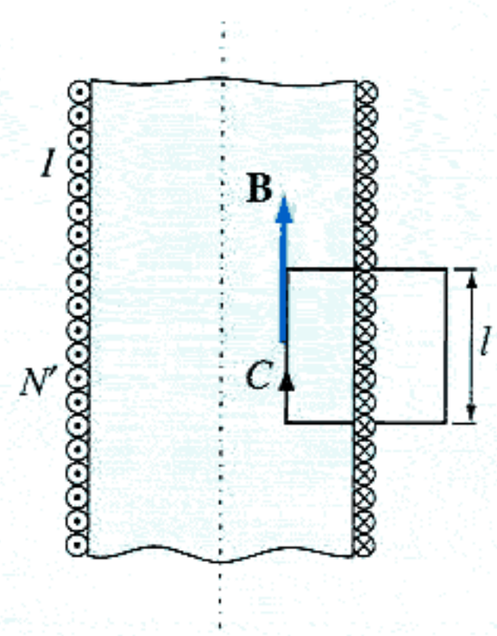

Figure 4.19 Evaluation of the magnetic field inside an infinite solenoid using Ampère's law; for Example 4.13.

Example 4.13 Magnetic Field inside an Infinite Solenoid from Ampère's Law

An infinitely long air-filled solenoid has N' turns of wire per unit of its length. A steady current of intensity I flows through the winding. Using Ampère's law, prove that the magnetic flux density inside the solenoid is given by the expression in Eq. (4.37).

Solution Knowing that the vector $\mathbf{B}$ inside an infinite solenoid is axial (parallel to the solenoid axis) and that it is zero outside the solenoid, it is now very simple to evaluate the magnitude of $\mathbf{B}$ in the solenoid from Ampère's law. The Amperian contour is a rectangle positioned partly inside the solenoid as shown in Fig. 4.19. The line integral of $\mathbf{B}$ along the vertical (axial) edge of the rectangle that is inside the solenoid equals Bl, because $\mathbf{B}$ is parallel to that edge and does not vary along it (the structure is infinitely long). The line integral of $\mathbf{B}$ along the remaining three edges of the rectangle is zero, because $\mathbf{B}$ is perpendicular to

portions of horizontal (perpendicular to the axis) edges that are inside the solenoid and is zero outside it. The net current enclosed by the contour, on the other hand, equals the number of turns over the length l, which is $N'l$, times I (the current through each turn). Hence, Ampère's law gives

$$Bl = \mu_0 N' l I, \tag{4.67}$$

i.e., the same as in Eq. (4.37). Note that we did not in any way restrict the location of the left edge of the contour C in Fig. 4.19 to be on the solenoid axis or at a specific distance from it, which means that Eq. (4.37) is valid across the entire cross section of the solenoid, and not only on the solenoid axis (in Example 4.5, the magnetic field is evaluated along the solenoid axis only). In other words, the magnetic field is uniform (the same) throughout the entire volume enclosed by the solenoid winding (while zero outside it). We also note that the cross section of the solenoid in this discussion and calculation is not in any way restricted to be of circular shape, which implies that the magnetic field is the same for arbitrary shape of the solenoid cross section (provided that the solenoid is very long).

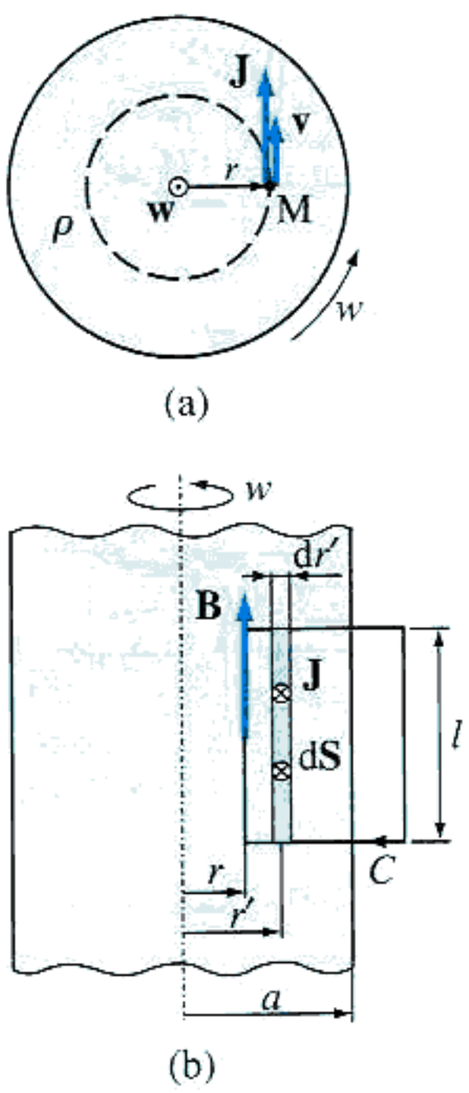

Figure 4.20 Evaluation of the magnetic field of a rotating charged cylinder: (a) equivalent impressed current density and (b) Amperian contour; for Example 4.14.

Example 4.14 Magnetic Field of a Rotating Charged Cylinder

A very long cylinder of radius a is uniformly charged over its volume by a charge of density ρ. The cylinder uniformly rotates about its axis with an angular velocity w. The permeability is μ_0 everywhere. Find the magnetic flux density vector inside and outside the cylinder, assuming that the charge distribution of the cylinder remains the same during the rotation.

Solution As the charges of the cylinder rotate with it, they form a volume electric current. Referring to Fig. 4.20(a), the velocity at which a point M that is r away from the cylinder axis moves is

$$\mathbf{v} = \mathbf{w} \times \mathbf{r} = wr\,\hat{\boldsymbol{\phi}}, \tag{4.68}$$

and the current density vector at that point can be found from Eq. (3.28). The current lines in the cylinder are circles centered at the cylinder axis [Fig. 4.20(a)], and the current density is a function of r given by

$$J(r) = \rho v(r) = \rho w r \qquad (0 \le r \le a). \tag{4.69}$$

We note that this current density, which is independent of the electric field, can be regarded as an impressed electric current density, $\mathbf{J}_i$ [Fig. 3.17(a)].

Because of the currents in the cylinder being circular, the cylinder can be visualized as a series of many very long coaxial solenoids of radii varying from $r = 0$ to $r = a$. That is why the magnetic flux density vector, $\mathbf{B}$, outside the cylinder (i.e., outside all equivalent solenoids) is zero, whereas $\mathbf{B}$ is axial inside the cylinder. Ampère's law, Eq. (4.49), applied to a rectangular contour C shown in Fig. 4.20(b) results in [left-hand side of the equation is the same as in Eq. (4.67)]

$$B(r)\,l = \mu_0 \int_{r'=r}^{a} J(r')\,\underbrace{l\,\mathrm{d}r'}_{\mathrm{d}S} = \mu_0 \rho w l \int_r^a r'\,\mathrm{d}r', \tag{4.70}$$

where $\mathrm{d}S$ is the surface area of a thin strip of length l and width $\mathrm{d}r'$ (r' is the integration variable). Hence, the magnitude of $\mathbf{B}$ at points that are r away from the cylinder axis comes out to be

$$B(r) = \begin{cases} \mu_0 \rho w (a^2 - r^2)/2 & \text{for } r < a \\ 0 & \text{for } r \ge a \end{cases}. \tag{4.71}$$

Example 4.15 Magnetic Field of an Infinite Current Sheet from Ampère's Law

Using Ampère's law, prove that the magnetic flux density vector due to an infinite planar current sheet with a uniform surface current density J_s in free space is given by the expression in Eq. (4.47).

Solution Because of symmetry, the magnetic field lines are parallel to the sheet and **B** does not vary in directions parallel to the sheet. We apply Ampère's law to a rectangular contour C portrayed in Fig. 4.21. The line integral of **B** along each of the two edges of the contour that are parallel to the sheet equals Bl and the enclosed current is $J_s l$ [Eq. (3.13)], so that

$$2Bl = \mu_0 J_s l, \tag{4.72}$$

from which the same result as in Eq. (4.47) is obtained.

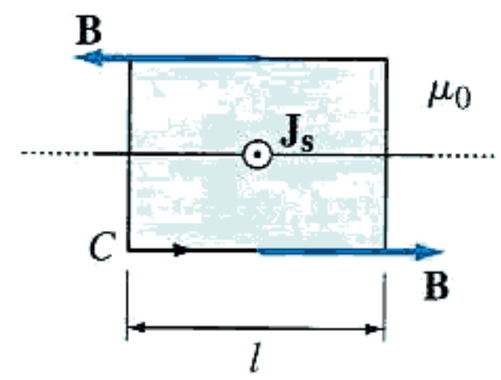

Figure 4.21 Evaluation of the magnetic field of an infinite current sheet using Ampère's law; for Example 4.15.

Problems: 4.10–4.19; *Conceptual Questions* (on Companion Website): 4.11–4.15; *MATLAB Exercises* (on Companion Website).

4.6 DIFFERENTIAL FORM OF AMPÈRE'S LAW

In electrostatics, we derived the differential form of Gauss' law [Eq. (1.163) or (1.166)] starting from its integral form [Eq. (1.135)]. Again, an analogous concept and transformation exist in magnetostatics. In this section, we shall utilize the integral form of Ampère's law, Eq. (4.49), to derive its differential equivalent. What we expect to obtain is a spatial differential relationship between the magnetic flux density vector, **B** (field), and the current density vector, **J** (source), at a point in space.

We consider first the one-dimensional case, and assume that **J** has only a z-component in the Cartesian coordinate system which is a function of the coordinate x only, that is, $\mathbf{J} = J_z(x)\,\hat{\mathbf{z}}$ (1-D current distribution). Then, by symmetry, the only present component of **B** is B_y (like in Example 4.15), i.e., $\mathbf{B} = B_y(x)\,\hat{\mathbf{y}}$. We apply Ampère's law [Eq. (4.49)] to a narrow rectangular contour C lying in the xy-plane, with edges parallel to the x- and y-axes, as shown in Fig. 4.22. The dimension of the contour in the x-direction is $\mathrm{d}x$ and the length of the edges parallel to the y-axis is l. The magnetic field is constant along both edges with length l (B_y does not vary with y), so that essentially no integration is needed on the left-hand side of Eq. (4.49), i.e., the integral along each edge reduces to $\mathbf{B}\cdot\mathbf{l}$ ($\mathbf{l}$ has the same direction as $\mathrm{d}\mathbf{l}$). No integration is needed on the right-hand side of Eq. (4.49) either, because $\mathrm{d}x$ is differentially small and we can take $J_z(x)$ as constant over the surface spanned over C. Finally, as **B** is tangential to both edges with length l, **B** and $\mathrm{d}\mathbf{l}$ are directed in opposite directions along the left edge, and in the same direction along the right edge, we can write

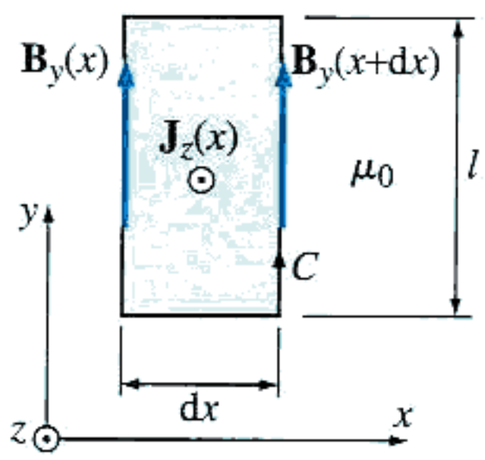

Figure 4.22 For the derivation of the one-dimensional Ampère's law in differential form.

$$-B_y(x)\,l + B_y(x+\mathrm{d}x)\,l = \mu_0 J_z(x)\,l\,\mathrm{d}x. \tag{4.73}$$

Noting that

$$\mathrm{d}B_y = B_y(x+\mathrm{d}x) - B_y(x), \tag{4.74}$$

Eq. (4.73) becomes a differential equation,

$$\boxed{\frac{\mathrm{d}B_y}{\mathrm{d}x} = \mu_0 J_z.} \tag{4.75}$$ *1-D differential Ampère's law*

This is the one-dimensional Ampère's law in differential form. We observe the analogy with the 1-D Gauss' law in Eq. (1.158).

We now generalize Eq. (4.75) to an arbitrary three-dimensional current distribution. The current density vector has now all three Cartesian components and all of them are functions of all three coordinates,

$$\mathbf{J} = J_x(x,y,z)\,\hat{\mathbf{x}} + J_y(x,y,z)\,\hat{\mathbf{y}} + J_z(x,y,z)\,\hat{\mathbf{z}}. \tag{4.76}$$

The Amperian contour C in Eq. (4.49) must, therefore, be differentially small in both dimensions. Additionally, one contour is not enough; we need three small contours, oriented perpendicularly to each of the three current density components, respectively. All edges of the contours being differentially small, the line integral along each of them can be approximated by taking a constant value of the field component tangential to the edge and multiplying it by plus or minus the edge length. This gives us the result for each pair of integrals along parallel edges within each contour that has exactly the same form as in the 1-D case [Eqs. (4.73)–(4.75)]. For the contour that lies entirely in the plane normal to the x-component of $\mathbf{J}$, shown in Fig. 4.23, we have

$$\oint_C \mathbf{B}\cdot d\mathbf{l} = -B_z(x,y,z)\,dz + B_y(x,y,z)\,dy + B_z(x,y+dy,z)\,dz$$
$$-B_y(x,y,z+dz)\,dy = \mu_0 J_x(x,y,z)\,dy\,dz, \tag{4.77}$$

which, divided by $dy\,dz$, results in

$$\frac{\oint_C \mathbf{B}\cdot d\mathbf{l}}{dy\,dz} = \frac{B_z(x,y+dy,z) - B_z(x,y,z)}{dy}$$
$$-\frac{B_y(x,y,z+dz) - B_y(x,y,z)}{dz} = \frac{\partial B_z}{\partial y} - \frac{\partial B_y}{\partial z} = \mu_0 J_x. \tag{4.78}$$

For contours that are oriented perpendicularly to each of the remaining two coordinate axes, y- and z-axes, analogous procedures lead to equations

$$\frac{\partial B_x}{\partial z} - \frac{\partial B_z}{\partial x} = \mu_0 J_y \quad \text{and} \quad \frac{\partial B_y}{\partial x} - \frac{\partial B_x}{\partial y} = \mu_0 J_z, \tag{4.79}$$

respectively. Multiplying Eq. (4.78) by the unit vector $\hat{\mathbf{x}}$, and Eqs. (4.79) by $\hat{\mathbf{y}}$ and $\hat{\mathbf{z}}$, respectively, and summing the three equations, we obtain the following equation with the vector $\mathbf{J}$ [Eq. (4.76)], multiplied by μ_0, on the right-hand side:

Ampère's law in differential form

$$\boxed{\left(\frac{\partial B_z}{\partial y} - \frac{\partial B_y}{\partial z}\right)\hat{\mathbf{x}} + \left(\frac{\partial B_x}{\partial z} - \frac{\partial B_z}{\partial x}\right)\hat{\mathbf{y}} + \left(\frac{\partial B_y}{\partial x} - \frac{\partial B_x}{\partial y}\right)\hat{\mathbf{z}} = \mu_0 \mathbf{J}.} \tag{4.80}$$

This partial differential equation (PDE) represents Ampère's law in differential form for an arbitrary steady current distribution. It relates the rate of change of $\mathbf{B}$ field components in spatial coordinates to the local current density vector, $\mathbf{J}$. We see that only those variations of individual components that are in directions

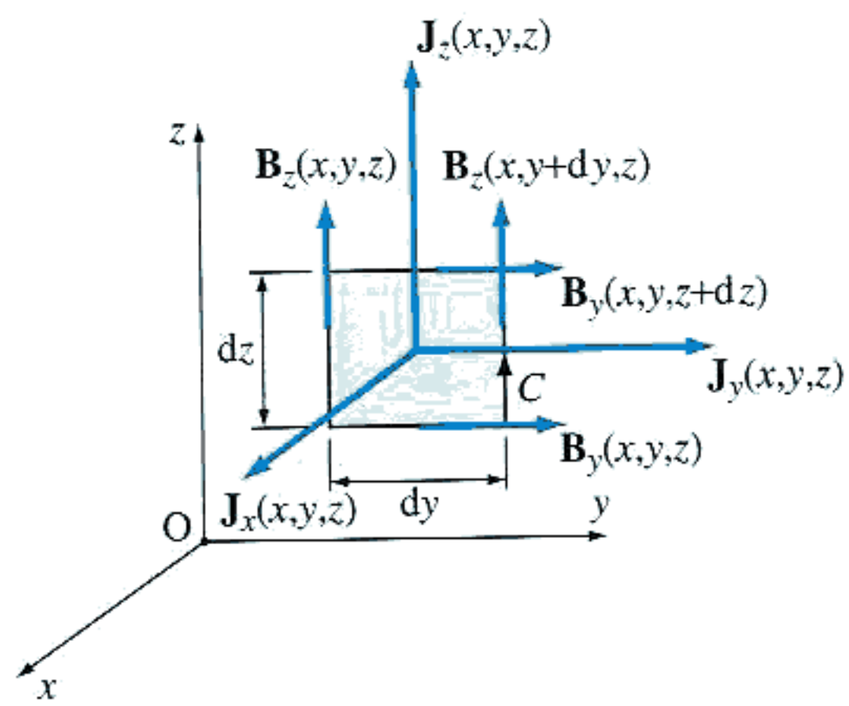

Figure 4.23 For the derivation of Ampère's law in differential form for an arbitrary current distribution.

perpendicular to the direction of the component (change of B_x along y and z, and not along x, etc.) contribute in this relationship, which is just opposite to the dependences in the differential Gauss' law [Eq. (1.163)].

4.7 CURL

The expression on the left-hand side of Eq. (4.80) is the so-called curl of a vector function ($\mathbf{B}$), written as curl $\mathbf{B}$,[4] analogous to the divergence of a vector field ($\mathbf{E}$) as used to express the differential form of Gauss' law [Eq. (1.166)]. In addition, we notice that applying formally the formula for the cross product of two vectors in the Cartesian coordinate system[5] to $\nabla \times \mathbf{B}$, where the del operator is given by Eq. (1.100), we obtain exactly curl $\mathbf{B}$. Hence,

$$\boxed{\begin{aligned}\operatorname{curl}\mathbf{B} = \nabla \times \mathbf{B} = &\left(\frac{\partial B_z}{\partial y} - \frac{\partial B_y}{\partial z}\right)\hat{\mathbf{x}} + \left(\frac{\partial B_x}{\partial z} - \frac{\partial B_z}{\partial x}\right)\hat{\mathbf{y}} \\ &+ \left(\frac{\partial B_y}{\partial x} - \frac{\partial B_x}{\partial y}\right)\hat{\mathbf{z}},\end{aligned}} \tag{4.81}$$

curl in Cartesian coordinates

which can also be written in the form of a determinant,

$$\operatorname{curl}\mathbf{B} = \nabla \times \mathbf{B} = \begin{vmatrix} \hat{\mathbf{x}} & \hat{\mathbf{y}} & \hat{\mathbf{z}} \\ \frac{\partial}{\partial x} & \frac{\partial}{\partial y} & \frac{\partial}{\partial z} \\ B_x & B_y & B_z \end{vmatrix} \tag{4.82}$$

(using the determinant form is a convenient way for memorizing the expression for $\nabla \times \mathbf{B}$ in the Cartesian coordinate system). Note that the curl is an operation that is performed on a vector, and the result is also a vector. Finally, the differential Ampère's law can now be written in a short form as

$$\boxed{\operatorname{curl}\mathbf{B} = \nabla \times \mathbf{B} = \mu_0 \mathbf{J}.} \tag{4.83}$$

Ampère's law using curl notation

In nonrectangular coordinate systems, the differentially small Amperian contour in Fig. 4.23 becomes curvilinear and with different expressions for lengths of its edges for different current density components in each of the systems. For instance, from Fig. 1.10, the contour perpendicular to the radial vector component $J_r\,\hat{\mathbf{r}}$ in spherical coordinates is a curvilinear quadrilateral of edge lengths $r\,\mathrm{d}\theta$ and $r\sin\theta\,\mathrm{d}\phi$. Carrying out similar derivations as in Eqs. (4.77)–(4.80) for this contour and contours oriented perpendicularly to other unit vectors in Figs. 1.25 and 1.26, the expression for the curl in cylindrical coordinates is obtained to be

$$\boxed{\begin{aligned}\operatorname{curl}\mathbf{B} = \nabla \times \mathbf{B} = &\left(\frac{1}{r}\frac{\partial B_z}{\partial \phi} - \frac{\partial B_\phi}{\partial z}\right)\hat{\mathbf{r}} + \left(\frac{\partial B_r}{\partial z} - \frac{\partial B_z}{\partial r}\right)\hat{\boldsymbol{\phi}} \\ &+ \frac{1}{r}\left[\frac{\partial}{\partial r}\left(rB_\phi\right) - \frac{\partial B_r}{\partial \phi}\right]\hat{\mathbf{z}},\end{aligned}} \tag{4.84}$$

curl in cylindrical coordinates

[4]Note that rot $\mathbf{B}$ is also used for curl $\mathbf{B}$, "rot" being a short for "rotation" (or "rotational").

[5]For vectors given by their Cartesian components,

$$\begin{aligned}\mathbf{a} \times \mathbf{b} &= \left(a_x\,\hat{\mathbf{x}} + a_y\,\hat{\mathbf{y}} + a_z\,\hat{\mathbf{z}}\right) \times \left(b_x\,\hat{\mathbf{x}} + b_y\,\hat{\mathbf{y}} + b_z\,\hat{\mathbf{z}}\right) \\ &= \left(a_y b_z - a_z b_y\right)\hat{\mathbf{x}} + \left(a_z b_x - a_x b_z\right)\hat{\mathbf{y}} + \left(a_x b_y - a_y b_x\right)\hat{\mathbf{z}}.\end{aligned}$$

and that for the spherical coordinate system

curl in spherical coordinates

$$\boxed{\begin{aligned}\operatorname{curl}\mathbf{B} = \nabla\times\mathbf{B} = \frac{1}{r\sin\theta}\left[\frac{\partial}{\partial\theta}(\sin\theta B_\phi) - \frac{\partial B_\theta}{\partial\phi}\right]\hat{\mathbf{r}} \\ + \frac{1}{r}\left[\frac{1}{\sin\theta}\frac{\partial B_r}{\partial\phi} - \frac{\partial}{\partial r}(rB_\phi)\right]\hat{\boldsymbol{\theta}} + \frac{1}{r}\left[\frac{\partial}{\partial r}(rB_\theta) - \frac{\partial B_r}{\partial\theta}\right]\hat{\boldsymbol{\phi}}.\end{aligned}} \tag{4.85}$$

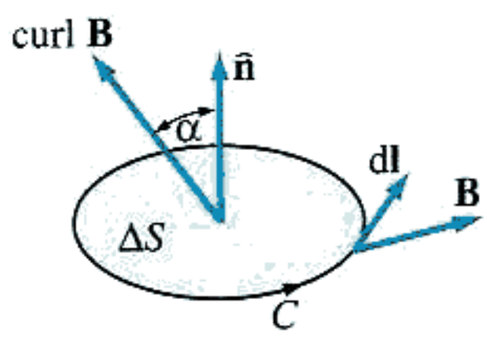

Figure 4.24 For the definition of the curl of a vector field in Eq. (4.87).

In the same way as with $\nabla\cdot\mathbf{E}$ in Section 1.15, we use the notation $\nabla\times\mathbf{B}$ in cylindrical and spherical coordinate systems not to refer to it as the actual cross product of vectors ∇ and $\mathbf{B}$, which is valid only in rectangular coordinates [Eq. (4.81)], but to merely symbolize the curl operation. With this, we also emphasize the fact that relations derived employing such vector formalism in the Cartesian coordinate system hold true (are identities) generally, in all coordinate systems (properties of physical quantities and relations between them are the facts that are independent of the choice of coordinate system).

Combining Eqs. (4.81) and (4.78), we find that the x-component of $\operatorname{curl}\mathbf{B}$, that is, $\hat{\mathbf{x}}\cdot\operatorname{curl}\mathbf{B}$, can be expressed as the net circulation (line integral) of $\mathbf{B}$ along the incremental contour C of Fig. 4.23 divided by the area of the surface spanned over the contour,

$$\hat{\mathbf{x}}\cdot\operatorname{curl}\mathbf{B} = \frac{\oint_C \mathbf{B}\cdot d\mathbf{l}}{dy\,dz}. \tag{4.86}$$

We can now formally proclaim the Cartesian x-axis to be an arbitrary linear axis (direction) in space and the contour C to be an arbitrarily shaped differentially small contour bounding a surface ΔS, as shown in Fig. 4.24, and write

alternative definition of the curl

$$\boxed{\hat{\mathbf{n}}\cdot\operatorname{curl}\mathbf{B} = \lim_{\Delta S\to 0}\frac{\oint_C \mathbf{B}\cdot d\mathbf{l}}{\Delta S},} \tag{4.87}$$

where $\hat{\mathbf{n}}$ is the unit vector normal to the surface ΔS ($\Delta\mathbf{S} = \Delta S\hat{\mathbf{n}}$) and determined using the right-hand rule. Eq. (4.87) is an equivalent mathematical definition of the curl of a vector. It enables us to obtain a component of the curl of $\mathbf{B}$ along a desired direction at a given point by computing the circulation of $\mathbf{B}$ along a contour in the plane perpendicular to that direction as the contour shrinks to zero about the point. The circulation of $\mathbf{B}$ about C, per unit area, appearing on the right-hand side of Eq. (4.87) equals $\hat{\mathbf{n}}\cdot\operatorname{curl}\mathbf{B} = |\operatorname{curl}\mathbf{B}|\cos\alpha$ ($|\hat{\mathbf{n}}| = 1$). Therefore, for the orientation of $\Delta\mathbf{S}$ defined by $\alpha = 0$, we get the maximum in the circulation ($\cos\alpha = 1$), and Eq. (4.87) becomes

physical meaning of the curl

$$\boxed{|\operatorname{curl}\mathbf{B}| = \left(\lim_{\Delta S\to 0}\frac{\oint_C \mathbf{B}\cdot d\mathbf{l}}{\Delta S}\right)_{\max} \qquad (\alpha = 0).} \tag{4.88}$$

This means that (1) the magnitude of $\operatorname{curl}\mathbf{B}$ equals the maximum (as the direction of the surface element $\Delta\mathbf{S} = \Delta S\hat{\mathbf{n}}$ is varied) net circulation of $\mathbf{B}$ per unit area with the area of the surface element tending to zero and (2) the direction of $\operatorname{curl}\mathbf{B}$ is in the direction that gives the maximum value for the magnitude of the net circulation per unit area ($\alpha = 0$). From it, we may regard the curl of a vector field (not only the magnetostatic field) physically as a measure of those local sources of the field at a point in space which produce circular field components with respect to that point. We recall that the divergence is a measure of sources that produce radial field components with respect to the point [Eq. (1.172)]. Ampère's law tells us that the sources producing locally circular field components in the case of the magnetostatic

field in free space are elemental currents of intensities $\mathbf{J}\,\Delta S$. Quantitatively, the curl represents the surface density of such sources, and in our case this density is $\mathbf{J}$. The concept of the curl of a vector field is used in numerous applications, in many areas of science and engineering.

Replacing $\mu_0\mathbf{J}$ by $\nabla \times \mathbf{B}$ [from Eq. (4.83)] in the integral form of Ampère's law, Eq. (4.49), leads to

$$\boxed{\oint_C \mathbf{B} \cdot d\mathbf{l} = \int_S (\nabla \times \mathbf{B}) \cdot d\mathbf{S}.} \tag{4.89}$$

Stokes' theorem

Although obtained here specifically for the magnetostatic field in free space, this equation is an identity, holding for any vector field (for which the appropriate partial derivatives exist). It is widely used in electromagnetics and other areas of science and engineering, and is known as Stokes' theorem. In words, it states that the net circulation of a vector field along an arbitrary contour is the same as the net flux of its curl through any surface bounded by the contour, where the reference orientations of the contour and the surface are interconnected by the right-hand rule. We notice the parallelism with the divergence theorem, Eq. (1.173), which applies to a closed surface and relates the flux of a vector field with a volume integral of its divergence.

To prove Stokes' theorem (for an arbitrary vector field $\mathbf{B}$), imagine the surface S subdivided into a large number of differentially small patches ΔS_i ($\Delta S_i \to 0$) which are bounded by infinitesimal contours C_i, as depicted in Fig. 4.25. By applying the definition of the curl in Eq. (4.87) to one of these patches, we can write

$$\oint_{C_i} \mathbf{B} \cdot d\mathbf{l} = \Delta S_i\, \hat{\mathbf{n}} \cdot \operatorname{curl} \mathbf{B} = (\nabla \times \mathbf{B}) \cdot \Delta S_i \hat{\mathbf{n}} = (\nabla \times \mathbf{B}) \cdot \Delta \mathbf{S}_i. \tag{4.90}$$

Now, let us determine this circulation for every ΔS_i comprising S and sum all the results. What we get on the left-hand side of the resulting equation is the line integral of $\mathbf{B}$ along the overall contour C bounding the surface S, since the terms arising from the sides of small contours shared by any two patches cancel out during the summation, as can be seen in Fig. 4.25, and the only boundaries for which the cancelation does not occur are those forming the contour C. Hence,

$$\oint_C \mathbf{B} \cdot d\mathbf{l} = \lim_{\Delta S_i \to 0} \sum_i (\nabla \times \mathbf{B}) \cdot \Delta \mathbf{S}_i. \tag{4.91}$$

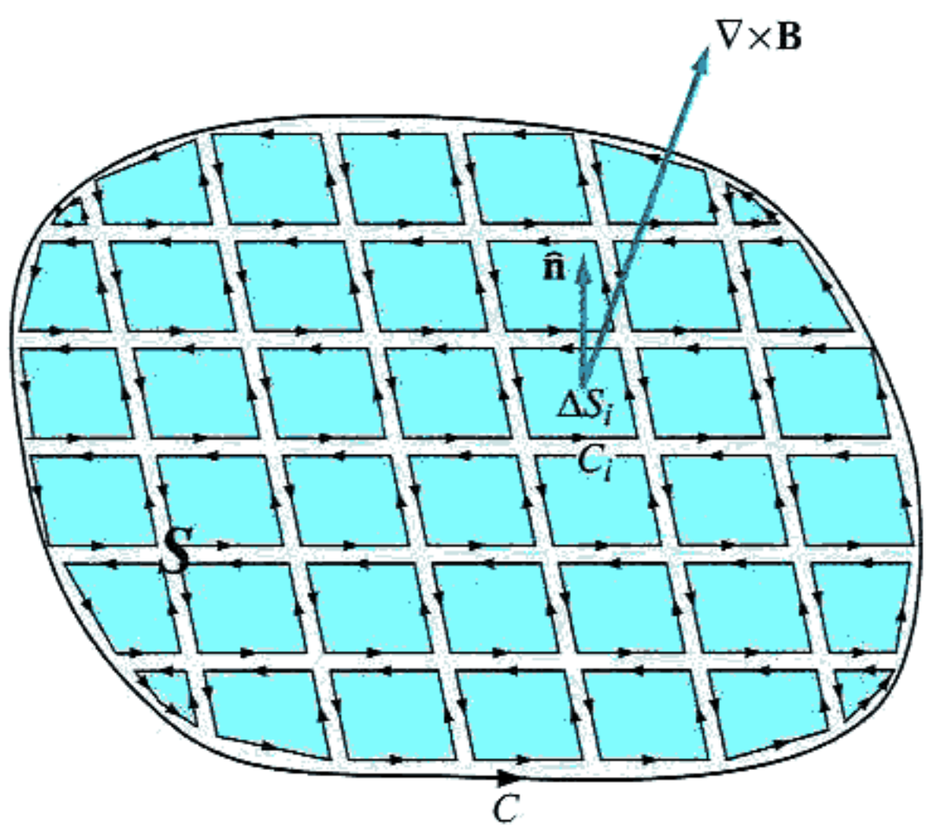

Figure 4.25 Open surface S subdivided into differentially small patches – for the proof of Stokes' theorem, Eq. (4.89).

In the limit, the summation on the right-hand side of this equation becomes an integral, $\Delta\mathbf{S}_i$ becomes $d\mathbf{S}$, and we have $\int_S (\nabla \times \mathbf{B}) \cdot d\mathbf{S}$, thus proving the theorem.

By applying Stokes' theorem to Eq. (1.75) or simply by analogy with the differential form of Ampère's law, Eq. (4.83), we arrive to the differential form of Maxwell's first equation for the electrostatic field:

curl of **E** *in electrostatics*

$$\boxed{\nabla \times \mathbf{E} = 0.} \tag{4.92}$$

We see that the electrostatic field is a curl-free or irrotational field, and this is a property of any conservative vector field (the field with zero circulation along any closed path).

Example 4.16 Cylindrical Current Conductor Using Differential Ampère's Law

Redo Example 4.9 but now using the differential form of Ampère's law.

Solution This is completely analogous to the application of the differential Gauss' law to solve an electrostatic problem with spherical symmetry in Example 1.22. For the interior of the conductor in Fig. 4.15 (where $\mathbf{J} = J\hat{\mathbf{z}}$ and $J = \text{const}$), combining Eqs. (4.53), (4.84), and (4.83), we now have in place of Eqs. (1.174) and (1.175)

$$\nabla \times \mathbf{B} = \frac{1}{r}\frac{\partial}{\partial r}[rB(r)]\hat{\mathbf{z}} = \mu_0 J\hat{\mathbf{z}} \quad \longrightarrow \quad rB(r) = \mu_0 J \int r\,dr + C_1 = \frac{\mu_0 J r^2}{2} + C_1$$

$$\longrightarrow \quad B(r) = \frac{\mu_0 J r}{2} + \frac{C_1}{r} \qquad (0 \le r < a)\,. \tag{4.93}$$

with $C_1 = 0$, since there exists no line current (of intensity I_0) along the z-axis (for $r = 0$) in Fig. 4.15 [otherwise, this constant would be $C_1 = \mu_0 I_0/(2\pi)$]. Similarly, in the surrounding space (with $\mathbf{J} = 0$),

$$\frac{\partial}{\partial r}[rB(r)] = 0 \quad \longrightarrow \quad rB(r) = C_2 \quad \longrightarrow \quad B(r) = \frac{C_2}{r} \qquad (a < r < \infty)\,. \tag{4.94}$$

where $C_2 = \mu_0 J a^2/2$, from $B(a^-) = B(a^+)$. Both Eqs. (4.93) and (4.94) give the same corresponding results as in Eq. (4.56).

Problems: 4.20–4.24; *Conceptual Questions* (on Companion Website): 4.16 and 4.17; *MATLAB Exercises* (on Companion Website).

4.8 LAW OF CONSERVATION OF MAGNETIC FLUX

As vector **B** is called the magnetic flux density vector, its flux through a surface S is called, accordingly, the magnetic flux. It is denoted as Φ,

magnetic flux (unit: Wb)

$$\boxed{\Phi = \int_S \mathbf{B} \cdot d\mathbf{S},} \tag{4.95}$$

and measured in webers (Wb), where $\text{Wb} = \text{T} \cdot \text{m}^2$. We recall that the electric flux, Ψ, is defined as the flux of the electric flux density vector, **D**, through a designated surface [Eq. (2.42)], and that the unit for Ψ is C.

The generalized Gauss' law, Eq. (2.43), tells us that the net outward electric flux through a closed surface is equal to the total charge enclosed by the surface. Our analogy between electric and magnetic fields naturally imposes a question: what

HISTORICAL ASIDE

Sir George Gabriel Stokes (1819–1903), a British mathematician and physicist, was a professor of mathematics at Cambridge University. Stokes was the oldest of the trio of Cambridge professors, James Clerk Maxwell (1831–1879) and Lord Kelvin (1824–1907) being the other two, who especially contributed to the fame of the Cambridge school of mathematical physics in the 19th century. His main contributions were in the areas of viscous fluids, sound, light, spectroscopy, fluorescence, and X rays. During a period of time, he held the post of the Lucasian Chair of Mathematics at Cambridge, was University's Member of Parliament, and President of the Royal Society, the three offices that had only once before been held by one person, Sir Isaac Newton (1642–1727).

Wilhelm Eduard Weber (1804–1891), a German physicist, was a professor at Göttingen University. Weber received his doctoral dissertation from the University of Halle in 1826, with a topic on the acoustic theory of reed organ pipes, and was appointed professor of physics at Göttingen in 1831. In collaboration with Karl Friedrich Gauss (1777–1855), he built the first practically useful telegraph (3 km long) in 1833, to connect his physics laboratory with Gauss' astronomical observatory at Göttingen. They also worked together on investigating terrestrial magnetism (earth's magnetic field). From 1836 to 1841, they organized a network of observation stations around the world to correlate measurements of terrestrial magnetism at different locations. In 1841, he developed the electrodynamometer, which could precisely measure the angular displacement of a coil with a current caused by another coil positioned perpendicularly to it and carrying the same current. Weber used this instrument for a final validation of Ampère's previous conclusions about magnetic forces due to currents in wire loops (in the coils). Furthermore, it was used, in the same or similar realizations, by many researchers and students over decades both to directly measure the magnetic forces and torques due to given currents and to determine (indirectly measure) the (unknown) current from the measured torque (as a sort of ammeter). During his later years at Göttingen, Weber worked on a theoretical generalization and unification of laws describing forces between charges at rest (Coulomb's law) and in motion (Ampère's force law), as well as Faraday's law of electromagnetic induction for time-varying currents (charges in accelerated motion). He also contributed to understanding the connection between light and electromagnetic phenomena and establishing the link between electromagnetism and optics, which was crucial for Maxwell's development of electromagnetic field theory (that includes light). Working again jointly with Gauss, Weber provided a significant impact in the early stage of the development of a new coherent system of units to also include electromagnetic phenomena, which gradually evolved into the present International System of Units (SI). The SI includes the weber, unit of magnetic flux, named in his honor. *(Portrait: AIP Emilio Segrè Visual Archives, Brittle Books Collection)*

is the net magnetic flux through a closed surface equal to? The answer is: zero. To prove this, we consider first the magnetic flux density $d\mathbf{B}$ of a single current element $\mathbf{J}\,dv$ in free space, as depicted in Fig. 4.26. From the Biot-Savart law and the expression for $d\mathbf{B}$ in Eq. (4.6), we know that the lines of this field are circles centered on the straight line containing the current element (Fig. 4.26). We can imagine the entire space surrounding the element divided into thin closed tubes of uniform cross section formed by bunches of field lines, where one such tube is shown in Fig. 4.26. According to Eq. (4.6), again, the magnitude of the magnetic

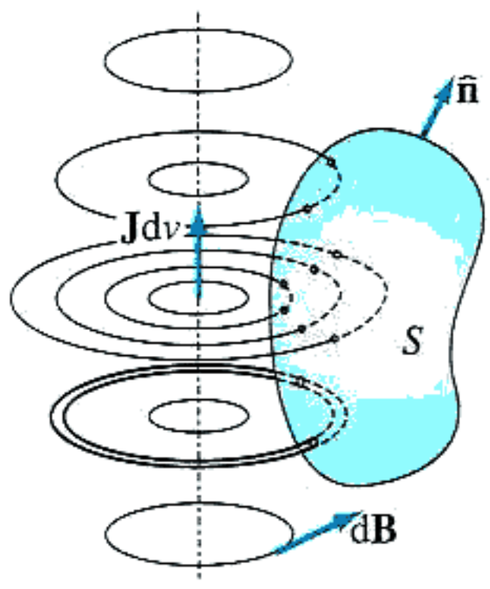

Figure 4.26 For the derivation of the law of conservation of magnetic flux.

flux density vector is constant along each field line, and thus over the entire volume of each tube (because the tubes are thin). Consequently, the magnetic flux through any tube is the same in magnitude at any cross section of the tube, regardless of whether that cross section is perpendicular to the tube axis or not.

Imagine now an arbitrary closed surface S in the field, Fig. 4.26. Some of the elementary tubes pass through S, but always an even number of times. Therefore, the net outward flux of $\mathrm{d}\mathbf{B}$ through all small surfaces representing intersections of thin tubes and the surface S equals zero. Since such intersections cover the entire surface S, we have

$$\oint_S \mathrm{d}\mathbf{B} \cdot \mathrm{d}\mathbf{S} = 0. \tag{4.96}$$

Our proof continues then by invoking the superposition principle, by means of which the actual magnetic flux density $\mathbf{B}$ of an arbitrary current distribution in free space can be decomposed into elementary flux densities $\mathrm{d}\mathbf{B}$ due to individual current elements making the current distribution, so that

$$\mathbf{B} = \int_{v_{\mathrm{cur}}} \mathrm{d}\mathbf{B}, \tag{4.97}$$

where v_{cur} is the domain with currents (sources of the magnetic field). Applying the integration over v_{cur} as an operator to Eq. (4.96), and interchanging the order of integral signs, we obtain

$$\oint_S \left(\int_{v_{\mathrm{cur}}} \mathrm{d}\mathbf{B} \right) \cdot \mathrm{d}\mathbf{S} = 0. \tag{4.98}$$

Finally, substituting Eq. (4.97),

law of conservation of magnetic flux

$$\boxed{\oint_S \mathbf{B} \cdot \mathrm{d}\mathbf{S} = 0,} \tag{4.99}$$

which completes our proof. This relation is known as the law of conservation of magnetic flux, and also as Maxwell's fourth equation. For obvious reasons, it is sometimes referred to as Gauss' law for the magnetic field. Together with Ampère's law (Maxwell's second equation), it forms a complete set of Maxwell's equations for the magnetostatic field in free space (or any nonmagnetic medium). We notice that the law of conservation of magnetic flux has the identical form as the continuity equation for steady currents, Eq. (3.40).

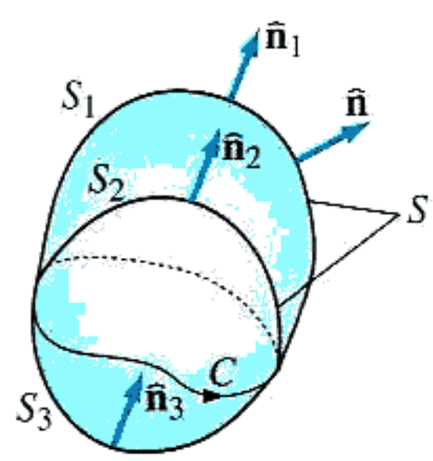

Figure 4.27 For the proof that the magnetic flux through a contour is unique.

Consider next an arbitrary contour C and two open surfaces, S_1 and S_2, with arbitrary shape that are both bounded by the contour and oriented in the same way – according to the right-hand rule with respect to the orientation of the contour, as shown in Fig. 4.27. The magnetic fluxes through the surfaces are

$$\Phi_1 = \int_{S_1} \mathbf{B} \cdot \mathrm{d}\mathbf{S} \quad \text{and} \quad \Phi_2 = \int_{S_2} \mathbf{B} \cdot \mathrm{d}\mathbf{S}, \tag{4.100}$$

respectively. The total outward flux through the closed surface S formed by S_1 and S_2 ($S = S_1 \cup S_2$) is

$$\oint_S \mathbf{B} \cdot \mathrm{d}\mathbf{S} = \Phi_1 - \Phi_2, \tag{4.101}$$

which is zero, from the law of conservation of magnetic flux. Hence,

flux through a contour, Fig. 4.27

$$\boxed{\Phi_1 = \Phi_2,} \tag{4.102}$$

meaning that the magnetic flux through any number of surfaces of arbitrary shape that all have a common contour bounding them is the same, provided that all the

surfaces are oriented in the same way. This enables us to link the flux to a contour rather than to a surface bounded by the contour (and there is an infinite number of such surfaces), and to use the term flux through a contour or flux linked by a contour. In other words, the flux (through a contour) is uniquely determined by the shape of a contour and by its orientation, and is the same for any surface spanned over the contour and oriented in accordance to the right-hand rule with respect to the orientation of the contour.

By analogy with the differential form of the continuity equation for steady currents, Eq. (3.41), the law of conservation of magnetic flux in differential form is given by

$$\boxed{\nabla \cdot \mathbf{B} = 0.} \tag{4.103}$$

flux conservation law in differential form

We see that the **B** field is another divergenceless (divergence-free) or solenoidal vector field. This means that there cannot be local sources of radial magnetic field components with respect to a point, i.e., that there exist no positive or negative "magnetic charges" and no free north or south magnetic poles, which would correspond to electric charges, with density ρ [Eq. (1.166)]. Equivalently, the magnetic field lines close upon themselves, as there are no "magnetic charges" for the lines to begin and terminate on.

We can now summarize the two Maxwell's differential equations governing the electrostatic field in free space,

$$\boxed{\nabla \times \mathbf{E} = 0 \quad \text{and} \quad \nabla \cdot \mathbf{E} = \frac{\rho}{\varepsilon_0},} \tag{4.104}$$

conservative field

and those for the magnetostatic field in free space,

$$\boxed{\nabla \times \mathbf{B} = \mu_0 \mathbf{J} \quad \text{and} \quad \nabla \cdot \mathbf{B} = 0,} \tag{4.105}$$

solenoidal field

which, in a condensed form, shows all the similarities and fundamental differences between the two fields.

Problems: 4.25 and 4.26; *Conceptual Questions* (on Companion Website): 4.18–4.23; *MATLAB Exercises* (on Companion Website).

4.9 MAGNETIC VECTOR POTENTIAL

In electrostatics, we introduced the electric scalar potential (V) to help us describe electric fields and evaluate the electric field intensity vector (**E**). The electric scalar potential due to a point charge Q, as an elementary source of the electric field, in free space is [Eq. (1.80)]

$$V = \frac{1}{4\pi\varepsilon_0}\frac{Q}{R}. \tag{4.106}$$

Following the analogy established in connection with Eq. (4.4), which is the basis of the Biot-Savart law, the potential due to an elementary source of the magnetostatic field, $Q\mathbf{v}$, is defined as

$$\boxed{\mathbf{A} = \frac{\mu_0}{4\pi}\frac{Q\mathbf{v}}{R}.} \tag{4.107}$$

magnetic vector potential (unit: T · m)

This quantity is called the magnetic vector potential, and its unit is T · m. It is a vector whose direction is very simple to determine – the same as the direction of $Q\mathbf{v}$, and whose magnitude is proportional to $1/R$ (and not to $1/R^2$, which is present in

the expression for **B** due to $Q\mathbf{v}$). By the same reasoning as with obtaining the three versions of the Biot-Savart law for volume, surface, and line currents, Eqs. (4.7)–(4.9), the corresponding integral expressions for the magnetic vector potential are:

A due to volume current

$$\mathbf{A} = \frac{\mu_0}{4\pi}\int_v \frac{\mathbf{J}\,\mathrm{d}v}{R}, \tag{4.108}$$

A due to surface current

$$\mathbf{A} = \frac{\mu_0}{4\pi}\int_S \frac{\mathbf{J}_s\,\mathrm{d}S}{R}, \tag{4.109}$$

A due to line current

$$\mathbf{A} = \frac{\mu_0}{4\pi}\int_l \frac{I\,\mathrm{d}\mathbf{l}}{R}. \tag{4.110}$$

In general, the solutions for the magnetic vector potential due to given current distributions are substantially simpler than the corresponding solutions for the magnetic flux density vector.

Let us find the curl of **A**. By representing the expression in Eq. (4.107) in the spherical coordinate system shown in Fig. 4.28, in which Q is at the coordinate origin, so $R = r$ (r being the radial spherical coordinate), and $\mathbf{v}$ is z-directed,

$$\mathbf{A} = A\,\hat{\mathbf{z}} = A\cos\theta\,\hat{\mathbf{r}} - A\sin\theta\,\hat{\boldsymbol{\theta}} = A_r\hat{\mathbf{r}} + A_\theta\hat{\boldsymbol{\theta}}, \quad A = \frac{\mu_0 Q v}{4\pi r}, \tag{4.111}$$

where

$$A_r = A\cos\theta = \frac{\mu_0 Q v\cos\theta}{4\pi r}, \qquad A_\theta = -A\sin\theta = -\frac{\mu_0 Q v\sin\theta}{4\pi r} \tag{4.112}$$

($A_\phi = 0$). Using the expression for the curl in spherical coordinates, Eq. (4.85), we have

$$\begin{aligned}\nabla\times\mathbf{A} &= \frac{1}{r}\left[\frac{\partial}{\partial r}(rA_\theta) - \frac{\partial A_r}{\partial\theta}\right]\hat{\boldsymbol{\phi}}\\ &= \frac{\mu_0 Q v}{4\pi r}\left[\frac{\partial}{\partial r}(-\sin\theta) - \frac{\partial}{\partial\theta}\left(\frac{\cos\theta}{r}\right)\right]\hat{\boldsymbol{\phi}} = \frac{\mu_0 Q v\sin\theta}{4\pi r^2}\,\hat{\boldsymbol{\phi}}.\end{aligned} \tag{4.113}$$

Noting that (Fig. 4.28)

$$Q\mathbf{v}\times\hat{\mathbf{r}} = Qv\,\hat{\mathbf{z}}\times\hat{\mathbf{r}} = Qv\,|\hat{\mathbf{z}}\times\hat{\mathbf{r}}|\,\hat{\boldsymbol{\phi}} = Qv\sin\theta\,\hat{\boldsymbol{\phi}}, \tag{4.114}$$

we obtain

$$\nabla\times\mathbf{A} = \frac{\mu_0}{4\pi}\frac{Q\mathbf{v}\times\hat{\mathbf{r}}}{r^2}, \tag{4.115}$$

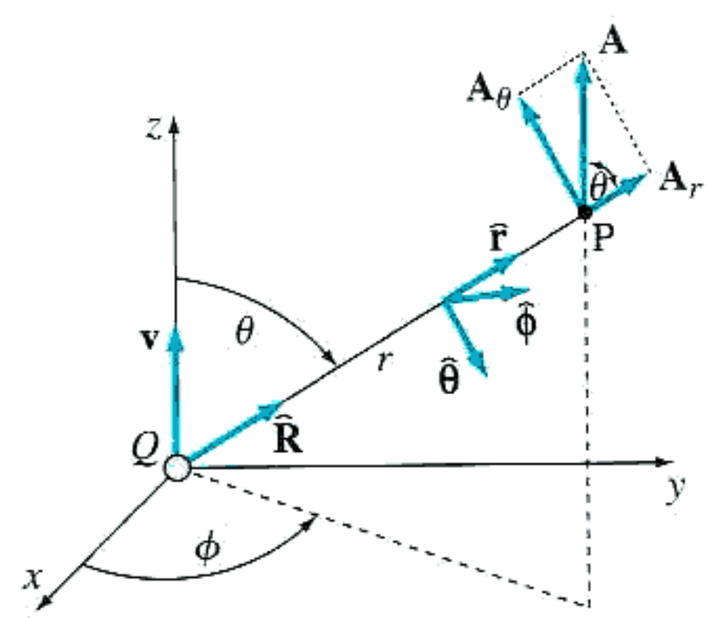

Figure 4.28 Magnetic vector potential due to a point charge moving in free space, and its components in a spherical coordinate system.

which is exactly the magnetic flux density vector due to $Q\mathbf{v}$, Eq. (4.4) with $R = r$ and $\hat{\mathbf{R}} = \hat{\mathbf{r}}$. Hence,

$$\boxed{\mathbf{B} = \nabla \times \mathbf{A},} \tag{4.116}$$

magnetic flux density from potential

and the same is true for the magnetic vector potential $\mathrm{d}\mathbf{A}$ due to an arbitrary volume, surface, or line current element, Eq. (4.10). Integrating the expression $\nabla \times \mathrm{d}\mathbf{A}$ over a domain v with volume currents, we have

$$\int_v (\nabla \times \mathrm{d}\mathbf{A}) = \nabla \times \left(\int_v \mathrm{d}\mathbf{A}\right) = \nabla \times \mathbf{A}, \tag{4.117}$$

where the integration and differentiation (del) operators can readily interchange places because they are completely independent – the integration is performed with respect to the coordinates of the source point (point at which the current density vector is $\mathbf{J}$), while the differentiation is carried out with respect to the coordinates of the field point (point at which the magnetic vector potential is $\mathbf{A}$). Consequently, the magnetic flux density vector ($\mathbf{B}$) and the magnetic vector potential ($\mathbf{A}$) due to an arbitrary volume current distribution, Eq. (4.108), are related at an arbitrary point in space as in Eq. (4.116), and similar proofs can be carried out for the magnetic potential due to surface currents, Eq. (4.109), and line currents, Eq. (4.110). This relationship, in conjunction with Eqs. (4.108)–(4.110), provides an alternative general method for evaluating the $\mathbf{B}$ field produced by steady currents, where $\mathbf{A}$ is evaluated first by integration, and then $\mathbf{B}$ is found from the potential by differentiation. Potentials, generally, are auxiliary quantities that are used to determine fields indirectly. Finally, we note that, contrary to V in electrostatics, $\mathbf{A}$ does not have any simple physical interpretation in magnetostatics.

On the other side, the divergence of the magnetostatic potential $\mathbf{A}$ is always zero, which is, essentially, a consequence of the steady current density $\mathbf{J}$ being a divergenceless vector, i.e., of the continuity equation in Eq. (3.41) or (3.40). Namely, in analogy to Eq. (4.117), we can apply the divergence operator to the integral expression in Eq. (4.108) and write

$$\nabla \cdot \mathbf{A} = \frac{\mu_0}{4\pi} \nabla \cdot \left(\int_v \frac{\mathbf{J}\,\mathrm{d}v}{R}\right) = \frac{\mu_0}{4\pi} \int_v \nabla \cdot \left(\frac{\mathbf{J}}{R}\right) \mathrm{d}v = \frac{\mu_0}{4\pi} \oint_S \frac{\mathbf{J}}{R} \cdot \mathrm{d}\mathbf{S}, \tag{4.118}$$

where S is the closed surface bounding v, and the use is made of the divergence theorem, Eq. (1.173), to convert the volume integral to a surface (flux) one. For the special case when v is a spherical domain centered at the field point (where the potential is being computed), $1/R$ can be brought out of the flux integral, as S in that case is a spherical surface of radius R, and the integral, in turn, becomes zero, $\oint_S \mathbf{J} \cdot \mathrm{d}\mathbf{S} = 0$, by virtue of the continuity equation, Eq. (3.40). In the general case, the arbitrary domain v can be subdivided into a stack of concentric spherical layers with each of them being a part of a full spherical shell of thickness $\mathrm{d}R$ centered at the field point, with the current of density $\mathbf{J}$ flowing through that part and no current in the rest of the shell, outside v. The same conclusion about a zero flux integral based on the continuity equation can then be derived for the surface of each shell, and thus

$$\boxed{\nabla \cdot \mathbf{A} = 0,} \tag{4.119}$$

divergence of $\mathbf{A}$ due to steady currents

which holds true for the magnetic potential due to surface and line steady currents as well.

The magnetic flux through an arbitrary contour, Eq. (4.95), can now be expressed in terms of the magnetic vector potential,

$$\Phi = \int_S \mathbf{B} \cdot d\mathbf{S} = \int_S (\nabla \times \mathbf{A}) \cdot d\mathbf{S}, \tag{4.120}$$

which, by using Stokes' theorem, Eq. (4.89), becomes

magnetic flux from the potential

$$\boxed{\Phi = \oint_C \mathbf{A} \cdot d\mathbf{l}.} \tag{4.121}$$

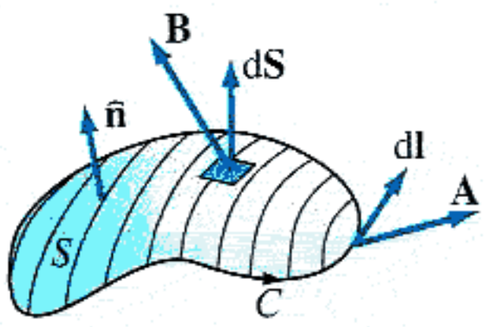

Figure 4.29 For the evaluation of the magnetic flux through a surface by integrating the magnetic vector potential along its boundary.

The orientation of the contour C and the surface S are in accordance to the right-hand rule, as shown in Fig. 4.29. Eq. (4.121) represents a means for determining the magnetic flux by evaluating a contour integral (of $\mathbf{A}$) rather than a surface integral (of $\mathbf{B}$), which is very convenient in some computations and derivations. Note that this is yet another proof that the magnetic flux through a contour is unique (the same for all surfaces bounded by C).

Problems: 4.27; *Conceptual Questions* (on Companion Website): 4.24 and 4.25; *MATLAB Exercises* (on Companion Website).

4.10 PROOF OF AMPÈRE'S LAW

We are now ready to prove Ampère's law by utilizing the magnetic vector potential, $\mathbf{A}$. On the left-hand side of the differential form of the law, Eq. (4.83), we have, by means of Eq. (4.116),

$$\nabla \times \mathbf{B} = \nabla \times (\nabla \times \mathbf{A}). \tag{4.122}$$

Applying formally (symbolically) the vector identity for expanding the vector triple product,[6]

$$\mathbf{a} \times (\mathbf{b} \times \mathbf{c}) = \mathbf{b}(\mathbf{a} \cdot \mathbf{c}) - \mathbf{c}(\mathbf{a} \cdot \mathbf{b}), \tag{4.123}$$

to the product $\nabla \times (\nabla \times \mathbf{A})$, we get the following identity for expanding the curl of the curl of an arbitrary vector field ($\mathbf{A}$):

$$\nabla \times (\nabla \times \mathbf{A}) = \nabla(\nabla \cdot \mathbf{A}) - (\nabla \cdot \nabla)\mathbf{A} = \nabla(\nabla \cdot \mathbf{A}) - \nabla^2 \mathbf{A}. \tag{4.124}$$

The first term in this expansion is grad(div $\mathbf{A}$), and in our case it is zero, because div $\mathbf{A} = \nabla \cdot \mathbf{A} = 0$ [Eq. (4.119)]. With this, Eq. (4.122) becomes

$$\nabla \times \mathbf{B} = -\nabla^2 \mathbf{A}. \tag{4.125}$$

Vector $\nabla^2 \mathbf{A}$ is called the Laplacian of the vector function $\mathbf{A}$, which, having in mind Eq. (1.100), can be written in Cartesian coordinates as

$$\nabla^2 \mathbf{A} = (\nabla \cdot \nabla)\mathbf{A} = \left(\frac{\partial^2}{\partial x^2} + \frac{\partial^2}{\partial y^2} + \frac{\partial^2}{\partial z^2} \right) (A_x \hat{\mathbf{x}} + A_y \hat{\mathbf{y}} + A_z \hat{\mathbf{z}})$$

[6] A cross (vector) product of a vector ($\mathbf{a}$) with a cross product of two (other) vectors ($\mathbf{b}$ and $\mathbf{c}$) is called the vector triple product. Note also that the vector triple product identity in Eq. (4.123) is known as the "bac-cab" or "back-cab" identity, as the word "bac-cab" can be read on the right-hand side of the equation.

$$= \left(\frac{\partial^2 A_x}{\partial x^2} + \frac{\partial^2 A_x}{\partial y^2} + \frac{\partial^2 A_x}{\partial z^2}\right)\hat{\mathbf{x}} + \left(\frac{\partial^2 A_y}{\partial x^2} + \frac{\partial^2 A_y}{\partial y^2} + \frac{\partial^2 A_y}{\partial z^2}\right)\hat{\mathbf{y}}$$
$$+ \left(\frac{\partial^2 A_z}{\partial x^2} + \frac{\partial^2 A_z}{\partial y^2} + \frac{\partial^2 A_z}{\partial z^2}\right)\hat{\mathbf{z}}. \tag{4.126}$$

We see that Cartesian components of the Laplacian of $\mathbf{A}$ equal the Laplacian of the corresponding components of $\mathbf{A}$, where the latter operator is the Laplacian of a scalar field, Eq. (2.94), and hence[7]

$$\boxed{\nabla^2 \mathbf{A} = \nabla^2 A_x\,\hat{\mathbf{x}} + \nabla^2 A_y\,\hat{\mathbf{y}} + \nabla^2 A_z\,\hat{\mathbf{z}}.} \tag{4.127}$$

Laplacian of a vector in Cartesian coordinates

From Eq. (4.108),

$$\mathbf{A} = A_x\,\hat{\mathbf{x}} + A_y\,\hat{\mathbf{y}} + A_z\,\hat{\mathbf{z}} = \frac{\mu_0}{4\pi}\int_v \frac{(J_x\,\hat{\mathbf{x}} + J_y\,\hat{\mathbf{y}} + J_z\,\hat{\mathbf{z}})\,\mathrm{d}v}{R}$$
$$= \frac{\mu_0}{4\pi}\left(\hat{\mathbf{x}}\int_v \frac{J_x\,\mathrm{d}v}{R} + \hat{\mathbf{y}}\int_v \frac{J_y\,\mathrm{d}v}{R} + \hat{\mathbf{z}}\int_v \frac{J_z\,\mathrm{d}v}{R}\right), \tag{4.128}$$

and we conclude that each Cartesian component of $\mathbf{A}$ is actually produced by the same component of the current density vector, namely, A_x is produced by J_x, and so on. Recalling the expression for the electric scalar potential due to a volume charge in free space, Eq. (1.82), we identify the duality between V due to ρ and A_x due to J_x:

$$V = \frac{1}{4\pi\varepsilon_0}\int_v \frac{\rho\,\mathrm{d}v}{R} \quad \longleftrightarrow \quad A_x = \frac{\mu_0}{4\pi}\int_v \frac{J_x\,\mathrm{d}v}{R}. \tag{4.129}$$

By the same duality principle, in turn, there must be a differential equation for A_x which has the same form as the differential equation for V, that is, Poisson's equation [Eq. (2.93)]. Therefore, by changing the variables, we get

$$\nabla^2 V = -\frac{\rho}{\varepsilon_0} \quad \longleftrightarrow \quad \nabla^2 A_x = -\mu_0 J_x. \tag{4.130}$$

Similarly,

$$\nabla^2 A_y = -\mu_0 J_y \quad \text{and} \quad \nabla^2 A_z = -\mu_0 J_z, \tag{4.131}$$

and substituting all these back in Eq. (4.127),

$$\boxed{\nabla^2 \mathbf{A} = -\mu_0 \mathbf{J}.} \tag{4.132}$$

vector Poisson's equation

This is a second-order vector partial differential equation (PDE) for the magnetic vector potential of a volume current in free space (or any nonmagnetic medium), usually referred to as the vector Poisson's equation. It can be used as a starting point in solving (analytically or numerically) for $\mathbf{A}$ due to a given current distribution $\mathbf{J}$. We use it here for deriving Ampère's law. Namely, returning to Eq. (4.125), we can now substitute for the Laplacian of $\mathbf{A}$ and obtain

$$\nabla \times \mathbf{B} = -\nabla^2 \mathbf{A} = \mu_0 \mathbf{J}. \tag{4.133}$$

[7]Note that the expansion in Eq. (4.127) does not have equally simple counterparts in cylindrical and spherical coordinate systems (Figs. 1.25 and 1.26). In these systems, the Laplacian of a vector function ($\mathbf{A}$), $\nabla^2\mathbf{A}$, is computed, from Eq. (4.124), as $\nabla^2\mathbf{A} = \nabla(\nabla\cdot\mathbf{A}) - \nabla\times(\nabla\times\mathbf{A}) = \text{grad}(\text{div}\,\mathbf{A}) - \text{curl}\,(\text{curl}\,\mathbf{A})$, namely, as the gradient of the divergence of $\mathbf{A}$ minus the curl of the curl of $\mathbf{A}$, using the expressions for the gradient, divergence, and curl in Eqs. (1.105), (1.108), (1.170), (1.171), (4.84), and (4.85).

which is Eq. (4.83), and this completes our proof of the Ampère's law in differential form. Stokes' theorem, Eq. (4.89), which is derived from the mathematical definition of the curl of a vector, gives its integral equivalent, Eq. (4.49).

Note that the proof carried out in this section is essentially based on the concept of the magnetic vector potential, which is defined by Eq. (4.107) and related to the magnetic flux density vector by Eq. (4.116). This latter relation is obtained from Eq. (4.4), which is the rudimentary version of the Biot-Savart law. This means that we have, in fact, derived Ampère's law from the Biot-Savart law.

4.11 MAGNETIC DIPOLE

A small loop with a steady current constitutes the magnetic equivalent of the electric dipole of Fig. 1.28, and is referred to as a magnetic dipole. The reason for this and what we mean by "small" will soon be evident. A magnetic dipole is characterized by its magnetic moment, defined as

magnetic dipole moment

$$\boxed{\mathbf{m} = I\mathbf{S},} \tag{4.134}$$

where I is the current intensity of the loop and $\mathbf{S} = S\hat{\mathbf{n}}$ is the loop surface area vector, oriented in accordance to the right-hand rule with respect to the reference direction of the current. Note that $\mathbf{m}$ is analogous to the electric dipole moment, $\mathbf{p}$, defined by Eq. (1.116). The unit for $\mathbf{m}$ is $\mathrm{A} \cdot \mathrm{m}^2$.

We would like to find the expressions for the magnetic vector potential and the magnetic flux density vector due to a magnetic dipole at large distances compared with the loop dimensions. To this end, we consider a rectangular loop with sides a and b, shown in Fig. 4.30. Let the axis of the loop coincide with the z-axis of a spherical coordinate system and the center of the loop be located at the origin of the system. Far away from the loop ($r \gg a, b$), the loop is observed as being small and the magnetic vector potential of the loop can be evaluated as that due to four line current elements, given by $I\mathbf{a}$, $I\mathbf{b}$, $I(-\mathbf{a})$, and $I(-\mathbf{b})$, using Eq. (4.110). Let us first calculate the potential at a point P due to the pair of parallel elements of length a, Fig. 4.30,

$$\mathbf{A}_{aa} = \mathbf{A}_1 + \mathbf{A}_2 = \frac{\mu_0}{4\pi}\frac{I\mathbf{a}}{r_1} + \frac{\mu_0}{4\pi}\frac{I(-\mathbf{a})}{r_2} = \frac{\mu_0 I\mathbf{a}}{4\pi}\left(\frac{1}{r_1} - \frac{1}{r_2}\right), \tag{4.135}$$

where r_1 and r_2 are the distances of the point P from the centers of the first and second element, respectively. Noting that the position vector of the first element with respect to the second element is $\mathbf{d} = -\mathbf{b}$, we can now use the same approximations

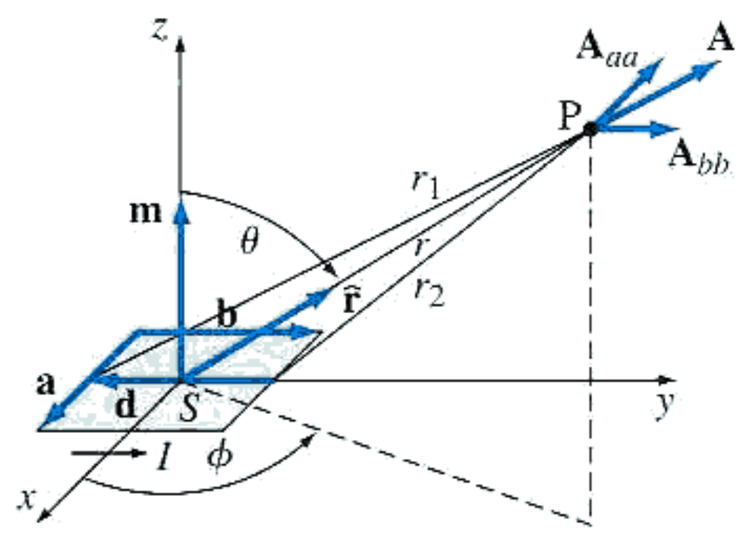

Figure 4.30 Magnetic dipole.

as in deriving Eq. (1.115) for an electric dipole, with which Eq. (4.135) becomes

$$\mathbf{A}_{aa} \approx \frac{\mu_0 I \mathbf{a}}{4\pi} \frac{\mathbf{d} \cdot \hat{\mathbf{r}}}{r^2} = -\frac{\mu_0 I \mathbf{a}(\mathbf{b} \cdot \hat{\mathbf{r}})}{4\pi r^2}. \tag{4.136}$$

Similarly, the potential due to the other pair of elements, those of length b, is given by

$$\mathbf{A}_{bb} \approx \frac{\mu_0 I \mathbf{b}(\mathbf{a} \cdot \hat{\mathbf{r}})}{4\pi r^2}. \tag{4.137}$$

By superposition and using the formula for the vector triple product in Eq. (4.123), the total magnetic vector potential of the dipole turns out to be

$$\mathbf{A} = \mathbf{A}_{aa} + \mathbf{A}_{bb} = \frac{\mu_0 I}{4\pi r^2} [\mathbf{b}(\mathbf{a} \cdot \hat{\mathbf{r}}) - \mathbf{a}(\mathbf{b} \cdot \hat{\mathbf{r}})] = \frac{\mu_0 I}{4\pi r^2} (\mathbf{a} \times \mathbf{b}) \times \hat{\mathbf{r}}. \tag{4.138}$$

As the magnetic moment of the loop is (Fig. 4.30)

$$\mathbf{m} = I\mathbf{S} = Iab\,\hat{\mathbf{z}} = I\mathbf{a} \times \mathbf{b}, \tag{4.139}$$

$\mathbf{A}$ can be expressed in terms of $\mathbf{m}$ as

$$\mathbf{A} = \frac{\mu_0}{4\pi} \frac{\mathbf{m} \times \hat{\mathbf{r}}}{r^2}. \tag{4.140}$$

We see that the magnetic potential depends on the dipole magnetic moment and the position of the field point with respect to the dipole, and not on the shape of the loop, which can be arbitrary (not only rectangular). Finally, since $\mathbf{m} \times \hat{\mathbf{r}} = m \sin\theta\, \hat{\boldsymbol{\phi}}$, which directly comes from Eq. (4.114), Eq. (4.140) can be rewritten as

$$\boxed{\mathbf{A} = A_\phi \hat{\boldsymbol{\phi}} = \frac{\mu_0 m \sin\theta}{4\pi r^2} \hat{\boldsymbol{\phi}}.} \tag{4.141}$$

magnetic dipole potential

We conclude that the magnetic vector potential due to the magnetic dipole has only a ϕ-component in the spherical coordinate system, which is a function of coordinates r and θ.

The magnetic flux density vector of the dipole is now determined applying the formula for the curl in spherical coordinates, Eq. (4.85), to the expression for $\mathbf{A}$ in Eq. (4.141),

$$\boxed{\begin{aligned}\mathbf{B} = \nabla \times \mathbf{A} &= \frac{1}{r\sin\theta} \frac{\partial}{\partial\theta} (\sin\theta A_\phi)\, \hat{\mathbf{r}} - \frac{1}{r} \frac{\partial}{\partial r} (r A_\phi)\, \hat{\boldsymbol{\theta}} \\ &= \frac{\mu_0 m}{4\pi r^3} \left(2\cos\theta\, \hat{\mathbf{r}} + \sin\theta\, \hat{\boldsymbol{\theta}}\right).\end{aligned}} \tag{4.142}$$

magnetic dipole field

Comparing Eqs. (1.117) and (4.142), we observe that the $\mathbf{E}$ and $\mathbf{B}$ field of the electric and magnetic dipoles, respectively, are identical in form, so that the corresponding field lines have identical shape. However, this is true only at large distances from the dipoles (relative to their dimensions), which is illustrated in Fig. 4.31. We see that, although identical far from the sources, the normalized field lines due to the two dipoles are fundamentally different close to them; the electric field lines terminate on the two charges forming the electric dipole, whereas the magnetic field lines close upon themselves through the current loop.

We shall see in the next chapter that the concept of a magnetic dipole is fundamental for understanding the behavior of magnetic materials, much like the electric dipole was used in Chapter 2 in studying the electric field in the presence of dielectric materials. The field of a magnetic dipole, Eq. (4.142), is also used, again in

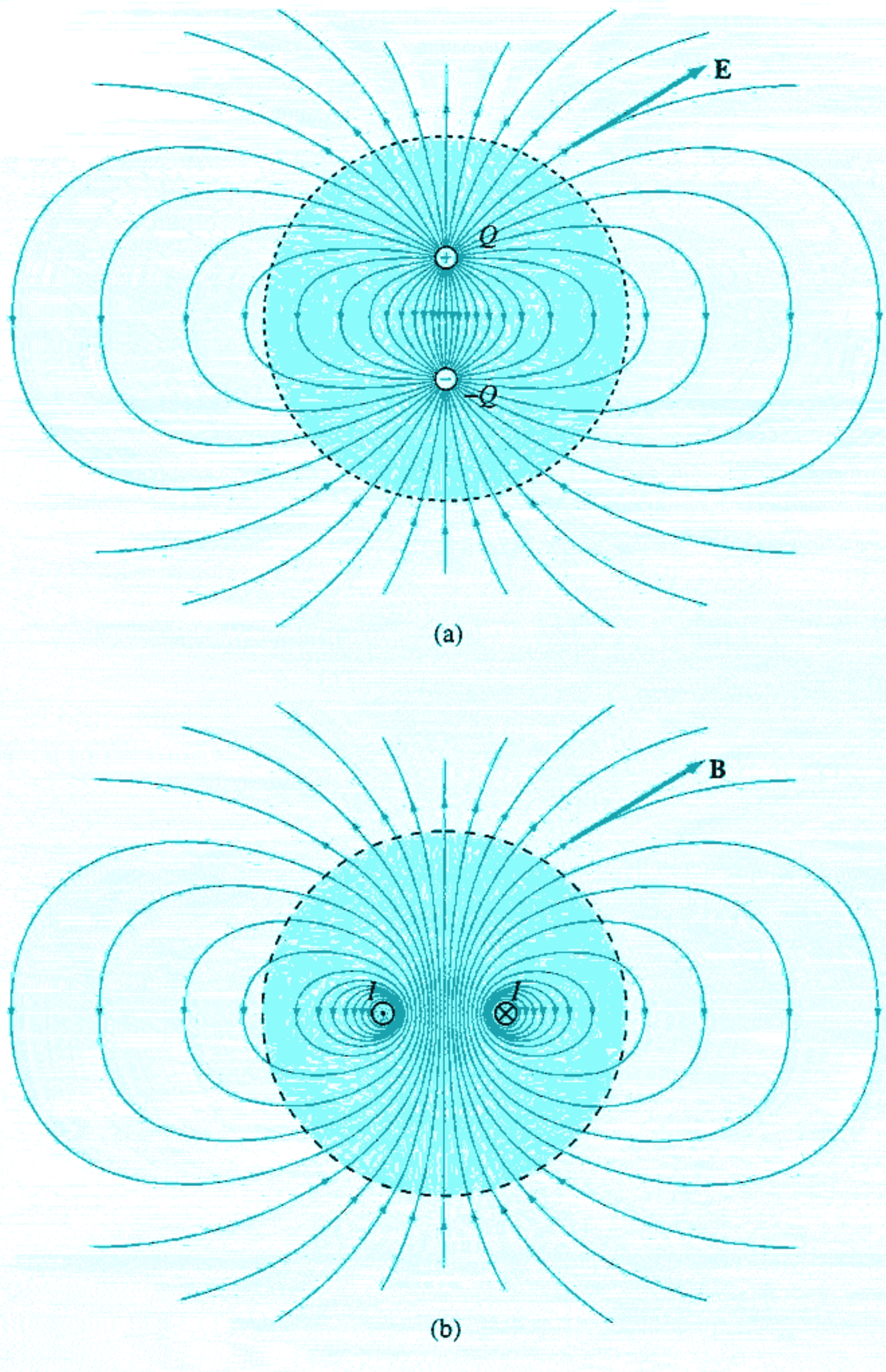

Figure 4.31 Normalized electric field lines of an electric dipole (a) and magnetic field lines of a magnetic dipole (b).

parallel to the electric field of an electric dipole, as an approximation for the static and quasistatic (low-frequency) magnetic field produced by an electrical device, which is important in EMI considerations.

Problems: 4.28–4.31; *Conceptual Questions* (on Companion Website); 4.26; *MATLAB Exercises* (on Companion Website).

4.12 THE LORENTZ FORCE AND HALL EFFECT

From the definition of the electric field intensity vector, Eq. (1.23), we have that the electric force on a point charge Q situated in an electric field of intensity $\mathbf{E}$ is

$$\boxed{\mathbf{F}_e = Q\mathbf{E}.} \tag{4.143}$$

electric force on a particle

Similarly, Eq. (4.1) tells us that the magnetic force on a point charge Q moving at a velocity $\mathbf{v}$ in a magnetic field equals

$$\boxed{\mathbf{F}_m = Q\mathbf{v} \times \mathbf{B},} \tag{4.144}$$

magnetic force on a particle

where $\mathbf{B}$ is the flux density vector of the field. Finally, the force on a moving charge due to both an electric and a magnetic field is obtained by superposition,

$$\boxed{\mathbf{F} = \mathbf{F}_e + \mathbf{F}_m = Q\mathbf{E} + Q\mathbf{v} \times \mathbf{B}.} \tag{4.145}$$

Lorentz force

This equation is known as the Lorentz force equation or law. The total (electric + magnetic = electromagnetic) force on the particle is called the Lorentz force.

An interesting and important manifestation of the motion of free charges in a material under the influence of the Lorentz force is the Hall effect, which we describe briefly here. We consider a conducting strip of width a situated in a uniform steady magnetic field of flux density vector $\mathbf{B}$ that is perpendicular to the strip, as depicted in Fig. 4.32. Let a steady current of density $\mathbf{J}$ flow through the strip. The free charges constituting the current can be positive or negative (e.g., holes and electrons in a semiconductor), and Fig. 4.32 shows both cases. Due to the magnetic force given by Eq. (4.144), the charges move (deflect) across the strip in the direction perpendicular to both $\mathbf{B}$ and $\mathbf{J}$, which results in a charge separation on the two sides of the strip. In Fig. 4.32(a), the free charges are positive ($Q > 0$), $\mathbf{v} = \mathbf{v}_d$ (drift velocity) is in the same direction as $\mathbf{J}$ [Eq. (3.11)], $\mathbf{v}_d \times \mathbf{B}$ is directed to the right, and so is $\mathbf{F}_m$; thus, the positive charges move to the right. In Fig. 4.32(b), on the other hand, the free charges are negative ($Q < 0$), $\mathbf{v}_d$ is in the direction opposite to $\mathbf{J}$, $\mathbf{v}_d \times \mathbf{B}$ is directed to the left, and $\mathbf{F}_m$ is again directed to the right (because $Q < 0$); hence, the negative charges end up at the right edge of the strip. Accumulated charges produce an electric field (of intensity $\mathbf{E}$) across the strip. This field, in turn, acts on the free charges with an electric force, Eq. (4.143), which is in the opposite direction to the magnetic force. In the equilibrium, the two forces are equal in magnitude, i.e., the Lorentz (total) force on the charges is zero,

$$\mathbf{F} = Q(\mathbf{E} + \mathbf{v}_d \times \mathbf{B}) = 0, \tag{4.146}$$

from which,

$$E = v_d B. \tag{4.147}$$

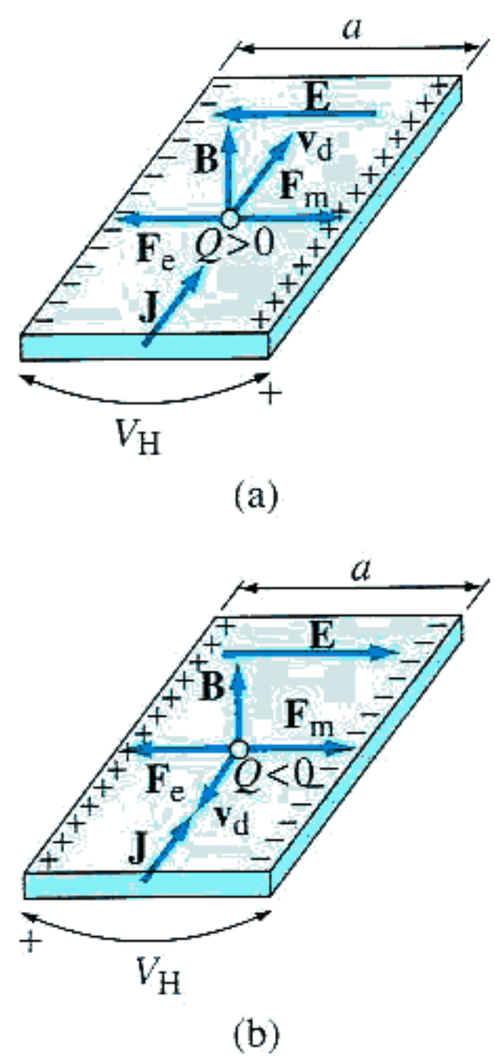

Figure 4.32 Hall effect in a material with (a) positive free charges and (b) negative free charges.

The voltage between the strip edges amounts to

$$\boxed{V_H = Ea = v_d B a.} \tag{4.148}$$

Hall voltage

This voltage is known as the Hall voltage, and the effect itself is called the Hall effect. The direction of the Hall voltage drop is different for positive and negative charges [from right to left in Fig. 4.32(a), and from left to right in Fig. 4.32(b)]. So, the polarity of the Hall voltage tells us the sign of free charge carriers in a material. Note that this represents a method for determining whether a given semiconductor is p-type or n-type.

HISTORICAL ASIDE

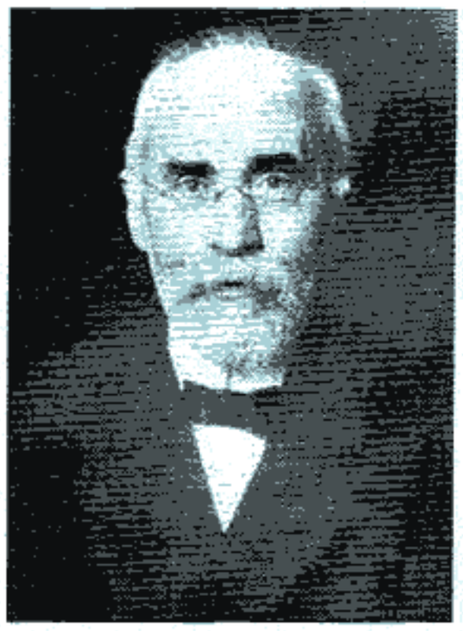

Hendrik Antoon Lorentz (1853–1928), a Dutch mathematician and physicist, a professor of mathematical physics at the University of Leiden, was the winner of the 1902 Nobel Prize in Physics. He further developed Maxwell's electromagnetic theory of light, and proposed the electron theory according to which oscillating electrons within atoms constitute miniature equivalent Hertzian radiators that emit light. In 1904, he introduced his famous Lorentz transformations (of space and time coordinates), which describe time dilation and length contraction for a body moving at velocities close to the speed of light and represent the foundation of Einstein's (1879–1955) special theory of relativity. He formulated the Lorentz force law for a moving charged particle in the presence of electric and magnetic fields. Lorentz is also the author of the so-called Lorentz-Lorenz formula, jointly with Danish physicist Ludwig Lorenz (1829–1891), who discovered it independently. The formula provides a mathematical relationship between the index of refraction (of light) and density of a medium. *(Portrait: AIP Emilio Segrè Visual Archives, Lande Collection)*

Edwin Herbert Hall (1855–1938), an American physicist, was a professor at Harvard University. He received his doctorate in physics from Johns Hopkins University under Professor Henry Augustus Rowland (1848–1901), who was one of the world's most brilliant physicist of the last quarter of the 19th century. As a part of his dissertation work, Hall pursued the question as to whether the resistance of a current-carrying conductor was affected by the presence of an external magnetic field. In experiments with guidance from Professor Rowland in 1879, he used a conductor in the form of a strip of a gold leaf mounted on a glass plate and placed it between the poles of an electromagnet such that the magnetic field lines were perpendicular to the current flow in the strip. What he observed was the development of a significant transverse electric field in the conductor and the associated voltage across the strip as the result of the applied magnetic field. Hall published his findings in the famous article "On a New Action of the Magnet on Electric Currents" in American Journal of Mathematics in November of 1879, and this phenomenon soon came to be known as the "Hall effect." He was appointed professor of physics at Harvard in 1895. *(Portrait: "Voltiana," Como, Italy - Sept. 10, 1927 issue, courtesy AIP Emilio Segrè Visual Archives)*

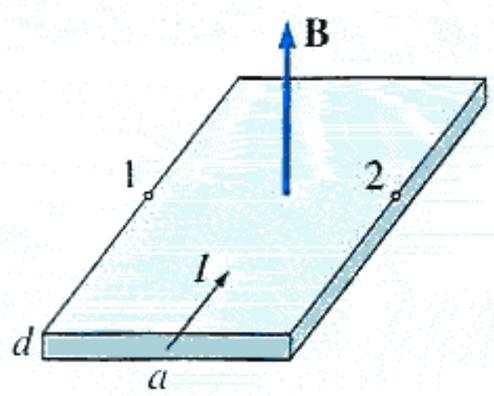

Figure 4.33 Hall element for measuring the magnetic flux density; for Example 4.17.

Example 4.17 Hall Element for Measuring the Magnetic Flux Density

A Hall element for measuring the magnetic flux density is in the form of a strip with width a and thickness d, shown in Fig. 4.33. The concentration of free charge carriers in the strip is N_v and the charge of each carrier is Q. The strip carries a steady current of intensity I, and the magnetic flux density vector is perpendicular to the strip. A voltmeter shows a voltage V_{12} between the strip edges. What is the algebraic intensity of the magnetic flux density vector (B) with respect to the reference direction indicated in Fig. 4.33?

Solution From Eqs. (3.11) and (3.5), the current density in the element can be written as

$$J = N_v Q v_d = \frac{I}{ad}. \tag{4.149}$$

which yields $v_d = I/(N_v a d Q)$. The Hall voltage is given in Eq. (4.148), and $V_H = V_{21}$ in Fig. 4.33, namely, it is opposite to the measured voltage V_{12}. Hence, the magnetic flux density turns out to be

$$B = \frac{V_H}{v_d a} = -\frac{V_{12}}{v_d a} = -\frac{N_v Q d V_H}{I}. \tag{4.150}$$

Example 4.18 **Lorentz Force due to a Rotating Charged Contour**

A uniformly charged circular contour of radius a and total charge Q rotates in free space about its axis with a uniform angular velocity $\mathbf{w} = w\,\hat{\mathbf{z}}$, as shown in Fig. 4.34. A charged particle q moves with a uniform velocity $\mathbf{v} = v\,\hat{\mathbf{y}}$ along a path that belongs to the plane $z = a$ and is parallel to the y-axis. Find the Lorentz force on the particle at an instant when it is at the point P(0, 0, a), above the center of the contour.

Solution The electric field intensity vector at the point P in Fig. 4.34 is given by Eq. (1.44) with $z = a$.

$$\mathbf{E} = \frac{Q\sqrt{2}}{16\pi\varepsilon_0 a^2}\,\hat{\mathbf{z}} = E\,\hat{\mathbf{z}}. \tag{4.151}$$

The time period for one rotation of the contour is

$$T = \frac{2\pi}{w} \tag{4.152}$$

(full angle divided by the angular velocity). Noting that the total charge of the contour, Q, passes any given reference point on the contour during the time T, we conclude that the rotating charged contour is equivalent to a line current along the contour of intensity [Eq. (3.4)]

$$I = \frac{Q}{T} = \frac{Qw}{2\pi}. \tag{4.153}$$

From Eq. (4.19), the magnetic flux density vector due to this current at the point P ($z = a$) is

$$\mathbf{B} = \frac{\mu_0 I\sqrt{2}}{8a}\,\hat{\mathbf{z}} = \frac{\mu_0 Q w\sqrt{2}}{16\pi a}\,\hat{\mathbf{z}} = B\,\hat{\mathbf{z}}. \tag{4.154}$$

Using Eq. (4.145), the Lorentz force on the charge q comes out to be (Fig. 4.34)

$$\mathbf{F} = q(\mathbf{E} + v\,\hat{\mathbf{y}} \times \mathbf{B}) = \underbrace{qE\,\hat{\mathbf{z}}}_{\mathbf{F}_e} + \underbrace{qvB\,\hat{\mathbf{x}}}_{\mathbf{F}_m} = \frac{qQ\sqrt{2}}{16\pi\varepsilon_0 a^2}\left(\varepsilon_0\mu_0 v w a\,\hat{\mathbf{x}} + \hat{\mathbf{z}}\right). \tag{4.155}$$

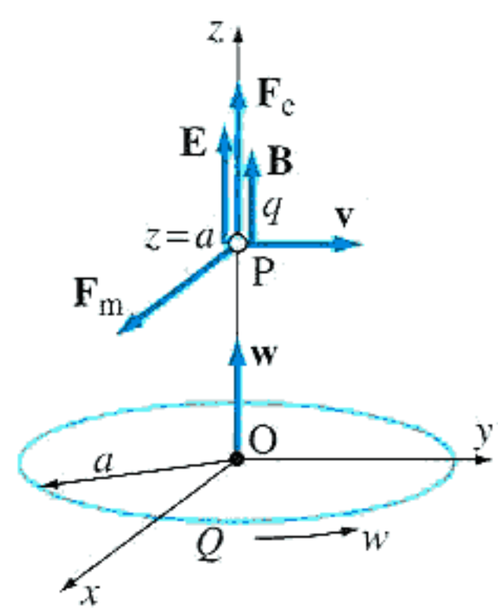

Figure 4.34 Lorentz force on a charged particle moving above a rotating charged contour; for Example 4.18.

Problems: 4.32.

4.13 EVALUATION OF MAGNETIC FORCES

Eq. (4.144) gives the Lorentz magnetic force (i.e., the magnetic component of the total Lorentz force) on a single point charge moving in a magnetic field. If we have many charges constituting a current in some domain, we utilize the superposition principle as in Eq. (4.5) and conclude that the magnetic force on a volume current element $\mathbf{J}\,dv$ is given by

$$d\mathbf{F}_m = (\mathbf{J}\,dv) \times \mathbf{B}, \tag{4.156}$$

where $\mathbf{B}$ is the flux density vector of the external magnetic field. Then, from Eq. (4.10), the magnetic force on a surface current element is

$$d\mathbf{F}_m = (\mathbf{J}_s\,dS) \times \mathbf{B}, \tag{4.157}$$

and that on a line current element

$$d\mathbf{F}_m = I\, d\mathbf{l} \times \mathbf{B}. \tag{4.158}$$

Integration of Eqs. (4.156)–(4.158) leads to the following integral formulations for the total magnetic force for volume, surface, and line current distributions:

magnetic force on volume current

$$\mathbf{F}_m = \int_v \mathbf{J} \times \mathbf{B}\, dv, \tag{4.159}$$

magnetic force on surface current

$$\mathbf{F}_m = \int_S \mathbf{J}_s \times \mathbf{B}\, dS, \tag{4.160}$$

magnetic force on line current

$$\mathbf{F}_m = \int_l I\, d\mathbf{l} \times \mathbf{B} = I \int_l d\mathbf{l} \times \mathbf{B}. \tag{4.161}$$

In the last integral, I can be taken out of the integral sign because it is always constant along the line (continuity equation for steady currents).

In the case of a straight homogeneous conductor of arbitrary cross section with a steady current placed in a uniform magnetic field, we have $\mathbf{J} = \text{const}$ [Eq. (3.82)] and $\mathbf{B} = \text{const}$, so that $\mathbf{J} \times \mathbf{B} = \text{const}$ and Eq. (4.159) becomes

$$\mathbf{F}_m = (\mathbf{J} \times \mathbf{B}) \int_v dv = (\mathbf{J}v) \times \mathbf{B} = (\mathbf{J}Sl) \times \mathbf{B} = (JS\mathbf{l}) \times \mathbf{B}, \tag{4.162}$$

where v and l are the volume and length of the conductor, respectively, S is the surface area of its cross section, the direction of the vector $\mathbf{l}$ is the same as the direction of the current flow along the conductor, and $|\mathbf{l}| = l$. Introducing the current intensity of the conductor, $I = JS$, we obtain

$\mathbf{F}_m$ on a straight conductor in a uniform magnetic field

$$\mathbf{F}_m = I\mathbf{l} \times \mathbf{B}. \tag{4.163}$$

Example 4.19 **Force Between Two Long Parallel Wires with Current**

Two parallel, very long and thin wires in air carry currents of intensities I_1 and I_2, both flowing in the same direction. The distance between the wire axes is d. Find the magnetic forces on wires per unit of their length.

Solution Fig. 4.35 shows the cross section of the two wires. From Eq. (4.22), the magnetic flux density vector due to the current in the first wire (I_1), assuming that it is infinitely long, at the axis of the second wire is

$$\mathbf{B}_1 = \frac{\mu_0 I_1}{2\pi d}\, \hat{\mathbf{y}}. \tag{4.164}$$

Since the wires are thin (as compared to the distance between their axes), we can assume that the magnetic field across the entire cross section of the second wire is uniform and given

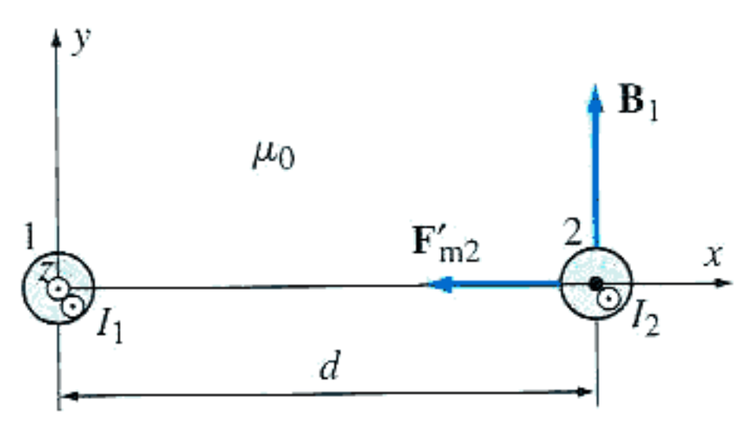

Figure 4.35 Evaluation of the force between two long parallel current-carrying wires; for Example 4.19.

by Eq. (4.164), so that Eq. (4.163) can be used. Hence, the force on the part of the second conductor that is l long equals

$$\mathbf{F}_{m2} = I_2(l\hat{\mathbf{z}}) \times \mathbf{B}_1 = \frac{\mu_0 I_1 I_2 l}{2\pi d}\,\hat{\mathbf{z}} \times \hat{\mathbf{y}} = -\frac{\mu_0 I_1 I_2 l}{2\pi d}\,\hat{\mathbf{x}}, \tag{4.165}$$

and the force per unit of its length

$$\mathbf{F}'_{m2} = \frac{\mathbf{F}_{m2}}{l} = -\frac{\mu_0 I_1 I_2}{2\pi d}\,\hat{\mathbf{x}}. \tag{4.166}$$

The per-unit-length force on the first conductor is $\mathbf{F}'_{m1} = -\mathbf{F}'_{m2}$.

We see that the magnetic force between the wires is attractive if the currents are in the same direction, i.e., if both I_1 and I_2 are either positive or negative, and repulsive if they are in opposite directions ($I_1 I_2 < 0$). So, just in contrary to charges Q_1 and Q_2 and Coulomb's law, "like" currents (in parallel wires) attract and "unlike" currents repel each other (also see Fig. 4.2).

Example 4.20 Force on a Loop near a Long Wire

A long straight wire carries a steady current of intensity I. A rectangular conducting loop lies in the same plane as the wire, with two sides (of length b) parallel to the wire and two sides (of length a) perpendicular. The distance between the wire and the closer parallel side of the loop is c. The loop carries a steady current of the same intensity, and the directions of currents are shown in Fig. 4.36. Determine the net magnetic force on the loop.

Solution The magnetic flux density vector due to the current in the long wire at any point in the plane of the loop is normal to the plane, and at a distance x from the wire its magnitude is

$$B(x) = \frac{\mu_0 I}{2\pi x}. \tag{4.167}$$

The forces on each side of the loop are obtained from Eq. (4.163), and their directions are given in Fig. 4.36. From symmetry, it is obvious that the forces on the sides 2 and 4 are equal in magnitude and with opposite directions,

$$\mathbf{F}_{m2} = -\mathbf{F}_{m4}. \tag{4.168}$$

The forces on the sides 1 and 3 are also in opposing directions, but their magnitudes are different because of their different distances from the long wire ($x = c$ and $x = c + a$),

$$F_{m1} = IbB(c) = \frac{\mu_0 I^2 b}{2\pi c} \quad \text{(repulsive)}, \tag{4.169}$$

$$F_{m3} = IbB(c+a) = \frac{\mu_0 I^2 b}{2\pi (c+a)} \quad \text{(attractive)}. \tag{4.170}$$

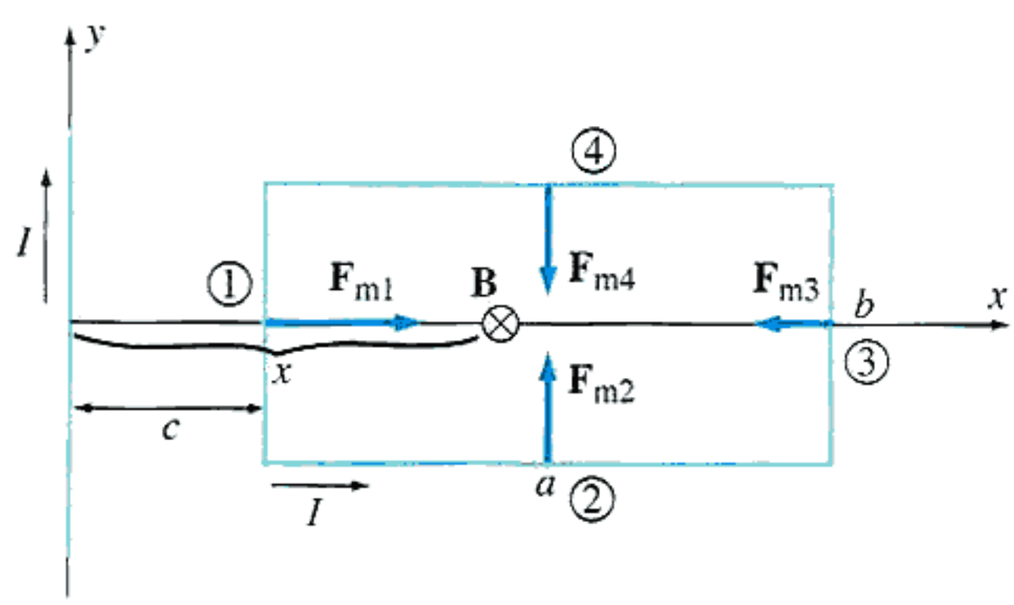

Figure 4.36 Evaluation of the magnetic force on a rectangular current loop near a long wire with current; for Example 4.20.

The total force on the loop, assuming that it is rigid (i.e., the loop maintains its shape even under the influence of the magnetic forces on its sides), is hence given by

$$\begin{aligned}\mathbf{F}_m &= \mathbf{F}_{m1} + \mathbf{F}_{m2} + \mathbf{F}_{m3} + \mathbf{F}_{m4} = \mathbf{F}_{m1} + \mathbf{F}_{m3} \\ &= \frac{\mu_0 I^2 b}{2\pi}\left(\frac{1}{c} - \frac{1}{c+a}\right)\hat{\mathbf{x}} = \frac{\mu_0 I^2 ab}{2\pi c(c+a)}\hat{\mathbf{x}}.\end{aligned} \tag{4.171}$$

Thus, the loop is pushed away from the long wire. Note that if the polarity of either (but not both) of the two currents (in the wire and the loop) were reversed, the loop would be pulled toward the long wire.

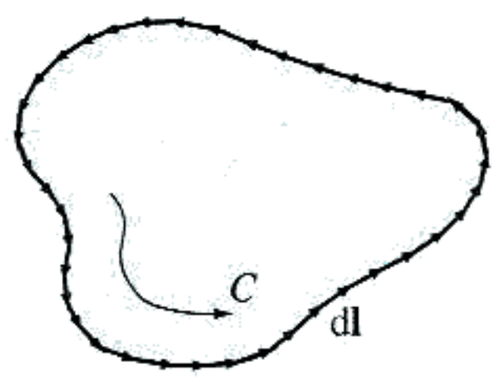

Figure 4.37 In view of the head-to-tail rule for vector addition, it is obvious that the integral of dl along a closed path is always zero; for Example 4.21.

Example 4.21 Force on a Loop in a Uniform Magnetic Field

Prove that the net magnetic force on a contour of arbitrary shape with a steady current in a uniform magnetic field is zero.

Solution For a uniform magnetic field, $\mathbf{B} = \text{const}$, so that Eq. (4.161) becomes

$$\mathbf{F}_m = I\oint_C d\mathbf{l} \times \mathbf{B} = I\left(\oint_C d\mathbf{l}\right) \times \mathbf{B}. \tag{4.172}$$

For any closed path,

$$\oint_C d\mathbf{l} = 0, \tag{4.173}$$

which is evident from Fig. 4.37, and hence $\mathbf{F}_m = 0$.

Example 4.22 Torque on a Current Loop in a Uniform Magnetic Field

A rigid square loop of side length a is situated in a uniform steady magnetic field of flux density $\mathbf{B}$, as shown in Fig. 4.38(a). There is a steady current of intensity I in the loop. The angle between the plane of the loop and the plane normal to the vector $\mathbf{B}$ is θ. The loop is mounted such that it is free to rotate about the axis O-O′ which is perpendicular to the plane of the drawing. Find (a) the net force and (b) the net torque on the loop.

Solution

(a) From Eq. (4.172), there is no net force on the loop, i.e., the vector sum of individual magnetic forces on the loop sides is zero.

(b) The forces on the sides of the loop that are normal to the axis O-O′ tend to stretch the loop, but do not produce torques on it. The torques (moments) of the forces on the sides 1 and 2 of the loop (sides parallel to the axis O-O′) calculated with respect to the center of the loop are

$$\mathbf{T}_1 = \mathbf{r}_1 \times \mathbf{F}_{m1} \quad \text{and} \quad \mathbf{T}_2 = \mathbf{r}_2 \times \mathbf{F}_{m2}, \tag{4.174}$$

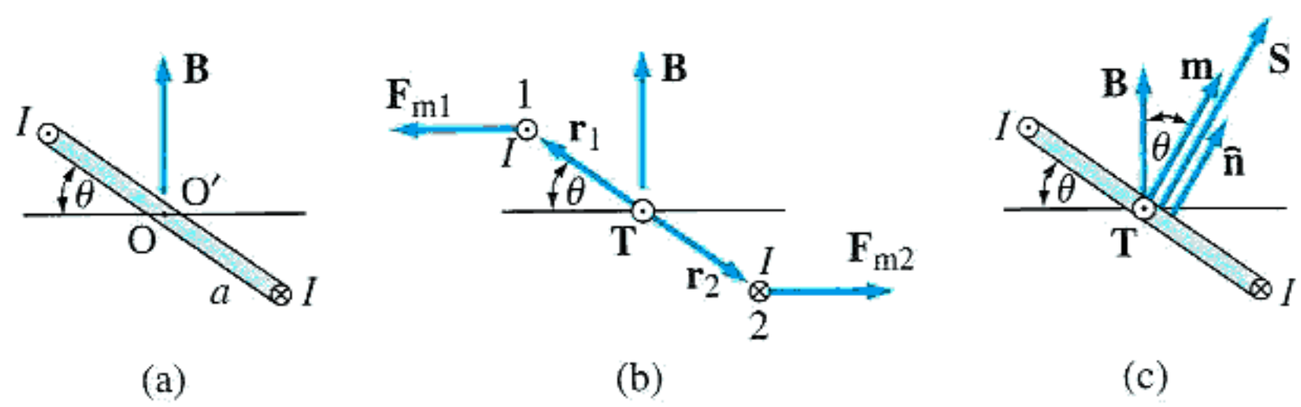

Figure 4.38 Evaluation of the torque $\mathbf{T}$ of magnetic forces on a current loop in a uniform magnetic field: (a) position of the loop relative to the magnetic field, (b) magnetic forces on loop sides producing a torque, and (c) the relationship with the magnetic moment $\mathbf{m}$ of the loop; for Example 4.22.

respectively, where $\mathbf{F}_{m1}$ and $\mathbf{F}_{m2}$ are the magnetic forces on the sides, and $\mathbf{r}_1$ and $\mathbf{r}_2$ are the position vectors of the centers of sides with respect to the loop center [Fig. 4.38(b)]. Since

$$\mathbf{F}_{m1} + \mathbf{F}_{m2} = 0, \tag{4.175}$$

the resultant torque on the loop is given by

$$\mathbf{T} = \mathbf{T}_1 + \mathbf{T}_2 = \mathbf{r}_1 \times \mathbf{F}_{m1} + \mathbf{r}_2 \times \mathbf{F}_{m2} = (\mathbf{r}_1 - \mathbf{r}_2) \times \mathbf{F}_{m1} = \mathbf{r}_{12} \times \mathbf{F}_{m1}. \tag{4.176}$$

The vector $\mathbf{r}_{12} = \mathbf{r}_1 - \mathbf{r}_2$ joins the point of application of $\mathbf{F}_{m2}$ to that of $\mathbf{F}_{m1}$ and is independent of the choice of origin of the two vectors $\mathbf{r}_1$ and $\mathbf{r}_2$. Therefore, the torque is also independent of the choice of origin, i.e., it is the same when calculated about any reference point, provided that the total force on the loop is zero.

Using Eq. (4.163), the magnitudes of the forces $\mathbf{F}_{m1}$ and $\mathbf{F}_{m2}$ are

$$F_{m1} = F_{m2} = IaB, \tag{4.177}$$

which, substituted in Eqs. (4.174), gives the magnitudes of the corresponding torque vectors:

$$T_1 = T_2 = |\mathbf{r}_1 \times \mathbf{F}_{m1}| = \frac{a}{2} F_{m1} \sin\theta = \frac{Ia^2 B \sin\theta}{2} \tag{4.178}$$

($|\mathbf{r}_1| = a/2$). Hence, the magnitude of the resultant torque vector $\mathbf{T}$ is

$$T = 2T_1 = Ia^2 B \sin\theta, \tag{4.179}$$

and its direction is shown in Fig. 4.38(b). Of course, the same is obtained from Eq. (4.176).

Noting that the angle between the unit normal $\hat{\mathbf{n}}$ on the loop surface oriented in accordance to the right-hand rule with respect to the reference direction of the loop current and the vector $\mathbf{B}$ is also θ [Fig. 4.38(c)], we conclude that the resultant torque of magnetic forces on the loop can be compactly expressed as

$$\boxed{\mathbf{T} = \mathbf{m} \times \mathbf{B},} \tag{4.180}$$

torque on a current loop in a uniform magnetic field

where $\mathbf{m}$ is the magnetic moment of the loop, given by Eq. 4.134, so that

$$T = |\mathbf{m} \times \mathbf{B}| = mB \sin\theta = Ia^2 B \sin\theta. \tag{4.181}$$

Eq. (4.180) is a general expression for the torque on a current loop of arbitrary shape and size in a uniform magnetic field. We see that the torque on the loop always tend to turn the loop so as to align the vectors $\mathbf{m}$ and $\mathbf{B}$. In other words, it tends to align the magnetic field produced by the loop current (which coincides with the direction of $\mathbf{m}$ – see Figs. 4.6 and 4.8) with the applied (external) magnetic field that is causing the torque. Finally, the magnetic field across a small current loop, i.e., a magnetic dipole (Fig. 4.30), can always be considered as locally uniform, which means that Eq. (4.180) gives us the torque on a magnetic dipole (with any shape and the magnetic moment $\mathbf{m}$) in any (generally nonuniform) magnetic field (with the local flux density $\mathbf{B}$). We observe the analogy with the torque on an electric dipole, $\mathbf{T} = \mathbf{p} \times \mathbf{E}$, in Eq. (2.3).

Problems: 4.33–4.39; *Conceptual Questions* (on Companion Website): 4.27–4.30; *MATLAB Exercises* (on Companion Website).

Problems

4.1. Rectangular current loop. Consider a rectangular loop with sides a and b in air. If the loop carries a steady current of intensity I, find the magnetic flux density vector at an arbitrary point along the axis of the loop perpendicular to its plane.

4.2. Triangular current loop. A loop in the form of a triangle representing a half of a square of side a carries a steady current of intensity I, as shown in Fig. 4.39. The medium is air. Calculate the magnetic flux density vector at a point P located at the fourth vertex of the square.

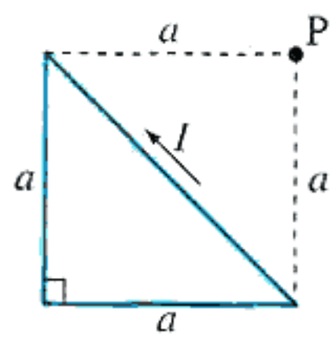

Figure 4.39 Triangular current loop; for Problem 4.2.

4.3. Current loop with circular and linear parts. Fig. 4.40 shows a wire contour composed from a half of a circle of radius a and a half of a square of side $2a$. The contour is situated in air and carries a steady current of intensity I. Find the magnetic flux density vector (a) at the central point O and (b) at a point $2a$ apart from the point O along the line perpendicular to the plane of the contour.

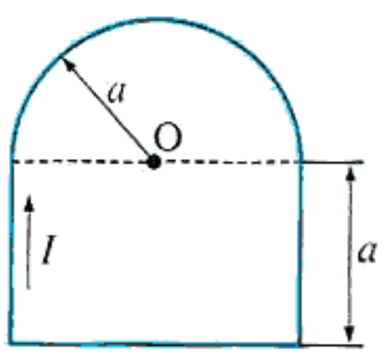

Figure 4.40 Current contour composed from a semicircle and three linear parts; for Problem 4.3.

4.4. Circular surface current distribution. There is a surface current over a circular surface of radius b with a hole of radius a ($a < b$) in free space. The surface lies in the plane $z = 0$ of a cylindrical coordinate system, with the coordinate origin coinciding with the surface center. The surface current density vector is $\mathbf{J}_s = J_{s0}(a/r)\hat{\boldsymbol{\phi}}$ ($a \le r \le b$), where J_{s0} is a constant. Compute the magnetic flux density vector along the z-axis.

4.5. Magnetic field of a rotating charged disk. A circular disk of radius a is uniformly charged over its surface by a charge of density ρ_s. The disk uniformly rotates in air about its axis (perpendicular to the disk) with an angular velocity w. Find the magnetic flux density vector at an arbitrary point along the axis of rotation. Assume that the charge distribution over the disk remains the same during the rotation.

4.6. Solenoids with different length-to-diameter ratios. Consider a solenoid with a nonmagnetic core and $N = 1000$ tightly wound turns of wire carrying a steady current $I = 1$ A. The length of the solenoid is $l = 50$ cm. Calculate the $\mathbf{B}$ field at the solenoid center, at the center of the 250th (or 750th) wire turn, and at the center of the first (or last) wire turn, and sketch the function $B(z)$ along the solenoid axis ($-\infty < z < \infty$) for the solenoid radius equal to (a) $a = 25$ cm and (b) $a = 2$ cm, respectively.

4.7. Helmholtz coils. Fig. 4.41 shows two identical very short coils, each with N circular turns of wire, in air. The distance between the centers of the coils is d, and the wire turn radii are a. The coils carry steady currents of equal intensities, I, and are oriented in the same way. When $d = a$, the magnetic field near the center of the structure (midway between the two coils) is approximately uniform, and the structure is referred to as Helmholtz coils. (a) For an arbitrary distance d ($d \neq a$), find the expression for the magnetic flux density $B(z)$ at an arbitrary point along the axis of the coils (z-axis), assuming that B due to each of the coils equals N times the flux density of a single turn of wire (circular current loop, Fig. 4.6) at the respective coil location. (b) Show that $dB/dz = 0$ at the center of the structure (point C), so for $z = d/2$ (and any d, relative to a). (c) Then verify that $d^2B/dz^2 = 0$ at the point C when $d = a$ (note that even $d^3B/dz^3 = 0$ at C in this case).

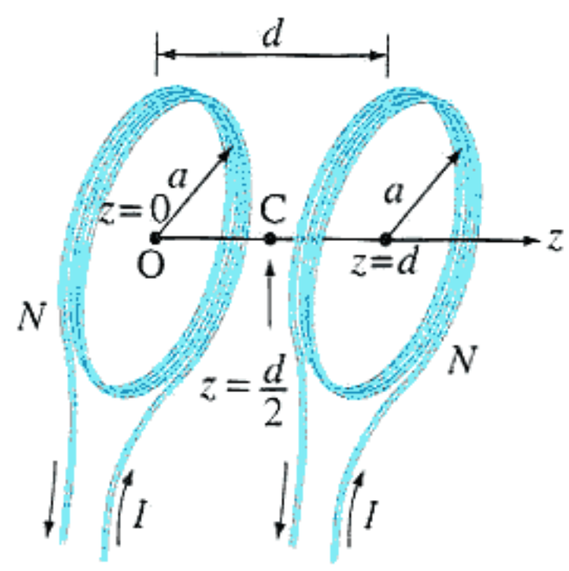

Figure 4.41 Helmholtz coils; for Problem 4.7.

4.8. Spherical coil. Consider a coil consisting of N turns of an insulated thin wire wound uniformly and densely in one layer on a nonmagnetic sphere of radius a. The current through the wire is I. The surrounding medium is air.

Find the magnetic flux density vector at the sphere center.

4.9. Two parallel strips with opposite currents. Two parallel, very long identical strip conductors of width $2a$ carry currents of the same intensity I and opposite directions. The distance between the strips is $2a$ as well. The cross section of the structure is shown in Fig. 4.42. The permeability everywhere is μ_0. Compute the **B** field at the center of the cross section (point O).

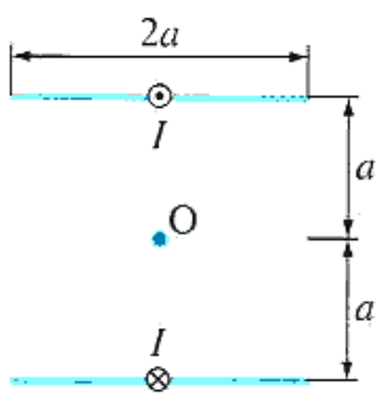

Figure 4.42 Cross section of two parallel strip conductors with currents of the same magnitude and opposite directions; for Problem 4.9.

4.10. Magnetic field of a hollow cylindrical conductor. A steady current of intensity I flows through an infinitely long hollow cylindrical copper conductor of radii a and b $(a < b)$. The cross section of the conductor is shown in Fig. 4.43. The medium in the hole and outside the conductor is nonmagnetic. Find the magnetic flux density vector everywhere.

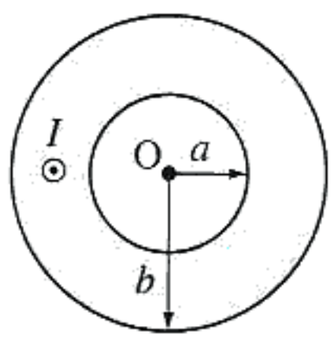

Figure 4.43 Cross section of a hollow cylindrical conductor with a steady current; for Problem 4.10.

4.11. Magnetic field of a triaxial cable. The cross section of a triaxial cable, having three coaxial cylindrical conductors, looks the same as the cross cut of the system of three concentric spherical conductors in Fig. 1.56. The radius of the inner conductor of the cable is $a = 1$ mm, the inner and outer radii of the middle conductor are $b = 2$ mm and $c = 2.5$ mm, and those of the outer conductor $d = 5$ mm and $e = 5.5$ mm. The cable conductors and dielectric, as well as the surrounding medium, are all nonmagnetic. Assuming that steady currents of intensities $I_1 = 2$ A, $I_2 = -1$ A, and $I_3 = -1$ A flow through the inner, middle, and outer conductor, respectively, all given with respect to the same reference direction, calculate the magnetic flux density vector everywhere $(0 \le r < \infty)$.

4.12. Rotating cylinder with a surface charge. An infinitely long conducting nonmagnetic cylinder of radius a is uniformly charged over its surface with a charge density ρ_s. The cylinder rotates in air about its axis with a uniform angular velocity w. Find the **B** field inside the cylinder and outside it.

4.13. Rotating nonuniformly charged hollow cylinder. An infinitely long hollow cylinder of inner radius a and outer radius b $(a < b)$ in air is charged with a volume charge density $\rho(r) = \rho_0 r/a$ $(a \le r \le b)$, where ρ_0 is a constant and r the radial distance from the cylinder axis. The cylinder uniformly rotates about its axis with an angular velocity w. Assuming that the charge distribution of the cylinder does not change during the rotation, determine the magnetic flux density vector everywhere.

4.14. Two parallel infinite planar current sheets. Two parallel infinite planar current sheets in air have the same uniform surface current density J_s. The distance between the sheets is d. Find the magnetic flux density vector everywhere if the currents of the sheets run in (a) the same direction and (b) opposite directions.

4.15. Magnetic field inside a thin plate with current. A thin copper plate of length b, width a, and thickness d $(d \ll a)$ carries a steady current of intensity I, as shown in Fig. 4.44. The plate is situated in air. Neglecting the end effects, use Ampère's law to find the distribution of the magnetic flux density vector inside the plate [note that this is mathematically completely analogous to the application of a similar integral equation in Eq. (6.146) and Fig. 6.25(b)].

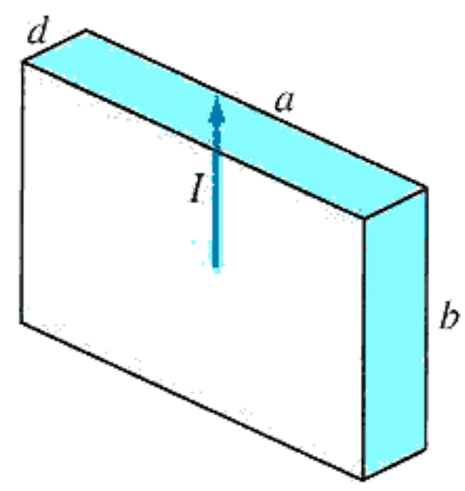

Figure 4.44 Thin conducting plate with a steady current; for Problem 4.15.

4.16. Magnetic field in a leaky parallel-plate capacitor. Calculate the magnetic flux density vector

in the imperfect dielectric of the parallel-plate capacitor from Problem 3.12 (Fig. 3.32).

4.17. Magnetic field in a leaky spherical capacitor. Find the magnetic flux density vector in the imperfect dielectric of the spherical capacitor from Example 3.3 (Fig. 3.6).

4.18. Magnetic field in a leaky coaxial cable. Determine the magnetic flux density vector in the imperfect dielectric of the coaxial cable from Problem 3.17 (Fig. 3.34).

4.19. Magnetic field around a grounding electrode. Find the magnetic flux density vector on the surface of the ground for the grounding electrode from Example 3.15 [Fig. 3.26(a)].

4.20. Current distribution from field distribution. Using the differential Ampère's law, show that the magnetic field given by Eqs. (4.53) and (4.56) is produced by a uniform volume current of density given by Eq. (4.52) along an infinitely long cylinder of radius a in free space.

4.21. Coaxial cable using differential Ampère's law. Redo Example 4.11 but employing Ampère's law in differential form.

4.22. Rotating charged cylinder by differential Ampère's law. Redo Example 4.14 but with the use of the differential form of Ampère's law.

4.23. Thin plate with current, differential Ampère's law. Redo Problem 4.15 but applying the differential Ampère's law [adopt the vector-component notation as in Fig. 4.22 and Eq. (4.75), and use the analogy with the application of the differential Gauss' law in Example 1.23].

4.24. Ampère's law in differential and integral form. In a certain region, the magnetic field is given by $\mathbf{B} = [4(z-1)^2\,\hat{\mathbf{x}} + 2x^3\,\hat{\mathbf{y}} + xy\,\hat{\mathbf{z}}]$ mT (x, y, z in m). The medium is air. (a) Find the current density. (b) From the result in (a), find the total current enclosed by a square contour lying in the xy-plane, with the center at the coordinate origin and sides, of length 2 m, parallel to the x- and y-axes. (c) Confirm Ampère's law in integral form and Stokes' theorem by evaluating the net circulation of $\mathbf{B}$ along the contour defined in (b).

4.25. Magnetic flux through a cylindrical surface. Calculate the outward magnetic flux through the lateral surface of a cylinder of radius $a = 10$ cm and height $h = 20$ cm in a uniform magnetic field of flux density $B = 1$ T. The vector $\mathbf{B}$ makes an angle of 60° with the cylinder axis.

4.26. Law of conservation of magnetic flux. For the magnetic field defined in Problem 4.24, confirm the law of conservation of magnetic flux in differential and integral forms by evaluating (a) the divergence of $\mathbf{B}$ and (b) the outward flux of $\mathbf{B}$ through the surface of a cube, respectively. Let the cube be centered at the coordinate origin, with edges parallel to coordinate axes and 2 m long.

4.27. Magnetic flux from vector potential. In a certain region, the magnetic vector potential is given as the following function in a cylindrical coordinate system: $\mathbf{A} = 2r^2\hat{\boldsymbol{\phi}}$ T · m (r in m). (a) Find the magnetic flux density vector in this region. (b) Obtain the magnetic flux through a circular contour 1 m in radius that lies in the plane $z = 0$ and is centered at the coordinate origin. (c) Check the results by evaluating the circulation of $\mathbf{A}$ along the contour.

4.28. Potential and field due to a magnetic dipole. A magnetic dipole with a moment $\mathbf{m} = 400\ \mu\text{Am}^2\,\hat{\mathbf{z}}$ is located at the origin of a spherical coordinate system. Calculate the magnetic potential $\mathbf{A}$ and flux density $\mathbf{B}$ at the following points defined by spherical coordinates: (a) (1 m, 0, 0), (b) (1 m, $\pi/2$, $\pi/2$), (c) (1 m, π, 0), (d) (1 m, $\pi/4$, 0), (e) (10 m, $\pi/4$, 0), and (f) (100 m, $\pi/4$, 0). The dipole dimensions are much smaller than 1 m.

4.29. Circular current loop as a magnetic dipole. Refer to the circular current loop in Fig. 4.6, and show that for $|z| \gg a$, Eqs. (4.19) and (4.142) become the same, the latter equation giving the magnetic flux density vector of a magnetic dipole far away from it.

4.30. Rectangular current loop as a magnetic dipole. Check the result for the $\mathbf{B}$ field due to a rectangular loop obtained in Problem 4.1 by comparing it with the corresponding dipole-field expression, from Eq. (4.142), at points far away from the loop.

4.31. Dipole equivalent to a surface current distribution. Consider the circular nonuniform surface current distribution from Problem 4.4, and show that far away along the z-axis ($|z| \gg a$),

this current distribution can be replaced by an equivalent magnetic dipole located at the coordinate origin. Find the moment, **m**, of the equivalent dipole.

4.32. Lorentz force due to a rotating charged disk. Refer to the rotating charged disk from Problem 4.5, and assume that a charged particle Q moves with a uniform velocity v along a path parallel to the plane of the disk. Find the Lorentz force on the particle at an instant when it is at the point that belongs to the axis of disk rotation and is at a distance a from the disk center.

4.33. Forces between three parallel wires with current. Three parallel very long and thin wires in air carry currents of intensities $I_1 = 1$ A, $I_2 = -1$ A, and $I_3 = 2$ A, all given with respect to the same reference direction. The distance between any two of the wires is $d = 1$ m, so their cross section constitutes an equilateral triangle (with sides d). (a) Determine the direction and magnitude of the per-unit-length magnetic force on the wire with current I_3. (b) Redo the problem if $I_2 = 1$ A.

4.34. Force on a wire due to a semicylindrical conductor. A very long aluminum conductor in the form of a half of a thin cylindrical shell of radius $b = 40$ mm and thickness $d = 0.5$ mm is situated in air. Another very long aluminum conductor, in the form of a very long wire of radius $a = 1$ mm, is positioned along the axis of the semicylinder. The two conductors carry steady currents of the same magnitude $I = 100$ A and opposite directions, as shown in Fig. 4.45. Find the magnetic force on the wire conductor per unit length.

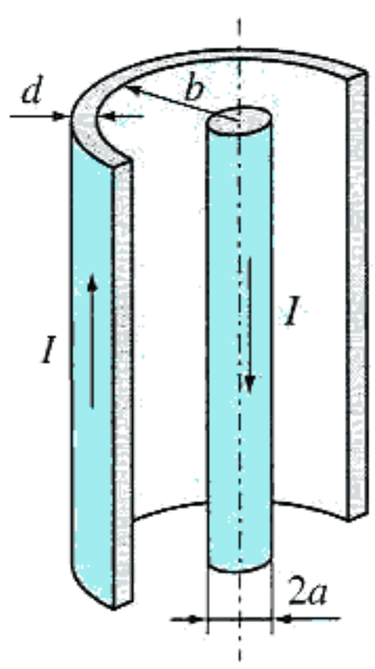

Figure 4.45 System composed of a wire conductor along the axis of a thin semicylindrical conductor; for Problem 4.34.

4.35. Wire-strip transmission line. Fig. 4.46 shows a cross section of a two-conductor transmission line consisting of a wire and a strip. The width of the strip is $2a$ and the separation between the conductors is a. The dielectric is air. If the current I runs along the line, calculate the magnetic force on the strip conductor per unit of its length.

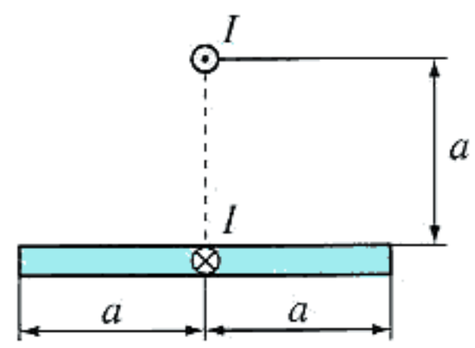

Figure 4.46 Cross section of a transmission line consisting of a wire and a strip; for Problem 4.35.

4.36. Line composed of a wire and a corner strip conductor. A wire and a 90° corner conductor, which is made from two identical strips of width a, carry steady currents of intensities I and $-I$ given with respect to the same reference direction. The distance of the wire from both ends of the corner conductor is a. A cross section of such a transmission line is portrayed in Fig. 4.47. The materials and the ambient medium are nonmagnetic. Find the per-unit-length magnetic force on the wire.

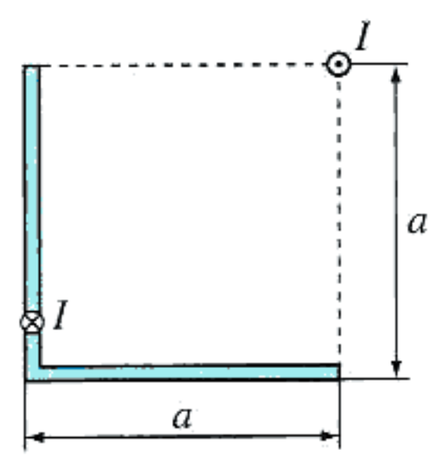

Figure 4.47 Cross section of a transmission line consisting of a wire and a 90° corner strip conductor; for Problem 4.36.

4.37. Coaxial cable with off-centered cavity. Shown in Fig. 4.48 is a cross section of a coaxial cable in which the cylindrical cavity of radius b representing the inner surface of the outer conductor is off-centered by a vector **d** with respect to the common axis of the inner conductor and the outer surface of the outer conductor. The other two radii are a and c, and the relationship $b + d \leq c$ is satisfied. The permeability everywhere is μ_0. If a steady current of intensity I is established in the cable, determine the magnetic force on the inner conductor per unit of its length.

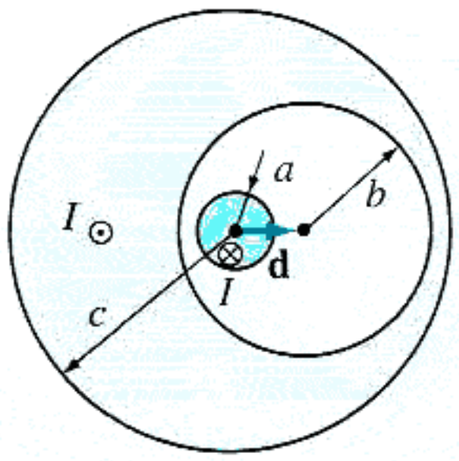

Figure 4.48 Coaxial cable with off-centered inner surface of the outer conductor; for Problem 4.37.

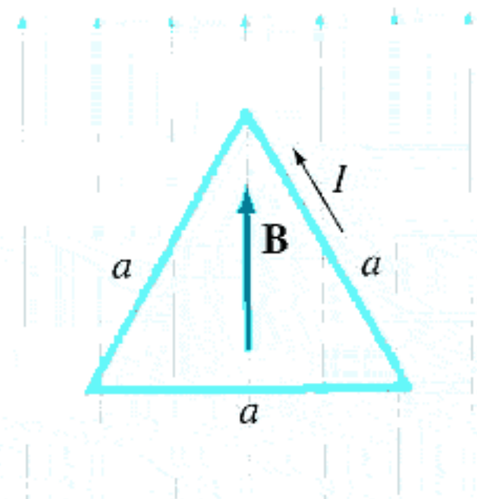

Figure 4.49 Triangular current loop in a uniform magnetic field; for Problem 4.38.

4.38. Force and torque on a triangular current loop. A rigid loop in the form of an equilateral triangle of side length a is situated in a uniform steady magnetic field of flux density $\mathbf{B}$. The magnetic field lines are parallel to the plane of the loop and are perpendicular to one of its sides, as shown in Fig. 4.49. If a steady current of intensity I is established in the loop, find (a) the force and (b) the torque on each of the loop sides, as well as (c) the net force and (d) the net torque on the loop.

4.39. Torque between two magnetic dipoles. Two small current loops are positioned in free space. The first loop has a magnetic moment $\mathbf{m}_1 = m\hat{\mathbf{z}}$ and is centered at the origin (O) of the Cartesian coordinate system. Obtain the torque on the second loop, for the following locations of its center P and directions of its magnetic moment $\mathbf{m}_2$: (a) P(0, a, 0) and $\mathbf{m}_2 = m\hat{\mathbf{z}}$, (b) P(0, a, 0) and $\mathbf{m}_2 = m\hat{\mathbf{y}}$, (c) P(0, 0, a) and $\mathbf{m}_2 = m\hat{\mathbf{z}}$, (d) P(0, 0, a) and $\mathbf{m}_2 = m\hat{\mathbf{x}}$, and (e) P(0, a, a) and $\mathbf{m}_2 = m\hat{\mathbf{z}}$. Take $m = 0.1$ Am^2 and $a = 10$ m.

5 Magnetostatic Field in Material Media

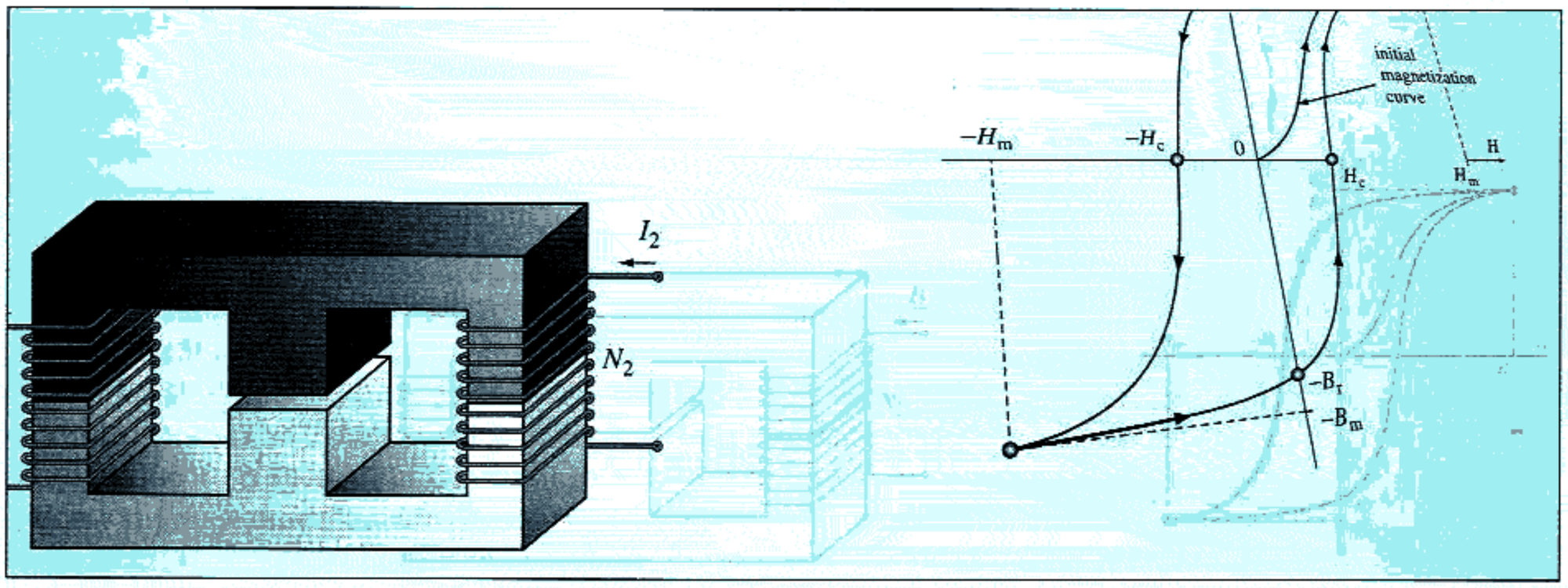

Introduction:

Our study of magnetostatics has so far been restricted to the magnetic field due to steady electric currents in a vacuum and other nonmagnetic media. In this chapter, we shall introduce and discuss phenomena associated with the magnetostatic field in the presence of magnetic materials. Many of the basic concepts, physical laws, and mathematical techniques constituting the analysis of materials in the magnetic field are entirely analogous to the corresponding concepts, laws, and techniques in electrostatics, which makes our discussions in this chapter much easier. The most important difference, however, with respect to the analysis of dielectric materials is the inherent nonlinear behavior of the most important class of magnetic materials, called ferromagnetics. This is a class of materials with striking magnetic properties (many orders of magnitude stronger than in other materials), with iron as a typical example.

We shall start with a qualitative characterization of microscopic magnetic phenomena in substances and describe the behavior of different types of magnetic materials based on the classical atomic model. By analogy with the polarization vector in electrostatics, the magnetization vector will be used to describe the magnetized state of a material on a macroscopic scale. Magnetization volume and surface current density vectors will be defined as macroscopic equivalents to a vast collection of tiny electric currents that are microscopic sources of the magnetization of a magnetic material. These current densities will enable us to evaluate the magnetic field due to magnetized materials using free-space formulas and techniques from the preceding chapter. We shall derive and discuss Maxwell's equations and boundary conditions for magnetostatic systems that include arbitrary media. The concept of permeability of a material will allow for additional macroscopic characterization of magnetic materials. Finally, a section on magnetic circuits (consisting of ferromagnetic cores of different shapes with current-carrying

windings) will represent a culmination of the theory of the magnetostatic field in the presence of magnetic materials. Most of the work of the chapter will be applied to perform the analysis of such circuits, which essentially resembles the dc analysis of nonlinear electric circuits.

5.1 MAGNETIZATION VECTOR

According to the elementary atomic model of matter, all materials are composed of atoms, each with a central fixed positively charged nucleus and a number of negatively charged electrons circulating around the nucleus in various orbits. Both these orbital motions and the inherent spins of the electrons about their own axes can be represented by small current loops, i.e., magnetic dipoles. These tiny currents are referred to as Ampère's currents. The magnetic moment of each elementary loop is given by Eq. (4.134).[1] In the absence of an external magnetic field, the equivalent magnetic dipoles have random orientations with respect to one another, resulting in no net magnetic moment. With an applied field, however, the equivalent current loops experience torques, which lead to a net alignment of microscopic magnetic dipole moments with the external magnetic field [see Eq. (4.180)] and a net magnetic moment in the material on a macroscopic scale. The process of inducing macroscopic magnetic moments by an external magnetic field is called the magnetization of the material. This process is practically instantaneous, and the material in the new magnetostatic state is said to be magnetized or in the magnetized state. When magnetized (by an external field), a material is a source of its own magnetic field, and the total field at an arbitrary point in space (inside or outside the material) is a sum of the external (primary) field and the field due to the magnetized material (secondary field). In the analysis, we can replace the material by a collection of microscopic Ampère's current loops (magnetic dipoles) residing in a vacuum, as the rest of the material does not produce any field. Then, the secondary field can, in principle, be determined using the expression for the magnetic field due to a magnetic dipole in free space, Eq. (4.142), and superposition.

Instead of analyzing every single atom and all microscopic magnetic dipole moments, however, we rather introduce a macroscopic quantity termed the magnetization vector to describe the magnetized state of a material and the resulting field. Analogously to the definition of the polarization vector (**P**) for electrically polarized dielectric materials, Eq. (2.7), the magnetization vector, **M**, is defined as the density of the equivalent elementary magnetic moments in a magnetic material at a given point:

magnetization vector (unit: A/m)

$$\boxed{\mathbf{M} = \frac{\left(\sum \mathbf{m}\right)_{\text{in } dv}}{dv}.} \tag{5.1}$$

We note that $\mathbf{M}\,dv$ represents the dipole moment of a magnetic dipole that is equivalent to an elementary volume dv in the material, i.e., to all the dipoles (microscopic Ampère's currents) within it. The unit for the magnetization vector is A/m.

[1] A third source of equivalent microscopic magnetic dipole moments in atoms is nuclear spin, but it provides a negligible contribution to the macroscopic magnetic properties of materials. Note, however, that nuclear spin represents the basis of magnetic resonance imaging (MRI), used in medicine, and also in many areas of science and engineering.

In any magnetic material, the magnetization vector at a point is a function of the magnetic flux density vector at that point,

$$\mathbf{M} = \mathbf{M}(\mathbf{B}), \tag{5.2}$$

and this relationship is a characteristic of individual materials. It is entirely analogous to the relationship between the polarization vector and the electric field intensity vector, Eq. (2.9), in electrostatics.

5.2 BEHAVIOR AND CLASSIFICATION OF MAGNETIC MATERIALS

A thorough understanding and precise quantitative characterization of microscopic magnetic phenomena in materials require a full quantum mechanical treatment. Here, however, we describe qualitatively the behavior of different types of magnetic materials based on the classical atomic model. Generally, materials can be classified according to their magnetic behavior into diamagnetic, paramagnetic, ferromagnetic, antiferromagnetic, ferrimagnetic, and superparamagnetic materials.

In diamagnetic materials, the magnetic moments of electrons orbiting about their nuclei are dominant compared to the magnetic moments attributed to electron spin. In order to describe diamagnetic behavior, which is present to a greater or lesser extent with all magnetic materials, we consider first a model of an atom with a single electron that circulates about the nucleus along an orbit of radius a with a uniform angular velocity $\mathbf{w}_0 = w_0\,\hat{\mathbf{z}}$, as shown in Fig. 5.1(a). In the absence of an external magnetic field, the outward centrifugal force on the electron, given by

$$F_{\mathrm{cf}} = \frac{m_{\mathrm{e}} v_0^2}{a} = m_{\mathrm{e}} w_0^2 a, \tag{5.3}$$

where m_{e} and v_0 are the mass and velocity of the electron ($v_0 = w_0 a$), respectively, is balanced by the centripetal (attractive) electric (Coulomb) force, F_{e}, between the nucleus and electron. Thus, the balance equation reads

$$F_{\mathrm{e}} = m_{\mathrm{e}} w_0^2 a. \tag{5.4}$$

The orbiting electron is equivalent to a small current loop (magnetic dipole), where the current I of the loop is given by Eq. (4.153) with $Q = -e$ and is

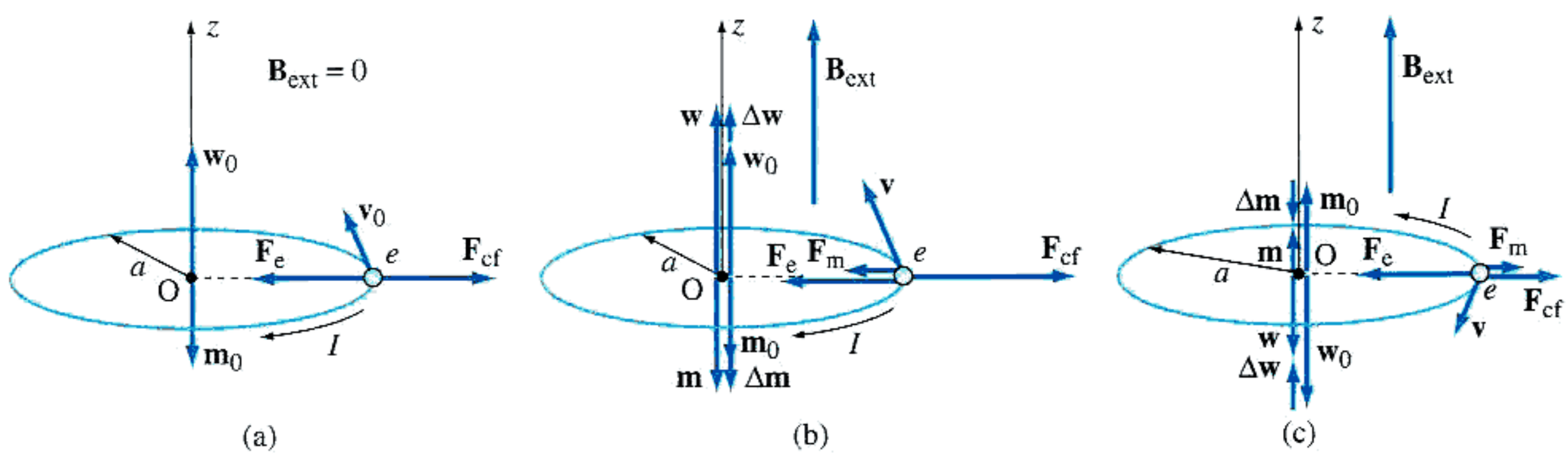

Figure 5.1 Atom with a single electron orbiting about the nucleus, in the absence of an external magnetic field (a), and with an applied magnetic field, whose direction coincides with the direction of the electron angular velocity vector (b) or is opposite to it (c).

directed oppositely to the direction of electron travel (because the electron charge is negative). From Eq. (4.134), the magnetic moment of the dipole is

$$\mathbf{m}_0 = I\pi a^2(-\hat{\mathbf{z}}) = -\frac{ew_0a^2}{2}\,\hat{\mathbf{z}}. \tag{5.5}$$

In the presence of an external magnetic field, there is an additional force on the electron – the magnetic force, Eq. (4.144),

$$\mathbf{F}_\mathrm{m} = Q\mathbf{v}\times\mathbf{B}_\mathrm{ext} = -e\mathbf{v}\times\mathbf{B}_\mathrm{ext}, \tag{5.6}$$

with $\mathbf{B}_\mathrm{ext}$ denoting the magnetic flux density vector of the applied field. For the situation in Fig. 5.1(b), where the electron angular velocity vector is in the same direction as the applied field $\mathbf{B}_\mathrm{ext} = B_\mathrm{ext}\,\hat{\mathbf{z}}$, the magnetic force is centripetal (inward), so that the new balance equation is

$$F_\mathrm{e} + ewaB_\mathrm{ext} = m_\mathrm{e}w^2a, \quad w = w_0 + \Delta w. \tag{5.7}$$

Here, the force unbalance created by the magnetic force is compensated for by an increase Δw of the orbital angular velocity ($\Delta w > 0$). Combining Eqs. (5.4) and (5.7) gives

$$m_\mathrm{e}(w^2 - w_0^2) = ewB_\mathrm{ext}. \tag{5.8}$$

Since the perturbation of the electron velocity is small, i.e., $\Delta w \ll w_0$, even for the strongest applied magnetic fields, we can write

$$w^2 - w_0^2 = (w + w_0)(w - w_0) \approx 2w\Delta w. \tag{5.9}$$

Substituting this into Eq. (5.8), the increase of the angular velocity comes out to be

$$\Delta w = \frac{eB_\mathrm{ext}}{2m_\mathrm{e}}. \tag{5.10}$$

In place of Eq. (5.5), the new equivalent magnetic dipole moment is

$$\mathbf{m} = -\frac{ewa^2}{2}\,\hat{\mathbf{z}} = -\frac{ea^2}{2}\,\mathbf{w}. \tag{5.11}$$

Introducing the angular momentum of the electron,

$$\mathbf{L} = m_\mathrm{e}\mathbf{r}\times\mathbf{v} = \mathcal{I}\mathbf{w}, \tag{5.12}$$

where $\mathbf{r}$ is the instantaneous position vector of the electron with respect to the origin O ($|\mathbf{r}| = a$) and $\mathcal{I} = m_\mathrm{e}a^2$ is the rotational inertia of the electron, Eq. (5.11) becomes

$$\mathbf{m} = -\frac{e}{2m_\mathrm{e}}\mathbf{L} = -\frac{e}{2m_\mathrm{e}}\mathcal{I}\mathbf{w}. \tag{5.13}$$

The increase of the dipole moment due to the increase of the orbiting velocity of the electron, in Eq. (5.10), is given by

$$\Delta\mathbf{m} = -\frac{e}{2m_\mathrm{e}}\mathcal{I}\Delta\mathbf{w} = -\left(\frac{e}{2m_\mathrm{e}}\right)^2\mathcal{I}\mathbf{B}_\mathrm{ext}, \tag{5.14}$$

and is called the induced magnetic moment of the electron. We note that $\Delta\mathbf{m}$ is antiparallel (i.e., in the opposite direction) to the applied magnetic field $\mathbf{B}_\mathrm{ext}$.

For an electron whose orbital angular velocity vector and the field $\mathbf{B}_\mathrm{ext}$ are opposed, as in Fig. 5.1(c), the force $\mathbf{F}_\mathrm{m}$ on the electron is in the outward direction, and the force unbalance is compensated for by a reduced velocity, i.e., $\Delta w < 0$. The new magnetic dipole moment is smaller in magnitude than $\mathbf{m}_0$, so that the induced moment $\Delta\mathbf{m}$ is again in the $-z$ direction, that is, still antiparallel to the applied

field, and given by the same expression in Eq. (5.14). This same expression for $\Delta\mathbf{m}$ is obtained also in the case of an arbitrary mutual position of the electron orbit and the applied magnetic field, as well as for the model of an atom with N electrons, which travel along orbits that are arbitrarily oriented with respect to the applied magnetic field, where $\mathcal{I}$ should be replaced by the average rotational inertia of all electrons in the atom, $\mathcal{I} = \mathcal{I}_{\text{av}}$.

With no external magnetic field applied, the magnetic dipoles of the atoms have random orientations, so that the net magnetic moment and the magnetization vector in the material are zero. With an applied field, however, each atom acquires a differential induced moment given by Eq. (5.14), with $\mathcal{I} = \mathcal{I}_{\text{av}}$, and all these moments are antiparallel to the magnetic flux density vector, $\mathbf{B}$, in the material. As a result, the net magnetic moment of the atoms opposes the applied field. Thus, a rod of a diamagnetic material placed in a magnetic field will orient itself perpendicular to the applied field, i.e., across the field lines. The term diamagnetism originates from the Greek word "dia" meaning "across." If a diamagnetic specimen is brought near either pole of a strong bar magnet, it will be repelled by the magnet. From Eqs. (5.1) and (5.14), the magnetization vector is

$$\mathbf{M} = N_{\text{v}}\,\Delta\mathbf{m} = -\frac{N_{\text{v}} e^2 \mathcal{I}_{\text{av}}}{4m_{\text{e}}^2}\,\mathbf{B}, \tag{5.15}$$

N_{v} being the concentration (number per unit volume) of atoms in the material. We note that this equation represents a special form of Eq. (5.2). In addition, it is customary to write

$$\mathbf{M} = \frac{\chi_{\text{m}}}{\mu_0}\,\mathbf{B}, \tag{5.16}$$

where χ_{m} is a dimensionless proportionality constant given by

$$\boxed{\chi_{\text{m}} = -\frac{\mu_0 N_{\text{v}} e^2 \mathcal{I}_{\text{av}}}{4m_{\text{e}}^2}.} \tag{5.17}$$

magnetic susceptibility of diamagnetic materials

It is called the magnetic susceptibility of the material. (For a vacuum, which is the only truly nonmagnetic medium, $\chi_{\text{m}} = 0$.) We see that the diamagnetic materials are linear magnetic media, because the relationship $\mathbf{M}(\mathbf{B})$ in Eq. (5.16) is a linear one. Typical diamagnetic materials are bismuth, silver, lead, copper, gold, silicon, germanium, graphite, sulfur, hydrogen, helium, sodium chloride, and water. Substituting typical values for the quantities involved in the expression in Eq. (5.17) indicates that χ_{m} of diamagnetic materials is of order -10^{-6} (water) to -10^{-4} (bismuth). We see that the magnetic susceptibility of diamagnetic materials is negative and very small. The macroscopic magnetic effect in diamagnetic substances is very weak and negligible in most practical situations. In general, the diamagnetic effect is present in all materials when placed in a magnetic field, because it arises from an interaction of orbiting electrons in atoms with the external field. However, in other types of magnetic materials, the diamagnetic reaction is completely masked by other effects.

In paramagnetic materials, the atoms have a small permanent net magnetic dipole moment associated with them, due almost entirely to spin magnetic dipole moments of electrons. In the absence of an external magnetic field, the random orientation of the atoms produces an average magnetic moment of a zero in a finite volume. When an external field is applied, however, there is a small torque given by Eq. (4.180) on each atomic moment, which tends to align the moment in the direction of the applied field. This alignment acts to increase the value of

the magnetic flux density vector, **B**, within the material over the external value. However, the external field also causes a diamagnetic effect of the orbiting electrons (all magnetic materials exhibit diamagnetic behavior), which counteracts the increase in **B**. The alignment process is also impeded by the forces of random thermal vibrations, and the resulting increase in **B** is quite small. The overall macroscopic effect is equivalent to that of a small positive magnetization. The magnetization vector, **M**, is in the same direction as the vector **B**. Eq. (5.16), then, tells us that the magnetic susceptibility of paramagnetic materials is positive and very small. When a rod of a paramagnetic material is placed in a magnetic field, it orients itself along the field lines, and hence the term paramagnetism (the word "para" in Greek means "along"). Additionally, if a paramagnetic substance is brought near a pole of a strong bar magnet, it will be attracted to it. Typical paramagnetic materials are palladium, aluminum, and oxygen, and typical values of χ_m are of orders 10^{-6} (oxygen) to 10^{-3} (palladium). Note that air is a paramagnetic medium as well. Obviously, the paramagnetic effect is also very weak and paramagnetic materials can be treated as nonmagnetic media ($\chi_m = 0$) in most practical applications.

The remaining four classes of magnetic materials (ferromagnetic, antiferromagnetic, ferrimagnetic, and superparamagnetic) all have strong atomic magnetic dipole moments caused primarily by uncompensated electron spin moments. The interaction of adjacent atoms leads to an alignment of the atomic moments in either an aiding (parallel) or opposing (antiparallel) manner.

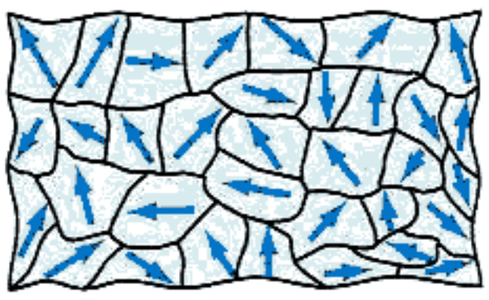

Figure 5.2 Magnetic domains in a polycrystalline ferromagnetic specimen with no external magnetic field applied.

The macroscopic magnetization of ferromagnetic materials can be many orders of magnitude larger than that of paramagnetic materials. Interatomic forces in a ferromagnetic sample cause the atomic moments to line up in a parallel fashion over regions containing large number of atoms (e.g., 10^{15} atoms). These regions, called the magnetic domains (or Weiss' domains), range in size from a few microns to several centimeters in each dimension. With no external field applied, the domain moments vary in direction from domain to domain, as indicated in Fig. 5.2 for a polycrystalline ferromagnetic specimen. Due to overall vector cancelations, the material as a whole has no net magnetization. Upon the application of an external magnetic field, however, the volumes of the domains that have moments aligned or nearly aligned with the applied field grow at the expense of their neighbors, and the magnetic flux density vector of the secondary field (that due to the material) increases greatly over that of the external field alone. For weak applied fields, the movements of magnetic domain walls are reversible, i.e., the domains go back to their initial states after the field is turned off. Above a certain (not large) field magnitude, however, this process becomes irreversible. Additionally, the domains start rotating toward the direction of the applied field, so that completely random domain orientations are no longer attained after the external field has been removed. In other words, there is a residual or remanent net magnetization of the material that remains after the complete removal of the primary field. This means that the magnetization of the material lags behind the field producing it, and also that the magnetization state of the material at an instant of time is a function not only of the magnetic field, i.e., its flux density vector, at that instant, but also of the magnetic history of the material. This phenomenon is called hysteresis (which is derived from a Greek word meaning "to lag"). As the applied field becomes even much stronger, a total alignment of all the domain moments with the applied field occurs. At this point, the ferromagnetic material is said to be saturated. In the state of saturation, further increase of the external magnetic flux density vector no longer causes an increase of the magnetization vector.

Typical ferromagnetic materials are iron, nickel, and cobalt, and their alloys. The name ferromagnetic comes from the Latin word for iron, "ferrum." Ferromagnetics are the most important magnetic materials in engineering. They are widely used in cores of inductors and transformers, and in electric motors, generators, electromagnets, relays, and other devices that use magnetic forces and torques, as well as in magnetic heads and tracks of computer hard disks and other magnetic storage (recording) devices. Note that above a certain (very high) temperature, called the Curie temperature, the thermal vibrations of atoms completely prevent the coupling (parallel alignment) of atomic magnetic moments, so that ferromagnetic materials lose all their ferromagnetic characteristics and revert to paramagnetic materials. The Curie temperature for iron is 770°C.

In antiferromagnetic materials, the forces between adjacent atoms cause the atomic magnetic moments to line up in opposite directions so that the net magnetic moment of a specimen is zero, even in the presence of an applied magnetic field. Chromium and manganese, as well as many oxides, sulfides, and chlorides, belong to this class of materials. Examples are manganese oxide (MnO_2), ferrous sulfide (FeS), and cobalt chloride ($CoCl_2$). Antiferromagnetism is not of practical importance.

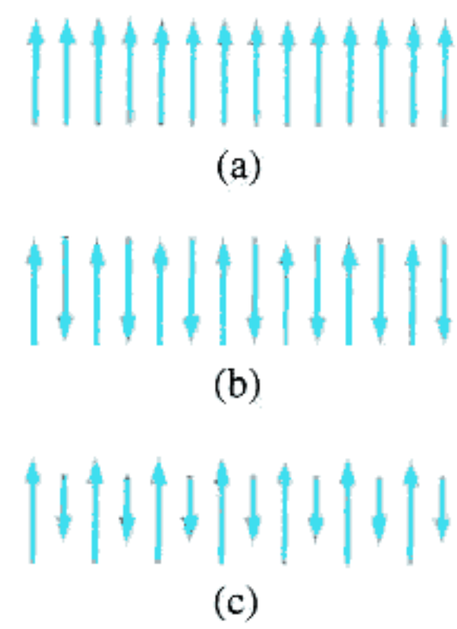

Figure 5.3 Schematic structures of atomic magnetic dipole moments for (a) ferromagnetic, (b) antiferromagnetic, and (c) ferrimagnetic materials.

In ferrimagnetic materials, the magnetic moments of adjacent atoms are also aligned antiparallel, but the moments are not equal, so there is a net magnetic moment of a specimen. A large response to an externally applied magnetic field therefore occurs, although it is substantially less than in ferromagnetic substances. Fig. 5.3 depicts schematically a comparison of the atomic magnetic dipole moment structure for ferromagnetic, antiferromagnetic, and ferrimagnetic materials. The most important subclass of ferrimagnetics are the ferrites, which have much lower electric conductivity (σ) than the ferromagnetics (for instance, 10^{-4} to 10^2 S/m, compared with 10^7 S/m for iron). Low conductivity limits induced currents in the material when alternating (ac) fields are applied (so-called eddy currents), and this is why the ferrites are used in many applications at high frequencies, such as cores for high-frequency transformers, AM, short-wave, and FM antennas, and phase shifters, in spite of their weaker magnetic effects (compared to ferromagnetics). The reduced eddy currents lead to lower Joule's (ohmic) losses in the material (core). Typical examples of ferrite substances are iron ferrite (Fe_3O_4), nickel ferrite ($NiFe_2O_4$), and cobalt ferrite ($CoFe_2O_4$). Ferrimagnetism also disappears at temperatures above a critical value – the Curie temperature.

Finally, superparamagnetic materials are composed of ferromagnetic particles suspended in a nonmagnetic (dielectric) matrix. Each particle contains many magnetic domains, but the domain walls cannot penetrate the matrix material and there is no coupling with adjacent particles. Thin dielectric (plastic) tapes with suspended ferromagnetic particles can store large amounts of information in magnetic form because the particles are independent from each other and it is possible to change the state of magnetization along the tape abruptly in very small distances. Such superparamagnetic tapes are widely used as audio, video, and data recording tapes.

5.3 MAGNETIZATION VOLUME AND SURFACE CURRENT DENSITIES

In this section, we shall obtain the expressions for evaluation of the macroscopic distribution of volume and surface current densities equivalent to microscopic Ampère's currents in a magnetized body – from a given distribution of the

magnetization vector, **M**. The vector **M**, in turn, is obtained by averaging the microscopic magnetic dipoles (magnetic moments of microscopic Ampère's current loops) in the magnetic material. The equivalent macroscopic current is called the magnetization current, and the corresponding volume and surface current densities are denoted by $\mathbf{J}_{\mathrm{m}}$ and $\mathbf{J}_{\mathrm{ms}}$, respectively. The expressions for these current densities are similar to the expressions for calculating the volume and surface bound (polarization) charge densities (ρ_{p} and ρ_{ps}) from the polarization vector (**P**) in a polarized dielectric body. They will be used later for free-space evaluations of the magnetic flux density vector (**B**) due to magnetized bodies.

Let us first find the intensity of the total magnetization current $I_{\mathrm{m}C}$ enclosed by an arbitrary imaginary contour C situated (totally or partly) inside a magnetized magnetic body, as depicted in Fig. 5.4. We note that $I_{\mathrm{m}C}$ is actually the current that passes through any surface S bounded by C. Let the magnetic moments of small Ampère's current loops in a vacuum that constitute the magnetization current be expressed as

$$\mathbf{m} = I\mathbf{S}_{\mathrm{m}}, \tag{5.18}$$

where $S_{\mathrm{m}} = |\mathbf{S}_{\mathrm{m}}|$ is the surface area of the loop. It is obvious in Fig. 5.4 that all the loops that pass through S twice, as well as those that do not pass through S at all, contribute with zero net current intensity to $I_{\mathrm{m}C}$. Only loops that pierce S only once, that is, the loops that encircle C, contribute actually to the total current intensity flowing through S. To evaluate $I_{\mathrm{m}C}$ in the general case, we therefore count the loops that are strung along C (like pearls on a string). In doing that, we count the contribution of such loops as either I or $-I$ (note that I, generally, differs from loop to loop), by inspecting whether the direction of the loop current traversing S is in agreement or disagreement with the reference orientation of S.

Consider an element $\mathrm{d}l$ of C and the case when the angle β between the vector **M** (or the average of elementary dipole moment vectors **m** near $\mathrm{d}l$) and vector $\mathrm{d}\mathbf{l}$, which is oriented in accordance to the orientation of C, is less than 90°, as shown in Fig. 5.5(a). Note that centers of loops that are positioned close to $\mathrm{d}l$ and encircle it are inside an oblique cylinder with bases S_{m} and height

$$\mathrm{d}h = \mathrm{d}l \cos\beta, \tag{5.19}$$

so that the total number of these loops equals the concentration of loops (magnetic dipoles), N_{v} [see Eq. (2.6)], times the volume of the cylinder, $\mathrm{d}v = S_{\mathrm{m}}\,\mathrm{d}h$. The reference orientation of the surface S is related to that of the contour C by means of the right-hand rule, so the reference direction of the unit normal vector $\hat{\mathbf{n}}$ on S in

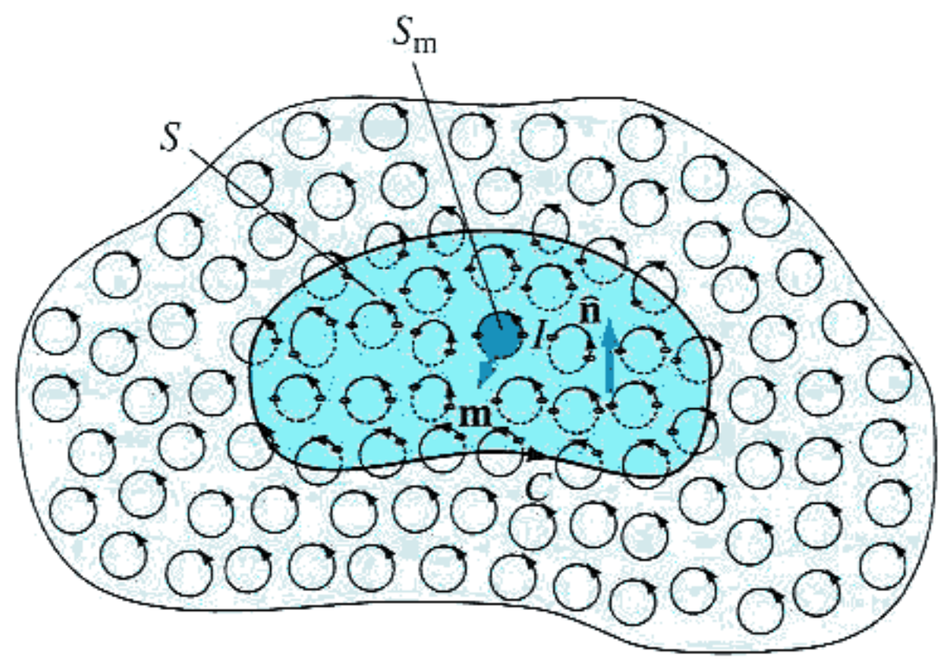

Figure 5.4 Contour C in a magnetized magnetic body.

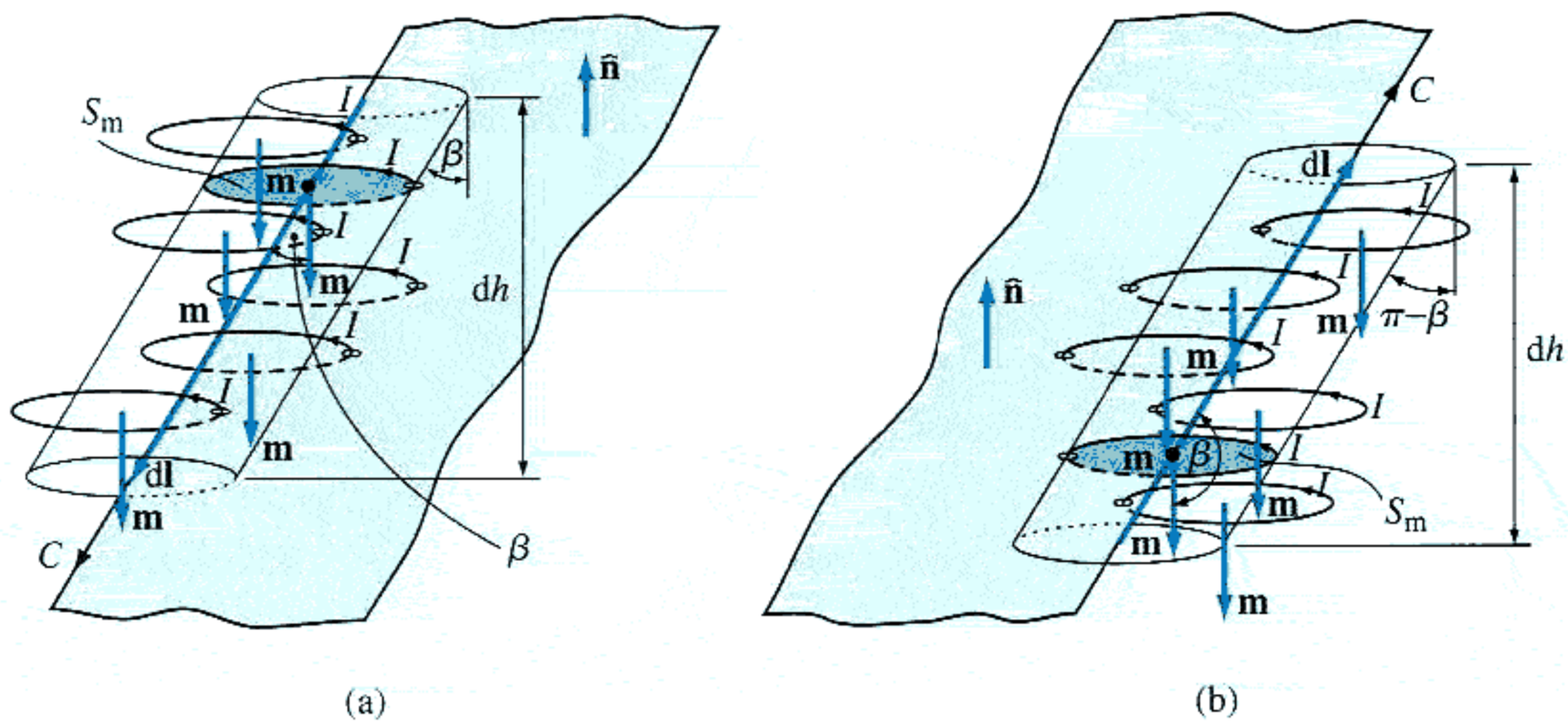

Figure 5.5 Element of the contour C in Fig. 5.4, in two cases with regards to the angle β between $\mathbf{M}$ and $\mathrm{d}\mathbf{l}$: (a) $0 \le \beta < 90°$ and (b) $90° < \beta \le 180°$.

Fig. 5.5(a) is from S upward. We then realize that all the loop currents encircling $\mathrm{d}l$ pass through S in the positive direction (direction in agreement with the orientation of S) and contribute to the total current with the intensity I (we assume that all the loops near $\mathrm{d}l$, which is differentially small, have the same moments and currents). Hence, the corresponding contribution to the magnetization current intensity through S is given by

$$\mathrm{d}I_\mathrm{m} = N_\mathrm{v} S_\mathrm{m}\, dl \cos\beta\, I \quad (0 \le \beta < 90°). \tag{5.20}$$

In the case when $\beta > 90°$, Fig. 5.5(b),

$$\mathrm{d}h = \mathrm{d}l\, \cos(\pi - \beta) = \mathrm{d}l\,(-\cos\beta), \tag{5.21}$$

and, because all the loop currents encircling $\mathrm{d}l$ pierce S in the negative direction and are taken as $-I$,

$$\mathrm{d}I_\mathrm{m} = N_\mathrm{v} S_\mathrm{m}\, \mathrm{d}l\,(-\cos\beta)\,(-I) \quad (90° < \beta \le 180°), \tag{5.22}$$

which is the same result as in Eq. (5.20).

Eq. (5.1) can be interpreted here as $\mathbf{M} = N_\mathrm{v}\mathbf{m}$, where $\mathbf{m}$ is given by Eq. (5.18), and hence, for an arbitrary β ($0 \le \beta \le 180°$), we have

$$\mathrm{d}I_\mathrm{m} = N_\mathrm{v} m\, \mathrm{d}l \cos\beta = N_\mathrm{v}\mathbf{m}\cdot\mathrm{d}\mathbf{l} = \mathbf{M}\cdot\mathrm{d}\mathbf{l} \tag{5.23}$$

[note that the boundary case, $\beta = 90°$ (the contour element $\mathrm{d}\mathbf{l}$ is tangential to the surfaces S_m of the loops) and $\mathrm{d}I_\mathrm{m} = 0$, is also properly included in this formula]. Finally, by integrating the result for $\mathrm{d}I_\mathrm{m}$ along the entire contour C, we get

$$\boxed{I_{\mathrm{m}C} = \oint_C \mathbf{M}\cdot\mathrm{d}\mathbf{l}.} \tag{5.24}$$

total magnetization current enclosed by a contour C

This is an integral equation similar in form to Ampère's law, Eq. (4.48). It tells us that the circulation (line integral) of the magnetization vector along an arbitrary contour in a magnetostatic system that includes magnetic materials is equal to the total magnetization current enclosed by that contour. The reference direction of the current flow is related to the reference orientation of the contour by the right-hand rule.

Eq. (5.24) is true for any contour C. Let us apply it to the contour C enclosing an elementary surface ΔS inside a magnetic material:

$$\frac{(I_{\mathrm{m}})_{\text{through } \Delta S}}{\Delta S} = \frac{\oint_C \mathbf{M} \cdot \mathrm{d}\mathbf{l}}{\Delta S} \quad (\Delta S \to 0), \tag{5.25}$$

where both sides of the equation are divided by ΔS. The expression on the left-hand side of the above equation represents the component of the magnetization volume current density vector normal to ΔS,

$$\hat{\mathbf{n}} \cdot \mathbf{J}_{\mathrm{m}} = \frac{(I_{\mathrm{m}})_{\text{through } \Delta S}}{\Delta S} \tag{5.26}$$

($\hat{\mathbf{n}}$ is the unit vector normal to the surface ΔS), while the expression on the right-hand side of the equation is, by definition [Eq. (4.87)], the component of the curl of $\mathbf{M}$ along $\hat{\mathbf{n}}$, that is, $\hat{\mathbf{n}} \cdot \operatorname{curl} \mathbf{M}$. Hence,

$$\hat{\mathbf{n}} \cdot \mathbf{J}_{\mathrm{m}} = \hat{\mathbf{n}} \cdot \operatorname{curl} \mathbf{M}, \tag{5.27}$$

and, since this is true for any $\hat{\mathbf{n}}$ and thus for all components of the vector $\mathbf{J}_{\mathrm{m}}$, it implies that

magnetization volume current density vector

$$\boxed{\mathbf{J}_{\mathrm{m}} = \operatorname{curl} \mathbf{M} = \nabla \times \mathbf{M}.} \tag{5.28}$$

This is a differential form of the integral relationship in Eq. (5.24). It tells us that the magnetization volume current density vector, in A/m^2, at an arbitrary point in a material is equal to the curl of the magnetization vector at that point.

If $\mathbf{M} = \text{const}$ inside the magnetic material (uniformly magnetized material), all spatial derivatives of $\mathbf{M}$ are zero, and from Eq. (5.28),

no volume magnetization current in a uniformly magnetized material

$$\boxed{\mathbf{M} = \text{const} \quad \longrightarrow \quad \mathbf{J}_{\mathrm{m}} = 0.} \tag{5.29}$$

Physically, the currents of adjacent Ampère's current loops that flow in opposite directions cancel everywhere in the interior of a uniformly magnetized material, and there is no net volume current. If $\mathbf{M} \neq \text{const}$, however, then volume macroscopic magnetization current exists only if the magnetization vector varies throughout the volume of the material (nonuniformly magnetized material) in a way that its curl is nonzero, otherwise $\mathbf{J}_{\mathrm{m}} = 0$.

On the surface of a magnetized magnetic body, there always exists surface macroscopic magnetization current (there are parts of small Ampère's current loops pressed onto the surface that cannot be compensated by oppositely flowing currents of neighboring loops). The only exception are parts of the surface where $\mathbf{M}$ and the microscopic magnetic dipoles are normal to the surface, that is, the surfaces S_{m} of the Ampère's current loops are laying in the surface of the body. To determine the magnetization macroscopic surface current density vector, $\mathbf{J}_{\mathrm{ms}}$ (in A/m), equivalent to the microscopic currents, we apply Eq. (5.24) to a narrow rectangular elementary contour, with length Δl and height Δh ($\Delta h \to 0$), shown in Fig. 5.6. The contour being differentially small, the magnetic moments $\mathbf{m}$ of Ampère's current loops near the contour are all parallel to each other. The resultant of all the corresponding Ampère's currents, and thus the vector $\mathbf{J}_{\mathrm{ms}}$, is perpendicular to the local magnetization vector, $\mathbf{M}$. The contour C in Fig. 5.6 is positioned such that $\mathbf{M}$ lies in the plane of the contour and $\mathbf{J}_{\mathrm{ms}}$ is perpendicular to that plane. There is no magnetization ($\mathbf{M} = 0$) in free space (a vacuum, air, or any other nonmagnetic medium) surrounding the body, so that the circulation of vector $\mathbf{M}$ in Eq. (5.24) is reduced to $\mathbf{M} \cdot \Delta\mathbf{l}$ along the lower side of C. By the definition of the surface current density vector

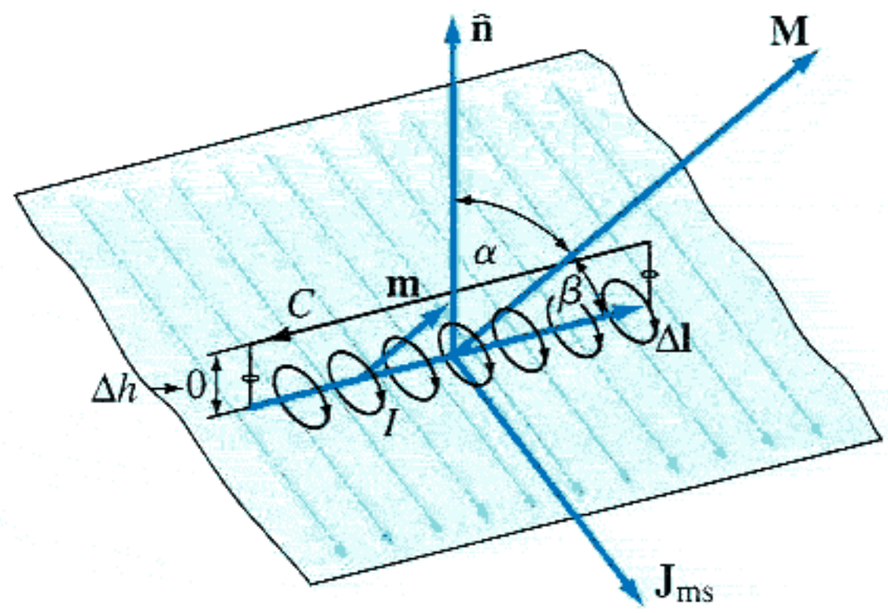

Figure 5.6 Elementary contour used for deriving the boundary condition for the vector **M** on the surface of a magnetic body.

[see Eq. (3.13)], the total current enclosed by C, appearing on the left-hand side of Eq. (5.24), equals $J_{ms}\Delta l$, and we have

$$J_{ms}\Delta l = \mathbf{M}\cdot\Delta\mathbf{l} = M\Delta l\cos\beta = M\Delta l\sin\alpha, \tag{5.30}$$

where α is the angle that **M** makes with the normal on the surface directed from the magnetic body outward ($\alpha = 90° - \beta$). Hence,

$$J_{ms} = M\sin\alpha, \tag{5.31}$$

or, in a vector form,

$$\boxed{\mathbf{J}_{ms} = \mathbf{M}\times\hat{\mathbf{n}},} \tag{5.32}$$

magnetization surface current density vector; $\hat{\mathbf{n}}$ outward normal on a magnetic body surface

with $\hat{\mathbf{n}}$ standing for the outward normal unit vector on the surface. This is the boundary condition for the vector **M** on the surface of a magnetic body, connecting the magnetization vector in the body near the surface and the magnetization surface current density vector on the surface. Note that only the tangential component of **M** contributes to $\mathbf{J}_{ms}$.

The expressions in Eqs. (5.28) and (5.32) can be used for determining the distribution of volume and surface magnetization current densities, $\mathbf{J}_m$ and $\mathbf{J}_{ms}$, of a magnetized body, assuming that the state of magnetization of the body is described by a given distribution of the magnetization vector, **M**, inside the body. We can then, considering these macroscopic currents to reside in a vacuum, calculate the magnetic flux density vector, **B**, due to the magnetized body (and any other related quantity of interest) using the appropriate free-space equations (e.g., various forms of the Biot-Savart law and Ampère's law) and solution techniques suitable to specific geometries and current distributions.

Example 5.1 Nonuniformly Magnetized Ferromagnetic Cube

The magnetization vector in a ferromagnetic cube shown in Fig. 5.7 is given by

$$\mathbf{M}(x, y) = M_0\frac{xy}{a^2}\,\hat{\mathbf{z}}, \tag{5.33}$$

where M_0 is a constant. The surrounding medium is air. Find the distribution of magnetization currents of the cube.

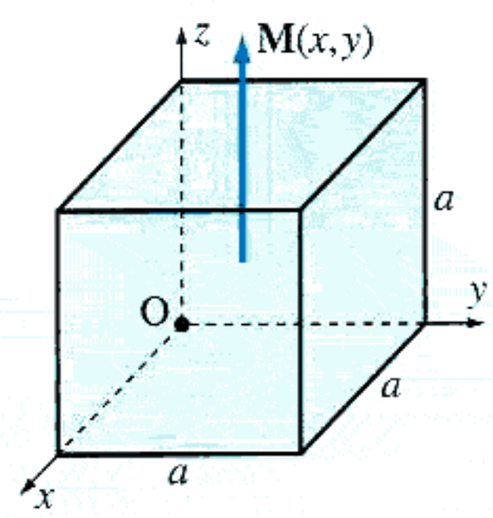

Figure 5.7 Ferromagnetic cube with magnetization $\mathbf{M}(x, y)$; for Example 5.1.

Solution From Eqs. (5.28) and (4.81), the magnetization volume current density vector inside the cube is

$$\mathbf{J}_m = \frac{\partial M_z}{\partial y}\,\hat{\mathbf{x}} - \frac{\partial M_z}{\partial x}\,\hat{\mathbf{y}} = \frac{M_0}{a^2}(x\,\hat{\mathbf{x}} - y\,\hat{\mathbf{y}}). \tag{5.34}$$

The magnetization surface current density vector is, by means of Eq. (5.32),

$$\mathbf{J}_{\mathrm{ms1}} = \mathbf{M}(a^-, y) \times \hat{\mathbf{x}} = \frac{M_0 y}{a}\,\hat{\mathbf{y}} \quad \text{and} \quad \mathbf{J}_{\mathrm{ms2}} = \mathbf{M}(x, a^-) \times \hat{\mathbf{y}} = -\frac{M_0 x}{a}\,\hat{\mathbf{x}} \tag{5.35}$$

on the front side and right-hand side of the cube, respectively, and $\mathbf{J}_{\mathrm{ms}} = 0$ on the remaining four sides of the cube [in terms of Eq. (5.31), $M = 0$ on the back side and left-hand side, whereas $\sin\alpha = 0$ on the top and bottom sides of the cube].

Example 5.2 Uniformly Magnetized Ferromagnetic Disk

A thin ferromagnetic disk of radius a and thickness d ($d \ll a$) is situated in air. The disk is uniformly magnetized throughout its volume. The magnetization vector is normal to disk bases and its magnitude is M. Determine (a) the distribution of magnetization currents of the disk and (b) the magnetic flux density vector at an arbitrary point along the disk axis normal to the bases.

Solution

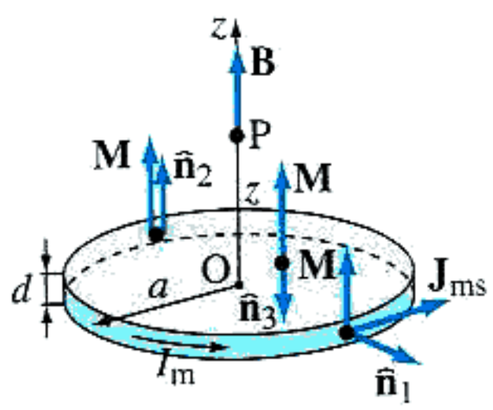

Figure 5.8 Magnetization surface current on a uniformly magnetized ferromagnetic disk; for Example 5.2.

(a) Eq. (5.29) tells us that there is no magnetization volume current inside the disk. According to Eq. (5.32) and Fig. 5.8, a magnetization surface current flows circumferentially along the side disk surface, with density

$$\mathbf{J}_{\mathrm{ms}} = \mathbf{M} \times \hat{\mathbf{n}}_1 = M\,\hat{\mathbf{z}} \times \hat{\mathbf{r}} = M\hat{\boldsymbol{\phi}}, \tag{5.36}$$

while on the upper and lower disk bases, $\mathbf{J}_{\mathrm{ms}} = 0$, because $\mathbf{M}$ is collinear with both $\hat{\mathbf{n}}_2$ and $\hat{\mathbf{n}}_3$.

(b) Since the ferromagnetic disk is thin, the circumferential sheet of magnetization current over its surface can be replaced by an equivalent circular current loop with radius a and current intensity

$$I_{\mathrm{m}} = J_{\mathrm{ms}} d = Md. \tag{5.37}$$

Assuming that the loop is in a vacuum, the magnetic flux density vector along the z-axis is given by Eq. (4.19), that is,

$$\mathbf{B} = \frac{\mu_0 M d a^2}{2\left(z^2 + a^2\right)^{3/2}}\,\hat{\mathbf{z}}. \tag{5.38}$$

Example 5.3 Cylindrical Bar Magnet

A cylindrical bar magnet of radius a and length l is permanently magnetized with a uniform magnetization. The magnetization vector, $\mathbf{M}$, is parallel to the bar axis. The medium around the magnet is air. Compute the magnetic flux density vector at the center of the magnet.

Solution The magnetization surface current density over the magnet is the same as that over the magnetized disk in Fig. 5.8, and the vector $\mathbf{B}$ both inside and outside the magnet can be found as that due to a cylindrical current sheet of radius a and length l in a vacuum with the surface current density given in Eq. (5.36). This sheet, on the other hand, is equivalent to the solenoid in Fig. 4.10, so that the flux density along the magnet axis is given by Eq. (4.36) with NI/l substituted by $J_{\mathrm{ms}} = M$ [see Eq. (4.30)]. Specifically, $\mathbf{B}$ at the center of the magnet equals

$$\mathbf{B} = \frac{\mu_0 l}{\sqrt{l^2 + 4a^2}}\,\mathbf{M}. \tag{5.39}$$

Example 5.4 Nonuniformly Magnetized Infinitely Long Cylinder

Fig. 5.9(a) shows an infinitely long cylinder of radius a in air, having a nonuniform magnetization given by $\mathbf{M} = M_0(1 - r^2/a^2)\,\hat{\mathbf{z}}$, where M_0 is a constant. Find (a) the distribution of

magnetization currents of the cylinder and (b) the magnetic flux density vector inside and outside the cylinder.

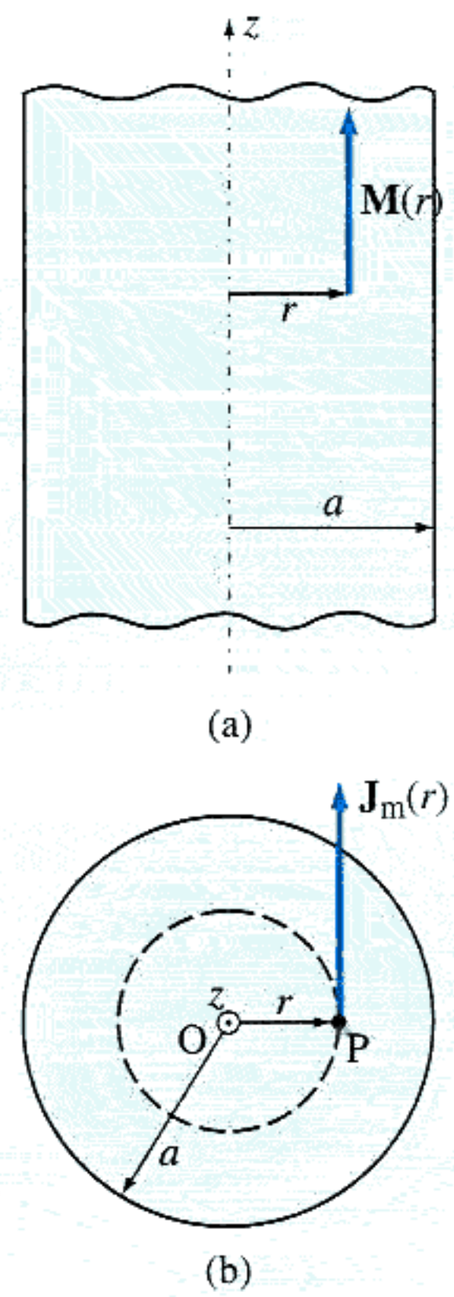

Figure 5.9 Magnetization vector (a) and magnetization volume currents (b) inside a nonuniformly magnetized infinitely long ferromagnetic cylinder; for Example 5.4.

Solution

(a) Applying the formula for the curl in cylindrical coordinates, Eq. (4.84), we obtain that the streamlines of the magnetization volume current inside the cylinder are circles centered at the cylinder axis, as indicated in Fig. 5.9(b), with the following current density vector:

$$\mathbf{J}_{\mathrm{m}} = \nabla \times \mathbf{M} = -\frac{\partial M_z}{\partial r}\,\hat{\boldsymbol{\phi}} = \frac{2M_0}{a^2}\,r\,\hat{\boldsymbol{\phi}}. \tag{5.40}$$

There is no magnetization surface current over the surface of the cylinder, because $M(a^-) = 0$ in the cylinder close to the surface.

(b) We note that the vector $\mathbf{J}_{\mathrm{m}}$ in Eq. (5.40) is of exactly the same form as the current density vector $\mathbf{J}$ inside the rotating charged cylinder in Fig. 4.20 computed in Eq. (4.69). The only difference are the multiplicative constants, ρw in Eq. (4.69) vs. $2M_0/a^2$ in Eq. (5.40). Consequently, the magnetic flux density vectors in the two systems are also of the same form, the only difference being those two multiplicative constants. [The magnetic field due to the rotating charged cylinder in Fig. 4.20 was obtained by visualizing the current distribution $\mathbf{J}$ as a series of coaxial infinitely long solenoids and applying Ampère's law, Eq. (4.49).] By substituting, therefore, ρw in Eq. (4.71) by $2M_0/a^2$, the flux density due to the magnetized cylinder in Fig. 5.9 turns out to be

$$\mathbf{B} = \mu_0 M_0 \left(1 - \frac{r^2}{a^2}\right)\hat{\mathbf{z}} = \mu_0 \mathbf{M} \tag{5.41}$$

inside the cylinder ($0 \le r \le a$) and $\mathbf{B} = 0$ outside it.

Example 5.5 Uniformly Magnetized Ferromagnetic Sphere

A ferromagnetic sphere of radius a is uniformly magnetized, and the magnetization vector is $\mathbf{M}$. The sphere is surrounded by air. Calculate (a) the magnetization surface current density vector at an arbitrary point on the sphere surface and (b) the magnetic flux density vector at the sphere center.

Solution

(a) For a spherical coordinate system with the origin at the sphere center and the z-axis parallel to the magnetization vector, as shown in Fig. 5.10, $\mathbf{M} = M\hat{\mathbf{z}}$ and the magnetization surface current density vector over the sphere surface at a point P defined by an angle θ is

$$\mathbf{J}_{\mathrm{ms}} = \mathbf{M} \times \hat{\mathbf{n}} = M \sin \angle(\mathbf{M}, \hat{\mathbf{n}}) = M \sin\theta, \quad 0 \le \theta \le \pi. \tag{5.42}$$

(b) After the ferromagnetic material has been removed, we apply the superposition principle to find the $\mathbf{B}$ field due to the spherical sheet of current described by the function in Eq. (5.42), which is analogous to the computation of the electric field due to a uniformly polarized dielectric sphere in Fig. 2.7. We subdivide the sphere surface into thin rings of width $\mathrm{d}l_{\mathrm{r}} = a\,\mathrm{d}\theta$, which is depicted in Fig. 5.10. Each such ring can be viewed as an equivalent circular wire loop with the same current. The current of the ring containing the point P equals

$$\mathrm{d}I_{\mathrm{m}} = J_{\mathrm{ms}}\,\mathrm{d}l_{\mathrm{r}} = Ma \sin\theta\,\mathrm{d}\theta. \tag{5.43}$$

Using Eq. (4.19), the magnetic flux density vector of this ring at the sphere center is

$$\mathrm{d}\mathbf{B} = \frac{\mu_0\,\mathrm{d}I_{\mathrm{m}} a_{\mathrm{r}}^2}{2a^3}\,\hat{\mathbf{z}}, \tag{5.44}$$

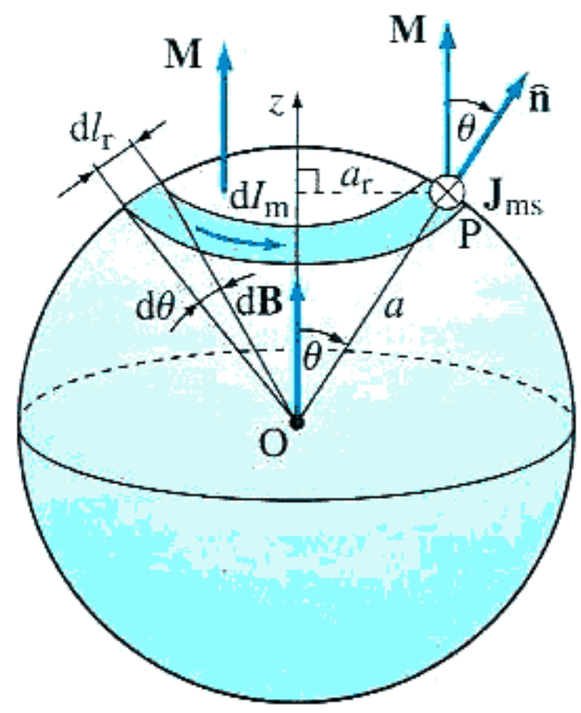

Figure 5.10 Ferromagnetic sphere with a uniform magnetization; for Example 5.5.

with $a_r = a \sin\theta$ standing for the ring radius. Hence, the resultant flux density comes out to be

$$\mathbf{B} = \frac{\mu_0 M}{2}\,\hat{\mathbf{z}} \int_{\theta=0}^{\pi} \sin^3\theta \, d\theta = \frac{2}{3}\,\mu_0 \mathbf{M}, \tag{5.45}$$

where the integral in θ is evaluated as [see also Eq. (2.32)]

$$\int_0^{\pi} \sin^3\theta \, d\theta = \int_0^{\pi} \left(1 - \cos^2\theta\right) \sin\theta \, d\theta = \left(-\cos\theta + \frac{\cos^3\theta}{3}\right)\Bigg|_0^{\pi} = \frac{4}{3}. \tag{5.46}$$

Problems: 5.1–5.6; *Conceptual Questions* (on Companion Website): 5.1–5.3; *MATLAB Exercises* (on Companion Website).

5.4 GENERALIZED AMPÈRE'S LAW

We now consider a general magnetostatic system where, in addition to equivalent magnetization currents (bound currents) inside magnetic bodies and over their surfaces, we have conduction currents (free currents) flowing through conductors (including conducting magnetic materials). As sources of the magnetic flux density vector, **B**, all these currents act as if they were in a vacuum, and Ampère's law, Eq. (4.48), becomes

Ampère's law for a system with conductors and magnetic materials

$$\boxed{\oint_C \mathbf{B} \cdot d\mathbf{l} = \mu_0 \left(I_C + I_{mC}\right),} \tag{5.47}$$

with I_C and I_{mC} standing for the total conduction current and the total magnetization current, respectively, enclosed by an arbitrary contour C. Dividing this equation by μ_0, moving I_{mC} to the left-hand side of the equation, then substituting it by the circulation of the magnetization vector, **M**, from Eq. (5.24), and finally joining the two integrals along C into a single integral, we get the equivalent integral equation:

$$\oint_C \left(\frac{\mathbf{B}}{\mu_0} - \mathbf{M}\right) \cdot d\mathbf{l} = I_C, \tag{5.48}$$

which is conveniently written as

generalized Ampère's law

$$\boxed{\oint_C \mathbf{H} \cdot d\mathbf{l} = I_C.} \tag{5.49}$$

This equation is referred to as the generalized Ampère's law. The new quantity on the left-hand side of the equation,

$$\boxed{\mathbf{H} = \frac{\mathbf{B}}{\mu_0} - \mathbf{M},} \tag{5.50}$$

magnetic field intensity vector (unit: A/m)

is called the magnetic field intensity vector and is measured in A/m. It is analogous to the electric flux density vector, **D**, in electrostatics, which is defined by Eq. (2.41). The generalized Ampère's law is valid for magnetostatic fields in arbitrary media, and is easier to use than the form in Eq. (5.47) because it has only free (true) currents on the right-hand side of the integral equation.

The most general representation of conduction current is that by means of the volume current density, **J**, which yields

$$\boxed{\oint_C \mathbf{H} \cdot d\mathbf{l} = \int_S \mathbf{J} \cdot d\mathbf{S},} \tag{5.51}$$

generalized Ampère's law in terms of the volume current density

where S is a surface of arbitrary shape bounded by the contour C (orientations of C and S are in accordance to the right-hand rule). Since this integral relation holds for any choice of C, applying Stokes' theorem, Eq. (4.89), results in the following differential relation:

$$\boxed{\nabla \times \mathbf{H} = \mathbf{J},} \tag{5.52}$$

generalized differential Ampère's law

namely, the differential form of the generalized Ampère's law. Eqs. (5.51) and (5.52) represent, respectively, the integral and differential Maxwell's second equation for the magnetostatic field in an arbitrary medium.

Example 5.6 Toroidal Coil with a Ferromagnetic Core

A uniform and dense winding with N turns of wire is placed over a thin toroidal ferromagnetic core of length l. If there is a steady current of intensity I through the winding, find the magnetic field intensity vector in the core.

Solution Due to symmetry, magnetic field lines in the core are circular as in the air-filled toroid in Fig. 4.18. Moreover, the field in the core is uniform, because the toroid is thin [see Eq. (4.66)]. Applying generalized Ampère's law, Eq. (5.49), to a circular contour C of length l along the toroid axis, as shown in Fig. 5.11, gives $Hl = NI$, from which,

$$H = \frac{NI}{l} \quad \text{(thin toroid with an arbitrary core).} \tag{5.53}$$

Note that this result holds true for a core made from an arbitrary magnetic material (including nonlinear and inhomogeneous media).

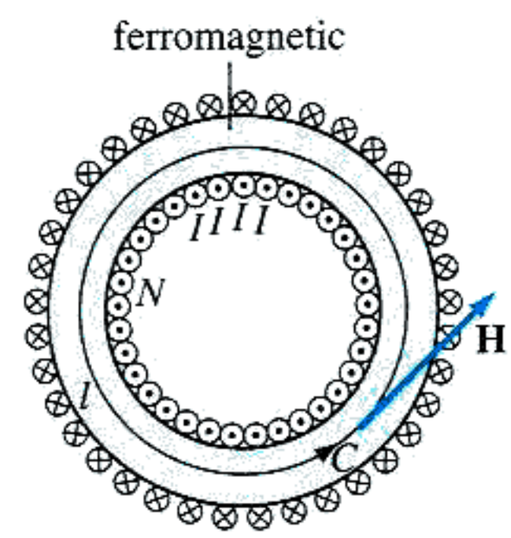

Figure 5.11 Evaluation of the magnetic field intensity vector in a toroidal coil with a ferromagnetic core; for Example 5.6.

Example 5.7 Closed Surface in a Uniformly Magnetized Material

Prove that the flux of the magnetic field intensity vector through a closed surface situated inside a uniformly magnetized ferromagnetic material equals zero.

Solution According to our experience so far with vector calculus and different forms of Maxwell's equations, the flux of a vector through a closed surface in integral notation corresponds, in differential notation, to the divergence of that same vector (with similar correspondence between the circulation along a contour and the curl). Let us therefore consider the divergence of the magnetic field intensity vector, **H**, in the material. Since the material is uniformly magnetized, the divergence of the magnetization vector, **M**, at an arbitrary point

in the material is zero ($\mathbf{M} = \text{const}$). The divergence of the magnetic flux density vector, $\mathbf{B}$, on the other hand, is always zero [Eq. (4.103)]. Consequently, the definition of the magnetic field intensity vector, Eq. (5.50), gives

$$\nabla \cdot \mathbf{H} = \frac{1}{\mu_0} \nabla \cdot \mathbf{B} - \nabla \cdot \mathbf{M} = 0, \tag{5.54}$$

i.e., the divergence of $\mathbf{H}$ is also zero in the material, which in integral notation [see Eq. (1.173)] reads

$$\oint_S \mathbf{H} \cdot d\mathbf{S} = 0, \tag{5.55}$$

for any closed surface S situated inside the material.

Problems: 5.7–5.11; *Conceptual Questions* (on Companion Website): 5.4–5.7; *MATLAB Exercises* (on Companion Website).

5.5 PERMEABILITY OF MAGNETIC MATERIALS

We now introduce the concept of permeability for macroscopic characterization of magnetic materials, which is analogous to the permittivity concept in electrostatics. Substituting Eq. (5.2) into Eq. (5.50), we obtain that the magnetic field intensity vector ($\mathbf{H}$) at a point in any magnetic material is a function of the magnetic flux density vector ($\mathbf{B}$) at that point, or vice versa,

constitutive equation of an arbitrary (nonlinear) magnetic material

$$\boxed{\mathbf{B} = \mathbf{B}(\mathbf{H}).} \tag{5.56}$$

This is the general constitutive equation for characterization of magnetic materials, parallel to Eq. (2.46) in electrostatics. For linear magnetic materials, the magnetization vector, $\mathbf{M}$, is linearly proportional to $\mathbf{B}$, and hence also to $\mathbf{H}$ [see Eq. (5.50)], which is customarily written as

$$\mathbf{M} = \chi_m \mathbf{H}. \tag{5.57}$$

Here, χ_m is the magnetic susceptibility of the material, that is, the same dimensionless quantity defined in Eq. (5.16). Note, however, that Eq. (5.16) holds only for diamagnetic and paramagnetic materials, where, as we shall see later in this section, $\mathbf{B} \approx \mu_0 \mathbf{H}$, while Eq. (5.57) holds for all linear magnetic media. Thus we have

$$\mathbf{B} = \mu_0(\mathbf{H} + \mathbf{M}) = \mu_0(1 + \chi_m)\mathbf{H} = \mu_0 \mu_r \mathbf{H}, \tag{5.58}$$

where $\mu_r = 1 + \chi_m$ is a dimensionless proportionality constant called the relative permeability of the material, which is entirely analogous to the relative permittivity ε_r in electrostatics. In practice, μ_r (or χ_m) for a given material can be determined experimentally. In analogy to Eq. (2.50) in electrostatics, we also introduce the permeability (or absolute permeability) of the material,

permeability (unit: H/m)

$$\boxed{\mu = \mu_r \mu_0,} \tag{5.59}$$

where the value of the permeability of a vacuum, μ_0, is given in Eq. (4.3), with which,

constitutive equation of a linear magnetic material

$$\boxed{\mathbf{B} = \mu \mathbf{H}.} \tag{5.60}$$

The unit for μ is henry per meter (H/m). For free space and other nonmagnetic media, $\mu_r = 1$ and

constitutive equation for free space

$$\boxed{\mathbf{B} = \mu_0 \mathbf{H}.} \tag{5.61}$$

For diamagnetic materials (see Section 5.2), the value of μ is slightly smaller than the permeability of a vacuum (e.g., $\mu_r = 0.999833$ for bismuth, a substance which shows diamagnetism more strongly than most materials), whereas μ of paramagnetic materials is slightly greater than μ_0 (e.g., $\mu_r = 1.0008$ for palladium, one of the strongest paramagnetic materials). Because μ differs only insignificantly from μ_0, it is very common to assume $\mu = \mu_0$ for diamagnetic and paramagnetic materials, as well as for antiferromagnetic substances, in most practical applications. Thus, these three classes of materials are commonly said to be nonmagnetic.

For ferromagnetic, ferrimagnetic, and superparamagnetic materials, on the other hand, μ is much larger than μ_0. These materials, especially ferromagnetic ones, often exhibit permanent magnetization, highly nonlinear behavior, and hysteresis effects, as we shall discuss in more detail in a later section. In ferromagnetics, the function $B(H)$ in Eq. (5.56) is in general nonlinear and has multiple branches. The magnetization properties of the material depend on the applied magnetic field intensity, H, and also on the history of magnetization of the material, i.e., on its previous states. In other words, the value of μ for a ferromagnetic material generally is not unique, but is a function of H and the previous history of the material. Typically, the maximum value of μ_r is around 250 for cobalt, 600 for nickel, and 5000 for iron (with 0.4% impurity), whereas it is as high as about 200,000 for purified iron (0.04% impurity) and 1,000,000 for supermalloy (79.5% Ni, 15% Fe, 5% Mo, 0.5% Mn). In many applications involving ferromagnetics, we assume

$$\boxed{\mu_r \to \infty,} \tag{5.62}$$

perfect magnetic conductor (PMC)

and such media are customarily referred to as perfect magnetic conductors (PMC). As we shall see in the next section, the magnetic flux density vector, **B**, in a nonmagnetic medium near the surface of a ferromagnetic (or PMC) body is always normal to the surface, the same as for the electric field intensity vector, **E**, near the surface of a perfect electric conductor (PEC), with $\sigma \to \infty$. Shown in Table 5.1 are values of the relative permeability of an illustrative set of selected materials,

Table 5.1. Relative permeability of selected materials

Material	μ_r	Material	μ_r
Bismuth	0.999833	Titanium	1.00018
Gold	0.99996	Platinum	1.0003
Mercury	0.999968	Palladium	1.0008
Silver	0.9999736	Manganese	1.001
Lead	0.9999831	Cast iron	150
Copper	0.9999906	Cobalt	250
Water	0.9999912	Nickel	600
Paraffin	0.99999942	Nickel-zinc ferrite (Ni-Zn-Fe_2O_3)	650
Wood	0.9999995	Manganese-zinc ferrite (Mn-Zn-Fe_2O_3)	1200
Vacuum	1	Steel	2000
Air	1.00000037	Iron (0.4% impurity)	5000
Beryllium	1.0000007	Silicon iron (4% Si)	7000
Oxygen	1.000002	Permalloy (78.5% Ni, 21.5% Fe)	7×10^4
Magnesium	1.000012	Mu-metal (75% Ni, 14% Fe, 5% Cu, 4% Mo, 2% Cr)	10^5
Aluminum	1.00002	Iron (purified – 0.04% impurity)	2×10^5
Tungsten	1.00008	Supermalloy (79.5% Ni, 15% Fe, 5% Mo, 0.5% Mn)	10^6

of considerable theoretical and/or practical interest – in terms of their magnetic properties.

A magnetic material is said to be homogeneous when its magnetic properties do not change from point to point in the region being considered. Otherwise, the material is inhomogeneous [e.g., $\mu = \mu(x, y, z)$ in the region]. Finally, some magnetic materials, such as ferrites, are anisotropic. Namely, an applied magnetic field (vector **B**) in one direction can produce magnetization (i.e., vector **M**) in another direction in a material. Accordingly, Eq. (5.60) becomes a matrix equation,

$[\mu]$ – permeability tensor of an anisotropic magnetic material

$$\boxed{\begin{bmatrix} B_x \\ B_y \\ B_z \end{bmatrix} = \begin{bmatrix} \mu_{xx} & \mu_{xy} & \mu_{xz} \\ \mu_{yx} & \mu_{yy} & \mu_{yz} \\ \mu_{zx} & \mu_{zy} & \mu_{zz} \end{bmatrix} \begin{bmatrix} H_x \\ H_y \\ H_z \end{bmatrix},} \tag{5.63}$$

where $[\mu]$ is the permeability tensor. It is analogous to the permittivity tensor, $[\varepsilon]$, defined by Eq. (2.52). However, Eq. (5.50) remains valid (it represents the definition of the **H** field), although **B**, **H**, and **M** are no longer parallel at a point. The anisotropy of ferrites is used in a number of microwave devices, including some types of gyrators, directional couplers, and isolators.

Note that in a linear, isotropic, and homogeneous magnetic material, we can substitute **H** by $\mathbf{B}/\mu$ in the generalized Ampère's law and bring $1/\mu$ (because it is constant) outside the integral sign in the integral form of the law, Eq. (5.49), or outside the operator (curl) sign in its differential form, Eq. (5.52), yielding

$$\oint_C \mathbf{B} \cdot \mathrm{d}\mathbf{l} = \mu I_C \quad \text{and} \quad \nabla \times \mathbf{B} = \mu \mathbf{J}, \tag{5.64}$$

respectively. We realize that these equations are identical to the corresponding free-space laws, Eqs. (4.48) and (4.83), except for μ_0 being substituted by μ. In the same way, replacing μ_0 with μ in Eq. (4.7) gives the version of the Biot-Savart law for a volume conduction current in a homogeneous magnetic medium of permeability μ:

$$\mathbf{B} = \frac{\mu}{4\pi} \int_v \frac{(\mathbf{J}\,\mathrm{d}v) \times \hat{\mathbf{R}}}{R^2}, \tag{5.65}$$

with $\mathbf{H} = \mathbf{B}/\mu$. Additionally, Eq. (4.132) and the concept of magnetic permeability imply that the Laplacian of the magnetic vector potential of a volume current in a homogeneous magnetic medium satisfies the following differential equation:

$$\nabla^2 \mathbf{A} = -\mu \mathbf{J}. \tag{5.66}$$

Finally, Eq. (4.108) becomes

$$\mathbf{A} = \frac{\mu}{4\pi} \int_v \frac{\mathbf{J}\,\mathrm{d}v}{R}. \tag{5.67}$$

From Eq. (5.50), we find that the magnetization vector in a linear and isotropic magnetic material can be expressed in terms of the magnetic field intensity vector as

$$\mathbf{M} = \frac{\mathbf{B}}{\mu_0} - \mathbf{H} = \left(\frac{\mu}{\mu_0} - 1\right)\mathbf{H} = (\mu_r - 1)\mathbf{H}. \tag{5.68}$$

If the material is also homogeneous, then the magnetization volume current density vector, $\mathbf{J}_m$, at a point in the material can be obtained directly from the conduction volume current density vector, **J**, at that point:

$$\mathbf{J}_m = \nabla \times \mathbf{M} = \nabla \times [(\mu_r - 1)\mathbf{H}] = (\mu_r - 1)\nabla \times \mathbf{H} = (\mu_r - 1)\mathbf{J}. \tag{5.69}$$

We see that there cannot be magnetization volume current ($\mathbf{J}_m = 0$) in a homogeneous linear magnetic medium with no free current ($\mathbf{J} = 0$).

Problems: 5.12–5.15; *Conceptual Questions* (on Companion Website): 5.8.

5.6 MAXWELL'S EQUATIONS AND BOUNDARY CONDITIONS FOR THE MAGNETOSTATIC FIELD

From the Biot-Savart law for the magnetic flux density $d\mathbf{B}$ of a single conduction current element $\mathbf{J}\,dv$ in free space and the superposition principle, we proved in Section 4.8 the law of conservation of magnetic flux, Eq. (4.99), for the magnetostatic field in free space. We can repeat here that same proof for a magnetization current element, $\mathbf{J}_m\,dv$ (or $\mathbf{J}_{ms}\,dS$), and get the same result, which means that the net magnetic flux (the flux of the vector $\mathbf{B}$) due to any distribution of conduction and magnetization currents (which, equivalently, reside in a vacuum) through a closed surface always equals zero. In other words, we conclude that the law of conservation of magnetic flux (Maxwell's fourth equation) holds for structures that include arbitrary magnetic materials.

We now write down the full set of Maxwell's equations governing the magnetostatic field in an arbitrary medium, together with the associated constitutive equation:

$$\boxed{\begin{cases} \oint_C \mathbf{H}\cdot d\mathbf{l} = \int_S \mathbf{J}\cdot d\mathbf{S} \\ \oint_S \mathbf{B}\cdot d\mathbf{S} = 0 \\ \mathbf{B} = \mathbf{B}(\mathbf{H})\ [\mathbf{B} = \mu\mathbf{H}] \end{cases}} \tag{5.70}$$

Maxwell's second equation, static field
Maxwell's fourth equation
constitutive equation for $\mathbf{B}$

The corresponding differential Maxwell's equations are:

$$\boxed{\nabla\times\mathbf{H} = \mathbf{J} \quad \text{and} \quad \nabla\cdot\mathbf{B} = 0.} \tag{5.71}$$

Maxwell's differential equations, magnetostatic field

In addition to integral and differential Maxwell's equations for any field, boundary conditions always represent the third form of field equations, and they are derived from the respective integral equations (differential equations apply only at a point). Let us derive here the boundary conditions for the magnetostatic field on the boundary surface between two arbitrary media. Let $\mathbf{J}_s$ be the density vector of a surface conduction (free) current that may exist on the boundary. We apply the generalized Ampère's law in integral form, Eq. (5.49), to a narrow rectangular elementary contour C positioned such that $\mathbf{J}_s$ is normal to the plane of the contour, as depicted in Fig. 5.12. Having in mind Eqs. (2.79) and (5.30), we obtain

$$\oint_C \mathbf{H}\cdot d\mathbf{l} = H_{1t}\,\Delta l - H_{2t}\,\Delta l = I_C = J_s\Delta l, \tag{5.72}$$

which yields

$$H_{1t} - H_{2t} = J_s. \tag{5.73}$$

In vector form [also see Eq. (2.84)],

$$\boxed{\hat{\mathbf{n}}\times\mathbf{H}_1 - \hat{\mathbf{n}}\times\mathbf{H}_2 = \mathbf{J}_s,} \tag{5.74}$$

boundary condition for $\mathbf{H}_t$: $\hat{\mathbf{n}}$ *directed from region 2 to region 1*

where $\hat{\mathbf{n}}$ is the normal unit vector on the surface, directed from region 2 to region 1. If no surface conduction current exists on the boundary, Eq. (5.73) becomes

$$H_{1t} = H_{2t} \quad (\mathbf{J}_s = 0), \tag{5.75}$$

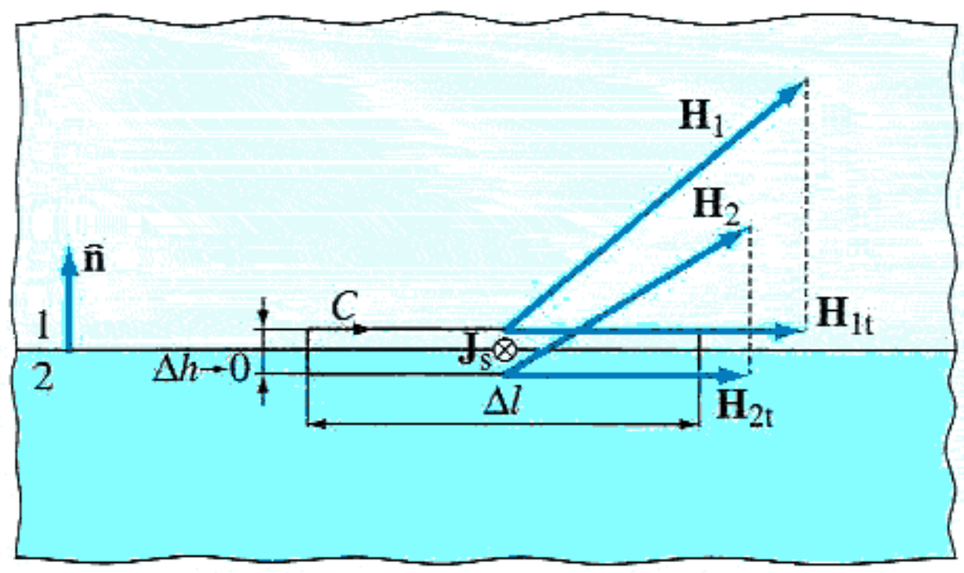

Figure 5.12 Deriving the boundary condition for tangential components of vector **H** on the boundary surface between two arbitrary magnetic media.

that is, the tangential component of **H** is continuous across the boundary free of conduction current.

Noting, on the other hand, that the law of conservation of magnetic flux, Eq. (4.99), and the continuity equation for steady currents, Eq. (3.40), have exactly the same form, we conclude that the corresponding boundary conditions must have exactly the same form as well. Therefore, from the boundary condition for normal components of the vector **J** in the steady current field, Eq. (3.55), we directly write the boundary condition for normal components of the vector **B** in the magnetostatic field:

boundary condition for $\mathbf{B}_n$

$$\boxed{\hat{\mathbf{n}} \cdot \mathbf{B}_1 - \hat{\mathbf{n}} \cdot \mathbf{B}_2 = 0 \quad \text{or} \quad B_{1n} = B_{2n}.} \tag{5.76}$$

It tells us that $\mathbf{B}_n$ is always continuous across a boundary.

At an interface between two linear magnetic media of permeabilities μ_1 and μ_2 with no surface conduction current ($\mathbf{J}_s = 0$), the law of refraction of the magnetic field lines holds that is entirely analogous to the corresponding laws in electrostatics, Eq. (2.87), and steady current field, Eq. (3.56). With α_1 and α_2 denoting the angles that field lines in region 1 and region 2 make with the normal to the interface, as shown in Fig. 5.13, we have

law of refraction of magnetic field lines

$$\boxed{\frac{\tan\alpha_1}{\tan\alpha_2} = \frac{\mu_1}{\mu_2}.} \tag{5.77}$$

This relationship indicates that magnetic field lines are bent farther away from the normal in the medium with the higher permeability. Bending of field lines is basically due to unequal magnetization surface currents on the two sides of the interface.

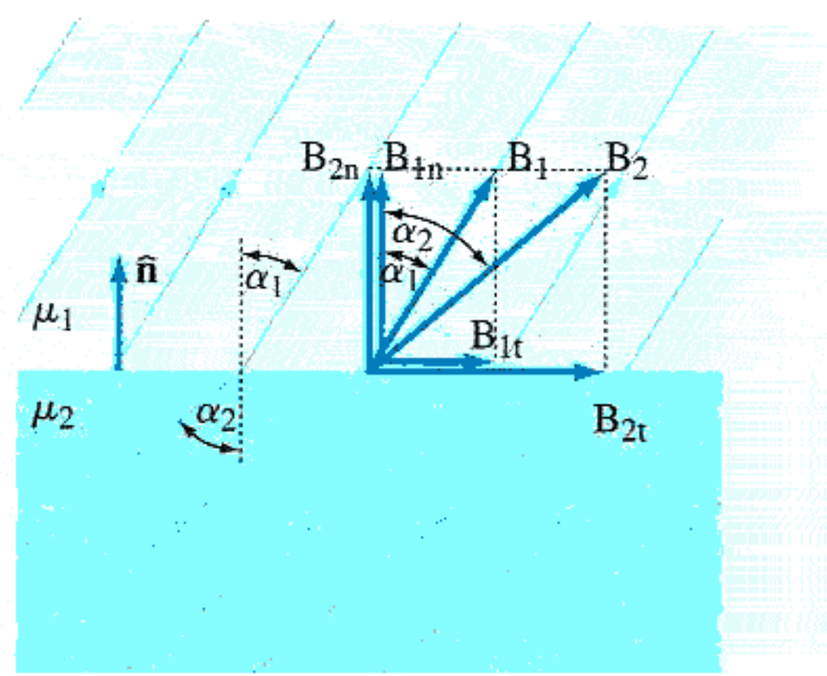

Figure 5.13 Refraction of magnetic field lines at a magnetic-magnetic interface.

Note that if region 2 is filled with a ferromagnetic material and region 1 with a nonmagnetic material, then $\mu_2 \gg \mu_1$ and $\mu_1/\mu_2 \approx 0$, and Eq. (5.77) results in

$$\alpha_1 \approx 0 \quad (\mu_2 \gg \mu_1) \tag{5.78}$$

for any α_2 (except for $\alpha_2 = 90°$, i.e., for field lines in region 2 parallel to the interface). This means that magnetic field lines in a nonmagnetic medium near the interface with a ferromagnetic medium (or PMC) are always normal to the interface.

Finally, using Eq. (5.32) and adding up the magnetization surface current density vectors that accumulate on the two sides of a magnetic-magnetic interface, analogously to deriving Eq. (2.89) in electrostatics, we arrive to the following boundary condition for the tangential components of the magnetization vector:

$$\boxed{\hat{\mathbf{n}} \times \mathbf{M}_1 - \hat{\mathbf{n}} \times \mathbf{M}_2 = \mathbf{J}_{\text{ms}},} \tag{5.79}$$

boundary condition for $\mathbf{M}_t$

where $\hat{\mathbf{n}}$ is directed from medium 2 to medium 1 (Figs. 5.12 and 5.13) and $\mathbf{J}_{\text{ms}}$ is the total magnetization surface current density vector at the interface.

Problems: 5.16; *Conceptual Questions* (on Companion Website): 5.9–5.12; *MATLAB Exercises* (on Companion Website).

5.7 IMAGE THEORY FOR THE MAGNETIC FIELD

Magnetostatic systems often include current conductors in the presence of large flat ferromagnetic bodies. By utilizing image theory, similarly to the procedure described in Section 1.21, we can remove the ferromagnetic body from the system and replace it by an image of the original current distribution. The equivalent problem is then much simpler to solve because it consists of a known current distribution (original plus image) in free space.

Consider a straight current conductor in a nonmagnetic half-space in the vicinity of an infinite planar interface with a ferromagnetic (or PMC) half-space. Let the conductor be parallel to the interface. Eq. (5.78) tells us that the ferromagnetic material in the lower half-space, i.e., the induced magnetization current in the material, influences the resultant magnetic flux density vector, **B**, such that it has no tangential component at the upper side of the interface, as shown in Fig. 5.14(a). This condition remains unaltered, however, if we replace the ferromagnetic block by another conductor parallel to the interface that is positioned symmetrically with respect to the original conductor and carries a current of the same intensity and the same direction, Fig. 5.14(b). We conclude thus that, as far as the magnetic field in the upper half-space is concerned, systems in Fig. 5.14(a) and Fig. 5.14(b) are equivalent. This is an example of the image theory (theorem) for the magnetic field.

The theory is not restricted to conductors parallel to the material interface only. It states that an arbitrary current configuration above an infinite ferromagnetic (or PMC) plane can be replaced by a new current configuration in free space consisting from the original current configuration itself and its positive image in the ferromagnetic plane. The equivalence is with respect to the magnetic field above the ferromagnetic plane, the component of that field due to the induced magnetization current in the ferromagnetic material being equal to the field of the image. As another example, Fig. 5.15 shows the image of a current conductor consisting of three segments with different orientations with respect to the ferromagnetic interface in Fig. 5.15(a), where it is a simple matter to conclude that the vector **B** in the plane of symmetry in Fig. 5.15(b) has no component tangential to the plane.

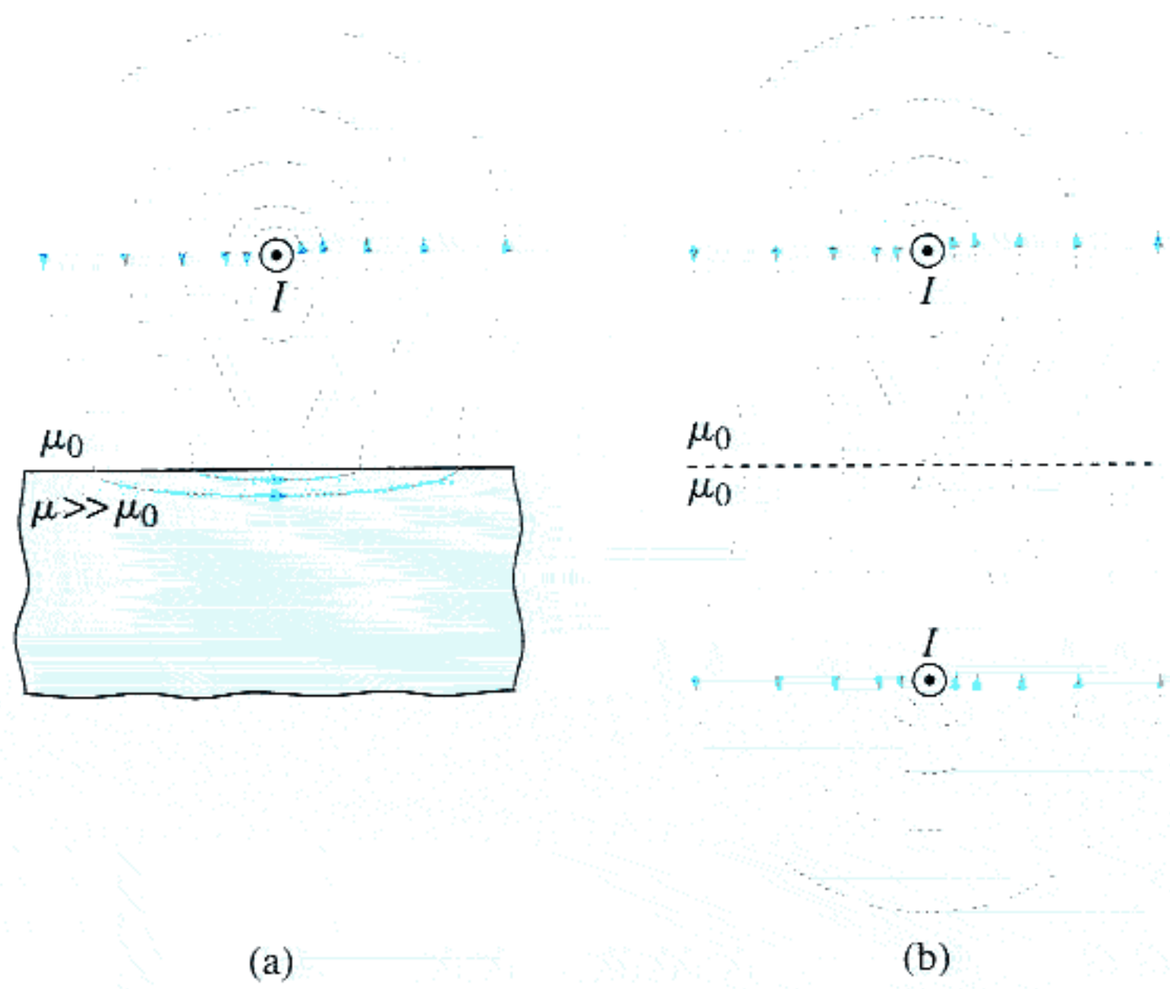

Figure 5.14 (a) Straight current conductor parallel to the interface of a ferromagnetic (or PMC) half-space. (b) By image theory, the influence of the ferromagnetic material on the magnetic field in the upper half-space can be represented by a positive image of the original current.

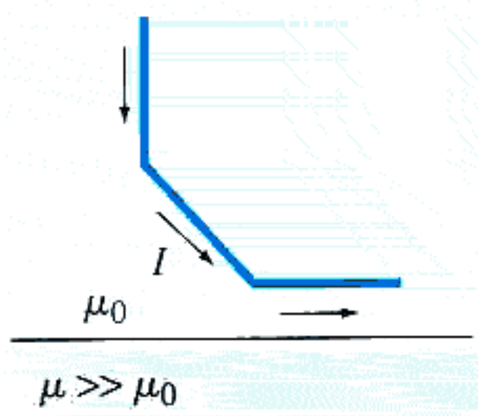

(a)

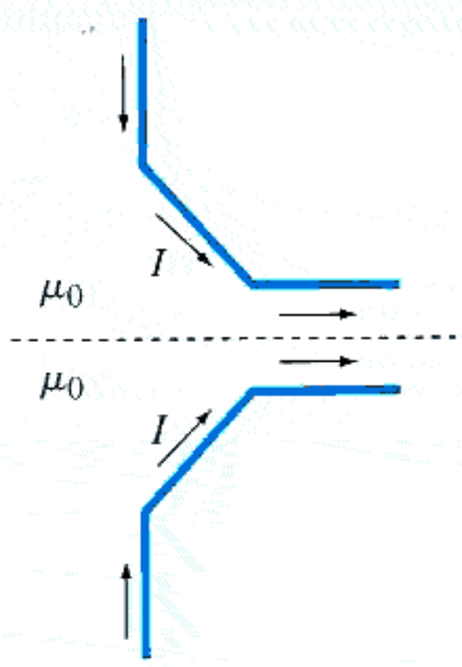

(b)

Figure 5.15 Image theory for the magnetic field due to a current conductor with arbitrarily oriented segments above a ferromagnetic (or PMC) plane: (a) original system with the material interface and (b) equivalent free-space system.

Example 5.8 Force on a Conductor above a Ferromagnetic Plane

A very long and thin wire is situated in air at a height h above a ferromagnetic half-space, parallel to its surface, and carries a current of intensity I. Determine the magnetic force on the wire per unit of its length.

Solution By image theory, the system wire-ferromagnetic is equivalent to a symmetric two-wire system in air, as shown in Fig. 5.16. The force on the upper (original) conductor per unit of its length is then obtained using Eq. (4.166) with $I_1 = I_2 = I$ and $d = 2h$, that is,

$$\mathbf{F}'_{\mathrm{m}} = IB = \frac{\mu_0 I^2}{4\pi h}. \tag{5.80}$$

Here, B is the magnetic flux density along the upper conductor due to the lower conductor, i.e., due to the magnetization current in the ferromagnetic material. We see that a large ferromagnetic (or PMC) block always attracts a current conductor running parallel to it.

Example 5.9 Strip Conductor between Two PMC Planes

An infinitely long thin strip conductor of width a carries a steady current of intensity I. The strip is placed between two parallel PMC planes, as shown in Fig. 5.17(a). Find the magnetic flux density vector in the space between the PMC planes, assuming that it is air-filled.

Solution By multiple applications of the image theory for the magnetic field, we obtain the equivalent system in Fig. 5.17(b), which represents an infinite planar current sheet with surface current density $J_s = I/a$ in free space. The magnetic field between the PMC planes is thus uniform, with flux density $B = \mu_0 J_s/2 = \mu_0 I/(2a)$ [see Fig. 4.21 and Eq. (4.47)].

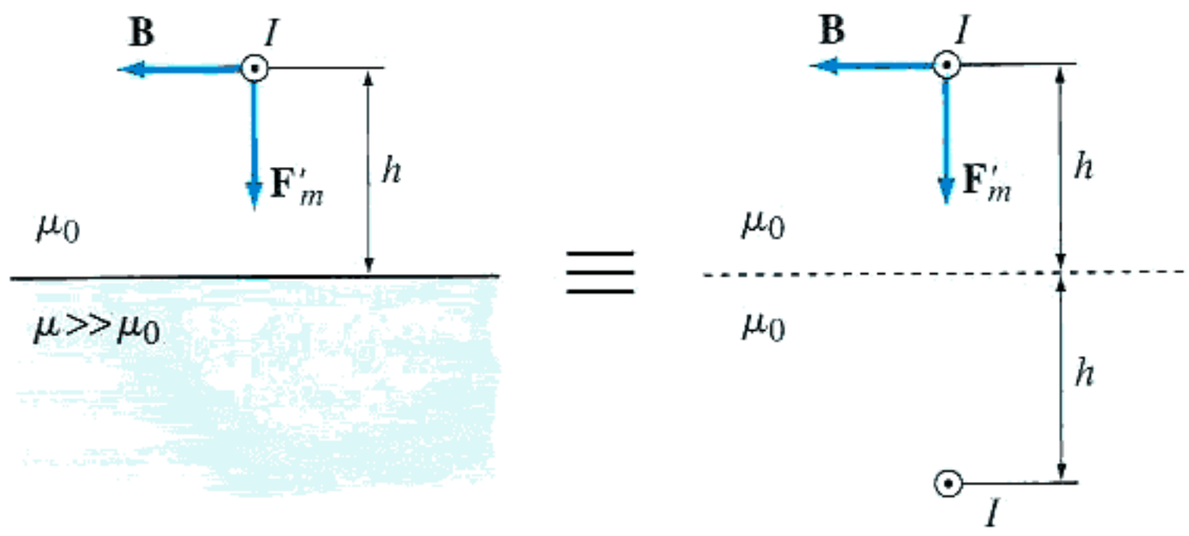

Figure 5.16 Evaluation of the force on a horizontal straight wire with a current above a ferromagnetic plane, using image theory; for Example 5.8.

Example 5.10 **Uniformly Magnetized Hemisphere on a PMC Plane**

A uniformly magnetized ferromagnetic hemisphere of radius a in air is lying on a PMC ($\mu_r \to \infty$) plane. The magnetization vector is $\mathbf{M}$, and it is perpendicular to the plane, as shown in Fig. 5.18. Calculate the magnetic flux density and field intensity vectors at the center of the bottom surface of the hemisphere (point O in the figure).

Solution We first evaluate the distribution of equivalent magnetization currents of the hemisphere. The magnetization volume current density vector inside the material and the magnetization surface current density vector on the bottom surface of the hemisphere are both zero. There is, however, a hemispherical sheet of magnetization current over the upper surface of the hemisphere given by Eq. (5.42), where now $0 \le \theta \le \pi/2$. Using the image theory for the magnetic field, we then supplement this sheet, considered to be in a vacuum, with another hemispherical sheet below the plane of symmetry, which is also described by the function in Eq. (5.42), but with $\pi/2 \le \theta \le \pi$ (note that $\sin\theta$ is symmetric with respect to $\theta = \pi/2$, which corresponds to a positive image of the current, exactly as required by the image theory). We thus obtain the full spherical sheet of magnetization current in Fig. 5.10, and conclude that the magnetized hemisphere on the PMC plane is equivalent to the magnetized sphere of Fig. 5.10, in free space. Hence, the magnetic flux density vector at the sphere center, as well as that at the point O in Fig. 5.18, is given by Eq. (5.45). Finally, by means of Eq. (5.50), the magnetic field intensity vector at the point O is

$$\mathbf{H} = \frac{\mathbf{B}}{\mu_0} - \mathbf{M} = \frac{2}{3}\mathbf{M} - \mathbf{M} = -\frac{\mathbf{M}}{3}. \tag{5.81}$$

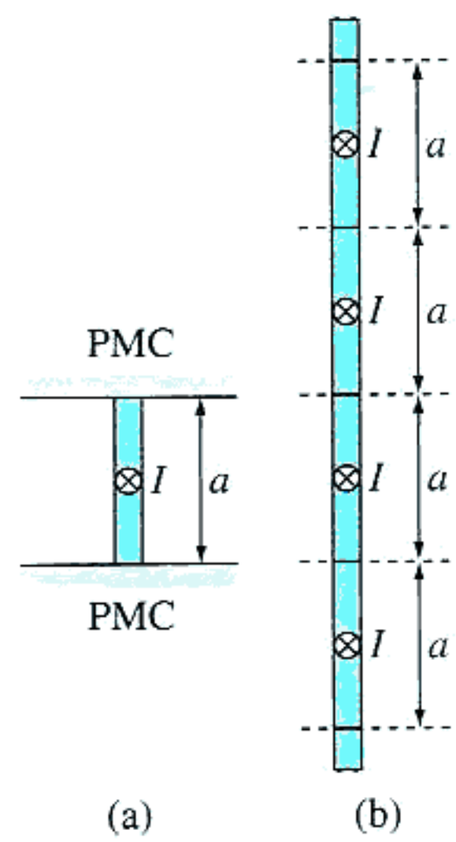

Figure 5.17 (a) Strip conductor between two parallel PMC planes and (b) equivalent infinite planar current sheet in free space; for Example 5.9.

Problems: 5.17–5.19; *Conceptual Questions* (on Companion Website): 5.13; *MATLAB Exercises* (on Companion Website).

5.8 MAGNETIZATION CURVES AND HYSTERESIS

In this section, we consider in more detail the B-H relationship, Eq. (5.56), for ferromagnetic materials. This relationship, being nonlinear in general, is usually given as a graph showing B (ordinate) as a function of H (abscissa). A curve representing

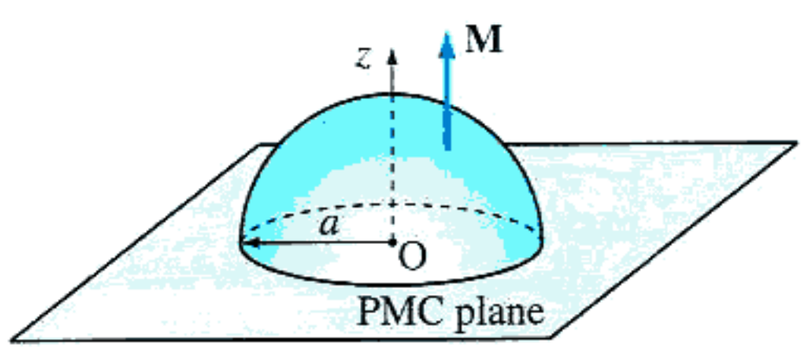

Figure 5.18 Ferromagnetic hemisphere with a uniform magnetization lying on a PMC plane; for Example 5.10.

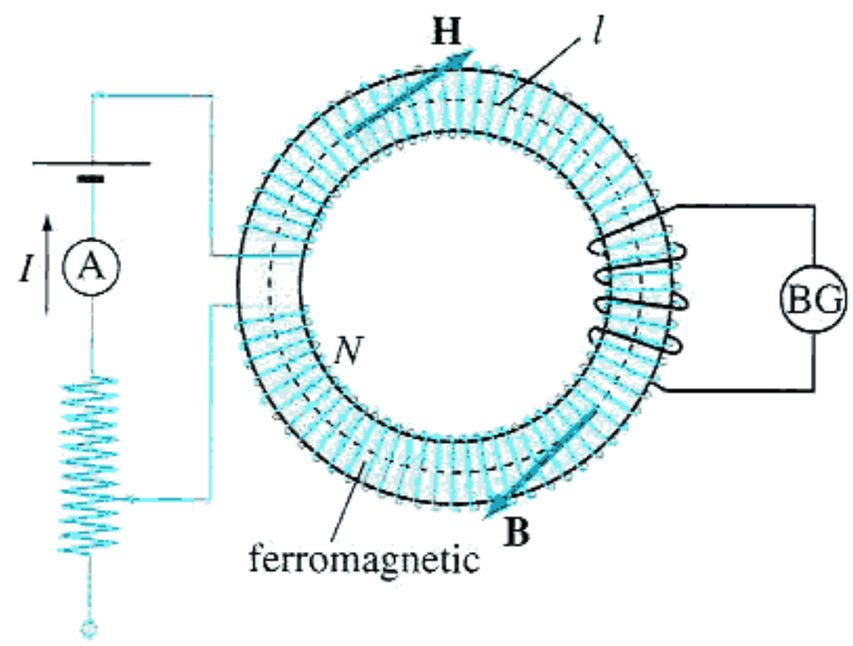

Figure 5.19 Simple apparatus for measurement of magnetization curves.

the function $B(H)$ on such a diagram is called a magnetization curve and is obtained by measurement on a given material specimen.

Fig. 5.19 shows the simplest apparatus for measurement of magnetization curves, where a uniform winding is placed over a thin toroidal core (ring) cut from a ferromagnetic sample we want to measure. If a current I is established in the toroid (primary coil), the magnetic field intensity H in the core is given by Eq. (5.53), where N is the number of wire turns of the coil and l is the mean length of the toroid. By varying I, therefore, we directly vary H (H is proportional to I). The magnetic flux density B in the core is then measured, as a response to H, by a ballistic galvanometer (BG) connected to another winding (secondary coil) that is placed over the core. Namely, the galvanometer measures the charge that passes through the secondary circuit, as a consequence of the change of magnetic flux through the secondary coil. This charge, as we shall see in the next chapter, is proportional to the flux change, so that the galvanometer actually serves as a fluxmeter. Thus, by changing, step by step, the current I in the primary coil and field H in the core, and measuring the corresponding values of the flux density B, we obtain, point by point, the magnetization curve of the material.

Shown in Fig. 5.20 is a typical initial magnetization curve for a ferromagnetic sample, where the material is completely demagnetized and both B and H are zero

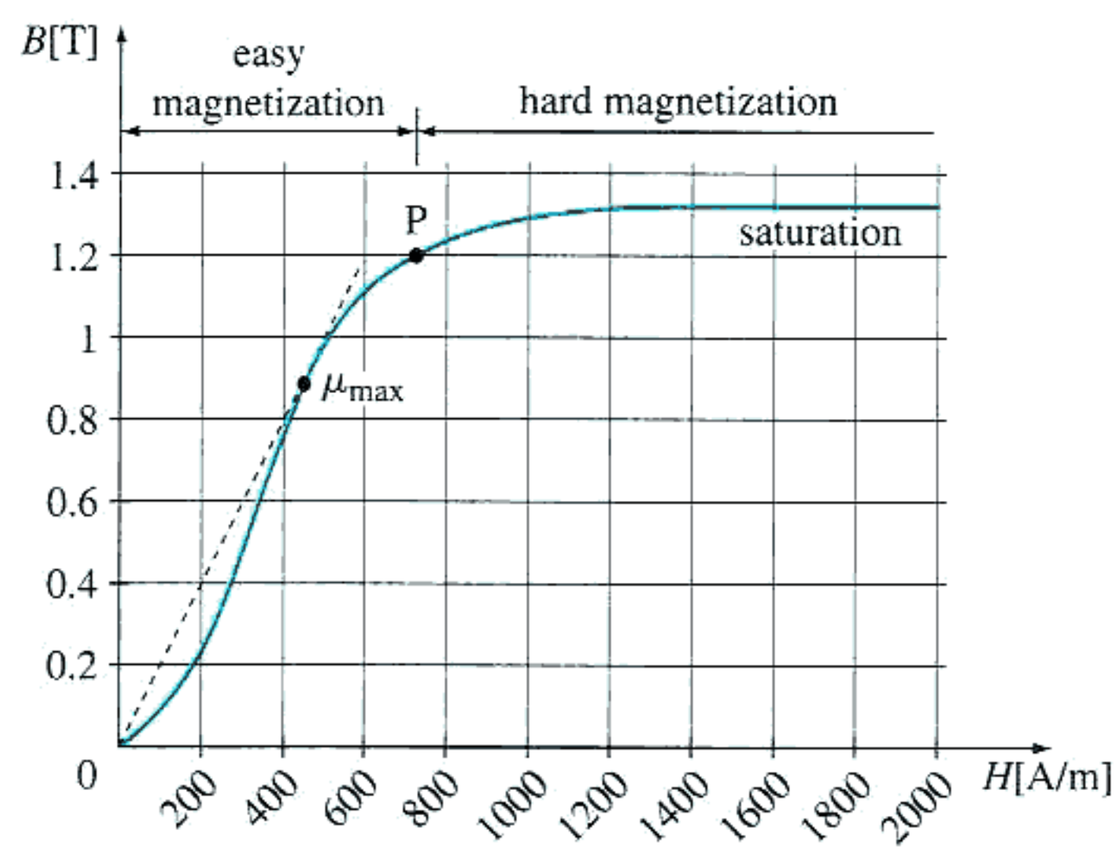

Figure 5.20 Typical initial magnetization curve for a ferromagnetic material.

before a field is applied. As we begin to apply a current in the primary circuit in Fig. 5.19, the magnetic flux density also rises, but not linearly. Moreover, the value of B rises rapidly at first and then more slowly. The first part of the initial magnetization curve (roughly up to the point P in Fig. 5.20) represents the region of easy (steep) magnetization. In the upper section of the curve, the increase in magnetization due to gradual rotations of magnetic domains in the material not already parallel to **H** is more difficult, and the curve tends to become flat. This is the region of hard (flat) magnetization. Very strong magnetic fields are usually required to reach the state of saturation, where all the moments of magnetic domains in the material are parallel to **H** and the magnetization curve flattens off completely.

The permeability at any point on the magnetization curve is given by

$$\mu = \frac{B}{H}, \tag{5.82}$$

where B is the ordinate of the point (in T) and H is the abscissa (in A/m). The relative permeability is then $\mu_r = \mu/\mu_0$. The maximum permeability is at the point on the curve with the largest ratio of B to H, i.e., at the point of tangency with the straight line of steepest slope that passes through the origin and intersects the magnetization curve (Fig. 5.20). Note that the maximum μ does not correspond to the steepest slope of the magnetization curve, because μ is not proportional to the slope of the curve ($\mathrm{d}B/\mathrm{d}H$), but equals the ratio B/H.

Having reached saturation, let us now turn to Fig. 5.21, where we continue our experiment – by reducing I and H. As we do so, the effects of hysteresis begin to show, and we do not retrace the initial-magnetization curve. Hysteresis means that B lags behind H, so that the magnetization curves for increasing and decreasing the applied field are not the same. Even after H becomes zero, B does not go to zero, but to a value $B = B_r$, termed the remanent (residual) magnetic flux density. Note that the existence of a remanent flux density in a ferromagnetic material makes permanent magnets possible. We then reverse H (by reversing the polarity of the battery in Fig. 5.19), and increase it in the negative direction, so that B comes to zero at $H = -H_c$, where H_c is the so-called coercive force. As H is increased in the negative direction further, the material becomes magnetized even more, with negative polarity. It passes through the stages of easy and hard magnetization, the magnetization curve flattens off, and negative saturation is reached. The end of the curve on the left-hand side of the diagram is for the field $H = -H_m$, after which

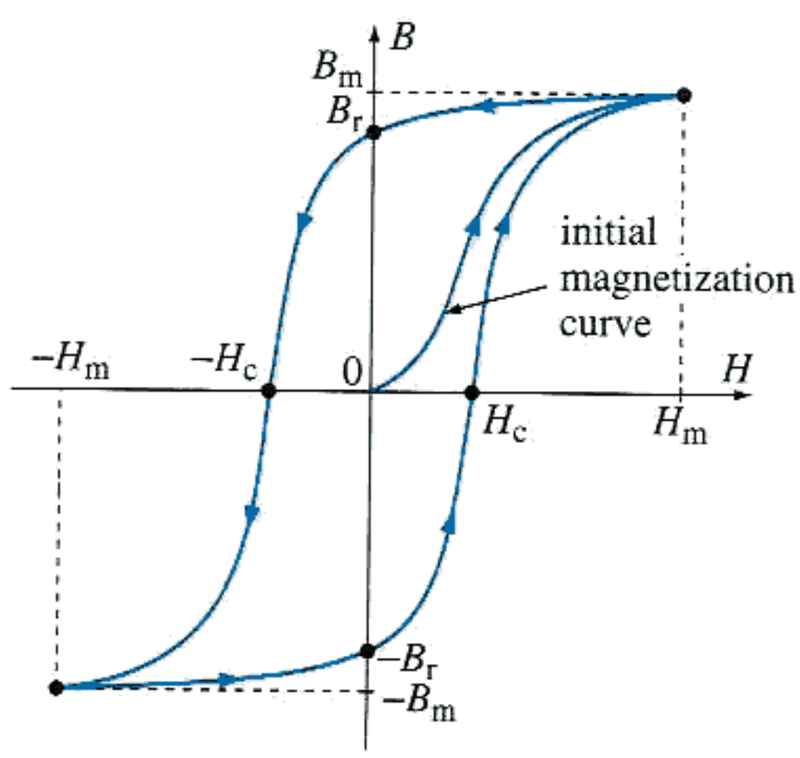

Figure 5.21 Typical hysteresis loop for a ferromagnetic material.

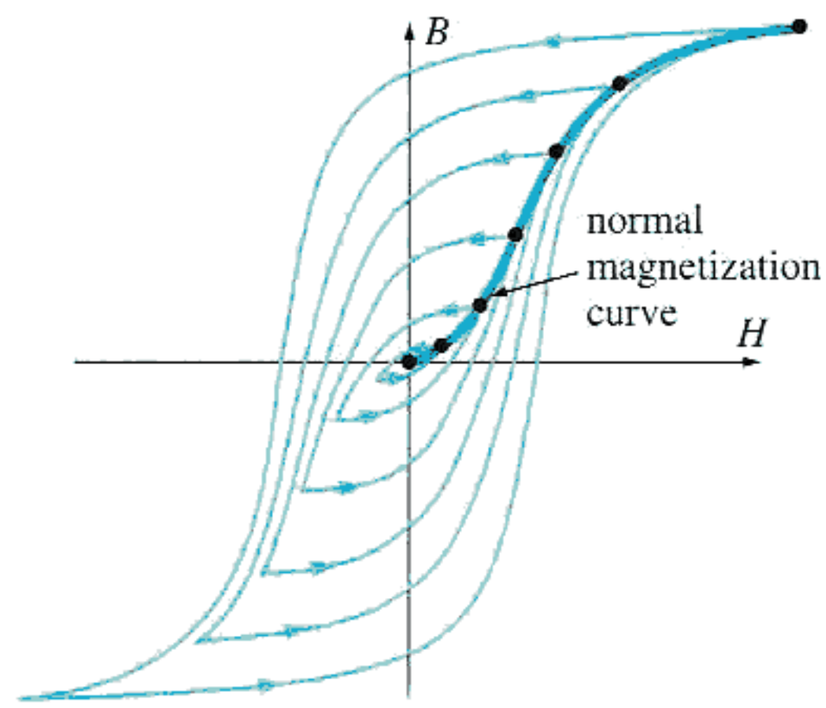

Figure 5.22 Demagnetization of a ferromagnetic sample by reversals of the applied field **H**; definition of the normal magnetization curve.

we start reducing H. The next intercept of the curve with the B axis (for $H = 0$) gives $B = -B_r$ (negative remanent flux density). At this point, we reverse the battery polarity again and continue – by increasing H in the positive direction. This makes the flux density zero at a positive field $H = H_c$ (coercive force). With a further increase in H, the material reaches positive saturation (at $H = H_m$), and a full cycle in the BH diagram is completed. The loop traced out by the magnetization curve during this cycle is referred to as the hysteresis loop.

Having carried our ferromagnetic specimen to saturation at both ends of the magnetization curve in Fig. 5.21, we now move on to Fig. 5.22, to continue to cycle the applied field H, but over successively smaller ranges ($\pm H$ is brought to smaller and smaller amplitudes on each reversal). We obtain thus a series of hysteresis loops that decrease in size, and the residual B for $H = 0$ eventually becomes zero, that is, the material is left in a demagnetized state. Such a process is used for demagnetization of objects that have a residual magnetization (i.e., remanent flux density) under conditions of zero applied magnetic field. In practice, the process can be carried out by inserting the object to be demagnetized inside a coil with a low-frequency ac current, and then gradually reducing the current amplitude in the coil or slowly removing the object from the coil with the current amplitude constant. The curve connecting the tips of the hysteresis loops in Fig. 5.22 is another characteristic of ferromagnetic materials known as the normal magnetization curve. For a particular ferromagnetic material, the normal and initial magnetization curves are very similar.

Ferromagnetic materials having small coercive forces H_c and therefore narrow (thin) hysteresis loops (with small loop areas), as illustrated in Fig. 5.23, are referred to as soft ferromagnetics. As we shall see in a later chapter, the area enclosed by the hysteresis loop is proportional to energy loss per unit volume of the material in one cycle of field variation. This is so-called hysteresis loss, which corresponds to the energy lost in the form of heat in overcoming the friction encountered during the movements of magnetic domain walls and rotations of the domains in a ferromagnetic material. Soft ferromagnetic materials have a large magnetization for a very small applied field and exhibit low hysteresis losses. Additionally, they have very large values of initial permeability [μ in Eq. (5.82) for a very small H]. For example, supermalloy, a typical soft ferromagnetic, has an initial relative permeability on the order of 10^5, $B_r = 0.6$ T, and $H_c = 0.4$ A/m. Soft ferromagnetic materials are used for building transformers and ac machines

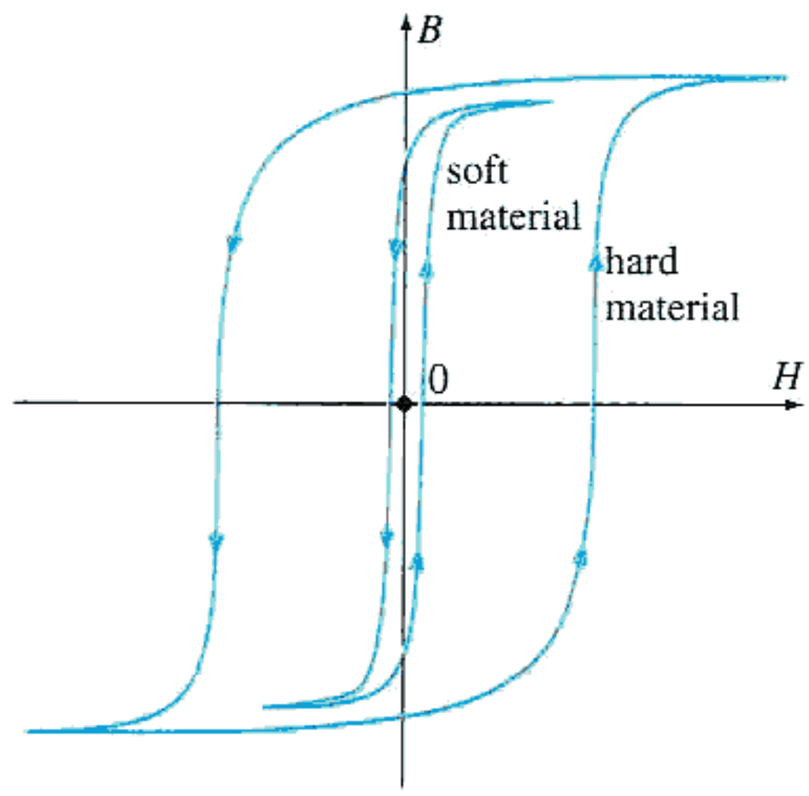

Figure 5.23 Hysteresis loops for soft and hard ferromagnetic materials.

(motors and generators), where the material is permanently exposed to alternating magnetization.

Hard ferromagnetic materials, on the other hand, have large coercive forces H_c and hence broad (fat) hysteresis loops (Fig. 5.23). They have small initial permeabilities, and are used for building permanent magnets and dc machines. In these applications, fields do not change frequently, and hysteresis losses, therefore, are not significant, in spite of large hysteresis loop areas. The essential characteristic of permanent-magnet materials is a high remanent flux density B_r (they are permanently magnetized even with no magnetic field applied), but it is also important that their coercive force be large, so that the material may not be easily demagnetized. Alnico, an aluminum-nickel-cobalt alloy with a small amount of copper, is a typical hard ferromagnetic, having an initial μ_r around 4, B_r around 1 T, and H_c on the order of 50,000 A/m.

Conceptual Questions (on Companion Website): 5.14–5.16.

5.9 MAGNETIC CIRCUITS – BASIC ASSUMPTIONS FOR THE ANALYSIS

Magnetic circuit in general is a collection of bodies and media that form a way along which the magnetic field lines close upon themselves, i.e., it is a circuit of the magnetic flux flow. The name arises from the similarity to electric circuits. In practical applications, including transformers, generators, motors, relays, magnetic recording devices, etc., magnetic circuits are formed from ferromagnetic cores of various shapes, that may or may not have air gaps, with current-carrying windings wound about parts of the cores. Fig. 5.24 shows a typical magnetic circuit.

The analysis of magnetic circuits with steady currents in the windings (dc magnetic circuits) is based, of course, on Maxwell's equations for the magnetostatic field in arbitrary media, Eqs. (5.70). Given, however, great complexity of the rigorous analysis of practical magnetic circuits, we introduce here a set of approximations that will, in conjunction with Maxwell's equations, make the analysis much simpler and yet accurate enough for engineering applications.

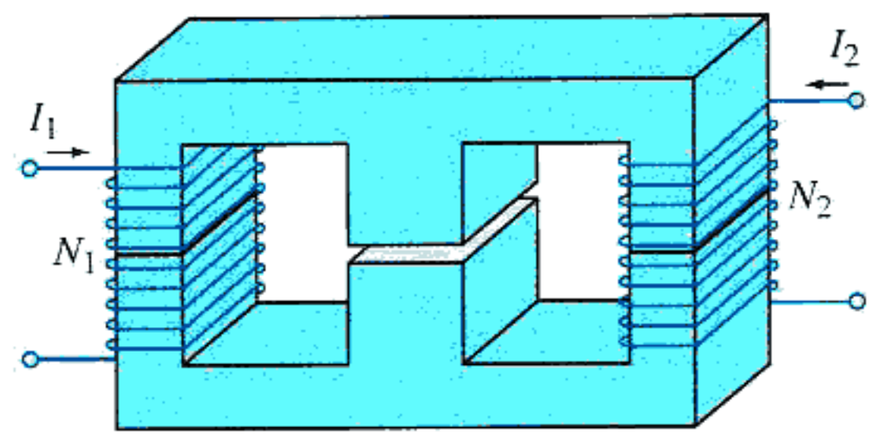

Figure 5.24 Typical magnetic circuit.

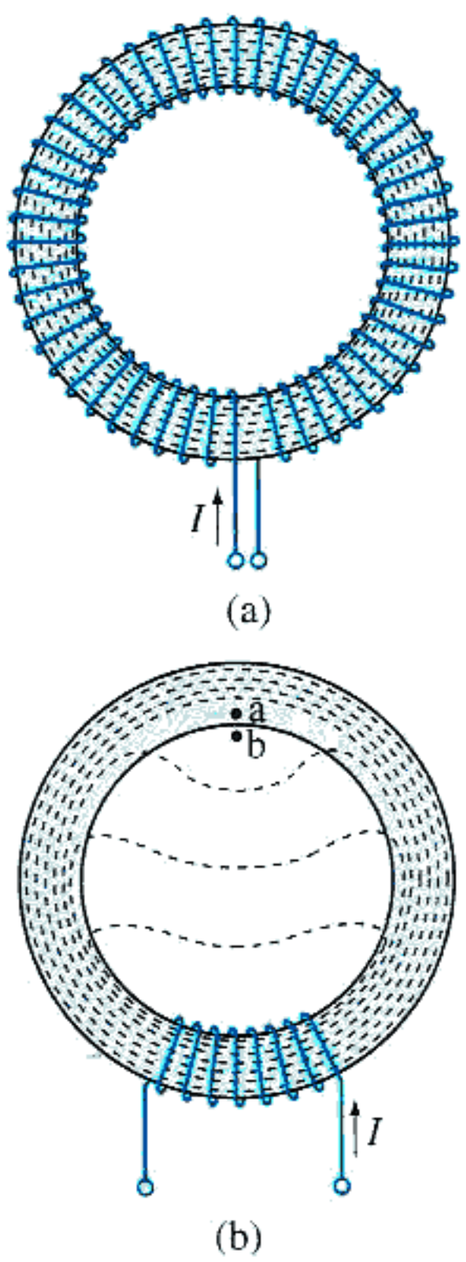

Figure 5.25 Toroidal ferromagnetic core with (a) a uniform winding and (b) concentrated winding.

Firstly, we assume that the magnetic flux is concentrated exclusively inside the magnetic circuit, i.e., in the branches of the ferromagnetic core and air gaps. This is never exactly true. For a toroidal ferromagnetic core with a uniform winding shown in Fig. 5.25(a), however, the flux is restricted to the interior of the toroid as a consequence of the geometrical symmetry of the structure, provided that the wire turns are very tightly wound over the core. In reality, there is always some leakage flux between the wire turns. In addition, in circuits containing coils placed only over parts of the core, some flux lines bridge the space between the core sections through air, as indicated in Fig. 5.25(b). Boundary conditions for the magnetostatic field applied to the interface between the ferromagnetic and air in Fig. 5.25(b) tell us that magnitudes of the magnetic flux density vector at points a and b in the figure are related as $B_a \approx \mu_r B_b$. As μ_r is very large for ferromagnetic materials, $B_a \gg B_b$, so we conclude that practically the entire magnetic flux is restricted to the ferromagnetic core, and the larger the μ_r the more accurate this assumption. Note that in electric circuits this is always true for the current flow because the conductivity of air is zero, whereas the permeability of air is not.

Secondly, we assume that air gaps in the magnetic circuit are narrow enough so that the fringing flux near the gap edges can be neglected. For more precise analysis, formulas for an effective length and cross-sectional area of the gap may be used to incorporate the fringing effects into the basic equations for the circuit.

Finally, we assume that the magnetic field is uniform throughout the volume of each branch of the circuit. Then, in applying Maxwell's equations, every cross section of a branch is assumed to have the same area, and the path of every flux line along the branch is assumed to be of the same length, equal to the mean length of that part of the circuit. This is true only for thin magnetic circuits. In many applications involving thick cores, however, the error due to thin magnetic circuit approximations is acceptable, which is illustrated in the following examples.

Example 5.11 Thick Toroid with a Linear Ferromagnetic Core

Assume that the toroidal coil in Fig. 4.18 is wound about a core made of a linear ferromagnetic material of permeability μ. (a) Determine the magnetic flux through the core. (b) Find the error made in the flux computation if the magnetic field in the core is assumed to be uniform, specifically for $b - a = 0.1a$ (thin toroid) and $b - a = a$ (thick toroid).

Solution

(a) The magnetic field intensity vector, **H**, is the same as in the air-filled toroid in Fig. 4.18. From Eq. (4.65),

H inside a thick toroidal coil

$$\boxed{H(r) = \frac{NI}{2\pi r}, \quad a \le r \le b.} \tag{5.83}$$

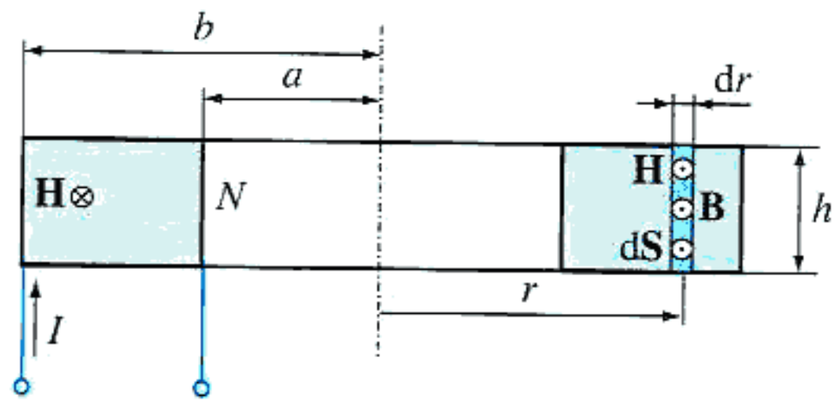

Figure 5.26 Evaluation of the magnetic flux through a cross section of a thick toroidal coil with a linear ferromagnetic core; for Example 5.11.

The magnetic flux through the core is then obtained by integrating the flux density $B(r) = \mu H(r)$ over a cross section of the toroid, as shown in Fig. 5.26,

$$\Phi = \int_{r=a}^{b} B(r)\,\mathrm{d}S = \frac{\mu N I h}{2\pi}\int_a^b \frac{\mathrm{d}r}{r} = \frac{\mu N I h}{2\pi}\ln\frac{b}{a}, \tag{5.84}$$

where $\mathrm{d}S$ is the surface area of a thin strip of length h and width $\mathrm{d}r$.

(b) Under the assumption of a uniform field distribution in the core, the path of every flux line is assumed to be of the same length, equal to the mean length of the toroid, $l = \pi(a+b)$, and the magnetic field intensity is given by Eq. (5.53). The approximate flux is then obtained by multiplying the constant flux density $B = \mu H$ by the surface area S of the core cross section,

$$\Phi_{\text{approx}} = BS = \mu H(b-a)h = \frac{\mu N I h}{\pi}\frac{b-a}{a+b}. \tag{5.85}$$

The associated relative error in the flux computation is computed as

$$\delta_\Phi = \frac{|\Phi_{\text{approx}} - \Phi|}{\Phi} = \left|\frac{2(b/a-1)}{(1+b/a)\ln(b/a)} - 1\right|. \tag{5.86}$$

For $b - a = 0.1a$, that is, $b/a = 1.1$, the error turns out to be $\delta_\Phi = 0.075\%$, while for $b - a = a$ $(b/a = 2)$, $\delta_\Phi = 3.8\%$. We see that even for a quite thick toroid (the latter case), the approximate expression in Eq. (5.85) is reasonably accurate.

Example 5.12 Thick Toroid with a Nonlinear Ferromagnetic Core

Let the toroidal coil of Fig. 4.18 be wound around a core made from a nonlinear ferromagnetic material. Fig. 5.27(a) shows the cross section of such a structure, with $a = 2$ cm, $b = 4$ cm, $h = 1$ cm, $N = 200$, and $I = 1$ A. Assume that the initial magnetization curve of the material can be approximated by the piece-wise linear curve shown in Fig. 5.27(b). Calculate the magnetic flux through the core (a) rigorously and (b) assuming that the field in the core is uniform.

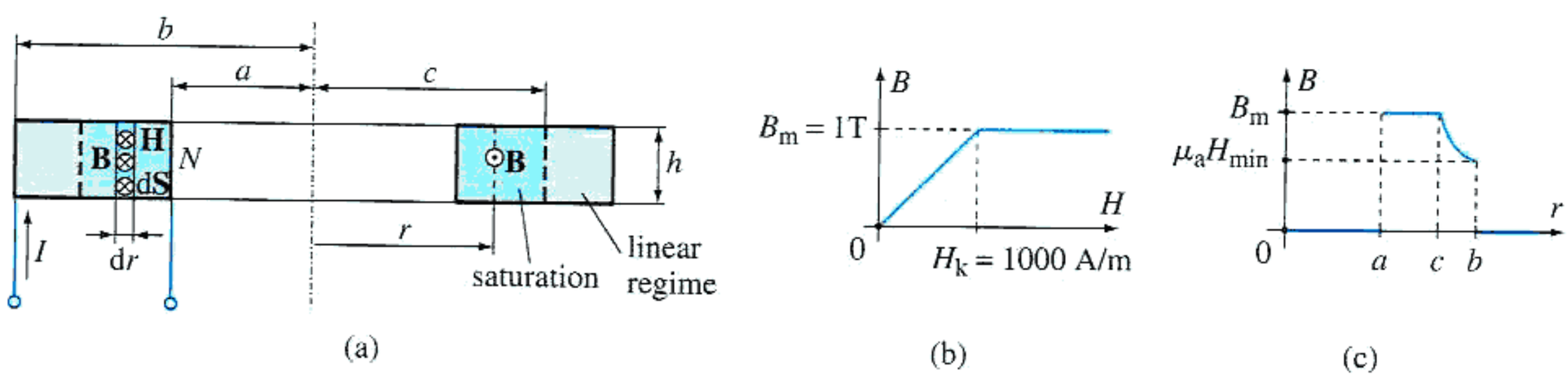

Figure 5.27 Analysis of a thick toroidal coil with a nonlinear ferromagnetic core: (a) cross section of the structure, (b) idealized initial magnetization curve of the material, and (c) distribution of the magnetic flux density along the radial axis; for Example 5.12.

Solution

(a) From Eq. (5.83), the minimum and maximum magnetic field intensities in the core are

$$H_{\min} = H(b) = 796 \text{ A/m} \quad \text{and} \quad H_{\max} = H(a) = 1592 \text{ A/m}, \tag{5.87}$$

respectively. Since the field value $H_k = 1000$ A/m, representing the limit on the magnetization curve in Fig. 5.27(b) up to which the material is in the linear regime and above which is in saturation ("knee" value), satisfies the condition

$$H_{\min} < H_k < H_{\max}, \tag{5.88}$$

we conclude that the part of the core for which $H(r) > H_k$ is in saturation $[B(r) = B_m]$, whereas the remaining part of the core is in the linear regime. In this latter case,

$$B(r) = \mu_a H(r), \quad \mu_a = \frac{B_m}{H_0} = 0.001 \text{ H/m}, \tag{5.89}$$

where μ_a is the initial permeability of the material. From the condition

$$H(c) = H_k, \tag{5.90}$$

we obtain the radial distance c that represents the boundary between the two parts of the core:

$$c = \frac{NI}{2\pi H_k} = 3.2 \text{ cm} \tag{5.91}$$

[see Fig. 5.27(a)]. Sketched in Fig. 5.27(c) is the distribution of the magnetic flux density, $B(r)$, along the radial axis.

The magnetic flux through the core is (see Fig. 5.26)

$$\Phi = \int_a^b B(r)\,\mathrm{d}S = \underbrace{B_m h(c-a)}_{\text{saturation}} + \underbrace{\frac{\mu_a NIh}{2\pi}\int_c^b \frac{\mathrm{d}r}{r}}_{\text{linear regime}}$$

$$= B_m h\left[(c-a) + \frac{NI}{2\pi H_k}\ln\frac{b}{c}\right] = 191.4\ \mu\text{Wb}. \tag{5.92}$$

(b) If we assume a uniform field distribution in the core, then the field intensity everywhere in the core equals that for $r = r_{\text{mean}} = (a+b)/2 = 3$ cm. That is, $H = H(r_{\text{mean}}) = 1061$ A/m, which, being greater than H_k, implies that the entire core is in saturation. The magnetic flux through the core is hence

$$\Phi_{\text{approx}} = B_m(b-a)h = 200\ \mu\text{Wb}. \tag{5.93}$$

The error relative to the result in Eq. (5.92) is $\delta_\Phi = 4.5\%$, and this is very reasonable given that the core is both thick and nonlinear.

Problems: 5.20; *Conceptual Questions* (on Companion Website): 5.17; *MATLAB Exercises* (on Companion Website).

5.10 KIRCHHOFF'S LAWS FOR MAGNETIC CIRCUITS

With the assumptions made (in the previous section) that the field is restricted to the branches of the magnetic circuit (flux leakage and fringing are negligible) and is uniform in every branch, we now specialize general Maxwell's equations for the magnetostatic field to obtain the laws analogous to Kirchhoff's laws in the electric circuit theory. Thus, applying the law of conservation of magnetic flux, Eq. (4.99), to

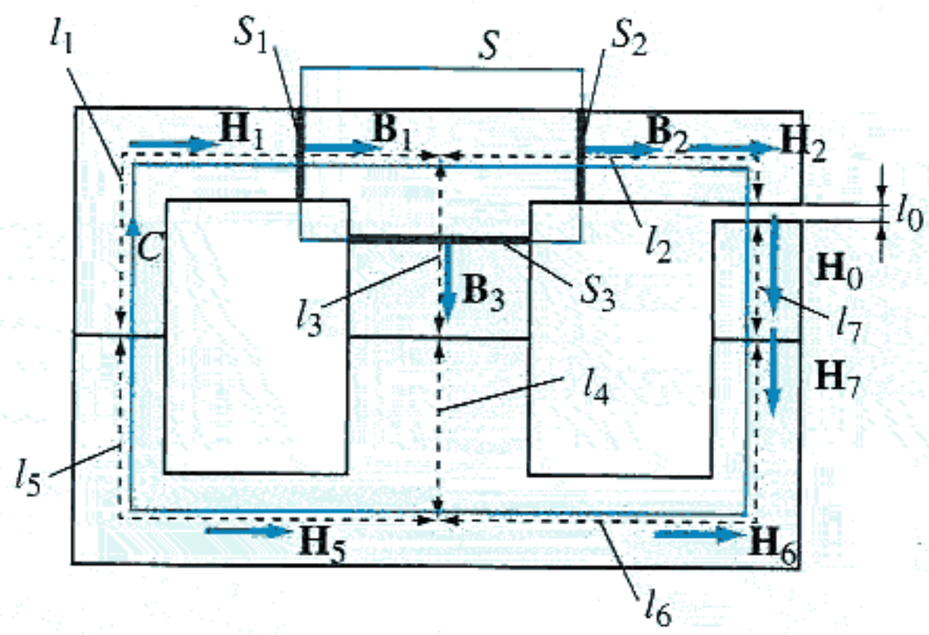

Figure 5.28 A closed surface S about a node and a closed path C along the axes of branches of a magnetic circuit – for the formulation of Kirchhoff's laws for magnetic circuits.

a closed surface S placed about a node (junction of branches) in a magnetic circuit, as shown in Fig. 5.28, yields

$$\oint_S \mathbf{B} \cdot d\mathbf{S} = 0 \quad \longrightarrow \quad \boxed{\sum_{i=1}^{M} B_i S_i = 0,} \tag{5.94}$$

Kirchhoff's "current" law for magnetic circuits

where S_i $(i = 1, 2, \ldots, M)$ are cross-sectional areas of the branches in the junction and B_i $(i = 1, 2, \ldots, M)$ are the magnetic flux densities in these branches.

Applying, on the other hand, the generalized Ampère's law, Eq. (5.49), to a contour C placed along a closed path of flux lines in the circuit (Fig. 5.28) gives

$$\oint_C \mathbf{H} \cdot d\mathbf{l} = I_C \quad \longrightarrow \quad \boxed{\sum_{j=1}^{P} H_j l_j = \sum_{k=1}^{Q} N_k I_k,} \tag{5.95}$$

Kirchhoff's "voltage" law for magnetic circuits

with l_j $(j = 1, 2, \ldots, P)$ standing for the lengths of the branches along the path and H_j $(j = 1, 2, \ldots, P)$ for the magnetic field intensities in the branches, whereas N_k and I_k $(k = 1, 2, \ldots, Q)$ are the numbers of wire turns and current intensities, respectively, in the coils that exist along the path. The product $N_k I_k$, expressed in ampere-turns, is termed a magnetomotive force (mmf), in analogy to an electromotive force (emf) in electric circuits.

Eqs. (5.94) and (5.95) are referred to as Kirchhoff's laws for magnetic circuits. In addition to these circuital laws, we need the "element laws" describing individual parts of the circuit, analogous to current-voltage characteristics for elements (e.g., resistors) in the analysis of electric circuits. These laws are the relationships $B = B(H)$, i.e., the magnetization curves, for the branches of the circuit, including air gaps (where $B = \mu_0 H$). Because of the nonlinear nature of the ferromagnetic portions of the magnetic circuit, and nonlinearity of magnetization curves, the analysis of magnetic circuits often resembles the analysis of nonlinear electric circuits which contain diodes and other elements with nonlinear current-voltage characteristics. This is, at the same time, the most important difference between the analysis of magnetic circuits and the electric circuit theory, which primarily deals with linear electric circuits.

In cases where the ferromagnetic materials in the circuit can be considered as linear, however, an equivalent electric circuit with linear resistors and time-invariant voltage generators can be introduced. By solving the equivalent circuit using some of the standard circuit-theory techniques, we obtain thus all required

quantities for the original magnetic circuit. As an illustration, note that the magnetic flux through a simple magnetic circuit in Fig. 5.29(a) can be expressed, having in mind Eq. (5.53), as

$$\Phi = BS = \mu HS = \frac{\mu NIS}{l} = \frac{NI}{\mathcal{R}}, \tag{5.96}$$

where

reluctance (unit: H^{-1})

$$\boxed{\mathcal{R} = \frac{l}{\mu S}} \tag{5.97}$$

is the so-called reluctance of the core. It is defined generally as the ratio of the magnetomotive force (ampere-turns) to the flux. The SI unit for reluctance is ampere per weber (A/Wb) or inverse henry (H^{-1}). We note that the final expression for Φ in Eq. (5.96) is analogous to the expression for the current in a simple electric circuit in which an ideal voltage source of emf NI is connected with a resistor of resistance $\mathcal{R}$, as indicated in Fig. 5.29(b). Eq. (5.97), moreover, has the same form as the expression for the resistance of a resistor with uniform cross section and conductivity σ in Eq. (3.85). The concept of reluctance can be used for the analysis of arbitrary linear magnetic circuits, where the equivalent electric circuit is obtained by replacing the individual parts of the core and the air gaps by resistors with resistances calculated from Eq. (5.97) and representing the coils by voltage generators with electromotive forces equal to the magnetomotive forces NI.

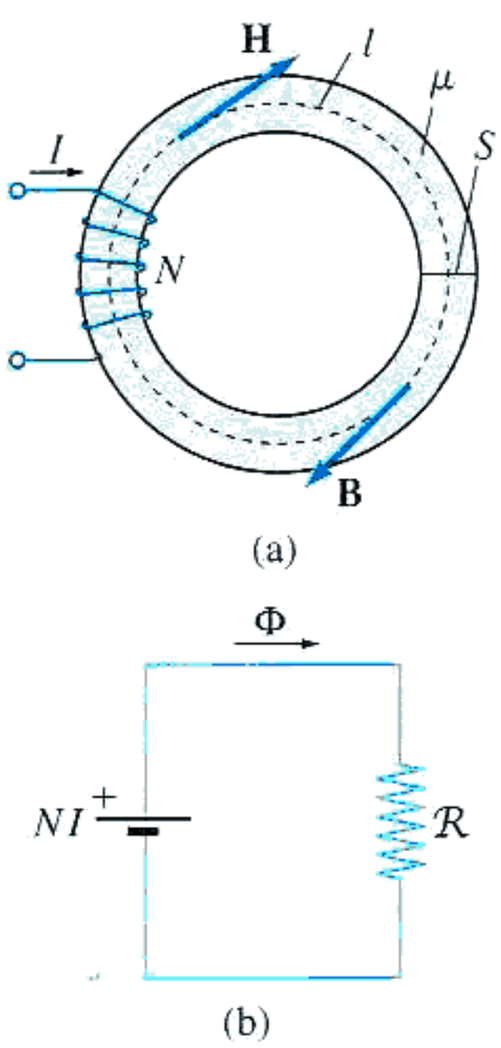

Figure 5.29 Reluctance concept: a simple linear magnetic circuit (a) and the equivalent electric circuit (b).

Example 5.13 Simple Nonlinear Magnetic Circuit with an Air Gap

Consider a magnetic circuit consisting of a thin toroidal ferromagnetic core with a coil and an air gap shown in Fig. 5.30(a). The coil has $N = 1000$ turns of wire with the total resistance $R = 50\ \Omega$. The length of the ferromagnetic portion of the circuit is $l = 1$ m, the thickness (width) of the gap is $l_0 = 4$ mm, the cross-sectional area of the toroid is $S = S_0 = 5\ \text{cm}^2$, and the emf of the generator in the coil circuit is $\mathcal{E} = 200$ V. The idealized initial magnetization curve of the material is given in Fig. 5.30(b). Find the magnetic field intensities in the core and in the air gap.

Solution We adopt standard approximations for the analysis of magnetic circuits and neglect the field nonuniformity in the ferromagnetic core, as well as the flux leakage from the core and fringing around the air gap edges (Section 5.9). Let (B, H) and (B_0, H_0) designate the magnetic flux density and field intensity in the core and the gap, respectively, as

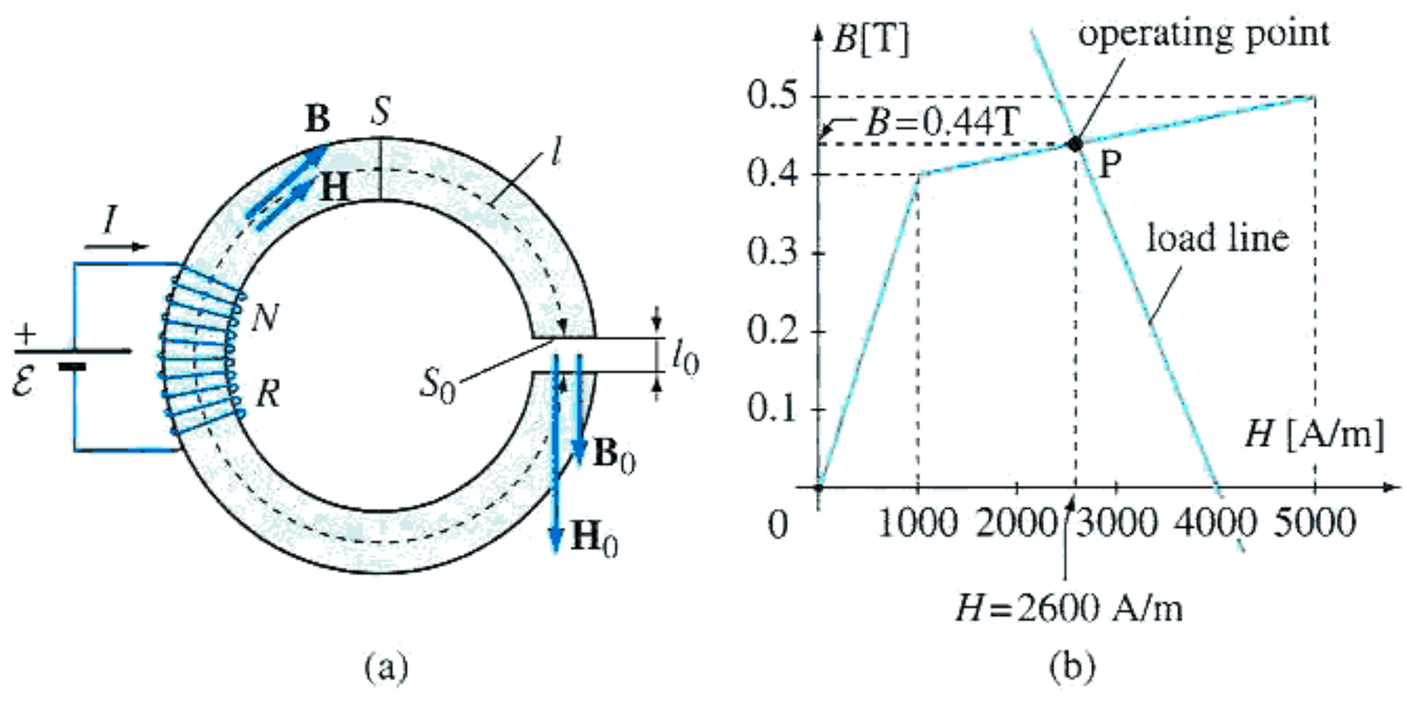

Figure 5.30 Analysis of a simple nonlinear magnetic circuit with an air gap: (a) circuit geometry, with flux density and field intensity vectors in the circuit, and (b) idealized initial magnetization curve of the material, with the load line and operating point for the circuit; for Example 5.13.

indicated in Fig. 5.30(a). From Kirchhoff's laws for magnetic circuits, Eqs. (5.94) and (5.95), we have

$$BS = B_0 S_0 \quad \longrightarrow \quad B = B_0 \tag{5.98}$$

and

$$Hl + H_0 l_0 = NI, \tag{5.99}$$

where $I = \mathcal{E}/R = 4$ A is the current intensity of the coil. The above equations, combined with the constitutive equation for the air gap,

$$B_0 = \mu_0 H_0, \tag{5.100}$$

result in the following relationship between the flux density and field intensity in the core:

$$Hl + B\frac{l_0}{\mu_0} = NI. \tag{5.101}$$

With the numerical data substituted,

$$H + 3183B = 4000 \quad (H \text{ in A/m}; \quad B \text{ in T}), \tag{5.102}$$

and this represents the equation of the load line for the magnetic circuit (the locus of all possible combinations of values B and H for this given circuit configuration and excitation, not yet taking into account the characteristics of the core material). Upon plotting this line in the BH chart [Fig. 5.30(b)], we conclude that its intersection with the magnetization curve of the core material belongs to the second part of the curve (hard magnetization section – also see Fig. 5.20). This intersection (point P) represents the operating point for the circuit, i.e., it determines the actual position of the ferromagnetic core on the magnetization curve for the given circuit configuration and excitation (NI). To find numerically the abscissa and ordinate of the point P, we solve the system of equations composed of the load line equation, Eq. (5.102), and the equation of the line describing the hard magnetization segment of the magnetization curve, read from Fig. 5.30(b),

$$B = 0.4 + 2.5 \times 10^{-5}(H - 1000), \tag{5.103}$$

and what we get is $B = 0.44$ T and $H = 2600$ A/m. By means of Eq. (5.98), $B_0 = 0.44$ T as well, and Eq. (5.100) then gives $H_0 = 350$ kA/m (field intensity in the air gap). We see that $H_0 \gg H$. This can also be concluded without actually solving the circuit, by introducing the permeability of the material at the point P, $\mu = B/H = 1.7 \times 10^{-4}$ H/m, into Eq. (5.98) and expressing the magnetic field intensity in the gap as

$$H_0 = \frac{\mu}{\mu_0} H = 135.3H. \tag{5.104}$$

(Note that μ here is a function of H, not a constant.) It is typical for magnetic circuits with air gaps, in general, that the magnetic field intensities in the gaps are much larger than those in the ferromagnetic material.

Example 5.14 **Simple Linear Magnetic Circuit with an Air Gap**

Assume that the core of the circuit of Fig. 5.30(a) is made from a linear ferromagnetic material of relative permeability $\mu_r = 1000$, and compute the magnetic flux through the core.

Solution Combining Eq. (5.101) with the relationship $B = \mu H$, we can write now

$$\Phi = BS = NI\left(\frac{l}{\mu S} + \frac{l_0}{\mu_0 S_0}\right)^{-1} = \frac{NI}{\mathcal{R} + \mathcal{R}_0}, \tag{5.105}$$

where the reluctances [Eq. (5.97)] of the core and the gap are

$$\mathcal{R} = \frac{l}{\mu_r \mu_0 S} = 1.6 \times 10^6 \text{ H}^{-1} \quad \text{and} \quad \mathcal{R}_0 = \frac{l_0}{\mu_0 S_0} = 6.37 \times 10^6 \text{ H}^{-1}, \tag{5.106}$$

respectively, and the equivalent electric circuit is shown in Fig. 5.31. Hence, the flux through the core amounts to $\Phi = 5 \times 10^{-4}$ Wb.

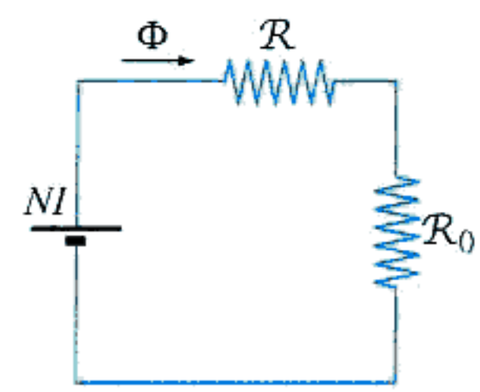

Figure 5.31 Equivalent electric circuit for the magnetic circuit of Fig. 5.30(a), assuming that the ferromagnetic material is linear; for Example 5.14.

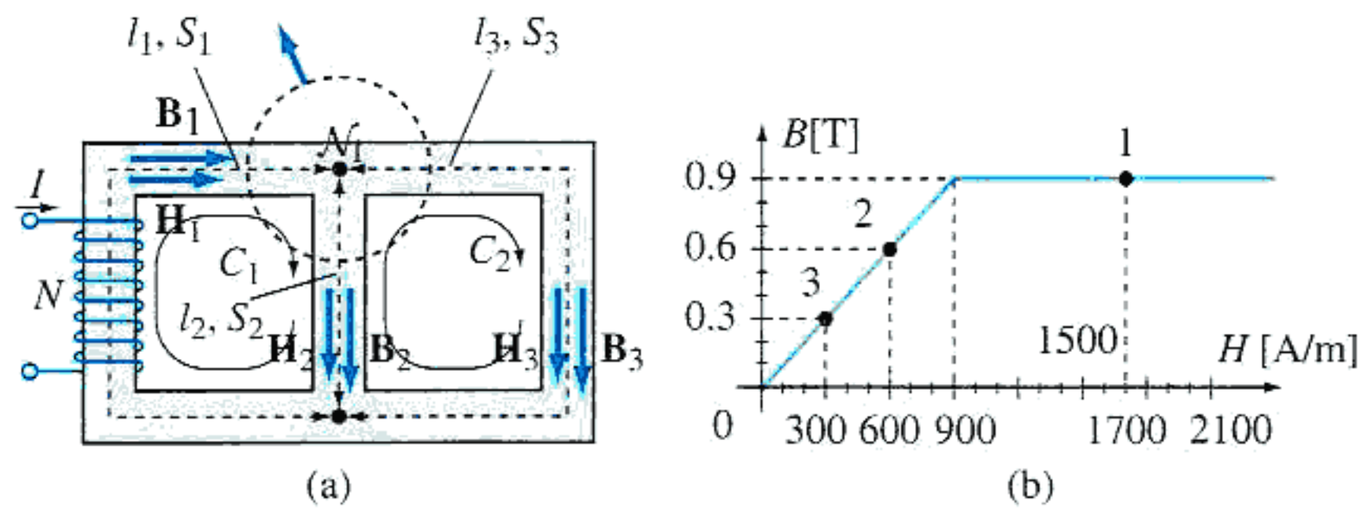

Figure 5.32 Analysis of a nonlinear magnetic circuit with three branches: (a) circuit geometry, with the adopted independent node and closed paths in the circuit, and (b) idealized initial magnetization curve of the material, with computed operating points for the branches; for Example 5.15.

Example 5.15 Nonlinear Magnetic Circuit with Three Branches

Dimensions of the magnetic circuit shown in Fig. 5.32(a) are $l_1 = l_3 = 2l_2 = 20$ cm and $S_1 = S_2 = S_3 = 1$ cm^2. The mmf in the first branch of the circuit is $NI = 400$ ampere-turns. The initial magnetization curve of the core can be linearized as in Fig. 5.32(b). Calculate the magnetic flux densities and field intensities in the three branches of the circuit.

Solution Let us orient the branches of the circuit as in Fig. 5.32(a). There is a total of two nodes and three closed paths in the circuit. Thus, in complete analogy with the analysis of electric circuits, Kirchhoff's "current" and "voltage" laws for magnetic circuits, Eqs. (5.94) and (5.95), are to be applied to one node (independent node) and two closed paths (independent closed paths), respectively. We choose the node $\mathcal{N}_1$ and closed paths C_1 and C_2 in Fig. 5.32(a). The corresponding equations are:

$$-B_1S_1 + B_2S_2 + B_3S_3 = 0 \quad \longrightarrow \quad B_1 = B_2 + B_3, \tag{5.107}$$

$$H_1l_1 + H_2l_2 = NI, \tag{5.108}$$

$$-H_2l_2 + H_3l_3 = 0. \tag{5.109}$$

Depending on whether the operating points for the individual branches of the circuit belong to the linear part or to the saturation part of the magnetization curve in Fig. 5.32(b), we may have

$$B_i = \begin{cases} \mu_a H_i & \text{for } H_i \le 900 \text{ A/m} \\ 0.9 \text{ T} & \text{for } H_i > 900 \text{ A/m} \end{cases}, \quad i = 1, 2, 3, \tag{5.110}$$

where the initial permeability of the material is $\mu_a = 0.9/900$ H/m $= 0.001$ H/m. So, there exist a total of eight combinations for the magnetization stages of the branches and only one of them is true.

Suppose, first, that none of the magnetizations in the branches is in saturation ($B = \mu_a H$ in all three branches). Eq. (5.107) then becomes

$$H_1 = H_2 + H_3, \tag{5.111}$$

and the solution of the system with Eqs. (5.111), (5.108), and (5.109) is $H_1 = 1500$ A/m, $H_2 = 1000$ A/m, and $H_3 = 500$ A/m. This is contradictory to the assumption of linearity in all three branches, since both H_1 and H_2 appear to be larger than 900 A/m. We conclude that our initial guess is not correct, and the circuit has therefore to be solved again, with another assumption, i.e., that some of the branches are in saturation.

To reduce the number of additional trials (out of remaining seven combinations) to a minimum, we note first that the adopted reference directions of the magnetic flux density vectors in Fig. 5.32(a) likely reflect the actual flux flow in the branches, meaning that B_1, B_2, and B_3 are all positive. Eq. (5.107) then tells us that B_1 must be larger than both B_2 and B_3 individually, so it is logical to expect that the branch with the coil would first reach saturation ($B_1 = 0.9$ T). The other two branches, however, must remain in the linear regime ($B_2 = \mu_a H_2$ and $B_3 = \mu_a H_3$), because $B_2 = 0.9$ T would imply $B_3 = 0$ and vice versa, which

is impossible. With this, Eq. (5.107) becomes

$$H_2 + H_3 = 900 \text{ A/m}, \tag{5.112}$$

and the solution of the new system of three equations is $H_1 = 1700$ A/m, $H_2 = 600$ A/m, and $H_3 = 300$ A/m. Obviously, these values are consistent with the new assumption made about the magnetization stages in the branches, and this is the true solution for the circuit. The actual positions of the operating points for the branches on the magnetization curve are indicated in Fig. 5.32(b). The remaining two flux densities in the circuit are $B_2 = 0.6$ T and $B_3 = 0.3$ T.

Example 5.16 Reverse Problem in the Magnetic Circuit Analysis

For the magnetic circuit shown in Fig. 5.33, $l_1 = l_3 = 20$ cm, $l_2 = l_2' + l_2'' = 10$ cm, $l_0 = 1$ mm, $S_1 = S_3 = 1$ cm^2, $S_2 = 2$ cm^2, and $N_2 I_2 = 1000$ A turns. The core is made from the material whose initial magnetization curve can be approximated analytically by the function

$$B = \frac{1.5H}{500 + H}, \quad H \geq 0 \quad (H \text{ in A/m}; \quad B \text{ in T}). \tag{5.113}$$

If the magnetic flux in the central branch of the circuit is $\Phi_2 = 200\ \mu$Wb with respect to the downward reference direction, find $N_1 I_1$.

Solution This is a reverse problem in the magnetic circuit analysis: for a given response (magnetic flux in one or more branches of the circuit), find the unknown excitation (one or more magnetomotive forces) that produces it. In the analysis of magnetic circuits with nonlinear magnetization curves (given either graphically or analytically), reverse problems are generally much simpler to solve than direct problems, because in the latter case we have to simultaneously solve the full set of equations written in accordance to Kirchhoff's circuital laws together with nonlinear material characteristics for individual parts of the circuit. In reverse problems, on the other hand, we start with the given field quantities for one or more branches and then applying the circuital and material equations one at a time we solve for other field quantities, one by one, and for the required magnetomotive forces.

With reference to the notation in Fig. 5.33, the flux densities in the ferromagnetic section of the second (central) branch of the circuit (B_2) and in the air gap (B_0) are

$$B_2 = B_0 = \frac{\Phi_2}{S_2} = 1 \text{ T}. \tag{5.114}$$

From the magnetization curve, i.e., by solving the magnetization equation, Eq. (5.113), for the corresponding field intensity in the material,

$$H_2 = \frac{500 B_2}{1.5 - B_2} = 1 \text{ kA/m}, \tag{5.115}$$

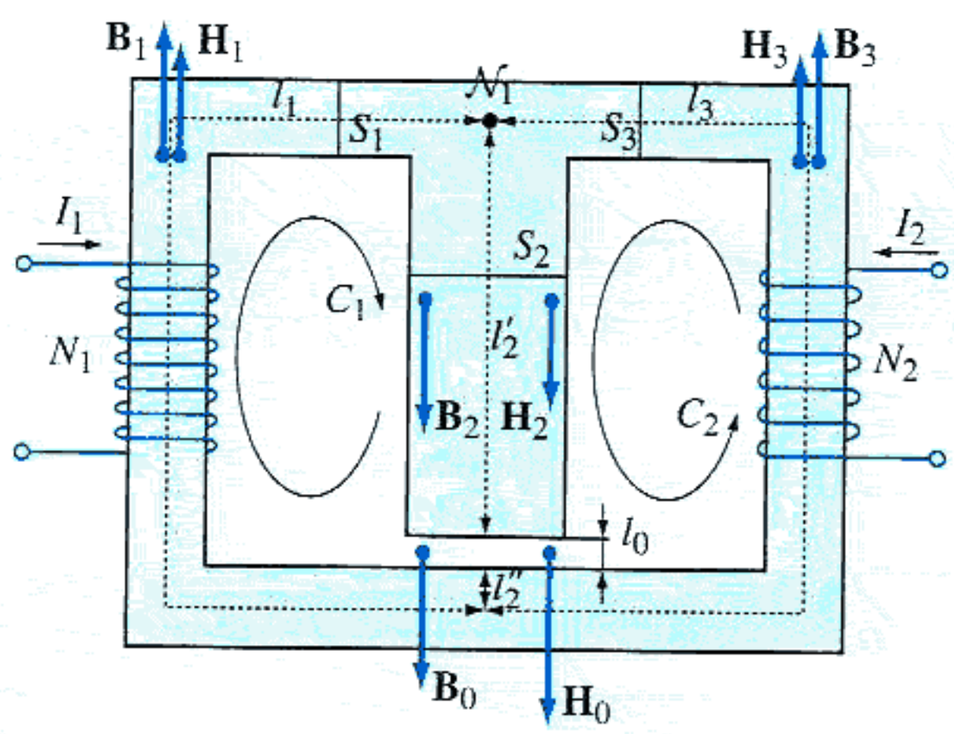

Figure 5.33 Magnetic circuit with a nonlinear magnetization curve given analytically; for Example 5.16.

whereas in the gap,

$$H_0 = \frac{B_0}{\mu_0} = 795.8 \text{ kA/m}. \tag{5.116}$$

Kirchhoff's "voltage" law for the closed path C_2 in Fig. 5.33 now yields

$$H_3 = \frac{N_2 I_2 - H_2 l_2 - H_0 l_0}{l_3} = 521 \text{ A/m}, \tag{5.117}$$

with the corresponding flux density in the third branch given by

$$B_3 = \frac{1.5 H_3}{500 + H_3} = 0.765 \text{ T}. \tag{5.118}$$

The flux density in the first branch is next obtained using Kirchhoff's "current" law for the node $\mathcal{N}_1$ in Fig. 5.33, and from it the associated H value,

$$B_1 = \frac{B_2 S_2 - B_3 S_3}{S_1} = 1.235 \text{ T} \quad \longrightarrow \quad H_1 = \frac{500 B_1}{1.5 - B_1} = 2.33 \text{ kA/m}. \tag{5.119}$$

Finally, we apply Kirchhoff's "voltage" law to the closed path C_1 and obtain the mmf we seek:

$$N_1 I_1 = H_1 l_1 + H_2 l_2 + H_0 l_0 = 1362 \text{ A turns}. \tag{5.120}$$

Example 5.17 Demagnetization in a Magnetic Circuit

The ferromagnetic core of the circuit shown in Fig. 5.34(a) has the cross-sectional area $S = 1 \text{ cm}^2$, mean length $l = 20$ cm, and air-gap thickness $l_0 = 1$ mm. The number of wire turns of the coil is $N = 1000$, the resistance of the winding is $R = 20\ \Omega$, and the emf of the generator is $\mathcal{E} = 20$ V. The core does not have residual magnetization and the switch K is in the off position (open). By turning the switch on, the mmf is applied to the circuit and the magnetic flux through it rises following the initial magnetization curve of the material. This curve can be considered as linear, as shown in Fig. 5.34(b), where the initial permeability is $\mu_a = 0.001$ H/m. The magnetic flux density in the core becomes $B = B_m$ in the stationary state. The switch is then turned off (opened) and a new stationary state established in the

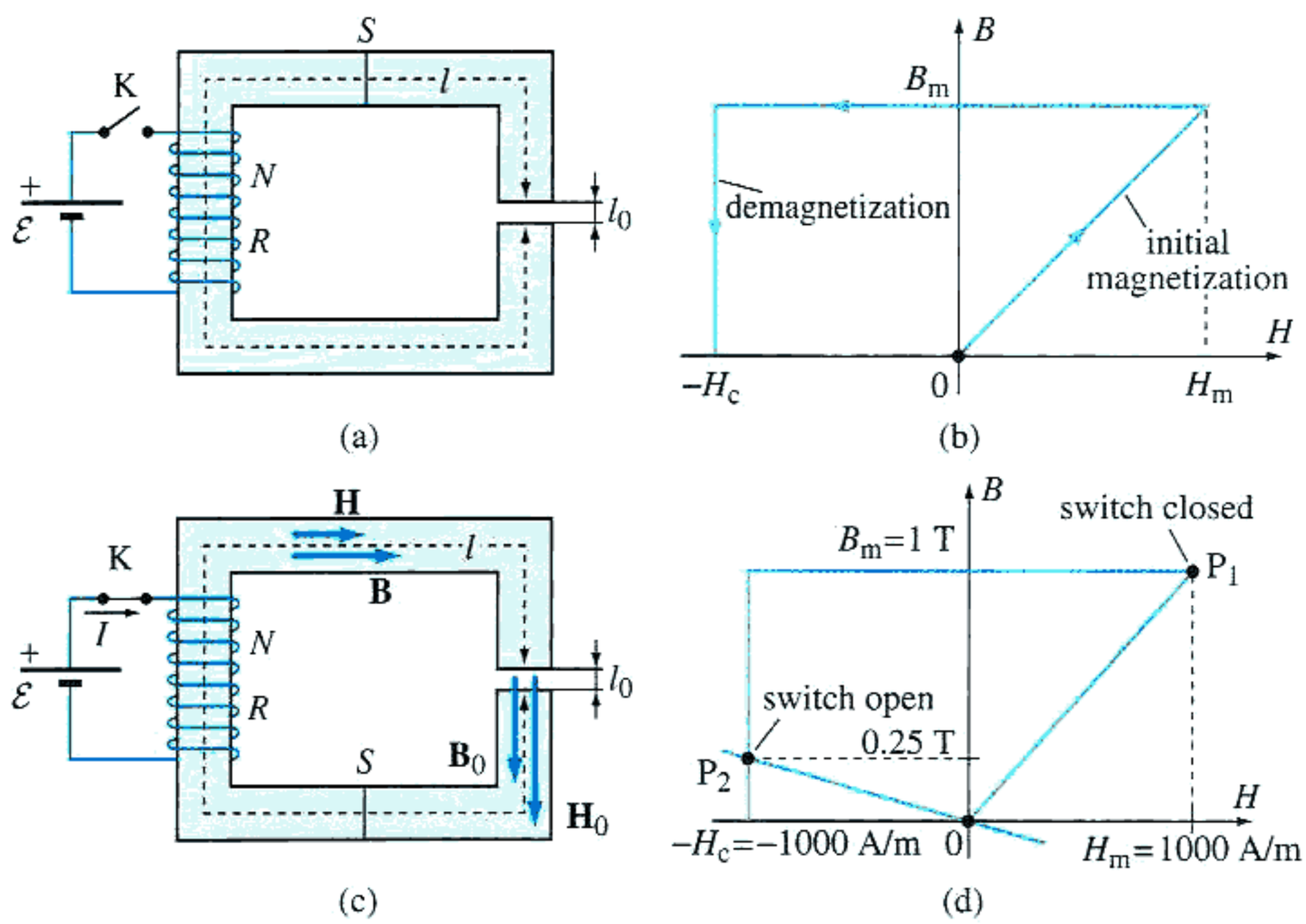

Figure 5.34 Magnetization and demagnetization in a magnetic circuit with an air gap: (a) circuit geometry, (b) idealized initial magnetization and demagnetization curves of the material, (c) magnetic flux density and field intensity vectors in the circuit, and (d) operating points for the circuit in two stationary states; for Example 5.17.

circuit. The demagnetization curve for the material can be approximated by two straight-line segments [Fig. 5.34(b)], where the coercive force is given by $H_c = H_m$. What is the magnetic field intensity in the gap in the new state?

Solution After the switch K is turned on (closed), the current in the winding is [Fig. 5.34(c)] $I = \mathcal{E}/R = 1$ A, and the relationship between the flux density B and field intensity H in the core is the same as in Eq. (5.101). Moreover, as

$$B = \mu_a H, \tag{5.121}$$

we obtain [see also Eq. (5.105)]

$$B = NI\left(\frac{l}{\mu_a} + \frac{l_0}{\mu_0}\right)^{-1} = 1\ \text{T}, \tag{5.122}$$

and this is the maximum value for the flux density, $B = B_m = 1$ T. Hence, $H_m = B_m/\mu_a = 1$ kA/m.

After the switch K is opened, Eq. (5.101) becomes

$$Hl + B\frac{l_0}{\mu_0} = 0, \tag{5.123}$$

and this represents the equation of the load line for the magnetic circuit in this state. We suppose first that the intersection of this line with the demagnetization curve in Fig. 5.34(b) belongs to the horizontal segment of the curve, i.e., that $B = B_m = 1$ T. From Eq. (5.123), $H = -4$ kA/m, which is impossible because $H < -H_c$ ($H_c = H_m = 1$ kA/m). We conclude thus that the operating point for the circuit belongs to the vertical segment of the demagnetization curve, as indicated in Fig. 5.34(d). The magnetic field intensity in the core is therefore $H = -H_c = -1$ kA/m. Eq. (5.123) then gives the corresponding flux density in the core, $B = 0.25$ T. The magnetic field intensity in the gap is $H_0 = B/\mu_0 = 200$ kA/m.

Example 5.18 Complex Linear Magnetic Circuit

For the magnetic circuit shown in Fig. 5.35(a), $l_1 = l_2 = 10$ cm, $l_3 = 5$ cm, $l_0 = 1$ mm, $N_1 = 1000$, $N_2 = 500$, and $I_1 = I_2 = 1$ A. The ferromagnetic material from which the core is made can be considered as linear, with relative permeability $\mu_r = 1000$. The cross-sectional area of all parts of the core is $S = 1$ cm^2. Find the magnetic field intensity in the air gap.

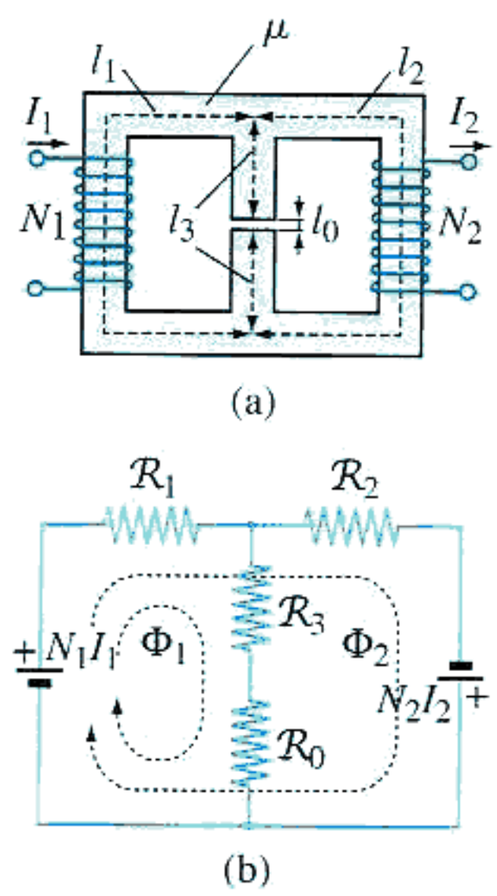

Figure 5.35 Analysis of a linear magnetic circuit with three branches: (a) circuit geometry and (b) equivalent electric circuit for loop analysis; for Example 5.18.

Solution Fig. 5.35(b) shows the equivalent electric circuit for the problem, with reluctances, Eq. (5.97),

$$\mathcal{R}_1 = \mathcal{R}_2 = 2\mathcal{R}_3 = \frac{l_1}{\mu_r\mu_0 S} = 8\times10^5\ \text{H}^{-1}, \quad \mathcal{R}_0 = \frac{l_0}{\mu_0 S} = 8\times10^6\ \text{H}^{-1}. \tag{5.124}$$

The figure also shows the adopted loops for the loop analysis of the (electric) circuit. The corresponding loop equations are

$$(\mathcal{R}_1 + \mathcal{R}_3 + \mathcal{R}_0)\Phi_1 + \mathcal{R}_1\Phi_2 = N_1 I_1, \tag{5.125}$$

$$\mathcal{R}_1\Phi_1 + (\mathcal{R}_1 + \mathcal{R}_2)\Phi_2 = N_1 I_1 + N_2 I_2, \tag{5.126}$$

and their solution for the flux through the central branch of the circuit

$$\Phi_1 = \frac{\mathcal{R}_2 N_1 I_1 - \mathcal{R}_1 N_2 I_2}{\mathcal{R}_0\mathcal{R}_1 + \mathcal{R}_0\mathcal{R}_2 + \mathcal{R}_1\mathcal{R}_2 + \mathcal{R}_1\mathcal{R}_3 + \mathcal{R}_2\mathcal{R}_3} = 2.84\times10^{-5}\ \text{Wb}. \tag{5.127}$$

The magnetic field intensity in the gap comes out to be

$$H_0 = \frac{\Phi_1}{\mu_0 S} = 226\ \text{kA/m}. \tag{5.128}$$

Problems: 5.21–5.27; *Conceptual Questions* (on Companion Website): 5.18–5.21; *MATLAB Exercises* (on Companion Website).

5.11 MAXWELL'S EQUATIONS FOR THE TIME-INVARIANT ELECTROMAGNETIC FIELD

Maxwell's equations for the magnetostatic field, Eqs. (5.70), represent a general mathematical model for determining the magnetic field (**H**) from a distribution of steady electric currents (**J**), which is considered to be known. The distribution of currents, however, for the geometry, material properties, and excitation of a given structure can be obtained from Eqs. (3.59), which also yield the solution for the electric field (**E**) in the system. In addition, Eqs. (3.60) provide a means for evaluating the associated distribution of charges (ρ) in the system from the electric field distribution. All these equations together represent a full set of Maxwell's equations that govern both the electric and the magnetic field due to steady electric currents. These two fields, moreover, can be considered as components of a more complex field – the electromagnetic field – produced by steady currents. The combined field is called the time-invariant electromagnetic field, and we summarize here the four Maxwell's equations in differential form for this field:

Maxwell's first equation, static field
Maxwell's second equation, static field
Maxwell's third equation
Maxwell's fourth equation

$$\boxed{\begin{cases} \nabla \times \mathbf{E} = 0 \\ \nabla \times \mathbf{H} = \mathbf{J} \\ \nabla \cdot \mathbf{D} = \rho \\ \nabla \cdot \mathbf{B} = 0 \end{cases}} \quad . \tag{5.129}$$

What is very important, the electric and magnetic fields constituting the time-invariant electromagnetic field are entirely unrelated and independent from each other, and can be analyzed separately, as we have done in Chapters 3 (electric part) and 5 (magnetic part). This is not the case, however, with the time-varying electromagnetic field, as we shall see in the following chapters. Under nonstatic conditions, the third and fourth Maxwell's equations retain the same form as in Eqs. (5.129), whereas the first two equations have additional terms on the right-hand side of equations, which are responsible for the coupling between the electric and magnetic fields that change in time. In chapters that follow, the electric and magnetic fields will always be treated together, as related integral parts of the time-varying electromagnetic field.

Example 5.19 Continuity Equation from Ampère's Law

Starting from Maxwell's second differential equation for the time-invariant electromagnetic field derive the corresponding form of the continuity equation.

Solution Let us take the divergence of both sides of the differential form of Maxwell's second equation (generalized Ampère's law) for static fields, in Eqs. (5.129):

$$\nabla \cdot (\nabla \times \mathbf{H}) = \nabla \cdot \mathbf{J}. \tag{5.130}$$

The second-order vector derivative on the left-hand side of this equation is equal to zero for any vector field,[2] so the right-hand side of the equation must be zero as well, $\nabla \cdot \mathbf{J} = 0$, and

[2]The divergence of the curl of an arbitrary vector function (**A**) is always zero, or, in terms of the del operator,

$$\nabla \cdot (\nabla \times \mathbf{A}) = 0.$$

This is obvious if **A** is the magnetic vector potential, because then $\mathbf{B} = \nabla \times \mathbf{A}$ [Eq. (4.116)] and $\nabla \cdot \mathbf{B} = 0$ [Eq. (4.103)]. To prove it for **A** representing any vector field, however, we apply formally the identity

$$\mathbf{a} \cdot (\mathbf{b} \times \mathbf{c}) = (\mathbf{a} \times \mathbf{b}) \cdot \mathbf{c}$$

this is exactly the differential form of the continuity equation under the static assumption, Eq. (3.41). We see now that Eq. (3.41) is actually included implicitly in the set of Maxwell's equations in Eqs. (5.129).

Problems: 5.28; *MATLAB Exercises* (on Companion Website).

Problems

5.1. Nonuniformly magnetized parallelepiped. A rectangular ferromagnetic parallelepiped is situated in air in the first octant of the Cartesian coordinate system ($x, y, z \geq 0$), with one vertex at the coordinate origin, and the edges, of lengths a, b, and c, parallel to coordinate axes x, y, and z, respectively. The magnetization vector in the parallelepiped is given by $\mathbf{M}(x, y, z) = M_0[\sin(\pi y/b)\,\hat{\mathbf{x}} + \sin(\pi z/c)\,\hat{\mathbf{y}} + \sin(\pi x/a)\,\hat{\mathbf{z}}]$, where M_0 is a constant. Compute (a) the volume magnetization current density vector in the parallelepiped and (b) the surface magnetization current density vector over its sides.

5.2. Hollow cylindrical bar magnet. A hollow cylindrical bar magnet of radii a and b ($a < b$), and length l, is permanently magnetized with a uniform magnetization and situated in air. The magnetization vector, of magnitude M, is parallel to the bar axis. Find (a) the distribution of magnetization currents of the magnet and (b) the magnetic flux density vector along the axis.

5.3. Uniformly magnetized square ferromagnetic plate. A uniformly magnetized square ferromagnetic plate of side length a and thickness d ($d \ll a$) is situated in air. With reference to the coordinate system in Fig. 5.36, the magnetization vector in the plate is given by $\mathbf{M} = M_0\,\hat{\mathbf{z}}$, where M_0 is a constant. Determine the magnetic flux density vector at an arbitrary point along the z-axis.

5.4. Magnetization parallel to plate faces. Consider the square ferromagnetic plate in Fig. 5.36, and

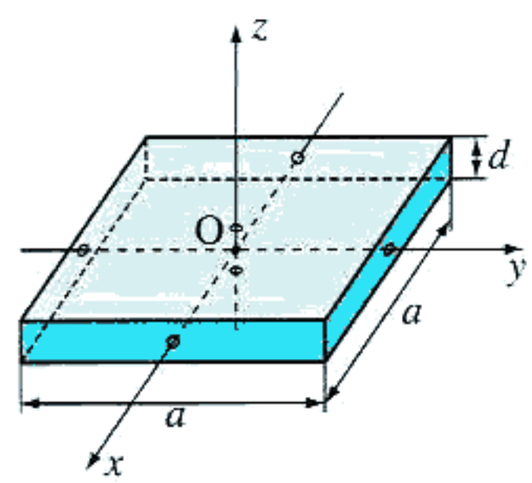

Figure 5.36 Uniformly magnetized square ferromagnetic plate; for Problem 5.3.

assume that the magnetization vector is $\mathbf{M} = M_0\,\hat{\mathbf{y}}$ ($M_0 = \text{const}$). Neglecting end effects, find the magnetic flux density vector at the plate center (point O).

5.5. Nonuniformly magnetized ferromagnetic disk. A thin ferromagnetic disk of radius a and thickness d ($d \ll a$) in air has a nonuniform magnetization, given by $\mathbf{M} = M_0(r/a)^2\,\hat{\mathbf{z}}$ (Fig. 5.37), where M_0 is a constant. Calculate (a) the distribution of magnetization currents of the disk and (b) the magnetic flux density vector along the z-axis.

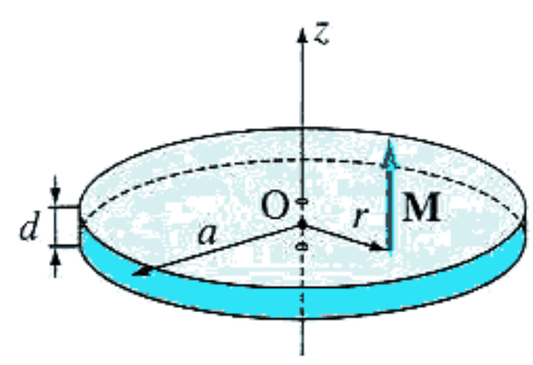

Figure 5.37 Nonuniformly magnetized thin ferromagnetic disk; for Problem 5.5.

5.6. Infinite cylinder with circular magnetization. An infinitely long ferromagnetic cylinder of radius a in air has a nonuniform magnetization.

(in a scalar triple product, the cyclic permutation of the order of the three vectors does not change the result) to the scalar triple product $\nabla \cdot (\nabla \times \mathbf{A})$, and obtain

$$\nabla \cdot (\nabla \times \mathbf{A}) = (\nabla \times \nabla) \cdot \mathbf{A} = 0$$

(cross product of a vector with itself is always zero). Alternatively, the divergence, using Eq. (1.167), of the expression for the curl (of any vector) in the Cartesian coordinate system in Eq. (4.81) turns out to be zero.

In a cylindrical coordinate system whose z-axis coincides with the cylinder axis, $\mathbf{M} = M_0(r/a)\hat{\boldsymbol{\phi}}$ $(0 \le r \le a)$, where M_0 is a constant. Find (a) the volume magnetization current density vector in the cylinder, (b) the surface magnetization current density vector on the cylinder surface, (c) the magnetic flux density vector in the cylinder, and (d) the magnetic flux density vector outside the cylinder.

5.7. Magnetic field intensity vector. Find the magnetic field intensity vector, $\mathbf{H}$, (a) along the axis of the magnetized disk from Example 5.2, (b) at the center of the cylindrical bar magnet from Example 5.3, and (c) inside and outside the nonuniformly magnetized infinitely long cylinder from Example 5.4.

5.8. Total (conduction plus magnetization) current density. The magnetic flux density vector, $\mathbf{B}$, in a ferromagnetic material is a known function of spatial coordinates. (a) Prove that the total (conduction plus magnetization) volume current density in the material, $\mathbf{J}_{\text{tot}} = \mathbf{J} + \mathbf{J}_{\text{m}}$, can be obtained as $\mathbf{J}_{\text{tot}} = \nabla \times \mathbf{B}/\mu_0$. (b) Specifically, compute $\mathbf{J}_{\text{tot}}$ for $\mathbf{B}$ given as the following function of Cartesian coordinates: $\mathbf{B}(x, y, z) = \{[(2x + z)/y^2]\,\hat{\mathbf{x}} + (2/y)\,\hat{\mathbf{y}} + (x + 2y)\,\hat{\mathbf{z}}\}$ T (x, y, z in m).

5.9. Constant flux density vector in a magnetic region. In a certain magnetic region, the magnetic flux density vector does not vary with spatial coordinates. The conduction volume current density vector is $\mathbf{J}$. Find the magnetization volume current density vector, $\mathbf{J}_{\text{m}}$.

5.10. Closed path in a uniform field. Considering an arbitrary contour in a magnetic field with no spatial variation of the magnetic flux density vector ($\mathbf{B} = \text{const}$), in a current-free ($\mathbf{J}_{\text{tot}} = 0$) region, prove the following vector identity: $\oint_C d\mathbf{l} = 0$.

5.11. Circulation of the magnetic flux density vector. The magnetization vector, $\mathbf{M}$, and conduction current density vector, $\mathbf{J}$, are known at every point of a magnetic body. Find the expression for the circulation of the magnetic flux density vector along a closed path C situated entirely inside the body.

5.12. Total magnetization and conduction current. Consider an imaginary closed path C inside a homogeneous magnetic material of relative permeability μ_{r}. The total conduction current enclosed by C is I_C. What is the total magnetization current $I_{\text{m}C}$ enclosed by C?

5.13. Thin toroidal coil with a linear ferromagnetic core. A coil with N turns of wire is wound uniformly and densely over a thin toroidal ferromagnetic core of permeability μ. If a steady current of intensity I is established in the coil, find the circulation of (a) the magnetic field intensity vector, (b) the magnetic flux density vector, and (c) the magnetization vector through the core, along its mean length.

5.14. Solenoidal coil with a linear ferromagnetic core. There is a uniform and dense solenoidal winding wound over a very long cylindrical ferromagnetic core of permeability μ. The number of wire turns per unit length of the core is N'. A steady current of intensity I flows through the winding. Determine (a) the magnetic field intensity vector, (b) the magnetic flux density vector, (c) the magnetization vector, and (d) the volume magnetization current density vector in the core, as well as (e) the surface magnetization current density vector over the surface of the core.

5.15. Ferromagnetic cylinder with a conduction current. A very long ferromagnetic cylinder of radius a and relative permeability μ_{r} is situated in air. There is a uniform conduction current of density J flowing along the cylinder. Find the distribution of (a) the magnetic field intensity vector, (b) the magnetic flux density vector, and (c) the magnetization vector inside and outside the cylinder, as well as (d) the distribution of magnetization currents of the cylinder.

5.16. Magnetic-magnetic boundary conditions. Assume that the plane $z = 0$ separates medium 1 ($z > 0$) and medium 2 ($z < 0$), with relative permeabilities $\mu_{\text{r}1} = 600$ and $\mu_{\text{r}2} = 250$, respectively. The magnetic field intensity vector in medium 1 near the boundary (for $z = 0^+$) is $\mathbf{H}_1 = (5\,\hat{\mathbf{x}} - 3\,\hat{\mathbf{y}} + 2\,\hat{\mathbf{z}})$ A/m. Calculate the magnetic field intensity vector in medium 2 near the boundary (for $z = 0^-$), $\mathbf{H}_2$, if (a) no conduction current exists on the boundary ($\mathbf{J}_{\text{s}} = 0$) and (b) there is a surface current of density $\mathbf{J}_{\text{s}} = 3\,\hat{\mathbf{y}}$ A/m on the boundary.

5.17. Force on a conductor above an infinite PMC corner. Two PMC ($\mu_{\text{r}} \to \infty$) half-planes are connected together at an angle of 90° with

respect to each other, as shown in Fig. 5.38. A very long and thin wire in air runs parallel to the half-planes, at a distance h from each of them. If a steady current of intensity I is established in the wire, find the per-unit-length magnetic force on it.

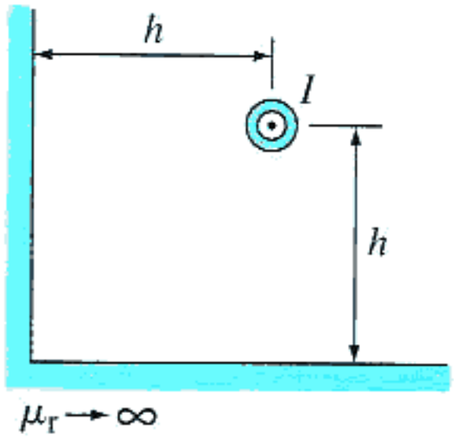

Figure 5.38 Cross section of a system consisting of a current-carrying wire and an infinitely large 90° PMC corner; for Problem 5.17.

5.18. Uniformly magnetized hollow disk on a PMC plane. A uniformly magnetized hollow ferromagnetic disk surrounded by air is lying on a PMC plane. The magnetization vector is **M**, and it is normal to the plane, as shown in Fig. 5.39. The disk radii are a and b, and thickness is d ($d \ll a, b$). Obtain the magnetic flux density vector along the z-axis for $z > 0$.

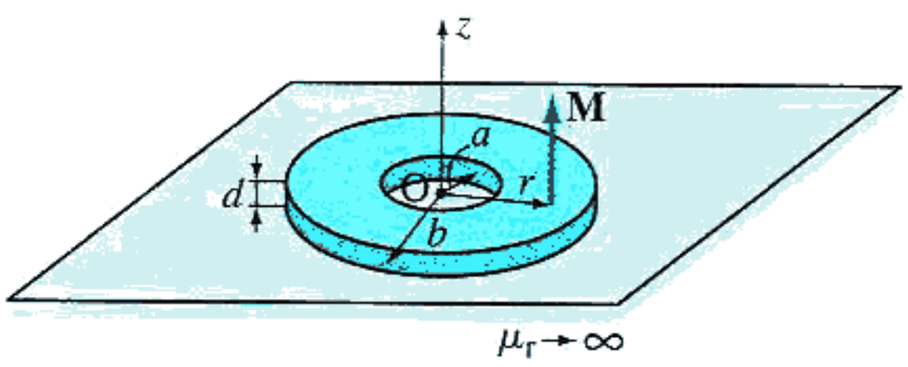

Figure 5.39 Hollow ferromagnetic disk with a uniform magnetization lying on a PMC plane; for Problem 5.18.

5.19. Magnetized cylinder between two PMC planes. A ferromagnetic cylinder of radius a and height h is placed between two parallel PMC planes, as portrayed in Fig. 5.40. The medium around the cylinder is air. The cylinder is uniformly magnetized throughout its volume, with the magnetization vector given as $\mathbf{M} = M_0\,\hat{\mathbf{z}}$, where M_0 is a constant. Find the magnetic flux density vector in the space between the PMC planes, both inside and outside the cylinder.

5.20. Magnetic flux through a thick toroid. Repeat Example 5.12 but for the piece-wise linear approximation of the initial magnetization curve of the core material given in Fig. 5.30(b).

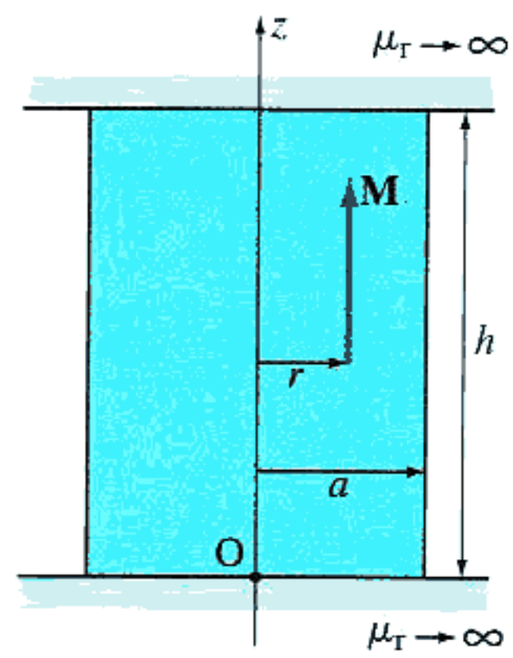

Figure 5.40 Uniformly magnetized cylinder between two parallel PMC planes; for Problem 5.19.

5.21. Simple nonlinear magnetic circuit. Fig. 5.41 shows a magnetic circuit consisting of a thin magnetic core of length $l = 40$ cm and cross-sectional area $S = 2.25$ cm^2 and an air gap of thickness $l_0 = 0.25$ mm. The winding has $N = 800$ turns of wire with a steady current of intensity $I = 1$ A. The core is made from a nonlinear ferromagnetic material whose initial magnetization curve can be linearized in parts as in Fig. 5.27(b). Find the magnetic field intensities in the core and in the air gap.

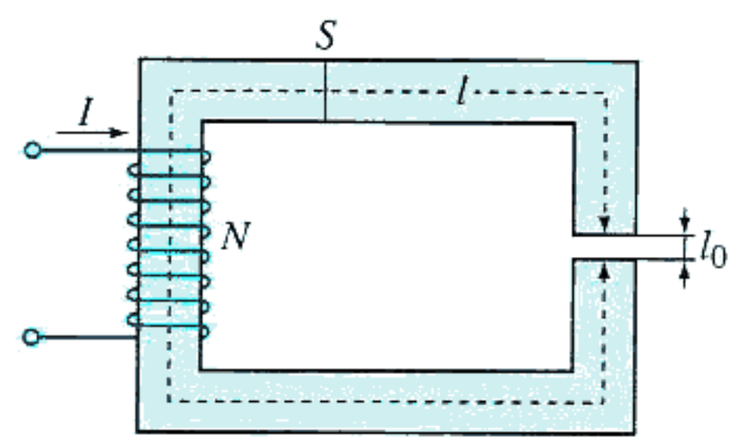

Figure 5.41 Simple nonlinear magnetic circuit with an air gap; for Problem 5.21.

5.22. Complex nonlinear magnetic circuit. Dimensions of the magnetic circuit shown in Fig. 5.42(a) are $l_1 = l_3 = 2l_2 = 20$ cm and $S_1 = S_2 = S_3 = 2$ cm^2. The magnetomotive forces in the circuit are $N_1 I_1 = 100$ ampere-turns and $N_2 I_2 = 300$ ampere-turns. The idealized initial magnetization curve of the core is shown in Fig. 5.42(b). Compute the magnetic flux densities and field intensities in each of the three branches of the circuit.

5.23. Magnetic circuit with a zero flux in one branch. Referring to the magnetic circuit in Fig. 5.42(a), let $l_1 = l_3 = 30$ cm, $l_2 = 10$ cm,

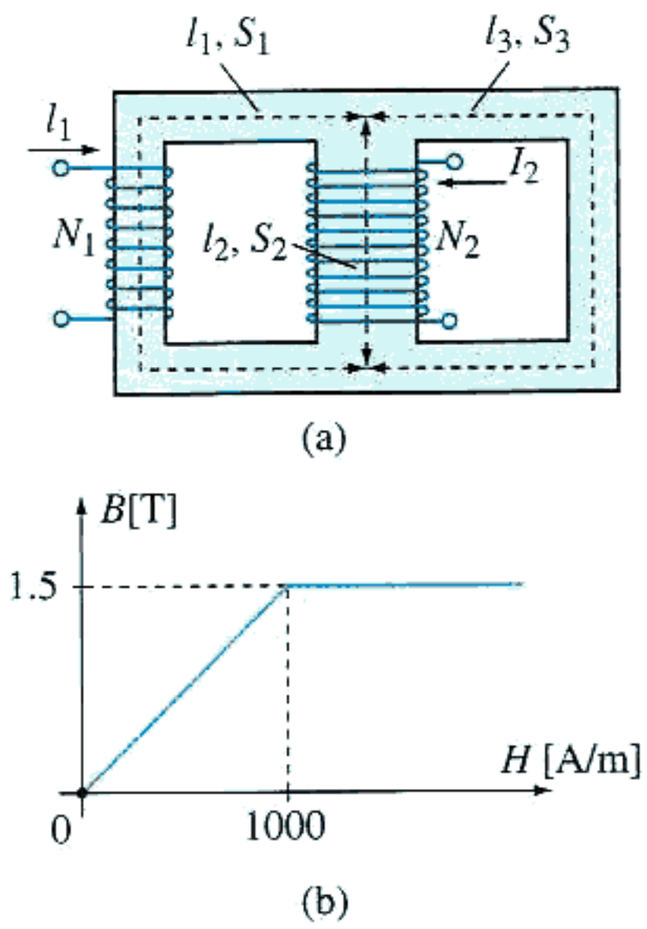

Figure 5.42 Nonlinear magnetic circuit with three branches and two mmf's: (a) circuit geometry and (b) idealized initial magnetization curve of the material; for Problem 5.22.

$S_1 = S_3 = 10\ \text{cm}^2$, $S_2 = 20\ \text{cm}^2$, $N_1 = 1500$, and $N_2 = 1000$. Let the idealized initial magnetization curve of the core be that in Fig. 5.27(b). If the current of the winding in the second branch of the circuit is $I_2 = 0.5$ A, find the current I_1 of the winding in the first branch such that the magnetic flux in that branch is zero.

5.24. Nonlinear magnetic circuit with two air gaps. For the magnetic circuit shown in Fig. 5.43, $l_1' = l_1'' = l_3' = l_3'' = 12$ cm, $l_2 = 5$ cm, $l_0 = 0.6$ mm, and $N_1 I_1 = 1100$ A turns. The cross-sectional area of each of the branches is $S = 2.5\ \text{cm}^2$. The initial magnetization curve of the core can be approximately represented as in Fig. 5.27(b). Determine the mmf $N_2 I_2$ of the second coil such that the magnetic flux through that coil is zero.

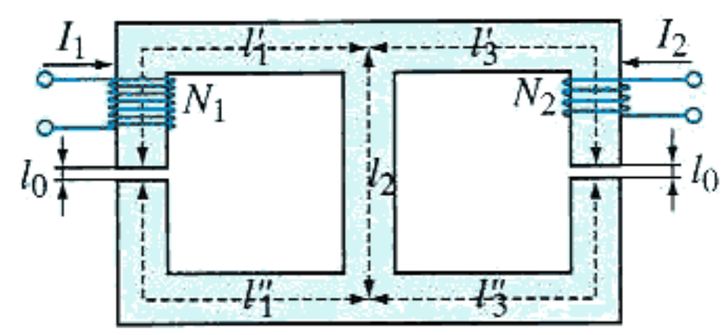

Figure 5.43 Nonlinear magnetic circuit with three branches, two air gaps, and two mmf's; for Problem 5.24.

5.25. Reverse problem with a nonlinear magnetic circuit. Refer to the magnetic circuit shown in Fig. 5.43 and described in the previous problem, and assume that the core is made out from the material whose initial magnetization curve can be approximated analytically by the function $B = \arctan(H/250)$ T (H in A/m), $H \geq 0$. Under these circumstances, find the mmf $N_2 I_2$ in the third branch such that the magnetic flux through the first branch (branch with the given mmf $N_1 I_1$) is $\Phi_1 = 125\ \mu$Wb with respect to the upward reference direction.

5.26. Remanent flux in a circuit with zero mmf. Repeat Example 5.17 but for $l = 50$ cm and $l_0 = 0.5$ mm.

5.27. Linear magnetic circuit with three branches. Assuming that the ferromagnetic material out of which the core of the magnetic circuit from Problem 5.24 is made can be considered as linear, with relative permeability $\mu_r = 1000$, and that $N_2 I_2 = 500$ A turns, (a) find the reluctances of the individual parts of the core and the air gaps and generate an equivalent electric circuit for the problem. (b) By solving the electric circuit in (a), find the magnetic field intensities in each of the air gaps.

5.28. Continuity equation from Ampère's law in integral form. Starting from Maxwell's second equation in integral form for the time-invariant electromagnetic field, derive the time-invariant integral form of the continuity equation.

6 Slowly Time-Varying Electromagnetic Field

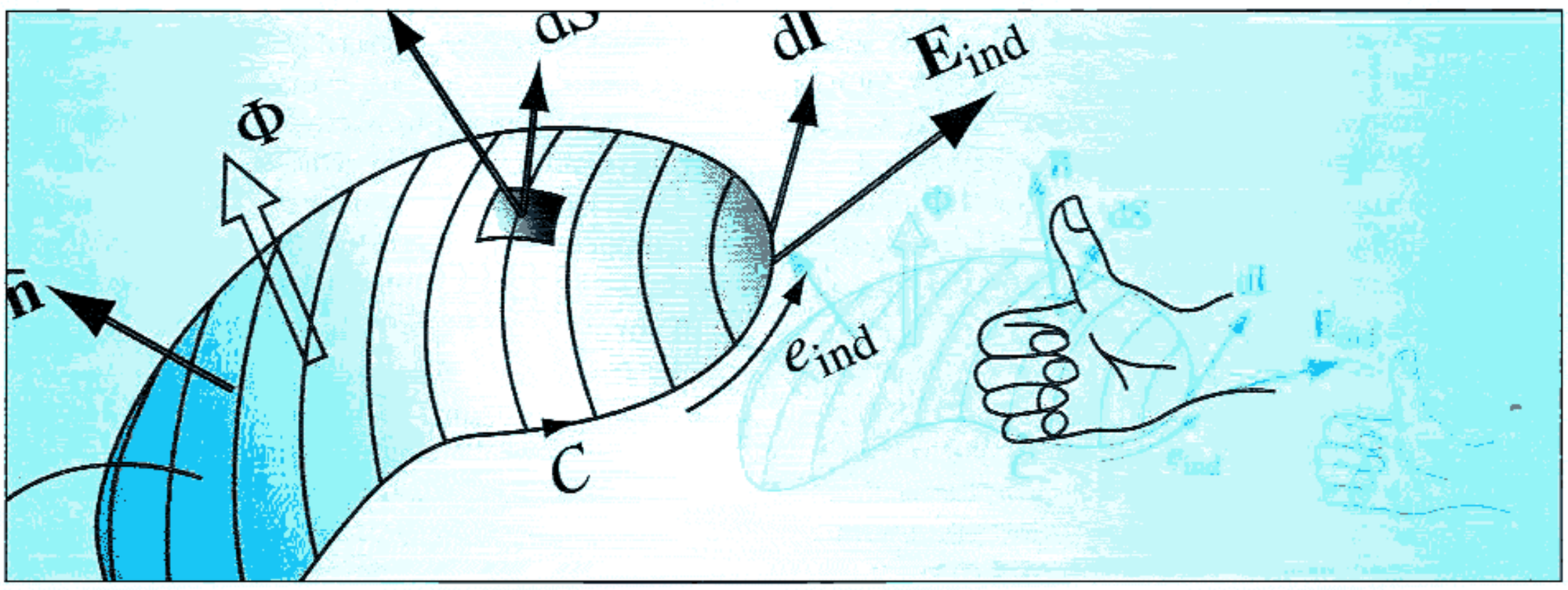

Introduction:

We now introduce time variation of electric and magnetic fields into our electromagnetic model. The new field is the time-varying electromagnetic field, which is caused by time-varying charges and currents. In the new model, all the quantities, in general, change in both space and time. As opposed to static fields, the electric and magnetic fields constituting the time-varying electromagnetic field are coupled to each other and cannot be analyzed separately. Namely, a magnetic field that changes in time produces (induces) an electric field and thus an electric current, and this phenomenon is known as electromagnetic induction. Additionally, a changing electric field induces a magnetic field. As we shall see in a later chapter, this mutual induction of time-varying electric and magnetic fields is the basis of time retardation in electromagnetic systems (lagging in time of time-varying electric and magnetic fields behind their sources), and as such of propagation of electromagnetic waves and of electromagnetic radiation.

The time-retardation concept is one of the most important phenomena in electromagnetics. It basically tells us that there is a time lag between a change of the field sources, i.e., of time-varying charges and currents, and the associated change of the fields, so that the values of field intensities at a distance from the sources depend on the values of charge and current densities at an earlier time. In other words, it takes some time for the effect of a change of charges and currents to be "felt" at distant field points. The time lag equals the time needed for electromagnetic disturbances to propagate over the corresponding distance. We shall see in a later chapter that the velocity of propagation of electromagnetic disturbances in a vacuum or air (free space) equals $c_0 = 3 \times 10^8$ m/s (speed of light and other electromagnetic waves in free space). Hence, the time lag in free space is $\tau = R/c_0$, where

R is the distance between the source and field (observation) points.

If the time τ for all combinations of source and field points in a domain of interest is much shorter than the time of change of the sources [e.g., the period of change of time-harmonic (steady-state sinusoidal) charges and currents, $T = 1/f$, where f is the frequency of the sources], the retardation effect in the system can be neglected. With D designating the maximum dimension of the domain of interest (containing all sources and all field points of interest for the analysis), which most often is the entire system under consideration, so that $R \leq D$, and τ the corresponding (maximum) time lag in the domain, we thus have $\tau = D/c_0 \ll T = 1/f$ as the condition under which the retardation is insignificant. This means that the system size and the rate of change of charges and currents are such that electromagnetic disturbances propagate over the entire system (or the useful part of the system) before the sources have changed significantly. We refer to such charges and currents as slowly time-varying sources and the corresponding electromagnetic fields as slowly time-varying fields, indicating that the rate of their change in time is slow when compared to the velocity of travel of electromagnetic disturbances (waves). In time-harmonic electromagnetics, a slow time variation corresponds to the low-frequency, and the field model in which the time retardation is negligible is called accordingly the low-frequency electromagnetic field. On the other side, the rapidly time-varying (e.g., high-frequency time-harmonic) field cannot be analyzed without taking into account the travel time of electromagnetic disturbances from one point in the system to another. In this chapter (and the following one), we restrict our attention to slow time variations and low frequencies of sources and fields.

The slowly time-varying (low-frequency) electromagnetic field has many formal similarities with the time-invariant (static) electromagnetic field. This is why it is also called the quasistatic electromagnetic field. In addition to all the quantities being now time-dependent, the only essentially new feature of the quasistatic electromagnetic field that is not present under the static assumption is electromagnetic induction, and the fundamental governing law of electromagnetics describing this new phenomenon is Faraday's law of electromagnetic induction. However, this law is probably the most important basic experimental fact of electromagnetics. It is the underpinning of all of the dynamic-field practical applications, from electric motors and generators, through propagation of electromagnetic waves, to antennas and wireless communication.

We shall start the study of the slowly time-varying electromagnetic field by introducing the induced electric field intensity vector due to a single point charge in accelerated motion as an experimental postulate, and then generalize this concept to the evaluation of the induced electric field intensity vector due to any spatial distribution of slowly time-varying currents. The Coulomb electric field component due to time-varying excess charge in the system, with the same form as in electrostatics, will be discussed and added to the field equations. The concept of the induced electromotive force will be introduced and Faraday's law of electromagnetic induction derived using the magnetic vector potential. The full set of Maxwell's equations for the slowly time-varying electromagnetic field will be completed, along with the associated version of the continuity equation. In parallel, the induced electric field due to motion of conductors in static magnetic fields will be introduced as an impressed electric field and discussed in the context of Faraday's law of electromagnetic induction. All new concepts and equations will be applied to the analysis of a whole variety of quasistatic electromagnetic systems. Examples will include systems based on transformer induction (stationary conductors in changing magnetic fields) and those involving motional induction (moving conductors in static magnetic fields), as well as structures in which both types of electromagnetic induction are present at the same time (moving conductors in changing magnetic fields).

6.1 INDUCED ELECTRIC FIELD INTENSITY VECTOR

We know from Chapter 1 that a point charge Q in free space is a source of an electric field, predicted by Coulomb's law and described by Eq. (1.24). On the other side, the Biot-Savart law (Chapter 4) tells us that there will also be a magnetic field, given

by Eq. (4.4), if this charge moves with some velocity $\mathbf{v}$ in space. We now introduce a third field, which will exist in the space around the charge whenever the velocity $\mathbf{v}$ changes in time, i.e., whenever the acceleration (or deceleration) $\mathbf{a} = \mathrm{d}\mathbf{v}/\mathrm{d}t$ of the charge is not zero. This new field is an electric field in its nature. It is called the induced electric field and its intensity vector is given by

$$\boxed{\mathbf{E}_{\text{ind}}(t) = -\frac{\mu_0}{4\pi}\frac{Q\,\frac{\mathrm{d}\mathbf{v}}{\mathrm{d}t}}{R},} \tag{6.1}$$

point charge in an accelerated motion

which is an experimental result as well. Of course, the unit for $\mathbf{E}_{\text{ind}}$ is V/m. This is a time-varying field, that is, $\mathbf{E}_{\text{ind}}$ is a function of time.[1] Comparing Eqs. (6.1) and (4.107), we conclude that the induced electric field intensity vector at any instant of time and any point of space is actually equal to the negative of the time rate of change of the magnetic vector potential, $\mathbf{A}$, at that point,[2]

$$\boxed{\mathbf{E}_{\text{ind}}(t) = -\frac{\partial \mathbf{A}}{\partial t}.} \tag{6.2}$$

induced electric field intensity vector (unit: V/m)

Combining then this temporal differential relationship between $\mathbf{A}$ and $\mathbf{E}_{\text{ind}}$ with the spatial integral relationship between the current density vector, $\mathbf{J}$, and $\mathbf{A}$ in Eq. (4.108), we obtain the following integral (more precisely, integro-differential) expression for the induced electric field intensity vector due to an arbitrary volume current distribution:

$$\boxed{\mathbf{E}_{\text{ind}}(t) = -\frac{\mu_0}{4\pi}\frac{\partial}{\partial t}\int_v \frac{\mathbf{J}\,\mathrm{d}v}{R} = -\frac{\mu_0}{4\pi}\int_v \frac{(\partial \mathbf{J}/\partial t)\,\mathrm{d}v}{R}.} \tag{6.3}$$

$\mathbf{E}_{\text{ind}}$ *due to volume current*

Here, the time derivative operator can be moved inside the integral sign and applied directly to the current density vector because the differentiation with respect to time and spatial integration over the volume v are entirely independent operations and can be performed in an arbitrary order. Similarly, Eqs. (4.109) and (4.110) yield the corresponding expressions for a surface current of density $\mathbf{J}_s$ and line current of intensity i:[3]

$$\mathbf{E}_{\text{ind}}(t) = -\frac{\mu_0}{4\pi}\int_S \frac{(\partial \mathbf{J}_s/\partial t)\,\mathrm{d}S}{R}, \tag{6.4}$$

$\mathbf{E}_{\text{ind}}$ *due to surface current*

$$\mathbf{E}_{\text{ind}}(t) = -\frac{\mu_0}{4\pi}\int_l \frac{(\mathrm{d}i/\mathrm{d}t)\,\mathrm{d}\mathbf{l}}{R}. \tag{6.5}$$

$\mathbf{E}_{\text{ind}}$ *due to line current*

We conclude from Eqs. (6.3)–(6.5) that an induced electric field will exist in a system whenever time-varying electric currents (representing accelerated or decelerated motion of electric charges) exist in the conductors. Such currents are said to induce

[1] While using the notation $\mathbf{E}_{\text{ind}}(t)$ for the induced electric field vector to emphasize its time dependence, and similarly designating other time-varying field quantities (field intensity vectors, flux density vectors, potentials, charge and current densities, etc.) that will be introduced in this chapter, we always keep in mind that all these quantities, in general, are functions of spatial coordinates as well, e.g., $\mathbf{E}_{\text{ind}} = \mathbf{E}_{\text{ind}}(x, y, z, t)$.

[2] When dealing with time-varying spatially distributed quantities, we use the partial derivative with respect to time (e.g., $\partial \mathbf{A}/\partial t$) rather than the ordinary (total) derivative ($\mathrm{d}\mathbf{A}/\mathrm{d}t$) to emphasize their multivariable character.

[3] As mentioned in Chapter 3, for circuit-theory quantities (e.g., current intensity and voltage) that vary in time, we use lowercase notation (e.g., i and v) to distinguish it from the same quantities in the time-constant (dc) regime, which are capitalized (I and V).

the field. On the other side, it will be zero at all instants of time when $\mathbf{J}$, $\mathbf{J}_S$, and I are constants with respect to time (time-invariant currents) at all points of the system.

Eqs. (6.3)–(6.5) represent a general means for evaluating (analytically or numerically) the electric field due to any spatial distribution of slowly time-varying currents in free space. In a later chapter, we shall introduce certain corrections in these expressions to extend their validity to rapidly time-varying current distributions. Essentially, these corrections introduce wave propagation effects in the computation of fields due to rapidly time-varying currents.

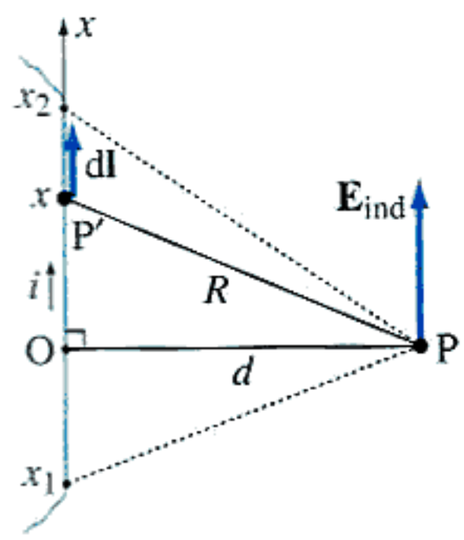

Figure 6.1 Evaluation of the induced electric field due to a finite straight wire conductor with a slowly time-varying current; for Example 6.1.

Example 6.1 Induced Electric Field of a Straight Wire Conductor

Find the expression for the electric field intensity vector at an arbitrary point in space induced by a slowly time-varying current $i(t)$ in a straight segment of length l representing a part of a wire structure in air.

Solution We use the integral expression in Eq. (6.5) and refer to Fig. 6.1. Let P′ and P denote, respectively, a source point along the segment and a field point positioned arbitrarily in space. The coordinate defining the position of the point P′ is x, $x_1 \le x \le x_2$, where x_1 and x_2 ($x_2 - x_1 = l$) are the coordinates of the starting and ending point of the segment, respectively. Note that both x_1 and x_2 can be either positive or negative, as well as zero, depending on the actual position of the point P with respect to the segment. Finally, let d mark the perpendicular distance of the point P from the segment. As $R = \sqrt{x^2 + d^2}$ and $\mathrm{d}\mathbf{l} = \mathrm{d}x\,\hat{\mathbf{x}}$ (Fig. 6.1), the induced electric field intensity vector at the point P is given by

$$\mathbf{E}_{\text{ind}} = -\frac{\mu_0}{4\pi}\frac{\mathrm{d}i}{\mathrm{d}t}\int_l \frac{\mathrm{d}\mathbf{l}}{R} = -\frac{\mu_0}{4\pi}\frac{\mathrm{d}i}{\mathrm{d}t}\,\hat{\mathbf{x}}\int_{x_1}^{x_2}\frac{\mathrm{d}x}{\sqrt{x^2+d^2}}, \tag{6.6}$$

where $\mathrm{d}i/\mathrm{d}t$ can be brought outside the integral sign because the current intensity $i(t)$ does not change along the wire (given that the current is slowly time-varying).[4] The solution of this integral[5] is

$\mathbf{E}_{\text{ind}}$ – *finite straight wire conductor*

$$\boxed{\mathbf{E}_{\text{ind}} = -\frac{\mu_0}{4\pi}\frac{\mathrm{d}i}{\mathrm{d}t}\ln\frac{x_2+\sqrt{x_2^2+d^2}}{x_1+\sqrt{x_1^2+d^2}}\,\hat{\mathbf{x}}.} \tag{6.7}$$

We note that the expression in Eq. (6.7) can be combined for computing the induced electric field due to structures containing any number of straight wire segments with a slowly time-varying current.

Example 6.2 Induced Electric Field of an EMI Source (Square Contour)

A source of electromagnetic interference (EMI) can be approximated by a square current contour of side length $a = 5$ cm in free space, as shown in Fig. 6.2(a). The contour carries a current whose intensity, $i(t)$, is a pulse function shown in Fig. 6.2(b). Compute the induced electric field intensity vector at the point M.

Solution We note that the time needed for electromagnetic disturbances to propagate over the domain of interest (from source points at the contour to the field point M) in Fig. 6.2(a) is on the order of $\tau = a/c_0 = 0.167$ ns ($c_0 = 3 \times 10^8$ m/s). Since this time is much shorter

[4] As we shall see in a later chapter, the intensity of a rapidly time-varying current in a wire conductor, in general, changes along the conductor.

[5] Note that $\int \mathrm{d}x/\sqrt{x^2+d^2} = \ln\left(x+\sqrt{x^2+d^2}\right) + C$ (C being the integration constant), which can be easily verified by differentiation.

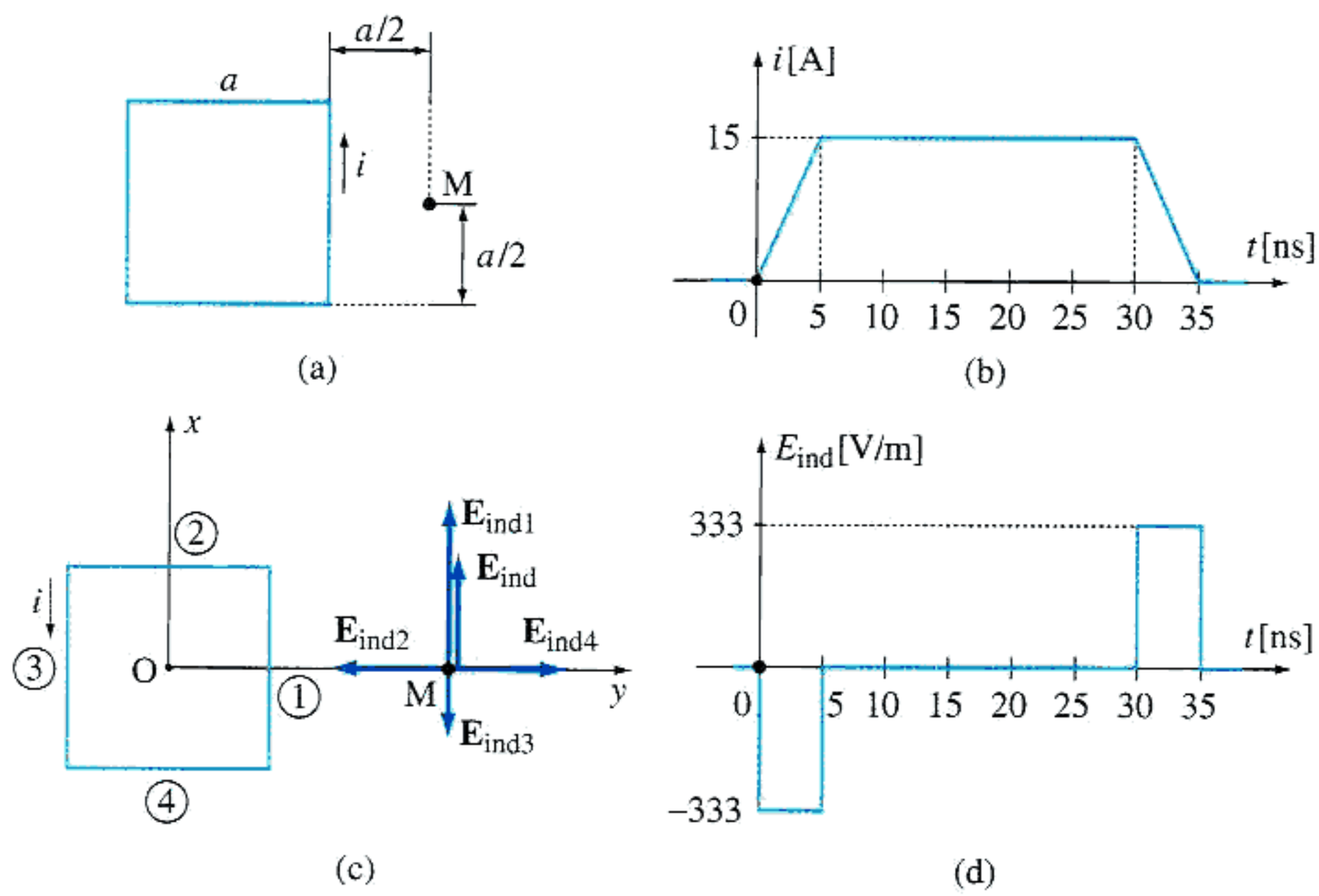

Figure 6.2 Evaluation of the induced electric field near a square current contour: (a) geometry of the problem, (b) contour current intensity as a function of time, (c) field intensity vectors due to individual sides of the contour, and (d) resultant field intensity as a function of time; for Example 6.2.

than the time of change (rise or fall) of the current intensity $i(t)$ in Fig. 6.2(b), $\Delta t = 5$ ns, the current can be considered as slowly time-varying and the system as quasistatic.

By means of the superposition principle, the total induced electric field intensity vector is given by [Fig. 6.2(c)]

$$\mathbf{E}_{\text{ind}} = \mathbf{E}_{\text{ind1}} + \mathbf{E}_{\text{ind2}} + \mathbf{E}_{\text{ind3}} + \mathbf{E}_{\text{ind4}}, \tag{6.8}$$

where the field intensity vectors due to individual sides of the contour, $\mathbf{E}_{\text{ind1}}, \ldots, \mathbf{E}_{\text{ind4}}$, are obtained from Eq. (6.7). Due to mutual antisymmetry of the second and fourth current segments with respect to the point M, $\mathbf{E}_{\text{ind2}} = -\mathbf{E}_{\text{ind4}}$. The distances d in the expressions for computing $\mathbf{E}_{\text{ind1}}$ and $\mathbf{E}_{\text{ind3}}$ equal $a/2$ and $3a/2$, respectively, whereas $x_1 = -a/2$ and $x_2 = a/2$ are the same in both expressions. Hence, the resultant $\mathbf{E}_{\text{ind}}$ at the point M comes out to be

$$\begin{aligned}\mathbf{E}_{\text{ind}} = \mathbf{E}_{\text{ind1}} + \mathbf{E}_{\text{ind3}} &= -\frac{\mu_0}{4\pi}\frac{\mathrm{d}i}{\mathrm{d}t}\left(\ln\frac{1+\sqrt{2}}{-1+\sqrt{2}} - \ln\frac{1+\sqrt{10}}{-1+\sqrt{10}}\right)\hat{\mathbf{x}} \\ &= -1.11\times 10^{-7}\frac{\mathrm{d}i}{\mathrm{d}t}\,\hat{\mathbf{x}}\ \text{V/m} \quad (\mathrm{d}i/\mathrm{d}t \text{ in A/s}).\end{aligned} \tag{6.9}$$

From Fig. 6.2(b), $\mathrm{d}i/\mathrm{d}t$ is nonzero only during the rise and fall intervals of the current pulse, when $\mathrm{d}i/\mathrm{d}t = \Delta i/\Delta t = \pm 15\ \text{A}/(5\ \text{ns}) = \pm 3\times 10^9$ A/s, which yields $E_{\text{ind}} = \mp 333$ V/m. The function $E_{\text{ind}}(t)$ is plotted in Fig. 6.2(d). We see that very strong pulses of the induced electric field in the form of "spikes" are generated in the vicinity of the contour. This field thus may cause a very strong undesirable interference (EMI) into the operation of neighboring circuits in the system.

Example 6.3 Induced Electric Field of a Circular Wire Segment (Arc)

Consider a wire conductor in the form of an arc representing a part of a wire contour with a slowly time-varying current of intensity $i(t)$ in free space. The arc is defined by its radius a and angle α, as shown in Fig. 6.3(a). Find the expression for the induced electric field intensity vector at the arc center (point O) due to this current conductor.

Solution Since the distance of the field point from the source point in this case is always the same, $R = a$ [see Fig. 6.3(a)], we can bring it outside the integral sign in Eq. (6.5), which

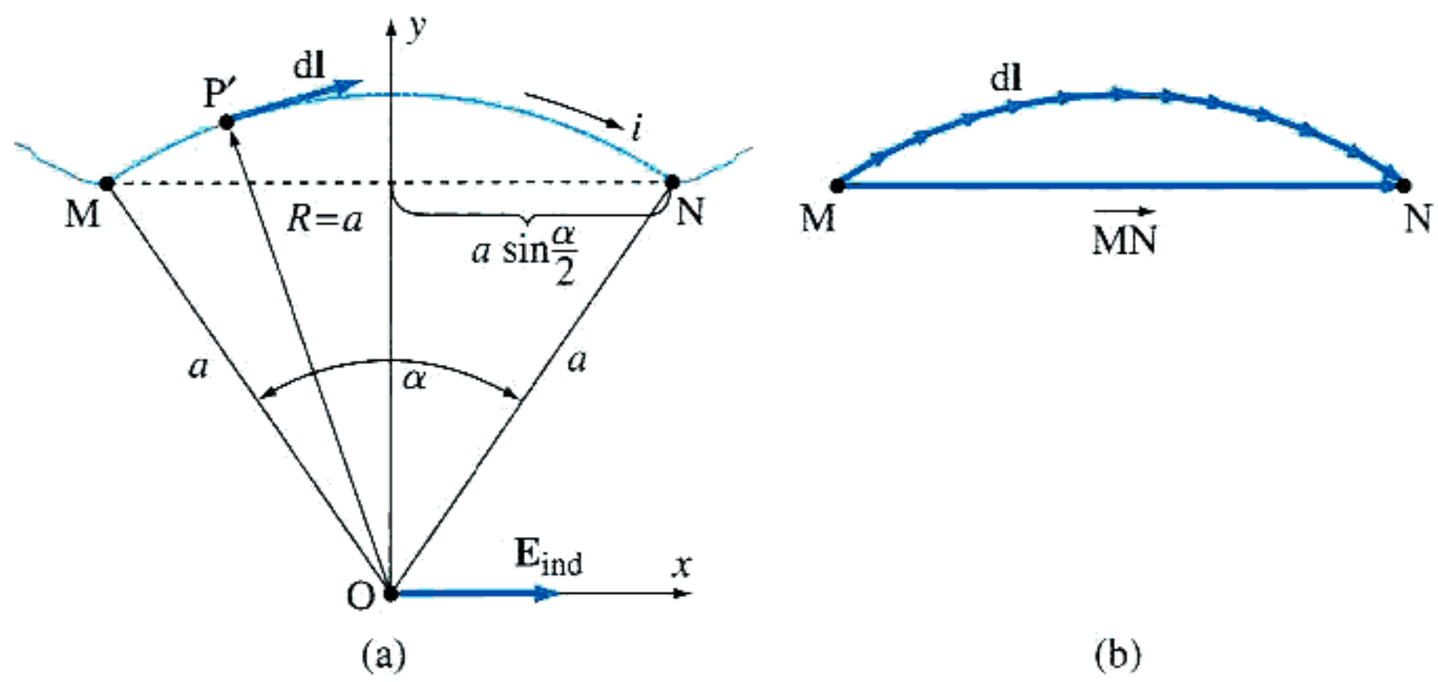

Figure 6.3 (a) Electric field induced by a slowly time-varying current along a circular wire segment and (b) application of the head-to-tail rule for vector addition to solve the integral of $\mathbf{dl}$ along the segment; for Example 6.3.

leads to

$$\mathbf{E}_{\text{ind}} = -\frac{\mu_0}{4\pi a}\frac{\mathrm{d}i}{\mathrm{d}t}\int_{\mathrm{M}}^{\mathrm{N}} \mathbf{dl}, \tag{6.10}$$

where M and N are the starting and ending points of the conductor, respectively. Using the head-to-tail rule for vector addition, we observe from Fig. 6.3(b) that

$$\int_{\mathrm{M}}^{\mathrm{N}} \mathbf{dl} = \overrightarrow{\mathrm{MN}} \tag{6.11}$$

(note that this result holds true not only for a path in the form of an arc but for an arbitrarily shaped path, planar or nonplanar, between points M and N). Finally, as the distance between points M and N equals $\overline{\mathrm{MN}} = 2a\sin(\alpha/2)$,

$\mathbf{E}_{\text{ind}}$ – *circular wire segment*

$$\boxed{\mathbf{E}_{\text{ind}} = -\frac{\mu_0}{4\pi a}\frac{\mathrm{d}i}{\mathrm{d}t}\overrightarrow{\mathrm{MN}} = -\frac{\mu_0}{2\pi}\sin\frac{\alpha}{2}\frac{\mathrm{d}i}{\mathrm{d}t}\hat{\mathbf{x}}.} \tag{6.12}$$

Example 6.4 Current Contour of Complex Shape

Consider the contour consisting of two semicircular and two linear parts in Fig. 1.51, and assume that it carries a time-harmonic current of intensity $i(t) = \cos(9 \times 10^6 t)$ A (t in s) with respect to the clockwise reference direction, as well as that $a = 10$ cm and $b = 20$ cm. Under these circumstances, determine the induced electric field intensity vector at the contour center (point O).

Solution Since the period of change of the current intensity $i(t)$, $T = 2\pi/\omega = 0.7\ \mu$s (where $\omega = 9 \times 10^6$ rad/s is the angular frequency), is much longer than the time $\tau = b/c_0 = 0.667$ ns needed for electromagnetic disturbances to propagate from source points at the larger semicircle to the field point O in Fig. 1.51, the time-harmonic current in the contour can be considered as a low-frequency (slowly time-varying) current.

Referring to Fig. 6.4 and employing the superposition principle, the resultant induced electric field intensity vector is given by Eq. (6.8). From Eq. (6.12),

$$\mathbf{E}_{\text{ind1}} = -\frac{\mu_0}{4\pi a}\frac{\mathrm{d}i}{\mathrm{d}t}\overrightarrow{\mathrm{QR}} = -\frac{\mu_0}{2\pi}\frac{\mathrm{d}i}{\mathrm{d}t}\hat{\mathbf{x}}, \quad \mathbf{E}_{\text{ind3}} = -\frac{\mu_0}{4\pi b}\frac{\mathrm{d}i}{\mathrm{d}t}\overrightarrow{\mathrm{SP}} = -\frac{\mu_0}{2\pi}\frac{\mathrm{d}i}{\mathrm{d}t}(-\hat{\mathbf{x}}), \tag{6.13}$$

that is, $\mathbf{E}_{\text{ind1}} + \mathbf{E}_{\text{ind3}} = 0$. From Eq. (6.7), on the other hand,

$$\mathbf{E}_{\text{ind2}} = -\frac{\mu_0}{4\pi}\frac{\mathrm{d}i}{\mathrm{d}t}\ln\frac{b+\sqrt{b^2+0}}{a+\sqrt{a^2+0}}\hat{\mathbf{x}} = -\frac{\mu_0}{4\pi}\frac{\mathrm{d}i}{\mathrm{d}t}\ln\frac{b}{a}\hat{\mathbf{x}}. \tag{6.14}$$

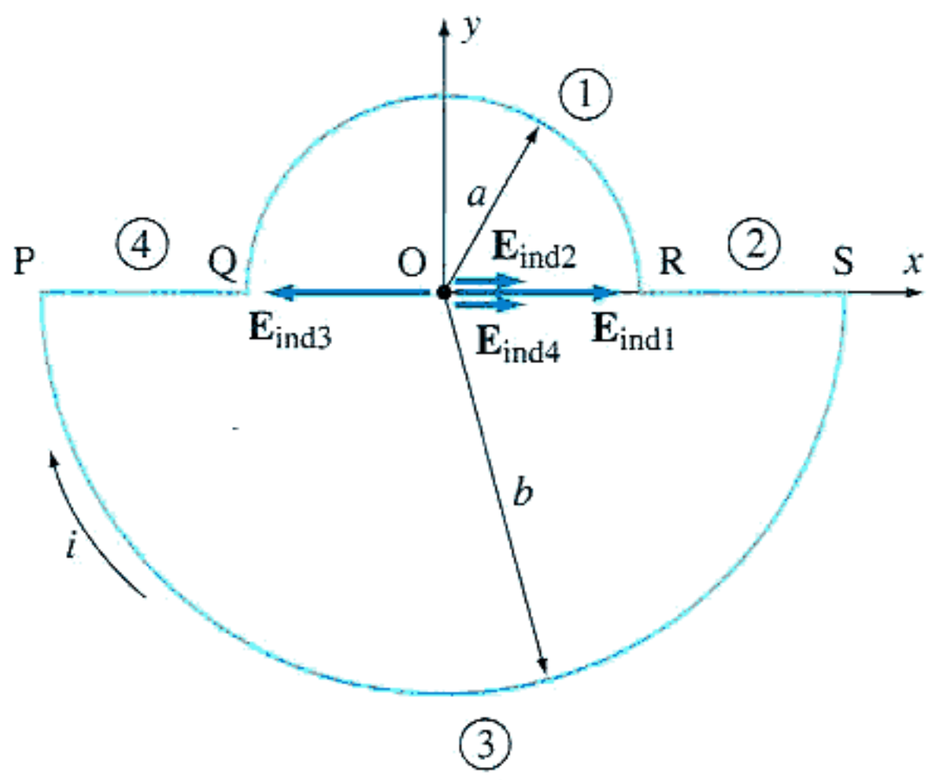

Figure 6.4 Evaluation of the induced electric field due to a current contour with two semicircular and two linear parts; for Example 6.4.

Due to symmetry, $\mathbf{E}_{\text{ind4}} = \mathbf{E}_{\text{ind2}}$, so that the total $\mathbf{E}_{\text{ind}}$ equals

$$\mathbf{E}_{\text{ind}} = 2\mathbf{E}_{\text{ind2}} = -\frac{\mu_0}{2\pi}\frac{\mathrm{d}i}{\mathrm{d}t}\ln\frac{b}{a}\,\hat{\mathbf{x}} = 1.25\sin(9\times 10^6 t)\,\hat{\mathbf{x}}\ \text{V/m} \quad (t \text{ in s}). \tag{6.15}$$

Problems: 6.1–6.9; *Conceptual Questions* (on Companion Website): 6.1–6.8; *MATLAB Exercises* (on Companion Website).

6.2 SLOWLY TIME-VARYING ELECTRIC AND MAGNETIC FIELDS

The slowly time-varying electric field, in general, is composed of two components: the induced electric field, given by Eqs. (6.3)–(6.5), and the Coulomb electric field – the field due to excess charge, which we denote here as $\mathbf{E}_q$. The total electric field intensity vector is thus

$$\boxed{\mathbf{E}(t) = \mathbf{E}_{\text{ind}}(t) + \mathbf{E}_q(t).} \tag{6.16}$$

total electric field = induced plus Coulomb fields

The Coulomb field component has the same form as in electrostatics, given by Eqs. (1.37)–(1.39), however, the charge densities are now time-dependent. For instance, the field due to excess volume charge in free space is obtained as

$$\mathbf{E}_q(t) = \frac{1}{4\pi\varepsilon_0}\int_v \frac{\rho(t)\,\mathrm{d}v}{R^2}\,\hat{\mathbf{R}}. \tag{6.17}$$

Equivalently,

$$\boxed{\mathbf{E}_q(t) = -\nabla V(t),} \tag{6.18}$$

electric field due to excess charge

where the electric scalar potential is expressed as

$$\boxed{V(t) = \frac{1}{4\pi\varepsilon_0}\int_v \frac{\rho(t)\,\mathrm{d}v}{R}} \tag{6.19}$$

slowly time-varying electric potential

[see Eqs. (1.101) and (1.82)].

As the spatial distribution of the field $\mathbf{E}_q(t)$ has all the properties of the electrostatic field, we can write

$$\oint_C \mathbf{E}_q(t) \cdot d\mathbf{l} = 0 \tag{6.20}$$

[Eq. (1.75)] or

$$\nabla \times \mathbf{E}_q(t) = 0 \tag{6.21}$$

[Eq. (4.92)], which are the mathematical expressions of the conservative character of the field $\mathbf{E}_q(t)$. In accordance to Eqs. (1.88) and (1.90), the time-varying potential difference (voltage) between points M and N in space is given by

$$v_{\mathrm{MN}}(t) = V_{\mathrm{M}}(t) - V_{\mathrm{N}}(t) = \int_{\mathrm{M}}^{\mathrm{N}} \mathbf{E}_q(t) \cdot d\mathbf{l}. \tag{6.22}$$

The field due to excess time-varying charge also obeys Gauss' law. In differential notation [Eq. (1.166)],

$$\nabla \cdot \mathbf{E}_q(t) = \frac{\rho(t)}{\varepsilon_0}. \tag{6.23}$$

However, a combination of Eqs. (6.2) and (4.119) leads to

$$\nabla \cdot \mathbf{E}_{\mathrm{ind}} = -\nabla \cdot \left(\frac{\partial \mathbf{A}}{\partial t}\right) = -\frac{\partial}{\partial t}(\nabla \cdot \mathbf{A}) = 0, \tag{6.24}$$

where the time derivative operator can be brought outside the divergence operator (which implies spatial differentiation) because these two operations are entirely independent from one another and can be performed in an arbitrary order. Hence, the divergence of the vector $\mathbf{E}(t)$ in Eq. (6.16) equals

$$\nabla \cdot \mathbf{E}(t) = \nabla \cdot \mathbf{E}_{\mathrm{ind}}(t) + \nabla \cdot \mathbf{E}_q(t) = \frac{\rho(t)}{\varepsilon_0}, \tag{6.25}$$

which means that Gauss' law holds for the total electric field as well.

In the case of dielectric materials in the time-varying electric field, the polarization vector [Eq. (2.7)] and bound charge densities [Eqs. (2.19) and (2.23)] in the material are time-dependent. The generalized Gauss' law in integral form, Eq. (2.44), is written as

$$\oint_S \mathbf{D}(t) \cdot d\mathbf{S} = \int_v \rho(t)\, dv, \tag{6.26}$$

where $\mathbf{D}(t)$ is the total electric flux density vector in the material, given by Eqs. (2.41) and (2.47) with $\mathbf{E}$ representing the total electric field intensity vector.

On the other side, the slowly time-varying magnetic field has the same form as the magnetostatic field. The magnetic flux density vector in free space can thus be obtained using the time-varying version of Eqs. (4.7)–(4.9). For instance, the field due to a volume current distribution in free space is given by

$$\mathbf{B}(t) = \frac{\mu_0}{4\pi} \int_v \frac{[\mathbf{J}(t)\, dv] \times \hat{\mathbf{R}}}{R^2}. \tag{6.27}$$

The field $\mathbf{B}(t)$ can also be obtained indirectly, via the magnetic vector potential, as [Eq. (4.116)]

slowly time-varying magnetic field

$$\boxed{\mathbf{B}(t) = \nabla \times \mathbf{A}(t),} \tag{6.28}$$

where

slowly time-varying magnetic potential

$$\boxed{\mathbf{A}(t) = \frac{\mu_0}{4\pi} \int_v \frac{\mathbf{J}(t)\, dv}{R},} \tag{6.29}$$

with analogous expressions for surface and line currents.

In magnetic materials, the magnetization vector [Eq. (5.1)] and magnetization current densities [Eqs. (5.28) and (5.32)] are now time-dependent. The integral form of the generalized Ampère's law, Eq. (5.51), can be rewritten as

$$\oint_C \mathbf{H}(t) \cdot d\mathbf{l} = \int_S \mathbf{J}(t) \cdot d\mathbf{S}, \tag{6.30}$$

and that of the law of conservation of magnetic flux, Eq. (4.99), as

$$\oint_S \mathbf{B}(t) \cdot d\mathbf{S} = 0. \tag{6.31}$$

Problems: 6.10.

6.3 FARADAY'S LAW OF ELECTROMAGNETIC INDUCTION

We now introduce Faraday's law of electromagnetic induction, as the most important governing law of the slowly time-varying electromagnetic field and the explicit relation between the electric and magnetic fields that change in time. Following Oersted's discovery in 1820 that electric currents produced magnetic fields, Michael Faraday was convinced that the reverse was also possible – that a magnetic field could produce an electric current. In 1831, Faraday set up an apparatus consisting of an iron toroidal core (ring), like the one in Fig. 5.19, with two coils wound on it. The primary coil was connected through a switch to a battery (voltaic cell) and the secondary coil was short-circuited by a wire running above a compass, as sketched in Fig. 6.5. Thus, any electric current in the secondary coil would, by means of its magnetic field, deflect the compass needle. Upon closing the switch, Faraday observed a momentary deflection of the needle, indicating a brief surge of current induced in the secondary coil. The same happened when the switch was opened, terminating the current in the primary coil, but the needle deflection was opposite in polarity with respect to the previous one. In steady states, however, i.e., once the current in the primary coil reached its final value (equal to the battery voltage divided by the resistance of the primary circuit or to zero), there was no current in the secondary coil and the compass needle was at its zero position. Faraday realized that a current was produced (induced) in the secondary coil by a changing magnetic field in the iron core (the field was changed from zero to a final steady value, corresponding to a steady current intensity established in the primary circuit, and then back to zero when the current was terminated). This extraordinary discovery led to the formulation of the law of electromagnetic induction, named after Faraday.

The mathematical statement of Faraday's law of electromagnetic induction describes the time variation of the magnetic flux through an arbitrary contour as

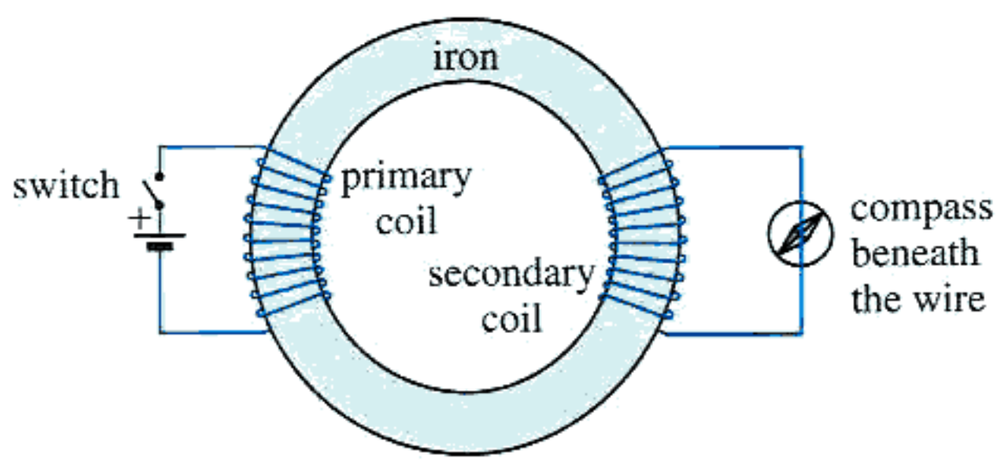

Figure 6.5 Sketch of the apparatus used in Faraday's 1831 experiment that led to the discovery of electromagnetic induction.

HISTORICAL ASIDE

Michael Faraday (1791–1867), an English physicist and chemist, self-educated from books he was binding to earn a living, became a member of the Royal Society at age 34. He was mostly unfamiliar with mathematics, but at the same time he was an enormously gifted experimentalist and imaginative thinker, and certainly one of the greatest scientists ever. Upon a recommendation by Sir Humphry Davy (1778–1829), the discoverer of six chemical elements, Faraday was appointed Chemical Assistant at the Royal Institution on March 1, 1813. After repeating Oersted's (1777–1851) 1820 experiment, he demonstrated in September of 1821 that the magnetic field around a straight wire with an electric current was circular, and, in the same set of experiments, went a large step further – by making a current-carrying wire suspended above a permanent magnet circle around the magnet, he invented the first electric motor. Generalizing from the patterns formed by iron filings around magnets, he introduced the concept of electric and magnetic field lines (he called them lines of force) as a new approach to studying electricity and magnetism. Faraday was elected to the Royal Society in 1824 and was made Director of the Laboratory at the Royal Institution in 1825. In 1826, he started Christmas Lectures for children at the Institution, which not only continue, but are now televised to giant audiences all over the world. In his famous August 29, 1831 experiment, he wound two coils of wire on the same iron ring (see Fig. 6.5) and discovered that a current in one coil if changed in time induced a current in the other coil. He concluded that an electric current could be produced by a time-varying magnetic field and thus discovered electromagnetic induction. Faraday's induction ring was the world's first electric transformer. In subsequent experiments in the fall of 1831, he attempted to create a current using a permanent magnet. He discovered that when a permanent magnet was moved in and out of a wire coil, a current was induced in the coil. He then demonstrated that a continuous current could be generated by rotating a copper disk between the poles of a large permanent magnet and taking leads off the rim and the center of the disk. This invention, referred to as Faraday's wheel (see Fig. 6.35), was the first dynamo (electric generator). Faraday used his concept of lines of force to explain the principle of electromagnetic induction observed in his experiments. He explained that an electric current was induced in a conductor only when magnetic lines of force cut across it, and this could be either because the lines of a changing magnetic field expanded and collapsed in space cutting thus across the conductor (transformer induction) or because the conductor moved across the static field lines (motional induction). He realized that the magnitude of the induced current was dependent on the number of lines of force cut by the conductor in unit time, which is a true equivalent to a more mathematical formulation of what is now known as Faraday's law of electromagnetic induction. It was the discovery of electromagnetic induction in 1831, more than any other, that allowed electricity to be turned, during the remainder of the 19th century, from a scientific curiosity into a powerful technology. In the 1830s, Faraday also studied the relationships between the amount of material deposited on electrodes of an electrolytic cell, the amount of electricity passed through the cell, and chemical properties of different elements, and formulated fundamental principles of electrochemistry (Faraday's laws of electrolysis). He also discovered that light could be affected by a magnetic force – he demonstrated in 1845 that a strong magnetic field could rotate the plane of polarization of polarized light – which later became known as the Faraday magneto-optical effect. In his famous lecture "Thoughts on Ray-vibrations" at the Royal Institution in April of 1846, he suggested that the propagation of light through space consisted of vibrations of lines of force, which, intuitively, was not far from Maxwell's (1831–1879) explanation, given much later (in 1865) and based on rigorous mathematical derivations,

that light was an oscillatory electromagnetic disturbance – electromagnetic wave. In a series of studies from 1846 to 1850, Faraday evolved his global theoretical electromagnetic model based on the "force field" – the field of lines of force in tension filling the space around charged bodies, current-carrying conductors, and permanent magnets, and thus established the field theory of electromagnetism. These concepts of electric and magnetic force fields were put into a mathematical form a generation later by Maxwell, who himself made it very clear in his texts that the basic ideas for his classical electromagnetic field equations came directly from Faraday. Despite his epochal scientific achievements and far-reaching contributions to humanity, Faraday remained a modest and humble person throughout his life. We honor Faraday also by using farad (F) as the unit for capacitance. *(Portrait: Edgar Fahs Smith Collection, University of Pennsylvania Libraries)*

the cause of the induced electromotive force along the contour. In developing the general electromagnetic model, it is usually taken as an experimentally based postulate. However, because we started our study of electromagnetic induction by taking the mathematical expression for the induced electric field intensity vector due to a point charge in accelerated motion as an experimental postulate, we are now able to actually derive Faraday's law from the facts that we already know about the induced electric field.

In a region with free charge carriers (e.g., in a conducting wire), the induced electric field intensity vector, $\mathbf{E}_{\text{ind}}$, acts on the carriers by the force $Q\mathbf{E}_{\text{ind}}$ [Eq. (4.143)], where Q is the charge of a carrier (e.g., a free electron). Therefore, the line integral of $\mathbf{E}_{\text{ind}}$ along a line joining any two points M and N in space represents the electromotive force (emf) induced in the line:

$$\boxed{e_{\text{ind}} = \int_{\text{M}}^{\text{N}} \mathbf{E}_{\text{ind}} \cdot \mathrm{d}\mathbf{l}.} \tag{6.32}$$

induced electromotive force (emf), in volts

The induced emf is measured in volts and defined in the same way as the emf of a voltage generator in Eq. (3.112). In fact, the line can be replaced by an equivalent voltage generator whose emf is e_{ind}, as shown in Fig. 6.6.

For a closed line (contour) that does not change or move in time, Fig. 6.7, we use Eq. (6.2) and write

$$e_{\text{ind}} = \oint_C \mathbf{E}_{\text{ind}} \cdot \mathrm{d}\mathbf{l} = -\oint_C \frac{\partial \mathbf{A}}{\partial t} \cdot \mathrm{d}\mathbf{l} = -\frac{\mathrm{d}}{\mathrm{d}t} \oint_C \mathbf{A} \cdot \mathrm{d}\mathbf{l}. \tag{6.33}$$

We now recall that the circulation of the magnetic vector potential along a contour equals the magnetic flux through the contour, Eq. (4.121), so that

$$\boxed{e_{\text{ind}} = -\frac{\mathrm{d}\Phi}{\mathrm{d}t}.} \tag{6.34}$$

Faraday's law of electromagnetic induction

This equation is known as Faraday's law of electromagnetic induction. It is one of the most important experimental pillars of electromagnetics. It shows, first of all, that the electric and magnetic fields are related to one another under nonstatic conditions. More specifically, it states that a magnetic field that changes with time produces (induces) an electric field and an electromotive force, as well as an electric current in conducting media [by virtue of Ohm's law in local form, Eq. (3.18)].

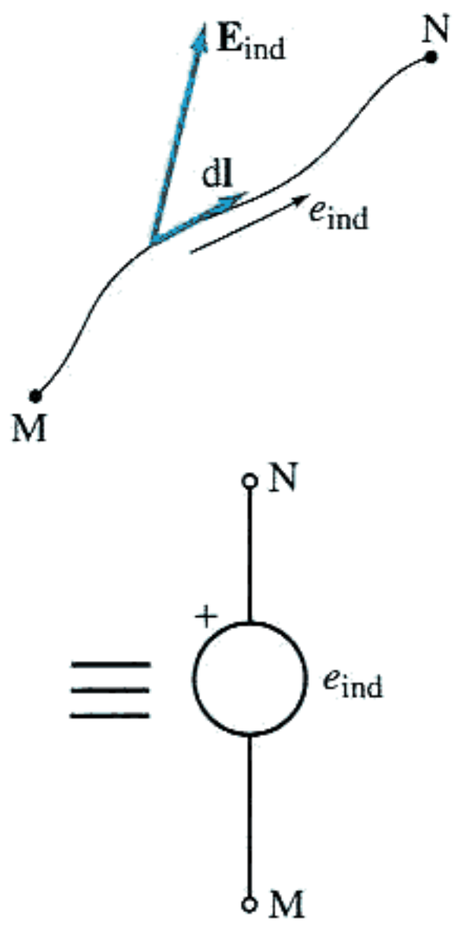

Figure 6.6 Induced emf in a line joining two points in space.

Finally, it quantifies the induced emf in an arbitrary contour as being equal to the negative of the time rate of change of the magnetic flux through the contour, i.e., through a surface of arbitrary shape spanned over the contour and oriented in accordance to the right-hand rule with respect to the orientation of the contour. This rule tells us that the flux is in the direction defined by the thumb of the right hand when the other fingers point in the direction of the emf, as indicated in Fig. 6.7.

Expressing the magnetic flux using the flux density vector [Eq. (4.95)] leads to

$$\oint_C \mathbf{E}_{\text{ind}} \cdot \mathrm{d}\mathbf{l} = -\frac{\mathrm{d}}{\mathrm{d}t} \int_S \mathbf{B} \cdot \mathrm{d}\mathbf{S}, \tag{6.35}$$

where the reference directions of $\mathrm{d}\mathbf{l}$ and $\mathrm{d}\mathbf{S}$ are interconnected by the right-hand rule: fingers – $\mathrm{d}\mathbf{l}$, thumb – $\mathrm{d}\mathbf{S}$ (see Fig. 6.7). Since the circulation of the field intensity vector due to excess charge is zero [Eq. (6.20)], we have that

$$\oint_C \mathbf{E} \cdot \mathrm{d}\mathbf{l} = \oint_C \mathbf{E}_{\text{ind}} \cdot \mathrm{d}\mathbf{l}, \tag{6.36}$$

which means that Faraday's law can be expressed in terms of the total electric field intensity vector as well. In addition, the time derivative on the right-hand side of Eq. (6.35) can be moved inside the surface integral, provided that the surface S does not change or move in time. Combining these two conclusions, we obtain the following version of Faraday's law of electromagnetic induction in integral form:

Faraday's law in integral form

$$\boxed{\oint_C \mathbf{E} \cdot \mathrm{d}\mathbf{l} = -\int_S \frac{\partial \mathbf{B}}{\partial t} \cdot \mathrm{d}\mathbf{S}.} \tag{6.37}$$

We note the formal similarity between this equation and the generalized Ampère's law in integral form, Eq. (6.30), where $-\partial \mathbf{B}/\partial t$ in Eq. (6.37) stands for $\mathbf{J}$ in Eq. (6.30) in the flux integrals, while the electric and magnetic field intensity vectors, $\mathbf{E}$ and $\mathbf{H}$, appear in the corresponding line integrals on the left-hand side of equations.

The contour C in Fig. 6.7 can be an imaginary (nonmaterial) contour, i.e., it does not need to be a conducting wire loop for Faraday's law of electromagnetic induction to be true. The electric field and emf are induced by a magnetic field that changes with time regardless of whether or not conducting wires are present. However, in the case when C does represent a conducting wire contour, there is a current of intensity

induced current

$$\boxed{i_{\text{ind}} = \frac{e_{\text{ind}}}{R}} \tag{6.38}$$

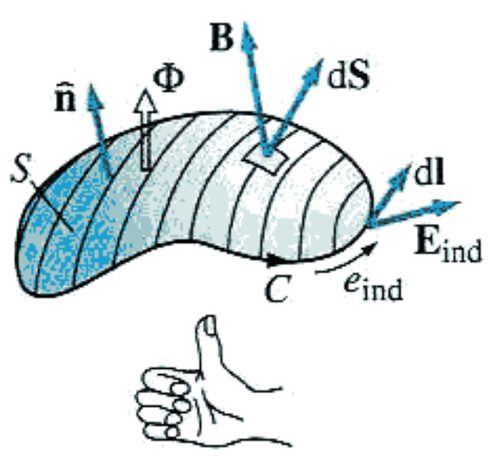

Figure 6.7 Arbitrary contour in a time-varying magnetic field – for the formulation of Faraday's law of electromagnetic induction.

in the wire, as shown in Fig. 6.8, where R is the total resistance of the contour and of the equivalent closed circuit including the ideal voltage generator with emf e_{ind} [this, basically, comes from the version of Kirchhoff's voltage law in Eq. (3.118)]. This current is called the induced current. We can say thus that, in general, time-varying magnetic fields, $\mathbf{B}(t)$, induce electric currents in conducting media, which also change with time.

On the other hand, if the conducting wire loop is not closed (e.g., there is a small air gap in the loop), there is no current flowing through it,[6] and the loop behaves like an open-circuited generator with emf e_{ind}, as in Fig. 6.6. The voltage across the gap equals the induced emf, i.e., $v_{\text{NM}}(t) = e_{\text{ind}}(t)$ [see Eq. (3.115)].

[6] As opposed to dc and slowly time-varying cases, as we shall see in a later chapter, a rapidly time-varying current can exist even in open-ended wire conductors that do not form closed current circuits.

HISTORICAL ASIDE

Heinrich Friedrich Emil Lenz (1804–1865), a Russian physicist, was a professor of physics at the University of St. Petersburg. He was one of the three great scientists, together with Faraday (1791–1867) and Henry (1797–1878), who independently from each other investigated electromagnetic induction at about the same time at three remote places on the globe. Lenz was born and educated in Dorpat (now Tartu), Estonia, then a part of Russian Empire. As geophysical scientist, he traveled around the world in the 1820s and made extremely accurate measurements of the salinity, temperature, and specific gravity of sea waters. He also studied electricity and magnetism, and discovered, in 1833, that the resistivity of metallic conductors increases with a rise in temperature [see Eq. (3.22)]. In 1834, he discovered that an induced current always produces effects that oppose its cause. This became to be known as Lenz's law. From 1840 to 1863, Lenz was the Dean of Mathematics and Physics at the University of St. Petersburg.

The minus sign in Eq. (6.34) indicates that the induced emf in the contour is in a direction that opposes the change in the magnetic flux through the contour that caused the emf in the first place. This fact, contained in Faraday's law, is an experimental result referred to as Lenz's law. To illustrate it, assume that at an instant t the flux in Fig. 6.8 increases in time, i.e., $d\Phi/dt > 0$. From Eq. (6.34), the emf $e_{\text{ind}}(t)$ at that instant is negative, and so is the induced current intensity $i_{\text{ind}}(t)$ in Eq. 6.38. The induced current produces a secondary magnetic field, whose reference direction is determined by another application of the right-hand rule: fingers – current, thumb – field [for example, see Fig. 4.31(b)]. Hence, given the reference direction of i_{ind} in Fig. 6.8, the reference direction of the secondary magnetic field, and its flux, will be the same as that of the primary (original) magnetic field $\mathbf{B}(t)$ and flux $\Phi(t)$. So, with respect to that reference direction, the secondary flux is negative, because $i_{\text{ind}}(t)$ is negative at the time instant considered. We conclude thus that the magnetic field due to the induced current opposes the change (increase in this case) in the primary magnetic field, which caused the induced emf and current in the first place, and this is the statement of Lenz's law. Generally, Lenz's law represents a rule for (quickly) determining the actual direction of an induced current in a loop (circuit), without fully applying Faraday's law. This direction is always such that the magnetic field due to the induced current opposes (tends to cancel) the change in the magnetic flux that induces the current.[7]

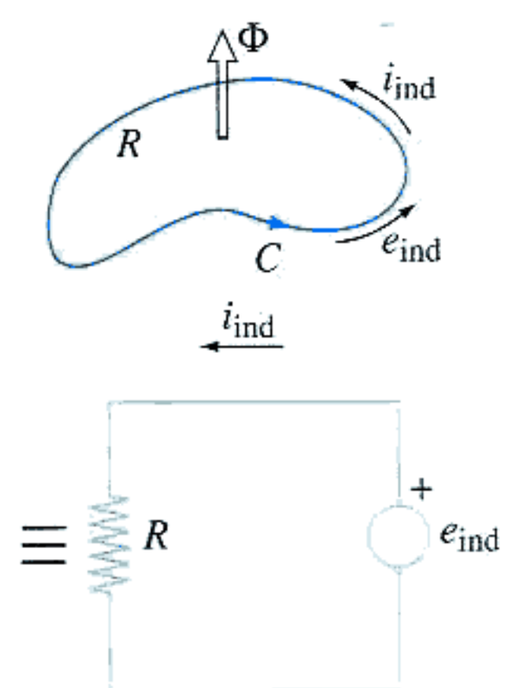

Figure 6.8 Induced current in a conducting wire loop situated in a time-varying magnetic field.

By virtue of Stokes' theorem, Eq. (4.89), or simply by analogy with the differential form of the generalized Ampère's law, Eq. (5.52), we obtain the differential equivalent of Eq. (6.37), namely, Faraday's law of electromagnetic induction in differential form:

$$\boxed{\nabla \times \mathbf{E} = -\frac{\partial \mathbf{B}}{\partial t}.} \tag{6.39}$$

Faraday's law in differential form

[7]The magnetic field due to the induced slowly time-varying current in typical thin-wire circuits is much weaker than the primary magnetic field inducing the current. Therefore, it is usually negligible with respect to the primary field and falls far short of fully canceling the flux change causing the electromagnetic induction.

In words, the curl of the time-varying electric field intensity vector existing at any point of space and any instant of time equals the negative of the time rate of change of the magnetic flux density vector at that point.

Note that the differential form of Faraday's law can also be derived by taking the curl of both sides of Eq. (6.2) and using Eq. (6.28). This results in

$$\nabla \times \mathbf{E}_{\text{ind}} = -\nabla \times \left(\frac{\partial \mathbf{A}}{\partial t}\right) = -\frac{\partial}{\partial t}(\nabla \times \mathbf{A}) = -\frac{\partial \mathbf{B}}{\partial t}, \tag{6.40}$$

which is the version of the law with the induced electric field intensity vector. Since the curl of the field intensity vector due to excess charge is zero [Eq. (6.21)], we conclude that

$$\nabla \times \mathbf{E} = \nabla \times \mathbf{E}_{\text{ind}} + \nabla \times \mathbf{E}_q = \nabla \times \mathbf{E}_{\text{ind}}, \tag{6.41}$$

which gives the version of the law with the total electric field intensity vector, Eq. (6.39).

6.4 MAXWELL'S EQUATIONS FOR THE SLOWLY TIME-VARYING ELECTROMAGNETIC FIELD

Faraday's law of electromagnetic induction, given by Eq. (6.37) or Eq. (6.39), represents Maxwell's first equation for the time-varying electromagnetic field. It is essentially different from Maxwell's first equation for the time-invariant electromagnetic field in Eqs. (5.129). It tells us that a magnetic field changing with time gives rise to an electric field. The remaining three Maxwell's equations are given by Eqs. (6.30), (6.26), and (6.31), and they retain the same form as in the time-invariant case. We now summarize the full set of Maxwell's equations in differential form along with the constitutive equations for the slowly time-varying electromagnetic field in a linear isotropic medium:

Maxwell's first equation

Maxwell's second equation, quasistatic field

Maxwell's third equation

Maxwell's fourth equation

constitutive equation for **D**

constitutive equation for **B**

constitutive equation for **J**

$$\boxed{\begin{cases} \nabla \times \mathbf{E}(t) = -\frac{\partial \mathbf{B}}{\partial t} \\ \nabla \times \mathbf{H}(t) = \mathbf{J}(t) \\ \nabla \cdot \mathbf{D}(t) = \rho(t) \\ \nabla \cdot \mathbf{B}(t) = 0 \\ \mathbf{D}(t) = \varepsilon \mathbf{E}(t) \\ \mathbf{B}(t) = \mu \mathbf{H}(t) \\ \mathbf{J}(t) = \sigma \mathbf{E}(t) \end{cases}} \tag{6.42}$$

Because of the new term on the right-hand side of the first equation, the time-varying electric and magnetic fields are coupled together and cannot be analyzed separately, as opposed to time-invariant electric and magnetic fields, which are entirely independent from each other. On the other hand, as we shall see in a later chapter, Maxwell's equations for the rapidly time-varying electromagnetic field differ from the corresponding equations for the slowly time-varying field only in the generalized Ampère's law (second equation). Namely, an additional term exists on the right-hand side of this equation in the general case, expressing the fact that an electric field rapidly changing with time gives rise to a magnetic field. Therefore, the second equation in the system of Eqs. (6.42) represents the quasistatic version of

Maxwell's second equation and is true for slowly time-varying (e.g., low-frequency time-harmonic) fields.

Eqs. (6.19) and (6.29) give the expressions for slowly-time varying electromagnetic potentials in free space. Substituting Eqs. (6.2) and (6.18) in Eq. (6.16) leads to the following expression for the electric field intensity vector, **E**, in terms of the potentials:

$$\boxed{\mathbf{E}(t) = -\frac{\partial \mathbf{A}}{\partial t} - \nabla V(t).} \tag{6.43}$$

electric field via potentials

We see that both potentials are needed for **E**, whereas **A** alone suffices for the magnetic flux density vector, **B**, in Eq. (6.28). Eqs. (6.43) and (6.28) represent a means for evaluating (by differentiation) the electromagnetic field (**E**, **B**) from potentials (V, **A**), the evaluation of potentials being, in general, considerably simpler than the direct evaluation of field vectors.

In addition to Maxwell's equations for a given class of electromagnetic fields, we always have in mind the associated version of the continuity equation, which represents one of the fundamental principles of electromagnetics – the principle of conservation of charge, but can also be derived from Maxwell's equations. Thus, by taking the divergence of both sides of the quasistatic version of the generalized Ampère's law in Eqs. (6.42), as in Eq. (5.130) for the static case, we obtain that

$$\nabla \cdot \mathbf{J}(t) = 0, \tag{6.44}$$

which is the differential form of the continuity equation for slowly time-varying currents. We note that it has the same form as the continuity equation for time-invariant (steady) currents, Eq. (3.41). We also note that it can be regarded as the special case of the general continuity equation for time-varying currents, Eq. (3.39), with $\partial\rho/\partial t \approx 0$. Namely, in the slowly time-varying field, the rate of the time-variation in excess charge is slow enough to be neglected while evaluating the current continuity balance. In integral notation,

$$\boxed{\oint_S \mathbf{J}(t) \cdot d\mathbf{S} = 0,} \tag{6.45}$$

continuity equation for slowly time-varying currents

which is the same as Eq. (3.40) for steady currents.

Eq. (6.45) implies that the slowly time-varying current intensity $i(t)$ along a wire conductor, just as the steady current intensity I along a wire, is the same in every cross section of the conductor – the fact that we have already used throughout this chapter. It also means that Kirchhoff's circuital law for slowly time-varying currents is given by

$$\sum_{k=1}^{N} i_k(t) = 0, \tag{6.46}$$

where N is the number of conductors (branches in a circuit) meeting at a node. We see that Kirchhoff's current law for low-frequency ac circuits has the same form as that for dc circuits [Eq. (3.42)].

6.5 COMPUTATION OF TRANSFORMER INDUCTION

This section is devoted to the application of Faraday's law of electromagnetic induction in evaluating the induced emf, e_{ind}, and electric field intensity vector, $\mathbf{E}_{\text{ind}}$, in stationary contours due to given slowly time-varying current distributions and their magnetic fields. This kind of electromagnetic induction is called transformer

induction, because it is the basis of current and voltage transformation by magnetic coupling between circuits. Namely, it enables time-varying currents and voltages in one circuit (primary circuit) to be transformed, by induction, to time-varying currents and voltages in another circuit (secondary circuit), where the transfer of energy between the circuits is actually performed by the magnetic field due to the currents in the primary circuit causing the induced electric field in the secondary circuit. The electromagnetic induction due to motion of conductors in magnetic fields will be introduced and studied in the next section.

In some applications, we are interested only in the total emf induced in a contour (e.g., a wire loop). In such cases, we apply the version of Faraday's law of electromagnetic induction in Eq. (6.34), where we only need to evaluate the magnetic flux through the contour and compute its time derivative, which is usually a simple task to do. However, to find the actual distribution of the emf along a contour or to find the distribution of the induced electric field intensity vector in space, which is necessary in many applications, we have to employ the version of the law in Eq. (6.35). This equation, although always true, enables us to analytically solve for the field $\mathbf{E}_{\text{ind}}$ only due to highly symmetrical primary current distributions. These are the cases where the vector $\mathbf{E}_{\text{ind}}$ is tangential to some (or all) sections of the contour and has a constant magnitude along such sections, while being perpendicular to the remaining sections of the contour (if such sections exist). In other words, these are the cases in which we are able to bring the induced electric field intensity, E_{ind}, outside the integral sign on the left-hand side of Eq. (6.35), and solve for it. Note that Eqs. (6.3)–(6.5), on the other hand, provide general solution procedures for computing $\mathbf{E}_{\text{ind}}$.

Because Faraday's law and Ampère's law have the same mathematical form, there is a complete formal analogy in their application. In solving for $\mathbf{E}_{\text{ind}}$ due to $\mathbf{B}$ in highly symmetrical situations, therefore, we shall exploit the parallelism with the application of Ampère's law in solving for $\mathbf{B}$ (or $\mathbf{H}$) due to $\mathbf{J}$, discussed in Section 4.5, whenever possible.

Example 6.5 Induced Electric Field of an Infinite Solenoid

An infinitely long solenoid with a circular cross section of radius a has N' turns of wire per unit of its length. The solenoid is wound about a ferromagnetic core of permeability μ. A slowly time-varying current of intensity $i(t)$ flows through the winding. The medium outside the solenoid is air. The magnetic field due to currents induced in the core can be neglected. Find the induced electric field intensity vector inside and outside the solenoid.

Solution Because of symmetry, the lines of the induced electric field due to the current in the solenoid winding are circles centered at the solenoid axis. To show this, consider an arbitrary point P inside the solenoid, at a distance r from the solenoid axis (Fig. 6.9). Let $d\mathbf{E}'_{\text{ind}}$ and $d\mathbf{E}''_{\text{ind}}$ be the field intensity vectors at this point due to two symmetrical current elements denoted as $i\,d\mathbf{l}'$ and $i\,d\mathbf{l}''$ and shown in Fig. 6.9. In accordance to Eq. (6.5), these two vectors are such that their sum $d\mathbf{E}'_{\text{ind}} + d\mathbf{E}''_{\text{ind}}$ is tangential to the circular contour C of radius r centered at the solenoid axis. The same is true for any other pair of symmetrical current elements, which can also be in a plane that does not contain the point P. As all current elements constituting the current $i(t)$ in the winding can be grouped in such symmetrical pairs, we conclude that the resultant vector $\mathbf{E}_{\text{ind}}$ at the point P is tangential to the contour C. This same conclusion holds for a point outside the solenoid. In addition, $E_{\text{ind}} = \text{const}$ along C, i.e., the magnitude of $\mathbf{E}_{\text{ind}}$ depends only on the radial coordinate r of the cylindrical coordinate system whose z-axis is the solenoid axis. Hence,

$$\mathbf{E}_{\text{ind}} = E_{\text{ind}}(r, t)\,\hat{\boldsymbol{\phi}}, \tag{6.47}$$

where $\hat{\boldsymbol{\phi}}$ is the circular unit vector in the system.

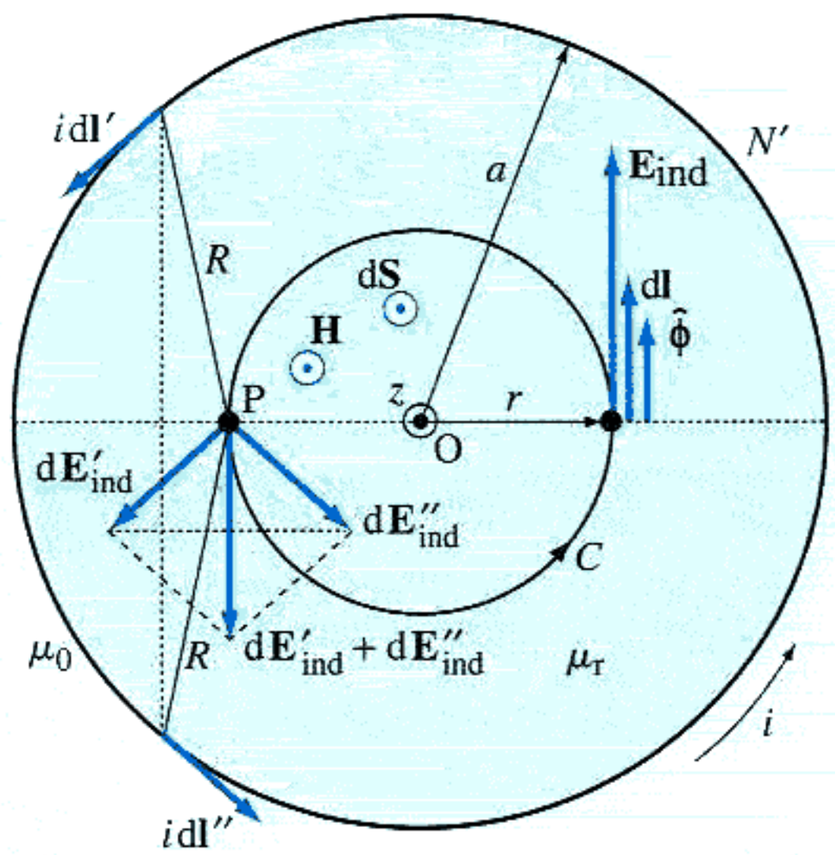

Figure 6.9 Evaluation of the induced electric field due to a slowly time-varying current in an infinite solenoid (cross-sectional view); for Example 6.5.

The magnetic field due to any spatial distribution of slowly time-varying currents has the same form as that due to the same spatial distribution of steady currents. Therefore, we can use the result of the analysis of a solenoid with a steady current of intensity I in the winding, performed in Example 4.13. This means that the magnetic field inside the solenoid is axial (field lines are parallel to the solenoid axis) and uniform, given by

$$\mathbf{H} = H(t)\,\hat{\mathbf{z}} = N' i(t)\,\hat{\mathbf{z}}, \tag{6.48}$$

while $\mathbf{H} = 0$ outside the solenoid. Note that this result does not take into account the magnetic field due to currents induced in the ferromagnetic core, which can be neglected.

We now use Faraday's law of electromagnetic induction, Eq. (6.35), and apply it to the contour C in Fig. 6.9 in a manner completely analogous to the application of Ampère's law in Eqs. (4.54)–(4.56). The circulation of $\mathbf{E}_{ind}$ along C equals

$$E_{ind}\,2\pi r = -\frac{d\Phi}{dt}. \tag{6.49}$$

The magnetic flux through the contour is

$$\Phi = \begin{cases} B\pi r^2 & \text{for } r \le a \\ B\pi a^2 & \text{for } r > a \end{cases} \tag{6.50}$$

(there is no flux outside the solenoid), where $B = \mu H$ and H is given in Eq. (6.48). The solutions for the induced electric field intensity inside and outside the solenoid come out to be

$$\boxed{E_{ind} = -\frac{\mu N' r}{2}\frac{di}{dt} \quad (r \le a) \quad \text{and} \quad E_{ind} = -\frac{\mu N' a^2}{2r}\frac{di}{dt} \quad (r > a),} \tag{6.51}$$

E_{ind} of an infinite solenoid

respectively.

We note that the magnetic field inside the solenoid varies synchronously with the current in the winding $[H(t) \propto i(t)]$, whereas the induced electric field varies synchronously with the time derivative of the current $[E_{ind}(t) \propto di(t)/dt]$.

Example 6.6 Inhomogeneous Conducting Loop around a Solenoid

Consider the solenoid from the previous example, and assume that a wire loop of radius b $(b > a)$ is placed coaxially around it, as shown in Fig. 6.10(a). The two halves of the loop are made from different materials, with conductivities σ_1 and σ_2. The cross-sectional area of both wire parts is S. The magnetic field due to currents induced in the core and in the wire

loop can be neglected. Calculate the voltage between the junctions of two wire parts (points M and N).

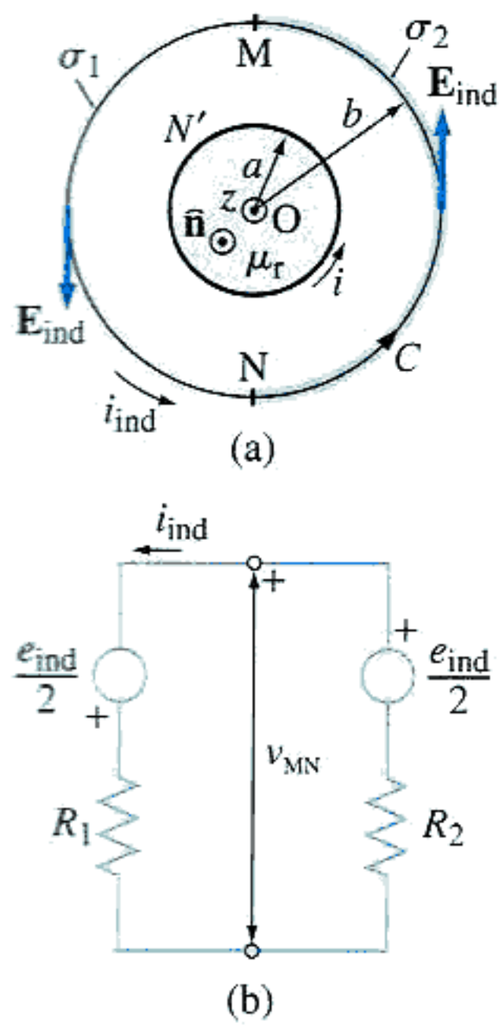

Figure 6.10 (a) Wire loop composed of two parts with different conductivities placed around an infinite solenoid carrying a slowly time-varying current and (b) equivalent circuit diagram; for Example 6.6.

Solution The system in Fig. 6.10(a) can be analyzed from the circuit-theory point of view, using the equivalent circuit diagram shown in Fig. 6.10(b), where e_{ind} is the induced emf in the contour C in Fig. 6.10(a), while R_1 and R_2 are resistances of the two wire parts constituting the contour. Having in mind the second expression in Eqs. (6.51), this emf amounts to

$$e_{\text{ind}} = -\frac{\mathrm{d}\Phi}{\mathrm{d}t} = -\pi\mu N' a^2 \frac{\mathrm{d}i}{\mathrm{d}t}. \tag{6.52}$$

Electromotive forces generated by the magnetic field due to the induced currents are neglected. By means of Eq. (3.85), the resistances are

$$R_1 = \frac{\pi b}{\sigma_1 S} \quad \text{and} \quad R_2 = \frac{\pi b}{\sigma_2 S}. \tag{6.53}$$

Employing Eq. (6.38), the current in the circuit, i.e., the induced current in the loop, is given by

$$i_{\text{ind}} = \frac{e_{\text{ind}}}{R_1 + R_2}. \tag{6.54}$$

Finally, the voltage between points M and N is obtained from Fig. 6.10(b) as

$$v_{\text{MN}} = R_1 i_{\text{ind}} - \frac{e_{\text{ind}}}{2} = \frac{R_1 - R_2}{2(R_1 + R_2)} e_{\text{ind}} = -\frac{\pi\mu(\sigma_2 - \sigma_1)N' a^2}{2(\sigma_1 + \sigma_2)} \frac{\mathrm{d}i}{\mathrm{d}t}. \tag{6.55}$$

Note that in the case of a homogeneous wire loop ($\sigma_1 = \sigma_2$), there is no voltage between different points along the loop.

Example 6.7 Magnetic Field due to Induced Current in a Loop

Refer to the system in Fig. 6.10(a), and assume that $i(t) = 2\cos 1000t$ A (t in s), $N' = 1000$ turns/m, $a = 10$ cm, $b = 20$ cm, $S = 1$ mm^2, $\sigma_1 = 57$ MS/m, $\sigma_2 = 15$ MS/m, and $\mu = \mu_0$ (air-filled solenoid). Under these circumstances, find the magnetic flux density vector at the loop center due to the induced current in the loop.

Solution Let us first check whether the current in the solenoid can be considered as slowly time-varying. Since the solenoid is infinitely long, this problem is actually a two-dimensional one, and the check of whether a low-frequency analysis is sufficiently accurate here should be performed in the cross section of the structure containing the wire loop. The maximum dimension of the structure relevant to the field computation in this cross section is $2b$, and the corresponding time of propagation of electromagnetic disturbances is $\tau = 2b/c_0 = 1.33$ ns. This time is much shorter than the period of change of $i(t)$, which equals $T = 2\pi/\omega = 6.28$ ms ($\omega = 1000$ rad/s). We conclude that this structure can indeed be analyzed as a low-frequency (quasistatic) problem. This means that we can use the results of the analysis of the structure performed in the previous example.

From Eq. (6.54), the induced current intensity in the loop is

$$i_{\text{ind}}(t) = -\frac{\mu_0\sigma_1\sigma_2 N' a^2 S}{(\sigma_1 + \sigma_2)b} \frac{\mathrm{d}i}{\mathrm{d}t} = 1.5 \sin 1000t \text{ A}. \tag{6.56}$$

The magnetic flux density vector due to this current at the center of the loop is obtained using Eq. (4.19) for the field point defined by $z = 0$ and the contour radius b:

$$\mathbf{B}_{\text{ind}}(t) = \frac{\mu_0 i_{\text{ind}}(t)}{2b} \hat{\mathbf{z}} = 4.7 \sin 1000t\, \hat{\mathbf{z}}\ \mu\text{T}. \tag{6.57}$$

Let us finally compare the field $\mathbf{B}_{\text{ind}}(t)$ to the primary magnetic field – that due to the current $i(t)$ in the solenoid winding. By means of Eq. (6.48), the flux density vector of the primary field inside the solenoid is

$$\mathbf{B}(t) = \mu_0 N' i(t)\, \hat{\mathbf{z}} = 2.5 \cos 1000t\, \hat{\mathbf{z}} \text{ mT}. \tag{6.58}$$

We see that $|\mathbf{B}_{\text{ind}}(t)|/|\mathbf{B}(t)| = 1.9 \times 10^{-3}$, i.e.,

$$|\mathbf{B}_{\text{ind}}(t)| \ll |\mathbf{B}(t)|. \tag{6.59}$$

In other words, the magnetic field due to the induced current in the loop is absolutely negligible with respect to the magnetic field of the solenoid, which caused the induced current in the first place. We also note that the waveforms of these two fields ($\sin 1000t$ and $\cos 1000t$) are such that $\mathbf{B}_{\text{ind}}(t)$ tends to compensate for the change in $\mathbf{B}(t)$, i.e., it opposes the action that actually created it. Of course, this is in accordance with Lenz's law.

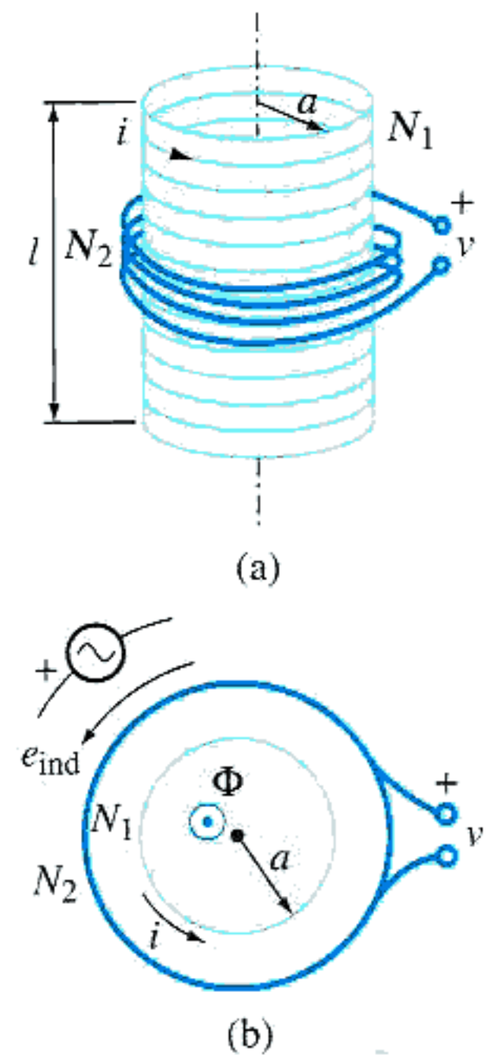

Figure 6.11 An open-circuited short coil placed around a very long solenoid carrying a low-frequency current: (a) three-dimensional view showing the windings and (b) cross-sectional view showing reference directions for the emf and voltage; for Example 6.8.

Example 6.8 Open-Circuited Coil around a Solenoid

An air-filled solenoid of length $l = 2$ m and circular cross section of radius $a = 10$ cm has $N_1 = 1750$ turns of wire. There is a low-frequency time-harmonic current of intensity $i(t) = I_0 \sin \omega t$ flowing through the winding, where $I_0 = 10$ A and $\omega = 10^6$ rad/s. An open-circuited short coil with $N_2 = 10$ turns of wire is placed around the solenoid, as shown in Fig. 6.11(a). Compute the voltage between the terminals of the coil.

Solution The solenoid is very long ($l \gg a$), so that the end effects can be neglected while computing the magnetic field about its center. This means that the solenoid can be considered as infinitely long while computing the magnetic flux through the short coil in Fig. 6.11(a). As the coil consists of N_2 wire turns, this flux is given by

$$\Phi = N_2 \Phi_{\text{single turn}}, \tag{6.60}$$

where $\Phi_{\text{single turn}}$ is the flux through a surface spanned over any of the turns. In other words, the electromotive forces induced in individual turns all add in series, and hence the total emf in the coil is N_2 times that in Eq. (6.52) with $\mu = \mu_0$ and $N' = N_1/l$, which results in

$$e_{\text{ind}} = -N_2 \frac{\mathrm{d}\Phi_{\text{single turn}}}{\mathrm{d}t} = -\frac{\pi \mu_0 N_1 N_2 a^2}{l} \frac{\mathrm{d}i}{\mathrm{d}t} = -\frac{\pi \omega \mu_0 N_1 N_2 a^2 I_0}{l} \cos \omega t. \tag{6.61}$$

There is no current in the coil, because it is open-circuited, so that the voltage across the coil terminals is [Fig. 6.11(b)]

$$v(t) = -e_{\text{ind}}(t) = \frac{\pi \omega \mu_0 N_1 N_2 a^2 I_0}{l} \cos \omega t = 3.45 \cos 10^6 t \text{ kV} \quad (t \text{ in s}). \tag{6.62}$$

Example 6.9 Rectangular Contour near an Infinite Line Current

An infinitely long straight wire carries a slowly time-varying current of intensity $i(t)$. A rectangular contour of side lengths a and b lies in the same plane with the wire, with two sides parallel to it, as shown in Fig. 6.12. The distance between the wire and the closer parallel side of the contour is c. Determine the emf induced in the contour.

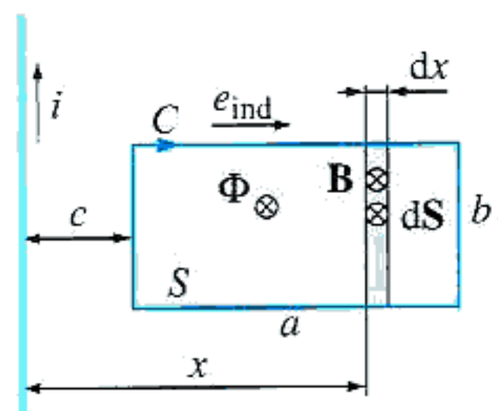

Figure 6.12 Evaluation of the emf in a rectangular contour in the vicinity of an infinitely long wire with a slowly time-varying current; for Example 6.9.

Solution The magnetic flux density vector produced by the current in the wire at any point in the plane of the contour is perpendicular to the plane and at a distance x from the wire (Fig. 6.12) and an instant t, its magnitude is [see Eq. (4.22)]

$$B(x, t) = \frac{\mu_0 i(t)}{2\pi x}. \tag{6.63}$$

By integrating this density across the flat surface spanned over the contour, we obtain the magnetic flux through the contour:

$$\Phi(t) = \int_{x=c}^{c+a} B(x, t) \underbrace{b\,\mathrm{d}x}_{\mathrm{d}S} = \frac{\mu_0 i(t) b}{2\pi} \int_c^{c+a} \frac{\mathrm{d}x}{x} = \frac{\mu_0 i(t) b}{2\pi} \ln \frac{c+a}{c}, \tag{6.64}$$

where $\mathrm{d}S$ is the surface area of a thin strip of length b and width $\mathrm{d}x$ in Fig. 6.12, and the flux is determined with respect to the reference direction into the plane of drawing (note that this integration is similar to that in Fig. 5.26).

For the adopted direction of the flux, the right-hand rule gives the clockwise reference direction for the induced emf in the contour, with respect to which,

$$e_{\text{ind}}(t) = -\frac{\mathrm{d}\Phi}{\mathrm{d}t} = -\frac{\mu_0 b}{2\pi} \ln \frac{c+a}{c} \frac{\mathrm{d}i}{\mathrm{d}t}. \tag{6.65}$$

Example 6.10 **Induced Emf in a Coil with a Nonlinear Core**

A coil with $N = 400$ turns of wire is wound uniformly and densely about a thin toroidal core of length $l = 40$ cm and cross-sectional area $S = 1$ cm^2, as shown in Fig. 6.13(a). A slowly time-varying current whose intensity, $i(t)$, is a periodic alternating triangular-pulse function sketched in Fig. 6.13(b) is established in the coil, where $I_0 = 0.1$ A and $T = 1$ ms. The core is made of a nonlinear ferromagnetic material that exhibits hysteresis effects. In steady state, the operating point (B, H) periodically circumscribes a hysteresis loop that can approximately be represented as in Fig. 6.13(c), where $B_\text{m}/H_\text{m} = \mu_\text{h} = 0.001$ H/m. The resistance of the coil can be neglected. Find the voltage across the coil terminals in the time interval $0 \le t \le T$.

Solution The magnetic field intensity in the core varies synchronously with the current in the winding $[H(t) \propto i(t)]$ and is given by

$$H(t) = \frac{Ni(t)}{l} \tag{6.66}$$

[see Eq. (5.53)]. The function $H(t)$ is plotted in Fig. 6.13(d), where $H_\text{m} = NI_0/l = 100$ A/m.

From the hysteresis loop in Fig. 6.13(c), we conclude that the magnetic flux density in the core, $B(t)$, first varies as a linear function of time from $B = -B_\text{m}$ (for $H = 0$) to $B = B_\text{m}$ (for $H = H_\text{m}$), then becomes time-invariant while H is reduced from $H = H_\text{m}$ to $H = 0$, afterwards it is again a linear (now decaying) function of time when $H(t)$ is reversed and increased in the negative direction from $H = 0$ to $H = -H_\text{m}$, and so on. The amplitude of

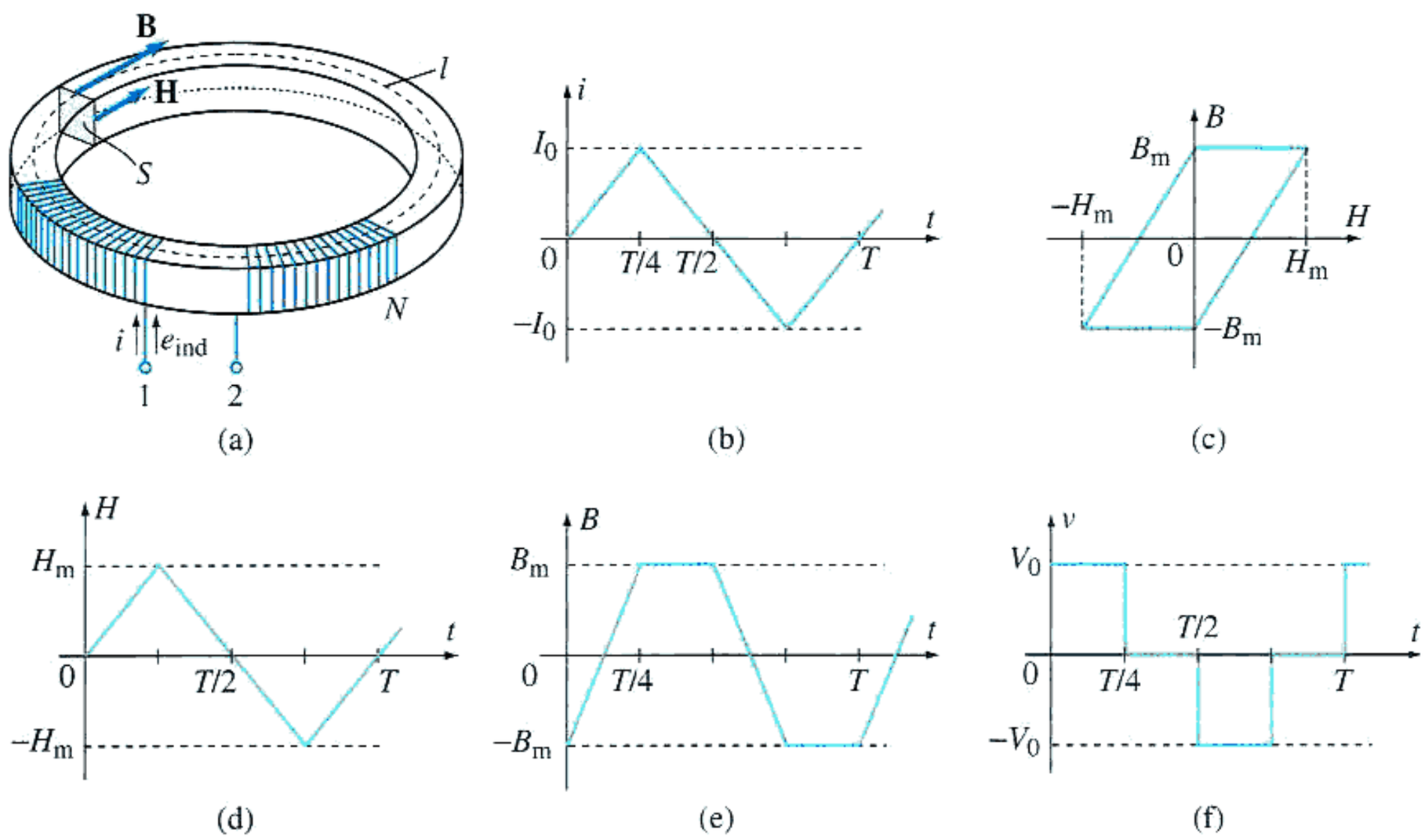

Figure 6.13 Analysis of electromagnetic induction in a coil with a core made from a nonlinear ferromagnetic material (note that $v = v_{12}$); for Example 6.10.

the periodic trapezoidal-pulse waveform of B is $B_m = \mu_h H_m = 0.1$ T, and $B(t)$ is plotted in Fig. 6.13(e).

The magnetic flux through the coil is $\Phi(t) = NB(t)S$ and the induced emf in the coil, $e_{ind}(t)$, is given by Faraday's law of electromagnetic induction, Eq. (6.34). As the resistance of the coil is negligible, the voltage across the coil terminals is

$$v(t) = v_{12}(t) = -e_{ind}(t) = \frac{d\Phi(t)}{dt} = NS\frac{dB(t)}{dt}. \tag{6.67}$$

This function is proportional to the slope of the function $B(t)$ and is plotted in Fig. 6.13(f). It is a periodic alternating rectangular-pulse function with the same period (T). The pulse amplitude is proportional to the slope of $B(t)$ in the first quarter of the period, that is, $V_0 = NS(2B_m)/(T/4) = 8NSB_m/T = 32$ V.

We see that the induced emf and voltage of the coil do not vary synchronously with the time derivative of its current, which is a consequence of the nonlinearity and hysteresis behavior of the core material.

Problems: 6.11–6.17; *Conceptual Questions* (on Companion Website): 6.9–6.16; *MATLAB Exercises* (on Companion Website).

6.6 ELECTROMAGNETIC INDUCTION DUE TO MOTION

Consider a conductor moving with a velocity $\mathbf{v}$ in a static (time-invariant) magnetic field of the flux density $\mathbf{B}$. The field exerts the magnetic Lorentz force, $\mathbf{F}_m$, given by Eq. (4.144), on each of the charge carriers in the conductor. This force "pushes" the carriers to move, and separates positive and negative excess charges in the conductor. We can formally divide $\mathbf{F}_m$ by the charge of a carrier and obtain $\mathbf{F}_m/Q = \mathbf{v} \times \mathbf{B}$. This new quantity, although expressed in V/m, is not a true electric field intensity vector, because it is not produced by an excess charge [Eq. (6.18)] or by a time-varying current [Eq. (6.2)]. By definition given by Eq. (3.107), it represents an impressed electric field intensity vector, which we term here the induced electric field intensity vector due to motion, and write

$$\boxed{\mathbf{E}_{ind} = \mathbf{v} \times \mathbf{B}.} \tag{6.68}$$

induced electric field intensity vector due to motion (unit: V/m)

This field generates an induced electromotive force, as given by Eq. (6.32). Hence, the emf along a line through a conductor between points M and N (Fig. 6.6) due to motion in a time-invariant magnetic field is

$$e_{ind} = \int_M^N \mathbf{E}_{ind} \cdot d\mathbf{l} = \int_M^N (\mathbf{v} \times \mathbf{B}) \cdot d\mathbf{l}. \tag{6.69}$$

This emf is referred to as the emf due to motional induction or simply motional emf. For a moving contour (closed line),

$$\boxed{e_{ind} = \oint_C (\mathbf{v} \times \mathbf{B}) \cdot d\mathbf{l}.} \tag{6.70}$$

motional emf (unit: V)

Note that the velocity of different parts of the contour need not be the same, including cases when some parts are stationary while other move in arbitrary directions. In other words, the motion of the contour may include translation, rotation, and deformation (changing shape and size) of the contour in an arbitrary manner.

When a contour moves and/or changes in a static magnetic field, the magnetic flux through the contour changes with time. It is possible to relate the total

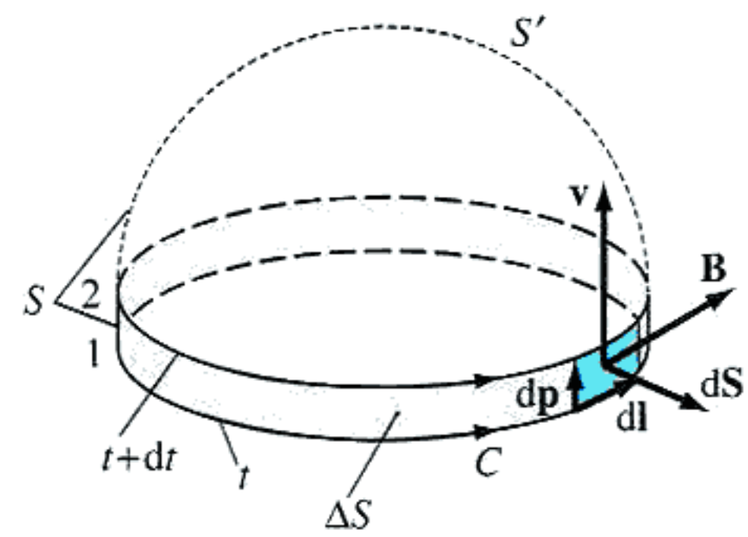

Figure 6.14 A contour moving in a time-invariant magnetic field.

emf induced in the contour to the rate of change of the flux, i.e., to express the motional emf in terms of Faraday's concept of changing flux through the contour, as in Eq. (6.34). To see this, consider the moving contour C in Fig. 6.14. Let $\mathbf{v}$ be the velocity of an element $\mathrm{d}\mathbf{l}$ of the contour. In a time interval $\mathrm{d}t$, this element moves a distance $\mathrm{d}\mathbf{p} = \mathbf{v}\,\mathrm{d}t$ (see Fig. 6.14). Eq. (6.70) thus becomes

$$e_{\text{ind}} = \oint_C (\mathbf{v} \times \mathbf{B}) \cdot \mathrm{d}\mathbf{l} = \frac{1}{\mathrm{d}t} \oint_C (\mathrm{d}\mathbf{p} \times \mathbf{B}) \cdot \mathrm{d}\mathbf{l}. \tag{6.71}$$

Applying the identity $(\mathbf{a} \times \mathbf{b}) \cdot \mathbf{c} = (\mathbf{c} \times \mathbf{a}) \cdot \mathbf{b}$ (scalar triple product is unaffected by cyclic permutation of the order of vectors) to the scalar triple product $(\mathrm{d}\mathbf{p} \times \mathbf{B}) \cdot \mathrm{d}\mathbf{l}$ and noting that $\mathrm{d}\mathbf{l} \times \mathrm{d}\mathbf{p}$ equals the vector surface element $\mathrm{d}\mathbf{S}$ shown in Fig. 6.14, we have

$$e_{\text{ind}} = \frac{1}{\mathrm{d}t} \oint_C \mathbf{B} \cdot (\mathrm{d}\mathbf{l} \times \mathrm{d}\mathbf{p}) = \frac{1}{\mathrm{d}t} \oint_C \mathbf{B} \cdot \mathrm{d}\mathbf{S}. \tag{6.72}$$

This last integral represents the magnetic flux through the strip ΔS swept out by the contour C during the interval $\mathrm{d}t$ (tinted strip between the positions 1 and 2 of the contour in Fig. 6.14). Let us mark this flux by $\mathrm{d}\Phi_{\text{through } \Delta S}$, so that

$$e_{\text{ind}} = \frac{\mathrm{d}\Phi_{\text{through } \Delta S}}{\mathrm{d}t}. \tag{6.73}$$

The strip ΔS represents the difference in area between the surface S bounded by the contour in position 1 (at instant t) and the surface S' bounded by the contour in position 2 (at instant $t + \mathrm{d}t$), as

$$S = S' \cup \Delta S. \tag{6.74}$$

Designating the magnetic flux through S and S' by Φ and Φ', respectively, the increment in flux from t to $t + \mathrm{d}t$ equals

$$\mathrm{d}\Phi = \Phi' - \Phi, \tag{6.75}$$

and this is exactly the negative of the flux through the strip ΔS, i.e., $\mathrm{d}\Phi = -\mathrm{d}\Phi_{\text{through } \Delta S}$. Finally, substituting this equation in Eq. (6.73) leads to $e_{\text{ind}} = -\mathrm{d}\Phi/\mathrm{d}t$, which is the same as in Eq. (6.34). We conclude that the same form of Faraday's law of electromagnetic induction holds for both transformer and motional emf in a contour.

Example 6.11 Moving Metallic Bar in a Static Magnetic Field

A metallic bar of length $a = 2$ m slides without friction at a constant velocity over parallel metallic rails, as shown in Fig. 6.15. The bar is perpendicular to the rails and the

mechanical force acting on the bar is $F_{\text{mech}} = 4$ N. The whole system is situated in a uniform time-invariant magnetic field of flux density $B = 1$ T. The field lines are perpendicular to the plane of the rails and directed out of the page. A load of resistance $R = 5\ \Omega$ is connected between the rails. The losses in the bar and in the rails, as well as the magnetic field due to induced currents in the system, can be neglected. (a) Find the velocity of the bar. (b) Evaluate the power of Joule's losses in the load and discuss the energy balance in this system.

Solution

(a) The bar moves in a static magnetic field and the emf is induced in it due to motional induction. Since the bar is straight and the field is uniform (i.e, the same everywhere), the expression for the motional emf in Eq. (6.69) becomes

$$\boxed{e_{\text{ind}} = (\mathbf{v} \times \mathbf{B}) \cdot \mathbf{l},} \tag{6.76}$$

emf in a straight conductor moving in a uniform magnetic field

where the emf is directed from point M to point N along the bar (Fig. 6.15), $\mathbf{l} = \overrightarrow{\text{MN}}$, and $\mathbf{v}$ is the velocity of the bar (which is to be determined). Moreover, since the vectors $\mathbf{v}$, $\mathbf{B}$, and $\mathbf{l}$ are all orthogonal with respect to each other and $|\mathbf{l}| = a$, we can write

$$e_{\text{ind}} = vBa. \tag{6.77}$$

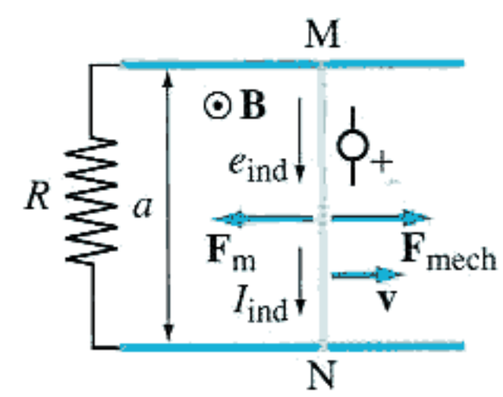

Figure 6.15 A metallic bar moving in a uniform time-invariant magnetic field (elementary electric generator); for Example 6.11.

The bar and the rails constitute a conducting loop, that is, an electric circuit of the form shown in Fig. 6.8. Hence, there will be a time-invariant induced current in the loop of intensity

$$I_{\text{ind}} = \frac{e_{\text{ind}}}{R} = \frac{vBa}{R} \tag{6.78}$$

[see Eq. (6.38)], given with respect to the same reference direction as the emf, where we neglect the resistance of the bar and the rails and the corresponding Joule's losses. The current I_{ind}, on the other hand, produces a secondary magnetic field, which is neglected in evaluating the emf in Eq. (6.76). Note that this field opposes the increasing flux of the primary field $\mathbf{B}$ through the loop, the area of which expands as the bar moves to the right, as yet another example of Lenz's law.

We know that, in the presence of a magnetic field, a current-carrying conductor experiences a magnetic force. From Eq. (4.163), the magnetic force on the metallic bar in Fig. 6.15 comes out to be

$$\mathbf{F}_{\text{m}} = I_{\text{ind}}\mathbf{l} \times \mathbf{B} \quad \longrightarrow \quad F_{\text{m}} = I_{\text{ind}}aB. \tag{6.79}$$

This force opposes the motion of the bar and the generation of the emf in it, which again is in accordance with Lenz's law. In other words, $\mathbf{F}_{\text{m}}$ is directed oppositely to the mechanical force $\mathbf{F}_{\text{mech}}$ on the bar. Furthermore, as the velocity of the bar is constant, these two forces must be exactly equal in magnitude (Newton's second law), that is,

$$F_{\text{mech}} = F_{\text{m}} = \frac{vB^2a^2}{R} \qquad (v = \text{const}). \tag{6.80}$$

Hence, the velocity we seek is

$$v = \frac{F_{\text{mech}}R}{a^2B^2} = 5 \text{ m/s}. \tag{6.81}$$

Eqs. (6.77) and (6.78) now give the values for the induced emf and current in the loop: $e_{\text{ind}} = 10$ V and $I_{\text{ind}} = 2$ A.

(b) By Joule's law, Eq. (3.77), the power of Joule's losses in the load resistor is

$$P_{\text{J}} = RI_{\text{ind}}^2 = 20 \text{ W}. \tag{6.82}$$

Note that, on the other side, the power generated by the induced emf in the bar, i.e., the power of the equivalent ideal voltage generator of emf e_{ind} in Fig. 6.8, equals

$$P_{\text{ind}} = e_{\text{ind}}I_{\text{ind}} = 20 \text{ W} \tag{6.83}$$

[see Eq. (3.121)]. Finally, the mechanical power used to move the bar at the velocity v is obtained as

$$P_{\text{mech}} = F_{\text{mech}} v = 20 \text{ W}. \tag{6.84}$$

We see that, as expected,

$$P_{\text{mech}} = P_{\text{ind}} = P_{\text{J}}, \tag{6.85}$$

which is in compliance with the principle of conservation of energy. The system in Fig. 6.15 is a simple example of an electric generator based on electromagnetic induction, where the applied mechanical energy is converted into the electric energy and delivered to the load. The agent by which the energy transfer is carried out is the induced emf in the moving bar, and the energy of this emf is ultimately dissipated to heat in the resistor.

Example 6.12 Rotating Wire Loop in a Static Magnetic Field

A rectangular wire loop of edge lengths a and b rotates with a constant angular velocity ω about its axis in a uniform time-invariant magnetic field of flux density B, as depicted in Fig. 6.16(a). The vector $\mathbf{B}$ is perpendicular to the plane of drawing and is directed out of the page. At an instant $t = 0$, the loop lies in the plane of drawing. The resistance of the loop is R. The magnetic field due to induced currents can be neglected. Calculate (a) the induced emf in the loop and (b) the instantaneous and time-average mechanical power of loop rotation.

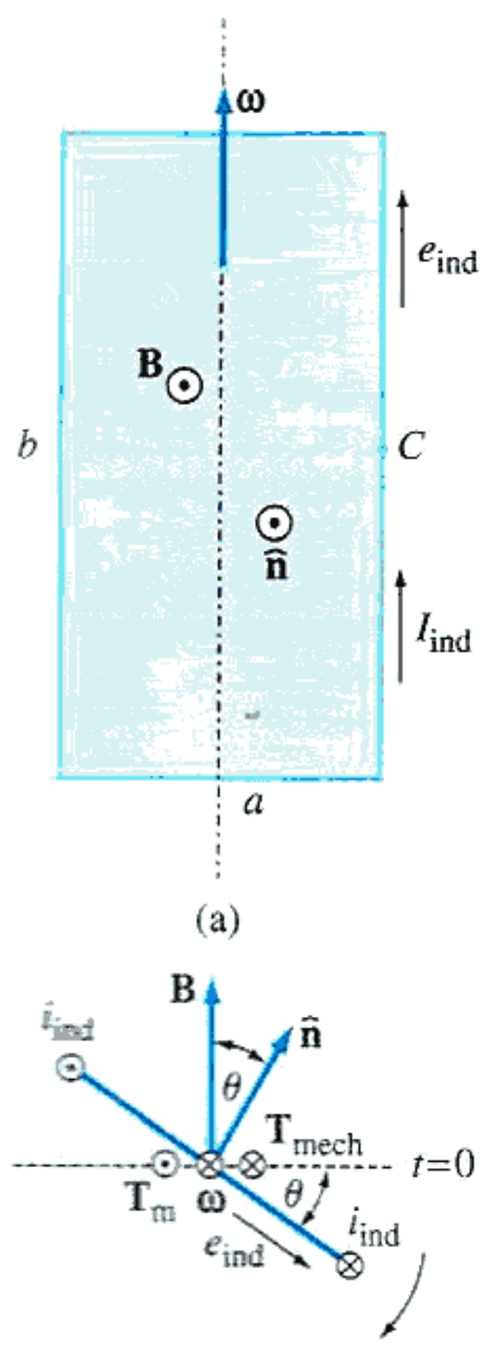

Figure 6.16 A wire loop rotating in a uniform time-invariant magnetic field (elementary ac generator): (a) top view at an instant $t = 0$ and (b) cross-sectional view at an arbitrary instant t; for Example 6.12.

Solution

(a) Referring to Fig. 6.16(b), the magnetic flux through the loop is

$$\Phi = \mathbf{B} \cdot \mathbf{S} = \mathbf{B} \cdot ab\hat{\mathbf{n}} = abB \cos\theta, \tag{6.86}$$

where θ is the angle between the plane of the loop at an instant t and the plane perpendicular to the vector $\mathbf{B}$. From the definition of angular velocity,

$$\frac{d\theta}{dt} = \omega. \tag{6.87}$$

Since $\omega = \text{const}$, the solution for θ is

$$\theta(t) = \theta_0 + \omega t, \tag{6.88}$$

where $\theta_0 = 0$ ($\theta = 0$ for $t = 0$). Thus,

$$\Phi(t) = abB \cos\omega t, \tag{6.89}$$

which, substituted in Eq. (6.34), leads to the following expression for the induced motional emf in the loop:

$$e_{\text{ind}}(t) = -\frac{d\Phi}{dt} = \omega abB \sin\omega t. \tag{6.90}$$

(b) The current intensity in the loop amounts to

$$i_{\text{ind}}(t) = \frac{e_{\text{ind}}}{R} = \frac{\omega abB}{R} \sin\omega t. \tag{6.91}$$

The magnetic field due to this current is neglected in the computation of the emf in Eq. (6.90).

From Fig. 4.38 and Eq. (4.181), the instantaneous torque of magnetic forces acting on the loop is given by

$$T_{\text{m}}(t) = i_{\text{ind}} abB \sin\theta = \frac{\omega a^2 b^2 B^2}{R} \sin^2 \omega t. \tag{6.92}$$

Eq. (4.180) tells us that the direction of this torque is such that it opposes the rotation of the loop (Lenz's law), i.e., it is opposite to the direction of an externally applied mechanical torque, $\mathbf{T}_{\text{mech}}$, that rotates the loop. In order to sustain the rotation at a constant rate,

$\mathbf{T}_{\text{mech}}$ must be exactly equal in magnitude to $\mathbf{T}_{\text{m}}$ (Newton's second law in angular form). Hence, the instantaneous mechanical power used to rotate the loop is

$$P_{\text{mech}}(t) = T_{\text{mech}}\omega = T_{\text{m}}\omega = \frac{\omega^2 a^2 b^2 B^2}{R} \sin^2 \omega t. \tag{6.93}$$

The same result can also be obtained from energy conservation, as the mechanical power of loop rotation equals the electric power of the circuit, i.e., the power of Joule's losses dissipated in the loop [as in Eq. (6.85)]. This yields

$$P_{\text{mech}}(t) = P_{\text{J}}(t) = R i_{\text{ind}}^2 = \frac{\omega^2 a^2 b^2 B^2}{R} \sin^2 \omega t. \tag{6.94}$$

Given that the time-average value of the function $\sin^2 \omega t$ is

$$\frac{1}{T}\int_0^T \sin^2 \omega t \, \mathrm{d}t = \frac{1}{T}\int_0^T \frac{1-\cos 2\omega t}{2} \, \mathrm{d}t = \frac{1}{2T}\left(\int_0^T \mathrm{d}t - \int_0^T \cos 2\omega t \, \mathrm{d}t\right) = \frac{1}{2}, \tag{6.95}$$

where $T = 2\pi/\omega$ is the period of time-harmonic variation of the emf and current in the loop, the time-average mechanical power of loop rotation equals

$$(P_{\text{mech}})_{\text{ave}} = \frac{\omega^2 a^2 b^2 B^2}{2R}. \tag{6.96}$$

Note that the system in Fig. 6.16 represents a rotational version of the generator based on translational motion in a static magnetic field in Fig. 6.15. It illustrates the basic principle of an alternating current (ac) generator, where the loop is mechanically rotated in a static magnetic field at a constant rate and the emf and current are induced in the loop of a sinusoidal (time-harmonic) waveform. The angular frequency of this waveform equals the angular velocity ω of the loop rotation.

Example 6.13 Moving Contour near an Infinite dc Line Current

Assume that the current in the straight wire conductor from Fig. 6.12 is time-invariant, with intensity I, and that the contour moves away from the wire at a constant velocity v, as shown in Fig. 6.17. At $t = 0$, the distance of the closer parallel side of the contour from the wire is $x = c$. Determine the emf induced in the contour.

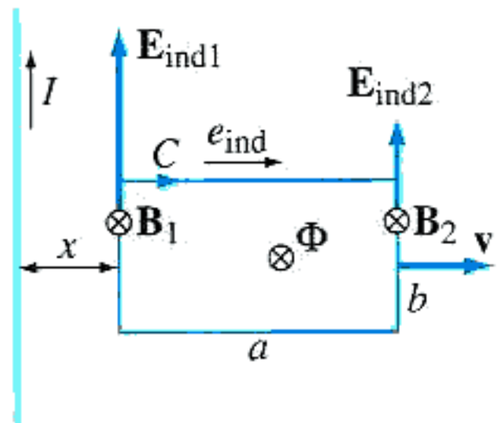

Figure 6.17 Evaluation of the emf in a rectangular contour moving in the magnetic field due to an infinitely long wire with a steady current; for Example 6.13.

Solution The magnetic field produced by the current in the wire is time-invariant, and the system in Fig. 6.17 represents a motional induction version of the same geometry with transformer induction in Fig. 6.12. The magnetic field is nonuniform (magnetic flux density changes in space), and that is why the magnetic flux through the contour is time-varying. As the contour moves uniformly away from the wire, the distance of its closer parallel side from the wire increases linearly in the course of time, and is given by

$$x(t) = c + vt. \tag{6.97}$$

The magnetic flux density vector around the wire has the same spatial distribution as in Fig. 6.12, so that the magnetic flux through the contour has the same form as in Eq. (6.64), with $i(t)$ substituted by I and c by $x(t)$:

$$\Phi(t) = \frac{\mu_0 I b}{2\pi} \ln \frac{x+a}{x} = \frac{\mu_0 I b}{2\pi} \ln \frac{c+a+vt}{c+vt}. \tag{6.98}$$

From Eq. (6.34), the motional emf induced in the contour, given with respect to the clockwise reference direction (Fig. 6.17), is

$$e_{\text{ind}}(t) = -\frac{\mathrm{d}\Phi}{\mathrm{d}t} = -\frac{\mathrm{d}\Phi}{\mathrm{d}x}\frac{\mathrm{d}x}{\mathrm{d}t} = -\frac{\mathrm{d}\Phi}{\mathrm{d}x} v = \frac{\mu_0 I a b v}{2\pi} \frac{1}{x(x+a)} = \frac{\mu_0 I a b v}{2\pi (c+vt)(c+a+vt)}. \tag{6.99}$$

The emf in the contour can also be computed using Eq. (6.70). Note that the induced electric field intensity vector $\mathbf{E}_{\text{ind}}$ due to motion, given by Eq. (6.68), is perpendicular to the

pair of contour edges of length a, and hence there is no emf in these edges. On the other hand, $\mathbf{E}_{\text{ind}}$ does not change along each of the remaining two contour edges, which are parallel to it. Its magnitude along the left and right edges in Fig. 6.17 equals

$$E_{\text{ind1}} = vB_1 = \frac{\mu_0 I v}{2\pi x} \quad \text{and} \quad E_{\text{ind2}} = vB_2 = \frac{\mu_0 I v}{2\pi (x+a)}, \tag{6.100}$$

respectively, where B_1 and B_2 are the corresponding magnetic flux densities. Finally, the total emf in the contour is obtained as

$$e_{\text{ind}} = \oint_C \mathbf{E}_{\text{ind}} \cdot d\mathbf{l} = E_{\text{ind1}} b - E_{\text{ind2}} b = \frac{\mu_0 I b v}{2\pi} \left(\frac{1}{x} - \frac{1}{x+a} \right), \tag{6.101}$$

which is the same result as in Eq. (6.99).

Example 6.14 Conducting Fluid Flow in a Static Magnetic Field

Fig. 6.18 shows a system for measurement of fluid velocity that consists of a parallel-plate capacitor situated in a uniform time-invariant magnetic field. A liquid flows between the capacitor plates and the voltage between the plates is measured by a voltmeter. The velocity of the fluid can be considered to be uniform. The magnetic field lines are parallel to the plates. The conductivity and permeability of the liquid are σ and μ_0, respectively. The capacitor plate area is S and the separation between plates is d. Fringing effects in the capacitor can be neglected. The flux density of the applied magnetic field is B. The internal resistance of the voltmeter is R_V, while the resistance of the interconnecting conductors is negligible. Show that the velocity of the fluid is linearly proportional to the voltage V indicated by the voltmeter and find the proportionality constant.

Solution We have a motion (flow) of the conducting liquid (with an unknown velocity $\mathbf{v}$) in the static magnetic field, and therefore an electric field due to motion is induced, given by Eq. (6.68). Vectors $\mathbf{v}$ and $\mathbf{B}$ are mutually orthogonal (Fig. 6.18), and we can write

$$E_{\text{ind}} = vB. \tag{6.102}$$

This field forces the charge carriers in the liquid to move perpendicularly to the direction of the liquid flow, so that positive and negative excess charges are accumulated on the lower and upper capacitor plates, respectively. These charges produce a Coulomb field $\mathbf{E}_q$ (field due to excess charge), which is perpendicular to the plates and practically uniform in the space between them.

Since the voltmeter is not ideal, i.e., its internal resistance is not infinite, there is a steady current flowing through its terminals. By the continuity equation for steady currents, this current continues with the current of the same intensity through the conducting liquid, that is,

$$I_V = I_{\text{liquid}} = JS, \tag{6.103}$$

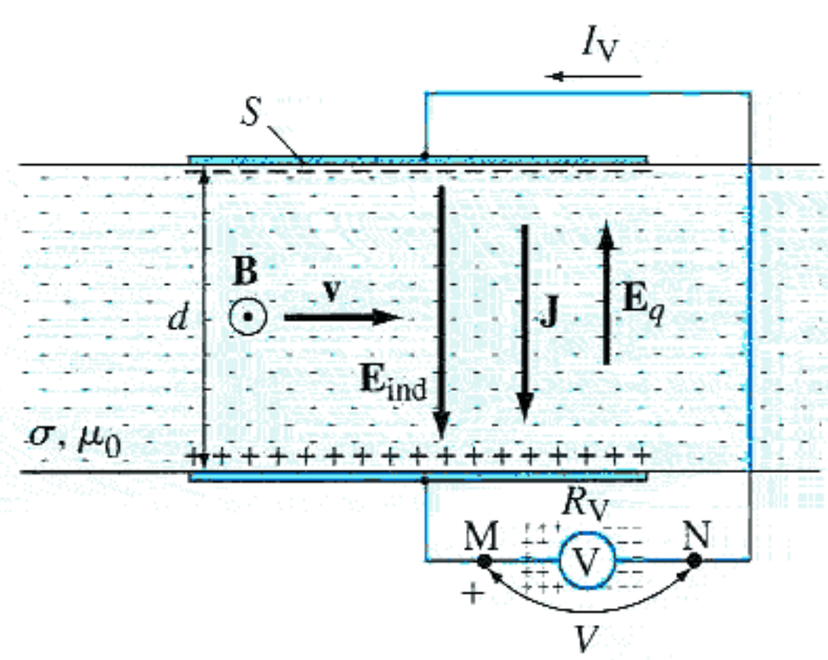

Figure 6.18 Measurement of fluid velocity based on motional electromagnetic induction; for Example 6.14.

with J standing for the current density in the liquid. This current density, in turn, can be expressed in terms of the total electric field in the liquid, given by Eq. (6.16), as follows:

$$\mathbf{J} = \sigma \mathbf{E} = \sigma(\mathbf{E}_q + \mathbf{E}_{\text{ind}}) \quad \longrightarrow \quad J = \sigma(E_{\text{ind}} - E_q), \tag{6.104}$$

where the scalar form of the equation is obtained for the reference directions of vectors $\mathbf{J}$, $\mathbf{E}_{\text{ind}}$, and $\mathbf{E}_q$ adopted in Fig. 6.18.

The voltage that the voltmeter indicates equals the potential difference between its terminals (M and N):

$$V = V_{\text{M}} - V_{\text{N}}, \tag{6.105}$$

which, if evaluated using Eq. (6.22) along a (straight) path through the liquid, can also be expressed as

$$V_{\text{M}} - V_{\text{N}} = E_q d \tag{6.106}$$

(the interconnecting conductors in the voltmeter circuit are ideal, and thus equipotential). Finally, Ohm's law gives

$$V = R_{\text{V}} I_{\text{V}} = R_{\text{V}} J S = R_{\text{V}} S \sigma (E_{\text{ind}} - E_q) = R_{\text{V}} S \sigma \left(vB - \frac{V}{d} \right), \tag{6.107}$$

from which the solution for the velocity of liquid flow turns out to be

$$v = \frac{\sigma S R_{\text{V}} + d}{\sigma S d R_{\text{V}} B} V. \tag{6.108}$$

We see that, indeed, v is linearly proportional to V, where the proportionality constant depends on the parameters of the system in Fig. 6.18 and the conductivity of the fluid.

Problems: 6.18–6.28; *Conceptual Questions* (on Companion Website): 6.17–6.22; *MATLAB Exercises* (on Companion Website).

6.7 TOTAL ELECTROMAGNETIC INDUCTION

Consider now the most general case of electromagnetic induction – that of a moving conductor in a time-varying magnetic field. This is the case where both sources of the induced electric field, namely, the magnetic field change and conductor motion, act simultaneously. Hence, the induced electromotive force in a contour that is moved and/or deformed in a magnetic field that itself varies with time is the sum of the transformer emf, Eq. (6.37), and the motional emf, Eq. (6.70). We thus write

$$e_{\text{ind}} = \underbrace{-\int_S \frac{\partial \mathbf{B}}{\partial t} \cdot d\mathbf{S}}_{\text{transformer emf}} + \underbrace{\oint_C (\mathbf{v} \times \mathbf{B}) \cdot d\mathbf{l}}_{\text{motional emf}}, \tag{6.109}$$

and call e_{ind} here the total (transformer plus motional) or complex (combined) emf in the contour.

The motional emf term of Eq. (6.109) can be transformed as described by Eqs. (6.71)–(6.75) and Fig. 6.14, so that the total emf in the contour can be expressed as $e_{\text{ind}} = -\,d\Phi/dt$ [same as in Eq. (6.34)], or

$$\boxed{e_{\text{ind}} = \oint_C \mathbf{E}_{\text{ind}} \cdot d\mathbf{l} = -\frac{d}{dt} \int_S \mathbf{B} \cdot d\mathbf{S}.} \tag{6.110}$$ *total induction*

This last expression on the right-hand side of the equation represents the total derivative of the magnetic flux through the contour with respect to time, where

the change in flux with time is partly due to a change in the magnetic field and partly due to a change in the shape, orientation, and/or position of the contour. These two parts of the flux change correspond to the transformer and motional emf terms of Eq. (6.109).[8] It appears, however, that Eq. (6.34) is the most general form of Faraday's law of electromagnetic induction, which includes both mechanisms by which the magnetic flux through a contour could change. These two mechanisms are the magnetic field variation and contour motion, and except for them, there are no other possibilities that may result in an induced emf in the contour.

Example 6.15 Moving Contour near a Time-Varying Line Current

Refer to Fig. 6.17 and assume that the current in the infinite wire conductor is slowly time-varying, with intensity $i(t)$. Find the emf induced in the moving contour.

Solution We now have a motion of the contour in a time-varying magnetic field, produced by the current in the wire, i.e., a combination of systems in Figs. 6.12 and 6.17. Therefore, the emf is induced in the contour due to combined (transformer plus motional) induction. Combining Eqs. (6.64) and (6.98), the magnetic flux through the contour is

$$\Phi(t) = \frac{\mu_0 i(t) b}{2\pi} \ln \frac{c + a + vt}{c + vt}. \tag{6.111}$$

From Eq. (6.110) [or Eq. (6.34)], the total (combined) emf in the contour is

$$e_{\text{ind}}(t) = -\frac{\mathrm{d}\Phi}{\mathrm{d}t} = \underbrace{-\frac{\mu_0 b}{2\pi} \ln \frac{c + a + vt}{c + vt} \frac{\mathrm{d}i}{\mathrm{d}t}}_{\text{transformer emf}} + \underbrace{\frac{\mu_0 i(t) abv}{2\pi(c + vt)(c + a + vt)}}_{\text{motional emf}}. \tag{6.112}$$

We note that the first term in this expression represents the transformer part of the total emf; it becomes zero in the case of a steady current in the wire and becomes the same as in Eq. (6.65) in the case of a stationary contour. The second term represents the motional part of the total emf; it becomes zero in the case of a stationary contour and becomes the same as in Eq. (6.99) in the case of a steady current in the wire.

Example 6.16 Rotating Loop in a Time-Harmonic Magnetic Field

Assume that the applied field in Fig. 6.16 is a low-frequency time-harmonic magnetic field with flux density $B(t) = B_0 \sin \omega t$, and obtain the emf induced in the rotating loop. Identify the parts of the emf corresponding to the transformer and motional induction.

Solution Obviously, we are now adding a transformer induction component to the system in Fig. 6.16. The magnetic flux in Eq. (6.86) becomes

$$\Phi(t) = abB(t) \cos\theta = abB(t) \cos \omega t. \tag{6.113}$$

Hence, the emf induced in the contour is

$$e_{\text{ind}}(t) = -\frac{\mathrm{d}\Phi}{\mathrm{d}t} = \underbrace{-ab\frac{\mathrm{d}B}{\mathrm{d}t} \cos \omega t}_{\text{transformer emf}} + \underbrace{\omega abB(t) \sin \omega t}_{\text{motional emf}}. \tag{6.114}$$

[8]Note that the division of the induced emf between the transformer and motional parts depends on the chosen frame of reference. The particular division in Eq. (6.109) is given for the stationary frame of reference, attached to the field **B**, with respect to which the contour moves at the velocity **v**. In other words, it is given as measured by a stationary observer (so-called laboratory observer). The total emf, however, is unique and the same for any chosen frame of reference and any observer, including the one moving with the contour.

For the given time-variation $B(t)$, the terms corresponding to the transformer and motional induction appear to be

$$e_{\text{ind(transformer)}} = -\omega abB_0 \cos^2 \omega t \quad \text{and} \quad e_{\text{ind(motional)}} = \omega abB_0 \sin^2 \omega t, \tag{6.115}$$

respectively, and the total emf

$$e_{\text{ind}}(t) = -\omega abB_0 \left(\cos^2 \omega t - \sin^2 \omega t\right) = -\omega abB_0 \cos 2\omega t = \omega abB_0 \cos(2\omega t + \pi). \tag{6.116}$$

We see that the frequency of the induced emf (and current) in the contour is twice the frequency of the applied magnetic field.

Example 6.17 Stationary Loop in a Rotating Magnetic Field

A rectangular loop of resistance R is situated in the magnetic field produced by two mutually perpendicular large coils with low-frequency time-harmonic currents. The field due to each coil can be considered to be uniform. The currents in the coils are of equal amplitudes and 90° out of phase, so that the magnetic flux densities they produce are given as $B_1(t) = B_0 \cos \omega t$ and $B_2(t) = B_0 \sin \omega t$, respectively, and shown in Fig. 6.19(a). The sides of the loop are a and b long. Neglecting the magnetic field due to induced current in the loop, find the time-average torque of magnetic forces on the loop.

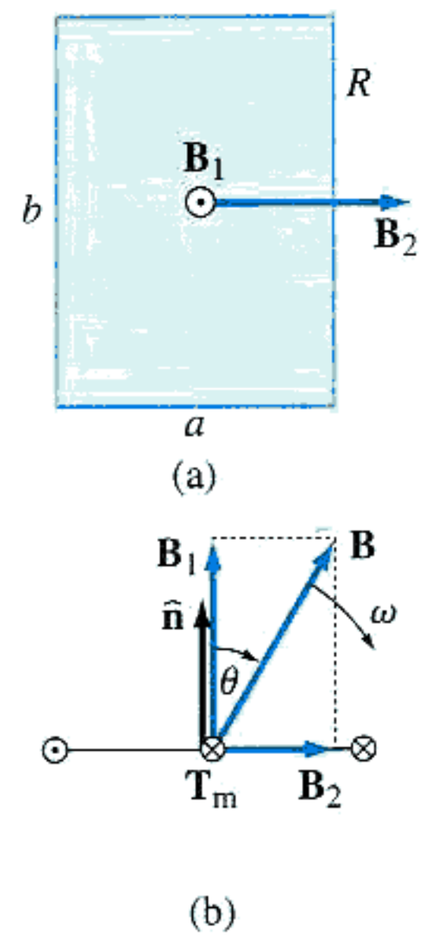

Figure 6.19 A rectangular wire loop exposed to two time-harmonic magnetic fields of equal amplitudes and 90° out of phase (a), which superposed to each other represent a rotating magnetic field (b); for Example 6.17.

Solution From Fig. 6.19(b), the magnitude of the resultant magnetic flux density vector,

$$\mathbf{B}(t) = \mathbf{B}_1(t) + \mathbf{B}_2(t), \tag{6.117}$$

at an arbitrary instant of time equals

$$|\mathbf{B}(t)| = \sqrt{B_1^2(t) + B_2^2(t)} = \sqrt{B_0^2(\cos^2 \omega t + \sin^2 \omega t)} = B_0, \tag{6.118}$$

i.e., it is constant with respect to time. This means that the tip of the vector $\mathbf{B}(t)$ traces a circle of radius B_0 in the course of time. Such a vector belongs to a class of so-called circularly polarized time-harmonic vectors. Let θ mark the angle between vectors $\mathbf{B}(t)$ and $\mathbf{B}_1(t)$ at time t, Fig. 6.19(b). The tangent of this angle is

$$\tan \theta(t) = \frac{B_2(t)}{B_1(t)} = \frac{B_0 \sin \omega t}{B_0 \cos \omega t} = \tan \omega t, \tag{6.119}$$

and hence the rate at which it changes in time is given by Eq. (6.87). This means that $\mathbf{B}$ rotates at a constant angular velocity, equal to the angular frequency ω of the individual magnetic flux densities and currents in the coils. At $t = 0$, $\mathbf{B}_2 = 0$ and $\mathbf{B} = \mathbf{B}_1$, which implies that $\theta(0) = 0$ and $\theta(t) = \omega t$ [see Eq. (6.88)].

As the contour is stationary and vector $\mathbf{B}$ changes in time (its magnitude is constant, but its direction changes), this is a system based on transformer induction. On the other hand, for the generation of emf it is irrelevant whether $\mathbf{B}$ rotates around a stationary loop or a loop rotates (at the same rate) in a static $\mathbf{B}$. This latter case is exactly the system based on motional induction in Fig. 6.16. Exploiting this equivalency,[9] the flux through the loop in Fig. 6.19, emf, current, and instantaneous torque of magnetic forces on the loop are given by Eqs. (6.89), (6.90), (6.91), and (6.92), respectively, with B substituted by B_0. Using Eq. (6.95), the time-average torque is

$$(T_{\text{m}})_{\text{ave}} = \frac{\omega a^2 b^2 B_0^2}{2R}. \tag{6.120}$$

The direction of this torque is the same as the direction of the field rotation [Fig. 6.19(b)], which is in accordance with Lenz's law. Namely, the induced current in the loop and the associated magnetic moment of the loop produce a torque ($\mathbf{T}_{\text{m}}$) that tends to rotate the loop

[9]The possibility to approach the problem of a stationary contour in a rotating magnetic field as a motional induction case is the reason for which we analyze it in the section devoted to total induction.

along with the applied rotating field [i.e., to rotate $\hat{\mathbf{n}}$ closer to $\mathbf{B}$ in Fig. 6.19(b) and thus decrease the angle θ], which is in opposition to the change in the magnetic flux through the contour (caused by the increase in θ) that generated the emf in the first place.

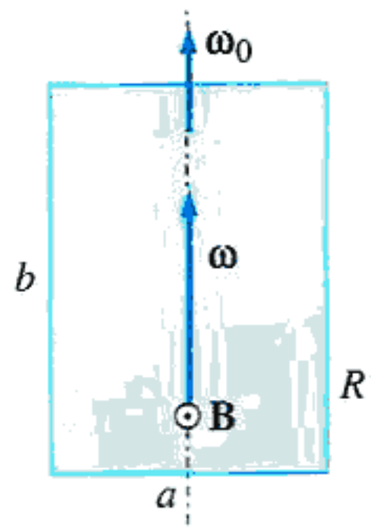

Figure 6.20 Elementary asynchronous motor in the form of a rectangular wire loop rotating with an angular velocity ω_0 in a rotating magnetic field of angular frequency ω, where $\omega > \omega_0$ (top view at $t = 0$); for Example 6.18.

Example 6.18 Rotating Loop in a Rotating Field – Asynchronous Motor

Assume that the loop exposed to the rotating magnetic field from Fig. 6.19 also rotates in the same direction with an angular velocity ω_0 ($\omega_0 < \omega$), as indicated in Fig. 6.20. This device represents an elementary asynchronous motor. Calculate (a) the time-average power of Joule's losses dissipated in the loop, (b) the time-average torque of magnetic forces on the loop, and (c) the efficiency of the motor.

Solution

(a) This is a system based on total (mixed) induction – the magnetic field changes (rotates) in time and the loop moves (rotates). It is called the asynchronous motor because the loop does not rotate in synchronism with the field. The relative rate of rotation of the field with respect to the rotating part of the motor (the loop in our case), called the rotor, equals

$$\Delta\omega = \omega - \omega_0, \tag{6.121}$$

which is referred to as the slipping angular velocity of the asynchronous motor. Consequently, this system can be replaced by either an equivalent system with a stationary loop and a magnetic field rotating with a velocity $\Delta\omega$ (transformer induction case, as in Fig. 6.19) or an equivalent system with a loop rotating with a velocity $\Delta\omega$ in a static magnetic field (motional induction case, as in Fig. 6.16). From Eqs. (6.89), (6.118), and (6.121), the magnetic flux through the loop in Fig. 6.20 is

$$\Phi(t) = ab|\mathbf{B}|\cos\Delta\omega t = abB_0\cos(\omega - \omega_0)t. \tag{6.122}$$

Eq. (6.94) then tells us that the time-average power of Joule's losses in the loop can be written as

$$(P_J)_{\text{ave}} = k(\omega - \omega_0)^2, \quad \text{where} \quad k = \frac{a^2b^2B_0^2}{2R}. \tag{6.123}$$

(b) By means of Eq. (6.92), the time-average torque of magnetic forces on the loop is

$$(T_m)_{\text{ave}} = k(\omega - \omega_0), \tag{6.124}$$

where the coefficient k is that in Eq. (6.123). This torque has the same direction as the slipping velocity of the motor.

(c) The rate of the loop rotation in Fig. 6.20 is ω_0, so that Eq. (6.93) gives the following expression for the time-average mechanical power used to rotate the loop:

$$(P_{\text{mech}})_{\text{ave}} = (T_m)_{\text{ave}}\,\omega_0 = k\,\omega_0(\omega - \omega_0). \tag{6.125}$$

The efficiency of the motor is given by

$$\eta = \frac{(P_{\text{mech}})_{\text{ave}}}{(P_{\text{mech}})_{\text{ave}} + (P_J)_{\text{ave}}} = \frac{\omega_0}{\omega}, \tag{6.126}$$

where we neglect the losses in the stationary part of the motor (the stator).

Example 6.19 Charge Flow due to a Magnetic Flux Change

Consider a wire contour of resistance R situated in a magnetic field, as shown in Fig. 6.21. If this field is changed and/or the contour is moved in the field during an arbitrary interval of time so that the corresponding net change of the magnetic flux through the contour is $\Delta\Phi$, find the total charge flow Q in the contour during this process.

Solution Since the magnetic flux of the contour, Φ, varies in time during the considered process, an emf e_{ind} is induced in the contour (due to the total induction in the general case), for which we can write

$$e_{\text{ind}} = -\frac{\mathrm{d}\Phi}{\mathrm{d}t} \quad \text{and} \quad e_{\text{ind}} = Ri, \tag{6.127}$$

where i is the intensity of current in the contour (Fig. 6.21). Combining these two equations gives

$$\mathrm{d}\Phi = -Ri\,\mathrm{d}t. \tag{6.128}$$

From Eq. (3.4), the charge that flows through the contour during an elementary time $\mathrm{d}t$ is $\mathrm{d}Q = i\,\mathrm{d}t$, resulting in

$$\mathrm{d}\Phi = -R\,\mathrm{d}Q. \tag{6.129}$$

We then integrate both sides of the above equation. On the left-hand side of the equation, we thus obtain the total change of flux, $\Delta\Phi$, from its starting value (Φ_1) to the ending value (Φ_2) in the process,

$$\int_{\Phi_1}^{\Phi_2} \mathrm{d}\Phi = \Phi_2 - \Phi_1 = \Delta\Phi. \tag{6.130}$$

On the right-hand side of the equation, the integral of $\mathrm{d}Q$ equals the total charge flow, Q, and hence

$$\boxed{Q = -\frac{\Delta\Phi}{R},} \tag{6.131}$$

charge flow in a wire contour due to a magnetic flux change

where the reference directions of the charge flow and the magnetic flux are interconnected by the right-hand rule, as indicated in Fig. 6.21.

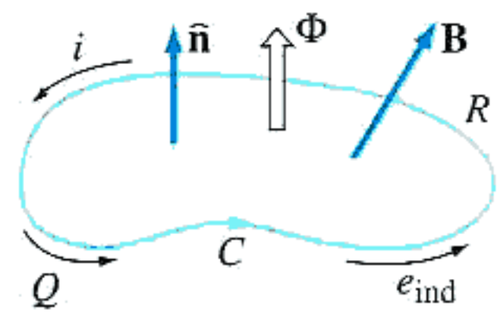

Figure 6.21 Evaluation of the charge flow in a wire contour as a consequence of a change of the magnetic flux through the contour; for Example 6.19.

Example 6.20 Fluxmeter Based on a Charge-Flow Measurement

A fluxmeter consists of a small coil (magnetic sonde) connected to a ballistic galvanometer, as in Fig. 6.22. The cross-sectional area of the coil is S and the number of wire turns is N. The total resistance of the coil and the galvanometer is R. The coil is placed in a uniform time-invariant magnetic field such that the magnetic field lines are perpendicular to the flat surface spanned over the coil cross section (Fig. 6.22). The coil is then removed from the field, and the charge flow indicated by the galvanometer is Q. What is the flux density of the magnetic field?

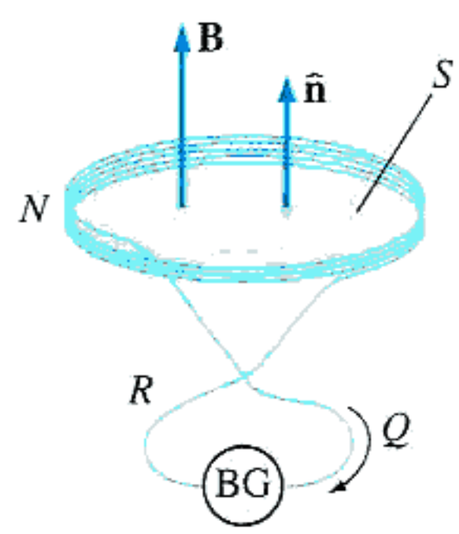

Figure 6.22 Fluxmeter consisting of a small coil and a ballistic galvanometer (BG); for Example 6.20.

Solution The magnetic flux of the coil while it is in the field is

$$\Phi_1 = NBS, \tag{6.132}$$

whereas $\Phi_2 = 0$ after the coil is removed from the field. Using Eq. (6.131), the charge flow through the galvanometer is given by

$$Q = -\frac{\Delta\Phi}{R} = -\frac{\Phi_2 - \Phi_1}{R} = \frac{\Phi_1}{R} = \frac{NBS}{R}, \tag{6.133}$$

which yields the following expression for the magnetic flux density of the field:

$$B = \frac{R}{NS}Q. \tag{6.134}$$

We see that B is linearly proportional to Q, where the proportionality constant is determined by the parameters (R, N, and S) of the fluxmeter in Fig. 6.22.

Thus, by directly measuring the charge flow through its terminals, a ballistic galvanometer connected to a magnetic sonde can be used to indirectly measure the flux density of an unknown magnetic field. In some cases, like in this example, the measurement is based on motional electromagnetic induction (field is time-constant and a coil is either removed from the field or brought into it). In other applications, like in the apparatus for measurement of magnetization curves in Fig. 5.19, a coil is stationary in a field that is either established from

zero to its final value B (to be measured) or reduced from some value (B) to zero, so that the measurement is based on transformer electromagnetic induction.

Example 6.21 Magnetic Flux through a Superconducting Contour

Prove that the magnetic flux through a superconducting wire contour cannot be changed.

Solution A superconducting wire has zero resistivity [see Eq. (3.23)] and zero total resistance, $R = 0$, so that Eqs. (6.127) give

Φ = const through a superconducting contour

$$\boxed{\frac{d\Phi}{dt} = 0 \quad (R = 0),} \tag{6.135}$$

that is, Φ = const, which completes our proof.

Having in mind that Φ denotes the total existing flux through the contour, this result can be explained as follows. If the magnetic field in which a superconducting contour resides (external or primary magnetic field) is changed and/or the contour is moved in the field, a current is induced in the contour whose magnetic field (secondary field) completely cancels the change of the magnetic flux through the contour (Lenz's law in its extreme form), such that the total flux Φ through the contour remains constant.

Problems: 6.29–6.33; *Conceptual Questions* (on Companion Website): 6.23–6.25; *MATLAB Exercises* (on Companion Website).

6.8 EDDY CURRENTS

Whenever electric field is induced in a conducting medium, electric current is also established, with the same time-dependence as the field (we assume that the medium is linear in terms of its conductivity). An example is a conducting wire loop in a time-varying magnetic field (Fig. 6.8), where the intensity of the induced current in the wire is given by Eq. (6.38). This section is devoted to studying volume induced currents in solid conducting bodies, where many current contours are established throughout the volume of the body as a result of the induced electric field. These currents are perpendicular to the magnetic flux in the body and, since they flow like "eddies" (in water), we call them eddy currents. The eddy current density vector, $\mathbf{J}_{\text{eddy}}$, is related to the electric field intensity vector, $\mathbf{E}$, through Ohm's law in local form:

density of eddy currents

$$\boxed{\mathbf{J}_{\text{eddy}} = \sigma \mathbf{E},} \tag{6.136}$$

where σ is the conductivity of the material. The vector $\mathbf{E}$ represents the actual (measurable) electric field in the material, which, in general, is composed of the induced electric field, $\mathbf{E}_{\text{ind}}$, and the field due to excess charge, $\mathbf{E}_q$ [see Eq. (6.16)]. The vector $\mathbf{J}_{\text{eddy}}$ in Eq. (6.136), therefore, is the actual (total) current density vector in the material, the corresponding components of which are $\sigma \mathbf{E}_{\text{ind}}$ and $\sigma \mathbf{E}_q$. Note that the component $\sigma \mathbf{E}_{\text{ind}}$ alone is usually identified as the induced current density vector in the material. However, as the accumulation of excess charge in the majority of practical systems with an induced electric field is also a result of electromagnetic induction, both components of the eddy current density vector can be said to be induced by the same cause that induces the field $\mathbf{E}_{\text{ind}}$ and electromotive force in the system, i.e., to represent the induced current in the material. This cause, on the other hand, can be related to either transformer or motional induction, as well as to total (combined) induction.

As a consequence of eddy currents, electric power is lost to heat in the material, according to Joule's law, and this is the principle of induction heating. In so-called induction furnaces, for instance, eddy currents are created on purpose to produce local heating in metal pieces and high enough temperatures to melt the metal. In ac machines and transformers, however, the power loss due to eddy currents induced in ferromagnetic[10] cores is undesirable. From Eq. (3.31), the volume density of the power of Joule's losses at a point in the material is proportional to the square of the density of eddy currents, J_{eddy}, at that point. Using Eq. (3.32), the total instantaneous power of Joule's (ohmic) losses in the entire body is obtained as

$$\boxed{P_{\text{J}} = \int_v \frac{J_{\text{eddy}}^2}{\sigma}\, \mathrm{d}v,} \tag{6.137}$$

Joule's (ohmic) losses due to eddy currents

where v denotes the volume of the body.

Another important consequence of eddy currents is the magnetic field that they produce. By Lenz's law, this field (secondary magnetic field) opposes the change in the primary magnetic flux inside the body, which caused the eddy currents in the first place. While the secondary magnetic field due to induced currents in thin-wire circuits is practically always negligible with respect to the primary magnetic field, this often is not the case with volume eddy currents in solid bodies. The larger the volume of the body and areas of eddy current contours (eddies) in the material the larger the induced emf along the contours and the current intensities, as well as the magnetic field they produce. This effect is also usually not desirable. For instance, the magnetic field due to eddy currents in ferromagnetic cores of ac machines and transformers tends to cancel the primary magnetic flux in the core and thus considerably reduces the efficiency of the device. As an illustration, consider a large core of a rectangular parallelepipedal shape in a uniform time-varying primary magnetic field $\mathbf{B}$, as depicted in Fig. 6.23(a). The secondary (induced) magnetic field, $\mathbf{B}_{\text{ind}}$, is the strongest at the center of the cross section of the core, i.e., at the center of all eddy current contours, where all the fields due to these contours add up. Hence, the resultant (primary plus secondary) magnetic flux density is not uniformly distributed over the core cross section; it is the smallest at the center and the largest near the core surface. In other words, practically only the "skin" region below the surface of the core carries the magnetic flux and is effectively used for the operation of the device. This phenomenon is referred to as the skin effect in ferromagnetic cores.

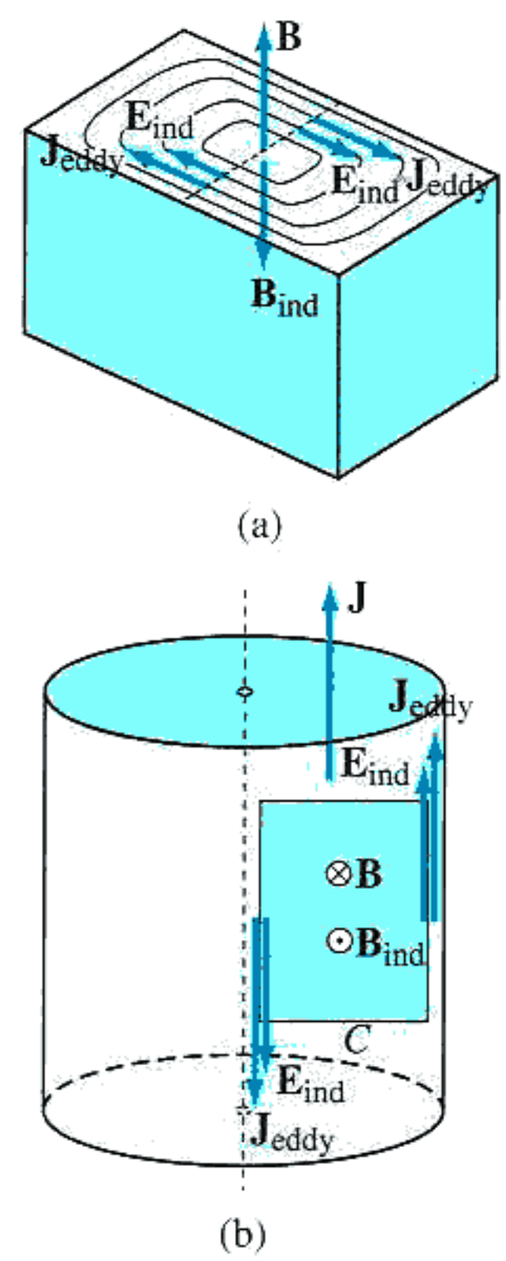

Figure 6.23 Illustration of the skin effect in a parallelepipedal ferromagnetic core with a time-varying magnetic field (a) and in a cylindrical conductor with a time-harmonic current (b).

Note that the skin effect in current conductors at high frequencies is also a consequence of induced (eddy) currents and their magnetic field. To show this, consider a cylindrical conductor carrying a time-harmonic (ac) current of density $\mathbf{J}$, Fig. 6.23(b). Using the analogy with the dc case in Fig. 4.15, the lines of the magnetic field $\mathbf{B}$ due to this current are circles centered at the conductor axis. This field induces an electric field $\mathbf{E}_{\text{ind}}$, which is axial in the conductor (field lines are parallel to the conductor axis) and can be qualitatively analyzed by applying Faraday's law of electromagnetic induction, Eq. (6.35), to the rectangular contour C shown in Fig. 6.23(b). The direction of vectors $\mathbf{E}_{\text{ind}}$ and $\mathbf{J}_{\text{eddy}}$ is determined by Lenz's law (i.e., by the minus sign in Faraday's law). It is such that the secondary magnetic field, $\mathbf{B}_{\text{ind}}$, opposes the primary field $\mathbf{B}$. Hence, the eddy current density vector tends to cancel

[10]Ferromagnetic materials are electrically conducting, with large conductivities (e.g., $\sigma_{\text{Fe}} = 10$ MS/m for iron).

the current density **J** inside the conductor volume, while adding to its magnitude near the conductor surface. Therefore, the magnitude of the total current density vector is small at the conductor axis and increases towards the conductor surface. The higher the frequency (i.e., the faster the time rate of change d/dt in Faraday's law) the larger the induced emf in the contour C and the more pronounced the skin effect. At very high frequencies, the current is restricted to a very thin layer ("skin") near the conductor surface,[11] practically on the surface itself, and can be considered therefore as a surface current and described using the surface current density vector, $\mathbf{J}_s$ [see Eqs. (3.12) and (3.13)].

Examples in this section include evaluation of eddy current distributions and Joule's losses in several characteristic systems based on each of the three types of electromagnetic induction (transformer, motional, and total induction). In all cases, we shall neglect the magnetic field due to eddy currents and the associated skin effect in conducting bodies. Taking this field into account in the evaluation of the distribution of eddy currents in the body would require a much more complex analysis based on numerical field-computation techniques.

Example 6.22 Eddy Currents in a Thin Conducting Disk

A thin conducting disk of radius a, thickness δ ($\delta \ll a$), conductivity σ, and permeability μ_0 is positioned inside an infinitely long air-filled solenoid, as shown in Fig. 6.24(a). A low-frequency time-harmonic current of intensity $i(t) = I_0 \cos \omega t$ flows through the winding. The number of wire turns per unit of the solenoid length is N'. (a) Determine the distribution of eddy currents induced in the disk, neglecting the magnetic field that they produce. (b) Find the time-average power of Joule's losses dissipated in the disk. (c) Evaluate the magnetic field due to eddy currents at the disk center.

Solution

(a) Eddy currents are induced in the disk due to transformer induction in this structure. The induced electric field inside the solenoid is given by the first expression in Eqs. (6.51). Using Eq. (6.136) and referring to Fig. 6.24(b), the distribution of eddy currents in the

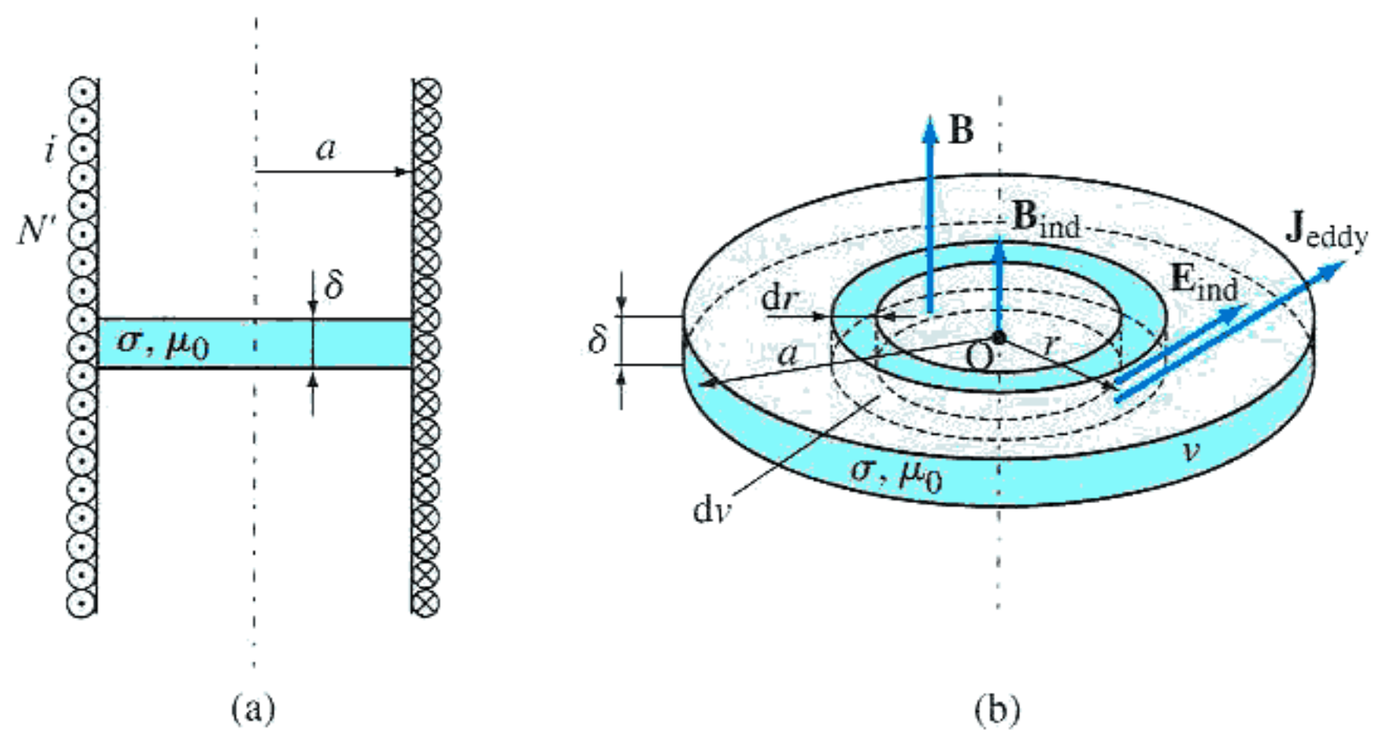

Figure 6.24 (a) Thin conducting disk inside an infinitely long solenoid with a low-frequency time-harmonic current and (b) evaluation of eddy currents in the disk and their magnetic field at the disk center; for Example 6.22.

[11] For example, we shall see in a later chapter that the thickness of the layer that carries most of the current in copper conductors at frequencies higher than about 1 MHz is less than a fraction of a millimeter.

disk is described by the following expression for the induced current density:

$$J_{\text{eddy}}(r,t) = \sigma E_{\text{ind}}(r,t) = -\frac{\mu_0 \sigma N' r}{2}\frac{\mathrm{d}i}{\mathrm{d}t} = \frac{\omega \mu_0 \sigma N' I_0 r}{2}\sin\omega t \quad (0 \le r \le a), \tag{6.138}$$

where r is the radial distance from the solenoid axis and we assume that the electric field due to excess charge is practically zero.

(b) From Eq. (6.137), the instantaneous power of Joule's losses in the disk is

$$P_{\text{J}}(t) = \int_{r=0}^{a} \frac{J_{\text{eddy}}^2(r,t)}{\sigma}\underbrace{2\pi r\,\mathrm{d}r\delta}_{\mathrm{d}v} = \frac{\pi\sigma(\omega\mu_0 N' I_0)^2\delta}{2}\sin^2\omega t\int_0^a r^3\,\mathrm{d}r$$

$$= \frac{\pi\sigma(\omega\mu_0 N' I_0)^2 a^4\delta}{8}\sin^2\omega t, \tag{6.139}$$

with $\mathrm{d}v$ being the volume of an elementary hollow disk of radius r, width $\mathrm{d}r$, and thickness (height) δ [Fig. 6.24(b)]. Having in mind Eq. (6.95), the time-average of this power amounts to

$$(P_{\text{J}})_{\text{ave}} = \frac{\pi\sigma(\omega\mu_0 N' I_0)^2 a^4\delta}{16}. \tag{6.140}$$

(c) As $\delta \ll a$, the elementary hollow disk of volume $\mathrm{d}v$ in Fig. 6.24(b) can be replaced by an equivalent circular current contour (wire) of radius r and current intensity

$$\mathrm{d}I_{\text{eddy}}(r,t) = J_{\text{eddy}}(r,t)\,\delta\,\mathrm{d}r \tag{6.141}$$

(cross section of the hollow disk through which the current of density $\mathbf{J}_{\text{eddy}}$ flows is a small rectangle of side lengths δ and $\mathrm{d}r$, and surface area $\delta\,\mathrm{d}r$). The magnetic flux density due to this current at the center of the disk is obtained using Eq. (4.19) for $z = 0$ and r substituting a:

$$\mathrm{d}B_{\text{ind}}(r,t) = \frac{\mu_0\,\mathrm{d}I_{\text{eddy}}(r,t)}{2r}. \tag{6.142}$$

By virtue of the superposition principle, the resultant magnetic field due to eddy currents is given by

$$B_{\text{ind}}(t) = \int_{r=0}^{a}\mathrm{d}B_{\text{ind}}(r,t) = \frac{\omega\mu_0^2\sigma N' I_0\delta}{4}\sin\omega t\int_0^a \mathrm{d}r = \frac{\omega\mu_0^2\sigma N' I_0 a\delta}{4}\sin\omega t. \tag{6.143}$$

Comparing the amplitude B_{ind0} of the field $B_{\text{ind}}(t)$ to the amplitude B_0 of the primary field $B(t) = \mu_0 N' I_0\cos\omega t$ [Eq. (6.48)] inside the solenoid, we see that

$$\frac{B_{\text{ind0}}}{B_0} = \frac{\omega\mu_0\sigma a\delta}{4}. \tag{6.144}$$

Hence, the magnetic field due to eddy currents in the disk is negligible with respect to the magnetic field due to primary currents in the solenoid only if

$$\frac{\pi f\mu_0\sigma a\delta}{2} \ll 1, \tag{6.145}$$

where $f = \omega/(2\pi)$ is the frequency of the currents, and whether or not this condition is satisfied depends on the numerical values of the parameters of the structure in Fig. 6.24(a). As an example, for $f = 60$ Hz (power frequency), $\sigma = 58$ MS/m (copper), and $\delta = a/20$, we obtain that only for disks with quite small radii ($a \ll 5$ cm), $B_{\text{ind0}} \ll B_0$, whereas eddy currents in larger disks produce magnetic fields that cannot be neglected with respect to primary fields (at least at the disk center, where the secondary magnetic field is maximum).

Note that the magnetic field $\mathbf{B}_{\text{ind}}$ in Eq. (6.143) is evaluated based on the distribution of eddy currents given by Eq. (6.138). However, in the case when the condition in Eq. (6.145) is not satisfied, this evaluation is not accurate enough and provides only qualitative results, because the starting expression for the induced electric field in Eqs. (6.51)

is obtained taking into account only the primary magnetic field on the right-hand side of Faraday's law of electromagnetic induction.

Example 6.23 Eddy Currents in a Thin Ferromagnetic Plate

A thin conducting ferromagnetic plate of length b, width a, and thickness d ($d \ll a$) is situated in a uniform low-frequency time-harmonic magnetic field of flux density $B(t) = B_0 \cos \omega t$. The field lines are perpendicular to the plate cross section, as shown in Fig. 6.25(a). The conductivity of the plate is σ. Neglecting the end effects and the magnetic field produced by eddy currents, find (a) the distribution of these currents throughout the plate and (b) the total time-average power of Joule's losses associated with them.

Solution

(a) This is another example of a structure with eddy currents due to transformer induction. By neglecting the end effects (since $d \ll a$), we assume that the current streamlines in the plate are straight and parallel to the plate surfaces, as indicated in Fig. 6.25(b). From Eq. (6.136), the same is true for the lines of the total electric field intensity vector, $\mathbf{E}$, in the plate. By the same token, the magnitude E of this vector does not depend on the coordinate y in Fig. 6.25(b). Applying Faraday's law of electromagnetic induction, Eq. (6.37), to the rectangular contour C shown in Fig. 6.25(b), we get

$$2E(x,t)\,l = -\frac{\mathrm{d}B}{\mathrm{d}t}\,2xl, \qquad -\frac{d}{2} < x < \frac{d}{2}, \tag{6.146}$$

which yields

$$E(x,t) = -x\,\frac{\mathrm{d}B}{\mathrm{d}t} = \omega B_0 x \sin \omega t, \tag{6.147}$$

where we neglect the magnetic field due to eddy currents in the plate. The density of these currents is given by

$$J_{\text{eddy}}(x,t) = \sigma E(x,t) = \omega \sigma B_0 x \sin \omega t. \tag{6.148}$$

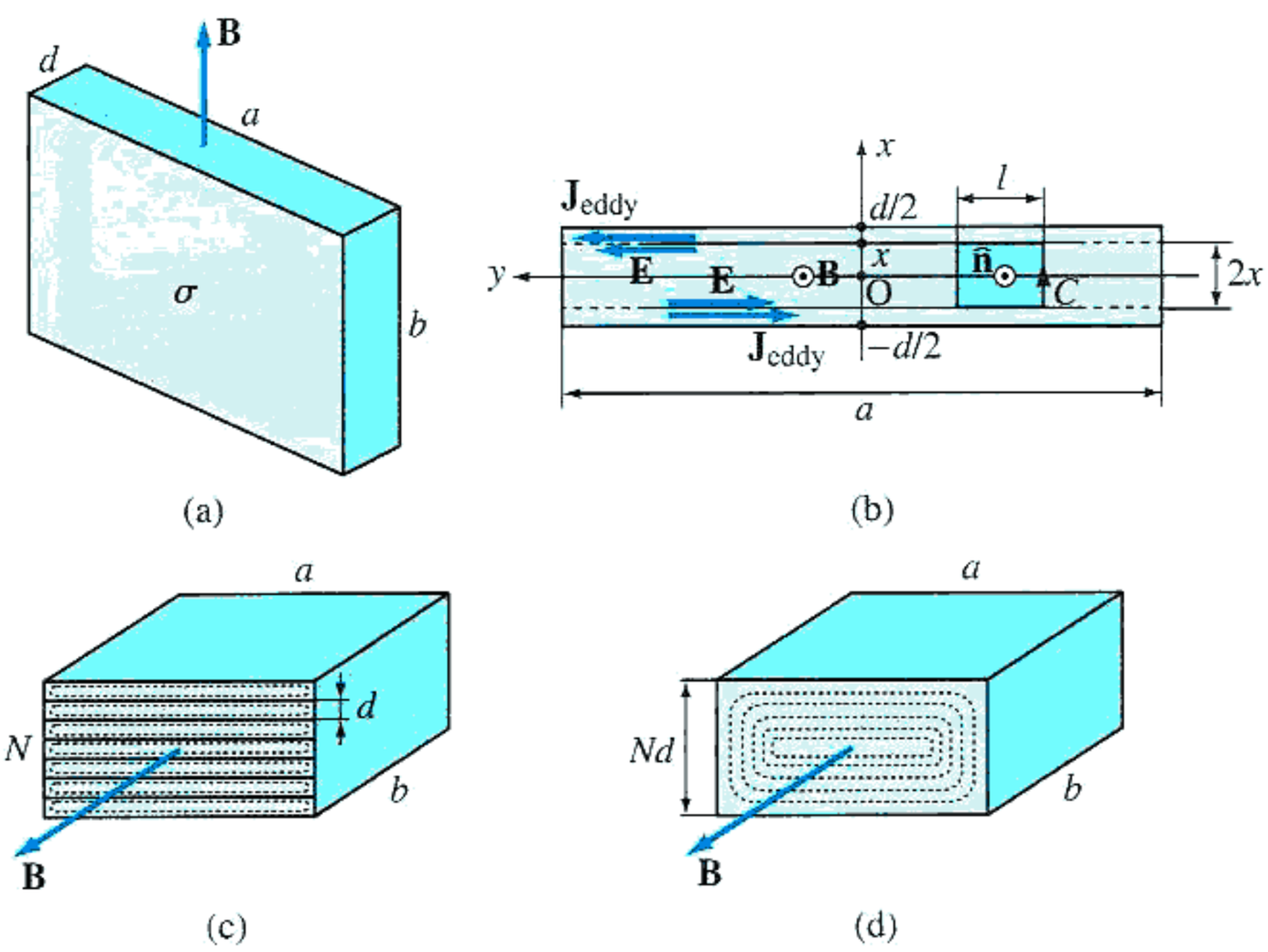

Figure 6.25 (a) Thin conducting ferromagnetic plate in a uniform low-frequency time-harmonic magnetic field, (b) distribution of eddy currents in the plate, (c) N insulated thin plates forming a core of an ac machine or transformer, and (d) a core with the same dimensions made of a single piece of material; for Example 6.23.

(b) The total instantaneous power of Joule's losses dissipated throughout the volume v of the plate is

$$P_J(t) = \int_v \frac{J^2_{\text{eddy}}(x,t)}{\sigma} \underbrace{ab\,\mathrm{d}x}_{\mathrm{d}v} = \omega^2 \sigma a b B_0^2 \sin^2 \omega t \int_{x=-d/2}^{d/2} x^2\,\mathrm{d}x = \frac{\omega^2 \sigma a b d^3 B_0^2}{12} \sin^2 \omega t, \tag{6.149}$$

where $\mathrm{d}v$ represents the volume of a differentially thin slab of thickness $\mathrm{d}x$ used in the volume integration. Finally, averaging in time [Eq. (6.95)] results in

$$(P_J)_{\text{ave}} = \frac{\omega^2 \sigma a b d^3 B_0^2}{24}. \tag{6.150}$$

Note that ferromagnetic cores of ac machines and transformers are made of mutually insulated stacked thin plates, as portrayed in Fig. 6.25(c), rather than of a single piece of material, shown in Fig. 6.25(d). With this, the areas of eddy current contours in the core are considerably reduced, and so are the electromotive forces and current intensities along the contours. Consequently, both undesirable effects of eddy currents (Joule's losses and secondary magnetic field) are reduced significantly as well. In specific, the time-average power of Joule's losses in the laminated core in Fig. 6.25(c) can be obtained as N times the power given in Eq. (6.150) for a single thin plate, where N is the number of insulated thin plates. On the other hand, the time-average power of Joule's losses in the homogeneous core in Fig. 6.25(d) can roughly be estimated using the same thin-plate expression in Eq. (6.150) for the plate thickness Nd. Hence, we can write

$$\boxed{(P_J)_{\text{ave1}} \propto Nd^3 \quad \text{and} \quad (P_J)_{\text{ave2}} \propto (Nd)^3,} \tag{6.151}$$

ohmic losses in a laminated core vs. homogeneous core – of an ac machine or transformer

respectively, for these two powers. We see that the reduction of Joule's losses in the laminated core is estimated to be as large as by roughly a factor of N^2 as compared to the homogeneous core with the same dimensions. Also, the skin effect caused by the magnetic field due to eddy currents is much more pronounced in the core in Fig. 6.25(d), where the resultant magnetic flux is "pushed" to the "skin" region near the surface of the core only, so that the entire interior of the core is practically flux-free. In the core in Fig. 6.25(c), on the other side, the "skin" regions are formed in each of the thin insulated plates, so that, although not entirely uniform over the cross section of the core, the resultant flux is much more densely distributed throughout the volume of the core and the ferromagnetic material is much more effectively used for the machine or transformer operation.

Note also that, from Eq. (6.150),

$$\boxed{(P_J)_{\text{ave}} \propto f^2 \sigma,} \tag{6.152}$$

dependence of ohmic losses due to eddy currents on frequency and conductivity

which means that the power loss due to eddy currents in the core increases very rapidly with an increase in the operating frequency of the device (f) and also that it can be reduced by using core materials that have low conductivity (σ). That is why ferrites (which have high permeability but low conductivity) are used instead of ferromagnetics in some applications at high frequencies (e.g., for the cores of high-frequency transformers or multiturn loop antennas).

Example 6.24 Eddy Currents in a Rotating Strip

A very long, thin conducting strip of length l, width a, and thickness δ ($\delta \ll a \ll l$) rotates about its axis at a constant angular velocity ω in a uniform time-invariant magnetic field of flux density B, as shown in Fig. 6.26(a). At an instant $t = 0$, the strip is perpendicular to the vector **B**. The conductivity of the strip is σ, and permeability μ_0. Determine (a) the distribution of eddy currents and (b) the instantaneous power of Joule's losses in the strip. Neglect the end effects and the magnetic field produced by eddy currents.

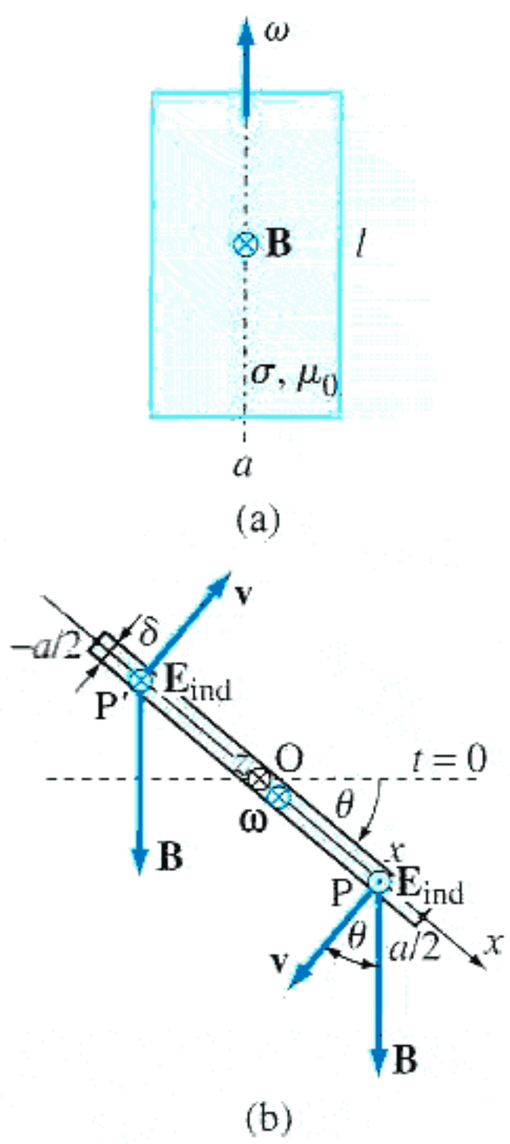

Figure 6.26 Evaluation of eddy currents in a strip rotating in a uniform time-invariant magnetic field: (a) top view at $t = 0$ and (b) cross-sectional view at an arbitrary time t; for Example 6.24.

Solution

(a) This is a structure with eddy currents generated because of motional induction. The induced electric field in the strip is given by Eq. (6.68), where we neglect the magnetic field due to currents in the strip. The vector $\mathbf{E}_{\text{ind}}$ is perpendicular to the cross section of the strip, shown in Fig. 6.26(b). At a point P, the velocity of which is $v = \omega x$,

$$\mathbf{E}_{\text{ind}} = \mathbf{v} \times \mathbf{B} = vB \sin\theta(-\hat{\mathbf{z}}) = -\omega x B \sin \omega t\, \hat{\mathbf{z}}, \qquad -\frac{a}{2} < x < \frac{a}{2}, \tag{6.153}$$

where $\theta = \omega t$ is the angle between the strip and the reference horizontal plane at time t [see Eq. (6.88)]. Note that, for the position of the strip in Fig. 6.26(b), the direction of $\mathbf{E}_{\text{ind}}$ is out of the page for $x > 0$ and into the page for $x < 0$ (point P′). The density of eddy currents in the strip, given with respect to the reference direction out of the page in Fig. 6.26(b), is

$$J_{\text{eddy}} = \sigma E_{\text{ind}} = \omega \sigma x B \sin \omega t, \tag{6.154}$$

where we neglect the end effects, i.e., the electric field due to excess charge that accumulates near the ends of the strip and causes the current streamlines to bend and close into themselves near the ends.

(b) The total instantaneous power of Joule's losses in the strip comes out to be

$$P_J(t) = \int_{x=-a/2}^{a/2} \frac{J_{\text{eddy}}^2}{\sigma}\, dv = \omega^2 \sigma l \delta B^2 \sin^2 \omega t \int_{-a/2}^{a/2} x^2\, dx = \frac{\omega^2 \sigma a^3 l \delta B^2}{12} \sin^2 \omega t, \tag{6.155}$$

where $dv = l\delta\, dx$ is the volume of an elementary strip of length l, thickness δ, and width dx.

Example 6.25 Rotating Cylinder in a Rotating Magnetic Field

A very long conducting cylinder of length l, radius a, and conductivity σ rotates at a constant angular velocity ω_0 about its axis, while being exposed to a rotating magnetic field of flux density B and angular frequency ω ($\omega > \omega_0$), as shown in Fig. 6.27(a). Neglect the end effects and the magnetic field due to eddy currents, and calculate the total instantaneous power of Joule's losses in the cylinder.

Solution This is a system based on total (transformer plus motional) induction. However, we can use the concept of slipping velocity given in Eq. (6.121) and replace this system by a cylinder rotating in a static magnetic field with the rate $\Delta\omega = \omega - \omega_0$ in the opposite

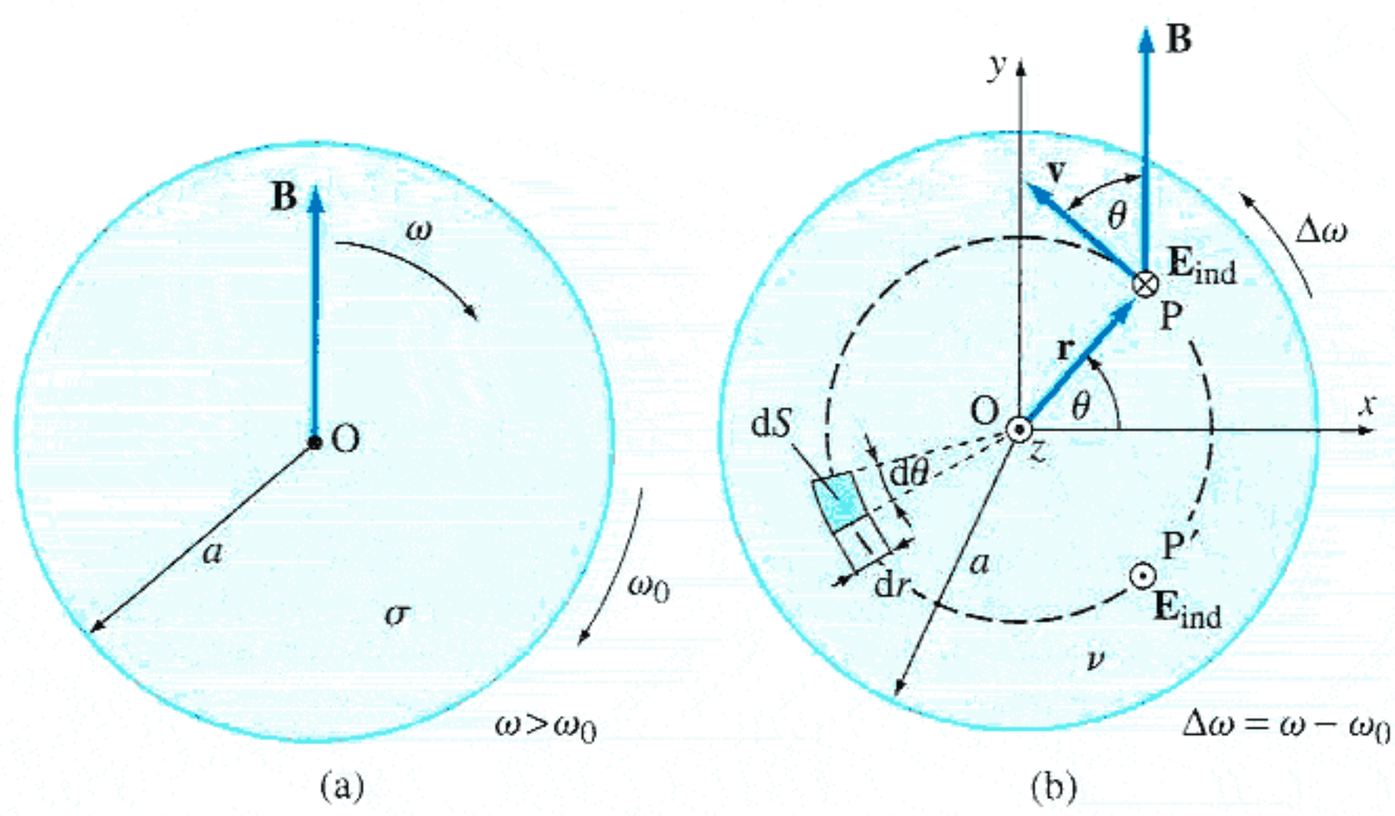

Figure 6.27 (a) Rotating cylinder in a rotating magnetic field and (b) equivalent system with the cylinder rotating in a static magnetic field; for Example 6.25.

direction, as depicted in Fig. 6.27(b). In the equivalent system, which is based on motional induction only, the induced electric field is found in a similar fashion as in Eq. (6.153). At a point P in Fig. 6.27(b),

$$\begin{aligned}\mathbf{E}_{\text{ind}} &= \mathbf{v} \times (B\,\hat{\mathbf{y}}) = vB\sin\theta(-\hat{\mathbf{z}}) = -\Delta\omega r B\sin\theta\,\hat{\mathbf{z}} \\ &= -\Delta\omega r B\sin(\Delta\omega t + \theta_0)\,\hat{\mathbf{z}}, \quad 0 \le r < a, \quad -\pi \le \theta < \pi, \end{aligned} \tag{6.156}$$

where r is the radial distance from the cylinder axis ($r = |\mathbf{r}|$), $v = \Delta\omega r$ is the velocity of the point, and θ is the angle between the vector $\mathbf{r}$ and the x-axis, which equals θ_0 at $t = 0$ and is given by Eq. (6.88) with $\Delta\omega$ as rotation rate. Note the opposite directions of $\mathbf{E}_{\text{ind}}$ at points P and P′ in the cylinder cross section, i.e., for θ positive and negative, respectively, which tells us how the streamlines of eddy currents ($\mathbf{J}_{\text{eddy}}$) close throughout the cylinder.

The total instantaneous power of Joule's losses dissipated in the cylinder is obtained by integration:

$$\begin{aligned}P_J(t) &= \int_v \sigma E_{\text{ind}}^2\,\mathrm{d}v = \int_{r=0}^{a}\int_{\theta=-\pi}^{\pi} \sigma E_{\text{ind}}^2(r,\theta)\,l\,\underbrace{r\,\mathrm{d}\theta\,\mathrm{d}r}_{\mathrm{d}S} \\ &= (\Delta\omega)^2\sigma B^2 l\int_0^a r^3\,\mathrm{d}r\int_{-\pi}^{\pi}\sin^2\theta\,\mathrm{d}\theta = \frac{\pi(\omega-\omega_0)^2\sigma a^4 l B^2}{4}, \end{aligned} \tag{6.157}$$

where $\mathrm{d}S$ is an elementary patch in the cylinder cross section [Fig. 6.27(b)], the sides of which are $\mathrm{d}r$ and $r\,\mathrm{d}\theta$ long, and $\mathrm{d}v = l\,\mathrm{d}S$. We see that the dissipated power is constant with respect to time, which is a consequence of the cylindrical (rotational) symmetry of this problem.

Problems: 6.34–6.45; *Conceptual Questions* (on Companion Website): 6.26–6.30; *MATLAB Exercises* (on Companion Website).

Problems

6.1. Induced electric field of a circular current loop. Assuming that the current in the circular loop in Fig. 4.6 is not steady but slowly time-varying, with intensity $i(t)$, find the induced electric field intensity vector at an arbitrary point along the z-axis (point P).

6.2. Induced electric field of a triangular current loop. For the triangular current loop in Fig. 4.39, calculate the electric field intensity vector at the point P induced by a slowly time-varying current of intensity $i(t)$ in the loop.

6.3. Magnetic field of an EMI source (square contour). Consider the square current contour described in Example 6.2, and find the magnetic field intensity vector at the point M in Fig. 6.2(a). Compare the result with that for the induced electric field intensity vector in Fig. 6.2(d).

6.4. Induced electric field above a square current contour. Determine the electric field intensity vector at a point N placed at a height a above the vertex representing the junction of sides 1 and 2 of the square contour in Fig. 6.2(c), the coordinates of the point thus being $x = y = a/2$ and $z = -a$, induced by the pulse current $i(t)$ in Fig. 6.2(b).

6.5. Magnetic field of a current contour of complex shape. For the wire contour with semicircular and linear parts carrying a low-frequency time-harmonic current from Example 6.4, compute the magnetic field intensity vector at the point O in Fig. 6.4.

6.6. Induced electric field of a semicircular-rectangular loop. Find the induced electric field intensity vector at the point O in Fig. 4.40, assuming that a slowly time-varying current of intensity $i(t)$ flows along the loop.

6.7. Current contour with circular and straight segments. A current of intensity $i(t) = \sin(10^8 t)$ A (t in s) flows along a wire contour with two circular (quarter-circle and 3/4-circle) and two linear parts, shown in Fig. 6.28, where $a = 3$ cm and $b = 9$ cm. (a) Verify that this is a low-frequency current, and compute (b) the induced electric field intensity vector and (c) the magnetic field intensity vector at the point O.

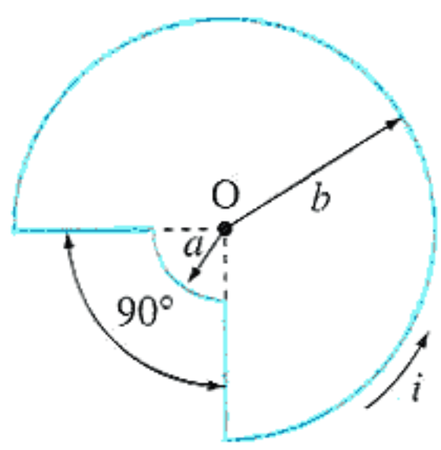

Figure 6.28 Wire contour with a quarter-circle, 3/4-circle, and two linear parts carrying a low-frequency time-harmonic current; for Problem 6.7.

6.8. Induced electric field at the axis of a circular segment. Repeat Example 6.3 but for the field point at an arbitrary location (defined by the coordinate z) along the z-axis (normal to the plane of drawing) in Fig. 6.3(a).

6.9. Induced electric field above or below a semicircular loop. Consider the wire contour made of a semicircle and a straight line from Example 4.4, and assume that it carries a slowly time-varying current of intensity $i(t)$. Determine the induced electric field intensity vector at an arbitrary point along the z-axis in Fig. 4.9(a).

6.10. Voltage from current distribution and total electric field. In a domain v in free space, there is a slowly time-varying distribution of volume currents and charges. We know the current density vector, $\mathbf{J}$, at every point of v, as well as the (total) electric field intensity vector (due to currents and charges in v), $\mathbf{E}$, at every point outside it. Find the voltage between any two points, M and N, outside v.

6.11. Voltage along a straight wire in a quasistatic field. A straight metallic wire is placed in a quasistatic electromagnetic field, for which the magnetic vector potential, $\mathbf{A}$, is known at every point of space. What are (a) the total electric field inside the wire and (b) the voltage between the ends, M and N, of the wire?

6.12. Rectangular wire loop around a solenoid. Consider the solenoid described in Example 6.5, and assume that a rectangular wire loop of edge lengths b and c is placed coaxially around it ($b, c > 2a$), as shown in Fig. 6.29. The magnetic field due to induced currents can be neglected. (a) What is the total induced emf in the loop? Find the emf in the edge MN of the loop, e_{indMN}, in the following two ways, respectively: (b) by integrating along the edge the induced electric field intensity vector due to the current in the solenoid winding [use the relationship in Eq. (4.43) to solve the integral] and (c) by showing that e_{indMN} equals the induced emf in the triangle $\triangle$OMN in Fig. 6.29, and then computing this latter emf as a part of the total emf from (a).

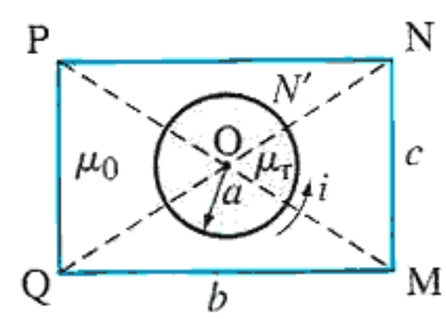

Figure 6.29 Rectangular wire loop placed coaxially around the solenoid in Fig. 6.9; for Problem 6.12.

6.13. Solenoid and a loop of wire with nonuniform cross section. Repeat Example 6.6 but assuming that the wire loop around the solenoid is composed of two parts with the same conductivity, σ, but with different cross-sectional areas, S_1 and S_2 ($S_1 \neq S_2$), and different lengths, determined by angles α and $2\pi - \alpha$, respectively, as shown in Fig. 6.30.

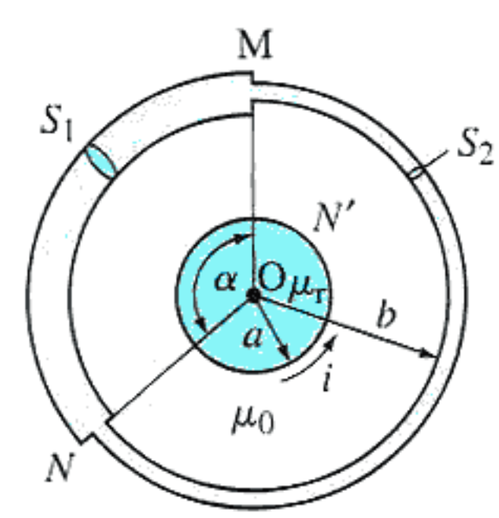

Figure 6.30 Structure in Fig. 6.10(a) but with a loop of wire of nonuniform cross section around the solenoid; for Problem 6.13.

6.14. Complex wire assembly inside a solenoid. Let the wire loop composed of two semicircular parts with conductivities σ_1 and σ_2 from Example 6.6 have radius $a/2$ and be placed coaxially inside an air-filled solenoid, and let two additional linear pieces of wire, with conductivities σ_3 and σ_4, be attached to it, at points M and N, as depicted in Fig. 6.31. Linear wire segments are positioned radially with respect to the solenoid axis, and their ends (points

P and Q) are very close to one another (the gap between them is much smaller than a). Compute the voltage between points P and Q.

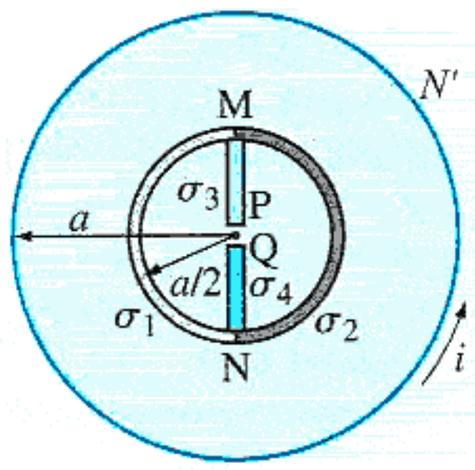

Figure 6.31 Wire assembly of four parts with different conductivities placed inside an air-filled solenoid (the gap between points P and Q is very small); for Problem 6.14.

6.15. Emf in a rectangular loop due to a two-wire line current. A very long lossless thin two-wire line in air, with distance between axes of conductors equal to $4a$, is fed at one end by an ideal current generator of low-frequency time-harmonic current intensity $i_g(t) = I_{g0} \cos \omega t$, while the other end of the line is short-circuited. A rectangular wire loop of side lengths a and b is placed in the plane of the line, such that its two sides are parallel to the line and the distance of one of the sides from one of the line conductors is a. Neglecting end and propagation effects, i.e., computing the magnetic field of the line as if it were infinitely long and assuming that the line current is the same in every cross section, as well as the magnetic field due to induced current, find the emf induced in the loop for situations in (a) Fig. 6.32(a) and (b) Fig. 6.32(b), respectively.

6.16. Large square and small circular concentric coplanar loops. Fig. 6.33 shows two concentric wire loops lying in the same plane, in free space, a large square loop of side length a and a small circular one of radius b ($b \ll a$). The loops are oriented in the same, counterclockwise, direction. The square loop carries a low-frequency time-harmonic current of intensity $i(t) = I_0 \sin \omega t$, and the resistance of the circular loop is R. Determine the induced current in the circular loop, neglecting its own magnetic field.

6.17. Electromagnetic induction in a nonlinear magnetic circuit. Consider a magnetic circuit in the form of a thin toroidal ferromagnetic core with two windings, like the one in Fig. 5.19. The length and cross-sectional area of the core are $l = 50$ cm and $S = 1$ cm^2, respectively. The primary coil, with $N_1 = 850$ turns of wire

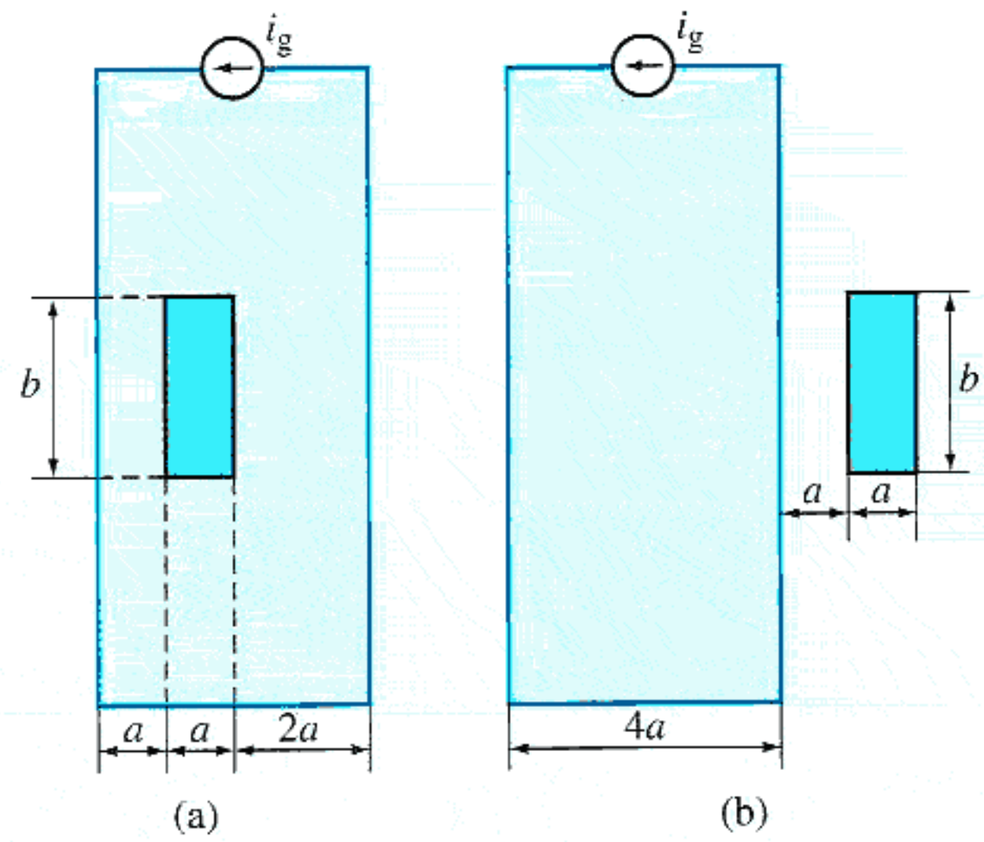

Figure 6.32 Electromagnetic induction in a rectangular loop due to a time-varying current of a thin two-wire line: (a) loop between line conductors and (b) loop on a side of the line; for Problem 6.15.

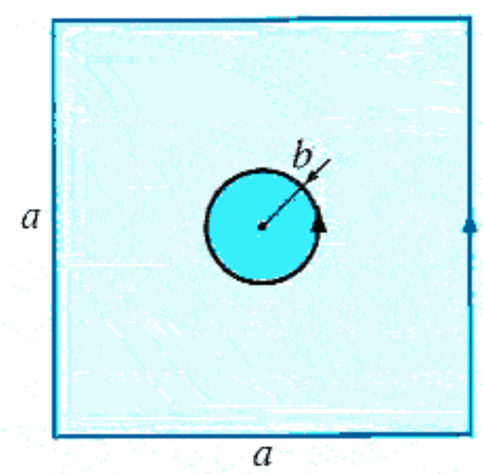

Figure 6.33 Magnetically coupled large square and small circular concentric coplanar loops in free space; for Problem 6.16.

wound uniformly and densely along the entire core, is fed by a low-frequency time-harmonic current of intensity $i(t) = I_0 \sin \omega t$, where $I_0 = 0.1$ A and $\omega = 10^6$ rad/s. The secondary coil has only $N_2 = 4$ wire turns encircling the primary winding, and is open-circuited. The idealized hysteresis loop of the core material is that in Fig. 6.13(c), with $B_m = 0.5$ T and $H_m = 170$ A/m. Sketch roughly the voltage waveform across the secondary coil terminals within one period of time-harmonic variation of the current in the primary circuit ($T = 2\pi/\omega$), that is, for $0 \le \omega t \le 2\pi$.

6.18. Rotating rod in a uniform magnetic field. A conducting rod rotates uniformly with angular velocity w about an axis that splits it onto two unequal parts of lengths l_1 and l_2 ($l_1 \neq l_2$) in a uniform time-invariant magnetic field of flux density B, as shown in Fig. 6.34. The axis of rotation is perpendicular to the rod, and

vector **B** is parallel to the axis. (a) Find the total induced emf in the rod. What is the total emf if (b) $l_1 = l_2$, (c) $l_2 = 0$, and (d) $l_1 = 0$, respectively?

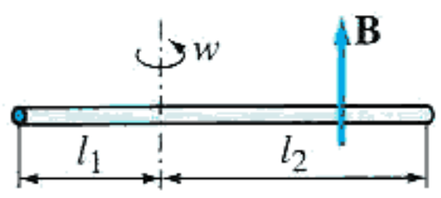

Figure 6.34 Conducting rod uniformly rotating about an excentric axis in a uniform static magnetic field; for Problem 6.18.

6.19. Faraday's wheel. Fig. 6.35 shows Faraday's wheel, consisting of a copper disk of radius a that rotates at a constant angular velocity w about its axis together with an attached axial copper rod, between the poles of a large permanent magnet producing a uniform magnetic field of flux density B, with **B** perpendicular to the disk surface. A pair of terminals, 1 and 2, is defined by taking leads off the rim and the center of the disk (via the rod), respectively. Neglecting the magnetic field due to induced currents in the disk and thickness of the rod, compute (a) the total induced emf in the disk with respect to the reference direction from the disk center to the rim, (b) the Coulomb electric field intensity vector (due to excess charge) at an arbitrary point of the disk, and (c) the voltage ($V = V_{12}$) across the open terminals of the wheel.

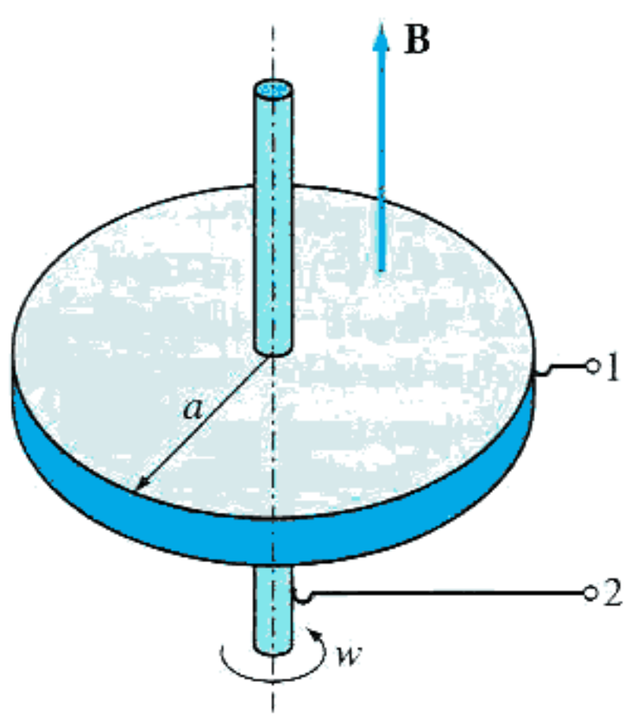

Figure 6.35 Faraday's wheel (a copper disk uniformly rotating between the poles of a large permanent magnet), with open terminals; for Problem 6.19.

6.20. Electric motor – with a linearly sliding bar in a magnetic field. Consider the system with a metallic bar moving in a uniform static magnetic field described in Example 6.11 (Fig. 6.15), and assume that an ideal voltage generator of time-constant emf $\mathcal{E}$ is added in series with the resistor (of resistance R), as shown in Fig. 6.36. Let the values of the system parameters $\mathcal{E}$, R, a, and B be all given and positive (disregard the concrete numerical values from Example 6.11), and perform the analysis of this new system as follows. (a) For the bar at rest ($v = 0$), find the current in the circuit (I) and mechanical force acting on the bar. (b) For the bar sliding (uniformly), sketch the dependence of I on the velocity of the bar (v), for v both positive and negative (movement away from and toward the voltage generator), respectively. (c) Determine the mechanical power of the bar movement (P_{mech}) in terms of the algebraic intensity of the mechanical force on the bar (F_{mech}), for $-\infty < F_{\text{mech}} < \infty$, and sketch this dependence (note that v is a function of F_{mech}). (d) What are the ranges of values of F_{mech} in which the system in Fig. 6.36 operates as a motor ($P_{\text{mech}} < 0$ – the main mode of operation of the system) and as a generator ($P_{\text{mech}} > 0$), respectively? (e) Compute F_{mech} for which the mechanical power of the motor ($|P_{\text{mech}}|$) is maximum. (f) If for the safe operation of the motor, its current has to be smaller in magnitude than $I_{\max}$ (so that the motor does not burn out), what is the corresponding range of velocity v? (g) Establish and discuss the power balance for the system, in both motor and generator mode of operation.

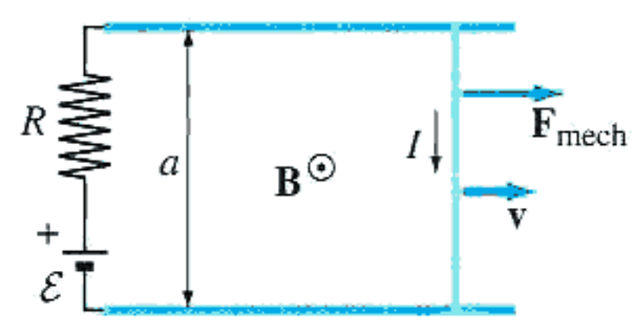

Figure 6.36 Electric motor – with a linearly sliding metallic bar in a static magnetic field (as in Fig. 6.15), and a dc voltage generator added in the circuit; for Problem 6.20.

6.21. Computation for a sliding-bar electric motor. For the electric motor from the previous problem, let $\mathcal{E} = 5$ V, $R = 2\ \Omega$, $a = 1$ m,

$F_{mech} = 2.5$ N, and $v = 10$ m/s. Find B and the power that the voltage generator $(\mathcal{E}, R)$ delivers to the rest of the structure.

6.22. Electric motor – with a rotating bar in a magnetic field. A metallic bar of length a is attached at its one end to a vertical metallic rod, about which, as an axis, it can rotate so that its other end slides without friction along a circular horizontal metallic rail (of radius a), as portrayed in Fig. 6.37. A voltage generator of time-invariant emf $\mathcal{E}$ and internal resistance R is connected between the rail and the rod (axis), and the whole system is situated in a uniform static magnetic field, whose field lines are perpendicular to the plane of the rail and flux density is B. The algebraic intensity of an externally applied mechanical torque on the rail is T_{mech}, for the reference direction of vector $\mathbf{T}_{mech}$ in Fig. 6.37. The losses in the bar, rod, and rail, and the magnetic field due to the current in the circuit (I) can be neglected. (a) What are I and T_{mech} for the bar at rest? (b) If the bar rotates uniformly, find its angular velocity (w). (c) Sketch the dependence of the mechanical power of the bar rotation (P_{mech}) on T_{mech}, for $-\infty < T_{mech} < \infty$, and mark the ranges of system operation as a motor and as a generator, respectively. (d) Compute all relevant powers in the system, and discuss the overall power balance.

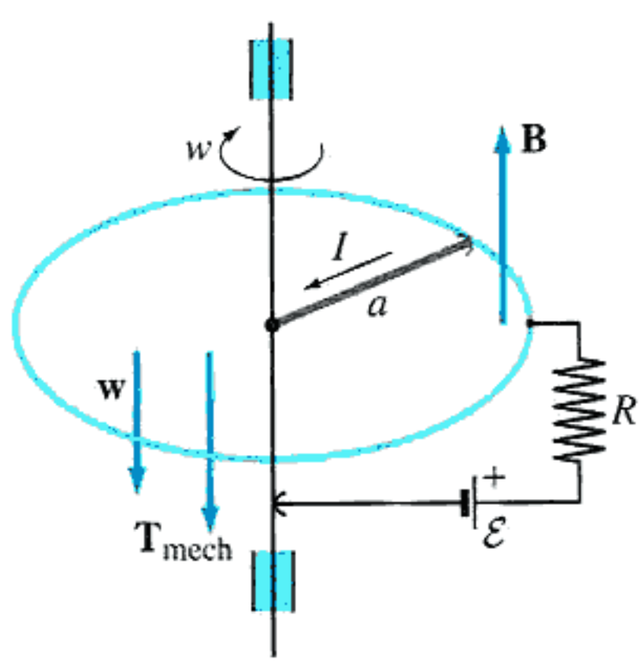

Figure 6.37 Electric motor – with a uniformly rotating metallic bar in a static magnetic field, forming an electric circuit with a dc voltage generator; for Problem 6.22.

6.23. Rotating loop near an infinite dc line current. An infinitely long straight wire conductor situated in air carries a time-invariant current of intensity I. A rectangular wire loop of edge lengths a and b and resistance R rotates with a constant angular velocity w about its axis that is parallel to the conductor and at a distance c from it, as shown in Fig. 6.38(a). At an instant $t = 0$, the loop and conductor lie in the same plane (plane of drawing). Neglecting the magnetic field due to induced currents in the loop, determine (a) the induced emf in the loop and (b) the instantaneous mechanical power of loop rotation. [To compute the magnetic flux through the loop, adopt the integration surface consisting of a cylindrical part of radius r_1 and a flat part of width $r_2 - r_1$, as indicated in Fig. 6.38(b), where r_1 and r_2 can be found using the cosine rule. See also the flux computation in Fig. 7.9(c).]

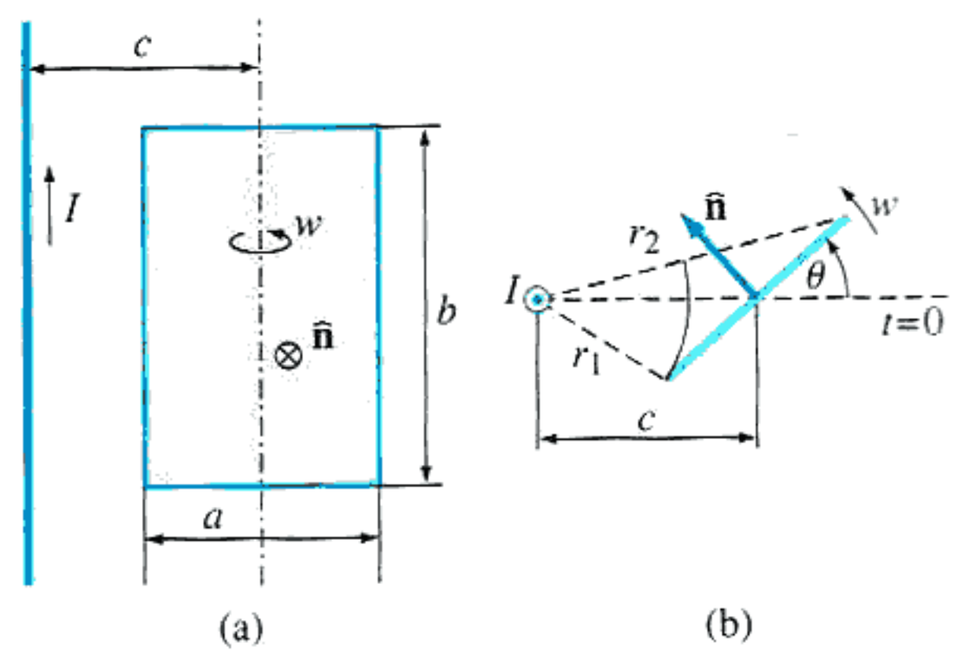

Figure 6.38 Rectangular loop rotating in the magnetic field due to an infinitely long wire with a steady current: (a) side view at an instant $t = 0$ and (b) top (cross-sectional) view at an arbitrary instant t, with a suggested integration surface (in two parts) bounded by the loop; for Problem 6.23.

6.24. System for measurement of fluid velocity with an ideal voltmeter. If in the system for measurement of fluid velocity based on motional electromagnetic induction described in Example 6.14 the voltmeter is ideal, i.e., the intensity of the current flowing through its terminals is so low that it can be assumed to be zero, express (a) the electric field due to excess charge in the region between the capacitor plates and (b) the voltage indicated by the voltmeter in terms of the fluid velocity, v, and other parameters of the system.

6.25. Thévenin generator for fluid flow in a magnetic field. Consider the Thévenin equivalent generator for the system with motional

electromagnetic induction from Example 6.14 – that replaces the rest of the system with respect to the voltmeter in Fig. 6.18, as indicated in Fig. 6.39. (a) Show that the emf and internal resistance of this generator, computed as the open-circuit voltage of the circuit (in Fig. 6.18) it represents and input resistance of the circuit (with all the excitations shut down), equal $\mathcal{E}_T = vBd$ and $R_T = d/(\sigma S)$, respectively. (b) Obtain the expression for the velocity of the fluid in Eq. (6.108) using the generator from (a).

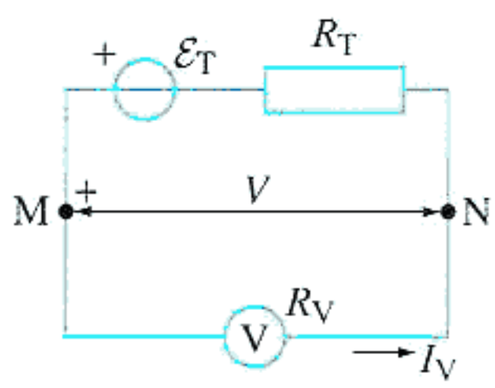

Figure 6.39 Thévenin equivalent generator at terminals (M and N) of the voltmeter in Fig. 6.18; for Problem 6.25.

6.26. Fluid flow through a cylindrical capacitor with dc current. A nonmagnetic liquid of conductivity σ flows between the conductors of a very long coaxial cable of conductor radii a and b ($a < b$), as depicted in Fig. 6.40. Both the inner conductor and the inner surface of the outer conductor of the cable are insulated by a thin layer of perfect dielectric. At one end, the cable is fed by an ideal current generator of time-constant current intensity I_g, while the other end is short-circuited. A cylindrical capacitor of length l is placed inside the cable such that its electrodes (thin cylindrical plates), with radii a and b, are tightly pressed against the respective (insulated) cable conductors. A voltmeter, whose internal resistance, including the resistance of the interconnecting conductors, is R_V, is connected to the capacitor. The velocity of the fluid, considered to be uniform, is v. Calculate (a) the magnetic flux density vector, (b) the induced electric field intensity vector, (c) the current density vector, and (d) the Coulomb electric field intensity vector (due to excess charge) – in the region between the electrodes of the cylindrical capacitor, as well as (e) the voltage indicated by the voltmeter.

6.27. Nonuniform fluid flow and motional induction. Consider the structure from Example 6.14, and assume that the velocity of the fluid is

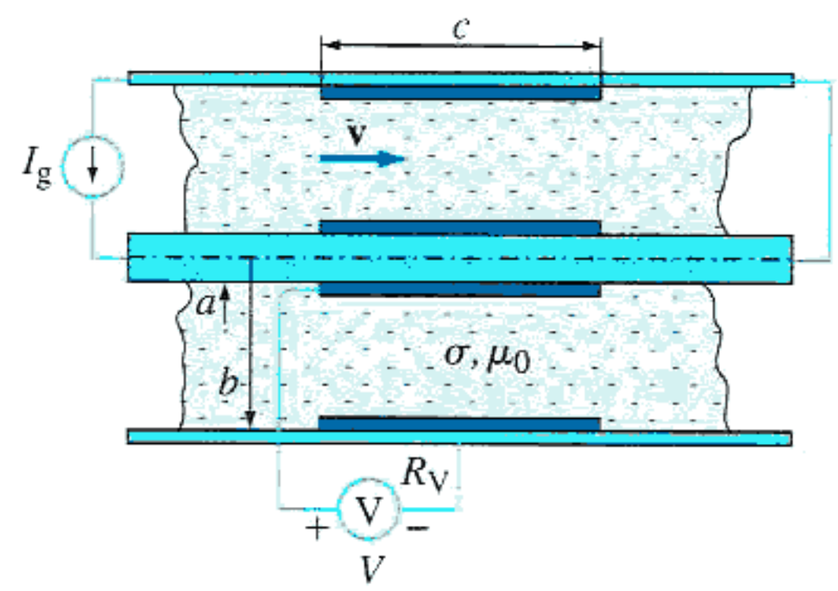

Figure 6.40 System for measurement of conducting fluid flow velocity using motional electromagnetic induction inside a cylindrical capacitor with steady current; for Problem 6.26.

nonuniform, given by $v(x) = v_0[1 - (2x/d)^2]$, $-d/2 \le x \le d/2$, where v_0 is a constant, as well as that a variable resistor (rheostat) is connected to the capacitor plates in place of the voltmeter in Fig. 6.18, as shown in Fig. 6.41. (a) Find the parameters of the Thévenin equivalent generator – to replace the rest of the structure with respect to the rheostat, as in Fig. 6.39. (b) If the resistance of the rheostat is R, what is the voltage across it?

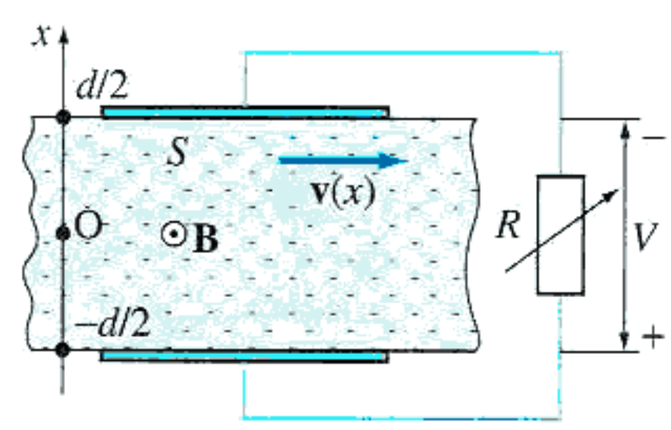

Figure 6.41 Structure in Fig. 6.18 but with a nonuniform fluid velocity, $v(x)$, and a variable resistor connected to the capacitor plates; for Problem 6.27.

6.28. Measurement of fluid velocity and conductivity. For the structure described in the previous problem, let $S = 0.5\ \text{m}^2$, $d = 10$ cm, and $B = 0.1$ T. When the resistance of the rheostat is set to $R = R_0 = 40\ \text{m}\Omega$, its voltage is $V = V_0 = 30$ mV, whereas $V = 2V_0$ if $R = 4R_0$. Based on these data, compute the central velocity (for $x = 0$), v_0, and conductivity, σ, of the fluid, using the Thévenin equivalent generator (from the previous problem).

6.29. Moving contour in a nonuniform dynamic magnetic field. A rectangular contour of side lengths a and b moves along the x-axis with a constant velocity v in a time-harmonic magnetic field of angular frequency ω, which can be considered to be low, and flux density $B(x, t) = B_0 \cos kx \cos \omega t$, where B_0 and k are constants, and vector $\mathbf{B}$ is normal to the plane of the contour, as shown in Fig. 6.42. At $t = 0$, the center of the contour coincides with the coordinate origin ($x = 0$). Find the emf induced in the contour.

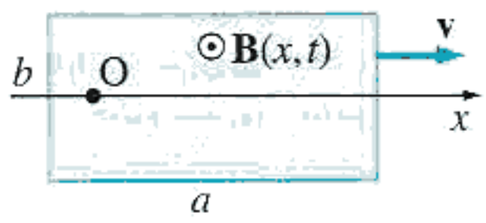

Figure 6.42 Rectangular contour moving in a nonuniform low-frequency time-harmonic magnetic field; for Problem 6.29.

6.30. Rotating loop near an infinite ac line current. Repeat Problem 6.23 but for a low-frequency time-harmonic current of intensity $i(t) = I_0 \cos \omega t$ flowing through the infinitely long wire conductor in Fig. 6.38(a), where $\omega = w$.

6.31. Small loop in the magnetic field of a rotating large loop. Assume that the current in the large square loop from Problem 6.16 is time-constant, of intensity I, and that this loop uniformly rotates with an angular velocity ω about its axis of symmetry that is parallel to a pair of its sides. At an instant $t = 0$, it is in the same plane with the small circular loop (as in Fig. 6.33). The magnetic field due to induced currents in the circular loop can be neglected. Find (a) the induced emf in the circular loop and (b) the instantaneous and time-average torque of magnetic forces acting on it.

6.32. Two rotating loops. If in the previous problem the small loop situated in the magnetic field of the rotating large loop also rotates in the same direction with an angular velocity ω_0 ($\omega_0 < \omega$), determine (a) the time-average power of Joule's (ohmic) losses in the small loop and (b) the time-average mechanical power of its rotation.

6.33. Charge flow through the secondary coil on a magnetic core. Fig. 6.43 shows a thin linear ferromagnetic core with cross-sectional area $S = 1\ \text{cm}^2$, mean length $l = 20$ cm, and two windings each having $N = 100$ wire turns and resistance $R = 10\ \Omega$. The first winding is connected via a switch K to a dc voltage generator of emf $\mathcal{E} = 9$ V and internal resistance $R_1 = 20\ \Omega$. The second winding is terminated in a ballistic galvanometer, whose resistance is $R_2 = 5\ \Omega$. The switch K is first open, and there is no residual magnetization in the core. The switch is then closed, and the charge flow indicated by the galvanometer is $Q = 600\ \mu$C. What is the relative permeability of the core?

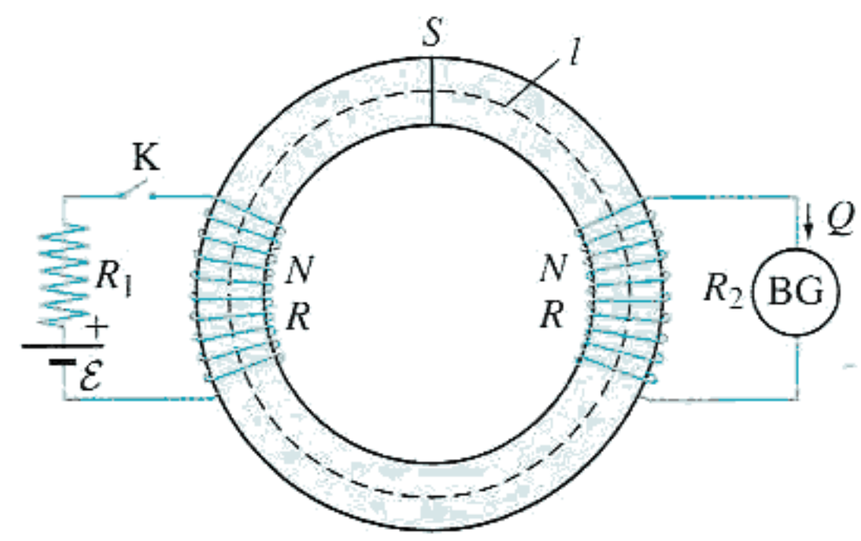

Figure 6.43 Linear ferromagnetic core with two coils, and a voltage generator and ballistic galvanometer (BG) in the primary and secondary circuits, respectively; for Problem 6.33.

6.34. Thin conducting disk in the gap of a magnetic circuit. For the simple linear magnetic circuit from Example 5.14, assume that the cross section of the core in Fig. 5.30(a) is a circle of radius a ($S = \pi a^2$), that the air gap is completely filled with a thin conducting disk of radius a, thickness l_0, conductivity σ, and permeability μ_0, like the one in Fig. 6.24, and that the current in the coil (with N turns of wire) is low-frequency time-harmonic, with intensity $i(t) = I_0 \cos \omega t$. The length and relative permeability of the ferromagnetic portion of the circuit are l and μ_r, respectively. Neglecting the magnetic field due to eddy currents in the disk and core, find l_0 such that the time-average power of Joule's losses dissipated in the disk is maximum, and find that maximum power.

6.35. Eddy currents in Faraday's wheel. (a) Compute the time-average power of Joule's losses due to induced (eddy) currents in Faraday's wheel described in Problem 6.19. (b) What is the magnetic field that these currents produce at the center of the wheel?

6.36. **Eddy currents in an infinite conducting cylinder.** An infinitely long solenoid with N' turns of wire per unit of its length is wound about a conducting ferromagnetic (infinitely long) cylinder of radius a, permeability μ, and conductivity σ. The winding carries a low-frequency time-harmonic current of intensity $i(t) = I_0 \sin \omega t$, and the medium outside the solenoid is air. (a) Determine the time-average per-unit-length power of ohmic losses due to eddy currents induced in the cylinder, neglecting the magnetic field they produce, and then (b) find this magnetic field at the axis of the cylinder (use the procedure from Example 4.14).

6.37. **Hollow disk in a triangular-pulse magnetic field.** A thin hollow conducting disk of radii a and b, thickness δ ($\delta \ll a < b$), conductivity σ, and permeability μ_0 is situated in a uniform slowly time-varying magnetic field, such that the field lines are perpendicular to the disk, as shown in Fig. 6.44. The intensity of this field, $H(t)$, is a periodic alternating triangular-pulse time function of amplitude H_m and period T, sketched in Fig. 6.13(d). Neglecting the magnetic field produced by eddy currents, find (a) the distribution of these currents throughout the disk and (b) the total instantaneous and time-average powers of Joule's losses associated with them, and then (c) compute the magnetic field due to eddy currents at the disk center (point O).

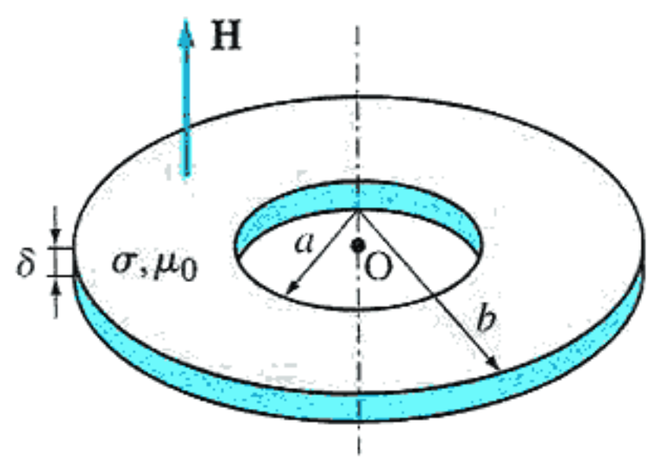

Figure 6.44 Thin hollow conducting disk in a uniform slowly time-varying magnetic field, whose intensity, $H(t)$, is sketched in Fig. 6.13(d); for Problem 6.37.

6.38. **Induction furnace.** Fig. 6.45 shows an induction furnace consisting of a very long air-filled solenoid, with circular cross section of radius a and length l ($l \gg a$), and a toroidal channel (carrying a metal piece that is heated), with a rectangular cross section, placed coaxially around the solenoid and centrally with respect to its length. The inner and outer radii of the toroid are b and c ($a < b < c$), and its height is h. The solenoid has N turns of wire with a low-frequency time-harmonic current of intensity $i(t) = I_0 \cos \omega t$. The channel is completely filled with a metal of conductivity σ and permeability μ_0. Neglecting the end effects (i.e., computing the induced electric field of a solenoid as if it were infinitely long) and the magnetic field due to eddy currents, find (a) the distribution of eddy currents in the channel (these currents produce local heating in the metal, namely, induction heating, that ultimately melts it) and (b) the total time-average power of Joule's losses dissipated to heat in the metal.

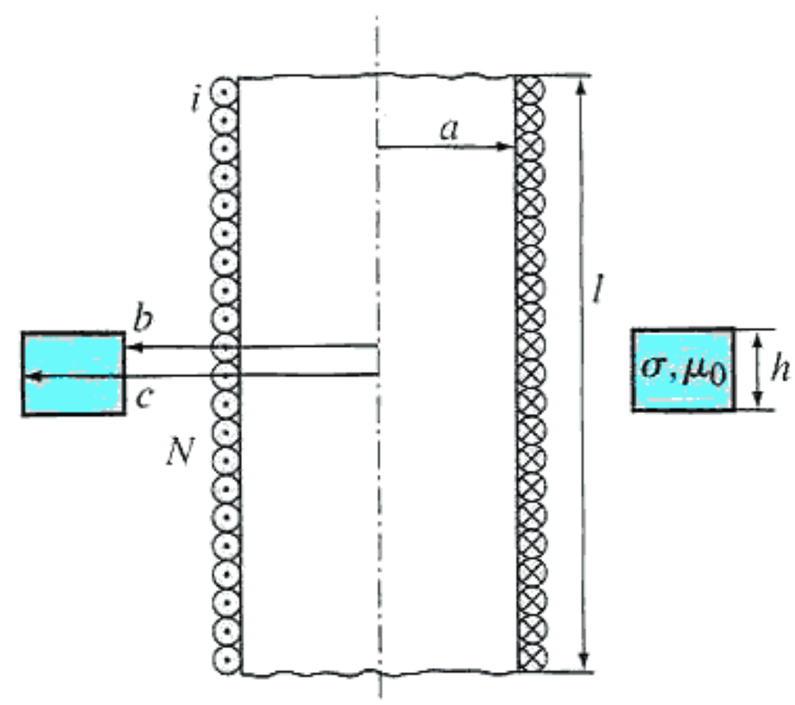

Figure 6.45 Induction furnace: eddy currents accompanying the induced electric field of a very long solenoid with a low-frequency time-harmonic current in the winding heat and melt metal in a toroidal channel of rectangular cross section placed around the solenoid; for Problem 6.38.

6.39. **Eddy currents in a thin conducting spherical shell.** Consider the solenoid described in Example 6.22, and assume that a thin conducting spherical shell of radius b ($b < a$), thickness δ ($\delta \ll b$), conductivity σ, and permeability μ_0 is placed inside it, such that the sphere center lies on the solenoid axis. Determine the time-average power of Joule's losses in the shell, due to eddy currents, neglecting the magnetic field that they produce.

6.40. **Loss power in a laminated ferromagnetic core.** A laminated conducting ferromagnetic core in

the form of a packet of N insulated stacked thin plates of length b, width a, thickness d ($d \ll a$), and conductivity σ is placed in a uniform slowly time-varying magnetic field, such that the field lines are perpendicular to the packet cross section, as shown in Fig. 6.25(c). The flux density of this field, $B(t)$, is a periodic alternating triangular-pulse time function of amplitude B_m and period T, like the function sketched in Fig. 6.13(d). End effects and magnetic field due to eddy currents can be neglected. (a) Find the total time-average power of Joule's losses in the core. (b) How large has to be N for a given total thickness of the packet, c, so that the total loss power does not exceed a given value P?

6.41. Torque on a rotating strip in a magnetic field. For the conducting strip rotating in a uniform time-constant magnetic field from Example 6.24, find the instantaneous torque of magnetic forces on the strip – (a) by integrating torques of magnetic forces on elementary strips (with eddy currents) of width dx in Fig. 6.26(b) (see Example 4.22) and (b) from energy conservation (see Example 6.12), respectively. (c) What is the time-average torque on the strip?

6.42. Inhomogeneous strip in two orthogonal magnetic fields. Fig. 6.46 shows a very long, thin nonmagnetic conducting strip of length l, width a, and thickness δ ($\delta \ll a \ll l$) lying in the xy-plane of a Cartesian coordinate system. The conductivity of the strip varies with the x coordinate, and is given by $\sigma(x) = 4\sigma_0 x^2/a^2$, $-a/2 \le x \le a/2$, where σ_0 is a positive constant. The strip is exposed to two uniform low-frequency time-harmonic magnetic fields of flux density vectors $\mathbf{B}_1(t) = B_0 \cos \omega t\, \hat{\mathbf{x}}$ and $\mathbf{B}_2(t) = B_0 \sin \omega t\, \hat{\mathbf{z}}$, respectively. Neglecting the end effects and the magnetic field due to eddy currents, compute (a) the time-average power of Joule's losses dissipated in the strip and (b) the time-average torque of magnetic forces acting on the strip.

6.43. Eddy currents in two crossed rotating strips. Fig. 6.47 shows a cross section of a very long conductor, of length l, conductivity σ, and permeability μ_0, consisting of two crossed (at a right angle) thin strips, each of width a and thickness δ ($\delta \ll a \ll l$). The conductor uniformly rotates in air about its axis, with an angular velocity ω, in a uniform magnetostatic field, of flux density B (Fig. 6.47). At $t = 0$, one of the strips is parallel to the field lines. Neglecting the end effects and the magnetic field due to eddy currents in the conductor, find (a) the induced electric field vector at an arbitrary point of each of the two strips, (b) the instantaneous power of Joule's losses in each of the strips, (c) the total instantaneous torque of magnetic forces on the conductor, and (d) the time-average torque on the conductor.

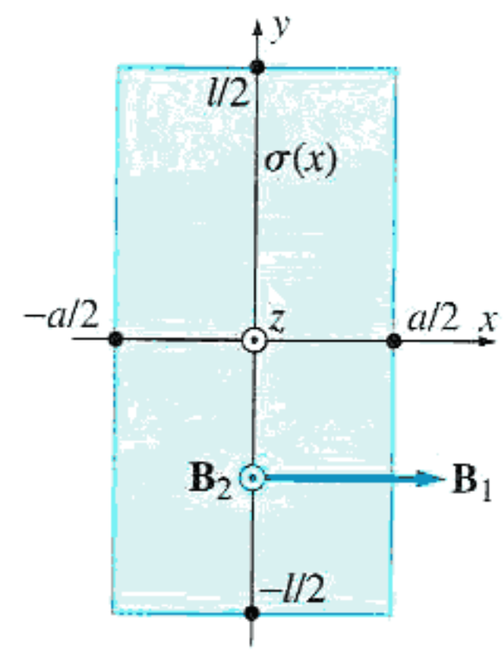

Figure 6.46 Continuously inhomogeneous conducting strip situated in two mutually orthogonal time-harmonic magnetic fields of equal amplitudes and 90° out of phase; for Problem 6.42.

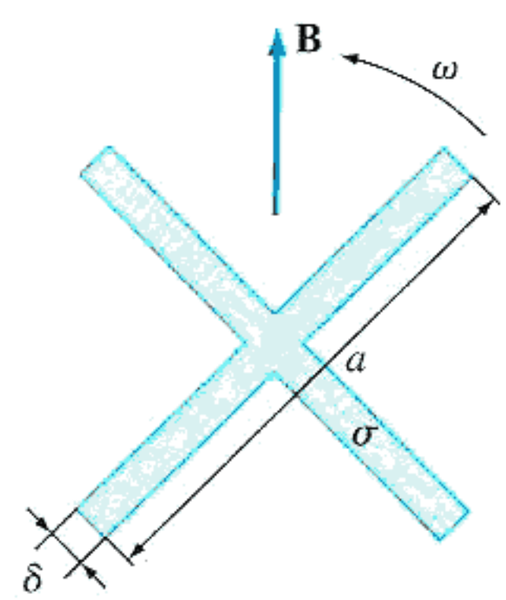

Figure 6.47 Cross section of a conductor composed of two crossed strips rotating in a uniform time-invariant magnetic field; for Problem 6.43.

6.44. Continuously inhomogeneous rotating cylinder. Repeat Example 6.25 but for a continuously inhomogeneous cylinder whose conductivity is given by the following function of the radial coordinate r [Fig. 6.27(b)]: $\sigma(r) = \sigma_0 r/a$, $0 \le r \le a$, where σ_0 is a positive constant.

6.45. Eddy currents in a rotating cylindrical shell. An infinitely long thin conducting cylindrical shell of radius a, thickness δ ($\delta \ll a$), conductivity σ, and permeability μ_0 is rotated in air uniformly about its axis by an externally applied mechanical torque, $\mathbf{T}'_{\text{mech}}$, per unit length of the shell and against the torque of forces of a uniform time-invariant magnetic field of flux

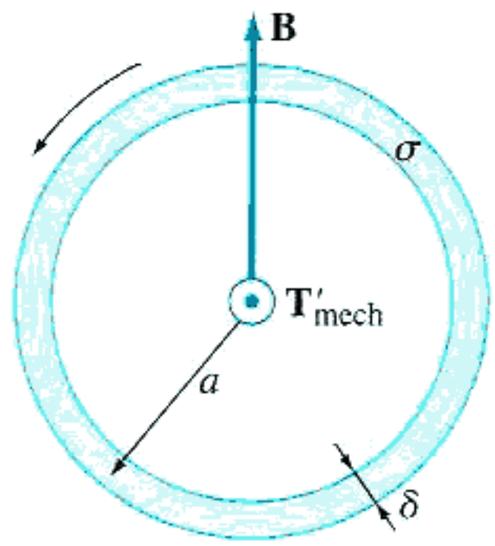

Figure 6.48
Rotating cylindrical conducting shell in a uniform time-invariant magnetic field; for Problem 6.45.

density B, in which the shell resides, as shown in Fig. 6.48. Neglecting the magnetic field due to eddy currents in the shell, find (a) the angular velocity of rotation of the shell (ω) and (b) the per-unit-length mechanical power used to rotate the shell (P'_{mech}).

7 Inductance and Magnetic Energy

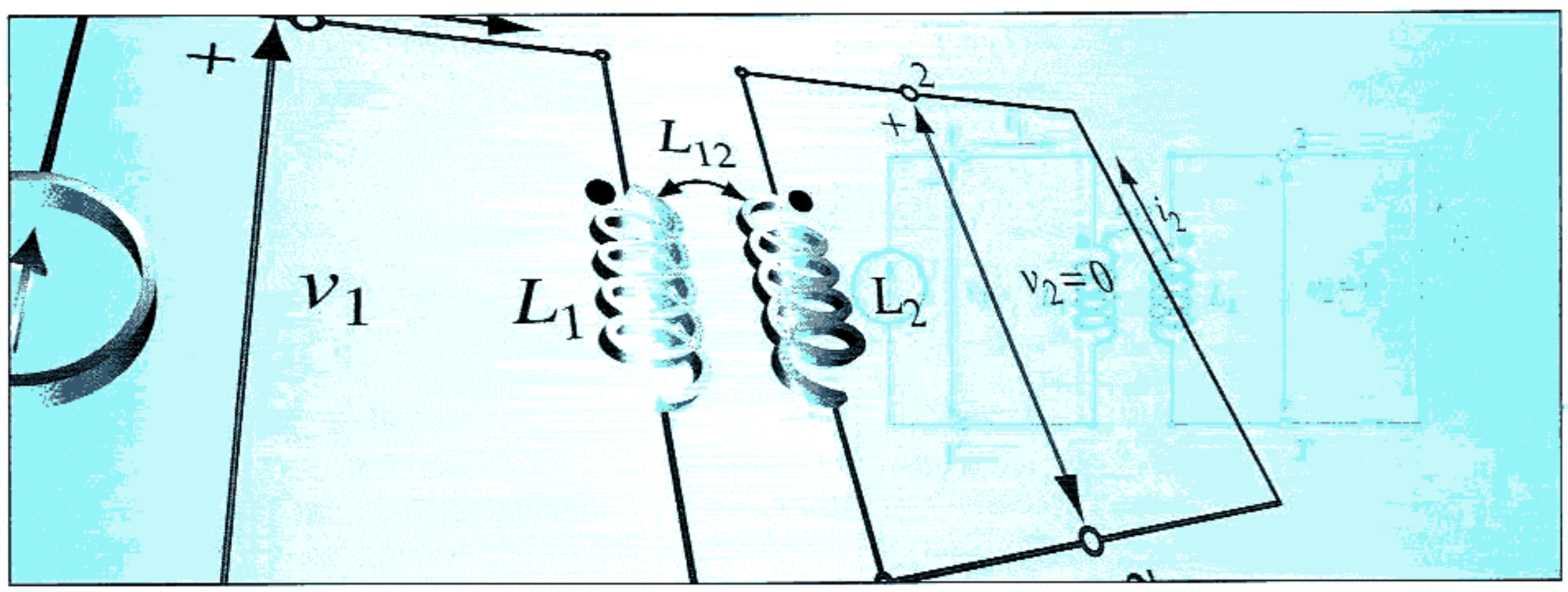

Introduction:

In this chapter, we introduce and study the concepts of self- and mutual inductance. In general, inductance can be interpreted as a measure of transformer electromagnetic induction in a system of conducting contours (circuits) with slowly time-varying currents in a linear magnetic medium. Briefly, self-inductance is a measure of the magnetic flux and induced emf in a single isolated contour (or in one of the contours in a system) due to its own current. Similarly, a current in one contour causes magnetic flux through another contour and induced emf in it, and mutual inductance is used to characterize this coupling between the contours. Some conductor configurations, called inductors, are specially designed to have a desired (large) inductance (they can have many turns of wire and can be loaded with magnetic cores). Along with the resistor and capacitor, the inductor represents another fundamental element in circuit theory and a basic building block for ac electric circuits. The inductance of an inductor is dual to the capacitance of a capacitor.

An equally important concept of energy in magnetic fields is also discussed. We shall see that, just as configurations of charged bodies store electric energy, configurations of current-carrying conductors store magnetic energy. Using circuit-theory terminology, inductors (magnetically coupled or uncoupled) in a circuit contain magnetic energy, in a manner analogous to capacitors as electric energy "containers." We shall introduce magnetic energy density as well. In the case of conductors in the presence of linear magnetic materials, magnetic energy will be related to self- and mutual inductances of the conductors. For systems that contain ferromagnetic materials with pronounced nonlinearity and hysteresis behavior, on the other side, special attention will be paid to establishing a clear physical understanding and precise mathematical characterization of the energy balance in the system, including so-called hysteresis losses in the material.

The material of this chapter represents a culmination of our investigations of steady and slowly

time-varying magnetic fields and electromagnetic induction (Chapters 4–6). On the other hand, it parallels, to a large extent, the electrostatic analysis of capacitors and other systems of charged conducting bodies, including electric energy considerations (Chapter 2). Therefore, a substantial portion of the previous work will be referenced and used here, in both the theoretical narrative and examples.

We shall first study self- and mutual inductance in two separate sections, and then analyze magnetically coupled circuits based on both concepts. Magnetic energy of current-carrying conductors and magnetic energy density in the field will bediscussed next. Finally, the concept of self-inductance will be revisited from the energy standpoint. Examples will include inductance and energy computation for a large variety of theoretically and practically important electromagnetic structures with slowly time-varying and time-invariant currents and fields, ranging from various contours and coils with cores of different shapes and material compositions to several types of transmission lines and circuits with magnetically coupled inductors.

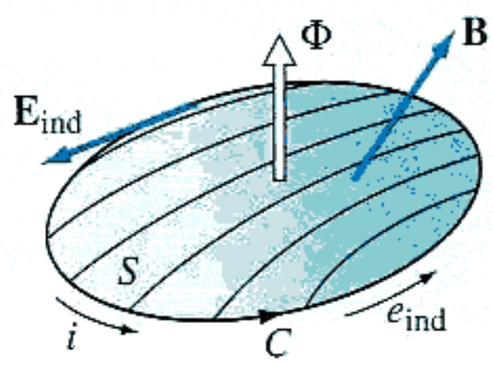

Figure 7.1 Current contour (loop) in a linear magnetic medium.

7.1 SELF-INDUCTANCE

Consider a stationary conducting wire contour (loop), C, in a linear, homogeneous or inhomogeneous, magnetic medium, and assume that a slowly time-varying current of intensity i is established in the contour, as shown in Fig. 7.1. This current produces a magnetic field whose flux density vector, $\mathbf{B}$, at any point of space and any instant of time is linearly proportional to i.[1] The magnetic field, as well as an induced electric field (see Section 6.1), of intensity $\mathbf{E}_{\text{ind}}$, exist both around the contour and inside the wire itself. The magnetic flux through a surface S bounded by C is given by Eq. (4.95) and is also linearly proportional to i. The proportionality constant,

self-inductance (unit: H)

$$\boxed{L = \frac{\Phi}{i},} \tag{7.1}$$

is termed the self-inductance or just inductance of the contour. More precisely, the inductance defined by Eq. (7.1) is the so-called external inductance, since it takes into account only the flux Φ of the magnetic field that exists outside the conductor of the loop. There is also an internal inductance of the loop, due to the flux inside the conductor. We shall introduce the concept of internal inductance in terms of the magnetic energy stored inside the conductor in a later section. Because the surrounding medium is magnetically linear, L depends only on the medium permeability and on the shape and dimensions of the contour, and not on the current intensity i. It is always positive, provided, of course, that the reference orientations of C and S (i.e., the reference directions of i and Φ) are interconnected by the right-hand rule, as in Fig. 7.1.

The induced emf along the loop C is given by Eq. (6.33) and is linearly proportional to $\mathrm{d}i/\mathrm{d}t$. It is interrelated with the flux Φ by means of Faraday's law of electromagnetic induction, and we can write

emf due to self-induction

$$\boxed{e_{\text{ind}} = -\frac{\mathrm{d}\Phi}{\mathrm{d}t} = -L\frac{\mathrm{d}i}{\mathrm{d}t}.} \tag{7.2}$$

This emf is referred to as the emf due to self-induction (or self-induced emf) in the circuit (it is caused by the magnetic field due to the current in the circuit

[1] Since the current is slowly time-varying, its intensity (i) is only a function of time and does not change along the contour.

itself, and not due to currents in other circuits). The unit for the self-inductance is henry (H). From Eqs. (7.1) and (7.2), which represent two equivalent definitions of L, $\mathrm{H} = \mathrm{Wb/A} = \mathrm{V \cdot s/A}$. One henry is a very large unit. Typical values of self-inductances in practice are on the order of mH, μH, and nH.

HISTORICAL ASIDE

Joseph Henry (1797–1878), an American physicist and one of the greatest scientists and inventors in the area of electricity and magnetism ever, was a professor of natural philosophy at Princeton and the first secretary of the Smithsonian Institution. From 1819 to 1822, he attended the Albany Academy, where he was appointed professor of mathematics and natural philosophy in 1826. Although his teaching duties were extremely heavy, Henry soon became the foremost American scientist of his time. He discovered electromagnetic induction independently of Faraday (1791–1867). In fact, Henry had performed the key experiments that led to the discovery of induction ahead of Faraday, in 1830, but Faraday published his discovery first, in 1831. On the other side, Henry is fully credited for the discovery of self-induction. It was his idea to wind many layers of insulated wire on an iron core and thus obtain electromagnets of unmatched power. In a demonstration at Yale University in 1831, his electromagnet lifted more than a ton of iron (previous electromagnets were capable of lifting only a couple of kilograms). Experimenting with electromagnets, he observed a large spark that was generated whenever the circuit was broken, and thus discovered self-induction (in 1831). He realized that, in general, a time-varying current in a circuit not only induces electromotive force in another circuit (mutual induction), but also in itself (self-induction). He also defined the associated property of a circuit, its self-inductance, as a measure of its ability to "self-induce" electromotive force. He found that "coiling" of the wire greatly enhances the self-inductance of the circuit. The same year, he demonstrated his electric motor based on a continuous oscillating motion of a straight electromagnet with two coils at its ends. The electromagnet rocked back and forth on a horizontal axis with its ends being alternately attracted and repelled by two vertical permanent magnets and its polarity being reversed automatically in the same rhythm by alternately connecting the coils to electrochemical cells (sources). Although still an experimental laboratory device, Henry's motor was much closer to a mechanically useful practical machine than Faraday's 1821 motor. It was just one year later, in 1832, that William Sturgeon (1783–1850) invented the commutator and the first motor with continuous rotary motion, which was a rotary analogue of Henry's oscillating motor and essentially a "prototype" of our modern dc motors. In another stunning demonstration to his students at the Albany Academy, in 1831, Henry strung a mile of wire all around the inside of the lecture hall to connect an electromagnet to a battery. The magnet was placed close to one end of a pivot mounted steel bar, whose other end, in turn, was next to a bell. After the circuit was closed and a current "sent" from the battery to the coil of the electromagnet, a steel bar swung toward the magnet, striking the bell on the other end. Breaking the connection, next, made the electromagnet lose its force and release the bar, which was then free to strike again. This was the world's first electrical relay (electromechanical switch). In addition, by connecting and disconnecting the battery to the circuit in a particular pattern, the steel bar, a mile away, could be made to ring the same series of signals on the bell, and this is nothing else but telegraphy. Although, obviously, Henry invented the telegraph in 1831, it is Samuel Morse (1791–1872) who is credited for this invention [Henry did not patent any of his devices, and actually helped Morse to put his telegraph model to practical use and transmit the first telegraph message using the Morse code (invented in 1838) from

Baltimore to Washington, D.C. on May 24, 1844]. In 1832, Henry became professor of natural philosophy (physics) at Princeton University (then College of New Jersey). After the Smithsonian Institution was established in 1846, Henry was named its first secretary (director). He was also the second president (elected in 1868) of the National Academy of Sciences, and he held both positions until his death. In his honor, we use henry (H) as the unit for inductance. *(Portrait: Library of Congress, Brady-Handy Photograph Collection)*

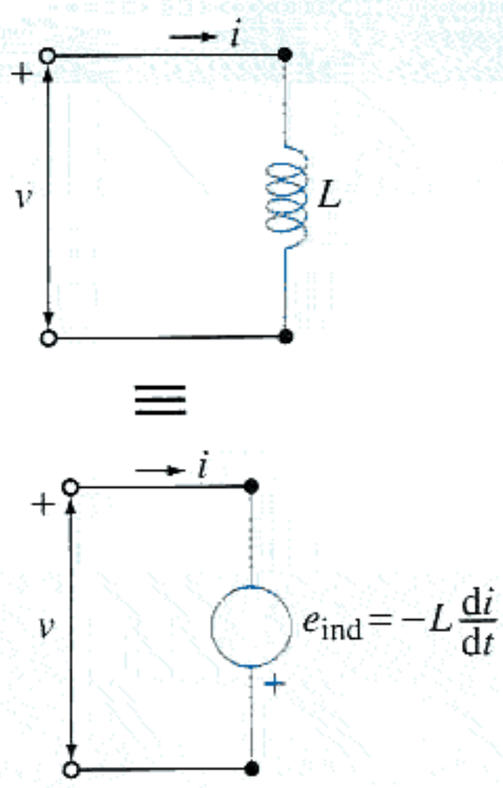

Figure 7.2 Circuit-theory representation of an inductor and equivalent controlled voltage generator.

Note that, while the emf definition of self-inductance in Eq. (7.2) does not make any sense for steady currents, the flux definition in Eq. (7.1) can be used in practically the same way under both dynamic and static conditions. Namely, a dc current I that is assumed to flow in the contour produces the flux Φ through the contour in the same way a (slowly) time-varying current does, and the inductance obtained as $L = \Phi/I$ is equal to that obtained, for the same contour, using either Eq. (7.1) or (7.2) and time-varying current. On the other hand, the flux Φ due to the current I is time-invariant, and thus no emf is generated in the contour.

Every conducting loop or circuit has some inductance (self-inductance), usually as an undesirable side effect, which can often be neglected. In practical applications, however, we frequently design and use conductors that are specially arranged and shaped (such as a conducting wire wound as a coil), and sometimes loaded with magnetic cores, to supply a certain (large) amount of inductance. Such a device, with its inductance L as its basic property, is called an inductor. Just as a capacitor can store electric energy, an inductor can store magnetic energy, as we shall see in a later section. Resistors, capacitors, and inductors are basic circuit elements that are combined, together with voltage and current generators, to form arbitrary RLC circuits.

Fig. 7.2 shows the circuit-theory representation of an inductor. When a time-varying current of intensity i flows through the inductor terminals, the emf e_{ind} is induced in the inductor, given by Eq. (7.2), where L is the inductance of the inductor. With respect to its terminals, the inductor can now be replaced by an equivalent ideal voltage generator whose emf equals e_{ind} (this is a voltage generator controlled by the time derivative of a current), as indicated in Fig. 7.2. The reference direction of this emf is the same as the reference direction of the current i (see Fig. 7.1). The voltage v across the inductor terminals in Fig. 7.2 is hence

element law for an inductor

$$\boxed{v = -e_{ind} = L\frac{di}{dt}.} \tag{7.3}$$

This is the element law (current-voltage characteristic) for an inductor. It tells us that v is linearly proportional to the rate of change of i in time, with L as the proportionality constant. Its form is just opposite to the element law for a capacitor, Eq. (3.45), and we say that an inductor and a capacitor are dual elements. These two laws, the element law for a resistor (Ohm's law), Eq. (3.72), Kirchhoff's current and voltage laws, Eqs. (3.42) and (1.92), and element laws for an ideal voltage generator, Eq. (3.116), and an ideal current generator, Eq. (3.127), represent a full set of basic equations of circuit theory for analysis of linear ac circuits.

Note that the model in Fig. 7.2 actually represents an ideal inductor, which does not include any parasitic effects, such as parasitic capacitances between the adjacent turns in a coil and Joule's losses (in wires and magnetic cores). These effects are present to a greater or lesser extent in all real inductors, but can be neglected in many practical situations. The only effect modeled by an ideal inductor is the emf

due to self-induction, e_{ind}. On the other side, it is assumed in circuit theory that the magnetic flux, induced emf, and magnetic energy are concentrated only in the inductors in a circuit, while the magnetic field and the associated flux, emf, and energy due to the connecting conductors are assumed to be negligible. In practice, there is always an induced emf distributed along conductors in the circuit (in the ac regime), and it depends on the shape and dimensions of the conductors. However, this emf, i.e., the inductance of the conductors, can, again, be neglected in many practical applications. We recall that similar assumptions of zero capacitance and zero resistance of the conductors have been made while introducing circuit-theory representations of a capacitor and a resistor in Figs. 2.15 and 3.9, respectively. The circuit-theory model, therefore, deals with connecting conductors (lines between the elements in circuit layouts) as if they were all ideal short-circuits, where the shape, dimensions, and material properties of the interconnects are assumed to be completely irrelevant for the operation (and analysis and design) of the circuit.

Finally, inductors filled with magnetically nonlinear materials (e.g., the coil of Fig. 6.13) are nonlinear circuit elements. In such cases, the magnetic properties (permeability) of the material depend on the applied magnetic field intensity, H, whereas H is always proportional to i. Consequently, the inductance of the inductor depends on the current intensity,

$$\boxed{L = L(i),} \tag{7.4}$$

nonlinear inductor

which is analogous to the relations in Eqs. (2.114) and (3.74) for a nonlinear capacitor and a nonlinear resistor, respectively.

Example 7.1 Inductance of a Very Long Air-Filled Solenoid

An air-filled solenoidal coil has $N = 200$ turns of wire. The length of the solenoid is $l = 20$ cm and the surface area of its cross section is $S = 4$ cm^2. The solenoid can be considered as very long, so that the end effects can be neglected. Under these circumstances, find the inductance of the coil.

Solution Let us assume a slowly time-varying current of intensity i in the coil, find the magnetic flux through all of its turns, and use Eq. (7.1) for the inductance. By neglecting the end effects, we also assume that the magnetic field produced by the current i is uniform inside the entire solenoid (as for an infinitely long solenoid). This field is given by Eq. (6.48), which leads to the following expressions for the magnetic flux through a surface spanned over a single turn of the coil and the total flux through the coil:

$$\Phi_{\text{single turn}} = \mu_0 HS \quad \longrightarrow \quad \Phi = N\Phi_{\text{single turn}} = \frac{\mu_0 N^2 Si}{l}, \tag{7.5}$$

where the reference direction for Φ is adopted in accordance to the right-hand rule with respect to the reference direction for i. The inductance of the coil is hence

$$\boxed{L = \frac{\Phi}{i} = \frac{\mu_0 N^2 S}{l},} \tag{7.6}$$

L – very long solenoid

that is, $L = 100\ \mu$H for the given numerical data. It is the same for any shape of the solenoid cross section (provided that the solenoid is very long).

Example 7.2 Coil on an Inhomogeneous Thick Toroidal Core

A coil with N turns of wire is wound over a thick toroidal core of rectangular cross section made of two ferromagnetic layers of permeabilities μ_1 and μ_2, as portrayed in Fig. 7.3. The

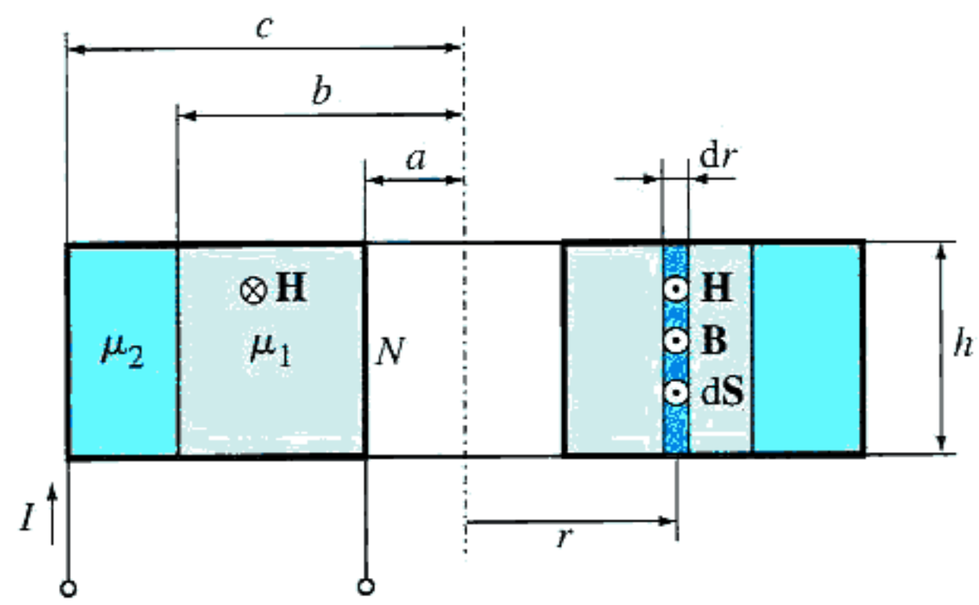

Figure 7.3 Evaluation of the inductance of a coil wound on a thick toroidal core with two linear ferromagnetic layers; for Example 7.2.

inner and outer radii of the toroid are a and c, its height is h, and the radius of the boundary surface between the layers is b ($a < b < c$). Calculate the inductance of the coil.

Solution If a steady current of intensity I is assumed to flow in the coil (Fig. 7.3), the magnetic field intensity $H(r)$ inside the core (in both ferromagnetic layers) is given by Eq. (5.83). The magnetic flux through the coil is then [see Fig. 7.3 and Eqs. (5.84) and (5.92)]

$$\Phi = N\int_{r=a}^{c} B(r)\,\mathrm{d}S = N\left[\int_a^b \mu_1 H(r)\,\mathrm{d}S + \int_b^c \mu_2 H(r)\,\mathrm{d}S\right] = \frac{N^2 I h}{2\pi}\left(\mu_1 \ln\frac{b}{a} + \mu_2 \ln\frac{c}{b}\right), \tag{7.7}$$

and the inductance of the coil

$$L = \frac{\Phi}{I} = \frac{N^2 h}{2\pi}\left(\mu_1 \ln\frac{b}{a} + \mu_2 \ln\frac{c}{b}\right). \tag{7.8}$$

Example 7.3 External Inductance p.u.l. of a Thin Two-Wire Line

Find the external inductance per unit length of a thin symmetrical two-wire transmission line in air. The conductor radii are a and the distance between their axes is d ($d \gg a$).

Solution The two-wire line can be considered as an infinitely long wire loop that closes upon itself at both ends of the line at infinity. Fig. 7.4 shows the cross section of the line. The procedure of evaluation of the line inductance (external self-inductance) per unit length is analogous (dual) to the procedure of evaluation of the capacitance per unit length of a thin two-wire line in Example 2.15. We assume that a slowly time-varying current of intensity i (or a steady current of intensity I) is established in the line (Fig. 7.4). At a point M in the plane containing the axes of conductors, the magnetic flux density vectors $\mathbf{B}_1$ and $\mathbf{B}_2$ due to currents (of the same magnitude and opposite directions) in individual conductors of the line are collinear, so that the resultant magnetic flux density is

$$B = B_1 + B_2 = \frac{\mu_0 i}{2\pi}\left(\frac{1}{x} + \frac{1}{d-x}\right), \tag{7.9}$$

where x is the distance from the axis of the first conductor.

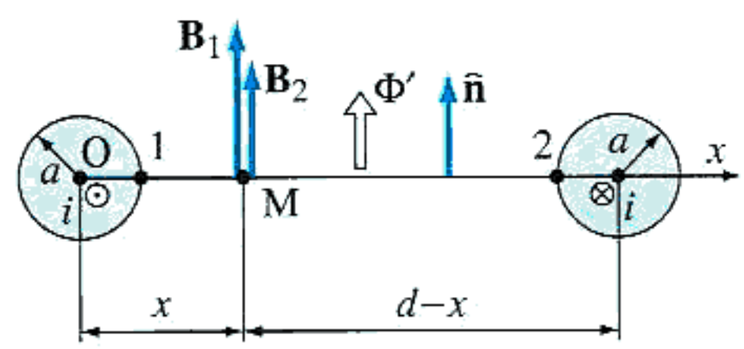

Figure 7.4 Evaluation of the external inductance per unit length of a thin two-wire transmission line in air (cross section of the structure); for Example 7.3.

As the structure is infinitely long, we consider only a part of it that is l long and compute the magnetic flux through the flat surface of length l that is spanned between the line conductors (such integration surface is the right choice because **B** is perpendicular to the surface) and oriented as required by the right-hand rule with respect to the adopted reference direction of the line current. This flux is given by

$$\Phi = \int_{x=a}^{d-a} B \underbrace{l\,\mathrm{d}x}_{\mathrm{d}S} = \frac{\mu_0 i l}{2\pi} \int_a^{d-a} \left(\frac{1}{x} + \frac{1}{d-x}\right) \mathrm{d}x = \frac{\mu_0 i l}{\pi} \ln \frac{d-a}{a} \approx \frac{\mu_0 i l}{\pi} \ln \frac{d}{a} \tag{7.10}$$

[see the integration in Eq. (2.140)]. Hence, the external inductance per unit length (per each meter) of the line comes out to be

$$\boxed{L' = L_{\text{p.u.l.}} = \frac{\Phi'}{i} = \frac{\Phi}{il} = \frac{\mu_0}{\pi} \ln \frac{d}{a},} \tag{7.11}$$

L' – thin two-wire line (unit: H/m)

where Φ' is the flux per unit length of the line.

As a numerical example, for $d/a = 30$, $L' = 1.36\ \mu\text{H/m}$. If the line is 100 m long, its total external inductance amounts to $L = 136\ \mu\text{H}$.

Example 7.4 External Inductance p.u.l. of a Coaxial Cable

Consider an air-filled coaxial cable. The radius of the inner conductor of the cable is a and the inner radius of the outer conductor is b ($b > a$). Obtain the expression for the external inductance per unit length of the cable.

Solution Let us assume a dc current of intensity I flowing through the line conductors, as shown in Fig. 7.5. The associated magnetic flux density vector, **B**, is circular with respect to the cable axis and its magnitude, $B(r)$, in the dielectric is given by the second expression in Eq. (4.61), where r is the distance from the axis and $a < r < b$. Computing the magnetic flux through a flat surface of length l spanned between the conductors (Fig. 7.5) then yields the following expression for the external inductance per unit length of the cable:

$$\boxed{L' = \frac{\Phi}{Il} = \frac{1}{Il} \int_{r=a}^{b} B(r)\,\mathrm{d}S = \frac{1}{Il} \int_a^b \frac{\mu_0 I}{2\pi r}\, l\,\mathrm{d}r = \frac{\mu_0}{2\pi} \ln \frac{b}{a},} \tag{7.12}$$

L' – coaxial cable

where the dielectric can be any nonmagnetic material ($\mu = \mu_0$). The procedure is dual to the voltage and capacitance computation in Example 2.10.

As a numerical example, the inductance per unit length of an RG-11 coaxial cable, having $a = 0.6$ mm and $b = 3.62$ mm (dielectric is polyethylene), is computed to be $L' = 359$ nH/m.

Comparing the expression for L' in Eq. (7.12) and the expression for the capacitance per unit length of the same cable, $C' = 2\pi\varepsilon_0/\ln(b/a)$ [see Eq. (2.123)], we note that the following

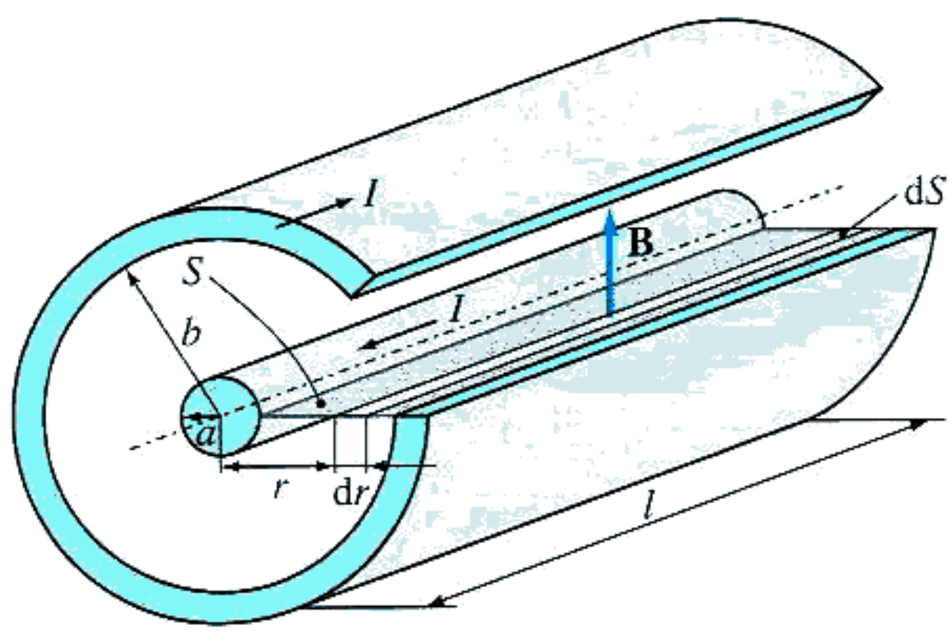

Figure 7.5 Evaluation of the external inductance per unit length of a coaxial cable; for Example 7.4.

relationship exists between the two parameters:

duality of L' and C' for air dielectric

$$\boxed{L'C' = \varepsilon_0\mu_0.} \tag{7.13}$$

Comparing then the expressions in Eqs. (7.11) and (2.141), we also note that the same is true for a thin two-wire line in air. As a matter of fact, as we shall prove in a later chapter, the same relationship exists between L' and C' for any two-conductor transmission line with air dielectric. For a transmission line having homogeneous linear dielectric of arbitrary permittivity and permeability, $L'C' = \varepsilon\mu$. Using these relations, we can now very easily obtain the inductance per unit length of transmission lines (with homogeneous linear dielectrics) for which we already have the capacitance per unit length (found in Chapter 2). For example, from the expression in Eq. (2.146) for the capacitance per unit length of the transmission line consisting of a thin wire conductor and a grounded conducting plane in Fig. 2.24(a), we can directly write the expression for the external inductance per unit length of this line:

$$L' = \frac{\varepsilon_0\mu_0}{C'} = \frac{\mu_0}{2\pi}\ln\frac{2h}{a}. \tag{7.14}$$

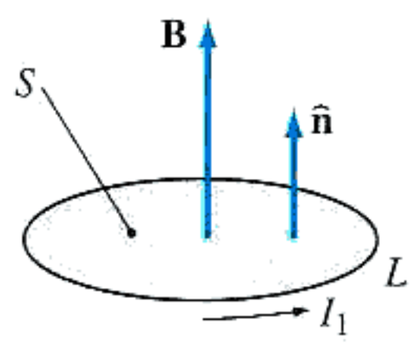

Figure 7.6 Superconducting contour of inductance L in a uniform magnetostatic field; for Example 7.5.

Example 7.5 Superconducting Contour in a Magnetic Field

A superconducting planar contour of area S and inductance L is situated in a uniform magnetostatic field of flux density B. The contour is first positioned such that the vector $\mathbf{B}$ is perpendicular to the plane of the contour, as in Fig. 7.6. In this state, a steady current of intensity I_1 flows along the contour. The contour is then turned such that its plane becomes parallel to $\mathbf{B}$. Find the current I_2 in the contour in the new steady state.

Solution The total magnetic flux through the contour in the first state is

$$\Phi_1 = LI_1 + BS, \tag{7.15}$$

where the first term is the flux due to the current (I_1) in the contour (self-flux) and the second term is the flux of the external magnetic field ($\mathbf{B}$), i.e., the flux due to other currents (or permanent magnets) in the system (mutual flux).

In the second state,

$$\Phi_2 = LI_2, \tag{7.16}$$

since the mutual flux is zero ($\mathbf{B}\cdot\mathbf{S} = 0$).

The total magnetic flux through a superconducting contour cannot be changed [see Eq. (6.135)], which means that

$$\Phi_1 = \Phi_2. \tag{7.17}$$

Combining Eqs. (7.15)–(7.17), the current in the contour in the second state is hence

$$I_2 = I_1 + \frac{BS}{L}. \tag{7.18}$$

Note that the increment in current between the two states, $\Delta I = BS/L$, is induced in the contour exactly at the amount that completely compensates, via the associated magnetic field, the change of the mutual flux (from BS to zero), maintaining thus a constant total flux through the contour.

Problems: 7.1–7.9; *Conceptual Questions* (on Companion Website): 7.1–7.10; *MATLAB Exercises* (on Companion Website).

7.2 MUTUAL INDUCTANCE

Consider now two stationary conducting wire contours, C_1 and C_2, in a linear (homogeneous or inhomogeneous) magnetic medium, as shown in Fig. 7.7. Let the first contour carry a slowly time-varying current of intensity i_1. As a result, a

magnetic field, of flux density $\mathbf{B}_1$, is produced everywhere, and $\mathbf{B}_1$, which is a function of both the spatial coordinates and time, is linearly proportional to i_1. Some of the lines of $\mathbf{B}_1$ pass through the second contour, i.e., through a surface S_2 bounded by C_2. These lines constitute the magnetic flux through the second contour due to the current i_1, which can be expressed as

$$\Phi_2 = \int_{S_2} \mathbf{B}_1 \cdot d\mathbf{S}_2. \tag{7.19}$$

The flux Φ_2 is linearly proportional to i_1 as well:

$$\Phi_2 = L_{21} i_1, \tag{7.20}$$

where the proportionality constant L_{21} is called the mutual inductance between the two contours and is obtained as

$$\boxed{L_{21} = \frac{\Phi_2}{i_1}.} \tag{7.21}$$

mutual inductance (unit: H)

Note that the symbol M is also used to denote mutual inductance. It is a measure of magnetic coupling between the contours. Its magnitude depends on the shape, size, and mutual position of the contours, and on the magnetic properties (permeability) of the medium. The mutual inductance can be both positive and negative, depending on the adopted reference orientation of each of the contours for their given mutual position. Namely, if a positive current i_1 in the contour C_1 gives rise to a positive magnetic flux Φ_2 for the orientation of the surface S_2 that is in accordance to the right-hand rule with respect to the orientation of the contour C_2, the mutual inductance is positive. Otherwise, it is negative.[2] The mutual inductance is also expressed in henrys.

By applying Faraday's law of electromagnetic induction, Eq. (6.34), to the flux in Eq. (7.20), we obtain the induced emf (due to transformer induction) in the contour C_2:

$$\boxed{e_{\text{ind2}} = -\frac{d\Phi_2}{dt} = -L_{21}\frac{di_1}{dt}.} \tag{7.22}$$

emf due to mutual induction

Eqs. (7.21) and (7.22) should be regarded as equivalent definitions of mutual inductance. They indicate that the mutual inductance between two magnetically coupled contours (circuits) can be evaluated by assuming a current (i_1) to flow in one contour (primary circuit) and computing or measuring the magnetic flux (Φ_2) or the induced emf (e_{ind2}) in the other contour (secondary circuit). Again, note that, while the flux definition of L_{21} in Eq. (7.21) can be used for both time-varying

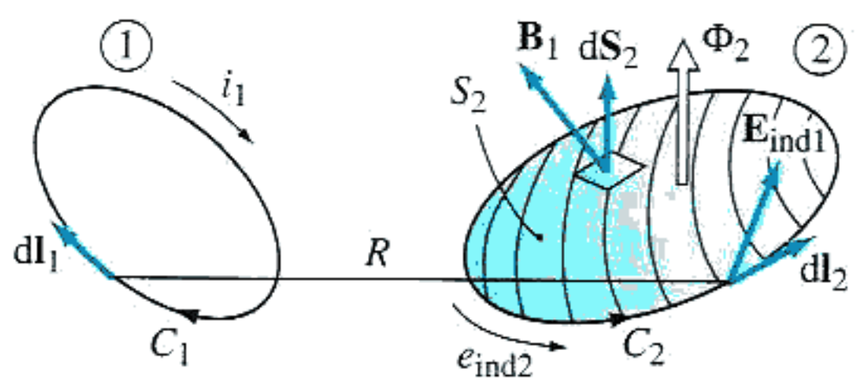

Figure 7.7 Two magnetically coupled conducting contours.

[2] In some texts, the information about the sign of the mutual inductance for specific reference orientations of contours is not included in its definition, i.e., mutual inductance is defined as always being nonnegative.

and steady currents, the emf definition in Eq. (7.22) makes sense for time-varying currents only.

Conversely, if we assume that a current i_2 flows along the contour C_2 and determine the associated magnetic flux Φ_1 through the contour C_1, the mutual inductance between the contours is given by

$$L_{12} = \frac{\Phi_1}{i_2}, \tag{7.23}$$

with an analogous expression using the induced emf e_{ind1} along the contour C_1. Because of reciprocity (in a linear system, transfer functions remain the same if the source location and the location at which the response to the source is observed are interchanged),

reciprocity of mutual induction

$$\boxed{L_{12} = L_{21}.} \tag{7.24}$$

If the medium around the contours is air (or any nonmagnetic medium), the induced electric field intensity vector due to the current in the first contour is given by [see Eq. (6.5) and Fig. 7.7]

$$\mathbf{E}_{\text{ind1}} = -\frac{\mu_0}{4\pi} \oint_{C_1} \frac{\mathrm{d}i_1}{\mathrm{d}t} \frac{\mathrm{d}\mathbf{l}_1}{R}, \tag{7.25}$$

so that the induced emf in the second contour can be written as [see Eq. (6.33)]

$$\mathbf{e}_{\text{ind2}} = \oint_{C_2} \mathbf{E}_{\text{ind1}} \cdot \mathrm{d}\mathbf{l}_2 = -\frac{\mu_0}{4\pi} \oint_{C_2} \oint_{C_1} \frac{\mathrm{d}\mathbf{l}_1 \cdot \mathrm{d}\mathbf{l}_2}{R} \frac{\mathrm{d}i_1}{\mathrm{d}t} = -L_{21} \frac{\mathrm{d}i_1}{\mathrm{d}t}. \tag{7.26}$$

This yields the following expression for the mutual inductance between the contours C_1 and C_2:

Neumann formula for mutual inductance

$$\boxed{L_{21} = \frac{\mu_0}{4\pi} \oint_{C_2} \oint_{C_1} \frac{\mathrm{d}\mathbf{l}_1 \cdot \mathrm{d}\mathbf{l}_2}{R},} \tag{7.27}$$

which is known as the Neumann[3] formula for mutual inductance. It implies the evaluation of a double line integral along the contours and underscores the fact that the mutual inductance is only a property of the geometrical shape and the physical arrangement of coupled contours, as well as of the permeability of the medium [if the contours are situated in a homogeneous linear magnetic medium of permeability μ, the constant μ_0 needs to be replaced by μ in Eq. (7.27)]. It is obvious from Eq. (7.27) that the change of the reference orientation of one of the contours in Fig. 7.7 (but not both of them), which means the change of the reference direction of one of the vectors $\mathrm{d}\mathbf{l}_1$ and $\mathrm{d}\mathbf{l}_2$, changes the polarity (sign) of the mutual inductance L_{21}. It is also obvious that interchanging the subscripts 1 and 2 in Eq. (7.27) does not change the algebraic value (which includes both the magnitude and the sign) of the double integral (since the dot product is commutative and the two line integrations can be performed in an arbitrary order). This proves the identity in Eq. (7.24). The Neumann formula represents a good basis for numerical evaluation of the mutual inductance of contours of arbitrary shapes, where the involved line integrals along the contours are computed using numerical integration methods.

[3]Franz Ernst Neumann (1798–1895), a German mineralogist, physicist, and mathematician, a professor of mineralogy and physics at the University of Königsberg. Neumann contributed to the theory of electromagnetic induction, and derived, in 1845, the formula for the mutual inductance between two equal parallel coaxial polygons of wire, the generalization of which is the Neumann formula for mutual inductance of arbitrary wire contours (loops), as we use it today.

Example 7.6 **Mutual Inductance between a Loop and an Infinite Wire**

Find the mutual inductance between the rectangular loop and the infinitely long straight wire in Fig. 6.12.

Solution The infinitely long wire can be considered as a loop that closes upon itself at infinity. Designating it as C_1 and the rectangular loop as C_2, the current i_1 and magnetic flux Φ_2 in Eq. (7.21) are actually the current i carried by the wire in Fig. 6.12 and the flux Φ through the rectangular contour given by Eq. (6.64), respectively. The mutual inductance between the contours for their reference orientations given in Fig. 6.12 (upward orientation for the infinitely long wire and clockwise direction for the rectangular loop) is hence

$$L_{21} = \frac{\Phi_2}{i_1} = \frac{\mu_0 b}{2\pi} \ln \frac{c+a}{c}. \tag{7.28}$$

Note that the same result is obtained by applying the emf definition of mutual inductance in Eq. (7.22) to the expression for the induced emf in the rectangular contour in Eq. (6.65). Note also that computing the mutual inductance as L_{12} in this case would be prohibitively complicated. It would require either finding the induced electric field intensity vector $\mathbf{E}_{\text{ind2}}$ at an arbitrary point of the infinite wire due to an assumed current i_2 in the rectangular contour, and then integrating it along the wire (which, in fact, is the Neumann formula for L_{12}) or finding and integrating the magnetic flux density vector $\mathbf{B}_2$ due to i_2 across a half-plane bounded by the loop C_1.

Example 7.7 **Mutual Inductance of Two Coils on a Thin Toroidal Core**

Two coils are wound uniformly and densely in two layers, one on top of the other, about a thin toroidal core (such as the one shown in Fig. 5.11). The core is made from a linear ferromagnetic material of relative permeability $\mu_r = 500$. Its length is $l = 50$ cm and cross-sectional area $S = 1$ cm^2. The number of wire turns is $N_1 = 400$ for the first coil and $N_2 = 600$ for the second one. Compute the mutual inductance of the coils.

Solution Let us adopt the same reference orientations for the two coils (this will give us a positive mutual inductance of the coils) and assume that the first coil carries a current of intensity i_1. This current produces a magnetic field of the same intensity (H_1) everywhere inside the core. From Eq. (5.53), $H_1 = N_1 i_1 / l$, so that the total magnetic flux through the second coil (Φ_2) is given by [see also Eq. (5.96)]

$$\Phi_{\text{single turn}} = \mu H_1 S \quad (\mu = \mu_r \mu_0) \quad \longrightarrow \quad \Phi_2 = N_2 \Phi_{\text{single turn}} = \frac{\mu N_1 N_2 S i_1}{l}, \tag{7.29}$$

and the mutual inductance between the coils comes out to be

$$\boxed{L_{21} = \frac{\Phi_2}{i_1} = \frac{\mu N_1 N_2 S}{l}.} \tag{7.30}$$

L_{21} – two coupled coils on a thin toroidal core

Finally, substituting the numerical data gives $L_{21} = 30$ mH.

Note that the same result is obtained by assuming a current i_2 to flow in the second coil and computing the mutual inductance L_{12} from the total magnetic flux through the first coil (Φ_1).

Example 7.8 **Magnetic Coupling between a Toroidal Coil and a Loop**

An open-circuited toroidal coil with a rectangular cross section has $N = 500$ turns of wire that are uniformly and densely wound about a ferromagnetic core. The relative permeability of the material is $\mu_r = 1000$. The inner and outer radii of the toroid are $a = 2$ cm and $b = 4$ cm (thick toroid), and its height is $h = 1$ cm. A wire loop is placed around the toroid, as shown in Fig. 7.8. There is a low-frequency time-harmonic current of intensity $i = I_0 \cos \omega t$

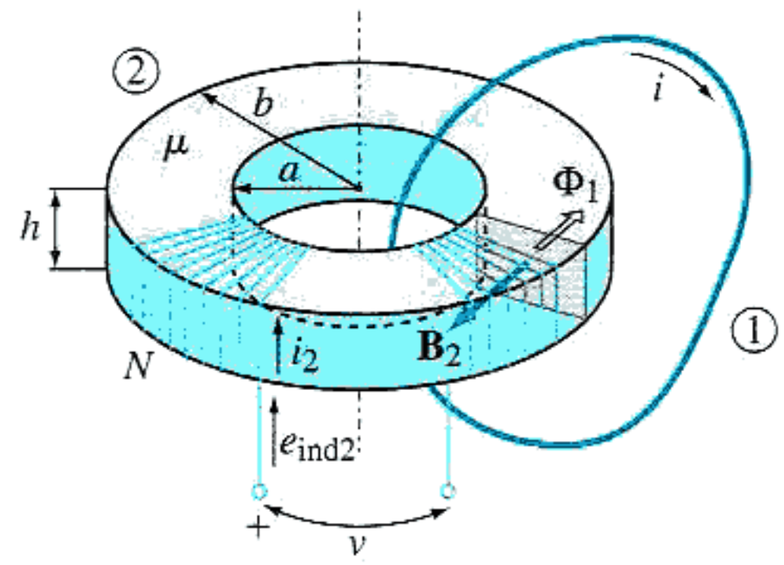

Figure 7.8 Magnetic coupling between a coil wound over a thick toroidal core and a wire loop encircling the toroid; for Example 7.8.

flowing along the loop, where $I_0 = 2$ A and $\omega = 7 \times 10^3$ rad/s. Find the voltage between the terminals of the coil.

Solution Let us denote the wire loop as circuit 1 and the toroidal coil as circuit 2. There is no current in the coil (it is open-circuited) and the voltage across the coil terminals is [see Eqs. (6.62) and (7.22)]

$$v = -e_{\text{ind2}} = L_{21}\frac{\mathrm{d}i_1}{\mathrm{d}t} \quad (i_1 \equiv i). \tag{7.31}$$

However, the mutual inductance L_{21} is extremely difficult to find using Eq. (7.21). Namely, the field $\mathbf{B}_1$ due to i_1, which would have to be integrated through each of the turns of the toroidal coil in order to compute the flux Φ_2, is not only highly nonuniform but also impossible to find analytically for a loop of arbitrary, irregular shape.

On the other side, we can use the identity in Eq. (7.24) and find the inductance L_{12} instead. To this end, we assume a current of intensity i_2 in the toroidal coil, and no current in the loop ($i_1 = 0$), find the flux Φ_1 through a surface bounded by the loop, and use Eq. (7.23). Under these circumstances, there is no field outside the coil [see Example 4.12], so that the flux Φ_1 equals the negative of the flux Φ through a cross section of the toroid given by Eq. (5.84), where the minus sign (negative) comes from different reference directions of the fluxes in Figs. 7.8 and 5.26. Hence,

$$L_{12} = \frac{\Phi_1}{i_2} = -\frac{\Phi}{I} = -\frac{\mu_r\mu_0 Nh}{2\pi}\ln\frac{b}{a} = -693\ \mu\text{H}. \tag{7.32}$$

Finally, combining Eqs. (7.31), (7.24), and (7.32), the time-harmonic voltage between the coil terminals in Fig. 7.8 comes out to be

$$v = L_{12}\frac{\mathrm{d}i_1}{\mathrm{d}t} = -\omega L_{12} I_0 \sin\omega t = 9.7\sin(7\times 10^3 t)\ \text{V} \quad (t \text{ in s}). \tag{7.33}$$

Note that the amplitude of the voltage v can be written as

Z_{21} – transfer impedance between two circuits (unit: Ω)

$$\boxed{V_0 = |Z_{21}|I_0,} \quad \text{where} \quad Z_{21} = \omega L_{21} = \omega L_{12} = -\frac{\omega\mu_r\mu_0 Nh}{2\pi}\ln\frac{b}{a} = -4.85\ \Omega. \tag{7.34}$$

This amplitude (or the corresponding rms value[4]) can be measured by a voltmeter connected to the terminals of the coil. Thus, by directly measuring V_0, we can indirectly measure the amplitude (or rms value) of the current (I_0) in an arbitrary conductor, without inserting an ammeter in its circuit. In such cases, the coil in Fig. 7.8 is used as a test transformer, where the current to be determined is transformed to the voltage that is indicated by the voltmeter by means of magnetic coupling and transformer electromagnetic induction. The constant Z_{21} in Eq. (7.34), expressed in ohms, is said to be the mutual impedance or transfer impedance

[4]Note that most instruments show rms (root-mean-square) values of measured quantities instead of their amplitudes (maximum values).

between the two circuits ($Z_{12} = Z_{21}$). It is negative here, as the mutual inductance between the circuits is, because of the particular reference orientations of the contours and reference directions of i and v in Fig. 7.8.

Example 7.9 **Mutual Inductance p.u.l. of Two Two-Wire Lines**

Fig. 7.9(a) shows a cross section of a system composed of two infinitely long thin two-wire lines running parallel to each other in air. The first line has conductors marked as 1 and 1′, and the second one as 2 and 2′. The distances between axes of the first and second conductor of the first line and each of the conductors of the second line are r_{12}, $r_{12'}$, $r_{1'2}$, and $r_{1'2'}$, respectively. Find the mutual inductance per unit length between the two lines.

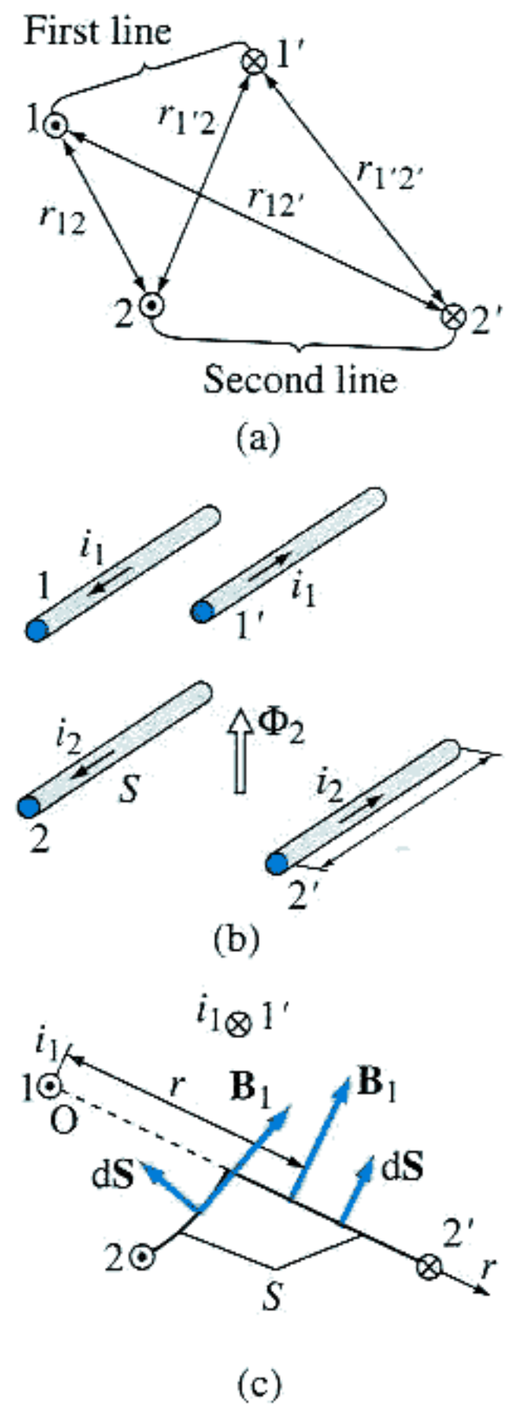

Figure 7.9 Evaluation of the mutual inductance per unit length of two parallel infinitely long thin two-wire lines in air: (a) cross section of the system with given geometrical data, (b) three-dimensional view showing a part of the system of length l that is only considered, and (c) integration of the magnetic field due to the conductor 1 over a conveniently chosen surface bounded by the conductors of the line 2–2′; for Example 7.9.

Solution We assume that the first line (line 1–1′) carries a current of intensity i_1, as indicated in Fig. 7.9(b). Our goal is to find the magnetic flux Φ_2 due to this current through a surface S of length l bounded by the conductors of the second line (line 2–2′), and to apply Eq. (7.21) for the mutual inductance between the lines.

Let us first find the flux Φ_a through S due to the conductor 1 alone. The corresponding magnetic flux density vector, $\mathbf{B}_1$, is circular with respect to the axis of the conductor and its magnitude is [Eq. (4.22)]

$$B_1 = \frac{\mu_0 i_1}{2\pi r}, \tag{7.35}$$

where r is the distance from the axis. To integrate $\mathbf{B}_1$, however, it is not convenient to adopt S simply as the flat surface spanned across the conductors 2 and 2′. Instead, a more complicated surface, the cross section of which is shown in Fig. 7.9(c), is adopted. It consists of a cylindrical part of radius r_{12} and a flat part (strip) whose width is equal to $r_{12'} - r_{12}$. The flux through the cylindrical part of the surface is zero, because $\mathbf{B}_1$ is tangential to the surface ($\mathbf{B}_1 \perp \mathrm{d}\mathbf{S}$) in this part of integration (note the analogy with the electric potential computation in Fig. 1.23). The integration over the rest of S (flat part) is quite simple to perform, because $\mathbf{B}_1$ is now perpendicular to the integration surface ($\mathbf{B}_1 \parallel \mathrm{d}\mathbf{S}$). Hence, the flux computation practically reduces to the one in Eq. (6.64), and we have

$$\Phi_a = \int_{r=r_{12}}^{r_{12'}} B_1 \, \mathrm{d}S = \int_{r_{12}}^{r_{12'}} \frac{\mu_0 i_1}{2\pi r} l \, \mathrm{d}r = \frac{\mu_0 i_1 l}{2\pi} \ln \frac{r_{12'}}{r_{12}}. \tag{7.36}$$

Similarly, the flux Φ_b due to the current i_1 in the conductor 1′ alone can be found by integrating the corresponding magnetic field through a surface conveniently placed with respect to this conductor. However, instead of repeating the above computation for a new position of the conductor (now conductor 1′), we can use the final result in Eq. (7.36) with just changing the notation:

$$\Phi_b = -\frac{\mu_0 i_1 l}{2\pi} \ln \frac{r_{1'2'}}{r_{1'2}}, \tag{7.37}$$

where the minus sign comes from the reference direction of the current i_1 in the conductor 1′ being opposite to the direction of the current in the conductor 1.

By superposition, the total magnetic flux through the line 2–2′ at the length l of the system amounts to

$$\Phi_2 = \Phi_a + \Phi_b = \frac{\mu_0 i_1 l}{2\pi} \ln \frac{r_{12'} r_{1'2}}{r_{12} r_{1'2'}}. \tag{7.38}$$

The corresponding flux per unit length (for one meter) of the system is obtained as

$$\Phi_2' = (\Phi_2)_{\text{p.u.l.}} = \frac{\Phi_2}{l}. \tag{7.39}$$

so that the mutual inductance per unit length of the two lines for the orientations of the lines given in Fig. 7.9 is

$$\boxed{L_{21}' = (L_{21})_{\text{p.u.l.}} = \frac{L_{21}}{l} = \frac{\Phi_2'}{i_1} = \frac{\mu_0}{2\pi} \ln \frac{r_{12'} r_{1'2}}{r_{12} r_{1'2'}}.} \tag{7.40}$$

L_{21}' – two parallel thin two-wire lines (unit: H/m)

Depending on the actual mutual position of the lines, L'_{21} can be both positive (when $r_{12'}r_{1'2} > r_{12}r_{1'2'}$) and negative (when $r_{12'}r_{1'2} < r_{12}r_{1'2'}$). The unit for L'_{21} is H/m.

This formula is of great importance in assessing (usually undesired) magnetic coupling and mutual electromagnetic induction between different combinations of parallel two-wire transmission lines in practical applications (e.g., coupling between a phone line and nearby power line or between pairs of wire conductors in an electronic device). It can be used also for other types of transmission lines that can be approximated by wire lines in some considerations (e.g., rough computation of mutual inductances within multiconductor microstrip and strip transmission lines that give rise to the so-called inductive "cross talk" between conductors in printed circuit boards in computers).

Problems: 7.10–7.15; *Conceptual Questions* (on Companion Website): 7.11–7.21; *MATLAB Exercises* (on Companion Website).

7.3 ANALYSIS OF MAGNETICALLY COUPLED CIRCUITS

Having now in hand the concepts of both self- and mutual inductance, let us assume that slowly time-varying currents exist in both contours (circuits) of Fig. 7.7 at the same time, as shown in Fig. 7.10. The total magnetic flux Φ_1 through the first circuit is now caused by both i_1 and i_2. Using Eqs. (7.1) and (7.23) and the superposition principle, we have

$$\Phi_1 = L_1 i_1 + L_{12} i_2, \tag{7.41}$$

with L_1 being the self-inductance of the first circuit and L_{12} the mutual inductance between the circuits. Similarly, the total magnetic flux through the second circuit is

$$\Phi_2 = L_{21} i_1 + L_2 i_2, \tag{7.42}$$

where $L_{21} = L_{12}$ and L_2 is the self-inductance of the second circuit. By the same token, the induced emf in each of the circuits is composed of both self-induction and mutual-induction terms, which can be written as

$$e_{\text{ind1}} = -\frac{\mathrm{d}\Phi_1}{\mathrm{d}t} = -L_1\frac{\mathrm{d}i_1}{\mathrm{d}t} - L_{12}\frac{\mathrm{d}i_2}{\mathrm{d}t}, \tag{7.43}$$

$$e_{\text{ind2}} = -\frac{\mathrm{d}\Phi_2}{\mathrm{d}t} = -L_{21}\frac{\mathrm{d}i_1}{\mathrm{d}t} - L_2\frac{\mathrm{d}i_2}{\mathrm{d}t}. \tag{7.44}$$

Finally, from Fig. 7.10 [see also Figs. 6.6 and 6.11(b)], voltages across the terminals of the circuits are given by

current-voltage characteristic of two magnetically coupled circuits

$$\boxed{v_1 = -e_{\text{ind1}} = L_1\frac{\mathrm{d}i_1}{\mathrm{d}t} + L_{12}\frac{\mathrm{d}i_2}{\mathrm{d}t},} \tag{7.45}$$

$$\boxed{v_2 = -e_{\text{ind2}} = L_{21}\frac{\mathrm{d}i_1}{\mathrm{d}t} + L_2\frac{\mathrm{d}i_2}{\mathrm{d}t}.} \tag{7.46}$$

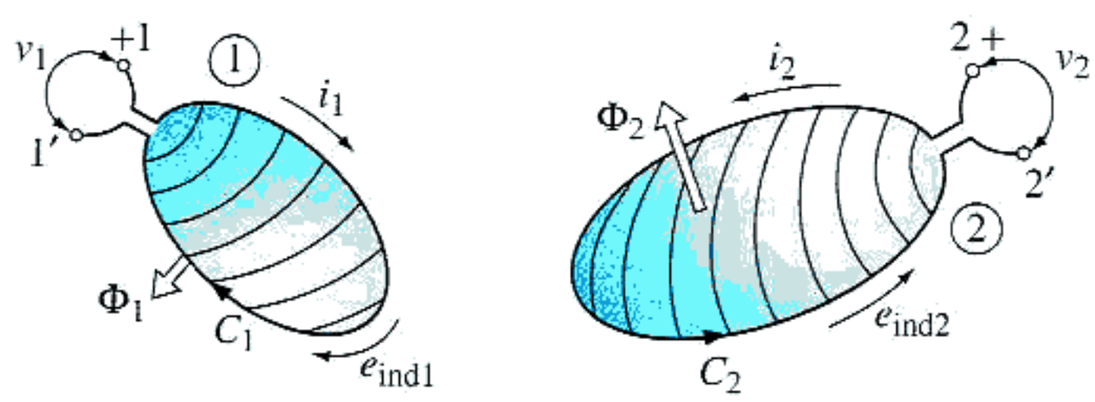

Figure 7.10 Analysis of two magnetically coupled circuits with slowly time-varying currents.

In words, the voltage across the terminals of each of the circuits is a linear combination of time derivatives of currents in both circuits, with L_1, L_2, and $L_{12} = L_{21}$ as linearity (proportionality) constants.

Shown in Fig. 7.11 is the circuit-theory representation of the two magnetically coupled circuits of Fig. 7.10. This is a two-port network whose current-voltage characteristic is given by Eqs. (7.45) and (7.46). It consists of two coupled ideal inductors, where, in addition to modeling the emf due to self-induction in each inductor, the effect of the emf due to mutual induction between the inductors is also modeled. The mutual inductance between the inductors is customarily written as

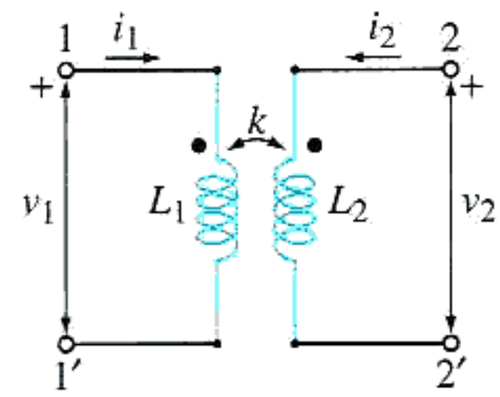

Figure 7.11 Circuit-theory representation of two coupled inductors.

$$L_{12} = \pm k\sqrt{L_1 L_2}, \tag{7.47}$$

where k is a positive dimensionless constant called the coefficient of (magnetic) coupling of the inductors (circuits) and defined as

$$\boxed{k = \frac{|L_{12}|}{\sqrt{L_1 L_2}}, \quad 0 \le k \le 1.} \tag{7.48}$$

coefficient of magnetic coupling between two circuits (dimensionless)

We shall see in the next section that k is always less than or eventually equal to unity. The coefficient k in Fig. 7.11 thus provides the information about the magnitude of the mutual inductance between the circuits of Fig. 7.10. The sign of L_{12}, however, depends on the adopted reference directions of currents i_1 and i_2, and therefore cannot be given as a single piece of information (positive or negative) along with k, independently from the current directions. That is why we use a so-called two-dot notation to include the information about the sign of L_{12} in the representation in Fig. 7.11, by placing two big dots near the particular ends of the two inductors. According to this notation (convention), if both currents (i_1 and i_2) enter the inductors at ends marked by a big dot (as in Fig. 7.11), the mutual inductance, for that particular combination of reference directions of currents, is positive (note that $L_{12} > 0$ in Fig. 7.10). The same is true if both currents leave the inductors at marked (dotted) ends. Otherwise, if one current enters and the other leaves the inductor at marked ends, the mutual inductance is negative (note that a change of the reference direction of one of the currents in Figs. 7.10 and 7.11 would result in L_{12} becoming negative). Finally, if $k = 0$, the two inductors in Fig. 7.11 become decoupled and independently described by the current-voltage characteristic in Eq. (7.3) for a single inductor [Eqs. (7.45) and (7.46) with $L_{12} = 0$].

Note that Eqs. (7.41) and (7.42) can be represented in matrix form:

$$[\Phi] = [L][i]. \tag{7.49}$$

where $[\Phi]$ and $[i]$ are column matrices whose elements are the fluxes and currents of the coupled circuits, respectively, and $[L]$ is a symmetrical square matrix of inductances,

$$\boxed{[L] = \begin{bmatrix} L_{11} & L_{12} \\ L_{21} & L_{22} \end{bmatrix} = \begin{bmatrix} L_1 & L_{12} \\ L_{12} & L_2 \end{bmatrix}} \tag{7.50}$$

inductance matrix

($L_{11} \equiv L_1$ and $L_{22} \equiv L_2$). Note also that these equations, as well as Eqs. (7.43)–(7.46) for the electromotive forces and voltages, can be generalized to the system with an arbitrary number (N) of coupled contours (circuits), in which case $[L]$ is an $N \times N$ matrix.

Example 7.10 **Two Coupled Inductors Connected in Series and Parallel**

Find the equivalent inductance of two coupled inductors of inductances L_1 and L_2 and coupling coefficient k if they are connected in (a) series, as in Fig. 7.12(a), and (b) parallel, as in Fig. 7.12(b).

Solution

(a) Voltages v_1 and v_2 of individual inductors are given by Eqs. (7.45) and (7.46). The current through the inductors in Fig. 7.12(a) is the same, $i_1 = i_2 = i$, so that the voltage across their connection is

$$v = v_1 + v_2 = \underbrace{L_1 \frac{di}{dt} + L_{12} \frac{di}{dt}}_{\text{inductor 1}} + \underbrace{L_{12} \frac{di}{dt} + L_2 \frac{di}{dt}}_{\text{inductor 2}} = (L_1 + L_2 + 2L_{12}) \frac{di}{dt}. \tag{7.51}$$

By comparison with the current-voltage characteristic for a single inductor, Eq. (7.3), we conclude that the total (equivalent) inductance of the connection in series equals

equivalent inductance of two coupled inductors in series

$$\boxed{L = L_1 + L_2 + 2L_{12},} \tag{7.52}$$

where the mutual inductance between the inductors, for the situation given in Fig. 7.12(a), is positive (the current enters both inductors at their ends marked by a big dot) and, using Eq. (7.47), amounts to

$$L_{12} = k\sqrt{L_1 L_2}. \tag{7.53}$$

(b) The voltage across the inductors in Fig. 7.12(b) is the same, $v_1 = v_2 = v$. Assuming it to be known, Eqs. (7.45) and (7.46) provide the following system of equations with di_1/dt and di_2/dt as unknowns:

$$L_1 \frac{di_1}{dt} + L_{12} \frac{di_2}{dt} = v \quad \text{and} \quad L_{12} \frac{di_1}{dt} + L_2 \frac{di_2}{dt} = v. \tag{7.54}$$

Its solution is

$$\frac{di_1}{dt} = \frac{L_2 - L_{12}}{L_1 L_2 - L_{12}^2} v \quad \text{and} \quad \frac{di_2}{dt} = \frac{L_1 - L_{12}}{L_1 L_2 - L_{12}^2} v. \tag{7.55}$$

As the current through the terminals of the parallel connection of inductors is $i = i_1 + i_2$, we have

$$\frac{di}{dt} = \frac{di_1}{dt} + \frac{di_2}{dt} = \frac{L_1 + L_2 - 2L_{12}}{L_1 L_2 - L_{12}^2} v. \tag{7.56}$$

By expressing v in terms of di/dt,

$$v = \frac{L_1 L_2 - L_{12}^2}{L_1 + L_2 - 2L_{12}} \frac{di}{dt}, \tag{7.57}$$

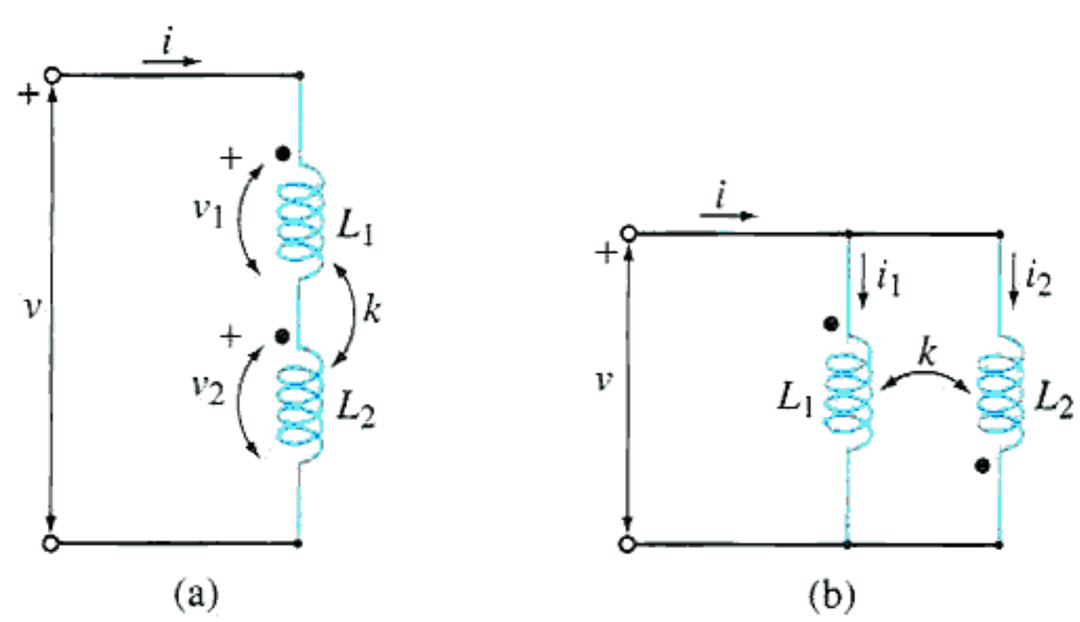

Figure 7.12 Evaluation of the equivalent inductance of two coupled inductors connected in (a) series and (b) parallel; for Example 7.10.

we conclude that the two coupled inductors of Fig. 7.12(b) can be replaced by a single equivalent inductor of inductance

$$\boxed{L = \frac{L_1 L_2 - L_{12}^2}{L_1 + L_2 - 2L_{12}}.} \tag{7.58}$$

equivalent inductance of two coupled inductors in parallel

The particular (given) placement of big dots in Fig. 7.12(b) tells us that the mutual inductance L_{12} is negative, and hence Eq. (7.47) yields

$$L_{12} = -k\sqrt{L_1 L_2}. \tag{7.59}$$

Note that for $k = 0$ and $L_{12} = 0$, Eqs. (7.52) and (7.58) reduce to expressions for equivalent inductances of two ordinary inductors of inductances L_1 and L_2 (that are not magnetically coupled together) connected in series and parallel, respectively. Note also that these expressions (with $L_{12} = 0$) have the same form as the corresponding expressions for two connected resistors of resistances R_1 and R_2 [see Eqs. (3.86) and (3.94)].

Example 7.11 Coupling Coefficient of Two Coils on a Toroidal Core

Compute the coefficient of coupling between the coils on the thin toroidal core from Example 7.7.

Solution Using the expression in Eq. (7.29) for the magnetic flux through the cross section of the core due to the current i_1 in the first coil, the self-inductance of the first coil is

$$\boxed{L_1 = \frac{\Phi_1}{i_1} = \frac{N_1 \Phi_{\text{single turn}}}{i_1} = \frac{\mu N_1^2 S}{l}.} \tag{7.60}$$

L – coil on a thin toroidal core

Similarly, the self-inductance of the second coil is $L_2 = \mu N_2^2 S/l$. The mutual inductance between the coils is given by Eq. (7.30). Hence, their coupling coefficient turns out to be

$$\boxed{k = \frac{|L_{12}|}{\sqrt{L_1 L_2}} = \frac{N_1 N_2}{\sqrt{N_1^2 N_2^2}} = 1.} \tag{7.61}$$

maximum coupling – coils on a toroidal core

This maximum coupling is a consequence of the magnetic flux due to the current of each of the coils being concentrated entirely inside the core (flux leakage from the core is negligible), so that the entire flux passes through every turn of both coils.

Example 7.12 Voltage Transformation by Two Coupled Coils

Consider a magnetic circuit in the form of a thin toroidal ferromagnetic core with two windings shown in Fig. 7.13(a). The windings have $N_1 = 1000$ and $N_2 = 500$ turns of wire, respectively. The ferromagnetic material can be considered to be linear. Losses in the

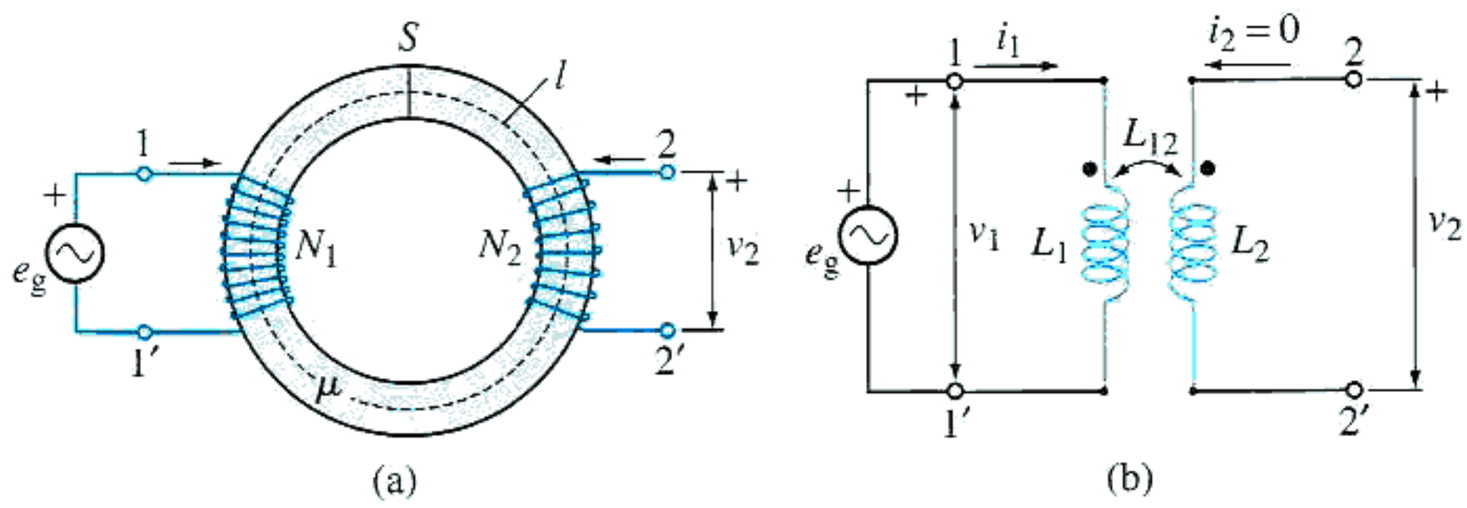

Figure 7.13 (a) Magnetic circuit with two windings and (b) equivalent schematic diagram with two coupled inductors; for Example 7.12.

windings and the core can be neglected. The primary winding is connected to an ideal ac voltage generator of emf $e_g = 100\cos 377t$ V (t in s). The secondary winding is open-circuited. Find the voltage across the secondary winding.

Solution Fig. 7.13(b) shows the equivalent schematic diagram with two coupled inductors, where L_{12} is positive for the reference orientations of windings in Fig. 7.13(a). As the secondary winding is open-circuited, Eqs. (7.45) and (7.46) give

$$v_1 = L_1 \frac{di_1}{dt} \quad \text{and} \quad v_2 = L_{21}\frac{di_1}{dt} \quad (i_2 = 0). \tag{7.62}$$

Using Eqs. (7.60) and (7.30), we can write

voltage transformation by coupled coils

$$\boxed{\frac{v_1}{v_2} = \frac{L_1}{L_{12}} = \frac{N_1^2}{N_1N_2} = \frac{N_1}{N_2},} \tag{7.63}$$

that is, the ratio of the voltages across the primary and secondary windings is equal to the ratio of the numbers of wire turns. The voltage across the secondary winding is hence

$$v_2 = \frac{N_2}{N_1}v_1 = \frac{N_2}{N_1}e_g = 50\cos 377t \text{ V} \quad (t \text{ in s}). \tag{7.64}$$

We can say that the circuit in Fig. 7.13 operates as a transformer of voltage from its primary port to its secondary port, with the transformation (multiplication) factor being equal to the wire turns ratio N_2/N_1.

Example 7.13 Current Transformation by Two Coupled Coils

Assume that the primary winding in the magnetic circuit in Fig. 7.13(a) is connected to an ideal ac current generator of current intensity $i_g = 15\sin 377t$ mA (t in s), while the secondary winding is short-circuited, and determine the current of the secondary winding.

Solution From the equivalent schematic diagram shown in Fig. 7.14 and Eq. (7.46),

$$L_{12}\frac{di_1}{dt} + L_2\frac{di_2}{dt} = 0 \quad (v_2 = 0). \tag{7.65}$$

This means that

current transformation by coupled coils

$$\boxed{\frac{i_1}{i_2} = -\frac{L_2}{L_{12}} = -\frac{N_2^2}{N_1N_2} = -\frac{N_2}{N_1}.} \tag{7.66}$$

i.e., the ratio of the currents in the primary and secondary windings is equal to the negative inverse ratio of the numbers of wire turns. Solving for the current in the secondary winding, we have

$$i_2 = -\frac{N_1}{N_2}i_1 = -\frac{N_1}{N_2}i_g = -30\sin 377t \text{ mA} \quad (t \text{ in s}). \tag{7.67}$$

We see that the circuit in Fig. 7.14 performs a transformation of current between its ports, with the magnitude transformation factor being the reciprocal of that for the voltage transformation in Eq. (7.64).

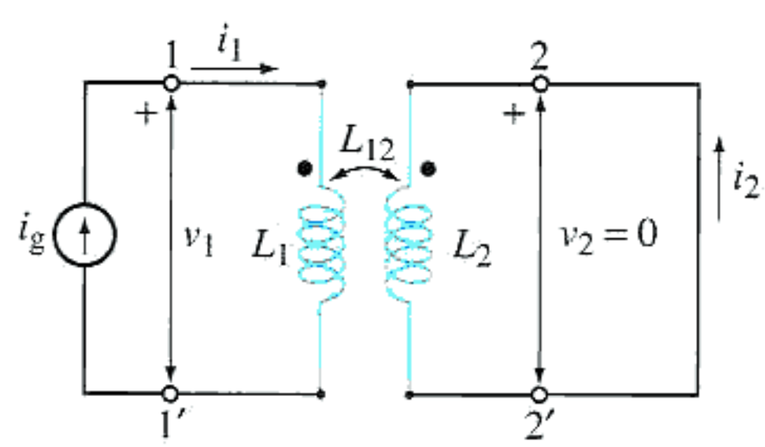

Figure 7.14 Current transformation by two magnetically coupled coils; for Example 7.13.

Example 7.14 **Coupling Coefficient of Two Coaxial Solenoids**

Fig. 7.15 shows a cross section of two very long solenoidal coils positioned coaxially with respect to each other. Radii of solenoids are a_1 and a_2, their length is the same, l, and numbers of wire turns are N_1 and N_2, respectively. The inner coil is wound on a core made of a linear ferromagnetic material of relative permeability μ_r, while the space between the coils is air-filled. Neglecting the end effects, calculate the coefficient of coupling between the two coils.

Solution Let us adopt counter-clockwise reference directions of currents in both coils (Fig. 7.15). Assume first that a current, of intensity I_1 (steady current), exists only in the first (inner) coil, while $I_2 = 0$. Under this assumption, the magnetic field is nonzero only inside the first coil and is given by [see Eq. (6.48)]

$$H_1 = \frac{N_1 I_1}{l}. \tag{7.68}$$

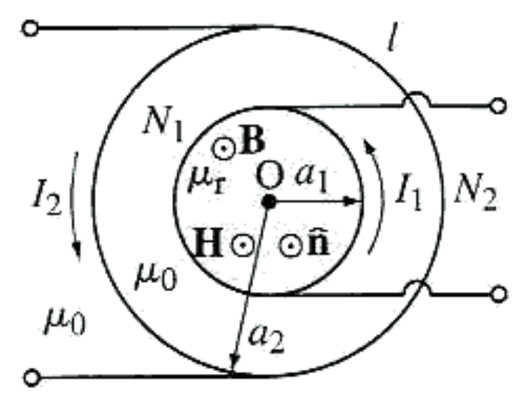

Figure 7.15 Cross section of two coupled coaxial solenoids; for Example 7.14.

Therefore, the magnetic fluxes through a single turn of both coils are the same,

$$\Phi_{\text{single turn}} = \mu_r \mu_0 H_1 \pi a_1^2 = \frac{\mu_r \mu_0 N_1 I_1 \pi a_1^2}{l}. \tag{7.69}$$

Using this expression, the self-inductance of the first coil is found to be

$$L_1 = \frac{\Phi_1}{I_1} = \frac{N_1 \Phi_{\text{single turn}}}{I_1} = \frac{\mu_r \mu_0 N_1^2 \pi a_1^2}{l} \tag{7.70}$$

[note that this can also be obtained by multiplying the inductance in Eq. (7.6) by μ_r]. Using the same expression (for $\Phi_{\text{single turn}}$), the mutual inductance between the coils is obtained as

$$L_{21} = \frac{\Phi_2}{I_1} = \frac{N_2 \Phi_{\text{single turn}}}{I_1} = \frac{\mu_r \mu_0 N_1 N_2 \pi a_1^2}{l}. \tag{7.71}$$

On the other hand, the assumption of a current, of intensity I_2, existing only in the second (outer) coil (while $I_1 = 0$) in Fig. 7.15 gives a nonzero magnetic field everywhere inside the second coil, of intensity

$$H_2 = \frac{N_2 I_2}{l}. \tag{7.72}$$

The magnetic flux density in the core is $B_2 = \mu_r \mu_0 H_2$, while $B_{20} = \mu_0 H_2$ in the air-filled space between the coils, which leads to the following for the total magnetic flux through the second coil:

$$\Phi_2 = N_2[\underbrace{B_2 \pi a_1^2}_{\text{core}} + \underbrace{B_{20}\pi(a_2^2 - a_1^2)}_{\text{air}}] = \frac{\mu_0 N_2^2 \pi I_2 (\mu_r a_1^2 + a_2^2 - a_1^2)}{l}. \tag{7.73}$$

The self-inductance of the second coil is hence

$$L_2 = \frac{\Phi_2}{I_2} = \frac{\mu_0 N_2^2 \pi [(\mu_r - 1)a_1^2 + a_2^2]}{l}, \tag{7.74}$$

whereas computing Φ_1 through the first coil and $L_{12} = \Phi_1/I_2$ would, of course, give the same result for the mutual inductance as in Eq. (7.71).

Finally, the coefficient of coupling between the coils, Eq. (7.48), comes out to be

$$k = \frac{|L_{12}|}{\sqrt{L_1 L_2}} = \sqrt{\frac{\mu_r}{\mu_r - 1 + (a_2/a_1)^2}}. \tag{7.75}$$

Note that for very large relative permeabilities μ_r (e.g., $\mu_r = 1000$), k is very close to unity (coupling is very strong), which is a consequence of the magnetic flux Φ_2 due to I_2 in the second coil being practically entirely concentrated in the core of the first coil for $\mu_r \gg 1$ [$\mu_r a_1^2 \gg a_2^2 - a_1^2$ in Eq. (7.73)].

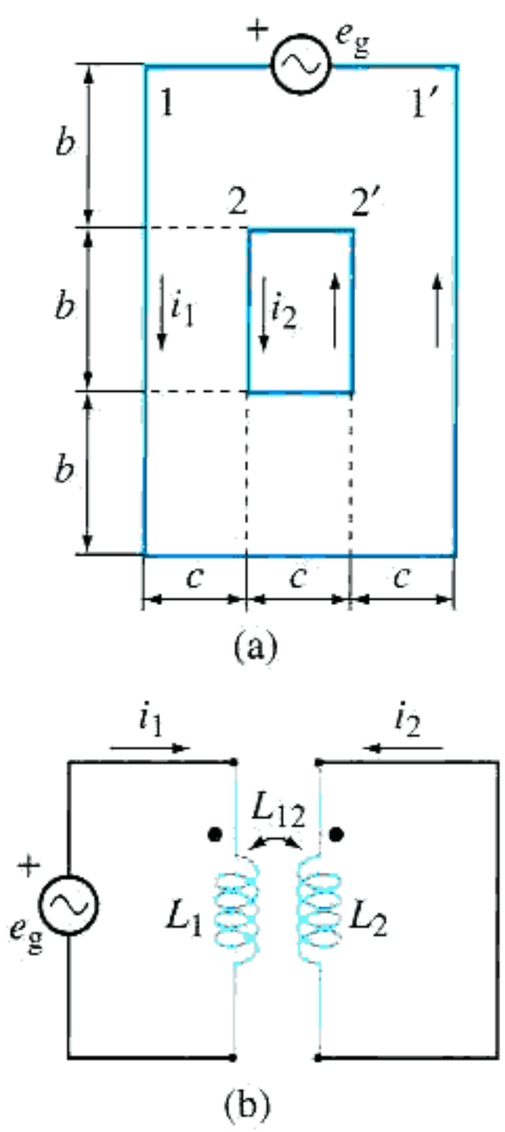

Figure 7.16 Analysis of magnetically coupled circuits containing two thin two-wire lines: (a) structure geometry and (b) equivalent schematic diagram with two coupled inductors; for Example 7.15.

Example 7.15 Magnetically Coupled Circuits Containing Two-Wire Lines

Fig. 7.16(a) depicts two parallel thin two-wire lines (1–1′ and 2–2′) in air, where $b = 20$ cm and $c = 5$ mm. The radii of all wires are $a = 0.3$ mm. The first line is connected at one end to an ideal voltage generator of time-harmonic emf $e_g(t) = \mathcal{E}_{g0} \cos \omega t$, where $\mathcal{E}_{g0} = 3$ V and $\omega = 10^6$ rad/s, and the other end of the line is short-circuited. The second line is short-circuited at both ends. Neglecting internal inductances, losses in the wires, capacitive coupling between the lines, end effects, and propagation effects, find the amplitudes of currents in the lines.

Solution Using Eq. (7.11), self-inductances per unit length of the lines in Fig. 7.16(a) are

$$L_1' = \frac{\mu_0}{\pi} \ln \frac{3c}{a} = 1.565\ \mu\text{H/m} \quad \text{and} \quad L_2' = \frac{\mu_0}{\pi} \ln \frac{c}{a} = 1.125\ \mu\text{H/m}, \tag{7.76}$$

respectively, where we neglect internal inductances of the lines. Eq. (7.40) gives the mutual inductance per unit length of the lines ($r_{12'} = r_{1'2} = 2c$ and $r_{12} = r_{1'2'} = c$):

$$L_{12}' = \frac{\mu_0}{2\pi} \ln \frac{(2c)^2}{c^2} = \frac{\mu_0}{\pi} \ln 2 = 277\ \text{nH/m}. \tag{7.77}$$

We neglect the end effects and the propagation effects, so that the total self-inductances and mutual inductance of the magnetically coupled circuits formed by the lines are obtained by multiplying the per-unit-length inductances by the corresponding lengths of the lines, $L_1 = L_1' 3b = 939$ nH, $L_2 = L_2' b = 225$ nH, and $L_{12} = L_{12}' b = 55.4$ nH (the length of the shorter of the two lines, b, is relevant for the mutual inductance between the lines).

Fig. 7.16(b) shows the equivalent schematic diagram of the two coupled circuits (we neglect the losses in wires and capacitive coupling between the circuits). According to this diagram,

$$L_1 \frac{di_1}{dt} + L_{12} \frac{di_2}{dt} = e_g, \quad L_{12} \frac{di_1}{dt} + L_2 \frac{di_2}{dt} = 0. \tag{7.78}$$

The solution of these two equations for the time derivatives of currents in the circuits is

$$\frac{di_1}{dt} = \frac{L_2}{L_1 L_2 - L_{12}^2} \mathcal{E}_{g0} \cos \omega t \quad \text{and} \quad \frac{di_2}{dt} = -\frac{L_{12}}{L_1 L_2 - L_{12}^2} \mathcal{E}_{g0} \cos \omega t. \tag{7.79}$$

which is then integrated with respect to time to obtain the solution for the currents. Integration in time of time-harmonic quantities results in an additional factor $1/\omega$ in the expressions for amplitudes, so that the amplitudes (peak-values) of the currents in the circuits (and the lines) are, respectively,

$$I_{01} = \frac{L_2 \mathcal{E}_{g0}}{\omega(L_1 L_2 - L_{12}^2)} = 3.24\ \text{A} \quad \text{and} \quad I_{02} = \frac{L_{12} \mathcal{E}_{g0}}{\omega(L_1 L_2 - L_{12}^2)} = 0.8\ \text{A}. \tag{7.80}$$

Example 7.16 Inductance p.u.l. of a Two-Wire Line above a PMC Plane

A symmetrical thin two-wire line is positioned in air over a ferromagnetic ($\mu \gg \mu_0$) plane, as shown in Fig. 7.17(a). The wire radii are a, the height of the axes of both wires with respect to the plane is h ($h \gg a$), and the distance between the wire axes is d ($d \gg a$). Compute the inductance per unit length of the line (in the presence of the plane).

Solution Assume that a slowly time-varying current of intensity i is established in the line [Fig. 7.17(a)]. By image theory for the magnetic field, Fig. 5.14, we can remove the ferromagnetic plane by introducing positive images of the original current conductors. The equivalent system in Fig. 7.17(b) is thus obtained, which consists of two (magnetically coupled) parallel thin two-wire lines with the same current (i) in air. The total magnetic flux per unit length of the upper (original) line is therefore [see Eq. (7.41)]

$$\Phi' = L_1' i + L_{12}' i, \tag{7.81}$$

where L'_1 is the self-inductance p.u.l. of the upper line when isolated in free space and L'_{12} is the mutual inductance p.u.l. of the upper and lower lines in the equivalent system in air. These inductances are computed using Eqs. (7.11) and (7.40), respectively, so that the inductance p.u.l. of the original line in Fig. 7.17(a) comes out to be

$$L' = \frac{\Phi'}{i} = L'_1 + L'_{12} = \frac{\mu_0}{\pi}\left(\ln\frac{d}{a} + \ln\frac{\sqrt{d^2+4h^2}}{2h}\right) = \frac{\mu_0}{\pi}\ln\frac{d\sqrt{d^2+4h^2}}{2ah}. \tag{7.82}$$

Obviously, L'_{12} represents the influence of the ferromagnetic material in the lower half-space on the line inductance.

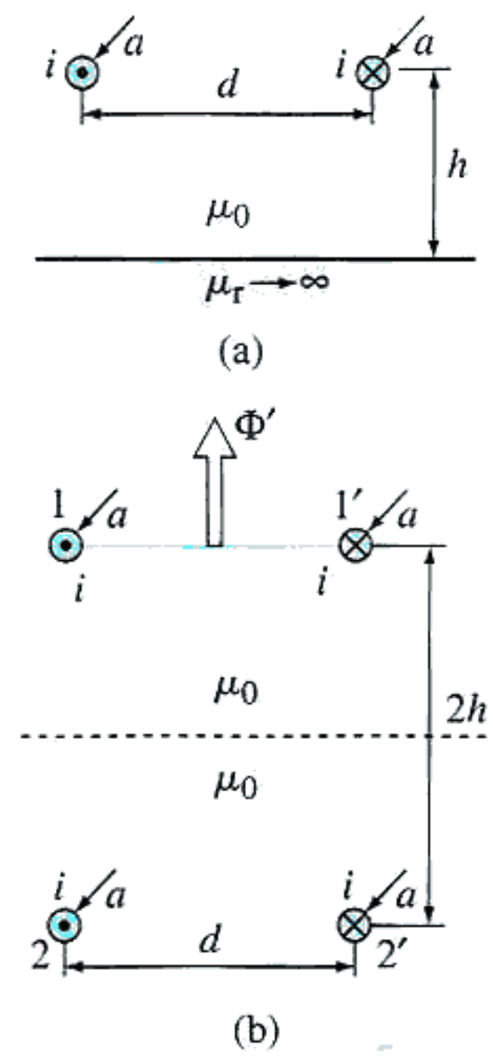

Figure 7.17 Evaluation of the inductance per unit length of a two-wire line above a ferromagnetic (or PMC) plane: (a) original system and (b) equivalent free-space system with two magnetically coupled two-wire lines; for Example 7.16.

Problems: 7.16–7.24; *Conceptual Questions* (on Companion Website): 7.22–7.28; *MATLAB Exercises* (on Companion Website).

7.4 MAGNETIC ENERGY OF CURRENT-CARRYING CONDUCTORS

Every system of conducting loops with currents contains a certain amount of energy, called magnetic energy, in a manner analogous to a system of charged conducting bodies storing electric energy. In other words, current-carrying (coupled or uncoupled) inductors in an ac or dc circuit store magnetic energy, much like charged capacitors store electric energy. By the principle of conservation of energy, the magnetic energy of a system of loops (or inductors) with currents equals the work done to the system in the process of establishing these currents from zero to their final values. Thus, by simulating this process of "loading" the loops by currents, we can find general expressions for computing the magnetic energy in terms of the current intensities and associated magnetic fluxes (final values) of the loops.

Let us consider first a single loop with a slowly time-varying current of intensity i. The current flow is maintained in the circuit by an ideal voltage generator of emf e_g, as shown in Fig. 7.18. As the magnetic flux through the loop, Φ, changes in time, an emf e_{ind} is induced in the loop, given by Faraday's law of electromagnetic induction, Eq. (6.34). Using Kirchhoff's voltage law, Eq. (3.119), we can write

$$e_g = Ri - e_{ind}, \tag{7.83}$$

where R is the resistance of the loop. The emf e_{ind} (emf due to self-induction) opposes the current change in the loop (Lenz's law), that is, it acts against the emf e_g. Therefore, an amount of work must be done in establishing the current in the loop to overcome this induced emf. This work is done by en external agent, with the energy transfer to the circuit being modeled by the generator (of emf e_g) in Fig. 7.18.

To investigate the energy balance in the circuit during a differentially short time interval dt, we multiply both sides of Eq. (7.83) by $i\,dt$,

$$e_g i\,dt = Ri^2\,dt + (-e_{ind} i\,dt). \tag{7.84}$$

By means of Eq. (3.121), the term on the left-hand side of this equation is the work done by the emf of the generator during the time interval dt. It equals the energy of external sources delivered to the circuit during that fraction of time. From Joule's law, Eq. (3.77), the first term on the right-hand side of the equation represents Joule's (ohmic) losses in the loop during dt. Finally, the last term in the equation (including the minus sign) is the work done against the emf e_{ind} in dt. Eq. (7.84) thus expresses the principle of conservation of energy for the circuit in Fig. 7.18,

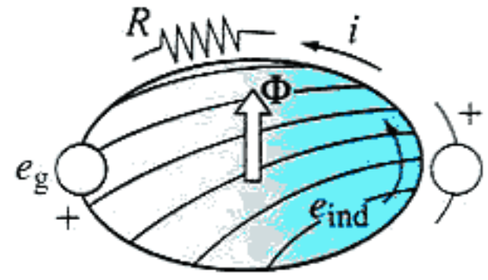

Figure 7.18 Wire loop of inductance L and resistance R with a slowly time-varying current of intensity i, maintained by an ideal voltage generator of emf e_g.

telling us that the work done by the generator during $\mathrm{d}t$ is partly converted into Joule's losses and partly used to overcome the induced emf in the loop. While the first part is lost to heat, the second part is given to the emf e_{ind}, i.e., to the flux Φ of the loop. Ultimately, it represents the energy delivered to the magnetic field of the current i in the loop during the time $\mathrm{d}t$. Using Eq. (6.34), $-e_{\text{ind}}\,\mathrm{d}t = \mathrm{d}\Phi$, so that the elementary work done by external sources to the magnetic field of the loop can be written as

$$\mathrm{d}W_{\text{m}} = -e_{\text{ind}} i\,\mathrm{d}t = i\,\mathrm{d}\Phi. \tag{7.85}$$

If the medium surrounding the loop is magnetically linear, the use of Eq. (7.1) yields

$$\mathrm{d}W_{\text{m}} = i\,\mathrm{d}\Phi = i\,\mathrm{d}(Li) = Li\,\mathrm{d}i, \tag{7.86}$$

where L is the inductance of the loop. The magnetic field, on the other hand, is capable of storing the received energy, and this stored energy is the magnetic energy of the loop, expressed in joules (J). Consequently, the work $\mathrm{d}W_{\text{m}}$ in Eq. (7.86) represents an increment of the magnetic energy of the circuit in Fig. 7.18.

When the current in the loop is zero, the loop has no energy. The total energy stored in the magnetic field of the loop when its current is i equals therefore the net work done to the magnetic field in changing the loop current from $i = 0$ to its final value i, and is obtained by adding up all elementary works $\mathrm{d}W_{\text{m}}$:

$$W_{\text{m}} = \int_{i=0}^{i} \mathrm{d}W_{\text{m}} = L\int_{0}^{i} i\,\mathrm{d}i = L\,\frac{i^2}{2}\bigg|_{0}^{i} = \frac{1}{2}Li^2. \tag{7.87}$$

From the circuit-theory standpoint, this is also the energy of a linear inductor of inductance L in an arbitrary electric circuit. Employing Eq. (7.1), the equivalent expressions for the energy of an inductor are

energy of inductor (unit: J)

$$\boxed{W_{\text{m}} = \frac{1}{2}Li^2 = \frac{1}{2}\Phi i = \frac{\Phi^2}{2L}.} \tag{7.88}$$

We note the complete analogy (duality) with the corresponding expressions for the electric energy (W_{e}) of a capacitor in Eq. (2.192).

Generally, for a system with N ($N \geq 1$) magnetically coupled loops (inductors),

energy of N magnetically coupled loops

$$\boxed{W_{\text{m}} = \frac{1}{2}\sum_{k=1}^{N} \Phi_k i_k.} \tag{7.89}$$

where the magnetic fluxes through the loops are given by linear relationships in Eqs. (7.41)–(7.42) or (7.49). Using these relationships, the energy of the system can be expressed only in terms of the currents and self- and mutual inductances of the loops. For example, for $N = 2$, the magnetic energy of two coupled loops can be written in the form

magnetic energy of two coupled inductors

$$\boxed{W_{\text{m}} = \frac{1}{2}[(\underbrace{L_1 i_1 + L_{12} i_2}_{\Phi_1})i_1 + (\underbrace{L_{12} i_1 + L_2 i_2}_{\Phi_2})i_2] = \frac{1}{2}L_1 i_1^2 + \frac{1}{2}L_2 i_2^2 + L_{12} i_1 i_2.} \tag{7.90}$$

This energy can be both larger and smaller than the sum of energies of the two loops when magnetically isolated from each other (when $L_{12} = 0$), because L_{12} can be both positive and negative. Note that the expression in Eq. (7.89) is entirely analogous to the expression for the electric energy of a linear multibody system in Eq. (2.195).

The magnetic energy can also be expressed in terms of distributions of the current density vector, **J**, and the magnetic vector potential, **A**, throughout the volume of current-carrying loops. Namely, the magnetic flux Φ_k through the loop C_k of the system with N loops equals the circulation of **A** along C_k [see Eq. (4.121)], so that Eq. (7.89) becomes

$$W_{\mathrm{m}} = \frac{1}{2}\sum_{k=1}^{N} i_k \underbrace{\oint_{C_k} \mathbf{A}\cdot \mathrm{d}\mathbf{l}_k}_{\Phi_k} = \frac{1}{2}\sum_{k=1}^{N} \oint_{C_k} \mathbf{A}\cdot i_k\,\mathrm{d}\mathbf{l}_k, \tag{7.91}$$

where the current i_k can be brought inside the integral sign in the line integral because it does not change along the wire (currents are slowly time-varying). As $i_k\,\mathrm{d}\mathbf{l}_k = \mathbf{J}\,\mathrm{d}v_k$, Eq. (4.10), we then have

$$W_{\mathrm{m}} = \frac{1}{2}\sum_{k=1}^{N} \int_{v_k} \mathbf{A}\cdot \mathbf{J}_k\,\mathrm{d}v_k, \tag{7.92}$$

with v_k standing for the volume of the kth loop. Finally, the sum of N integrals over volumes of individual loops can be joined together into a single volume integral:

$$\boxed{W_{\mathrm{m}} = \frac{1}{2}\int_{v_{\mathrm{current}}} \mathbf{J}\cdot\mathbf{A}\,\mathrm{d}v.} \tag{7.93}$$

magnetic energy in terms of volume currents

Since any slowly time-varying volume current distribution can be considered as consisting of an infinite number of filamentary current loops, this is a general expression for evaluation of the magnetic energy of a system of current conductors of arbitrary shapes in a linear medium. In general, the volume integration is performed over all parts of the system populated by current (v_{current}). We again note the duality with the corresponding expression for the electric energy, namely, with the volume integral expression in Eq. (2.196) for W_{e} in terms of the charge density (ρ) and the electric scalar potential (V) for an electrostatic system with a volume charge.

Example 7.17 Magnetic Energy of Two Coupled Two-Wire Lines

Find the time-average magnetic energy of the system of two coupled two-wire lines shown in Fig. 7.16 and described in Example 7.15.

Solution From Eqs. (7.79), instantaneous intensities of currents in the lines have the following forms: $i_1(t) = I_{01}\sin\omega t$ and $i_2(t) = -I_{02}\sin\omega t$, where the current amplitudes I_{01} and I_{02} are given in Eqs. (7.80). Using Eq. (7.90), the instantaneous magnetic energy contained in the magnetic field of the two lines is

$$\begin{aligned} W_{\mathrm{m}}(t) &= \frac{1}{2}L_1 i_1^2(t) + \frac{1}{2}L_2 i_2^2(t) + L_{12} i_1(t) i_2(t) \\ &= \frac{1}{2}L_1 I_{01}^2 \sin^2\omega t + \frac{1}{2}L_2 I_{02}^2 \sin^2\omega t - L_{12} I_{01} I_{02}\sin^2\omega t, \end{aligned} \tag{7.94}$$

where the self-inductances and mutual inductance of the coupled circuits in Fig. 7.16(b) are also found in Example 7.15. Eq. (6.95) tells us that the time-average value of the function $\sin^2\omega t$ is 1/2, so that the time-average magnetic energy of the system is

$$(W_{\mathrm{m}})_{\mathrm{ave}} = \frac{1}{2}\left(\frac{1}{2}L_1 I_{01}^2 + \frac{1}{2}L_2 I_{02}^2 - L_{12} I_{01} I_{02}\right) = 2.43\ \mu\mathrm{J}. \tag{7.95}$$

This energy can also be obtained using the equivalent inductance, L, seen by the generator in Fig. 7.16. To find L, we rewrite the first equation of Eqs. (7.79) in the following

form:

$$e_g = \left(L_1 - \frac{L_{12}^2}{L_2}\right)\frac{di_1}{dt} = L\frac{di_1}{dt}. \tag{7.96}$$

Hence,

$$L = L_1 - \frac{L_{12}^2}{L_2} = 925.4 \text{ nH}. \tag{7.97}$$

In other words, this is the inductance of an inductor that, as far as the generator is concerned, can replace the two coupled inductors in Fig. 7.16(b). Consequently, the energy of the two coupled two-wire lines is the same as the energy of the equivalent inductor, and Eq. (7.88) can be used. Since the current of the equivalent inductor is i_1,

$$W_m(t) = \frac{1}{2}Li_1^2(t), \tag{7.98}$$

which, averaged in time, gives the same result as in Eq. (7.95).

Example 7.18 Proof that the Maximum Coupling Coefficient is Unity

Prove that the largest possible value for the magnitude of the mutual inductance of two magnetically coupled circuits equals the geometric mean of the self-inductances of circuits.

Solution The inequality that we have to prove, $|L_{12}| \le \sqrt{L_1L_2}$, is a consequence of the simple fact that the stored magnetic energy is always positive (or eventually zero). To show this, we start with the expression for the energy stored in the magnetic field of the two circuits in Eq. (7.90) and write it in the following form:

$$W_m = \frac{1}{2}L_1i_1^2\left[1 + \frac{L_2}{L_1}\left(\frac{i_2}{i_1}\right)^2 + 2\frac{L_{12}}{L_1}\frac{i_2}{i_1}\right] = \frac{1}{2}L_1i_1^2 f(x), \tag{7.99}$$

where

$$f(x) = ax^2 + bx + 1, \quad x = \frac{i_2}{i_1}, \quad a = \frac{L_2}{L_1}, \quad \text{and} \quad b = 2\frac{L_{12}}{L_1}. \tag{7.100}$$

From the fact that $W_m \ge 0$, we conclude that the quadratic function $f(x)$ must be nonnegative for all values of x. This, in turn, is satisfied only if the minimum of f, given by

$$f_{\min} = f(-b/2a) = f(-L_{12}/L_2) = \frac{L_2}{L_1}\frac{L_{12}^2}{L_2^2} - 2\frac{L_{12}}{L_1}\frac{L_{12}}{L_2} + 1 = -\frac{L_{12}^2}{L_1L_2} + 1, \tag{7.101}$$

is nonnegative. Hence,

$$f_{\min} \ge 0 \quad \longrightarrow \quad L_{12}^2 \le L_1L_2 \quad \text{or} \quad |L_{12}| \le \sqrt{L_1L_2} \quad \longrightarrow \quad k \le 1, \tag{7.102}$$

which concludes our proof. We realize that these inequalities can also be written in terms of the coefficient of coupling of the two circuits, defined by Eq. (7.48), as $k \le 1$ (that the coupling coefficient cannot be larger than unity we noted earlier, in Section 7.3, but without a proof).

Problems: 7.25 and 7.26; *Conceptual Questions* (on Companion Website): 7.29 and 7.30; *MATLAB Exercises* (on Companion Website).

7.5 MAGNETIC ENERGY DENSITY

In analogy with the concept of electric energy density (Section 2.16), we shall now define and use the magnetic energy density to describe the actual localization and distribution of the magnetic energy of a system of current-carrying conductors, the total amount of which is given by Eqs. (7.89) and (7.93). To this end, let us consider first a simple case of a magnetic field of uniform intensity in a thin toroidal

ferromagnetic core with a winding that carries a slowly time-varying current of intensity i. Let the number of wire turns of the winding be N, the length of the core l, and its cross section S in area. From Eq. (5.53), the current in the winding can be expressed in terms of the magnetic field intensity H in the core as $i = Hl/N$. On the other hand, the magnetic flux through the winding (all of its turns) can be written as $\Phi = N\Phi_{\text{single turn}} = NBS$, where B is the magnetic flux density in the core. Substituting these two expressions in Eq. (7.85) leads to the following expression for the work of external sources needed for a change $\mathrm{d}\Phi$ in the magnetic flux of the winding (not counting Joule's losses in the winding):

$$\mathrm{d}W_{\mathrm{m}} = i\,\mathrm{d}\Phi = \frac{Hl}{N}\,\mathrm{d}(NBS) = H\,\mathrm{d}B\,Sl = H\,\mathrm{d}B\,v, \tag{7.103}$$

where $v = Sl$ is the volume of the core, i.e., the volume of the domain where the magnetic field exists. The net work in changing the flux from zero to its final value Φ or, equivalently, the flux density from zero to the final value B is hence

$$W_{\mathrm{m}} = \int_{B=0}^{B} \mathrm{d}W_{\mathrm{m}} = v\int_{0}^{B} H\,\mathrm{d}B. \tag{7.104}$$

Dividing it by v, we get the magnetic energy density (energy per unit volume) of the core (in J/m^3),

$$\boxed{w_{\mathrm{m}} = \frac{W_{\mathrm{m}}}{v} = \int_{0}^{B} H\,\mathrm{d}B.} \tag{7.105}$$

magnetic energy density, arbitrary medium (unit: J/m^3)

More precisely, for an arbitrary magnetic material of the core, this is the energy per unit volume of the material spent by external sources in establishing the field, and not the energy stored in the field per unit volume of the material. Namely, as we shall see later in this section, in the case of materials that exhibit hysteresis effects (see Fig. 5.21), this energy can only partially be returned by the field to the sources in the reverse process of reducing the field intensity H to zero, because of losses occurring during the magnetization (while establishing H) and demagnetization (while reducing H) of the material. These losses, appearing as heat, are a consequence of microscopic frictions encountered as elementary magnetic domains (see Fig. 5.2) change their size and rotate in the magnetization-demagnetization process of the material and are known as hysteresis losses. For materials with no hysteresis losses, on the other side, Eq. (7.105) gives the energy that is contained in the field per unit volume of the core and can be obtained from it at any time in its entirety by reducing to zero the current in the coil. While using the term magnetic energy density for the integral expression in Eq. (7.105), we shall always keep in mind this distinction in its actual meaning between materials with pronounced hysteresis behavior and those for which hysteresis effects are not present or can be neglected.

Although derived for a special case of a coil on a thin toroidal core, the result in Eq. (7.105) can be generalized to an arbitrary magnetic field, which can be visualized as a collection of elementary flux tubes (toroids) formed by the lines of vector **B** [see Fig. 4.26 and the proof of the law of conservation of magnetic flux, Eq. (4.99)]. In general, the magnetic energy of a differentially small cell of volume $\mathrm{d}v$ in an arbitrary (nonuniform) magnetic field in an arbitrary (nonlinear) material is

$$\mathrm{d}W_{\mathrm{m}} = w_{\mathrm{m}}\,\mathrm{d}v, \tag{7.106}$$

where the energy density is given by Eq. (7.105). By summing up the energies of all of the cells, that is, by integrating the energy $\mathrm{d}W_{\mathrm{m}}$ over the entire domain with the

magnetic field (volume v), we obtain the total magnetic energy of the system:

$$W_{\mathrm{m}} = \int_v w_{\mathrm{m}}\,\mathrm{d}v = \int_v \left(\int_0^B H\,\mathrm{d}B \right) \mathrm{d}v. \tag{7.107}$$

In the case of a linear magnetic material of permeability μ, $\mathbf{B} = \mu\mathbf{H}$, so that the integral with respect to B in the expression for the magnetic energy density in Eq. (7.105) can easily be solved,

magnetic energy density, linear medium

$$\boxed{w_{\mathrm{m}} = \int_0^B H\,\mathrm{d}B = \frac{1}{\mu}\int_0^B B\,\mathrm{d}B = \frac{B^2}{2\mu} = \frac{1}{2}BH = \frac{1}{2}\mu H^2.} \tag{7.108}$$

Note that these expressions are entirely analogous to the corresponding expressions in Eq. (2.199) for the electric energy density w_{e} in a linear dielectric of permittivity ε.[5] The expression for the total magnetic energy becomes

$$W_{\mathrm{m}} = \frac{1}{2}\int_v \mathbf{B}\cdot\mathbf{H}\,\mathrm{d}v. \tag{7.109}$$

For nonlinear magnetic materials, the integral in Eq. (7.105), in general, cannot be solved analytically (in a closed form). Having in mind a typical initial magnetization curve of a nonlinear ferromagnetic material (e.g., that in Fig. 5.20), we note that $H\,\mathrm{d}B$ is proportional to the area of a thin strip of "length" H (length measured in A/m) and "width" $\mathrm{d}B$ (width measured in T) positioned between the curve and the B-axis at the "height" B with respect to the H-axis, as indicated in Fig. 7.19(a). This means that the integral in Eq. (7.105) represents the sum of areas of all such strips as the point P′ with abscissa H and ordinate B moves in the integration process from the coordinate origin to its final position (P). We conclude, thus, that the magnetic energy density in the material is proportional to the area between the magnetization curve and the B-axis, that is, to the area of the curvilinear triangle OPQ in Fig. 7.19(a). The proportionality constant (w_{m}/area) can be expressed in terms of the ratio of the magnetic field intensity H in A/m that corresponds to a certain physical length along the H-axis and the length (e.g., a 1-cm division along the axis may represent a 100-A/m field intensity) and the similar ratio (B/length) for the B-axis. This conclusion, of course, applies also to linear materials, which can always be considered as a special case of nonlinear ones. In a linear case, the hypotenuse of the triangle OPQ becomes straight, and the area of the triangle is computed as $BH/2$, Fig. 7.19(b), which is the same result as in Eq. (7.108).

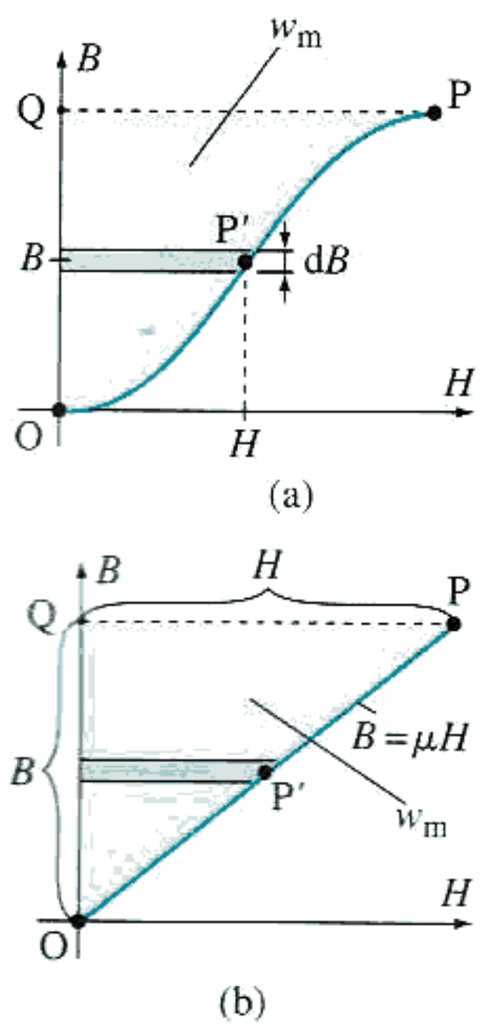

Figure 7.19
Correspondence between the magnetic energy density given by the integral in Eq. (7.105) and the area between the magnetization curve and the B-axis for (a) nonlinear and (b) linear magnetic materials.

In ferromagnetic materials that exhibit hysteresis effects, the function $B(H)$ is not only nonlinear, but also has multiple branches. Thus, if H is reduced from its value at the point P in Fig. 7.19(a) to zero, B does not go to zero, but to the remanent

[5] As in the electrostatic case, the magnetic energy of a system of current-carrying conductors might alternatively be viewed to reside in the system current, and not the magnetic field [see the corresponding discussion on the two energy localization viewpoints (field-based and charge-based) for an electrostatic system, in Section 2.16]. With this approach, the magnetic energy density would be evaluated as being equal to $\mathbf{J}\cdot\mathbf{A}/2$ at points where the current exists in the system [from Eq. (7.93)] and would be zero elsewhere. Although this viewpoint is also "correct" and has its merit, we choose to describe the magnetic energy localization of a system in terms of the magnetic field distribution (energy exists wherever and whenever the field exists) and use the associated energy density expressions in Eq. (7.108). As noted in the discussion of the electric energy localization, the field-based approach is much better suited to modeling electromagnetic wave propagation and the associated energy flow, where both electric and magnetic fields of a wave exist (and carry energy) independent of the charge and current that produced them at previous instants of time.

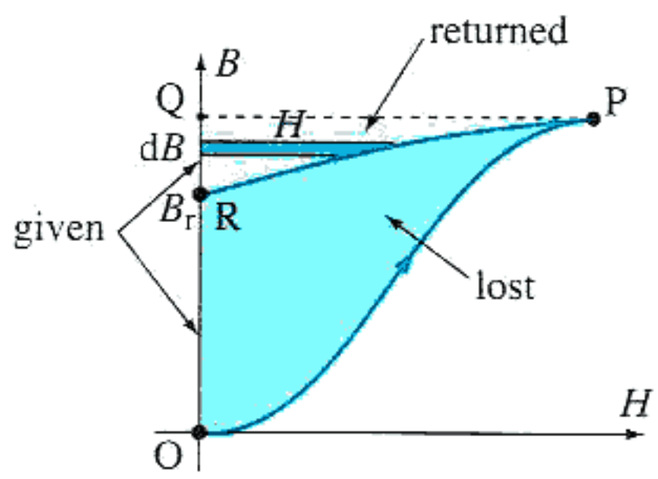

Figure 7.20 Evaluation of hysteresis losses in a ferromagnetic material as the difference between the energy given to the field and the energy returned to the sources in the process of magnetization and demagnetization of the material.

magnetic flux density $B = B_r$ (see Fig. 5.21). As B also decreases, dB is negative. This means that the energy $H\,dB$ per unit volume of the material given to the magnetic field in this process is negative, that is, the field is returning its energy to the external sources (e.g., to the generator in Fig. 7.18). However, this returned energy, which is proportional to the area of the curvilinear triangle RPQ shown in Fig. 7.20, is smaller than the energy spent by the sources in increasing the magnetic field in the material (curvilinear triangle OPQ). The difference in energy is lost to heat in the material in the process of its magnetization and demagnetization (hysteresis losses), and the difference in area in Fig. 7.20 is the area of the curvilinear triangle OPR. Consequently, the energy of hysteresis losses per unit volume of the material is proportional to the area of the triangle OPR.

Finally, let us consider a full hysteresis cycle in the material. The density of energy spent on changing the magnetic field in this cycle is given by the integral in Eq. (7.105) with the integration being carried out all around the hysteresis loop. Dividing the loop (contour C_h) into four characteristic segments, as indicated in Fig. 7.21, we note that $H\,dB > 0$ along the first line segment ($H > 0$ and $dB > 0$) and the third segment ($H < 0$ and $dB < 0$), while $H\,dB < 0$ along the second line segment ($H > 0$ and $dB < 0$) and the fourth one ($H < 0$ and $dB > 0$). The areas between line segments 1 and 3 and the B-axis are therefore a measure of the energy density given to the field at a point in the material, while the areas between line segments 2 and 4 and the B-axis correspond to the energy density returned to the sources at the same point. The difference, the area enclosed by the hysteresis loop, S_h, represents hysteresis losses in the material. In other words, the energy density

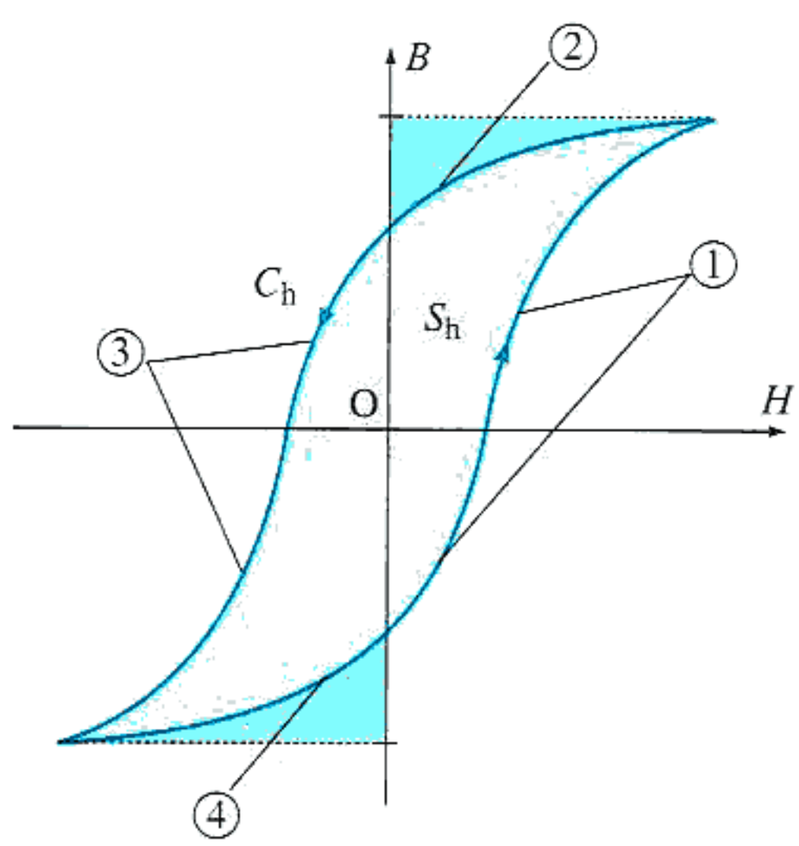

Figure 7.21 Evaluation of hysteresis losses in a complete magnetization-demagnetization hysteresis cycle of the material.

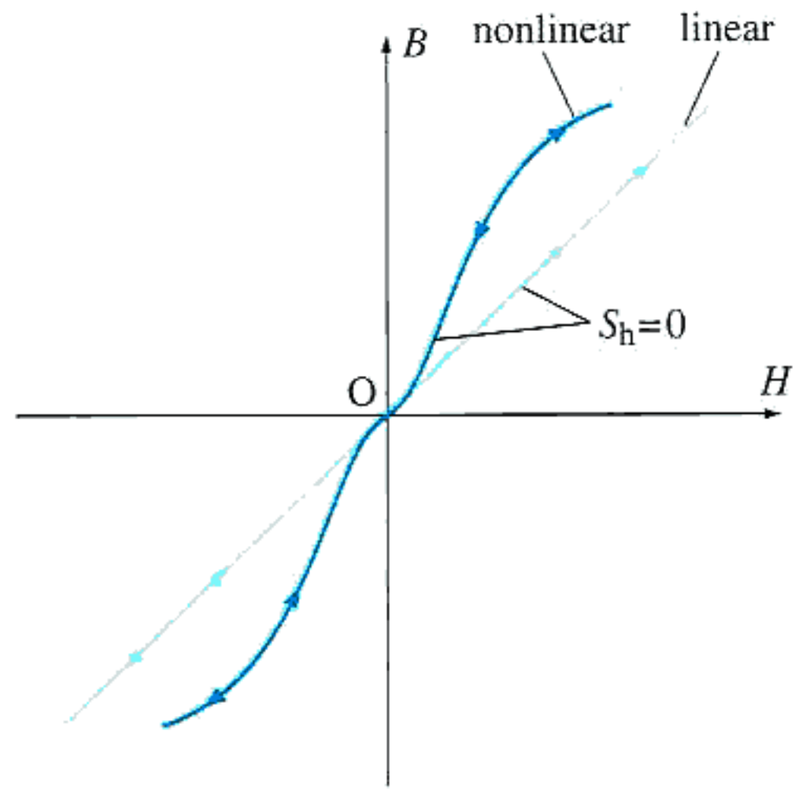

Figure 7.22 Cases with no hysteresis losses: nonlinear material with retracing of the initial magnetization curve in the periodic magnetization-demagnetization of the material, which results in zero loop area, and linear material (or material whose magnetization curve can be approximated by a linear function).

of hysteresis losses, w_h, in one complete magnetization-demagnetization hysteresis cycle is proportional to the area S_h,

energy density of hysteresis losses (see Fig. 7.21)

$$\boxed{w_h = w_m = \oint_{C_h} H\,dB \propto S_h.} \tag{7.110}$$

If the field is time-harmonic (ac field), with a frequency f, the time of one cycle of the periodic magnetization-demagnetization of the material, that is, the time during which the point P′ circumscribes once the hysteresis loop, equals the period of the field variation, $T = 1/f$. The time-average power of hysteresis losses, $(P_h)_{ave}$, is obtained by dividing the energy lost within a cycle by T, i.e., by multiplying it by f. Thus, in the case of a uniform field intensity in the material, we can write

time-average power of hysteresis losses for an ac field

$$\boxed{(P_h)_{ave} \propto f\,S_h v,} \tag{7.111}$$

where v is the volume of the material with losses.

We now recall that hard ferromagnetic materials, having large S_h (see Fig. 5.23), are used primarily for dc applications, so that $f = 0$ in Eq. (7.111) and hysteresis losses do not represent any problem. Soft ferromagnetic materials have small S_h, and that is why they are very suitable for ac applications. In the limiting case, if no hysteresis is present and the initial magnetization curve is retraced, as depicted in Fig. 7.22, $S_h = 0$ in Eq. (7.111) and the periodic magnetization-demagnetization process is accomplished with no hysteresis losses. Finally, $S_h = 0$ for linear magnetic materials as well (Fig. 7.22).

In general, total losses in a ferromagnetic material in an ac field are the sum of hysteresis losses and Joule's losses due to eddy currents, given by Eq. (6.137). We recall that the time-average power of eddy-current losses is proportional to the frequency squared [Eq. (6.152)].

Example 7.19 Energy Distribution in a Thick Linear Toroidal Core

Consider the toroidal coil from Example 5.11, and assume that a slowly time-varying current of intensity i is established in the coil. Under these circumstances, find (a) the distribution of magnetic energy in the core and (b) the total energy of the coil.

Solution

(a) The distribution of energy in the core is described by the magnetic energy density, w_m. As the material of the core is linear, we use Eq. (7.108). The magnetic field intensity in the core is given by Eq. (5.83), and hence

$$w_m(r) = \frac{1}{2}\mu H^2(r) = \frac{\mu N^2 i^2}{8\pi^2 r^2} \quad (a < r < b), \tag{7.112}$$

where r is the distance from the toroid axis.

(b) The energy of the coil, that is, the total magnetic energy stored in the core, can be obtained by integrating the energy density w_m over the volume v of the core [Eq. (7.109)]. Because w_m is a function of the coordinate r only, we adopt dv in the form of a differentially thin toroid of radius r and thickness dr, the cross section of which is the thin strip of length h and width dr shown in Fig. 5.26. The volume of this elementary toroid is thus $dv = l\,dS$, where $l = 2\pi r$ (length of the toroid) and $dS = h\,dr$, so that the magnetic energy comes out to be

$$W_m = \int_{r=a}^{b} w_m(r)\underbrace{2\pi r h\,dr}_{dv} = \frac{\mu N^2 i^2 h}{4\pi}\int_a^b \frac{dr}{r} = \frac{\mu N^2 i^2 h}{4\pi}\ln\frac{b}{a}. \tag{7.113}$$

The above result can also be obtained from Eq. (7.88), as $W_m = \Phi_{total} i/2$, where Φ_{total} is N times the flux through the cross section of the core, found in Eq. (5.84).

Example 7.20 Energy of a Simple Nonlinear Magnetic Circuit

Calculate the energy spent for establishing the field in the magnetic circuit shown in Fig. 5.30 and described in Example 5.13.

Solution Final (established) values of the magnetic flux density and field intensity in the ferromagnetic core and the air gap, (B, H) and (B_0, H_0), are found in Example 5.13. As the material of the core is nonlinear and the operating point P of the circuit, in Fig. 5.30(b), does not belong to the first segment of the idealized initial magnetization curve (which could be described by an initial permeability), we must use Eq. (7.105) for the density of energy spent to change the field in the core from zero to (B, H). Having in mind Fig. 7.19(a), this density is proportional to the area of a polygon formed by the curve and the B-axis, from the coordinate origin to the point P, as shown in Fig. 7.23. This polygon, in turn, is a sum of a triangle and a trapezoid, which gives the following solution for the integral in Eq. (7.105):

$$w_m = \int_0^B H\,dB = \underbrace{\frac{1}{2}H_k B_k}_{\text{triangle}} + \underbrace{\frac{1}{2}(H_k + H)(B - B_k)}_{\text{trapezoid}} = 272\ \text{J/m}^3, \tag{7.114}$$

where $B_k = 0.4$ T and $H_k = 1000$ A/m are the magnetic flux density and field intensity at the point K ("knee" point between the two segments of the curve) in Figs. 7.23 and 5.30(b).

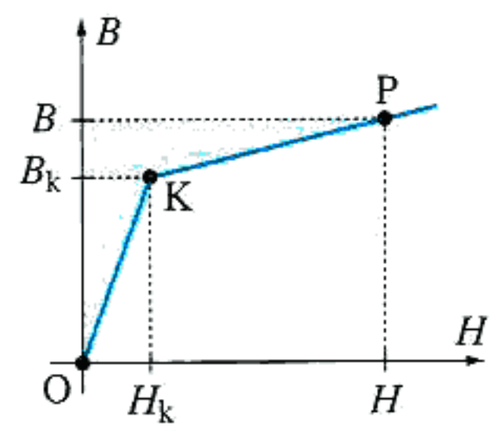

Figure 7.23 Evaluation of the density of energy spent for establishing the field in the core in Fig. 5.30; for Example 7.20.

Air is a linear medium, so that the magnetic energy density in the gap can be obtained using Eq. (7.108),

$$w_{m0} = \frac{1}{2}B_0 H_0 = 77\ \text{kJ/m}^3. \tag{7.115}$$

Finally, the total magnetic energy of the circuit amounts to

$$W_m = w_m S l + w_{m0} S_0 l_0 = 290\ \text{mJ}. \tag{7.116}$$

This energy can be completely returned by the field only if the initial magnetization curve is retraced in the process of reducing the field intensities in the circuit, as in Fig. 7.22.

Example 7.21 Energy Lost in Magnetization and Demagnetization

In a thin toroidal core of cross-sectional area $S = 1$ cm^2 and length $l = 20$ cm, a magnetic field is established of intensity $H_m = 1$ kA/m, and then reduced to $H = 0$. In this process,

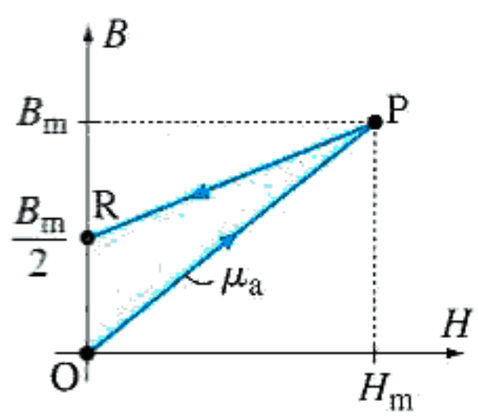

Figure 7.24 Evaluation of the net magnetic energy spent in the magnetization-demagnetization of a ferromagnetic core; for Example 7.21.

the operating point described the path shown in Fig. 7.24, where the initial permeability is $\mu_a = 0.001$ H/m. Find the net magnetic energy spent in the magnetization-demagnetization of the core.

Solution The magnetic energy spent to establish $H = H_m$ is positive, while it is negative in the process of reducing H to zero. The net magnetic energy, W_m, spent in the entire magnetization-demagnetization process represents hysteresis losses in the core (see Fig. 7.20). Its density is proportional to the area of the shaded triangle OPR in Fig. 7.24 and is given by

$$w_m = \underbrace{\int_O^P H\,dB}_{\text{magnetization}} + \underbrace{\int_P^R H\,dB}_{\text{demagnetization}} = \underbrace{\frac{1}{2}\frac{B_m}{2}H_m}_{\triangle OPR} = \frac{1}{4}B_m H_m = 250\ \text{J/m}^3, \tag{7.117}$$

where $B_m = \mu_a H_m = 1$ T, so that $W_m = w_m Sl = 5$ mJ.

Example 7.22 Time-Average Power of Hysteresis Losses in a Core

Consider the core depicted in Fig. 6.13(a) and (c), and assume that a low-frequency time-harmonic current of intensity $i = I_0 \sin(2\pi f t)$ is established in the coil, where $I_0 = 0.1$ A and $f = 1$ kHz. Compute the time-average power of hysteresis losses in the core.

Solution The energy density of hysteresis losses in one magnetization-demagnetization hysteresis cycle of the material is given by Eq. (7.110), with S_h now being the area of the parallelogram in Fig. 6.13(c). The current amplitude is the same as in Example 6.10, so that the peak-values of $H(t)$ and $B(t)$ are also the same, $H_m = 100$ A/m and $B_m = 0.1$ T [note that $B(t)$ is not a time-harmonic function, due to the nonlinearity and hysteresis behavior of the core material]. Thus, computing the parallelogram area, we obtain

$$w_h = \oint_{C_h} H\,dB = 2B_m H_m = 20\ \text{J/m}^3. \tag{7.118}$$

Based on Eq. (7.111), the time-average power of hysteresis losses in the volume $v = Sl$ of the core is

$$(P_h)_{ave} = f w_h Sl = 0.8\ \text{W}. \tag{7.119}$$

Example 7.23 Evaluation of Force from Energy for an Electromagnet

An electromagnet consisting of an iron core in the shape of a horseshoe and a coil is sketched in Fig. 7.25. The cross-sectional area of the core is S. With a steady current established in the coil, the electromagnet is capable of lifting a weight W (made also of iron). Assuming that there are two tiny air gaps between the core and the weight and that the magnetic flux density in the core and the gaps is B, find the lifting force of the electromagnet.

Solution The lifting force of the electromagnet is a consequence of the magnetic field in the magnetic circuit in Fig. 7.25, namely, it is the magnetic force, $\mathbf{F}_m$, on the lower part of the circuit that is lifting its weight. This force can be determined from the magnetic energy of the system using the principle of conservation of energy. Let us suppose that $\mathbf{F}_m$ moves the weight by an elementary distance dx upward. We recall the energy considerations in connection with Fig. 7.18. Here, however, the elementary work of external sources $i\,d\Phi$ from Eq. (7.85) is split to the change in the magnetic energy of the system dW_m and the work dW_F of the force $\mathbf{F}_m$ along the displacement dx. As $dW_F = F_m\,dx$, we can write

$$i\,d\Phi = dW_m + dW_F = dW_m + F_m\,dx. \tag{7.120}$$

If the magnetic flux is maintained at a constant value (Φ) in this experiment, which means that the current i in the coil is varied appropriately, then $d\Phi = 0$ and the above equation yields

magnetic force from energy

$$\boxed{F_m = -\left.\frac{dW_m}{dx}\right|_{\Phi=\text{const}}}. \tag{7.121}$$

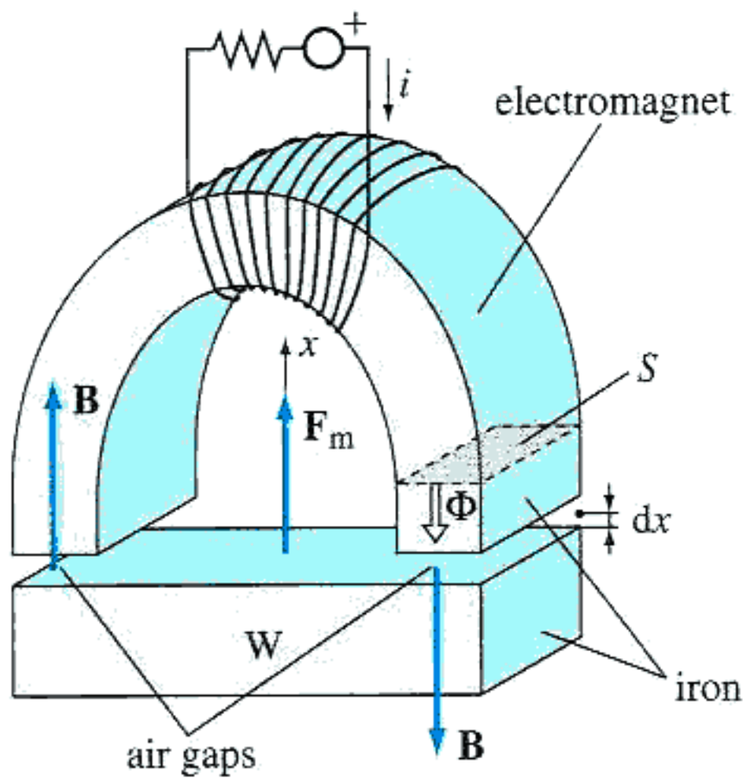

Figure 7.25 Evaluation of the lifting force of an electromagnet from the magnetic energy contained in the air gaps; for Example 7.23.

When the weight is moved upward by dx, the only change in magnetic energy of the system is the reduction in energy contained in the two air gaps due to their decreased length. The energy change dW_m in Eq. (7.121) is thus negative and corresponds to the energy contained in the parts of the air gaps that are dx long and that vanish in our experiment. In other words, it equals the negative of the magnetic energy density w_m in the air gaps, given by Eq. (7.108) with $\mu = \mu_0$, times the change in the volume of the gaps:

$$dW_m = -\underbrace{\frac{B^2}{2\mu_0}}_{w_m} \underbrace{2S\,dx}_{dv} = -\frac{B^2 S\,dx}{\mu_0} \tag{7.122}$$

($2S$ is the total cross-sectional area of the gaps). From Eq. (7.121), the lifting force of the electromagnet is

$$F_m = -\frac{dW_m}{dx} = \frac{B^2 S}{\mu_0}. \tag{7.123}$$

As a numerical example, for $B = 1$ T and $S = 0.125$ m^2, $F_m \approx 100$ kN, which means that this electromagnet can lift a weight of $m = F_m/g \approx 10$ tons ($g = 9.81$ m/s^2 – standard acceleration of free fall). Such powerful electromagnets are used in cranes for lifting large pieces of iron.

Example 7.24 Magnetic Pressure

(a) For the electromagnet of Fig. 7.25, determine the magnetic pressure, that is, the pressure of the lifting force $\mathbf{F}_m$, on the surface of the iron piece that is being lifted. (b) Based on the result in (a), compare the maximal values of the magnetic and electric pressures attained in practical situations.

Solution

(a) The force acts on the parts of the surface of the iron piece that form the air gaps with the core in Fig. 7.25, that is, on the surface of area $2S$ in total. The corresponding pressure is therefore given by

$$\boxed{p_m = \frac{F_m}{2S} = \frac{B^2}{2\mu_0},} \tag{7.124}$$ *magnetic pressure (unit: Pa)*

and is called the magnetic pressure. This expression is valid for any boundary surface between a ferromagnetic material (with $\mu \gg \mu_0$) and air (or any other nonmagnetic

medium), with B being the local magnetic flux density in air near the surface. We see that the pressure p_m actually equals the local magnetic energy density on the nonmagnetic side of the surface. It acts from the ferromagnetic material toward the medium with $\mu = \mu_0$.

(b) Note that the expression in Eq. (7.124) is entirely analogous to the expression in Eq. (2.133) for the electric pressure on a metallic surface in air. These two expressions provide us now with an opportunity to compare the electric and magnetic pressures and forces. Combining them, we get

$$\frac{p_m}{p_e} = \frac{1}{\varepsilon_0 \mu_0}\left(\frac{B}{E}\right)^2. \tag{7.125}$$

To estimate the ratio of the maximal magnetic and maximal electric pressure attained in practical situations, we recall that the maximal permissible electric field intensity, E, is determined by the dielectric strength of air, Eq. (2.53), and we take therefore $E_{max} = 3$ MV/m in this estimation. On the other side, there is no such limit for B. However, maximal magnetic flux densities that are normally attained in typical magnetic circuits are on the order of one tesla and it is reasonable to assume that $B_{max} = 1$ T for the comparison. Hence,

ratio of maximal magnetic and electric pressures attained in practice

$$\boxed{\frac{(p_m)_{max}}{(p_e)_{max}} = \frac{1}{\varepsilon_0 \mu_0}\left(\frac{B_{max}}{E_{max}}\right)^2 \approx 10{,}000.} \tag{7.126}$$

We conclude that practically attainable magnetic pressures are several orders of magnitude stronger than electric ones. This is why magnetic forces, and not electric ones, are the actual workhorses of our industrial world. Practically all devices for electromechanical energy conversion, such as different types of electric motors and generators, are based on magnetic forces and their work and power.

Problems: 7.27–7.35; *Conceptual Questions* (on Companion Website): 7.31–7.33; *MATLAB Exercises* (on Companion Website).

7.6 INTERNAL AND EXTERNAL INDUCTANCE IN TERMS OF MAGNETIC ENERGY

In this section, we revisit the concept of self-inductance and techniques to compute it, now from the energy standpoint. We consider, thus, an arbitrary conductor in a linear magnetic medium. From Eq. (7.88), if we assume a slowly time-varying (or steady) current of intensity i to flow in the conductor, the inductance (self-inductance) of the conductor, L, can be expressed in terms of the energy contained in the magnetic field due to i, W_m, as

inductance from magnetic energy

$$\boxed{L = \frac{2W_m}{i^2}.} \tag{7.127}$$

This expression can be viewed as the third equivalent definition of self-inductance, the other two being the flux definition in Eq. (7.1) and emf definition in Eq. (7.2). It can hence be used, as an alternative general means for computing the inductance of different structures, where the magnetic energy of the structure is computed using the integral expression in Eq. (7.109).

Since the energy W_m can be written as the sum of energies localized inside and outside the conductor,

$$W_m = W_{mi} + W_{me}, \tag{7.128}$$

the inductance L can be decomposed accordingly into the internal inductance, L_i, and external inductance, L_e, of the conductor:

$$L = L_i + L_e. \tag{7.129}$$

In other words,

$$\boxed{L_i = \frac{2W_{mi}}{i^2} \quad \text{and} \quad L_e = \frac{2W_{me}}{i^2},} \tag{7.130}$$

internal and external inductances

where the internal and external magnetic energies of the conductor are obtained by integrating the energy density over the conductor interior (volume v_i) and exterior (volume v_e), respectively, that is,

$$W_{mi} = \frac{1}{2}\int_{v_i} \mathbf{B}\cdot\mathbf{H}\,dv \quad \text{and} \quad W_{me} = \frac{1}{2}\int_{v_e} \mathbf{B}\cdot\mathbf{H}\,dv. \tag{7.131}$$

More precisely, v_e is only that part of the conductor exterior which is occupied by the magnetic field (there is no need to integrate zero energy density).

In all of the examples of Section 7.1, we only evaluated the external inductance of conductors, by employing the flux (or emf) definition of self-inductance with only the external magnetic flux taken into account. Evaluation of L_i from the internal magnetic flux is also possible, but is physically less clear and mathematically more complicated than from the internal stored magnetic energy.

At high frequencies, due to skin effect (see Fig. 6.23), the current and magnetic field in a conductor are confined to a very thin region on the surface of the conductor, which considerably reduces the high-frequency value of the internal inductance of the conductor from its low-frequency (or dc) value. Therefore, in most high-frequency applications, L_i is negligible as compared to L_e, and assumption that $L \approx L_e$ yields very accurate results.

Example 7.25 **Internal Inductance p.u.l. of a Cylindrical Conductor**

Find the internal inductance per unit length of an infinitely long cylindrical conductor of radius a. The permeability of the conductor is μ. Skin effect is not pronounced.

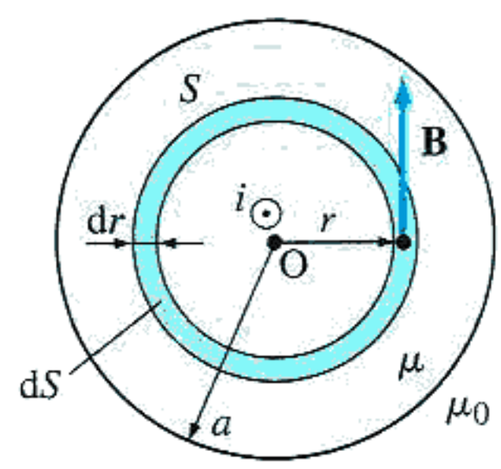

Figure 7.26 Evaluation of the low-frequency internal inductance per unit length of an infinitely long cylindrical conductor of permeability μ; for Example 7.25.

Solution Assume that the conductor carries a current of intensity i that is uniformly distributed over its cross section (skin effect not pronounced). The magnetic flux density in the conductor is given by the expression for $r < a$ in Eq. (4.56) with μ_0 substituted by μ and I by i, that is,

$$B(r) = \frac{\mu i r}{2\pi a^2}, \tag{7.132}$$

with r being the distance from the conductor axis, as shown in Fig. 7.26. From the first expression in Eqs. (7.131), the internal magnetic energy per unit length of the conductor is obtained by integrating the magnetic energy density over the cross section S of the conductor [see Eqs. (2.206) and (2.207) for the similar integration of the electric energy density],

$$W'_{mi} = (W_{mi})_{p.u.l.} = \int_S w_m\,dS = \int_0^a \frac{B^2(r)}{2\mu}\underbrace{2\pi r\,dr}_{dS} = \frac{\mu i^2}{4\pi a^4}\int_0^a r^3\,dr = \frac{\mu i^2}{16\pi}, \tag{7.133}$$

where dS is the surface area of an elementary ring of radius r and width dr (Fig. 7.26).

The first equation of Eqs. (7.130) then gives the following expression for the low-frequency internal inductance per unit length of the conductor:

$$\boxed{L'_i = \frac{2W'_{mi}}{i^2} = \frac{\mu}{8\pi}.} \tag{7.134}$$

low-frequency internal inductance p.u.l. of a cylindrical conductor

We note that this inductance is independent of the conductor radius. For nonmagnetic conductors, $L'_{\mathrm{i}} = \mu_0/(8\pi) = 50$ nH/m.

Example 7.26 **Internal Inductance p.u.l. of a Thin Two-Wire Line**

Determine the total (internal plus external) low-frequency inductance per unit length of the two-wire line in Fig. 7.4, assuming that the conductors are nonmagnetic.

Solution Since the distance between the conductors of the line is much larger than the conductor radii, the internal magnetic energies of individual conductors (for an assumed low-frequency current in the line) can be evaluated independently from each other. Therefore, the low-frequency internal inductance per unit length of the line can be found as twice that of a single isolated conductor, Eq. (7.134) with $\mu = \mu_0$ (conductors are nonmagnetic), which yields

$$L'_{\mathrm{i}} = L'_{\mathrm{i1}} + L'_{\mathrm{i2}} = 2L'_{\mathrm{i1}} = \frac{\mu_0}{4\pi} = 100 \text{ nH/m}. \tag{7.135}$$

Using the expression for the external inductance p.u.l. of the line, Eq. (7.11), its total low-frequency per-unit-length inductance is

low-frequency total inductance p.u.l. of a thin two-wire line

$$\boxed{L' = L'_{\mathrm{i}} + L'_{\mathrm{e}} = \frac{\mu_0}{\pi}\left(\frac{1}{4} + \ln\frac{d}{a}\right).} \tag{7.136}$$

Example 7.27 **Inductance from Energy for a Coaxial Cable**

Find the total low-frequency inductance per unit length of the coaxial cable from Example 4.11.

Solution If we assume that a dc current of intensity I is established in the cable conductors, as in Fig. 4.17, the magnetic flux density at a distance r from the cable axis, $B(r)$, is given by Eqs. (4.61)–(4.63). We use the energy definition of inductance, Eq. (7.127). The total (internal plus external) magnetic energy per unit length of the cable can be obtained by integrating the magnetic energy density over the cross section of the cable (the magnetic field outside the cable, for $r > c$, is zero) in the same manner as in Eq. (7.133),

$$W'_{\mathrm{m}} = \int_{r=0}^{c} \underbrace{\frac{B^2(r)}{2\mu_0}}_{w_{\mathrm{m}}} \underbrace{2\pi r\,\mathrm{d}r}_{\mathrm{d}S}. \tag{7.137}$$

As the function $B(r)$ for $0 \le r \le c$ is given by three different expressions in Eqs. (4.61) and (4.62), we break the integration with respect to r up into three parts: from 0 to a, from a to b, and from b to c. This yields

$$W'_{\mathrm{m}} = \underbrace{\frac{\mu_0 I^2}{16\pi}}_{W'_{\mathrm{mi1}}} + \underbrace{\frac{\mu_0 I^2}{4\pi}\ln\frac{b}{a}}_{W'_{\mathrm{me}}} + \underbrace{\frac{\mu_0 I^2}{4\pi(c^2-b^2)}\left(\frac{c^4}{c^2-b^2}\ln\frac{c}{b} - \frac{3c^2-b^2}{4}\right)}_{W'_{\mathrm{mi2}}}. \tag{7.138}$$

where W'_{mi1}, W'_{me}, and W'_{mi2} are the magnetic energies residing in the inner conductor, dielectric, and outer conductor of the cable per unit of its length, respectively. The total dc (or low-frequency) inductance per unit length of the cable is hence

low-frequency total inductance p.u.l. of a coaxial cable

$$\boxed{L' = \frac{2W'_{\mathrm{m}}}{I^2} = \underbrace{\frac{\mu_0}{2\pi}\left[\frac{1}{4} + \frac{1}{c^2-b^2}\left(\frac{c^4}{c^2-b^2}\ln\frac{c}{b} - \frac{3c^2-b^2}{4}\right)\right]}_{L'_{\mathrm{i}}} + \underbrace{\frac{\mu_0}{2\pi}\ln\frac{b}{a}}_{L'_{\mathrm{e}}},} \tag{7.139}$$

where L'_{i} and L'_{e} are the internal and external inductance, respectively, per unit length of the cable.

The above result for L'_e is, of course, the same as that in Eq. (7.12), which was obtained using the flux definition of inductance. Note that the first component of L'_i, that corresponding to the magnetic energy in the inner conductor, equals the internal inductance per unit length of an isolated cylindrical conductor in air, Eq. (7.134) with $\mu = \mu_0$.

As a numerical example, the internal and external inductances per unit length of a coaxial cable with $a = 1$ mm, $b = 4$ mm, and $c = 5$ mm amount to $L'_i = 66.6$ nH/m and $L'_e = 277.3$ nH/m.

Problems: 7.36–7.38; *Conceptual Questions* (on Companion Website): 7.34; *MATLAB Exercises* (on Companion Website).

Problems

7.1. Induced emf and voltage of an inductor. A current of intensity $i(t) = I_0\, e^{-t/\tau}$, where I_0 and $\tau > 0$ are constants, flows through an inductor of inductance L. Calculate (a) the magnetic flux, (b) the induced emf, and (c) the voltage of the inductor. Specify the reference directions/orientations for all quantities.

7.2. Inductance of a solenoid with a two-layer core. If the solenoidal coil described in Example 7.1 is wound over a ferromagnetic core with two coaxial layers of relative permeabilities $\mu_{r1} = 500$ and $\mu_{r2} = 1000$, as shown in Fig. 7.27, where the cross-sectional area of the inner layer is $S_1 = 1$ cm^2, find the inductance of the coil.

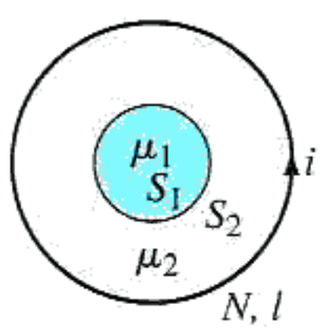

Figure 7.27 Solenoid with a core composed of two coaxial linear ferromagnetic layers; for Problem 7.2.

7.3. Toroidal coil with a two-layer core. Repeat Example 7.2 but for the two-layer core shown in Fig. 7.28.

7.4. Inductance of a coil in a simple linear magnetic circuit. Find the inductance of the coil in the simple linear magnetic circuit with an air gap from Example 5.14.

7.5. Two-wire line with ferromagnetic coatings over conductors. Let the conductors of the thin symmetrical two-wire transmission line in Fig. 7.4 be coated by ferromagnetic layers of permeability μ and thickness a, analogously to the line with dielectrically coated conductors in Fig. 2.31. Determine the external inductance per unit length of the new line.

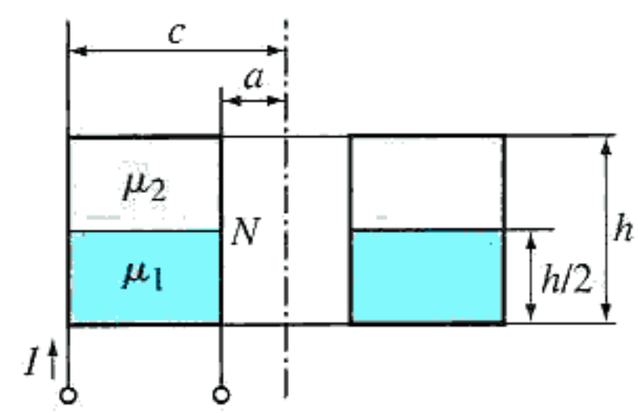

Figure 7.28 The same toroidal coil as in Fig. 7.3 but with ferromagnetic layers stacked on top of one another; for Problem 7.3.

7.6. Coaxial cable filled with an inhomogeneous magnetic material. Compute the external inductance per unit length of a coaxial cable filled with a piece-wise homogeneous ferromagnetic material composed of two coaxial layers of relative permeabilities μ_{r1} and μ_{r2} and dimensions as in Fig. 2.50.

7.7. Planar line with two magnetic layers. For the planar transmission line in Fig. 3.24, assume that the two material layers between metallic strips are lossless ($\sigma_1 = \sigma_2 = 0$), but magnetic, with permeabilities μ_1 and μ_2. Let $w \gg d_1 + d_2$, so that fringing effects can be neglected, i.e., the magnetic field of the line can be considered to be uniform and localized only in the two layers, and not in the air around (also see the magnetic field computation in

Example 11.10). Under these circumstances, find the p.u.l. external inductance of the line.

7.8. External inductance p.u.l. of a three-wire line. What is the external inductance per unit length of the transmission line consisting of an isolated wire and two short-circuited wires in air described in Example 2.16?

7.9. Bringing a superconducting contour in a magnetic field. A superconducting square contour of edge length a and inductance L is first situated outside any magnetic field, and there is no current in it. The contour is then brought in a uniform time-invariant magnetic field of flux density B and positioned so that the vector $\mathbf{B}$ is perpendicular to the plane of the contour. Orienting the contour in accordance to the right-hand rule with respect to the direction of $\mathbf{B}$, find (a) the magnetic flux through the contour and (b) the current intensity along it – in the new steady state.

7.10. Mutual inductance between a loop and two-wire line. Find the mutual inductance between the rectangular loop and the two-wire line in both cases in Fig. 6.32, in the following two ways: (a) from the definition of mutual inductance in Eq. (7.21) or (7.23) and (b) using Eq. (7.40), respectively.

7.11. Mutual inductance of two coils on a thick toroidal core. Repeat Example 7.7 but for a thick toroidal core of a rectangular cross section, as the one shown in Fig. 5.26, with the inner and outer radii and height of the toroid being $a = 3$ cm, $b = 6$ cm, and $h = 2$ cm, respectively.

7.12. Mutual inductance between a toroidal coil and axial wire. Consider the thick toroidal coil with a rectangular cross section in Fig. 4.18, and assume that an infinitely long straight wire runs along the axis of the toroid (z-axis). Find the mutual inductance between the coil and the wire, computing it both as (a) L_{12} and (b) L_{21}.

7.13. Mutual inductance between a solenoid and rectangular loop. Assume that the length of the solenoid in Fig. 6.29 is l ($l \gg a$), so that the total number of wire turns amounts to $N = N'l$, as well as that its terminals are open. If the rectangular loop positioned around the solenoid at the middle of its length (Fig. 6.29) carries a low-frequency time-harmonic current of intensity $i = I_0 \cos \omega t$, determine the voltage between the terminals of the solenoid.

7.14. Mutual inductance between large and small concentric loops. If in the two-loop system in Fig. 6.33 a slowly time-varying current of intensity $i(t)$ flows along the small circular loop, while the large square loop is open-circuited, compute the induced emf in the large loop.

7.15. Emf in a phone line due to a nearby power line. A power conductor of a cable car and track form a transmission line that can be approximated by a two-wire line, in a vertical plane, with distance between wire axes $h = 5$ m. In the same horizontal plane containing the power conductor, running in parallel to it, there is a two-wire telephone line, and the distances of axes of wires of this line from the power-conductor axis are $d_1 = 5.5$ m and $d_2 = 5.9$ m, respectively. Both lines can be considered to be thin. If a time-harmonic current of amplitude (peak-value) $I_0 = 150$ A and frequency $f = 60$ Hz is established in the power line, find the amplitude of the induced emf per $l = 1$ km length of the phone line, neglecting the influence of the earth, i.e., assuming that the two lines are in free space.

7.16. Equivalent input inductance of structures with coupled coils. Two magnetically coupled coils, wound on a cardboard core, have inductances $L_1 = L_2 = 50\ \mu$H and coupling coefficient $k = 0.1$. Calculate the equivalent inductance between terminals 1 and 2 of the structure for connections between coils as in Fig. 7.29(a), (b), and (c), respectively.

7.17. Equivalent inductance for a unity coupling coefficient. Repeat the previous problem assuming that the cardboard core is replaced by a linear ferromagnetic one, with which $L_1 = L_2 = 60$ mH and $k = 1$.

7.18. Coupling coefficient of two circuits from charge flow. Fig. 7.30 shows the circuit-theory representation of two magnetically coupled circuits, where the inductances of the circuits are $L_1 = 10$ mH and $L_2 = 3$ mH, and their resistances $R_1 = 10\ \Omega$ and $R_2 = 8\ \Omega$, respectively. When the switch K in

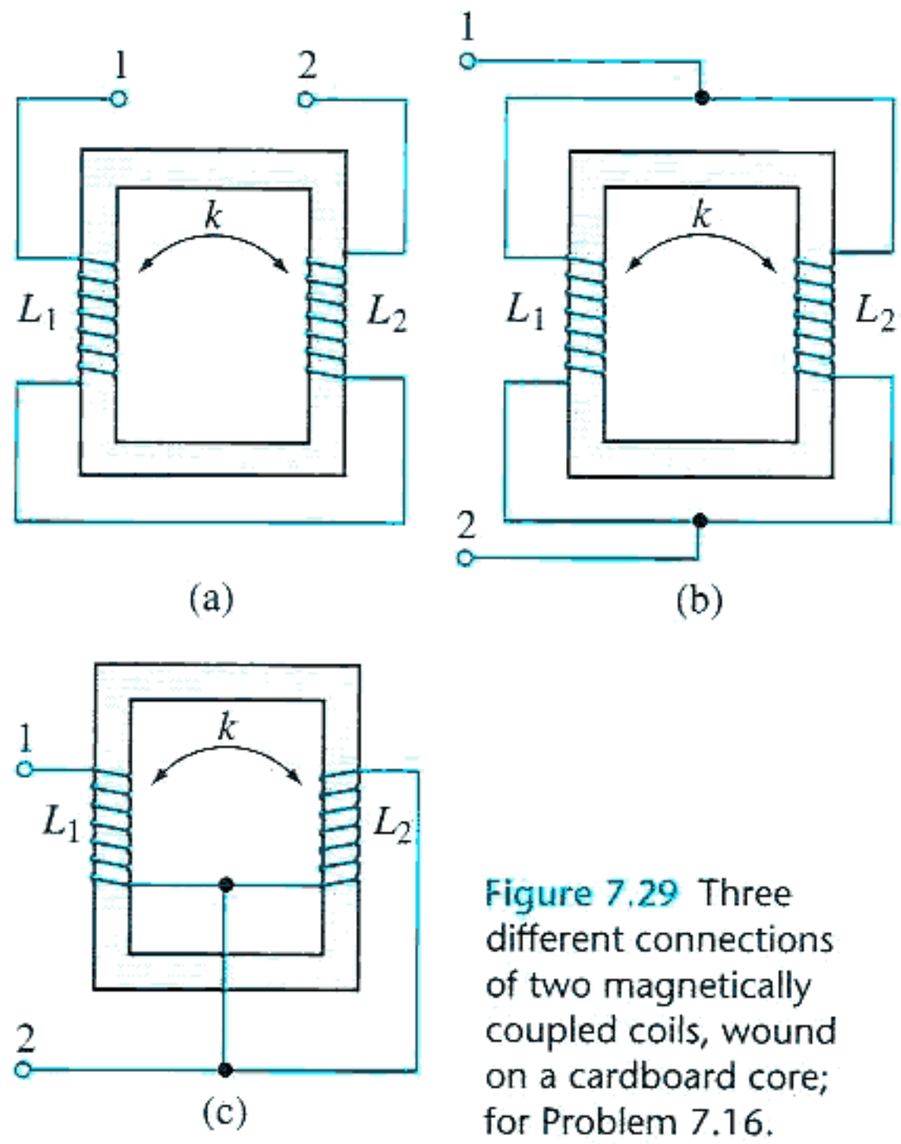

Figure 7.29 Three different connections of two magnetically coupled coils, wound on a cardboard core; for Problem 7.16.

the primary circuit is closed, connecting it to an ideal dc voltage generator of emf $\mathcal{E} = 20$ V, the charge flow indicated by the ballistic galvanometer (whose resistance is included in R_2) in the secondary circuit is $Q = 1$ mC. What is the coefficient of coupling (k) between the circuits?

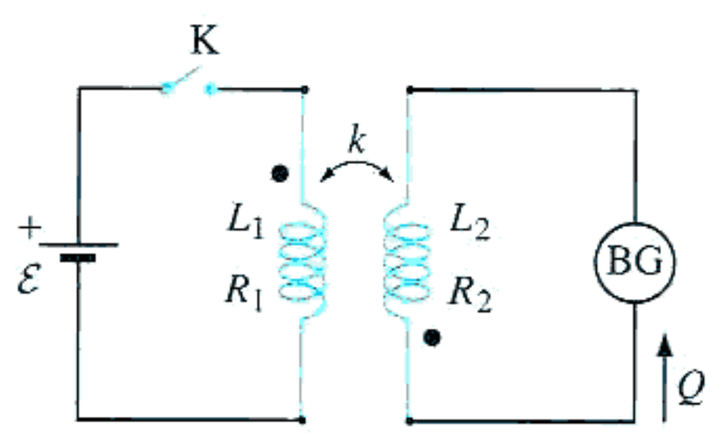

Figure 7.30 Magnetically coupled circuits with a dc voltage generator and a ballistic galvanometer (BG) on the primary and secondary sides, respectively; for Problem 7.18.

7.19. Thick toroidal coil and three-turn loop around it. An air-filled thick toroidal coil of a rectangular cross section, defined by the inner and outer radii $a = 5$ cm and $b = 15$ cm and height $h = 7$ cm of the toroid, has $N = 1800$ wire turns of negligible resistance. The toroid is encircled by three turns of wire that are connected to an ideal low-frequency time-harmonic current generator, as shown in Fig. 7.31. When the switch K between the terminals P and Q of the coil is open, the voltage across it is $v_{PQ} = 100 \sin 377t$ mV (t in s). (a) What is the current intensity $i_g(t)$ of the current generator? (b) If the switch K is then closed, find the current through it in the new steady state.

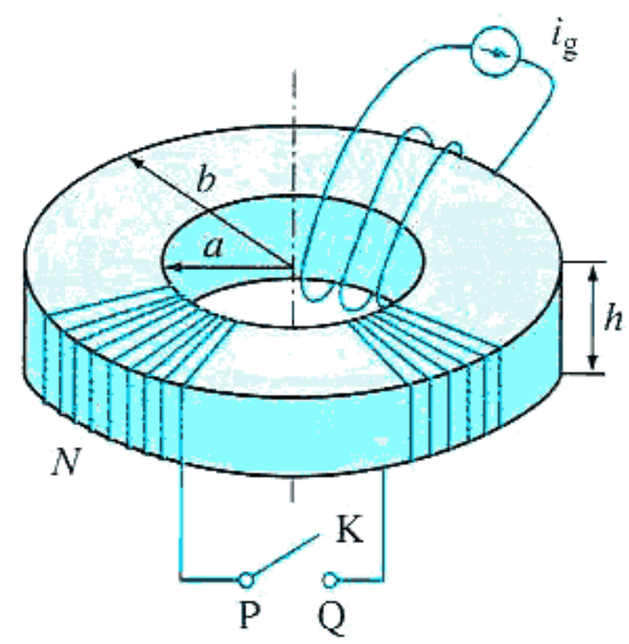

Figure 7.31 Magnetically coupled circuits with a thick toroidal coil and a three-turn loop around it; for Problem 7.19.

7.20. Coupling coefficient of two coaxial toroidal coils. Shown in Fig. 7.32 is a system of two air-filled thick toroidal coils, wound uniformly and densely on cardboard cores with rectangular cross sections, that are positioned coaxially one inside the other. The inner and outer radii of the inner toroid are a_1 and b_1, while those of the outer toroid are a_2 and b_2 ($a_2 < a_1 < b_1 < b_2$), and the heights of the

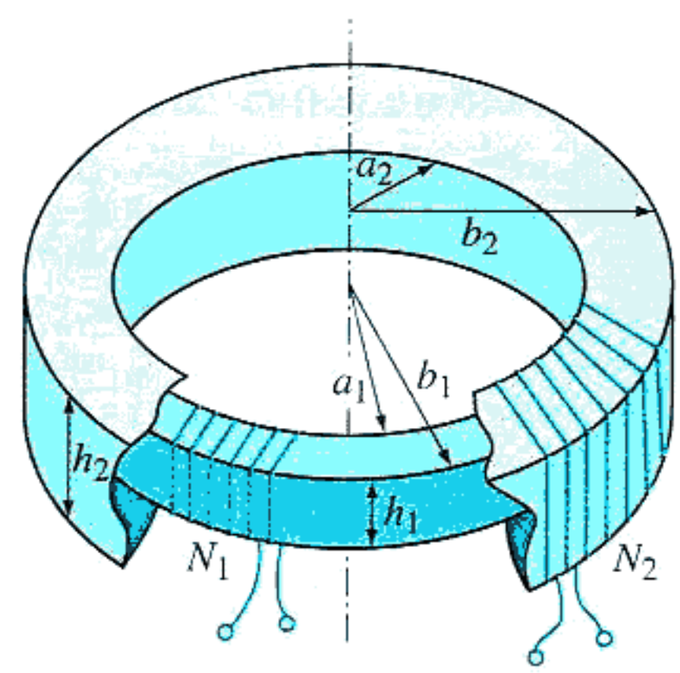

Figure 7.32 Two coupled coaxial air-filled thick toroidal coils; for Problem 7.20.

toroids are h_1 and h_2 ($h_1 < h_2$), respectively. The numbers of wire turns are N_1 for the inner and N_2 for the outer coil. Determine the coefficient of coupling between the two coils.

7.21. Magnetically coupled circuits with coaxial solenoids. For the system of two coupled coaxial solenoids in Fig. 7.15, let $a_1 = 2$ cm, $a_2 = 6$ cm, $l = 1$ m, $N_1 = 2000$, $N_2 = 4000$, and $\mu_r = 200$. In addition, let the outer solenoid be connected to an ideal time-harmonic voltage generator of emf $e_g = 50 \cos 377t$ V (t in s), and the inner solenoid be short-circuited. Compute (a) the equivalent input inductance seen by the generator and (b) the amplitudes of currents in the solenoids.

7.22. Voltage transformation by two coupled two-wire lines. If the second (inner) two-wire line in Fig. 7.16 is short-circuited at one end but open at the other, compute the amplitude of the current in the first line and voltage across the open terminals of the second circuit.

7.23. Current transformation by two coupled two-wire lines. Considering the system in Fig. 6.32 as two magnetically coupled circuits containing two two-wire lines, assume that $a = 8$ mm, $b = 25$ cm, $I_{g0} = 1$ A, and $\omega = 10^5$ rad/s, as well as that the length of the longer line is $l = 90$ cm and the radii of all wires $r_w = 0.4$ mm, and compute the amplitude of the current in the shorter line (of length b) for cases in Fig. 6.32(a) and Fig. 6.32(b), respectively. Neglect internal inductances, losses in the wires, capacitive coupling between the lines, end effects, and propagation effects.

7.24. Two-wire line in a vertical plane above a PMC surface. Repeat Example 7.16 but for a two-wire line in a vertical plane above the horizontal PMC plane, with the wires running in parallel to it, and h denoting the height of the axis of the lower wire with respect to the material surface and equaling $d/2$. Does the presence of the ferromagnetic material increase or decrease the p.u.l. inductance of the line?

7.25. Energy of magnetically coupled coil and loop. For magnetically coupled circuits containing an air-filled thick toroidal coil of a rectangular cross section and three-turn wire loop around it shown in Fig. 7.31 and described in Problem 7.19, find the total instantaneous and time-average magnetic energies of the circuits in both steady states, namely, with the switch K open and closed, respectively.

7.26. Energy of magnetically coupled two-wire lines – three cases. Compute the time-average magnetic energy of systems with two coupled two-wire lines from (a) Problem 7.22, (b) Problem 7.23 for the case in Fig. 6.32(a), and (c) Problem 7.23 for the case in Fig. 6.32(b), respectively.

7.27. Magnetic energy of two coupled coaxial solenoids. Consider the system of two coupled coaxial solenoids described in Problem 7.21, and find the time-average magnetic energy of the system – in the following three ways, respectively: (a) using the equivalent input inductance seen by the voltage generator, (b) by means of self- and mutual inductances of the coupled circuits and Eq. (7.90), and (c) from the magnetic field intensity and energy density throughout the system. (d) What portion of the total energy is stored in the ferromagnetic core, inside the inner coil, and what in the air-filled region between the two coils?

7.28. Energy distribution in thick linear two-layer toroidal cores. Find the magnetic energy density in the material, energy stored in each linear ferromagnetic layer, and total energy of the coil for thick toroidal coils with two-layer cores in (a) Fig. 7.3 and (b) Fig. 7.28, respectively, assuming that a slowly time-varying current of intensity $i(t)$ is established in the coil. Compute the energies by integrating the energy density throughout the volumes of individual layers, as well as using the expressions for inductances where appropriate.

7.29. Energy distribution in a planar line with two magnetic layers. Assuming that the planar transmission line with two magnetic layers between metallic strips described in Problem 7.7 carries a dc current of intensity I, compute the magnetic energy density and total energy per unit length of each of the layers, as well as the p.u.l. energy of the entire line.

7.30. Energy of a nonlinear magnetic circuit with three branches. Compute the magnetic

energy spent for establishing the field in each of the three branches, as well as the total energy, of the nonlinear magnetic circuit shown in Fig. 5.32 and described in Example 5.15.

7.31. Energy of another nonlinear magnetic circuit. Repeat the previous problem but for the magnetic circuit from Problem 5.22 (Fig. 5.42).

7.32. Magnetization-demagnetization energy of a thick toroidal core. Consider the thick toroidal coil with a rectangular cross section and nonlinear ferromagnetic core described in Example 5.12, and assume that its current is first established at an intensity of $I = 1$ A, so that the distribution of the magnetic flux density, $B(r)$, in the core is exactly that in Fig. 5.27(c), and then reduced to $I = 0$. In this process, the operating point at different locations in the core first moves up the idealized initial magnetization curve, and then back to the B-axis, where the magnetic flux densities drop to a half of the previously reached value, so either to $B_m/2$ in the part of the core that is in saturation ($r \leq c$) or to $B(r)/2$ [$B(r) < B_m$] in the part of the core in the linear regime ($r > c$), as indicated in Fig. 7.33 (similarly to the process in Fig. 7.24). Find (a) the density of the net magnetic energy spent in the magnetization-demagnetization process at every point of the core (for every r, $a \leq r \leq b$) and (b) the energy spent in the entire core.

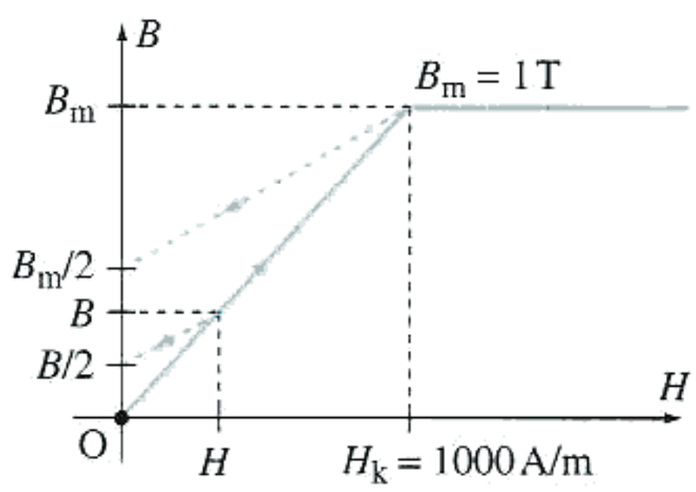

Figure 7.33 Magnetization and demagnetization of the thick toroidal nonlinear ferromagnetic core in Fig. 5.27; for Problem 7.32.

7.33. Power of hysteresis losses in the core of a solenoid. An infinitely long solenoid with a circular cross section of radius a and N' turns of wire per unit of its length is wound about a nonlinear ferromagnetic core whose idealized hysteresis loop is shown in Fig. 7.34, where $B_m/H_m = \mu_h =$ const. There is a low-frequency time-harmonic current of amplitude I_0 and angular frequency ω flowing through the winding. Saturation is not reached in the core. Determine the time-average power of hysteresis losses per unit length of the core.

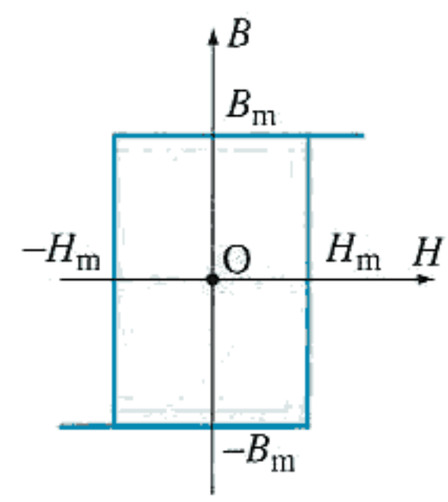

Figure 7.34 Idealized hysteresis loop of a ferromagnetic core filling an infinite solenoid; for Problem 7.33.

7.34. Power of hysteresis losses in a thick toroidal core. Assume that a low-frequency time-harmonic current of intensity $i = I_0 \cos(2\pi f t)$ is established in the thick toroidal coil with a nonlinear ferromagnetic core in Fig. 5.27(a), where $I_0 = 1$ A and $f = 10$ kHz (a, b, h, and N are specified in Example 5.12), that the idealized hysteresis loop of the core material is that in Fig. 6.13(c), where $B_m/H_m = \mu_h = 0.001$ H/m for all locations in the core, and that saturation is not reached at any location. Note that, from Eq. (5.83), $H_m = NI_0/(2\pi r)$ ($a \leq r \leq b$). Under these circumstances, find (a) the energy density of hysteresis losses in one magnetization-demagnetization hysteresis cycle at every point of the material (for every r) and (b) the total time-average power of hysteresis losses in the core.

7.35. Frequency dependence of hysteresis and eddy-current losses. A conducting ferromagnetic body is placed in a uniform low-frequency time-harmonic magnetic field, and the total time-average power of losses in the body is measured to be P_1 and P_2 at two different frequencies, f_1 and f_2, respectively, for the same amplitude of the applied magnetic flux density. What are the time-average powers of (a) hysteresis losses and (b) Joule's losses due to eddy currents in the body, at each of the frequencies?

7.36. Magnetic energy p.u.l. of a triaxial cable. Find the internal, external, and total magnetic energy per unit length of the triaxial cable from Problem 4.11.

7.37. Internal inductance p.u.l. of a hollow cylindrical conductor. Determine the dc or low-frequency internal inductance per unit length of the infinitely long hollow cylindrical copper conductor in Fig. 4.43.

7.38. Total inductance of a coaxial cable with magnetic inhomogeneity. From energy, find the total low-frequency inductance per unit length of a coaxial cable filled with two coaxial magnetic layers, described in Problem 7.6. Assume that the conductors of the cable are nonmagnetic and that the inductance of the outer conductor (which is very thin) is negligible.

Quantities, Symbols, Units, and Constants

APPENDIX 1

Symbol	Quantity or Parameter	SI Unit (and Value)	Defined In:
$\mathbf{A}$	Magnetic vector potential	T · m (tesla-meter)	Section 4.9
A_{dB}	Decibel attenuation (attenuation in dB)	dB (decibel)	Section 9.7
A_{eff}	Antenna effective aperture	m^2 (meter squared)	Section 14.13
$\mathbf{a}$	Acceleration (vector)	m/s^2 (s – second)	Section 6.1
$\mathbf{B}$	Magnetic flux density vector	T (tesla)	Section 4.1
B	Susceptance	S (siemens)	Section 12.6
b	Normalized transmission-line susceptance	dimensionless	Section 12.6
C	Capacitance	F (farad)	Section 2.12
C'	Capacitance per unit length (p.u.l.)	F/m	Section 2.12
c	Velocity of electromagnetic (EM) waves	m/s	Section 8.9
c_0	Velocity of EM waves in free space	299,792,458 m/s	Section 9.3
$\mathbf{D}$	Electric flux density (displacement) vector	C/m^2 (C – coulomb)	Section 2.5
D	Antenna directivity	dimensionless	Section 14.6
e	Charge of electron, magnitude	1.602×10^{-19} C	Section 1.1
$\mathbf{E}$	Electric field intensity vector	V/m (volt per meter)	Section 1.2
E_{cr}	Dielectric strength of a material	V/m	Section 2.6
E_{cr0}	Dielectric strength of air	3 MV/m ($M \equiv 10^6$)	Section 2.6
$\mathbf{E}_i$	Impressed electric field intensity vector	V/m	Section 3.10
$\mathbf{E}_{ind}$	Induced electric field intensity vector	V/m	Section 6.1
$\mathbf{E}_q$	Field due to excess charge	V/m	Section 6.2
$\mathcal{E}, e$	Electromotive force (emf) of a generator	V (volt)	Section 3.10
e_{ind}	Induced electromotive force (emf)	V	Section 6.3
$\mathbf{F}_e$	Electric (Coulomb) force	N (newton)	Section 1.1
$\mathbf{F}_m$	Magnetic force	N	Section 4.1
f	Frequency	Hz (hertz)	Ch. 6, Intro
f_p	Plasma frequency	Hz	Section 9.12
f_{res}	Resonant frequency of an EM resonator	Hz	Section 10.1
f_c	Cutoff frequency of a waveguide mode	Hz	Section 13.2
$\underline{\mathbf{F}}$	Antenna characteristic radiation function	dimensionless	Section 14.5
f	Antenna normalized field pattern	dimensionless	Section 14.5
$\underline{F}_a$	Antenna array factor (AF)	dimensionless	Section 14.15
G	Conductance	S	Section 3.8

(Continued)

Symbol	Quantity or Parameter	SI Unit (and Value)	Defined In:
G'	Conductance per unit length	S/m	Section 3.12
g	Normalized transmission-line conductance	dimensionless	Section 12.6
G	Antenna gain	dimensionless	Section 14.6
g	Standard acceleration of free fall	$9.81\ \mathrm{m/s^2}$	Example 7.23
$\mathbf{H}$	Magnetic field intensity vector	A/m (amp per meter)	Section 5.4
HPBW	Half-power beamwidth of an antenna	degree (°)	Section 14.5
I, i	Current intensity (or current)	A (ampere or amp)	Section 3.1
I_m	Magnetization current	A	Section 5.3
$\mathbf{J}$	Current density vector (conduction current)	$\mathrm{A/m^2}$	Section 3.1
$\mathbf{J}_i$	Impressed current density vector	$\mathrm{A/m^2}$	Section 3.10
$\mathbf{J}_m$	Magnetization volume current density vector	$\mathrm{A/m^2}$	Section 5.3
$\mathbf{J}_{eddy}$	Density of eddy currents	$\mathrm{A/m^2}$	Section 6.8
$\mathbf{J}_d$	Displacement current density vector	$\mathrm{A/m^2}$	Section 8.1
$\mathbf{J}_s$	Conduction surface current density vector	A/m	Section 3.1
$\mathbf{J}_{ms}$	Magnetization surface current density vector	A/m	Section 5.3
k	Coefficient of magnetic coupling	dimensionless	Section 7.3
l	Length	m (meter)	Section 1.3
l_e	Electrical length	dimensionless	Section 12.6
L	Self-inductance	H (henry)	Section 7.1
L_{21}	Mutual inductance	H	Section 7.2
L_i	Internal inductance	H	Section 7.6
L'	Inductance per unit length	H/m	Example 7.3
$\mathbf{m}$	Magnetic dipole moment	$\mathrm{A \cdot m^2}$	Section 4.11
$\mathbf{M}$	Magnetization vector	A/m	Section 5.1
m	Mass	kg (kilogram)	Section 5.2
N_v, N	Concentration (number/$\mathrm{m^3}$) of particles	$\mathrm{m^{-3}}$	Section 2.2
n	Index of refraction	dimensionless	Example 9.18
$\mathbf{p}$	Electric dipole moment	$\mathrm{C \cdot m}$	Section 1.11
$\mathbf{P}$	Polarization vector	$\mathrm{C/m^2}$	Section 2.2
p_e	Electric pressure	$\mathrm{Pa = N/m^2}$ (pascal)	Example 2.12
p_m	Magnetic pressure	Pa	Example 7.24
P	Power (instantaneous)	W (watt)	Section 8.12
P_J	Power of Joule's losses or ohmic losses	W	Section 3.3
P_{mech}	Mechanical power	W	Example 6.11
P_{ave}	Time-average power	W	Example 6.12
P_f	Power flow (transfer)	W	Section 8.11
p_J	Ohmic power density	$\mathrm{W/m^3}$	Section 3.3
P'_J	Power of Joule's losses per unit length	W/m	Section 3.12
$\mathcal{P}$	Poynting vector	$\mathrm{W/m^2}$	Section 8.11
$\underline{\mathcal{P}}$	Complex Poynting vector	$\mathrm{W/m^2}$	Section 8.12

Symbol	Quantity or Parameter	SI Unit (and Value)	Defined In:
$\mathcal{P}_{ave}$	Time-average Poynting vector	W/m^2	Section 8.12
Q, q	Charge	C (coulomb)	Section 1.1
Q_p	Bound (polarization) charge	C	Section 2.3
Q'	Line charge density (charge per unit length)	C/m	Section 1.3
Q	Reactive power	W	Section 8.12
Q	Quality factor of a resonator	dimensionless	Section 12.10
Q_c	Q factor for structure conductors	dimensionless	Section 12.10
Q_d	Q factor for structure dielectric	dimensionless	Section 12.10
R	Source-to-field distance	m	Section 1.2
R	Resistance	Ω (ohm)	Section 3.8
R_{gr}	Grounding resistance	Ω	Section 3.13
R_{rad}	Radiation resistance of an antenna	Ω	Section 14.4
R_{ohmic}	Ohmic resistance of an antenna	Ω	Section 14.4
R_s	Surface resistance of a good conductor	Ω/square (or Ω)	Section 10.3
R'	Resistance per unit length	Ω/m	Section 3.12
r	Normalized transmission-line resistance	dimensionless	Section 12.6
$\mathcal{R}$	Reluctance	H^{-1}	Section 5.10
S	Surface area	m^2	Section 1.3
$\underline{S}$	Complex power	W	Section 8.12
s	Standing wave ratio (SWR)	dimensionless	Example 10.9
t	Time	s (second)	Section 3.1
T	Period of time-harmonic oscillation	s	Ch. 6, Intro
T	One-way time delay period of a tr. line	s	Section 12.14
T	Temperature	K (kelvin) or °C	Section 3.2
$\mathbf{T}$	Torque	$N \cdot m$	Section 2.1
U	Antenna radiation intensity	W/sr (W per steradian)	Section 14.6
v	Volume	m^3	Section 1.3
V	Electric scalar potential (at a point)	V	Section 1.6
V, v	Voltage (between two points)	V	Section 1.8
V_{cr}	Breakdown voltage	V	Section 2.17
V_{step}	Voltage of a step (for a grounding electrode)	V	Section 3.13
$\underline{V}$	Complex rms (root-mean-square) voltage	V	Section 8.7
$\underline{V}_{oc}$	Open-circuit voltage of a receiving antenna	V	Section 14.12
$\mathbf{v}$	Velocity (vector)	m/s	Section 3.1
v_p	Phase velocity	m/s	Section 9.4
v_g	Group velocity	m/s	Section 9.13
W	Work or energy	J (joule)	Section 1.6
W_e	Electric energy	J	Section 2.15
W_m	Magnetic energy	J	Section 7.4
W_{em}	Electromagnetic energy	J	Section 8.11

(*Continued*)

Symbol	Quantity or Parameter	SI Unit (and Value)	Defined In:
w_e	Electric energy density	J/m^3	Section 2.16
w_m	Magnetic energy density	J/m^3	Section 7.5
$\mathbf{w}$	Angular velocity (vector)	rad/s (radian per second)	Section 5.2
X	Reactance	Ω	Example 8.20
x	Normalized transmission-line reactance	dimensionless	Section 12.6
$\underline{Y}$	Complex admittance	S	Section 12.6
Y_0	Characteristic admittance of a tr. line	S	Section 11.4
$\underline{y}_n$	Normalized transmission-line admittance	dimensionless	Section 12.6
$\underline{Z}$	Complex impedance	Ω	Example 8.20
Z_0	Characteristic impedance of a tr. line	Ω	Section 11.4
Z_{TEM}	TEM wave impedance	Ω	Section 11.1
Z_{TE}	TE wave impedance	Ω	Section 13.7
Z_{TM}	TM wave impedance	Ω	Section 13.7
$\underline{Z}_A$	Antenna input impedance	Ω	Section 14.4
$\underline{z}_n$	Normalized transmission-line impedance	dimensionless	Section 12.6
α	Attenuation coefficient	Np/m (neper per meter)	Section 9.7
α_c	Attenuation coeff. due to conductor losses	Np/m	Section 11.6
α_d	Attenuation coeff. due to dielectric losses	Np/m	Section 11.6
β	Phase coefficient or wavenumber	rad/m	Section 8.10
$\underline{\gamma}$	Complex propagation coefficient	m^{-1}	Section 9.7
$\underline{\Gamma}$	Reflection coefficient	dimensionless	Section 10.2
δ	Skin depth	m	Section 9.11
$\tan \delta_d$	Loss tangent	dimensionless	Section 9.9
ε	Permittivity of a dielectric material	F/m	Section 2.6
ε_0	Permittivity of a vacuum (free space)	$8.8542\ \mathrm{pF/m}\ \ (\mathrm{p} \equiv 10^{-12})$	Section 1.1
$\underline{\varepsilon}_e$	Equivalent complex permittivity	F/m	Section 9.7
$\underline{\varepsilon}$	High-frequency complex permittivity	F/m	Section 9.9
ε_p	Plasma effective permittivity	F/m	Section 9.12
ε_r	Relative permittivity	dimensionless	Section 2.6
ε_{reff}	Effective relative permittivity of a tr. line	dimensionless	Section 11.9
η	Intrinsic impedance of a medium	Ω	Section 9.3
η_0	Intrinsic impedance of free space	$\approx 120\pi\ \Omega \approx 377\ \Omega$	Section 9.3
$\underline{\eta}$	Complex intrinsic impedance	Ω	Section 9.7
$\underline{\eta}_w$	Wave impedance	Ω	Example 10.11
η_{rad}	Radiation efficiency of an antenna	dimensionless	Section 14.4
$\eta_{aperture}$	Antenna aperture efficiency	dimensionless	Section 14.13
λ	Wavelength	m	Section 8.10
λ_0	Free-space wavelength	m	Section 9.5
λ_z	Wavelength along a tr. line or waveguide	m	Section 12.1
μ	Permeability of a magnetic material	H/m	Section 5.5

Symbol	Quantity or Parameter	SI Unit (and Value)	Defined In:
μ_0	Permeability of a vacuum (free space)	$4\pi \times 10^{-7}$ H/m	Section 4.1
μ_r	Relative permeability	dimensionless	Section 5.5
ρ	Volume charge density (free charge)	C/m^3	Section 1.3
ρ_p	Bound volume charge density	C/m^3	Section 2.3
ρ_s	Surface charge density	C/m^2	Section 1.3
ρ_{ps}	Bound surface charge density	C/m^2	Section 2.3
ρ	Resistivity of a medium	$\Omega \cdot m$	Section 3.2
σ	Conductivity of a medium	S/m	Section 3.2
τ	Relaxation time or time constant	s	Section 3.7
$\underline{\tau}$	Transmission coefficient	dimensionless	Section 10.2
Φ	Magnetic flux	Wb (weber)	Section 4.8
χ_e	Electric susceptibility of a medium	dimensionless	Section 2.2
χ_m	Magnetic susceptibility of a medium	dimensionless	Section 5.2
Ψ	Electric flux	C	Section 2.5
ψ	Phase angle of a reflection coefficient	rad (radian)	Section 10.2
ω	Angular or radian frequency	rad/s	Example 6.4
Ω	Solid angle	sr (steradian)	Section 1.12
Ω_A	Beam solid angle of an antenna	sr	Section 14.6

Powers of Ten as Multipliers of Fundamental Units

Multiple	Prefix	Symbol	Multiple	Prefix	Symbol
10^{18}	Exa	E	10^{-2}	centi	c
10^{15}	Peta	P	10^{-3}	milli	m
10^{12}	Tera	T	10^{-6}	micro	μ
10^{9}	Giga	G	10^{-9}	nano	n
10^{6}	Mega	M	10^{-12}	pico	p
10^{3}	kilo	k	10^{-15}	femto	f
10^{2}	hecto	h	10^{-18}	atto	a

APPENDIX

2 Mathematical Facts and Identities

A2.1 TRIGONOMETRIC IDENTITIES

$\sin(\alpha \pm \beta) = \sin\alpha\cos\beta \pm \cos\alpha\sin\beta$ $\cos(\alpha \pm \beta) = \cos\alpha\cos\beta \mp \sin\alpha\sin\beta$ $2\sin\alpha\sin\beta = \cos(\alpha-\beta) - \cos(\alpha+\beta)$ $2\sin\alpha\cos\beta = \sin(\alpha+\beta) + \sin(\alpha-\beta)$ $2\cos\alpha\cos\beta = \cos(\alpha+\beta) + \cos(\alpha-\beta)$ $\sin\alpha \pm \sin\beta = 2\sin\frac{\alpha\pm\beta}{2}\cos\frac{\alpha\mp\beta}{2}$ $\cos\alpha + \cos\beta = 2\cos\frac{\alpha+\beta}{2}\cos\frac{\alpha-\beta}{2}$ $\cos\alpha - \cos\beta = -2\sin\frac{\alpha+\beta}{2}\sin\frac{\alpha-\beta}{2}$	$\sin 0 = 0$ $\sin 30° = \frac{1}{2}$ $\sin 45° = \frac{\sqrt{2}}{2}$ $\sin 60° = \frac{\sqrt{3}}{2}$ $\sin 90° = 1$ $\sin 180° = 0$	$\cos 0 = 1$ $\cos 30° = \frac{\sqrt{3}}{2}$ $\cos 45° = \frac{\sqrt{2}}{2}$ $\cos 60° = \frac{1}{2}$ $\cos 90° = 0$ $\cos 180° = -1$
$\sin^2\alpha = \frac{1-\cos 2\alpha}{2}$ $\cos^2\alpha = \frac{1+\cos 2\alpha}{2}$ $\sin^2\alpha + \cos^2\alpha = 1$ $\sin 2\alpha = 2\sin\alpha\cos\alpha$ $\cos 2\alpha = \cos^2\alpha - \sin^2\alpha$	$\sin(-\alpha) = -\sin\alpha$ $\cos(-\alpha) = \cos\alpha$ $\sin(\alpha \pm 90°) = \pm\cos\alpha$ $\cos(\alpha \pm 90°) = \mp\sin\alpha$	
$\tan\alpha = \frac{\sin\alpha}{\cos\alpha}$ $\cot\alpha = \frac{1}{\tan\alpha}$	$\sec\alpha = \frac{1}{\cos\alpha}$ $\csc\alpha = \frac{1}{\sin\alpha}$	

$c^2 = a^2 + b^2 - 2ab\cos\gamma$ (cosine formula, arbitrary triangle; angle γ is opposite to side c)

$c^2 = a^2 + b^2$ (Pythagorean theorem, right triangle; c is hypotenuse)

A2.2 EXPONENTIAL, LOGARITHMIC, AND HYPERBOLIC IDENTITIES

$e^x e^y = e^{x+y}$	$e = 2.71828$ (base of natural logarithm)
$(e^x)^a = e^{ax}$	$j = \sqrt{-1}$ (imaginary unit)
$e^{jx} = \cos x + j \sin x$ (Euler's identity) $e^{jx} + e^{-jx} = 2\cos x$ $e^{jx} - e^{-jx} = 2j \sin x$	
$\log x = \log_{10} x$ (common logarithm) $\ln x = \log_e x$ (natural logarithm) $\ln e^x = x$	True for a logarithm of any base: $\log(xy) = \log x + \log y$ $\log \frac{x}{y} = \log x - \log y$ $\log x^a = a \log x$
Hyperbolic sine and cosine: $\sinh x = \frac{e^x - e^{-x}}{2}$ $\cosh x = \frac{e^x + e^{-x}}{2}$ $\sinh jx = j \sin x$ $\cosh jx = \cos x$	Hyperbolic tangent and cotangent: $\tanh x = \frac{\sinh x}{\cosh x}$ $\coth x = \frac{1}{\tanh x}$

A2.3 SOLUTION OF QUADRATIC EQUATION

$$ax^2 + bx + c = 0 \quad \longrightarrow \quad x = \frac{-b \pm \sqrt{b^2 - 4ac}}{2a}$$

A2.4 APPROXIMATIONS FOR SMALL QUANTITIES

For $|x| \ll 1$,

$(1+x)^a \approx 1 + ax$ $\sin x \approx x$ $\cos x \approx 1 - \frac{x^2}{2}$	$e^x \approx 1 + x$ $\ln(1+x) \approx x$

A2.5 DERIVATIVES

$\frac{d}{dx} x^c = cx^{c-1}$	$\frac{d}{dx} \sin x = \cos x$
$\frac{dc}{dx} = 0 \quad (c = \text{const})$	$\frac{d}{dx} \cos x = -\sin x$
$\frac{d}{dx} e^x = e^x$	$\frac{d}{dx} \tan x = \sec^2 x$
$\frac{d}{dx} \ln x = \frac{1}{x}$	

For $f = f(x)$ and $g = g(x)$,

$\frac{d}{dx}(f+g) = \frac{df}{dx} + \frac{dg}{dx}$	$\frac{d}{dx}\left(\frac{f}{g}\right) = \frac{\frac{df}{dx} g - f \frac{dg}{dx}}{g^2}$
$\frac{d}{dx}(fg) = \frac{df}{dx} g + f \frac{dg}{dx}$	Chain rule for taking derivatives:
$\frac{d}{dx}(cf) = c \frac{df}{dx}$	$\frac{d}{dx} f[g(x)] = \frac{df}{dg} \frac{dg}{dx}$

A2.6 INTEGRALS

$\int x^c \, dx = \frac{x^{c+1}}{c+1} + C \quad (c \neq -1)$	$\int \sin x \, dx = -\cos x + C$
$\int \frac{dx}{x} = \ln \lvert x \rvert + C$	$\int \cos x \, dx = \sin x + C$
$\int e^x \, dx = e^x + C$	$\int \frac{dx}{\sqrt{x^2 + c^2}} = \ln\left(x + \sqrt{x^2 + c^2}\right) + C$
	$\int x e^{-x} \, dx = -(1+x) e^{-x} + C$

$$\int cf \, dx = c \int f \, dx$$

$$\int (f+g) \, dx = \int f \, dx + \int g \, dx$$

$$\int f \, dg = fg - \int g \, df \quad \text{(integration by parts)}$$

A2.7 VECTOR ALGEBRAIC IDENTITIES

For vectors **a** and **b**, and angle α between them,

$\mathbf{a}\cdot\mathbf{b} = \lvert\mathbf{a}\rvert\lvert\mathbf{b}\rvert\cos\alpha$ (dot product of vectors)	
$\mathbf{a}\times\mathbf{b} = \lvert\mathbf{a}\rvert\lvert\mathbf{b}\rvert\sin\alpha\,\hat{\mathbf{n}}$ (cross product of vectors; $\hat{\mathbf{n}}$ is the unit vector normal to the plane of **a** and **b**, and its direction is determined by the right-hand rule when **a** is rotated by the shortest route toward **b**)	
$\mathbf{a}\cdot\mathbf{a} = \lvert\mathbf{a}\rvert^2 = a^2$ $\hat{\mathbf{a}} = \dfrac{\mathbf{a}}{a}$ (unit vector of **a**; $\lvert\hat{\mathbf{a}}\rvert = 1$)	$\mathbf{a}\cdot\mathbf{b} = \mathbf{b}\cdot\mathbf{a}$ $\mathbf{a}\times\mathbf{b} = -\mathbf{b}\times\mathbf{a}$
$(\mathbf{a}\times\mathbf{b})\cdot\mathbf{c} = (\mathbf{b}\times\mathbf{c})\cdot\mathbf{a} = (\mathbf{c}\times\mathbf{a})\cdot\mathbf{b}$ (scalar triple product) $\mathbf{a}\times(\mathbf{b}\times\mathbf{c}) = \mathbf{b}(\mathbf{a}\cdot\mathbf{c}) - \mathbf{c}(\mathbf{a}\cdot\mathbf{b})$ (vector triple product)	

For vectors in the Cartesian coordinate system,

$$\mathbf{a} = a_x\,\hat{\mathbf{x}} + a_y\,\hat{\mathbf{y}} + a_z\,\hat{\mathbf{z}} \quad (\hat{\mathbf{x}},\ \hat{\mathbf{y}}, \text{ and } \hat{\mathbf{z}} \text{ are coordinate unit vectors})$$

$$a = \lvert\mathbf{a}\rvert = \sqrt{a_x^2 + a_y^2 + a_z^2}$$

$$\mathbf{a}+\mathbf{b} = (a_x + b_x)\,\hat{\mathbf{x}} + (a_y + b_y)\,\hat{\mathbf{y}} + (a_z + b_z)\,\hat{\mathbf{z}}$$

$$\mathbf{a}\cdot\mathbf{b} = a_x b_x + a_y b_y + a_z b_z$$

$$\mathbf{a}\times\mathbf{b} = (a_y b_z - a_z b_y)\,\hat{\mathbf{x}} + (a_z b_x - a_x b_z)\,\hat{\mathbf{y}} + (a_x b_y - a_y b_x)\,\hat{\mathbf{z}}$$

A2.8 VECTOR CALCULUS IDENTITIES

For a scalar function f (and g) and a vector function **a** (and **b**),

$\nabla f \equiv \operatorname{grad} f$ (gradient of f) $\nabla\cdot\mathbf{a} \equiv \operatorname{div}\mathbf{a}$ (divergence of **a**) $\nabla\times\mathbf{a} \equiv \operatorname{curl}\mathbf{a}$ (curl of **a**) $\nabla\cdot(\nabla f) \equiv \nabla^2 f$ (Laplacian of f)	
$\nabla\times(\nabla f) = 0$ $\nabla\cdot(\nabla\times\mathbf{a}) = 0$ $\nabla(fg) = (\nabla f)\,g + f\nabla g$ $\nabla f(g) = \frac{df}{dg}\nabla g$ (chain rule)	$\nabla\cdot(f\mathbf{a}) = (\nabla f)\cdot\mathbf{a} + f\nabla\cdot\mathbf{a}$ $\nabla\times(f\mathbf{a}) = (\nabla f)\times\mathbf{a} + f\nabla\times\mathbf{a}$ $\nabla\cdot(\mathbf{a}\times\mathbf{b}) = \mathbf{b}\cdot(\nabla\times\mathbf{a}) - \mathbf{a}\cdot(\nabla\times\mathbf{b})$ $\nabla\times(\nabla\times\mathbf{a}) = \nabla(\nabla\cdot\mathbf{a}) - \nabla^2\mathbf{a}$ ($\nabla^2\mathbf{a}$ – Laplacian of **a**)
$\int_v \nabla\cdot\mathbf{a}\,dv = \oint_S \mathbf{a}\cdot d\mathbf{S}$ (divergence theorem; S is the boundary surface of v) $\int_S (\nabla\times\mathbf{a})\cdot d\mathbf{S} = \oint_C \mathbf{a}\cdot d\mathbf{l}$ (Stokes' theorem; C is the boundary contour of S)	

A2.9 GRADIENT, DIVERGENCE, CURL, AND LAPLACIAN IN ORTHOGONAL COORDINATE SYSTEMS

Cartesian coordinate system $[f(x, y, z), \quad \mathbf{a} = a_x(x, y, z)\,\hat{\mathbf{x}} + a_y(x, y, z)\,\hat{\mathbf{y}} + a_z(x, y, z)\,\hat{\mathbf{z}}]$

$$\nabla = \frac{\partial}{\partial x}\,\hat{\mathbf{x}} + \frac{\partial}{\partial y}\,\hat{\mathbf{y}} + \frac{\partial}{\partial z}\,\hat{\mathbf{z}} \quad \text{(del operator)}$$

$$\nabla f = \frac{\partial f}{\partial x}\,\hat{\mathbf{x}} + \frac{\partial f}{\partial y}\,\hat{\mathbf{y}} + \frac{\partial f}{\partial z}\,\hat{\mathbf{z}}$$

$$\nabla \cdot \mathbf{a} = \frac{\partial a_x}{\partial x} + \frac{\partial a_y}{\partial y} + \frac{\partial a_z}{\partial z}$$

$$\nabla \times \mathbf{a} = \left(\frac{\partial a_z}{\partial y} - \frac{\partial a_y}{\partial z}\right)\hat{\mathbf{x}} + \left(\frac{\partial a_x}{\partial z} - \frac{\partial a_z}{\partial x}\right)\hat{\mathbf{y}} + \left(\frac{\partial a_y}{\partial x} - \frac{\partial a_x}{\partial y}\right)\hat{\mathbf{z}}$$

$$\nabla^2 f = \frac{\partial^2 f}{\partial x^2} + \frac{\partial^2 f}{\partial y^2} + \frac{\partial^2 f}{\partial z^2}$$

$$\nabla^2 \mathbf{a} = \nabla^2 a_x\,\hat{\mathbf{x}} + \nabla^2 a_y\,\hat{\mathbf{y}} + \nabla^2 a_z\,\hat{\mathbf{z}}$$

Cylindrical coordinate system $[f(r, \phi, z), \quad \mathbf{a} = a_r(r, \phi, z)\,\hat{\mathbf{r}} + a_\phi(r, \phi, z)\,\hat{\boldsymbol{\phi}} + a_z(r, \phi, z)\,\hat{\mathbf{z}}]$

$$\nabla f = \frac{\partial f}{\partial r}\,\hat{\mathbf{r}} + \frac{1}{r}\frac{\partial f}{\partial \phi}\,\hat{\boldsymbol{\phi}} + \frac{\partial f}{\partial z}\,\hat{\mathbf{z}}$$

$$\nabla \cdot \mathbf{a} = \frac{1}{r}\frac{\partial}{\partial r}(r a_r) + \frac{1}{r}\frac{\partial a_\phi}{\partial \phi} + \frac{\partial a_z}{\partial z}$$

$$\nabla \times \mathbf{a} = \left(\frac{1}{r}\frac{\partial a_z}{\partial \phi} - \frac{\partial a_\phi}{\partial z}\right)\hat{\mathbf{r}} + \left(\frac{\partial a_r}{\partial z} - \frac{\partial a_z}{\partial r}\right)\hat{\boldsymbol{\phi}} + \frac{1}{r}\left[\frac{\partial}{\partial r}(r a_\phi) - \frac{\partial a_r}{\partial \phi}\right]\hat{\mathbf{z}}$$

$$\nabla^2 f = \frac{1}{r}\frac{\partial}{\partial r}\left(r\frac{\partial f}{\partial r}\right) + \frac{1}{r^2}\frac{\partial^2 f}{\partial \phi^2} + \frac{\partial^2 f}{\partial z^2}$$

$$\nabla^2 \mathbf{a} = \nabla(\nabla \cdot \mathbf{a}) - \nabla \times (\nabla \times \mathbf{a})$$

Spherical coordinate system $[f(r, \theta, \phi), \quad \mathbf{a} = a_r(r, \theta, \phi)\,\hat{\mathbf{r}} + a_\theta(r, \theta, \phi)\,\hat{\boldsymbol{\theta}} + a_\phi(r, \theta, \phi)\,\hat{\boldsymbol{\phi}}]$

$$\nabla f = \frac{\partial f}{\partial r}\,\hat{\mathbf{r}} + \frac{1}{r}\frac{\partial f}{\partial \theta}\,\hat{\boldsymbol{\theta}} + \frac{1}{r\sin\theta}\frac{\partial f}{\partial \phi}\,\hat{\boldsymbol{\phi}}$$

$$\nabla \cdot \mathbf{a} = \frac{1}{r^2}\frac{\partial}{\partial r}\left(r^2 a_r\right) + \frac{1}{r\sin\theta}\frac{\partial}{\partial \theta}(\sin\theta\, a_\theta) + \frac{1}{r\sin\theta}\frac{\partial a_\phi}{\partial \phi}$$

$$\nabla \times \mathbf{a} = \frac{1}{r\sin\theta}\left[\frac{\partial}{\partial \theta}(\sin\theta\, a_\phi) - \frac{\partial a_\theta}{\partial \phi}\right]\hat{\mathbf{r}} + \frac{1}{r}\left[\frac{1}{\sin\theta}\frac{\partial a_r}{\partial \phi} - \frac{\partial}{\partial r}(r a_\phi)\right]\hat{\boldsymbol{\theta}} + \frac{1}{r}\left[\frac{\partial}{\partial r}(r a_\theta) - \frac{\partial a_r}{\partial \theta}\right]\hat{\boldsymbol{\phi}}$$

$$\nabla^2 f = \frac{1}{r^2}\frac{\partial}{\partial r}\left(r^2\frac{\partial f}{\partial r}\right) + \frac{1}{r^2\sin\theta}\frac{\partial}{\partial \theta}\left(\sin\theta\frac{\partial f}{\partial \theta}\right) + \frac{1}{r^2\sin^2\theta}\frac{\partial^2 f}{\partial \phi^2}$$

for $\nabla^2\mathbf{a}$, see the formula above

APPENDIX 3

Vector Algebra and Calculus Index

Concept	Page Numbers	Concept	Page Numbers
Unit vector	4	Line, surface, volume integrals	8–10
Magnitude of a vector	4	Line integral of a vector	16–17
Position vector of a point	4	Circulation of a vector	17
Decomposition of a vector	4–6	Flux (surface integral) of a vector	28–30
Graphical addition of vectors	6	Gradient	23–25
Dot product of vectors	16, 36	Directional derivative	25
Cross product of vectors	174, 195	Divergence	36–38
Scalar triple product	258–259	Divergence theorem	38
Vector triple product	204	Curl	195–197
Cartesian coordinate system	3–4	Stokes' theorem	197–198
Cylindrical coordinate system	24	Laplacian of a scalar	82–83
Spherical coordinate system	24–25	Laplacian of a vector	205

APPENDIX 4

Answers to Selected Problems

CHAPTER 1

1.2. $Q_3 = -4$ pC and $d = 2$ cm. **1.7.** $F_e = Q^2(6\sqrt{3} + 3\sqrt{6} + 2)/(24\pi\varepsilon_0 a^2)$ along the cube diagonal containing the charge. **1.11.** $Q = \pi\rho_{s0}a^2/2$. **1.15.** $E = Q(b - a)/\{2\pi\varepsilon_0 ab[\pi(a + b) + 2(b - a)]\}$, direction toward the midpoint of the larger semicircle. **1.19.** $\mathbf{E} = Q'[\hat{\mathbf{x}}/\sqrt{x^2 + y^2} + (1 - x/\sqrt{x^2 + y^2})\,\hat{\mathbf{y}}/y]/(4\pi\varepsilon_0)$. **1.23.** $\mathbf{E} = \rho_{s0}z[\sqrt{z^2 + a^2} - |z| + z^2(1/\sqrt{z^2 + a^2} - 1/|z|)]\,\hat{\mathbf{z}}/(2\varepsilon_0 a^2)$ (z-axis as in Fig. 1.14). **1.27.** $\mathbf{E} = Q'[(\theta_2 - \theta_1)\,\hat{\mathbf{x}} + \hat{\mathbf{y}}\ln(R_1/R_2)]/(2\pi\varepsilon_0 a)$ (notation in Fig. 4.11). **1.30.** $W_e = 526.5$ nJ. **1.35.** $V = \rho_s a/(2\varepsilon_0)$. **1.37.** $V = -99.27$ kV. **1.44.** (a) $0.793\hat{\mathbf{x}} + 0.637\hat{\mathbf{y}}$ and (b) $6.27°$. **1.46.** (a) $V = 0$ and $\mathbf{E} = -17.984\,\hat{\mathbf{z}}$ V/m, (b) $V = 0$ and $\mathbf{E} = -6.355\,\hat{\mathbf{z}}$ V/m, and (c) $V = 346\ \mu$V and $\mathbf{E} = 3.459(\hat{\mathbf{x}} + \hat{\mathbf{y}})\ \mu$V/m. **1.49.** $\mathbf{E} = p'(\cos\phi\ \hat{\mathbf{r}} + \sin\phi\ \hat{\boldsymbol{\phi}})/(2\pi\varepsilon_0 r^2)$. **1.55.** $V = \rho_0(4a^3 - r^3)/(12\varepsilon_0 a)$ $(r \le a)$ and $V = \rho_0 a^3/(4\varepsilon_0 r)$ $(r > a)$. **1.58.** $V = -\rho a^2/(4\varepsilon_0)$. **1.63.** (a) $\mathbf{E} = -\rho_0 a[1 + \cos(\pi x/a)]\,\hat{\mathbf{x}}/(\pi\varepsilon_0)$ $(|x| \le a)$ and $\mathbf{E} = 0$ $(|x| > a)$, and (b) $V = -2\rho_0 a^2/(\pi\varepsilon_0)$. **1.64.** $\mathbf{E} = \rho_0 a\, e^{-|x|/a}\,\hat{\mathbf{x}}/\varepsilon_0$ $(-\infty < x < \infty)$. **1.72.** (a) For the notation as in Fig. 1.35, $\mathbf{E} = \rho x\,\hat{\mathbf{x}}/\varepsilon_0$ $(|x| \le d/2)$ and (b) $\mathbf{E} = \rho_s(x/|x|)\,\hat{\mathbf{x}}/(2\varepsilon_0)$, with $\rho_s = \rho d$ $(|x| > d/2)$. **1.76.** (a) $Q_a = -2Q$ and $Q_b = 3Q$, and (b) $V = 3Q/(4\pi\varepsilon_0 b)$. **1.79.** $Q_1' = -88.5$ nC/m and $Q_3' = 450$ nC/m. **1.80.** $Q_1 = 1.85$ pC and $Q_2 = 24.85$ pC. **1.82.** Adopting an x-axis such that the plane $x = 0$ coincides with the first surface of the first slab, (a) $\rho_s = 1\ \mu\text{C/m}^2$ at $x = 0$, $\rho_s = 1\ \mu\text{C/m}^2$ at $x = 1$ cm, $\rho_s = -1\ \mu\text{C/m}^2$ at $x = 4$ cm, and $\rho_s = 1\ \mu\text{C/m}^2$ at $x = 5$ cm, (b) $\mathbf{E} = -112.94\,\hat{\mathbf{x}}$ kV/m for $x < 0$, $\mathbf{E} = 0$ for $0 < x < 1$ cm, $\mathbf{E} = 112.94\,\hat{\mathbf{x}}$ kV/m for 1 cm $< x <$ 4 cm, $\mathbf{E} = 0$ for 4 cm $< x <$ 5 cm, and $\mathbf{E} = 112.94\,\hat{\mathbf{x}}$ kV/m for $x >$ 5 cm, and (c) $V = 3.39$ kV. **1.89.** $V = Q'\ln(h\sqrt{2}/a)/(2\pi\varepsilon_0)$.

CHAPTER 2

2.3. $\mathbf{E} = Ph\,\hat{\mathbf{z}}(1/\sqrt{b^2 + h^2} - 1/\sqrt{a^2 + h^2})/\varepsilon_0$. **2.6.** (a) $\rho_p = -2P_0 x/a^2$, $\rho_{ps1} = -P_0$ $(x = -a)$, and $\rho_{ps2} = P_0$ $(x = a)$, (b) $\mathbf{E} = -P_0 x^2\,\hat{\mathbf{x}}/(\varepsilon_0 a^2)$ $(|x| \le a)$ and $\mathbf{E} = 0$ $(|x| > a)$, and (c) $V = -2P_0 a/(3\varepsilon_0)$. **2.9.** $\rho_p = -\rho$. **2.16.** (a) $\mathbf{E}_2 = (4\,\hat{\mathbf{x}} - 2\,\hat{\mathbf{y}} + 10\,\hat{\mathbf{z}})$ V/m and (b) $\mathbf{E}_2 = (4\,\hat{\mathbf{x}} - 2\,\hat{\mathbf{y}} + 7\,\hat{\mathbf{z}})$ V/m. **2.20.** (a) $\rho = -4\varepsilon_0 V_0 x^{-2/3}/(9d^{4/3})$, (b) $\rho_{s1} = 0$, (c) $\rho_{s2} = 4\varepsilon_0 V_0/(3d)$, and (d) $Q = 0$. **2.22.** (a) $V = (-2.5 + 0.125/r)$ V and (b) $\mathbf{E} = (0.125/r^2)$ V/m (r in m). **2.30.** (a) $C = 132.8$ nF, (b) $V = 2.26$ GV, and (c) $E = 2.26$ MV/m. **2.32.** $C' = 2\pi\varepsilon_0/\ln[d^2/(ab)]$. **2.35.** $C' = 9.86$ pF/m. **2.42.** $V_{new} = 136.5$ V. **2.44.** (a) $C = 2.224$ pF, (b) $\rho_s = 1.77\ \mu\text{C/m}^2$, (c) $\rho_p = 0$, and (d) $\rho_{ps1} = -1.327\ \mu\text{C/m}^2$ $(r = a)$ and $\rho_{ps2} = 147.6\ \text{nC/m}^2$ $(r = b)$. **2.46.** $V_{new} = 8.571$ kV. **2.50.** (a) $C' = 211$ pF/m and (b) $\rho_{s1} = 531.3\ \text{nC/m}^2$, $\rho_{s2} = 177\ \text{nC/m}^2$, $\rho_{s3} = 88.54\ \text{nC/m}^2$, and $\rho_{s4} = 885.4\ \text{nC/m}^2$ for the parts of the conductor surface interfacing dielectric sectors with ε_{r1}, ε_{r2}, ε_{r3}, and ε_{r4}, respectively. **2.55.** $C = 2ab\varepsilon_0(1 + 6/\pi)/d$. **2.59.** $b = 5$ cm. **2.63.** $W_{e1}/W_e = 66.1\%$. **2.68.** $W_e = \rho_0^2 a^3 S/(2\varepsilon)$. **2.71.** (a) $V_{cr} = 158.8$ kV, (b) $W_e' = 130$ mJ/m, and (c) $F_e' = 25$ mN/m. **2.73.** $V_{cr} = 80.67$ kV. **2.79.** $\varepsilon_{r1}E_{cr1}a = \varepsilon_{r2}E_{cr2}b$. **2.81.** (a) $V_{cr} = 440$ kV and (b) $W_e' = 8.15$ J/m.

CHAPTER 3

3.4. $G = 2\pi\sigma ab/(b - a)$. **3.8.** $R = a/[\sigma_0 bc(1 + 18/\pi)]$. **3.12.** (a) $\mathbf{J} = 2\sigma_0 V\,\hat{\mathbf{z}}/(5d)$, (b) $G = 2\pi\sigma_0 a^2/(5d)$, (c) $P_J = 2\pi\sigma_0 a^2 V^2/(5d)$, (d) $\rho = 24\varepsilon_0 V(1 + 3z/d)/(5d^2)$, $\rho_{s1} = 4\varepsilon_0 V/(5d)$ $(z = 0)$, and $\rho_{s2} = -64\varepsilon_0 V/(5d)$ $(z = d)$, and (e) $\rho_p = -18\varepsilon_0 V(1 + 4z/d)/(5d^2)$, $\rho_{ps1} = -2\varepsilon_0 V/(5d)$ $(z = 0)$, and $\rho_{ps2} = 56\varepsilon_0 V/(5d)$ $(z = d)$. **3.16.** In the spherical coordinate system adopted as in Fig. 2.7, $\mathbf{J}_s = \sigma bV(1 + \cos\theta)\,\hat{\boldsymbol{\theta}}/[(b - a)\sin\theta]$. **3.18.** (a) $G' = 4\pi\sigma_0/[2\ln(b/a) + b^2/a^2 - 1]$ and (b) $\rho = 8\varepsilon_0 V(1 + r^2/a^2)/\{a^2[2\ln(b/a) + b^2/a^2 - 1]\}$. **3.24.** (a) $R_{gr} = 31.85\ \Omega$, and (b) $P_{J1} = 15.92$ kJ and $P_{J2} = 63.69$ kJ. **3.27.** $R = 1/(2\pi\sigma a)$. **3.28.** $(V_{step})_{max} = 119.2$ V.

CHAPTER 4

4.4. $\mathbf{B} = \mu_0 J_{s0} a(1/\sqrt{z^2 + a^2} - 1/\sqrt{z^2 + b^2})\,\hat{\mathbf{z}}/2$. **4.8.** $B = \mu_0 NI/(4a)$, the direction of $\mathbf{B}$ with respect to wire turns as in Fig. 4.10. **4.15.** With the rectangular coordinate system as in Fig. 6.25(b), $\mathbf{B} = \mu_0 Ix\,\hat{\mathbf{y}}/(ad)$. **4.17.** With the spherical coordinate system as in Fig. 2.7,

$\mathbf{B} = -\mu_0 \sigma abV(1+\cos\theta)\,\hat{\boldsymbol{\phi}}/[(b-a)\,r\sin\theta]$. **4.18.** With the cylindrical coordinate system as in Fig. 3.20 [also see Fig. 8.12(a)], $\mathbf{B} = \mu_0 \mathcal{E}[G'(l-z) + 1/R_L]\,\hat{\boldsymbol{\phi}}/(2\pi r)$ ($G' = 6.84$ pS/m). **4.24.** (a) $\mathbf{J} = 795.8\,[x\,\hat{\mathbf{x}} + (-y+8z-8)\,\hat{\mathbf{y}} + 6x^2\,\hat{\mathbf{z}}]$ A/m^2 (x, y, z in m), (b) $I_C = 6.366$ kA, and (c) $\oint_C \mathbf{B}\cdot d\mathbf{l} = 8$ mT $\cdot$ m. **4.32.** With the Cartesian coordinate system as in Fig. 4.34, $\mathbf{F} = Q\rho_s(\sqrt{2}-1)[\varepsilon_0\mu_0 vwa(\sqrt{2}-1)\,\hat{\mathbf{x}} + \hat{\mathbf{z}}]/(2\sqrt{2}\varepsilon_0)$. **4.34.** $F'_m = 31.83$ mN/m (repulsive, symmetrically with respect to the semicylinder). **4.36.** $F'_m = \mu_0 I^2\sqrt{2}(\pi/4 + \ln\sqrt{2})/(4\pi a)$ (repulsive, symmetrically with respect to the corner conductor). **4.38.** Adopting a Cartesian coordinate system with origin at the orthocenter of the triangle, x-axis along $\mathbf{B}$ ($\mathbf{B} = B\,\hat{\mathbf{x}}$), and z-axis out of the page, and denoting the loop side perpendicular to $\mathbf{B}$ as side 1, and the other two sides as 2 and 3 in the counterclockwise order, (a) $\mathbf{F}_{m1} = IaB\,\hat{\mathbf{z}}$, $\mathbf{F}_{m2} = -IaB\,\hat{\mathbf{z}}/2$, and $\mathbf{F}_{m3} = -IaB\,\hat{\mathbf{z}}/2$, (b) $\mathbf{T}_1 = Ia^2B\sqrt{3}\,\hat{\mathbf{y}}/6$, $\mathbf{T}_2 = Ia^2B\sqrt{3}(\sqrt{3}\,\hat{\mathbf{x}} + \hat{\mathbf{y}})/24$, and $\mathbf{T}_3 = Ia^2B\sqrt{3}(-\sqrt{3}\,\hat{\mathbf{x}} + \hat{\mathbf{y}})/24$, (c) $\mathbf{F}_m = 0$, and (d) $\mathbf{T} = Ia^2B\sqrt{3}\,\hat{\mathbf{y}}/4$.

CHAPTER 5

5.3. $\mathbf{B} = 2\sqrt{2}\mu_0 M_0 a^2 d\,\hat{\mathbf{z}}/[\pi(4z^2+a^2)\sqrt{2z^2+a^2}]$. **5.5.** (a) $\mathbf{J}_m = -2M_0 r\,\hat{\boldsymbol{\phi}}/a^2$ and $\mathbf{J}_{ms} = M_0\hat{\boldsymbol{\phi}}$, and (b) $\mathbf{B} = \mu_0 M_0 d\,\hat{\mathbf{z}}\{[|z| - \sqrt{z^2+a^2} + z^2(1/|z| - 1/\sqrt{z^2+a^2})]/a^2 + a^2/[2(z^2+a^2)^{3/2}]\}$. **5.9.** $\mathbf{J}_m = -\mathbf{J}$. **5.16.** (a) $\mathbf{H}_2 = (5\,\hat{\mathbf{x}} - 3\,\hat{\mathbf{y}} + 4.8\,\hat{\mathbf{z}})$ A/m and (b) $\mathbf{H}_2 = (2\,\hat{\mathbf{x}} - 3\,\hat{\mathbf{y}} + 4.8\,\hat{\mathbf{z}})$ A/m. **5.19.** $\mathbf{B} = \mu_0 M_0\,\hat{\mathbf{z}}$ ($r < a$) and $\mathbf{B} = 0$ ($r > a$). **5.22.** For reference directions of vectors $\mathbf{B}$ and $\mathbf{H}$ as in Fig. 5.32(a), $B_1 = -0.375$ T, $H_1 = -250$ A/m, $B_2 = -1.5$ T, $H_2 = -1500$ A/m, $B_3 = 1.125$ T, and $H_3 = 750$ A/m. **5.24.** $N_2 I_2 = -107.3$ A turns.

CHAPTER 6

6.2. With the x- and y-axes oriented as in Fig. 6.2, $\mathbf{E}_{ind} = 3.651\times10^{-8}(di/dt)(-\hat{\mathbf{x}} + \hat{\mathbf{y}})$ V/m (di/dt in A/s). **6.7.** With the Cartesian coordinate system adopted as in Fig. 6.4, (a) $\tau = b/c_0 = 0.3$ ns $\ll T = 2\pi/\omega = 62.8$ ns, (b) $\mathbf{E}_{ind} = 11\cos 10^8 t\,(-\hat{\mathbf{x}} + \hat{\mathbf{y}})$ V/m, and (c) $\mathbf{H} = 8.33\sin 10^8 t\,\hat{\mathbf{z}}$ A/m (t in s). **6.9.** $\mathbf{E}_{ind} = \mu_0(di/dt)\{\ln[(\sqrt{a^2+z^2}+a)/(\sqrt{a^2+z^2}-a)] - 2a/\sqrt{a^2+z^2}\}\,\hat{\mathbf{y}}/(4\pi)$. **6.13.** $v_{MN} = \mu N' a^2\alpha(di/dt)\{(S_1 - S_2)/[S_1 + S_2\alpha/(2\pi-\alpha)]\}/2$. **6.19.** (a) $e_{ind} = wBa^2/2$, (b) $E_q = -wBr$, with respect to the (outward) radial reference direction (r is the radial distance from the disk center), and (c) $V_{12} = wBa^2/2$. **6.21.** $B = 0.5$ T or $B = -1$ T, and $P_{gen} = -25$ W (in both cases). **6.26.** In the cylindrical coordinate system adopted as in Fig. 3.20 [or Fig. 8.12(a)], (a) $\mathbf{B} = \mu_0 I_g\,\hat{\boldsymbol{\phi}}/(2\pi r)$, (b) $\mathbf{E}_{ind} = -v\mu_0 I_g\,\hat{\mathbf{r}}/(2\pi r)$, (c) $\mathbf{J} = \sigma(\mathbf{E}_q + \mathbf{E}_{ind})$, (d) $\mathbf{E}_q = \sigma\mu_0 R_V I_g v l\,\hat{\mathbf{r}}/\{r[2\pi\sigma R_V l + \ln(b/a)]\}$, and (e) $V = \sigma\mu_0 R_V I_g v l\ln(b/a)/[2\pi\sigma R_V l + \ln(b/a)]$. **6.30.** $e_{ind} = \mu_0\omega b I_0 \sin 2\omega t\,\{ac(c^2 + a^2/4)\cos\omega t/[(c^2+a^2/4)^2 - a^2c^2\cos^2\omega t] + \ln[(c^2 + a^2/4 + ac\cos\omega t)/(c^2 + a^2/4 - ac\cos\omega t)]\}/(4\pi)$. **6.34.** $l_0 = l/\mu_r$ and $[(P_J)_{ave}]_{max} = \pi\sigma\mu_r\mu_0^2\omega^2N^2a^4I_0^2/(64l)$. **6.38.** (a) With the same reference direction as in Fig. 6.24, $J_{eddy} = \sigma\omega\mu_0 N a^2 I_0 \sin\omega t/(2lr)$ and (b) $(P_J)_{ave} = \pi\sigma\mu_0^2\omega^2N^2a^4hI_0^2\ln(c/b)/(4l^2)$. **6.42.** (a) $(P_J)_{ave} = \sigma_0\omega^2a^3l\delta B_0^2/40$ and (b) $(T_m)_{ave} = -\sigma_0\omega a^3 l\delta B_0^2\,\hat{\mathbf{y}}/40$. **6.45.** (a) $\omega = \mathbf{T}'_{mech}/(\pi\sigma a^3\delta B^2)$ and (b) $P'_{mech} = \mathbf{T}'^2_{mech}/(\pi\sigma a^3\delta B^2)$.

CHAPTER 7

7.5. $L' = [\mu\ln 2 + \mu_0\ln(d/2a)]/\pi$. **7.7.** $L' = \mu_1 d_1/w + \mu_2 d_2/w$. **7.11.** $L_{21} = 332.7$ mH. **7.13.** $v = -\pi\mu\omega N' a^2 I_0 \sin\omega t$. **7.16.** (a) $L = 110\ \mu$H, (b) $L = 22.5\ \mu$H, and (c) $L = 49.5\ \mu$H. **7.23.** (a) $I_0 = 183.3$ mA and (b) $I_0 = 85.3$ mA. **7.25.** Switch K open: $W_m(t) = 706\cos^2 377t$ mJ (t in s) and $(W_m)_{ave} = 353$ mJ, switch K closed: $W_m(t) = 0$ and $(W_m)_{ave} = 0$. **7.32.** (a) $w_m = 250$ J/m^3 for $a \le r \le c$ and $w_m = (0.2536/r^2)$ J/m^3 (r in m) for $c \le r \le b$ ($c = 3.2$ cm), and (b) $W_m = 8.45$ mJ. **7.34.** (a) $w_h = (2.026/r^2)$ J/m^3 (r in m) and (b) $(P_h)_{ave} = 882.5$ W. **7.36.** $W'_{mi} = 157.9$ nJ/m, $W'_{me} = 346.6$ nJ/m, and $W'_m = 504.5$ nJ/m.

CHAPTER 8

8.1. (a) $J_{d01} = J_{d02} = I_0/S$, (b) $E_{01} = I_0/(2\pi\varepsilon_1 fS)$ and $E_{02} = I_0/(2\pi\varepsilon_2 fS)$, and (c) $V_0 = (\varepsilon_1 d_2 + \varepsilon_2 d_1)I_0/(2\pi\varepsilon_1\varepsilon_2 fS)$. **8.5.** In the cylindrical coordinate system whose z-axis coincides with the cable axis, (a) $\mathbf{J}_d = \varepsilon(dv/dt)\,\hat{\mathbf{r}}/[r\ln(b/a)]$ and $\mathbf{J}_{tot} = \mathbf{J}_d$, and (b) $\mathbf{J}_d$ the same as in (a) and $\mathbf{J}_{tot} = \sigma v\,\hat{\mathbf{r}}/[r\ln(b/a)] + \mathbf{J}_d$. **8.9.** $\mathbf{H} = \sqrt{\varepsilon_0/\mu_0}\,E_0\sin\theta\cos(\omega t - \beta r)\,\hat{\boldsymbol{\phi}}/r$. **8.20.** (a) $\underline{Q}' = -jI_0\sin\phi/(\omega a)$, (b) $\underline{V} = -jI_0\,e^{-j\beta R}/(2\pi\varepsilon_0\omega R)$, (c) $\underline{\mathbf{A}} = \mu_0 a I_0\,e^{-j\beta R}\,\hat{\mathbf{x}}/(8R)$, (d) $\underline{\mathbf{E}} = -jI_0\,e^{-j\beta R}[\omega\mu_0 a\,\hat{\mathbf{x}}/8 + z(1+j\beta R)\,\hat{\mathbf{z}}/(2\pi\varepsilon_0\omega R^2)]/R$, (e) $\underline{\mathbf{H}} = -azI_0(1+j\beta R)\,e^{-j\beta R}\,\hat{\mathbf{y}}/(8R^3)$, and (f) $\mathbf{A}(t) = \mu_0 a I_0\sqrt{2}\cos(\omega t - \beta R)\,\hat{\mathbf{x}}/(8R)$ and $\mathbf{E}(t) = \omega\mu_0 a I_0\sqrt{2}\cos(\omega t - \beta R - \pi/2)\,\hat{\mathbf{x}}/(8R) + zI_0\sqrt{2}\sqrt{1+\beta^2R^2}\cos(\omega t - \beta R + \arctan\beta R - \pi/2)\,\hat{\mathbf{z}}/(2\pi\varepsilon_0\omega R^3)$, where $R = \sqrt{z^2+a^2}$. **8.22.** (a) $\beta a = \omega/c_0 = 3.33$, so the condition $\beta a \ll 1$ is not met, (b) $\underline{Q}' = -1.061$

$\sin(3\phi/2)$ nC/m $(0 < \phi < 2\pi)$ and $\underline{Q}_0 = 141$ pC, (c) $\underline{V} = 0$ and $\underline{\mathbf{A}} = -\mathrm{j}11.31\, \mathrm{e}^{-\mathrm{j}33.33\sqrt{z^2+0.01}}\, \hat{\mathbf{x}}/\sqrt{z^2+0.01}$ nT · m (z in m), and (d) since $\underline{\mathbf{A}}$ has only an x-component and $\underline{V}$ is constant (zero) along the z-axis, $\underline{E}_z = -\mathrm{j}\omega\underline{A}_z - \partial\underline{V}/\partial z = 0$. **8.23.** $\underline{\mathbf{B}} = \mu_0 J_{s0} a(\mathrm{e}^{-\mathrm{j}\beta\sqrt{a^2+z^2}}/\sqrt{a^2+z^2} - \mathrm{e}^{-\mathrm{j}\beta\sqrt{b^2+z^2}}/\sqrt{b^2+z^2})\,\hat{\mathbf{z}}/2$. **8.25.** $\underline{\mathbf{A}} = \mathrm{j}2\mu_0 a J_{s0}\, \mathrm{e}^{-\mathrm{j}\beta a}\,\hat{\mathbf{z}}/3$. **8.32.** $\Psi_{\mathcal{P}} = 848.27$ kW, into the earth. **8.36.** (a) $\mathbf{H}(t) = \sqrt{\varepsilon/\mu}\, E_0 \cos(\omega t - \beta z)\,\hat{\boldsymbol{\phi}}/r$ and $\underline{\mathbf{H}} = \sqrt{\varepsilon/\mu}\, E_0\sqrt{2}\,\mathrm{e}^{-\mathrm{j}\beta z}\,\hat{\boldsymbol{\phi}}/(2r)$, (b) $\underline{\mathcal{P}} = \sqrt{\varepsilon/\mu}\, E_0^2\,\hat{\mathbf{z}}/(2r^2)$, (c) $\underline{S} = \pi\sqrt{\varepsilon/\mu}\, E_0^2 \ln(b/a)$, and (d) $P_{\text{ave}} = \pi\sqrt{\varepsilon/\mu}\, E_0^2 \ln(b/a)$. **8.39.** First term (integral) in Eq. (8.196) equals zero, second term $\sigma\pi a^2 V_0^2/(2d)$, third one $-\mathrm{j}\omega\varepsilon\pi a^2 V_0^2/(2d)$ (approximately), and the last (complex power flow) $(-\sigma + \mathrm{j}\omega\varepsilon)\pi a^2 V_0^2/(2d)$. **8.41.** $\mathcal{P}(t) = \sqrt{\varepsilon_0/\mu_0}\, E_0^2 \sin^2\theta \cos^2(\omega t - \beta r)\,\hat{\mathbf{r}}/r^2$, $\underline{\mathcal{P}} = \sqrt{\varepsilon_0/\mu_0}\, E_0^2 \sin^2\theta\,\hat{\mathbf{r}}/(2r^2)$, and $\mathcal{P}_{\text{ave}} = \mathrm{Re}\{\underline{\mathcal{P}}\} = \sqrt{\varepsilon_0/\mu_0}\, E_0^2 \sin^2\theta\,\hat{\mathbf{r}}/(2r^2)$ [see Eq. (6.95)].

CHAPTER 9

9.5. (a) $f = 1.5$ GHz, and $\theta_0 = 150°$ or $\theta_0 = 30°$, (b) $\underline{\mathbf{H}} = 28.2\,\mathrm{e}^{\mathrm{j}\theta_0}\,\mathrm{e}^{\mathrm{j}10\pi z}\,\hat{\mathbf{x}}$ mA/m (z in m), and (c) $\mathcal{P}_{\text{ave}} = -0.3\,\hat{\mathbf{z}}$ W/m^2. **9.6.** (a) $\varepsilon_r = 3.6$ and $\mu_r = 2.5$. **9.11.** $I_{\text{ind}} = 3.39$ mA. **9.15.** $W = 95.69$ mJ and (b) $W = 47.84$ mJ. **9.17.** $r = 18.2$ m. **9.24.** (a) $\varepsilon_r = 81$ and $\sigma = 4$ S/m, (b) $\underline{\gamma} = (78.72 + \mathrm{j}204)$ m^{-1}, (c) $\mathbf{H} = 27.8\,\mathrm{e}^{78.72y}\cos(6.28 \times 10^9 t + 204y - 21°)\,\hat{\mathbf{z}}$ mA/m (t in s; y in m), and (d) $\mathcal{P}_{\text{ave}} = -12.93\,\mathrm{e}^{157.44y}\,\hat{\mathbf{y}}$ mW/m^2. **9.26.** (a) $\varepsilon_r = 3$ and $\tan\delta_d = 10^{-3}$, (b) $\underline{\gamma} = (0.1814 + \mathrm{j}363)$ m^{-1}, and (c) $\mathcal{P}_{\text{ave}} = 1.035\,\mathrm{e}^{-0.363z}\,\hat{\mathbf{z}}$ W/m^2. **9.31.** (a) $\delta_{1\%} = 1.91$ μm and (b) $A_{\text{dB}} = 20{,}910$ dB (perfect shielding). **9.33.** $h_b = 161.7$ km. **9.38.** (a) $\Delta t = 34.5$ ns and (b) $\Delta t = 0.0152$ ps. **9.42.** (a) RHEP, (b) LP, (c) LHEP, (d) LP, (e) LHEP, (f) LP, (g) LP, (h) RHEP, and (i) LHEP.

CHAPTER 10

10.3. $W_{\text{em}}(t) = \varepsilon E_{i0}^2 S(2\beta l + \sin 2\beta l \cos 2\omega t)/\beta$ $(\beta = 2\pi/\lambda$ and $\omega = \beta/\sqrt{\varepsilon\mu_0})$. **10.6.** $f = 375$ MHz and $E_{i0} = 0.51$ V/m. **10.9.** (a) $f = 1.5$ GHz, (b) $\lambda_{\text{glass}} = 10$ cm, (c) $\mathbf{E}_{\text{air}}(t) = 1.777[\cos(9.425 \times 10^9 t + 31.42x + 90°) - \sin 31.42x \cos(9.425 \times 10^9 t)]\,\hat{\mathbf{y}}$ kV/m (t in s; x in m) and $\underline{\mathbf{E}}_{\text{air}} = 1.257(\mathrm{j}\,\mathrm{e}^{\mathrm{j}31.42x} - \sin 31.42x)\,\hat{\mathbf{y}}$ kV/m, (d) $|\underline{\mathbf{H}}_{\text{air}}|_{\max} = 6.67$ A/m, $|\underline{\mathbf{H}}_{\text{air}}|_{\min} = 3.33$ A/m, and $|\underline{\mathbf{H}}_{\text{glass}}|_{\max} = |\underline{\mathbf{H}}_{\text{glass}}|_{\min} = 6.67$ A/m, (e) $\mathcal{P}_{\text{ave}} = -8.378\,\hat{\mathbf{x}}$ kW/m^2 everywhere, and (f) $\underline{\eta}_w = 188.5\ \Omega$. **10.14.** $d_{\max} = 38$ m. **10.19.** $(W_{\text{em}})_{\text{ave}} = 8.854 \times 10^{-14}$ J. **10.23.** $\delta_{\text{violet}} = 53.64°$, $\delta_{\text{blue}} = 52.19°$, $\delta_{\text{green}} = 51.29°$, $\delta_{\text{yellow}} = 50.83°$, $\delta_{\text{orange}} = 50.68°$, and $\delta_{\text{red}} = 50.16°$; $\gamma = 3.48°$. **10.28.** $\underline{\mathcal{P}} = (83.3\,\hat{\mathbf{x}} - 249.9\,\hat{\mathbf{z}})$ W/m^2. **10.31.** $\theta_{\text{accept}} = \arcsin[(n_{\text{core}}^2 - n_{\text{cladding}}^2)^{1/2}/n_0]$; from air, $\theta_{\text{accept}} = 17.31°$; from water, $\theta_{\text{accept}} = 12.92°$. **10.34.** $h_r = 4.59$ km. **10.38.** $(\Gamma_e)_{\text{dB}} = -9.42$ dB.

CHAPTER 11

11.4. $(P_{\text{cr}})_{\max} = 317$ MW and $P_l = 295$ MW. **11.7.** (a) $C' = 9.476$ pF/m, $L' = 1.174$ μH/m, $R' = 1.079\ \Omega$/m, and $G' = 0$, and (b) $Z_0 = 352.1\ \Omega$ and $\alpha = 1.532 \times 10^{-3}$ Np/m. **11.10.** (a) $C' = 13.24$ pF/m, $L' = 840$ nH/m, $R' = 0.657\ \Omega$/m, and $G' = 0$, and (b) $|\underline{\rho}_s| = 67.9$ nC/m^2 and $|\underline{\mathbf{J}}_s| = 20.37$ A/m. **11.14.** (a) $(P_{\text{cr}})_{\max} = 15.31$ MW and (b) $P_l = 5.426$ MW. **11.19.** $C' = 203.9$ pF/m, $L' = 218$ nH/m, $R' = 7.15\ \Omega$/m, and $G' = 384.5$ μS/m.

CHAPTER 12

12.4. (a) $f = 300$ MHz and $\underline{Z}_L = (38.46 + \mathrm{j}92.31)\ \Omega$, and (b) $f = 300$ MHz and $\underline{Z}_L = (38.46 - \mathrm{j}92.31)\ \Omega$. **12.8.** (a) $l_{\max} = 3.69$ cm and $R_{\max} = 130.9\ \Omega$, $l_{\min} = 28.69$ cm and $R_{\min} = 19.1\ \Omega$; (b) $l_{\min} = 18.75$ cm and $R_{\min} = 8.58\ \Omega$, $l_{\max} = 43.75$ cm and $R_{\max} = 291.4\ \Omega$. **12.11.** (a) With reference to Fig. 12.8, $l_c = 12.08$ cm, $Z_{0t} = 115.1\ \Omega$, and $l = 37.5$ cm, assuming that all transmission-line sections have air dielectric. **12.14.** $P_{L1} = 22.41$ W, $P_{L2} = 31.73$ W, and $P_{L3} = 10.97$ W. **12.19.** $l_{\text{stub}} = 2.09$ mm. **12.21.** (a) $W_{\text{em}}(0) = 0.2$ μJ, (b) $t = 1.36$ ns, and (c) $t = 624.7$ ns. **12.29.** First solution: $l_1 = 9.3$ mm and $l_{\text{stub1}} = 8.9$ mm; second solution: $l_2 = 24$ mm and $l_{\text{stub2}} = 41.1$ mm. **12.33.** $l_{\text{damage}} = 10$ m and $R_{\text{eq}} = 1.02\ \Omega$. **12.35.** $v_g = 5$ V $(0 \le t \le 9$ ns); $v_L = 0$ $(0 \le t < 1.5$ ns), $v_L = 3.33$ V $(1.5$ ns $< t < 4.5$ ns), $v_L = 4.44$ V $(4.5$ ns $< t < 7.5$ ns), and $v_L = 4.81$ V $(7.5$ ns $< t \le 9$ ns). **12.38.** During time intervals $0 \le t < 1$ ns, 1 ns $< t < 2$ ns, ..., 9 ns $< t \le 10$ ns, v_g assumes values 6 V, 0, 10 V, 0, 6.66 V, 0, 4.45 V, 0, 2.96 V, and 0, respectively; the corresponding values of v_L are 0, 12 V, 0, 7.98 V, 0, 5.33 V, 0, 3.56 V, 0, and 2.37 V. **12.41.** Starting at $t = 1$ ns, v_L is a sequence of trapezoidal pulses of durations 2 ns and magnitudes 4 V, −1.33 V, 0.444 V, and −0.148 V,

respectively (each new pulse starts exactly at the end of the preceding one). **12.46.** $C = 40$ pF. **12.48.** $v_L(t) = 0.75[e^{-(t-T)/\tau}h(t-T) - e^{-(t-t_1)/\tau}h(t-t_1)]$ V and $v_g(t) = 0.5[h(t) - h(t-t_0)] - 0.5[h(t-t_2) - h(t-t_3)] + 0.75[e^{-(t-t_2)/\tau}h(t-t_2) - e^{-(t-t_3)/\tau}h(t-t_3)]$ V, where $T = 1.17$ ns, $\tau = 2.4$ ns, $t_0 = 2$ ns, $t_1 = 3.17$ ns, $t_2 = 2.34$ ns, and $t_3 = 4.34$ ns.

CHAPTER 13

13.8. (a) For $\varepsilon_r = 1$, dominant frequency range $1.5\text{ GHz} < f \le 3\text{ GHz}$, first three TE modes TE_{10}, TE_{01}, and TE_{11}, first three TM modes TM_{11}, TM_{21}, and TM_{12}, $(f_c)_{10} = (f_c)_{01} = 1.5$ GHz, $(f_c)_{11} = 2.12$ GHz, and $(f_c)_{21} = (f_c)_{12} = 3.35$ GHz; at $f = 2$ GHz, possible TE_{10} and TE_{01}; (b) for $\varepsilon_r = 2.5$, dominant frequency range $0.949\text{ GHz} < f \le 1.897$ GHz, first three TE and first three TM modes as in (a), $(f_c)_{10} = (f_c)_{01} = 0.949$ GHz, $(f_c)_{11} = 1.34$ GHz, and $(f_c)_{21} = (f_c)_{12} = 2.12$ GHz; at $f = 2$ GHz, possible TE_{10}, TE_{01}, TE_{11}, TE_{20}, TE_{02}, and TM_{11}. **13.12.** (a) $\underline{\mathcal{P}} = -j\omega\mu|\underline{H}_0|^2[(m\pi/a)\sin(2m\pi x/a)\cos^2(n\pi y/b)\,\hat{\mathbf{x}} + (n\pi/b)\cos^2(m\pi x/a)\sin(2n\pi y/b)\,\hat{\mathbf{y}}]/(2k^2) + \omega\mu\beta|\underline{H}_0|^2[(n\pi/b)^2\cos^2(m\pi x/a)\sin^2(n\pi y/b) + (m\pi/a)^2\sin^2(m\pi x/a)\cos^2(n\pi y/b)]\,\hat{\mathbf{z}}/k^4$, (b) $P = q\eta ab(f^2/f_c^2)\sqrt{1 - f_c^2/f^2}|\underline{H}_0|^2$, where $f_c = (f_c)_{02} = c/b$ and $q = 1/2$ for TE_{02} and $f_c = (f_c)_{11} = c\sqrt{1/a^2 + 1/b^2}/2$ and $q = 1/4$ for TE_{11}, and (c) the flux of $\underline{\mathcal{P}}$ into each wall is zero. **13.14.** $P_{max} = P_{cr} = 210.3$ MW. **13.16.** (a) $\alpha = 1.3 \times 10^{-3}$ Np/m and (b) $\alpha = 2.88 \times 10^{-4}$ Np/m. **13.17.** (a) $\alpha = 4.15 \times 10^{-3}$ Np/m and (b) $\alpha = 3.33 \times 10^{-3}$ Np/m. **13.21.** At $f = 22.5$ GHz: $v_p = 2.59 \times 10^8$ m/s, $v_g = 1.54 \times 10^8$ m/s, $\lambda_z = 11.5$ mm, and $\lambda = 8.9$ mm; at $f = 18$ GHz: $v_p = 3.29 \times 10^8$ m/s, $v_g = 1.22 \times 10^8$ m/s, $\lambda_z = 18.3$ mm, and $\lambda = 11.1$ mm; at $f = 27$ GHz: $v_p = 2.36 \times 10^8$ m/s, $v_g = 1.7 \times 10^8$ m/s, $\lambda_z = 8.7$ mm, and $\lambda = 7.4$ mm. **13.27.** (a) $a = 50$ mm and $d = 20.23$ mm, and (b) TE_{102}. **13.34.** $(W_{em})_{cr} = 29.9$ mJ. **13.35.** $\mathcal{E}_{ind} = 3.16$ kV and $W_{em} = 23.2$ mJ. **13.38.** (a) $P_c = 17.37$ mW and (b) $P_c = 30.19$ mW. **13.39.** $P_d = 70.6$ mW.

CHAPTER 14

14.8. $\mathcal{P}_{ave} = 18.62\sin^2\theta\,\hat{\mathbf{r}}/r^2$ W/m^2 (r in m). **14.10.** $\underline{\mathcal{P}} = \sqrt{\mu_0/\varepsilon_0}\beta^2|\underline{I}_0|^2\sin^2\theta\{1 + e^{-2\alpha l} - 2e^{-\alpha l}\cos[\beta l(1-\cos\theta)]\}\,\hat{\mathbf{r}}/\{(4\pi r)^2[\alpha^2 + \beta^2(1-\cos\theta)^2]\}$. **14.11.** $\underline{\mathbf{E}} = \underline{E}_\theta\,\hat{\boldsymbol{\theta}} = j\omega\mu_0\underline{I}_u\,l[e^{-j\beta r}/(4\pi r)]\sin\theta\,\hat{\boldsymbol{\theta}}\sin u/u$, where $u = \beta h\cos\theta$ ($h = l/2$), $\underline{\mathbf{H}} = H_\phi\,\hat{\boldsymbol{\phi}} = (\underline{E}_\theta/\eta_0)\,\hat{\boldsymbol{\phi}}$, and $\underline{\mathcal{P}} = \mathcal{P}_{ave} = (|\underline{E}_\theta|^2/\eta_0)\,\hat{\mathbf{r}}$ ($\eta_0 = 377\ \Omega$). **14.15.** $\underline{\mathcal{P}} = \eta\beta^2 I^2 l^2(1 + \cos^2\theta - \sin^2\theta\sin 2\phi)\,\hat{\mathbf{r}}/(32\pi^2 r^2)$. **14.19.** $R_{rad} = 0.8\ \Omega$, $R_{ohmic} = 6.46\ \Omega$, and $\eta_{rad} = 11\%$. **14.24.** (a) $D = 10$, and (b) $\text{HPBW}_{elevation} = 114.5°$ and $\text{HPBW}_{azimuth} = 65.5°$. **14.29.** $R_{ohmic} = R'[l/2 - (\sin\beta l)/(2\beta)]$, where $R' = \sqrt{\pi\mu f/\sigma}/(2\pi a)$ and $\beta = 2\pi f/c_0$ ($c_0 = 3 \times 10^8$ m/s). **14.33.** (a) $|\underline{\mathbf{E}}_{direct}| = 60$ mV/m and (b) $|\underline{\mathbf{E}}_{reflected}| = 26.6$ mV/m. **14.35.** $|\underline{\mathbf{E}}_{iono\ twice}|_{tot} = 243.2\ \mu$V/m. **14.41.** $|\underline{V}_{oc}| = 1.9$ mV. **14.44.** $|\underline{V}_{oc}| = 1.9$ mV. **14.46.** (a) $|(\underline{V}_{oc})_{direct}| = 0$ and $|(\underline{V}_{oc})_{reflected}| = 9.35\ \mu$V; (b) $|(\underline{V}_{oc})_{direct}| = 33.5\ \mu$V and $|(\underline{V}_{oc})_{reflected}| = 23.7\ \mu$V. **14.52.** $r_{max} = 1.191$ km. **14.57.** $f(\theta) = \sin\theta\sin[(\pi/2)\cos\theta]$. **14.60.** $f(\theta) = \{\cos[(\pi/2)\cos\theta]\cos(\pi\sin\theta\cos\phi)\}/\sin\theta$ for $0 \le \theta \le 90°$, and $f(\theta) = 0$ for $90° < \theta \le 180°$. **14.63.** $f(\theta) = \{\cos^3[(\pi/2)\cos\theta]\}/\sin\theta$. **14.66.** (a) $\theta_{max} = 90° \to \alpha = 0$ (broadside N-element array), and (b) $\theta_{max} = 0 \to \alpha = -\beta d$ (endfire radiation in $+z$ direction) and $\theta_{max} = 180° \to \alpha = \beta d$ (endfire radiation in $-z$ direction).

Bibliography

Notaroš, B. M., *Electromagnetic Theory I*, University of Massachusetts, Dartmouth, MA, 2002.

Notaroš, B. M., *Electromagnetic Theory II*, University of Massachusetts, Dartmouth, MA, 2003.

Notaroš, B. M., V. V. Petrović, M. M. Ilić, and A. R. Djordjević, B. M. Kolundžija, and M. B. Dragović, *Collection of Examination Questions and Problems in Electromagnetics*, Department of Electrical Engineering, University of Belgrade, Belgrade, 1998 (in Serbian).

Djordjević, A. R., G. N. Božilović, and B. M. Notaroš, *Collection of Examination Problems in Fundamentals of Electrical Engineering with Solutions, Part I*, Department of Electrical Engineering, University of Belgrade, Belgrade, 1997 (in Serbian).

Djordjević, A. R., G. N. Božilović, and B. M. Notaroš, *Collection of Examination Problems in Fundamentals of Electrical Engineering with Solutions, Part II*, Department of Electrical Engineering, University of Belgrade, Belgrade, 1997 (in Serbian).

Popović, B. D., *Electromagnetics*, Gradjevinska Knjiga, Belgrade, 1986, 2nd edition (in Serbian).

Surutka, J., *Electromagnetics*, Gradjevinska Knjiga, Belgrade, 1978, 5th edition (in Serbian).

Djordjević, A. R., *Electromagnetics for Computer Engineering*, University of Belgrade, Belgrade, 1996 (in Serbian).

Popović, Z., and B. D. Popović, *Introductory Electromagnetics*, Prentice Hall, Upper Saddle River, NJ, 2000.

Inan U. S., and A. S. Inan, *Engineering Electromagnetics*, Addison Wesley Longman, Menlo Park, CA, 1999.

Inan U. S., and A. S. Inan, *Electromagnetic Waves*, Prentice Hall, Upper Saddle River, NJ, 2000.

Sadiku, M. N. O., *Elements of Electromagnetics*, Oxford University Press, New York, 2001, 3rd edition.

Hayt, W. H., Jr. and J. A. Buck, *Engineering Electromagnetics*, McGraw-Hill, New York, 2001, 6th edition.

Ulaby, F. T., *Fundamentals of Applied Electromagnetics*, Prentice Hall, Upper Saddle River, NJ, 1999 edition.

Asimov, I., *Asimov's Biographical Encyclopedia of Science and Technology*, Doubleday, New York, 1982, 2nd revised edition.

Popović, B. D., *Collection of Problems in Electromagnetics*, Gradjevinska Knjiga, Belgrade, 1985, 6th edition (in Serbian).

Dragović, M. B., *Antennas and Propagation of Radio Waves*, Kontekst, Belgrade, 1994 (in Serbian).

Kraus, J. D., and D. A. Fleisch, *Electromagnetics with Applications*, McGraw-Hill, New York, 1999, 5th edition.

Rao, N. N., *Elements of Engineering Electromagnetics*, Pearson Prentice Hall, Upper Saddle River, NJ, 2004, 6th edition.

Cheng, D. K., *Field and Wave Electromagnetics*, Addison-Wesley, Reading, MA, 1989, 2nd edition.

Božilović, H. A., Ž. A. Spasojević, and G. N. Božilović, *Collection of Problems in Fundamentals of Electrical Engineering – Electrostatics, Steady Currents*, Naučna Knjiga, Belgrade, 1983 (in Serbian).

Božilović, H., Ž. Spasojević, and G. Božilović, *Collection of Problems in Fundamentals of Electrical Engineering – Electromagnetism, ac Currents*, Department of Electrical Engineering, University of Belgrade, Belgrade, 1998, 7th edition (in Serbian).

Iskander, M. F., *Electromagnetic Fields and Waves*, Waveland Press, Prospect Hills, IL, 2000.

Haus, H. A., and J. R. Melcher, *Electromagnetic Fields and Energy*, Prentice Hall, Upper Saddle River, NJ, 1989.

Stutzman, W. L., and G. A. Thiele, *Antenna Theory and Design*, John Wiley & Sons, New York, 1998, 2nd edition.

Balanis, C. A., *Antenna Theory: Analysis and Design*, John Wiley & Sons, New York, 1997, 2nd edition.

Kraus, J. D., and R. J. Marhefka, *Antennas for All Applications*, McGraw-Hill, New York, 2002, 3rd edition.

Pozar, D. M., *Microwave Engineering*, John Wiley & Sons, New York, 2005, 3rd edition.

Demarest, K. R., *Engineering Electromagnetics*, Prentice Hall, Upper Saddle River, NJ, 1998.

Wentworth, S. M., *Fundamentals of Electromagnetics with Engineering Applications*, John Wiley & Sons, New York, 2005.

Paul, C. R., *Electromagnetics for Engineers with Applications*, John Wiley & Sons, New York, 2004.

Lonngren, K. E., S. V. Savov, and R. J. Jost, *Fundamentals of Electromagnetics with MATLAB*, SciTech Publishing, Raleigh, NC, 2007, 2nd edition.

Johnk, C. T. A., *Engineering Electromagnetic Fields and Waves*, John Wiley & Sons, New York, 1988, 2nd edition.

Ida, N., *Engineering Electromagnetics*, Springer, New York, 2004, 2nd edition.

Ramo, S., J. R. Whinnery, and T. Van Duzer, *Fields and Waves in Communication Electronics*, John Wiley & Sons, New York, 1994, 3rd edition.

Griffiths, D. J., *Introduction to Electrodynamics*, Pearson Addison Wesley, Upper Saddle River, NJ, 1999, 3rd edition.

Index

A

Active power, 398
Air breakdown, 74
Ampère, André-Marie, 186
Ampère's currents, 222
Ampère's law, 185–186
  applications of, 187–188
  corrected generalized, 354
  1-D differential, 193–194
  differential form of, 193–195
  generalized, 234–236, 271
  proof of, 204–206
  for system with conductors and magnetic materials, 234
  in terms of volume current density, 235
  using curl notation, 195
Angular or radian frequency, 367
Anisotropic media, 72
Antennas, 713
  arrays of, 772–776
  beam solid angle of, 792
  characteristic radiation functions of, 736–739
  directivity and gain of, 740–745
  effective aperture of, 766–768
  far zone of, 720–721
  general theory of receiving, 760–763
  input impedance of, 732–733
  monopole, 754–755
  near zone of, 721–722
  normalized field pattern of, 736
  normalized power pattern of, 737
  ohmic resistance of, 750–751
  open-circuit voltage of receiving, 761
  polarization of, 745
  radiation efficiency of, 733
  radiation resistance of, 730
  straight wire, 731–732
  wire dipole, 745–749
Arc discharge, 109
Array factor for waves, 488
Arrays of antennas
  array factor, 773
  broadside, 775
  endfire, 776
  pattern multiplication for, 774
  uniform linear, 782
Asynchronous motor, 292
Attenuation coefficient, 550–552
  for losses in dielectric, 569–570
  of transmission line, 551
  for transmission-line conductors, 551
  for transmission-line dielectric, 552
  for uniform plane waves, 430–431
  of wave-guiding structure, 551
Attenuation in free space, 770

B

Bell, Alexander Graham, 432
Biot, Jean Baptiste, 178
Biot-Savart law
  defined, 177
  for line current, 178–179
  for surface current, 178
  for volume current, 178
Bounce diagrams, 646–648
Boundary conditions
  for conductor-free space, 41–42, 80
  for dielectric-conductor surfaces, 534
  for rapidly time-varying electromagnetic field, 363
  for steady current fields, 137
  for surface dielectric-free space, 67
  between two arbitrary media, 80–81
Bound (or polarization) charge(s), 61–67, 355, 438
Bound surface charge density, 67–70, 76, 81, 795
Bound volume charge density, 66–70, 76, 795
Breakdown
  in air, 73–74
  of dielectric, 74, 108–109, 683–684
  voltage, 110–111, 554–555
Brewster, Sir David, 517
Brewster angle, 516–517, 520

C

Capacitance
  of capacitor, 86–87, 90, 311, 356
  duality relationship between conductance and, 146–148, 159
  of isolated metallic body, 87
  p.u.l. of transmission line, 87, 542–543, 564, 577
Capacitors, 86
  circuit-theory representation of, 87
  element law for, 135
  energy of, 103
  with homogeneous dielectrics, analysis, 88–94
  with imperfect inhomogeneous dielectrics, analysis, 152–156
  with inhomogeneous dielectrics, analysis, 95–101
  with nonlinear dielectric, analysis, 102
  parallel-plate, 90
  self-discharging of nonideal, 148
  spherical, 88
Cardioid radiation pattern, 780–781
Cartesian coordinate system, 3–4, 799–800
  curl in, 195–196
  del operator in, 24
  divergence in, 36–37
  dot product of two vectors in, 36
  gradient in, 24
  Helmholtz equations in, 410–411
  Laplacian in, 82
  Laplacian of vector in, 204–205

Cavity resonators, 614, 696
electromagnetic energy stored in, 700–703
quality factor of, 703–705
rectangular, 696–700
Chain rule for taking derivatives, 798
Characteristic impedance of transmission line, 542–544, 580–582
Charge density
bound surface, 67–70, 76, 81, 795
bound volume, 66–70, 76, 795
line, 8
surface, 8
volume, 8
Charge(s)
distribution on metallic bodies of arbitrary shapes, 48–49
distribution in steady current field, 138–139
of electron, 3
per unit length, 9
point, 3–8
Circuit analysis
of lossless transmission lines, 581
of low-loss transmission lines, 581–582
of transmission lines using Smith chart, 618–622
Circuit-theory representation
of capacitor, 87, 96
of generator, 149–152
of inductor, 314–315
of magnetically coupled circuits, 325
of resistor, 142, 148
of transmission line in ac regime, 577
of transmission line in dc regime, 158
Circular polarization (CP), 458–459, 520, 764
Coaxial cable, 89–90
Coefficient of (magnetic) coupling of inductors (circuits), 325, 334
Coercive force, 245–247
Complex domain, 370–375, 381–389
Complex power, 398
Complex representatives of field and circuit quantities, 369–373
Conductance, 142, 146
of capacitors with imperfect inhomogeneous dielectrics, 153–154
p.u.l. of transmission line, 157–162, 549, 577
Conductivity, 128, 130–131
Conductors, 39, 125, 140
Constitutive equations, 138, 236, 239, 357
Continuity equation, 133–135, 138–139
complex-domain, 374
differential form of, 134
for rapidly time-varying currents, 364–366
for steady currents, 134
for surface currents (for plates), 366
for wires, 385
Continuous charge distributions, 8–9
Convection current density, 131
Copper, surface resistance of, 495
Corona discharge, 109
Cosine reference for time-harmonic quantities, 367
Coulomb, Charles Augustin de, 2
Coulomb force, 3
Coulomb's law, 2–7
Couplers, waveguide, 692–695
Critical angle, 514–515
Critical (breakdown) field intensities, 73–74
Curl, 195–197
Current density vector, 126–129
total (conduction plus displacement), 353
Current generator, 151
Current intensity (or current), 126–127
Current transformation by coupled coils, 328
Cutoff or critical frequency of waveguides, 667, 677–679
Cutoff wavelength, 667
Cylindrical coordinate system, 24, 800
curl in, 195
divergence in, 37
gradient in, 24
Laplacian in, 82

D

Decibel attenuation, 433
in wireless link, 770–771
Decibel reflection coefficient, 485
Del operator, 24–25, 366, 535
Diamagnetism, 225, 237
Dielectric breakdown, 62
in electrostatic systems, 108–114
in transmission lines, 554
in waveguides, 683
Dielectric-dielectric boundary conditions, 79–81, 363
Dielectric materials, characterization of, 71–74
Dielectric permittivity. *See* Permittivity
Dielectric strength, 73–74, 791
Dielectric waveguides, 515–516
Dipole moment, 27, 63–66, 206, 224–227
Direct currents, 124
Directional derivative, 25
Dispersion, 452–457
Dispersion diagram, 452–453, 689
Displacement current, 351–356
density in vacuum, 355
density vector, 353, 355
Divergence, 36–38
Divergence theorem, 38
Dominant cavity mode, 698
Dominant frequency range, 668, 678
Dominant waveguide mode, 668
Drift velocity, 126
Duality relationship between conductance and capacitance, 146–148, 159

E

Eddy currents, 294–301
Electrical effective aperture, 768
Electric current, defined, 125
Electric dipole, 26–27, 62–63, 792
Electric displacement vector. *See* Electric flux density vector
Electric energy, 102
of capacitor, 103
of electromagnetic system, 105
Electric energy density, 104–105, 414, 418, 477
Electric field, 7
due to charged conductors, 43–46
due to excess charge, 269
due to line charge, 10
due to polarized dielectric bodies, 68–70
due to surface charge, 10
due to volume charge, 10
Electric field intensity vector
definition, 7–8
impressed, 149
induced, 265, 283, 791
Electric flux, 71

Electric flux density vector, 71
Electric forces, 3–7, 15, 90–91, 209
Electric induction vector. *See* Electric flux density vector
Electric potential. *See* Electric scalar potential
Electric probe, 481
Electric-probe waveguide couplers, 695
Electric scalar potential, 16–18, 269, 380
due to line charge, 20
due to polarized dielectric bodies, 68–70
due to surface charge, 20
due to volume charge, 19
Electric susceptibility, 64
Electrolytes, 129–130
Electromagnetic interference (EMI), 27
Electromagnetic spectrum, 425–427
Electromagnetic waves, 361–362
Electromotive force (emf) of generator, 150
Electrostatic field
conductors in, 39–42
conservative nature of, 17
Electrostatic induction, 40
Electrostatic shielding, 46–47
Elliptical polarization (EP), 459–460, 765
Energy velocity, 454
E-plane pattern, 737, 739
Equipotential surfaces, 19
Euler's identity, 371
Evanescent attenuation, 667
Exponential identities, 797

F

Fabry-Perot resonator, 476
quality factor of, 707–708
Faraday, Michael, 272–273
Faraday cage, 46–47
Faraday's law of electromagnetic induction, 271–276, 284, 290
Far field, 720–721
Ferrites, 227, 238
Ferroelectric materials, 72
Ferromagnetic materials, 226–227, 246–247
hysteresis effects in, 336
Finite-difference (FD) method, 84–86
Fluxmeter, 293–294
Flux of vector function, 28–29
Franklin, Benjamin, 111
Free-space wavelength, 425, 445, 565, 794
Fresnel, Augustin Jean, 517
Fresnel's coefficients for normal polarization, 511
Fresnel's coefficients for parallel polarization, 511
Friis, Harald T., 769
Friis transmission formula, 768–770

G

Gauss, Johann Karl Friedrich, 29
Gaussian surface, 31
Gauss' law, 270, 353
applications of, 31–34
differential form of, 35–39
formulation and proof of, 28–31
generalized, 70–71, 138, 270, 357
for magnetic field, 173
for system with conductors and dielectrics, 70
in terms of volume charge density, 71
using divergence notation, 36
Gauss-Ostrogradsky theorem. *See* Divergence theorem
General duality principle for electromagnetic fields, 759
General impedance load, 401–402
Good conductors,439–445, 492–499
Good dielectrics, 436–438
Gradient, 23–25
Grating lobes, 776–777
Grazing incidence, 514
Grounding electrodes, 162–164
Grounding resistance, 164–167, 793
Group velocity, 454–456, 690, 793
Guided TEM wave, 534–538
Guide wavelength, 689

H

Half-power (or –3-dB) beamwidth (HPBW), 738–739
Half-wave dipole, 747–754, 763–767, 779–781
Half-wave matching, 525
Hall, Edwin Herbert, 210
Hall effect, 209
Hall voltage, 209
Hard ferromagnetic materials, 247
Heaviside, Oliver, 536
Heaviside function, 634
Helical antennas, 459, 461
Helmholtz equations, 410–411, 418–419, 431, 672–676
Helmholtz, Hermann von, 432
Henry, Joseph, 313–314
Hertz, Heinrich Rudolf, 717
Hertzian dipole, 714–720
H-plane pattern, 738
Hybrid waves, 534, 548, 563
Hyperbolic identities, 796–797
Hysteresis, 226, 245
Hysteresis loop, 245–247, 337–338
Hysteresis losses in material, 246, 335, 337

I

Ideal current generator, 151
Ideal voltage generator, 150
Image theory
for antennas in presence of conducting plane, 751–752
for charges above conducting plane, 51–52
for currents above conducting plane, 560
for magnetic field, 241
for steady currents, 163
Impedance matching, 607–608
Impedance transformers, 593
Impressed electric field intensity vector, 283
Index of refraction, 444–445, 509, 792
Induced electric field intensity vector, 265, 283, 791
Induced electromotive force (emf), 273, 481
due to motional induction, 283–289
due to self-induction, 312
due to transformer induction, 277–283
total, 289–294
Inductance. *See also* Self-inductance
external, 312–318, 543, 557–566
internal, 312, 343–344, 543, 556–557
mutual, 318–324
per unit length of transmission lines, 317–318, 330–331, 344–345, 543, 556–566
Inductance matrix, 325
Induction furnace, 295
Inductor, 314

Inductor (*Continued*)
circuit-theory representation of, 314
element law for, 314
nonlinear, 315
Infinitesimal dipole, 717
Internal resistance of generator, 150
Intrinsic impedance, 414, 490
complex, 432
of free space, 414
of good conductors, 440, 492
of good dielectrics, 437
of plasma medium, 450
Ionosphere, 448, 450–451, 756–757

J

Joule, James Prescott, 144
Joule (J), 103
Joule's heat, 132, 149
Joule's law, 143, 331
in local (point) form, 132
in "surface" form, 496

K

Kirchhoff, Gustav Robert, 22
Kirchhoff's current law, 134, 277
for magnetic circuits, 250–252
Kirchhoff's voltage law, 22, 150

L

Laplace, Pierre Simon de, 83
Laplace's equation, 82–86
Laplacian, 82–83
of vector function, 204
Law of conservation of magnetic flux, 198–201
Law of refraction
of electric field lines, 81
of magnetic field lines, 240
of steady current lines, 137
Left-hand circularly polarized (LHCP) waves, 459
Left-hand elliptically polarized (LHEP) waves, 460
Lenz, Heinrich Friedrich Emil, 275
Lenz's law, 275, 295
Lightning arrester, 111–113
Linear polarization (LP), 458
Line charge density, 8
Line dipole, 27
Line integral of electrostatic field vector, 18
Logarithmic identities, 797
Lorentz, Hendrik Antoon, 210
Lorentz force equation, 209
Lorentz magnetic force, 211
Lorenz, Ludwig Valentine, 378
Lorenz condition (or Lorenz gauge) for potentials, 376–378
Lorenz electromagnetic potentials, 376–389
Losses in transmission lines, 547–550
Lossless transmission lines
circuit analysis of, 581
pulse excitations of, 640–646
step response of, 634–640
Loss tangent, 437
Low-loss transmission lines
attenuation coefficient of, 582
characteristic impedance of, 582
load voltage reflection coefficient of, 583
load voltage transmission coefficient of, 584
phase coefficient of, 582
return loss (RL) of, 584
standing wave patterns for, 588–589

M

Magnetically coupled circuits, 324–331
Magnetic circuits
assumptions and analysis, 247–248
demagnetization in, 256–257
Kirchhoff's laws for, 250–252
reverse problem in, 255–256
Magnetic dipole, 206–208, 224–227, 792
Magnetic dipole (small loop) antenna, 758–760
Magnetic energy
of current-carrying conductors, 331–333
of inductor, 332
spent in magnetization-demagnetization, 339–340
in terms of volume currents, 333
Magnetic energy density, 334–338, 414, 418, 477
Magnetic field, 174
Magnetic field intensity vector, 235
Magnetic flux
through contour, 200
law of conservation, 198–201
through magnetic circuit, 250–255
Magnetic flux density vector, 174
due to given current distributions, 179–185
due to line current, 178
due to magnetized bodies, 231–234
due to moving point charge, 175–176
for loop and field point in one plane, 179
Magnetic force, 174
on current distributions, 211–215
Magnetic materials, behavior and classification of, 223–227
Magnetic moment of loop, 207
Magnetic pressure, 341–342
Magnetic susceptibility, 225
Magnetic vector potential, 201–204, 270, 380
Magnetization currents, 232
Magnetization curve, 243–247
Magnetization surface current density vector, 230–234
Magnetization vector, 222, 225, 228
Magnetization volume current density vector, 230
Magnetostatic field, 174
Magnetostatics, 239–241
Maxwell, James Clerk, 358–359
Maxwell's equations
in complex domain, 373–375
in differential form, 359, 374
for electrostatic field, 75
for magnetostatic field, 239
for rapidly time-varying electromagnetic field, 357–360, 373–375
for slowly time-varying electromagnetic field, 276–277
source-free, 409, 535
for time-invariant electromagnetic field, 258
Metallic conductors, 39, 125, 140
Metallic waveguides, 505–507, 663
Method of moments (MoM), 49–51
Microscopic magnetic dipoles, 228
Microscopic magnetic phenomena, 222–227
Microstrip line, including fringing effects, analysis and design, 570–572
Microstrip line, neglecting fringing effects, 91–92
Microwave oven, 706–707
Mobility of electrons, 126
Modal fields. *See* Modes

Modes, 665, 671–679
MoM matrix equation, 49–51
Multilayer printed circuit board, 567–570
Multimode propagation, 668
Mutual inductance, 318–324

N

Nabla operator. *See* Del operator
Napier, John, 432
Near field, 721–722
Newton's second law, 448
Newton's third law, 3
Nonlinear capacitors, 87
Nonlinear dielectrics, 72
Nonlinear resistors, 142
Nonpropagating waves, 450, 667
Nonrectangular coordinate systems, 24–25, 800
Normal incidence
  on penetrable planar interface, 483–492, 520–526
  on perfectly conducting plane, 472–483
Normalized transmission line admittance, 594
Normalized load impedance, 616
Normalized transmission-line impedance, 594
Normally dispersive media, 455
Normal polarization of obliquely incident waves, 499–503

O

Oblique incidence on dielectric interface, 507–520
Oblique incidence on PEC, 499–504
Oersted, Hans Christian, 175
Ohm, Georg Simon, 141–142
Ohmic losses. *See* Power of Joule's losses
Ohm's law, 128–129, 141–142
One-dimensional (1-D) differential Gauss' law, 37
One-dimensional scalar wave equation, 413
One-dimensional source-free wave equation, 378–379
Onnes, Heike Kamerlingh, 129, 132
Open-ended waveguide antennas, 694
Optical anti-reflective coatings, 524–525
Optical fibers, 515–516
Overlapping pulses, 643–644
Overmoded operation of waveguides, 669

P

Parallel-plate waveguide, 505
Parallel polarization of obliquely incident waves, 499–500, 503–504
Paramagnetic materials, 225
Pattern multiplication theorem, 774
Perfect electric conductors (PEC), 130, 361, 363
Perfect magnetic conductors (PMC), 237, 241
Permeability
  of magnetic materials, 236–239
  on magnetization curve, 245, 250
  of vacuum, 174
Permittivity
  effective relative of transmission line, 564, 569
  equivalent complex, 430
  of good dielectrics, 438
  high-frequency, 438
  of medium, 72–73
  plasma effective, 449
  tensor, 72
  of vacuum (free space), 3
Perturbation method for computation of losses in good conductors, 497–499, 547–556, 610–614, 684–687, 703–705, 731–732
Per-unit-length dipole moment, 27
Phase coefficient
  in plasma medium, 449
  in transmission line, 537, 544, 565, 581–582
  in unbounded lossless media, 381
  in unbounded lossy media, 434, 437, 440
  in waveguide, 666
Phase velocity, 417
  in dispersive media, 452
  in good conductors, 444
  in nondispersive media, 455
  in transmission line, 537, 544, 565, 579
  in waveguide, 689
Phasors, 369–370
Planar multilayer media, 520–526
Plasma effective permittivity, 449
Plasma frequency, 449
Plasmas
  propagation of electromagnetic waves in, 447–450
  wave dispersion in, 456–457
pn junction, 77–79, 130
Point charges, 3–8
Poisson, Siméon Denis, 83
Poisson's equation, 82, 205
Polar dielectrics, 62
Polarization charges. *See* Bound (or polarization) charges
Polarization current density vector, 355
Polarization ellipse, 460
Polarization of antennas, 745, 762
Polarization of dielectrics, 62–63
Polarization of uniform plane waves
  circular (CP), 458–459, 520, 764
  elliptical (EP), 459–460, 765
  handedness of, 459–460, 463
  linear (LP), 458, 460–461
Polarization vector, 63–64, 67, 76
Position vector of point, 4
Power balance in circuit, 124
Power of Joule's losses, 132–133, 143, 792
  in antennas, 731–732
  in capacitor, 136
  in cavity resonator, 704
  density, for plane waves, 433
  due to eddy currents, 295
  in good conductors, 493–499
  in resistor with time-varying current, 368
  time-average, 368
  in transmission lines in ac regime, 547–551
  in transmission lines with steady currents, 159
  in waveguides, 685
Poynting, John Henry, 391
Poynting's theorem, 389–402
Poynting vector, 392
  complex, 398
Principle of conservation of charge, 133
Principle of conservation of energy, 17, 102, 331
Pulse excitations, transmission lines with, 640–646

Q

Quadratic equation, 797
Quality factor (or Q factor) of resonators, 610–614

Quality factor (or Q factor) of resonators (*Continued*)
of cavity resonators, 703–705
of Fabry-Perot resonator, 707–708
of transmission-line resonators, 612–614
Quarter-wave transformer, 594–597
Quasistatic (low-frequency) complex potentials and fields, 384
Quasistatic electromagnetic systems, 384–385
Quasi-TEM waves, 548, 563

R

Radian frequency, 367
Radiation efficiency of antenna, 733
Radio-frequency (RF) waves, 427
Radio waves, 427
Rapidly time-varying electromagnetic field
boundary conditions for, 363
Maxwell's equations for, 357–360, 373–375
Reactive power, 398, 495, 733
Rectangular cavity resonators, 696–708
Rectangular waveguides, 663
analysis based on multiple reflections, 664–671
dominant mode in, 668–671
general TE modal analysis of, 671–676
general TM modal analysis of, 676–677
Reflection coefficient, 485, 511, 522, 583–585, 632–633
Relative permeability, 236. *See also* Permeability
Relative permittivity, 72. *See also* Permittivity
Relaxation time, 139–140, 611
Reluctance, 252
Remanent flux density, 245
Resistance
antenna ohmic, 750–751
of conductor, 141
dc resistance p.u.l. of transmission lines, 157–159
grounding, 164–167
high-frequency resistance p.u.l. of transmission lines, 549, 577
radiation, 730
surface resistance of good conductors, 492–496, 548, 685
Resistance-capacitance analogy, 148
Resistors, 140–146
circuit-theory representation of, 142
parallel, 145–146
power of Joule's losses in, 143
series, 145
Resonators
Fabry-Perot resonators, 476, 707–708
transmission-line resonators, 608–614
waveguide cavity resonators, 696–708
Retarded potentials. *See* Lorenz electromagnetic potentials
Right-hand circularly polarized (RHCP) waves, 459
Right-hand elliptically polarized (RHEP) waves, 460
Right-hand rule for induced electromotive force, 274
Rms (root-mean-square) value, of time-harmonic function, 367–368

S

Savart, Fèlix, 178
Scalar triple product, 284, 799
Scattered electromagnetic field, 473
Self-inductance, 312–318, 342–345
Semiconductors, 130
Shunt stubs, 604–605
SI units, 791–795
Siemens, Ernst Werner Von, 142
Siemens, Karl Wilhelm Von, 142
Skin depth
for copper, 442
definition, 441
for good conductors, 442
one-percent depth of penetration, 444
Skin effect, 295–296, 441–447
in ferromagnetic cores, 295
in good conductors, 492, 497
Slowly time-varying electromagnetic field, 264
Maxwell's equations for, 276–277
Smith chart, 614–628
Snell, Willebrord van Royen, 517
Snell's law of reflection, 501
Snell's law of refraction, 508–509, 511, 513
Soft ferromagnetic materials, 246
Solid angle, 28
Spherical coordinate system, 24–25, 800
curl in, 196
divergence in, 37
gradient in, 25
Laplacian in, 82
Spherical electromagnetic waves, 380
Standing wave patterns, transmission lines, 586–587, 603–604
Standing wave ratio (SWR), 490, 586
Standing waves, 474–483
Steady electric currents, 124
Step response of transmission lines, 634–640, 646–655
Stokes, Sir George Gabriel, 199
Stokes' theorem, 197–198
Stored electromagnetic energy, 391
Strip line, including fringing effects, analysis and design, 570, 572–573
Strip line, neglecting fringing effects, 92
Stubs, 604–605
Superconductors, 129, 294, 318
Superposition principle, 3–4
Surface charge density, 8
Surface current
continuity equation for, 366
density vector, 127–128
magnetization, 230–234
Surface density of reactive power, 495
Surface divergence, 366
Surface reactance of good conductors, 492–499
Surface wave, 514

T

Telegrapher's equations, 577–580, 629
TEM (transverse electromagnetic) waves, 413, 536
Tesla, Nikola, 176–177
Thales of Miletus, 2
Thévenin equivalent generator, 631–632, 649–651, 761
Thévenin impedance of receiving antenna, 761–762
Thin two-wire line, 92–93
Three-layer medium, propagation in, 521

Time-average power, 368, 398
Time-domain reflectometer (TDR), 638, 652–653
Time-harmonic electromagnetics, 366–369
Time-invariant (dc) regime, 124
Time period, 140
Time-varying electromagnetic field, 263
Torque, 214–215
Total (conduction plus displacement) current, 353
Total internal reflection, 514–516
Total transmission, 519
Transformer induction, 277–278
Transients on transmission lines, 628–630
Transmission coefficient, 485
Transmission-line resonators, 608–614
Transmission lines
  bounce diagram for, 646–648
  circuit analysis of, 577–582
  generalized reflection coefficient of, 585
  input impedance of, 593
  load reflection coefficient of, 583
  with nonlinear terminations, transient analysis of, 652, 655
  one-way delay time of, 631
  power computations of, 589–591
  pulse excitations, analysis of, 640–646
  with reactive loads, transient analysis of, 649–654
  with resistive loads, transient analysis of, 634–648
  Smith chart for, 614–628
  standing wave ratio (SWR) of, 586
  with steady currents, 156–162
  step response of, 634–640, 646–655
  transient analysis of, 628–630
Transmission lines, field theory of, 533
  circuit parameters of, 557–566
  effective relative permittivity of, 564, 569
  with inhomogeneous dielectric, 563–570
  propagation coefficient of, 537, 544
  small losses in, 547–556
Transverse electric (TE) waves, 671
Transverse magnetic (TM) waves, 676
Trigonometric identities, 796
Two-conductor transmission lines, 540–546, 577, 579

U

Uniform plane electromagnetic waves
  in good conductors, 439–447
  in good dielectrics, 436–439
  in ionosphere, 450–451
  in lossless media, 412–429
  in lossy media, 429–436
  in multilayer media, 520–526
  in plasma, 447–451
  polarization of, 458–465
Units, 791–795

V

Vector addition, 3
Vector algebraic identities, 799
Vector calculus identities, 799
Vector product, 174
Velocity of electromagneticwaves, 378, 413–414
Volta, Alessandro, 22
Voltage, 21

W

Watt, James, 132
Wave equations, 377, 409–410
Waveguide(s), 662
  aspect ratio, 678
  attenuation coefficient, 686–687
  couplers, 692–695
  cutoff or critical frequency of, 667, 677–679
  dielectric breakdown and power-handling capacity of, 683–684
  dominant mode in, 668–671
  group velocity, 690–692
  overmoded operation of, 669
  phase coefficient, 666
  phase velocity, 689
  power flow along, 681–684
  with small losses, 684–688
  standard, 678–679
  TE wave impedance, 680–681
  TM wave impedance, 680–681
  usable frequency range of, 686
  wave dispersion in, 688–690
Wave impedance
  of TE and TM waves, 680–681
  of TEM wave, 491–492, 522, 537
Wavelength, 381, 416–417, 425, 537, 544, 579, 689–690
Wavenumber. *See* Phase coefficient
Weber, Wilhelm Eduard, 199